GEOLOGICAL SURVEY OF CANADA
COMMISSION GÉOLOGIQUE DU CANADA

PAPER 83-1A
ÉTUDE

CURRENT RESEARCH
PART A

RECHERCHES EN COURS
PARTIE A

Canada

1983

Notice to Librarians and Indexers

The Geological Survey's thrice-yearly *Current Research* series contains many reports comparable in scope and subject matter to those appearing in scientific journals and other serials. All contributions to the Scientific and Technical Report section of *Current Research* include an abstract and bibliographic citation. It is hoped that these will assist you in cataloguing and indexing these reports and that this will result in a still wider dissemination of the results of the Geological Survey's research activities.

Avis aux bibliothécaires et préparateurs d'index

La série Recherches en cours *de la Commission géologique paraît trois fois par année; elle contient plusieurs rapports dont la portée et la nature sont comparable à ceux qui paraissent dans les revues scientifiques et autres périodiques. Tous les articles publiés dans la section des rapports scientifiques et techniques de la publication* Recherches en cours *sont accompagnés d'un résumé et d'une bibliographie, ce qui vous permettra, nous l'espérons, de cataloguer et d'indexer ces rapports, d'où une meilleure diffusion des résultats de recherche de la Commission géologique.*

Technical editing and compilation
Rédaction et compilation techniques
R.G. Blackadar
H. Dumych
P.J. Griffin
W.C. Morgan
N.C. Ollerenshaw
L.E. Vincent

Production editing and layout
Préparation et mise en page
M.J. Kiel
Leona R. Mahoney

Typed and checked by
Dactylographie et vérification
Jacinthe Caron
Janet Legere
Janet Gilliland
Shirley Kostiew
Sharon Parnham

GEOLOGICAL SURVEY
PAPER 83-1A

COMMISSION GÉOLOGIQUE
ÉTUDE 83-1A

CURRENT RESEARCH
PART A

RECHERCHES EN COURS
PARTIE A

1983

Available in Canada through

authorized bookstore agents
and other bookstores

or by mail from

Canadian Government Publishing Centre
Supply and Services Canada
Hull, Québec, Canada K1A 0S9

and from

Geological Survey of Canada
601 Booth Street
Ottawa, Canada K1A 0E8

A deposit copy of this publication is also available
for reference in public libraries across Canada

Cat. No. M44-83/1AE Canada: $12.00
ISBN 0-660-11257-4 Other countries: $14.40

Price subject to change without notice

Geological Survey of Canada – ***Commission géologique du Canada***

R.A. PRICE
Director General
Directeur général

J.G. FYLES
Chief Geologist
Géologue en chef

M.J. KEEN
Director, Atlantic Geoscience Centre, Dartmouth, Nova Scotia
Directeur du Centre géoscientifique de l'Atlantique, Dartmouth (Nouvelle-Ecosse)

J.A. MAXWELL
Director, Central Laboratories and Technical Services Division
Directeur de la Division des laboratoires centraux et des services techniques

R.G. BLACKADAR
Director, Geological Information Division
Directeur de la Division de l'information géologique

W.W. NASSICHUK
Director, Institute of Sedimentary and Petroleum Geology, Calgary, Alberta
Directeur de l'Institut de géologie sédimentaire et pétrolière, Calgary (Alberta)

J.C. McGLYNN
Director, Precambrian Geology Division
Directeur/par int. de la Division de la géologie du Précambrien

A.G. DARNLEY
Director, Resource Geophysics and Geochemistry Division
Directeur de la Division de la géophysique et de la géochimie appliquées

J.S. SCOTT
Director, Terrain Sciences Division
Directeur de la Division de la science des terrains

D.C. FINDLAY
Director, Economic Geology Division
Directeur de la Division de la géologie économique

R.B. CAMPBELL
Director, Cordilleran Geology Division, Vancouver, British Columbia
Directeur de la Division de la géologie de la Cordillère, Vancouver (Colombie-Britannique)

Separates

A limited number of separates of the papers that appear in this volume are available by direct request to the individual authors. The addresses of the Geological Survey of Canada offices follow:

601 Booth Street,
OTTAWA, Ontario
K1A 0E8

Institute of Sedimentary and Petroleum Geology,
3303-33rd Street N.W.,
CALGARY, Alberta
T2L 2A7

Cordilleran Geology Division
100 West Pender Street,
VANCOUVER, B.C.
V6B 1R8

Atlantic Geoscience Centre,
Bedford Institute of Oceanography,
P.O. Box 1006,
DARTMOUTH, N.S.
B2Y 4A2

When no location accompanies an author's name in the title of a paper, the Ottawa address should be used.

Tirés à part

On peut obtenir un nombre limité de "tirés à part" des articles qui paraissent dans cette publication en s'adressant directement à chaque auteur. Les adresses des différents bureaux de la Commission géologique du Canada sont les suivantes:

601, rue Booth
OTTAWA, Ontario
K1A 0E8

Institut de géologie sédimentaire et pétrolière
3303-33rd, St. N.W.,
CALGARY, Alberta
T2L 2A7

Division de la géologie de la Cordillère
100 West Pender Street
VANCOUVER, Colombie-Britannique
V6B 1R8

Centre géoscientifique de l'Atlantique
Institut océanographique de Bedford
B.P. 1006
DARTMOUTH, Nouvelle-Ecosse
B2Y 4A2

Lorsque l'adresse de l'auteur ne figure pas sous le titre d'un document, on doit alors utiliser l'adresse d'Ottawa.

SCIENTIFIC AND TECHNICAL REPORTS
RAPPORTS SCIENTIFIQUES ET TECHNIQUES

ECONOMIC GEOLOGY/GÉOLOGIE ÉCONOMIQUE

GEOCHEMISTRY/GÉOCHIMIE

GEOMATHEMATICS/GÉOMATHÉMATIQUES

GEOPHYSICS/GÉOPHYSIQUE

MARINE GEOSCIENCE/ÉTUDES GÉOSCIENTIFIQUES DU MILIEU MARIN

PETROLOGY/PÉTROLOGIE

QUATERNARY GEOLOGY/GÉOLOGIE DU QUATERNAIRE

Inventory Mapping and Stratigraphic Studies/Inventaire cartographique et stratigraphique

Paleoecology and Geochronology/Paléoécologie et géochronologie

Sedimentology and Geomorphology/Sédimentologie et géomorphologie

REGIONAL GEOLOGY/GÉOLOGIE RÉGIONALE

Appalachian Region/Région des Appalaches

Cordilleran Region/Région de la Cordillère

Precambrian Shield/Bouclier précambrien

SCIENTIFIC AND TECHNICAL NOTES
NOTES SCIENTIFIQUES ET TECHNIQUES

DISCUSSIONS AND COMMUNICATIONS
DISCUSSIONS ET COMMUNICATIONS

1. # SOME CHEMICAL ASPECTS OF THE REGOLITHIC AND HYDROTHERMAL ALTERATIONS ASSOCIATED WITH THE URANIUM MINERALIZATION IN THE ATHABASCA BASIN, SASKATCHEWAN

Project 750058

L.P. Tremblay
Economic Geology Division

Tremblay, L.P., Some chemical aspects of the regolithic and hydrothermal alterations associated with the uranium mineralization in the Athabasca Basin, Saskatchewan; in Current Research, Part A, Geological Survey of Canada, Paper 83-1A, p. 1-14, 1983.

Abstract

Chemical analyses were carried out on 45 pairs of whole-rock samples from intensely altered and less altered basement in the vicinity of the major known unconformity-type uranium deposits in Saskatchewan. The results indicate that magnesia was depleted when the rocks underwent regolithic alteration and was later added when the rocks were altered by the mineralizing solutions, that is, when the uranium deposits were formed after deposition of the Athabasca rocks. Other chemical changes indicated are an apparent decrease in silica and an apparent increase in alumina, water, TiO_2 and, in most locations potash. Soda appears to have been removed completely. The above changes should be taken as trends only. These trends also remained when the data were treated with Al_2O_3 concentrations assumed to be constant.

Introduction

During the last five years I made one to three day visits to most of the uranium deposits associated with the Athabasca Basin in Saskatchewan to evaluate the uranium resources for the Department of Energy, Mines and Resources. The deposits visited were Rabbit Lake, Collins Bay A and B zones, West Bear, Raven and Horseshoe, McClean Lake, Midwest Lake, Dawn Lake, Key Lake, Cluff Lake, Maurice Bay, Stewart Island and Fond-du-Lac (Tremblay, 1982).

Because all the deposits are under a thick cover of overburden and also in most places under a thick cover of Athabasca strata, the examination of most was based on diamond drill cores only, except for Rabbit Lake and Cluff Lake D orebody which were also inspected in open pits.

This paper presents preliminary results of whole-rock chemical analyses of a suite of samples selected from various deposits and presents broad chemical characteristics of the two main alteration types (regolithic and hydrothermal) associated with these deposits (Tremblay, 1978).

Geological Setting

All the deposits are spatially related to the Athabasca Basin and to the sub-Athabasca unconformity, although the unconformity between Archean and Aphebian rocks recognized in the vicinity of most deposits is not regarded as significant in the deposit genesis.

The Athabasca Basin is a broad east-west structure, 425 km by 225 km, containing about 1500 m of flat-lying Helikian sandstones of the Athabasca Group. It lies with marked angular unconformity upon a Hudsonian basement of intensely deformed and metamorphosed Archean and Aphebian sedimentary, plutonic and volcanic rocks.

The basement is made up of a stable craton of mainly Archean rocks under the northwestern two-thirds of the basin and of a northeasterly trending belt of mainly Aphebian metasedimentary rocks enclosing areas and domes of Archean granite gneiss under the southeastern third of the basin.

Below the sub-Athabasca unconformity, basement rocks are altered in a thin red hematite-rich zone which changes downward over a metre or so into a light-coloured zone rich in kaolinite, chlorite, and illite or sericite. This changes gradationally downward over a few metres into unaltered rock. The alteration is assumed to be due to weathering and to indicate the presence of a regolith at the unconformity at the base of the Athabasca rocks (Macdonald, 1980). The regolithic zone is not present everywhere, since it was locally eroded before deposition of the Athabasca rocks.

The Athabasca Basin is filled mainly with quartz-rich pebbly sandstone, together with minor conglomerate, and shale or siltstone of the Athabasca Group. The sandstone is poorly sorted near the base and in the upper half of the succession is interbedded with larger amounts of shale and siltstone (Fahrig, 1961; Lerand, 1970). Conglomerate occurs as discontinuous layers of various thicknesses throughout the succession. The Athabasca rocks are unmetamorphosed, but locally may be silicified and indurated or argillized and softened. The Athabasca Group was probably deposited between 1500 and 1650 Ma (Fahrig and Loveridge, 1981). It has been subdivided into nine formations by Ramaekers (1980). It is cut by a few gabbro dykes that strike mainly northwesterly and that are about 1200 Ma old (Fahrig and Jones, 1969). The Athabasca succession is intersected in the western half of the basin by the Carswell Circular Structure, a multiring structure, 35 km in diameter, consisting of an uplifted core of basement granitic gneisses surrounded by two rings of deformed but unmetamorphosed Athabasca strata.

The basement rocks and the Athabasca strata at the unconformity are mineralized locally with uranium or with uranium and abundant nickel, cobalt and arsenic and locally some gold, silver, selenium and tellurium. This mineralization is assumed to be spatially related to the unconformity as it occurs where there are irregularities on the unconformity surface and where there are zones of intense clay alteration. It is the only type of mineralization treated in this study which excludes other types of Pb-Zn, Cu-U and U-P mineralization found in basement rocks of northern Saskatchewan that are not related to the sub-Athabasca unconformity.

The clay alteration zones (Tremblay, 1978) are considered to result from both regolithic and mineralizing processes. The rocks affected by the regolithic processes are characterized in hand specimen by a grey white colour, by a clay-like very fine grained appearance, by softness and by little cohesion. The rocks affected by the mineralizing processes are similar except that they are grey to light yellowish green, their grain size is relatively coarser and they are better lithified, though soft. The mineralizing processes are assumed to have caused these differences or changes, because of the close spatial relationship between the intensity of mineralization and the intensity of clay alteration. As there is an obvious increase in uranium content with increase of clay alteration (Table 1.1), the alteration is believed to be related directly to the mineralizing process. Altered rocks with coarse sericite were dated by the K-Ar method at 1260 Ma (Tremblay, 1982). Pagel et. al. (1979) suggested that the mineralizing solutions were hydrothermal, because fluid inclusion studies on quartz and carbonate associated with the mineralization indicated temperatures between 60 and 260°C. The mineralizing solutions altered both basement and Athabasca rocks and appear to have circulated mainly along the sub-Athabasca unconformity and related faults, since it is there that the alteration is strongest. The altered areas resulting from the mineralizing solutions are found mainly in coarse grained basement rocks rich in feldspar and in regolithic areas of basement rocks. In general the mineralizing alteration does not extend much more than 100 m below the unconformity into the basement rocks, nor much more than 40 m above the unconformity into Athabasca strata.

Present Work

Information supplied by the various mine operators was used in the selection of the cores studied in this project. In most cases, cores from four to twelve holes were examined at each deposit. Generally the holes selected were distributed along a line of section that extended from barren or weakly mineralized rock across the rich part of the ore zone into relatively unmineralized rock. Some cores from barren rocks were also examined. In rare instances the positions of the holes studied were erratic because of unavailability of core due to previous sampling or loss of core during drilling. Generally, cores were examined to determine the types and intensity of alteration, the nature and age of host rocks (basement or Athabasca), the type and grade of mineralization and any other significant geological features such as the colour of the rocks, the colour of the clay-altered section and the coarseness of the clay minerals particularly sericite and chlorite. Where it was possible, samples of the above various features were collected for future reference and use. Altogether about 1200 samples were obtained, most of them 3 to 7 cm long by 1 to 3 cm across. All samples were from core except in the case of Rabbit Lake and Cluff Lake D orebody, where samples were also obtained from the open pits.

In examining drill core the criteria used to distinguish between the two main types of alteration (regolithic and mineralizing-hydrothermal) were as follows:

1. The regolithic alteration was assumed to be present where, at and below the sub-Athabasca unconformity there is a thin red hematitic zone of weathered material which varies downward, over a metre or so, into a light-coloured zone and thence gradationally downward over a few metres into unweathered rock. This weathered profile is assumed to be typical of the regolithic alteration. However, if the red zone at the unconformity is missing, possibly removed by erosion, and if the remaining part of the weathered profile is present, the alteration was assumed to be regolithic provided that the core is not mineralized or only weakly mineralized, and that its alteration minerals are clay-sized. Possibly core samples from some such doubtful weathered profiles should not have been used in this study, as they could have been affected by the mineralizing solutions, but nevertheless they were retained and analyzed in an attempt to detect characteristics of both types of alteration.
2. The alteration associated with the mineralizing solutions was assumed to be present where the core came from a particularly U-rich, highly clay-altered area. This is based on the apparent general spatial relationship between the clay-altered areas and the mineralization (Table 1.1). This alteration is referred to later in this paper as hydrothermal alteration. Generally the core from such areas is composed of clay-size particles, is grey to light yellowish green, and is somewhat fissile because of the abundance of flakes of sericite and chlorite. These flakes are somewhat coarser (still generally much less than 1 mm) than those of the regolithic altered zones.

Table 1.1

Uranium content of a few of the samples in Table 1.3 showing that altered rocks are richer in U. Analyzed by delayed neutron activation in the AECL Laboratory in Ottawa

Weakly Altered Rock		Intensely Altered Rock		
Sample no.	U in ppm	Sample no.	U in ppm	Deposit
254	5.3	245	15.8	McClean Lake
252	341.0	251	869.0	McClean Lake
181	7.7	179	65.3	Maurice Bay
89	26.7	88	71.5	Collins Bay A
116	4.3	112	240.0	Collins Bay B
129	3.1	125	441.0	Collins Bay B
99	9.0	97	128.0	Rabbit Lake
92	7.2	91	21.6	Raven
103	9.6	102	60.2	West Bear
202	93.8	155	142.0	Midwest Lake
211	12.2	208	59.4	Midwest Lake
170	26.0	169	36.9	Cluff Lake
271	94.0	269	863.0	Key Lake
284	34.6	282	1250.0	Key Lake
290	4.6	286	307.0	Key Lake

Table 1.2

Chemical analyses of selected 21 pairs of core samples from 21 holes in areas of known uranium deposits throughout the Athabasca Basin*

Deposit	Collins Bay A zone		West Bear		Collins Bay B zone								Conwest	
Pair no.	1		2		3		4		5		6		7	
Lab no.	87	89	101	103	116	117	128	130	134	135	139	141	232	234
SiO_2	22.2	68.0	57.1	69.1	69.7	70.6	67.8	70.2	72.9	74.6	73.6	73.9	66.7	78.0
TiO_2	1.36	0.37	0.63	0.81	0.38	0.25	0.36	0.26	0.26	0.18	0.32	0.27	0.78	0.55
Al_2O_3	17.1	19.5	18.5	15.9	19.9	16.3	21.0	15.0	19.2	12.8	18.7	13.7	18.1	12.8
Fe_2O_3	41.0	0.8	9.8	0.6	0.1	2.4	0.6	0.6	0.0	0.4	0.2	0.2	2.3	1.1
FeO	1.3	0.0	0.0	0.1	0.1	0.0	0.1	1.4	0.2	0.0	0.0	2.0	0.0	0.0
MnO	0.07	0.01	0.01	0.01	0.01	0.01	0.00	0.02	0.00	0.01	0.00	0.03	0.01	0.01
MgO	0.38	2.28	3.54	3.94	0.35	1.89	0.40	2.03	0.09	2.93	0.26	1.28	0.51	0.42
CaO	0.22	0.03	0.07	0.16	0.02	0.10	0.01	0.13	0.00	0.15	0.01	2.01	0.06	0.02
Na_2O	0.0	0.0	0.0	0.0	0.0	0.0	0.0	0.0	0.0	0.0	0.0	3.5	0.0	0.0
K_2O	1.23	1.11	2.44	2.78	3.00	4.31	2.97	6.49	0.78	2.84	1.58	1.99	5.17	3.81
H_2O	9.6	7.2	6.3	5.2	6.1	4.1	6.3	4.6	6.7	5.6	5.3	1.1	5.0	2.3
P_2O_5	1.24	0.03	0.08	0.11	0.01	0.04	0.07	0.06	0.00	0.05	0.02	0.00	0.06	0.04
CO_2	0.6	0.1	0.5	0.1	0.0	0.3	0.0	0.0	0.0	0.8	0.1	0.1	0.0	0.0
S	0.29	0.20	0.15	0.20	0.00	0.00	0.00	0.01	0.01	0.01	0.04	0.01	0.09	0.05
Volat.	0.0	0.0	0.0	0.0	0.0	0.0	0.0	0.0	0.0	0.0	0.0	0.0	0.0	0.0
Rb	0.003	0.002	0.004	0.008	0.004	0.012	0.004	0.008	0.002	0.009	0.002	0.003	0.011	0.011
Zn	0.014	0.003	0.008	0.010	0.001	0.005	0.000	0.002	0.000	0.001	0.001	0.002	0.013	0.001
Total	98.1	99.6	99.3	99.1	99.8	100.4	99.7	100.9	100.2	100.4	100.1	100.3	98.9	99.2
Distance below unconform. in m.	0.3	5.5	0.3	11	4	21	1	28	0.3	7.6	1	14.3	0.6	5.8

Deposit	Midwest				McClean Lake		Key Lake							
Pair no.	8		9		10		11		12		13		14	
Lab no.	149	147	213	214	250	253	229	226	258	256	277	276	294	293
SiO_2	65.6	71.0	38.9	55.5	32.8	76.6	66.5	75.8	72.4	81.3	68.8	72.4	59.8	79.3
TiO_2	1.22	0.72	1.71	1.91	1.61	0.00	0.58	0.46	0.72	0.48	0.64	0.47	2.88	0.32
Al_2O_3	18.5	16.5	31.2	21.6	20.6	14.1	16.8	11.2	15.3	9.2	16.3	13.3	25.7	13.8
Fe_2O_3	0.4	0.3	2.3	0.4	28.4	0.6	6.2	0.2	0.0	0.5	0.1	0.8	0.5	0.1
FeO	0.0	0.0	0.9	0.6	0.0	0.0	0.5	3.0	0.5	0.3	0.8	0.2	0.0	0.6
MnO	0.00	0.00	0.01	0.01	0.08	0.00	0.02	0.03	0.00	0.01	0.01	0.01	0.01	0.00
MgO	4.81	2.69	9.73	8.24	1.22	3.18	0.72	1.38	3.59	3.90	4.06	4.67	0.18	0.05
CaO	0.07	0.09	0.11	0.56	0.14	0.10	0.32	0.06	0.09	0.04	0.22	0.82	0.02	0.00
Na_2O	0.0	0.0	0.0	0.0	0.0	0.0	0.0	0.3	0.0	0.0	0.0	0.1	0.0	0.0
K_2O	2.40	3.02	3.24	1.50	5.75	1.82	2.40	5.14	2.70	0.30	2.77	0.95	0.66	0.44
H_2O	5.5	4.5	12.0	8.8	6.9	3.2	5.0	1.6	4.4	4.2	5.0	5.2	9.4	5.3
P_2O_5	0.06	0.06	0.03	0.38	0.1	0.04	0.27	0.02	0.03	0.05	0.12	0.02	0.10	0.07
CO_2	0.0	0.3	0.0	0.1	0.2	0.3	0.8	0.0	0.2	0.2	0.1	1.3	0.0	0.0
S	0.13	0.13	0.03	0.06	0.00	0.00	0.02	0.05	0.09	0.03	0.45	0.00	0.04	0.04
Volat.	0.0	0.0	0.0	0.0	0.0	0.0	0.0	0.0	0.0	0.0	0.0	0.0	0.0	0.0
Rb	0.003	0.004	0.007	0.003	0.009	0.002	0.008	0.017	0.004	0.001	0.005	0.005	0.002	0.002
Zn	0.000	0.001	0.003	0.002	0.004	0.000	0.006	0.002	0.000	0.012	0.002	0.002	0.001	0.001
Total	98.8	99.5	100.2	99.8	98.1	100.0	100.2	99.4	100.1	100.6	99.5	100.3	99.4	100.0
Distance below unconform. in m.	9.8	3.7	5.5	24.7	0.3	3.7	2	7	20.4	3	27.5	15	4	1.6

Deposit	Key Lake				Cluff Lake						Maurice Bay			
Pair no.	15		16		17		18		19		20		21	
Lab no.	297	296	300	298	159	160	161	163	196	197	189	186	224	221
SiO_2	68.2	69.7	43.0	66.2	74.5	76.5	73.2	79.5	73.2	74.5	69.6	71.7	31.1	44.4
TiO_2	0.72	0.64	2.00	0.48	0.01	0.26	0.57	0.51	0.06	0.62	0.80	0.68	1.58	1.13
Al_2O_3	17.0	15.0	32.0	16.7	15.7	10.3	14.8	8.7	17.8	15.4	15.9	15.9	26.6	29.9
Fe_2O_3	0.4	0.4	1.0	0.4	0.3	0.1	0.9	0.8	0.2	0.3	3.7	1.2	20.5	1.5
FeO	0.2	0.3	0.6	0.6	0.0	2.3	0.0	2.0	0.0	0.1	0.3	0.0	0.0	0.4
MnO	0.01	0.00	0.00	0.01	0.01	0.01	0.02	0.01	0.00	0.00	0.0	0.01	0.01	0.01
MgO	4.23	5.77	5.00	6.43	1.15	3.04	2.07	4.34	0.41	3.23	1.97	2.53	5.52	8.38
CaO	0.16	0.03	0.10	0.09	0.14	0.04	0.13	0.07	0.05	0.03	0.08	0.26	0.20	0.08
Na_2O	0.0	0.0	0.0	0.0	0.0	0.2	0.0	0.0	0.0	0.0	0.0	0.0	0.0	0.0
K_2O	3.36	1.26	7.00	0.32	4.34	4.89	3.54	1.24	5.23	2.35	3.09	3.67	2.69	3.50
H_2O	4.9	5.1	8.1	6.6	4.2	2.0	4.0	3.3	3.2	4.0	3.9	4.0	8.9	10.0
P_2O_5	0.07	0.01	0.30	0.11	0.05	0.03	0.02	0.04	0.03	0.04	0.16	0.21	0.50	0.09
CO_2	0.1	0.0	0.3	0.1	0.0	0.0	0.0	0.0	0.2	0.3	0.3	0.1	0.0	0.0
S	0.05	0.10	0.20	0.05	0.03	0.24	0.14	0.15	0.00	0.00	0.00	0.00	0.08	0.04
Volat.	0.0	0.0	0.0	0.0	0.0	0.0	0.0	0.0	0.0	0.0	0.0	0.0	0.0	0.0
Rb	0.007	0.005	0.000	0.002	0.007	0.009	0.010	0.004	0.008	0.004	0.006	0.011	0.004	0.014
Zn	0.002	0.005	0.000	0.002	0.000	0.003	0.003	0.001	0.001	0.001	0.001	0.001	0.001	0.002
Total	99.4	98.6	100.1	98.1	100.5	100.0	99.5	100.7	100.3	100.9	100.0	100.3	98.1	98.7
Distance below unconform. in m.	4.0	3	24.7	7.3	3	30.5	31.4	66.8	7.6	30.5	1	34	2	12

* These samples are believed to represent the chemical changes that took place when the unconformity was formed before the deposition of the Athabasca strata. The analysis on the right of each sample pair is from the less altered rock whereas the other is from the altered rock. The changes are regarded as regolithic. All samples are basement rock.

Table 1.3

Chemical analyses of selected 24 pairs of core samples from 24 holes in areas of known uranium deposits throughout the Athabasca Basin*

Deposit	McClean Lake				Maurice Bay				Collins Bay A zone		Rabbit	
Pair no.	1		2		3		4		5		6	
Lab no.	245	254	251	252	179	181	185	186	88	89	97	99
SiO_2	40.4	72.5	55.9	69.9	37.0	64.8	70.0	71.7	40.6	68.0	36.6	81.4
TiO_2	0.04	0.01	0.02	0.01	0.70	0.56	0.68	0.68	1.16	0.37	0.93	0.26
Al_2O_3	33.5	15.6	17.5	18.2	35.0	18.4	17.0	15.9	33.4	19.5	21.2	6.7
Fe_2O_3	0.9	0.6	8.5	3.2	3.0	1.9	0.7	1.2	1.3	0.8	1.4	1.5
FeO	0.0	0.0	0.0	0.3	0.0	0.0	0.2	0.0	0.3	0.0	0.8	0.1
MnO	0.01	0.01	0.02	0.01	0.00	0.00	0.01	0.01	0.01	0.01	0.03	0.01
MgO	9.17	4.59	2.88	0.79	8.73	2.23	2.86	2.53	7.56	2.28	25.12	4.65
CaO	0.26	0.12	0.19	0.04	0.17	1.12	0.05	0.26	0.10	0.03	0.49	0.32
Na_2O	0.0	0.0	0.0	0.0	0.0	0.0	0.0	0.0	0.0	0.0	0.0	0.0
K_2O	3.71	1.41	2.62	2.86	2.71	4.52	3.54	3.67	2.55	1.11	0.02	0.03
H_2O	12.4	5.3	6.9	4.8	9.4	4.3	3.9	4.0	11.7	7.2	12.0	4.5
P_2O_5	0.12	0.04	0.02	0.01	0.63	0.82	0.06	0.21	0.12	0.03	0.28	0.12
CO_2	0.0	0.1	0.2	0.2	0.7	0.4	0.2	0.1	0.0	0.1	0.1	0.1
S	0.08	0.00	4.88	0.01	0.06	0.00	0.00	0.00	0.26	0.20	0.35	0.12
Volat.	0.0	0.0	0.0	0.0	0.0	0.0	0.4	0.0	0.0	0.0	0.0	0.0
Rb	0.005	0.003	0.004	0.004	0.003	0.007	0.009	0.011	0.004	0.002	0.022	0.000
Zn	0.001	0.001	0.005	0.001	0.000	0.000	0.002	0.001	0.008	0.003	0.001	0.002
Total	100.6	100.4	99.8	100.3	98.4	99.1	99.7	100.3	99.2	99.6	99.4	99.9
Distance below unconform. in m.	6.7	10	1	3.7	4.6	20	9	34	5.5	6	12	17

Deposit	Raven		Horseshoe		West Bear				Midwest			
Pair no.	7		8		9		10		11		12	
Lab no.	91	92	93	92	102	103	105	106	155	202	208	211
SiO_2	62.9	82.6	42.6	82.6	63.4	69.1	68.7	73.4	44.8	93.8	44.8	55.5
TiO_2	0.67	0.18	0.49	0.18	0.76	0.81	0.65	0.63	0.82	0.02	1.98	1.11
Al_2O_3	21.2	9.5	30.1	9.5	20.0	15.9	16.7	14.9	31.6	3.2	31.0	20.2
Fe_2O_3	0.2	0.7	2.5	0.7	0.7	0.6	0.9	0.8	0.0	0.0	0.9	3.8
FeO	0.0	0.0	0.0	0.0	0.3	0.1	0.2	0.0	1.5	0.4	0.3	0.0
MnO	0.01	0.01	0.01	0.01	0.01	0.01	0.01	0.00	0.01	0.00	0.02	0.01
MgO	3.94	2.68	8.59	2.68	5.29	3.94	4.40	2.80	2.92	0.41	2.11	4.63
CaO	0.34	0.06	0.38	0.06	0.08	0.16	0.07	0.05	0.15	0.01	0.19	0.16
Na_2O	0.0	0.0	0.0	0.0	0.0	0.0	0.0	0.0	0.0	0.0	0.0	0.0
K_2O	3.72	1.09	3.76	1.09	2.43	2.78	2.32	2.95	8.41	0.65	8.50	3.61
H_2O	6.1	3.7	10.4	3.7	6.9	5.2	6.0	4.6	6.9	0.9	8.9	7.7
P_2O_5	0.21	0.03	0.10	0.03	0.05	0.11	0.04	0.06	0.07	0.01	0.04	0.03
CO_2	0.1	0.0	0.0	0.0	0.2	0.1	0.3	0.0	0.3	0.2	0.1	0.9
S	0.13	0.13	0.18	0.13	0.15	0.20	0.04	0.00	0.88	0.15	0.04	3.02
Volat.	0.0	0.0	0.0	0.0	0.0	0.0	0.0	0.0	0.0	0.0	0.0	0.0
Rb	0.004	0.002	0.008	0.002	0.005	0.008	0.005	0.008	0.008	0.003	0.007	0.004
Zn	0.001	0.001	0.004	0.001	0.011	0.010	0.010	0.003	0.002	0.000	0.002	0.002
Total	99.6	100.7	99.2	100.7	100.4	99.1	100.5	100.3	98.5	99.9	98.5	100.8
Distance below unconform. in m.	136	235	338	235	3	11	7.6	11.6	2.4	6	3.4	42

Deposit	Cluff Lake								Collins Bay B zone			
Pair no.	13		14		15		16		17		18	
Lab no.	166	167	169	170	201	200	174	143	112	116	122	124
SiO_2	74.8	77.9	63.8	73.4	72.0	73.7	29.6	40.8	39.7	69.7	52.0	69.1
TiO_2	0.80	0.28	0.06	0.01	0.02	0.01	0.75	1.53	1.47	0.38	2.80	0.30
Al_2O_3	13.9	9.2	18.4	14.2	14.9	13.7	20.7	31.2	25.6	19.9	24.6	21.4
Fe_2O_3	0.1	0.8	1.0	0.0	0.2	0.6	3.9	5.8	13.6	0.1	3.5	0.3
FeO	0.2	2.3	0.5	0.5	0.3	0.2	7.5	0.6	0.0	0.1	0.3	0.1
MnO	0.01	0.03	0.02	0.02	0.01	0.01	0.02	0.02	0.17	0.01	0.02	0.01
MgO	2.46	2.36	6.71	0.44	4.61	2.54	22.29	0.57	1.77	0.35	0.90	0.26
CaO	0.10	0.10	0.23	0.44	0.11	0.21	0.17	0.17	0.17	0.02	0.11	0.02
Na_2O	0.0	0.0	0.0	3.2	0.0	0.0	0.0	0.0	0.0	0.0	0.0	0.0
K_2O	2.72	3.40	1.63	5.63	1.82	4.60	0.01	8.60	6.81	3.00	7.09	1.41
H_2O	4.1	2.9	6.6	1.0	5.2	3.6	14.4	5.8	9.2	6.1	7.2	7.6
P_2O_5	0.01	0.03	0.13	0.08	0.06	0.12	0.05	0.59	0.07	0.01	0.27	0.03
CO_2	0.1	0.1	0.0	0.0	0.3	0.3	0.9	1.4	0.0	0.0	0.0	0.0
S	0.07	0.08	0.08	0.02	0.00	0.07	0.16	0.31	0.02	0.00	0.18	0.00
Volat.	0.0	0.0	0.0	0.0	0.0	0.0	0.0	0.0	0.0	0.0	0.0	0.0
Rb	0.004	0.008	0.003	0.016	0.005	0.011	0.046	0.007	0.009	0.004	0.000	0.003
Zn	0.001	0.002	0.005	0.000	0.002	0.003	0.001	0.007	0.010	0.001	0.000	0.002
Total	99.3	99.5	99.1	99.0	99.5	99.6	100.6	98.1	98.9	99.8	99.8	100.6
Distance below (+ above) unconform. in m.	12	28.4	31.4	61	16.8	23.8	+9	+17	+14	4	+17	4.3

Deposit	Collins Bay B zone		Key Lake									
Pair no.	19		20		21		22		23		24	
Lab no.	125	129	262	263	261	259	269	271	282	284	286	290
SiO_2	44.0	67.5	37.0	70.2	34.0	69.8	36.7	75.1	21.6	68.0	55.0	73.2
TiO_2	1.39	0.38	2.03	0.49	10.00	0.17	0.08	0.34	0.66	0.62	0.60	0.34
Al_2O_3	14.0	22.9	30.6	15.0	28.0	15.7	29.3	11.6	19.1	15.8	21.0	13.9
Fe_2O_3	25.6	0.3	0.7	0.7	3.0	0.2	3.0	0.8	1.3	0.4	1.0	0.3
FeO	0.8	0.0	1.2	0.1	1.3	0.3	2.1	0.3	3.3	0.3	2.7	0.2
MnO	0.44	0.00	0.01	0.00	0.00	0.00	0.02	0.01	0.16	0.01	0.00	0.00
MgO	1.17	0.23	13.03	7.45	10.00	6.05	9.71	4.96	12.27	6.39	7.00	3.87
CaO	0.13	0.01	0.09	0.02	0.10	0.14	0.22	0.51	13.28	0.54	0.30	0.11
Na_2O	0.0	0.0	0.0	0.0	0.0	0.0	0.0	0.0	0.0	0.0	0.1	0.0
K_2O	4.10	2.11	1.51	0.82	0.40	0.48	0.73	0.62	0.62	0.53	0.30	1.58
H_2O	6.8	7.3	12.2	5.7	12.6	6.0	15.2	5.3	7.7	6.7	8.9	4.8
P_2O_5	0.02	0.01	0.01	0.00	0.00	0.11	0.01	0.11	0.11	0.05	0.10	0.07
CO_2	0.6	0.0	0.1	0.1	0.3	0.4	0.1	0.8	18.4	0.7	1.5	0.0
S	0.00	0.01	0.17	0.02	0.00	0.23	0.50	0.01	0.09	0.03	0.40	0.00
Volat.	0.0	0.0	0.0	0.0	0.0	0.0	0.6	0.0	0.0	0.0	0.0	0.0
Rb	0.006	0.004	0.000	0.001	0.000	0.001	0.001	0.002	0.004	0.002	0.000	0.004
Zn	0.012	0.001	0.001	0.001	0.000	0.001	0.003	0.001	0.017	0.005	0.100	0.005
Total	99.3	100.8	98.7	100.7	99.8	99.7	98.6	100.5	98.7	100.1	99.8	98.6
Distance below (+ above) unconform. in m.	+23	3.4	62	68	47	28	18	31	8.2	10.7	5	23

* These samples are considered to be typical of the transformation that took place when the host basement rocks were altered by the hydrothermal solutions related to the U mineralization. The analysis on the right of each sample pair is from the less altered rock whereas the other is from the altered rock. All samples, except pair no. 16, are basement rock.

Table 1.4

Amount of relative increase or decrease in per cent obtained from the 21 pairs of core samples given in Table 1.2*

Deposit	CBA	WB	CBB				CW	MW		ML	
Pair no.	1	2	3	4	5	6	7	8	9	10	
SiO_2	-67.3	-17.4	-1.3	-3.4	-2.3	-0.4	-14.5	-7.6	-29.9	-59.2	
TiO_2	267.6	-22.2	52.0	38.5	44.4	18.5	44.8	68.4	-10.5	?	
Al_2O_3	-9.3	16.4	22.1	40.0	50.0	36.5	41.4	12.1	44.4	46.1	
MgO	-83.3	-11.1	-81.5	-80.3	-97.0	-79.7	21.4	78.8	18.1	-61.6	
K_2O	10.8	-12.2	-30.4	-54.2	-72.5	-20.6	35.6	-20.5	116.	215.9	
H_2O	33.3	21.2	48.8	37.0	19.6	381.8	117.4	22.2	36.4	115.6	
Deposit	Key Lake						Cluff Lake			MB	
Pair no.	11	12	13	14	15	16	17	18	19	20	21
SiO_2	-12.7	-11.0	-5.0	-24.6	-2.2	-35.1	-2.6	-7.9	-1.8	-2.9	-30.0
TiO_2	26.1	50.0	36.2	800.0	12.5	316.7	-96.1	11.8	-90.3	17.7	39.8
Al_2O_3	50.0	66.3	22.6	86.2	13.3	91.6	52.4	70.1	15.6	0.0	-8.6
MgO	-47.8	-8.0	-13.1	260.0	-26.7	-22.2	-62.2	-52.3	-87.3	-22.1	-34.1
K_2O	-53.3	(800.)	191.6	50.0	166.7	(2087.)	-11.3	185.5	122.6	-15.2	-23.1
H_2O	212.5	4.7	-3.8	77.4	-3.9	22.7	110.0	21.2	-20.	-2.5	-11.0

* These samples are from the known uranium deposit areas associated with the unconformity at the base of the Athabasca Basin. The results are the products of the regolithic alteration that affected the basement rocks at the unconformity before deposition of the Athabasca strata. Minus sign means decrease. Brackets indicate figures rejected in the calculation of the means of Table 1.6. CBA, Collins Bay A zone; CBB, Collins Bay B zone; WB, West Bear; ML, McClean Lake; CW, Conwest; MW, Midwest Lake; MB, Maurice Bay; RL, Rabbit Lake; R, Raven; H, Horseshoe.

Table 1.5

Amount of relative increase or decrease in per cent obtained from the 24 pairs of core samples given in Table 1.3*

Deposit	ML		MB		CBA	RL	R	H	WB		MW	
Pair no.	1	2	3	4	5	6	7	8	9	10	11	12
SiO_2	-44.3	-20.0	-42.9	-2.4	-40.3	-55.0	-23.9	-48.4	-8.3	-6.4	-52.2	-20.0
TiO_2	300.0	100.0	25.0	0	213.5	257.7	272.2	172.2	-6.2	3.2	(4000.)	78.4
Al_2O_3	114.7	-3.8	90.2	6.9	71.3	216.4	123.2	216.8	25.8	12.1	(887.5)	53.5
MgO	99.8	264.6	291.5	13.0	231.6	440.0	47.0	220.5	34.3	57.1	612.2	-45.6
K_2O	163.1	-8.4	-40.0	-3.5	129.3	-33.3	241.3	245.	-12.6	-21.4	(1193.8)	135.5
H_2O	134.	43.7	118.6	-2.5	62.5	166.7	64.9	181.1	32.7	30.4	666.7	15.6
Deposit	Cluff Lake				CBB			Key Lake				
Pair no.	13	14	15	16	17	18	19	20	21	22	23	24
SiO_2	-4.0	-13.1	-2.3	-27.5	-43.1	-24.8	-34.8	-47.3	-51.3	-51.1	-68.2	-24.9
TiO_2	185.7	500.0	100.0	-51.0	286.8	833.3	265.8	314.3	(5783.)	-76.5	6.5	76.5
Al_2O_3	51.1	29.6	8.8	-33.8	28.6	13.9	-38.9	104.0	78.3	152.6	20.9	51.1
MgO	4.3	1425.0	81.5	(3810.0)	405.7	246.2	408.7	74.9	65.3	95.8	92.0	80.9
K_2O	-20.	-71.1	-60.4	-99.9	127.	402.8	94.3	84.1	-16.7	16.1	17.0	-81.0
H_2O	41.4	560.	44.4	148.3	50.8	-5.3	-6.8	114.0	110.0	186.8	14.9	85.4

* These samples are from the known uranium deposit areas associated with the unconformity at the base of the Athabasca Basin. The results are the products of the hydrothermal alteration that affected the basement rocks near the unconformity where the uranium deposits were formed. Brackets indicate figures rejected in the calculation of the means of Table 1.6.CBA, Collins Bay A zone; CBB, Collins Bay B zone; WB, West Bear; ML, McClean Lake; CW, Conwest; MW, Midwest Lake; MB, Maurice Bay; RL, Rabbit Lake; R, Raven; H, Horseshoe.

As examples of the assessment of the above criteria in some deposits the following observations are presented. At Key Lake, although the criteria of both alterations are present, those due to the hydrothermal solutions appear to be most important and appear to mask in part the features of the regolithic alteration. In the Collins Bay A zone the alteration seems to be typical of both regolithic and hydrothermal solutions. At Cluff Lake, although the alteration effects are also characteristic of both regolithic and hydrothermal solutions, their intensities vary so erratically from place to place that it is difficult to assess the effects of either type separately and to be sure which alteration is the main one in most deposits, except in the D orebody where the effects of hydrothermal alteration appear dominant.

The specific gravity of the intensely altered specimens used in this study could not be determined by the usual water immersion method because of their high clay content. Attempts on powders with a porosimeter and air as the medium were also unsuccessful. Although no calculations involving specific gravity were made in this study I feel that their use would not have changed the trends indicated.

Results

The 89 samples selected appear to be representative of the changes that took place when the rocks were affected by the two main alterations (regolithic and hydrothermal). The analyses of the 89 samples are grouped in Tables 1.2 and 1.3 in 45 pairs of related samples, (one sample, no. 92, appears twice): 21 pairs display changes associated with regolithic alteration (Table 1.2) and 24 pairs display those associated with hydrothermal alteration (Table 1.3). Each pair came from a different diamond drillhole and in each case both samples are of similar rock type; it is not known, however, if they are from the same band or layer of the basement succession. Most of the samples are medium- to coarse-grained granitoid rocks, probably meta-arkose. The table form used is to facilitate comparison of the altered rock with the corresponding somewhat less altered rock and of the changes that characterized the two main alterations. The amounts of relative increase or decrease in per cent of the various elements, relative to their content in the less altered sample, are given in Tables 1.4 and 1.5. Table 1.6 summarizes the relative increases and decreases that characterize the two main alterations (regolithic and hydrothermal) and that differentiate them from each other. The means in Table 1.6 are arithmetic means; some values were rejected in the calculation of the means as being anomalously high and are bracketed in Tables 1.4 and 1.5. Furthermore, to test the results of Table 1.6, alumina was considered immobile and the rock compositions recalculated so that the amount of alumina in each sample stayed constant. These calculations are presented in Table 1.7.

Finally because very few of the analyses presented in this paper are of fresh rocks, some chemical analyses of fresh rocks published by Hoeve and Sibbald (1978) and Harper (1978) are incorporated in Table 1.8.

The chemical determinations, except those in Table 1.1, were done by XRF rapid chemical methods in the Analytical Chemistry Laboratory, Geological Survey of Canada, Ottawa. The volatile components comprise all compounds lost on ignition other than CO_2 and H_2O.

Discussion

The basement rocks below the unconformity at the base of the Athabasca Basin underwent regolithic alteration before deposition of the Athabasca rocks and hydrothermal alteration after deposition (Tremblay, 1978) of the Athabasca. These two alterations are characterized by features that were observed in core samples and by chemical changes that were recognized in the chemical analyses listed in Tables 1.2 and 1.3. Some of these chemical changes have similar trends for both alterations and others have different trends for each. The differences in relative compositional changes, that is, their apparent gains and losses, are the characteristic features that permit distinction and differentiation of one alteration from the other, and explanation of the appearance of each alteration type. The amount of relative increase and decrease of the elements probably varied with the degree of intensity of the two alterations (regolithic and hydrothermal). The main chemical changes are presented in Table 1.6 and are briefly discussed and evaluated below. These changes represent trends only, and their values indicate only their relative order of magnitude. Similar chemical trends are apparent in some of Hoeve and Sibbald's (1978) analyses of rocks from the Rabbit Lake area. Also de Carle (1981) has suggested some similar trends for rocks in the Key Lake area. At least Hoeve and Sibbald's (1978) analyses, of their "red alteration" appear to be of rocks that were affected by both alterations as defined here.

Briefly, both types of alteration display a general relative decrease in silica (SiO_2) and a general apparent increase in alumina (Al_2O_3), water (H_2O) and titania (TiO_2) although an occasional pair may display the converse. Both alterations also display differences in relative compositional changes for MgO and K_2O. Thus the hydrothermal alteration is characterized by a general relative increase in MgO whereas a general relative decrease in MgO characterizes the regolithic alteration. The relative changes in K_2O are quite erratic: they vary with the types of alteration, with the deposits and in some cases with the sample pair. In general, however, the K_2O changes (Table 1.6) display an overall relative increase when all the samples of both the regolithic and hydrothermal altered zones are assessed together. If the alumina content is assumed constant, however, the relative amount of increase or decrease in weight per cent of SiO_2, TiO_2, and MgO (Table 1.7) may vary appreciably from those presented in Table 1.6, but their trends remain about the same except for potash, which shows a general relative decrease (Table 1.7). In this study it is not known if the rock has undergone volume changes.

Na_2O

Soda appears to have been removed completely as it was not detected in most samples analyzed (Table 1.2, 1.3). Exceptions occur in five samples which appear to have been only weakly affected by both types of alteration. The very low soda content of most of the samples in this study indicates that they are of altered rocks. For comparison, chemical analyses of relatively fresh rocks from this study and from the Rabbit Lake and Cluff Lake areas (Hoeve and Sibbald, 1978; Harper, 1978) are given in Table 1.8. They show soda contents ranging from about 1 to 4.3% and averaging about 2.5%.

SiO_2

The amount of silica has apparently decreased as a result of the effects of both types of alteration, and the amount of the decrease due to either effect can locally be the same. However, it appears that on the average the hydrothermal solutions more effectively removed silica than did the regolithic process. In the hydrothermally altered rocks the apparent decrease in silica averages 23 per cent of the amount of silica in the less altered rocks, whereas in the rocks affected by the regolithic alteration the apparent decrease is about 11 per cent. The effects of the regolithic alteration on silica as indicated by the chemical analyses

Table 1.6

Amounts of relative increases and decreases in per cent of the main chemical elements of the rocks resulting from the alterations of basement rocks in areas of the main known uranium deposits of the Athabasca Basin

	Chemical elements	Regolithic alteration				Hydrothermal alteration			
		Δ %		Actual change in wt. %		Δ %		Actual change in wt. %	
		Mean	Range	Mean	Range	Mean	Range	Mean	Range
Relative increase	Al_2O_3	36	-8.5 to 92	5	-1.8 to 15.3	60	-4 to 216	11	-10.5 to 28.4
	MgO					225	-45 to 1425	5	-2.5 to 21.7
	TiO_2	81	-96 to 800	0.46	-0.56 to 16.1	175	-76 to 833	0.56	-0.78 to 2.5
	H_2O	59	-2.5 to 382	2.2	-1.1 to 4.2	119	-6.8 to 667	5	-0.5 to 9.9
	K_2O	41	-71 to 216	0.6	-3.42 to 6.68[1]	52	-100 to 403	0.56	-8.59 to 7.76[1]
	K_2O	139	-53 to 800	1.6	-2.74 to 6.68[2]	100	-81 to 403	2	-1.28 to 7.76[3]
Relative decrease	SiO_2	-16	-0.4 to -67	-11.	-0.3 to -45.8	-32	-2 to -68	-23	-1.7 to -49
	MgO	-23	-87 to 260	-1.5	-2.86 to 2.12				
	K_2O	-33	-12 to -72	-1.3	-0.34 to -3.42[4]	-40	-3.5 to -100	-2.4	-0.13 to -8.59[5]

[1]All deposits
[2]ML, MW, KL, CBA, CW and Cluff Lake
[3]ML, MW, KL, CBA, CBB and RL
[4]WB, MB, and CBB
[5]WB, MB and Cluff Lake

CBA, Collins Bay A zone; CBB, Collins Bay B zone; WB, West Bear; ML, McClean Lake; CW, Conwest; MW, Midwest Lake; MB, Maurice Bay; RL, Rabbit Lake; R, Raven; H, Horseshoe.

Table 1.7

Assuming aluminum immobile amount of relative increases and decreases of the main chemical elements of the rocks resulting from the alterations of basement rocks in areas of the main known uranium deposits of the Athabasca Basin

	Chemical elements	Regolithic alteration				Hydrothermal alteration			
		Δ %		Actual change in wt. %		Δ %		Actual change in wt. %	
		Mean	Range	Mean	Range	Mean	Range	Mean	Range
Relative increase	MgO					75.5		2.19	-3.26 to 33.03
	TiO_2	34		0.185	-0.73 to 1.23	107		0.43	-.0.4 to 5.43
	H_2O	2		0.09	-2.37 to 3.7	9		0.43	-1.9 to 4.1
	Fe_2O_3	641		4.2	-3.0 to 21.5	175		1.93	-3.2 to 41.6
	FeO					268		0.67	-2.17 to 10.7
	P_2O_5	66		0.06	-0.5 to 1.38				
Relative decrease	SiO_2	-37		-26.3	-54.2 to -2.1	-47.5		-33.9	-69.8 to 26.3
	MgO	-47		-1.53	-3.83 to 2.0				
	K_2O	-8.6		-0.22	-4.37 to 3.33	-13		-0.34	-8.58 to 4.79
	FeO	-3.5		-0.023	-2.67 to 7.8				
	CaO	-83		-0.19	-2.0 to 0.22	-36		-0.07	-1.03 to 0.2
	P_2O_5					-82		-0.09	-0.83 to 0.2

appear to have been small at Collins Bay B zone, Cluff Lake and Key Lake, but have been important at West Bear and Maurice Bay. Figures 1.1 and 1.2 show that the silica content of the samples from both alterations decreases with an increase in alteration and on approaching the unconformity and related fault zones, suggesting that these features were the main circulating paths for the alteration solutions.

Al_2O_3

Alumina generally exhibits an apparent increase in relation to the other elements in rocks affected by either alteration, except in samples with a high Fe_2O_3 content, as seen locally in the regolithic zone. This suggests that the regolithic alteration is responsible for an apparent decrease and that the apparent increases are due mainly to the hydrothermal alteration. The apparent changes in the alumina content also suggest that alumina was not immobile as is commonly assumed and that rock volumes did not remain constant. This is shown on Figures 1.3 and 1.4 and is suggested by the large amount of sericite in the altered rocks. The increase in alumina content averages 5% in regolithic altered pairs and 11% in hydrothermally altered pairs. The relative increases are 36% and 60%, respectively. Alumina content is probably represented by the large amount of sericite, illite and kaolinite abundantly developed in some parts of the altered areas associated with the ore zones and was probably derived from the feldspar in the altered rocks.

H_2O

Samples from the more altered rocks also show an increase in the water content relative to the amount of water in the less altered samples. The increase is 5% H_2O for the hydrothermal alteration and only 2% for the regolithic one, that is 120% and 60% respectively of the amount of water in the less altered rocks. This added water occurs mainly in the clay minerals including sericite and chlorite and possibly indicates an increase in the content of these minerals.

TiO_2

There were also apparent increases in the TiO_2 content as a result of both alterations. The relative increase is almost 200% in the hydrothermally altered rocks, and 80% in the regolithic rocks. However, the total amount of TiO_2 present is so small that it is difficult to assess its changes accurately and to regard the values of these changes as meaningful. Most of the titanium is thought to be in sphene and titanium oxides, probably mainly anatase (Dahlkamp and Tan, 1977; Rimsaite, 1979).

Table 1.8

Chemical analyses of core specimens of relatively fresh basement rocks in the area of the Athabasca Basin

Deposit	KL		MB	CBB		RL		CL	
	264*	230	195	118	136	1a	3a	2	4
SiO_2	73.7	75.2	65.7	72.9	70.8	69.1	71.5	64.28	70.2
TiO_2	0.25	0.16	0.48	0.14	0.23	0.60	0.30	0.43	0.02
Al_2O_3	12.9	13.1	15.8	14.7	14.5	15.5	10.1	17.40	16.30
Fe_2O_3	0.3	0.4	0.5	0.2	0.4	0.70	0.20	1.71	0.57
FeO	2.0	0.7	3.0	1.0	2.1	0.33	0.82	6.21	0.69
MnO	0.02	0.01	0.03	0.01	0.04	0.02	0.02	0.09	0.02
MgO	1.61	1.21	2.53	0.99	1.23	1.65	3.63	2.29	0.61
CaO	0.37	1.23	0.57	1.74	1.47	0.68	2.70	0.60	0.42
Na_2O	1.9	2.4	1.2	3.6	4.3	1.48	1.31	0.98	4.06
K_2O	5.21	4.21	6.6	2.97	3.71	5.99	5.25	2.89	5.16
H_2O	1.8	1.4	2.5	1.6	1.2	3.13	2.40	2.18	0.88
P_2O_5	0.04	0.05	0.09	0.06	0.05			0.05	0.14
CO_2	0.1	0.0	1.0	0.2	0.0	0.05	3.84	0.24	0.15
S	0.05	0.04	0.03	0.00	0.01				
volatiles	0.0	0.0	0.0	0.0	0.0				
Rb	0.009	0.012	0.015	0.004	0.011				
Zn	0.002	0.001	0.003	0.001	0.003				
Total	100.4	100.3	100.2	100.3	100.2	99.24	102.07	99.35	99.22
Depth below unconformity in metres	86	?	44	25	17	?	?	?	?

*264 - coarse grained granitoid
230 - medium grained quartz-feldspar-biotite gneiss
195 - medium- to coarse-grained quartz-feldspar-biotite gneiss
136 - medium grained biotite-quartz-feldspar gneiss
118 - coarse grained quartz-feldspar rock
1a, pegmatite, and 3a, meta-arkose, from Hoeve and Sibbald (1978)
2, quartzofeldspathic gneiss (mean of 7 analyses)
4, pegmatoid, (mean of 4) from Harper (1978)

CBA, Collins Bay A zone; CBB, Collins Bay B zone; WB, West Bear; ML, McClean Lake; CW, Conwest; MW, Midwest Lake; MB, Maurice Bay; RL, Rabbit Lake; R, Raven; H, Horseshoe.

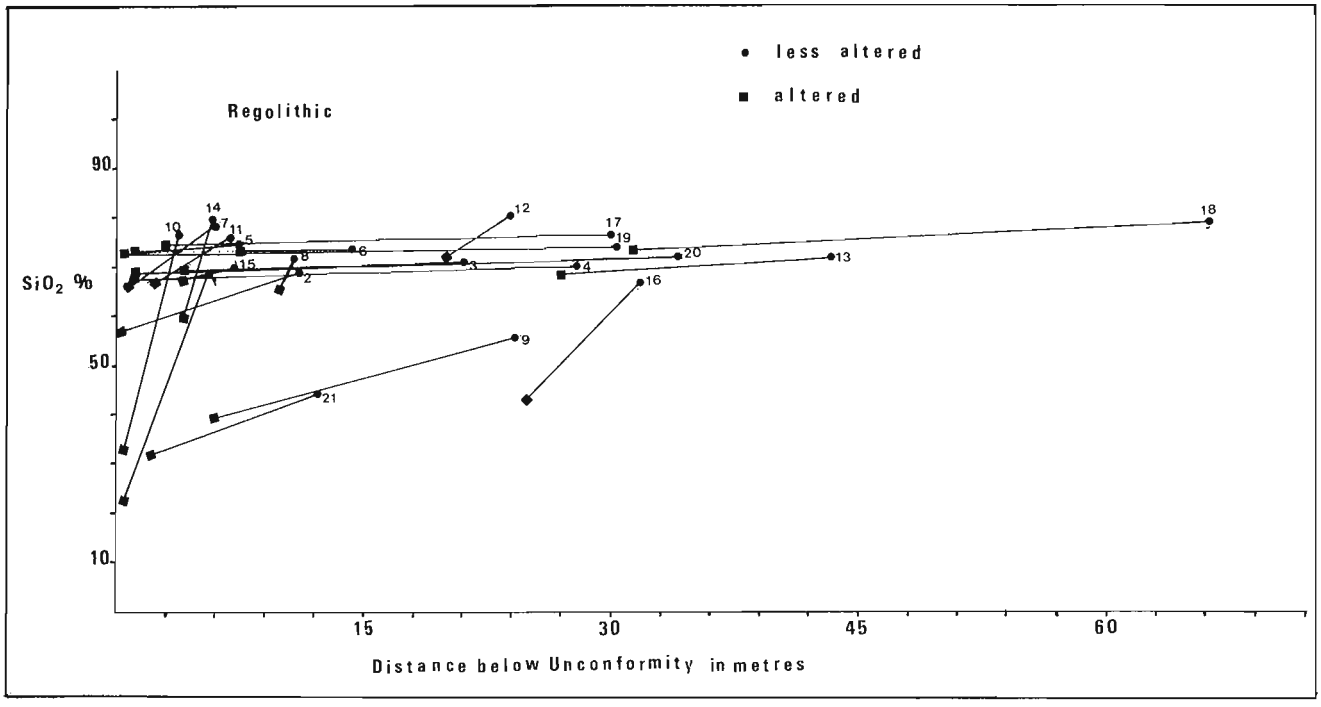

Figure 1.1. Diagram showing that the silica content of the regolithic altered rocks increases slightly with depth below the unconformity. The slope is not as pronounced as that of the lines of Figure 1.2. It is assumed that the lines with a steeper slope are of samples from rocks that have also been affected by hydrothermal alteration (see Fig. 1.2). 21 pairs of related samples were used.

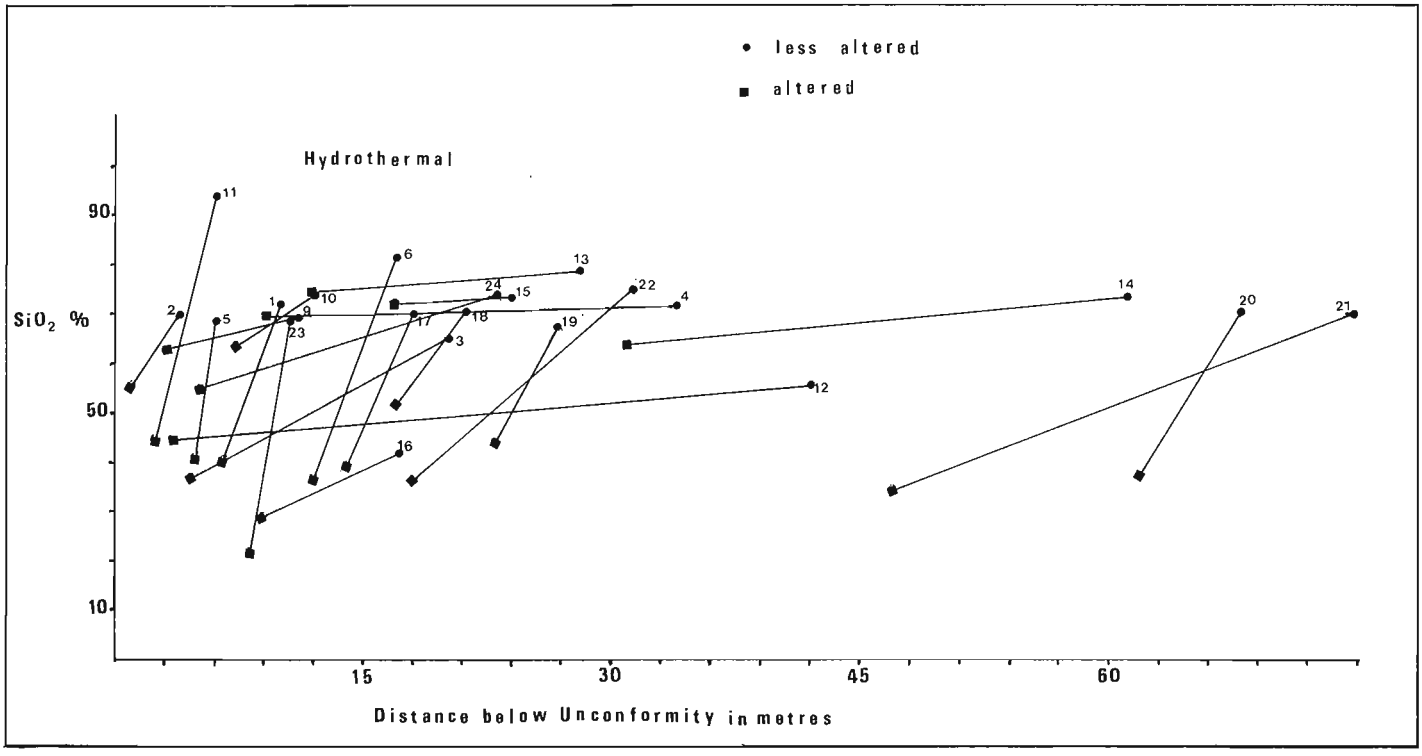

Figure 1.2. Diagram showing that the silica content of the hydrothermally altered rocks increases appreciably with depth below the unconformity. The slope of the lines is in general steeper than those of the regolithic altered rocks (see Fig. 1.1). 22 pairs of related samples were used.

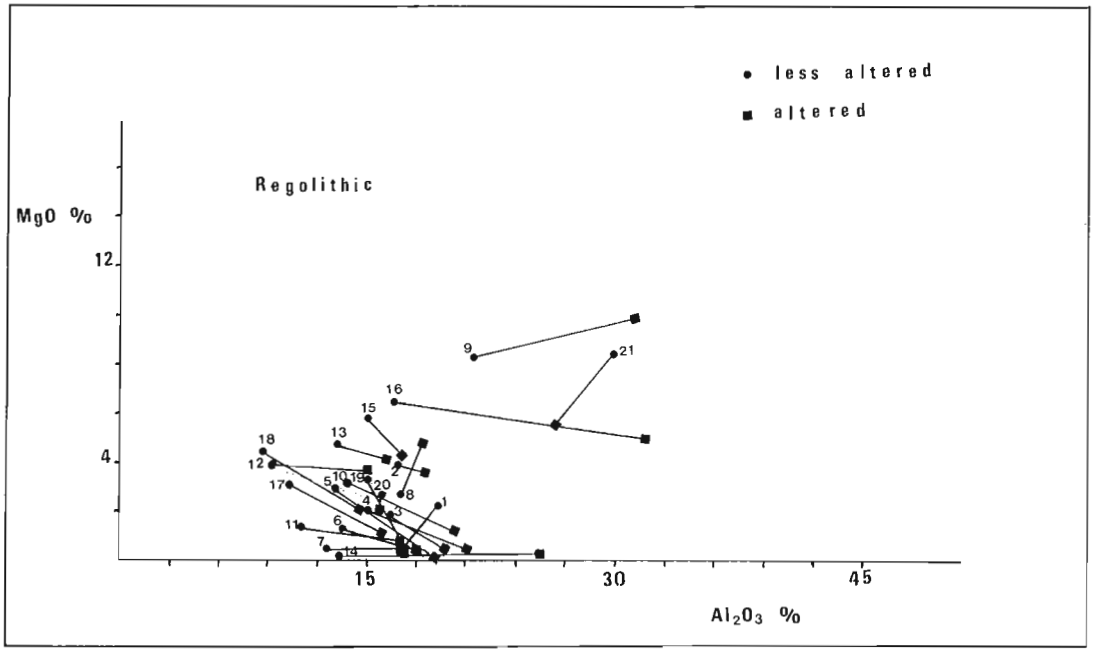

Figure 1.3. *Diagram showing that magnesia and alumina have moved in opposite directions when the rocks underwent regolithic alteration at the unconformity. Some samples (nos. 8 and 9) show the converse. They suggest that they were also affected by the hydrothermal alteration. 21 pairs of related samples were used.*

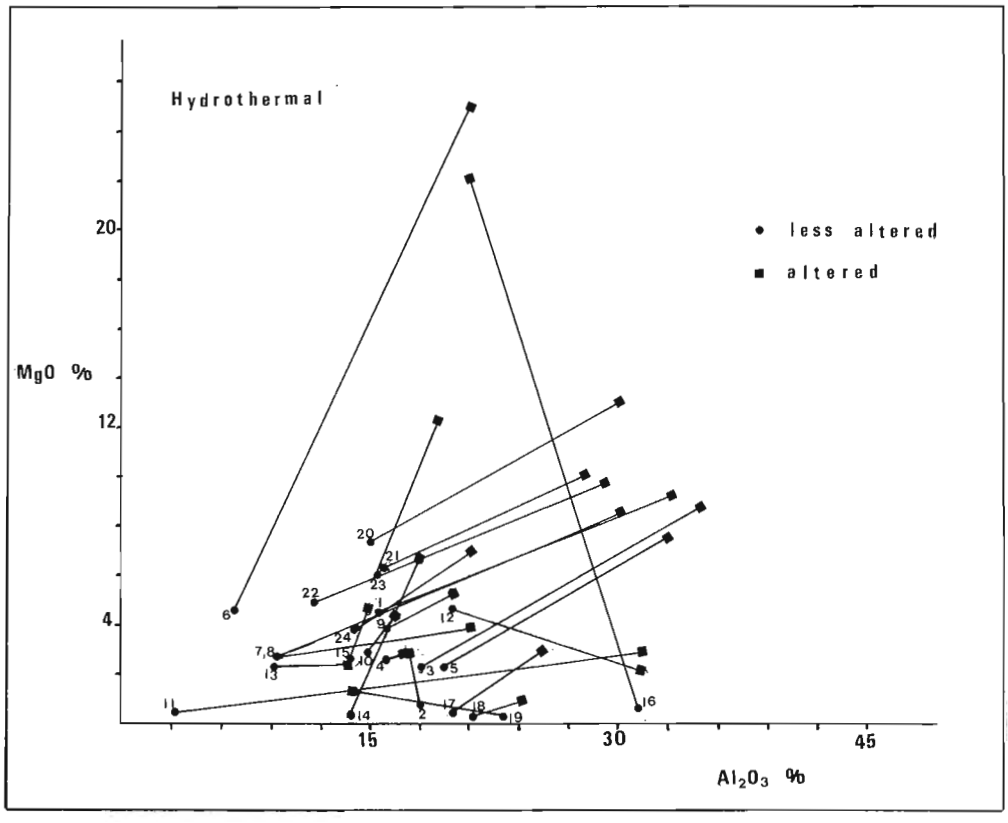

Figure 1.4. *Diagram showing that magnesia and alumina have moved together when the rocks were hydrothermally altered at the unconformity. Some samples (nos. 12 and 16) show the converse. They suggest that they were not affected by the hydrothermal alteration but only by the regolithic alteration. 24 pairs of related samples were used.*

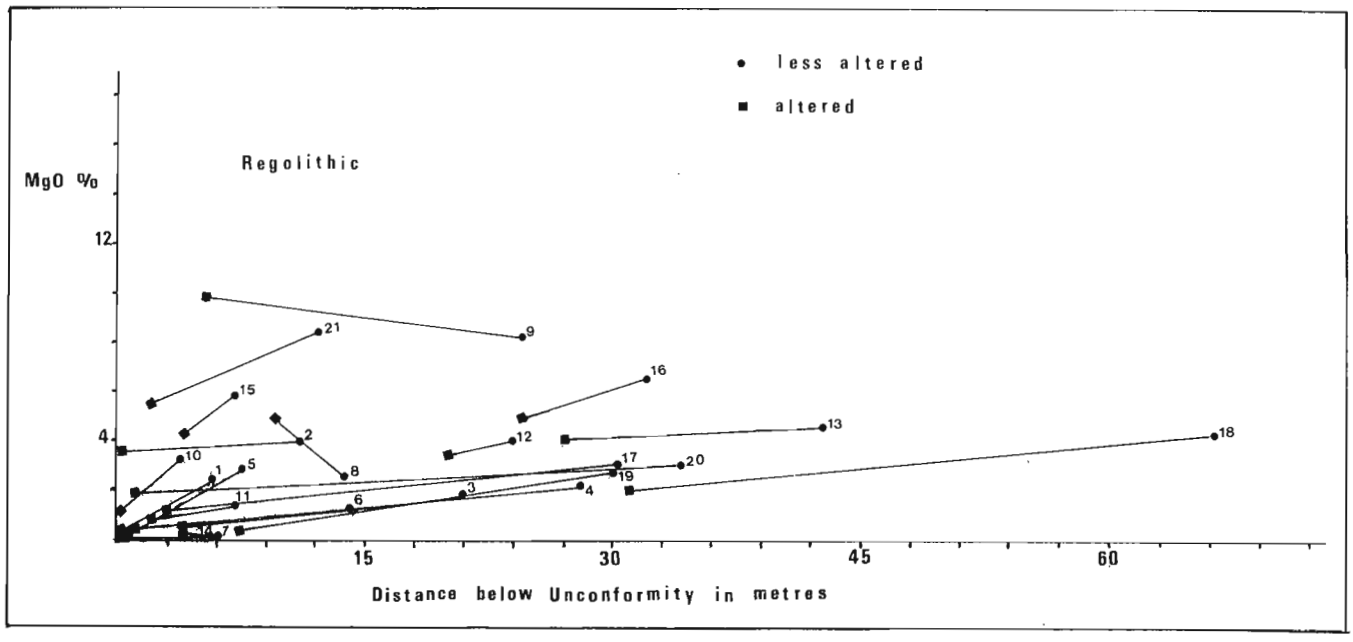

Figure 1.5. Diagram showing that the magnesia content of the regolithic altered rock increases with depth below the unconformity. The slope of the lines representing sample pairs nos. 8 and 9 suggests that these rock samples were also affected by the hydrothermal alteration (see Fig. 1.6 for slope comparison). 21 pairs of related samples were used in this diagram.

K_2O

The K_2O content of the altered rocks is higher in 60% of the samples than that of the less altered ones, except in the areas of the West Bear and Maurice Bay deposits. Conflicting results in some deposits may indicate superimposed effects of the hydrothermal alteration on regolithic rocks. The increase in K_2O content averages 2% in rocks affected by hydrothermal alteration and 1.5% in those affected by regolithic alteration. The relative increases are 100% and 139% respectively. In addition it is possible that these increases are the result of the regolithic alteration only, because most feldspars appear to have weathered readily to illite (sericite) and other clay minerals. On the other hand, when this apparent increase is assessed assuming that the alumina was immobile (Table 1.7), it appears that there was no increase in the K_2O content, but rather a decrease of the order of less than 0.4% K_2O for both alterations. Thus what happens to K_2O during the two alterations is still not clear. The K_2O content of the altered rocks from both alterations probably occurs mainly in the sericite flakes that are abundant everywhere in both the regolithic and the hydrothermal zones. Also the locally enlarged size of the sericite flakes suggests that the hydrothermal alteration near the mineral deposits was very effective.

MgO

The MgO content shows a substantial increase of about 5% in hydrothermally altered rocks. The relative increase is of the order of 225%. The magnesia is probably present in the chlorite which occurs abundantly with the sericite in most hydrothermally altered areas. In contrast, where the alteration is regolithic, the MgO content has decreased by about 1.5%; the relative decrease being about 25% of the content of the less altered rocks. In areas of regolithic alteration chlorite is generally not abundant. These relations are shown in Figures 1.5 and 1.6, the magnesia content decreasing with depth away from the unconformity (Fig. 1.6) for the hydrothermal alteration and increasing with depth for the regolithic alteration (Fig. 1.5). Some chemical analyses related to paleoweathering along the sub-Athabasca unconformity, presented by Fahrig and Loveridge (1981) support the relation of the regolithic alteration. Moreover magnesia and alumina appear to have moved together when the alteration was hydrothermal (Fig. 1.4) and to have moved in separate directions during the regolithic alteration (Fig. 1.3). Similar deposits in Australia are reported to be closely associated with magnesium-rich chloritic alteration (Hegge and Rowntree, 1978).

Conclusions

The main conclusions drawn from this study are:

1. Most deposits studied are spatially associated with regolithic alteration in basement rocks at the sub-Athabasca unconformity and related structures. This alteration is generally easily recognized where the weathering profile is intact but is difficult to ascertain where the characteristic upper red zone of the profile is missing. Regolithic altered rocks are soft, dense and made up of white clay-altered material.
2. Hydrothermally altered rocks are recognized in the vicinity of all deposits studied. This alteration also is closely related in space to the sub-Athabasca unconformity and occurs in both basement rocks and Athabasca strata. It is generally indicated by the abundance of sericite and chlorite flakes in a white clay base, by sericite and chlorite flakes somewhat larger in size than those of the regolithic white clay-altered rock, and in most instances by a greenish white fissile clay appearance. Hydrothermally altered rocks generally have a higher U content (Table 1.1).

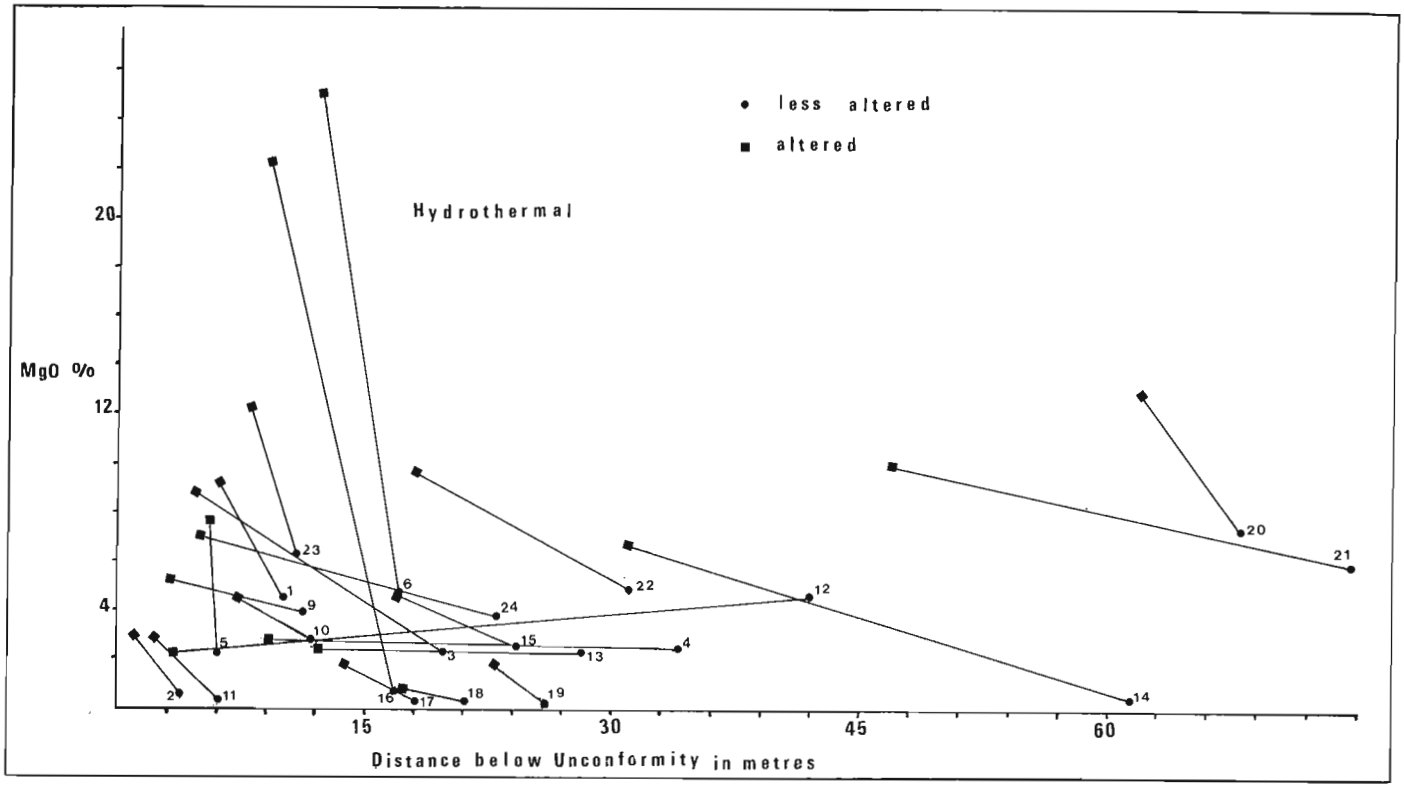

Figure 1.6. *Diagram showing that the magnesia content of the hydrothermally altered rocks decreases with depth below the unconformity. Sample pair no. 12 slopes in the same direction as the sample pairs regarded as affected only by the regolithic alteration (see Fig. 1.5). 22 pairs of related samples were used for this diagram.*

3. The minerals that developed during these changes are mainly sericite, chlorite, kaolinite, other clay minerals and anatase.

4. As suggested by the present analyses the apparent chemical changes that characterize both types of alteration are a decrease in silica and an increase in water, titania and alumina in the more altered rocks.

5. The hydrothermally altered rocks in the vicinity of all deposits, particularly those near the rich ore zones, appear to be enriched in magnesia (MgO), whereas the regolithic altered areas exhibit a magnesia decrease. The apparent decrease in MgO probably accompanied the removal of soda from the rocks whereas its enrichment appears to have taken place when the U deposits were formed as a result of hydrothermal action. The relative increase in magnesia is represented in the altered mineralized rock by the development of Mg-chlorite and the amount of the increase appears proportional to the size and grade of the deposit. This is suggested by the high MgO content of samples 20-24, 6 and 16 and by the abundances of Mg-chlorite at Key Lake, Rabbit Lake and Cluff Lake D orebodies. This high Mg-enrichment may suggest that the mineralizing solutions were not diagenetic (Macdonald, 1980).

6. Magnesia (MgO) enrichment appears to be a good indicator of U mineralization, and may therefore warrant investigation as an exploration tool.

7. The altered rocks in the vicinity of most deposits appear to have been completely depleted of soda (Na_2O). At the same time most deposits appear to have been enriched in potash (K_2O). These two features (soda depletion and potash enrichment) probably took place at about the same time, that is when the rocks underwent regolithic alteration because all the feldspars are completely altered to sericite and other clay minerals. It is also possible, however, that further enrichment in K_2O took place when the U was deposited from the hydrothermal solutions. This is suggested by the abundance of sericite associated with these deposits and by the larger size of the sericite flakes. The latter may have become larger when the U deposits formed from hydrothermal solutions, that is, when the temperature of the rock was presumably higher. Most of the K_2O probably was derived from the fine grained sericite (illite) of the surrounding altered host rocks.

References

Dahlkamp, F.J. and Tan, B.
1977: Geology and mineralogy of the Key Lake U-Ni deposits, northern Saskatchewan, Canada; in Geology, Mining and Extraction Processing of Uranium, ed. M.J. Jones; London Institute of Mining and Metallurgy, p. 145-158.

de Carle, A.L.
1981: Geology of the Key Lake Deposits – an overview; in Canadian Institute of Mining and Metallurgy Geology Division Uranium Field Excursion Guidebook, Sept. 8-13, p. 115.

Fahrig, W.F.
1961: The geology of the Athabasca Formation; Geological Survey of Canada, Bulletin 68, 41 p.

Fahrig, W.F. and Jones, D.L.
1969: Paleomagnetic evidence for the extent of Mackenzie igneous events; Canadian Journal of Earth Sciences, v. 6, no. 4, pt. 1, p. 679-688.

Fahrig, W.F. and Loveridge, W.D.
1981: Rb-Sr isochron age of weathered pre-Athabasca Formation basement gneiss, northern Saskatchewan; in Rb-Sr and U-Pb Isotopic Age Studies, Report 4; in Current Research, Part C, Geological Survey of Canada, Paper 81-1C, p. 127-129.

Harper, C.T.
1978: Geology of the Cluff Lake Uranium Deposits; Canadian Institute of Mining and Metallurgy, Bulletin, v. 71, p. 68-78.

Hegge, M.R. and Rowntree, J.C.
1978: Geological setting and concepts on the origin of uranium deposits in the East Alligator River region, N.T., Australia; Economic Geology, v. 73, p. 1420-1429.

Hoeve, J. and Sibbald, T.I.I.
1978: On the genesis of the Rabbit Lake and other unconformity-type uranium deposits in northern Saskatchewan, Canada; Economic Geology, v. 73, p. 1450-1473.

Lerand, M.M.
1970: Athabasca Formation Rumpel Lake stratigraphic test, lithologic description; Geological Survey of Canada, Open File Report 668.

Macdonald, C.C.
1980: Mineralogy and geochemistry of a Precambrian regolith in the Athabasca Basin; unpublished M.Sc. thesis, University of Saskatchewan.

Pagel, M., Poty, B., and Sheppard, S.M.F.
1979: Contributions to some Saskatchewan uranium deposits mainly from fluid inclusions and isotopic data; International Symposium on the Pine Creek Geosyncline, N.T., Australia, June.

Ramaekers, P.
1980: Stratigraphy and tectonic history of the Athabasca Group (Helikian) of northern Saskatchewan; in Summary of Investigations, Saskatchewan Geological Survey, Miscellaneous Report 80-4.

Rimsaite, J.Y.H.
1979: Petrology of basement rocks at the Rabbit Lake deposit and progressive alteration of pitchblende in an oxidation zone of uranium deposits in Saskatchewan; in Current Research, Part B, Geological Survey of Canada, Paper 79-1B, p. 281-299.

Tremblay, L.P.
1978: Uranium subprovinces and types of uranium deposits in the Precambrian rocks of Saskatchewan; in Current Research, Part A, Geological Survey of Canada, Paper 78-1A, p. 427-435.

1982: Geology of the uranium deposits related to the sub-Athabasca unconformity, Saskatchewan; Geological Survey of Canada, Paper 81-20, 56 p.

THE TOPSAILS IGNEOUS TERRANE OF WESTERN NEWFOUNDLAND

Project 730044

J.B. Whalen and K.L. Currie
Precambrian Geology Division

Whalen, J.B. and Currie, K.L., The Topsails igneous terrane of western Newfoundland; in Current Research, Part A, Geological Survey of Canada, Paper 83-1A, p. 15-23, 1983.

Abstract

The Topsails igneous terrane consists of a central core of high-level leucocratic potassic granite and porphyry, locally peralkaline, presumed to be of Devonian age. With distance from the core the rocks become older and more mafic, although there are local exceptions. The oldest exposed rocks, possibly Precambrian in age, are mafic to ultramafic with ophiolitic affinities. The variety and juxtaposition of igneous rocks implies that the underlying crust must be complexly laminated or tessellated. The Topsails terrane is separated from neighbouring terranes, from which it differs profoundly in lithology and structure, by major tectonic breaks which have, in some cases, been affected by later igneous activity. This pattern suggests that western Newfoundland may consist of a mosaic of roughly equant terranes, rather than an assemblage of thin strips as previously supposed.

The peralkaline granites of the Topsails region appear to have been derived by partial melting of volatile-depleted continental crust. The peralkaline character was a primary feature of the magma, generally destroyed by subsequent evolution of the magma, and not a late, local feature due to volatile interactions.

Introduction

The Canadian Appalachians exhibit a roughly symmetrical pattern (Williams, 1964), so that linear zones can be defined running from northeast to southwest. With the advent of plate tectonic theory, the zones received an explanation in terms of continental collision in early Paleozoic time (Bird and Dewey, 1970). Despite the success and fertility of the zonal scheme, the exact location and nature of the zone boundaries remains dubious and controversial. In western Newfoundland, the Great Northern Peninsula, extending as far south as Stephenville (Fig. 2.1) consists of Precambrian rocks of the Grenville Province veneered by continental shelf deposits of Eocambrian to Ordovician age, and locally structurally overlain by large nappes emplaced from the east during Ordovician time.

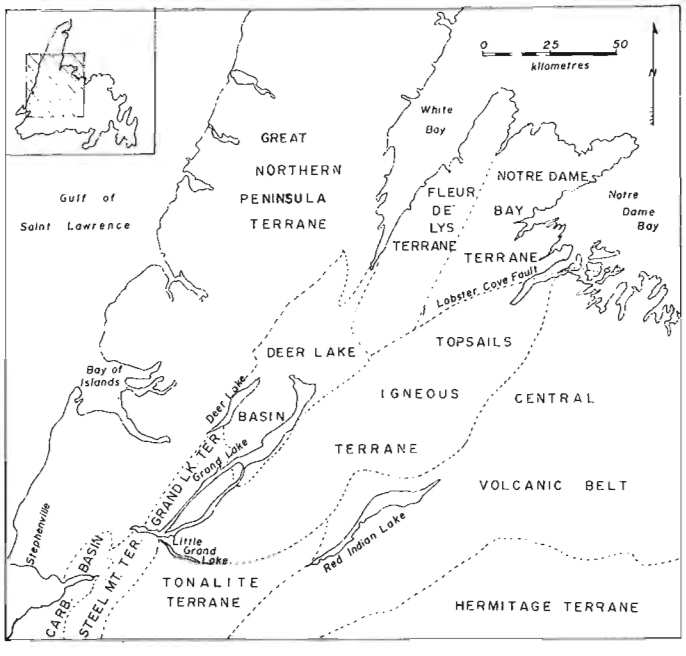

Figure 2.1. *Location of the Topsails igneous terrane and other geological terranes of western Newfoundland.*

Along its eastern edge this terrane contacts a fault-bounded basin of Carboniferous rocks. To the east of this 'Humber zone' (Williams, 1979) lie two disparate terranes. To the north, the Fleur de Lys terrane has generated a large polemic literature concerning the presence of basement, the nature and significance of ophiolitic complexes, and the grade of metamorphism (Hibbard, 1978, 1979). No final assessment can yet be made, but most geologists appear to concur with Williams (1978) in regarding this terrane as "the precarious continental margin of North America". South of the Fleur de Lys terrane, extending from the Birchy Lake-Indian Brook line to Little Grand Lake, and from Grand Lake east to Buchans, lies the Topsails terrane which consists mainly of salic, leucocratic igneous rocks, including significant amounts of alkali granite. Formerly the Topsails terrane was regarded as a Devonian batholith, and hence irrelevant to the definition of pre-Devonian zones. We previously showed this view to be erroneous (Whalen and Currie, 1982). The Topsails terrane exhibits a complex sequence of intrusive relations suggesting that it is as old as contiguous terranes, although of quite different character. The remarkably salic and leucocratic character of the igneous activity demonstrates an unusual basement.

General Geology of the Topsails Terrane

The Topsails terrane exhibits (a) an almost total lack of sedimentary and regionally metamorphosed rocks, (b) generally massive igneous rocks, and (c) a predominance of potassic and leucocratic granitoid rocks. All of these characteristics differ strongly from those of juxtaposed terranes. The Topsails terrane consists of a central core of massive, high level, pink to red granite and correlative porphyries (Fig. 2.2), which contains within it screens of older rocks, probably as separators of various plutons. Around the central core, older rocks appear as relict fringes. In a general way the rocks are more mafic and older the farther they lie from the central core, although there are local exceptions. The oldest rocks are probably of Precambrian age.

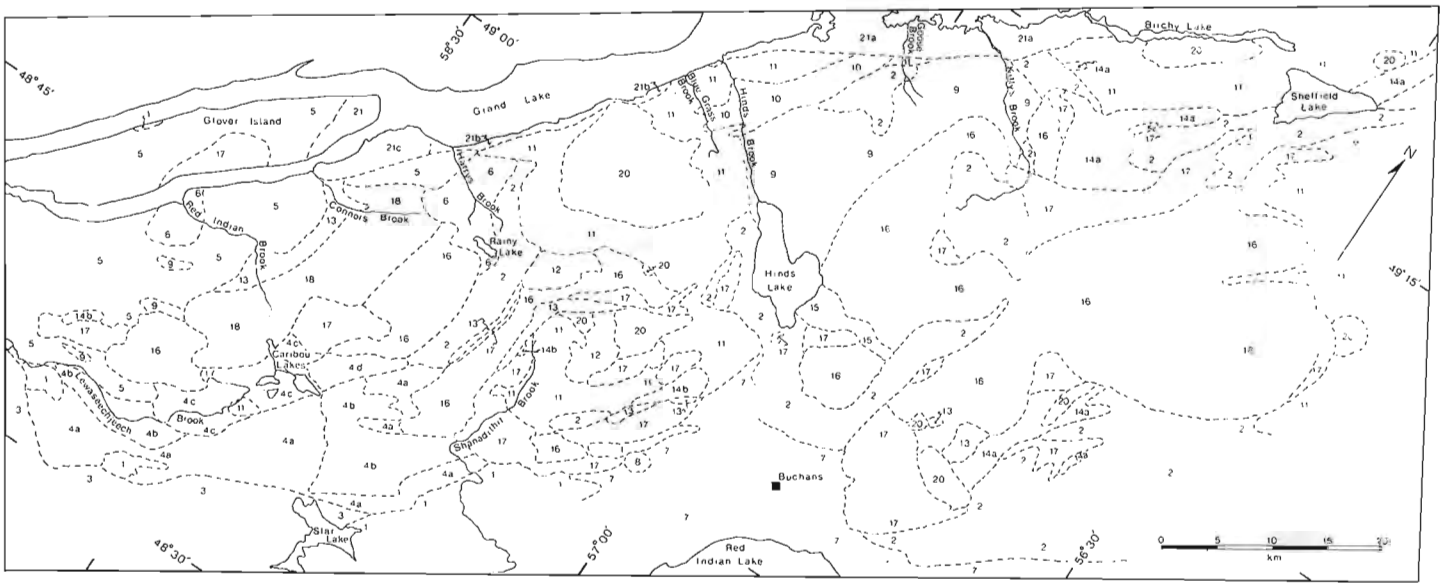

LEGEND

Period	Unit	Description	Symbol
Carboniferous	Howley Beds	Grey sandstone, minor conglomerate and siltstone	21c
	Little Pond Brook Formation	Grey to green muscovitic sandstone, quartz pebble conglomerate	21b
	North Brook and Rocky Brook Fms.	Pink to orange conglomerate and sandstone, granite wash	21a
		unconformity	
Devonian (?)		Quartz feldspar porphyry, rhyolite, minor basalt, composite dykes	20
		relations uncertain	
		diabase and porphyry dykes	19
		intrusive contact	
		Massive white biotite-amphibole, two-feldspar granite	18
		gradational to intrusive contact	
		fine- to medium-grained amphibole ± pyroxene, amphibole-biotite and biotite one or two-feldspar granites and minor granodiorite (marginal and contaminated phases of unit 16)	17
		intrusive to gradational contacts	
		coarse white to red amphibole ± pyroxene, one feldspar granite	16
		intrusive contact	
		pink biotite-amphibole two-feldspar granite	15
		relations uncertain	
Silurian (?)		red amphibole-biotite syenite to granite	14a
		grey to orange amphibole ± pyroxene gabbro to syenite	14b
		relations uncertain	
		agmatite of mafic to ultramafic blocks in granitoid matrix. Blocks may be as old as unit 1. Matrix may be as young as unit 18	13
		intrusive to gradational relations	
		red epidotized and chloritized granophyric aplite	12
		intrusive to gradational relations	
	Springdale Group (?)	red rhyolite, rhyolite breccia, laharic breccia, minor subaerial basalt	11
		unconformity	

Period	Unit	Description	Symbol
Ordovician (?)		pink biotite (-muscovite) granite and aplite	10
		relations uncertain	
		pink biotite-amphibole potash feldspar porphyritic, two-feldspar granite	9
		relations uncertain	
	Feeder Granodiorite	pink to red, biotite-amphibole, two feldspar granite	8
		intrusive contact	
	Buchans Group	basalt, rhyolite, tuff, breccia, minor subaqueous conglomerate	7
		relations uncertain	
	Rainy Lake complex	gabbro, diorite, minor granodiorite; may be equivalent to 5 in part	6
		intrusive contact	
	Glover Formation	pillow, basalt, massive basalt, minor rhyolite, tuff and shale. Probably equivalent to 7 in part	5
		mainly tectonic contacts	
		massive to moderately foliated granodiorites with many small mafic to ultramafic fragments. Relations between sub-units uncertain 4a-biotite granite to granodiorite, minor amphibole granodiorite 4c-amphibole-biotite quartz-eye porphyritic granite to granodiorite 4b-white amphibole granodiorite 4d-biotite-muscovite granodiorite and migmatite	4
		relations uncertain	
		hornblende-biotite tonalite to diorite moderately to strongly foliated, with many small to large mafic to ultramafic inclusions	3
		relations uncertain	
	Hungry Mountain complex	hornblende gabbro, diorite, tonalite, amphibole-biotite granodiorite, minor biotite-muscovite gneiss, moderately to strongly foliated with many small to large mafic inclusions. Probably equivalent to units 3, 4	2
		intrusive to gradational relations	
		mafic to ultramafic rocks; basalt, gabbro hornblendite, ophiolitic suites	1

Geology by J.B. Whalen 1981, 1982, K.L. Currie 1981, 1982, J.G. Graves 1981, and P. Barrette 1982

Figure 2.2. *Preliminary geological map of the Topsails igneous terrane.*

The Topsails terrane appears to be tectonically separated from neighbouring terranes. The drift-filled valley of Birchy Lake, thought to contain the Lobster Cove fault (Dean and Strong, 1977), separates the Topsails and Fleur de Lys terranes. To the west, a steeply dipping fault, exposed in Connors Brook and thought to extend the length of Grand Lake (Hyde and Ware, 1981), separates the Topsails terrane from a Carboniferous basin. To the south and east, investigations in the Buchans camp (Thurlow, 1981), and our own observations farther to the southwest, show that the Topsails terrane is thrust to the southeast over the central volcanic belt of Newfoundland, and over a gneissic, much more mafic, igneous terrane to the south of Lewaseechjeech Brook.

Description of Units

The oldest rocks exposed in the Topsails terrane comprise moderately to strongly deformed ultramafic to granodioritic intrusive rocks (map units 1-4). Rocks of mafic to ultramafic composition (unit 1) occur as small to large inclusions in units 2, 3 and 4. Southeast of the Topsails terrane, Dunning (1981) and Dunning et al. (1982) identified larger fragments occurring in units 3 and 4 as being of ophiolitic affinities, and suggested that the smaller mafic inclusions in these units were also oceanic crustal material. Similar mafic to ultramafic inclusions occur in the Hungry Mountain complex (unit 2) and younger igneous breccias (unit 13). Some gabbroic bodies west of Buchans, here included in unit 1, may be as young as unit 16.

In the northern part of the Topsails terrane the oldest rocks have been grouped together into the Hungry Mountain complex (unit 2), as described by Thurlow (1981). Bell and Blenkinsop (1981) obtained a rather uncertain Rb-Sr isochron age of 660 ± 60 Ma for this unit north of Buchans. Even in the type area near Buchans, the Hungry Mountain complex is very heterogeneous on both large and small scales. The rocks consist principally of hornblende gabbro, diorite and tonalite with numerous mafic to ultramafic inclusions. Significant amounts of various types of younger granodiorite also occur, together with minor amounts of biotite-muscovite gneiss. The mafic portions of the complex and the most abundant granodiorite type strikingly resemble unist 3 and 4c respectively. The Hungry Mountain complex may be equivalent to undifferentiated units 1, 3 and 4, but we believe it to be a significantly older, possibly Precambrian complex. Structurally, the complex varies from massive to strongly foliated, but epidote veins and patches are ubiquitous and characteristic.

South of the Topsails terrane, an extensive mafic to tonalitic terrane (unit 3) has been described by Herd and Dunning (1979), Dunning (1981) and Dunning et al. (1982). This terrane consists of moderately to strongly foliated hornblende-biotite tonalite to diorite with numerous small to large mafic to ultramafic inclusions of unit 1. A massive to moderately foliated granodiorite terrane (unit 4) separates this mafic terrane from the Topsails. The granodiorite can be subdivided into four types; (a) medium grained white to pink biotite granodiorite to granite, (b) coarse grained, acicular amphibole granodiorite, (c) and (d) medium granined biotite-muscovite granodiorite. The latter unit contains large inclusions of quartz, obviously derived from older veins, and locally appears to be a remobilized migmatite complex. We believe this body to represent basement only slightly remobilized. Contact relationships between the tonalite terrane (unit 3) and the granodiorite terrane (unit 4) are very poorly exposed, but the granodiorites appear to be younger.

The Glover Formation (unit 5) underlies much of Glover Island, and a large area on the east side of Grand Lake extending as far north as Harrys Brook. On Glover Island and the eastern shore of Grand Lake the formation consists mainly of pillowed basalts, but farther to the east, acid tuffs and flows with thin shale and siltstone units become a major component. South of Red Indian Brook the rocks closely resemble the Buchans Group (unit 7). A fossil locality at the southwest margin of the mapped area yielded a middle to late Arenig fauna (G.S. Nowlan, personal communication, 1982). Close to contacts with younger granitic rocks the Glover Formation loses primary features and becomes massive, fine grained rock, presumably due to contact metamorphism, although such metamorphism is not obvious in the field. Knapp et al. (1979) found the Glover Formation on Glover Island to rest on ultramafic rocks.

The Rainy Lake complex (unit 6) outcrops well in Harrys Brook and Red Indian Brook, but is poorly exposed from Harrys Brook to Rainy Lake and southwards. The complex consists of distinctive, mildly saussuritized gabbro with clots of pyroxene, biotite and amphibole, which is cut by various mesocratic diorites, leucocratic tonalites and granodiorites. The western parts of the complex in Harrys and Red Indian brooks contain basaltic enclaves, and the sequence is bounded to the west by west-facing pillow lavas with minor interstitial red chert. Riley (1957) and Knapp et al. (1979) mapped these areas as Glover Formation. We interpret the Rainy Lake complex to be the roots of the Glover Formation.

The Buchans Group (unit 7), which borders the central part of the Topsails terrane has been recently mapped in detail by Kean (1979), described by Thurlow (1981) and Thurlow and Swanson (1981), and dated by a Rb/Sr whole-rock isochron at 447 ± 18 Ma (Bell and Blenkinsop, 1981). The Buchans Group consists of a sequence of pillowed basalts, dacites, rhyolites, fragmental tuffs and breccias, with minor conglomerate of subaqueous origin. Thurlow (1981) showed that the Hungry Mountain complex (unit 2) was thrust over the Buchans Group, and that younger granites (units 14 and 16) intrude the group. Parts of the Buchans Group may be correlative with the Glover Formation, which it lithologically resembles, but the available ages suggest that the Buchans Group is slightly younger.

Rather diverse granitoid rocks (units 8, 9, 10) outcropping at various places in the Topsails terrane, appear to be roughly of similar age to the Glover Formation, Rainy Lake complex and Buchans Group. These rocks are generally near massive, or weakly foliated, and lack the small scale heterogeneity characteristic of units 2 and 3. Some of the granitic portion of the Hungry Mountain complex (unit 2) may be equivalent to these units. All of these units exhibit fracture-related chlorite and epidote alteration. The Feeder Granodiorite (unit 8), celebrated in accounts of the Buchans camp (Thurlow, 1981) forms a small body between the Topsails and the Buchans Group, and dykes of this body cut the Buchans Group. The pink, two-feldspar, biotite-amphibole granitoid rock is characterized by 5 to 10 mm, rounded to subhedral, quartz grains. Bell and Blenkinsop (1981) obtained a Rb/Sr isochron of 410 ± 80 Ma from this rock. Granite of this type has not been observed in the Topsails terrane, lending support to the suggestion of Thurlow (1981) that it may be genetically related to the Buchans Group acid volcanics, which are likewise absent from the Topsails terrane.

White to pink, potash feldspar porphyritic, two-feldspar biotite-amphibole granite comprises unit 9. The largest body lies west of Hinds Lake, extending from Hinds Brook to Kittys Brook, where Neale and Nash (1963) reported a muscovite K-Ar age of 484 Ma from this granite. At the sampled locality, we interpret the muscovite to be a secondary, fracture-related phase, not a primary mineral. The reported age presumably refers to some alteration event, and sets a minimum age for this unit. In the southern part of the Topsails terrane, small bodies of very similar granodiorite intrude the Glover Formation.

West of unit 9, a large body of pink, roughly equigranular, biotite and biotite-muscovite two-feldspar granite extends from Blue Grass Brook to Goose Brook. This body contains aplitic zones with coarse grained muscovite rosettes and patchy, greisen-like, muscovite alteration. Contact relations between units 9 and 10 were not observed, but the units are thought to be of similar age. In Blue Grass Brook volcanics and sediments of unit 11 unconformably overlie the granite. The basal conglomerate contains rounded cobbles of locally derived granite, red rhyolite and oxidized basalt, and is in turn overlain by flows of similar rhyolite and basalt. The intrusive rocks of units 9 and 10 thus appear to form a basement for the volcanic and sedimentary rocks of the Springdale Group (unit 11).

A thick volcanic section younger than the Glover Formation and Rainy Lake complex outcrops in the central part of the Topsails terrane. We have observed unconformable contacts with the Glover Formation and older granitic rocks (unit 10). The lithological composition and stratigraphic position of this volcanic section strongly suggest that it is equivalent to the Springdale Group of presumed Silurian age. Neale and Nash (1963) mapped the Springdale Group from its type area southwest to the vicinity of Sheffield Lake, where they truncated it by a rather arbitrary boundary, possibly because they recognized the presence of subvolcanic porphyries (unit 20) in this area. However, we have been able to separate the Springdale-type lithologies from these younger rocks. Near-massive red rhyolite, with little layering or flow banding, forms the lowest part of this section and is overlain by reddened basalt flows with frothy vesicular tops indicating subaerial extrusion. The upper part of the section consists of bright, orange to red rhyolites with sparse, small phenocrysts. Spectacular rhyolite-basalt mixtures occur, including a flow composed of globules of basalt and rhyolite, and composite dykes grading from rhyolite cores to basalt edges. The upper part of the section also contains rhyolite breccias with well sized, angular fragments, and laharic breccias with both rhyolite and basaltic boulders in chaotic rhyolitic matrix. We interpret a small area of similar volcanics at the southeast edge of the Topsails terrane (Caribou Lakes) to be part of the Springdale Group, since they exhibit unconformable relations with the older granodiorite (unit 4c) and are associated with flow-banded rhyolite dykes. Dunning et al. (1982) believed these rocks to be younger and associated with 'Topsails granite' (units 16 and 17).

The volcanic assemblage is intruded by, and grades into, red aplitic to granophyric amphibole-biotite granite (unit 12), thought to be the plutonic equivalent of the volcanic rocks. This granite contains many rhyolitic enclaves and patches, and much of the body is fine grained with miarolitic cavities, suggesting high level to subvolcanic intrusion. Fluorite occurs in cavities in the granite, and as vuggy fracture fillings in the rhyolite. The volcanic-plutonic assemblage has been folded at least twice, but the fold axes are sinuous and appear to wrap around neighbouring younger plutons, suggesting that the assemblage forms screens or pendants to younger granite intrusions.

The central part of the Topsails terrane contains several elongate belts of agmatite (unit 13) consisting of extraordinarily complex mixtures of diverse mafic fragments and variously hybridized granitoid rocks. The mafic fragments range from fine grained but featureless basalt, through various gabbroic rock types, to ultramafic blocks. Fragments range in size from a few millimetres to more than 10 m, and shapes range from extremely angular to almost spherical. The edges of the mafic blocks commonly show physical disintegration so that mafic grains are strewn through the salic host, producing hydridization. The salic host is itself composite, consisting of at least two different phases, an older granodioritic rock of coarse grained texture, and a younger alaskitic rock of aplitic texture. The whole unit is cut by mafic dykes which are themselves sinuous, and locally broken up, suggesting that they were emplaced into a still plastic mass. The agmatite zones presumably sample material originally at greater depth. The mafic fragments could be, in part, derived from unit 1, whereas the salic matrix appears more likely equivalent to units 16, 17 and 18. Although one poorly exposed example northeast of Buchans fringes syenite (unit 14a), the others appear to form screens separating plutons of hornblende-bearing granite.

Two syenite-bearing suites occur within the Topsails terrane, namely a gabbro-syenite suite (unit 14b) and a granite-syenite suite (unit 14a). Based on intrusive relationships and degree of alteration, both appear older than unit 16, but the two suites do not appear genetically related. The gabbro-syenite suite occurs as an elongate body east of Shanadithit Brook, as an isolated hill, possibly a large fragment in an agmatite zone, west of Shanadithit Brook, and as a small body on the southwest margin of the Topsails terrane. The gabbros contain elongate clinopyroxenes with amphibole rims, euhedral plagioclase and interstitial potash feldspar. The more salic parts of the unit are deep orange with minor acicular amphibole. A petrographically identical rock, the Skull Hill syenite, a few kilometres east of the mapped area gave a zircon age of 415 ± 2 Ma (Kean and Jayasinghe, 1982). The syenite-granite suite (unit 14a) around Sheffield Lake exhibits an apparent continuum of compositions from red, two-feldspar, biotite-amphibole-clinopyroxene syenite to biotite-amphibole granite. The syenite contains abundant, small, partially disaggregated mafic inclusions, which decrease in abundance with increasing quartz content. Granite of unit 17 clearly intrudes the syenite. Northeast of Buchans, the poorly exposed syenite to granite sequence appears to belong to a different suite than the Sheffield Lake occurrences, although it is also older than unit 16.

Southeast of Hinds Lake a small body of pink two-feldspar biotite-amphibole granite (unit 15) is cut by fine grained peralkaline dykes of unit 17.

Coarse grained, white to red, alkali feldspar, amphibole granite with prominent quartz grains and a distinctive interstitial habit to the mafic minerals (unit 16) outcrops over a very large area of the Topsails terrane, extending from Lewaseechjeech Brook for more than 100 km to the northeast to the vicinity of Sheffield Lake. The unit appears to be quite lithologically and chemically homogeneous over this large area, although thin section examination shows that it varies from biotite-bearing through biotite-absent to aegirine-bearing granite. Closely associated with unit 16 is a spectrum of fine- to medium-grained granitic to granodioritic phases which have been grouped into one map unit (unit 17). These phases occur mainly at the margins of the coarse grained amphibole granite, and vary from amphibole-poor or amphibole-free biotite granite to peralkaline amphibole-aegirine granite. Both one-feldspar and two-feldspar types occur. Contact relationships, where observed, show that these phases are younger than unit 16, although in many areas the contacts appear to be gradational. Adjacent to agmatite zones (unit 13), the marginal rocks of unit 17 exhibit dioritic or granodioritic phases. Field observations and chemistry indicate that these compositions result from mixing of amphibole granite (unit 16) and solid basaltic fragments. The distribution of other phases of unit 17 suggests that they also result from contamination or hydridization of amphibole granite by host rocks.

Throughout the whole Topsails terrane, substantial parts, although by no means all of unit 16, are peralkaline. The peralkaline character of unit 16 mainly resides in spongy mafic clots of alkali pyroxene and riebeckite with occasional

aenigmatite and 'exotic' sodium titanium silicates and phosphates. These clots, whether 'restite' from an older source, or cumulates resulting from crystallization, are indisputably older than their salic surroundings. The evidence therefore suggests that the magma was initially peralkaline, but lost this character by crystallization and/or interaction with host rocks. Since petrography and chemistry demonstrate that most phases of unit 17 are not peralkaline, they cannot simply be chilled marginal zones of unit 16.

In the southern part of the Topsails terrane, biotite-dominant, two-feldspar granite, readily recognized in the field by the white plagioclase crystals on a weathered surface, is a major rock type (unit 18). Last year we noted that this material intruded unit 16 southwest of Rainy Lake. However further mapping suggests that in other areas the two units grade into one another. Unit 18 may therefore be an unusual variant of unit 17.

Units 16, 17 and 18 are locally cut by numerous dykes (unit 19) including basalt, diabase, gabbro, quartz-feldspar porphyry and composite dykes. These dykes, which are too small to show on the present map, are essentially restricted to the southern half of the Topsails terrane. Only one 7 cm basalt dyke was observed cutting units 16 and 17 north of Hinds Lake. Unlike the host rocks, which appear fresh, many of the dykes are perceptibly altered, and on large outcrop surfaces can be seen to be broken up into segments, presumably by movement within a still hot or reheated granitic host.

High level intrusive and extrusive quartz-feldspar porphyries form substantial, presumably subvolcanic plutons west of Hinds Lake, south of Birchy Lake and northeast of Buchans. Phenocrysts of quartz up to 1 cm across have the characteristic bipyramidal high temperature form. Mafic minerals appear as rare clotty aggregates, or within the matrix. The porphyries locally exhibit poorly developed flow banding and grade to rhyolite with rare interbedded basalt. Petrographic and chemical studies show that some parts of the porphyries are peralkaline, whereas others, including most of the rhyolite, are not. Therefore the rhyolite may not be chilled equivalents of the porphyries. West of Sheffield Lake however, a 30 to 60 m section of riebeckite-aegirine-aenigmatite rhyolite overlies and is cut by peralkaline quartz-feldspar porphyry. The peralkaline rhyolite is structureless and very fine grained with 1 to 3 cm spongy, dendritic mafic aggregates. Thin section study indicates that only rare aegirine cores of some mafic clots are free of matrix inclusions. This observation, together with the delicate structure of the clots suggest that they may have developed by subsolidus reactions, and this rhyolite may therefore be a chilled equivalent of the peralkaline porphyry.

Age relationships between this unit and the amphibole granite (unit 16) remain unclear. Last year we suggested that the porphyries may be younger, citing the porphry dykes cutting unit 16. These dykes are not peralkaline, however, and may not be equivalent to unit 20. Field relations still suggest that the porphyries are not high level equivalents of the amphibole granite but represent a younger intrusive episode.

Spectacular composite dykes up to 50 cm in width cut the porphyries. Aphanitic basalt margins pass gradationally inward through basaltic zones with potash feldspar phenocrysts, to a zone of globules of basalt up to 5 cm across in an intermediate matrix, and ultimately to a central core or rhyolite porphyry.

A thin fringe of Carboniferous clastic sedimentary rocks (unit 21) fringes the eastern edge of Grand Lake, varying in width from 0 to 2 km (Hyde and Ware, 1981). At the northeast end of Grand Lake the Howley Beds (unit 21c) consist mainly of sandstone with minor conglomerate, siltstone and coaly beds. Clasts within the conglomerate appear to have been locally derived from biotite-muscovite granite (unit 10).

Between Hinds Brook and Harrys Brook the main rock type is grey-green coarse sandstone and pebble conglomerate (unit 21b, Little Pond Brook Formation of Hyde and Ware, 1981). Little of this material comes from the nearby granitic hills, although it might come from farther northeast in the Topsails. South of Harrys Brook, a distinctive conglomerate (unit 21a, North Brook Formation of Hyde and Ware, 1981) forms virtually all of the Carboniferous section exposed inland. This material appears entirely derived from nearby granites, and locally consists of granite wash. Due to nonexistent outcrop we saw no relations between units 21b and 21c, but the contrast is sufficiently striking to suggest the presence of a sizeable dislocation in the Carboniferous section near the north end of Glover Island.

Economic Geology

The Topsails terrane has received little prospecting attention, presumably due to its relative remoteness and poorly known geology. We believe, however, that some units have significant economic potential. We noted last year the similarity of the Rainy Lake complex to recent island arc intrusive complexes (Whalen and Currie, 1982). Such intrusions have known potential for porphyry copper mineralization. The Glover Formation, and the Buchans Group both contain considerable volumes of pillow lavas. We have mapped significant amounts of volcaniclastic sediments and rhyolites in the Glover Formation. Since the Glover Formation appears to be similar in age to the Buchans Group, and contains probable island-arc type intrusions, we suggest that the Glover Formation, like the Buchans Group, has potential for island-arc type massive sulphide mineralization.

Biotite-muscovite granite west of Hinds Lake (unit 10) has numerous pegmatitic to aplitic zones with patchy muscovite alteration. Since the granite is clearly an S-type body in the classification of Chappell and White (1974), and exhibits greisen-like alteration, we suggest it has potential for Sn mineralization.

The younger supracrustal rocks of the Springdale (?) Group are subaerial in origin, and therefore lack potential for massive sulphide mineralization. However, both the rhyolites and genetically related aplite contain vuggy fracture fillings of fluorite in the central part of the Topsails terrane. We consider there is potential for other vein-type mineralization in these rocks.

In the northwest corner of the Star Lake 1:50 000 sheet (NTS 12A/11, grid reference 53975000N/467300E) a molybdenite showing occurs in a drusy granophyric aplite of unit 17. The showing consists of coarse grained (1-2 cm) molybdenite rosettes in a drusy matrix. The host rocks and the mode of mineralization closely resemble molybdenite showings in the Ackley City batholith (Whalen, 1980). The diverse fine grained phases (unit 17) associated with the amphibole granite (unit 16) probably represent marginal and high-level phases, as is the case for the Ackley showings, and have potential not only for molybdenum but also for tin.

Relation of the Topsails Terrane to Juxtaposed Terranes

The boundaries of the Topsails terrane to the north, west and south can be easily defined by topographic features, namely the valleys of Birchy Lake, Grand Lake, and Little Grand Lake-Lewaseechjeech Brook. On the southeastern side the boundary clearly lies west of Red Indian Lake, close to the topographic drop off from the Topsails plateau to the lowlands around Red Indian Lake. Examination along these boundaries reveals both abrupt changes in the geology and

complex relations between the juxtaposed terranes. To the north of Birchy Lake the rocks consist of biotite diorite to granodiorite with a local fabric, and large migmatite zones. These rocks are intruded into quartz pebble conglomerates of the Fleur de Lys Group. None of these lithologies occurs anywhere in the Topsails terrane. However, Silurian acid volcanics of the Springdale Group and equivalents cross the Birchy Lake line, if not into the Fleur de Lys terrane, then clearly into the Notre Dame Bay terrane to the east. Along Grand Lake the Topsails terrane is in contact with Carboniferous sedimentary rocks. We have recognized no tight folding along the eastern side of the lake, although similar rocks are isoclinally folded west of the lake. Together with the unexplained change in provenance of the rocks near Glover Island, noted above, these relations suggest that the Carboniferous basin may be composed of several segments.

South of Grand Lake, the Topsails terrane clearly includes the Glover Formation. Riley (1957) showed the Glover Formation extending onto the southern shore of Little Grand Lake. The highlands southeast of Little Grand Lake consist of an assemblage of granodiorite, tonalite and diorite (unit 3) grading northeastward to granodiorite (unit 4a). All of these rocks are foliated and contain substantial amounts of agmatized mafic material. We believe unit 3 to be correlative, and probably continuous, with the tonalite gneiss terrane described by Herd and Dunning (1979) farther to the south. North of Lewaseechjeech Brook the massive granites of the Topsails terrane can be seen to project southward over the more mafic material in a thin sheet. Although the actual contact is not exposed, in one stream highly fractured, sheared and altered brick red amphibole granite (unit 16) lies in proximity to granodiorite of unit 4c. Field relations on both large and small scale strongly suggest southeasterly directed, low angle thrusting. Similar thrusting of the Topsails terrane over the Buchans Group of Ordovician acid and mafic volcanics has been documented by Thurlow (1981). From observations of the relative positions of massive granite on the hilltops and gneissic granodiorite in the valleys, we believe that similar relationships may extend around much of the southeastern margin of the Topsails.

The contact cannot be a simple thrust everywhere. Northeast of Caribou Lakes, sparse outcrop of gabbro and foliated biotite-muscovite granite suggest that such rocks probably form a continuous zone from the Rainy Lake complex (unit 6) south to the granodiorite terrane, an interpretation supported by aeromagnetic data (Geological Survey of Canada, 1956). This zone is flanked on both sides by hills of massive granite (unit 16) presumed to be intrusive into the older rocks. At the southern end of the zone, a hill of coarse amphibole granite is surrounded on three sides by foliated granodiorite. The coarse grained nature of the granite, and the presence of major zones of shearing and alteration, contrast sharply with the nearby outcrops of this phase. We interpret the hill to be a deeper level portion of unit 16 faulted into its present position by movement along the contact between the Topsails terrane and the granodiorite terrane.

The observations of the uniqueness of the Topsails terrane, and its isolation from neighbouring terranes by tectonic features, permit two very different, although not completely incompatible, models for the relation of the Topsails terrane to its surroundings. If the differences between the terranes are emphasized, then it might be assumed that the Topsails terrane is totally foreign in its present position, and entirely bounded by faults of unknown displacement. If this view is adopted, the Topsails terrane must have been joined to the Notre Dame Bay terrane prior to the Silurian, since Silurian igneous activity crosses the Lobster Cove fault west of Springdale. Junction with the granodiorite terrane must have occurred prior to Devonian, since presumed Devonian intrusives of the Topsails terrane are emplaced in the edges of the granodiorite terrane. On this view, if the breaks in the Carboniferous Grand Lake basin are significant, the geology gives no clues on the junction time of the Topsails and Great Northern Peninsula terranes, which could have been post-Carboniferous.

The alternative view emphasizes similarities, such as the continuity of the Glover Formation across Little Grand Lake, and the possible continuity of the Hungry Mountain complex beneath the Topsails terrane into the tonalite gneiss terrane of Herd and Dunning (1979). On this view the Topsails terrane could be continuous with the terranes to the northeast and southwest. The sharp boundaries of the terrane would then be ascribed to original composition differences, possibly accentuated by essentially vertical movements. The Topsails terrane clearly is a high-level terrane compared to the tonalite gneiss terrane to the south, but relatively deep seated compared to the central volcanic belt. Hence vertical movements between the three terranes would be expected. In our initial report (Whalen and Currie, 1982), we adopted the second model. Further mapping, however, suggests that the first may also be viable, and if correct would lead to a radical reinterpretation of Newfoundland geology. We prefer to withhold judgement until more information becomes available.

Granite Classification

Recent work indicates the prime importance of source rock variation in explaining major and minor differences between granites. A major distinction has been made by Chappell and White (1974) between granites formed from igneous sources (I-type) and those formed from sedimentary sources (S-type). A further subdivision, termed mantle or M-type, has been suggested for continental margin I-types which have chemical and isotopic compositions similar to those of island-arc volcanic rocks, and may form by anatexis of subducted ocean crust (White, 1979). Yet another type, anorogenic or A-type, may form in regions where the crust has been dehydrated and depleted by previous melting events (Loiselle and Wones, personal communication, 1982). These four types are based mainly on chemical criteria, but can be distinguished in the field by geological and petrographic differences.

Based on field mapping and preliminary chemical data, the Topsails terrane contains all four granite types. The biotite-muscovite granite west of Hinds Lake (unit 10), the biotite-muscovite granodiorite and migmatite north of Caribou Lakes (unit 4d) and the biotite-muscovite gneiss component of the Hungry Mountain complex (unit 2) are clearly S-type granites. The other bodies all appear to be I-type. The gabbroic to tonalitic intrusive rocks of the Hungry Mountain complex (unit 2), the tonalite terrane (unit 3) and the Rainy Lake complex (unit 6) all appear to be M-type. Much of the younger granite of the Topsails (units 16, 17 and 20) is alkaline to peralkaline, that is A-type. This juxtaposition of diverse types in a relatively small area clearly shows that the terrane has undergone a complex igneous history, and suggests that not all of the granitoid rocks can have developed from the same protolith.

Igneous History of the Topsails Terrane

The presence of such a diversity of granite types in a restricted area indicates the presence of a complex lower crust. The central part of the terrane must possess siliceous and potassic basement to produce the observed succession of siliceous and potassic melts. Such a basement was clearly not the source for the M-type granites, ophiolite-related Glover Formation, and island-arc-related Buchans Group

which fringe the southern two thirds of the terrane. These 'primitive' igneous rocks are mainly older than the potassic igneous rocks, and it seems unlikely that they were generated and emplaced in their present sites. Wholesale lateral transport and/or a laminated character of the crust is implied by the mixing of rock types in the Topsails terrane. The presence of mafic to ultramafic fragments in the agmatite zones (unit 13) within the potassic granites shows that mafic crust must be present at depth, whereas the presence of alkali granite within the Glover Formation shows that siliceous and potassic crust must be present below these 'primitive' rocks.

The source of the Topsails siliceous and potassic rocks must have been of continental character. Since this source appears to be surrounded by, or perhaps interlayed with, crust of more oceanic character, it seems to be an isolated continental fragment. This fragment must have retained a reasonable degree of rigidity during successive extractions of melt, since the superficial rocks are massive. To appreciate this point one need only consider the tonalite terrane to the south where all units are gneiss and clearly flowed relatively readily. Perhaps the relatively large scale melting of the tonalite may explain its relatively high level, compared to the subvolcanic Topsails terrane, since large scale melting leads to an overall reduction in density, and hence to relative uplift of deep-seated material.

Large scale melting of the relatively mafic tonalite terrane must have required high temperatures, yet initial dating (Dunning et al., 1982) suggests that most of the igneous rocks are of early to middle Ordovician age. Hence a large amount of energy was injected into the terrane relatively quickly. In the Topsails terrane, in Ordovician and later time, melts tended to stay near 'minimum melt' composition, but reappeared many times, commonly accompanied by small amounts of basic magmatism in the form of dykes and occasional basalt flows. These observations can be integrated into a model in which heat is transferred from below into cold granitoid crust, presumably by motion of basic magma, until the melting point is reached. Transport of the acid magma is assumed to be rapid relative to the heating rate, so that the newly generated magma moves away upward, bringing magmatic activity to a halt until the heat source is recharged. On this model, the continental fragment acts as a sort of 'thermal tap' so that an amount of energy sufficient to produce one episode of intensive melting in the tonalite is let into the crust in small amounts sufficient to produce repeated episodes of granite magmatism.

Finally, we note that peralkaline magmatism occurs in relatively small, widely separated bodies, and may possibly have occurred at more than one time. Peralkaline chemical analyses are in a minority in the Topsails terrane, even within the amphibole granite of unit 16. Preliminary work on the chemistry shows that the peralkaline rocks are extremely poor in Ca and Mg, with moderate Al and Na content, and relatively high K/Na ratios for peralkaline rocks. These observations suggest that a calcic, moderately aluminous phase with low K/Na ratio was extracted from the developing peralkaline melt. The only plausible phase fitting this description is hornblendic amphibole, a phase well known in the granites associated with the peralkaline rocks. Extraction may have occurred either by leaving solidus hornblende behind during partial melting (Huang and Wyllie, 1981) or by fractional crystallization of hornblende. Since the peralkaline phases tend to be relatively old, and the field evidence clearly suggests that they lost their peralkaline character with time, we are inclined to favour the first hypothesis. We suggest that this peralkaline granite formed by repeated partial melting of leucocratic amphibole granite under conditions such that amphibole was stable on the solidus. Continued, more extensive, partial melting destroyed the peralkaline character by incorporating the calcic and aluminous phases into the melt. Similarly, assimilation of more aluminous host rocks will destroy the peralkaline character of the melt, as observed where the amphibole granite contacts agmatite zones. We consider the finer grained phases (unit 17) of the locally peralkaline amphibole granite (unit 16) to represent not only marginal phases, but also higher level and more evolved portions of the magma. They may represent remnants of a roof zone complex, similar to that described for the Ackley City batholith (Whalen, 1980).

Taylor et al. (1980) suggested a model for formation of the peralkaline rocks based on the ideas of Hildreth (1979). They supposed the peralkaline character to be superimposed by a volatile phase at a late magmatic or subsolidus (metosomatic) stage. According to the thermogravitational model of Hildreth (1979) for felsic magmas, the chemically most evolved magmas occur at the top of the magma chamber. This model can be used to explain the field and chemical relationships within the Ackley City batholith (Whalen, in press), but in the case of Topsails peralkaline granites, the younger phases are not peralkaline. According to the model of Taylor et al. (1980) such younger, higher level phases should most clearly bear the signature of the volatile phase, and hence be most peralkaline. Field relationships therefore show this model to be inadequate.

Implications for Tectonic Models of Newfoundland

Last year we put forward a model for the tectonic development of the Topsails terrane based on the assumption the terrane was essentially autochthonous with respect to the juxtaposed terranes to the north and south. This model might be called the Japan model, since it was based on the present day example of Japan as an old continental fragment separated by a major oceanic region (Japan Sea) from its source. In the Newfoundland case, the central volcanic belt was suggested to be a back-arc basin (although the tentative age of the Hungry Mountain complex suggests that it was in existence prior to Cambro-Ordovician time), and an east-dipping subduction zone was suggested beneath the Topsails, surfacing along the Baie Verte-Brompton line, which was considered to pass down Birchy and Grand Lakes. The rather embarassing proliferation of ophiolitic fragments east of this line could then be explained by assuming that they were parts of the floor of the back-arc basin emplaced by late compression. We still believe this to be a viable, indeed necessary, model if one is to retain that classical view that Newfoundland geology can be correlated in northeast-southwest zones. The only refinement we would add is to note that fits could be improved by about 30 km of right hand movement on the east-west Grand Lake-Little Grand Lake Lineament. This would return the highly potassic and leucocratic Hare Hill region to the Topsails terrane, which it strongly resembles, and line up the scarp bounding the southern Long Range with the Cabot Fault, whose abrupt loss of topographic expression at the south end of Grand lake now poses an embarassment. On the opposite side of the Topsails terrane, we believe the boundary to pass from the region of Buchans, through an area of very little outcrop, northeast to the Hall Hill complex (Currie, 1976) which appears to be correlative to the Hungry Mountain complex, and thence past the 600 Ma Mansfield Head complex (Bostock et al., 1979) to the Lobster Cove fault.

While we believe this to be a reasonable model, we wish to draw attention to a more radical possibility, suggested by abandoning the assumption that west Newfoundland geology can be correlated along northeast-southwest zones. This assumption has clearly been weakened by the demonstration that Topsails geology is essentially unrelated to the

Fleur-de-Lys terrane to the north or to the tonalite terrane to the south. If we abandon the zonal hypothesis and draw boundaries around regions of mappably similar geology (Fig. 2.1) the picture looks very different. West Newfoundland falls into a number of discrete terranes separated by major discontinuities in the geology, presumably faults. Carboniferous basins appear as separate units, since our experience suggests that it is a dangerous and unjustified assumption to suppose that they represent only debris from surrounding terranes. Many of the terranes have a northeast elongation, although this is by no means universal. The overall picture is of a tessellate pattern in which each fragment bears no obvious relation to the one beside it. Correlations can be suggested. For example Williams et al. (1982) suggested that the sedimentary section can be correlated from the Fleur de Lys terrane to the Great Northern Peninsula terrane. However, all students from Newfoundland geology know how tenuous lithological correlation can be, and how much the correlations can be influenced by the desired zonal scheme. Tessellate terranes have been accepted for some time in the Cordillera, and in the Wopmay Orogen of the Northwest Territories. There seems no obvious reason why they should be absent from the Appalachians. These considerations suggest that fundamental discoveries in Newfoundland geology remain to be made. The Topsails terrane suggests that the answers may lie within the igneous rocks, rather than the more studied sedimentary rocks.

References

Bell, K. and Blenkinsop, J.
1981: A geochronologic study of the Buchans area, Newfoundland; Geological Association of Canada, Special Paper 22, p. 91-111.

Bird, J.M. and Dewey, J.F.
1970: Lithosphere plate-continental margin tectonics and the evolution of the Appalachian orogen; Geological Society of America, Bulletin 81, p. 1031-1060.

Bostock, H.H., Currie, K.L., and Wanless, R.K.
1979: The age of the Roberts Arm Group, north central Newfoundland; Canadian Journal of Earth Sciences, v. 16, p. 599-606.

Chappell, B.W. and White, A.J.R.
1974: Two contrasting granite types; Pacific Geology, v. 8, p. 173-174.

Currie, K.L.
1976: Studies of granitoid rocks in the Canadian Appalachians: Part 2; in Report of Activities, Part A, Geological Survey of Canada, Paper 76-1A, p. 155-163.

Dean, P.L. and Strong, D.F.
1977: Folded thrust faults in Notre Dame Bay, central Newfoundland; American Journal of Science, v. 77, p. 97-108.

Dunning, G.R.
1981: The Annieopsquotch ophiolite complex, southwestern Newfoundland, and its regional relationships; in Current Research, Part B, Geological Survey of Canada, Paper 81-1B, p. 11-15.

Dunning, G.R., Carter, P.J., and Best, M.A.
1982: Geology of Star Lake (west half), southwest Newfoundland; in Current Research, Part B, Geological Survey of Canada, Paper 82-1B, p. 21-26.

Geological Survey of Canada
1956: Rainy Lake, Newfoundland; Aeromagnetic map 273G.

Herd, R.K. and Dunning, G.R.
1979: Geology of the Puddle Pond map area, southwestern Newfoundland; in Current Research, Part A, Geological Survey of Canada, Paper 79-1A, p. 305-310.

Hibbard, J.
1978: Geology east of the Baie Verte lineament; Newfoundland Department of Mines and Energy, Mineral Development Division, Report 78-1, p. 103-109.

1979: Geology of the Baie Verte map area west (12H16/W); Newfoundland Department of Mines and Energy, Mineral Development Division, Report 79-1, p. 58-63.

Hildreth, E.W.
1979: The Bishop Tuff: evidence for the origin of zoned magma chambers; in Ash Flow Tuffs, ed. C.E. Chapin and W.E. Elston; Geological Society of America; Special Paper 180, p. 43-72.

Huang, W.L. and Wyllie, P.J.
1981: Phase relationships of S-type granite with H_2O to 35 kbars; muscovite granite from Harney Peak, South Dakota; Journal of Geophysical Research, v. 86, p. 10515.

Hyde, R.S. and Ware, M.J.
1981: Notes on the geology of parts of the Deer Lake (12H 3) and Rainy Lake (12A14) map areas; Newfoundland Department of Mines and Energy, Mineral Development Division, Map 81-17.

Kean, B.F.
1979: Buchans, Newfoundland; Newfoundland Department of Mines and Energy, Mineral Development Division, Map 79-125.

Kean, B.F. and Jayasinghe, N.R.
1982: Geology of the Badger Map area (12A16), Newfoundland; Newfoundland Department of Mines and Energy, Mineral Development Division, Report 81-2.

Knapp, D., Kennedy, D., and Martineau, Y.
1979: Stratigraphy, structure and regional correlation of rocks at Grand Lake, western Newfoundland; in Current Research, Part A, Geological Survey of Canada, Paper 79-1A, p. 317-325.

Neale, E.R.W. and Nash, W.A.
1963: Sandy Lake (east half), Newfoundland; Geological Survey of Canada, Paper 62-28.

Riley, G.C.
1957: Red Indian Lake (west half), Newfoundland; Geological Survey of Canada, Map 8-1957.

Taylor, R.P., Strong, D.F., and Kean, B.F.
1980: The Topsails igneous complex: Silurian and Devonian peralkaline magmatism in western Newfoundland; Canadian Journal of Earth Sciences, v. 17, p. 425-439.

Thurlow, J.G.
1981: The Buchans Group: its stratigraphic and structural setting; Geological Association of Canada, Special Paper 22, p. 79-90.

Thurlow, J.G. and Swanson, E.A.
1981: Geology and mineral deposits of the Buchans area, central Newfoundland; Geological Association of Canada, Special Paper 22, p. 113-142.

Whalen, J.B.
1980: Geology and geochemistry of the molybdenite showings of the Ackley City batholith, southeast Newfoundland; Canadian Journal of Earth Sciences, v. 17, p. 12461258.

– The Ackley City batholith, southeast Newfoundland: evidence for liquid state fractionation; Geochimica et Cosmochimica Acta. (in press)

Whalen, J.B. and Currie, K.L.
1982: Volcanic and plutonic rocks in the Rainy Lake area, Newfoundland; in Current Research, Part A, Geological Survey of Canada, Paper 82-1A, p. 17-22.

White, A.J.R.
1979: Sources of granite magmas; Geological Society of America, Abstracts with Program, 92nd Annual General Meeting, p. 539.

Williams, H.
1964: The Appalachians in northeastern Newfoundland – a two sided symmetrical system; American Journal of Science, v. 262, p. 1137-1158.

1978: Tectonic-lithofacies map of the Appalachian orogen; Memorial University of Newfoundland, Map 1.

1979: The Appalachian orogen in Canada; Canadian Journal of Earth Sciences, v. 16, p. 792-807.

Williams, H., Gillespie, R.T., and Knapp, D.A.
1982: Geology of Pasadena map area, Newfoundland; in Current Research, Part A, Geological Survey of Canada, Paper 82-1A, p. 281-288.

3. REGIONAL GEOLOGICAL SYNTHESIS, CENTRAL SUPERIOR PROVINCE: RECONNAISSANCE INVESTIGATIONS IN THE NAKINA AREA, ONTARIO

Project 770070

K.D. Card
Precambrian Geology Division

Card, K.D., Regional geological synthesis, central Superior Province: reconnaissance investigations in the Nakina area, Ontario; in Current Research, Part A, Geological Survey of Canada, Paper 83-1A, p. 25-27, 1983.

Abstract

Helicopter-supported reconnaissance investigations in a largely unmapped part of Superior Province about Nakina, Ontario, show that the English River, Wabigoon, and Quetico subprovinces continue eastward to, and extend beneath, the Phanerozoic cover rocks of the Moose River Basin. The southern boundary of the Moose River Basin is a fault zone that juxtaposes rocks as young as Cretaceous against the Archean basement. Several mafic gneiss units, probably the highly metamorphosed equivalents of the Tashota and Geraldton metavolcanic-metasedimentary sequences, are present in Wabigoon subprovince near Nakina. The eastern part of the Melchett Lake greenstone belt in English River subprovince contains intermediate and felsic metavolcanics with zones of sericitic and garnet-amphibole alteration.

Introduction

The geology of the area about Nakina, Ontario is poorly known; bedrock exposures are sparse and much of the area bounded by Highway 11 and latitude 51°N, and longitude 87°W and the contact with Phanerozoic rocks of the Moose River Basin has never been mapped. Diagram A of Ontario Geological Map 2196 (Ayres et al., 1970) shows the Wabigoon subprovince ending at about longitude 85°30'W with migmatitic metasediments of the English River subprovince extending southward to join with similar rocks of the Quetico subprovince. This configuration would contradict evidence that the Wabigoon subprovince continues eastward, possibly into Quebec (Card, 1982).

There are several metavolcanic belts with noteworthy deposits of gold and base metals west of Nakina and it is possible that these rocks, or their metamorphic equivalents, extend eastward. Reconnaissance investigations by the writer in 1980 along some of the roads south and east of Nakina revealed mafic gneiss of probable metavolcanic origin at several localities. In 1982, these reconnaissance investigations were extended using a helicopter. The results of this reconnaissance work are portrayed in Figures 3.1 and 3.2.

More detailed mapping should be carried out in parts of the area, especially the eastern end of the Melchett Lake greenstone belt and east of Highway 584 between Highway 11 and the CNR, to better define the geology and economic potential of the greenstones and their metamorphic equivalents.

Acknowledgments

Gordon Collette, pilot, Verrault Aviation Ltd. provided very capable and efficient service. Information from J.S. Fox, Teck Corporation, and R.P. Sage, Ontario Geological Survey, is gratefully acknowledged.

General Geology

Archean rocks of the Superior Province constitute the bedrock of most of the area. To the east, Phanerozoic rocks of the Moose River Basin are in fault and unconformable contact with the Archean (Fig. 3.2).

Superior Province is divisible into several east-trending litho-tectonic domains. Uchi subprovince in the north comprises low- to medium-grade metavolcanic-metasedimentary sequences of the Fort Hope greenstone belt, tonalitic and granodioritic gneiss of mainly plutonic origin, and foliated to massive plutons of mafic to felsic composition.

English River subprovince consists largely of metasedimentary rocks, or their high grade gneissic and migmatitic equivalents, with tonalitic orthogneiss and massive granitic plutons. Within English River subprovince there is a sizeable greenstone belt, the Melchett Lake belt. Although volcanic rocks are present in other parts of the

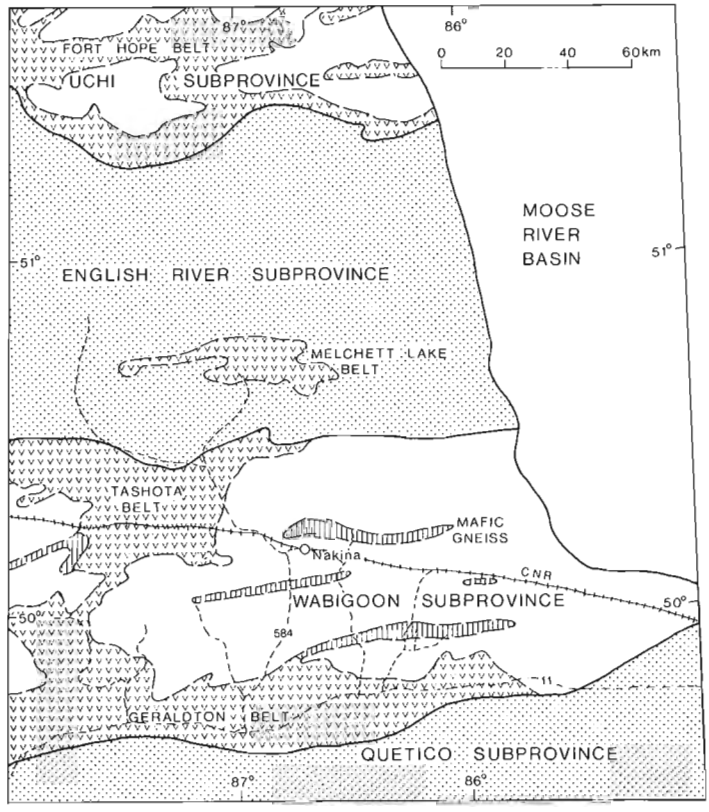

Figure 3.1. *Major geological subdivisions.*

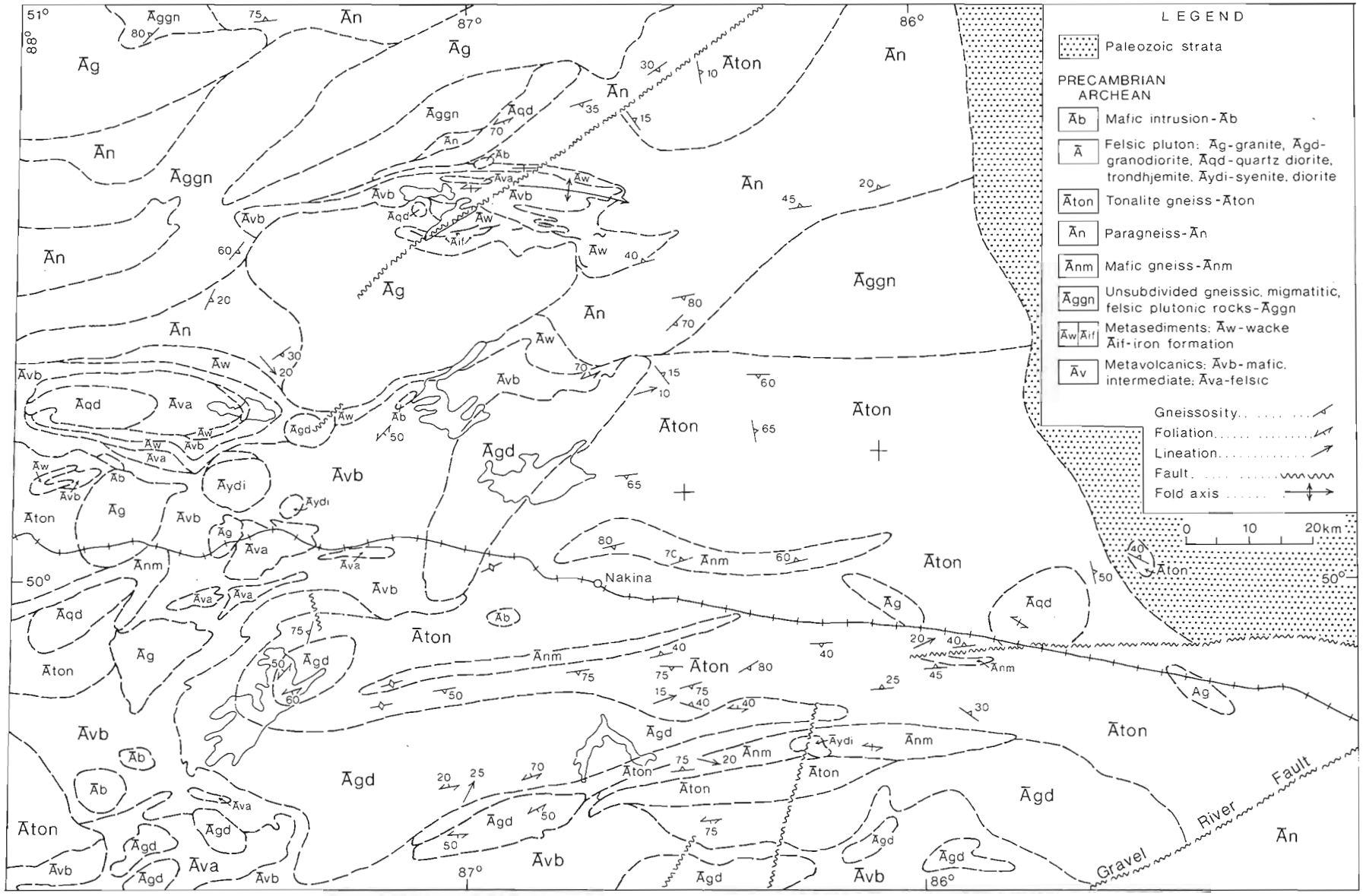

Figure 3.2. *General geology of the Nakina, Ontario area.*

dominantly metasedimentary English River and Quetico subprovinces, Melchett Lake belt is the largest known in Ontario.

Wabigoon subprovince is a typical greenstone-granite terrane consisting of thick metavolcanic-metasedimentary accumulations, tonalitic and granodioritic gneiss, and plutons ranging in composition from gabbro to granite and syenite. In addition to the known greenstone belts, here called the Tashota and Geraldton belts, there are several bodies of mafic gneiss (Anm in Fig. 3.2) which are probably the highly deformed, metamorphosed, and intruded equivalents of the better-preserved greenstone belts.

Quetico subprovince in the south is similar to the English River subprovince, consisting mainly of metasediments.

The boundaries between the various subprovinces are based mainly on changes in lithology, but also coincide, in part, with changes in structural style and trend, and metamorphic grade. In the western part of the area, the English River-Wabigoon boundary is placed at the contact between dominantly metavolcanic rocks in the south and metasedimentary rocks in the north. A short distance north of this lithological boundary there is an abrupt increase in metamorphic grade, as inferred from the presence of metasedimentary migmatite. The eastward extension of this boundary is not well defined on account of lack of outcrop, but is taken to coincide with the contact between metasedimentary migmatite to the north and tonalitic orthogneiss to the south. The Wabigoon-Quetico boundary is a lithological transition from metavolcanics to metasediments in the western part of the area, and a major fault, the Gravel River Fault, in the east (Fig. 3.2).

Structural Geology

Major structural elements, including subprovince boundaries, lithological units, faults, and fold axes trend generally east-west. In gneiss terranes, both the tonalitic orthogneiss units of the Wabigoon subprovince and the metasedimentary gneiss of the English River, foliations are variable in trend and dips of less than 45° are common. This suggests that the structure of the gneiss domains consists of domes and basins of various dimensions. Lineations in the gneiss belts generally trend and plunge eastward (Fig. 3.2).

Faults striking east-northeast and north-northeast are recognized or interpreted from topographic lineaments and aeromagnetic trends. One interpreted ENE fault passes through the Melchett Lake belt. Another, the continuation of the Gravel River fault, forms part of the Wabigoon-Quetico boundary.

A major east-trending fault in the eastern part of the area (Fig. 3.2) forms part of the Phanerozoic-Precambrian contact. North trending Ordovician-Silurian strata are in contact with Archean rock units along this fault, and immediately east of this area rocks as young as lower Cretaceous are juxtaposed against the Archean (Sanford et al., 1979). Significant Phanerozoic movement on this structure has therefore taken place, presumably with the north side moving down relative to the south. At Ogahalla Rapids on the Kenogami River some 40 km west of the Phanerozoic contact there are fault rocks consisting of granitoid augen gneiss with cataclastic foliation striking N85E and dipping 40°N. A rodding lineation in the foliation plane trends N70E and plunges shallowly east. These structures imply an ENE-WSW transport direction that could be attributed either to low angle, normal faulting (north side down) or thrusting (north side up and southwest). It is possible that both Precambrian and Phanerozoic movements have occurred.

North-northeast faults in the southeastern part of the area probably belong to a fault system extending north from Lake Superior that may have controlled emplacement of Proterozoic alkalic rock-carbonatite complexes and diatreme breccias such as the Port Coldwell, Killala, and Prairie Lake bodies (R.P. Sage, personal communication, 1981). In the Nakina area at Chipman Lake, one of the faults is spatially associated with a diorite-syenite body of probable Archean age and carbonatite and lamprophyre dykes of probable Proterozoic age.

Some Observations on the Melchett Lake Belt

Part of the Melchett Lake belt has recently been mapped in detail by Bond and Foster (1981) and earlier reconnaissance mapping in the area was carried out by Kindle (1931), and Thurston and Carter (1970). The present compilation (Fig. 3.2) is primarily from those sources. During the present survey, a number of observations were made in the eastern part of the belt around Colpitts and Bury lakes. Here, there are units of lapilli tuff and tuff breccia of intermediate and felsic composition and quartz-feldspar porphyry of probable intrusive origin. These rocks are regionally metamorphosed under amphibolite facies conditions. Sericitic alteration is present and there are patches and dyke-like bodies of mafic, garnet-amphibole material in the felsic rocks that may represent the product of regional metamorphism of metasomatically altered fragmental volcanics.

Sedimentary rocks of the Melchett Lake belt include metamorphosed wacke, pelite, and oxide-facies iron formation. Although these rocks have biotite, garnet, and staurolite porphyroblasts, primary structures such as bedding, graded bedding, ripples, load casts, and flames are locally well preserved. The structure of the northeastern part of the belt is interpreted as an east-plunging anticline, partly on the basis of top determinations in the metasediments. The structure of the Melchett Lake greenstone belt as a whole is probably a doubly-plunging antiform.

References

Ayres, L.D., Lumbers, S.B., Milne, V.G., and Robeson, D.W.
1970: Diagram A. Generalized distribution of major lithologic units and structures; scale 1 inch equals 100 miles; Ontario Department of Mines and Northern Affairs, Map 2196, Ontario Geological Map.

Bond, W.D. and Foster, J.R.
1981: Precambrian geology of the Melchett Lake area, Thunder Bay District; Ontario Geological Survey, Preliminary Maps P.2392, P.2393, scale 1:15 840.

Card, K.D.
1982: Progress report on regional geological synthesis, central Superior Province; in Current Research, Part A, Geological Survey of Canada, Paper 82-1A, p. 23-28.

Kindle, L.F.
1931: Kowkash-Ogoki gold area; Ontario Department of Mines, v. 40, pt. 4, p. 55-104.

Sanford, B.V., Grant, A.C., Wade, J.A., and Barss, M.S.
1979: Geology of Eastern Canada and Adjacent Areas; Geological Survey of Canada, Map 1401A, scale 1:2 000 000.

Thurston, P.C. and Carter, M.W.
1970: Operation Fort Hope; Ontario Department of Mines, M.P. 42, 64 p.

4. A RECONSIDERATION OF THE CARBONIFEROUS ROCKS OF SAINT JOHN, NEW BRUNSWICK

Project 730044

K.L. Currie and R.D. Nance[1]
Precambrian Geology Division

Currie, K.L. and Nance, R.D., A reconsideration of the Carboniferous rocks of Saint John, New Brunswick; in Current Research, Part A, Geological Survey of Canada, Paper 83-1A, p. 29-36, 1983.

Abstract

The Carboniferous Mispec Group consists of an alluvial fan redbed sequence of conglomerate, sheet-flood sandstones, and siltstone and shale (Balls Lake Formation) which grades laterally and vertically to grey, parallel-bedded, fluvial lithic arenite (Lancaster Formation). The Mispec Group was probably derived from a northwest-advancing thrust sheet, so that the fan deposits overlap and interdigitate with their distal fluvial deposits. The Mispec Group rests unconformably upon late Hadrynian volcano-sedimentary rocks of the Coldbrook Group (=West Beach Formation) which in Carboniferous time were weathered under arid conditions. The Mispec Group forms part of a large autochthonous terrane over-ridden in late Carboniferous time by a major thrust sheet advancing from the southeast and producing cleavage and flattening (S_{1C}) in the rocks beneath, as well as rare and local F_{1C} folds. At some point in its advance, the motion changed to eastward underthrusting, developing west-dipping cleavage (S_{2C}) and folds (F_{2C}). The folded sole thrust is exposed at Cape Spencer and other places, but it remains uncertain whether remnants of the overriding sheet are preserved, or only portions of an imbricate zone.

Introduction

Although many geologists have studied the rocks of the Saint John area during the past 150 years, no consensus exists on the stratigraphy or significance of a crescent-shaped belt of rocks extending along the shore of the Bay of Fundy (Fig. 4.1) and including the celebrated "Fern Ledges" of West Saint John. This lithologically diverse belt locally contains abundant fossils of Westphalian age, but parts of it have been repeatedly suggested to be of older, even Precambrian, age. Recently Rast and Grant (1973) and Rast et al. (1975) suggested the belt to form a different tectonic terrane from the rocks to the west, separated by a major tectonic break, the "Variscan front". A multidisciplinary study of the terrane to the west of this break (Currie et al., 1981) proved able to unravel many of the complexities of these rocks. We have therefore applied the same methods to the area east of the break.

Stratigraphy

The rocks in question fall naturally into three divisions, namely the plant-bearing grey lithic arenites of the Lancaster Formation, a unit of redbeds, particularly polymict conglomerate with lesser siltstone and sandstone (Balls Lake Formation), and a mainly volcanic unit (West Beach Formation), which can be further subdivided as shown below. For more than a century these units have been grouped together as the Mispec (or Mispek) Series or Group, but complete disagreement reigns over the relative order of the units. Hayes and Howell (1937) believed the Lancaster (their Little River series) to be the oldest, and the West Beach the youngest. Alcock (1938) claimed the Balls Lake to be the oldest and the Lancaster the youngest. Since he also found plant remains in his Balls Lake, he concluded that the whole series must be of Carboniferous age. McCutcheon (in Ruitenberg et al., 1979) claimed to agree with Alcock, but achieved agreement only by ignoring Alcock's definition of the Balls Lake Formation as mainly composed of red conglomerate and sandstone. When this definition is applied to McCutcheon's measured section, the order he observed becomes, in ascending order, West Beach-Balls Lake-Lancaster, or the exact reverse of Hayes and Howell.

We believe that the term Mispec Group has had a mischievous effect on attempts to determine the stratigraphy and structure. As will become evident, all three units cannot belong to a single stratigraphic group, and the traditional three-fold division is insufficient to describe the geology. We shall first present our broad conclusions on the stratigraphy, and then the detailed evidence supporting them.

The West Beach Formation, consisting of intercalated acid and mafic volcanic fragments, rhyolitic flows and minor redbeds, capped by basalt flows, is unconformably overlain by red conglomerates of the Balls Lake Formation, which grade laterally and by digitation into the Lancaster Formation grey arenites. Only the age of the Lancaster Formation is known from fossil evidence and all published fossil localities lie within this formation. West Beach Formation is a junior synonym of Coldbrook Group, and presumably has a similar Late Precambrian age. The "granite" bodies thought previously to intrude the West Beach Formation between Cape Spencer and Black River form klippen of a thrust sheet, or possibly an imbricate zone, formerly overlying the sedimentary and volcanic terrane.

The confusion over stratigraphy evident in the older literature arose mainly from three causes; incorrect grouping of Balls Lake and Lancaster strata, confusion of red clastic sediments of the Balls Lake with red, mainly tuffaceous, strata of the West Beach, and confusion of intensely sheared and deformed rocks whose correct attribution can only be ascertained by tracing them into less deformed material. Our basis for the drastic reorganization of the stratigraphy is summarized in the following description of units.

West Beach Formation (unit H_C)

Alcock (1938) coined the name West Beach Formation for a narrow belt of rocks along the seashore from Black River to West Saint John in which volcanic rocks are dominant. He also considered sedimentary and intrusive rocks to occur within this formation. Alcock defined no type section for the formation, and West Beach itself is a poor place to examine it due to the presence of complex fault slivers and intense deformation. A fine section of the formation can be examined on Taylor Island in the southern outskirts of Saint John. Together with a nearby section in

[1] Department of Geology, Ohio University, Athens, Ohio 45701

West Saint John, the rocks here exhibit the range and variability of the formation. The Taylor Island section, about 1100 m in total, consists of alternating sequences of mainly fragmental or tuffaceous acid and mafic volcanic rocks. The mafic sequences (unit H_{cb}) varying from 30 to 100 m in thickness, consist of thick, homogeneous units of tuff, fine to coarse pyroclastics, agglomerate and minor flows. These sequences have greenish black fresh surfaces and pale apple-green weathered surfaces. The acid parts of the formation (unit H_{ca}) consist of red lithic crystal tuffs, red flow-banded rhyolite, and interbedded red to maroon siltstone and sandstone. Individual beds rarely exceed 5 cm in thickness, although the aggregate thickness of the red sequences may exceed 100 m. Some of the red sequences contain thin conglomerate horizons with red siltstone 'rip-ups', rhyolite and quartz pebbles. Such conglomerates must be distinguished from the thicker polymict conglomerates of the overlying Balls Lake Formation. Redbeds of the West Beach Formation exhibit a variety of preserved sedimentary structures, including large rotated or slumped blocks, presumably resulting from penecontemporaneous volcanic earthquakes. The Taylor Island section clearly shows that the redbeds form large lenses within an enveloping more mafic, darker matrix.

The upper part of the West Beach Formation consists principally of basalt flows and associated gabbroic rocks (unit H_{cg}). Hayes and Howell (1937) distinguished this unit as the Courtenay Bay Formation. Basalt flows occur throughout the volcanic sequence, but are markedly more abundant toward the top. Many of the flows are distinctive amygdaloidal varieties and readily traceable. Pillows and pillow breccia occur locally, as on Victoria Street in West Saint John. Gabbroic rocks with grain size up to 2 mm are intimately associated with the basalts, to which they grade by appearance of amygdales and fining of grain. The basaltic rocks can be readily recognized in outcrop by the persistent appearance of coarse epidote in a characteristic pattern of green veins and blotches.

In West Saint John, the West Beach Formation appears relatively undeformed in most outcrops, although alteration may be strong. East of Saint John some outcrops have been reduced to schists. Acid schists can commonly be recognized by colour and texture, even where highly deformed, but the distinction between intermediate to mafic volcanic schists and schists of sedimentary derivation tends to be difficult, and locally impossible.

The base of the West Beach Formation has nowhere been observed, and the rocks underlying it can be identified only by inference. We believe that the carbonates of the Green Head Group south of Taylor Island underlie the West Beach Formation on Lorneville Point, presumably with some minor relative movement on the contact as is observed on virtually all stratigraphic contacts in the Saint John region. The top of West Beach Formation can be observed west of the mapped area on the road to Chance Harbour, as documented by McCutcheon (in Ruitenberg et al., 1979). At this locality the top of the West Beach is much reddened, and overlain by about a metre of red siltstone containing pale grey lenticular to pipe-like masses of fine grained carbonate (caliche horizon). This material is abruptly truncated upward by very coarse conglomerate of the Balls Lake Formation which contains boulders up to 30 cm across of the underlying basalt, rhyolite and siltstone. We interpret this sequence to be a regolith developed in Carboniferous time on the West Beach, overlain by alluvial fan deposits of the Balls Lake. A similar, but intensely sheared, succession of lithologies can be observed on the sea cliff at Ploughshare Rock.

The presence of pillows and extensive tuff layers suggests that much, if not all, of the West Beach Formation formed underwater. Strong et al. (1979) have investigated the geochemistry of the upper basaltic unit of the West Beach Formation, and shown it to be unequivocally calc-alkaline. They also showed that the rocks have been significantly metamorphosed to prehnite-pumpellyite grade. They noted that these relations seemed anomalous in strata supposedly interbedded with unmetamorphosed, plant-bearing redbeds. The obvious solution to this difficulty, namely that the West Beach Formation is not Carboniferous, but Precambrian in age and correlative to the Coldbrook Group, was pointed out more than 100 years ago by T. Sterry Hunt, quoted but brusquely dismissed by Alcock (1938). However we have been able to match the West Beach Formation unit by unit with the undisputed Coldbrook Group near Garnett Settlement, including such distinctive units as the vesicular basalts and red lithic crystal tuffs. We have further found the West Beach Formation appears structurally in the correct position and orientation for the Coldbrook Group, including the internal stratigraphy noted above. Finally, we note that the chemical analyses of the basaltic parts of the formation, as reported by Strong et al. (1979) agree tolerably well with the basaltic parts of the Coldbrook Group as reported by Ruitenberg et al. (1979). Clearly it would be desirable to confirm this correlation by isotopic age dating, and we hope to do so in future. Nevertheless, we believe the field evidence is sufficiently strong to establish the West Beach Formation as a junior, hence redundant, synonym of Coldbrook Group.

Balls Lake Formation (unit MP_{bl})

Hayes and Howell (1937) introduced the name Balls Lake Series as a synonym for their Little River Series, in which they included the "Fern Ledges". Alcock (1938) put the "Fern Ledges" in his Lancaster Formation along with most of Hayes and Howell's Little River Series. However he reserved the name Balls Lake Formation for the red, coarsely clastic rocks extending along the sea coast from Cranberry Point to Mispec Bay. Unfortunately he made no distinction between these red clastic sedimentary units and the red volcanogenic units of the West Beach Formation. We follow Alcock's definition, but restrict the Balls Lake Formation to the red, upward-fining, clastic sedimentary rocks. Typically the formation consists of red, polymict conglomerate fining upward to siltstone or shale. Where little deformed, crossbeds, channelling and grading are abundant. A typical, though incomplete, section of the formation can be observed along the seacoast from Cranberry Point to Mispec Bay.

The lowest parts of the Balls Lake Formation consist predominantly of coarse conglomerate with boulders up to 30 cm across, derived mainly from the local West Beach Formation, and including such characteristic lithologies as amygdaloidal basalt and red lithic tuff. Higher in the section lenses of conglomerate are thinner, and the clasts smaller and rounded. In addition, the proportion of red siltstone increases, such that in the upper part of the formation it is the principal lithology, and contains some thin graded sand layers (sheetflood deposits) and small, wispy conglomerate lenticles. East of Brandy Brook the top of the formation contains about 10 m of red tuffaceous beds overlying a pale grey rhyolite flow or sill about 2 m thick.

The Balls Lake Formation rests unconformably on weathered West Beach Formation as previously described. The top of the formation is not as easy to define because the unmistakeable Balls Lake lithology appears to grade laterally and vertically to Lancaster Formation. Fine exposures of this transition can be examined east of Mispec Bay along the sea cliff and in large inland exposures. At the top of the typical red Balls Lake lithologies, lenses of pale grey, rather fine grained lithic arenite up to a metre thick appear, and gradually increase in proportion upward. We follow the suggestion of McCutcheon (in Ruitenberg et al., 1979) and

define the top of the Balls Lake Formation at the first occurrence of fine grained, grey lithic arenite. Following this definition, the rhyolite horizon previously noted lies within the Balls Lake Formation on Brandy Brook, but within the Lancaster Formation south of Mispec River. It is therefore probable that the boundary is time transgressive. We have measured no sections within the Balls Lake Formation, but the map pattern clearly shows that the thickness decreases westward from possibly 200 m near Ploughshare Rock to a few metres at most in downtown Saint John. We believe this variation to be primary, resulting from deposition on an alluvial fan whose provenance lay to the southeast.

Alcock (1938) showed two fossil localities within the Balls Lake Formation, one on East Branch Black River, and the other at Ploughshare Rock. Ruitenberg et al. (1979) reported a further locality on the Old Black River Road west of Mispec River. We find all of these localities to lie in grey lithic arenite typical of the Lancaster Formation. We have seen no organic remains within the Balls Lake Formation as defined above, nor do we consider such remains likely to be abundant in view of the coarsely clastic, oxidized nature of the formation. Since fossils are not present, the age of the formation is uncertain, but the nature of the contact with the fossiliferous Lancaster Formation strongly suggests that the Balls Lake Formation is of Carboniferous age, probably Namurian or Westphalian.

The Balls Lake Formation forms a distinctive lithology within the section where the polymict conglomerate predominates. However where red shale and siltstone predominate, the redbeds of the Balls Lake can be confused with those of the West Beach. The latter commonly have a more maroon shade than the former, the proportion of siltstone is higher, volcanic detritus may be recognizable, and crystal tuff or flow-banded rhyolite is commonly present in extensive outcrops. We found these criteria to successfully distinguish the two formations, except for small isolated outcrops of red siltstone, which in some cases cannot be assigned except by their map pattern.

Lancaster Formation (unit P_l)

Alcock (1938) introduced the term Lancaster Formation for the fine to medium-grained grey lithic arenite comprising the celebrated "Fern Ledges" of West Saint John (formerly Lancaster). Alcock considered this unit to include the strata at the mouth of Little River (the Little River Series of Hayes and Howell, 1937), as well as rocks farther northeast along Little River, and a miscellaneous group of red sandstones and conglomerates lying east of Emerson Creek. On the basis of material at Duck Cove (the Fern Ledges), and excellent exposures at the foot of Sydney Street in downtown Saint John, we consider the Lancaster Formation to comprise well-sorted, pale to dark grey lithic arenite, locally grading to coarse sandstone or pebble conglomerate. The formation consistently contains red sandstone or pebble conglomerate layers up to a metre thick, but they do not comprise more than 5-10 per cent of the section in typical exposures. Beds of black shale or siltstone up to 60 cm thick occur locally, and consistently contain poorly preserved plant remains. According to this definition the Lancaster Formation is much more widespread in the Little River-Black River area than shown by either Alcock (1938) or Hayes and Howell (1937). Our view of the distribution of the Lancaster Formation is one of our major differences with previous mapping. However in our view, the strata east of Emerson Creek do not belong to the Lancaster Formation, since they are mainly composed of red conglomerate, red to green sandstone, and red siltstone. Beds of Lancaster type occur at the base of the section along Emerson Creek. We therefore consider this section to be slightly younger than the Lancaster Formation, in accordance with the views of van de Poll, as quoted by Ruitenberg et al. (1979). The fossil evidence shows the Lancaster Formation to be of Westphalian age (Hayes and Howell, 1937), at least at Duck Cove.

The contact relations of the Lancaster and Balls Lake formations were discussed above. The Lancaster Formation grades rather abruptly into younger conglomerates and brightly coloured sandstones on the east side of Emerson Creek. At Duck Cove the Lancaster appears to rest directly and unconformably on basalts of the West Beach Formation (upright east-facing Lancaster on inverted west-facing basalt). The section on upper Little River may rest unconformably on the Ordovician Saint John Group, although a sufficient interval is covered that a thin Balls Lake section could be present. We have nowhere seen a complete section of the Lancaster Formation, but from the map pattern we estimate that its maximum thickness probably exceeds 400 m.

The Lancaster Formation is a notably hard and indurated sandstone. Locally quartz veins up to 3 m across are abundant, but as noted by Alcock (1938), such veins are less common than in underlying formations.

Upper Carboniferous (unit P_u)

East of Emerson Creek a series of red to brown conglomerates, red and green sandstones and rare schistose, organic-rich, black shales overlie a thin sequence of Lancaster-like grey sandstone. These rocks are less indurated than the Lancaster, exhibit little or no penetrative deformation, and appear to be slightly younger (Ruitenberg et al., 1979). The strata appear to occur in fault-bounded slivers with little relation to the geology west of Emerson Creek. We have not studied these strata in detail, and consider them to belong to a different structural setting or level than the older rocks.

Triassic (unit T_q)

Following Alcock (1938), we consider an area of coarse, poorly indurated, uncleaved conglomerate lying east of the mouth of Little River to be correlative to the Triassic Quaco Formation. Unlike the southeasterly derived Balls Lake Formation, these conglomerates contain northwesterly derived boulders (Green Head Group carbonates), as well as various granites and volcanics. Although Alcock's suggestion of a Triassic age is plausible, it remains speculative in the absence of fossil evidence.

Granitoid Rocks (unit C_t)

Previous studies of this terrane have repeatedly drawn attention to "granites" said to intrude the Carboniferous sedimentary rocks. These en echelon bodies occur in a narrow belt extending from Cape Spencer across the mouth of Black River. According to our mapping the granites all occur within the West Beach Formation, with none emplaced in the demonstrably Carboniferous rocks. Further, completely exposed contacts of the bodies at Cape Spencer and the mouth of Black River are not intrusive, but rather show the granites have been thrust northwest over the West Beach Formation. Just west of Cape Spencer a small granitic body outcrops at the top of the sea cliff, but not at its base, being truncated along a folded V-shaped tectonic surface plunging into the cliff. We argue below that all the en echelon granite bodies represent synclinal keels of this kind in a single folded thrust sheet emplaced above the West Beach Formation.

The granitic rocks vary in outcrop from intensely shattered, but still igneous-textured, material, to barely recognizable muscovite (phengite) schists. Commonly the

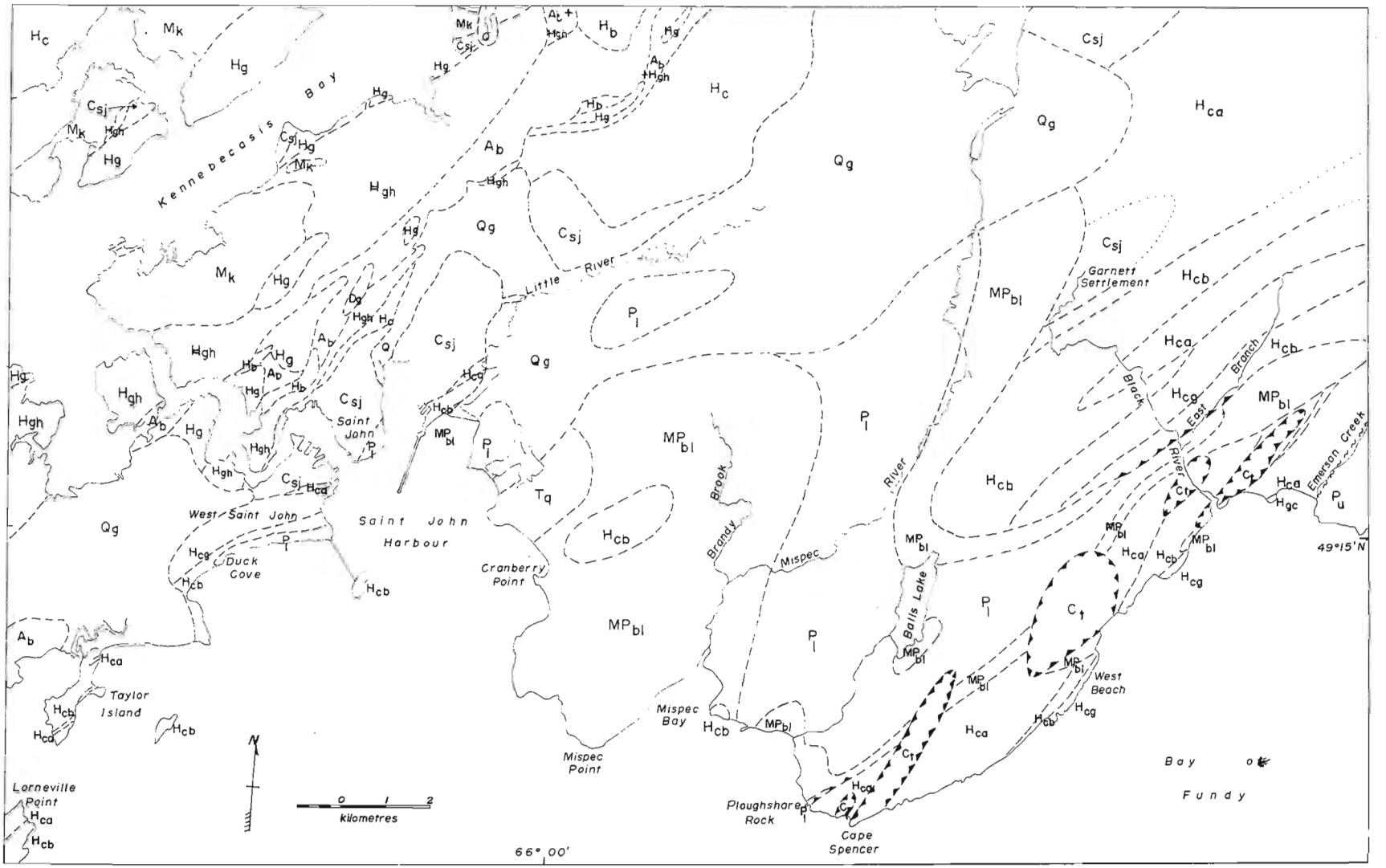

Figure 4.1. *Preliminary geological map of the Saint John region, New Brunswick (Geology between Little River and Kennebecasis Bay after Currie et al., 1981).*

LEGEND

Quaternary

Q_g — gravel, sand, stratified sand, till
--- unconformity ---

Triassic (?)

T_q — red to brown coarse conglomerate with marble boulders; minor sandstone
--- unconformity ---

Carboniferous

P_u — red sandstone and conglomerate, minor coaly beds and siltstone.
Grades to P_l at base
--- relations uncertain ---

C_t — allochthonous thrust slices bounded beneath by thrust faults.
Mainly shattered to sheared granodiorite to quartz diorite and granitic schist, possibly equivalent to H_g, minor limestone; thin conglomerate slices, probably equivalent to MP_{bl}
--- fault contact ---

P_l — LANCASTER FORMATION: grey lithic arenite, minor quartz pebble conglomerate, red sandstone and shale
--- gradational contact ---

MP_{bl} — BALLS LAKE FORMATION: red polymict conglomerate, red siltstone and shale; minor red to pink sandstone; no marble boulders
--- relations uncertain ---

M_k — KENNEBECASIS FORMATION: red to chocolate conglomerate, minor sandstone; typically rich in marble boulders
--- unconformity ---

Devonian

D_g — Hornblende leucogranite, massive pink granite with large square quartz
--- intrusive contact ---

Cambrian and Ordovician

C_{sj} — SAINT JOHN GROUP: Minor basal conglomerate, orthoquartzite, greenish grey sandstone and greywacke, black shale, quartz-rich siltstone
--- unconformity or disconformity ---

Hadrynian

H_c — COLDBROOK GROUP: (a) acid tuff, crystal tuff, agglomerate, flow-banded rhyolite; minor red shale and siltstone, conglomerate; (b) greenish-black tuff, lapilli tuff, agglomerate; minor intermediate to mafic flows; (g) basalt flows, amygdaloidal basalt, pillow basalt, gabbro; All units moderately to strongly epidotized.
--- unconformity, locally intrusive contact ---

H_g — granitoid plutonic rocks; biotite-hornblende quartz diorite to granodiorite, minor epidote alaskite; migmatite of H_g and H_b
--- intrusive contact ---

H_b — gabbro, diorite, hornblendite; altered mafic rocks and amphibolite, mafic rocks with alkali feldspar megacrysts; dykes and dyke complexes
--- intrusive contact ---

Helikian (?)

H_{gh} — GREEN HEAD GROUP: grey-blue to buff calcite and dolomite marble, fine quartzite, rusty black siltstone and semi-pelitic schist
--- unconformity ---

Aphebian (?)

A_b — BROOKVILLE GNEISS: mesocratic quartz-feldspar-hornblende-biotite gneiss with amphibolite lits; metasomatized equivalents of A_b; minor gneissic biotite leucogranite

geological contact, approximate

high angle fault, approximate

thrust fault, hachures on thrust plate

Geology by K.L. Currie 1980, 1982, R.D. Nance 1980, 1982, R.K. Pickerill 1980, G.E. Pajari 1980

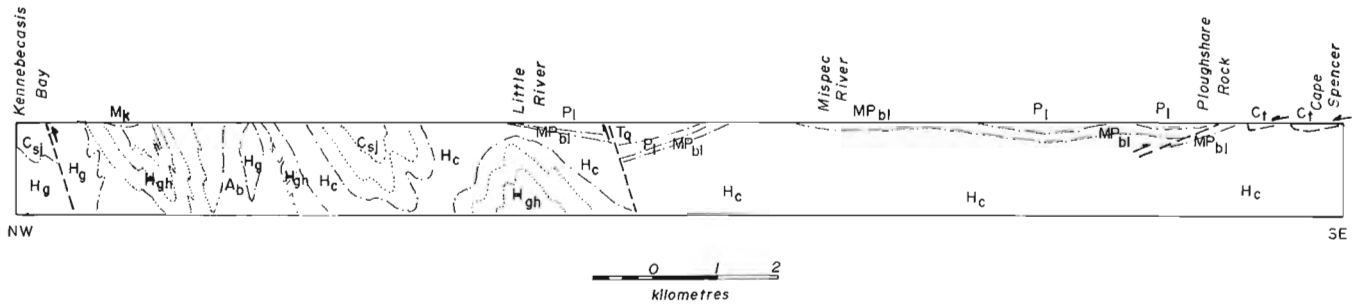

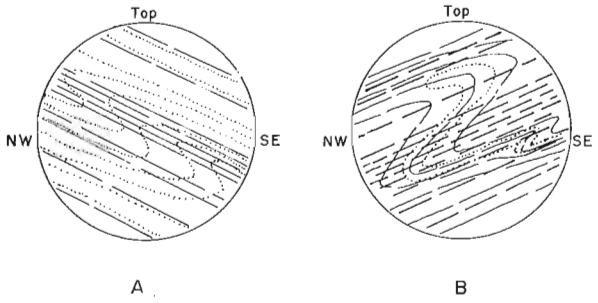

Figure 4.2

Structure cartoon from Kennebecasis Bay to Cape Spencer. (No vertical exaggeration). The structure of the Coldbrook Group beneath the Mispec Group is not well known, but is probably dominated by steeply dipping, near isoclinal folds similar to those in pre-Carboniferous rocks west of Little River.

Inset A shows small structure where only S_{1c} is present. The cleavage (broken lines) is commonly subparallel to bedding (dotted lines), but locally axial planar to isoclinal folds in the bedding.

Inset B shows the structure where both S_{1c} and S_{2c} are developed. S_{2c} is axial planar to tight to isoclinal folds with S_{1c} as folded element, and where bedding is still recognizable it has been refolded.

Note that both insets A and B depict minor structures which do not significantly affect the broad, open warps in the Mispec Group or the older folds in the Coldbrook Group unconformably beneath. Letter symbols same as Figure 4.1.

schists form an envelope around less deformed material. On the cliffs at Cape Spencer substantial compositional variation can be seen ranging from rather calcium-rich, strongly epidotized rock to leucogranite, together with a network of pegmatitic schlieren and quartz veins. This exposure appears to have formed part of a major intermediate to deep-seated pluton. No features typical of high-level granites (granophyric texture, rhyolitic or porphyritic patches, miarolitic cavities) were observed in any of the bodies. The granitoid rocks are variably, but generally strongly, altered. Plagioclase has been converted to epidote, or a peculiar purplish mineral, possibly thompsonite. Potash feldspar is partially converted to white mica, and all mafic minerals have been converted to chlorite, uralite and epidote. Hand specimen examination suggests that few of the rocks contained abundant potash feldspar. The variation was probably from quartz diorite to granodiorite, with some minor amounts of granitic material. Some of the more plagioclase-rich parts resemble inclusions found within basalts of the West Beach Formation.

At Cape Spencer the granitoid rocks contain inclusions of a quartz diorite reminiscent of the Mayflower Lake pluton (Currie et al., 1981) and a pelitic sediment at relatively high metamorphic grade, possibly derived from the Green Head Group. This locality also exhibits dykes of boundinaged but not penetratively deformed rhyolite very similar to the rhyolite within the Balls Lake Formation. The body at the mouth of Black River contains dykes identical in appearance and metamorphic grade to the nearby basalts of the West Beach Formation. These dykes show much less penetrative deformation than their host. Such relations strongly suggest that the granitoid rocks possess a penetrative fabric older than that imposed by their Carboniferous emplacement, and possibly older than the West Beach Formation. We consider that the texture and composition of the bodies demonstrate a deep-seated origin. Their contact relations and their high degree of deformation suggest that they may be older, not younger, than the other consolidated rocks of this region. We think it possible that they formed part of the basement to the West Beach Formation, perhaps as a major Hadrynian pluton of the type discussed by Currie et al. (1981). They may alternatively be completely foreign to this region, and form part of a far-travelled allochthon. In any event they are clearly not sills within the West Beach Formation as was previously supposed.

Quaternary (unit Q_g)

A major difficulty in mapping the bedrock arises from very widespread and thick gravel deposits of Quaternary age. Not only do these deposits hide the bedrock, but due to the local presence of very large blocks, they can give an erroneous impression of outcrop where none exists. We believe that some of the key outcrops of Coldbrook Group mapped by Alcock (1938) were large glacial erratics.

Structure

Accurate structural mapping depends on precise stratigraphy, which for the Carboniferous rocks cannot yet be considered firmly established. Further, determination of structure becomes impossible in regions of little or no outcrop, such as cross the mapped region. In these circumstances we have elected to consider the broad structures defined by regional mapping, and the detailed structures observed in particular areas of complete outcrop. We believe this procedure to give a reliable representation of the structural style, although it doubtless overlooks some local, poorly-exposed complexities. We have attempted to portray this overall picture in the cross-sectional cartoon of Figure 4.2.

The geological map (Fig. 4.1) clearly shows that the most prominent structures within the Carboniferous terrane are a series of open, northeast-trending domes and basins. The limb dips of these structures vary from 10 to 40 degrees, although dips as steep as 60 degrees occur locally. Plunges generally range from 5 to 30 degrees, with a few local plunges of minor structures as steep as 40 degrees. At the present exposure level the domes and basins mainly involve the Balls Lake and Lancaster formations, but the dome east of Little River brings up West Beach Formation in the core. The reappearance of West Beach Formation at Ploughshare Rock can likewise be attributed to gentle folding, although complicated by faulting in this instance.

Such structures are insufficient to account for observed minor structures. The most obvious is a widespread, approximately bedding-parallel cleavage (S_{1C}) which appears to intensify to the southeast from barely perceptible at Little River to very strong at Cape Spencer. Conglomerate pebbles are variously flattened but rarely lineated in this cleavage. In extreme cases, as at Ploughsare Rock, the diameter to thickness ratio may reach 20:1. The cleavage is locally observed to be axial planar to mesoscopic, west-verging recumbent isoclines (F_{1C}), a splendid example of which is exposed at the mouth of Little River. As first pointed out by Rast and Grant (1973), such structures are compatible with westward overthrusting of material onto the Carboniferous terrane. The cleavage can then be ascribed to loading of the terrane by the now almost entirely eroded allochthon. However this model does not account for younger minor structures. Along the seacoast from Little River to Mispec Bay a second cleavage (S_{2C}) locally cuts S_{1C} and parallels the axial surfaces of folds in S_{1C} (F_{2C}). To the south of Mispec Bay the S_{2C} cleavage gradually intensifies, and the F_{2C} folds become recumbent isoclines that verge to the southeast. South of Ploughshare Rock the second cleavage partially to completely overprints the first. At Ploughshare Rock the contact of the Balls Lake and West Beach formations is parallel to this cleavage, although there is little reason to suspect substantial movement along it. The attitude of the S_{2C} cleavage remains regular, striking 045 degrees and dipping 035 degrees to the northwest, except where it is refracted locally in coarse clastic beds. Perhaps the most spectacular example of interplay betweeen S_{1C} and S_{2C} can be seen at Cape Spencer. The lower bounding surface of the granite exposed here is an S_{1C} surface along which the granite was thrust to the west. However both S_{1C} and the thrust surface have been folded about a mesoscopic F_{2C} structure with strong S_{2C} axial planar cleavage. A few hundred metres to the west the thrust is brought back to the topographic surface by another F_{2C} fold which produces a small keel of granite on the sea cliff.

The broad domes and basins which dominate the map pattern must separate the two periods of mesoscopic folding, because they deform the S_{1C} cleavage, but not S_{2C}, and do not themselves possess an axial plane cleavage. The thrust fault at Cape Spencer must be a major structure, since it contains imbricate slices in the form of slivers of limestone east of Black River, and slivers of conglomerate (probably Balls Lake) and rhyolite to the west of Black River. On the other hand we see no necessity whatever for significant faulting between the western edge of the former "Mispec Group" (that is our Mispec Group plus the West Beach Formation) and rocks to the west (the 'Variscan front' of Rast et al., 1975). North of the dry dock in East Saint John the contact between the West Beach Formation and the Saint John Group can be fixed stratigraphically within less than 3 m. Both sequences young to the west and there is no unusual deformation on either side of the contact. On Minette Street in West Saint John the contact is covered, but both sequences young to the west, and deformation of the West Beach redbeds is very local, since they are stratigraphically underlain within less than 10 m by essentially underformed pillow lavas. We believe these relations are consistent with an unconformity or disconformity and support our correlation of the West Beach Formation and Coldbrook Group. Furthermore, at Duck Cove the contact between the Lancaster Formation and West Beach Formation can be fixed within 2 m, and the rocks on either side do not appear strongly deformed. Lancaster strata at Duck Cove, Sydney Street and elsewhere consistently young east, implying a change in facing direction across the contact that can only be accounted for by a further unconformity. At none of these localities does the degree and scale of deformation compare to those at Cape Spencer or other exposures of the sole thrust. Rather contact relations are completely compatible with minor movements along unconformities.

We have observed high angle faults within the Carboniferous section along the seacoast. In general these faults strike northeast and tend to bring the southeast side up. They appear to be very late, essentially brittle structures. Similar faults occur at least as far west as Kennebecasis Bay (Currie et al., 1981). We have also observed minor structures within the West Beach Formation and the granites which appear to be older than those deforming the Carboniferous rocks. We have made no detailed study of these structures, but they may be related to the structural history of the older rocks of this region (see Nance, 1982).

Discussion

According to our mapping the West Beach Formation is correlative to the Coldbrook Group, and hence virtually all of the area mapped by us is autochthonous or parautochthonous. The Carboniferous section was thus deposited on a basement which had been previously sutured to continental North America. However the material comprising the sedimentary section came from the southeast, from rocks which were, in part, unrelated to those to the northwest. The character of the Balls Lake Formation (red colour, coarse conglomerate, thin graded sand sheets, basal caliche horizon) implies that it formed as mid and distal alluvial fan deposits, with the characteristic grey, parallel-bedded arenites of the Lancaster Formation forming the distal fluvial deposits. If the fan was fed, as seems likely, from advancing thrust sheets, the detailed relations between the Balls Lake and Lancaster formations may be quite complex, since Balls Lake lithologies would advance westward with the thrust sheets, overlapping older fluvial deposits at their foot. Such relations seem to be implied by local enclaves of Lancaster-type sandstone within conglomerate, as at Mispec Point, and the presence of Visean-Namurian spores in eastern Lancaster Formation on East Branch Black River (M.S. Barss, written communication to W.H. Poole, 1979) compared to the well established Westphalian age of the formation at Duck Cove. In any event, the present work makes it clear that the Mispec Group consists only of the Lancaster and Balls Lake formations, and that the West Beach Formation cannot be included. Since the Mispec Group is essentially autochthonous, all of the area from Kennebecasis Bay southeast to Black River must have formed a unified terrane in Carboniferous time, the older rocks of which had undergone a long complex history previously outlined by Currie et al. (1981). The area examined this year extends the previously noted tendency for the rocks to young away from a central crystalline core.

In late Carboniferous time this terrane was subjected to thrusting from the southeast which led to the emplacement of a large overthrust sheet, now almost entirely removed by erosion, whose former presence is clearly demonstrated by structural evidence. We are uncertain whether any remnants of the allochthon now remain. Possibly the granite bodies at

Cape Spencer may be remnants of the allochthon, but we note that they might equally be fragments of local basement. If the latter is the case, the observed bodies are large imbricate slices similar in character to the sedimentary slices observed around Black River. To the west of the mapped area, at the Coleson Cove generating plant, we observed a spectacular shuppen zone of imbricate slices, most of which are exotic to this region, and hence were presumably detached in some manner from the overthrust sheet.

We also draw attention to the similarity in style of deformation across the whole of the autochthonous terrane. The syncline preserving the Ordovician Saint John Group relates to Carboniferous folds in style and orientation. Northeast trending, high-angle reverse faults occur all the way from Cape Spencer to Kennebecasis Bay. We do not suggest that all of these structures originated in Carboniferous time, but we consider it probable that they were modified and/or intensified at this time. Consequently we would not know where to put a "front" of deformation within this area. If the most westerly related structure is chosen, it lies northwest of any ground examined by us. If the sole thrust is chosen, its trace runs from Cape Spencer to Coleson Cove, and lies mainly beneath the Bay of Fundy.

Finally we draw attention to the complete lack of metamorphism and plutonism associated with the deformation. We have found no dykes or plutons cutting the Balls Lake or Lancaster formations, and their metamorphic grade is negligible. Even most of the (probably Precambrian) West Beach Formation lies below greenschist grade (Strong et al., 1979). The deformation must either be of superficial "thin-skinned" type, or only the leading edge of a much larger block has been observed. The former alternative could be reconciled with a version of the local deformation model of Poole et al. (1970), while the latter would correspond to a modified version of the "Variscan front" model of Rast and Grant (1973). There seems to be no reason to limit this latter model to a metamorphic or orogenic event, since the docking of a 'suspect' terrane should serve equally well.

In either case we believe that the apparent reversal of transport directions betweeen S_{1C} and S_{2C}, first noted by Rast (Rast et al., 1975), does not require radical explanations. Westerly directed transport (overthrusting) took place on shear fractures dipping east. But development of one set of such fractures implies at least potential development of the complementary (west-dipping) set. Which set is actually used seems to be, in many cases, almost a matter of chance, involving very small energy differences (Hobbs et al., 1976, p. 325). Hence small changes, for example in the density of the rocks of the overthrust sheet, could make it energetically favourable to develop the complementary set of fractures leading to easterly directed transport (underthrusting) in the same stress field. This reversal leads to no space problems because the net effect is the lifting up of the overlying sheet whether overthrusting or underthrusting is considered.

Acknowledgments

Financial support for field work was provided to Nance by Ohio University grant OURC 9637, which is hereby gratefully acknowledged. We have also benefited from discussions with Saifullah Tanoli, Ishmael Patel and Ron Pickerill.

References

Alcock, F.J.
1938: Geology of the Saint John region, New Brunswick; Geological Survey of Canada, Memoir 216.

Currie, K.L., Nance, R.D., Pajari, G.E., Jr., and Pickerill, R.K.
1981: Some aspects of the pre-Carboniferous geology of Saint John, New Brunswick; in Current Research, Part A, Geological Survey of Canada, Paper 81-1A, p. 23-30.

Hayes, A.O. and Howell, B.F.
1937: Geology of Saint John, New Brunswick; Geological Society of America, Special Paper 5.

Hobbs, B.E., Means, W.D., and Williams, P.F.
1976: An outline of structural geology; John Wiley and Sons, New York, 571 p.

Nance, R.D.
1982: Structural reconnaissance of the Green Head Group, Saint John, New Brunswick; in Current Research, Part A, Geological Survey of Canada, Paper 82-1A, p. 37-43.

Poole, W.H., Sanford, B.V., Williams, H., and Kelley, D.G.
1970: Geology of southeastern Canada; Geological Survey of Canada, Economic Geology Report 1 (5th edition) p. 228-304.

Rast, N. and Grant, R.H.
1973: Transatlantic correlation of the Variscan-Appalachian orogeny; American Journal of Science, v. 273, p. 572-579.

Rast, N., Pajari, G., Grant, R., Wardle, R., O'Brien, B., and Patel, I.
1975: Geology of southwestern New Brunswick – Field Guide; Geological Society of America, Penrose Conference Field Guide.

Ruitenberg, A.A., Giles, R.S., Venugopal, D.V., Buttimer, S.M., McCuthcheon, S.R., and Chandra, J.
1979: Geology and mineral deposits, Caledonia area; New Brunswick Department of Natural Resources, Mineral Resources Branch Memoir 1.

Strong, D.F., Dickson, W.L., and Pickerill, R.K.
1979: Chemistry and prehnite-pumpellyite facies metamorphism of calc-alkaline Carboniferous volcanic rocks of southeastern New Brunswick; Canadian Journal of Earth Sciences, v. 16, p. 1071-1085.

5.

TRACE ELEMENT CONTENTS OF TILL AND GOSSANOUS MUD IN THE BAKER LAKE REGION, DISTRICT OF KEEWATIN

Project 800008

Mikkel Schau
Precambrian Geology Division

Schau, M., Trace element contents of till and gossanous mud in the Baker Lake region, District of Keewatin; in Current Research, Part A, Geological Survey of Canada, Paper 83-1A, p. 37-41, 1983.

Abstract

In the Baker Lake region, surficial materials contain characteristic trace element signatures which reflect the underlying bedrock units. Of particular interest are the elevated levels of lead associated with the underlying Ketyet River Group and of uranium similarly associated with late granites. This contrasts with the low trace element contents of Quaternary sediments overlying the Dubawnt Group.

Introduction

A preliminary study by Shilts and Cunningham (1977) indicated that the clay fraction of till in the area north of Baker Lake contained values of U and Mo, and other elements in excess of those reported for similar materials in the region south of Baker Lake by Klassen and Shilts (1977a). The results south of Baker Lake were surprising because the Dubawnt Group hosts many uranium showings (Miller, 1980). Shilts and Cunningham (1977) suggested three hypotheses to explain the anomalous values in the till north of Baker Lake. The uraniferous till may have resulted from:

1. Erosion of fluorite-bearing granites or syenites with elevated U, or
2. Erosion of unknown uranium-bearing beds in what they termed "Aphebian quartzites and related rocks", which now constitute the Archean Ketyet River Group (Schau et al., 1982), or
3. Enhanced cation exchange capacity due to a difference in clay minerals between tills in the Baker Lake region and the rest of the District of Keewatin. The authors favoured the second hypothesis, although they were unable to eliminate the other hypotheses, in part because their sample spacing was too large.

During the course of regional bedrock mapping (Heywood and Schau, 1981; Schau et al., 1982) samples of surficial materials were acquired to check the original findings of Shilts and Cunningham (1977). During the 1980 and 1981 summers some 165 samples were collected in NTS map area 56D (Fig. 5.1a). Their clay fractions were analyzed by Bondar-Clegg and Co. Ltd. for trace elements (Shilts, 1980).

Acknowledgments

I thank members of the Terrain Sciences Division for their extensive help in the analyzing, interpreting and presenting of this material.

Results

Table 5.1 presents the averages obtained for each element in till samples grouped according to underlying bedrock type, their grand mean values and the average for 17 gossans not included in the grand mean. A detailed map of sample locations and all chemical data are available in GSC Open File 883.

Inspection of Table 5.1 shows that till collected on the metasedimentary rocks of the Ketyet River Group has values of Cu, Pb, Fe above the grand mean values, whereas till collected on the sediments of the Dubawnt Group is consistently below the mean for all elements except Mn. Till collected on the late granites is higher in uranium than till on the other units and zinc is marginally higher in till on the gneisses. The data that yielded these results (Open File 883) have been analyzed by discriminant analysis. A set of functions has been derived based on a separation into the groups shown in Table 5.1, which successfully classify 55 per cent of the till samples correctly. This is compared with 16 per cent classification success if the procedure was random. Thus, one can conclude that the chemical composition of clays in the till does reflect the bedrock on which it resides.

Factor analysis of the data determined from the gossans yield three factors that account for 80 per cent of the variability (Fig. 5.2A). The most important factor shows a reciprocal relation between easily dissolved transition elements (Mn, Ni, Zn, Cr, Co, and Cu) and more insoluble Mo and As complexes. A second factor shows a reciprocal relationship between U and Fe which probably indicates that as the gossan was being oxidized, and iron being accumulated, U was being removed in solution. Gossans form when pyrite and related sulphides are weathered and the country rock is leached by the resulting acid, strongly oxidizing solutions. Such solutions could give rise to the relationships between elements shown by the factor analysis noted above. The third factor shows the concentration of Pb to be independent of other elements; however, silver is partly associated with each factor and the Mo-As part of factor 1.

Similarly, a factor analysis has been performed on the data set from the till (Fig. 5.2B). The first factor is again one based on the divalent elements (Mn, Ni, Zn, Co) and the second is one that includes As, Mo, and Ag. The third indicates that Cu and U are associated with Pb and Ag. These factors account for 62 per cent of the variability (Fig. 5.2B). The inverse relations noted in the gossans (i.e. Mn vs. Mo and Fe vs. U) are not as prominent in these samples, suggesting that solution and oxidation, as seen in the gossans, are not important in the till. Therefore, a conclusion from the numerical analysis above is that chemical modification in clays from the till has not been important. This would tend to suggest that hypothesis 3 of Shilts and Cunningham (1977) is not a likely explanation for the anomalous values.

The levels of Mo, Pb, and U in till are shown on Figure 5.1b,c,d along with the distribution of the rock units mentioned in Table 5.1, to show the close geographical relationships between the concentrations of the elements in till and the underlying bedrock type. The areas shown here are included in the regional Thelon River Anomaly (Shilts, 1980) and the values are higher than those usually

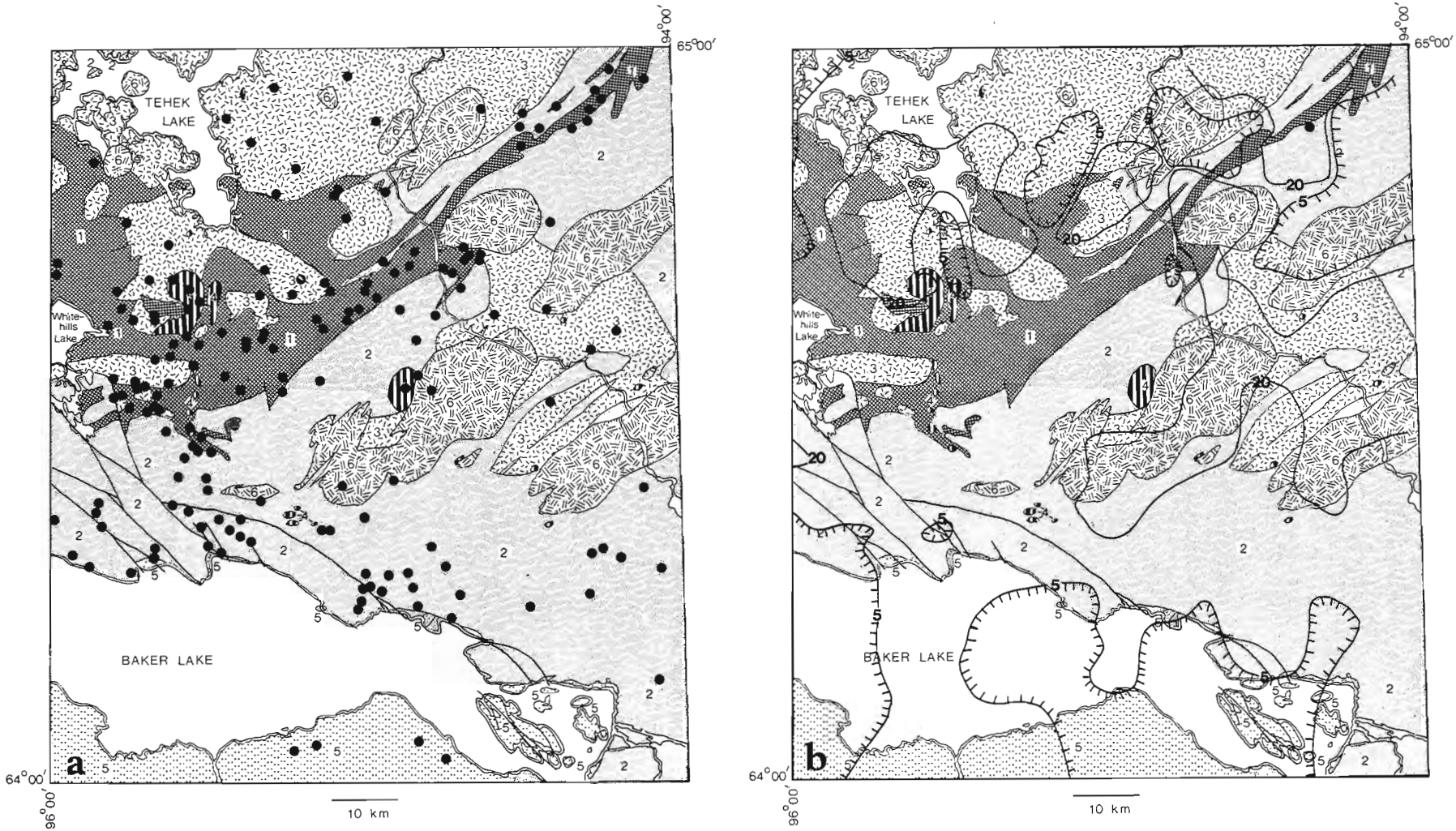

6 Late granite

5 Dubawnt Group

4 Hornblende syenite stocks

3 Tehek Plutonic Complex

2 Granitoid gneisses

1 Ketyet River Group

40 5 Contour lines with value in ppm; teeth point to region of lower value.

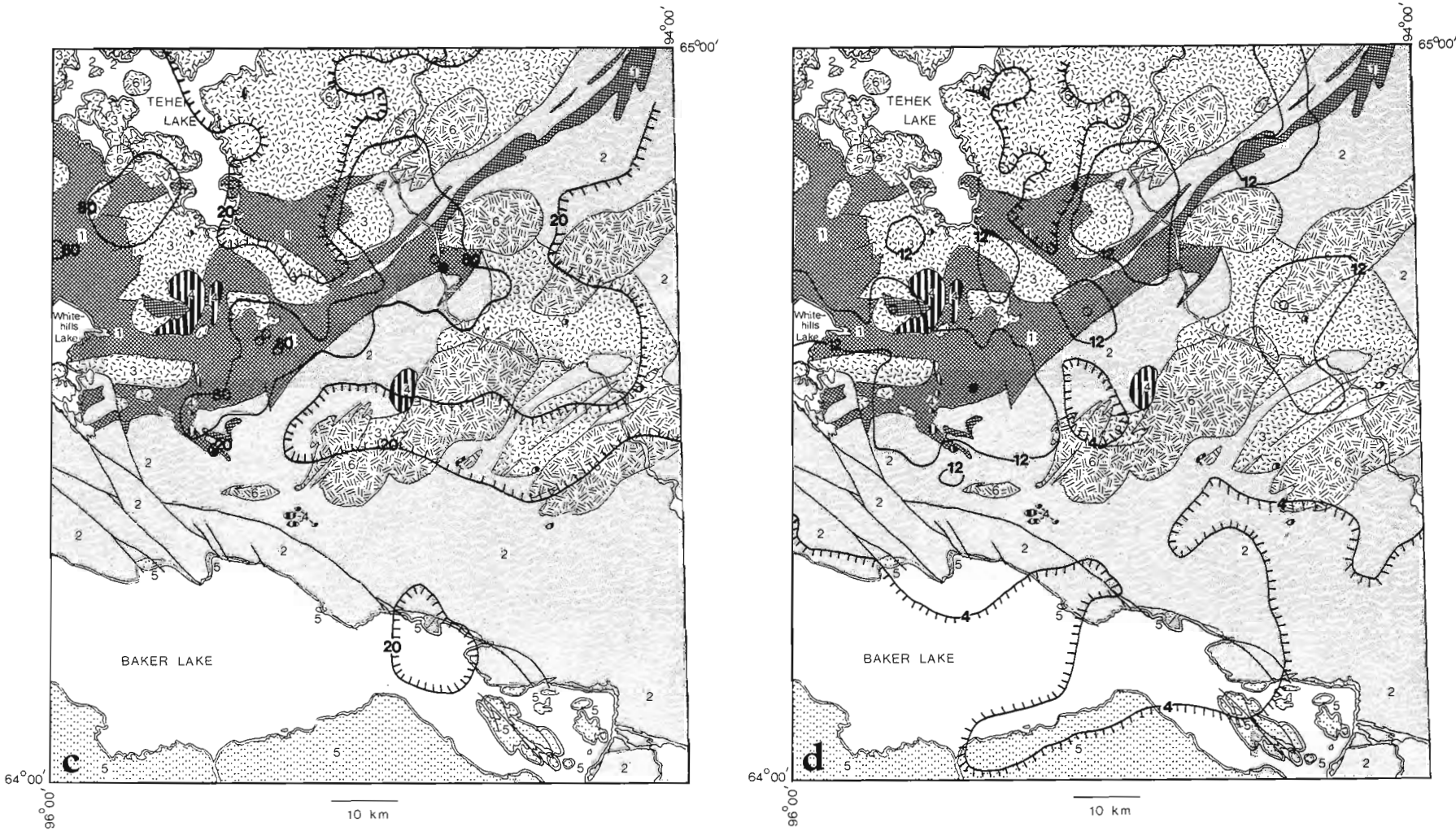

Figure 5.1. *Contour maps of elements in clays superposed on simplified map of geology of Baker Lake (modified after Schau et al., 1982). a. location and legend. b. U in clay. c. Pb in clay. d. Mo in clay. Open circles 2x or more highest contour level – solid dot highest value reported.*

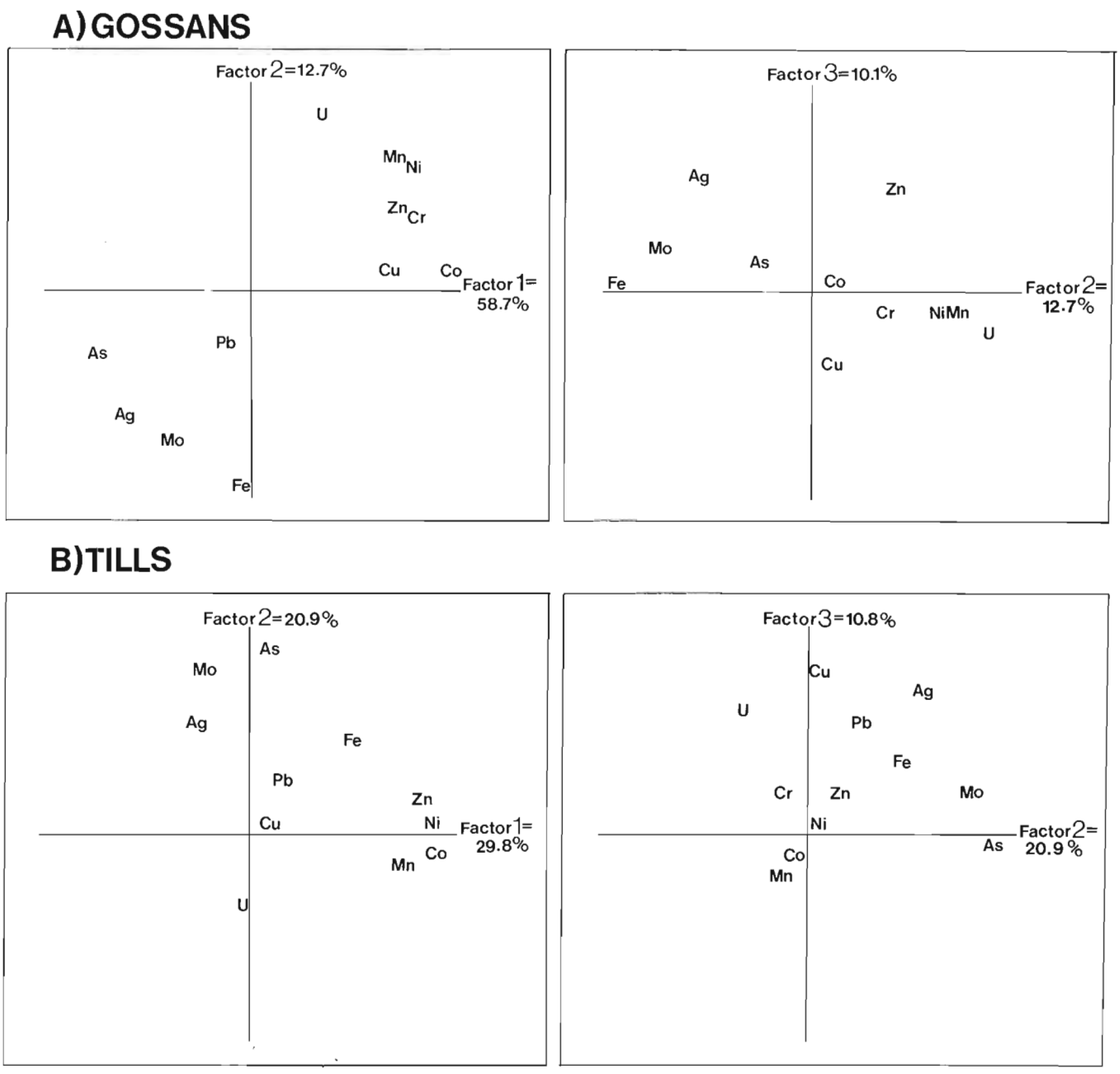

Figure 5.2. *Diagrams showing factors resulting from analysis of data from gossans (A) and till (B).*

encountered in the District of Keewatin (Klassen and Shilts, 1977b; Shilts, 1980; also see bottom line of Table 5.1). Variation within the map area shows that the elements from clay in till are associated with the underlying bedrock types. The U and Pb distribution (in clay, Fig. 5.1b,c) shows association with materials found over late granite and metasediments of Ketyet River Group respectively but uraninite deposits were located in Dubawnt Group. Galena showings, however, were found in the Ketyet River metasediments. Mo in clay (Fig. 5.1d) seems associated with deposits found over both the oldest metasediments and latest granites whereas molybdenite showings were found in granites of intermediate age.

Hypothesis 1 of Shilts and Cunningham (1977) linked U to fluorite-bearing granites and syenites in the area. Table 5.1 and Figure 5.1b suggest that the late granites (unit 6 on Fig. 5.1; or unit 11, Schau et al., 1982) may be uraniferous. These granites do not carry fluorite, as does one of the gneissic granitoid bodies (unit 2 on Fig. 5.1; or unit 6A, Schau et al., 1982) associated with gneiss, nor are they syenitic (as unit 9, Schau et al., 1982). The late granites are probably responsible for the enhanced airborne radiometric response shown on GSC map 35456G and ground-based gamma ray spectroscopy confirms the higher U values in this unit. U-bearing accessories such as sphene have been recognized to be radioactive (A. Miller, personal communication, 1982).

Table 5.1

Average values of elements in clay fraction from till classified by underlying bedrock

Bedrock	Cu	Pb	Zn	Co	Ni	U	Mo	Mn	Fe
Late granite (11); (N=6)	63	35	132	23	42	37	10	620	5.1
Dubawnt Group (10); (N=6)	35	27	98	17	34	5	3	860	3.3
Hornblende syenite (9); (N=6)	75	35	130	24	39	14	7	790	5.9
Tehek Plutonic Complex (4); (N=25)	80	40	123	22	45	16	9	663	5.4
Granitoid gneisses of various units (2,3,5,6,7); (N=63)	67	34	147	22	43	12	6	739	5.2
Ketyet River Group metasediments (1); (N=68)	131	88	135	21	42	14	17	525	6.6
Average (N=174)	93+106	56 ± 88	136 ± 42	21 ± 9	42 ± 19	14 ± 14	11 ± 21	647 ± 261	5.7 ± 1.9
Gossans (N=17) (Ag=5.1 ± 6.6 ppm) (As=23 ± 23 ppm)	111 ± 40	721 ± 894	84 ± 58	10 ± 9	16 ± 12	4 ± 3	80 ± 98	226 ± 137	21.1 ± 7.8
Regional value (Shilts, 1980)	45	10	150	ND*	ND	3	4	less than 900	less than 5

*No regional values currently available.

Hypothesis 2 of Shilts and Cunningham (1977) suggested unknown uraniferous beds may lie within the Ketyet River Group. Although none were found, there may, of course, be unknown beds rich in U present in the Ketyet, perhaps in the northeast corner (Fig. 5.1c), but the association of galena with the sulphidic and black (graphitic?) metasiltstones of the group would appear to be economically more interesting.

Conclusion

On the basis of a more detailed analysis of a larger data set than was available to Shilts and Cunningham (1977) it is concluded that the composition of the clay fraction of till in the Baker Lake area reflects the chemistry of underlying bedrock or mineralized zones within the bedrock. In particular, the elevated U values in the samples may be related to the minor accessory phases in late granites, and the Pb values to locally enriched layers within the metasediments of the Ketyet River Group.

References

Heywood, W.W. and Schau, M.
1981: Geology of Baker Lake region, District of Keewatin; in Current Research, Part A, Geological Survey of Canada, Paper 81-1A, p. 259-264.

Klassen, R.A. and Shilts, W.W.
1977a: Uranium exploration using till, District of Keewatin; in Report of Activities, Part A, Geological Survey of Canada, Paper 77-1A, p. 471-477.

1977b: Glacial dispersal of uranium in the District of Keewatin, Canada; in Prospecting in Areas of Glaciated Terrain; Institution of Mining and Metallurgy, London.

Miller, A.R.
1980: Uranium geology of the eastern Baker Lake Basin, District of Keewatin, Northwest Territories; Geological Survey of Canada, Bulletin 330, 63 p.

Schau, M., Tremblay, F., and Christopher, A.
1982: Geology of the Baker Lake map area, District of Keewatin: a progress report; in Current Research, Part A, Geological Survey of Canada, Paper 82-1A, p. 143-150.

Shilts, W.W.
1980: Geochemical profile of till from Longlac, Ontario to Somerset Island; Canadian Institute of Mining and Metallurgy, Bulletin, v. 77.

Shilts, W.W. and Cunningham, C.M.
1977: Anomalous uranium concentrations in till north of Baker Lake, District of Keewatin; in Report of Activities, Part B, Geological Survey of Canada, Paper 77-1B, p. 291-292.

6.

STRATIGRAPHY OF THE RAE GROUP, CORONATION GULF AREA, DISTRICTS OF MACKENZIE AND FRANKLIN

Project 770012

F.H.A. Campbell
Precambrian Geology Division

Campbell, F.H.A., Stratigraphy of the Rae Group, Coronation Gulf area, districts of Mackenzie and Franklin; in Current Research, Part A, Geological Survey of Canada, Paper 83-1A, p. 43-52, 1983.

Abstract

The Hadrynian Rae Group of the Coronation Gulf area consists predominantly of a shallow-water succession of fine grained sandstones, siltstones, dolomites and shales that accumulated in a broad, NNW-facing basin. Earlier correlations suggested that the group is equivalent to similar rocks in the Richardson Islands area of southern Victoria Island and in the Jameson Islands at the north end of Bathurst Inlet. The dolomite-dominated unit intercalated with the diabase sills, which makes up the bulk of the islands in Coronation Gulf, has been traced from the type area at the Rae River north of Coppermine to Victoria Island. A basal quartzite in the group, initially recognized in northern Bathurst Inlet has been traced westward into the lower part of the Rae Group, thus confirming the earlier interpretation of Rae sediments in the Bathurst Inlet region. Worm burrows, but more importantly trilobite tracks, in the uppermost two units of the initially-defined Rae Group demonstrate that these two units at least are Cambrian in age, and that a redefinition of the Rae Group is required.

Paleocurrent data from the underlying Husky Creek Formation of the Coppermine River Group suggest the formation was deposited in a generally southwest-trending valley during a pause(s) in extrusion of the partially coeval Copper Creek lavas.

Introduction

The Rae Group, which outcrops throughout the western Coronation Gulf area, was formally defined by Baragar and Donaldson (1973) who suggested that the group was deposited prior to 675 Ma, based on the age of the Coronation sills (Fahrig et al., 1971). Thorsteinsson and Tozer (1962) outlined areas of Precambrian rocks on southern Victoria Island and suggested that the islands comprising the Duke of York Archipelago were also all Precambrian. Later workers (Young, 1974, 1977; Young and Jefferson, 1975; Campbell, 1979; Dixon, 1979) suggested that the Rae in the type area is lithostratigraphically correlative with the rocks on and near southern Victoria Island and northern Bathurst Inlet (Fig. 6.1).

An examination of the Husky Creek Formation (Baragar and Donaldson, 1973) of the underlying Coppermine River Group was undertaken to determine the general sense of orientation of the basin or valley of sediment accumulation during the pause in the eruption of the Copper Creek Formation lavas.

Prior to identification of inarticulate brachiopods in the upper part of the Rae Group (Dixon, 1979), the units of Baragar and Donaldson (1973) had all been interpreted as Hadrynian. One of the main purposes of this examination was to confirm the age of the Paleozoic units previously assigned to the Rae, as well as to delineate any physical continuity, and thus correlation of various similar sequences in the Coronation Gulf region.

Husky Creek Formation

The Husky Creek Formation conformably overlies and is interstratified with lavas of the partially coeval Copper Creek Formation. The sediments of the Husky Creek are best exposed and occur primarily in the valley of the Coppermine River, but are discontinuously exposed in the flanking regions.

The Husky Creek sediments are predominantly medium- to coarse-grained immature red sandstones, siltstones, and minor mud-chip conglomerate. Ubiquitous trough or planar crossbedding, and desiccation features occur throughout.

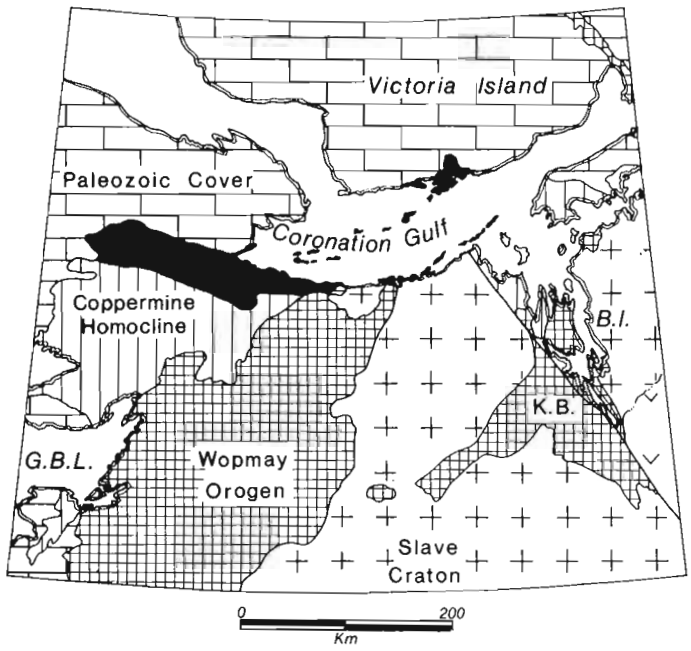

Figure 6.1. *Distribution of Rae Group sediments (black) in the northwestern part of the Canadian Shield. The Coppermine Homocline contains the Hornby Bay, Dismal Lakes and Coppermine River groups. K.B. is the designation for the Kilohigok Basin; B.I. is Bathurst Inlet and G.B.L. is Great Bear Lake.*

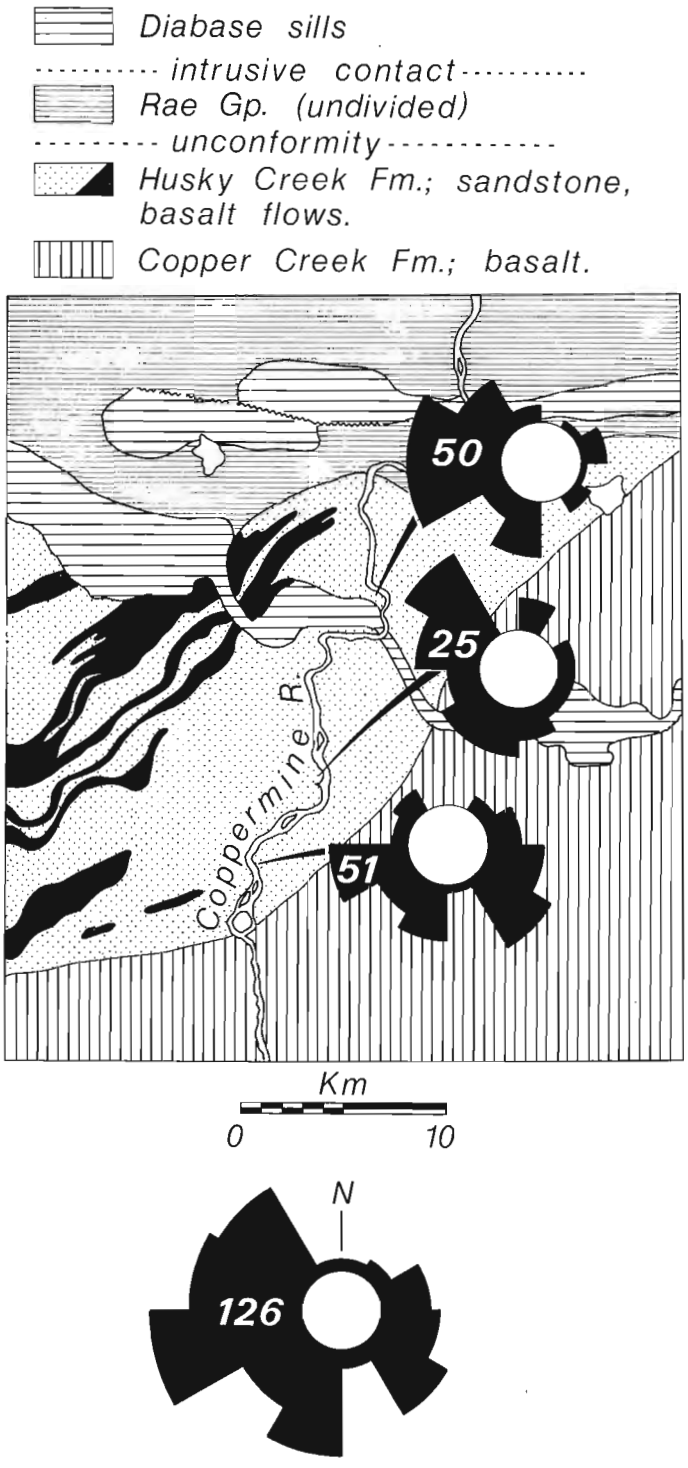

Figure 6.2. *Paleocurrent rose diagrams from the trough-crossbedded sandstones of the Husky Creek Formation. The numbers of readings is shown on the individual rose; the roses on the map are from individual outcrops, and the diameter of their centre circles is 20%. The diameter of the centre of the composite rose at the bottom of the figure is 10%. The outcrop locations on the Coppermine River are shown.*

Kerans (1982) documented evidence that the Muskox Intrusion and the Copper Creek lavas were nearly coeval. However, it is not possible, using presently available data, to determine the location of the vent(s) of lava extrusion. As the Husky Creek sediments were coeval with at least part of the lavas of the Copper Creek Formation, paleocurrent data in the sandstones may provide evidence of the orientation of the paleovalley in which these immature clastics were deposited. Crossbeds in the formation are polymodal (Fig. 6.2), but appear to have a predominantly southwesterly directed trend, with approximately 80 per cent of the cross-beds in the 150-330° range. The overall distribution, from an admittedly small sample, suggests that the Husky Creek sediments accumulated in a generally SW-trending valley, which was filled with volcaniclastic detritus derived from the flanking lavas and possibly associated pyroclastics. With stream/river transportation from the flanks into this valley, the variously directed contributing streams resulted in deposition of sands with multimodal crossbeds, which together show only a broad general trend to the southwest. Caution must be exercised, however, in over-interpreting these data, derived from a single "section" through the formation, as additional information from the formation margins to the east and west may provide contradictory interpretations.

Rae Group

The Rae Group is the youngest Precambrian succession in the region, and unconformably overlies rocks which range in age from Archean to Helikian (Fig. 6.1). From west to east, it rests progressively on Coppermine River Group sediments and volcanics, Dismal Lake Group sediments (both ca. 1200 Ma), Coronation Supergroup rocks (ca. 1860 Ma), metamorphosed Archean rocks (ca. 2500 Ma), and the Ekalulia, Parry Bay and Ellice formations in the Bathurst Inlet area (all ca. 1200 Ma). At all localities where it is exposed, the contact between the Rae Group and the underlying rocks is gently undulating, and a regolith is only locally preserved.

Following the informal designation of the uppermost two units of the initially defined Rae Group as Paleozoic, the various redefined units of Rae Group are described below in ascending stratigraphic order, following the original nomenclature of Baragar and Donaldson (1973).

Unit 19

This unit, as originally described by Baragar and Donaldson (1973) in the Coppermine River area, consists of "fine-grained greenish grey and greyish brown sandstone interbedded with grey to black shales". This description is valid for the westernmost part of the unit, but the basal part changes markedly to the east. Campbell (1979) described the succession of quartzites and siltstones on the Jameson Islands at the north end of Bathurst Inlet and suggested that these were the eastern equivalent of the Rae Group. During the course of mapping, equivalent rocks were traced laterally into unit 19 sensu stricto, with the quartzites pinching out approximately half-way between Port Epworth and Coppermine (Fig. 6.3).

A typical complete sequence of unit 19 in the eastern part of the Rae Group consists of, from the top to the base:

greenish-grey and grey fine grained sandstone, siltstone and shale, (90 + m);

buff, pink or grey weathering grey medium- to coarse-grained quartzite (5-20 + m);

massive, crossbedded, thick bedded, coarse grained, pebbly white quartzite and minor conglomerate (10-30 m);

a variously developed regolith, which ranges from white to pink to reddish, depending on the nature of the underlying material; where present, it is rarely more than 5 m thick.

The lower two quartzites are best developed and thickest in the eastern part of the area, and both pinch out to the west, where the lower part of the unit consists entirely of the typical fine grained sediments described by Baragar and Donaldson (1973).

Trough crossbeds are locally well developed in these quartzites and show a near unimodal transport to the west and west-northwest (Fig. 6.3). The beds in the basal white quartzite are typically thick (up to 1.5-2 m), massive, and contain few sedimentary structures other than large-scale crossbeds (up to 3 m wide). No fining-upward cycles were observed in the succession, and the entire lower part is remarkably devoid of fine grained detritus. In the eastern part of the region (Jameson Islands) cobbles to 5 cm of quartz and granitoid rocks of presumed Archean age are scattered throughout the quartzite.

As well as the sedimentary structures initially identified in the unit by Baragar and Donaldson (1973), mud cracks are common in the Coppermine area. Rippled surfaces are locally abundant and show a generally WSW-ENE transport pattern (Fig. 6.3). Locally there are thick (2-3 m) sequences of interbedded siltstone and shale which are chaotically slump folded. These sections are overlain and underlain by "normally bedded" sediments characteristic of the remainder of the unit.

Unit 20

This unit was originally described by Baragar and Donaldson (1973) as "red and green sandstone, siltstone, and mudstone. The unit is thinly laminated, locally crossbedded, and in places is ripple-marked". This unit is the most recessive in the Rae Group and outcrops well only in the valley of the Coppermine River, where it forms vertical cliffs.

Between Coppermine and Port Epworth to the east, the unit pinches out, and units 19 and 21 appear to be in conformable contact (Fig. 6.3).

Unit 21

This unit, originally described by Baragar and Donaldson as "Rusty and greenish grey to black shaly sandstone, siltstone, shale and argillite (Unit 21) overlie the red and green shales and closely resemble the basal unit in lithology".

The lithology and structures of this unit appear uniform throughout the area and it is nearly identical to the upper part of unit 19, particularly in the east. If the interpreted pinchout of unit 20 is correct, unit 21 is the equivalent of the upper part of unit 19. Unit 20 thus becomes a member of the basal Rae Group unit, but is present only in the western part of the area.

As well as the typical structures and sediments outlined by earlier workers, unit 21 locally contains abundant mud cracks, ubiquitous rippled beds, ball and pillow structures, flute marks, and rare thin crossbeded fine grained sandstones. Thin (1-3 cm) discontinuous dolomite beds in the upper part of the unit contain cone-in-cone structures.

Ripple marks are the most abundant transport indicator in the unit, and data in the western part of the area suggest that sediment transport directions were similar to those of unit 19 (Fig. 6.3).

Unit 22

This unit was originally described by Baragar and Donaldson (1973) as "...composed of well-bedded calcilutites and dololutites. ...Zones of stromatolites are locally abundant, particularly in the upper part of the section".

This is the most continuous unit in the Rae Group and extends from the type area near the Rae River to the southern part of Victoria Island. It typically outcrops as thin (2-30 m) lensoid stringers intercalated between the cliff-forming diabase sills (to 160 m) that form the bulk of the islands in Coronation Gulf. Where accessible, the unit consists of the same lithologies as described by Baragar and Donaldson (1973).

The contact between the dolomite and overlying quartzite (unit 23) on the Rae River is conformable but is defined by broad (4-6 m) shallow scours to 0.5 m deep incised into the dolomite beneath the quartzite. The contact between these same two units is exposed on the east side of Murray Island (Fig. 6.3) beneath a diabase sill. They are apparently conformable, with no evidence of erosion prior to deposition of the quartzite. A rusty weathering to buff quartzite, exposed on the shore on the southeast side of Murray Point, is identical to the overlying quartzite (unit 23). There is one striking difference, however, in that the relatively thin bedded (0.1-0.5 m) massive quartzites apparently intercalated with the dolomite contain vermiform structures up to 10 cm long and 1 cm wide. These occur in the basal 5-8 cm of the beds and are always horizontal to subhorizontal.

Stromatolites, reported by Baragar and Donaldson (1973), occur scattered throughout the sequence. However, the uniformity of the succession, together with the similarity of stromatolite types, renders them useless as a means of subdivision. For the most part, the stromatolites occur in broad mounds (1-3 m), with shallow intermound distributary channels. The mounds are weakly elongated (L:W = 1.5-3:1), and the contained stromatolites show little if any preferred elongation orientation. Individual stromatolites typically have a well developed lateral linkage and occur primarily as poorly developed pseudocolumnar forms; rare individuals show a pronounced branching.

The few elongations noted in the stromatolites of this unit suggest that the paleoshoreline trended approximately E-W in the northern part of the basin, and roughly NE-SW in the southwestern part of the basin (Fig. 6.3). It should be noted, however, that this interpretation is based on minimal data from both areas and variable stratigraphic positions.

It would appear, however, that this interpreted shoreline orientation is consistent with the paleoslope shown by the trough crossbeds in the overlying quartzites, particularly in the Victoria Island region (see below).

The identical nature of the unit from the southwestern to the northeastern extremities strongly suggests that the "Coppermine-Richardson Islands" line is approximately the original depositional strike. The absence of features typical of wave-resistant structures, together with the paucity of contained widespread stromatolite banks throughout the unit suggests that it was a continuous shallow-water platform, with stromatolites developing in areas of minimal clastic deposition. The lack of continuous outcrop of contained marker units renders this interpretation speculative.

Unit 23

This unit originally described by Baragar and Donaldson (1973) as "Typical sandstones of this unit are quartzose, medium grained, moderately well-indurated and display prominent blocky jointing ... Ripple marks and cross-bedding are the main sedimentary structures". Dixon (1979)

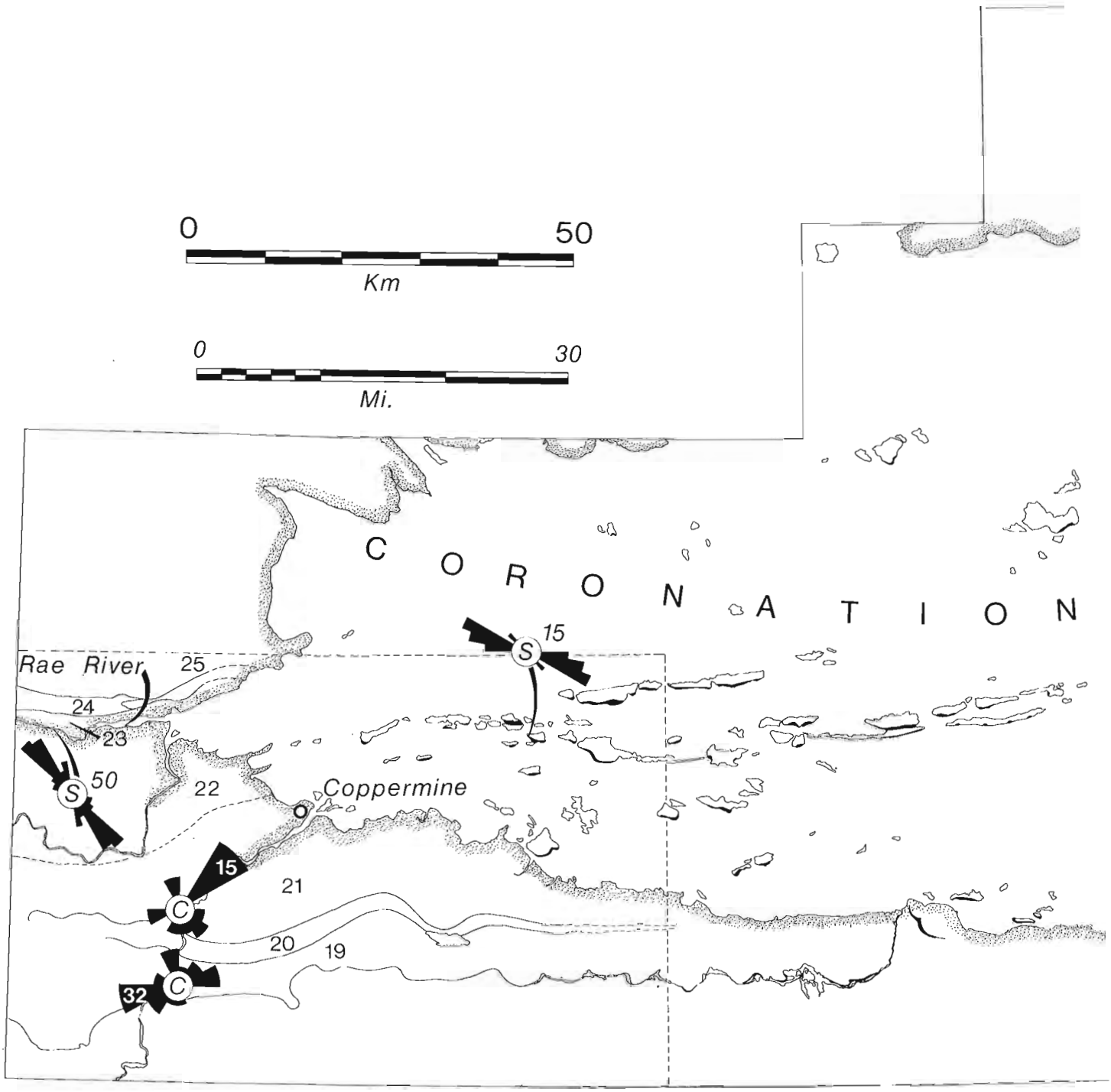

Figure 6.3. *Distribution of the sediments of the Rae Group (solid black) in the Coronation Gulf region; the Rae Group on southern Victoria Island is not patterned (see Fig. 6.1). The unpatterned parts of the islands in the gulf are entirely diabase. The area outlined in the southwestern corner was mapped by Baragar and Donaldson (1973), and the unit numbers shown are taken from their work. The paleocurrent roses are from locations beneath the centre of the rose unless otherwise indicated. The designations for the roses are: C = current ripples; S = stromatolite elongations; Open = trough crossbeds. The number of readings is as indicated for each rose, and the diameter of the centre circles is 20%. Units 24 and 25 north of the Rae River are in whole or in part Paleozoic.*

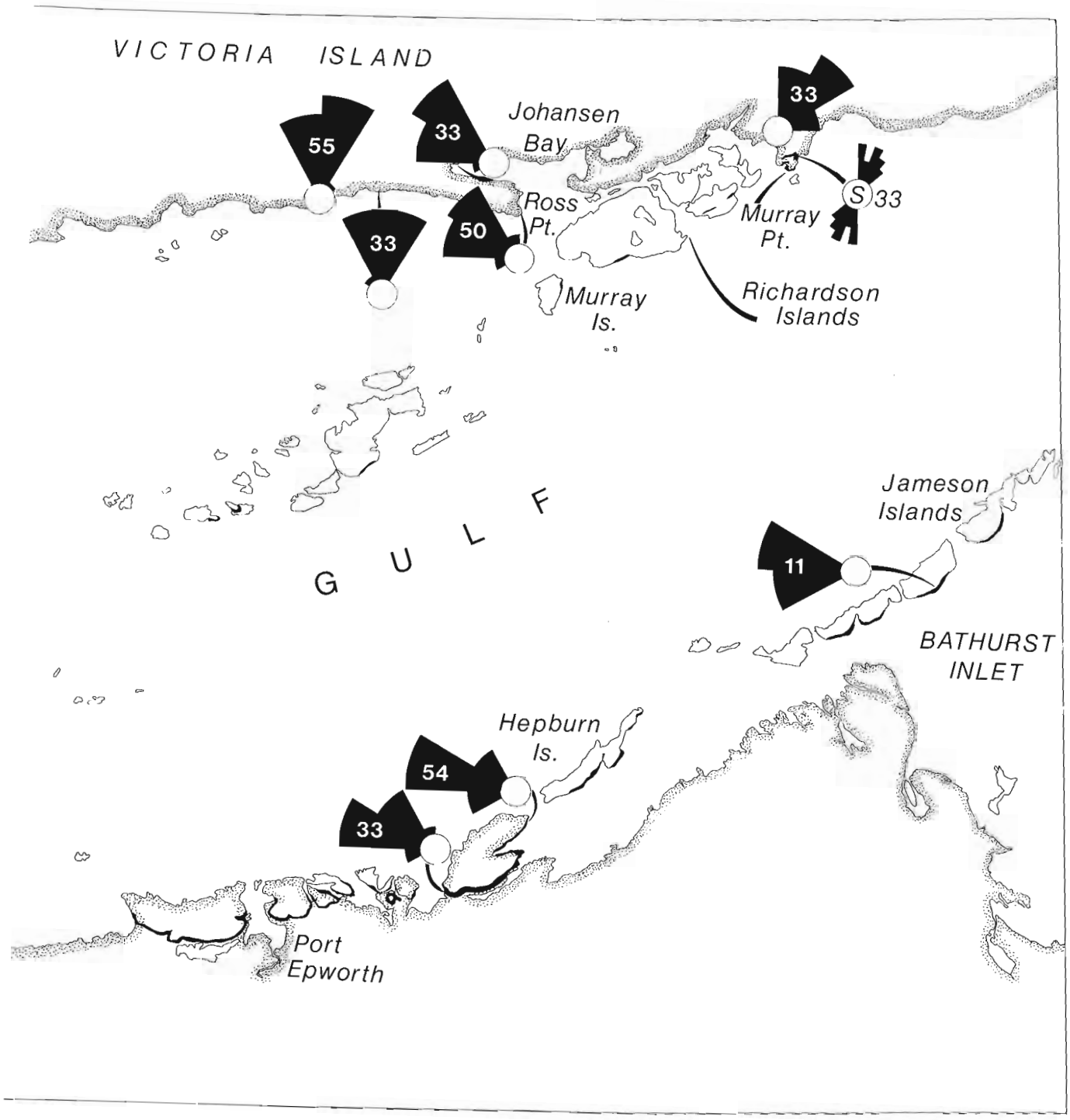
VICTORIA ISLAND
Johansen Bay
Ross Pt.
Murray Pt.
Murray Is.
Richardson Islands
Jameson Islands
G U L F
BATHURST INLET
Hepburn Is.
Port Epworth
55
33
33
50
33
S 33
11
54
33

Figure 6.4. *Large salt hoppers from unit 23 (GSC 203657).*

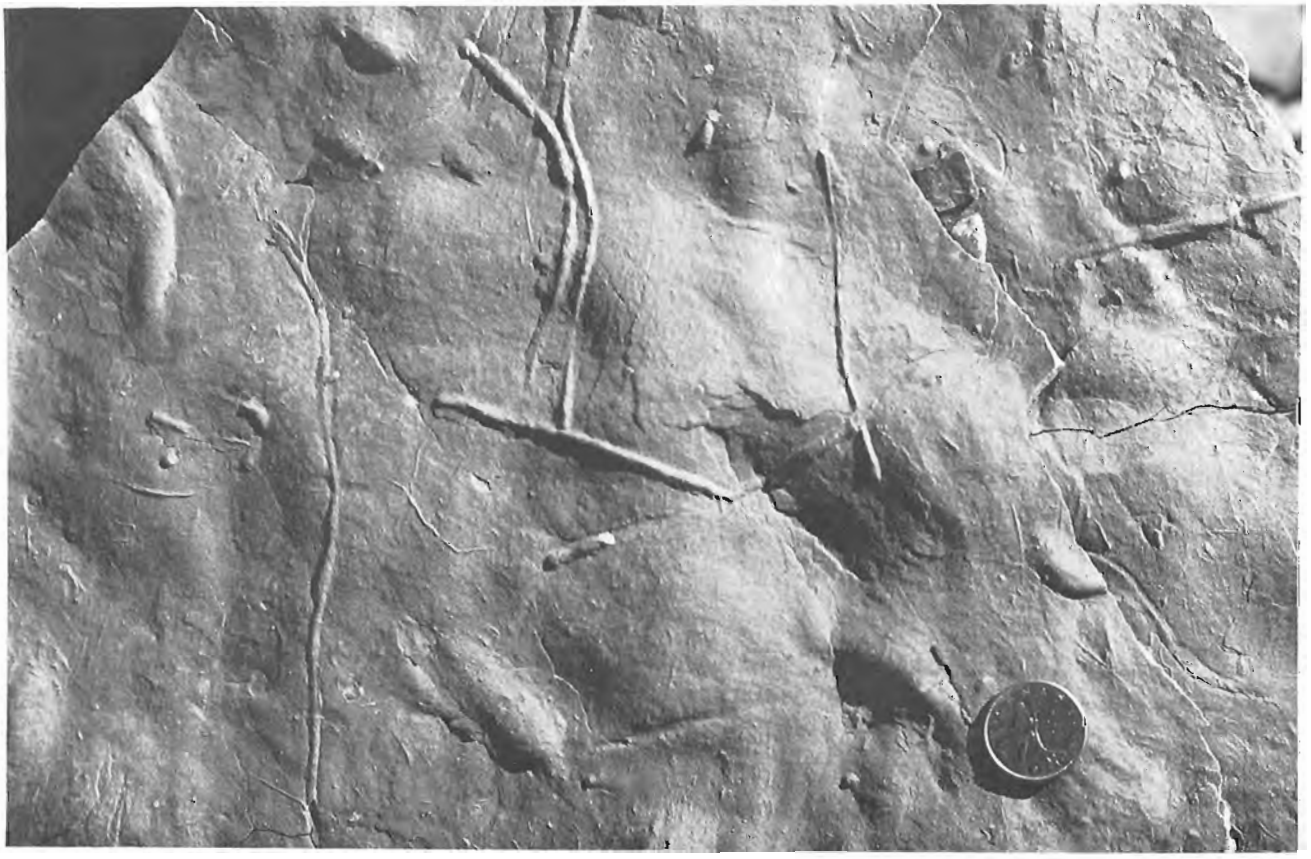

Figure 6.5. *Plan view of two varieties of burrows in unit 23. The larger type is typical, and occurs throughout the unit. The smaller, dendritic variety, is rarer, but is most abundant in the lower part of the section (GSC 203656-y).*

described the sandstones of southern Victoria Island as "...light pink to grey weathering, thickly bedded to massive, fine- and medium-grained quartzose sandstones interbedded with shale" and suggested that they were correlative with unit 23 in the Rae Group, based on the structural continuity between the Duke of York Archipelago and the Coppermine area. As outlined above, this interpretation has been confirmed, based on the outcrop continuity of unit 22 and the contact relationship with unit 23. The basal contact of the quartzites with the underlying dolomite appears conformable in both of these widely spaced locations.

The contact between units 22 and 23 is exposed on the east side of Murray Island, south of the larger of the Richardson Islands. There, the dolosiltites and dololutites of unit 22 are apparently conformably overlain by the buff and white quartzites of unit 23. These sandstones are identical in all respects to those which overlie the dolomitic unit in the eastern part of this same area and also to those to the west around Ross Point.

There are minor differences within the sandstone succession in the Richardson Islands region. The primary difference is in the scale of the crossbeds and the thickness of individual units. In the Murray Point area, where crossbeds are present, they typically have troughs up to 0.5 m wide and less than 1.25 m long; beds are invariably less than 0.75 m thick. In contrast, in the Ross Point area to the west, the trough crossbeds where present are up to 2.0 m wide and are of indeterminate length. In this same area, there are also massive, apparently structureless beds of white, rusty or buff quartzite interstratified with the trough crossbedded units. Typically, the crossbeds show a unimodal paleoflow pattern, generally to the NE-NW (Fig. 6.3). Rarely, there are small (2-5 cm) quartz pebbles contained in the basal parts of the troughs, but these nowhere form pebble lags or conglomerate beds. There are rare intercalated beds of grey-green siltstone and shale (to 20 cm) that typically show soft-sediment deformation structures.

Paleozoic Sediments

Unit 24

Typically, the unit consists of thin bedded to laminated grey-green, rarely red, shale, siltstone, mudstone, minor sandstone and doloarenite and rare thin (1-1.5 cm) beds of orange gypsum. Salt casts (Fig. 6.4) and mudcracks are ubiquitous. Ripple marks occur in the mudstones, and the grey-green shales are typically draped over these sands.

The lower contact of unit 24 is rarely exposed in the area, due to the fissile nature of the sediments. Where the lowermost exposed part of this member was examined along the Rae River west of Coppermine, the lower part of the unit contains fine grained, thin-bedded to laminated quartzose sandstones which rapidly decrease in abundance upwards. In the Ross point area, and in particular at the western end of Johanssen Bay, the stromatolitic dolomite of unit 25 appears to rest conformably on the quartzites of unit 23. Exposure, however, is poor in the intervening area between these two units, and a thin section of unit 24 could be drift covered.

The upper contact of unit 24 is poorly exposed in the regions examined. In the vicinity of the Rae River, the stromatolitic dolomite of unit 25 conformably overlies the lower part of unit 24, but is in turn overlain in the eastern part of the area by identical grey-green sediments. This relationship strongly suggests that this stromatolitic part of the Rae Group is a member within unit 24.

Dixon (1979) identified small (3-5 mm) inarticulate brachiopods in the section north of the Rae River. Dixon (personal communication, 1981) supplied me with additional information on the location of the sections he examined. Although the sequence Dixon examined is well exposed, no inarticulate brachiopods were found. However, burrows are ubiquitous throughout the succession. The structures are typically 1.5-3.0 mm wide, up to 15 cm long, and have a circular cross-section (Fig. 6.5). Also, there are small (0.5 mm) dendritic markings on the same soles which are always shorter (3 cm), but typically occur on the same bedding planes (Fig. 6.6) and there are larger structures which display a characteristic "U-tube" shape. These are generally 5-8 mm in diameter, and extend 2-4 cm below the base of the overlying beds (Fig. 6.6).

The structures also extend down into the underlying sediment, and they are visible in cross-section cutting across the internal laminations in the containing sediments. Rare, entire bedding plane areas are covered with small (1-2 mm) elliptical to near-circular pellets(?), (Fig. 6.7). These are confined to single laminae and nowhere appear to be the terminations of individual borings or tubes. Although rare, these occurrences appear to be accumulations of fecal pellets. Similar pellets may be scattered throughout the sediments in which the burrows occur, but are not so readily apparent as where they are concentrated in a single bedding plane surface.

Additional evidence of burrowing that generated these tubes is suggested by the paired nature of many of the bedding-plane-perpendicular elliptical cross-sections. Although these are not everywhere well developed, there appears to be a definite relationship between them and the associated casts displayed in plan view.

The shales and siltstones also display short, parallel evenly-spaced linear depressions (Fig. 6.6) which H.J. Hofmann (personal communitcaiton, 1982) has identified as trilobite tracks. These trilobite tracks indicate that this unit at least is Cambrian in age.

Unit 25

This unit, originally described by Baragar and Donaldson (1973) as the uppermost unit in the Rae Group is reinterpreted here as a subdivision of unit 24, based on the data outlined above. In the type area north of the Rae River, the subunit consists of orange to rusty weathering bioherms composed of weakly branching, upright to slightly inclined columnar stromatolites.

Where exposed, the basal contact of the stromatolite unit is sharp and conformable with the underlying burrowed shales and siltstones. Near the contact, there is a slight increase in the amount of dolomite in the uppermost part of unit 24, but the stromatolites commence directly on the terrigenous clastics. The upper contact was not observed in the area examined, but immediately north of Rae River the unit is apparently conformably overlain by grey-green, burrowed and mud-cracked siltstones and shales identical to those of the lower part of unit 24.

Reddish to orange-red stromatolites overlie unit 23 quartzites at the west end of Johanssen Bay on southern Victoria Island. Although the contact is not exposed, these appear identical to those in the Rae River area. There are, however, no shales and siltstones exposed which separate the two units. In the Johanssen Bay stromatolite succession, there are thin units (15-25 cm) of mud-cracked dark grey to black shales.

The bioherms appear weakly elongated at both localities, but the disaggregation of the uppermost surfaces precluded determination of preferred elongation directions.

As noted by Dixon (1979) unit 23 quartzite of Victoria Island is considerably thicker that the same unit in the Coppermine River area. The deposition of these relatively coarse clastics could account for the lack of accumulation of fines, which were deposited in the southern part of the basin.

Figure 6.6. *Plan view from below of complete and broken "U Tubes" from the upper part of unit 23. Note the short, parallel depressions scattered at random across the slab surface (centre and lower left). These have been interpreted as trilobite marks, indicating a Cambrian age (GSC 203656-Z).*

Figure 6.7. *Pellet(?)-covered bedding plane in the lower part of unit 23. The origin of the vermiform to straight marking is unknown (GSC 203657-B).*

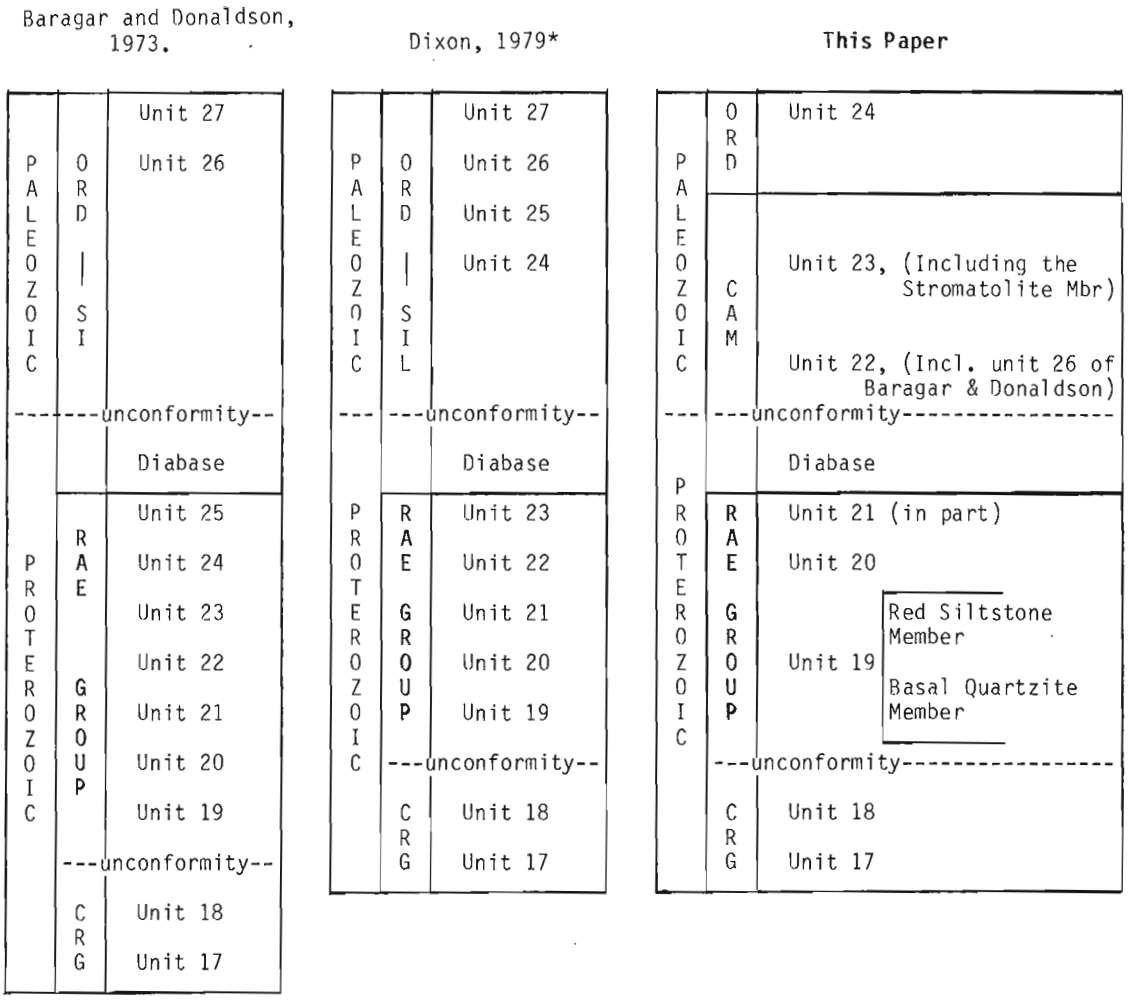

* Utilizing the same numerical scheme as Baragar and Donaldson.

Figure 6.8. *Evolution of the stratigraphic terminology for the Rae Group, showing the proposed revision, and reassignation of some of the Paleozoic units as well as Proterozoic units. CRG is the designation for the Coppermine River Group. Aside from the changes in the unit numbers and the redefinition of the units within the Rae Group, the lithological descriptions for the units as initially defined remain the same.*

Age of the Rae Group

As initially noted by Dixon (1979), and confirmed by this study, at least the upper two units of the initially-defined Rae Group (units 24 and 25) are undoubtedly Paleozoic. The lack of well-defined contact relationships between units 23 and 24 precludes accurate delineation of the position of the Cambrian-Precambrian boundary. As the diabase dykes and sills demonstrably intrude quartzites of unit 23 in both the Coppermine and Victoria Island areas, at least some of the rocks mapped as this unit are Rae Group as originally defined by Baragar and Donaldson (1973). However, similar quartzites south of Coppermine (unit 26 of Baragar and Donaldson, 1973) unconformably overlie the Coppermine Group lavas. This suggests that the basal Phanerozoic unit in the region is quartzite and that it may be very difficult to distinguish this unit from the possible source – unit 23.

Dixon (personal communication, 1982) could not identify the upper units of the Rae Group of Baragar and Donaldson west of 116°. His mapping suggested that the basal Paleozoic units rest directly on the quartzites of unit 23. If correct, this interpretation reinforces the present data on the distribution of the lowermost Paleozoic sediments, in that they are preserved in a depositional "valley" and that there was a regional erosional episode prior to deposition of the Ordovician-Silurian limestones and dolomites of unit 27.

This same relationship may also occur on southern Victoria Island, particularly in the Johanssen Bay region. Near the westernmost end of the bay, diabase dykes intrude the quartzite at the shoreline. However, the relationship between this "lower" quartzite and any overlying succession was not observed. If it is assumed that the lowermost Phanerozoic unit is a similar quartzite of unknown thickness, then the boundary would be very difficult to define, in particular with the near-conformable relationships between the two units and the lack of a recognized paleosoil or basal conglomerate.

During the course of this investigation, it was assumed, perhaps incorrectly, that the lowermost Phanerozoic rocks were in unit 24. Given these considerations, together with the possible worm burrows in the quartzites at Murray Point

on southern Victoria Island, the Cambrian-Precambrian boundary may be "within" the rocks presently identified as unit 23. Until the relationship between these units is unequivocally determined in both the northern and southern outcrop areas, units 24 and 24a and part of unit 23 are considered to be at least Cambrian. The Rae Group is therefore redefined to include only units 19 to 23 where the latter demonstrably predates the diabase sills and dykes (terminology of Baragar and Donaldson, 1973).

Thus, the interpretation of Dixon (1979) is followed here, with the addition of an unknown thickness of quartzite below unit 24 as part of the Phanerozoic column. The revised stratigraphic column is shown in Figure 6.8.

Evolution of the Rae Group

Following a protracted period of uplift and erosion during which the earlier sediments and volcanics were stripped from their common Archean basement, uplift to the east and south of Coronation Gulf supplied coarse quartzose detritus to broad braided rivers which gradually filled an approximately east-trending valley. These sediments now occupy the eastern part of the basin, approximately east of the vicinity of Port Epworth and at least as far east as the Jameson Islands. Isolated quartzose sediments in the Melville Sound-Elu Inlet area (Campbell, 1979) may be remnants of a once continuous basal sand sheet marking the beginning of Rae Group deposition.

Coeval with deposition of the coarse clastics, fine grained lateral equivalents accumulated in the distal parts of the basin. With initial marine transgression and burial of the braidplain valley, the shallow marine fine grained clastics accumulated over the peneplained basement as unit 19. Deposition of these sediments continued uninterrupted in the eastern part of the basin, but in the western part, periodic emergence resulted in the deposition of the eastward-thinning red muds, silts and shales of unit 20 (Fig. 6.3). Renewed subsidence resulted in the continued regional deposition of unit 19, earlier mapped as unit 21.

With decreasing supply of terrigenous clastics, coupled with basinal stabilization, the continuous shallow carbonate platform spread across the basin as unit 22. This, the most continuous unit of the group, extends from the southern to the northern limits of the redefined Rae Group (Fig. 6.3). The intraclast breccias, sporadic desiccation features, and scattered stromatolites strongly suggest that the carbonate platform was nearly continuous intertidal to shallow subtidal.

Renewed uplift in the source areas spread coarse terrigenous quartzose clastics (unit 23) into the basin as the carbonate platform foundered and the uppermost unit (23) of the redefined Rae Group accumulated in the formerly dominantly marine basin. As there are no precursory quartzose clastics in the uppermost part of unit 22, close to unit 23, there may have been a lengthy hiatus between deposition of the two apparently conformable units.

The upper contact of unit 23 with the basal overlying Paleozoic clastics was not observed in this study. However, as outlined above, it is quite probable that the basal Paleozoic unit is a quartzite identical to unit 23, from which it was in large part derived. Without detailed examination, the nature of this contact relationship cannot be unequivocally defined.

The redefinition of the Rae Group, initiated through the studies of Dixon (1979), together with the results of this examination necessitates a re-examination of the regional correlation of both the late Proterozoic and lowermost Paleozoic of the region.

Economic Geology

No new mineral deposits of economic significance were located in the region examined during this study. It is noteworthy, however, that gold-bearing quartz veins in the Archean basement could have been one of the sources for the basal quartz sands of both the Aphebian Odjick Formation and the Hadrynian Rae Group. Although no placer deposits were noted, the large scale sampling program that would be required to identify possible economic targets was beyond the scope of this investigation.

Acknowledgments

W.A. Gibbins (DIAND, Yellowknife) kindly assisted in all phases of this investigation. J. Dixon of the Institute of Sedimentary and Petroleum Geology, Calgary, supplied unpublished information on details of the successions in the uppermost part of the Rae Group north of the Rae River. J.A. Donaldson of Carleton University supplied airphotographs utilized in his original investigation. Helicopter support was provided through the facilities of Polar Continental Shelf Project, whose continuing support is gratefully acknowledged. Our pilot, Roger Frost of Quasar Helicopter, provided excellent service.

References

Baragar, W.R.A. and Donaldson, J.A.
1973: Coppermine and Dismal Lakes map area; Geological Survey of Canada Paper 71-39.

Campbell, F.H.A.
1979: Stratigraphy and sedimentation in the Helikian Elu Basin and Hiukitak Platform, Bathurst Inlet-Melville Sound, Northwest Territories; Geological Survey of Canada, Paper 79-8, 18 p.

Dixon, J.
1979: Comments on the Proterozoic stratigraphy of Victoria Island and the Coppermine area, Northwest Territories; in Current Research, Part B, Geological Survey of Canada, Paper 79-1B, p. 263-267.

Fahrig, W.F., Irving, E., and Jackson, G.D.
1971: Paleomagnetism of the Franklin Diabases; Canadian Journal of Earth Sciences, v. 8, p. 455-467.

Kerans, C.
1982: Sedimentology and stratigraphy of the Dismal Lakes Group; unpublished Ph.D. thesis, Carleton University, Ottawa, Ontario, 404 p.

Thorsteinsson, R. and Tozer, E.T.
1962: Banks, Victoria and Stefansson Islands, Arctic Archipelago; Geological Survey of Canada, Memoir 330, 83 p., 2 maps.

Young, G.M.
1974: Stratigraphy, paleocurrents and stromatolites of the Hadrynian (Upper Precambrian) rocks of Victoria Island, Arctic Archipelago; Precambrian Research, v. 1, p. 13-41.

1977: Stratigraphic correlation of upper Proterozoic rocks of northwestern Canada; Canadian Journal of Earth Sciences, v. 14, p. 1771-1787.

Young, G.M. and Jefferson, C.W.
1975: Late Precambrian shallow water deposits, Banks and Victoria Islands, Arctic Archipelago; Canadian Journal of Earth Sciences, v. 12, p. 1734-1748.

7.

INTERACTIVE PROCESSING OF GEOLOGICAL IMAGES

Project 720089

A.G. Fabbri and R. Wahl
Economic Geology Division

Fabbri, A.G. and Wahl, R., Interactive processing of geological images; in Current Research, Part A, Geological Survey of Canada, Paper 83-1A, p. 53-63, 1983.

Abstract

This paper introduces the reader to an interactive package for processing geological images (GIAPP). This package is currently installed on the CDC Cyber computer of the Department of Energy, Mines and Resources. The organization of user interaction and an example of digitizer data for input to a sample session are described. Considerations are made on capture and digitization of map data for image processing. The interactive session shows the type of interaction presently available.

Introduction

The objective of this paper is to describe a geological image processing system developed at the Geological Survey of Canada and currently implemented on the CDC Cyber System of the Department of Energy, Mines and Resources. Preliminary descriptions of the system and its initial interaction were given by Fabbri and Kasvand (1978), Fabbri et al. (1978), and Fabbri (1980). Among a variety of applications, it has been used in thematic mapping for mineral resource assessment (see Fabbri 1982a, in press).

Key features of the system are:

1. wide availability: it is operational on a time-sharing mainframe and therefore available to all interested scientists with access to a (Tektronix) graphics terminal and modem;
2. user friendliness: the user interaction has recently been made more 'friendly' so that the research worker may now devote more time to solving his image processing problems and less to using the computer system;
3. wide selection: the system is divided into five packages, each containing related families of algorithms. The packages are:
   1. Analysis of binary images compressed to one bit per pixel
   2. Processing of nonbinary images
   3. Interactive phase labelling of images
   4. Interactive editing of binary compressed images
   5. Processing of data from an x-y digitizer: creation and assemblage of large binary images from vectors.

Because all packages are connected with each other through a common file system, they can all be applied to a single problem.

The remainder of the paper is devoted to the organization of user interaction, an example of digitizer data for input to a sample session, and remarks on how to capture image data from geological maps.

Organization of the Interaction

The package of programs was originally intended as a laboratory tool designed for a minicomputer and for a single user or for a small number of users. For this reason the interactive conversation was kept to a minimum and a user's manual had to be constantly used during the sessions.

The image processing packages have recently been made more 'user friendly'. This has been achieved by inserting a hierarchical system of menus and options into the program code. The option to run the packages with the pre-existing minimal user interaction is nevertheless retained.

The organization of the user interaction is schematically represented as follows.

```
------------------------------------------------------------------------------
                                  level – 0
                                --------------
                                : OPTIONS :
                                --------------
 pre-existing minimal          menu driven               menu driven
     interaction             no menu display             menu display
------------------------------------------------------------------------------
------------------------------------------------------------------------------
                                  level – 1
                         ---------------------------
                         : OPERATION MENUS :
                         ---------------------------
menu redisplay    data manipulation    image manipulation    program exit
and extensions       operations            operations
------------------------------------------------------------------------------
------------------------------------------------------------------------------
                                  level – 2
                        -----------------------------
                        : PARAMETER SETTING :
                        -----------------------------
          value setting                control setting

                                       1-operation abort option
                                       2-redisplay settings
                                       3-perform operation
------------------------------------------------------------------------------
```

Level - 0

The three levels of user interaction allowed at 'level-0' are:

1. Pre-Existing Minimal Interaction. This is the original interaction which requires a detailed (external) manual and may be used by research workers familiar with the program code.
2. Menu-Driven Option With No Menu Display. This option allows the experienced user to avoid some of the time-consuming menu displays, and is especially useful on slow (300 baud) terminals.
3. Menu Driven With Menu Display. This provides full descriptive menus to be displayed together with parameter-setting routines.

In addition, the ability to switch from any level to any other level is provided.

Level - 1

The three types of operations allowed at 'level-1' are:

1. data and image manipulation operations
2. menu redisplay and extension operations
3. program termination.

The menu extension operation displays a menu for infrequently used data manipulation operations.

Level - 2

Parameter setting at 'level-2' allows both value settings and control operations to be performed. These routines are imposed (only during the menu review option) before each operation that may require value parameters to be set. Therefore, the user needs not explicitly call them nor is there any provision for doing so.

In addition to allowing values to be set, three types of control operations may be performed. They are as follows:

1. redisplaying the values of the parameters
2. aborting the intended operation
3. performing the intended operation.

Example of Data from a Digitizer

A simple way of digitizing map boundary data may consist of computing a file like the one shown in Figure 7.1. In the table contained in the illustration there are 687 pairs of tablet coordinate points and markers. The markers with value 1 indicate the end of a sequence of connected points, i.e., the location of the digitizing pen (cursor) when lifting the pen from the tablet. Markers with value 3 indicate points either at the beginning or within a sequence of connected points. A vector is to be computed only between point pairs with markers 3 and 3 or 3 and 1, but not 1 and 3.

The number of points collected was kept relatively small by choosing an appropriate value of tablet coordinate units as the longest distance interval permitted before collecting a new pair of coordinates or a new point (the value of 30 in the present example). This procedure would be followed unless a preselected angle difference (of 2.5 degrees) between adjacent vectors was exceeded, in which case a new point would be collected. While the first point at the beginning of a chain was collected immediately at pen contact with the tablet, the second point was collected when a smaller preselected distance (of 10 tablet units) was exceeded ('dead zone'). This first point pair represents the first vector of a chain which describes a line segment in the original map.

The additional tabular information in Figure 7.1, preceding the point coordinates, represents the necessary data for establishing a relationship between the 6 control points on a rectangular submap which can be placed on the tablet as shown in the diagram in Figure 7.2a. The data termed 'header' also contain some values which are simply reminders from the specific file (used for the example) which was transferred on a magnetic tape from a different computer equipped with a 34 cm x 34 cm graphic tablet digitizer.

The tabular data in Figure 7.1, correspond to the digitized geological boundaries of the southwestern part of Geological Survey of Canada, Map 1195A (Anderson and Williams, 1970). From the vectors generated by processing the data in Figure 7.1, a simple algorithm will compute a binary image of boundaries (see example in Fig. 7.2b), in which, for a desired resolution corresponding to a grid or raster of square cells, all cells crossed by one or more vectors will become black pixels with values of binary 1. Subsequent processing will generate thin boundaries (line thinning) as shown in Figure 7.2c. In addition, a large map may be broken down into a number of adjacent sub-images, and subsequently merged into a complete mosaic, as described in the next section and in Figure 7.3.

The data in Figure 7.1 comprise a simple example of how geological data from maps can be digitized in order to compute binary images of boundaries to be later processed and analyzed by using GIAPP as described by Fabbri (in press).

An Interactive Session for Processing Map Boundaries

To show the interaction with the image analysis programs presently available for geological applications on the Departmental CYBER general purpose computer, a sequence of operational steps is illustrated in Figure 7.3. In brief, the interactive steps are:

i) Initial procedure for fetching and selecting the desired data and program files;

ii) Display of a menu of options for processing;

iii) Initilization procedure for building a file input/output directory for the session;

iv) Input of digitizer data from formatted file external to the program directory in (iii);

v) Computation of dimensions in pixels of image corresponding to a given resolution, and test of horizontality of upper side of rectangle enclosing a submap;

vi) Computation of a binary image according to the parameters selected in the previous step (v);

vii) Storage of binary image as file for the directory generated in step (iii) above;

viii) Display of the binary image just stored;

ix) Assembly of a larger image containing the sub-image displayed in step (viii);

x) Display of the mosaic just assembled;

xi) Assembly of a mosaic of two adjacent rectangular submaps;

xii) Display of the mosaic computed and stored in step (xi).

Figure 7.3 shows the actual display on a Tektronix 4014/1 graphic terminal during the interactive execution of the 12 steps listed above. Note that each step is labelled in Figure 7.3 by the corresponding Roman numerals.

Concluding Remarks

The original reasons for programming the assemblage of smaller images into a larger mosaic of about 1000 pixels x 1000 pixels were as follows:

1. Limited computer memory. Because the transformation of vectors to raster is easily computed by storing an entire image in memory, the size of the image is restricted by the computer memory.
2. The availability of only a small graphic tablet digitizer online with a minicomputer.

Although the programs were developed when only 64 kilowords (16 bits/words) were available on a minicomputer, they retain their value in the current situation of a mainframe on which 28 kilowords (60 bits/words) are available for regular interactive usage. Note that a 540 pixels x 540 pixels sub-image (compressed to one bit per pixel) requires 4.86 kilowords (60 bits/words) and 18.36 kilowords (16 bits/words).

```
   4.00000   103.00000    35.00000
   9.00000     1.00000     0.00000
   0.00000     0.00000     0.00000
   0.00000   256.00000    16.00000
2059.00000     4.00000     1.00000
   0.00000     0.00000     0.00000
   0.00000     0.00000     0.00000
   0.00000  -613.75000    27.00000
  26.00000  -612.75000  -293.25000
-132.75000   432.25000   432.50000
-526.50000  -527.00000   -46.50000
 -47.25000 10000.00000     0.00000
   0.00000     0.00000     0.00000
   0.00000     0.00000     0.00000
   0.00000     0.00000     0.00000
   0.00000     0.00000     0.00000
   0.00000     0.00000     0.00000
   0.00000     0.00000     0.00000
   0.00000     0.00000     0.00000
   0.00000     0.00000     0.00000
   0.00000     0.00000     0.00000
   0.00000     0.00000     0.00000
   0.00000     0.00000     0.00000
   0.00000     0.00000     0.00000
   0.00000     0.00000     0.00000
   0.00000     0.00000     0.00000
   0.00000     0.00000     0.00000
   0.00000     0.00000     0.00000
   0.00000     0.00000     0.00000
   0.00000     0.00000     0.00000
   0.00000     0.00000     0.00000
   0.00000     0.00000     0.00000
   0.00000     0.00000     0.00000
   0.00000
```

Header

```
-433   291   3
-443   290   3
-453   288   3
-463   285   3
-473   281   3
-481   275   3
-483   267   3
-496   261   3
-503   253   3
-511   246   3
-516   237   3
-520   227   3
-518   217   3
-514   211   1
-436   292   3
-426   290   3
-418   284   3
-412   276   3
-410   266   3
-412   256   3
-413   246   3
-419   238   3
-427   230   3
-436   223   3
-446   217   3
-457   212   3
-467   209   3
-477   207   3
-487   206   3
-497   206   3
-507   205   3
-515   211   3
-520   220   3
-520   225   1
..

1,697,1,s
-315  -422   3
-305  -421   3
-275  -420   3
-245  -419   3
-214  -419   3
-204  -420   3
-193  -419   3
-182  -419   3
-172  -418   3
-162  -418   3
-132  -417   3
-122  -418   3
-112  -417   3
-102  -417   3
 -91  -416   3
 -81  -416   3
 -51  -417   3
 -41  -416   3
 -31  -416   3
 -21  -417   3
 -11  -416   3
  -1  -416   3
  10  -415   3
  20  -416   3
  27  -416   1
..
```

Point coordinates

X Y Z

Figure 7.1

Example of data generated by a graphic tablet digitizer. These data are the input to the 'tablets' programs (option 5 in Figure 7.3), and represent in the first and second columns and X and Y coordinates of points on the geological boundaries of a map. The third column, Z, of values holds a code for pen up (=1) or pen down (=3). The first 34 lines represent the 'header' information, which is as follows:

4.0	*= fourth file on storage device (reminder);*
103.0	*= file name or number (reminder)*
35.0	*= number of valid words in header (of 100 words in total);*
9.0	*= type of data in file: 9 is for table of values;*
1.0	*= data type: 1 for one computer word per value in table;*
256.0	*= 256 x 16 = 3096 which is the maximum number of values that can be stored in the table;*
16.0	*= see above line;*
2059.0	*= number of stored values in table – 2;*
4.0	*= number of points for computing the average coordinates of points 1 to 6 (reminder);*
1.0	*= pen contact "on" used for reading points (2 for "off": reminder);*
-613.75 to -132.75	*= X1 to X6 digitizer coordinates for points 1 to 6 in Figure 7.2a;*
432.00 to 47.25	*= Y1 to Y6 as in line above;*
10000.0	*= distance in map units (here m) corresponding to scaling interval between points 5 and 6 in Figure 7.2a.*

Lines 35-68, (-315 -422 3) to (-520 225 1) contain the data for the first 34 points digitized; lines 697-721, (-315 -422 3) to (27 -416 1), contain the data for the last 25 points digitized. The values in line 35 are the X-coordinate, the Y-coordinate and the Z-value marker for the first point at the beginning of the first chain of consecutive points. The values in line 36 (-443 290 3) are the corresponding coordinates and marker for the second point of a chain. These two lines of data allow the first vector in the file to be computed.

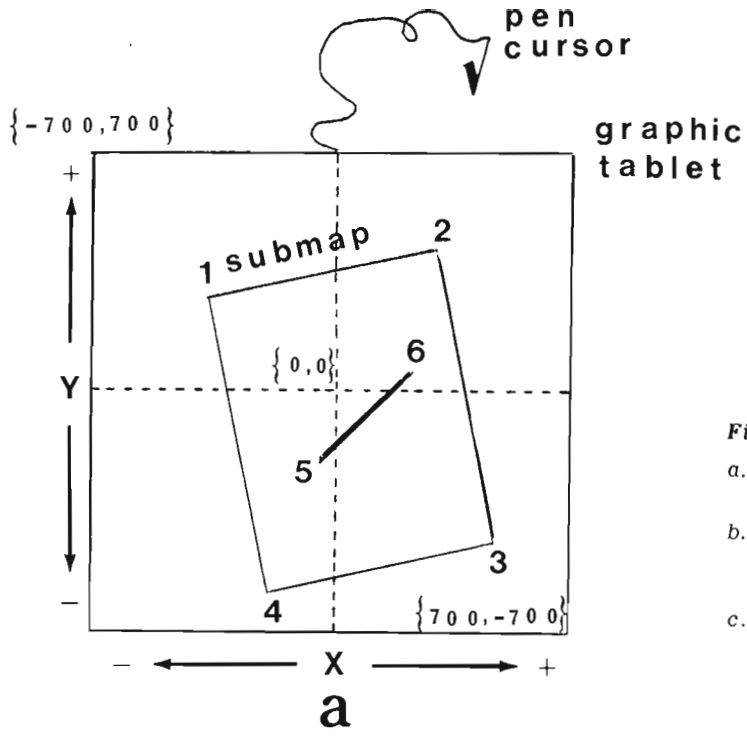

Figure 7.2

a. *Simplified diagram of the graphic tablet digitizer used for collecting the data in Figure 1, and*

b. *A fictitious example of vector to raster transformation in which the white squares indicate the white picture elements or pixels, and the black squares and black pixels.*

c. *Black pixels representing a boundary in (b) have been transformed into thin lines (line thinning).*

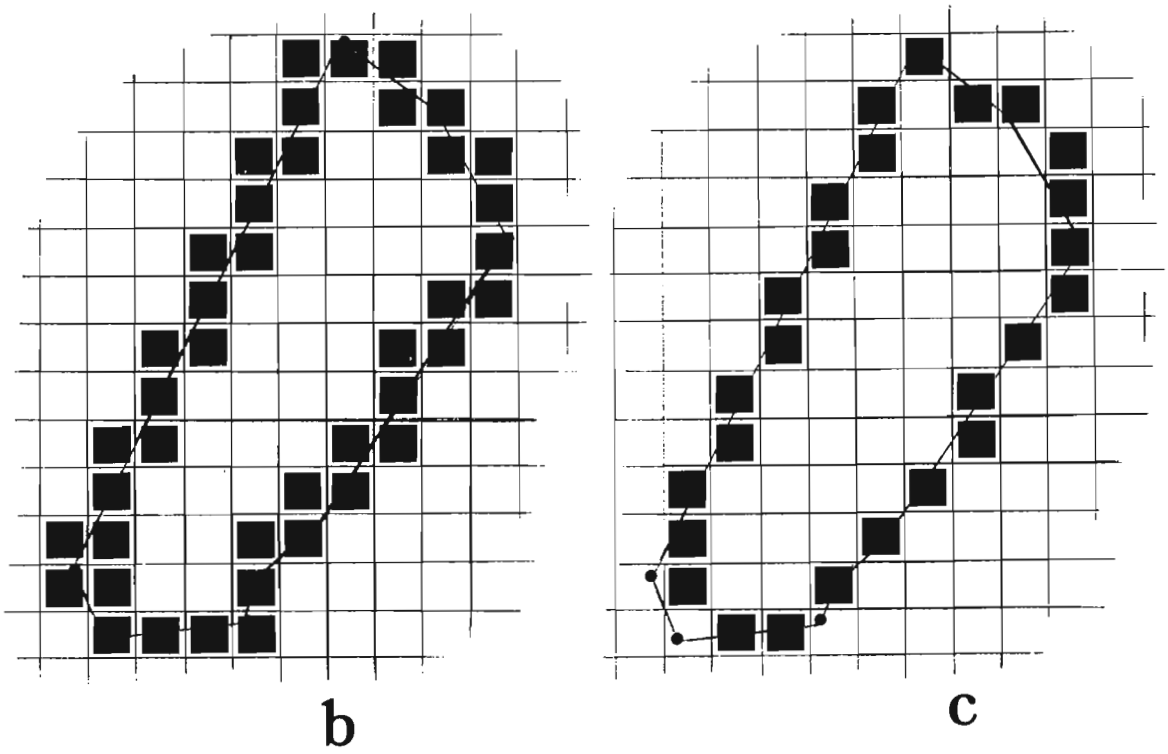

Figure 7.3. Conversational text and image displays obtained during an interactive session with "tablets" subpackage of programs for processing data from a graphic tablet digitizer. The program prompts in the illustration are in upper case characters, while the user's commands are in lower cases characters. The Roman numerals I to XII added to the "hard copies" of the Tektronix 4014/1 monitor, indicate the beginning of the twelve interactive steps listed in the text. The list of 18 choices available in step (i) represent image files from other interactive sessions. As it can be seen from the menu of operations in step (II), other alternative steps are also available. Arrows indicate particulars of poor resolution (a pixel represents a square of 250 m on the ground). Other small defects visible but not marked can be easily avoided by a careful usage of the graphic tablet.

I

```
COMMAND- attach,tape2,g1195av,cy=6,id=agf
COMMAND- begin,wrkproc,wrkproc/agf

-P 120 30

  WELCOME TO IMAGE ANALYSIS
INTERACTIVE COMPUTER PROGRAMS.
 WHAT PACKAGE DO YOU WANT TO RUN?
 CHOOSE FROM 1 TO 5
 1 - GIAPP
 2 - PHASE LABEL
 3 - EDIT BINARY IMAGE
 4 - NONBINARY ANALYSIS
 5 - TABLET5
 YOU NEED TO CHOOSE MT11 AND MT12.
 THE AVAILABLE CHOICES ARE:
                 MT11                          MT12
                 ----                          ----
             1   INITT1                    1   INITT2
             2   TESTS1                    2   TESTS2
             3   GRANUL1                   3   GRANUL2
             4   SKULLS1                   4   SKULLS2
             5   SKULLB1                   5   SKULLB2
             6   SKULLC1                   6   SKULLC2
             7   BATHU1                    7   BATHU2
             8   WJGEOL1                   8   WJGEOL2
             9   WJGEOL1A                  9   WJGEOL2A
            10   WJGEOL1B                 10   WJGEOL2B
            11   WJGEOL1C                 11   WJGEOL2C
            12   WJGRAV1                  12   WJGRAV2
            13   WJAERO1                  13   WJAERO2
            14   WJTOPO1                  14   WJTOPO2
            15   WJUREQ1                  15   WJUREQ2
            16   WJTHEQ1                  16   WJTHEQ2
            17   WJURTH1                  17   WJURTH2
            18   WJMINE1                  18   WJMINE2
 DO YOU WANT ANY OF THE ABOVE FILES? (0 = NO, 1 = YES)0
 WHAT IS THE PFN FOR MT11?initt1
 WHAT IS THE ID FOR MT11?mt11
 WHAT IS THE PFN FOR MT12?vec2
 WHAT IS THE ID FOR MT12?mt12
 MENUS REQUIRED?
 0=NO,1=YES1
*** TABLET ***
 MODE OF OPERATION?
 0 = MANUAL OPERATION
 1 = MENU DRIVEN, NO MENU DISPLAY
 2 = DISPLAY MENU2
**********************  TABLET  **********************
          MENU OF OPERATIONS
          ------------------
 1 - INITIALIZATION 'COOL START'
 2 - COPY COMPRESSED IMAGE
 3 - RUB DATA SET
 4 - READ VECTORS FROM TAPE2(RVECT2)
 5 - CREATE DS WITH TABLET VECTOR IN MEMORY(GEST3M)
 6 - READ DS TO MEM. WITH TABLET VECT TABLE(GEST3L)
 7 - ROTATE OR NOT DECISION PROGRAM (TABLT7)
 8 - CONSTRUCT BINARY PICT. FROM VECTOR TABLE(HPR52)
 9 - SAME AS (8) BUT WITH ROTATION(HPR52A)
10 - CREATE DS WITH BINARY IMAGE IN MEMORY(HPR78B)
11 - CREATE DS WITH COMPOSITE PICTURE(HPR85B)
12 - DISPLAY COMPRESSED IMAGE ON TEKTRONIX
13 - TYPE FILE OCCUPANCY TABLE
```

II

```
14 - INITIALIZE LLIO TABLE
15 - RECONSTRUCT LLIO TABLE
16 - PREPARE TAPE11
17 - PREPARE TAPE12
18 - EXIT FROM PROGRAM
19 - REDISPLAY THIS MENU
 >>> TYPE YOUR CHOICE.1
COOL START,YOU SURE?

1=YES,2=BYPASS DEFAULTS1
SLLIO  30  14   2   2   3
PREPD  0  0 13 14 17
RLIO1, RECON LLIO FROM MT= 11
DATA START
DATA END
RLIO1, RECON LLIO FROM MT= 12
DATA START
DATA END
 MODE OF OPERATION?
 0 = MANUAL OPERATION
 1 = MENU DRIVEN, NO MENU DISPLAY
 2 = DISPLAY MENU1
 >>> TYPE YOUR CHOICE.4
PRINT=1, NO PRINT =01
4 103 35
 MORE?, 1=YES, 0=NO.1
9 1 0
 MORE?, 1=YES, 0=NO.1
0 0 0
 MORE?, 1=YES, 0=NO.0
 MODE OF OPERATION?
 0 = MANUAL OPERATION
 1 = MENU DRIVEN, NO MENU DISPLAY
 2 = DISPLAY MENU1
 >>> TYPE YOUR CHOICE.7
 ROTATE OR NOT DECISION PROGRAM (TABLT7)
 DO YOU WANT TO SET PARAMETERS?
 0=NO, 1=YES1
 ERASE SCREEN AND TYPE 1 TO CONTINUE1
                  *** PARAMETER SETTINGS ***

        TYPE OF SETTING                                  CURRENT VALUE

        ---------------                                  -------------

        0  NO MORE SETTINGS
        1  ABORT THIS OPERATION
        2  NUMBER OF PIXELS ON THE SCALING INTERVAL.....    100

        3  SET  1    FOR MINIMUM CORNERS.....................     2

              2    FOR AVERAGE CORNERS
        4  SCALING INTERVAL LENGTH.....................10000.

        5  REDISPLAY THIS MENU
>>> TYPE YOUR CHOICE.2
>>>TYPE THE NEW VALUE OF THE PARAMETER.41
>>> TYPE YOUR CHOICE.0
```

III

IV

V

Figure 7.3 (continued)

```
TABLT7     41     2
PIXEL,FPIXEL,DPIXEL =     41    250.0000      4.0125
AVERAGE DIMENSIONS:IDIMA,JDIMA =    160   240
CORNERS =  -613    432     26  -526
  -613.26844    432.48943    26.48166  -526.63549
T,CO,SI =     .390168E-03    .100000E+01    .390168E-03
 MODE OF OPERATION?
 0 = MANUAL OPERATION
 1 = MENU DRIVEN, NO MENU DISPLAY
 2 = DISPLAY MENU1
 >>> TYPE YOUR CHOICE.8
 CREATE BINARY IMAGE FROM VECTOR TABLE,NO ROTATION(HPR52)
 DO YOU WANT TO SET PARAMETERS?
 0=NO, 1=YES1
 ERASE SCREEN AND TYPE 1 TO CONTINUE1
                    *** PARAMETER SETTINGS ***

        TYPE OF SETTING                                  CURRENT VALUE
        ---------------                                  -------------
        0  NO MORE SETTINGS
        1  ABORT THIS FUNCTION
        2  LAST FILLED ENTRY IN VECTOR TABLE.............  2059
           (-'VE ZEROS THE BINARY IMAGE IN MEMORY)
        3  NUMBER OF PIXELS WIDE.........................   160
        4  NUMBER OF PIXELS DEEP.........................   240
        5  TOP    COORD. OF ACTIVE TABLET AREA...........  432.
        6  BOTTOM COORD. OF ACTIVE TABLET AREA........... -527.
        7  LEFT   COORD. OF ACTIVE TABLET AREA........... -613.
        8  RIGHT  COORD. OF ACTIVE TABLET AREA...........   26.
        9  STEP SIZE ALONG VECTORS (IN TABLET UNITS).....   .50
       10  REDISPLAY THIS MENU
 >>> TYPE YOUR CHOICE.0
 HPR52  2059   160   240  -613   432    26  -526  4320     9   540   540 9
    .50000
 MODE OF OPERATION?
 0 = MANUAL OPERATION
 1 = MENU DRIVEN, NO MENU DISPLAY
 2 = DISPLAY MENU1
 >>> TYPE YOUR CHOICE.10
 CREATE DS FROM BINARY IMAGE IN MEMORY(HPR78B)
 DO YOU WANT TO SET PARAMETERS?
 0=NO, 1=YES1
 ERASE SCREEN AND TYPE 1 TO CONTINUE.1
                    *** PARAMETER SETTINGS ***

        TYPE OF SETTING                                  CURRENT VALUE
        ---------------                                  -------------
        0  NO MORE SETTINGS
        1  ABORT THIS OPERATION
        2  OUTPUT DS.....................................   300
        3  NUMBER OF PIXELS/ROW..........................   160
        4  NUMBER OF ROWS................................   240
        5  TOP    COORD OF ACTIVE TABLET AREA............  -613
        6  BOTTOM COORD OF ACTIVE TABLET AREA............   432
        7  LEFT   COORD OF ACTIVE TABLET AREA............    26
        8  RIGHT  COORD OF ACTIVE TABLET AREA............  -526
        9  REDISPLAY THIS MENU
 >>> TYPE YOUR CHOICE.2
 >>> TYPE THE NEW VALUE OF THE PARAMETER.100
 >>> TYPE YOUR CHOICE.0
 HRP78B   100   160   240   540  -613   432    26  -526     9   540
 GIVE NAME OF DATA(20 CHARACTERS) g1195a sw part
 >PICT-0160 0240  ID= G1195A SW PART
```

VI

VII

```
 IS IT OK? 1=YES, 2=NO, 3=ABORT1
 MODE OF OPERATION?
 0 = MANUAL OPERATION
 1 = MENU DRIVEN, NO MENU DISPLAY
 2 = DISPLAY MENU1
 >>> TYPE YOUR CHOICE.12
 PLOT COMPRESSED IMAGE ON TEKRONIX
 DO YOU WANT TO SET PARAMETERS?
 0=NO, 1=YES1
 ERASE SCREEN AND TYPE 1 TO CONTINUE.1
                    *** PARAMETER  SETTINGS ***

        TYPE OF SETTING                                  CURRENT VALUE
        ---------------                                  -------------
        0  NO MORE SETTINGS
        1  DATA SET TO DISPLAY...........................   100
        2  BAUD RATE (30 TO 960 CHARS/SEC)...............   960
        3  BLACK ON WHITE = 1.............................     1
           WHITE ON BLACK = 2
        4  SQUARE    PLOT = 1 OR 2........................     1
           HEXAGONAL PLOT = 3
        5  VECTOR DISPLAY(FAST)  = 1.....................     2
           POINT  DISPLAY(SLOW)  = 2
        6  SPACING BETWEEN PIXELS (USE A REAL VALUE).....   3.0
        7  MODEL OF TEKTRONIX............................     3
              1 = MOD 4006,4010 AND 4012/4013
              2 = MOD 4014/4015
              3 = MOD 4014/4015 + ENHANCED GRAPHICS MODE
        8  ADDRESSABLE POINTS............................     2
              1 = 1024 ADDRESSABLE POINTS
              2 = 4096 ADDRESSABLE POINTS
        9  SCREEN X-COORD. TOP LEFT CORNER...............   100
       10  SCREEN Y-COORD. TOP LEFT CORNER...............  3050
       11  ABORT THIS OPERATION
       12  REDISPLAY THIS MENU

    >>> TYPE YOUR CHOICE.5
    >>> TYPE THE NEW VALUE OF THE PARAMETER.1
    >>> TYPE YOUR CHOICE.6
    >>> TYPE THE NEW VALUE OF THE PARAMETER.9.
    >>> TYPE YOUR CHOICE.9
    >>> TYPE THE NEW VALUE OF THE PARAMETER.500
    >>> TYPE YOUR CHOICE.0
   PICTC   100   500  3050       9.000000          1     1     1
           0
              1  4095  3071   960     3
              2  4096
     TYPE 1 TO CONTINUE.1
```

VIII

Figure 7.3 (continued)

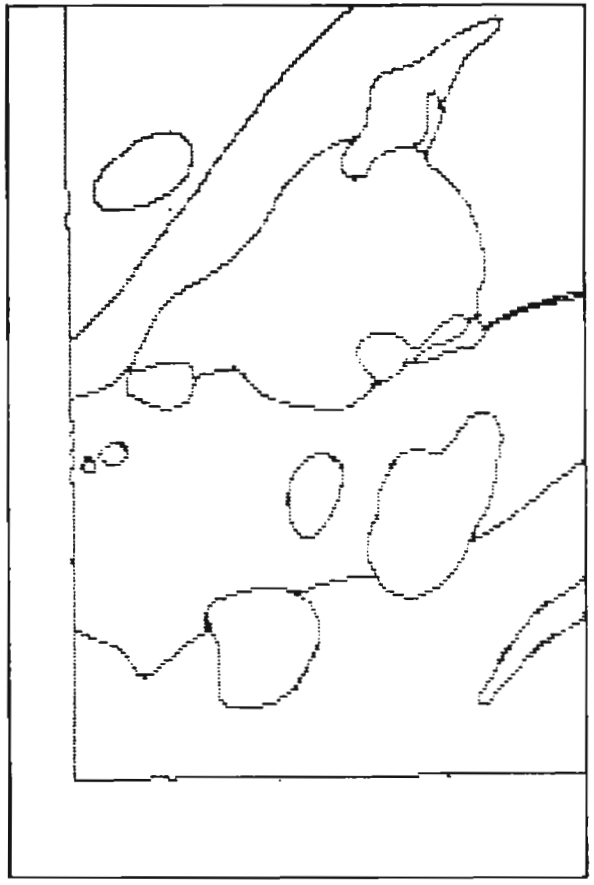

```
MODE OF OPERATION?
0 = MANUAL OPERATION
1 = MENU DRIVEN, NO MENU DISPLAY
2 = DISPLAY MENU1
>>> TYPE YOUR CHOICE.11                    <-- IX
CREATE DS WITH COMPOSITE PICTURE(HPR85B)
DO YOU WANT TO SET PARAMETERS?
0=NO, 1=YES1
ERASE SCREEN AND TYPE 1 TO CONTINUE1
                  *** PARAMETER SETTINGS ***

        TYPE OF SETTING                                  CURRENT VALUE

        ---------------                                  -------------

        0  NO MORE SETTINGS
        1  ABORT THIS OPERATION
        2  INPUT DS(USE '0' THE FIRST TIME).....            0

        3  INPUT DS WITH PATCH.....                       100

        4  OUTPUT DS.....                                 400

           BINARY PICTURE RANGE IN X
        5             START.....                          1

        6             END.....                            160

           BINARY PICTURE RANGE IN Y
        7             START.....                          1

        8             END.....                            240

        9  REDISPLAY THIS MENU
 >>> TYPE YOUR CHOICE.4
 >>> TYPE THE NEW VALUE OF THE PARAMETER.500
 >>> TYPE YOUR CHOICE.0
HPR85B:      0   100   500     1   160     1   240
CREATE COMPOSITE BINARY COMPRESSED PICTURE
GIVE NAME OF COMBO:30 CHARACTERS map g1195a south half
>PICT=COMBO:          MAP G1195A SOUTH HALF
ISITOK& 1=YES, 2=NO, 3=ABORT:I11
GIVE:IDIMBN,JDIM:216   320   240
   320   240
ISITOK& 1=YES, 2=NO, 3=ABORT:I11
 NO. OF 60-BIT WORDS/ROW= 6
 1 = PRESENT VALUE, 2 = 18 WORDS2
 MODE OF OPERATION?
 0 = MANUAL OPERATION
 1 = MENU DRIVEN, NO MENU DISPLAY
 2 = DISPLAY MENU1
 >>> TYPE YOUR CHOICE.12                   <-- X
 PLOT COMPRESSED IMAGE ON TEKRONIX
 DO YOU WANT TO SET PARAMETERS?
 0=NO, 1=YES0
PICTC   500   500  2800       9.000000          1     1     1
5     5
          1  4095  3071   960     3
          2  4096
TYPE 1 TO CONTINUE.1
```

Figure 7.3 (continued)

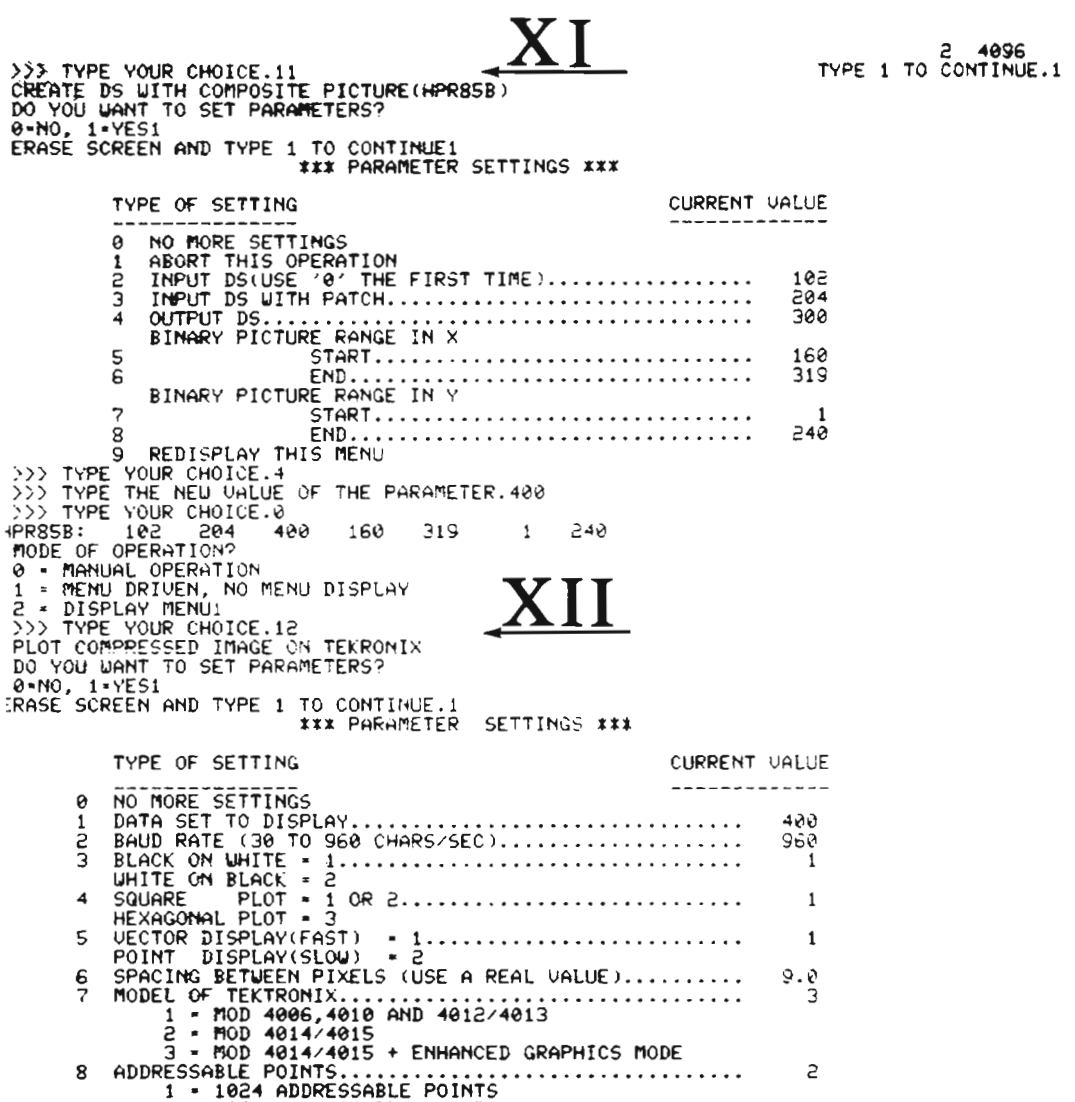

Figure 7.3 *(continued)*

```
MODE OF OPERATION?
0 = MANUAL OPERATION
1 = MENU DRIVEN, NO MENU DISPLAY
2 = DISPLAY MENU1
>>> TYPE YOUR CHOICE.11
```

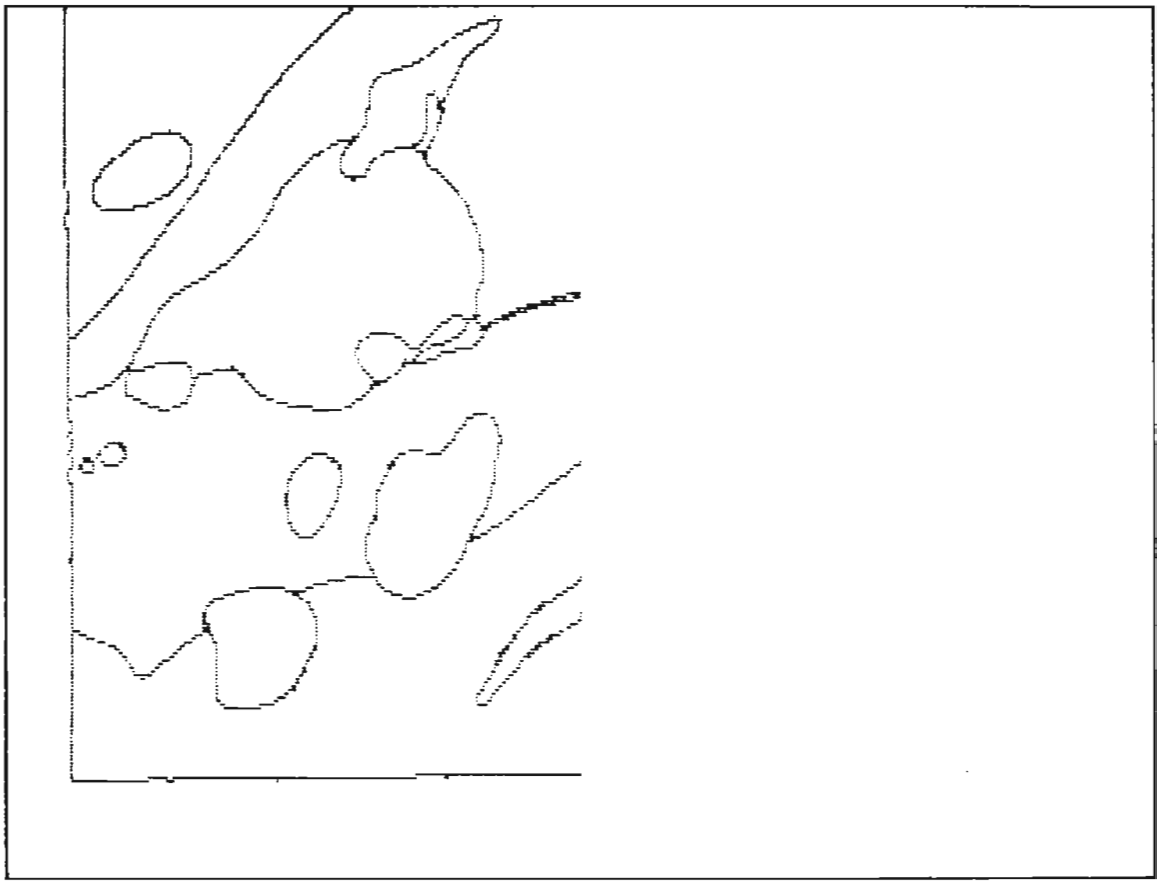

Figure 7.3 (*continued*)

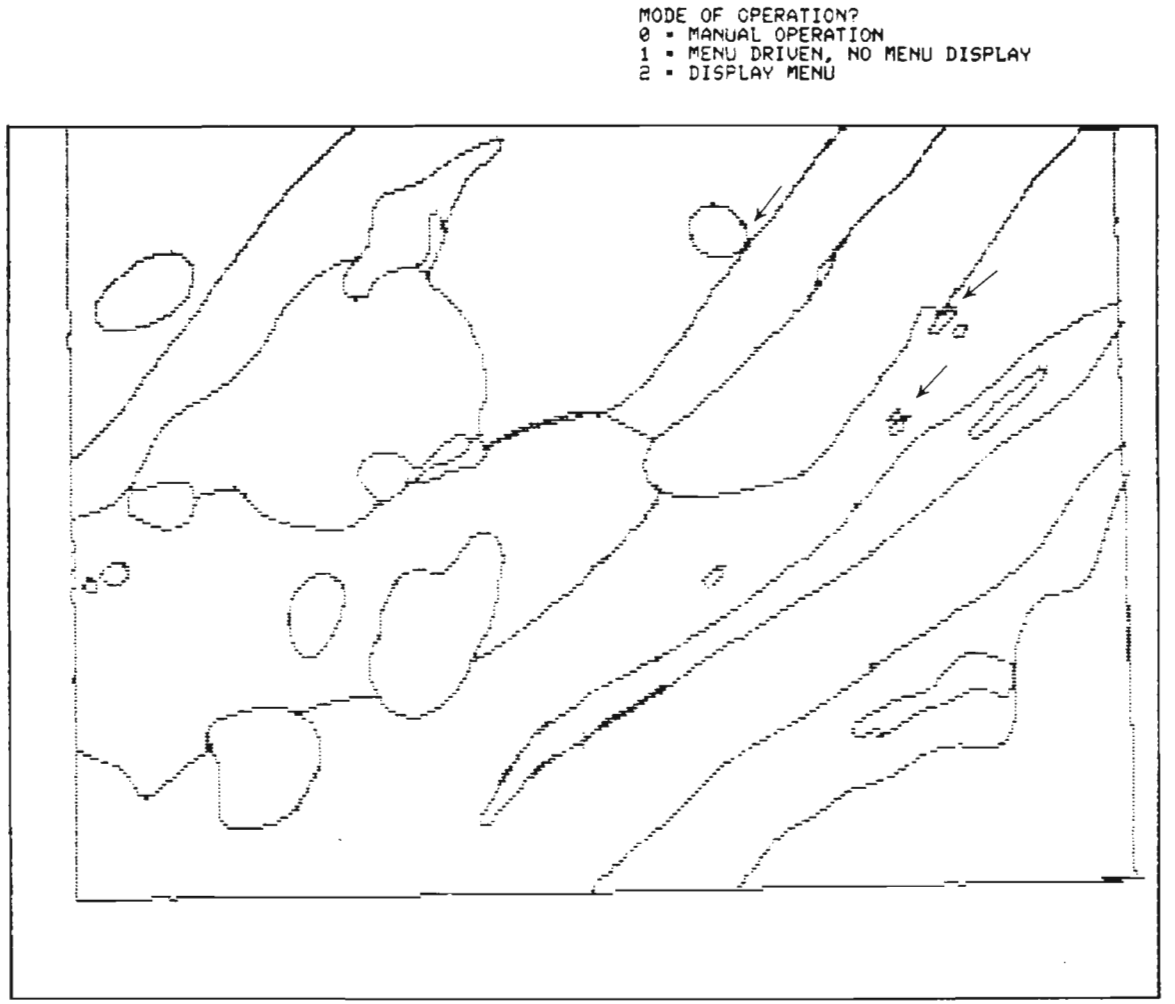

At present it is possible to easily assemble mosaics of images of map data from different maps, so that the resulting images are all in registration with one another: same resolution, same orientation and positioning, i.e., same correspondence with ground truth. Registration means a point-to-point correspondence between pixels from different images, and it is a necessary requirement for performing cross-correlations or matchings as described by Fabbri (in press). A description and discussion of the procedure developed for digitization and processing of large regional maps was made by Kasvand et al. (1981). Alternative approaches to the procedure here illustrated are as follows:

1. If the digitization is done on a large tablet, submap generation can be avoided. It would, however, be highly advisable to carry out the area identification (phase labelling) also as part of that procedure thus eliminating most of the successive work in interactive labelling. The latter would be only required for possible online corrections or editing.
2. Contour maps may also be raster scanned to create or obtain binary formatted mosaics directly. The maps, however, must be adequately registered on the scanner to avoid subsequent interpolation (resampling).
3. The vectorial data produced on a graphic tablet (or a raster scanned image of boundaries) is transformed into a binary image of thinned lines (see Fig. 7.2c). Subsequent processing permits the following steps: (a) to edit the image in places of poor resolution, (b) to identify junctions and segments in the "tessellation" of areas or to identify the areas surrounded by boundary pixels (component labelling), (c) to identify interactively all types of areas (phase labelling), and (d) to extract a binary image for each area type. At this stage it becomes an easy procedure (e) to go from raster back to vectors and to compute a graphic data base for generating aesthetically pleasing plots for automated geological cartography.

Preference for such alternate procedures clearly depends on the availability of equipment; in the present case only a minimal equipment situation is considered, namely a time shared situation on a general purpose mainframe.

Image processing methods provide some solutions to the problems of geological data capture and integration from maps and ancillary pictorial information. Such images can be used to develop quantitative thematic maps. The present paper provides a simple example for transforming vector data into binary images of map boundaries, i.e., into raster data (digital images) in order to use "GIAPP", a geological image analysis program package developed by Fabbri (1980, 1982b). The interactive session shows the type of 'user friendly' interaction presently available on the Departmental Cyber computer.

Acknowledgments

The authors are grateful to the Electrical Engineering Division of National Research Council Canada for the collaboration and assistance offered in this research. The Computer Science Center of the Department of Energy, Mines and Resources has generously supported this work.

References

Anderson, F.D. and Williams, H.
1970: Geology, Gander Lake (west half), Newfoundland; Geological Survey of Canada, Map 1195A, scale 1:250 000.

Fabbri, A.G.
1980: GIAPP: geological image analysis program package for estimating geometrical probabilities; Computers and Geosciences, v. 6, p. 153-161.

1982a: Image processing of coincident binary patterns from geological and geophysical maps of mineralized areas; in Uranium in Granites, editor Y.T. Maurice; Geological Survey of Canada, Paper 81-23, p. 157-165.

1982b: GIAPP: image analysis program and applications, 1977-1981; in Current Research, Part A; Geological Survey of Canada, Paper 82-1A, p. 421-424.

– Application of image processing for the detection of areas favourable to the occurrence of mineral resources; Proc. of VI Symposium of the International Association on the Genesis of Ore Deposits, Tbilisi, U.S.S.R.., Sept. 6-12, 1982. (in press)

Fabbri, A.G. and Kasvand, T.
1978: Picture processing of geological images; in Current Research, Part B, Geological Survey of Canada, Paper 78-1B, p. 169-174.

Fabbri, A.G., Kasvand, T., and Stray, J.H.
1978: Implementation of an interactive system for computer processing of geological images; in Current Research, Part C, Geological Survey of Canada, Paper 78-1C, p. 123-124.

Kasvand, T., Fabbri, A.G., and Nel, L.D.
1981: Digitization and processing of large regional geological maps; National Research Council Canada, Electrical Engineering Division, Report ERB-938, 91 p.

8. PISCES IV SUBMERSIBLE DIVES ON THE SCOTIAN SLOPE AT 63°W

Project 810047

Philip R. Hill, David J.W. Piper, and William R. Normark[1]
Atlantic Geoscience Centre, Dartmouth

*Hill, P.R., Piper, D.J.W., and Normark, W.R., **Pisces IV** submersible dives on the Scotian Slope at 63°W; in Current Research, Part A, Geological Survey of Canada, Paper 83-1A, p. 65-69, 1983.*

Abstract

*The upper continental slope and outermost continental shelf, in water depths of 700 to 300 m, were examined on two **Pisces** submersible dives. Observations confirm that the seabed morphology on the upper slope is irregular, as a result of late Pleistocene slumping. Sand is predominant to depths of 450 m on the slope, and to 500 m in a shallow slope valley. Gravel ribbons and current scour around boulders were found to water depths of 450 m, suggesting active contemporary currents. Bioturbated muds occur in deeper water.*

Introduction

Geological Setting

This report describes two submersible dives made on the upper part of the Scotian Slope, as part of a broader study of the late Quaternary history of selected areas of the slope. The dives were made within a 15 by 20 km area (Fig. 8.1) at 63°W investigated in detail by Hill (1979, 1981). This area lies immediately seaward of a deep water saddle on the continental shelf between Emerald Bank and LaHave Bank where the shelf break is around 260 m.

The overall morphology of this western part of the Scotian Slope is relatively smooth: deeply incised submarine canyons occur only east of 62°W. About 170 km of high resolution sparker profiles within the detailed study area show seabed geology to be complex, and suggest the presence of slump scars and allochthonous blocks cut by a shallow valley that lead to a lobe-like feature in 1000 m water depth. Piston cores show a complex sequence of late Pleistocene turbidite sand and mud deposits, and chaotic debris flow deposits (Hill et al., 1982). These are overlain disconformably by 1-2 m of rather uniform Holocene mud that grades upslope into sand.

Surficial sediment grades from gravelly sand at the shelf break, through sand to silty sand at about 400 m depth and then to silty mud. Detailed textural analysis and comparison with current meter data suggest that sand transport is dominated by suspension, and the sediment is deposited in equilibrium with the modern current regime (Hill and Bowen, 1982).

The late Quaternary glacial history of the Scotian Shelf has presumably had a major impact on sedimentation on the continental slope. Ice may have been grounded on the outer banks during the early or mid-Wisconsinan, with a floating ice shelf extending over deeper areas of the shelf; during the late Wisconsinan the ice margins receded (King, personal communication, 1981). The maximum amount of late Wisconsinan lowering of sea level is disputed, but lies between 70 m (Quinlan and Beaumont, 1981) and 115 m (King, 1970).

Purpose of Submersible Dives

Bathymetric and subbottom seismic data lack sufficient resolution of mesotopographic features (scales of tens of metres) in the study area because of the wide areas of insanification in deep water. Without an adequate understanding of the mesotopography, the origin of valleys and slump features remains largely unknown. Submersibles provide a means of investigating these features.

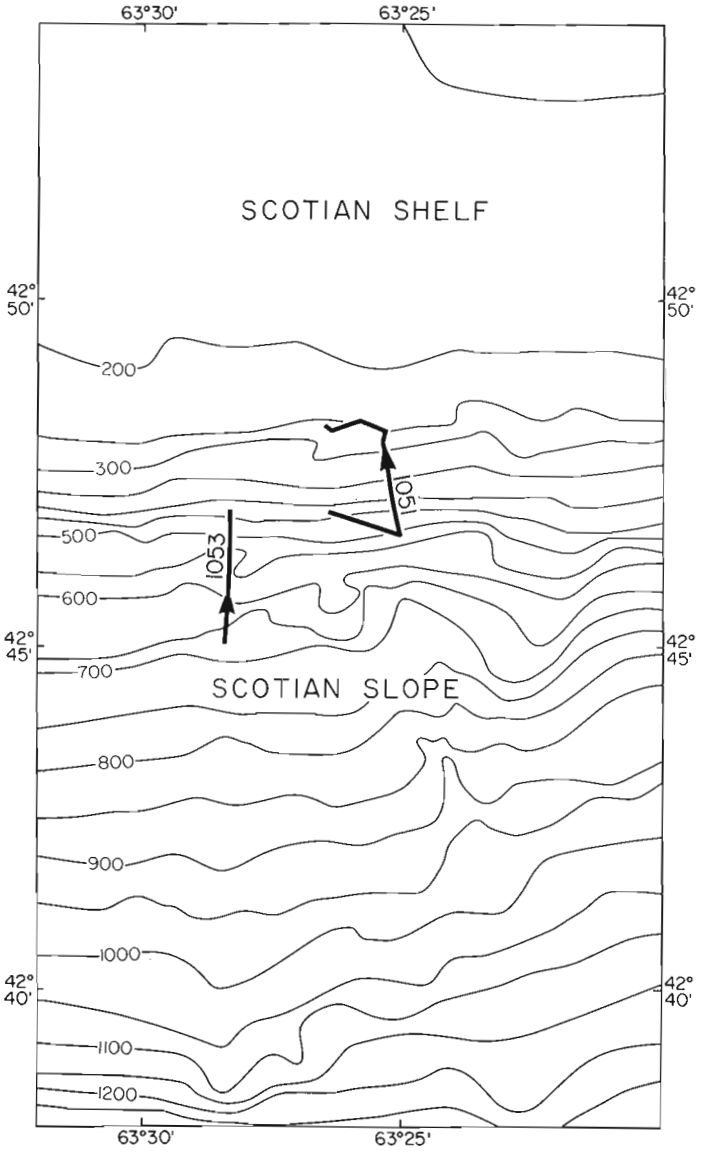

Figure 8.1. *Bathymetric map of study area showing location of dives.*

[1] United States Geological Survey, 345 Middlefield Road, Menlo Park, Ca 94025, U.S.A.

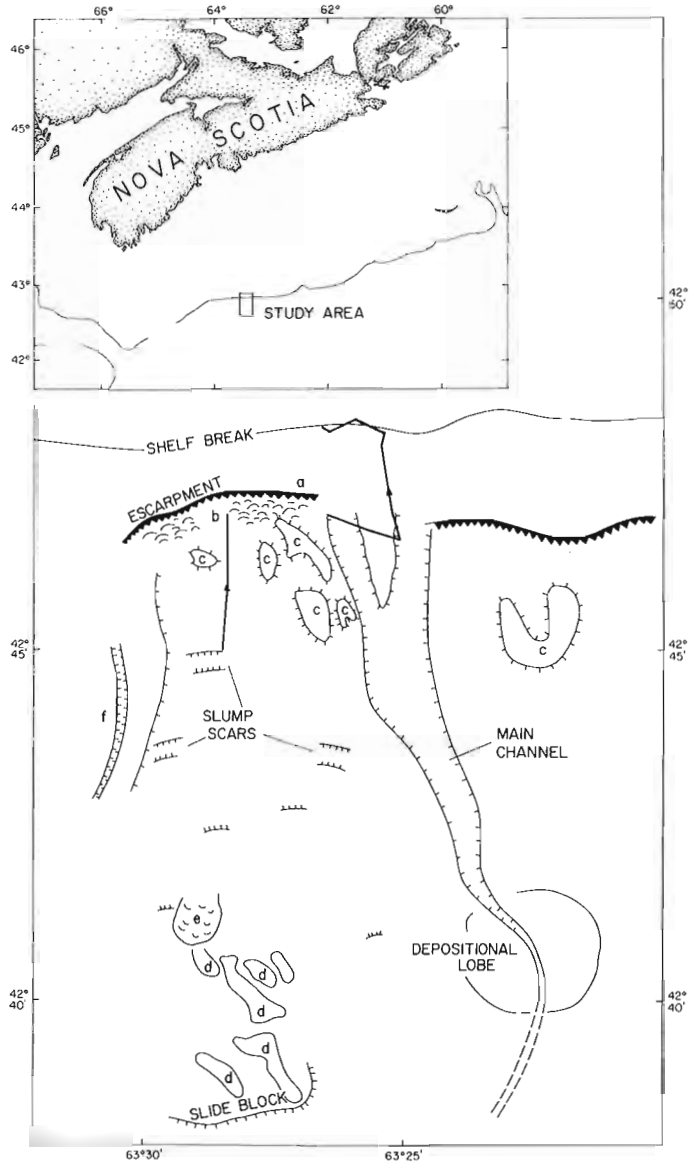

Figure 8.2. *Morphological interpration of study area (from Hill, 1981), based on GLORIA long-range side-scanning sonar records and high-resolution sparker profiles. (a) steep escarpment; (b) area of high relief and hyperbolic reflectors; (c) slide block surfaces identified from GLORIA records; (d) relief features on large slide block; (e) debris flow; (f) constructional channel on undisturbed slope area. Inset shows location of study area off eastern Canada.*

Furthermore, estimates of seabed roughness (hence drag coefficients) are desirable (Hill and Bowen, 1982), in order to relate observed surficial sediment distribution to measured currents on the uppermost slope. Previous attempts at photography and conventional side-scan sonar did not provide adequate information on bedforms and coarse sediment distribution in this area. In particular, it had not been possible to relate sediment samples to seabed mesotopography or to bedforms. Submersible dives were planned to resolve such questions.

Operation of **Pisces IV**

The operational features of **Pisces IV** are described by Levings and McDaniel (1973). It holds a pilot and two observers, each with forward-viewing ports with overlapping fields of view. It is equipped with two mechanical arms which can be used for sampling. Maximum operating depth was 800 m. The submersible did not have a positioning system. Dives were navigated by dead reckoning between the start and end of the dive, which were positioned from the mother ship, **Pandora II**, using Loran-C. Heading, estimated speed, submersible depth and estimated height off the bottom were recorded every minute during the dive; and were subsequently compiled to produce a dive profile (Fig. 8.3). Photographs were taken from handheld cameras through the ports.

Description of Dives

Dive 1051

The dive started on the mid-slope in a water depth about 470 m (Fig. 8.1, 8.3). It ran parallel to the slope across relatively rough topography for about 1.5 km and then dropped into the floor of the top of the eastern branch of the slope valley, which has too little relief to show up clearly on the bathymetric map (Fig. 8.1). The traverse followed the valley floor upslope for a short distance, and then ran obliquely up the wall of the valley, over a low sharp marking the shelf break, and finally westward along the outermost continental shelf.

The early part of the dive was over a mud bottom, but the valley floor at 500 m water depth was sandy mud. The seabed was sandy with some boulders and cobbles on the wall of the valley and shelf break escarpment. The outermost continental shelf was again sandy, with common patches of boulders and gravel, and some low ridges of large boulders.

Dive 1053

Dive 1052 was aborted before reaching bottom after a technical malfunction in the submersible. Dive 1053 started in 700 m water depth and traversed due north up the continental slope to 400 m water depth on the uppermost slope (Fig. 8.1, 8.3). The bottom was muddy, with abundant biogenic pits and mounds on the mid-slope to about 480 m.

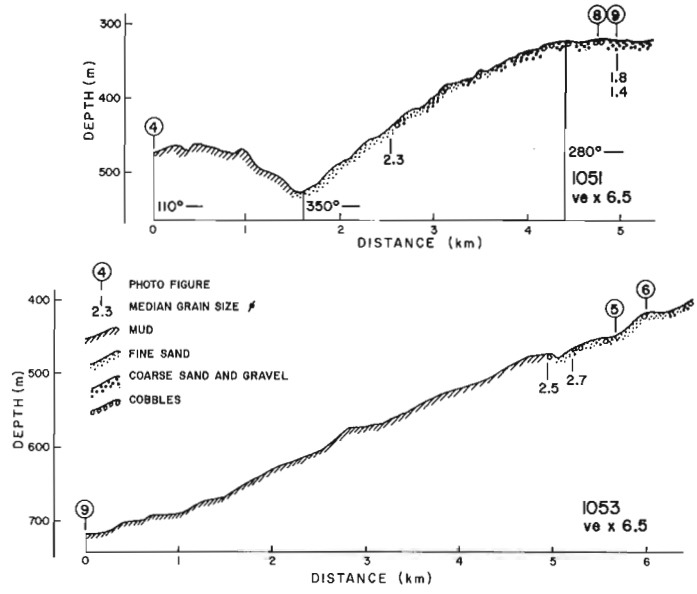

Figure 8.3. *Profile of dives 1051 and 1053, showing median grain size of sediment samples, location of photographs in Figures 8.4 to 8.9, and type of surficial sediments.*

Figure 8.5. *Gravel ribbon, upper slope, 425 m, photo P1-21, dive 1053.*

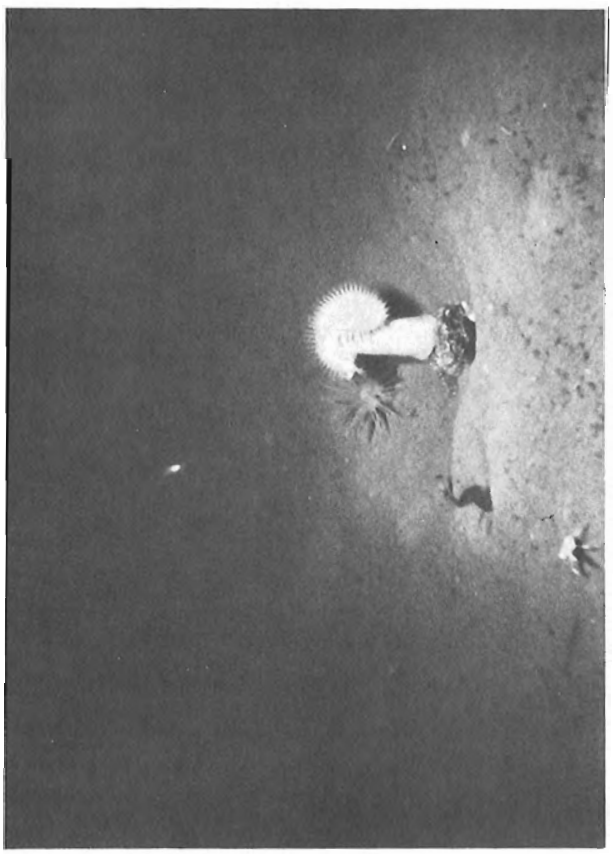

Figure 8.4. *Isolated cobble in mud, mid-slope, 480 m, photo N1-8, dive 1051.*

Local relief on the seafloor was irregular, appearing to rise in a series of steps, but with sloping surfaces that face in all directions from east through southwest and gradients of up to 1 in 3. The upper slope consisted of silty sand with scattered gravel and larger clasts. A 5 m-deep depression was crossed at about 480 m water depth, near the beginning of the sand and gravel bottom (Fig. 8.3). Whether the depression is a continuous valley feature, or merely a result of a local north-dipping slope is not clear.

Observations and Discussions

Pleistocene Slump Blocks

On both dives, the seafloor was observed to be irregular on a horizontal scale of tens or hundreds of metres and a vertical scale of metres to tens of metres. The seafloor along dive traverse 1053 appeared to rise in a series of steps, with slopes in a variety of directions at angles of up to 1 in 3. These variable slope directions suggest irregular slump blocks, not continuous slope valleys. This scale of irregularity is invisible in our bathymetric and seismic-reflection profiles. The observations from **Pisces** support the interpretation of an irregular late Pleistocene slump-block morphology masked by a veneer of Holocene sediment.

Slope Valleys

Dive 1051 traversed up one branch of the main slope valley. The valley walls were continuous, with side gradients of tens of degrees, and no definite layered outcrops were seen. Locally linear ridges up to 10 cm high and several metres long had steep faces in the downslope direction, transverse to the valley. These are tentatively interpreted as extensional features related to surficial slumping.

At about 500 m water depth the valley appeared to contain sandier sediment than the muddy seafloor to the west. It also showed more biogenic disturbance of the bottom sediments. These observations suggest normal currents may be concentrated in the valley. Currents of up to 25 cm were estimated on the upper slope during the dives.

Several scraps of cable, chain, iron and plastic were seen in the channel axis but nowhere else on the dives. Their significance is unclear.

Boulders in Deep Water

There are isolated areas of rocks, commonly cobble size, but locally boulders up to 2 m diameter, on the muddy bottom of the mid-slope. These rocks are often partly buried in mud (Fig. 8.4). Some rocks were isolated, but many occur associated with pebbles, in clusters less than 1 m across. These clasts could result from either ice rafting or are remnants of down-slope slump deposits winnowed by bioturbation and not completely masked by Holocene sediment. In either case, the boulders are probably relict late Pleistocene features.

Coarse Clasts on the Upper Slope

The surficial sediment on much of the upper slope, in water depths of less than 450-500 m, is silty sand, with sand content increasing up slope. There are scattered gravel clasts and shell debris. Cobbles and boulders, similar to those described above, occur locally. The only bedforms observed were gravel ribbons oriented along slope (Fig. 8.5) and scour pits on the southeast sides of large boulders (Fig. 8.6).

Figure 8.6. *Boulder and scour pit, upper slope, 410 m, photo P1-26, dive 1053.*

Figure 8.7. *Gravel patches, outer shelf, 330 m, photo N2-7, dive 1051.*

Figure 8.8. *Boulder ridges, outer shelf, 330 m, photo N2-3, dive 1051.*

Figure 8.9. *Surface bioturbation in mud showing pit 15 cm deep, 60 cm diameter, mid-slope, 707 m, photo P1-3, dive 1053.*

Sediments of the Outermost Shelf

Sediment on the outermost shelf is generally sand with patchy areas of gravelly sand or sandy gravel (Fig. 8.7). Gravel ribbons were observed commonly concentrated near large boulder fields (discussed below). No other distinctive bedforms were observed.

Boulder Ridges on the Outer Shelf

Low ridges of boulders and associated cobbles and gravel are common on the outer shelf. Individual boulders are as large as 1.5 m in diameter, and the ridges were metres to tens of metres wide, with steep sides (Fig. 8.8). The long dimension of the ridges is approximately east-west, parallel to the shelf edge. Gravel is concentrated around the ridges and grades laterally into gravel patches. The ridges presumably have a glacial origin and may be related to de Geer moraines or a terminal moraine feature at a calving ice-front, or to iceberg scour.

Bioturbation

Bioturbation is intense on the muddy mid-slope, producing a hummocky bottom of pits and mounds (Fig. 8.9). Pits have relief of as much as 10 to 20 cm and are up to 50 cm wide. Smaller, steep-walled burrows are common. Some burrows have brought red (possibly late Pleistocene) sediment to the surface.

The scale of the burrows is larger than expected. This has important implications for estimating bottom roughness and drag coefficients, as used by Hill and Bowen (1982) in relating surficial sediment distribution to measurements of modern currents. It is surprising that with such large scale bioturbation Hill (1979, 1981) could easily correlate beds only a few tens of centimetres thick in almost all cores from this area.

The frequency with which fish nosed into the bottom, thereby stirring up clouds of muddy sediment up to 20 cm thick was also unexpected. In these water depths it appears that fish, not burrowing or sessile filter feeding organisms, are probably the dominant cause of resuspension.

Conclusions

The two submersible dives on the Scotian Slope at longitude 63°W are consistent with the slump-block character of the area previously inferred from high-resolution seismic-reflection profiles. Evidence of current scour around boulders and the development of gravel ribbons near the shelf edge and to water depths of 450 m, confirm that the modern current regime actively moves coarse sediments in substantial water depths. Boulder ridges on the outermost continental shelf are probably of glacial moraine origin. The shelf edge appears to be an area of net sediment removal, with the development of lag gravels, in contrast to deeper areas where Holocene muds have accumulated.

Acknowledgments

We thank the Pisces pilots and the Master and crew of **Pandora II.** This manuscript was reviewed by M. Hampton, H. Josenhans and J.P.M. Syvitski.

References

Hill, P.R.
1979: Late Quaternary sediments on the Nova Scotian continental slope; Unpublished report, Department of Geology, Dalhousie University, Halifax, N.S., 109 p.

1981: Detailed morphology and late Quaternary sedimentation of the Nova Scotian slope, south of Halifax; Unpublished Ph.D. thesis, Dalhousie University, Halifax, N.S., 300 p.

Hill, P.R. and Bowen, A.J.
1982: Modern sediment dynamics at the Shelf-Slope boundary off Nova Scotia; in The Shelf-Slope Boundary: critical interface in continental margins, editors D.J. Stanley and G.T. Moore, Society of Economic Paleontologists and Mineralogists, Special Publication.

Hill, P.R., Aksu, A.E., and Piper, D.J.W.
1982: The deposition of thin bedded subaqueous debris flow deposits; in Marine Slides and other Mass Movements, editors S. Saxvo and J.K. Nieuwenhuis, NATO Conference Series, Series IV: Marine Sciences, v. 6, Plenum Press, N.Y., p. 273-287.

King, L.H.
1970: Surficial geology of the Halifax-Sable Island map area; Marine Sciences Directorate, Department of the Environment, Marine Sciences Paper 1, 16 p.

Levings, C.D. and McDaniel, N.
1973: Biological observations from the submersible Pisces IV near Britannia Beach, Howe Sound, B.C.; Fisheries Research Board of Canada, Technical Report 409.

Quinlan, G. and Beaumont, C.
1981: A comparison of observed and theoretical post-glacial sea level in Atlantic Canada; Canadian Journal of Earth Sciences, v. 18, p. 1146-1163.

9.

GEOLOGICAL DEVELOPMENT AND ECONOMIC EVALUATION OF THE SYDNEY COAL BASIN, NOVA SCOTIA[1]

Projects 680103 and 750096

Peter A. Hacquebard
Atlantic Geoscience Centre, Dartmouth

Hacquebard, P.A., Geological development and economic evaluation of the Sydney Coal Basin, Nova Scotia; in Current Research, Part A, Geological Survey of Canada, Paper 83-1A, p. 71-81, 1983.

Abstract

The Sydney Basin, which is almost entirely submarine, extends from northeastern Cape Breton Island almost as far as Newfoundland. It contains coal measures of Westphalian C, D and Stephanian ages, which have characteristics associated with paralic basins.

The structural style of the Sydney Basin is relatively simple and essentially saucer-shaped with the beds dipping towards the centre. A main feature is the (offshore) Boisdale Anticline, a pre-Westphalian high, which divides the western part of the Basin into the Ingonish and Glace Bay Subbasins.

The exploited part of the coalfield lies at the southern fringe of the Glace Bay Subbasin, which has its centre about 22 km from the coast. In the onshore area there are twelve mineable seams, whereas offshore there are only five. Four of these have been encountered in two oil exploration wells, drilled some 35 km seaward.

The centre of coal deposition in the nearshore area is located on the eastern side, where in the Donkin area four successive seams reach their greatest developments, with thicknesses of up to 4.3 m.

Cross-sections through five seams illustrate the development of coal and show the phenomenon of depositional splitting and rejoining. From detailed studies on two major seams it is apparent that the 'hinge lines' on succeeding terrigenous partings of the same seam run subparallel, while on partings of different seams they trend in different directions.

All coal is classed as high volatile 'A' bituminous, but there are significant changes within and beyond this category. These are related to the observation that the coalification is essentially postdeformational. This has resulted in an increase of rank with depth, as well as regionally from west to east within the same seam. Coke stability data indicate rank changes are economically favourable, because the coking characteristics of the coal improve with depth, and towards the east.

Total 'demonstrated' resources, present in ten seams, to a depth of 1220 m and/or 11 km from shore, amount to 1.6 x 10^9 t, when calculated on clean coal exclusive of partings and impure roof or bench coal. Of these in situ tonnages about 317 x 10^6 t may be suitable for metallurgical purposes, and 1.29 x 10^9 t can be classed as thermal coal. Some 82 per cent of the total estimate is contributed by four seams, namely the Phalen, Harbour, Hub and Lloyd Cove seams.

Introduction

Much new information has been gained on the extent and development of the Sydney coal basin from recent offshore exploration for oil, gas and coal. It is now realized that the detailed geology and the data acquired during some 200 years of mining relate only to a small region that lies on the fringe of an extensive offshore Carboniferous basin. Information on this basin is still limited, but interpretation of the new data in light of existing knowledge has considerably broadened the geological picture, as will be shown in this paper.

Location, Age and Stratigraphy

The Sydney coal basin is situated in northeastern Nova Scotia on and offshore Cape Breton Island (Fig. 9.1). It consists of two parts: a small land area of about 520 km^2 (200 square miles) and a region where mining is carried out below the sea. Both form part of a large Carboniferous basin that extends almost as far as Newfoundland, occupying some 36 300 km^2 (14 000 square miles). It is referred to as the Sydney Basin and its extent was determined by King and MacLean (1976) using shipboard geophysical and acoustic methods.

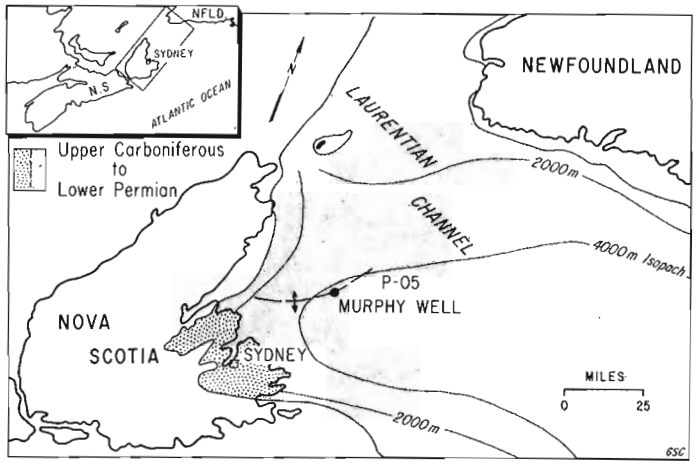

Figure 9.1. *Sydney coalfield and adjacent Carboniferous Basin (after King and MacLean, 1976).*

[1] Presented at the Ninth International Congress of Carboniferous Stratigraphy and Geology, Urbana, Illinois, May 22, 1979.

The coal-bearing rocks of the onshore part of the coal basin belong to the Morien Group, which, on the basis of the megaflora and spore florule, has been assigned a Westphalian C and D age (Bell, 1938; Hacquebard et al., 1960). The Group reaches its maximum thickness of around 1966 m (6450 feet) in the Glace Bay and Port Morien Districts, and has been subdivided into three biostratigraphic zones (A to C). These zones, which are based on plant and spore fossils (Barss and Hacquebard, 1967), are transgressive towards the northwest, where the younger zones overstep the older ones.

In the offshore part additional (post-Morien) coal measures are present. They comprise spore zone D which has an assemblage indicative of Stephanian age. This zone, which was first encountered in the uppermost seam of the shore section at Point Aconi, was intersected in several offshore wells where it ranged in thickness from 183-271 m (600-890 feet). It is followed by a sequence of red beds that may extend into the Permian (Fig. 9.2).

The coal-bearing sequence contains thirteen seams that are 0.9-4.3 m (3-14 feet) thick, nine of which occur in spore zones B and C, and three seams are present in zone D. All but the youngest three coals, of which two do not outcrop in the land area, have been mined in the past. The two most productive seams have been the Harbour and Phalen seams, which have been worked extensively in the submarine area adjacent to the coast.

Structure of Sydney Basin

As the basin is almost entirely offshore, its structure could be determined only with the aid of shipboard geophysical methods, principally seismic reflection techniques. King and MacLean (1976) have pointed out that the structural style of the Sydney Basin is relatively simple and, except for local folding, essentially saucer-shaped with the beds dipping towards the deeper and central parts of the basin. Along its southern boundary, however, a marginal fold belt is present, which is manifested by folding and faulting in the land area of the Sydney coalfield (Fig. 9.3). Here the beds are flexed in open folds that trend easterly to northeasterly with prevailing dips on the flanking beds of 4-15°, reaching 30° in a few instances. This folding likely was initiated by warping during deposition, because in general the coal seams are a little thicker in the synclines than on the anticlines. Apart from two boundary faults with considerable vertical displacement, located at the western and southeastern corners of the land area, only minor thrust faulting has been observed in the coalfield. Therefore, the main structures are probably the result of variable subsidence due to sediment load enhanced by differential compaction of the coal measure strata.

The structure of the western part of the Sydney Basin has become much better known from extensive seismic reflection work, carried out for Murphy Oil Co. in 1972. A contour map was prepared from the seismic profiles on a phantom Horizon "J", which in the known part of the coalfield corresponds to the pavement of the Phalen seam. This map proved accurate during the 1977 and 1978 offshore drilling program, when the determined positions of the Phalen seam checked closely with those predicted by the map. Also the proposed correlation of the Murphy et al. P-05 well closely conformed with the predicted position. Therefore, considerable reliance can be placed on the seismic interpretation and a similar map with contours of the Harbour seam is presented as Figure 9.3. This map was derived from the Horizon "J" map by raising each contour 450 feet (137 m), which is equal to the average vertical distance between the Harbour and Phalen seams. The Harbour seam horizon was selected because it has better continuity than the Phalen seam and is the best producing coal seam with the largest reserves.

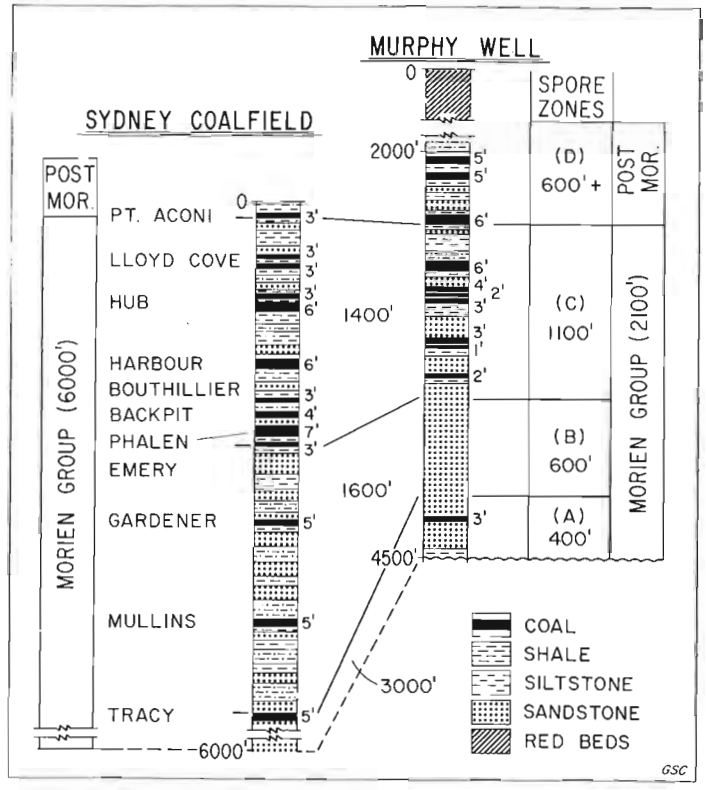

Figure 9.2. Coal bearing sequence of Sydney coalfield and correlation with Murphy et al. North Sydney P-05 well (after Hacquebard, 1979).

The main structural feature of the western part of the Sydney Basin is the Boisdale Anticline, which caused the formation of the Ingonish and Glace Bay subbasins (Fig. 9.3). The anticlinal structure is considered to be the continuation of the Boisdale Anticline of Bell and Goranson (1938) of Boularderie Island, which in turn is an extension of the pre-Carboniferous Boisdale Hills to the south and can be related to a pre-Morien high. This is revealed by the correlation of the section encountered in the Murphy et al. P-05 well with the sequence of the Sydney coalfield. Figure 9.2 shows a reduction in thickness of the individual spore zones in the Murphy et al. well as compared with the average thickness known from previous onshore geological studies. Zone A shows a thinning from 3000 to 400 feet (914-122 m), zone B from 1600 to 600 feet (488-183 m) and zone C from 1400 to 1100 feet (427-335 m) (Barss et al., 1979).

As the seismic interpretation shows a thrust fault on the south side of the (offshore) Boisdale Anticline, some lateral movement towards the southeast must have occurred. Similar faults are present on the south side of the Glace Bay Subbasin, but there the direction of movement was both to the southeast and to the southwest. The latter faults probably postdated the folding, whereas the former may have been contemporaneous with it.

The interpretation of the structure in the Morien Bay area (Fig. 9.4) was achieved by correlating the drilling results of borehole H-3 with those obtained from a shallow seismic survey, which was done with an acoustic transmitter (sparker) from a fishing boat. Drilling was carried out in Morien Bay with the expectation of intersecting the Harbour seam with sufficient cover to permit submarine mining. The 2.7 m (9 foot) thick seam was previously worked in a small land area, but could not be followed under the sea because of insufficient cover (it should be at least 55 m (180 feet) at the shoreline). Borehole H-3 was spotted in the projected

seaward extension of the eastward plunging syncline and depths of -274 m (-900 feet) for the Harbour seam and -451 m (-1480 feet) for the Phalen seam were predicted (Fig. 9.4A). The drilling results were different than expected and the sequence encountered posed a correlation problem. Palynological studies showed that the top of spore zone B occurs near -305 m (-1000 feet) and therefore the coal at -198 m (-650 feet) correlates with the Phalen seam which is in spore zone C (Fig. 9.2; M.S. Barss, personal communication). Apparently the well started in the subsea outcrop of the Harbour seam and as a result no coal was obtained in the core.

A subsequent seismic survey (Howells, 1977) provided the data for the interpretation shown in Figure 9.4B. The structure can be explained by a thrust fault with movement towards the southeast. A similar thrust fault, but with much less lateral displacement, was reported by Haites (1951) in the workings of Dominion Nos. 6 and 20 Collieries in the Glace Bay area. This fault can be extended to meet the disturbed zone that was recorded by the seismic survey in the centre of Morien Bay. It caused a lateral displacement of the synclinal axis to the south and also reversed the plunge from east to west, as was recorded seismically. As a result the Harbour seam underlies only a very small area in Morien Bay, which is delineated by the assumed subsea outcrop shown in Figure 9.4B. This body of coal is too small and shallow for submarine mining and since borehole H-3 did not intersect any other coals of mineable thickness, the Morien Bay area can no longer be regarded as a potential future reserve.

Environment of Deposition and Development of Coal Seams

Although no marine horizons are known in the Sydney succession, the coalfield is genetically a paralic basin. Such basins normally occupied coastal lowland areas of regions that were tectonically stable. In such regions, normal-banded autochthonous coals accumulated in extensive peat bogs that were formed and buried where the vegetation grew.

The development of such bogs at the present time has been described by Fisk (1960). In that paper on recent Mississippi deltaic deposits he showed that vegetation and peat formation are related to the distribution and nature of the clastic sediments. An important factor in this relationship is the variation in relief due to differential compaction. The effect of compaction by itself can provide areas of subsidence and poor drainage necessary for the accumulation of thick peat deposits. According to Fisk, the most favourable areas are interdistributary troughs and levee-flank depressions along active and abandoned river channels. Such areas would be those underlain by fine clastic sediments. Similar observations can be made on the fossil peat bogs of the Sydney floodplain, as was revealed by detailed depositional studies of the coal seams.

Isopachs on the Harbour seam (Fig. 9.5) show a general thinning towards the west and eventual termination due to splitting. The optimum seam development occurs in the Glace Bay-Donkin area, although in part this is offset in the synclinal region by post Band I erosion or nondeposition.

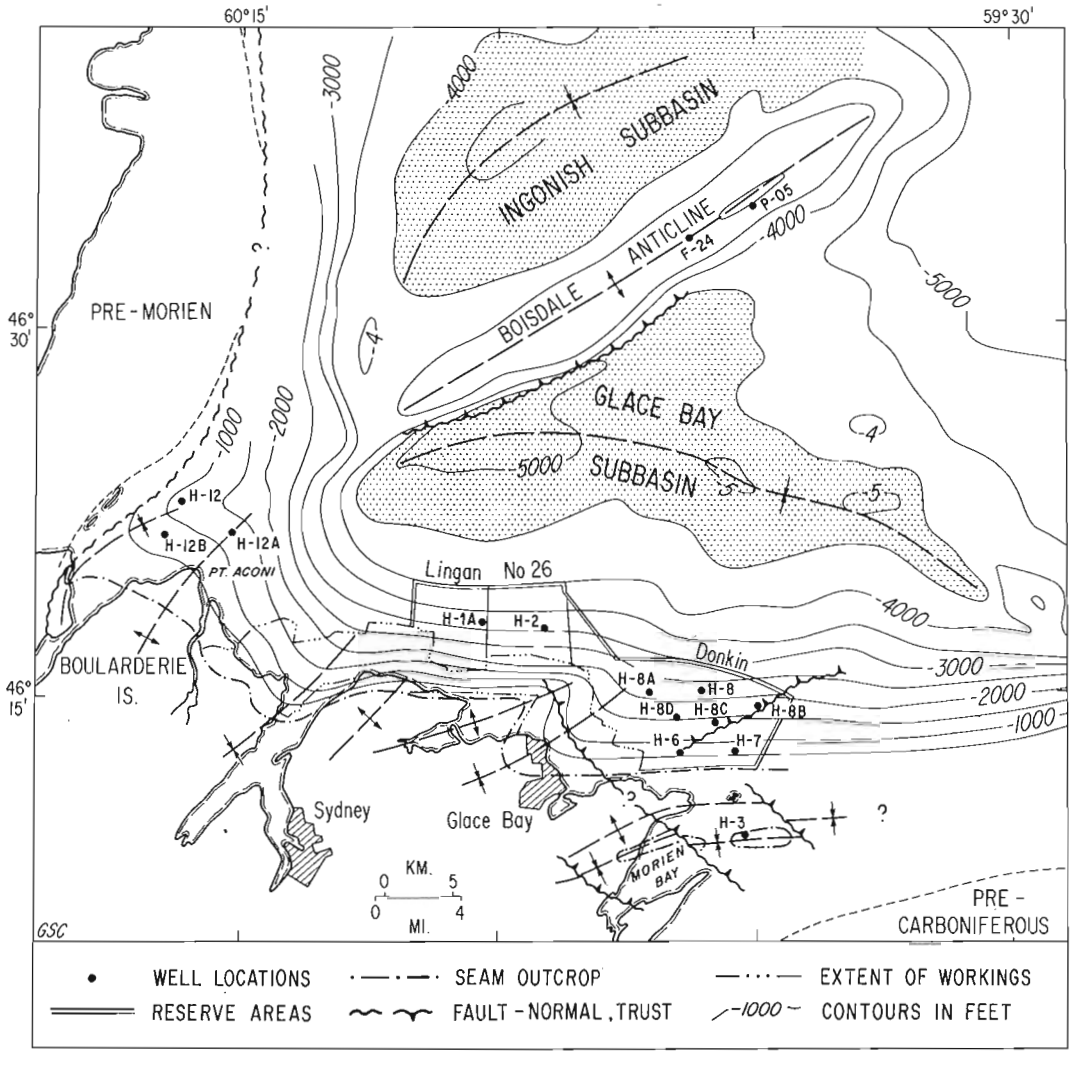

Figure 9.3. *Structural development of western part of Sydney Basin shown with Harbour seam contours.*

The depositional pattern of the Harbour seam was controlled by the underlying sediments, as is shown in Figure 9.6. The borehole sections of Figure 9.6 reveal that the decrease in seam thickness is accompanied by an increase in the thickness of clastic rocks between the main seam and Lower Bench coal. This phenomenon is related to the paleotopography that existed during the early stages of the Harbour peat accumulation. Higher ground was present in the western region due to the greater influx of clastic materials. Differential compaction, caused by differences in sedimentation, produced a localized basin in the Glace Bay-Donkin area. In this basin active peat accumulation started in the centre, while clastic sediments were still being laid down in the western part of the region. As time progressed the peat-forming vegetation migrated outward from the trough or subbasin, crossed the postulated levee and distributary channel of New Waterford, then went across the Sydney Mines interdistributary trough, and finally covered the 'Boularderie River' channel. It was only after this point was reached that peat growth occurred simultaneously over the entire areal extent of the Harbour bog.

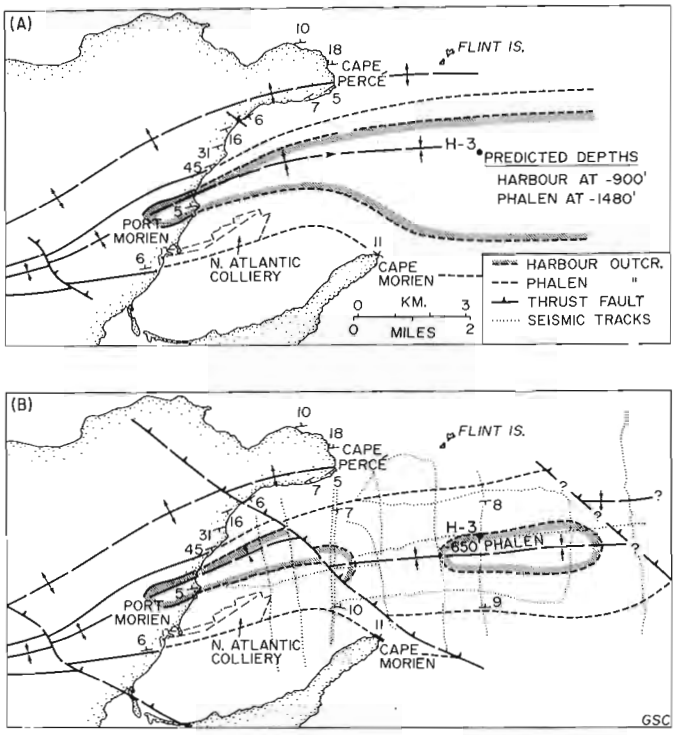

Figure 9.4. Structural interpretation of Morien Bay District; A. Before drilling; B. After drilling of borehole H-3 and seismic survey.

The development of the other major seams of the Sydney coalfield is shown by the cross-sections in Figure 9.7. The many different patterns that are represented reveal the ever changing interaction between fluvial sedimentation and peat accumulation. Some of the seams, notably the Phalen and Hub seams, show the influence of a very active river by their pronounced splitting, rejoining, and digitation. Others like the Harbour and Point Aconi seams were much less affected. However, a common characteristic of all these autochthonous coal seams is their termination by the process of subdividing and the eventual "pinching out" of individual benches.

The vertical arrangements of the seam sections in Figure 9.7 show two significant depositional features, namely:

1. A general westward seam extension from older to younger seams, reaching maximum coverage of the coalfield from the Harbour seam upwards. This includes four seams below the Phalen seam that are not shown in Figure 9.7, but which all have their nucleus of coal deposition in the eastern part of the coalfield. The western seam extensions are related to the transgressive nature of the

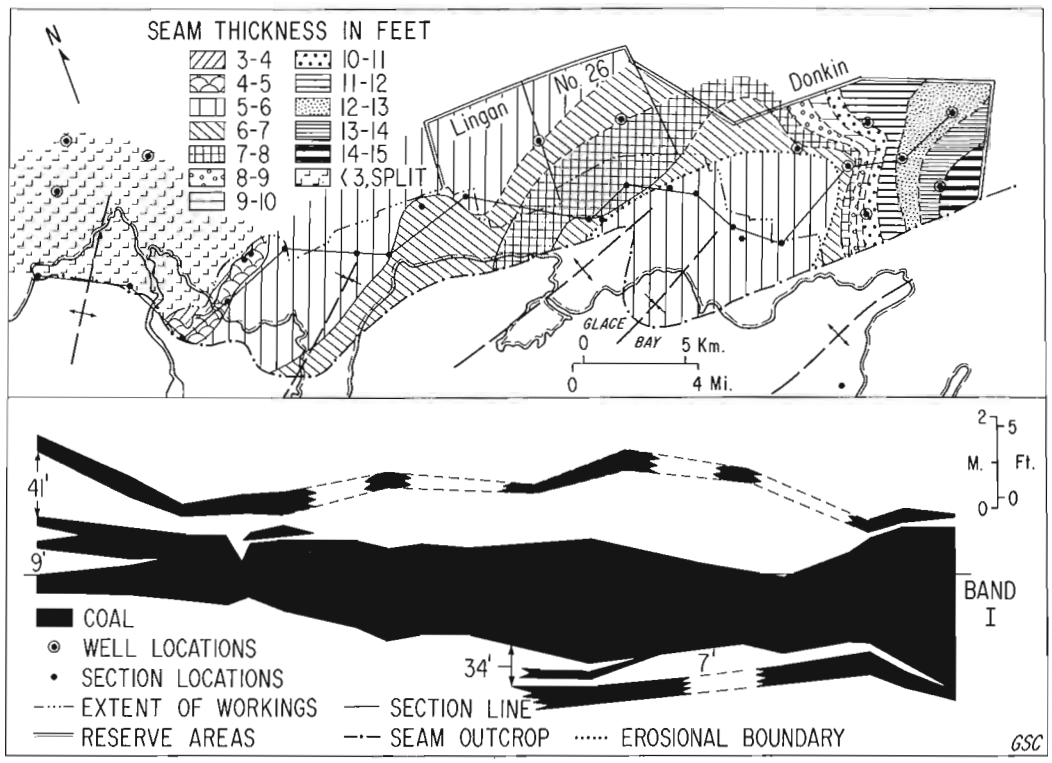

Figure 9.5. Isopach map and cross-section of the Harbour seam, Sydney coalfield.

upper biostratigraphic zones of the Morien Group (containing the younger coals), which overstep the lowest zone towards the west. The oldest coal deposition started where the basin was initiated in the eastern part of the coalfield, where below the Tracy seam some 914 m (3000 feet) of zone A sediments were laid down that are not present in the west.

2. The four uppermost seams, from Harbour to Point Aconi, all have their greatest development in the Donkin area. Here the different benches of the seams join together and form thicknesses of 3 m (10 feet) and more. The formation of this favourable area of coal accumulation was initiated during the deposition of the Harbour seam and its origin has been discussed with reference to Figure 9.5. The reason that the centre was maintained through four successive seams is probably the fact that the Donkin area was situated near the relatively steeply inclined northern limb of the Cap Percé Anticline.

Information concerning the presence of coal in the farther regions of the offshore Glace Bay Subbasin is available only from two oil exploration wells drilled on the Boisdale Anticline (North Sydney F-24 and P-05, Fig. 9.3). These wells intersected the known Sydney succession and as shown by the correlation of well P-05 (Fig. 9.2) contain the equivalents of the Harbour, Hub, Lloyd Cove and Point Aconi seams. In addition, there are two seams in spore zone D that do not occur in the land area. The thicknesses of these coals are uncertain because the formation-density logs were run at too great a speed for accurate measurements and only cuttings were provided. Nevertheless estimates of 0.9-1.8 m (3-6 feet) seem reasonable and are encouraging considering the fact that the coals occur on an anticline, where normally the seam thicknesses are reduced somewhat. Seam continuity through the Glace Bay Subbasin can be expected and an increase in thickness towards the centre is a fair assumption. However, the nature of the seam sections with regard to partings, and therefore their mineability, cannot be assessed without considerably more offshore drilling.

It would appear from the available information that a vast amount of coal may be present in the Glace Bay Subbasin and that, with the exception of the central area, a considerable part of this coal lies above the -1220 m (4000 feet) depth of mining limitation. Figure 9.3 shows that in the centre of the Subbasin the Harbour seam is projected to -1524 m (-5000 feet), which places the Point Aconi seam at -1250 m (-4100 feet), when using a 274 m (900 feet) stratigraphic separation. The coals between the Harbour and Point Aconi seams have progressively smaller areas in the centre that are below the -1219 m (-4000 feet) contour, with the younger coals all lying above it. The Glace Bay Subbasin occupies about 1300 km^2 (500 square miles) and a seam that is uniformly 1.2 m (4 feet) thick would contain 2.1×10^9 tonnes of coal. This illustrates the quantities of coal that could lie below the ocean floor within 56 km (35 miles) of the coastline.

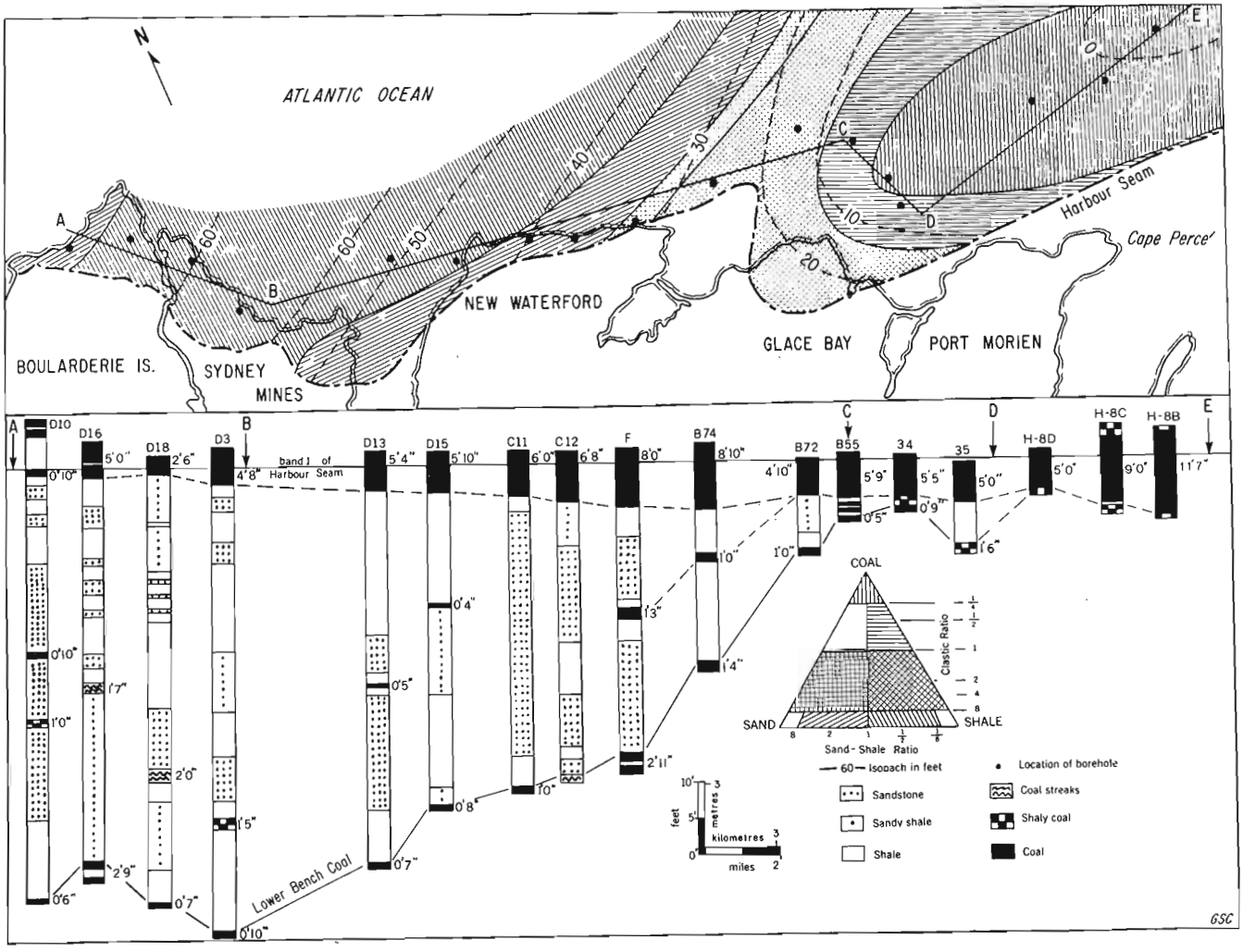

Figure 9.6. *Lithofacies map and sections of interval between Harbour seam (Band I) and Lower Bench coal (after Hacquebard and Donaldson, 1969; updated).*

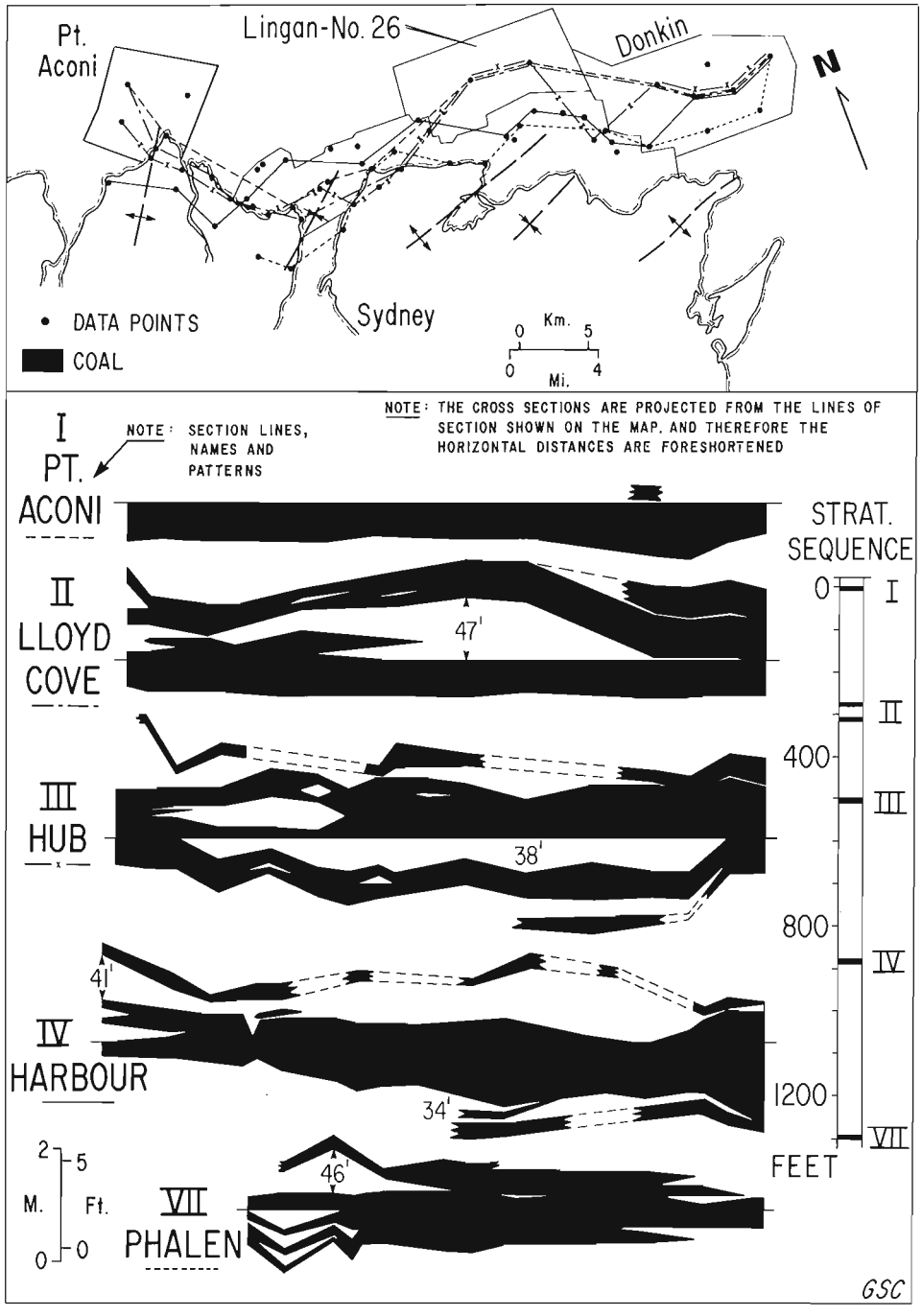

Figure 9.7. *Cross-sections through five upper seams of the Sydney coalfield (after Hacquebard and Donaldson, 1969; updated).*

Splitting of Seams

In the Sydney coalfield seam splitting is the principle reason for seam deterioration. Therefore, it is important to find the underlying cause of this phenomenon and if possible to predict its extent in the submarine area ahead of the present workings.

Seam splitting is a common feature of all coals deposited in paralic basins, and is the result of the interaction between fluvial sedimentation and peat deposition. Streams meandering through extensive lowland areas deposited sand, silt and clay on top of the peat, which afterwards continued to accumulate. After burial and compaction, these terrigenous deposits formed the stone partings within the coal. Sometimes renewed peat formation was limited, or entirely absent, leading to seam termination. It is of critical importance to determine the main river channel and its general course in order to outline the areas of seam splitting. Figure 9.8 shows how this can be determined with a detailed facies study of the Phalen and Harbour seams.

The pillars shown in the three-dimensional diagrams represent seam secitons that were measured in previously worked areas. They show the position of stone partings and splint bands. In the Phalen seam the optimum section is 2.7-3 m (8.8-10.0 feet) thick and has four partings

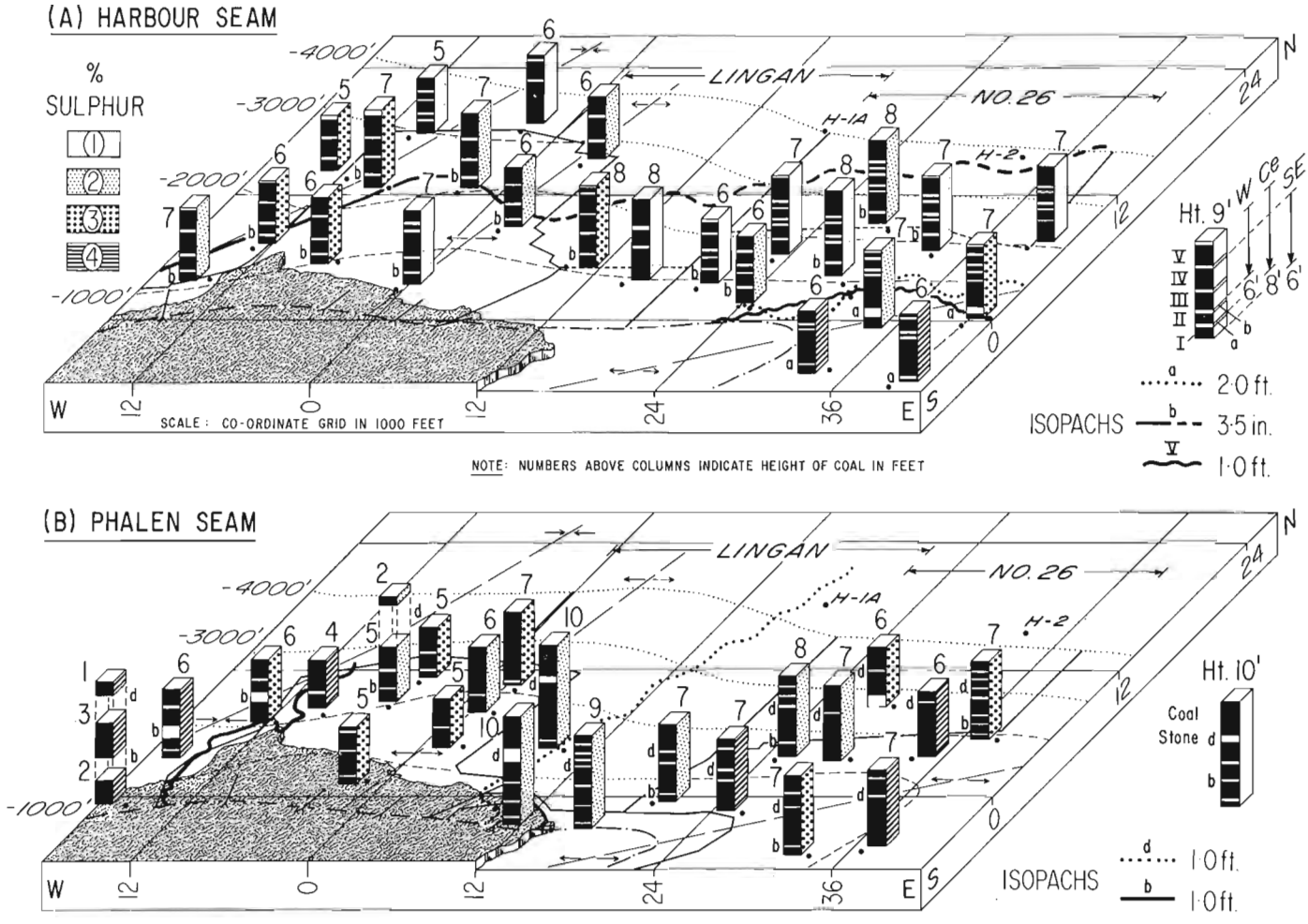

Figure 9.8. *Development of the Harbour and Phalen seams in central part of the Sydney coalfield.*

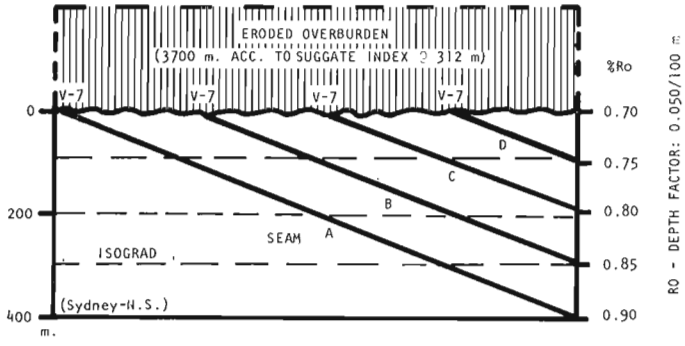

Figure 9.9. *Diagnostic features of postdeformational coalification (after Hacquebard, 1975).*

(Fig. 9.8B). Correlation of these partings shows that those marked 'b' and 'd' thicken on the west side of the Lingan area to such an extent that the individual benches of coal can no longer be mined. In the case of parting 'b' this caused the termination of mining entirely; in relation to parting 'd' it reduced the height of coal by 0.6-0.9 m (2-3 feet). For each parting a 'hinge line' has been constructed. This line is an isopach on the critical thickness of the parting, beyond which the entire seam can no longer be mined as one unit. It should be noted that the 'hinge lines' on partings 'b' and 'd' are subparallel and trend in a northerly direction. It was concluded from this that parting 'd' would only affect the western part of the Lingan Reserve, and that heights of coal of between 2.1 and 2.4 m (7 and 8 feet) can be expected to the east. This interpretation was confirmed by the offshore drilling carried out in 1977, where borehole H-1A found the equivalent of parting 'd' to be 25 cm (10 inches) thick. The 'Phalen River', responsible for partings 'b' and 'd' in this part of the field, occurs west of the study area but swings to the east in the Donkin area. This can be seen from the cross-section of the Phalen seam in Figure 9.7.

The development of the Harbour seam in the same study area is shown in Figure 9.8A. The optimum seam development is 2.7 m (9 feet) thick and consists of five benches separated by four stone partings or splint bands. The optimum thickness, however, is not present at any one locality because different parts of the seam section occur in different collieries. Collieries to the west possess benches III to V, those in the centre contain benches II to V and those in the southeast (in Glace Bay district) have benches I to IV. This variation in the thickness of the Harbour seam has been mentioned previously when discussing Figures 9.6 and 9.7. The 'hinge lines' on partings 'a' and 'b' are subparallel, as was the case in the Phalen seam, but they trend from west to east. As a result, less favourable conditions can be expected in the Lingan and No. 26 reserve areas with regard to parting 'b' of the Harbour seam, than with regard to parting 'd' of the Phalen seam. In the northern and deepest part of the reserve area only benches III to V, with a thickness of 1.8 m (6 feet) or less can be expected. This prognosis was substantiated with borehole H-1A, which intersected the Harbour seam with a thickness of 1.77 m (5.8 feet).

As a result of this comparative study it can be stated that, within specific areas of the coalfield, 'hinge lines' plotted on succeeding partings within the same coal seam run subparallel, whereas on partings of different seams they trend in different directions. This observation permits predictions on seam development ahead of existing workings, because it can indicate the approximate location of the river channels that are responsible for deterioration by seam splitting.

Coalification and Variations in Rank

In Carboniferous coals of Eastern Canada the coalification is predominantly postdeformational. Hacquebard and Donaldson (1970) showed that the rank of coal increases with the present depth below the surface but does not alter in surface exposures in relation to stratigraphic occurrence.

Figure 9.9 shows the results of a study of four coals (A to D) in the Sydney coalfield. At the surface these coals have the same Ro rank, namely V-7, notwithstanding a total stratigraphic separation of some 300 m (985 feet). However in boreholes the rank increases with depth from 0.75 to 0.80, 0.85 and 0.90 per cent Ro, respectively (or from V-7 to V-9). In underground mines the rank of individual seams increases with the depth of mining. The isograds, therefore, run horizontally and are not parallel to the seams as is the case in predeformational coalification. This means that the coal obtained its present rank from the maximum overburden that existed after deformation. In the example shown the eroded overburden was calculated at 3700 m (12 140 feet), using the method employed by Suggate (1959).

The Sydney coal is classed as high volatile 'A' bituminous but within and even beyond this broad category there are significant changes. These variations can be judged most accurately by vitrinite reflectance measurements which can be closely related to the content of volatile matter, the commonly used rank parameter. Within the high volatile 'A' class the reflectance ranges from 0.8 to 1.1 per cent Ro, or from V-8 to V-10. Medium volatile coal shows variations of V-11 to V-14 (M. Teichmüller in Stach et al., 1975, p. 42).

Previous studies by Hacquebard and Donaldson (1970) showed an increase in rank of the Harbour seam in Dominion Nos. 14 and 12 Collieries of V-8 to V-10 over a depth of 610 m (2000 feet). Comparable increases have been recorded recently on samples obtained from the 1977 and 1978 offshore coal drilling program. An increase was noted from 0.90 per cent Ro in workings of the Lingan mine at a depth of -350 m (-1150 feet) to 1.11 per cent Ro at -914 m (-3000 feet) in borehole H-1A. In the Donkin area the Harbour seam showed variations from 0.91 per cent Ro at -227 m (-744 feet) to 1.13 per cent Ro at -707 m (2321 feet).

In addition to these vertical changes in rank there also exists a regional increase from west to east, although it is less pronounced. The Harbour seam shows a change of two V-types over the width of the coalfield, namely from V-7 on Boularderie Island to V-9 at Donkin. This change occurs in coal that lies at about the same depth below the surface. It is also apparent by comparing readings obtained in the offshore area at greater depth. The Harbour seam intersected at -914 m (-3000 feet) in borehole H-1A at Lingan has a rank of 1.11 per cent Ro, whereas at -707 m (2321 feet) in borehole H-8 at Donkin it reached a rank of 1.13 per cent Ro. This means that it requires 207 m (679 feet) less depth of mining at Donkin than at Lingan to encounter coal of the same rank.

This double effect on rank changes, vertically and regionally, is illustrated in Figure 9.10. This rank map is based on a limited number of data and therefore only gives a general outline. It is noteworthy that the areas of equal rank cross the structure contours, which is further evidence for postdeformational coalification. As was mentioned previously, such coalification is caused by the maximum amount of overburden that existed after the deformation. The observed regional increase in rank, therefore, indicates that there existed less depth of burial in the western than in

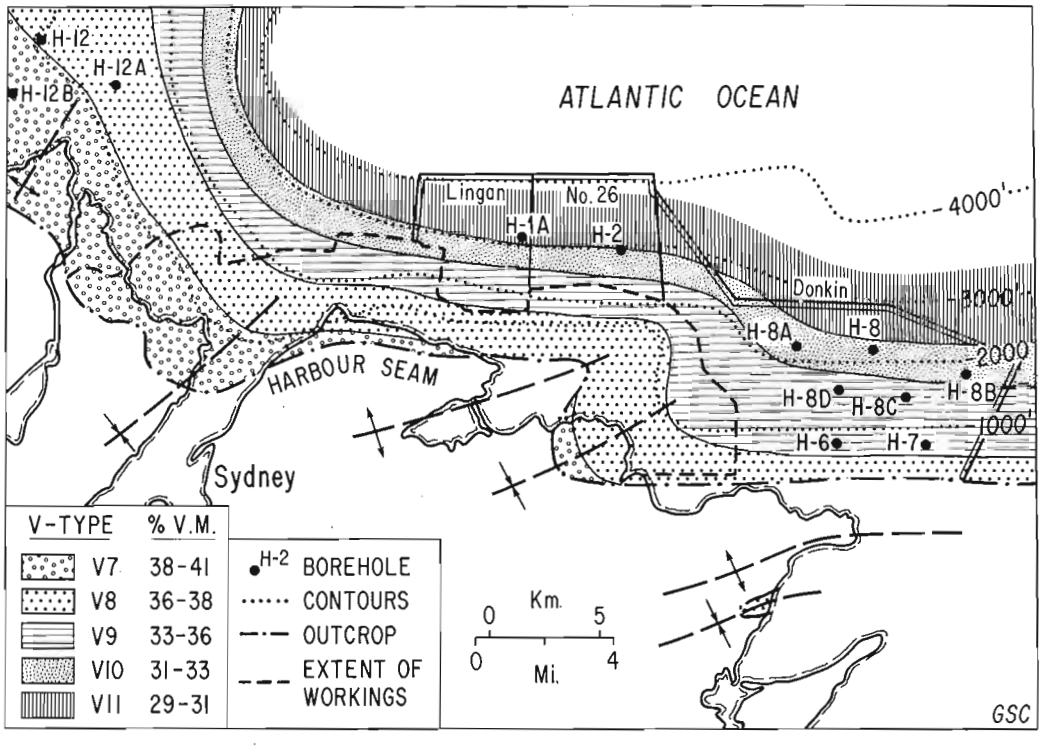

Figure 9.10. *General outline of rank variations in Sydney coalfield, illustrated with areas of equal vitrinite reflectance in Harbour seam.*

the eastern part of the coalfield. Calculations according to the method of Suggate (1959) gave 3700 m (12 140 feet) of eroded overburden in the Boularderie Island region (Fig. 9.9) as compared to 4200 m (13 776 feet) at Donkin (for locations see Fig. 9.3). This calculation is in agreement with the previously mentioned transgressive nature of the Morien Group, resulting in a regional thickening of the different spore zones from west to east.

Coal Resource Estimates

Since Dowling (1915) first published an estimate of the coal resources of the Sydney field, revisions have been made by MacKay (1947), Latour (1960), and Hacquebard (1976, 1979). The revisions were necessary as new data became available from borehole records and underground workings and because of changes in the resource parameters made in recent years.

The most significant change in the resource evaluations of the Sydney coalfield resulted from 13 wells drilled with a drillship in the offshore area during 1977 and 1978. This program provided much needed information on the submarine extension of existing workings and on those areas where seam continuity could not readily be predicted from onshore observations.

The new coal resource estimates here presented follow the format and parameters used by the Coal Division of the Cape Breton Development Corporation in their 1978 calculations. However, the author's figures (Table 9.1) are considerably lower because the heights of coal used in the calculations refer to 'clean' coal devoid of partings and impure roof or bench coal (with 15-50 per cent ash), whereas the Devco data were based on the entire opening between roof and pavement. In addition, not the seam outcrop but the -500 foot (152 m) contour was regarded as the upper boundary for resource estimates in the submarine areas.

The common parameters used in both calculations are as follows: (a) a 2.4 km (1.5 mile) influence radius of data points for coal included in the category of 'demonstrated' resources; (b) a maximum depth of mining of 1220 m (4000 feet) and/or a distance of 11 km (7 miles) from shore; (c) a minimum seam thickness of 1.2 m (4 feet) in the submarine areas.

Table 9.1

Sydney Coalfield – 'Demonstrated' Coal Resources
(In Million Tons)

Seam		Areas			Totals	
		Donkin	Lingan 26	Other	Short Tons	Tonnes (metric)
Pt. Aconi		96	-	-	96	87
Lloyd Cove		268	-	61	329	298
Hub		195	47	140	382	347
Harbour		352	180	-	532	483
Backpit		-	-	30	30	27
Phalen		-	210	-	210	190
Emery		-	-	14	14	13
Gardener		-	-	34	34	31
Mullins		-	-	100	100	91
Tracy		-	-	40	40	36
TOTALS	Short Tons	911	437	419	1767	-
	Tonnes (metric)	827	396	380	-	1603

Table 9.1 shows that after nearly 200 years of mining about 1603 x 10^6 t of 'demonstrated' coal resources remain in the (nearshore part of) Sydney coalfield. Some ten seams contribute to the grand total, but large amounts are present in only four seams, namely in the Phalen, Harbour, Hub and Lloyd Cove seams. Of these, the Harbour seam is the most important. It possesses the largest resources, amounting to 483 x 10^6 t, and has the lowest sulphur content of all the seams in the Sydney field (varying from 1-3 per cent). Parts of this seam and probably the Phalen seam as well have a good potential for metallurgical coal. The other resources, being too high in sulphur content (in excess of 3 per cent), are classed as thermal coal and after cleaning are excellent for electric power generation because of their high heating value (ranging from 7389-7778 Kcal/kg, on raw coal).

The table also reveals the significance of the Donkin area, which possesses 827 x 10^6 t in four seams. This large reserve became known entirely from the 1977-1978 offshore coal drilling program, because its potential could not be predicted from existing geological information.

Availability of Coking Coal

For the production of metallurgical coke it is necessary to have suitable coking coals available. Such coals have to be of a particular quality and grade and should possess specific properties in order to produce coke that meets the requirements of the steel industry. Foremost of these are good coking and coal blending properties, resulting in strong, non-expanding cokes with high stability factors, and coals possessing a low sulphur content. These factors are controlled by the rank and petrographic composition of the coal.

The coal presently mined in the Sydney coalfield is a high volatile 'A' bituminous coal and because of its high fluidity, has excellent blending characteristics. It is therefore valuable for the export market as metallurgical coal when the sulphur content is low.

To obtain coke of a strength required by the Sydney Steel Plant, it is necessary to add 25 per cent low volatile bituminous coal to the coal mined locally. This L.V. coal is imported from the United States as it is not available from the Sydney field at the present time. With an increase in rank of the domestic coal, less L.V. coal is needed for blending, and for medium volatile bituminous coal blending can be dispensed with altogether. Figure 9.10 shows that M.V. coal (V-11 to V-14) occurs below the -3000 foot (-914 m) contour in the Lingan-No. 26 area and below -2300 foot (-701 m) in the Donkin area. This is economically very favourable, because as mining proceeds to greater depths better metallurgical coal from a rank point of view will be produced, and less L.V. coal will need to be imported for blending purposes.

Figure 9.11 illustrates how the petrographic composition, in combination with the rank of coal, is of critical importance to the strength of the resultant coke. The rank curves of the H.V. and M.V. coals in the reflectance ranges of V-7 to V-12 (three curves) peak at about 75 per cent reactive macerals (consisting of vitrinite plus exinite plus part of semifusinite). The respective optimum stability factors that can be attained are 37, 48 and 62. It can be seen that the coke stability factors decline rapidly with lower and with higher amounts of reactive macerals.

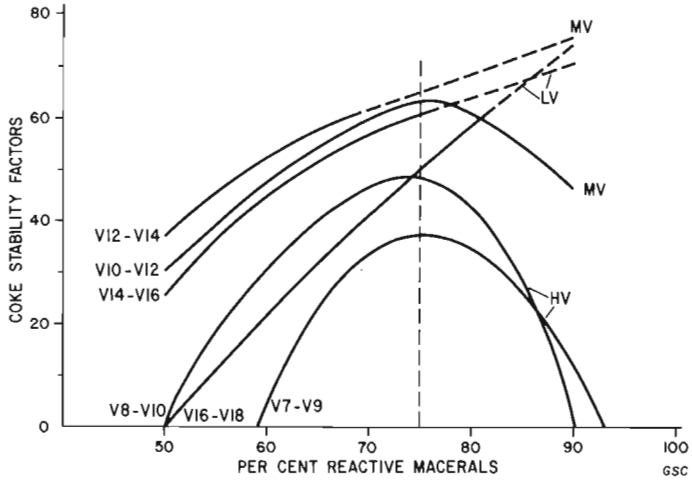

Figure 9.11. *Relationship of petrographic composition and rank to coke stability (after Cameron, 1975).*

The metallurgical coal presently produced at Sydney is from the Harbour seam in the Lingan and No. 26 Collieries. It has a rank of V-7 to V-9, averages about 80 per cent reactive macerals, and without blending with L.V. coal would yield a coke with a stability factor of 33 to 39.

Detailed petrographic and rank determinations have been made on the offshore samples to appraise the coking qualities of the Harbour seam in the reserve areas of Lingan-No. 26 and Donkin. The results show that petrographically the seam is rather stable when considered in its overall composition. The reactive components vary between 81 to 87 per cent, indicating that a change in rank is the prime factor affecting the alteration in coke stability. The latter shows a marked improvement with depth, namely from 33 in borehole H-6 at -238 m (-780 feet), to 54 in borehole H-8 at -707 m (2321 feet). As a coke stability of 55 is acceptable in a commercial operation, these results indicate that for the deeper Harbour coal samples only the addition of a small amount of L.V. coal would be necessary to achieve the desired coke strength.

From the point of view of rank and coke stability, the prospects of the Harbour seam being of metallurgical quality in the offshore reserve areas are excellent. The critical factor that remains to be considered is the sulphur content. In the Sydney coals the amount of sulphur varies considerably, both vertically through the seam section and regionally between sections. Changes of 1 to 4 per cent per seam total, sometimes 5 per cent, have been observed in the worked areas. This can be seen from the pillars in Figure 9.8 for the Harbour and Phalen seams. In general it can be stated that the highest amount of sulphur occurs in areas that are affected by seam splitting. The Phalen seam, which splits on both the eastern and western side of the coalfield, shows this relationship in Figure 9.8B.

Metallurgical coal should have less than 1 per cent sulphur, which in raw coal occurs only rarely in the Sydney coalfield. However, with the new coal cleaning facilities recently installed, it is now possible to reduce raw coal with 2 to 2.5 per cent sulphur to metallurgical standards. This means that the Harbour seam in the Lingan-No. 26 and (eastern part of) Donkin reserve areas very likely has a sulphur content that can be reduced to acceptable standards for the production of metallurgical coke. Resource calculations of these areas show 169 x 10^6 t of recoverable coal, possessing 2 per cent sulphur or less.

The sulphur content of the other seams in the reserve areas is considered too high for metallurgical use, with the possible exception of the Phalen seam in the Lingan-No. 26 area. It has 2.5 to 2.9 per cent sulphur in some locations and 1.5 to 1.7 per cent in others. In borehole H-1A the Phalen has reached the rank of M.V. bituminous coal; it has a vitrinite reflectance of 1.24 per cent and a calculated coke stability factor of 62. The resources of the Phalen seam in the 'high coal' area of the Lingan-No. 26 reserve that may possess 2 per cent sulphur or less are estimated at 36 x 10^6 t of recoverable coal.

From the preceding it is concluded that on the basis of our present knowledge, there may be as much as 212 x 10^6 t of recoverable coal resources of metallurgical quality available in the Sydney coalfield.

Acknowledgments

The author gratefully acknowledges contributions to this paper by the following personnel of the Atlantic Geoscience Centre, Geological Survey of Canada, in Dartmouth, Nova Scotia. M.P. Avery for making available the petrographic data essential for the evaluation of the coking properties of metallurgical coal. G.M. Grant for assisting with the compilation of the diagrams and M.S. Barss and A.C. Grant for their constructive comments and critical review of the manuscript.

References

Barss, M.S., Bujak, J.P., and Williams, G.L.
1979: Palynological zonation and correlation of sixty-seven wells, Eastern Canada; Geological Survey of Canada Paper 78-24, 118 p.

Barss, M.S. and Hacquebard, P.A.
1967: Age and the stratigraphy of the Pictou Group in the Maritime Provinces as revealed by fossil spores; Geological Association of Canada, Special Paper 4, p. 267-282.

Bell, W.A.
1938: Fossil flora of Sydney coalfield, Nova Scotia; Geological Survey of Canada, Memoir 155, 334 p.

Bell, W.A. and Goranson, E.A.
1938: Geological maps with marginal notes of Bras D'Or (359A) and West Half Sydney (360A); Geological Survey of Canada, Maps 359A, 360A.

Cameron, A.R.
1975: Principles of coal petrography; Symposium on coal evaluation, Calgary 1974; Alberta Research, Edmonton, Alberta, p. 51-67.

Dowling, D.B.
1915: Coalfields and coal resources of Canada; Geological Survey of Canada, Memoir 59.

Fisk, H.N.
1960: Recent Mississippi River sedimentation and peat accumulation; Compte Rendu, 4th Carboniferous Congress., Heerlen, 1958, Tome I, p. 187-199.

Hacquebard, P.A.
1975: Pre- and postdeformational coalification and its significance for oil and gas exploration; C.N.R.S. Paris, 1973 International Colloquium on: Pétrographie de la matière organique des sédiments, etc., p. 225-241.

Hacquebard, P.A. (cont.)
1976: Distribution and amounts of thermal and metallurgical coal resources in the Sydney field of Nova Scotia; Geological Survey of Canada, Atlantic Geosc. Centre, Dartmouth, N.S., Internal Technical Rpt. no. 11-K/G-76-1, 29 p.

1979: A geological appraisal of the coal resources of Nova Scotia; Canadian Mining and Metallurgical Bulletin, v. 72, no. 802, p. 76-87.

Hacquebard, P.A., Barss, M.S., and Donaldson, J.R.
1960: Distribution and stratigraphic significance of small spore genera in the Upper Carboniferous of the Maritime Provinces of Canada; Compte Rendu, 4th Carboniferous Congress, Heerlen, 1958, Tome I, p. 237-245.

Hacquebard, P.A. and Donaldson, J.R.
1969: Carboniferous coal deposition associated with floodplain and limmic environments in Nova Scotia; Geological Association of America, Special Paper 114, p. 143-191.

1970: Coal metamorphism and hydrocarbon potential in the Upper Paleozoic of the Atlantic Provinces, Canada; Canadian Journal of Earth Sciences, v. 7, p. 1139-1163.

Haites, T.B.
1951: Some geological aspects of the Sydney coalfield with reference to their influence on mining operations; Canadian Mining and Metallurgical Bulletin, v. 44, no. 469, p. 329-339; Canadian Institute of Mining and Metallurgy, Transactions, v. 54, p. 215-225.

Howells, K.
1977: A marine seismic profiling Survey to determine geological structures in coal bearing sediments in Morien Bay and adjacent offshore areas, Cape Breton Island, Nova Scotia; Nova Scotia Research Foundation Corp., Report 7-77, Project 2445, 9 p., one map.

King, L.H. and MacLean, B.
1976: Geology of the Scotian Shelf; Geologicaly Survey of Canada, Paper 74-31, 31 .

Latour, B.A.
1960: Coal reserves of Canada, prepared for the Royal Commission on Coal (1959); Geological Survey of Canada, Topical Report 17, 40 p., 12 tables.

MacKay, B.R.
1947: Coal reserves of Canada; Chapter 1 and Appendix A of the Royal Commission on Coal, 1946; Published by Geological Survey of Canada, Ottawa, Ontario, Canada, 113 p.

Murphy Oil Company, Ltd.
1972: Reflection seismic survey of a part of Cabot Strait offshore Cape Breton Island; Interpreted and reported by International Geophys. Consultants Ltd., Calgary, Project no. 79-EC-200-72-2, Map 11, Horizon "J" within Pictou.

Stach, E., Mackowsky, M.-Th., Teichmüller, M., Taylor, G.H., Chandra, D., and Teichmüller, R.
1975: Stach's textbook of coal petrology; Gebrüder Borntraeger, Berlin, Stuttgart, Germany, 428 p.

Suggate, R.P.
1959: New Zealand coals. Their geological setting and its influence on their properties; New Zealand Department of Scientific and Industrial Research, Bulletin 134, 113 p.

10.

SYSTEM OF INTERACTIVE COMPUTER PROGRAMS FOR QUANTITATIVE STRATIGRAPHIC CORRELATION

Project 690038

F.P. Agterberg[1] and F.M. Gradstein[2]

Agterberg, F.P. and Gradstein, F.M., System of interactive computer programs for quantitative stratigraphic correlation; in Current Research, Part A, Geological Survey of Canada, Paper 83-1A, p. 83-87, 1983.

Abstract

A new system of interactive computer programs expands the use of the RASC (Ranking and Scaling) (bio)stratigraphy of exploratory wells or sections. The objective of this system is to achieve quantitative stratigraphic correlation and to aid in tracing the depositional history of sedimentary basins.

Introduction

During the past five years we have developed several statistical models for the ranking and scaling of biostratigraphic events. This work was largely performed under the auspices of Project 148 (Quantitative Stratigraphic Correlation Techniques) of the International Geological Correlation Project, which will be completed in 1983.

The resulting computer algorithms (1) rank fossil events in wells or outcrop sections to arrive at the average sequence in time, (2) scale the average sequence along a relative time scale, (3) test the stratigraphic-normality of the individual (well) sequences, and (4) allow participation of rare index fossil events or of a marker horizon occurrence in the scaled sequence. The program also prints the fossil name dictionary and a regional occurrence table of the events.

The new program has been used to erect the Cenozoic foraminiferal stratigraphy of the Canadian Atlantic Margin (Gradstein and Agterberg, 1982) and to establish a quantitative range chart for Cretaceous nannofossils in the same region (Doeven et al., 1982).

The algorithms for the RASC computer program for RAnking and SCaling were written in FORTRAN IV (Agterberg and Nel, 1982a, b). Recently, M. Heller Consultants, Halifax, N.S. have edited the RASC program for release on tape and has prepared a detailed Syllabus.

Early in 1982, a 3-year project was commenced with the objective to develop a new system of interactive computer programs. This project will attempt to achieve quantitative stratigraphic correlation of sections using the RASC biozonations and will also perform geohistory analysis in the sense of Van Hinte (1978; see also Gradstein and Srivastava, 1980).

The present contribution describes initial methodology and results. Assistance in programming by Jacqueline Oliver is gratefully acknowledged.

Spline-Fitting of RASC Results

Table 10.1 contains the "distances" from origin (at the top of the composite section) for highest occurrences (disappearance events) of microfossils as estimated using RASC in 18 wells on the Labrador Shelf and Grand Banks off Newfoundland. In this paper the standard of Table 10.1 will be applied to 5 wells on the Labrador Shelf only (Fig. 10.1). These relative distances between successive events in Table 10.1 were estimated from cross-over frequencies between the events. For example, if the difference between the successive events A and B is nearly zero, this probably means that the cross-over frequency is about 50 per cent.

Table 10.1

RASC distances estimated for highest occurrences of microfossils occurring in 18 wells, Labrador Shelf and northern Grand Banks

Fossil Name	Event Code	RASC Distance	Successive Difference	Cluster Code
Elphidium sp	77	0.0000	0.0000	1
Cassidulina teretis	228	0.0000	0.1795	1
Uvigerina canariensis	10	0.1759	0.1838	1
Coscinodiscus sp1	65	0.3633	0.1215	1
Asterigerina gurichi	17	0.4848	0.5405	1
Ceratobulimina contraria	16	1.0253	0.0245	2
Coscinodiscus spp	22	1.0498	0.1788	2
Scaphopod sp1	67	1.2286	0.3874	2
Spiroplectammina carinata	18	1.6160	0.0511	3
Epistomina elegans	71	1.6672	0.1592	3
Guttulina problema	21	1.8264	0.1382	3
Gyroidina girardana	20	1.9646	0.2301	3
Globigerina praebulloides	15	2.1946	0.1037	3
Uvigerina dumblei	26	2.2983	0.3424	3
Alabamina wolterstorffi	70	2.6407	0.1216	4
Turrilina alsatica	24	2.7623	0.2160	4
Coarse arenaceous spp	25	2.9783	0.1883	4
Eponides umbonatus	27	3.1666	0.2490	4
Globigerina venezuelana	81	3.4156	0.2569	4
Globigerina linaperta	82	3.6725	0.0260	5
Pteropod sp1	31	3.6985	0.0918	5
Turborotalia pomeroli	33	3.7903	0.0219	5
Nodosaria sp8	69	3.8122	0.3061	5
Cyclammina amplectens	29	4.1183	0.1289	5
Pseudohastigerina micra	85	4.2472	0.0289	5
Marginulina decorata	34	4.2761	0.0153	5
Bulimina alazanensis	40	4.2914	0.2141	5
Epistomina sp5	118	4.5050	0.1603	5
Plectofrondicularia sp1	41	4.6659	0.2133	
Cibicidoides blanpiedi	30	4.8792	0.1418	6
Quadrimorphinella incauta	32	5.0209	0.0705	6
Cibicidoides alleni	42	5.0914	0.0517	6
Spiroplectammina dentata	35	5.1431	0.1303	6
Turrilina brevispira	86	5.2734	0.0625	6
Uvigerina batjesi	53	5.3359	0.0465	6
Osangularia expansa	49	5.3824	0.3780	6
Acarinina densa	90	5.7603	0.0247	6
Bulimina midwayensis	43	5.7850	0.0792	6
Pseudohastigerina wilcoxensis	36	5.8642	0.0899	6
Spiroplectammina spectabilis	57	5.9541	0.0047	6
Bulimina trigonalis	45	5.9587	0.3116	6
Acarinina aff. broedermanni	93	6.2703	0.0010	7
Megaspore sp1	46	6.2714	0.0655	7
Textularia plummerae	54	6.3368	0.4009	7
Subbotina patagonica	50	6.7377	0.3058	7
Acarinina soldadoensis	52	7.0435	0.5844	7
Glomospiria corona	56	7.6279	0.4045	
Gavelinella beccariformis	55	8.0324	0.2045	8
Rzehakina epigona	59	8.2369		8

Successive difference represents difference between successive RASC distances.

Clusters codes 1-8 were defined as in Gradstein and Agterberg (1982, Fig. 10.9 based on 16 wells) with 1) Pliocene-Pleistocene; 2) Late Miocene; 3) Early-Middle Miocene; 4) Oligocene; 5) (Late) Middle-Late Eocene; 6) (Early) Middle Eocene; 7) Early Eocene; 8) Paleocene.

[1] Economic Geology Division, Ottawa.
[2] Atlantic Geoscience Centre, Dartmouth.

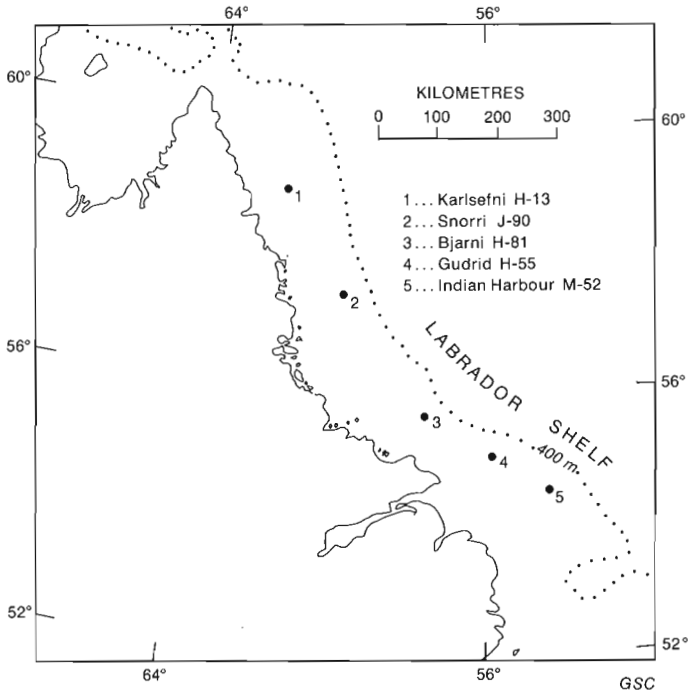

Figure 10.1. *Locations of 5 wells on Labrador Shelf used for examples in this paper.*

This situation arises if A and B are coeval in some wells, and if A is observed to occur about as many times above B as B above A in the wells used for comparison.

Clusters of events with distances which are close in value were defined on the basis of Table 10.1 and can be interpreted as biostratigraphic assemblage zones. these RASC zones can be used to compare and correlate individual wells and display sediment accumulation patterns as shown below.

One of the options of the RASC program is the so-called normality test. It consists of comparing individual well sequences of events with the standard which was computed from the cross-over frequencies for a number of sections in a larger region. Table 10.2 shows results of the normality test applied to the Karlsefni well (Fig. 10.1) in comparison with the standard shown in Table 10.1. The first column of Table 10.2 contains the codes (see Table 10.1 for fossil names) of the 24 Cenozoic microfossil events observed in Karlsefni. If an event is preceded by a hyphen, this indicates that it is coeval to the event situated immediately above it. The 24 events were observed on 16 stratigraphically successive levels down the well here numbered 1 to 16 (see column 2 of Table 10.2). The distances of all 24 events are shown in column 3. If the order of events in Karsefni were the same as that of the events in the standard (Table 10.1), the distance would never decrease in the downward direction. In reality, there is only a general increase in distance and locally events are out of place in comparison with the standard because of various types of uncertainties (Gradstein and Agterberg, 1982). Anomalous events can be identified. In the RASC output these are defined as events which are either too high or too low in a particular section with a probability of 95 or 99 per cent. Events 55 and 43 were identified as out of place in Karlsefni with a probability of 99 per cent and omitted from subsequent calculations. Distances of coeval events were averaged. The resulting unique distance values were related to their 16 stratigraphically successive levels in Karlsefni by using the spline-fitting program ICSSCU from the IMSL Library maintained by the Computer Science Centre of the Department of Energy, Mines and Resources.

The program ICSSCU is based on an algorithm originally written in ALGOL by Reinsch (1967). A FORTRAN version of this same algorithm has been published by De Boor (1978, p. 240-242). The input consists of N values X_i for the independent variable and corresponding values Y_i, i = 1, ..., N for the dependent variable. These values have the property $X_i < X_{i+1}$, i = 1, ..., N - 1. Also part of the input is a set of values D_i which are estimates of the standard deviations $(Y_i - S_{ti})$ where S_{ti} represent the true (population) values of the dependent variable which are to be estimated. Another input parameter is SM representing the sum of squares of standardized residuals of Y_i. As a guideline, Reinsch (1967) suggested that SM should lie within $N \pm (2N)^{\frac{1}{2}}$ which represents a 68 per cent confidence interval. If the values of D_i are unknown they can all be set equal to 1.0 as was done in our applications. Then the parameter SM can be considered as a knob which can be regulated. It is desirable to work with a parameter which is independent of the sample size N. For this reason, we have defined a smoothing factor SF = SM/N. This parameter merely serves to rescale the residuals. Suppose that the values D_i were set equal to a constant C instead of 1.0, then SF/C^2 will yield identical estimates of S_{ti}. The latter estimates can be written as S_i. They are part of the output, as well as (N - 1) sets of 3 coefficients for the (N - 1) cubic polynomials fitted to the data. The fitted spline function has the properties that it is continuous everywhere (also at the "knots" X_i), and that its first and second derivative are also continuous everywhere. The latter two variables assume zero values at the points where i = 1 and i = N. In our applications, the first derivative can be interpreted as the inverse of the rate of sedimentation.

Table 10.2

Events observed in Karlsefni H-13 well
(No. 1 in Fig. 10.1) compared to standard in Table 10.1

Event Code	Level Number	RASC Distance	Cluster Code
228	1	0.0000	1
22	2	1.0498	2
67	3	1.2286	2
25	4	2.9783	4
41	5	4.6659	
-118	(4.5858)	4.5056	5
69	6	3.8122	5
29	7	4.1183	5
57	8	5.9541	7
53	9	5.3359	6
86	10	5.2734	6
-30	(4.5318)	4.8792	6
-31		3.6985	5
-34		4.2761	5
42	11	5.0914	6
-46	(5.6814)	6.2714	7
36	12	5.8642	6
50	13	6.7377	7
52	14	7.0435	7
45	15	5.9587	6
-54	(6.1478)	6.3368	7
55	16	(8.0324)	8
-43	(7.6279)	(5.7850)	6
-56		7.6279	

Hyphens in column 1 indicate coeval events for which RASC distances were averaged (see values in brackets in column 2).

The 16 pairs of values that remain after averaging and omitting two anomalies (see text) are plotted in Fig. 10.2.

Figure 10.2a shows the ordinary cubic spline function fit which is obtained for smoothing factor SF = 0. In this situation, the fitted curve passes exactly through the 16 distance values used as input. Figures 10.2b to 10.2e show fits for larger values of SF. The amount of smoothing increases as a function of SF until the best-fitting least-squares straight line is obtained for SF = 1, 2, and all greater values. This straight line forms the upper limit of smoothing. Figures 10.2a to 10.2e were redrawn from displays generated on the screen of a Tektronix 4014-1. Because the RASC scale is related to geologic time, distances should in reality never decrease in the down-well direction (event scale). A decrease would violate the law of superposition of sedimentary strata. The fact that the observed distances do show local downward decreases is due to various types of uncertainties.

The pattern of Figure 10.2d (SF = 0.4) might be selected for further work because it satisfies the condition of no down-well decrease. It is noted that Figure 10.2c represents a border-line situation with approximately no decrease. However, from levels 9 to 11, the fitted RASC curve remains constant in Figure 10.2c. This would represent an infinitely large rate of sedimentation which is physically impossible. Consequently, the pattern of Figure 10.2d can be considered as the more realistic one. Similar sequences of displays where generated for 4 other wells. Non-decreasing curves were obtained for SM = 0.04 (Snorri and Bjarni) and SM = 0.2 (Herjolf and Gudrid).

Specific values along the horizontal distance scale of Figure 10.2d for Karlsefni can be selected for correlation with other wells. Use of the values 1 to 7 resulted in the pattern of Figure 10.3. The event scale in Figure 10.3 is the same as the vertical scale in Figure 10.2. The levels 1 to 7 were plotted along the event scale at values corresponding to the values 1-7 along the horizontal (RASC distance) scale using the spline-curve of Figure 10.2d. These levels were connected between adjacent wells in Figure 10.3. Although a pattern of the type shown in Figure 10.3 may be useful as an intermediate step in an interactive session for the quantitative stratigraphic correlation of a number of wells, it cannot be readily interpreted from a stratigraphic point of view. For this reason, the following additional steps should also be performed.

Construction of Age-Depth Diagrams

In Figure 10.4, the RASC distance of Table 10.1 is related to the numerical time scale as follows. The approximate age in millions of years is known for a number of the biostratigraphic events used. These dates are shown as circles in Figure 10.4. Distances for the same age were averaged and a spline-function was fitted by means of the ICSSCU program with SM = 1.0. For this purpose, age was used as the dependent variable. The curve of Figure 10.4 served to replace all distances of Tables 10.1 and 10.2 by ages (in Ma).

Only the relative order of events in wells is used in the RASC computer program for constructing standards such as Table 10.1 because rates of sedimentation differed significantly from well to well during geologic time. However, for purposes of correlation, the actual depth of the biostratigraphic events should be employed instead of relative levels along the event scale. Figure 10.5 for Karlsefni is equivalent to Figure 10.2 with distance replaced by age along the horizontal scale, and relative level of events replaced by actual depth along the vertical scale. Spline-fits for SF = 0.4 and 40.0 are also shown. In this type of diagram, a hiatus would be represented by a horizontal line. The pattern for SF = 0.4 suggests the existence of a long hiatus at about 6700 ft. Although the curve for SF = 40 is non-decreasing with depth, this spline function is not sufficiently flexible to show discontinuation in the rate of sedimentation such as hiatuses. Similar displays (all for SM = 0.4) were generated for the other four wells (Fig. 10.5). The SM = 0.4 spline-curves were intersected by vertical lines for multiples of 10 Ma. (The SF = 40 curve in Figure 10.5a was used for 50 Ma only.) The corresponding depth values can then be used for correlation.

Figure 10.6 is equivalent to Figure 10.3 with the RASC distance replaced by absolute age for 6 levels, and using depth instead of relative events order in the vertical direction. This pattern readily displays the conclusion of Gradstein and Srivastava (1980) that a broad shelf regression occurred in the Oligocene (37.5-23 Ma) probably accentuated by eustatic sea-level lowering.

Figure 10.7 (from Gradstein and Srivastava) illustrates depositional history at the site of the Karlsefni well. Cumulative sediment accumulation is plotted relative to the paleoseafloor through time. It is noted that the accumulated thickness was assumed to remain constant at about 6700 ft during the Oligocene in Figure 10.7 and this is in agreement with the pattern of Figure 10.5.

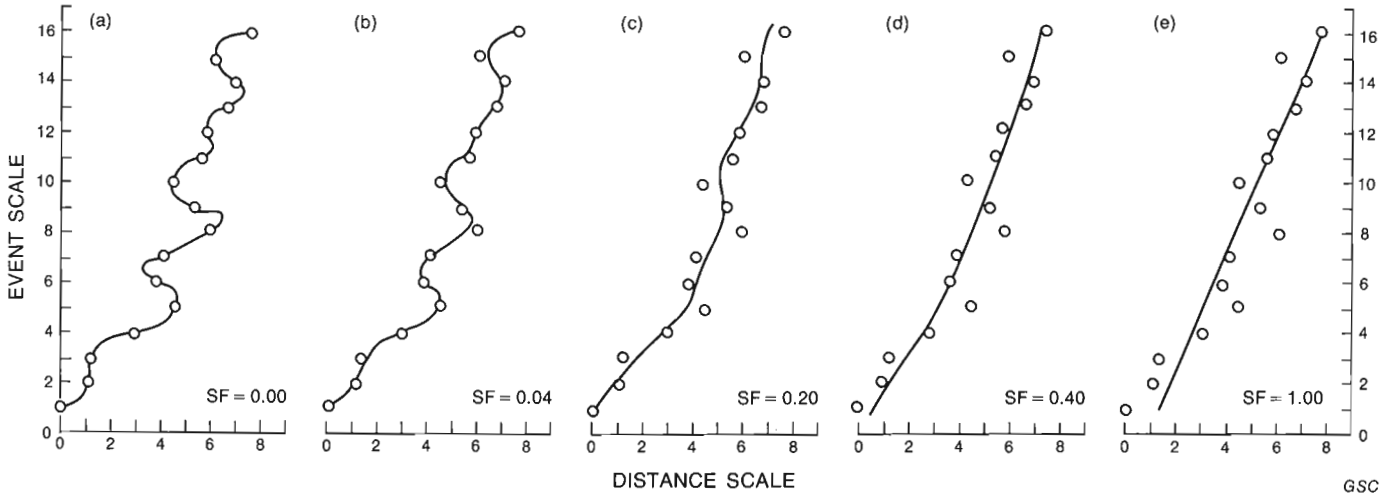

Figure 10.2. *Succession of spline curves fitted to Karlsefni data of Table 10.2 using different smoothing factors (SF). Figure 10.2d was selected for correlation in Figure 10.3.*

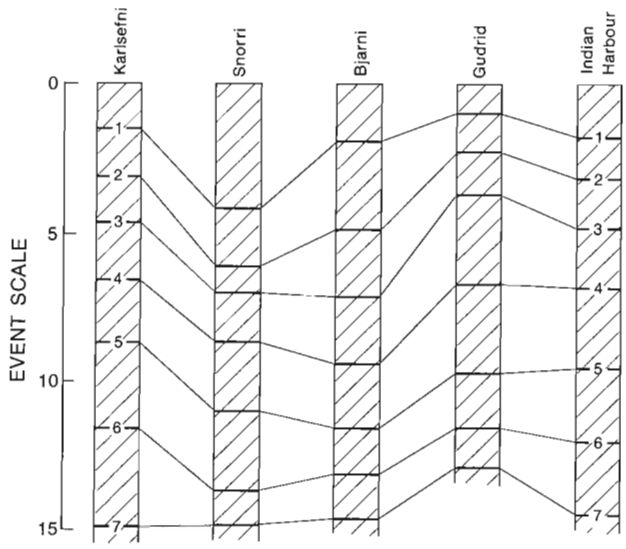

Figure 10.3. *Correlation of 5 wells shown in Figure 10.1. Levels 1-7 plotted along event scale represent RASC distances, e.g. those for Karlsefni were taken from Figure 10.2d.*

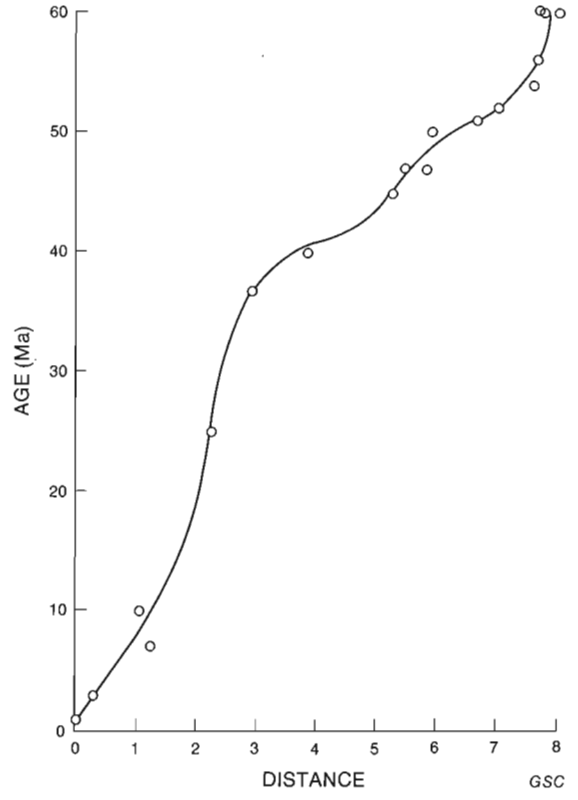

Figure 10.4. *Relation between age in Ma and RASC distance. Spline-curve with SF = 1.0 was fitted to crosses representing biostratigraphic events. Distances for events with same age were averaged.*

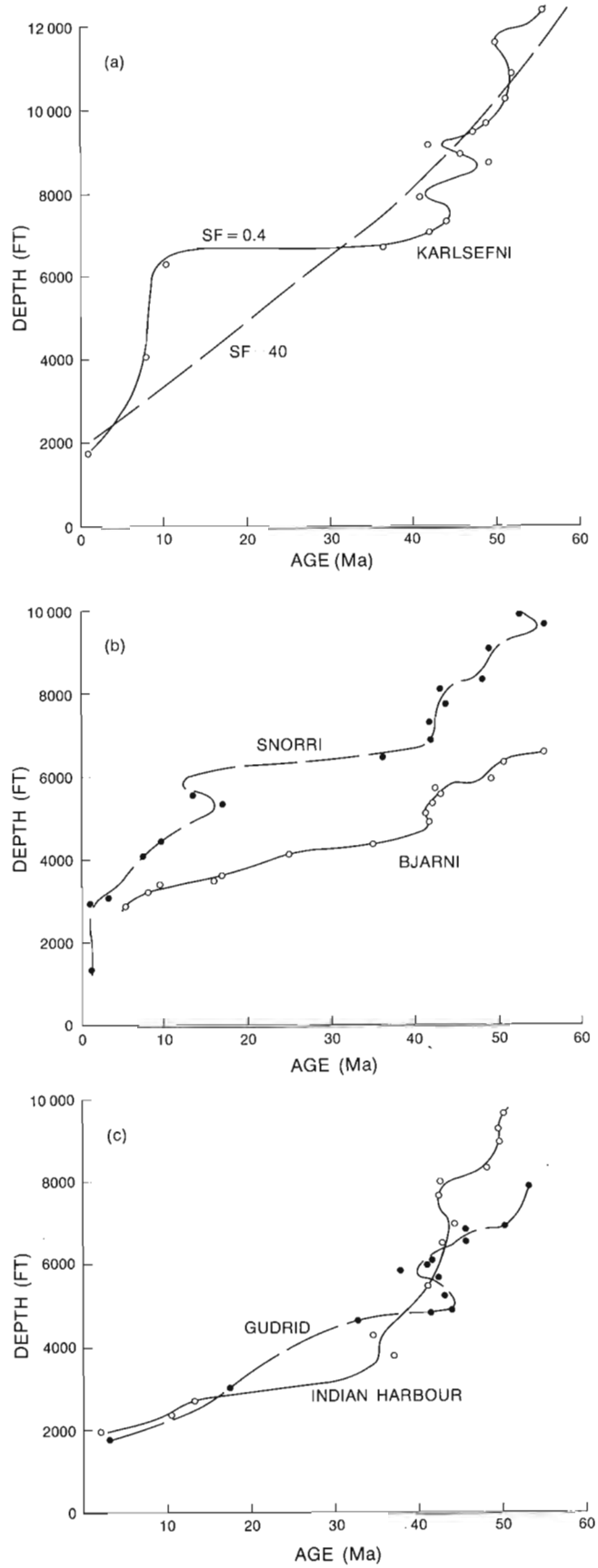

Figure 10.5. *Age-Depth diagrams of 5 wells. For Karlsefni, Figure 10.5a is equivalent to Figure 10.2 with replacement of horizontal distance scale by age (using relation shown in Fig. 10.4), and vertical event scale by depth.*

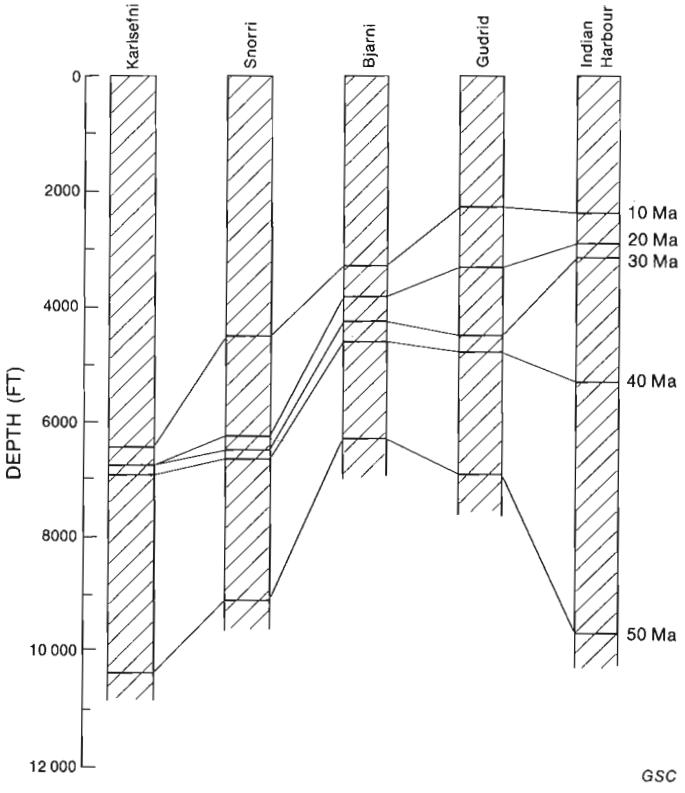

Figure 10.6. *Correlation of 5 wells shown in Figure 10.1. Levels for multiples of 10 Ma were taken from Figure 10.5a to 10.5c.*

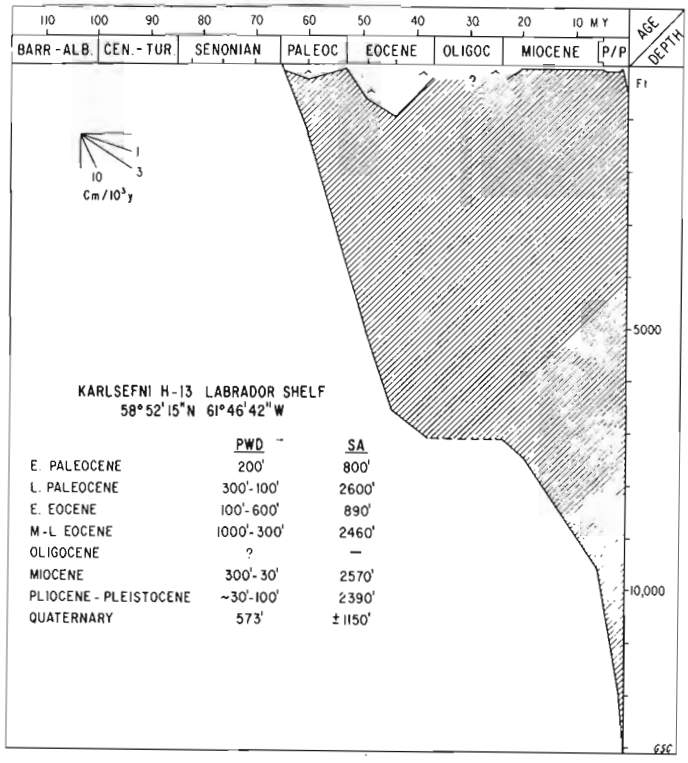

Figure 10.7. *Cumulative sediment accumulation (SA) is plotted relative to paleoseafloor through time, as derived from paleowaterdepth (PWD) interpretations to illustrate subsidence and depositional history. Well site is Karlsefni H-13 (from Gradstein and Srivastava, 1980, Fig. 10.4d, p. 274). Note similarity with Fig. 10.5a if age scale is reversed.*

Concluding Remarks

A system of interactive computer programs for quantitative stratigraphic correlation is under development. Upon completion this system should generate the types of displays shown as Figures 10.2 to 10.7 of this paper. The development and application of algorithms in addition to the subroutine ICSSCU for spline-fitting is being considered.

Additional factors including estimated paleoseafloor depth and compaction should be used to perform more refined geohistory analysis. For this purpose, information on lithology and actual depth of samples along the wells will have to become part of the input for the RASC computer program. Special attention should be paid to the problem of relating observed stratigraphic events and their average positions along the RASC distance scale to the numerical time scale in order to arrive at the best possible RASC biochronology.

By means of this interactive system, it should not only be possible to perform quantitative stratigraphic correlation and geohistory analysis but also to evaluate the propagation of errors due to uncertainties in the original data and the assumptions made.

References

Agterberg, F.P. and Nel, L.D.
1982a: Algorithms for the ranking of stratigraphic events: Computers & Geosciences, v. 8, no. 1, p. 69-90.

Agterberg, F.P. and Nel, L.D. (cont.)
1982b: Algorithms for the scaling of stratigraphic events: Computers & Geosciences, v. 8, no. 2, p. 163-189.

De Boor, C.
1978: A Practical Guide to Splines: Springer-Verlag, New York, 392 p.

Doeven, P.H., Gradstein, F.M., Jackson, A., Agterberg, F.P., and Nel, L.D.
1982: A quantitative nannofossil range chart: Micropaleontology, v. 28, no. 1, p. 85-92.

Gradstein, F.M. and Agterberg, F.P.
1982: Models of Cenozoic foraminiferal stratigraphy – Northwestern Atlantic Margin; in Quantitative Stratigraphic Correlation, J.M. Cubitt and R.A. Reyment, eds., Wiley, Chichester, England.

Gradstein, F.M. and Srivastava, S.P.
1980: Aspects of Cenozoic stratigraphy and paleoceanography of the Labrador Sea and Baffin Bay: Palaeogeography, Paleoclimatology, Palaeoecology, v. 30, p. 261-295.

Reinsch, C.H.
1967: Smoothing by spline functions: Numerische Mathematik, v. 10, p. 177-183.

Van Hinte, J.E.
1978: Geohistory analysis – Application of micropaleontology in exploration geology: American Association of Petroleum Geologists Bulletin, v. 62, no. 2, p. 201-222.

11.

DESCRIPTION ET NOTES SUR LA PÉTROLOGIE DES GRANITES DE LA RÉGION DU DÉTROIT DE FURY ET HECLA, NORD-OUEST DE L'ÎLE BAFFIN

Projet 790029

A. Ciesielski
Division de la géologie du Précambrien

Ciesielski, A., Description et notes sur la pétrologie des granites de la région du détroit de Fury et Hecla, nord-ouest de l'île Baffin; dans Recherches en cours, partie A, Commission géologique du Canada, Étude 83-1A, p. 89-101, 1983.

Résumé

Des granites cartographiés pendant l'été 1979 sont l'objet d'une étude géologique et géochimique portant sur les éléments majeurs et sur certains éléments traces. Il s'agit de granites roses mis en place dans un socle tonalitique à la fin de la dernière phase majeure de déformation. L'auteur met l'accent sur quelques diagrammes binaires et ternaires sur lesquels il se base pour évaluer les paramètres pression et température d'équilibre, le type de mise en place et le mode génétique des granites étudiés. On peut distinguer une hétérogénéité chimique relative par rapport à plus d'homogénéité macroscopique, on note aussi une ressemblance entre les granites roses de Fury et Hecla et certains granites tarditectoniques archéens de la province du Supérieur. Les hautes teneurs en uranium du granite sont liées à une phase de fracturation est-ouest postérieure à la déposition de sédiments d'âge protérozoïque ayant recouvert la partie sud du socle de Fury et Hecla.

Introduction

La campagne de cartographie menée pendant l'été 1979 dans la région du détroit de Fury et Hecla, a conduit à la découverte d'un stock de granite (sensu lato, monzonite quartzique ou adamellite) rose anormalement riche en uranium (Chandler et al., 1980). La carte géologique (Ciesielski, 1980) met en relief un bloc est où le granite est très bien défini dans l'espace ainsi qu'une zone ouest où il est caractérisé par des unités mixtes et des pegmatites. La fig. 11.1A montre un batholite rectangulaire de 35 km de côté recoupé par des failles est-ouest et des dykes-fractures nord-ouest et oblitéré au sud par des sédiments protérozoïques. L'encaissant est constitué essentiellement d'orthogneiss de composition tonalitique. À l'ouest, fig. 11.1B, le granite homogène ne se retrouve qu'en petits amas et règle générale, les grandes unités granitiques sont toujours mixtes, c'est-à-dire granites ou pegmatites et gneiss. L'encaissant est constitué de gneiss para- et orthogénétiques de composition tonalitique et granodioritique, dominé par des fractures nord-ouest. Bien que le granite rose présent à l'est montre de légères différences avec celui de l'ouest, le peu de pegmatites entre autre; l'auteur est d'avis qu'il s'agit de roches co-génétiques, bien que l'on ne connaisse pas leur extension en dehors de la région de Fury et Hecla. La ressemblance entre les contextes géologiques d'une partie de la péninsule de Melville (Schau, 1977) et ceux de la région de Fury et Hecla laisse présager un âge archéen pour ces derniers. La filiation probable entre les sédiments du secteur de Agu Bay (région de Fury et Hecla) avec le groupe de Prince Albert ainsi que des relations lithologiques d'âges et des datations géochronologiques de roches comparables mais situés à l'ouest de la péninsule de Melville (Frisch, 1980) sont d'autant de raisons laissant croire à un âge archéen pour les roches de Fury et Hecla.

Pétrographie

Dans les deux blocs, est et ouest, mis à part les roches dans lesquelles il fait intrusion, le granite rose contient souvent des enclaves, généralement métriques ou décimétriques, d'ultrabasites (amphibolites) et d'amphibolites. Les enclaves sont de type gneissique surtout dans le cas des amphibolites, mais peuvent être massives ou litées dans le cas des ultrabasiques. Les enclaves micacées (paragneiss) qui sont absentes dans le granite rose se retrouvent à quelques endroits dans les orthogneiss du bloc ouest. Tous ces divers types d'enclaves n'appartiennent à aucune grande unité cartographiable sur le terrain, si ce n'est quelques dykes de dimensions restreintes localisés sur la carte ouest. Une unité de composition monzonitique est présente dans le batholite est uniquement. Il s'agit d'enclaves de dimensions métriques, à grain moyen ou grossier, à phénocristaux ayant un contact souvent flou avec le granite rose. Elles sont réparties surtout à la périphérie du granite rose et plus rarement à l'intérieur; la ressemblance de cette roche avec le granite rose rend son identification difficile sur le terrain d'où la possibilité que son étendue en surface soit plus importante que celle décelée. Le granite rose, que ce soit à l'est ou à l'ouest, ne présente pas de particularité par rapport à d'autres roches du même type si ce n'est son contenu en uranium. Généralement, il s'agit d'une roche homogène, à grain moyen ou fin, à pegmatites associées et montrant des contacts intrusifs nettes dans les gneiss tonalitiques encaissants.

La minéralogie est relativement simple et classique, plagioclase An 8-15, souvent séricitisé, quartz, feldspaths potassiques mâclés à microcline non altérés, biotites chloritisées, muscovite probablement secondaire, apatite, allanite, opaques (magnétite et thorite) zircon et sphène. La texture est de type magmatique avec des contacts intergranulaires principalement courbes et quelquefois linéaires. Les plagioclases altérés montrent une fine zonation de bordure quand ils sont en contact avec les microclines. Des études ont démontrées qu'il s'agit d'un enrichissement relatif en Na, déjà décrit dans des granites du même type et dans des granites migmatitiques (Ciesielski, 1978). Les plagioclases à bordures zonées, à habitus trapus, plus ou moins corrodés, sont primaires comme les biotites. Les feldspaths potassiques mâclés microclines contiennent parfois des reliques de plagioclases et ont cristallisé tardivement malgré leur taille de phénocristaux (Swanson, 1977). Les seuls minéraux vraiment zonés sont les zircons, les muscovites pour leur part associées parfois à des fractures, sont considérées comme secondaires ou à tout le moins tardives. Notons que les symplectites et les perthites sont pratiquement absentes. L'ordre de cristallisation est le suivant: plagioclase An 8-15/biotite/quartz/microcline.

Les monzonites à phénocristaux enclavées dans le granite rose ont une minéralogie semblable, c'est-à-dire oligoclase, quartz, microcline en phénocristaux, biotite, amphibole, apatite, sphène, opaques et zircon. La texture et l'ordre de cristallisation sont tout à fait semblable aux

Figure 11.1A. *Carte géologique, bloc est, de la région du détroit de Fury et Hecla, île Baffin.*

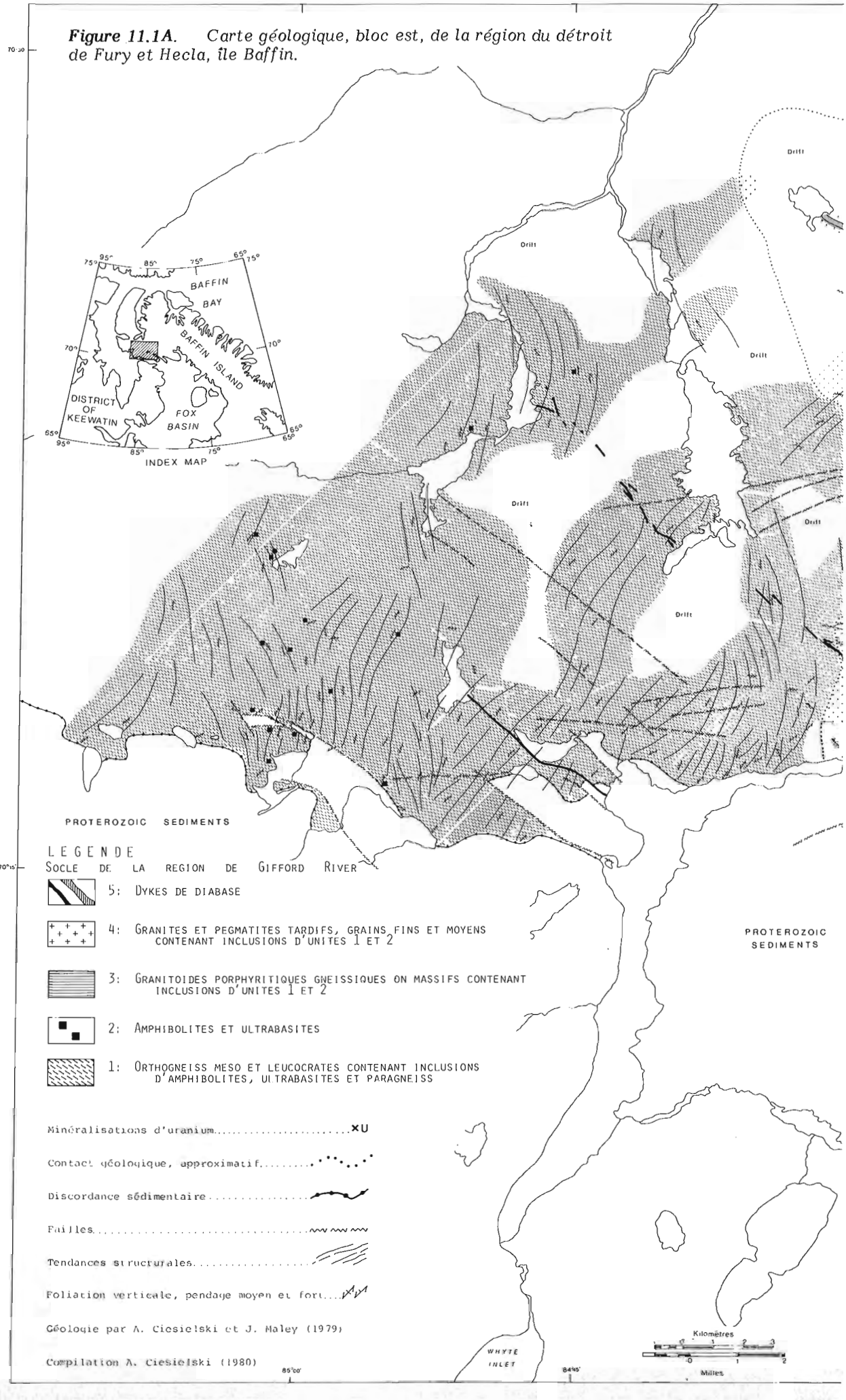


GIFFORD RIVER
Drift
Drift
Drift
Drift
Drift
Drift
Drift
Drift
PROTEROZOIC
SEDIMENTS
70°30'
70°15'
84°30'
84°15'
84°00'
83°45'

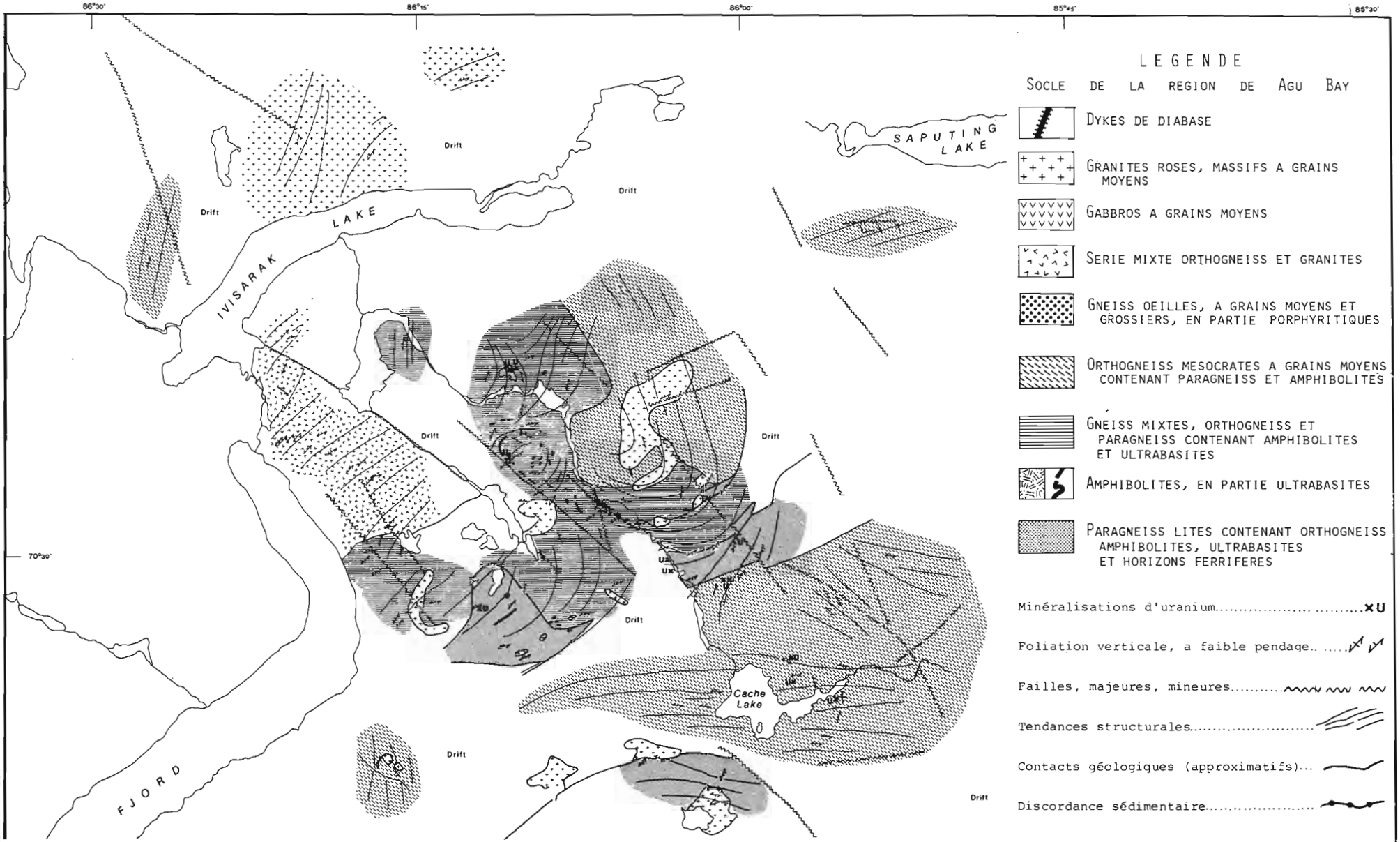
86°30'
86°15'
86°00'
85°45'
85°30'
70°30'
SAPUTING LAKE
IVISARAK LAKE
Drift
Cache Lake
FJORD
LEGENDE
SOCLE DE LA REGION DE AGU BAY
DYKES DE DIABASE
GRANITES ROSES, MASSIFS A GRAINS MOYENS
GABBROS A GRAINS MOYENS
SERIE MIXTE ORTHOGNEISS ET GRANITES
GNEISS OEILLES, A GRAINS MOYENS ET GROSSIERS, EN PARTIE PORPHYRITIQUES
ORTHOGNEISS MESOCRATES A GRAINS MOYENS CONTENANT PARAGNEISS ET AMPHIBOLITES
GNEISS MIXTES, ORTHOGNEISS ET PARAGNEISS CONTENANT AMPHIBOLITES ET ULTRABASITES
AMPHIBOLITES, EN PARTIE ULTRABASITES
PARAGNEISS LITES CONTENANT ORTHOGNEISS AMPHIBOLITES, ULTRABASITES ET HORIZONS FERRIFERES
Minéralisations d'uranium
Foliation verticale, a faible pendage
Failles, majeures, mineures
Tendances structurales
Contacts géologiques (approximatifs)
Discordance sédimentaire

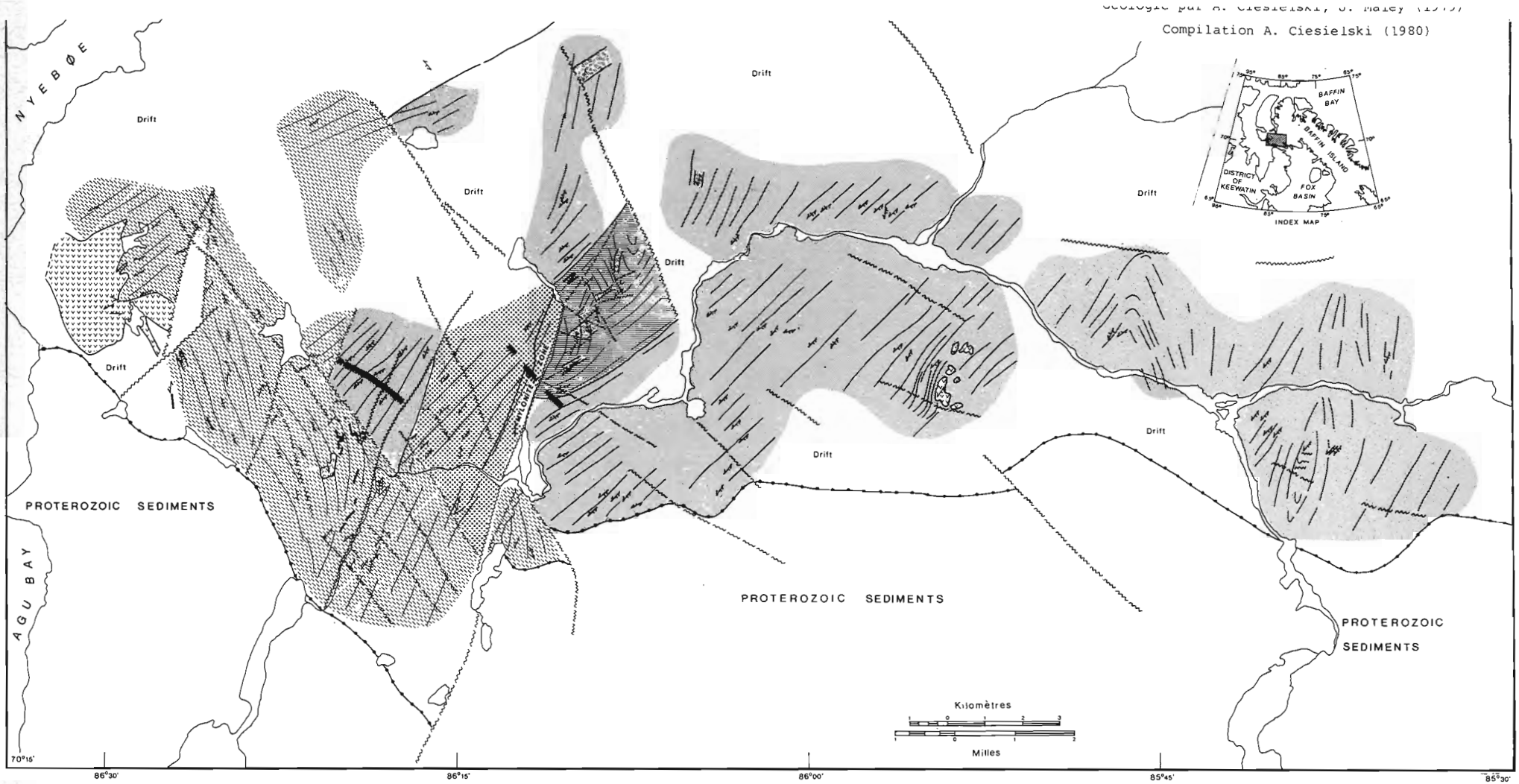

Figure 11.1B. *Carte géologique, bloc ouest, de la région du détroit de Fury et Hecla, île Baffin.*

granites roses, le contenu en biotite, amphibole et les phénocristaux les différencie toutefois. Notons que les amphiboles y sont peu répandues bien que primaires alors que dans le granite rose, la présence des amphiboles est essentiellement due à une contamination par les enclaves d'amphibolites. En plus des enclaves de tonalites qu'elle recoupe, cette unité contient aussi des enclaves d'amphibolites et d'ultrabasiques (amphibolite). Cette roche de composition monzonitique (quartzique) se retrouve un peu partout dans le granite rose mais en plus grande concentration le long du contact avec les gneiss tonalitiques. Sans phénocristaux elle ne se différencie du granite que par une couleur d'altération légèrement plus claire. Notons que l'on connaît des pegmatites associées à cette monzonite ayant une granulométrie décimétrique.

La déformation affecte peu les granites qui sont généralement massifs. Le bloc est est affecté par des grandes failles est-ouest qui sont postérieures à la déposition des sédiments et par une série de fractures nord-ouest reliées à la mise en place des dykes de diabase, aussi postérieurs aux sédiments. La minéralisation en uranium est associée à la fracturation est-ouest (Maurice, 1982) et n'affecte en rien le comportement des éléments majeurs et en traces. Le granite est affecté quelquefois par une foliation locale (en relation avec la présence d'enclaves toujours très déformées) pouvant être importante et par quelques plis dont l'origine semble régionale et en relation avec la phase de déformation qui affecte les tonalites encaissantes. Notons qu'à l'ouest, les pegmatites sont nettement plus déformées, et sont tantôt concordantes avec la foliation tantôt sécantes, laissant croire à une mise en place tardi-tectonique, ce qui est en accord avec la faible déformation du granite, étant donné son volume plus important. La fracturation est essentiellement nord-ouest, en relation elle aussi avec la mise en place de dykes de diabases quoique nettement moins évidente qu'à l'est, la phase de fracturation est-ouest étant pratiquement absente.

Études chimiques

Outre la cartographie géologique, la campagne de terrain menée en 1979 a permis la réalisation d'une étude géophysique de surface sur les anomalies uranifères (Charbonneau, 1982) ainsi qu'un échantillonnage systématique du granite à différentes échelles (Maurice, 1982). Les analyses (tableau 11.1) ainsi obtenues permettent une représentation suffisante de la composition générale du batholite est et des amas granitiques et pegmatitiques ouest. L'auteur présente ici quelques données sur la chimie des granites.

Les granites roses de Fury et Hecla ne montrent que peu de différences avec le nombre de granites roses tardi-tectoniques appartenant aux contextes volcano-sédimentaires/plutoniques du sud de la province du Supérieur (Dubé, 1978).

La fig. 11.2 donne la position des analyses catanormatives (tableau 11.1) dans la projection Qz-Ab-Or issue du tétrahèdre des granites. On notera une concentration évidente sur la ligne cotectique Qz-Or. La dérive est importante par rapport aux minima expérimentaux.

Tableau 11.1. (partie 1)

	ID	SIO2	TIO2	AL2O3	FE2O3	FEO	MNO	MGO	CAO	NA2O	K2O	P2O5	CR2O3	S	CO2	H2O
GRANITE WEST	15	72.72	.14	14.28	.40	.90	.02	.29	1.64	3.63	4.05	.05	.01	.07	0.00	.40
	16	72.13	.17	14.87	1.09	.40	.02	.35	.47	3.33	6.68	.09	.01	.05	0.00	.60
	18	73.20	.14	14.01	1.11	.30	.02	.13	1.05	3.36	4.96	.05	.01	.02	0.00	.40
	101	73.40	.16	14.72	.27	1.30	.04	.44	.56	3.37	5.16	.05	0.00	.02	0.00	.50
	139	71.78	.25	14.09	1.50	.90	.05	.26	1.25	3.14	5.06	.08	.00	.04	.20	.50
	140	72.27	.15	15.07	1.04	.30	.03	.40	1.85	3.97	3.87	.07	.01	.03	.20	.60
	141	74.45	.11	14.49	.55	.40	.02	.15	1.18	3.59	4.43	.04	.01	.01	.10	.30
	142	71.45	.25	14.91	1.24	.70	.03	.35	1.26	3.17	5.63	.09	.01	.01	0.00	.30
	143	72.17	.21	14.58	.76	1.30	.03	.52	1.47	3.06	4.82	.10	.01	.02	.20	.50
	144	73.35	.16	14.08	.84	.40	.02	.25	1.10	3.06	5.10	.07	.01	.03	.10	.50
	147	71.43	.24	14.78	.62	1.30	.05	1.02	1.14	3.83	4.31	.08	.01	.02	.20	.80
	148	72.38	.16	14.05	1.07	.50	.03	.33	.96	3.11	5.21	.05	.00	.01	.10	.70
	150	73.03	.02	13.59	.25	0.00	.00	0.00	.07	1.80	8.83	.03	.00	.03	.10	.10
	156	73.17	.14	14.19	1.34	.10	.03	.26	1.11	3.46	5.07	.06	.01	.02	0.00	.80
	157	72.28	.16	14.03	.92	.60	.03	.26	.98	3.03	5.26	.04	.00	.02	.20	1.20
	158	71.81	.16	14.18	1.19	.50	.04	.25	.97	3.21	5.24	.06	.01	.03	.10	1.00
	159	72.01	.17	14.20	.78	.80	.04	.32	.40	3.29	5.70	.05	.01	.04	.10	.70
	160	68.66	.02	19.03	.26	0.00	.00	.07	1.94	7.20	2.29	.10	.01	.04	.20	.90
GRANITE EAST	69	69.14	.49	15.49	1.57	1.80	.05	.96	1.08	3.77	5.08	.15	.01	.04	0.00	.50
	70	72.93	.21	14.65	.77	.80	.02	.63	.68	3.59	5.03	.07	.01	.05	0.00	.60
	45	71.76	.20	14.35	.87	1.00	.03	.52	.64	3.15	5.72	.07	.01	.05	.10	1.00
	43	71.08	.25	14.04	1.46	1.00	.03	.84	.51	3.19	6.13	.10	.00	.05	.10	.70
	41	72.54	.20	14.49	.83	.90	.01	.88	.47	3.21	5.60	.08	.01	.03	.40	.80
	46	71.72	.17	15.76	.89	.50	.04	.41	1.13	4.15	5.13	.08	.01	.03	0.00	.50
	68	72.30	.19	15.12	.74	.70	.02	.36	1.00	3.25	5.68	.07	.00	.07	.40	.50
	67	74.07	.24	13.46	1.14	.30	.01	.26	.31	2.26	7.50	.06	.01	.04	.20	.60
	71	71.35	.20	14.50	1.63	.40	.01	.60	.45	3.23	6.14	.06	.01	.03	.30	.60
	47	74.02	.10	13.83	.57	.40	.02	.19	.87	3.23	5.01	.04	0.00	.02	.10	.50
	102	71.70	.25	14.22	.93	1.00	.03	.51	.73	3.33	5.70	.08	0.00	.02	.20	.40
	106	73.85	.15	13.53	.70	.70	.03	.35	.59	3.11	5.05	.04	.01	.03	0.00	.40
	72	72.02	.18	14.14	1.37	.50	.02	.27	.73	3.36	5.20	.05	.00	.03	.20	.60
	48	63.75	.44	16.66	2.84	1.40	.05	1.42	.87	3.95	5.67	.16	.01	.03	0.00	1.30
	64	73.40	.18	14.33	.57	.70	.01	.41	.20	2.17	7.35	.06	.01	.04	.30	.90
	63	74.80	.10	13.89	1.37	.10	.01	.24	.22	2.96	6.49	.03	.01	.01	0.00	.40
	103	73.11	.12	13.96	.64	.60	.02	.17	.87	3.34	5.07	.05	.01	.05	.20	.50
	105	72.34	.12	15.10	.46	.70	.01	.36	.64	3.74	5.53	.04	.01	.01	0.00	0.00
	65	70.39	.47	14.79	1.71	1.20	.03	.56	1.55	3.52	4.97	.13	.00	.04	0.00	.60
	73	70.23	.26	14.60	1.25	1.00	.03	.26	1.32	3.68	4.94	.07	.01	.04	.20	.70
	74	73.58	.09	14.14	.84	0.00	.01	.27	.46	2.98	6.00	.04	.01	.02	.20	.50
	75	74.09	.12	13.96	.50	.80	.02	.51	1.12	3.55	3.74	.06	.01	.03	.10	.40
	77	72.25	.31	14.23	1.15	.70	.02	.73	.84	3.26	4.86	.07	.01	.03	0.00	.20
	79	70.22	.39	14.93	.77	1.00	.05	1.01	1.00	3.15	5.93	.13	.01	.03	.10	.80

Analyses par fluorescence X et par voie humide effectuées à la CGC

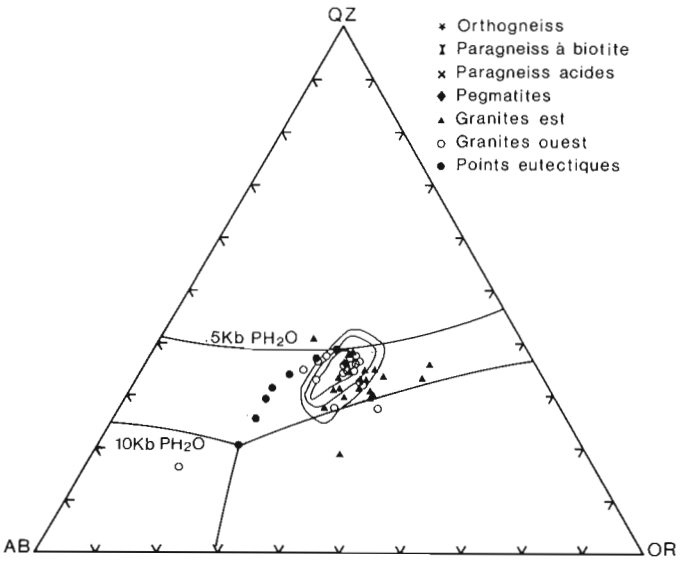

Figure 11.2. *Analyses catanormatives des granites est et ouest de Fury et Hecla dans la projection Qz-Ab-Or. Les points représentent la position des eutectiques dans Luth et al., 1964. Les champs concentriques représentent 571 analyses de granites selon des courbes de fréquence 4, 5, 6-7% (Mehnert, 1968, p. 178).*

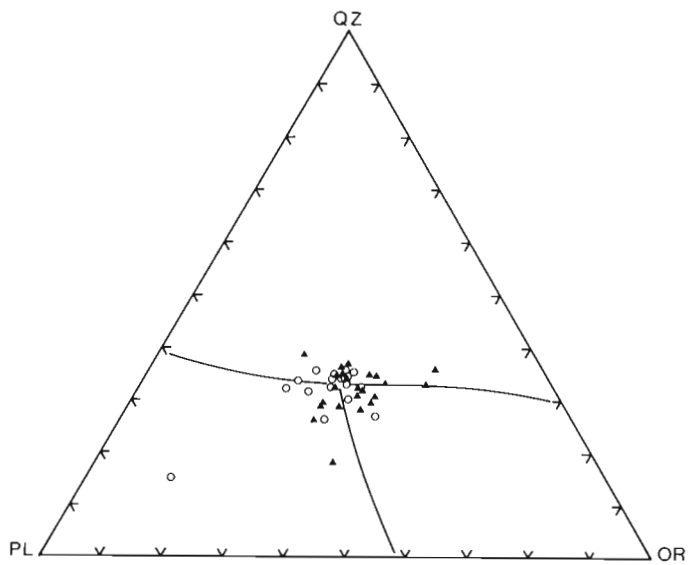

Figure 11.3. *Analyses catanormatives des granites est et ouest de Fury et Hecla dans la projection Qz-Pl-Or. Positions des lignes cotectiques, Ciesielski (1978) modifié. Voir légende fig. 11.2.*

Tableau 11.1. (partie 2)

ZR	SR	RB	ZN	NI	BA	C.I.P.W. ID	OR	AB	AN	Q	HY	AP	IL	C	MT	HEM
.014	.017	.018	.005	.006	.054	15	23.93	30.75	7.96	31.75	1.71	.12	.27	1.00	.58	0.00
.017	.018	.030	.007	.002	.167	16	39.49	28.14	2.12	25.77	.96	.20	.32	1.39	.68	.62
.013	.015	.025	.007	.005	.064	18	29.34	28.42	5.06	32.27	.33	.11	.27	1.25	.55	.73
.013	.012	.028	.008	.004	.045	101	30.48	28.49	2.54	31.44	3.03	.12	.30	2.67	.40	0.00
.026	.019	.021	.007	.004	.086	139	29.93	26.59	4.69	31.72	.66	.19	.47	1.74	2.17	0.00
.005	.024	.014	.005	.005	.089	140	22.88	33.62	7.67	30.43	.99	.16	.28	1.53	.50	.69
.008	.013	.020	.004	.001	.054	141	26.20	30.40	5.08	34.11	.47	.09	.20	1.92	.81	0.00
.024	.016	.021	.006	.008	.105	142	33.25	26.84	5.91	28.38	.88	.20	.47	1.44	1.59	.14
.025	.020	.018	.009	.002	.102	143	28.50	25.87	5.63	32.06	2.72	.22	.39	2.26	1.10	0.00
.030	.016	.020	.004	.005	.073	144	30.14	25.89	4.52	33.69	.52	.16	.30	1.87	.77	.31
.009	.016	.018	.007	.005	.048	147	25.48	32.44	4.04	28.67	4.06	.17	.45	2.32	.90	0.00
.014	.014	.026	.007	.003	.057	148	30.77	26.32	3.90	32.18	.32	.12	.29	1.87	1.21	.23
.000	.013	.044	.001	.002	.072	156	29.96	29.31	5.22	30.96	.65	.14	.23	1.09	0.00	1.34
.016	.012	.026	.005	.006	.050	157	31.09	25.60	3.43	32.64	.74	.10	.29	2.11	1.33	0.00
.015	.013	.027	.009	.004	.052	158	30.97	27.20	3.92	30.99	.52	.13	.30	1.79	1.16	.39
.014	.012	.027	.009	.003	.047	159	33.67	27.80	1.21	29.84	1.32	.10	.32	2.16	1.14	0.00
.020	.012	.027	.006	.001	.065	160	13.53	60.93	7.75	14.57	.16	.23	-.09	1.66	0.00	.26
.012	.012	.010	.002	.007	.011											
.036	.015	.024	.010	.007	.080	69	30.02	31.92	4.54	23.80	3.58	.36	.93	2.13	2.27	0.00
.014	.015	.024	.006	.003	.089	70	29.73	30.40	3.14	30.28	1.39	.16	.40	2.14	1.11	0.00
.018	.014	.028	.008	.004	.099	45	33.80	26.63	2.31	29.46	2.04	.16	.39	2.13	1.26	0.00
.026	.024	.025	.008	.006	.134	43	36.21	26.97	1.58	27.06	2.27	.23	.47	1.59	2.11	0.00
.015	.011	.023	.004	.005	.071	41	33.12	26.14	0.00	31.53	2.79	.18	.37	3.34	1.20	0.00
.008	.015	.027	.007	.009	.080	46	30.33	35.13	5.26	25.04	1.01	.19	.32	1.44	1.13	.11
.015	.024	.021	.005	.005	.071	68	33.59	27.49	2.15	30.06	1.15	.17	.36	2.93	1.08	0.00
.017	.028	.024	.005	.007	.207	67	44.35	19.08	.34	31.69	.56	.13	.45	1.50	.17	1.03
.017	.015	.027	.004	.007	.139	71	36.27	27.29	.22	28.16	1.50	.14	.37	2.47	.64	1.19
.007	.019	.019	.005	.005	.075	47	29.59	27.29	3.62	34.21	.56	.09	.19	1.78	.82	0.00
.021	.015	.028	.007	.009	.062	102	33.66	22.18	2.02	28.58	1.93	.18	.48	1.83	1.35	0.00
.012	.013	.029	.006	.008	.060	106	29.86	26.30	2.83	34.50	1.30	.09	.29	1.91	1.02	0.00
.019	.016	.024	.006	.007	.071	72	30.71	28.41	2.16	31.25	.68	.12	.34	2.20	1.09	.65
.067	.017	.027	.008	.007	.110	48	33.50	33.45	3.51	15.41	3.52	.37	.93	2.73	3.27	.59
.013	.009	.035	.005	.009	.061	64	43.45	16.20	0.00	33.30	1.46	.14	.35	3.22	.83	0.00
.008	.011	.027	.001	.005	.064	63	38.34	25.02	1.07	31.95	.59	.06	.18	1.61	.03	1.35
.010	.012	.028	.005	.006	.044	103	29.99	28.23	2.84	32.66	.73	.12	.23	1.94	.93	0.00
.012	.012	.028	.003	.001	.055	105	32.70	31.66	3.06	27.19	1.61	.10	.23	1.83	.67	0.00
.043	.021	.022	.010	.005	.133	65	29.38	29.82	7.16	26.91	1.40	.30	.89	.99	2.48	0.00
.027	.025	.023	.009	.004	.100	73	29.18	31.12	5.08	27.18	1.00	.17	.49	1.35	1.81	0.00
.005	.013	.025	.002	.003	.059	74	35.45	25.23	.90	32.48	.68	.09	-.03	2.41	0.00	.84
.008	.017	.008	.005	.006	.091	75	22.11	30.06	4.72	35.92	2.10	.15	.23	2.33	.73	0.00
.014	.020	.021	.006	.005	.076	77	28.72	27.58	3.88	31.96	1.32	.17	.59	2.19	1.31	.25
.021	.026	.027	.010	.006	.182	79	35.06	26.65	3.89	25.74	3.09	.29	.74	1.90	1.11	0.00

Ces derniers prévoient une concentration en Ab plus grande dans les produits de fusion que celle détectée dans les granites naturels (voir en autre Mehnert, 1968, Roubault et de la Roche, 1975). Il est pratiquement impossible d'évaluer le paramètre pression d'après ce diagramme puisqu'il y a une dispersion relative des deux groupes d'analyses est et ouest entre les lignes cotectiques correspondantes à 0.5 et 10 Kb p H_2O et qu'il n'y a aucune correspondance entre les minima expérimentaux et naturels. On ne peut en outre s'attendre à ce que les magmas comme ceux qui ont généré les granites de Fury et Hecla terminent leur course de différenciation dans le champ de l'albite.

La position des analyses dans ce diagramme dépend du type de norme utilisé pendant le traitement des données. Leur représentation est rendu tout à fait partielle par l'absence de la composante anorthite. Cette dernière est essentielle pour fixer l'eutectique réel des granites (voir Wyllie, 1977, p. 45).

La fig. 11.3 donne la composante An du plagioclase dans la projection Qz-Pl-Or. Malgré une concentration sur l'eutectique, on note une dispersion relative des deux blocs est et ouest.

Bien que montrant des lignes cotectiques approximatives, ce diagramme donne une image beaucoup plus réaliste de la position des granites dans le tétrahèdre Qz-Ab-An-Or. La composition des plagioclases (An_{20}) sert de repère sur la ligne Ab-An pour tracer la projection Qz-Pl-Or (voir Winkler, 1976, p. 280).

En comparaison, la fig. 11.4 donne la position spatiale de quelques granites d'anatexie, des paragneiss à biotite dont ils sont issus ainsi que les granites roses de Fury et Hecla. Notons que les paragneiss sont dans le champ des plagioclases, les leucogranites d'anatexie ainsi qu'un groupe des granites de Fury et Hecla se situent immédiatement au-dessus du plan E_5-E_4-P_1-P l'autre groupe se situant un peu plus haut dans le tétrahèdre à cause d'un plagioclase plus riche en An.

Les flèches a b c indiquent l'évolution des granitoïdes récents appartenant au Coastal Batholith (Atherton et al., 1979), la flèche d indique l'évolution des paragneiss à biotite vers les leucogranites. Notons que pour bien représenter la cristallisation issue de la fusion partielle, une fois touché la zone du quartz, la flèche d se doit de rester dans le plan $E_1E_2E_5P$ jusqu'ayant rejoint la position des leucogranites d'anatexie. Quelque soit le chemin réel de la cristallisation, on note un enrichissement des paragneiss en Or et un appauvrissement relatif en anorthite, lors de l'anatexie.

La distribution des alcalins dans les granites de Fury et Hecla est donnée dans la fig. 11.5. Une concentration relative des roches du bloc est et ouest apparait accompagnée d'un étalement des pegmatites de part et d'autre d'une moyenne centrale[1]. Étant donné le type de mise en place tardive des pegmatites et leurs associations à la fracturation (voir Maurice, 1982), il apparait évident que les compositions s'équilibrent par rapport à la moyenne donnant des concentrations tantôt riches en soude et pauvres en potasse et tantôt inversement dépendant de la concentration relative en orthose et en plagioclase.

Les granites roses de Fury et Hecla ont été comparés avec ceux décrits par Chappel (1978). La fig. 11.6 donne la position des analyses dans le diagramme CaO/SiO_2 en comparaison avec quelques granites d'anatexie issues de métagrauwackes. On note une concentration importante sous la tendance des granites de type S. La variation de la teneur en silice est nettement moins importante en proportion que la variation du calcium. Bien que la dispersion des analyses soit assez importante, elle ne constitue en aucun cas une

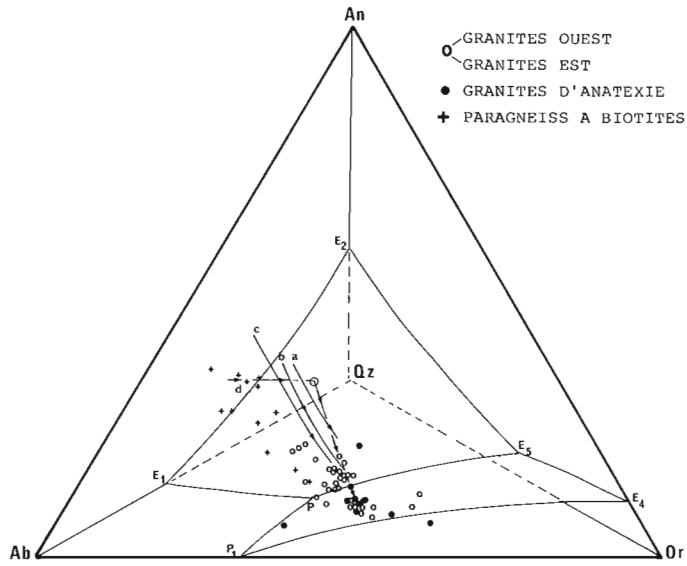

Figure 11.4. *Analyses catanormatives des granites est et ouest de Fury et Hecla, des paragneiss et leucogranites des migmatites de la baie James. Les flèches a b c représentent l'évolution de suites modernes (granodiorites de marges continentales), la flèche d représente l'évolution des migmatites (paléosome vers le néosome).*
D'après Hoffmann (1976), Winkler (1975), (1977) modifié.

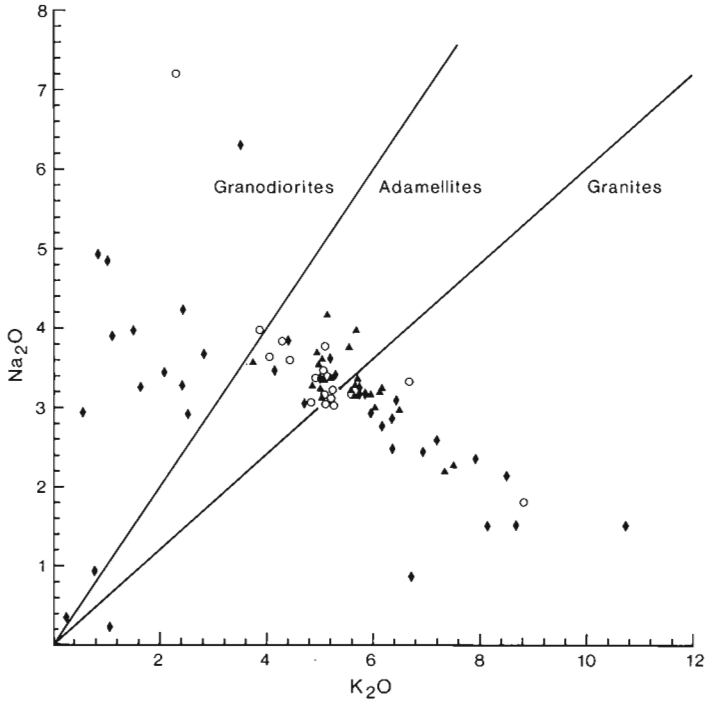

Figure 11.5. *Position des granites est et ouest et des pegmatites de Fury et Hecla dans le diagramme des alcalins. Notez la dispersion symétrique des pegmatites par rapport aux granites. Les champs de classification sont de Anhaeusser (1973). Voir légende fig. 11.2.*

[1] Les analyses chimiques détaillées des pegmatites sont disponibles auprès de l'auteur.

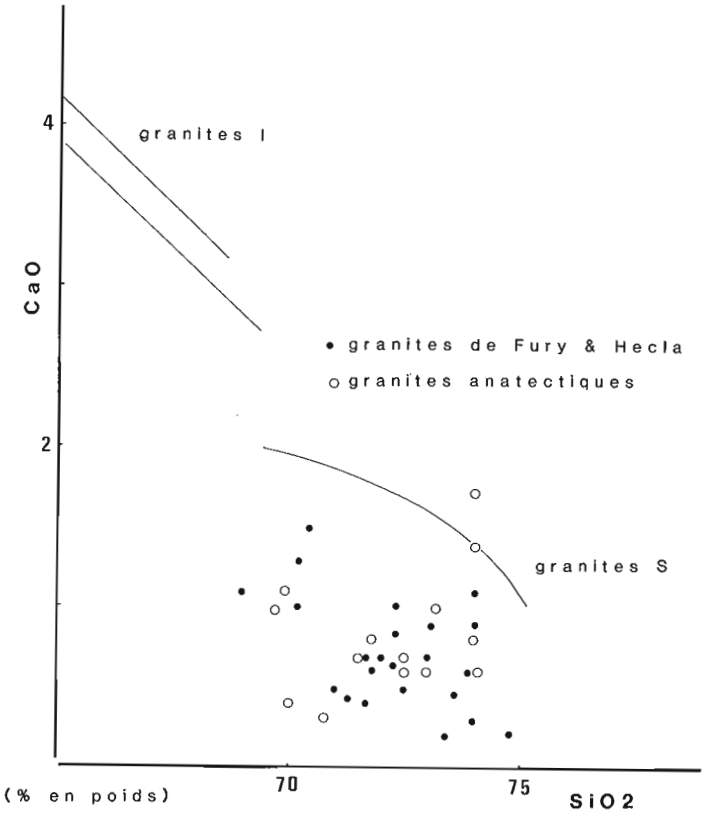

Figure 11.6. *Position des granites roses de Fury et Hecla dans le diagramme CaO/SiO_2, en comparaison avec des leucogranites d'anatexie de Ciesielski (1978). Les lignes continues donnent les tendances de suites récentes de Chappell, 1978.*

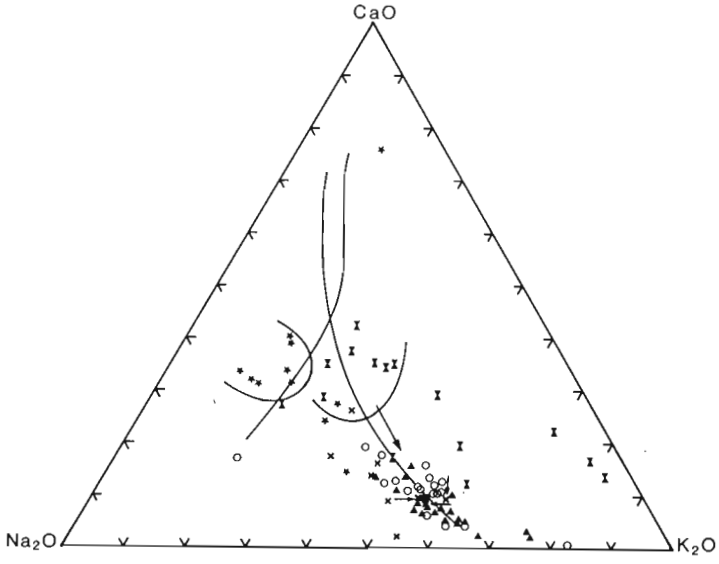

Figure 11.7. *Granites roses, gneiss ortho et paragénétiques de Fury et Hecla dans le diagramme des calco-alcalins. La grande flèche indique la provenance possible des granites. Les petites flèches marquent trois analyses de gneiss acides dans le champ des granites. Les tendances calco-alcalines et trondjhémitiques sont de Ermanovics et al., 1979. Notez la dispersion des gneiss à biotite et leur richesse relative en potassium. Voir légende fig. 11.2.*

tendance quelconque, et il est remarquable que les leucogranites d'anatexie qui sont indubitablement d'origine S ne suivent absolument pas la tendance prédite par les auteurs. Il y a donc en première approximation une incompatibilité avec le modèle I et S (voir Hine et al., 1978) de l'origine des suites granitiques. La division des granites en I et S semble fonctionnelle pour des complexes granitiques différenciés relativement récents (Strong et al., 1978; Beckinsale, 1979; Griffin et al., 1978; Lameyre, 1980), mais il n'en est pas de même pour tous les granites tardi-tectoniques archéens dont la mise en place ne forme pas toujours des batholites aussi bien circonscrits (voir par ex. Wallach, 1973; Dubé, 1978). La division en granite I et S de Chappel et White, est basée en premier lieu sur des critères chimiques tel l'alumine par rapport aux alcalins et le fer ferrique par rapport au fer ferreux. Or les comparaisons faites entre les granites tardi-tectoniques de Fury et Hecla et les leucogranites d'anatexie ne montre aucune différence notable bien que d'après leurs enclaves respectives et selon le modèle I et S on devrait pouvoir les différenciés.

Il devient impossible d'établir clairement la provenance des amphiboles des granites, car celles-ci peuvent être d'origine magmatique (autochtones) ou allochtones, c'est-à-dire, provenant de la digestion par le granite d'enclaves préexistantes de type amphibolite. Ces dernières, retrouvées aussi dans les tonalites encaissantes, ont souvent des allures de dykes, et il est donc possible que plusieurs des enclaves basiques et même ultrabasiques appartenant aux tonalites et aux granites de Fury et Hecla aient pour origine des dykes issus d'une phase de distention antétectonique. Les types d'enclaves n'ont pas de signification réelle en ce cas-ci puisque les granites roses de Fury et Hecla ne contiennent généralement que des enclaves de type amphibolites litées et que les tonalites de l'encaissant contiennent à la fois des enclaves basiques et ultrabasiques litées et des enclaves surmicacées de type paragneiss à biotite. Le litage vraisemblablement métamorphique (donc anté-mise-en-place du granite rose,) des amphibolites, nous oblige à les considérer non pas comme un produit primaire de différenciation (on le ferait pour des roches basiques impliquées dans des complexes immiscibles, voir Goldie, 1978, par exemple) mais comme des roches basiques prédatant la mise en place des granites et pouvant avoir des origines variées. D'ailleurs l'association quoique non spatiale des ultrabasites, amphibolites et paragneiss à biotite dans les tonalites de l'encaissant nous laisse déjà envisager une origine antétectonique et probablement supracrustale pour certaines de ces enclaves.

La représentation des granites dans le triangle des éléments calco-alcalin, nous amène à la figure 11.7 qui montre un nuage de points se situant à la terminaison de la tendance évolutive calco-alcaline, en opposition avec la tendance trondjhémitique. On notera que la répartition est la même pour les granites du bloc est et ouest de Fury et Hecla. En outre, les sédiments et les gneiss que le granite recoupe, ont été rapportés afin de déterminer si une relation génétique est probable entre ces trois types de roches. La grande flèche indique la trajectoire de provenance possible par fusion partielle des gneiss para-génétiques. Les gneiss d'origine ignée se situent près de la fin de la tendance trondjhémitique alors qu'une partie seulement des sédiments se situent au milieu de la lignée calco-alcaline. Les petites flèches indiquent la présence de trois analyses de paragneiss acides ayant des rapports calco-alcalin identiques à ceux des granites roses de Fury et Hecla. La dispersion des analyses des méta-sédiments est remarquable ainsi que leur richesse relative en potassium.

Tableau 11.2*

	SECTION CZ-H-5-79A				SECTION CZ-H-5-79A*				SECTION CZ-32-79				SECTION CZ-205-79			
	1		2		1		2		1		2		1		2	
	Plag.	K-spar	Plag.	K-spar	Plag.	K-spar	Plag.	K-spar	Plag.	K-spar	Plag.	K-spar	Plag.	K-spar	Plag.	K-spar
SiO_2	65.40	65.45	68.29	65.15	64.27	63.84	67.72	64.65	63.66	64.91	66.39	64.69	64.18	64.48	63.84	64.96
Al_2O_3	21.34	18.70	18.83	18.78	21.98	18.47	19.70	18.66	22.61	18.45	19.94	18.56	22.94	18.83	22.53	18.66
Fe as FeO	0.07	0.00	0.06	0.00	0.00	0.01	0.00	0.00	0.02	0.00	0.05	0.01	0.00	0.00	0.00	0.00
CaO	2.27	0.11	0.14	0.07	2.84	0.34	0.43	0.25	3.59	0.23	1.02	0.16	3.71	0.23	3.36	0.19
Na_2O	11.07	1.34	12.63	1.36	10.07	1.45	11.28	1.05	9.98	1.47	11.35	1.45	9.57	1.36	9.79	1.58
K_2O	0.25	15.88	0.25	15.65	0.19	15.78	0.21	16.18	0.22	15.61	0.23	15.77	0.15	15.36	0.14	15.60
Total	100.40	101.68	101.20	100.96	99.33	99.89	99.34	100.79	100.08	100.67	98.98	100.64	100.55	100.26	99.66	100.99
Mol % An	10.0	0.5	0.6	0.3	13.3	1.6	2.0	1.2	16.4	1.1	4.6	0.8	17.5	1.1	15.8	0.9
Ab	88.6	11.3	98.1	11.6	85.6	12.1	96.8	8.6	82.5	12.3	94.1	12.1	81.7	11.7	83.4	13.2
Or	1.3	88.2	1.3	88.1	1.1	86.4	1.2	89.9	1.2	86.6	1.3	87.1	0.8	87.2	0.8	85.9

	SECTION CZ-304-79				SECTION CZ-118-79									
	1		2		1		2		3		4		5	
	Plag.	K-spar	Plag.	K-spar	Plag.	K-spar	Plag.	K-spar	Plag.	K-spar	Plag.	K-spar	Plag.	K-spar
SiO_2	63.71	64.70	61.79	64.41	66.27	64.05	67.40	64.90	69.00	65.18	67.63	65.25	66.33	64.04
Al_2O_3	22.65	18.86	23.74	18.66	21.03	18.30	19.74	18.58	19.77	18.58	20.29	18.52	20.80	18.40
Fe as FeO	0.07	0.00	0.04	0.00	0.01	0.00	0.00	0.00	0.03	0.00	0.00	0.00	0.04	0.01
CaO	3.76	0.20	4.72	0.16	1.57	0.25	0.36	0.22	0.17	0.20	0.86	0.20	1.69	0.21
Na_2O	9.28	1.16	8.50	1.22	10.22	1.20	10.87	1.11	11.37	1.50	10.96	1.15	10.29	1.16
K_2O	0.17	15.67	0.30	15.23	0.18	15.38	0.11	15.67	0.12	15.44	0.13	15.58	0.13	15.54
Total	99.64	100.59	99.09	99.68	99.28	99.18	98.48	100.68	100.46	100.90	99.87	100.70	99.37	99.36
Mol % An	18.1	1.0	23.1	0.8	7.8	1.2	1.8	1.0	0.8	0.9	4.1	1.0	8.3	11.0
Ab	80.9	10.0	75.2	10.8	91.2	10.5	97.6	9.6	98.5	12.8	95.1	10.0	91.0	10.1
Or	1.0	89.0	1.7	88.4	1.0	88.3	0.7	89.3	0.7	86.3	0.8	89.0	0.8	88.9

	SECTION 8234						SECTION 8239					
	1		2		3		1		2		3	
	Plag.	K-spar	Plag.	K-spar	Plag.	K-spar	Plag.	K-spar	Plag.	K-spar	Plag.	K-spar
SiO_2	68.89	64.53	67.61	64.11	64.87	64.12	67.61	65.04	67.85	64.85	67.74	65.12
Al_2O_3	20.42	18.58	20.54	18.35	22.39	18.54	19.77	18.66	20.27	18.81	20.48	18.72
Fe as FeO	0.06	0.06	0.05	0.00	0.03	0.02	0.00	0.00	0.03	0.00	0.05	0.00
CaO	0.42	0.12	0.89	0.14	2.95	0.10	0.27	0.21	0.73	0.11	0.82	0.18
Na_2O	11.32	1.18	10.46	1.18	9.57	1.10	11.22	1.16	10.83	1.19	10.88	1.05
K_2O	0.15	16.11	0.13	15.79	0.17	16.12	0.15	15.51	0.15	15.35	0.13	15.49
Total	101.26	100.58	99.68	99.57	99.98	100.00	99.02	100.58	99.86	100.31	100.08	100.56
Mol % An	2.0	0.6	4.4	0.7	14.4	0.5	1.3	1.0	3.6	0.5	3.9	0.9
Ab	97.2	10.0	94.8	10.1	84.6	9.3	97.8	10.1	95.6	10.5	95.3	9.2
Or	0.8	89.5	0.8	89.2	1.0	90.2	0.9	88.9	0.9	89.0	0.8	89.9

	SECTION 8242						SECTION 225					
	1		2		3		1		2		3	
	Plag.	K-spar	Plag.	K-spar	Plag.	K-spar	Plag.	K-spar	Plag.	K-spar	Plag.	K-spar
SiO_2	68.15	64.57	64.67	64.80	67.93	65.15	67.82	64.85	68.89	65.51	68.43	65.26
Al_2O_3	19.81	18.71	22.68	18.70	20.29	18.88	19.59	18.59	19.77	18.68	19.81	18.68
Fe as FeO	0.01	0.02	0.03	0.00	0.01	0.00	0.02	0.00	0.08	0.00	0.00	0.00
CaO	0.21	0.00	3.21	0.00	0.80	0.00	0.23	0.00	0.20	0.02	0.21	0.02
Na_2O	10.77	1.26	9.26	1.09	10.65	1.02	11.30	1.07	10.96	1.17	10.75	1.12
K_2O	0.27	15.20	0.23	15.31	0.13	15.66	0.13	15.60	0.14	15.51	0.04	15.65
Total	99.22	99.76	100.08	99.90	99.81	100.71	99.09	100.11	100.04	100.84	99.24	100.73
Mol % An	1.0	0.0	15.9	0.0	3.9	0.0	1.1	0.0	1.0	0.1	1.1	0.1
Ab	97.4	11.1	82.8	9.8	95.3	9.0	98.1	9.4	98.2	10.3	98.7	9.8
Or	1.6	88.9	1.4	90.2	0.8	91.0	0.7	90.6	0.9	89.6	0.2	90.1

	SECTION KF-112-79				SECTION KF-269-79					
	1		2		1		2		3	
	Plag.	K-spar	Plag.	K-spar	Plag.	K-spar	Plag.	K-spar	Plag.	K-spar
SiO_2	65.03	64.86	67.78	64.61	63.34	63.72	63.14	63.72	63.49	64.05
Al_2O_3	21.39	18.69	19.93	18.65	22.61	18.38	22.20	18.66	22.46	18.57
Fe as FeO	0.05	0.00	0.00	0.00	0.00	0.00	0.01	0.00	0.01	0.00
CaO	2.22	0.23	0.42	0.18	3.53	0.33	3.35	0.37	3.48	0.29
Na_2O	9.99	1.22	11.05	1.31	9.83	1.47	10.06	1.44	9.89	1.53
K_2O	0.16	15.98	0.10	15.81	0.17	15.69	0.14	16.02	0.15	15.88
Total	98.84	100.98	99.28	100.56	99.48	99.59	99.00	100.21	99.48	100.32
Mol % An	10.8	1.1	2.0	0.9	16.4	1.5	15.4	1.7	16.2	1.3
Ab	88.2	10.3	97.4	11.1	82.7	12.2	83.8	11.8	83.0	12.6
Or	0.9	88.6	0.6	88.0	0.9	86.2	0.8	86.5	0.8	86.1

* Analyses à la sonde effetuées à la CGC

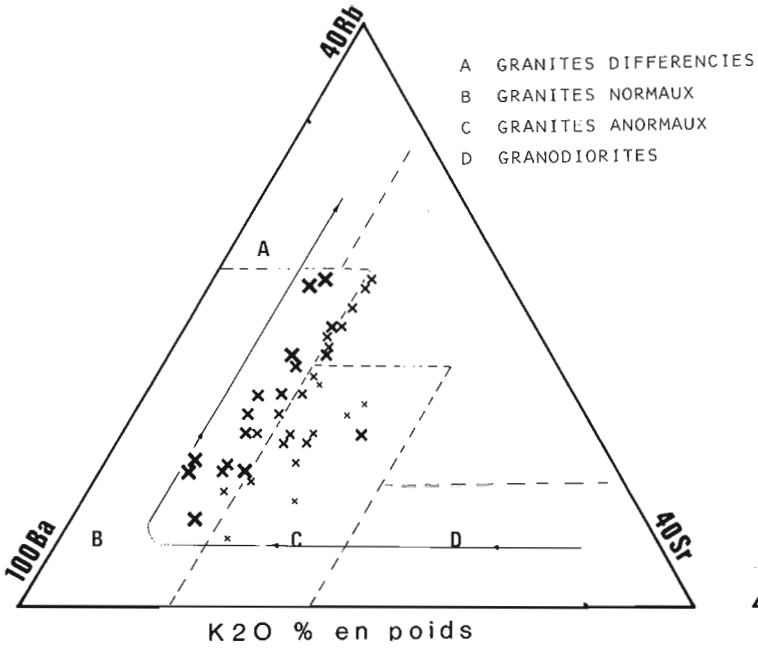

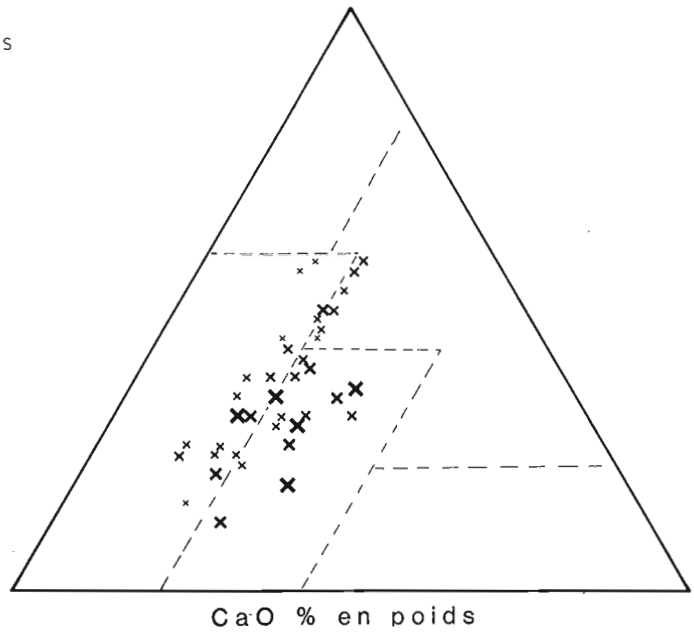

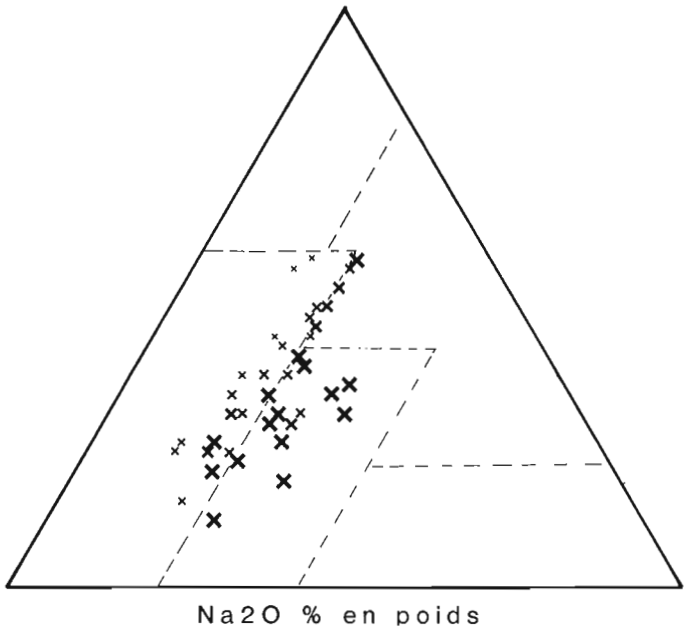

Figure 11.8

Position des granites roses de Fury et Hecla dans le diagramme Ba Rb Sr en fonction des éléments calco-alcalins. La taille relative marque l'augmentation de la concentration de l'élément majeur en % selon:

K_2O	Na_2O	CaO
- 4.5	- 3.0	- .25
4.5 - 5.0	3.0 - 3.25	.25 - .50
5.0 - 5.5	3.25 - 3.50	.50 - .75
5.5 - 6.0	3.50 - 3.75	.75 - 1.0
6.0 -	3.75 -	1.0 -

La flèche représente la variation relative en fonction de la différenciation. Les champs sont de El Bouseily et al., 1975.

Une première analyse du comportement de certains éléments traces a été effectuée en se servant du diagramme ternaire Ba-Rb-Sr d'après El Bouseily et al. (1975).

La figure 11.8 a, b, c montre le rapport qui existe entre d'une part les éléments traces Rb-Sr-Ba et d'autre part les éléments majeurs K-Na-Ca.

Fig. 11.8a: on note un étalement important des analyses selon l'axe Ba-Rb et une dérive par rapport à la tendance de différenciation prévue par l'auteur. Seul le strontium est lié de façon inverse au potassium.

Fig. 11.8b: le sodium est lié proportionnellement au strontium et de façon moins évidente au barium.

Fig. 11.8c: le calcium ne montre aucun lien vraiment évident sur ce diagramme si ce n'est un rapport problématique au strontium.

L'étalement important des analyses n'est pas lié à un processus de différenciation des granites de Fury et Hecla. Ces derniers sont globalement homogènes du point de vue des éléments majeurs. Les variations dans la teneur des éléments trace sont plutôt dues à des hétérogénéités internes, comme la variation de composition du plagioclase ou la teneur en microcline des échantillons.

Les analyses à la sonde effectuées sur les minéraux des granites ont permi de déterminer la quantité d'albite contenue dans les deux felspaths en présence. La méthode de Stormer et Whitney (1977) permet d'évaluer la température d'équilibre ou de refroidissement d'un granite par son contenu en albite. La fig. 11.9 montre deux nuages de points distincts qui correspondent à une dizaine d'échantillons semblables minéralogiquement, échantillonnés selon une ligne nord-sud dans le bloc est et montrant le même écart de température. Les analyses (tableau 11.2) montrent une grande variation dans le contenu en anorthite du plagioclase, allant de 2 à 20 par rapport à des taux d'albite dans le microline beaucoup plus constant. La température d'équilibre est évaluée à 550 ± 50°C. Le granite du bloc est n'étant ni zoné ni différencié macroscopiquement, il apparait peu probable qu'une zonation apparaisse au niveau minéralogique même avec une analyse systématique de tout le batholite. Les variations importantes dans le contenu en albite du plagioclase apparaissant à l'intérieur d'une même lame mince peuvent être dues en partie au moins à des réactions de contact avec des microclines.

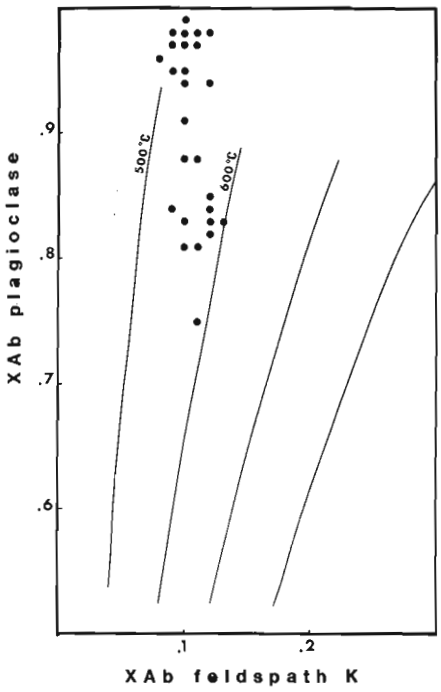

Figure 11.9. *Compositions des différents couples plagioclase/microline provenant des granites de Fury et Hecla dans le diagramme "composante albite versus température" de Stormer et Whitney (1977) donnant les températures d'équilibre.*

Discussions

Les granites de Fury et Hecla, s'il ne sont pas encore datés, montrent de grandes similitudes avec les granites tardi-tectoniques archéens du Supérieur. Il existe différents types de granitoïdes archéens qu'il est possible de classifier selon:

- qu'ils sont syn-tectoniques ou post-tectoniques
- qu'ils sont zonés et circonscrits
- qu'ils possèdent des auréoles de métamorphisme
- qu'ils sont liés ou non à des ceintures volcano-sédimentaires.

La génèse des granites récents (post-précambrien) s'inscrit relativement bien dans le modèle des marges continentales. La relation entre la production des magmas granitiques et les orogènes est devenue évidente, par exemple, les granitoïdes andinotypes et hercynotypes de Pitcher (1979), les granitoïdes associés à une tectonique profonde de Leake (1978), les granites de la chaîne Varisque de Didier et Lameyre (1977).

Il n'en va pas de même pour les granites plus anciens (Lameyre, 1980; Brown et Henessy, 1978).

S'il est possible de déterminer s'il sont post-tectoniques ou orogéniques leur affiliation à une tectonique globale n'est qu'analogique (Anderson et al., 1980).

En ce qui concerne les granitoïdes archéens, leur comparaison avec leurs analogues paléozoïques est difficile et due entre autre à l'importance que prend le socle granitique dans la province du Supérieur par exemple. Des modèles tectonogénétiques spécifiques à l'Archéen doivent être invoqués pour expliquer la naissance des magmas granitiques dans le contexte des alternances "ceintures gneissiques/ceintures volcano-sédimentaires" (voir en autre Schwertdner, 1978). Une hypothèse génétique concernant les granites roses tardi-tectoniques ne sera valable que quand il sera possible de les comparer chimiquement et tectoniquement avec leurs contextes géologiques et d'en dater les différentes unités.

Les granites roses uranifères de Fury et Hecla:

- sont tardi-tectoniques et d'âge thermique encore indéterminé, le contexte géologique est présumé archéen.
- sont microscopiquement homogènes, mais présentent des variations internes relativement grande en ce qui concerne l'albite du plagioclase, l'alumine et certains éléments traces par exemple.
- ne sont zonés ni minéralogiquement ni chimiquement.
- sont considérés comme des granites minimum, ne concordent pas avec le modelé des suites I et S de Chappel et White et présentent de grandes similitudes chimiques avec les granites d'anatexie.
- ont une température d'équilibre relativement froide de 550°C et sont considérés d'après le contexte géologique comme des roches de moyenne ou faible profondeur ayant cristallisées à la faveur de la remontée du socle.
- ont une source probablement hybrides ortho- et paragneissiques bien que leur filiation aux roches sédimentaires environnantes ne soit pas évidente.

Collaboration

Ont collaboré de près ou de loin à ce travail F.W. Chandler (CGC) pour entre autre, la logistique pendant l'été 1979, M.J. Maley (CGC) pour le traitement des données, messieurs Davidson, Emslie, Maurice et Thompson (tous de la CGC) pour leur revue critique du manuscrit.

Bibliographie

Anderson, J.L., Cullers, R.L., and Van Schmus, W.R.
1980: Anorogenic metaluminous and peraluminous granite plutonism in the Mid-Proterozoic of Wisconsin, U.S.A.; Contributions to Mineralogy and Petrology, v. 74, p. 311-328.

Anhaeusser, C.R.
1973: Geology and geochemistry of the Archean granites and gneisses of the Johannesburg-Pretoria dome; Geological Society of South-Africa, Special Publication 3.

Atherton, M.P. et al.
1979: The Geochemical character of the segmented Peruvian coastal Batholith and associated volcanics; in Origin of Granite Batholiths, Geochemical Evidence; ed. M.P. Atherton and J. Tarney; Shiva Publications Ltd.

Beckinsale, R.D.
1979: Granite magmatism in the tin belt of South-East Asia; in Origin of Granite Batholiths, Geochemical Evidence; ed. M.P. Atherton and J. Tarney; Shiva Publications Ltd.

Brown, G.C. and Hennessy, J.
1978: The initiation and thermal diversity of granite magmatism; Royal Society of London, Philosophical Transactions, Series A. 288, p. 631-643.

Chandler, F.W., Charbonneau, B.W., Ciesielski, A., Maurice, Y.T., and White, S.
1980: Geological studies of the Late Precambrian supracrustal rocks and underlying granitic basement, Fury and Hecla Strait area, Baffin Island, District of Franklin; in Current Research, Part A, Geological Survey of Canada, Paper 80-1A, p. 125-132.

Chappell, B.W.
1978: Granitoids from the Moonbi District, New England Batholith, eastern Australia; Geological Society of Australia, Journal, v. 25, p. 267-283.

Charbonneau, B.W.
1982: Radiometric study of three radioactive granites in the Canadian Shield: Elliot Lake, Ontario, Forth Smith, and Fury and Hecla, N.W.T.; in Uranium in Granites, ed. Y.T. Maurice; Geological Survey of Canada, Paper 81-23, p. 91-99.

Ciesielski, A.
1978: Les migmatites de la rivière Broadback ... baie James, Québec; thèse de doctorat inédite, Laboratoire de pétrologie, université de Paris (Pierre et Marie Curie).

1980: Cartes géologiques de la région du détroit de Fury et Hecla, Terre de Baffin; dossier public 687 de la CGC.

Didier, J. et Lameyre, J.
1977: Le noyau arverne du massif central français dans l'orogène varisque; Coll. intern. CNRS, Rennes, nº 243, p. 39-55.

Dubé, C.Y.
1978: Région des lacs Champion, Tésécau, et la rivière Rupert...MRN Québec, DPV 585.

El Bouseily, A.M. and El Sokkary, A.A.
1975: The Relation between Rb, Ba and Sr in Granitic Rocks; Chemical Geology, v. 16, p. 207-219.

Ermanovics, I.F., McRitchie, W.D., and Houston, W.N.
1979: Petrochemistry and tectonic setting of plutonic rocks of the Superior Province in Manitoba; in Trondjhemites, Dacites and Related Rocks, ed. Barker; Elsevier, Amsterdam.

Frisch, T.
1980: Tonalite gneisses, western Melville Peninsula, District of Franklin; in Loveridge, W.D., Rubidium-strontium and uranium-lead isopotic age studies Report 3; in Current Research, Part C, Geological Survey of Canada, Paper 80-1C, p. 217-219.

Goldie, R.
1978: Magma mixing in the Flavrian pluton, Noranda area, Quebec; Canadian Journal of Earth Sciences, v. 15, p. 132-144.

Griffin, T.J., White, A.J.R., and Chappell, B.W.
1978: The Moruya Batholith and Geochemical Contrasts between the Moruya and Jindabyne Suites; Geological Society of Australia, Journal, v. 25, p. 325-247.

Hine, R., Williams, I.S., Chappell, B.W., and White, A.J.R.
1978: Contrasts between I- and S-Type Granitoids of the Kosciusko Batholith; Geological Society of Australia, Journal, v. 25, p. 219-234.

Hoffmann, C.
1976: Natural granitic rocks and the granite systems Qz-Or-Ab-An(H_2O) and Qz-Ab-An-(H_2O); Neves Jahrbuch fuer Mineralogie, Monatshefte, H 7 p. 289-306.

Lameyre, J.
1980: Les magmas granitiques: leurs comportements, leurs associations et leurs sources; Mém. h. sér. Soc. géol. de France, nº 10.

Leake, B.E.
1978: Crustal evolution in northwestern Britain and adjacent regions; Geological Journal Special Issue No. 10.

Luth, W.C. et al.
1964: The Granite system at pressure of 4 to 10 Kb; Journal of Geophysical Research, v. 69, p. 759-773.

Maurice, Y.T.
1982: Uraniferous granites and associated mineralization in the Fury and Hecla Strait area, Baffin Island, N.W.T.; in Uranium in Granites, ed. Y.T. Maurice; Geological Survey of Canada, Paper 81-23, p. 101-113.

Mehnert, K.R.
1968: Migmatites and the Origin of Granitic Rocks; Elsevier Publishing Company, Amsterdam.

Pitcher, W.S.
1979: The nature, ascent and emplacement of granitic magmas; Geological Society of London, Journal, v. 136, p. 627-662.

Roubault, M. and de la Roche, H.
1975: Gneisses, migmatites, and granites in the system Q-Or-Ab; in Recent Contributions to Geochemistry and Analytical Chemistry, ed. Tugarinov, John Wiley and Sons.

Schau, M.
1977: Komatiites and quartzites in the Archean Prince Albert Group; Geological Association of Canada, Special Paper 16.

Schwertdner, W.M. et al.
1978: Structure of Archean rocks in western Ontario; in 1978 Archean Geochemistry Conference; University of Toronto Press, ed. Smith and Williams.

Stormer, J.C., Jr. and Whitney, J.A.
1977: Two-feldspar geothermometry in granulite facies metamorphic rocks; sapphirine granulites from Brazil; Contributions to Mineral Petrology, v. 65, p. 123-133.

Strong, D.F. and Dickson, W.L.
1978: Geochemistry of Paleozoic granitoid plutons from contrasting tectonic zones of northeast Newfoundland; Canadian Journal of Earth Sciences, v. 15, p. 145-156.

Swanson, S.E.
1977: Relation of nucleation and crystal-growth rate to the development of granitic textures; American Mineralogist, v. 62, p. 966-978.

Wallach, J.L.
1973: Némiscau Lake Area...MRN Québec DP 146.

Winkler, H.G.F.
1976: Petrogenesis of Metamorphic rocks; 4th ed., Springer Verlag, New York, Berlin, 334 p.

Winkler, H.G.F., Boese, M., and Marcopoulos, T.
1975: Low temperature granitic melts; Neves Jahrbuch fur Mineralogie, Monatschefte. H 6 p. 245-268.

Winkler, H.G.F., Das, K.B., and Breitbart, R.
1977: Further data of low-temperature melts existing on the quartz + plagiocase + liquid + vapour isobaric cotectic surface within the system Qz-Ab-Or-An-H_2O; Neves Jahrbuch fur Mineralogie, Monatshefte. H 6 p. 241-247.

Wyllie, P.J.
1977: Crustal anatexis: an experimental review; in Experimental Petrology Related to Extreme Metamorphism, ed. D.H. Green, Tectonophysics, v. 43, p. 41-71.

12. PRELIMINARY ACCOUNT OF THE GEOLOGY OF THE MONTRESOR RIVER AREA, DISTRICT OF KEEWATIN

Project 820008

Thomas Frisch and Judith G. Patterson
Precambrian Geology Division

Frisch, T. and Patterson, J.G., Preliminary account of the geology of the Montresor River area, District of Keewatin; in Current Research, Part A, Geological Survey of Canada, Paper 83-1A, p. 103-108, 1983.

Abstract

The map area is underlain by a variety of plutonic gneisses and greatly subordinate supracrustal rocks, which form a basement to two lower grade metasedimentary belts. K-feldspar augen gneiss grading into porphyroblastic granite predominates in the central and western regions. Much of the northern part is occupied by a "straight" zone of northeasterly trending, interlayered felsic and mafic gneisses, bordered by strongly flattened to mylonitic augen gneiss of the Slave-Chantrey mylonite belt. In contrast to the general northeasterly structural grain of the area, gneisses, in part supracrustal(?), in the east are folded about easterly plunging axes. Supracrustal rocks of lower amphibolite(?) grade and in part possibly postdating the gneisses, occur in the southern part of the area.

A sequence of moderately deformed, greenschist grade quartzitic rocks, schist and marble forms a 60 km long, 8 km wide synclinal belt striking northeast across the southern half of the area. This belt of shallow marine rocks is named the Montresor belt and is correlated with the Aphebian Amer group to the south.

Highly deformed, greenschist grade metasedimentary rocks of the Aphebian(?) Chantrey Group outcrop in the northeast. Quartz-pebble metaconglomerate, pelitic schist, fuchsitic orthoquartzite, and marble form a northeast-trending belt that breaks up southwestward into a zone of mylonitic gneisses belonging to the Slave-Chantrey mylonite belt.

Introduction

Mapping of the Montresor River area (NTS 66I) in 1982 constituted the first phase of a project on the Aphebian(?) Chantrey belt of supracrustal rocks and its environs. The map area lies astride the Arctic Circle some 240 km north-northwest of Baker Lake, bounded by longitudes 96° and 98°W and latitudes 66° and 67°N.

More than three-quarters of the area was mapped at a scale of 1:250 000 between June 14 and August 22, 1982.

Previous Work

The Montresor River area was reconnoitred during 1:506 880 scale geological mapping in 1960 (Heywood, 1961). Maps (1:250 000 scale) of the aeromagnetics and surficial geology are available (Geological Survey of Canada, 1977, 1982). Areas to the south and east have been mapped at 1:250 000 scale (Tella and Heywood, 1978; J.A. Fraser, personal communication, 1982).

Physiography

The Montresor River map area shows typical "barren lands" topography of low hills (relief rarely exceeds 100 m), innumerable lakes and minor streams, and eskers. Some regions, particularly in the central portion of the map area, are heavily drift covered. The Back River, a relatively major waterway, flows eastward through the southern part of the area (Fig. 12.1).

Acknowledgments

We thank our field assistants, John Gartner and Angela Dobson, for their excellent work; Rob Pritchard, of Les Hélicoptères Verreault, for indefatigable flying and, at times, looking after (and for?) the base camp; Gordon Collett, also of Les Hélicoptères Verreault, for moving us into our first base camp; our colleagues, A.N. LeCheminant and S. Tella, for co-operation and assistance at all times; and B. and E. Kotelewitz, of Baker Lake, for expediting services and numerous courtesies.

General Geological Features

Most of the Montresor River area is underlain by Archean and/or Aphebian gneissic, granitic to granodioritic rocks of plutonic origin. No age determinations are available from the map area but K-Ar mineral ages from neighbouring areas range from about 1600 to 1800 Ma (Heywood, 1961; Tella and Heywood, 1978).

Poorly to well foliated K-feldspar augen gneiss is the major rock type in the western and central parts. The northwestern sector is occupied by highly foliated and layered "straight" gneisses, which appear to be bordered by mylonitic rocks. The augen and straight gneisses trend mainly northeasterly (Fig. 12.1).

In contrast to the limited lithological variety elsewhere in the gneissic terrane, rocks in the east-central part of the map area form a heterogeneous assemblage of gneisses and granites with a strong easterly trend.

Metamafic rock occurs as amphibolite metadykes in gneiss and, in the northern part of the area, as larger bodies of amphibolite and metagabbro.

Rocks of supracrustal aspect forming part of the basement complex are relatively uncommon. Two of the larger exposures of such rocks are found in the southern third of the map area.

The gneisses and supracrustal rocks together constitute a basement complex to two northeast-trending belts of low grade, predominantly quartzose metasediments (Fig. 12.1): a moderately deformed belt, here termed the Montresor belt, 60 km long in the southern half of the area, and the highly deformed Chantrey belt in the northeast. At its

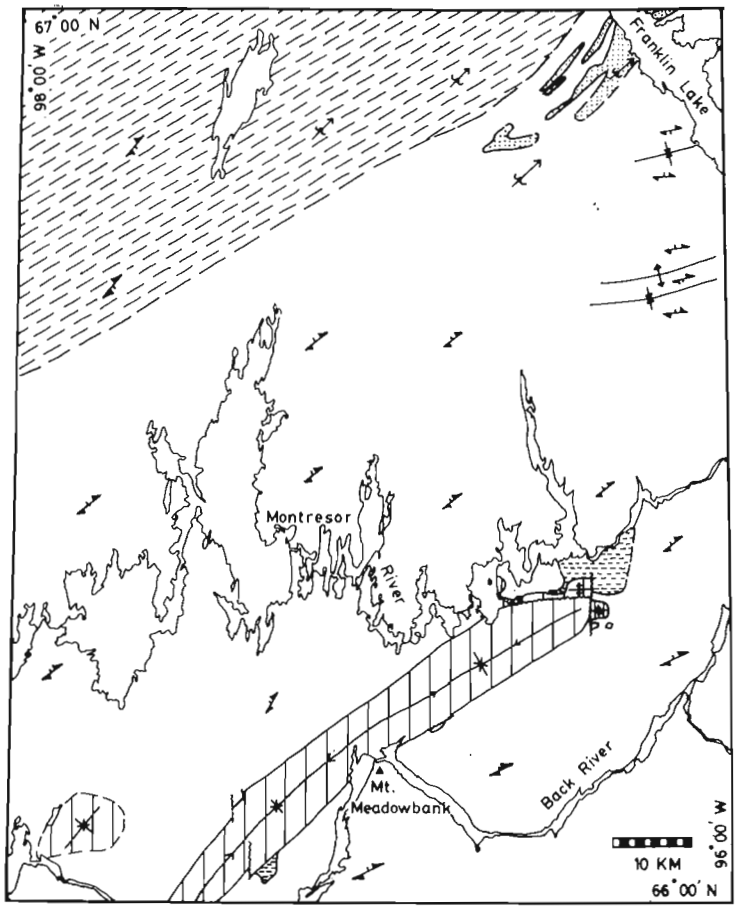

LEGEND

- Montresor belt of metasediments
- Chantrey belt of metasediments
- Undifferentiated basement complex
- Older metasediments
- Layered straight gneisses
- Gneissosity
- Anticline, syncline; direction of plunge
- Fault
- Antiform, synform
- Multiple folds

Figure 12.1. *Geological sketch map of the Montresor River map area.*

southwestern end, the Chantrey belt is broken up, degenerating into a shear/mylonite belt of gneisses that extends to the western border of the map area.

No assemblages diagnostic of greenstone belts and no significant late tectonic granitic bodies were recognized.

Basement Complex

Augen Gneiss

Medium- to coarse-grained gneiss composed of pink to white K-feldspar porphyroblasts in a dark, biotite-rich matrix is the most common rock in the central and western parts of the map area. Depending on degree of deformation, the porphyroblasts range from euhedral tablets to stretched augen, but the typical rock of this unit is an augen gneiss in which the augen are pink and 1 to 3 cm long. In places, such a rock appears to grade into massive, structureless, porphyroblastic, biotite-rich granite, and hence the augen gneiss is considered to be of igneous origin.

The augen gneiss commonly is cataclastically deformed and locally even mylonitized, particularly southwest, and along the strike, of the Chantrey belt. Thin layers of biotite schist intercalated with augen gneiss may have developed during shearing. Pegmatitic layers and pods in the plane of foliation of the gneiss are abundantly developed in many outcrops.

Foliation in the augen gneiss over the bulk of its outcrop area strikes north-northeasterly to northeasterly.

Layered Straight Gneiss

Interlayered grey, locally pink, biotite-feldspar-quartz gneiss and black, schistose biotite(-hornblende) gneiss underlie northwestern and northern parts of the map area. The well developed layering, strongly gneissic structure, consistent northeasterly strike and moderate to steep southeast dips stand in marked contrast to the augen gneiss to the south.

Layering in the straight gneiss is on the metre scale, mafic layers being 1 to 2 m thick and generally subordinate in number to quartzofeldspathic layers. In numerous outcrops, however, mafic and felsic rocks occur in roughly equal amounts. Contacts between layers are sharp and almost without exception concordant with the foliation. Local slight discordances and margins finer grained than centres suggest that some at least of the mafic layers are metadykes.

Stretched and flattened feldspars and quartz, long, fine grained crush zones, mylonite, and boudinaged mafic layers all attest to intense deformation, possibly related to movements in the Slave-Chantrey mylonite zone (Heywood and Schau, 1978). Although not commonly seen, fold closures suggest that the straight gneisses form an isoclinally folded sequence.

Eastern Sector

Rocks between Franklin Lake and the eastern reaches of the Montresor River exhibit lithologies and structural trends that are anomalous in comparison to the rest of the area. Associated with augen gneisses which are similar, but not necessarily related, to those to the west, are garnet-biotite gneisses of possibly supracrustal origin. The gneisses in this sector trend easterly and are deformed into open folds with easterly plunging axes. To the north, gneissic trends appear to swing northeasterly to conform with the Chantrey belt. The Chantrey rocks are bordered on the south in part by gneissic to massive hornblende granodiorite-diorite, a rock type not found to any extent elsewhere.

Farther south, towards the Montresor River, pink, leucocratic, K-feldsparphyric granite, locally studded with magnetite crystals up to 1 cm long, and sporadically gneissic, is the predominant rock.

Judged by the above, the eastern sector may have a tectono-metamorphic history different from the remainder of the map area. Further mapping is planned to resolve these questions.

Metasedimentary Rocks

Basement rocks of undoubted supracrustal origin occur near the eastern and western ends of the Montresor belt. In addition, some minor exposures of calc-silicate gneiss were observed in the southeastern corner of the map area.

The metasediments near the Montresor belt include dark biotite schist, locally with porphyroblasts of a bluish mineral (cordierite?); biotite-quartz schist; actinolite-bearing, impure quartzite; and minor amounts of white marble. Contacts with basement gneisses tend to be

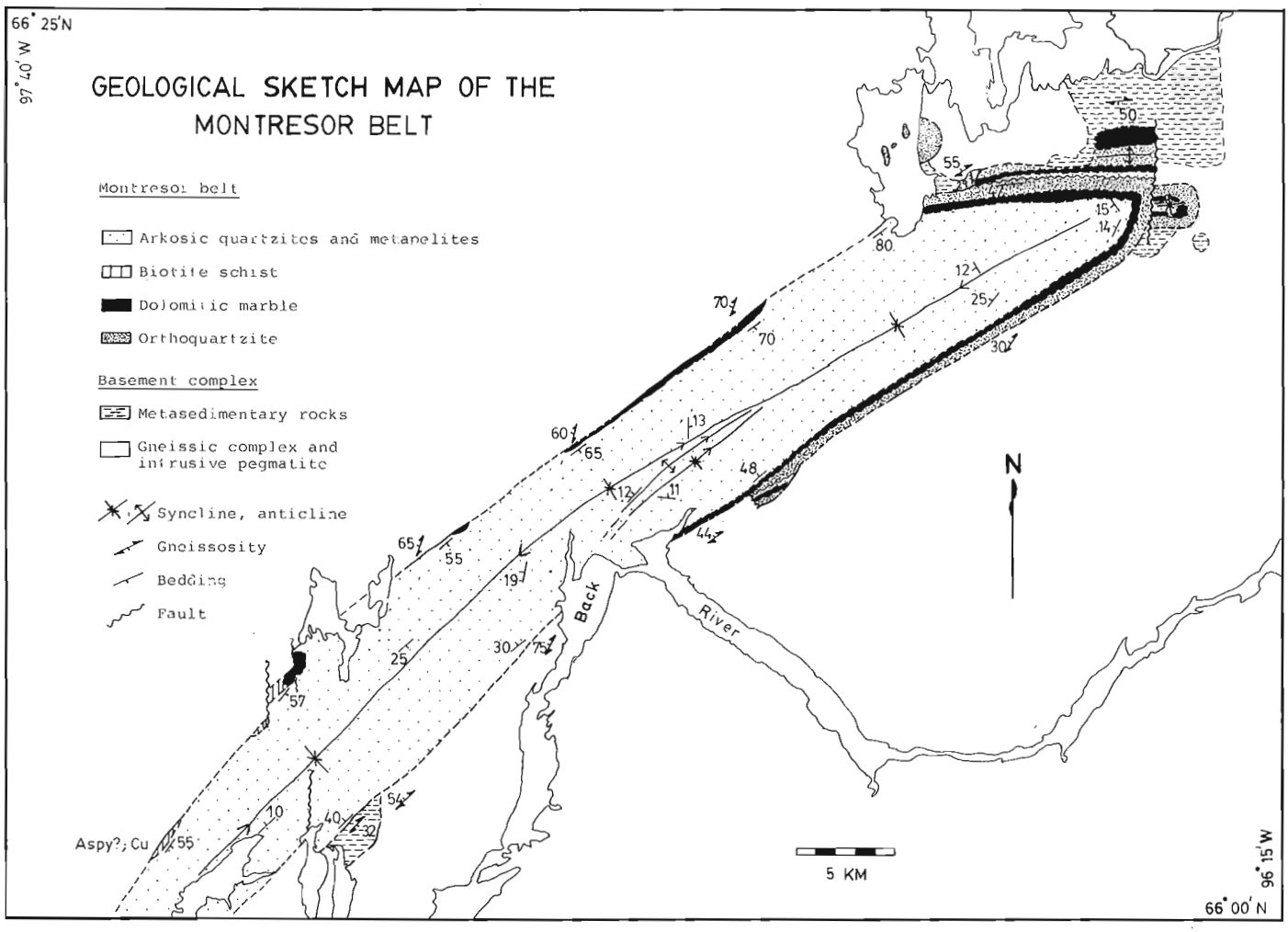

Figure 12.2. *Geological sketch map of the Montresor belt.*

conformable but age relations are uncertain. The metasediments appear to be less deformed and thus may be younger than the gneisses. The metasediments unconformably underlie the Montresor belt and are metamorphosed to a higher grade (lower amphibolite facies?). Therefore, they are considered to predate the Montresor rocks and to probably postdate at least part of the gneissic complex. Possible correlatives may be the Mackenzie Lake metasediments in the Kaminak Lake area (Bell, 1971).

Metamafic and Other Supracrustal Rocks

Amphibolite dykes or remnants thereof occur throughout the area but are nowhere abundant. They locally show slightly discordant contacts with host rocks and fine grained, sheared margins. A dyke seen cutting Chantrey Group metaconglomerates at a high angle exhibits stretching parallel to that of pebbles in the host rock.

Bodies of flaser textured metagabbro, composed of hornblende and plagioclase, outcrop in the northern part of the map area. They dip steeply to vertically and generally form resistant, easterly trending ridges up to 200 m thick. Although no intrusive features were observed, these dyke-like bodies are slightly discordant to the Chantrey belt; the crosscutting dyke mentioned above is probably an offshoot of one of these larger bodies nearby. Large sill-like metagabbro bodies also occur within the Chantrey belt, intrusive into the metasediments.

Mount Meadowbank (Fig. 12.1) is made up of a highly siliceous, poorly foliated gneiss, flanked on one side by amphibolite, on the other by mafic biotite schist. If the gneiss is an acid metavolcanic and the mafic rocks are basic metavolcanics, this restricted exposure may be a remnant of a greenstone belt assemblage.

Montresor Belt

The Montresor belt of low grade metasediments, 8 km wide, trends northeast across the southern half of the map area. It was informally named the Back River Belt by Bell (1970, Fig. 1) but because of possible confusion with the Back River greenstone belt in the Slave Province, we suggest that it be renamed the Montresor belt.

Figure 12.2 is a simplified sketch map showing the main features of the belt which consists predominantly of meta-arkose (field identification), underlain by a much thinner sequence of pelitic schist/phyllite, marble and ortho-quartzite. Metamorphic grade does not exceed that of the greenschist facies. The rocks overlie the basement complex

with profound unconformity and have been folded into an open syncline. Bedding commonly dips 10° to 20° but steepens to 60° and more at the margins of the belt.

Two small outliers of Montresor meta-arkose and micaceous quartzite outcrop in the southwestern corner of the map area. Drift cover is heavy in this region and the extent of Montresor rocks (Fig. 12.1) is inferred from the aeromagnetic pattern.

Lithology

A schematic stratigraphic column is presented in Figure 12.3. Resistant, bright white, glassy orthoquartzite forms the basal unit of the Montresor belt at its eastern end but is not found west of 96°50'W. The orthoquartzite is fine- to medium-grained but strongly recrystallized, slightly micaceous in places, nonconglomeratic, and thick bedded. Estimated maximum thickness of the orthoquartzite unit is 400 m.

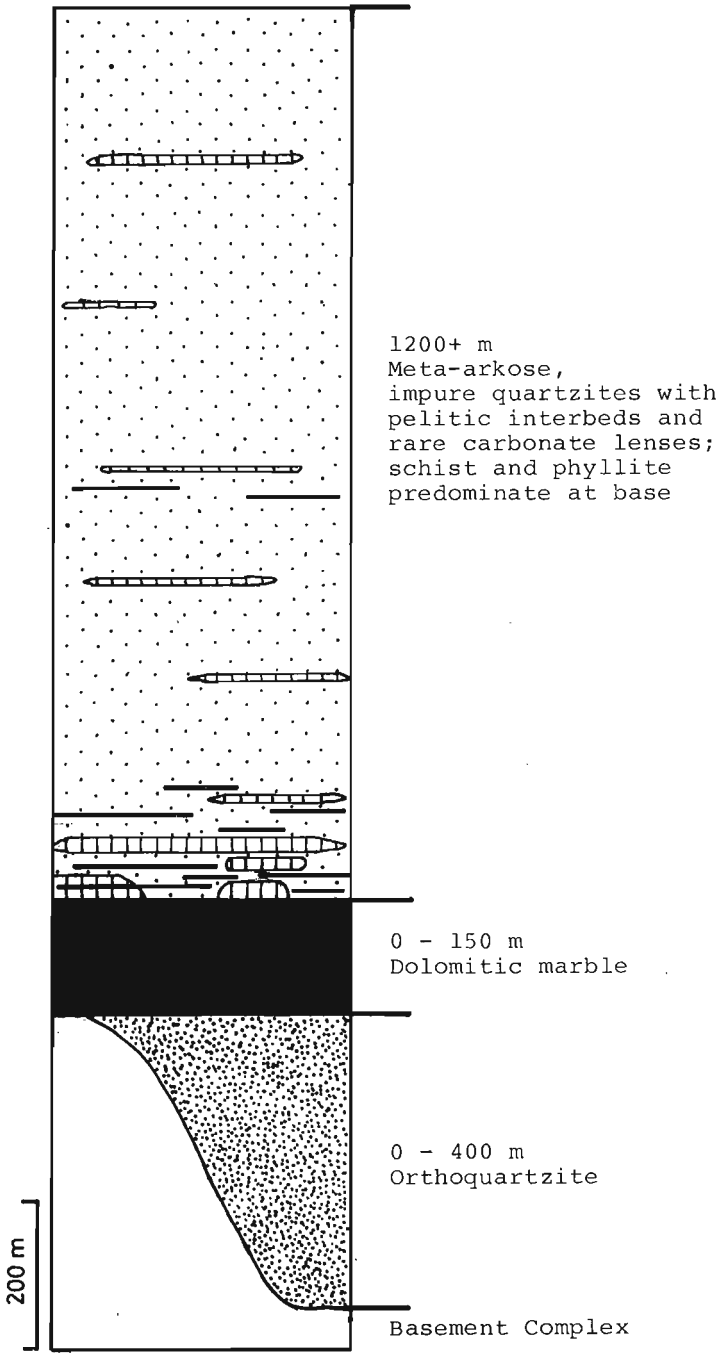

Figure 12.3. Composite stratigraphic column of the Montresor belt. Legend corresponds to that of Figure 12.2.

Overlying the orthoquartzite and present in many places along the margins of the belt is white, grey or buff impure dolomite marble with siliceous layers and pods. The marble is medium grained and contains quartz and tremolite. Original layering shown by siliceous layers is generally contorted and the low competency of the marble has given rise to intricate small scale folds with shallow plunges and to boudinage of siliceous layers. Crossbedding and conglomeratic zones occur sporadically. Estimated maximum thickness of the marble unit is 150 m.

Easily eroded, the marble unit generally outcrops poorly and its original extent is uncertain. Marble appears to have been reasonably persistent along the eastern half of the Montresor belt but it is absent in at least one locality at the western end, where dark biotite schist, which elsewhere overlies the marble unit, is in direct contact with the basement sequence. Further details of this contact zone are given later in the report.

The marble unit is in part directly overlain by impure and arkosic quartzite, but more commonly grades upward into dark, fine grained biotite schist and phyllite and locally is also underlain by thin layers of such micaceous rocks. The schist and phyllite are nondescript rocks of greatly varying thickness (rarely exceeding 50 m), which themselves grade into, or become interlayered with, meta-arkose and impure quartzite. On the present scale of mapping, the basal schist at most localities is included with the overlying quartzitic rock. Disseminated magnetite in the schist causes magnetic anomalies that help to outline the Montresor belt on the aeromagnetic map (Geological Survey of Canada, 1977).

Grey or pink meta-arkose and impure quartzite, commonly with pelitic laminae and interbeds, make up the remaining three-quarters or more of the Montresor belt – a thickness in excess of 1200 m. The rocks are medium grained and recrystallized, medium to thick bedded (typically 1 ± 0.5 m), crossbedded and ripple marked, and locally show graded, convolute or flaser bedding. Dark pelitic interbeds, in places pyritic, or pelitic laminae occur chiefly in the lower part of the quartzitic unit but may be found elsewhere, as well. Calcareous lenses are common near the base; higher in the section, they tend to be confined to one or two levels.

Conglomerate has been found in the quartzitic unit at only one locality, near the western end of the belt. A conglomerate lens, a few hundred metres long and up to 20 m thick, occurs well up in the section at one of the calcareous levels. It consists of well rounded pebbles and cobbles (up to 20 cm diameter) of white quartz and granite in a calcareous, sandy matrix.

Basement-Montresor Belt Contact

The contact of the Montresor belt with the basement is rarely seen. Wide divergence of gneissic foliation and bedding at a number of localities indicates a marked unconformity.

On the northern border of the Montresor belt near its western end, basal biotite schist containing scattered, rounded clasts of white quartz and granite (up to 2 m long), rests either directly on weakly gneissic granite or on a silicified zone of pyritic and chloritic quartzite, which itself overlies basement granitic gneiss.

At another locality, basal marble rests on basement gneiss and carbonate, apparently derived from the marble,

has filled a paleocrack in the gneiss. At the eastern end of the belt, the gneisses are everywhere overlain by orthoquartzite.

Typically, basement and Montresor metasediments are separated by a covered interval. Some contact zones are marked by pegmatite, which appears to have been injected along the contact and to have sent out apophyses into the bordering rocks.

Structure

The open syncline into which the Montresor sequence has been deformed plunges alternately northeast and southwest along its length (Fig. 12.2). The plunge is uniformly gentle and the disappearance of orthoquartzite southwestward is attributed not to structural, but to depositional controls. One major parasitic fold (northeast of Mount Meadowbank) and a few minor ones add little complexity to the fold structure.

Several north-trending faults have caused relatively minor offsets. The scarcity of marker beds in the predominant impure quartzitic unit hinders recognition of faulting. An easterly trending fault near the eastern end of the belt repeats the lower stratigraphy.

Origin and Correlation

The Montresor rocks are interpreted to represent a miogeoclinal sequence, laid down in a supratidal to subtidal depositional environment.

Heywood (1961) suggested correlation of the Montresor rocks with the Hurwitz Group. Subsequently, considerable work has been done on the Amer belt (Tippett and Heywood, 1978; Patterson, 1981) of metasediments in the Amer Lake area (NTS 66H), which lies immediately south of the Montresor River area. These rocks have been named the Amer group and are considered to be Aphebian (Tippett and Heywood, 1978; Patterson, 1981). The stratigraphy of the Montresor belt can be closely correlated with the Amer group and we suggest that the rocks described in this report be referred to as the Montresor belt of the Amer group.

Chantrey Belt

Heywood (1961) proposed the name Chantrey Group for a belt of highly deformed, metamorphosed supracrustal rocks that was found to extend 175 km northeasterly from west of Chantrey Inlet, the head of which lies 50 km northeast of Franklin Lake.

Mapping in 1982 resulted in the discovery of outliers of the Chantrey belt on both sides of Franklin Lake (Fig. 12.1). Chantrey Group rocks found include conglomerate, orthoquartzite, pelitic schist and carbonate rock, metamorphosed in the greenschist facies and strongly deformed.

Northwest of Franklin Lake, stretched-pebble metaconglomerate bordered by dark green quartz-biotite schist forms a tight isoclinal fold, whose limbs dip 40° to 60°NW, in conformity with the bordering gneissic foliation. The metaconglomerate consists of quartz pebbles, generally 1 to 2 cm long, elongated in the plane of the foliation of the matrix, a dark, fine grained, chlorite-biotite-quartz schist. Concordant veining by white quartz is locally intense.

A contact between Chantrey schist and the basement gneiss is exposed just north of the map area. The quartz-biotite schist is calcareous and contains rare augen-shaped clasts of white quartz and granite and minor carbonate lenses. The schist is interlayered, over a distance of 15 or 20 m, with sheets of grey biotite gneiss, which is a highly sheared variety of the gneiss farther from the contact zone. No evidence of intrusion of gneiss into schist was observed.

Southwest of Franklin Lake, a wider belt of steeply dipping Chantrey rocks is exposed, with interleaving of gneiss on a broad scale. The structure is complex, however, and exposure only moderately good. Dolomitic marble with contorted and strongly boudinaged quartzose laminae appears to form the northern margin of the belt. The marble is separated from the more central Chantrey rocks by amphibolite. White orthoquartzite, highly strained and locally fuchsite-bearing, is bordered by pelitic schist or marble. Much of the southern side of the belt appears to be underlain by quartz-pebble conglomerate, like that described above. Pelitic schist structurally overlain by orthoquartzite borders gneiss along part of the southern margin of the belt.

Farther southwest and separated from the main belt by drift and cataclastic-mylonitic gneiss lie poorly defined outliers (shown as a single mass on Figure 12.1) of metaconglomerate and minor quartz-feldspar-biotite schist. Although extremely stretched (length:width 12:1), quartz pebbles are easily recognized and bedding is preserved. The nose of one folded outlier plunges northeast beneath cataclastic basement gneiss.

No remnants of the Chantrey Group have been found farther southwest but this zone is made up of strongly flattened augen gneiss and mylonite that extend to the western border of the map area. The cataclastic belt is part of the Slave-Chantrey mylonite zone (Heywood and Schau, 1978).

A pegmatite sill intrusive into the Chantrey Group east of Chantrey Inlet gave a K-Ar age of 1680 Ma (Heywood, 1961). Bell (1970) considered the Chantrey Group to be Aphebian. On present evidence, the Chantrey Group could equally well be Archean.

Late Intrusive Rocks

Pegmatite

Discordant, muscovite-bearing pegmatite dykes are common throughout the area cutting all rocks except unmetamorphosed mafic dykes. Thus many basement rocks show two phases of pegmatite intrusion: older deformed, concordant pegmatites and younger crosscutting ones.

Larger bodies of white, muscovite-bearing pegmatite, containing abundant, irregularly distributed small garnets, seem to follow some of the Montresor-basement contacts. Pegmatites cutting the Montresor belt are restricted largely to its margins.

Mafic Dykes

Northwest-trending dykes, not more than 3 m thick, of lamprophyre and altered mafic rock of undetermined composition cut basement and Montresor rocks at scattered localities.

One or more diabase dykes, 30 m thick, follow the western shore of Franklin Lake. Another major diabase dyke with a similar trend is inferred from aeromagnetic patterns to traverse the south-central part of the map area.

Economic Geology

Some mineralization was noted at the Montresor-basement contact at the western end of the belt (Fig. 12.2).

A layer of quartz-biotite schist at the base of the Montresor sequence contains traces of native copper, and a little arsenopyrite? (Aspy? Cu in Fig. 12.2) occurs in the immediately adjacent leucogranitic rock. Richly pyritiferous lenses are found in the sheared, rusty quartzite – thought to be a recrystallized silicified zone – separating basement and Montresor rocks at the same locality.

References

Bell, R.T.

1970: The Hurwitz Group – a prototype for deposition on metastable cratons; in Symposium on Basins and Geosynclines of the Canadian Shield, ed. A.J. Baer; Geological Survey of Canada, Paper 70-40, p. 159-169.

1971: Geology of Henik Lake (east half) and Ferguson Lake (east half) map-areas, District of Keewatin (with a contribution by J.L. Talbot); Geological Survey of Canada, Paper 70-61, 31 p.

Geological Survey of Canada

1977: Montresor River, District of Keewatin, Northwest Territories; Geophysical Series (Aeromagnetic), Sheet 66I; Geological Survey of Canada, Map 7888G.

1982: Surficial Geology, Montresor River, District of Keewatin; Geological Survey of Canada, Map 10-1981.

Heywood, W.W.

1961: Geological notes, northern District of Keewatin; Geological Survey of Canada, Paper 61-18, 9 p.

Heywood, W.W. and Schau, M.

1978: A subdivision of the northern Churchill Structural Province; in Current Research, Part A, Geological Survey of Canada, Paper 78-1A, p. 139-143.

Patterson, J.G.

1981: Amer Lake: an Aphebian fold and thrust complex; unpublished M.Sc. thesis, University of Calgary, 106 p.

Tella, S. and Heywood, W.W.

1978: The structural history of the Amer Mylonite Zone, Churchill Structural Province, District of Keewatin; in Current Research, Part C, Geological Survey of Canada, Paper 78-1C, p. 79-88.

Tippett, C.R. and Heywood, W.W.

1978: Stratigraphy and structure of the northern Amer group (Aphebian), Churchill Structural Province, District of Keewatin; in Current Research, Part B, Geological Survey of Canada, Paper 78-1B, p. 7-11.

13. URANIUM AND THORIUM DISTRIBUTION PATTERNS AND LITHOGEOCHEMISTRY OF DEVONIAN GRANITES IN THE CHEDABUCTO BAY AREA, NOVA SCOTIA

Project 760045

K.L. Ford and S.B. Ballantyne
Resource Geophysics and Geochemistry Division

Ford, K.L. and Ballantyne, S.B., Uranium and thorium distribution patterns and lithogeochemistry of Devonian granites in the Chedabucto Bay area, Nova Scotia; in Current Research, Part A, Geological Survey of Canada, Paper 83-1A, p. 109-119, 1983.

Abstract

Follow-up investigations of airborne gamma ray spectrometric surveys confirmed the elevated levels of uranium and high eU/eTh ratios in some phases of the Devonian peraluminous granites of the Chedabucto Bay area. The high eU/eTh ratio is the result of increasing levels of uranium and/or decreasing levels of thorium associated with increasing differentiation.

Limited surficial geochemical sampling failed to distinguish two radiometrically distinct granites (Sangster Lake and Eastern Brook). The fact that uranium is not concentrated in either the aqueous or surficial sedimentary environment suggests that it may be in a non-labile form.

Lithogeochemical sampling indicated that some of the Chedabucto Bay granites are in the "specialized" granite class of Tischendorf. Characteristics of increased differentiation and/or autometasomatic alteration were best shown by enrichment of U, Be, Sn, Nb, and Rb, depletion of TiO_2, MgO, CaO, Sr, Ba, and Th, and an increasing Na_2O/K_2O ratio. An albitized cassiterite-bearing granitic dyke was found to exhibit these characteristics. Other granite phases showing some characteristics of increased differentiation (high eU/eTh) have high background levels of particular lithophile elements such as Sn and Be. These may be examples of "precursors" to mineralization.

Introduction

In 1978 a reconnaissance airborne gamma ray spectrometric survey (5 km line spacing) was flown over the eastern half of mainland Nova Scotia (Geological Survey of Canada, Geophysical Series Maps 35411G, 35511G, 35611G, and 35821G).

In 1979 and 1980, airborne gamma ray spectrometric data were collected with a north-south flight line and a line spacing of 1 km in the area of Chedabucto Bay, Nova Scotia (Geological Survey of Canada, Geophysical Series Maps 35611(3)G, 35611(4)G, 35611(5)G, and 35611(6)G). The survey area (Fig. 13.1) is covered by 1:50 000 scale N.T.S. maps 11F/3,4,5 and 6. These more detailed surveys provided increased resolution of the radioelement distribution patterns indicated in the 1978 reconnaissance.

Subsequent ground follow-up studies (Ford et al., 1981; Ford, 1982) and data within this report confirmed the significant radioelement variations within and among the various Devonian-Carboniferous granites of Nova Scotia. These radioelement variations are related to varying degrees of differentiation within the granites. Chatterjee and Muecke (1982) in their studies of the South Mountain Batholith of southwestern Nova Scotia showed that the airborne gamma ray spectrometric maps could be correlated with enrichment of elements such as Sn, Rb, Li, Be, F and Cs.

The Chedabucto Bay area has also been incorporated in regional lake sediment surveys (Bingley and Richardson, 1978) which cover all of south-central and southern Nova Scotia (Geological Survey of Canada, Open File 847, 1982). Elevated levels of uranium in lake sediments also reflect a general correlation with the underlying Devonian-Carboniferous granites.

This report examines previously defined regional radioelement distribution patterns, including uranium in lake sediments, and initial results of ground follow-up investigations conducted in 1981 in the Chedabucto Bay area.

Regional Geology and Structure

The geology of the Chedabucto Bay area is dominated by quartzites and slates of the Cambro-Ordovician Meguma Group (units 1 and 2 in Fig. 13.1), which have been folded into a series of tight folds with east-striking, steeply dipping axial planes (Stevenson, 1964; Schiller, 1961). The Meguma Group comprises the predominately quartzitic Goldenville Formation, overlain by dark, alumina-rich slates of the Halifax Formation. Rocks of the group are intruded by granites (unit 5, Fig. 13.1) of Devonian age (Fairbairn et al., 1960). These granites vary considerably in colour (grey to pink), texture (medium- to coarse-grained with aplitic, pegmatitic and porphyritic phases), structure (massive to locally foliated) and composition (see Table 13.1). The Meguma Group and associated granites occupy the eastern extremity of the Meguma Zone of central and southern Nova Scotia. Metamorphic grade within the Meguma Zone of the Chedabucto Bay area is predominantly middle amphibolite, but drops to lower greenschist south of Sherbrooke (Keppie and Muecke, 1979; Smith, 1981).

North of the Meguma Zone the geology is dominated by continental sediments of the Horton Group (unit 8) of early Mississippian age with minor amounts of possible pre-Mississippian volcanics and sediments (unit 6), and late Carboniferous diabase and gabbroic intrusions (unit 11). The Horton and Meguma strata are separated by an east-striking fault which forms the southern edge of the Glooscap Fault System (Keppie, 1977).

Airborne Gamma Ray Spectrometric Survey Results

Examination of the airborne gamma ray spectrometric survey data from the Chedabucto Bay area reveals the presence of several interesting radioelement distribution patterns.

Figure 13.2 shows that several portions of the study area exceed 3 ppm equivalent uranium. These areas are underlain by the Devonian granites or phases of these granites, and include the southwestern side of the Sherbrooke granite, the western edge of the Halfway Cove West granite, the Tom Lake granite, the east and east-central portions of the Sangster Lake granite and the Fox Island West granite.

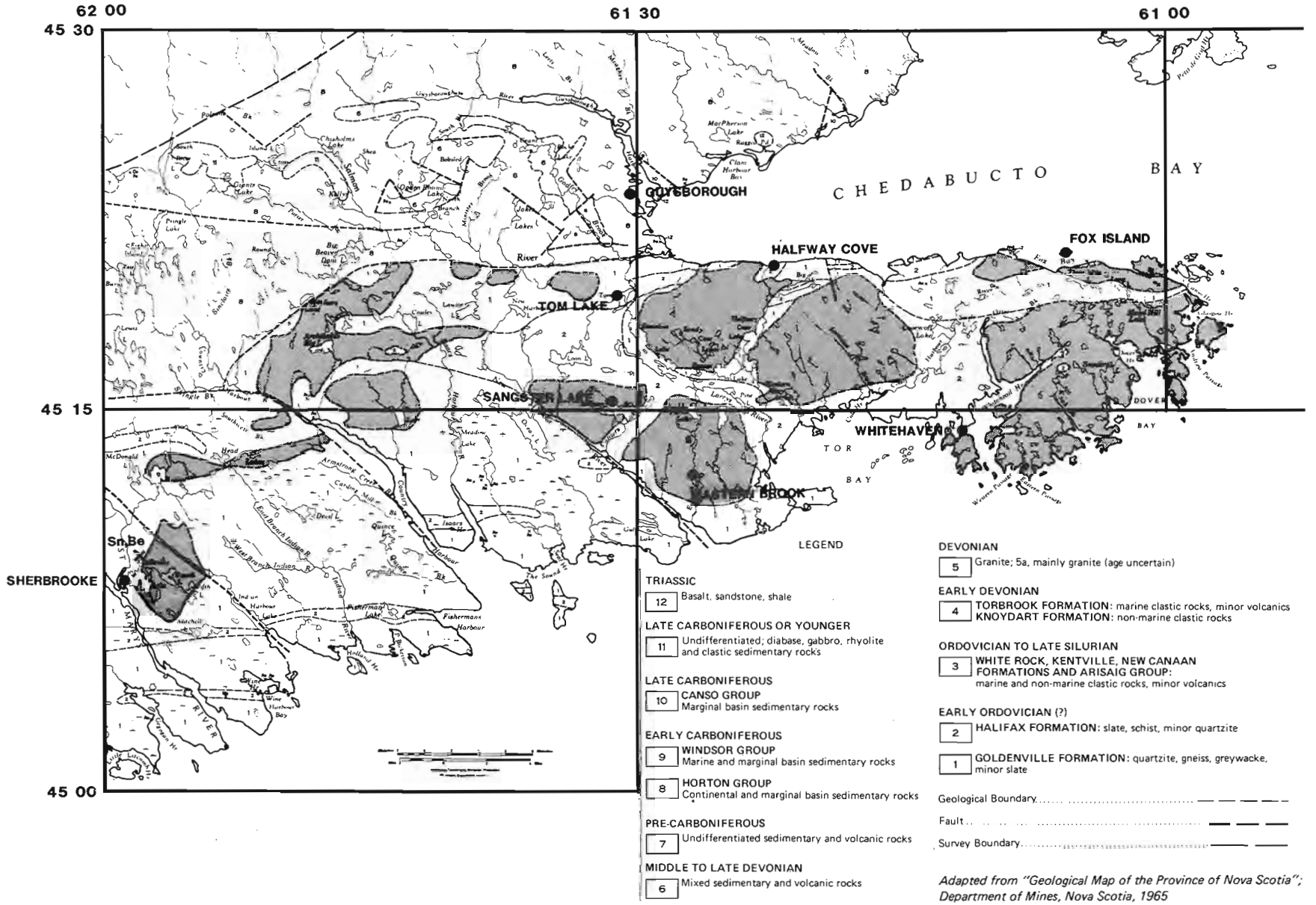

Figure 13.1. *Geology of the Chedabucto Bay area (adapted from Geological Map of the Province of Nova Scotia, Department of Mines, Nova Scotia, 1965). Total area coverd by north-south, 1 km line spaced airborne gamma ray spectrometric surveys. Devonian granites have been shaded.*

In contrast to these elevated levels of equivalent uranium, equivalent thorium levels are generally low over most of these areas (Fig. 13.3). Only the central area of the Halfway Cove East and eastern half of the Whitehaven-Dover Bay granites have relatively high levels of equivalent thorium. This general inverse correlation between equivalent uranium and equivalent thorium concentrations is an unusual characteristic of most, but not all, granitoids of the Meguma Zone of Nova Scotia.

In general the high equivalent uranium/equivalent thorium (eU/eTh) ratios (Fig. 13.4) are restricted to granitic areas, characterized by either elevated levels of uranium and/or depleted levels of thorium.

Such general relationships between uranium and thorium, however, are not characteristic of all Chedabucto Bay area granites. An example of the general trend is shown by the southwestern margin of the Sherbrooke granite where increased uranium concentrations (1-2 ppm for the northeastern side, to greater than 3 ppm for the southwestern edge) are superimposed on decreasing thorium concentrations (2-4 ppm to less than 2 ppm). Examples of contrasting trends include the peripheral areas of the Whitehaven-Dover Bay granite where decreased thorium levels (2-4 ppm for the peripheral areas compared to 6-8 ppm for the interior areas) are superimposed on relatively constant uranium levels (2-3 ppm for both peripheral and interior areas), and the Sangster Lake granite where sharply increased uranium concentrations (1-2 ppm at the western margin compared to greater than 5 ppm in the east and east-central areas) are superimposed on constant thorium concentrations (2-4 ppm). In each case high eU/eTh ratios are generated, but in each case by a slightly different relationship between the two radioelements.

Ground Follow-up Investigations and Results

In Situ Gamma Ray Spectrometric Results

One hundred and thirty in situ measurements utilizing a portable Disa 400 (Exploranium) gamma ray spectrometer were made on the granites of the Chedabucto Bay study area. These ground measurements reveal the same inverse relationship between uranium and thorium as the airborne data. Figures 13.5A, B, and C are log-log plots of equivalent uranium (eU) vs. equivalent thorium (eTh), eU/eTh ratio vs. eU, and eU/eTh vs. eTh, respectively. These plots show the wide range of uranium and thorium concentrations encountered in the Chedabucto Bay area granites. For comparison, the average concentrations of eU and eTh measured by in situ gamma ray spectrometry in and around the New Ross-Vaughn complex of the South Mountain Batholith (SMB) are also shown, as are the average abundances of U and Th in granites as reported by Taylor (1965). For those phases of the granites studied in the Chedabucto Bay area, the overall average eU and eTh concentrations are approximately 10 and 6 ppm respectively. These averages reflect the generally high eU/eTh ratio of most of the Chedabucto Bay area granites. The Halfway Cove East and Whitehaven-Dover Bay granites, characterized by relatively high eTh were not extensively studied during ground follow-up investigations. However, limited measurements yielded concentration levels of eU and eTh which are similar to those found for the granodioritic phase of the South Mountain Batholith (Chatterjee and Muecke, 1982; Ford, 1982) and Taylor's (1965) global average for granodioritic rocks (3 ppm U, 10 ppm Th). Keppie (personal communication, 1982) has indicated that dioritic phases were encountered in the area of the Halfway Cove East granite.

As indicated on Figures 13.5A, B, and C radioelement variations within individual granite plutons can be considerable. For example, concentrations in the Sangster Lake granite vary from 3 ppm eU in the western portion, to 9 ppm eU in the east-central portion, to 12 ppm eU in the extreme eastern part of the granite, while eTh concentrations remain constant at 5 ppm. Average eU/eTh ratios range from 0.6 in the west to 2.4 in the east. Variations in the ratio reflect zones of variable uranium content superimposed on a constant thorium content within the granite. In contrast to the Sangster Lake granite, the Sherbrooke granite is characterized by an increasing uranium concentration superimposed on a decreasing thorium concentration. Average radioelement concentrations range from 8 ppm eU and 11 ppm eTh in the northeast portion of the granite to 16 ppm eU and 5 ppm eTh in the southwest. In some areas this drastic variation in radioelement content is not accompanied by any obvious variations in texture or alteration in the granite. There may, in some cases, be an increase in the muscovite/biotite ratio with muscovite becoming the predominant micaceous phase in the high eU/eTh ratio portions of these granites. Ford (1982) referred to a similar feature for the Beadle Mountain granite in central New Brunswick. It has been suggested that such a variation in muscovite and biotite may reflect a high temperature water-rock interaction (Plant et al., 1980).

Studies conducted in other areas of Nova Scotia underlain by Devonian-Carboniferous granites (Chatterjee and Muecke, 1982; Ford, 1982), have also noted significant internal radioelement variation. In the New Ross-Vaughn area of the South Mountain Batholith, variations in uranium and thorium concentrations have been related to differentiation within a cogenetic suite of granitic rocks. In general, concentrations of uranium have been shown to increase, and thorium to decrease, with increasing differentiation proceeding from biotite granodiorite to biotite-muscovite and leucocratic adamellites, to dykes and irregular masses of aplite, pegmatite and porphyries. Superimposed on this cogenetic suite of granitic rocks is a series of argillitized, sericitized and albitized granites and greisens called para-intrusives by Chatterjee and Muecke (1982). Normal differentiation trends of some elements of the cogenetic suite tend to break down in the para-intrusive suite possibly as the result of interaction between a late stage fluid phase and residual magma or crystalline rocks. For the granites investigated in the Chedabucto Bay area there does not appear to be the same range of rock types as that encountered in the South Mountain Batholith. Dioritic or granodioritic phases may be present in the Halfway Cove East or Whitehaven-Dover Bay granitic bodies which have relatively higher concentrations of equivalent thorium as indicated on the airborne survey results.

The in situ gamma ray measurements within the Chedabucto Bay area clearly verify the distribution patterns observed in the regional airborne data.

Regional and Follow-up Stream and Lake Geochemistry

In the Chedabucto Bay area, anomalous levels of uranium in lake sediments are generally restricted to areas underlain by Devonian granites. The regional data (Bingley and Richardson, 1978; Geological Survey of Canada, Open File 847, 1982) show differences in the concentration levels of uranium both within and between the granitic bodies of the study area. Lake sediments associated with the Sherbrooke, Halfway Cove, and parts of the Whitehaven-Dover Bay granites have elevated levels of uranium compared to those for the Eastern Brook or Sangster Lake granites.

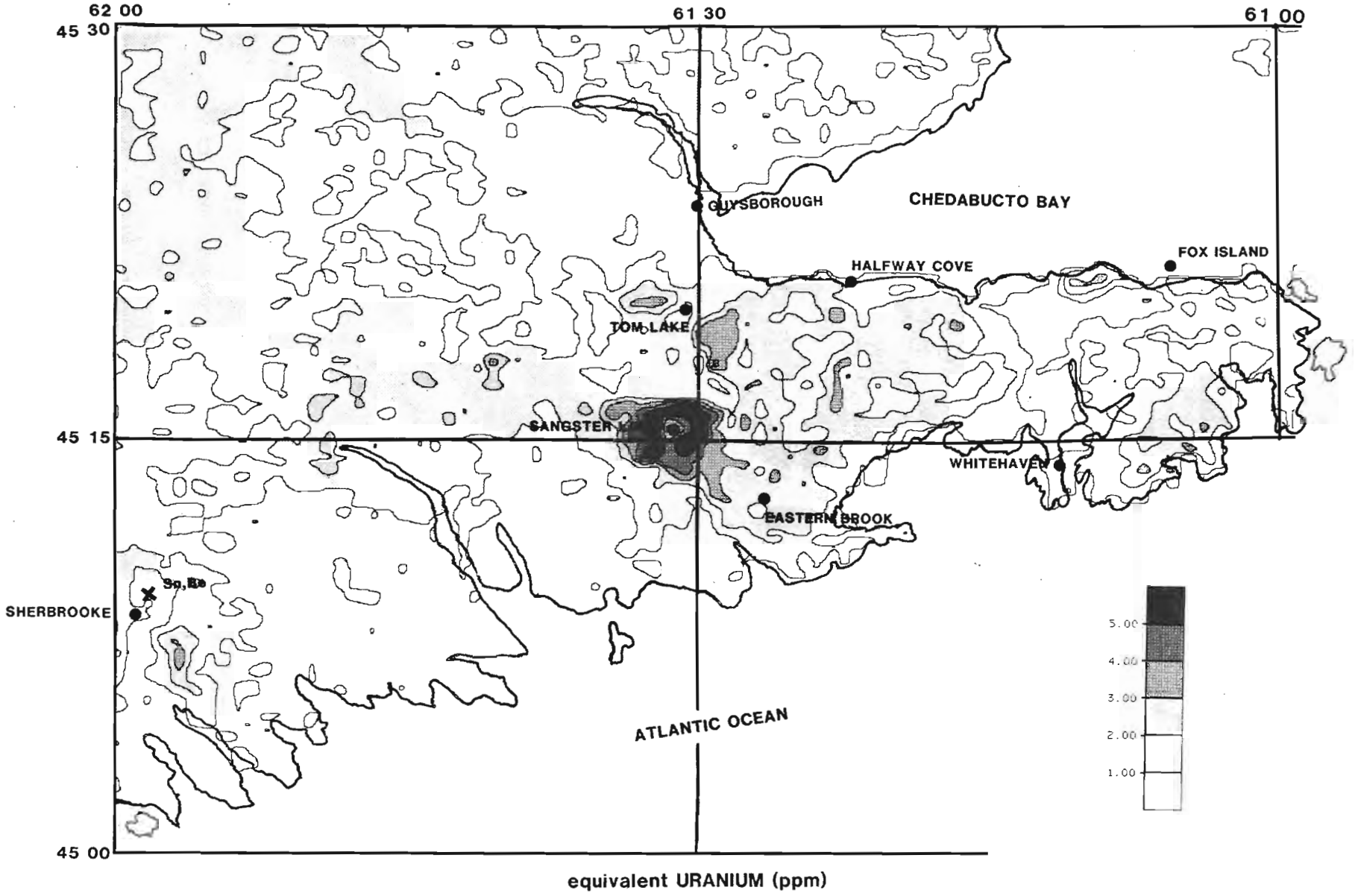

Figure 13.2. *Equivalent uranium (ppm) map for the Chedabucto Bay area compiled from 1 km line spaced airborne gamma ray spectrometric surveys.*

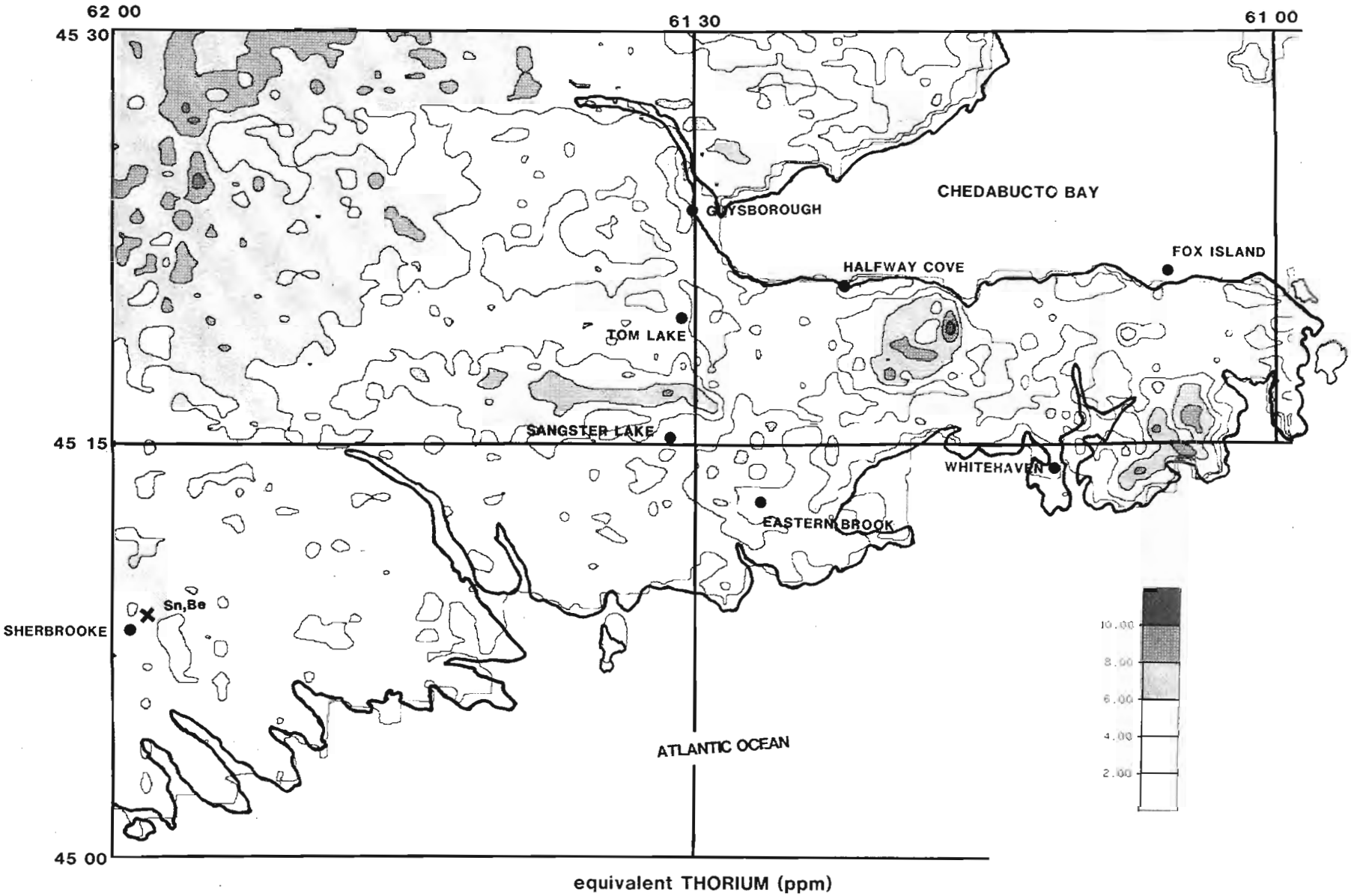

Figure 13.3. Equivalent thorium (ppm) map for the Chedabucto Bay area compiled from 1 km line spaced airborne gamma ray spectrometric surveys.

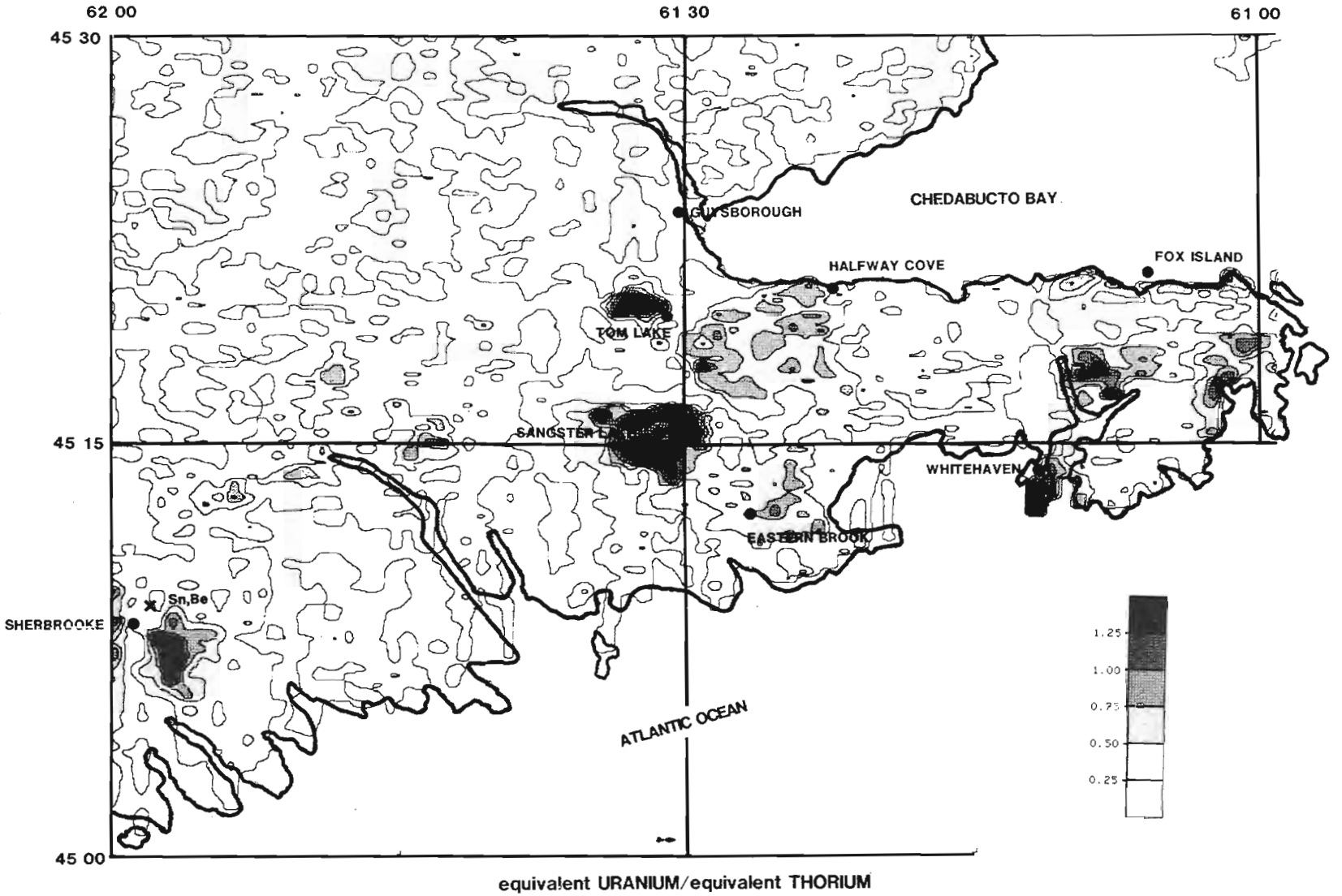

Figure 13.4. *Equivalent uranium/equivalent thorium ratio maps for the Chedabucto Bay area compiled from 1 km line spaced airborne gamma ray specrometric surveys.*

Table 13.1

Average major and minor element compositions (%) and selected trace element concentrations (ppm) of some Chedabducto Bay area granites

	Sangster Lake			Eastern Brook		Tom Lake	Halfway Cove	Whitehaven	Fox Island		Sherbrooke		A		B
	West	East I	East II	I	II				West	East	I	II			
	N=3	N=13	N=11	N=8	N=4	N=5	N=6	N=4	N=2	N=4	N=1	N=1			
SiO_2	74.13	72.55	73.57	73.00	74.00	73.40	71.67	74.42	61.35	73.95	74.00	74.30	73.38	1.39	73.02
TiO_2	.17	.20	.06	.24	.10	.11	.26	.10	.21	.12	.03	0.02	0.16	0.10	0.21
Al_2O_3	14.30	15.49	15.61	14.88	15.18	14.58	15.27	14.30	21.00	14.55	15.70	15.40	13.97	1.07	13.90
Fe_2O_3TOTAL	1.06	1.52	.69	1.60	.62	.86	1.70	1.08	1.70	.98	.31	.31	1.90	0.94	2.08
MnO	.03	.05	.04	.05	.03	.02	.06	.03	.03	.03	.02	.04	0.045	0.040	0.05
MgO	.33	.36	.13	.53	.18	.21	.59	.14	.42	.23	.02	.03	0.47	0.56	0.52
CaO	.64	.38	.29	.64	.54	.48	.97	.42	.84	.51	.30	.53	0.75	0.41	1.24
Na_2O	3.66	3.88	4.49	3.85	4.58	3.79	3.61	3.86	5.44	4.04	6.62	7.85	3.20	0.61	3.28
K_2O	4.55	4.16	3.95	4.32	4.19	4.76	4.23	4.45	7.54	4.43	2.20	.89	4.69	0.68	4.57
H_2O	.60	.70	.52	.49	.28	.75	.65	.48	.90	.68	.40	.30		-	0.90
CO_2	-	-	-	.10	.18	.30	.28	-	.20	.22	.10	.10		-	
P_2O_5	.29	.35	.38	.26	.43	.34	.24	.33	.46	.35	.30	.34		-	0.15
TOTAL	99.76	99.64	99.73	99.96	100.31	99.60	99.53	99.61	100.09	100.09	100.00	100.11			
Sr	67	18	47	78	17	54	117	12	100	25	10	50		285*	100**
Ba	263	89	84	321	137	206	350	90	430	152	40	40		600	840
Rb	207	335	412	239	313	254	223	390	370	288	690	390		150	170
Zr	27	45	11	61	17	28	63	18	80	32	-	40		180	175
Cu	5	5	4	4	4	5	7	5	6	6	6	9		10	10
Pb	27	12	11	22	18	15	25	14	14	20	8	15		20	19
Zn	31	57	23	32	15	14	56	47	16	19	52	45		40	39
Mo	2	3	3	6	5	-	2	-	-	-	-	-		2	1.3
F	342	800	538	690	702	430	478	871	578	555	295	300		735	850
W	2	3	3	2	2	2	5	4	4	4	4	4		2	2.2
Be	3.8	10.5	25.3	4.4	7.9	4.7	4.2	1.5	3.0	1.6	103.0	182.0		5	3
Li	52	180	64	97	38	78	96	125	46	36	4	7		30	40
Sn	8	21	32	18	18	10	7	11	10	10	126	218		3	3
Nb	3	16	18	4	7	13	9	10	14	14	8	14		20	21
U	3.7	9.5	9.8	5.7	6.9	3.3	5.6	3.6	6.0	6.9	7.0	12.0		4.8	4.8
Th	3.0	4.1	1.7	8.4	2.0	2.4	6.0	4.0	15.0	5.8	1	1		17	20
U/Th	1.23	2.32	5.76	.68	3.45	1.37	.93	.90	.40	1.19	7.0	12.00		.28	.28

Analytical Methods:

Majors, Minors, Sr, Ba, Rb, Zr, Nb, and Sn analyzed by x-ray flourescence, Cu, Pb, Zn, Mo, Be, and Li by atomic absorption, F by fusion and specific-ion electrode, W by colorimetric methods, U and Th by delayed neutron counting.

N = Number of samples analyzed

Rock type description:

Sangster Lake – West: Massive, coarse grained, pale pink, biotite-muscovite granite.
– East I: Foliated (locally massive), medium grained, buff coloured, biotite-muscovite granite.
– East II: Foliated (locally massive), fine grained, pale pink, muscovite leucogranite (minor biotite).

Eastern Brook – I: Massive porphyritic (Kspar), grey to pink, biotite granite (minor muscovite).
II: Massive, fine grained (locally medium to coarse), grey, muscovite leucogranite (minor biotite).

Tom Lake: Foliated, medium grained, grey to pink, muscovite granite (minor biotite).

Halfway Cove: Massive, medium to coarse grained (locally porphyritic), grey to pink, biotite granite (minor muscovite).

Whitehaven: Massive, medium grained, grey to pink, biotite-muscovite granite.

Fox Island – West: Foliated, medium grained, pink, biotite-muscovite syenite.
East: Foliated, medium grained, pink, muscovite-biotite granite.

Sherbrooke – I: Massive, coarse grained, inequigranular, pink, muscovite, leucogranite dyke.
II: Banded, fine to coarse granined, inequigranular, pink, leucogranite dyke (same as Sherbrooke I).

* Granites (average abundance): Taylor(1961)

** Low-calcium granites: Turekian and Wedepohl (1961)

(-) Dashes indicate no data are available.

A - Tischendorf's (1977) Specialized or Stannigne Granites (Group I)

B - Stemprok and Skvor (1974) Weighted mean of tin-bearing granites of the world (without Boliva)

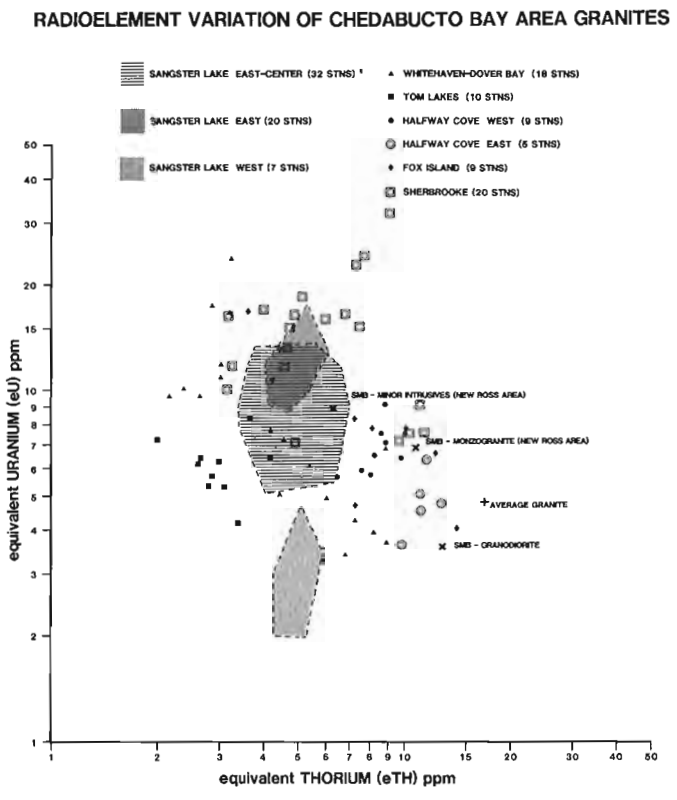

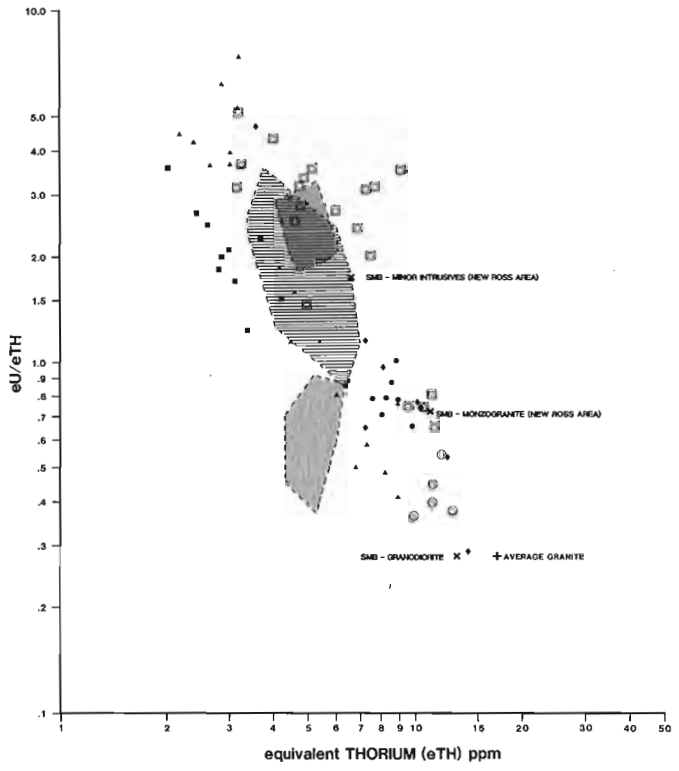

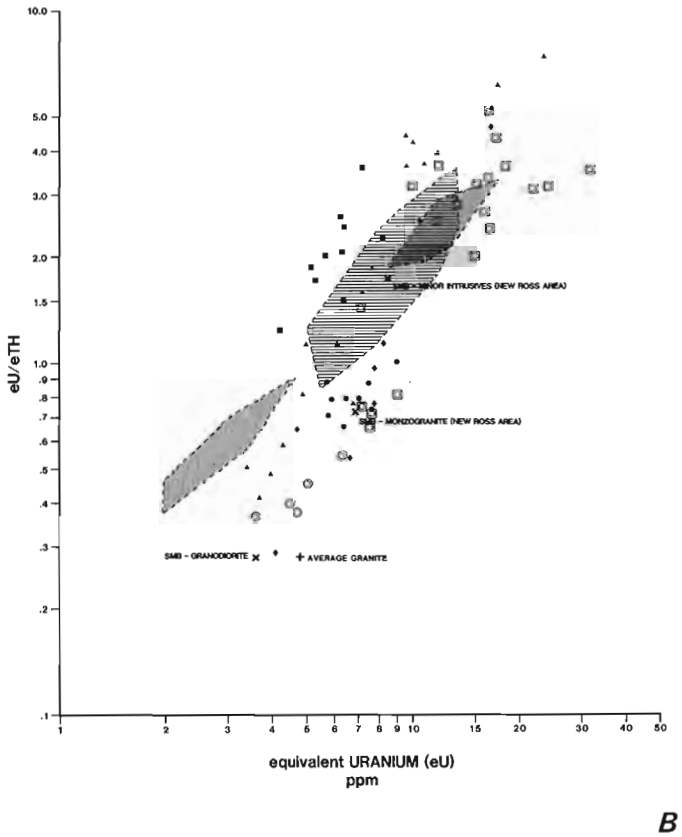

Figures 13.5A, B and C

Log-log plots of individual in situ gamma ray spectrometric measurements showing the equivalent uranium vs. equivalent thorium, eU/eTh vs. equivalent uranium, and the eU/eTh vs. equivalent thorium respectively for nine granite localities in the Chedabucto Bay area. The spread in concentrations encountered in the three areas of the Sangster Lake granite is indicated by shaded areas to reduce congestion in the diagram.

A visual examination of the unpublished regional raw data for uranium in lake sediments and corresponding loss on ignition (LOI) values reveals that the differences in uranium concentrations between and within the study area granitoids are not related to variations in organic content as measured by LOI. Sediment data from three lakes underlain by the Sangster Lake granite contain uranium concentrations in the range of 6.6-7.9 ppm while their corresponding LOI values range from 14.4 to 70.2%. Sediments from lakes underlain by the Halfway Cove granite have uranium concentrations ranging from 4.6-50.9 ppm, yet the LOI values for the two lakes which exhibit the minimum and maximum of this range are 27.8% and 33.2% respectively.

Examination of the remainder of the multielement regional lake sediment data (Geological Survey of Canada, Open File 847, 1982) failed to show any obvious associated geochemical anomalies or zoning patterns, identified by Davenport (1982) as being characteristic of Newfoundland mineralized granitoids.

In an effort to explain some of the differences between the regional lake sediment and the airborne gamma ray spectrometric patterns, a limited lake water and sediment sampling, stream water and sediment sampling, and heavy mineral panned concentrate sampling project was conducted in the Chedabucto Bay study area. The main foci of this follow-up were the Sangster Lake and Eastern Brook areas.

The apparent specialized nature of the Sangster Lake granite, as suggested by its anomalous appearance on the regional gamma ray spectrometric surveys had been verified previously by ground measurements and limited litho-geochemical sampling (Ford et al., 1981).

Nineteen surface lake water and twenty stream water samples collected in the Sangster Lake and Eastern Brook areas yielded surprisingly low concentrations on both U and F (less than 0.1 and 10 ppb respectively), and showed no significant differences between the two granite bodies. The pH of both surface lake waters and stream waters averaged 4.6 and conductivity measured less than 50 mhos/cm.

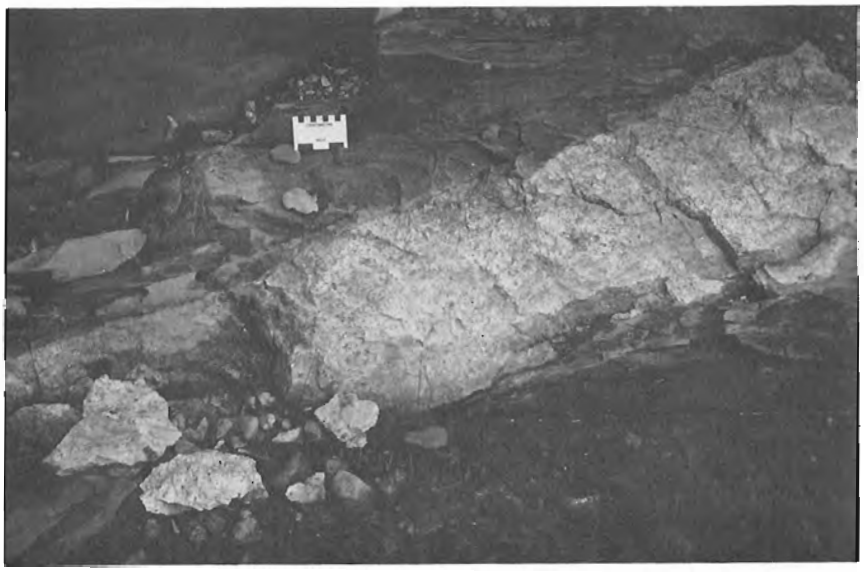

Figure 13.6. *Sn-Be-bearing leucogranite dyke west of the Sherbrooke Granite.*

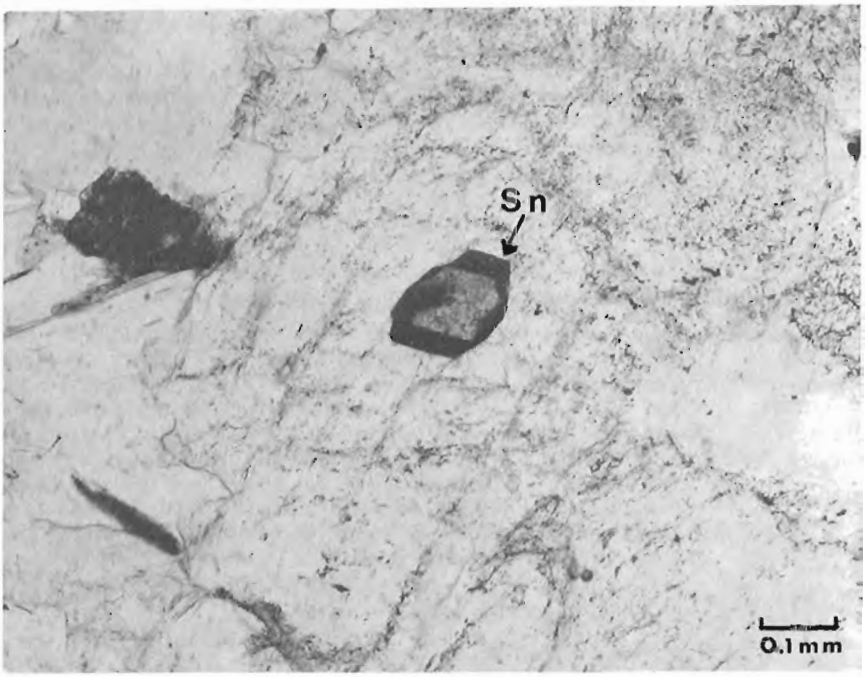

Figure 13.7. *Average major and minor (%) element and selected trace element (ppm) concentrations of some Chedabucto Bay area granites.*

Nine nearshore and centre lake sediment samples collected in the Sangster Lake area confirmed the levels of U indicated in the regional data. These samples averaged 6.1 ppm U (ranging from 2.5-9.0) with LOI ranging from 8.1% (nearshore) to 45.0% (centre of lake). Sn and F contents showed no significant variation within or between the two granite bodies, averaging 6.5 and 205 ppm respectively, with ranges of 1-14 and 50-490 ppm respectively.

Twenty stream sediment samples from the Sangster Lake and Eastern Brook granitic areas yielded an average uranium content of 4.3 ppm (ranging 0.5-13.0 ppm) and an average LOI of 22.9% (ranging 7.9-54.1%). Sn and F levels averaged 8.1 and 266 ppm respectively with ranges of 1-13 and 60-500 ppm respectively. Again there was no significant variation between samples collected from either granite body. Mo and W levels also showed no significant variation between the two granite areas, while other trace elements showed no significant enrichment or depletion with respect to the regional data already available (Bingley and Richardson, 1978; Geological Survey of Canada, Open File 847, 1982).

Four different size fractions from each of seven heavy mineral panned concentrates from the Sangster Lake area also gave disappointing results. Sn and W concentrations were similar to levels for corresponding stream sediments (less than 10 ppm). Examination of the concentrates failed to reveal the presence of cassiterite or other tin-bearing minerals. Even though the Sangster Lake granite is enriched in tin (Ford et al., 1981) it may not be in the form of cassiterite. Studies of the East Kemptville tin deposit of the Davis Lake pluton, South Mountain Batholith, have shown that rocks may contain 100-200 ppm Sn not as cassiterite (Richardson et al., 1982).

Limited surficial geochemistry failed to outline any differences between the Sangster Lake and Eastern Brook granites. The fact that uranium, in both waters and sediments is present in very low concentrations suggests that uranium may be present in a non-labile form in the Sangster Lake granite.

Lithogeochemistry and Mineralization

A limited rock sampling program (Ford et al., 1981) showed that the Sangster Lake granite exhibits elevated levels of U, Sn, Li, Nb, and Rb, and depleted levels of Th, Sr and Ba compared to Taylor's (1965) global average abundances for granites.

Table 13.1 is a summary of the major, minor and selected trace element analyses for some of the Chedabucto Bay area granites. For comparative purposes, trace element data from Taylor (1965), and Turekian and Wedepohl (1961), and major and minor element data from Tischendorf (1977) and Stemprok and Skvor (1974) as well as descriptions of the various phases for the granite bodies are given. The samples collected for this study do not represent all of the granitic phases, styles of alteration, or mineralization which might be found within the study area.

The Chedabucto Bay area granites are peraluminous and are low in TiO_2, MgO and CaO as are the "specialized" granites of Tischendorf (1977). They also show a general enrichment in U, Sn, Rb, and Li and a depletion in Th, Sr, Ba, and Zr compared to the average low calcium granites of Turekian and Wedepohl (1961).

Evidence of igneous differentiation within individual granitic bodies is shown by the analyses of the Sangster Lake and Eastern Brook samples. Minor dykes and/or irregular masses of finer grained leucogranite exhibit the characteristics of increased differentiation. Sangster Lake West and Eastern Brook I phases are less differentiated than the Sangster Lake East I and II and Eastern Brook II phases which generally show a marked enrichment in U, Be, Sn, Nb, and Rb and depletion in TiO_2, CaO and Ba.

We observed little alteration in the Sangster Lake granite. Milky white quartz veins locally containing abundant medium to coarse black tourmaline cut the various phases, as do barren quartz veins. Where observed these late veins caused no apparent alteration of the granite. Evidence of greisenization was not observed during limited traversing.

Table 13.1 shows that some phases of the Chedabucto Bay area granites have a variable Na_2O/K_2O ratio. Albitization in varying degrees has been suggested by staining techniques and confirmed, in extreme cases, in thin section. Albitized granitic rocks of the South Mountain Batholith are thought to be of autometasomatic rather than postmagmatic origin (Chatterjee, 1981). The significance of the albitization with respect to possible mineralizing processes within the Chedabucto Bay granites is not known. However, examination of a granitic dyke located just outside the western margin of the Sherbrooke granite (UTM co-ordinates 5000440N, 581020E) may provide some evidence. This 20 cm wide, nonsymmetrically zoned, leucogranitic dyke (Fig. 13.6) cross-cuts the slaty cleavage of the Goldenville Formation with no apparent alteration of the host rock. The high Na_2O/K_2O ratio is apparently due to intense albitization, as shown in stained rock slabs and confirmed in thin section. Chemical analyses of two samples (Table 13.1) from this dyke exhibit some of the characteristics of increased differentiation, as well as enrichment in SiO_2, Al_2O_3, and Na_2O and depletion in TiO_2, Fe_2O_3 (Total), MgO, and K_2O compared to other granitic rocks of the Chedabucto Bay area. Trace element analyses show little difference in the uranium concentrations of this dyke compared to the other granitic rocks, although thorium concentrations are extremely low. Depletion of F, Sr, Ba and Li is accompanied by significant enrichment in Sn, Be, and Rb as compared to the other Chedabucto Bay granites. Cassiterite has been identified in heavy mineral concentrates from the two dyke samples by X-ray diffraction and confirmed by microprobe studies of polished thin sections (Fig. 13.7). Although discrete Be phases have bene identified to date, a semi-quantitative optical emission analysis of mica separates from the two samples gave the following values, 150 ppm Be and 500 ppm Sn for sample I, and 700 ppm Be and 700 ppm Sn for sample II. By comparison, Beus (1965) reports a range of Be contents for muscovites from Be-bearing pegmatites of 30 to 140 ppm.

High concentrations of Sn, Be, Nb, and Ta in phases of the Sangster Lake granite may be related to the presence of ixiolite, $(Ta,Nb,Fe,Mn,Sn)_4O_8$ and tapiolite, $(Fe^{+2}(Ta,Nb)_2O_6)$ whose presence has been verified by super-panning and X-ray diffraction techniques. These minerals were found in leucogranite phases containing high Sn (20-50 ppm), Ta (14-37 ppm) and often elevated Be and Nb concentrations. All other granitic samples were found to contain Ta concentrations less than 3 ppm. Cassiterite has not been identified in the super-panned heavy mineral separates or thin sections of the Sangster Lake leucogranite phases to date. Concentrations of minerals such as ixiolite and tapiolite may explain the anomalous Sn concentrations. Although most of the fine grained or leucogranite samples from the Sangster Lake showed no W enrichment, one sample, containing 30 ppm W yielded wolframite (confirmed by X-ray diffraction) in a super-panned concentrate. These examples illustrate that the heavy mineral separation approach can help to explain variations in whole-rock lithogeochemistry which may not be revealed by thin section examination.

Initial results of fission-track and scanning electron microscope studies on the uranium enriched fine grained leucogranite phase of the Sangster Lake granite indicate that chlorine-bearing apatite and a uranium-bearing Fe phosphate phase contain the highest concentrations of uranium.

Summary

The results illustrate the capability of airborne gamma ray spectrometric surveys to delineate those granites or phases within larger granite plutons, which exhibit characteristics of increased differentiation. In the Chedabucto Bay area more differentiated granite phases are characterized by high eU/eTh ratios due to an inverse relationship between uranium and thorium. The reason for the high eU/eTh ratio (normally much less than 1 for most igneous rocks) is not fully understood, but may be related to some degree of late-stage water-rock interaction, possibly autometasomatic. Associated with these enrichment and depletion trends in the radioelements are similar trends in other lithophile elements. In the case of the Chedabucto Bay area granites, Sn and Be appear to have the most obvious correlation with the radioelement trends.

Those phases delineated by the airborne gamma ray spectrometric surveys and in situ measurements as showing characteristics of increased differentiation (high eU/eTh ratio) and confirmed by lithogeochemical sampling as having elevated levels of other lithophile elements (e.g. Sangster Lake granite) may be precursors to, or are spatially related to, potentially economic concentrations. An illustration of this relationship may be the southwestern edge of the Sherbrooke granite and the Sn-Be occurrence situated off its western margin.

Acknowledgments

We thank A.C. Roberts, G.J. Pringle, and Mrs. G.M. Le Cheminant of the Central Laboratories and Technical Services Division for carrying out mineral identification (XRD) and microprobe analysis.

Analytical work was carried out largely in the laboratories of the Geological Survey of Canada, Resource Geochemistry Subdivision under the direction of Ms. G.E.M. Hall. J.L. Bouvier and K.A. Church supervised the chemical analysis of rocks in the Central Laboratories and Technical Services Division. P.J. Lavergne was responsible for the methods development and preparation of the rock sample heavy mineral separates. Discussions with personnel of the Nova Scotia Department of Mines and Energy, Mineral Resources Division, were a valuable asset in this study. The paper was reviewed by D.R. Boyle, B.W. Charbonneau, and K.A. Richardson.

References

Beus, A.A.
1965: Geochemistry of beryllium and genetic types of beryllium deposits; ed. L.R. Page; W.H. Freeman and Company, San Fransisco, 401 p.

Bingley, J.M. and Richardson, K.A.
1978: Regional lake sediment geochemical surveys for Eastern Mainland Nova Scotia; Nova Scotia Department of Mines and Energy, Open File 371, 13 geochemical maps for each of 3-1:100 000 map sheets.

Chatterjee, A.K.
1981: Polymetallic Sn-Be, Sn-W-U, Sn-U, and U-P-F mineralization related to peraluminous acid magmatism – Southwestern Nova Scotia; in Mineral Resources Division Report of Activities, 1980; Nova Scotia Department of Mines and Energy, Report 81-1, p. 33.

Chatterjee, A.K. and Muecke, G.K.
1982: Geochemistry and the distribution of uranium and thorium in the granitoid rocks of the South Mountain Batholith, Nova Scotia: some genetic and exploration implications; in Uranium in Granites, ed. Y.T. Maurice; Geological Survey of Canada, Paper 81-23, p. 11-17.

Davenport, P.H.
1982: The identification of mineralized granitoid pluton from ore-element distribution patterns in regional lake sediment geochemical data; Canadian Institute of Mining and Metallurgy, Bulletin, v. 75, no. 840, p. 79-90.

Fairbairn, H.W., Hurley, P.M., Pinson, W.H., and Comier, R.F.
1960: Age of the granitic rocks of Nova Scotia; Geological Society of America, Bulletin, v. 71, p. 399-414.

Ford, K.L., Carson, J.M., and Holman, P.B.
1981: Preliminary airborne gamma ray spectrometric map and ground investigations, central Nova Scotia; Geological Survey of Canada, Open File 789.

Ford, K.L.
1982: Investigation of regional airborne gamma ray spectrometric patterns in New Brunswick and Nova Scotia; in Current Research, Part B, Geological Survey of Canada, Paper 82-1B, p. 177-194.

Keppie, J.D.
1977: Tectonics of Southern Nova Scotia; Nova Scotia Department of Mines, Paper 77-1.

Keppie, J.D. and Muecke, G.K.
1979: Metamorphic Map of Nova Scotia, 1979; in Folio of Geological Maps of Nova Scotia, scale 1:2 000 000, Nova Scotia Department of Mines and Energy.

Plant, J., Brown, C.G., Simpson, P.R., and Smith, R.T.
1980: Signature of metalliferous granites in the Scottish Caledonides; Institution of Mining and Metallurgy, Transactions, Section B, Applied Earth Science, v. 89, November 1980, p. B198-B210.

Richardson, J.M.G., Spooner, E.T.C., and McAuslan, D.A.
1982: The East Kemptville tin deposit, Nova Scotia: an example of a large tonnage, low grade greisen-hosted deposit in the endocontact zone of a granite batholith; in Current Research, Part B, Geological Survey of Canada, Paper 82-1B, p. 27-32.

Schiller, E.
1961: Geology, Guysborough, Nova Scotia (11F/5); Geological Survey of Canada, Map 27-1961, scale 1 inch to 1 mile.

Smith, P.K.
1981: Geology of the Sherbrooke area, Guysborough County, Nova Scotia; in Mineral Resources Division, Report of Activities, 1980; Nova Scotia Department of Mines and Energy, Report 81-1, p. 77-94.

Stemprok, M. and Skvor, P.
1974: Composition of tin-bearing granites from the Krusne Hory metallogenic province of Czechoslovakia; Journal of Geological Sciences, Economic Geology, Mineralogy, Prague, v. 16, p. 7-87.

Stevenson, I.M.
1964: Geology, Chedabucto Bay, Nova Scotia, (11F/6); Geological Survey of Canada, Map 1156A, scale 1 inch to 1 mile.

Taylor, S.R.
1965: The application of trace element data to problems in petrology; in Physics and Chemistry of the Earth, v. 6, ed. L.H. Ahrens, F. Press, S.K. Runcorn, and H.C. Urey, p. 135-213.

Tischendorf, G.
1977: Geochemical and petrographic characteristics of silicic magmatic rocks associated with rare-earth mineralization; in Metallization Associated with Acid Magmatism, ed. M. Stemprok, L. Burnol, and G. Tischendorf; International Geological Correlation Programme, v. 2, p. 41-96.

Turekian, K.K. and Wedepohl, K.H.
1961: Distribution of the elements in some major units of the earth's crust; Geological Society of America, Bulletin, v. 72, no. 2, p. 175-191.

14. A REACTION GRID FOR POTASSIUM-POOR PELITIC AND MAFIC ROCKS

Project 780011

E. Froese and R.D. Hall[1]
Precambrian Geology Division

Froese, E. and Hall, R.D., A reaction grid for potassium-poor pelitic and mafic rocks; in Current Research, Part A, Geological Survey of Canada, Paper 83-1A, p. 121-124, 1983.

Abstract

Reactions in potassium-poor pelitic and mafic rocks may be combined into a common grid which provides a convenient correlation of mineral assemblages in pelitic and mafic rocks and accommodates the rarely observed coexistence of hornblende with highly aluminous minerals.

In potassium-poor rocks, biotite is the only potassium-bearing mineral at medium and high grades of metamorphism. The composition of other minerals is given approximately in terms of the oxides SiO_2-TiO_2-Al_2O_3-Fe_2O_3-FeO-MgO-CaO-Na_2O-H_2O. At constant pressure, temperature, and activity of H_2O, and in the presence of quartz, plagioclase of constant composition, magnetite, and ilmenite, phase relations among these minerals may be shown in the following system (Froese, 1969):

$A = Al_2O_3-(Na_2O+CaO)$
$F = FeO-(Fe_2O_3+TiO_2)$
$M = MgO$

In Figure 14.1, mineral compositions are plotted on a diagram of A/(F+M) vs. M/(F+M) similar to the representation used by Stout (1972). The compositions of chlorite, almandine, gedrite, cummingtonite, and hornblende were taken from analyses (Table 14.1) of minerals found in a metamorphosed mafic volcanic rock from Limerick Township, Ontario (Hall, 1980). In hornblende analyses reported by Jen and Kretz (1981), the ratio of weight % Fe_2O_3 to weight % FeO ranges from 0.24 to 0.38. Taking these values as a guide, a ratio of 0.20 has been assumed for the hornblende analysis in Table 14.1. The compositions of staurolite and cordierite were taken from analyses (no. 6 and 7) in Percival et al. (1982). The composition of chloritoid is shown with a M/(F+M) ratio slightly greater than that of staurolite (Fox, 1971). The composition of orthopyroxene is plotted with a M/(F+M) ratio somewhat smaller than that of gedrite (Savolahti, 1966). This composition is consistent with gedrite falling inside the triangle almandine-cordierite-orthopyroxene (Grant, 1981). The composition of clinopyroxene is based on the Fe-Mg distribution between orthopyroxene and clinopyroxene (Jen and Kretz, 1981).

Korikovskii (1970) presented a reaction grid for quartz-bearing rocks, involving aluminum silicate, staurolite, chloritoid, cordierite, almandine, chlorite, and gedrite. This grid includes invariant points 1 to 6 shown in Figure 14.2. Invariant point 5 had been proposed previously by Robinson and Jaffe (1969). Trzcienski (1971) deduced invariant point 3 from field evidence; see also Carmichael et al. (1978). The grid for potassium-poor rocks has been expanded by the addition of cummingtonite (Spear, 1978; Percival et al., 1982). The grid of Spear (1978) includes invariant points 3,4, and 5 and several invariant points with anthophyllite. In Figure 14.2, anthophyllite has been ignored and invariant point 7 is metastable with respect to reactions involving anthophyllite. The grid developed by Percival et al. (1982) includes invariant points 3,4,5 and 6 of Korikovskii's (1970) grid as well as new invariant point 8.

Froese and Jen (1979), Froese (1980), and Froese and Goetz (1981) proposed reaction grids for mafic rocks including invariant points 9,10, and 11. In metamorphic studies, it is of interest to relate sequences of reactions in pelitic and mafic rocks. Also in some rocks, hornblende occurs with the aluminous minerals staurolite (Jan et al., 1971; Spear, 1982), kyanite (Demange, 1976; Moore, 1976), staurolite-kyanite (Frey, 1974; Gibson, 1978), cordierite (Goroshnikov and Yur'yev, 1965; Morton et al., 1970; Schumacher, 1981) and, at lower grade, chloritoid (Thompson, 1972; see also Carmichael et al., 1978; Fox, 1974; Leclair, 1982). These assemblages are not accommodated in the separate grids for pelitic and mafic rocks. Consequently, an attempt has been made to combine reactions in pelitic and mafic rocks into one grid (Fig. 14.2). One link is provided by invariant point 12 suggested by the existence of the assemblage chlorite-almandine-cummingtonite-gedrite-hornblende (Hall, 1980). At this invariant point a reaction from the pelitic grid (Spear, 1978)

chlorite+almandine+cummingtonite $\rightleftharpoons$ gedrite

intersects with a reaction in the mafic grid (Froese, 1980)

chlorite+almandine+hornblende $\rightleftharpoons$ cummingtonite.

The remainder of the grid has been completed in a schematic fashion but in a manner consistent with Schreinemakers' rules (Zen, 1966; Lindsley et al., 1968). Invariant point 13 is

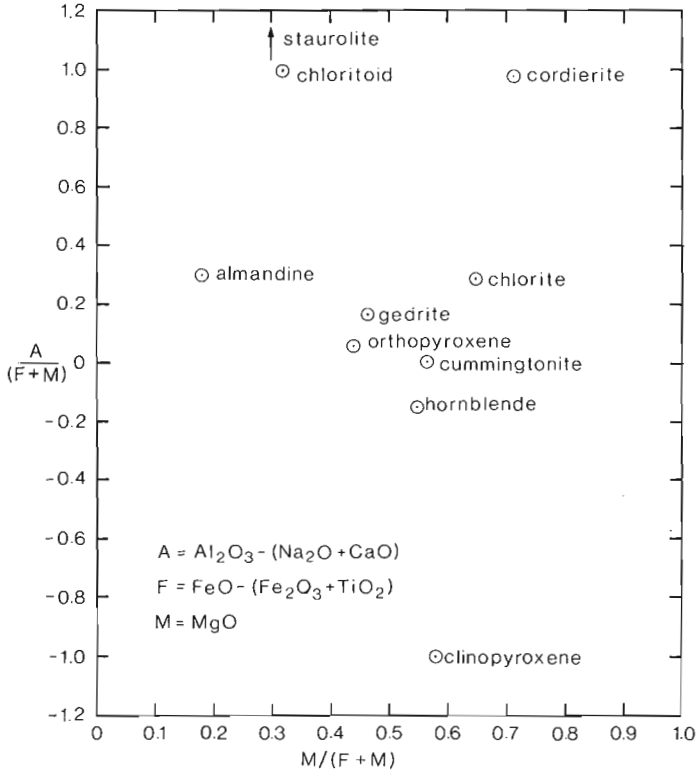

Figure 14.1. *Composition of minerals.*

[1]Anaconda Canada Exploration Limited, 1500 West Georgia Street, Vancouver, British Columbia, V6G 2Z6

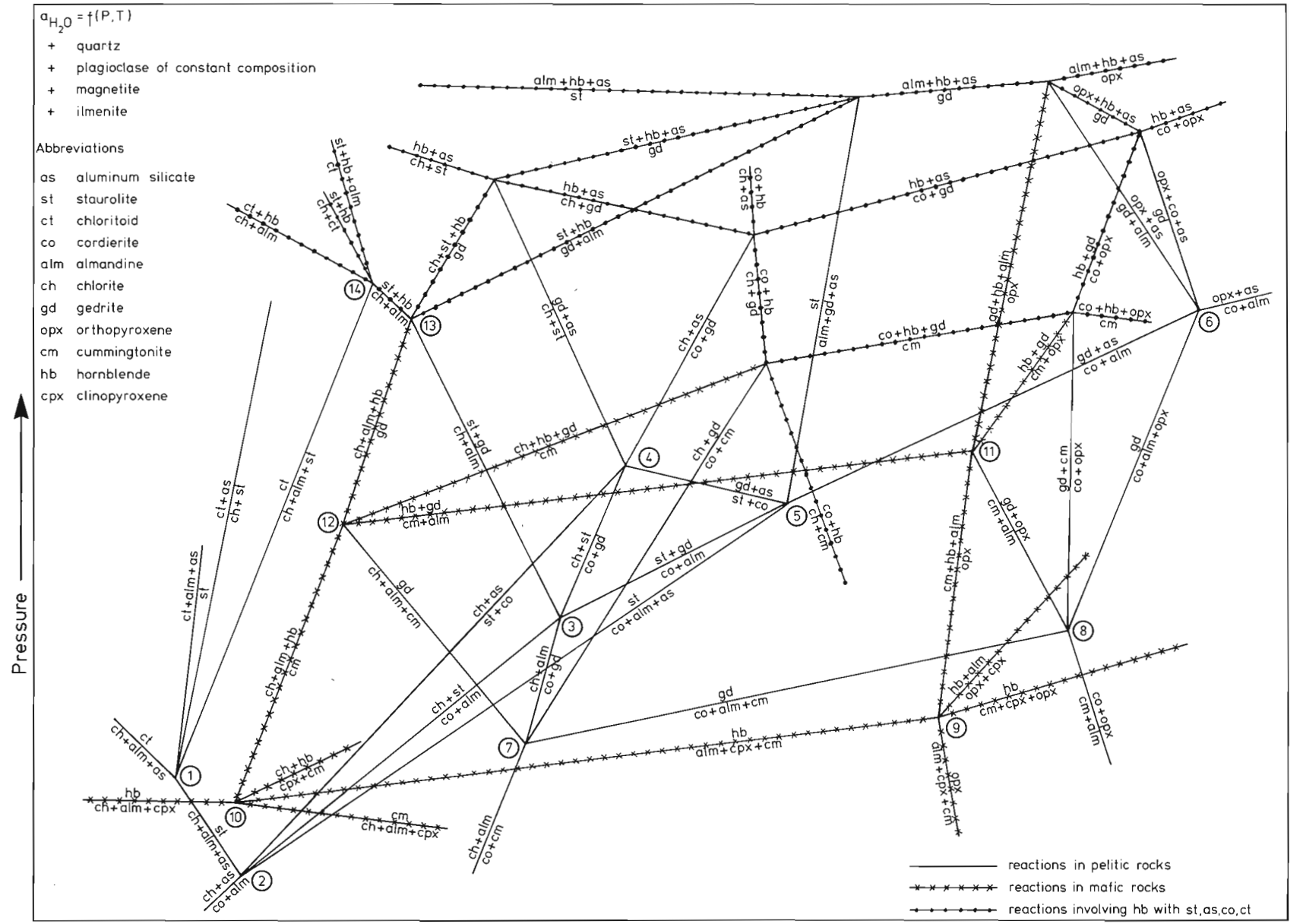

Figure 14.2. *Reaction grid for potassium-poor pelitic and mafic rocks.*

Table 14.1

Composition of minerals from a metamorphosed mafic volcanic rock (specimen 7998)

	chlorite	almandine	hornblende	cummingtonite	gedrite	biotite
SiO_2	26.29	36.70	42.13	53.42	41.14	36.27
TiO_2	0.09	0.06	0.35	0.04	0.21	1.32
Al_2O_3	22.34	21.64	15.29	1.04	16.22	16.85
FeO	19.57	32.15	18.62	24.79	25.43	17.30
MnO	-	2.00	0.07	0.22	0.23	-
MgO	20.04	3.97	9.56	18.05	12.31	14.09
CaO	-	2.89	9.80	0.33	0.49	0.16
Na_2O	-	-	2.45	0.39	2.59	0.56
K_2O	-	-	0.20	-	-	8.35
Total	88.33	99.41	98.47	98.28	98.62	94.90

Total iron expressed as FeO. Assuming a ratio of weight % Fe_2O_3 to weight % FeO = 0.2 in hornblende gives 3.16% Fe_2O_3 and 15.78% FeO.

Mineral assemblage: quartz, plagioclase An_{16-27}, and ilmenite in addition to analyzed minerals. Electron microprobe analysis by M. Bonardi, Mineralogy Section, Geological Survey of Canada.

supported by the observed assemblage chlorite-almandine-hornblende-gedrite-staurolite (Spear, 1982) and invariant point 14 by the occurrence of the association chloritoid-hornblende.

Acknowledgments

Beneficial discussions with J.A. Percival and R.K. Herd are gratefully acknowledged.

References

Carmichael, D.M., Moore, J.M., and Skippen, G.B.
1978: Isograds around the Hastings Metamorphic "Low"; in GSA-GAC-MAC Field Trips Guidebook, p. 325-346.

Demange, M.
1976: Une paragenèse à staurotide et tschermakite d'Ovala (Gabon); Bulletin de la Société française de Minéralogie et Cristallographie, v. 99, p. 379-402.

Fox, J.S.
1971: Coexisting chloritoid and staurolite and the staurolite-chlorite isograd from the Agnew Lake area, Ontario, Canada; Geological Magazine, v. 108, p. 205-219.

1974: Petrology of some low-variance meta-pelites from the Lukmanier Pass area, Switzerland; unpublished Ph.D. thesis, Cambridge University, Cambridge.

Frey, M.
1974: Alpine metamorphism of pelitic and marly rocks of the Central Alps; Schweizerische Mineralogische und Petrographische Mitteilungen, v. 54, p. 489-506.

Froese, E.
1969: Metamorphic rocks from the Coronation mine and surrounding area; Geological Survey of Canada, Paper 68-5, p. 55-77.

1980: A reaction grid for medium grade mafic rocks; in Current Research, Part A, Geological Survey of Canada, Paper 80-1A, p. 53-55.

Froese, E. and Goetz, P.A.
1981: Geology of the Sherridon Group in the vicinity of Sherridon, Manitoba; Geological Survey of Canada, Paper 80-21.

Froese, E. and Jen, L.S.
1979: A reaction grid for biotite-bearing granulites; in Current Research, Part A, Geological Survey of Canada, Paper 79-1A, p. 83-85.

Gibson, G.M.
1978: Staurolite in amphibolite and hornblendite sheets from the Upper Seaforth River, central Fiordland, New Zealand; Mineralogical Magazine, v. 42, p. 153-154.

Goroshnikov, V.I. and Yur'yev, L.D.
1965: Cordierite-polyamphibole and anthophyllite-cordierite rocks of the North Krivoy Rog district; Doklady of the Academy of Sciences of the U.S.S.R., Earth Science Sections, v. 163, p. 140-143.

Grant, J.A.
1981: Orthoamphibole and orthopyroxene relations in high-grade metamorphism of pelitic rocks; American Journal of Science, v. 281, p. 1127-1143.

Hall, R.D.
1980: Metamorphism of sulfide schists, Limerick Township, Ontario; unpublished Ph.D. thesis, University of Western Ontario, London, Ontario.

Jan, M.Q., Kempe, D.R.C., and Tahirkheli, R.A.K.
1971: Corundum, alterating to margarite, in amphibolite from Dir, West Pakistan; Mineralogical Magazine, v. 38, p. 106-109.

Jen, L.S. and Kretz, R.
1981: Mineral chemistry of some mafic granulites from the Adirondack region; Canadian Mineralogist, v. 19, p. 479-491.

Korikovskii, S.P.
1970: The influence of depth on the parageneses of K_2O – undersaturated, alumina-rich metapelites; Contributions to Physico-Chemical Petrology, v. 2, p. 59-87, Nauka Press, Moscow. (Translation available in the library of the Geological Survey of Canada, Ottawa.)

Leclair, A.D.
1982: Low to medium grade metamorphism in the central part of the Hastings Basin, southeastern Ontario: An evaluation of metamorphic conditions in chloritoid and staurolite-bearing schists; unpublished M.Sc. thesis, Queen's University, Kingston.

Lindsley, D.H., Speidel, D.H., and Nafziger, R.H.
1968: P-T-f_{O_2} relations in the system Fe-O-SiO_2; American Journal of Science, v. 266, p. 342-360.

Moore, R.L.
1976: Metamorphic petrology of the area between Mattawa, North Bay and Temiscaming, Ontario; unpublished Ph.D. thesis, Carleton University, Ottawa.

Morton, R.D., Batey, R., and O'Nions, R.K.
1970: Geological investigations in the Bamble sector of the Fennoscandian Shield, South Norway. 1. The Geology of eastern Bamble; Norges Geologiske Undersøkelse, no. 263.

Percival, J.A., Carmichael, D.M., and Helmstaedt, H.
1982: A petrogenetic grid for calcium and alkali-deficient bulk compositions; in Current Research, Part A, Geological Survey of Canada, Paper 82-1A, p. 169-173.

Robinson, P. and Jaffe, H.W.
1969: Chemographic exploration of amphibole assemblages from Central Massachusetts and southwestern New Hampshire; Mineralogical Society of America, Sepcial Paper no. 2, p. 251-274.

Savolahti, A.
1966: On rocks containing garnet, hypersthene, cordierite and gedrite in the Kiuruvesi region, Finland. Part 1: Juurikkajärvi; Comptes Rendus de la Société géologique de Finlande, no. 38, p. 343-386.

Schumacher, J.C.
1981: Coexisting hornblende-cordierite-gedrite in gedrite-cordierite gneiss, southwestern New Hampshire (abstract); EOS, v. 62, p. 422.

Spear, F.S.
1978: Petrogenetic grid for amphibolites from the Post Pond and Ammonoosuc Volcanics; Carnegie Institution of Washington Year Book 77, p. 805-808.

1982: Phase equilibria of amphibolites from the Post Pond Volcanics, Mt. Cube quadrangle, Vermont; Journal of Petrology, v. 23, p. 383-426.

Stout, J.H.
1972: Phase petrology and mineral chemistry of coexisting amphiboles from Telemark, Norway; Journal of Petrology, v. 13, p. 99-145.

Thompson, P.H.
1972: Stratigraphy, structure and metamorphism of the Flinton Group in the Bishop Corners – Madoc area, Grenville Province, eastern Ontario; unpublished Ph.D. thesis, Carleton University, Ottawa.

Trzcienski, W.E.
1971: Staurolite and garnet parageneses and related metamorphic reactions in metapelites from the Whetstone Lake area, southeastern Ontario; unpublished Ph.D. thesis, McGill University, Montreal.

Zen, E-an
1966: Construction of pressure-temperature diagram for multicomponent systems after the method of Schreinemakers – a geometric approach; United States Geological Survey, Bulletin 1225.

15. PRELIMINARY RESULTS OF GEOLOGICAL SYNTHESIS IN THE WESTERN SUPERIOR PROVINCE

Project 820006

J.A. Percival
Precambrian Geology Division

Percival, J.A., Preliminary results of geological synthesis in the western Superior Province; in Current Research, Part A, Geological Survey of Canada, Paper 83-1A, p. 125-131, 1983.

Abstract

Reconnaissance investigations were carried out in parts of the Wawa, Quetico, Wabigoon and English River subprovinces west of Lake Nipigon. In the Sunbar-Batwing Lakes granitoid complex south of the Shebandowan greenstone belt, units of gneissic rock define structural patterns that are partly related to the presence of crescentic plutons of intermediate composition. The contact between metavolcanic rocks of the Shebandowan belt and metasedimentary rocks of the Quetico subprovince is conformable and north-facing west of Shabaqua but facing directions are south in the Quetico belt farther east. Low-angle offset along large-scale fold limbs could account for the configuration. The Sowden-Wabikimi Lakes granitoid complex of the Wabigoon subprovince is made up of metavolcanic remnants, tonalitic gneiss, foliated and massive granitoid plutons and late mafic intrusions. In the Ogoki Reservoir area, a zone of granulite facies, some 60 x 16 km, was recognized in metasedimentary migmatite and tonalitic intrusions of the English River subprovince.

Introduction

Detailed studies of supracrustal rocks in the Superior Province have provided many insights into the nature of the Archean crust. In recent years, studies of granitoid and gneissic terranes (e.g. Breaks et al., 1978; Schwerdtner et al., 1979; Card, 1979) have attempted to balance geological coverage of the Province and integrate the history of these areas into regional syntheses. With the advent of precise dating techniques (e.g. Krogh et al., 1982), a more rigid geochronological framework for the Superior Province has emerged. One significant result is that regional deformation, metamorphism and plutonism occurred not during one Province-wide orogeny ("Kenoran" or "Algoman") but rather at different times in various subprovinces (Krogh et al., 1974; Nunes and Thurston, 1980; Davis et al., 1982; Turek et al., 1982) and possibly sequentially, in the manner envisioned by Langford and Morin (1976). This finding raises at least two pertinent questions: 1) if the structural-metamorphic-plutonic patterns in the individual subprovinces evolved independently, how do they differ? and 2) what effect, if any, did regional tectonism in adjacent subprovinces have on more stable parts of the crust? The scale of investigation of these questions is regional, involving several subprovinces. Thus, in the course of compilation of the geology of northwestern Ontario, parts of the Wawa, Quetico, Wabigoon and English River subprovinces (Fig. 15.1) were visited and are described below.

Acknowledgments

Field guidance and helpful discussions were provided by R.H. Sutcliffe, P.C. Thurston (Ontario Geological Survey), and R.A. Bernatchez (Steep Rock Iron Mines Ltd.). The help and co-operation of G.C. Patterson (Resident Geologist, Thunder Bay) and staff is greatly appreciated. P. Maenz provided capable field assistance.

Sunbar-Batwing Lakes Granitoid Complex, Wawa Subprovince

The Sunbar-Batwing Lakes complex (Schwerdtner and Goodwin, 1977), part of the Wawa subprovince, is bounded to the north and west by Archean metavolcanic rocks and to the south and east by flat-lying Proterozoic sedimentary and intrusive rocks (Fig. 15.2). The terrane is made up of four major lithological components: 1) hornblende-plagioclase amphibolite and mafic gneiss; 2) tonalite- to granodiorite gneiss, commonly with amphibolite xenoliths; 3) foliated plutonic rocks, including complex plutons of intermediate to mafic composition; and 4) massive to weakly-foliated leucocratic granite and granodiorite. Amphibolite is common in the margins of metavolcanic belts and also occurs as thin to discontinuous layers in tonalitic gneiss throughout the granitoid complex. The Northern Light gneiss (Grout, 1929) is made up of 1-50 mm layers of hornblende, biotite or hornblende-biotite-rich rock in leucocratic tonalite or granodiorite. Textural gradation from foliated homogeneous tonalite to tonalitic gneiss is evident locally at Weikwabinonaw Lake (Fig. 15.2). Homogeneous foliated rocks include tonalite, granodiorite, granite and a suite of coarse grained, variably foliated rocks ranging from syenite through diorite to biotite-hornblende gabbro. Clinopyroxene is present in the intermediate and mafic rock types and is commonly rimmed by hornblende. The intermediate plutons form circular plugs, such as the Icarus pluton (Goldich et al., 1972) and Hood Lake syenite (Schwerdtner, 1976) or crescent-shaped bodies such as the Greenwater (Stott and Schwerdtner, 1981), Perching Gull and Sleigh Lake plutons (Fig. 15.2). Massive leucocratic (<5% biotite) granite and granodiorite form discrete plutons with wide xenolith-rich haloes whose country rock is cut by dykes and sills of granite

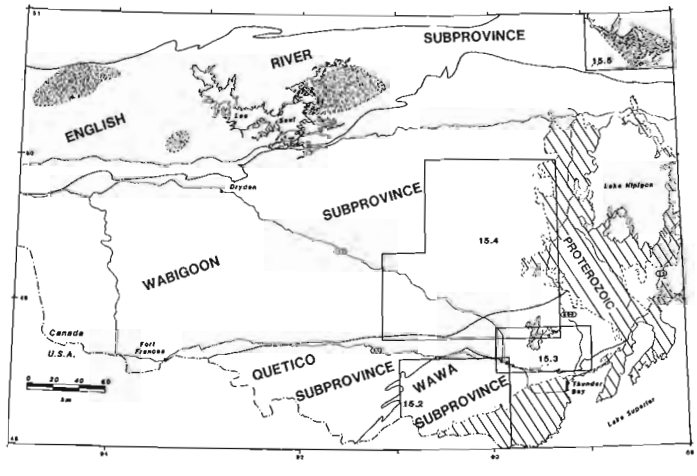

Figure 15.1. *Location map for part of western Superior Province. Areas of granulite facies in English River subprovince stippled after Thurston and Breaks (1978).*

or granodiorite. The proportion of this phase is difficult to estimate in contact zones but is higher than shown in Figure 15.2.

Discontinuous inclusion trains of amphibolite in tonalitic gneiss extend between the Shebandowan belt to the north and Saganagons belt to the south (Fig. 15.2). The gneissic rocks form continuous belts outlining large-scale structures. The Flatrock Lake pluton occupies the core of a major northwest-plunging structural culmination. The internal structure of the suite of foliated intermediate bodies suggests that fabrics developed during emplacement (Schwerdtner, 1976; Davidson, 1980; Stott and Schwerdtner, 1981), although subsequent deformation by intrusion of later plutons is possible. Foliation in the Perching Gull Lake pluton and surrounding rocks is concordant with the margins of the body and dips inward,

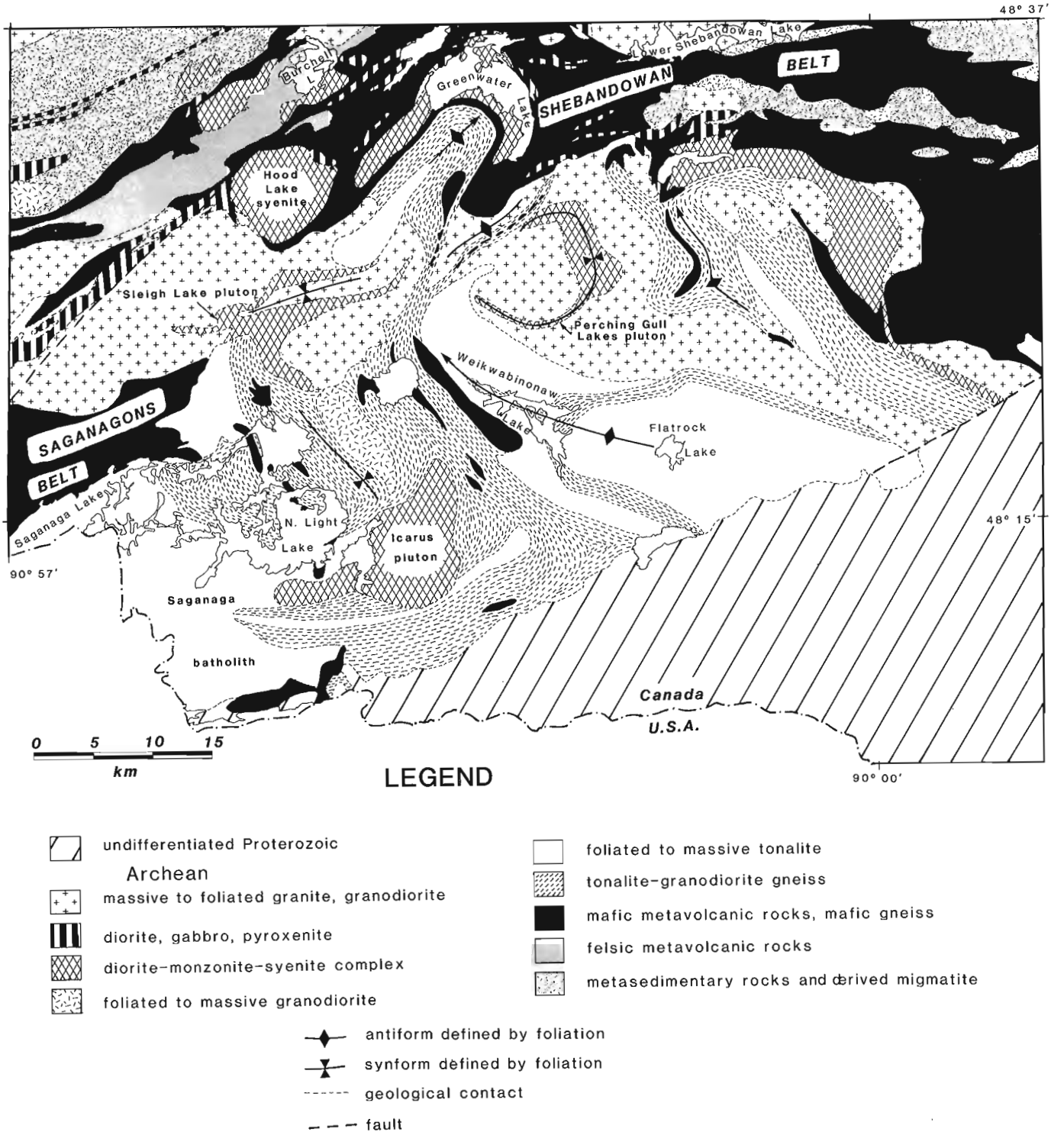

Figure 15.2. *Sunbar-Batwing Lakes granitoid complex. Small Proterozoic outliers omitted for clarity.*

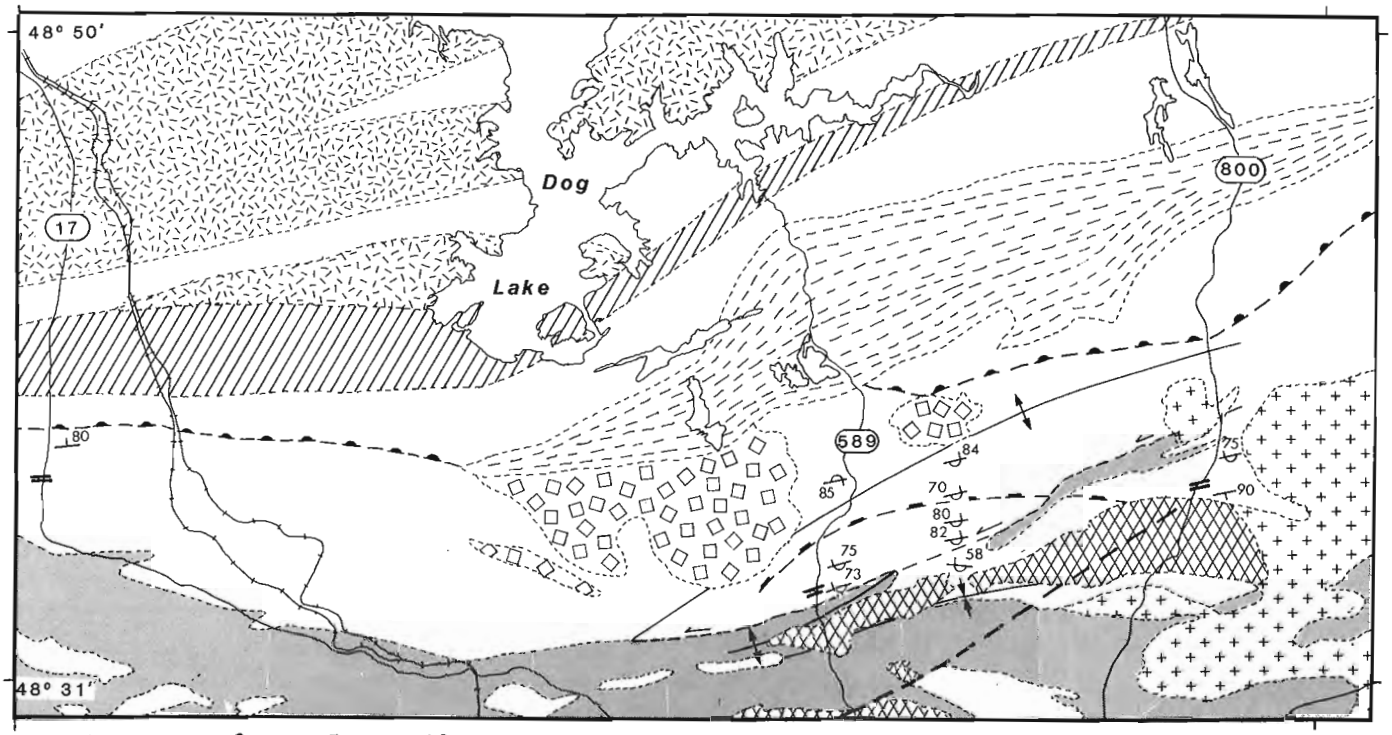

LEGEND

Archean

- hornblende-biotite granite
- hornblende monzonite,syenite
- foliated to mylonitic granite
- K-feldspar porphyritic granite
- peraluminous granite- contains muscovite, garnet, cordierite and paragneiss xenoliths
- interlayered migmatitic paragneiss, tonalitic gneiss, amphibolite, dioritic rocks
- metasedimentary rocks: mainly greywacke below the migmatite isograd, and migmatitic paragneiss above
- mafic to intermediate metavolcanic rocks
- rhyolite- dacite sills
- staurolite isograd (teeth point up-grade)
- migmatite isograd
- strike and dip of bedding, tops known; inclined, vertical, overturned
- anticline
- syncline
- geological contact
- fault, movement sense known; unknown

Figure 15.3. *Major features of Quetico subprovince northwest of Thunder Bay, Ontario.*

defining a crescentic synform. Similar configurations are indicated in the Sleigh Lake body (Fig. 15.2) and in the Saganaga batholith (Davidson, 1980).

The Greenwater pluton has a primary strain fabric and strain aureole (Stott and Schwerdtner, 1981), probably developed during forceful emplacement. This style of emplacement, characteristic of the intermediate bodies, contrasts sharply with that of the later, massive granite-granodiorite plutons which appear to have no structural effect on the country rock. The orientation of foliation in tonalite xenoliths in granite is generally unrotated from the regional trend.

Quetico Subprovince

The Quetico subprovince is made up predominantly of metasedimentary rocks and granitic intrusions, many of anatectic origin. North of Thunder Bay, low-grade metagreywackes with well-preserved sedimentary structures are in contact with metavolcanics of the Shebandowan belt. The dip of bedding, layering and foliation is steep and generally northerly adjacent to the boundary. Facing directions are consistently south (Fig. 15.3), as determined from graded beds, crossbeds, scour structures and flame casts in metagreywacke and mudstone with A, A-E and D-E (Bouma, 1962) turbidite sequences. This evidence would suggest that the metavolcanics of the Shebandowan belt stratigraphically overlie the metasedimentary rocks. However, to the west, facing directions are consistently north throughout the Quetico subprovince (Giblin, 1964; Pirie and Mackasey, 1978). These conflicting relationships suggest a complicated fold-fault geometry such as that indicated in Figure 15.3. Northeast-striking bodies of massive syenite to monzonite intrude the boundary zone.

Chlorite-grade metasediments of the Quetico belt are cut by sills up to 4 m wide of aphanitic rhyolite or dacite. The concordant bodies with rare apophyses are restricted to a zone some 1-4 km north of the main volcanic contact where they are present over a strike length of at least 135 km, from north of Burchell Lake to highway 800. The composition and fine grain size of the sills suggest that they may be cogenetic with volcanic rocks to the south. Several small bodies of K-feldspar megacrystic granite (e.g. Kehlenbeck, 1977) cut metasedimentary rocks containing porphyroblasts of garnet, andalusite and staurolite. The metamorphic minerals may be the result of contact metamorphism or of northward-increasing regional grade. A migmatite isograd is shown on Figure 15.3 to represent the first appearance of granitic pods and layers which are abundant to the north. The isograd is cut by foliated, locally protomylonitic biotite granite which locally contains inclusions of K-feldspar megacrystic granite. Within the metasedimentary migmatites to the north is a

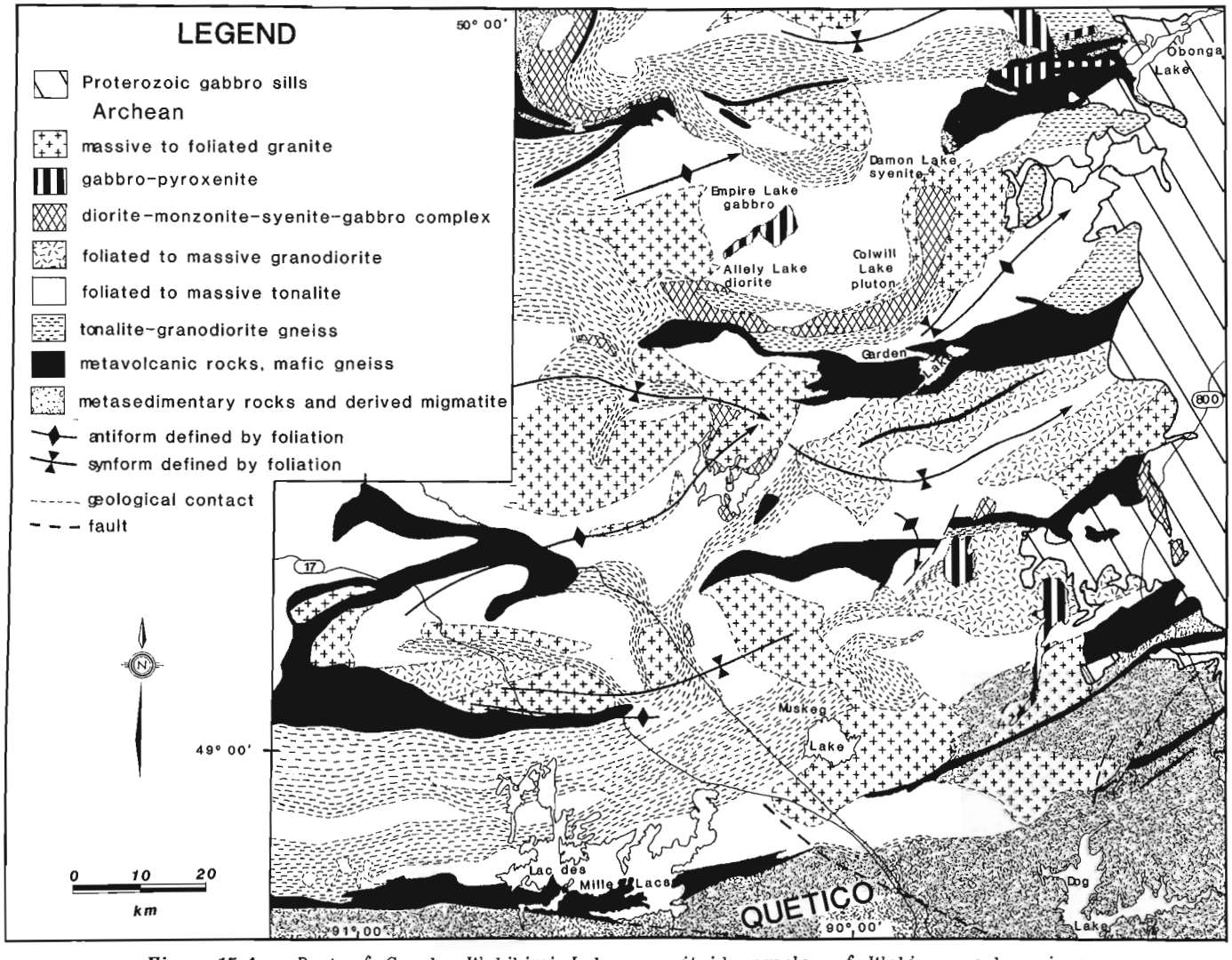

Figure 15.4. *Part of Sowden-Wabikimi Lakes granitoid complex of Wabigoon subprovince. Many small Proterozoic outliers have been omitted from the eastern side of the map.*

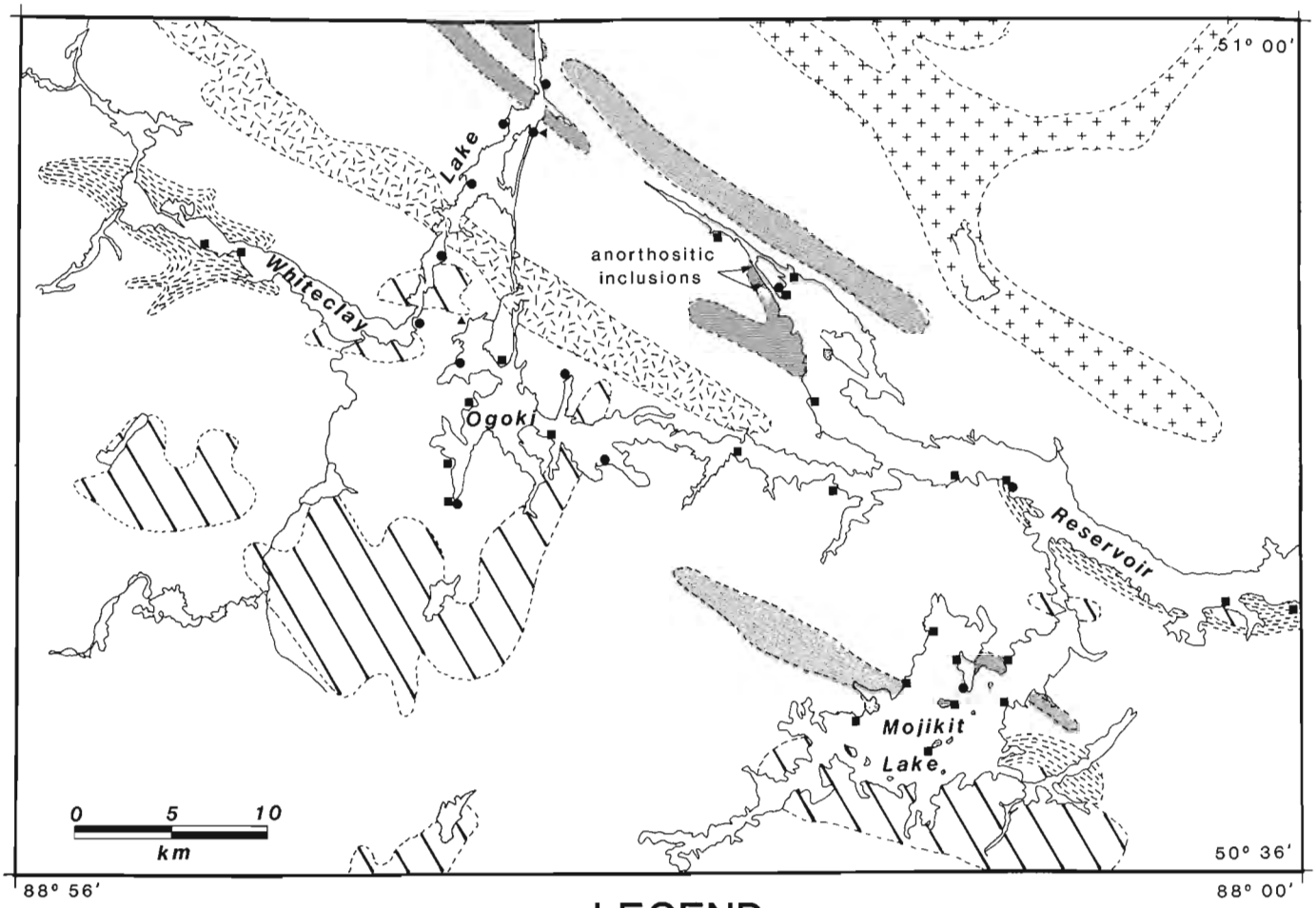

LEGEND

- Proterozoic gabbro

Archean

- biotite-magnetite gneissic granite
- homogeneous diatexite -peraluminous granite with metasedimentary inclusions
- hornblende-biotite-orthopyroxene-clinopyroxene tonalite
- tonalitic gneiss with mafic xenoliths
- metasedimentary migmatite (inhomogeneous diatexite)
- ▪ orthopyroxene occurrence
- • garnet-cordierite
- ▸ muscovite

Figure 15.5. *Lithological map with assemblage data for the Ogoki Reservoir-Mojikit Lake area (modified after Thurston et al., 1969). The area is the most easterly of four major occurrences of granulite-facies rocks in the English River subprovince of Ontario.*

lithologically heterogeneous unit up to 5 km wide of paragneiss, amphibolite, tonalitic gneiss and foliated diorite and tonalite. Metasedimentary migmatites are interlayered with peraluminous and biotite granites for approximately 25 km farther to the north, where metamorphic grade generally decreases in proximity to the Wabigoon subprovince.

Wabigoon Subprovince

The Sowden-Wabikimi Lakes granitoid complex as defined by Sage et al. (1975) consists of five main lithologic components: 1) small metavolcanic belts and inferred metavolcanic remnants, consisting of mafic gneiss; 2) tonalite-granodiorite gneiss; 3) foliated homogeneous rocks of tonalitic, mafic tonalitic, granitic and intermediate composition; 4) massive granite and granodiorite, occurring as discrete plutons and as dykes or sills in the gneisses, and 5) late gabbroic bodies containing fresh pyroxene. Gabbro with 5-100 mm thick layers of orthopyroxene-clinopyroxene-plagioclase and magnetite occurs in the Empire Lake body (Fig. 15.4). The Colwill Lake pluton is a composite body composed of massive to foliated, coarse grained syenite, diorite, gabbro and hornblende-pyroxenite. In addition to hornblende and biotite, clinopyroxene is present both as discrete grains and as cores to hornblende grains in most rock types. Near the core of the body, compositional gradation from hornblende-clinopyroxenite through mafic gabbro to gabbro and leuco-gabbro faces west. The Colwill Lake pluton appears to be continuous to the west with the Allely Lake diorite and to the north with the Damon Lake syenite, thus defining a composite crescentic pluton. The Empire Lake gabbro may also be related to the composite pluton.

Foliation and gneissosity in foliated and gneissic rocks generally dip 45-90° and define broadly east-trending, sinuous antiforms and synforms (Fig. 15.4). The small metavolcanic belts and remnants are generally homoclinal panels on the limbs of regional structures.

English River Subprovince

A 60 x 15 km region in the Mojikit Lake-Ogoki Reservoir area (Fig. 15.5) represents a fourth major occurrence of granulite-facies rocks in the English River subprovince of Ontario (Fig. 15.1, 15.5). The rocks are dominantly metasedimentary migmatite, locally with concordant layers and boudins of mafic gneiss, metagabbro and gabbroic anorthosite. Small bodies of foliated mafic tonalite at Mojikit Lake contain metasedimentary inclusions and are cut by granitic leucosome.

Metasedimentary migmatite is mainly inhomogeneous diatexite according to the criteria used by Breaks et al. (1978). Paleosome consists of garnet-biotite-plagioclase-quartz assemblages with some K-feldspar, sillimanite and cordierite. Associated coarse grained leucosome contains garnet-cordierite or orthopyroxene ± clinopyroxene in addition to quartz, feldspars and biotite. Pyroxenes and cordierite in leucosome are variably altered. Local layers of meta-iron formation are coarse grained garnetite or garnet-clinopyroxene-amphibole-quartz-Fe-oxide rocks. Migmatitic mafic gneiss consisting of orthopyroxene-clinopyroxene-hornblende-plagioclase ± garnet ± quartz assemblages is locally interlayered with metasedimentary migmatite. Boudins of layered gabbro and anorthositic rock occur locally in migmatite. Gabbro is granoblastic, coarse grained hornblende-orthopyroxene-plagioclase (An_{85}; 40%) rock and gabbroic anorthosite consists of plagioclase (An_{45}; 70%), hornblende, orthopyroxene and biotite. These small bodies may represent dismembered layered sills. Tonalitic rocks are medium- to coarse-grained, homogeneous to migmatitic, and generally have orthopyroxene-clinopyroxene-hornblende-biotite-plagioclase-quartz assemblages.

The presence of orthopyroxene in migmatite leucosome, in tonalitic and mafic rocks, and in a reaction zone between a mafic inclusion and granitic leucosome indicates prograde metamorphism of the entire lithological assemblage to the granulite facies. The north-south sequence of mineral assemblages in leucosome of paragneiss is muscovite-biotite, garnet-cordierite, and orthopyroxene-clinopyroxene (Fig. 15.5), characterizing the amphibolite-granulite transition. The coincidence between the location of intrusive bodies and the high-grade metamorphic assemblages suggests the possibility that the addition of magmatic heat during regional metamorphism was responsible for establishing granulite-facies conditions.

References

Bouma, A.H.
1962: Sedimentology of Some Flysch Deposits; Elsevier, Amsterdam, 168 p.

Breaks, F.W., Bond, W.D., Stone, D.
1978: Preliminary geological synthesis of the English River subprovince, northwestern Ontario and its bearing upon mineral exploration; Ontario Geological Survey, Miscellaneous Paper 72, 55 p.

Card, K.D.
1979: Regional geological synthesis, central Superior Province; in Current Reseach, Part A, Geological Survey of Canada, Paper 79-1A, p. 87-90.

Davidson, D.M., Jr.
1980: Emplacement and deformation of the Archean Saganaga batholith, Vermilion district, northeastern Minnesota; Tectonophysics, v. 66, p. 179-195.

Davis, D.W., Blackburn, C.E., and Krogh, T.E.
1982: Zircon U-Pb ages from the Wabigoon-Manitou Lakes region, Wabigoon subprovince, northwest Ontario; Canadian Journal of Earth Sciences, v. 16, p. 254-266.

Giblin, P.E.
1964: Burchell Lake area; Ontario Department of Mines, Geological Report 19, 39 p.

Goldich, S.S., Hanson, G.N., Hallford, C.R., and Mudrey, M.G. Jr.
1972: Early Precambrian rocks in the Saganaga Lake-Northern Light Lake area, Minnesota-Ontario: Part 1: Petrology and structure; Geological Society of America, Memoir 135, p. 151-177.

Grout, F.F.
1929: The Saganaga granite of Minnesota-Ontario; Journal of Geology, v. 37, p. 562-591.

Harris, F.R.
1968: Geology of the Saganagons Lake area; Ontario Department of Mines, Geological Report 66, 30 p.

Kehlenbeck, M.M.
1977: The Barnum Lake pluton, Thunder Bay, Ontario; Canadian Journal of Earth Sciences, v. 14, p. 2157-2167.

Krogh, T.E., Ermanovics, I.F., and Davis, G.L.
1974: Two episodes of metamorphism and deformation in the Archean rocks of the Canadian Shield; Carnegie Institution of Washington Yearbook, 73, p. 573-575.

Krogh, T.E., Davis, D.W., Nunes, P.D., and Corfu, F.
1982: Archean evolution from precise U-Pb isotopic dating (Abstract); Geological Association of Canada, Program with Abstracts 7, p. 61.

Langford, F.F. and Morin, J.A.
1976: The development of the Superior Province of northwestern Ontario by merging island arcs; American Journal of Science, v. 276, p. 1023-1034.

Nunes, P.D. and Thurston, P.C.
1980: Two hundred and twenty million years of Archean evolution: a zircon U-Pb age stratigraphic study of the Confederation Lakes greenstone belt, northwestern Ontario; Canadian Journal of Earth Sciences, v. 17, p. 710-721.

Pirie, J. and Mackasey, W.O.
1978: Preliminary examination of regional metamorphism in parts of Quetico metasedimentary belt, Superior Province, Ontario; in Metamorphism in the Canadian Shield, J.A. Fraser and W.W. Heywood (eds.); Geological Survey of Canada, Paper 78-10, p. 37-48.

Sage, R.P., Blackburn, C.E., Breaks, F.W., McWilliams, G.M., Schwerdtner, W.M., and Stott, G.M.
1975: Internal structure and composition of two granite complexes in Wabigoon subprovince; Geotraverse Workshop Proceedings, Precambrian Research Group, Department of Geology, University of Toronto, p. 24-32.

Schwerdtner, W.M.
1976: Hood Lake syenite – a diapiric body in the Shebandowan belt; Proceedings of the 1976 Geotraverse Conference, Precambrian Research Group, University of Toronto, p. 28-33.

Schwerdtner, W.M. and Goodwin, A.M.
1977: Structural geology of geotraverse region; Proceedings of the 1977 Geotraverse Conference, Precambrian Research Group, University of Toronto, p. 10-24.

Schwerdtner, W.M., Stone, D., Osadetz, K., Morgan, J., and Stott, G.M.
1979: Granitoid complexes and the Archean tectonic record in the southern part of northwestern Ontario; Canadian Journal of Earth Sciences, v. 16, p. 1965-1977.

Stott, G.M. and Schwerdtner, W.M.
1981: A structural analysis of the central part of the Shebandowan metavolcanic-metasedimentary belt; Ontario Geological Survey, Open File Report 5349, 44 p.

Thurston, P.C., Carter, M.W., and Riley, R.A.
1969: Operation Fort Hope, Attwood-Caribou Lakes Sheet, Districts of Kenora, Patricia Portion, and Thunder Bay, Ontario; Ontario Department of Mines, Map P-564.

Thurston, P.C. and Breaks, F.W.
1978: Metamorphic and tectonic evolution of the Uchi-English River subprovince; in Metamorphism in the Canadian Shield, J.A. Fraser and W.W. Heywood (eds.); Geological Survey of Canada, Paper 78-10, p. 49-62.

Turek, A., Smith, P.E., and Van Schmus, W.R.
1982: Rb-Sr and U-Pb ages of volcanism and granite emplacement in the Michipicoten belt – Wawa, Ontario; Canadian Journal of Earth Sciences, v. 9, p. 1608-1626.

16. DEEP MULTIFREQUENCY E.M. SOUNDING AT A SITE NEAR BOWMANVILLE, ONTARIO

Project 810003

Ajit K. Sinha
Resource Geophysics and Geochemistry Division

Sinha, A.K., Deep multifrequency E.M. sounding at a site near Bowmanville, Ontario; in Current Research, Part A, Geological Survey of Canada, Paper 83-1A, p. 133-137, 1983.

Abstract

A deep sounding multifrequency ground electromagnetic survey was carried out along two lines at the site of the proposed Darlington nuclear generating station during the summer of 1980 to evaluate the E.M. system in terms of its capabilities for detecting layerings in the limestone horizons and to compare the results with the lithological log from a deep borehole in the area. Seven soundings were carried out and interpreted in terms of resistivity and thickness parameters of the layers.

Most of the horizontal lithological boundaries in the area were detected by the E.M. survey. The agreement between the interpreted depth section and the borehole log was good although some sounding points were located up to 800 m away from the hole. Several conductive horizons not indicated in the borehole log were also mapped by the system. These are probably caused by saline water-filled fracture zones or zones in bedrock rich in shale or clays. Interpretation of field data on the two lines suggests an absence of faults in the area between the lines.

Introduction

For the last five years, the Terrain Geophysics Section of the Resource Geophysics and Geochemistry Division has been testing and evaluating a deep sounding multifrequency electromagnetic system called the Maxi-Probe to find its capabilities for mapping conducting horizons at depth in different areas of Canada. As part of that program, the system was tested in 1980 at the site of the proposed Darlington Nuclear Generating Station near Bowmanville, Ontario. An obvious advantage of this location is that a deep borehole (304 m deep) has been drilled and logged here by Ontario Hydro. Hence, a comparison of any new survey data with borehole data provides a measure of the accuracy and reliability of the survey results.

The survey was carried out in July, 1980, along two lines near the deep borehole UN1 shown in Figure 16.1. On the two survey lines (lines 1 and 2) are indicated the two transmitter locations designated by Tx_1 and Tx_2 and several receiver locations designated by Rx_1, Rx_2, Rx_1', Rx_2' etc. The entire survey was carried out in three days by the author with the help of a student assistant.

Acknowledgments

The author would like to thank Ontario Hydro for permission and facilities to carry out the test survey. Appreciation is expressed to Mr. E.M. Taylor, Manager, Geotechnical Engineering, Ontario Hydro, for supplying the lithological log of hole UN1 and Mr. J. Bowlby of the Geotechnical section for his assistance with the survey. The author is thankful to Mr. Scott MacRitchie, a summer student who helped with the field operations.

Description of the Area and Accessibility

The Darlington generating station site is near Bowmanville, Ontario, off Highway 401 about 60 km northeast of Toronto. The area is mostly flat except on the southern edge near the shores of Lake Ontario where the topography is undulating. The area is easily accessible from Highway 401 via Holt and Park roads which meet the East Access Road (see Fig. 16.1). At the time of this survey, much of the area near the proposed power house and construction parking had been excavated and filled with gravel and sand. Because of some restrictions on accessibility and the presence of Lake Ontario on two sides of the borehole UN1, it was not possible to carry out any soundings exactly over the drill hole location. As a compromise, two areas close to this hole were selected with the transmitters being placed at locations Tx_1 and Tx_2 as shown in Figure 16.1. Since the sounding positions do not coincide with the location of the hole UN1, an exact correspondence between borehole logs and the Maxi-Probe interpretation was not expected. However, the differences were not expected to be large considering the small lateral separations between them and the expectation of small dips in the underlying strata.

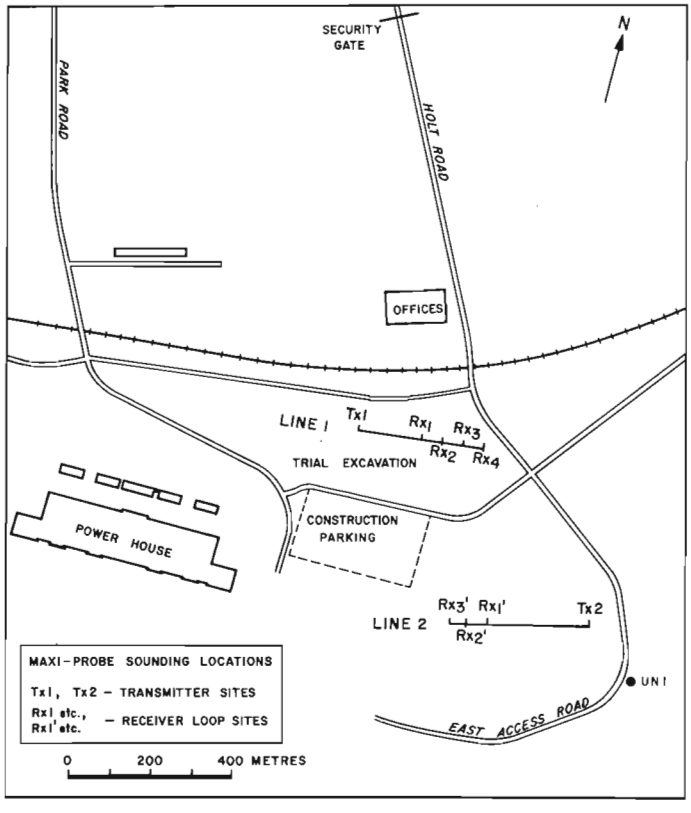

Figure 16.1. *Site plan and location map of the proposed Darlington Generating Station.*

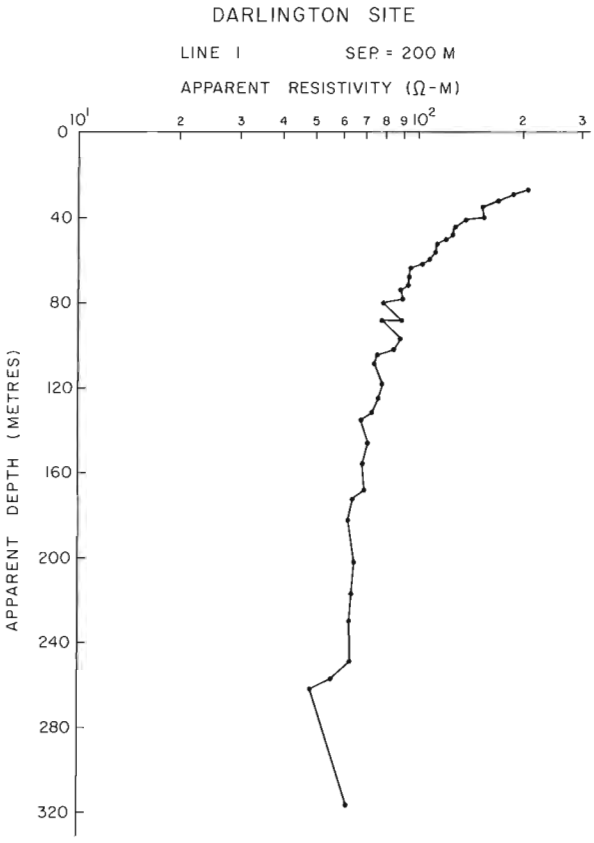

Figure 16.2. *Variation of apparent resistivity with depth on line 1 for a transmitter-receiver separation of 200 m.*

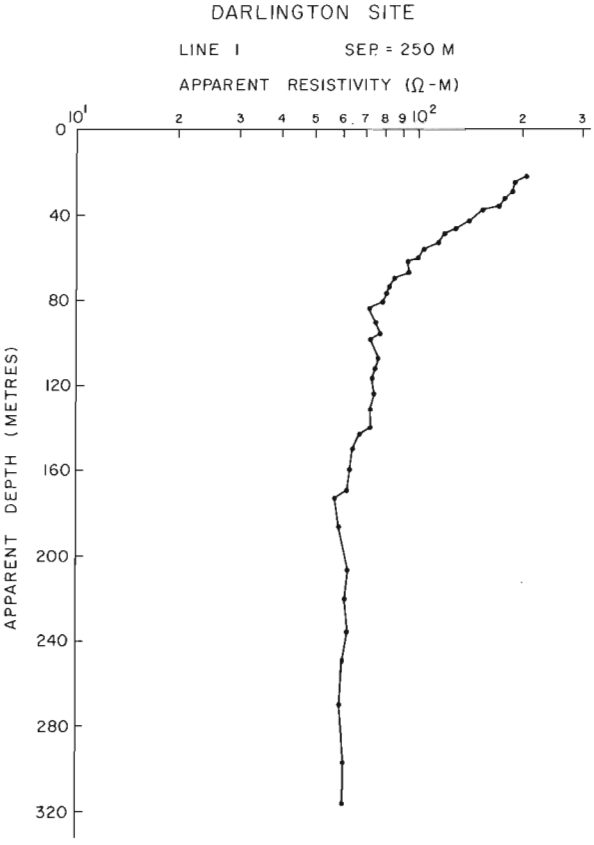

Figure 16.3. *Variation of apparent resistivity with depth on line 1 for a transmitter-receiver separation of 250 m.*

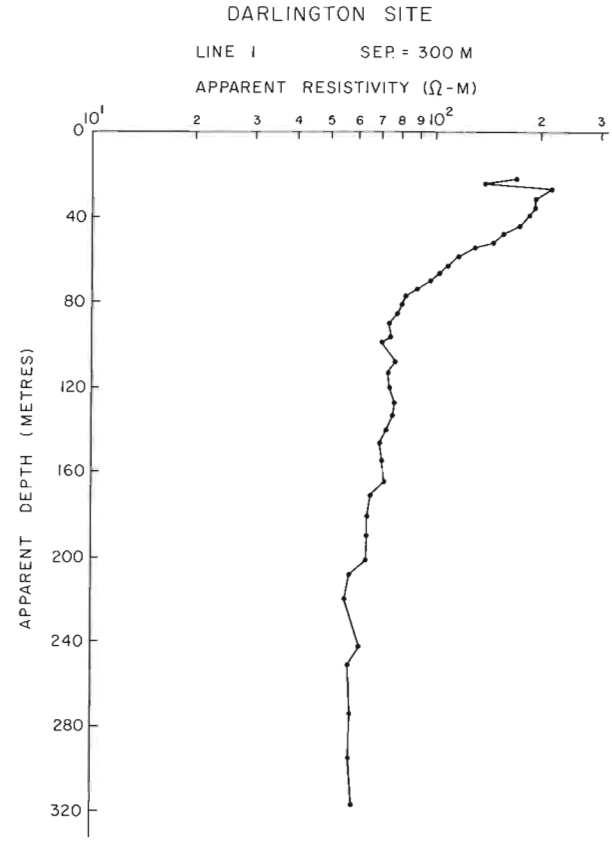

Figure 16.4. *Variation of apparent resistivity with depth on line 1 for a transmitter-receiver separation of 300 m.*

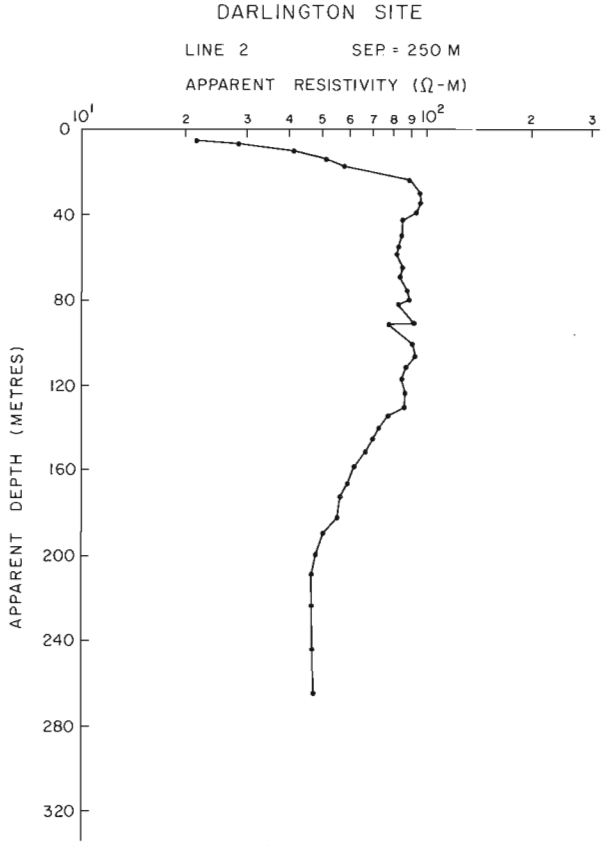

Figure 16.5. *Variation of the apparent resistivity with depth on line 2 for a transmitter-receiver separation of 250 m.*

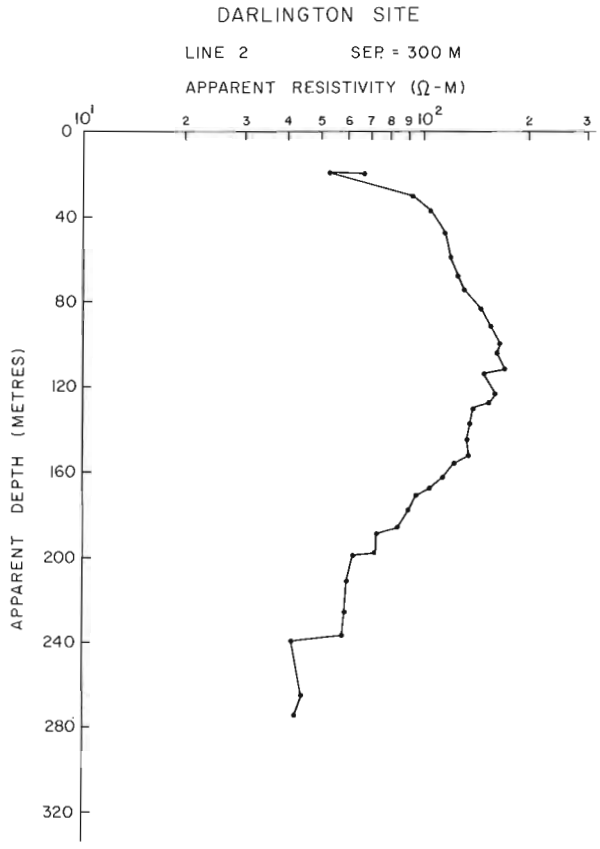

Figure 16.6. Variation of the apparent resistivity with depth on line 2 for a transmitter-receiver separation of 300 m.

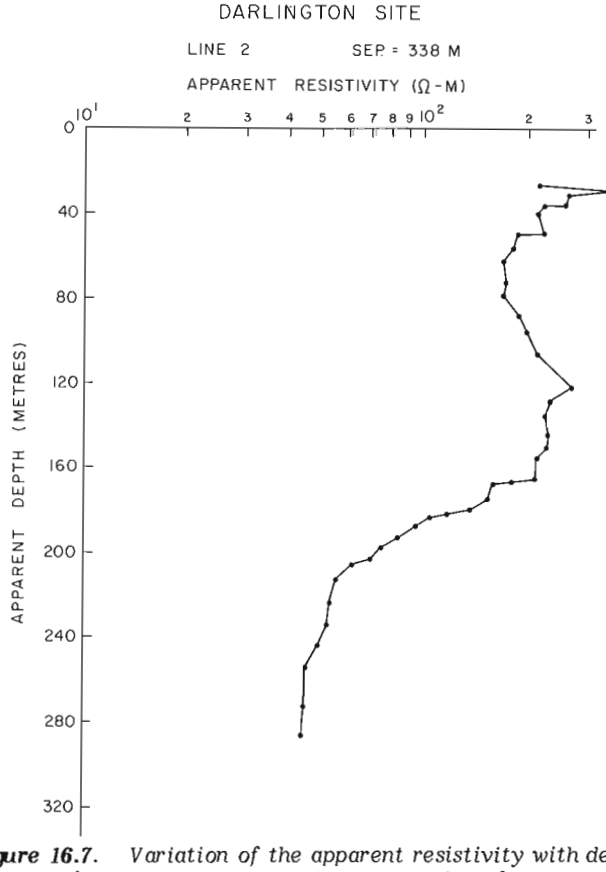

Figure 16.7. Variation of the apparent resistivity with depth on line 2 for a transmitter-receiver separation of 338 m.

Description of the System and Field Results

The Maxi-Probe is a deep sounding multifrequency ground electromagnetic system. The transmitter consists of one, two or three horizontal loops, placed on the ground which behave like vertical magnetic dipoles when the receiver is placed at a distance more than five times the loop diameter. For the survey at Darlington, the transmitter consisted of two loops, connected in parallel, each being 11 m in diameter. However, it is not necessary in this system to place the loops along any particular geometry. The transmitter is powered by a gasoline-driven generator of 2.5 kw capacity. The transmitter operator can select any of the 128 frequencies from 1 Hz to 60 kHz from the transmitter console. The receiver consists of a horizontal and a vertical coil enclosed in a fibre glass spherical shell for minimizing the wind noise. The receiver ball antenna is normally placed on a fibreglass tripod stand for stability. By using a built-in bubble level and a directional arrow on the antenna ball, it is possible to ensure that the measured fields are the true vertical and radial components of the total magnetic field. The output from the receiver antenna is transferred to the receiver console via a 5 m cable. The power for the receiver console is supplied by a rechargeable gell cell battery that lasts for 6-8 hours per charge. The receiver operator can either measure the in-phase and quadrature components of the magnetic field components or the ratios of their magnitudes. The operating principle of the Maxi-Probe system and the theory behind it have been described earlier (Sinha, 1979, 1980).

Four soundings were performed along line 1 and three along line 2. The ground in both areas had been excavated, filled with gravel and loose rock and levelled for future construction. On line 1 the receivers were placed at distances of 150 m, 200 m, 250 m and 300 m from the transmitter. For this system the sounding point is considered to be the middle point between the transmitter and the receiver. On line 2, the receiver locations were at 250 m, 300 m and 338 m from transmitter location Tx_2. The maximum transmitter to receiver separation could not be greater than 338 m along this line due to proximity of sources of electrical noise emanating from heavy construction machinery and from electrical powerlines.

The field data were interpreted graphically (Sinha, 1979) at the site, and later were analyzed on a computer which inverted the ratios of vertical and horizontal magnetic fields into apparent depth versus apparent resistivity plots for each frequency at every sounding. The data for sounding on line 1 at 150 m separation was quite noisy presumably because it was taken on a rainy and windy day. It was therefore omitted from any further analysis. The six remaining soundings yielded consistent interpretation for the area.

Discussions of the Results

Figures 16.2, 16.3 and 16.4 illustrate the apparent depth versus apparent resistivity plots for three soundings with the transmitter-receiver separations of 200, 250 and 300 m, respectively, on line 1. Our model simulations indicate that while the apparent depth values are very close to the true depths of the interfaces, the apparent resistivity values are not the resistivity values at that depth but rather a function of all resistivities encountered to that depth value. In fact, the apparent resistivity values are greatly influenced by the resistivities of the top layers of the ground. However, in a qualitative sense, the highs and lows of the apparent resistivity plots correctly reflect the variation of the resistivity at any particular depth. Efforts are underway to extract true resistivity values of different layers from Maxi-Probe sounding results. An average of 40 frequencies from 40 Hz to 51kHz were used at each sounding station and depths in excess of 300 m were probed.

All three plots indicate the presence of a relatively high resistivity material at the top presumably reflecting the presence of dry gravel and other fill material. The resistivity values are rather uniform at extremely low frequencies (greater depth values) reflecting the fact that the energy is going into a homogeneous medium, presumably the granitic gneiss layer which is encountered at a depth of 220 m according to the borehole lithology log for UN1. Interestingly, a strong conductive zone was detected at a depth of about 240 m at all three sounding locations. This zone may be due to an increase in water salinity within the granitic gneiss or the presence of a water-saturated fault or shear zone.

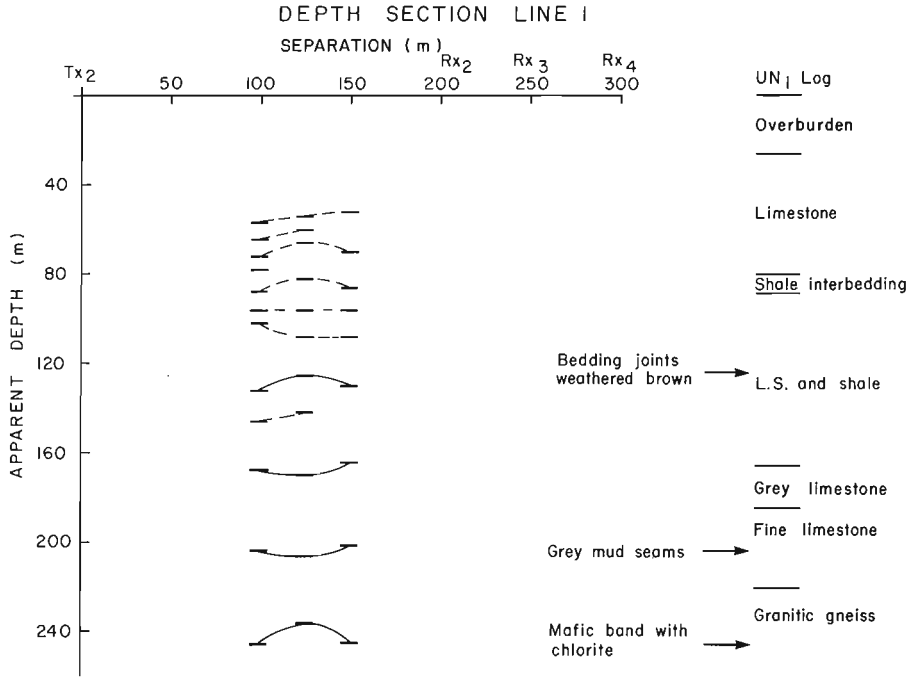

Figure 16.8. Maxi-Probe depth-section over line 1 at Darlington.

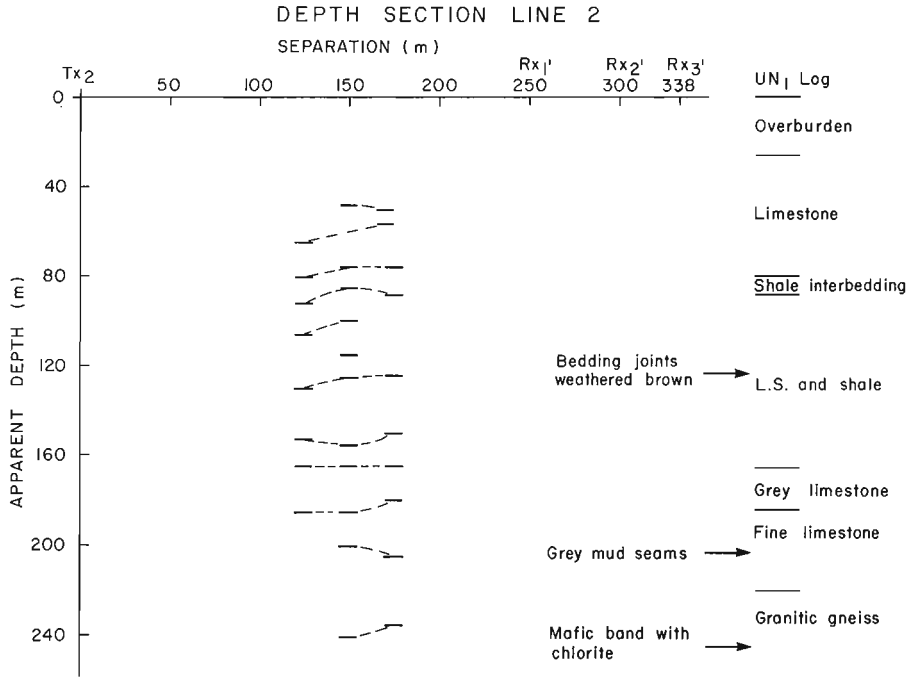

Figure 16.9. Maxi-Probe depth-section over line 2 at Darlington.

Figures 16.5, 16.6 and 16.7 illustrate the variations of apparent resistivity with depth for three soundings on line 2 for transmitter-receiver separations of 250, 300 and 338 m, respectively. Figures 16.5 and 16.6 indicate the presence of some conductive material at very shallow depths. But Figure 16.7, (separation of 338 m) gives only a mild indication of the presence of that layer. However, this is characteristic of the Maxi-Probe and many other frequency-domain systems where the apparent resistivity values are less dependent on the resistivity of the top layer for large separations between the transmitter and the receiver. Since the low resistivity of the top layer would have less influence on the apparent resistivity values with increasing coil separations, we should expect the apparent resistivity values in Figure 16.7 to be somewhat higher than those in Figure 16.6, which in turn should be higher than those in Figure 16.5. This is exactly what is shown in these figures. The presence of high conductivity material at shallow depths on line 2 reduces the depth of investigation to some extent.

Figures 16.8 and 16.9 illustrate depth sections for lines 1 and 2, respectively, based on Maxi-Probe sounding data. For plotting purposes, the mid-point between the transmitter and the receiver is taken as the sounding point. The 'tick' marks indicate the positions of conductive discontinuities as seen by the Maxi-Probe system. They are picked manually by the interpreter wherever the apparent resistivity shows a definite decrease. Good conductive interfaces are indicated by sharp breaks in the resistivity plots and are joined by solid lines while the weaker ones are joined by dashed lines. Since the depth of investigation depends on the separation between the transmitter and the receiver along with the conductivities of shallow materials, the deeper interfaces are not seen for the smaller separation of 250 m in Figure 16.9. On the right side of Figures 16.8 and 16.9 is a lithological log for the hole UN1. A comparison of the interpreted depths with the well-log shows great similarity between them. In fact, the Maxi-Probe survey results detect most of the lithological boundaries plus a few additional ones. This is because Maxi-Probe detects not only the conductivity discontinuities at lithological boundaries, but also conductivity discontinuities within lithological units which may be due to the presence of saline water in fracture zones or cracks. The latter almost certainly seems to be the case for the conductive feature at a depth of approximately 240 m which is within the granitic gneiss.

The consistency of interpreted depths between the six different soundings from two lines and the fact that the lines are separated from each other by almost 0.5 km suggests the presence of horizontal layering in the area. Minor discrepancies between the well log and the Maxi-Probe results may be explained

by the fact that (a) the soundings were not done over the drill hole location and hence the depths to the interfaces are likely to be somewhat different and, (b) the conductivity contrasts depend not only on change in lithology but also on the presence of water-filled fractures and the presence of shale and clay horizons within each formation even when they are quite thin.

As seen in Figures 16.8 and 16.9, the material between depths of 60 m to 100 m has several thin conductors. The lithologic log indicates that the limestone horizon in this depth range has several bands of silty mud and shaly limestone. These minor bands may not be laterally continuous over any great distance. Hence it becomes difficult to correlate them between different sounding points and from line to line. These conductive interfaces are indicated by dashed lines.

Conclusions

The multifrequency survey at the Darlington generating station site demonstrates the effectiveness of this technique for deep electromagnetic sounding over sedimentary strata, particularly since the electrical contrasts between the different formations in the area are small, especially between different varieties of limestone horizons.

On the basis of sounding results over two lines, it looks unlikely that a major fault system exists in the area bounded by the two lines. The conductive feature at a depth of 240 m, however, suggests the presence of horizontal fractures of some extent within the massive granitic gneiss or an abrupt increase in salinity. More extensive field tests over a wider area along several profiles will be needed to define the extent of these fractures.

References

Sinha, A.K.

1979: Maxi-Probe EMR-16: A new wide-band multifrequency ground EM system; in Current Research, Part B, Geological Survey of Canada, Paper 79-1B, p. 23-26.

1980: A study of topographic and misonentration effects in multifrequency electromagnetic soundings; Geoexploration, v. 18, p. 111-133.

17. THE CORONITIC MICHAEL GABBROS, LABRADOR: ASSESSMENT OF GRENVILLIAN METAMORPHISM IN NORTHEASTERN GRENVILLE PROVINCE

Project 790025

R.F. Emslie
Precambrian Geology Division

Emslie, R.F., The coronitic Michael gabbros, Labrador: assessment of Grenvillian metamorphism in northeastern Grenville Province; in Current Research, Part A, Geological Survey of Canada, Paper 83-1A, p. 139-145, 1983.

Abstract

Neohelikian Michael gabbros in southeastern Labrador display well defined progressive development of corona structures southward from their northern limit of exposure at the Grenville Front. The sequence of corona reactions is similar to those described from many other localities with the exception that pargasitic amphibole partly or entirely replaces clinopyroxene + spinel. At advanced stages of corona development corundum plates occur abundantly within sodic plagioclase, and their formation appears linked to breakdown of the anorthite component of plagioclase at elevated pressures. The reactions involved in corona formation place important constraints on interpretation of the intensity and extent of Grenvillian regional metamorphism in southeastern Labrador.

Introduction

Regionally metamorphosed rocks in the northeastern Grenville Province of southern Labrador form a complex distribution pattern. Although nonductile deformation attributable to Grenvillian tectonism has been widely recognized as marking the northern boundary of the Grenville Province (e.g. Gower et al., 1980), documentation of a synchronous or diachronous regional metamorphism has remained elusive, except in the immediate vicinity of the Labrador Trough (Brooks et al., 1981; Dallmeyer, 1982). A number of K-Ar mica ages around 950 ± Ma have been determined in the region but at face value these imply nothing more than tectonic uplift which cooled deep-seated rocks through the blocking temperature for diffusion of radiogenic argon in mica. Regional metamorphism of the Seal Lake Group, for example, whose depositional age is about 1323 ± 92 Ma is for the most part no higher than subgreenschist grade which could have been achieved largely by basin subsidence alone (Baragar, 1981). Delineation of the

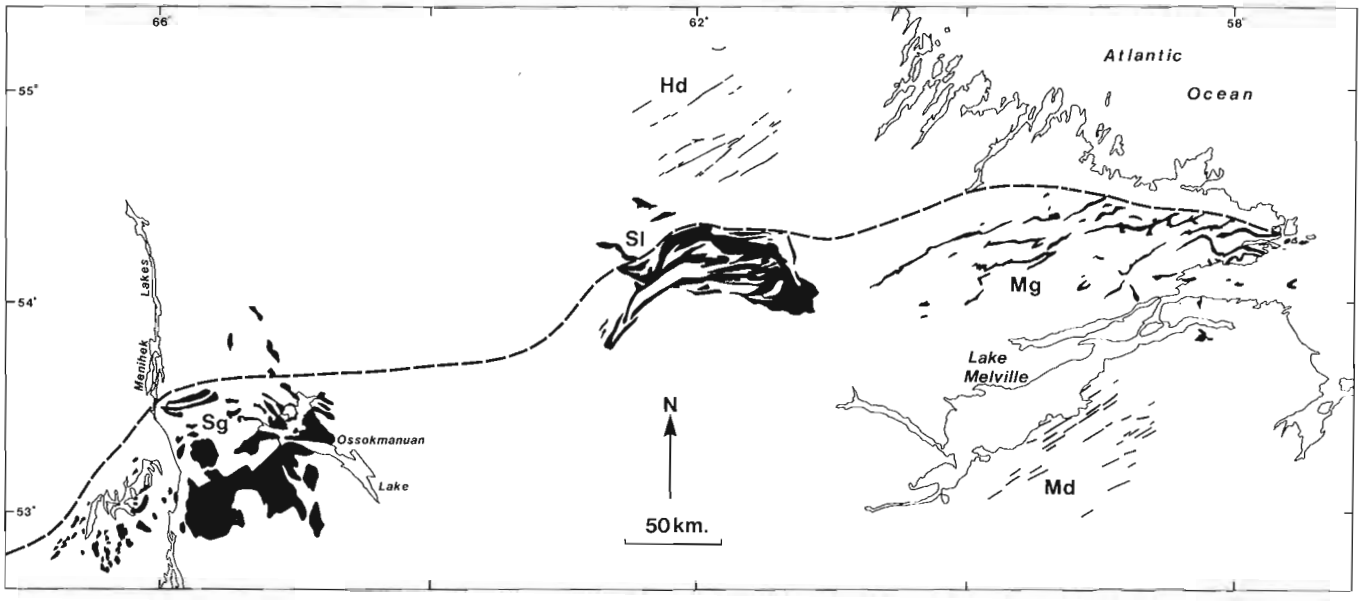

Figure 17.1. *Distribution of Neohelikian basic rocks in southern Labrador. Heavy dashed line is the approximate northern boundary of the Grenville Province adapted from Gower et al. (1980) and Brooks et al. (1981).*

Sg	*Shabogamo Intrusive Suite ('Shabogamo gabbro')*	*Hd*	*Harp dykes*
Sl	*Seal Lake Group*	*Md*	*Mealy dykes*
		Mg	*Michael gabbros*

All have mineral assemblages and/or rock chemistry consistent with crystallization from continental olivine tholeiite magmas. Their distribution within a zone some 600 km long and 250 km wide has been suggested to be related to Neohelikian continental rifting (Baragar, 1977, 1981; Meyers and Emslie, 1977). This magmatism closely followed the widespread major anorthosite suite magmatic event that ended prior to 1400 Ma ago.

intensity and extent of Grenvillian metamorphism is essential for the formulation of a realistic tectonic model of the Grenvillian Orogeny in this region.

The Michael gabbros, originally mapped by Stevenson (1970), and more recently by Gower (1981), were named informally by Fahrig and Larochelle (1972) who studied their paleomagnetism. The general distribution of the Michael gabbros is shown in Figure 17.1 along with other mafic intrusive and extrusive suites of similar age. The crystallization age of the gabbros has been estimated at 1461 ± 96 Ma (Rb-Sr, whole-rock) by Fahrig and Loveridge (1981). The Michael gabbros are of particular interest because of their relatively broad distribution extending southward for more than 50 km from the structural Grenville Front and because of their apparent increase in metamorphic grade toward the south (Fahrig and Larochelle, 1972). The intrusions consist of sheet-like bodies with both southerly and northerly dips and are accompanied by some subvertical dykes.

The present study is part of a co-operative investigation with J.K. Park, Geomagnetic Laboratory, Earth Physics Branch, and C.F. Gower, Newfoundland Department of Mines and Energy. During July, 1982 we sampled some 65 localities for petrological, paleomagnetic and age investigations. This report is a preliminary account of the petrography and mineral chemistry of the gabbros emphasizing some features of corona development that have an important bearing on interpretation of metamorphic history.

Petrography

Mineral assemblages in the least metamorphosed Michael gabbros are fairly typical of continental olivine tholeiites. Olivine, augite and plagioclase are the most abundant silicate minerals. Primary hypersthene is only rarely present in more than minor amounts but the central parts of thicker bodies contain hypersthene to the exclusion of olivine. In thin sections augite is dark grey or slightly brown, heavily charged with fine exsolved opaque inclusions. Primary plagioclase is also heavily clouded with very fine dusty inclusions giving it a brownish cast, particularly in cores. Red-brown biotite, apatite and opaque oxides are typical accessory minerals. Primary olive-brown hornblende occurs rarely but is locally abundant (Fig. 17.2D).

A variety of corona types is present in the Michael gabbros and these display a progression in development from north to south. The most northerly samples contain narrow double coronas separating olivine from plagioclase (Fig. 17.2A,B,C). Adjacent to olivine, the inner corona is prismatic, colourless hypersthene with elongation perpendicular to olivine margins. The outer rim is amphibole generally of pale to medium green shades. Very fine spinel may be present within the amphibole close to the hypersthene boundary. Sporadic rims bearing garnet and amphibole are present around opaque oxide grains.

Progressing southward, coronas become wider and central olivine kernels decrease in size. The hypersthene corona is followed outward by a zone consisting of a mixture of intergrown clinopyroxene and amphibole. Very thin necklaces of small garnets form an outermost rim in some assemblages. Garnet plus fine grained amphibole reaction zones increase in size between opaque oxides and plagioclase.

In the southernmost samples olivine is no longer present although forms implying its former existence are common. In some of these forms hypersthene can be seen to have grown inward to constitute a complete inner kernel. This is commonly surrounded by a green clinopyroxene rim or one containing a mixture of clinopyroxene and orthopyroxene with minor olive amphibole. This zone is commonly followed by a narrow moat of sodic plagioclase which is succeeded by a wide zone of relatively coarse garnets (Fig. 17.2H,I). A striking feature of large plagioclase grains is that they are replete with clear, colourless corundum plates up to a few hundred µm across but only a few µm thick (Fig. 17.2I). Relict subophitic textures are still visible in some samples (Fig. 17.2.G) and large dark inclusion-packed relict augite grains persist (Fig. 17.2I), distinct from clear green recrystallized augite.

Figure 17.2. *Progressive corona development in Michael gabbros.*

A. Specimen EC82-7. About 12 km south of the Benedict Fault zone and about 10 km due west of Lake Michael. Primary texture is nearly perfectly preserved except for very narrow double coronas separating olivine from plagioclase. Bar is 1 cm long.

B. Specimen EC82-7. Double coronas are shown in greater detail. Inner, lighter zone is fine prismatic orthopyroxene elongated perpendicular to the olivine margin. Outer rim of variable thickness is pale to medium green amphibole. Reaction between opaque oxides and plagioclase producing garnet and amphibole has begun but is sporadic in occurrence. Bar is 1 mm long.

C. Specimen EC82-7. Dark cloudy, subophitic clinopyroxene is heavily charged with fine exsolved opaque oxides. Contacts between clinopyroxene and olivine or plagioclase are sharp. Only rarely are fine lamellae of low-Ca pyroxene visible within the clinopyroxene. Bar is 1 mm long.

D. Specimen EC82-5. About 3 km south of Benedict Fault zone, on narrow peninsula, northeast part of Lake Michael. This is an unusually mafic sample from the interior of a large sheet. Olivine, clinopyroxene and minor orthopyroxene are enclosed by large poikilitic hornblende. Plagioclase is rare and has interstitial habit. Bar is 1 mm long.

E. Specimen EC82-1A. About 25 km south of Benedict Fault zone. Intermediate stage of corona development. Most olivine is gone from core areas which are now largely or entirely orthopyroxene. Reaction zones on opaque oxides are strongly developed. Cloudy brown plagioclase cores are still apparent. Bar is 1 mm long.

F. Specimen EC82-30. About 35 km south of the Benedict Fault zone, just north of Tom Luscombe Brook. Another example of an intermediate stage of corona development. Olivine cores are still present followed successively by zones of orthopyroxene, aluminous clinopyroxene plus amphibole, and an outer narrow fringe of small garnets. Bar is 1 mm long.

G. Specimen EC82-10A. About 45 km south of Benedict Fault zone, north shore of Double Mer. Olivine is no longer present. Advanced corona development has involved all silicate and oxide minerals. Plagioclase is not recrystallized and relict subophitic texture is still evident. Bar is 1 cm long.

H. Specimen EC82-8. Island in Double Mer about 1 km southwest of previous locality. Plagioclase has not recrystallized and is heavily charged with clear, colourless corundum plates (they appear darker because of their high relief). Well developed garnet coronas separate plagioclase from other mafic silicates. Note the narrow moats of sodic plagioclase present on the mafic mineral side of garnet coronas. Bar is 1 mm long.

I. Specimen EC82-8. Higher magnification of the previous specimen illustrates the platy forms of corundum in plagioclase. Cloudy, dark, triangular clinopyroxene grain (lower middle) appears to be a primary igneous relic. Bar is 1 mm.

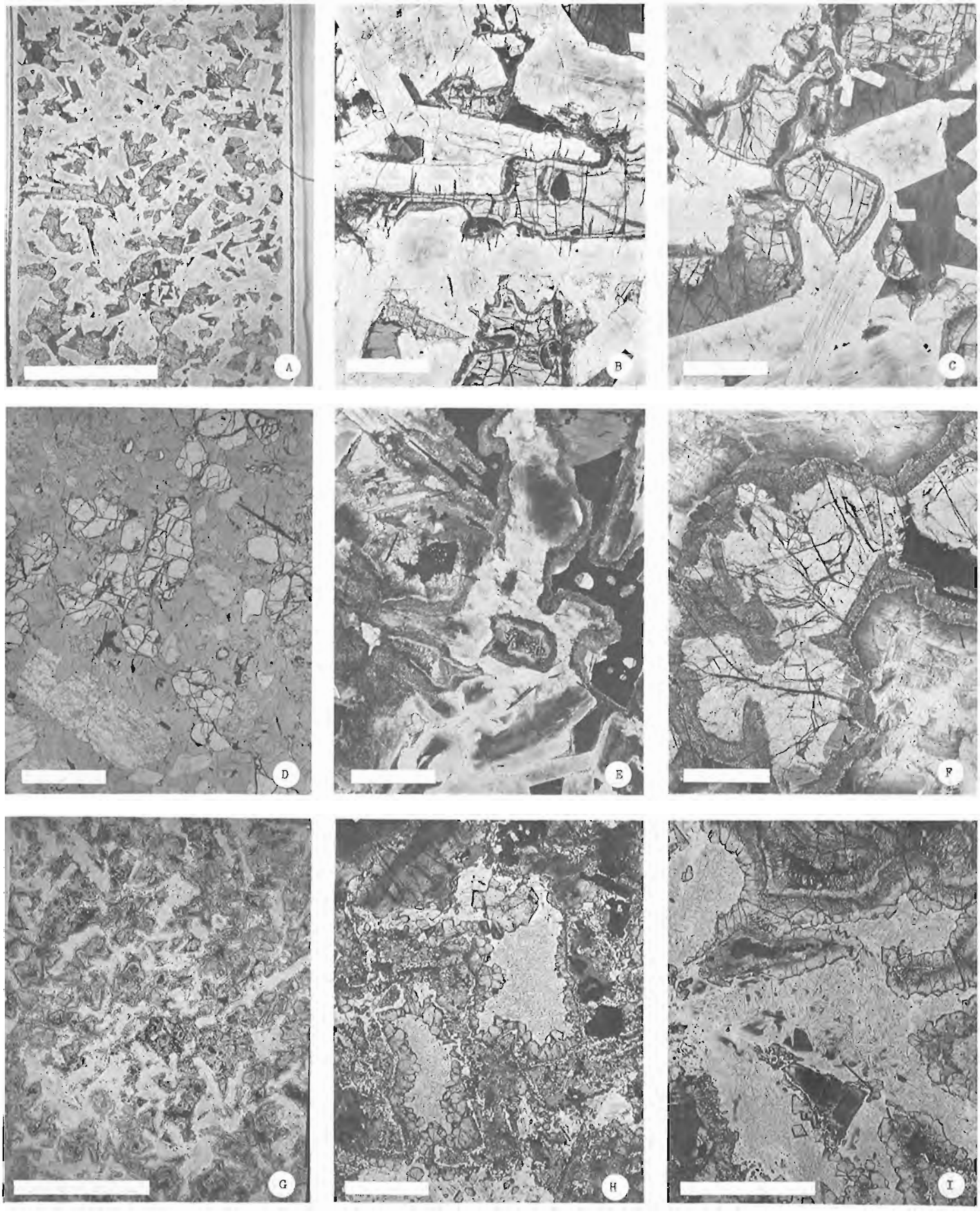
A
B
C
D
E
F
G
H
I

Table 17.1

Mineral chemistry of coronitic Michael gabbros

	EC82-7					EC82-30						EC82-8		
	oliv	cpx	opx	amph	biot	oliv	cpx	opx	cpx	amph	gar	cpx	cpx	gar
	1.	2.	3.	4.	5.	6.	7.	8.	9.	10.	11.	12.	13.	14.
	(4)	(1)	(2)	(2)	(3)	(4)	(3)	(2)	(2)	(1)	(2)	(5)	(3)	(3)
SiO_2	35.0	49.4	52.3	39.1	36.0	36.3	50.5	53.2	49.8	39.5	39.7	51.1	52.0	37.9
TiO_2	0.04	0.77	0.01	0.07	5.72	0.01	0.86	0.02	0.02	0.99	0.03	1.03	0.17	0.08
Al_2O_3	-	2.71	1.18	17.6	13.8	-	3.36	1.40	7.71	16.9	21.0	3.74	3.87	20.5
Cr_2O_3	0.03	0.06	0.03	0.00	0.03	0.01	0.03	0.01	0.03	0.01	0.03	0.06	0.05	0.05
FeO*	37.7	11.8	21.0	11.0	17.2	32.6	10.7	18.5	11.0	9.01	20.4	12.7	9.36	27.7
MnO	0.41	0.26	0.42	0.14	0.01	0.15	0.09	0.13	0.21	0.00	0.38	0.07	0.02	0.63
MgO	27.7	14.6	24.4	12.8	12.3	32.2	14.8	26.4	13.6	14.3	8.42	12.2	12.4	7.25
CaO	-	18.1	0.49	11.7	0.04	-	16.6	0.16	17.4	11.8	10.6	17.3	20.3	5.85
Na_2O	-	0.84	-	2.41	0.48	-	1.33	-	1.13	2.27	-	2.90	2.42	-
K_2O	-	0.04	-	1.62	9.59	-	0.01	-	0.02	1.99	-	0.03	0.04	-
Total	100.88	98.58	99.83	96.44	95.17	101.27	98.28	99.82	100.92	96.77	100.56	101.13	100.63	99.96
O	4	6	6	23	22	4	6	6	6	23	24	6	6	24
Si	0.977	1.888	1.942	5.845	5.479	0.981	1.911	1.947	1.836	5.845	6.029	1.908	1.931	5.948
Al^{iv}		0.112	0.052	2.155	2.480		0.089	0.053	0.164	2.155	0.000	0.092	0.069	0.052
Al^{vi}		0.010	0.000	0.954	0.000		0.061	0.007	0.171	0.798	3.764	0.072	0.101	3.736
Ti	0.001	0.022	0.000	0.008	0.656	0.000	0.024	0.001	0.001	0.110	0.003	0.029	0.005	0.009
Cr	0.001	0.002	0.001	0.000	0.004	0.000	0.001	0.000	0.001	0.001	0.004	0.002	0.001	0.006
Fe^{2+}	0.880	0.376	0.654	1.378	2.194	0.737	0.338	0.565	0.340	1.116	2.599	0.395	0.291	3.634
Mn	0.010	0.008	0.013	0.018	0.002	0.003	0.003	0.004	0.007	0.000	0.049	0.002	0.001	0.084
Mg	1.154	0.835	1.351	2.855	2.798	1.297	0.838	1.439	0.749	3.151	1.908	0.682	0.684	1.694
Ca		0.742	0.020	1.875	0.006		0.674	0.006	0.688	1.878	1.730	0.691	0.809	0.983
Na		0.062		0.699	0.143		0.098		0.081	0.652		0.210	0.174	
K		0.002		0.309	1.864		0.000		0.001	0.376		0.001	0.002	
Σ cations	3.022	4.059	4.032	16.097	15.627	3.018	4.038	4.022	4.037	16.082	16.084	4.086	4.067	16.146
Atom% Ca	-	38.0	1.0	30.7	0.1	-	36.4	0.3	38.7	30.6	27.7	39.1	45.3	15.6
Mg	56.7	42.8	66.7	46.7	56.0	63.8	45.3	71.6	42.2	51.3	30.6	38.6	38.4	26.8
Fe	43.2	19.3	32.3	22.6	43.9	36.2	18.3	28.1	19.1	18.2	41.7	22.4	16.3	57.6

FeO* = Total Fe as FeO.
Brackets enclose number of analyses averaged.

Specimen EC82-7

1. Olivine cores and rims
2. Cloudy brown clinopyroxene, broad beam scan
3. Secondary orthopyroxene, inner corona adjacent to olivine
4. Secondary amphibole, pale green, in outer corona
5. Primary red-brown biotite

Specimen EC82-30

6. Olivine cores and rims
7. Cloudy dark clinopyroxene, broad beam scans
8. Secondary orthopyroxene, inner corona adjacent to olivine
9. Fine grained clear clinopyroxene with amphibole in mid corona
10. Secondary amphibole, olive green, in mid corona
11. Secondary garnet in outermost corona

Specimen EC82-8

12. Cloudy dark clinopyroxene, broad beam scans
13. Pale green, clear clinopyroxene in corona cores
14. Secondary garnet in outermost coronas

Mineral Chemistry

Reconnaissance electron microprobe study of representative mineral assemblages in the Michael gabbros are summarized in Table 17.1 and Figures 17.3 and 17.4.

Olivines show a substantial range of composition, are unzoned, and probably represent a close approach to their primary compositions. Secondary orthopyroxenes vary systematically in composition with coexisting olivine and the regularity of tie line dispositions suggests a close approach to equilibrium between the two minerals (Fig. 17.3a).

Primary plagioclase compositions are concentrated in the range An_{50} to An_{60}. Little zoning is evident in some specimens but normal zoning has been measured with rims up to 20 mole per cent less An-rich than cores (Fig. 17.3c). Metamorphic plagioclase at advanced stages of reaction is markedly more sodic than primary compositions and zoning is not prominent (Fig. 17.3b).

Except for one relatively Mg-rich composition from an apparent cumulate zone, primary clinopyroxenes are low-Ca augites (Fig. 17.4). Recrystallized clear clinopyroxenes from more highly reacted assemblages are notably more Ca-rich reflecting lower temperature equilibration. Fine grained corona clinopyroxene intergrown with amphibole at an intermediate stage of corona development is exceedingly aluminous, having subequal amounts of tetrahedral and octahedral Al (Table 17.1, column 9).

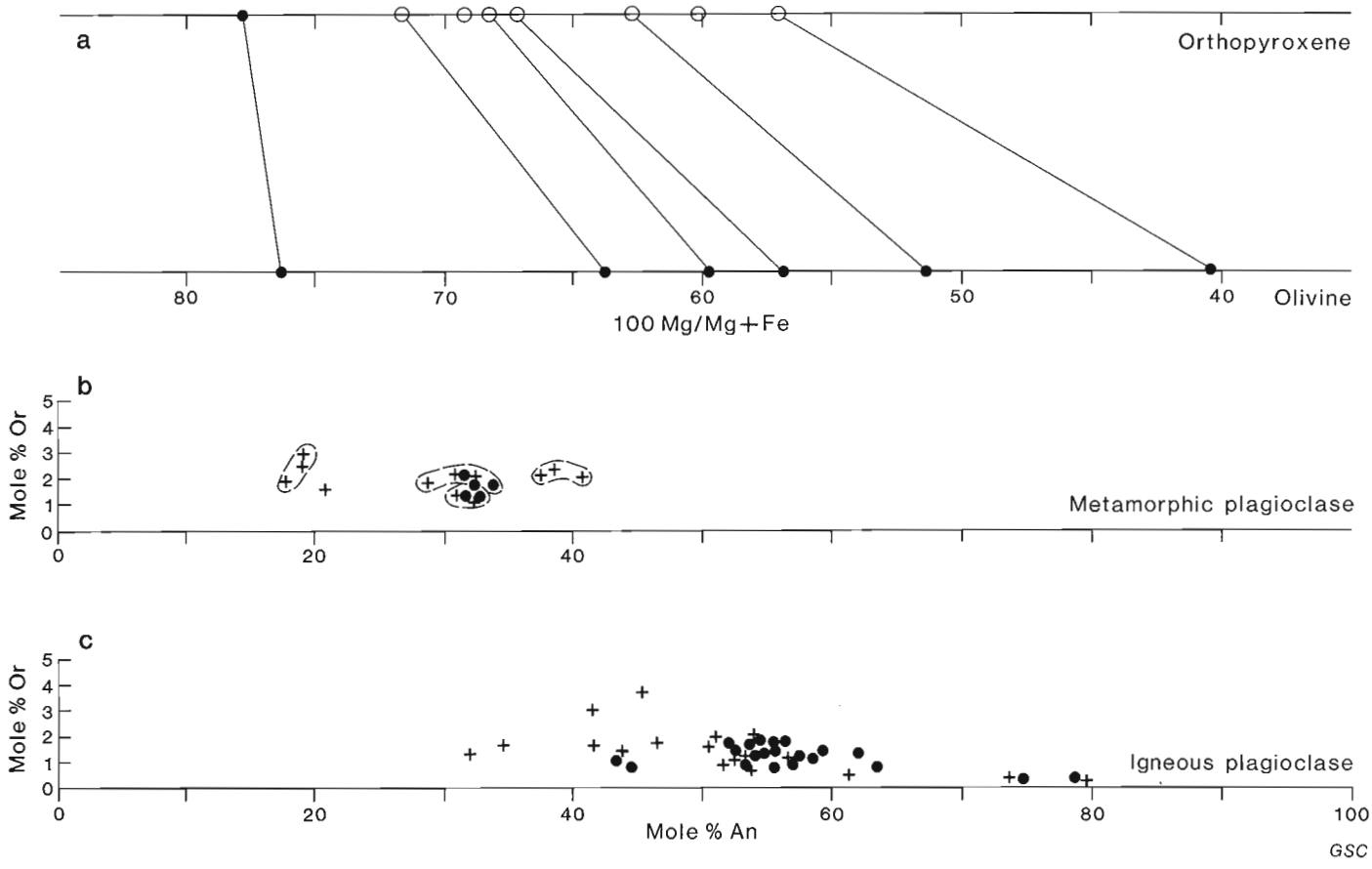

Figure 17.3. *Igneous and metamorphic mineral compositions in coronitic Michael gabbros.*

a. Olivines (assumed to approximate primary igneous compositions) and metamorphic orthopyroxenes (open circles) that form innermost coronas adjacent to olivine (each point is the average composition for an individual specimen). The lines join coexisting pairs. The most magnesian pair comprises primary orthopyroxene (solid circle) and olivine from a very mafic zone in the central part of a sheet, and suggests that crystal-liquid fractionation took place in larger magma volumes.

b. Compositions of plagioclase in advanced stages of corona development. Solid dots are cores of grains, crosses are rims. Dashed lines enclose analyses of different grains from the same sample. Compositions near An_{40} are plagioclase rims from a sample (EC82-30, Fig. 17.2, Table 17.1) approaching the limit of olivine stability; plagioclase cores in the same sample retain their primary compositions near An_{54}. The two samples near An_{30} (EC82-8, EC82-10A, Fig. 17.2, Table 17.1) are at a significantly more advanced stage where original plagioclase compositions are lost entirely and plagioclase is heavily charged with corundum plates; plagioclase near An_{20} from the same samples occurs as narrow continuous or discontinuous moats just inside the outer garnet coronas.

c. Cores and rims of plagioclase from least modified gabbros. Data points are individual analyses for 7 specimens. Zoning, when present, is normal and continuous. Plagioclase An_{75-80} is interstitial in the same rock with magnesian olivine and orthopyroxene in Figure 17.3a.

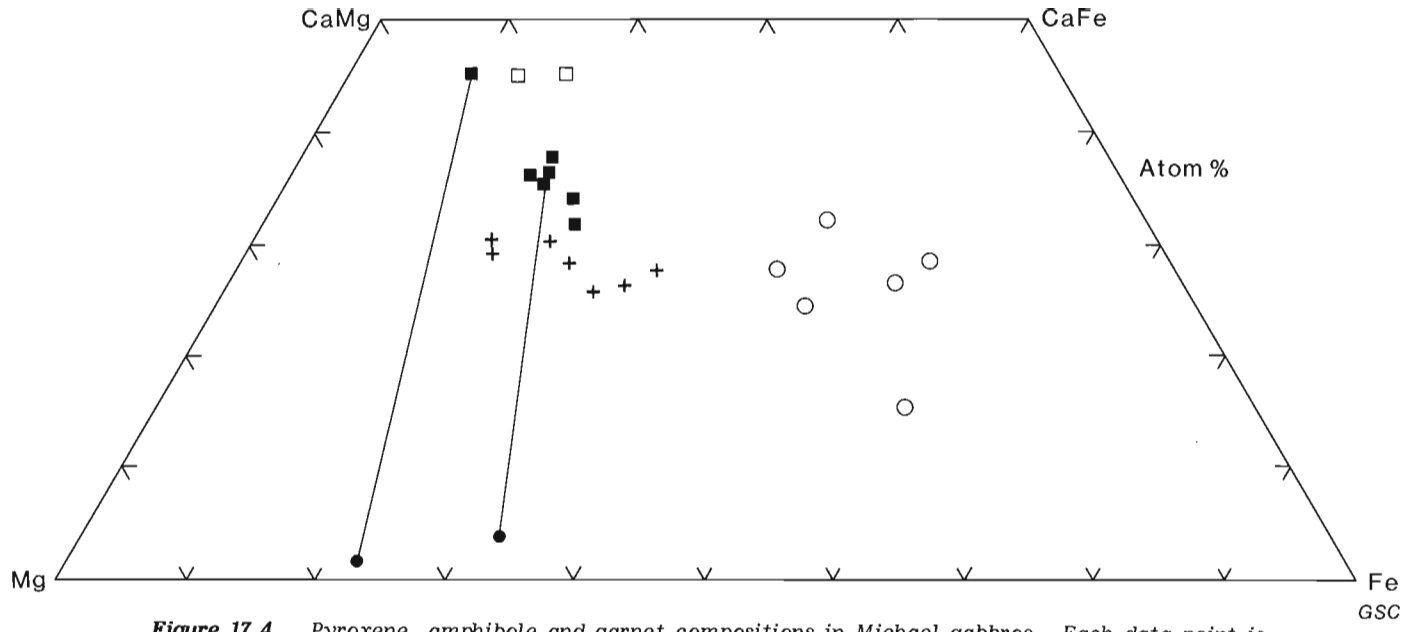

Figure 17.4. *Pyroxene, amphibole and garnet compositions in Michael gabbros. Each data point is an average composition for a single specimen. Solid squares are bulk compositions of primary, dark, subophitic clinopyroxenes estimated by broad beam microprobe scanning. Open squares are pale green, clear, metamorphic clinopyroxenes enclosed within garnet coronas at highest grades. Solid dots are relatively rare primary orthopyroxene; tie lines indicate coexisting pairs. Crosses are amphiboles from coronas. Open circles are garnets from coronas; the low-Ca Fe-rich garnet composition is from an advanced stage in which plagioclase contains abundant corundum plates (EC82-8, Figure 17.2, Table 17.1). The most magnesian pyroxene pair coexists with the most Mg-rich olivine (Fig. 17.3a) and An-rich plagioclase (Fig. 17.3c). Divisions are at 10 per cent intervals.*

Secondary amphiboles in coronas are highly aluminous calcic varieties (pargasites) even in the least modified Michael gabbros (Table 17.1, column 4). Red-brown biotite in the same specimen is rich in Ti (Table 17.1, column 5), typical of primary, high temperature biotites in basic rocks. Garnets from outermost coronas display not only a range in Fe/Fe + Mg but also considerable differences in grossularite contents (Table 17.1, Fig. 17.4).

Discussion

Reduced to its simplest terms, interpretation of the metamorphism of the Michael gabbros can be viewed as testing two distinct hypotheses:

1. Observed progressive corona development is the result of prograde regional heating during the Grenvillian Orogeny. The expected metamorphic gradient would be such that temperature and possibly pressure increased toward the south. This has been the conventional, favoured interpretation (e.g. Fahrig and Larochelle, 1972; Gower, 1981).
2. Progressive corona development is the result of subsolidus reactions during lower temperature re-equilibration of Michael gabbro assemblages because of their intrusion, crystallization and cooling at considerable (and probably variable) crustal depths.

Confirmation or rejection of one or other of these hypotheses has profound significance for the correct interpretation of effects of the Grenvillian Orogeny in the northeastern Grenville Province. Although hypothesis 1 has received more attention, there are several reasons why hypothesis 2 must be given serious consideration:

a. K-Ar whole-rock ages of 1323 ± 52 and 1348 ± 120 Ma have been determined from fine grained margins of Michael gabbros in the vicinity of Indian Harbour on the coast (Fahrig and Loveridge, 1981). These rocks have the double orthopyroxene-pargasite coronas on olivines and it is very difficult to imagine that such ages could have survived an amphibolite grade regional Grenvillian metamorphism.

b. Evidence for a penetrative deformation fabric is completely absent in thin sections of the Michael gabbros; delicate features of coronas are clearly preserved at all stages of development. This is not readily reconciled with a regional Grenvillian metamorphism of amphibolite or higher grade.

c. In the Mealy Mountains to the southwest, hornblende ages of 1400 ± 57 and 1533 ± 45 Ma in rocks of the Mealy Mountains complex (R.K. Wanless, personal communication, in Emslie, 1978) strongly suggest that Grenvillian metamorphism as high as amphibolite grade did not affect those rocks. In the Red Wine Mountains to the west regional heating that can be attributed to the Grenvillian Orogeny is limited to low grade (Emslie, 1981).

Corona reactions in the Michael gabbros are closely analogous to those typically seen in anhydrous coronitic gabbros:

olivine + Ca-Na plag = opx + cpx + spinel + Na-Ca plag
opx + cpx + spinel + Na-Ca plag = cpx + garnet + Na plag (± opx)

The chief difference in Michael gabbro coronas is that pargasitic amphibole appears to take the place of cpx + spinel partly or entirely. This suggests that low fluid pressures played a rôle in promoting reactions but P_{H_2O} must have been very much lower than P_{total}. More highly reacted assemblages are not more hydrous so that increasing hydration was not a controlling factor in progressive reaction. The stability of pargasitic amphibole in coronas of the least modified Michael gabbros indicates that conditions equivalent to at least amphibolite grade prevailed even at that stage.

Although positions and slopes for the anhydrous equilibria in P-T space are not closely defined for natural compositions, the slopes are known to be positive (e.g. Griffin and Heier, 1973; Whitney and McLelland, 1973; Gardner and Robins, 1974; Herzberg, 1978) with garnet-cpx associations at higher P, lower T, relative to olivine-plagioclase. Because corona development in the Michael gabbros increases progressively from north to south, some preliminary constraints can be placed on conditions of reaction:

a. If reactions occurred during cooling of the gabbros from igneous temperatures, the southern assemblages continued to react to somewhat lower T or higher P or both.

b. If reactions occurred during prograde regional metamorphism, the southern assemblages must reflect markedly higher P and T than those to the north.

c. If little or no temperature gradient existed from north to south the southern assemblages reacted under higher P.

The apparent breakdown of the anorthite component of plagioclase to form corundum plus more sodic plagioclase is expected to be a reaction promoted by relatively high pressures (Goldsmith, 1980). The required accompanying exchange of Ca and Na by plagioclase with its surroundings can presumably be related to garnet- and clinopyroxene-forming reactions.

Rigorous testing of the models outlined above will require more detailed analysis of the corona assemblages. In addition, isotopic dating of amphiboles and biotites should help further constrain possible ages of metamorphism and cooling intervals.

References

Baragar, W.R.A.
1977: Volcanism of the stable crust; in Volcanic Regimes in Canada, ed. W.R.A. Baragar, L.C. Coleman, and J.M. Hall; Geological Association of Canada, Special Paper 16, p. 377-405.

1981: Tectonic and regional relationships of the Seal Lake and Bruce River magmatic provinces; Geological Survey of Canada, Bulletin 314, 72 p.

Brooks, C., Wardle, R.J., and Rivers, T.
1981: Geology and geochronology of Helikian magmatism, western Labrador; Canadian Journal of Earth Sciences, v. 18, p. 1211-1227.

Dallmeyer, R.D.
1982: $^{40}Ar/^{39}Ar$ incremental-release age of biotite from a gabbro of the Shabogamo intrusive suite, southwestern Labrador; Canadian Journal of Earth Sciences, v. 19, p. 1877-1881.

Emslie, R.F.
1978: Elsonian magmatism in Labrador: age, characteristics and tectonic setting; Canadian Journal of Earth Sciences, v. 15, p. 438-453.

Emslie, R.F. (cont.)
1981: Exceptionally high grade metapelitic gneisses in the Red Wine Mountains, southern Labrador; Geological Association of Canada, Annual Meeting Abstracts, v. 6, p. A-17.

Fahrig, W.F. and Larochelle, A.
1972: Paleomagnetism of the Michael gabbro and possible evidence of the rotation of Makkovik Subprovince; Canadian Journal of Earth Sciences, v. 9, p. 1287-1296.

Fahrig, W.F. and Loveridge, W.D.
1981: Rb-Sr study of the Michael Gabbro, Labrador; in Rb-Sr and U-Pb Isotopic Age Studies, Report 4; in Current Research, Part C, Geological Survey of Canada, Paper 81-1C, p. 99-103.

Gardner, P.M. and Robins, B.
1974: The olivine-plagioclase reaction: geological evidence from the Seiland petrographic province, northern Norway; Contributions to Mineralogy and Petrology, v. 44, p. 149-156.

Goldsmith, J.R.
1980: The melting and breakdown reactions of anorthite at high pressures and temperatures; American Mineralogist, v. 65, p. 272-284.

Gower, C.F.
1981: The geology of the Benedict Mountains, Labrador; Newfoundland Department of Mines and Energy, Report 81-3, 26 p.

Gower, C.F., Ryan, A.B., Bailey, D.G., and Thomas A.
1980: The position of the Grenville Front in eastern and central Labrador; Canadian Journal of Earth Sciences, v. 17, p. 784-788.

Griffin, W.L. and Heier, K.S.
1973: Petrological implications of some corona structures; Lithos, v. 6, p. 315-335.

Herzberg, C.T.
1978: Pyroxene geothermometry and geobarometry: experimental and thermodynamic evaluation of some subsolidus phase relations involving pyroxenes in the system $CaO-MgO-Al_2O_3-SiO_2$; Geochimica et Cosmochimica Acta, v. 42, p. 945-957.

Meyers, R.E. and Emslie, R.F.
1977: The Harp dikes and their relationship to the geological record in central Labrador; Canadian Journal of Earth Sciences, v. 14, p. 2683-2696.

Stevenson, I.M.
1970: Rigolet and Groswater Bay map-areas, Newfoundland (Labrador); Geological Survey of Canada, Paper 69-48, 23 p.

Whitney, P.R. and McLelland, J.M.
1973: Origin of coronas in metagabbros of the Adirondack Mts., N.Y.; Contributions to Mineralogy and Petrology, v. 39, p. 81-98.

18.

GEOLOGY, REDROCK LAKE AND EASTERN CALDER RIVER MAP AREAS, DISTRICT OF MACKENZIE: THE CENTRAL WOPMAY OROGEN (EARLY PROTEROZOIC), BEAR PROVINCE, AND THE WESTERN ARCHEAN SLAVE PROVINCE

Project 810020

M.R. St-Onge, A.E. Lalonde[1], and J.E. King[2]
Precambrian Geology Division

St-Onge, M.R., Lalonde, A.E., and King, J.E., Geology, Redrock Lake and eastern Calder River map areas, District of Mackenzie: the central Wopmay Orogen (early Proterozoic), Bear Province, and the western Archean Slave Province; in Current Research, Part A, Geological Survey of Canada, Paper 83-1A, p. 147-152, 1983.

Abstract

Archean basement involvement in the early Proterozoic deformational history of Wopmay Orogen can be documented west of the Asiak fold-thrust belt probably as far as the main thermal culmination, which to the north is the locus of Hepburn Batholith emplacement. The Scotstoun Massif is not unlike Carousel Massif, a disharmonic fold structure cored by Archean basement in the Asiak fold-thrust belt. The Acasta Lake antiform located in the axis of the Hepburn thermal culmination is also a candidate for another basement-cored structure in Wopmay Orogen, although this will have to be tested with further work to the south. Within the Archean terrane centred on Redrock Lake, a mafic volcanic belt is intruded on the north side by the granite coring Carousel Massif and is fault bounded on the south side against the Point Lake granitoid terrane by the northeast-trending dextral transcurrent Redrock fault. To the west, the composite Hepburn Batholith has undergone a significant reduction in number and volume of plutons over that seen to the north. Between the Hepburn Batholith and the Wopmay Fault Zone, in the high grade units of the Akaitcho Group is emplaced a suite of hornblende diorites and biotite-hornblende granites centred on Bishop Lake. This suite is massive and petrographically unlike the Hepburn Batholith. The Wopmay Fault Zone is a 5-7 km wide belt of proto- to ultramylonites that has been broken by a set of north-south anastomosing brittle faults. These late faults juxtapose blocks of contrasting rock types, metamorphic grade and degree of deformation.

Introduction

The Redrock Lake and the eastern portion of the Calder River map areas combined provide a complete transect of the internal zone of the early Proterozoic Wopmay Orogen (McGlynn, 1970; Fraser et al., 1972) that flanks the western edge of the Archean Slave craton in the northwest corner of the Canadian Shield. Studies of the internal zone of Wopmay Orogen were initiated during systematic mapping of the Hepburn Lake map area (86 J) north of the present project area (Hoffman, 1972, 1973; Hoffman et al., 1978, 1980, 1981; St-Onge and Carmichael, 1979; Easton, 1980, 1981a,b; Hoffman and St-Onge, 1981; St-Onge, 1981). Work in the Redrock Lake and Calder River map areas was started during the summer of 1981 (St-Onge et al., 1982) and is expected to be completed by the end of the 1983 field season.

Three and a half months of work in the area in 1982 has carried the stratigraphy and structure established in 1981 southward, below 65°30', yielding the following set of results:

1. The Archean basement rocks, well exposed in Carousel Massif (St-Onge et al., 1982) and in the area south and southwest of Redrock Lake (Fig. 18.1) consists of a series of foliated syeno- and monzogranites (Streckeisen, 1976), two of which have an intrusive relationship with a basic volcanic section bounded on the south side by the Redrock Lake Fault.
2. Two other large scale folds of probable Archean basement occur west of Carousel Massif. The first, the Scotstoun structure (Fig. 18.1) is overlain by Odjick Formation siltstones, and the second, the Acasta structure (Fig. 18.1), is overlain by amphibolite and high grade paragneisses of the Akaitcho Group.
3. The basal sole fault or décollement first mapped around the hinge area of Carousel Massif (St-Onge et al., 1982) is now documented on the west side of the anticline to a point 12 km southwest of Redrock Lake. A similar fault (probably the western continuation of the décollement) is found around the north end of the Scotstoun Massif.
4. The composite Hepburn Batholith, with plutons ranging in composition from hornblende diorite to biotite syenogranite (Hoffman et al., 1980; St-Onge et al., 1982), as previously described to the north extends southward into the area mapped this year, but undergoes a significant reduction in size. As a result, the Akaitcho Group-Epworth Group transition, elsewhere obliterated by plutons of the Hepburn Batholith except in two localities (Easton, 1980), is exposed west of Scotstoun Lake. The transition, however, is coincident with the axis of the thermal high that characterizes the internal zone of Wopmay Orogen, making it difficult to determine if it is a conformable contact or a premetamorphic structural juxtaposition.
5. A suite of hornblende diorites and biotite-hornblende granites is centred on Bishop Lake (Fig. 18.2). The various plutons are all massive and are completely separate from the main axis of the Hepburn Batholith. Emplacement of the Bishop suite is either of late Hepburn Batholith age or Great Bear Batholith age.
6. The Wopmay Fault Zone is a 5-7 km wide zone of proto- to ultramylonites, which has been broken by a set of north-south anastomosing brittle faults. The late brittle faults juxtapose contrasting blocks of internally consistent stratigraphy and character. The Wopmay Fault "proper" is the westernmost fault mapped, which places the Dumas Group of the Great Bear Batholith against the low grade rocks of the Grant Group or against mylonites and granites of the Hepburn metamorphic-plutonic zone.

[1] Department of Geological Sciences, McGill University, Montréal, Québec
[2] Department of Geological Sciences, Queen's University, Kingston, Ontario, K7L 3N6

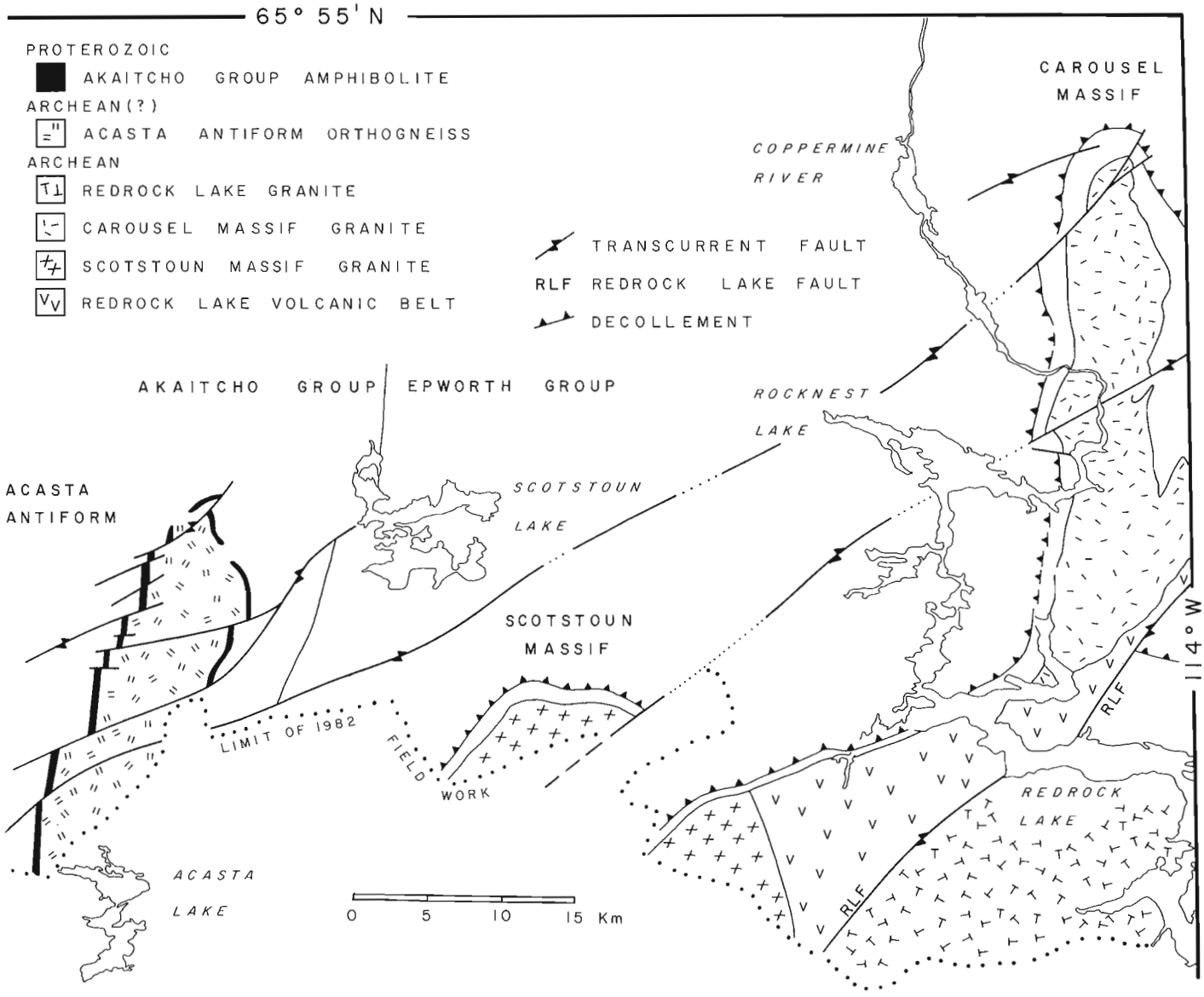

Figure 18.1. *Extent of Archean basement involvement in the early Proterozoic deformation of Wopmay Orogen as documented to date in the Redrock Lake map area. Note that the (D-4) collision event (Hoffman, 1982) recorded by the northeast-striking dextral faults affects both Proterozoic and Archean units.*

Redrock Lake Archean Basement

The Archean of the Redrock Lake-Carousel Massif area (Fig. 18.1) can be subdivided into three distinct units; the Carousel Massif granite, the Redrock Lake granite, and the Redrock Lake volcanic belt.

The Carousel Massif granite is predominantly a foliated to gneissic biotite monzogranite with a tectonic fabric that invariably strikes southwest and dips 60-80° west. Locally, the fabric is protomylonitic and in some cases it can be seen overprinted by a north-south spaced cleavage correlated with the folding of the massif. Amphibolite xenoliths that vary in length from 10-50 m occur in the granite and are most conspicuous within 0.5 km of the contact with the Redrock Lake volcanic belt. Minor phases of the granite body are K-feldspar megacrystic.

The Redrock Lake granite is a biotite syenogranite that only locally has a well developed lepidoblastic fabric. The granite can be K-feldspar megacrystic and in places contains two ferromagnesian minerals (biotite and hornblende). Amphibolite enclaves and mafic schlieren are very common but show no systematic regional distribution. The Redrock Lake granite is correlated with the late Archean granites to the east (Easton et al., 1981) which form a large part of the Archean granitoid terrane of Easton et al. (1982).

The Redrock Lake volcanic belt, separated from the Redrock Lake granite by a major northeast-striking dextral transcurrent fault (Fraser, 1960, 1974), consists predominantly of mafic, massive and pillowed flows with some intraflow, silty and tuffaceous beds. Mafic dykes and sills are found throughout the section and carbonate beds are

present north of Redrock Lake. Carbonatization of the volcanics is common and malachite staining was noted in some quartz veins. In contrast to the fault bounded contact on the south side, which is characterized by a network of quartz vein breccias, the western and northern boundaries of the volcanic belt show definite intrusive relationships with the granites (Fig. 18.1). The contact is gradual, the number and size of mafic enclaves in the granite increasing over a 0.5 km wide zone towards the volcanic belt proper. The metamorphic grade in the belt as documented in the mafic rocks is variable from amphibolite to transitional greenschist-amphibolite facies.

Scotstoun and Acasta Fold Structures

Southeast of Scotstoun Lake, Archean basement is exposed in the core of another large-scale north-plunging upright fold (Fig. 18.1) that is similar in geometry to Carousel Massif.

The Archean rocks consist predominantly of a pink biotite syenogranite that is often schlieric, with a well developed gneissic fabric striking southwest and dipping west. Amphibolite xenoliths are present but rare.

The granite is overlain on the north and west sides by Odjick Formation siltstones interbedded with dolomite. The strike of bedding in the sediments is conformable to the outline of the underlying granite. The maximum-phase mineral assemblage in pelitic layers is biotite-chlorite(?)-plagioclase-quartz-graphite. Although the actual contact with the granite is not exposed, the attitude and the low grade of the siltstone/dolomite beds point to the granite as being basement to the overlying section.

The southeast side of the Scotstoun Massif appears fault bounded. Whether this fault is part of the (D-4) conjugate transcurrent fault set that affects all pre-Cleaver Dykes and possibly all pre-Hornby Bay Group units (Hoffman, 1980, 1982), or whether the fault is an east-verging, west-dipping (D-1) thrust fault juxtaposing Archean basement on early Proterozoic Odjick Formation, will be resolved by extending the mapping south in 1983. The outcome of that work will have an important bearing on documenting to what extent, if any, the Archean basement of the Scotstoun Massif is itself allochthonous and whether or not there are further indications of significant shortening in the basement, in addition to that given by the large north-plunging granite-cored folds.

Fifteen kilometres west of Scotstoun Lake is another large scale north-plunging fold structure (Fig. 18.1) that is presently mapped as far south as Acasta Lake. The antiform is cored by an orthogneiss with a variable composition that ranges from granodiorite to syenogranite. Amphibolite layers and xenoliths are common in the deformed granitic unit. A tectonic fabric is generally present, striking north-south with steep dips.

The orthogneiss is structurally overlain by a thick unit of massive amphibolite intercalated with metamorphosed mafic sediments (Fig. 18.1). Associated with this mafic unit are calc-silicate and pelitic migmatite layers. Surrounding and structurally conformable with the outline of the orthogneiss and the amphibolite unit are the easternmost migmatites of the Akaitcho Group. The migmatites are derived from a number of protoliths that include pelites, semipelites, impure quartzites, mafic sediments and massive mafic flows or dykes. The tectonic fabric in the amphibolite unit and in the migmatites consistently dips away from the orthogneiss unit in the core of the antiform. The regional metamorphic grade is documented in pelitic layers by the maximum-phase assemblage sillimanite-biotite-K-feldspar-plagioclase-quartz.

The metamorphic grade and the degree of structural transposition of all units in the Acasta Lake area makes the identification of Archean basement more difficult than in the case of the Scotstoun Massif and the Carousel Massif. However, since we are dealing with an antiform structure, cored by an orthogneiss and rimmed by a consistent amphibolite/carbonate/pelitic migmatite unit, and since the scale is similar to other known basement-cored structures such as the Carousel Massif, it seems reasonable to suggest that the Acasta Lake orthogneiss is possibly Archean basement. This, of course, is only a hypothesis that will be verified with further mapping to the south, and proved if the Acasta Lake granitic unit can be shown to be part of the same domain as the granite coring the Scotstoun Massif and eventually the Archean units south of Redrock Lake.

Basal Décollement

The décollement surface mapped around the nose of Carousel Massif (St-Onge et al., 1982) has been traced along the west limb of the Carousel anticline across Redrock Lake and southwest of the lake as far as the mapping was taken. The décollement surface is best constrained in areas where the basement contact is at a high angle to the (D-1) north-south structural trend of the thrusted and folded early Proterozoic sequence. More specifically, the hinge zone of Carousel Massif and the area centred on Redrock Lake both have the needed contrast in the amount of E-W shortening above and below the décollement surface to enable an accurate location. In the hinge zone of the Scotstoun Massif (Fig. 18.1) strikes of bedding are north-south and dips are moderate to steep (60-90°) above the décollement. Structurally below the décollement, beds strike parallel to the contact of the Archean block and have dips of 20-25°N.

It is probable that the décollement "capping" the Scotstoun Massif is the westerly equivalent of the décollement present around the Carousel Massif and that with future mapping to the south, the offset of this structure by the fault that bounds the southeast side of the Scotstoun basement structure will become evident.

Hepburn Batholith

Field work during 1982 revealed the southward continuation of the Hepburn Batholith as defined by previous studies (Hoffman et al., 1980; St-Onge et al., 1982). The volume and number of intrusions within the batholith, however, is considerably reduced to the south (Fig. 18.2).

Petrographically, the batholith is not much different from the rocks described to the north. The dominant rock type remains a coarse grained, massive to well foliated biotite syenogranite or monzogranite, which commonly displays K-feldspar megacrysts. The common presence of garnet or sillimanite in this unit reflects its peraluminous (inherited?) composition. The rocks are intimately associated with migmatized pelitic sediments.

A large tonalite pluton is centred on Scotstoun Lake and is offset by one of the late (D-4) northeast-striking dextral transcurrent faults (Fig. 18.2). Petrographically the rock is grey, massive or faintly foliated, and is biotite-bearing. Accessory K-feldspar occurs as large poikilitic crystals and is distinctive of this particular pluton.

An elongate pluton northwest of Scotstoun Lake (Fig. 18.2) is composed dominantly of hornblende diorite with minor amounts of biotite-hornblende tonalite. Both rock types are massive.

Epworth Group-Akaitcho Group Transition

The Epworth Group-Akaitcho Group transition has always been masked north of 65°45' by plutons of the Hepburn Batholith, except in two localities northwest and southwest of Hepburn Lake. In both locations the two groups appear to be structurally conformable, the lower Odjick Formation overlying upper Akaitcho Group units (Easton, 1980). Due to the reduction in the number and volume of Hepburn Batholith plutons going south and to a slight shift westward of the main axis of pluton emplacement, the Akaitcho Group-Epworth Group transition has been mapped over a distance of 20 km near Scotstoun Lake (Fig. 18.2).

The sedimentary rocks north and south of Scotstoun Lake are a succession of metamorphosed semipelites and pelites with local quartzite beds up to 0.5 m in thickness. Commonly, lenses or discontinuous layers of quartz grit and quartz pebble conglomerate incorporated within the finer clastic material occur north and west of Scotstoun Lake. The regional metamorphic grade as documented in the pelitic layers is that of the maximum-phase assemblage sillimanite-biotite-K-feldspar-plagioclase-quartz-granitic melt. Due to the east-west shortening that has accompanied the formation of the migmatites, bedding is completely transposed and the quartz pebbles are flattened into the dominant east-dipping gneissic foliation. Despite the high grade of metamorphism and the transposition of bedding structures, it is evident from the nature and variety of protoliths that make up the sedimentary sequence north and south of Scotstoun Lake that the Odjick Formation is a likely parent.

Immediately west of the migmatized Odjick clastic sediments a sequence of migmatized semipelites, impure quartzites, amphibolites with locally calc-silicate and carbonate layers, and mafic sediments is found (Fig. 18.2). Structure is dominated by a steep east-dipping gneissic foliation and the metamorphic grade is that of sillimanite-K-feldspar-granitic liquid. These rock types, however, are not typical of the Odjick Formation, but rather are high grade equivalents of the easternmost Akaitcho Group as seen south of Hepburn Lake in the Hepburn Lake map area (Easton, 1981b).

Thus, the transition from the Akaitcho Group to the Epworth Group west of Scotstoun Lake, in addition to being exposed, can further be refined to a transition from units typical of the easternmost Akaitcho Group to rock types characteristic of the Odjick Formation. To the north this transition at lower metamorphic grades has been interpreted by Easton (1981b) to represent a conformable contact. Evidence from Scotstoun Lake does not contradict this but, because of the structural transposition in the high grade rocks, neither can the possibility of a premetamorphic fault contact be eliminated.

Bishop Plutonic Suite

The Bishop plutonic suite is a post-tectonic composite intrusion approximately 8 km wide and over 30 km long. The plutons are emplaced in the high grade rocks of the Akaitcho Group east of the Wopmay Fault Zone (Fig. 18.2).

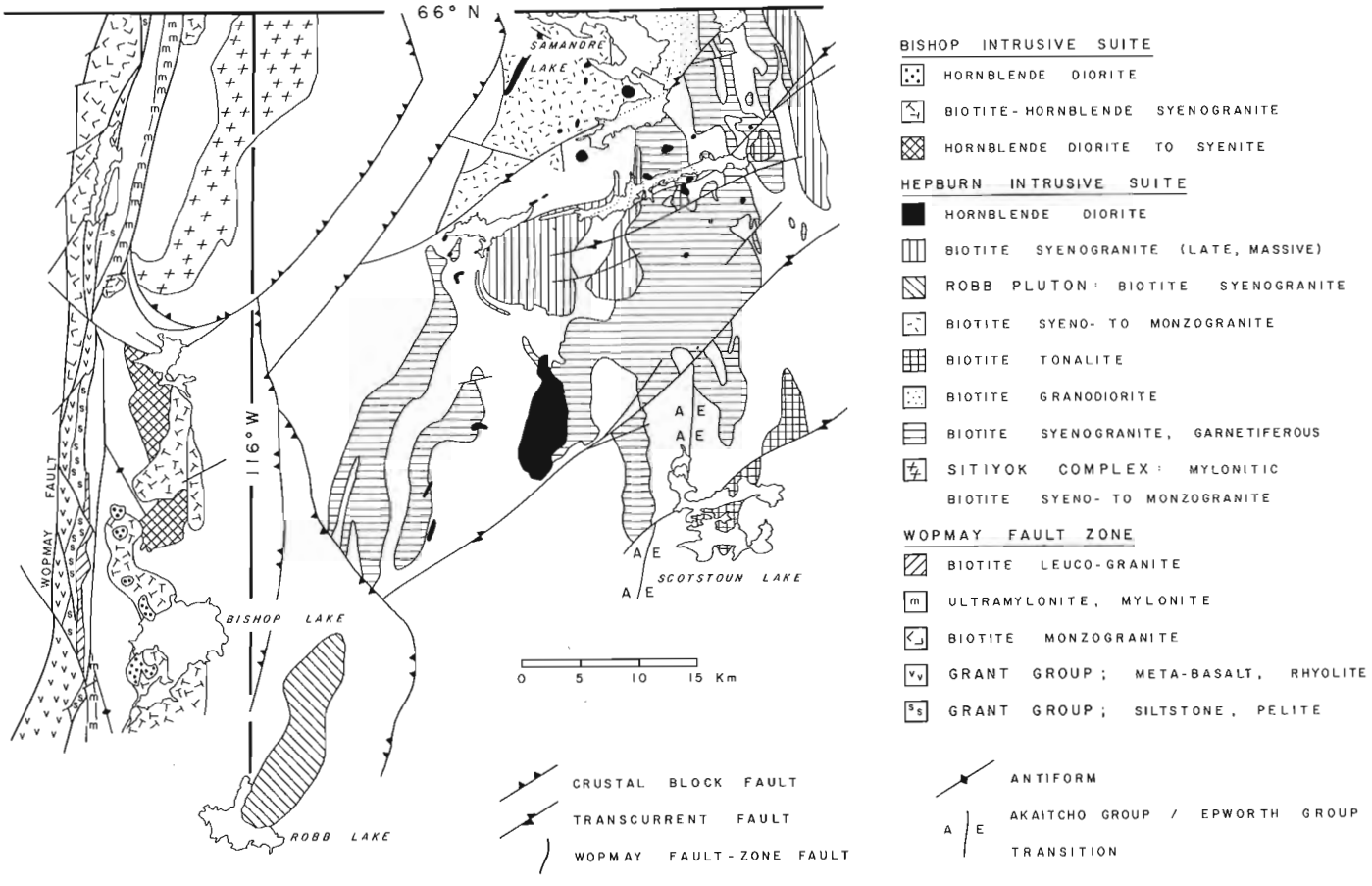

Figure 18.2. *Plutons of the Hepburn Batholith and Bishop plutonic suite shown with the major transcurrent faults, the Akaitcho Group-Epworth Group transition and the principal features of the Wopmay Fault Zone.*

The northern end of the plutonic suite is truncated by one of the curved faults associated with the south end of the high grade crustal block "D" of Hoffman and St-Onge (1981) and St-Onge et al. (1982).

Three rock types dominate in the Bishop suite. The earliest plutons occupy the northern part of the complex and are massive hornblende diorites, monzonites and syenites. The high variability in plagioclase-K-feldspar ratios is a characteristic feature of this unit. Xenoliths of foliated amphibolite are common. Intruding the early diorites are coarse grained, massive, biotite-hornblende syenogranites which constitute the bulk of the Bishop suite. In turn, a series of small circular plutons of compositionally homogeneous hornblende diorite cuts the granites in the central and southern parts of the complex (Fig. 18.2). The presence of hornblende in all units of the Bishop suite distinguishes it from the Hepburn Batholith. In addition, the pink colour of the Bishop granites contrasts with the grey Hepburn granites. The lack of any tectonic fabric in the Bishop suite plutons strongly suggests that their emplacement postdated the bulk of the east-west compression that affected most of the Hepburn Batholith units. The Bishop suite therefore is probably of late Hepburn Batholith or of Great Bear Batholith age.

Robb Granite

The late, massive Robb granite forms a single pluton emplaced in the medium grade rocks of the Akaitcho Group (Fig. 18.2). Contacts with the host rocks are always sharp and in one case tourmaline-bearing pegmatite dykes intrude foliation planes in the metasedimentary host rocks. The pluton is a coarse grained biotite syenogranite with well developed K-feldspar megacrysts. The lack of hornblende or garnet and sillimanite distinguishes it respectively from the Bishop and most Hepburn granites.

Wopmay Fault Zone

The Wopmay Fault Zone (Easton, 1981a) is a 5-7 km wide belt of proto- to ultramylonites which has been broken by an extensive set of north-south anastomosing brittle faults.

Regionally, the mylonite fabric superposed on the gneissic foliation of the high grade clastic sediments and mafic rocks of the western Akaitcho Group increases in intensity from east to west. At the outcrop scale the degree of mylonitization can be variable over 4-5 m. Ultramylonites are restricted to two belts shown on Figure 18.2.

Two southeast-plunging folds in the Akaitcho gneisses were mapped north and west of Bishop Lake. The mylonitic fabric is folded in these antiforms and both the fabric and folds are truncated by the plutons of the Bishop suite and by the late brittle faults of the Wopmay Fault Zone.

Within a series of blocks delineated by the late brittle faults is found the Grant subgroup of Easton (1981a) who proposed that the subgroup represents a lower grade western equivalent of the Akaitcho Group. The Grant subgroup is confined to the Wopmay Fault Zone and is completely fault bounded. Its structural position within the zone is varied. At 66°N it is sandwiched between a foliated to mylonitic granite (west side) and a high grade clastic sediment migmatite belt (east side). To the south at 65°30'N it occurs between the Dumas Group of Great Bear age (west side) and mylonitized Akaitcho gneisses (east side). The stratigraphy of the Grant subgroup is very consistent from block to block and can be matched across the brittle faults. The west portion of the Grant subgroup consists of a sequence of massive and pillow basalts at greenschist facies metamorphism. Minor amounts of rhyolite are intercalated with the mafic units. To the east the Grant subgroup consists of a folded sequence of interbedded siltstones and pelites, in which are emplaced a few large, coarse gabbroic sills or dykes. The metamorphic grade in the sedimentary sequence increases from chlorite to andalusite grade towards the east. Pillow tops and graded bedding in the siltstones suggest the sequence faces west but this should be confirmed with a detailed study of the Grant subgroup where it is best preserved at the latitude of Wopmay Lake.

The Grant subgroup then is a recognizable package, with a consistent internal stratigraphy. Mapping to date in the Calder sheet, however, also shows that it is a non-correlatable block. It is considered therefore not advisable at this stage of mapping to correlate the Grant subgroup with the Akaitcho Group. Rather, the Grant package should be considered a separate group until the internal stratigraphy and the tectonic framework is better understood.

Discussion

The net result of the 1982 field season was to establish some important facts pertaining to the tectonic framework of the internal zone of an orogenic belt. In the Wopmay Orogen, Archean basement is extensively exposed in the Redrock Lake map area and is involved in early Proterozoic deformation, mostly in the form of basement-cored large disharmonic folds. In the Asiak fold-thrust belt, Carousel Massif, and to the west, the Scotstoun Massif, both are capped by a décollement which seems to accommodate the bulk of the east-west shortening recorded in the overlying strata.

Farther west a décollement surface in the Acasta fold structure, also possibly cored by Archean basement, has not been recognized and may be difficult to document given the prevailing high grade metamorphism. Nevertheless, there is a distinct possibility that the Acasta structure is allochthonous and further work to the south in 1983 should clarify whether or not basement is autochthonous in the internal zone of Wopmay Orogen.

The Bishop plutonic suite is very different from the Hepburn Batholith in petrography, extent of deformation, and location in the metamorphic zone. If the suite is Great Bear in age one must explain why Great Bear intrusions were emplaced both east and west but not within the Wopmay Fault Zone. If the suite is of late Hepburn age then an explanation must be sought for the presence of two differing magmatic suites within the same collision belt.

The Wopmay Fault Zone has had a varied history, movement in the zone first yielding protomylonites to ultramylonites and eventually resulting in an impressive set of north-south anastomosing brittle faults. This could suggest the zone represents an important break in the crust along which movement from time to time was focused. It will be interesting to see to the south how close to the Wopmay Fault Zone Archean basement can be recognized in the Hepburn metamorphic-plutonic belt.

Acknowledgments

It is with pleasure that we thank Peter Harmathy, Steven Jackson, Lesia Zalusky and Martin St. Pierre for their independent mapping and assistance. Herb Helmstaedt (Queen's) and Robert Martin (McGill) both made useful visits with their respective Ph.D. students. Once again, field work was facilitated with the skillful expediting of Win Bowler and then Martin Irving for DIAND in Yellowknife.

References

Easton, R.M.
1980: Stratigraphy and geochemistry of the Akaitcho Group, Hepburn Lake map area, District of Mackenzie: An initial rift succession in Wopmay Orogen (early Proterozoic); in Current research, Part B, Geological Survey of Canada, Paper 80-1B, p. 47-57.

1981a: Geology of Grant Lake and Four Corners Lake map areas, Wopmay Orogen, District of Mackenzie; in Current Research, Part B, Geological Survey of Canada, Paper 81-1B, p. 83-94.

1981b: Stratigraphy of the Akaitcho Group and the development of an early Proterozoic continental margin, Wopmay Orogen, Northwest Territories; in Proterozoic Basins of Canada, ed. F.H.A. Campbell; Geological Survey of Canada, Paper 81-10, p. 79-95.

Easton, R.M., Boodle, R.L., Zalusky, L., Eiche, G., and McKinnon, D.
1981: Geology of 86H/3, 86H/4, 86H/5 and 86H/6, District of Mackenzie, Department of Indian Affairs and Northern Development, Preliminary Geological Map EGS-1981-5a,b,c,d, 1:30 000 scale with descriptive notes.

Easton, R.M., Boodle, R.L., and Zalusky, L.
1982: Evidence for gneissic basement to the Archean Yellowknife Supergroup in the Point Lake area, Slave Structural Province, District of Mackenzie; in Current Research, Part B, Geological Survey of Canada, Paper 82-1B, p. 33-41.

Fraser, J.A.
1960: North-central District of Mackenzie, N.W.T.; Geological Survey of Canada, Map 18-1960.

1974: The Epworth Group, Rocknest Lake area, District of Mackenzie; Geological Survey of Canada, Paper 73-39, 23 p.

Fraser, J.A., Hoffman, P.F., Irvine, T.N., and Mursky, G.
1972: Bear Structural Province; in Variations in Tectonic Styles in Canada, ed. R.A. Price and R.J.W. Douglas; Geological Association of Canada, Special Paper 11, p. 453-503.

Hoffman, P.F.
1972: Cross-section of the Coronation Geosyncline (Aphebian), Tree River to Great Bear Lake, District of Mackenzie; in Report of Activities, Part A, Geological Survey of Canada, Paper 72-1A, p. 119-125.

1973: Evolution of an early Proterozoic continental margin: the Coronation Geosyncline and associated aulacogens of the northwestern Canadian Shield; in A Discussion on the evolution of the Precambrian crust, organized by J. Sutton and B.F. Windley; The Royal Society of London, Philosophical Transactions, Series A, v. 273, p. 547-581.

1980: Conjugate transcurrent faults in north-central Wopmay Orogen (early Proterozoic) and their dip-slip reactivation during post-orogenic extension, Hepburn Lake map area, District of Mackenzie; in Current Research, Part A, Geological Survey of Canada, Paper 80-1A, p. 183-185.

Hoffman, P.F. (cont.)
1982: The Northern Internides of Wopmay Orogen (Sloan River, Hepburn Lake and part of Coppermine Map-areas, N.W.T.); Geological Survey of Canada, 1:250 000 scale map, Open File 832.

Hoffman, P.F. and St-Onge, M.R.
1981: Contemporaneous thrusting and conjugate transcurrent faulting during the second collision in Wopmay Orogen: implications for the subsurface structure of post-orogenic outliers; in Current research, Part A, Geological Survey of Canada, Paper 81-1A, p. 251-257.

Hoffman, P.F., St-Onge, M.R., Carmichael, D.M., and de Bie, I.
1978: Geology of the Coronation Geosyncline (Aphebian), Hepburn Lake sheet (86J), Bear Province, District of Mackenzie; in Current Research, Part A, Geological Survey of Canada, Paper 78-1A, p. 147-151.

Hoffman, P.F., St-Onge, M.R., Easton, R.M., Grotzinger, J., and Schulze, D.E.
1980: Syntectonic plutonism in north-central Wopmay Orogen (early Proterozoic), Hepburn Lake map area, District of Mackenzie; in Current Research, Part A, Geological Survey of Canada, Paper 80-1A, p. 171-177.

Hoffman, P.F., St-Onge, D.A., Easton, R.M., and St-Onge, M.R.
1981: Preliminary geological map of Hepburn Lake, District of Mackenzie; Geological Survey of Canada, Open File 784.

McGlynn, J.C.
1970: Bear Province; in Geology and Economic Minerals of Canada, ed. R.J.W. Douglas; Geological Survey of Canada, Economic Geology Report 1, p. 77-84.

St-Onge, M.R.
1981: "Normal" and "inverted" metamorphic isograds and their relations to syntectonic Proterozoic batholiths in the Wopmay Orogen, Northwest Territories, Canada; Tectonophysics, v. 76, p. 295-316.

St-Onge, M.R. and Carmichael, D.M.
1979: Metamorphic conditions, northern Wopmay Orogen, N.W.T.; Aureole de contact de l'intrusion du Muskox, T.N.O.; Geological Association of Canada, Program with Abstracts, v. 4, p. 81.

St-Onge, M.R., King, J.E., and Lalonde, A.E.
1982: Geology of the central Wopmay Orogen (Early Proterozoic), Bear Province, District of Mackenzie; Redrock Lake and the eastern portion of Calder River map areas; in Current research, Part A, Geological Survey of Canada, Paper 82-1A, p. 99-108.

Streckeisen, A.
1976: To each plutonic rock its proper name; Earth Science Reviews, v. 12, p. 1-33.

19. GEOLOGY OF THE SMOKEY ARCHIPELAGO, GRENVILLE FRONT ZONE, LABRADOR

EMR Research Agreement 241/4/82

V. Owen [1] and T. Rivers [1]
Precambrian Geology Division

Owen, V. and Rivers, T., Geology of the Smokey archipelago, Grenville Front Zone, Labrador; in Current Research, Part A, Geological Survey of Canada, Paper 83-1A, p. 153-161, 1983.

Abstract

The junction between the Grenville Front Zone and Makkovik Subprovince on the Labrador coast is marked by a 3 km wide transition zone across which south-dipping Grenvillian LS-fabrics give way northwards to N- to NE-trending Ketilidian (?) fabrics. Three major groups of rock units have been identified:

1. *A basement complex comprising pre-Ketilidian paragneisses, orthogneisses, and foliated intrusive rocks, metamorphosed from amphibolite to granulite facies.*
2. *A differentiated suite of layered gabbros to monzonites, probably of Paleohelikian age.*
3. *Paleohelikian granitoids of the Benedict Mountain Intrusive Suite.*

Members of the basement complex, although predominant in the Grenville Front Zone, have been identified throughout the study area. Paleohelikian plutonites characterize Makkovik Subprovince but are also represented within the Grenville Front Zone, where they locally contain amphibolite facies mineral assemblages along Grenvillian high strain zones.

Ketilidian (?) metamorphism attained granulite grade in the basement complex, but was locally retrogressed to amphibolite facies. In the north of the study area, some Paleohelikian intrusives exhibit NE-trending fabrics, indicating either late Ketilidian deformation, or the existence of a previously unknown Paleohelikian orogeny.

Effects of Grenvillian metamorphism and deformation are zonal in the central part of the map area, but become pervasive towards the south, a feature characteristic of the Grenville Front Zone elsewhere.

Introduction

The islands of the Smokey archipelago straddle the northern margin of the Grenville Front Zone in eastern Labrador, as positioned by Gower et al. (1980). Previous mapping on a reconnaissance scale by Stevenson (1970) and Gower (1981, personal communication, 1982) resulted in a subdivision of the region into (1) a northern region (Makkovik Subprovince) characterized by granitic, syenitic, and monzonitic rocks of the Benedict Mountain Intrusive Suite; and (2) a southern terrane (Grenville Province) dominated by gneissic rocks. The junction between these terranes coincides approximately with the Benedict Fault, a major E- to SE-trending shear zone interpreted by Stevenson (1970) as a south-dipping thrust fault.

This report outlines the preliminary results of 1:50 000 scale mapping in the Smokey archipelago during summer 1982. Emphasis was placed on determining the distribution and relative chronology of major rock units and their possible correlation within, and to the north of, the Grenville Front Zone.

Lithologies and Stratigraphic Relations

The present investigation largely confirms the stratigraphic relations described by Gower (1981). Three volumetrically important groups of rocks have been recognized: (a) a basement complex postulated to predate the Ketilidian orogeny[2]; (b) a differentiated sequence of gabbroic to monzonitic rocks, probably of Paleohelikian age; and (c) granitoids of the Benedict Mountain Intrusive Suite, emplaced about 1650 Ma (B.J. Fryer, personal communication, 1982). These have all been intruded by a series of gabbroic dykes known as the Michael gabbro (Fahrig and Larochelle, 1972), which has been dated at 1461 ± 96 Ma (Rb-Sr whole-rock; Fahrig and Loveridge, 1981). The distribution of lithologies and their relative field chronology are presented in Figure 19.1.

The Basement Complex

The basement complex includes all rocks interpreted to predate Paleohelikian intrusives. The earliest rocks are screens and rafts of migmatitic biotite gneiss (units 1 and 2, Fig. 19.1) within orthogneiss (unit 3) and younger, less deformed, foliated plutonic rocks (e.g. units 4 to 6).

Unit 1 is a leucocratic, grey to rose biotite quartzofeldspathic gneiss, which probably includes tectonites of both igneous and sedimentary parentage. Paragneissic rocks include sillimanite-bearing biotite gneiss and local diatexites. C.F. Gower (personal communication, 1982) reports that a sample collected by Stevenson (1970), and previously described as containing sillimanite-kyanite-and/or hypersthene (GSC unpublished data) actually contains all three minerals, although the sillimanite and kyanite may not be in equilibrium.

Unit 2 is a melanocratic garnet-biotite gneiss, locally containing up to 40 per cent (garnetiferous) leucosomes. Sillimanite- and cordierite-hypersthene ± sillimanite bearing varieties of the unit occur in the White Bear Islands, suggesting that the unit has, at least in part, a sedimentary protolith. Unit 2 is probably a lithological variant of unit 1.

---

[1] Department of Earth Sciences, Memorial University of Newfoundland, St. John's, Newfoundland, A1B 3X5.

[2] The Ketilidian orogeny is defined in southern Greenland, and is dated at approximately 1810 to 1770 Ma (late to post-kinematic granites; Rb-Sr whole-rock and U-Pb), with slow cooling in the belt indicated by K-Ar and Rb-Sr mineral ages ranging from 1700 to 1500 Ma (Allaart, 1976). Tectonothermal activity of about this age in the Makkovik Subprovince is herein referred to as Ketilidian rather than Hudsonian, since the relationship of the Makkovik Subprovince to the Churchill Province is uncertain.

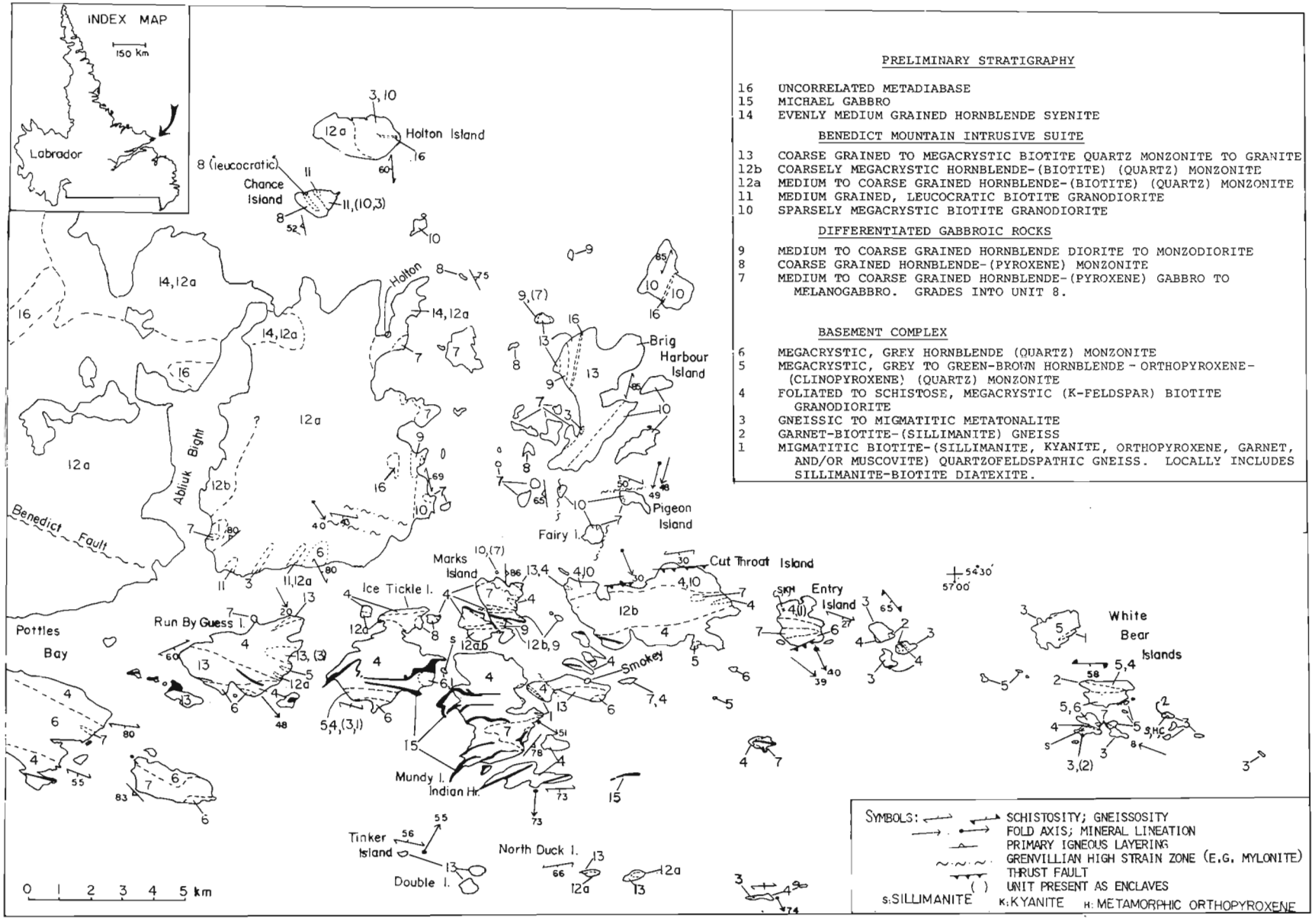

Figure 19.1. *Preliminary geological map of the Smokey archipelago. Geology near Holton and west of Abliuk Bight adapted from Gower (1981). "C" denotes cordierite.*

Migmatitic biotite-hornblende metatonalite (unit 3) is the most extensive gneissic unit of the basement complex, and is widely distributed as enclaves in granodiorites of various ages (units 4, 10 and 11; Fig. 19.2). The metatonalite is fine grained (0.5 mm) and is characterized by the presence of up to 30 per cent quartz-plagioclase leucocratic segregations bearing stubby (5 mm) hornblende crystals. Gower (1981) has correlated gneissic metatonalite cropping out on Chance and Holton islands with similar lithologies of the Cape Harrison Metamorphic Suite, the type locality of which is some 70 km NW of this area.

Unit 4, a foliated to schistose K-feldspar megacrystic biotite granodiorite, has been dated at 1824 ± 51 Ma (this study; Rb-Sr whole-rock, seven point isochron; initial ratio = 0.70311 ± 0.00040). The unit typically contains 5 to 15 per cent microcline megacrysts, ranging in size from 8 to 30 mm. Megacrysts are commonly augen-shaped where the unit has a schistose fabric.

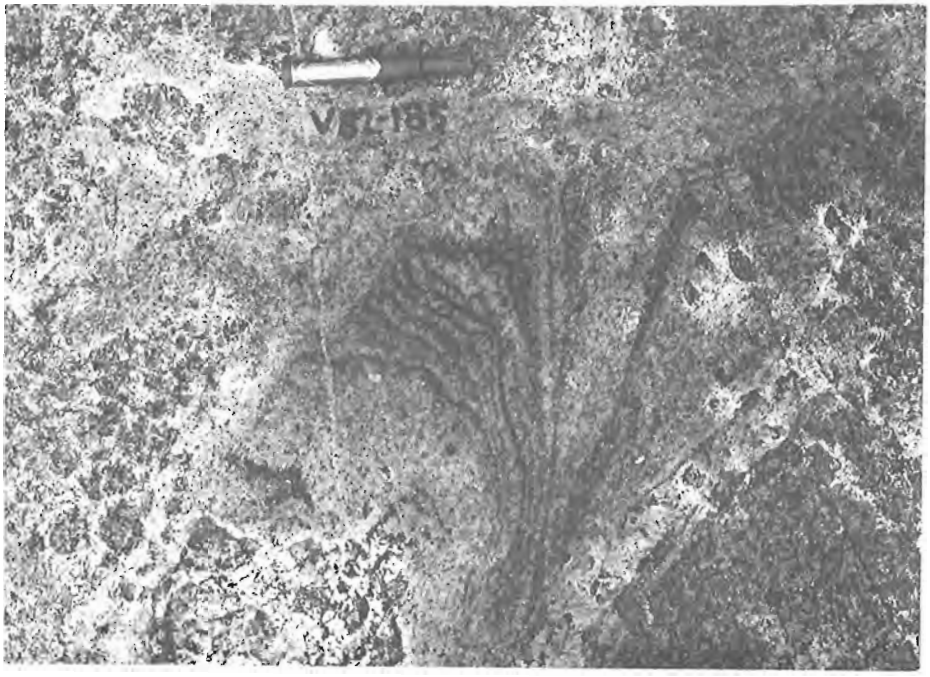

Figure 19.2. *Inclusion of gneissic metatonalite (unit 3) in sparsely megacrystic biotite granodiorite (unit 10; texture partly obscured by lichen). Fairy Island. Pen is 13 cm long.*

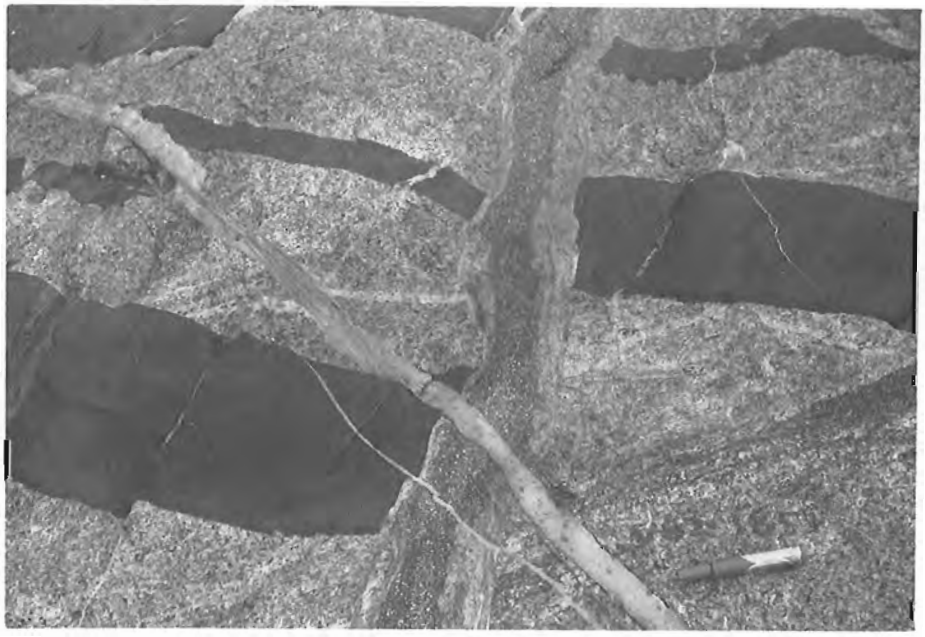

Figure 19.3. *Mafic dykes trending N45E are crosscut and offset along a plagioclasephyric mafic dyke, itself crosscut by a late aplite vein. Along strike (out of photo) the plagioclasephyric dyke is crosscut by a net-veined, fine grained mafic dyke. Host rock is megacrystic biotite granodiorite (unit 10). Fairy Island. Pen is 13 cm long.*

Unit 5 is a green-brown, granulite facies, sparsely megacrystic quartz-bearing monzonite to monzodiorite, containing hornblende-mantled ortho-pyroxene, minor biotite, and in places clinopyroxene ± garnet. The unit is foliated, and locally has a layered aspect defined by irregularly spaced pyroxene-bearing feldspathic pegmatoids, possibly of local derivation.

Unit 6 is a grey, sparsely megacrystic hornblende-biotite quartz-bearing monzonite to monzodiorite, texturally similar to unit 5. Relations between the two units are discussed below. Both units contain gneissic enclaves (units 1, 2, and/or 3) on Ice Tickle Island, and an isolated enclave of megacrystic biotite granodiorite (unit 4?) was noted in unit 6, south of Pottles Bay.

Paleohelikian Rocks

Units 7 to 9 include a diverse variety of differentiated gabbroic to monzonitic and dioritic rocks. Gower (1981) noted that this suite escaped (postdates?) most effects of the Ketilidian orogeny and predates the granitoids of the Benedict Mountain Intrusive Suite. He also recognized a westward gradation of gabbroic rocks through (granophyric) diorite and quartz monzodiorite.

Unit 7 includes the gabbroic members of the suite. Within the study area, the principal varieties are all amphibole bearing, and include: (a) melanocratic (CI about 50-70), biotite bearing, two-pyroxene gabbro with 1-2 cm amphibole megacrysts; (b) mesocratic (CI about 35-45) gabbro with 1-4 cm amphibole euhedra set in a medium grained (1 mm) plagioclase-amphibole-(pyroxene?) ground-mass; and (c) mesocratic to leucocratic (CI about 15-35) gabbro with amphibole-mantled pyroxenes, plagioclase laths to 1 cm, and locally with interstitial K-feldspar.

Unit 8 typically is a green-grey monzodiorite to quartz-bearing monzonite. On Chance Island, two varieties of monzonitic rocks occur: light grey ("leucocratic" – Fig. 19.1) biotite-amphibole monzonite with aligned tabular K-feldspars as blocks and disrupted bands in layered amphibole-

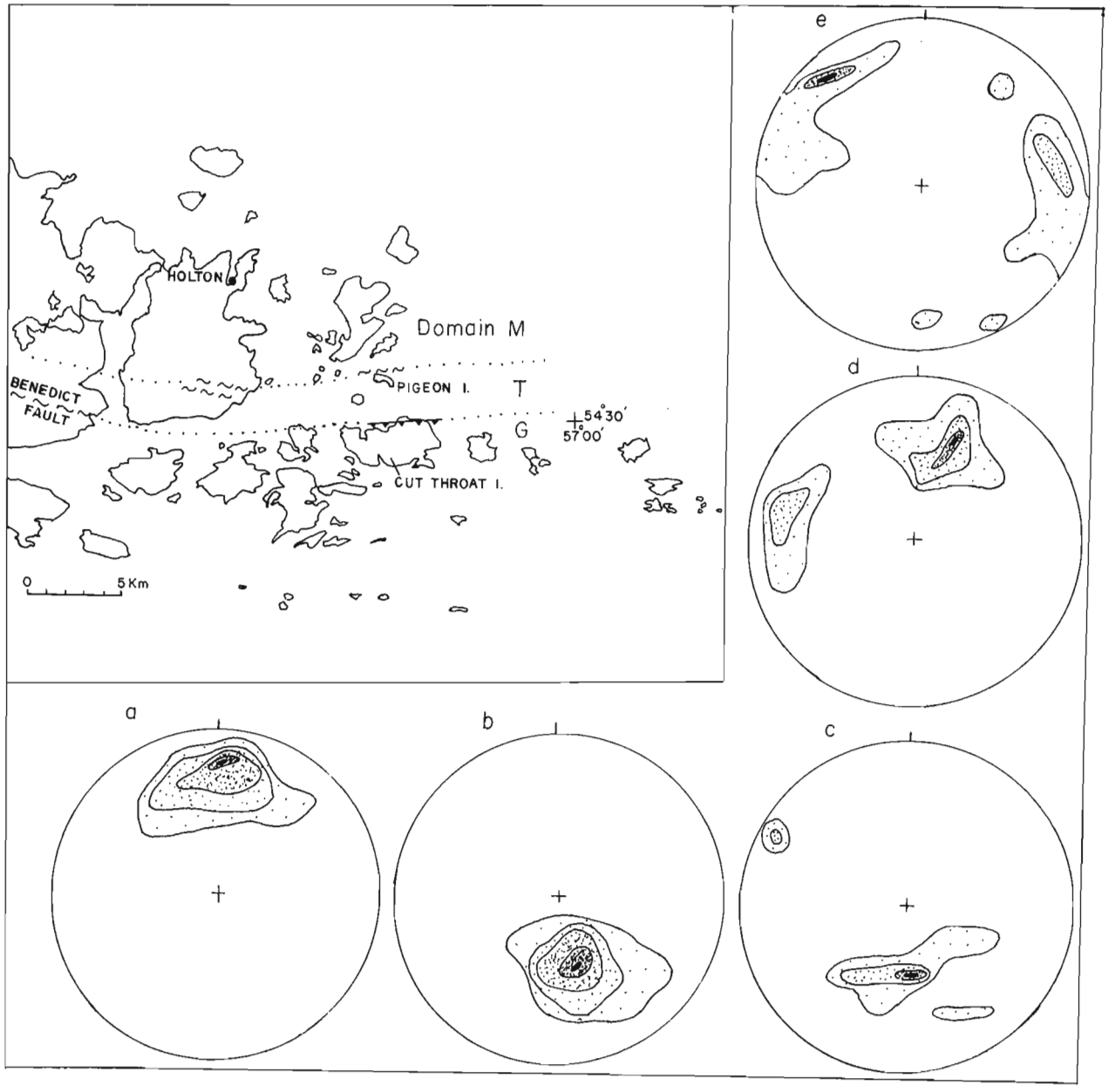

Figure 19.4. *Preliminary structural subdivision of the Smokey archipelago. The dotted lines connecting Grenvillian high strain zones and faults separate domains of characteristic structural pattern, and do not necessarily imply along strike continuity of individual Grenvillian structures.*

a. Domain G: 170 poles to planar structures; contours at 3%, 5%, 8%, 12% per 1% area, maximum 13%.

b. Domain G: 45 linear structures; contours at 3%, 5%, 10%, 20% per 1% area, maximum 24%.

c. Domain G: 33 fold axes; contours at 5%, 9%, 12% per 1% area, maximum 15%. The SSE-plunging folds postdate shallowly WNW-plunging folds.

d. Domain T: 40 poles to planar structures; contours at 3%, 6%, 9% per 1% area, maximum 10%.

e. Domain M: 24 poles to planar structures; contours at 4%, 8%, 10% per 1% area, maximum 12%.

clinopyroxene-biotite quartz-bearing monzonite with green-brown feldspars. Both monzonites have a colour index of 12-15. Both units 7 and 8 may show primary igneous layering formed by variations in the proportion of mafic minerals to feldspars. Less commonly, layering is defined by a phase and granulometric banding, where, for example, amphibole megacrysts are restricted to centimetre scale relatively melanocratic bands. The thickness of melanocratic layers typically ranges from 1-15 cm, whereas more leucocratic layers may exceed 1 m.

Unit 9 is a grey, medium- to coarse-grained hornblende-biotite diorite to monzodiorite. The diorite locally contains inclusions of gabbro (unit 7), and is tentatively placed with the differentiated gabbroic-monzonitic rocks of units 7 and 8, although it is possible that it represents an early phase of the Benedict Mountain Intrusive Suite.

The oldest member of the Benedict Intrusive Suite recognized within the study area is a medium grained, sparsely megacrystic biotite granodiorite (unit 10). Although distinction between units 4 and 10 is difficult where the latter has a strong Grenvillian fabric, unit 4 is more megacrystic and invariably has a fine grained (<1 mm) sucrose groundmass, even in areas of relatively low Grenvillian strain. Unit 10 contains gabbroic enclaves (unit 7) on the south coast of Brig Harbour Island and on an islet on the north shore of Marks Island.

Unit 11 comprises leucocratic (CI <5), medium grained biotite-(chlorite) granodiorite to granite, characteristically with traces of rusty weathering iron sulphides. Inclusions of gneissic metatonalite (unit 3) and sparsely megacrystic biotite granodiorite (unit 10) occur in the granodiorite on Chance Island, indicating the relative ages of these units.

Southeast of Abliuk Bight, a thin dyke of coarse grained plagioclase-rich hornblende-biotite monzonite crosscuts unit 11. We correlate this dyke with the medium- to coarse-grained monzonite (unit 12a) that dominates this area (Fig. 19.1). Unit 12b is a megacrystic (K-feldspar) textural variant of unit 12a. Both units locally contain quartz.

Unit 13 is a coarse grained to megacrystic, pink biotite quartz monzonite to granite. Its age relative to other members of the Benedict Mountain Intrusive Suite has not been ascertained, however, unit 13 crosscuts hornblende-biotite diorite (unit 9) on Brig Harbour Island.

Gower (1981, personal communication, 1982) describes unit 14 as a clinopyroxene-amphibole-bearing alkali feldspar syenite to ferrosyenite, locally with igneous layering. The unit is chemically distinct from the Benedict Mountain Intrusive Suite. It is not known, however, if the unit postdates younger members of the intrusive suite, although Gower (1981) reports that NW of Abliuk Bight the syenite intrudes megacrystic biotite granodiorite (unit 10).

Dykes of Michael gabbro up to 50 m thick occur in the south of the map area (Fig. 19.1). These dykes generally trend east, are rectiplanar along part of their length, and have well preserved chilled margins. A sample of Michael gabbro from Indian Harbour consists predominantly of clinopyroxene + plagioclase, although elsewhere the Michael gabbro has been reported to contain olivine (e.g. Gower, 1981; Fahrig and Loveridge, 1981), locally with coronas developed by reaction with plagioclase (B. Ryan and C. Gower, personal communication, 1982).

Unit 16 includes a variety of uncorrelated mafic intrusives, in part postdating the Benedict Mountain Intrusive Suite, and of uncertain relative age with respect to the Michael gabbro. Layered and net-veined lamprophyric dykes have been described from Brig Harbour and Holton Islands (Elders and Rucklidge, 1969), and Grasty et al. (1969) report a wide range of K-Ar whole-rock ages for (olivine) diabase and lamprophyric dykes in the area. Excluding the Michael gabbro and lamprophyres, at least three generations of mafic dykes postdate megacrystic biotite granodiorite (unit 10; Fig. 19.3).

Structural Geology

Distribution of Fabric Orientations

In reviewing possible criteria for defining the northern margin of the Grenville Province in eastern Labrador, Gower et al. (1980, p. 787) chose to define the Grenville Front as a gradational zone several to many kilometres wide, whose northern boundary "is taken as the limit of widespread Grenvillian deformation". The distribution of structural trends within the Smokey archipelago suggests that the northern boundary of the Grenville Front Zone is itself transitional over a 3 km zone, south of which E-W Grenvillian fabrics predominate, and north of which NE-SW Ketilidian (?) fabrics predominate (see below).

Domain G (Fig. 19.4) comprises the Grenville Front Zone as defined by Gower et al. (1980) and extends south of a line connecting the Benedict Fault with the thrust fault on the north side of Cut Throat Island. The domain is characterized by a predominantly E-striking, moderately to steeply south-dipping Grenvillian LS-fabric (Fig. 19.4a). Contained linear elements (mineral lineations, stretching fabrics) plunge moderately toward the SSE (Fig. 19.4b), roughly coincident with the orientation of one generation of Grenvillian fold axes (Fig. 19.4c; see below). North of this domain is the roughly 3 km wide transition zone (domain T) whose northern boundary is taken to coincide with Grenvillian high strain zones south of Holton and on Pigeon Island. This zone is characterized by two populations of planar fabric orientations (Fig. 19.4d): a south- to southwest-dipping Grenvillian foliation, developed along high strain zones, which overprint a NNE-striking Ketilidian (?) fabric. Similarly oriented Ketilidian (?) planar fabrics with variable dip directions (Fig. 19.4e) characterize domain M north of the transition zone, and are approximately coincident with foliation orientations described elsewhere in the Makkovik Subprovince (e.g. Ermanovics et al., 1982, Fig. 21.8a).

Pre-Grenvillian Deformation

Fabrics and structural elements present in the basement complex crosscut by unequivocally discordant mafic dykes predating and including the Michael gabbro are interpreted to be of pre-Grenvillian age. Two episodes of pre-Grenvillian deformation have been recognized in the area. The development of an early S-fabric was locally accompanied by the disruption of mafic dykes and enclaves (Fig. 19.5a), and may in part correspond with the development of the gneissosity typical of units 1 to 3, and the foliate to schistose fabric of units 4 to 6. These fabrics are locally folded (Fig. 19.5b), in places with the partial mobilization and/or recrystallization of quartz-feldspar along nonpenetrative slip surfaces. Subsequent refolding of these early small scale folds (amplitude about 10-50 cm) can generally be attributed to Grenvillian effects, particularly within domain G. These early fabrics and folds have been identified in basement rocks throughout the area, although their regional pre-Grenvillian orientation has not been determined.

Not all high strain zones in the study area can be assumed to be of Grenvillian age. For example, Gower (1981) noted that shear zones in megacrystic biotite granodiorite (unit 10) west of Abliuk Bight are crosscut by amphibole-clinopyroxene syenite (unit 14). These shear zones, along with the north- to northeast-trending tectonite fabrics

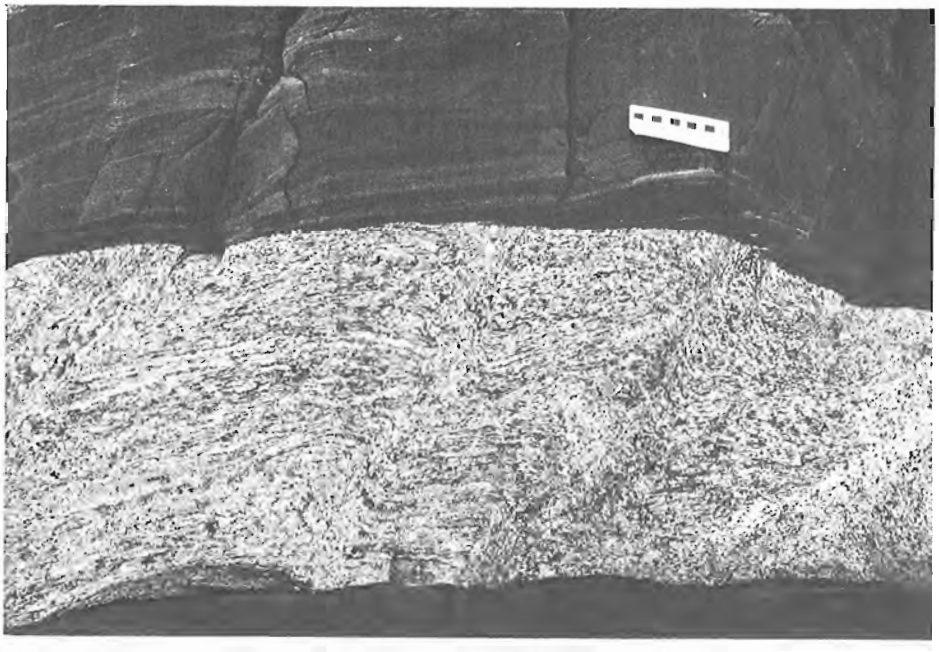

Figure 19.5

Pre-Grenvillian structural elements.

a. An amphibolite-enclave-rich zone (left foreground) in megacrystic biotite granodiorite (unit 4) crosscut by a series of subvertical mafic dykes trending N25E, subsequently crosscut by Michael gabbro (background). Mundy Island.

b. Same outcrop as Figure 19.5a. Pre-Grenvillian (Ketilidian?) folds are crosscut by N25E-trending mafic dykes. Scale in centimetres.

characterizing domain M, and also well represented in domain T, may be late Ketilidian features, or may imply a Paleohelikian orogenic event, although evidence for such an event is lacking (Gower, 1981). North- to northeast-trending tectonic foliations have not been identified within the differentiated gabbroic, monzonitic and dioritic rocks of units 7 to 9, possibly because these intrusions may be preferentially strained along their margins.

Grenvillian Deformation

Grenvillian deformation predominates in domain G, and is of minor importance north of domain T. At least two phases of Grenvillian folding are indicated by outcrop scale refolded folds in Paleohelikian and basement rocks in domain G, and by the large scale pattern of deformed dykes of Michael gabbro on Mundy and Ice Tickle islands. Although the geometry of large scale folds has not yet been determined, outcrop scale relations suggest that early, shallow-WNW-plunging folds with steep axial planes have been refolded about moderately SE- to SW-plunging axes (Fig. 19.4c). The predominant Grenvillian LS-fabric of domain G is the south dipping axial surface of these younger folds (Fig. 19.6a). Folded mylonitic zones with locally mylonitic axial surfaces suggest at least two periods of pronounced Grenvillian strain.

Grenvillian thrust faults have been identified on Cut Throat and Entry islands. These are moderately south-dipping features with mylonitic fabrics (Fig. 19.6b) in zones up to about 3 m wide, grading rapidly into their less highly strained protoliths. Rotated megacrysts and overturned small scale folds indicate the relative northerly sense of

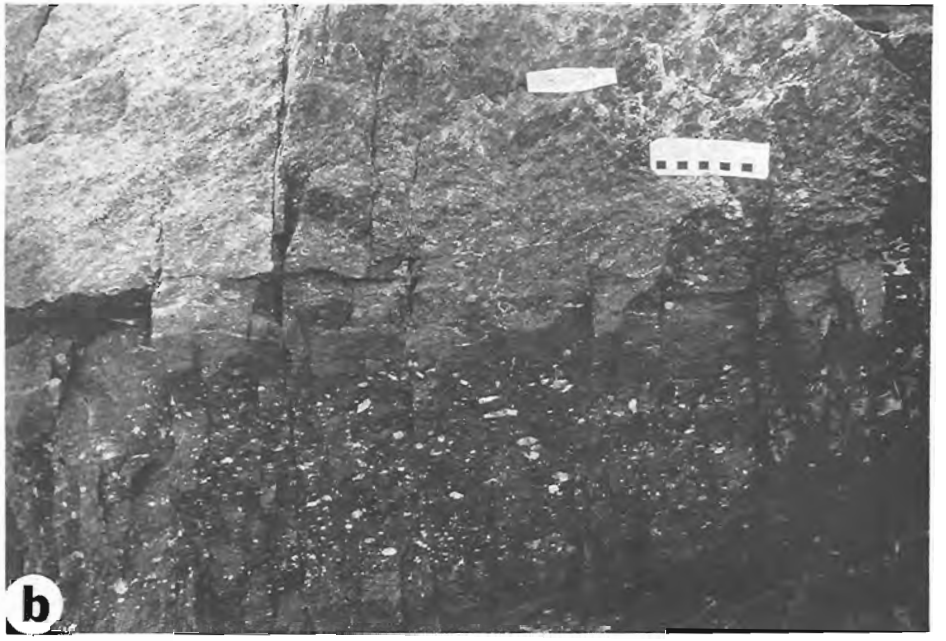

Figure 19.6. *Grenvillian structural elements.*

a. Grenvillian fold with limbs attenuated and detached parallel to the axial surface. Elsewhere in the outcrop, detached limbs of Grenvillian folds are isolated in a mylonitic axial planar fabric. The folded lithology is megacrystic biotite granodiorite (unit 4), layered by mafic dykes and pegmatite veins. Entry Island. Scale in centimetres.

b. Mylonite formed in megacrystic biotite granodiorite (unit 4) along thrust fault on Cut Throat Island. Scale in centimetres.

c. South-dipping Grenvillian brittle fracture zone incompletely overprinting a N-trending subvertical Ketilidian (?) fabric (subparallel to hammer handle) in megacrystic biotite granodiorite (unit 10). Looking south, Fairy Island.

movement of the hanging wall of the fault, and are consistent with the direction of movement inferred from stretching lineations within the mylonitic fabric of the thrust surface.

Grenvillian high strain zones have variable orientation (Fig. 19.1). The sense of movement across minor (width <1 m) high strain zones may be inferred from displaced mafic dykes or pegmatite veins. These zones typically are represented by a lineated and schistose fabric, and may anastomose around lens-shaped, metre-scale zones of relatively low strain.

Both ductile and brittle behaviour have been recognized within Grenvillian high strain zones in the area. Ribbon mylonites predominate in domain G, whereas both ribbon mylonites and rubbly fracture zones (Fig. 19.6c) occur in domain T. Grenvillian deformation in domain M appears to be restricted to a few minor brittle shear zones.

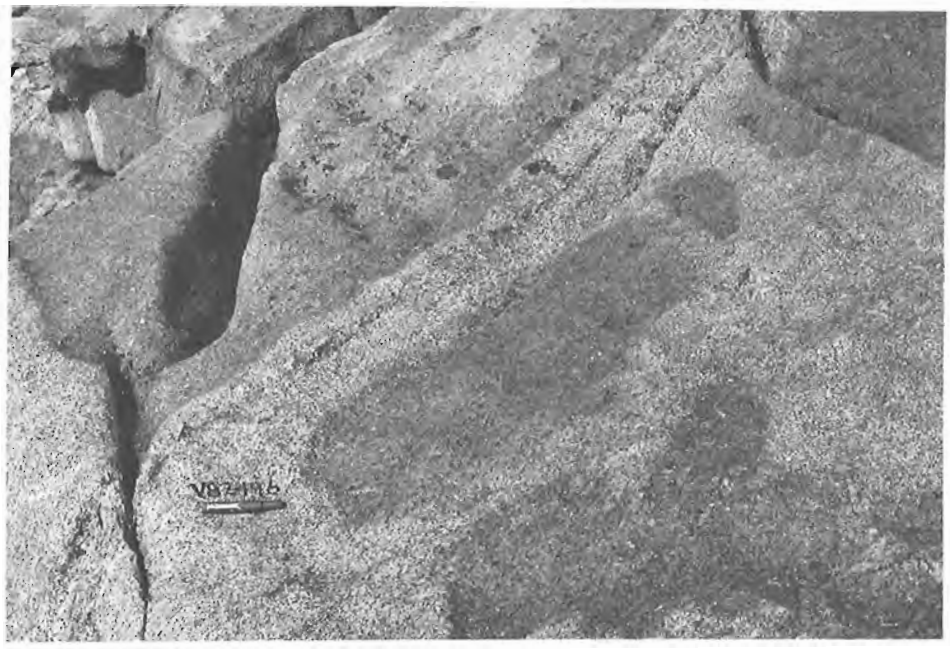

Figure 19.7. Incomplete passive retrogression of green-brown orthopyroxene-bearing monzonite (unit 5, dark patches) to bleached grey hornblende-biotite monzonite (unit 6). Note the continuity of pegmatoid veins across the outcrop. White Bear Islands. Pen is 13 cm long.

Pre-Grenvillian Metamorphism

The basement complex includes, by definition, all rocks predating the Paleohelikian intrusive suites. Various members of the complex contain metamorphic parageneses diagnostic of upper amphibolite to granulite facies, attributable, at least in part, to the Ketilidian orogeny. Granulite facies mineral assemblages have been observed only in basement rocks in domain G, and include sillimanite-kyanite-hypersthene (pelitic paragneiss, unit 1), hypersthene-cordierite (garnet-biotite gneiss, unit 2), and orthopyroxene-biotite ± clinopyroxene ± garnet (orthopyroxene-hornblende monzonite, unit 5). More commonly, however, amphibolite facies assemblages occur, and in some cases these can be attributed to a period of retrogression predating that associated with Grenvillian high strain. In particular, field evidence suggests that hornblende-biotite monzonite (unit 6) is the passively retrograded equivalent of orthopyroxene-hornblende monzonite (unit 5). In the White Bear Islands, the foliated to pegmatoid-layered fabric of unit 5 is preserved where the unit is incompletely retrograded. In this case, patches of green-brown orthopyroxene-bearing monzonite (unit 5) occur in bleached grey hornblende-biotite monzonite (unit 6; see Fig. 19.7). Subsequent retrogression of a dynamic nature is associated with Grenvillian high strain zones (see below).

Associated with the basement complex are a diverse assemblage of metamorphosed mafic dykes and enclaves. In some cases the oldest generations of the metabasites retain high grade mineral assemblages: two-pyroxene, biotite-bearing mafic enclaves occur in unit 5 in the White Bear Islands.

There is as yet no evidence either supporting or refuting pre-Ketilidian metamorphism or deformation of the basement complex. However, it should be noted that only the oldest units (units 1 to 3) are pervasively gneissic or migmatitic.

North- to northeast-trending Ketilidian (?) tectonic fabrics characterizing domain M are defined by a preferred orientation of biotite, amphibole, and/or feldspar in various members of the Benedict Mountain Intrusive Suite. The grade of metamorphism associated with the development of this fabric is unclear, since no differences in the mineralogy of unfoliated rocks and their foliated equivalents have been noted in hand sample.

Grenvillian Metamorphism

Metamorphic mineral assemblages of Grenvillian age are most readily identified where associated with Grenvillian fabrics, particularly those developed along high strain zones. Apart from parageneses associated with structural features of demonstrably Grenvillian age, the age of metamorphic mineral assemblages in Paleohelikian rocks is uncertain since, as described above, the age of north- to northeast-trending Ketilidian (?) fabrics characterizing domain M is uncertain. We have noted, however, two styles of metamorphic mineral assemblages in Paleohelikian rocks. The first of these is of uncertain age; the second is demonstrably Grenvillian. (1) Passive metamorphic overprinting of igneous fabrics reflects a grade of metamorphism up to amphibolite facies. An example of this is the occurrence of amphibole, locally with symplectic quartz intergrowths, mantling clinopyroxene of apparent igneous origin in the gabbroic to monzonitic rocks of units 7 and 8. This texture has been identified in these units within domains G, T and M, and may correspond with the passive retrogression (late Ketilidian?) noted in various members of the basement complex (e.g. unit 5). Alternatively, the metamorphism may be Grenvillian in age, but appear passive due to the rigid behaviour of relatively anhydrous intrusives during regional metamorphism; preservation of igneous textures and the development of corona textures are common in Grenvillian deformed gabbros elsewhere (Whitney and McClelland, 1973; Rivers, 1980). (2) Amphibolite facies mineral assemblages associated with high strain zones forming an LS-fabric of Grenvillian orientation (e.g. Fig. 19.4a,b) which occurs in Paleohelikian rocks within domains G and T. An example of this is a biotite-garnet-amphibole-bearing assemblage occurring along high strain zones developed in hornblende-biotite monzonite (unit 12a) on Marks Island.

Grenvillian schistose to mylonitic fabrics developed locally in orthopyroxene-hornblende monzonite (unit 5) and hornblende-biotite monzonite (unit 6), and developed pervasively in megacrystic biotite granodiorite (unit 4) are characterized by the assemblage biotite-epidote ± hornblende ± garnet, suggesting dynamic retrogression to epidote amphibolite facies.

The dominance of biotite in the shear zones contrasts with predominant hornblende in the relatively undeformed protoliths, and suggests that metasomatism, probably a result of fluid flux, is an important feature of Grenvillian metamorphism at this grade.

Distribution of Lithologies

To a first approximation, the domainal distribution of structural orientations in the Smokey archipelago does not have a direct analogue in the distribution of major rock types (Fig. 19.1, 19.4). For example, gneissic metatonalite (unit 3) locally dominates outcrops and occurs as enclaves in domains T and M, although it, along with other members of the basement complex, predominates in domain G. Similarly, various Paleohelikian intrusives are well represented within domain G. Within the study area, however, dykes of Michael gabbro have not been identified in domain M. Nevertheless, as noted by previous workers (Stevenson, 1970; Gower, 1981, personal communication, 1982), the regional distribution of major lithologies suggests a gradation from gneissic rocks in the Grenville Front Zone to predominantly Paleohelikian plutonites to the north.

Acknowledgments

The first author thanks R. Healey and D. Mitsuk, who provided reliable assistance in the field. C.F. Gower introduced us to the geology of the Smokey archipelago, provided suggestions for improving the manuscript at this early stage of interpretation, and made available the samples used in dating unit 4.

References

Allaart, J.H.
1976: Ketilidian mobile belt in South Greenland; in Geology of Greenland, ed. A. Escher and W.S. Watt, The Geological Survey of Greenland.

Elders, W.A. and Rucklidge, J.C.
1969: Layering and net veining in hornblende lamprophyre intrusions from the coast of Labrador; Journal of Geology, v. 77, p. 721-729.

Ermanovics, I.F., Korstgård, J.A., and Bridgwater, D.
1982: Structural and lithological chronology of the Archean Hopedale block and the adjacent Proterozoic Makkovik Subprovince, Labrador: Report 4; in Current Research, Part B, Geological Survey of Canada, Paper 82-1B, p. 153-165.

Fahrig, W.F. and Larochelle, A.
1972: Paleomagnetism of the Michael gabbro and possible evidence of the rotation of Makkovik Subprovince; Canadian Journal of Earth Sciences, v. 9, p. 1287-1296.

Fahrig, W.F. and Loveridge, W.D.
1981: Rb-Sr study of the Michael Gabbro, Labrador; in Rb-Sr and U-Pb Isotopic Age Studies, Report 4; in Current Research, Part C, Geological Survey of Canada, Paper 81-1C, p. 99-103.

Gandhi, S.S., Grasty, R.L., and Grieve, R.A.F.
1969: The geology and geochronology of the Makkovik Bay area, Labrador; Canadian Journal of Earth Sciences, v. 6, p. 1019-1034.

Gower, C.F.
1981: The geology of the Benedict Mountains, Labrador (13/J northeast and 13/I northwest); Newfoundland Department of Mines and Energy, Mineral Development Division, Report 81-3, 26 p.

Gower, C.F., Ryan, A.B., Bailey, D.G., and Thomas, A.
1980: The position of the Grenville Front in eastern and central Labrador; Canadian Journal of Earth Sciences, v. 17, p. 784-788.

Grasty, R.L., Rucklidge, J.C., and Elders, W.A.
1969: New K-Ar age determinations on rocks from the east coast of Labrador; Canadian Journal of Earth Sciences, v. 6, p. 340-344.

Rivers, T.
1980: Geological mapping in the Evening Lake-Wightman Lake area, western Labrador; in Current Research, ed. C.F. O'Driscoll and R.V. Gibbons; Newfoundland Department of Mines and Energy, Mineral Development Division, Report 80-1, p. 201-205.

Stevenson, I.M.
1970: Rigolet and Groswater Bay map-areas, Newfoundland (Labrador); Geological Survey of Canada, Paper 69-48.

Whitney, P.R. and McClelland, J.M.
1973: Origin of coronas in metagabbros of the Adirondack Mts., N.Y.; Contributions to Mineralogy and Petrology, v. 39, p. 81-98.

20. MULTIPARAMETER MAPPING OFF THE EAST COAST OF CANADA

Project 730081

R.F. Macnab
Atlantic Geoscience Centre, Dartmouth

Macnab, R.F., Multiparameter mapping off the east coast of Canada; in Current Research, Part A, Geological Survey of Canada, Paper 83-1A, p. 163-171, 1983.

Abstract

Since 1964, a large part of Canada's east coast offshore has been mapped in a joint program undertaken by DEMR and DFO components resident at the Bedford Institute of Oceanography. The data collected on these surveys have consisted for the most part of bathymetry, gravity, and magnetics, with single-channel seismic reflection measurements in selected areas. In the early years of the program, Decca Lambda was the primary means of navigation; with advances in computer technology, ship positioning is now accomplished largely by a combination of satellite navigation and Loran-C.

Multiparameter survey data satisfy a range of scientific and technical information needs, and are published in a variety of forms to suit these needs: navigation and bathymetric charts, Natural Resource Maps, regional compilations for scientific interpretations, and Open Files containing data in both digital and map form.

A number of technical developments are currently related to the multiparameter survey program: acquisition and field-testing of a new all-digital sea gravimeter; improvements in techniques and instrumentation for data logging and real-time navigation; creation of new software packages for handling geophysical data at sea and ashore; and implementation of procedures for the computer production of high quality contour maps in colour.

Introduction

The marine multiparameter mapping project is designed to collect bathymetric and geoscientific data over Canada's continental shelves and margins, and parts of adjacent deep ocean basins. These data form the bulk of a growing information bank that is used for the production of maps and for various scientific and technical studies.

Mapping is carried out off the east and west coasts of Canada. While the project has similar aims and end products on either coast, it varies in its regional organization and implementation. Only the east coast program will be described in this report.

The east coast project is a co-operative effort involving components of two Federal Government Departments: Energy, Mines and Resources (DEMR), and Fisheries and Oceans (DFO). This collaboration began in 1964, when geophysicists at the Bedford Institute of Oceanography operated a gravimeter and magnetometer aboard the Canadian Scientific Ship **Baffin** during a hydrographic survey in the Bay of Fundy. This proved to be a very efficient and cost-effective technique for acquiring potential field data, capitalizing as it did on a systematic mapping program that required a large ship to operate under precise navigational control.

From that beginning, the program has expanded and developed to the point where a large portion of the Canadian east coast offshore has been mapped. Figure 20.1 shows the extent and density of coverage to 1981, with a projection for the 1982 field program. Figure 20.2 shows the yearly accumulation of line-kilometres over which data have been collected, also with a projection for 1982. For the most part, these figures represent areas and distances over which three parameters have been measured on a routine basis: bathymetry, gravity, and total magnetic field. Some surveys have incorporated single-channel seismic reflection measurements on selected tracks (using 655 to 3277 cm^3 airguns), and high resolution reflection work (e.g. Huntec Deep Tow System) has been done to a lesser extent.

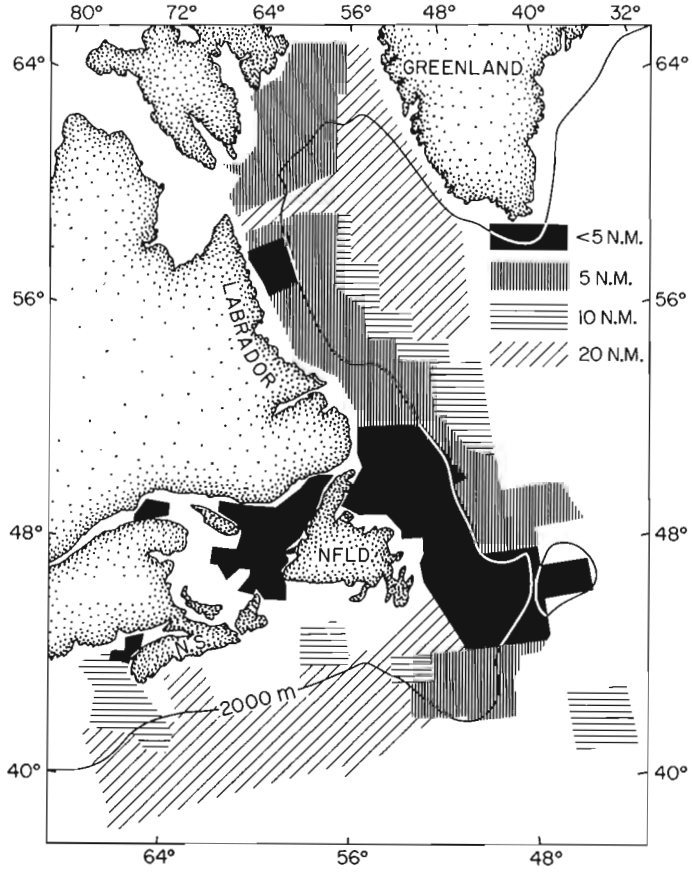

Figure 20.1. *Extent and density of multiparameter survey coverage from 1964 to 1982. Data comprise bathymetry, magnetics and gravity for the most part, with shallow seismic reflection on selected tracks.*

Individual cruises are described briefly in Table 20.1, which lists salient information such as area of operations, number of data points, and total line-kilometres.

Organizational and Policy Responsibilities

Departmental components involved in the east coast mapping project are the Geological Survey of Canada and the Earth Physics Branch of DEMR, and the Canadian Hydrographic Service of DFO (see Fig. 20.3). The primary DEMR mandate addressed by the project is to investigate the geological and geophysical characteristics of the seafloor and subfloor; the main DFO interest is to map water depths.

National hydrographic and geoscience priorities are formulated by the respective Branch Headquarters. Overall policy and strategy for the survey program are then shaped by an interdepartmental guiding committee which meets annually.

Operational Responsibilities

Responsibility for year by year planning, organization, and execution of these surveys is jointly shared by regional DEMR and DFO divisions. These are situated at the Bedford Institute of Oceanography (BIO) in Dartmouth, Nova Scotia: the Atlantic Geoscience Centre (AGC) of the Geological Survey of Canada, and the Atlantic Region of the Canadian Hydrographic Service.

Prior to each year's project, survey specifications relating to factors such as areas, parameters to be measured, line spacing and orientation, and choice of vessel, are discussed and mutually agreed upon, taking into account national and local needs and priorities. Also considered are the availability of ship time and the adequacy of positioning systems in the proposed survey area.

Initial survey coverage in a new area tends to consist of widely spread tracks (20 nautical miles apart) and tie lines, in order to acquire regional geophysical coverage at an early stage. Subsequent operations then concentrate on interlining between the original tracks, in order to pick up bathymetric detail and to further delineate interesting geophysical anomalies that appeared in the regional survey. Density of interlining is most often a function of water depth, with line spacing going down to one nautical mile or less on the shallower part of the continental shelf.

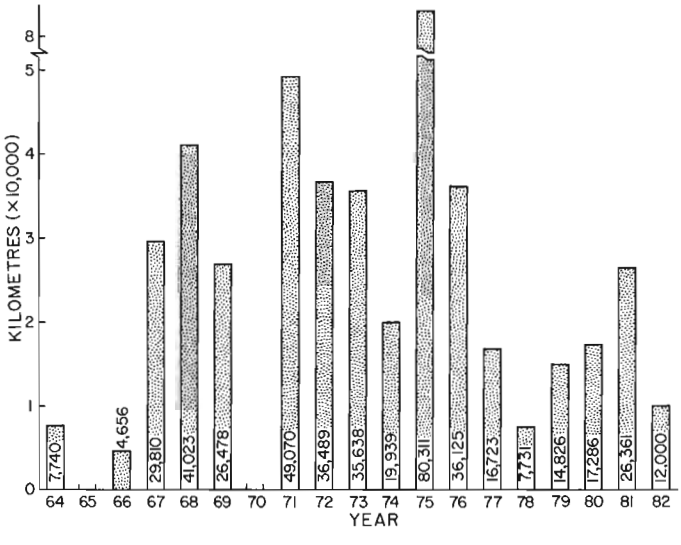

Figure 20.2. *Annual accumulation of line-kilometres on multiparameter survey cruises from 1964 to 1982.*

Most of shipboard survey team consists of hydrographic staff who are responsible for navigating the ship whilst running survey lines, and for operating the primary survey instrumentation: echo sounder, gravimeter, and magnetometer. Hydrographic personnel also perform routine shipboard processing of bathymetric and potential field data. On cruises where seismic reflection profiling is included in the program, a special support and operating team will also be in attendance; depending on the equipment in use, this team could be made up of AGC or contracted personnel. On some cruises, sea gravimeters belonging to the Earth Physics Branch have formed part of the equipment configuration, with EPB support staff in attendance. On all cruises, a geophysicist from AGC is in attendance for at least the first phase, in order to initiate procedures for the collection and handling of geophysical data, and to train hydrographic staff in these procedures.

Ships

A mix of Government-owned and chartered vessels has been deployed as survey platforms (Fig. 20.4). Of the **BIO Fleet,** which is owned and operated by DFO, the two ships that have been most used are **CSS Baffin** and **CSS Hudson.** Both are icebreakers with displacements approaching 5000 t and can carry a scientific/survey complement of up to 25 (though in practice the usual survey team rarely approaches that size). A smaller BIO vessel, the **CSS Dawson,** has also been used on occasion; it displaces 2700 t and has room for a scientific complement of 13.

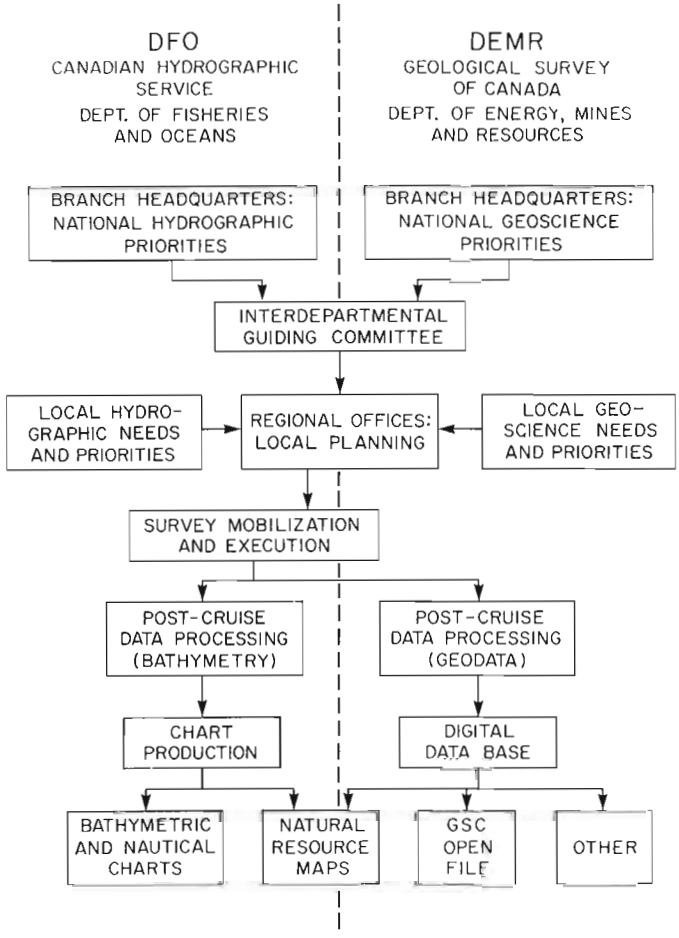

Figure 20.3. *Allocation of multiparameter survey responsibilities and functions between the Department of Fisheries and Oceans (DFO) and the Department of Energy, Mines and Resources (DEMR).*

CSS Baffin

CSS Hudson

CSS Dawson

M/V Minna

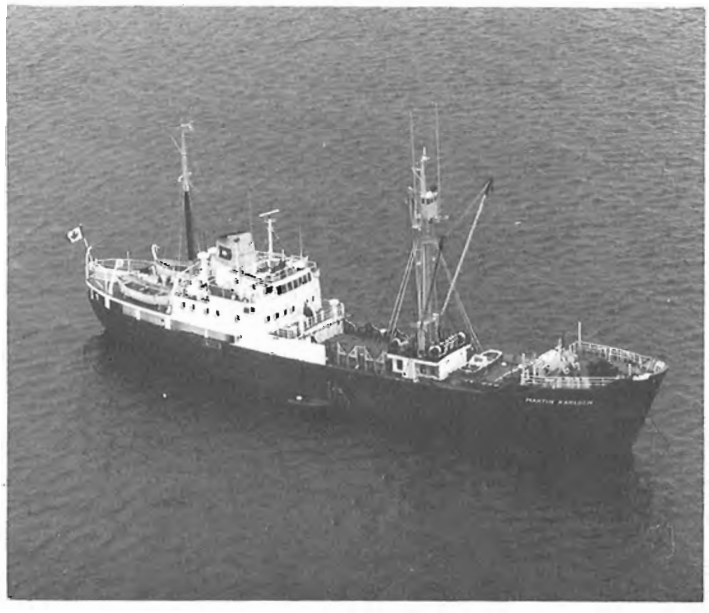

M/V Martin Karlsen

Figure 20.4. *Ships that are or have been engaged in multiparameter surveys. See text for brief descriptions.*

Table 20.1

Multiparameter survey cruises off the east coast of Canada

YEAR CRUISE NO.	VESSEL	AREA	NAVIGATIONS	NO. OF DATA POINTS			SEIS. REFL'N	TOTAL KM
				BATHY.	MAGNETICS	GRAVITY		
64-019	BAFFIN	BAY OF FUNDY	DECCA LAMBDA	9685	11499	8198	NO	4827
64-027	HUDSON	ORPHEUS BASIN	DECCA	199	7579	6446	NO	1913
66-008	BAFFIN	TAIL OF THE BANKS	DECCA LAMBDA	11562	11543	10307	NO	4656
67-014	BAFFIN	GRAND BANKS	DECCA LAMBDA	83836	81881	58767	NO	29810
68-021	BAFFIN	GULF OF ST. LAWRENCE	DECCA LAMBDA	75143	74673	58144	NO	29398
68-022	HUDSON	GRAND BANKS		28677	28591	20251	NO	11625
69-021	BAFFIN	GULF OF ST. LAWRENCE	DECCA LAMBDA	61853	65179	46360	NO	26478
71-014	HUDSON	GULF OF MAINE	SATNAV	35618	35359	28137	NO	12047
71-017	BAFFIN	FLEMISH CAP	DECCA LAMBDA	94598	92962	60046	YES	37023
72-015	MINNA	GRAND BANKS	DECCA LAMBDA	75324	75152	54564	NO	24075
72-025	HUDSON	LABRADOR SEA	SATNAV-LORAN/C	40769	40196	31839	YES	12414
73-014	BAFFIN	GULF OF ST. LAWRENCE	DECCA HIFIX	6600	6515	5570	NO	2699
73-019	MINNA	NE NFLD. SHELF	LAMBDA-LORAN/C	84134	84373	50929	YES	25851
73-034	DAWSON	TAIL OF THE BANKS	SATNAV-LORAN/C	19796	19723	18373	NO	7088
74-015	BAFFIN	GULF OF ST. LAWRENCE	HIFIX	7000	6630	6889	NO	2444
74-023	MINNA	LABRADOR SEA	SATNAV-LORAN/C	57903	59745	37774	YES	17495
75-009	HUDSON	NFLD. SEAMOUNTS, FLEMISH CAP	SATNAV-LORAN/C	67600	65490	58297	YES	18798
75-009	HUDSON	GULF OF ST. LAWRENCE NE NFLD. SHELF	SATNAV-LORAN/C	37176	30309	28500	YES	10431
75-009	HUDSON	LABRADOR SEA	SATNAV-LORAN/C	38340	36548	30969	YES	12601
75-018	MARTIN KARLSEN	LABRADOR SEA	DECCA LAMBDA SATNAV-LORAN/C	109449	107409	104211	YES	38481
76-012	BAFFIN	GULF OF ST. LAWRENCE	SATNAV-LORAN/C	20000	19437	0	NO	6033
76-019	MARTIN KARLSEN	LABRADOR SEA	SATNAV-LORAN/C	96618	95291	92116	NO	30092
77-008	BAFFIN	GULF OF ST. LAWRENCE	HIFIX	15000	14769	0	NO	4755
77-016	MARTIN KARLSEN	LABRADOR SEA	SATNAV-LORAN/C	42903	43479	36987	NO	11968
78-019	MARTIN KARLSEN	LABRADOR SEA	SATNAV-LORAN/C	25528	24495	24115	NO	7731
79-015	BAFFIN	SCOTIAN MARGIN	BIONAV	49435	46630	45555	NO	14826
80-028	HUDSON	DAVIS STRAIT	BIONAV + ACCUFIX	32216	32216	30097	YES	6517
80-031	BAFFIN	DAVIS STRAIT	BIONAV + ACCUFIX	25336	23596	20564	YES	6112
80-035	HUDSON	DAVIS STRAIT	BIONAV + ACCUFIX	17169	15906	16328	YES	4657
81-038	DAWSON	DAVIS STRAIT	BIONAV + ACCUFIX	51592	49486	48297	NO	18869
81-045	HUDSON	DAVIS STRAIT	BIONAV	26048	20536	19959	YES	7492

During the 1972-78 survey seasons, two smaller charter vessels were engaged: **M/V Minna** and **M/V Martin Karlsen.** Both were in the 2500-3000 t displacement range, with room for 12 to 15 scientific personnel. Designed and constructed as ice-reinforced cargo vessels, these ships didn't feature ready-made and suitable space for drawing offices and laboratories. Nor did they provide much in the way of specialized facilities such as stable electrical power, antenna mounts, echo-sounding transducers, and arrangements for towing instruments. Mobilization of these vessels for survey use therefore required considerable planning and innovation, particularly in the design and construction of portable laboratory modules for the conversion of cargo holds into work and equipment spaces.

Navigation

DFO has the direct responsibility for procurement, operation, and maintenance of all navigation equipment used in this program.

In the early years of the program, ship positioning was accomplished largely through use of Low-Ambiguity Decca (Lambda) operating in the range-range mode. This system consisted of a ship-mounted master station and two shore-based slave stations. Ship positions were derived by triangulation, using the measured times of master-slave transmissions.

With a well-calibrated chain, Lambda yielded positional accuracies in the order of 50-150 m. Under good conditions, ranges of up to 300 nautical miles were possible.

In the range-range mode, Decca Lambda had many drawbacks: only one ship could use the system at any time, and the ship had to be large enough to mount a sizeable master antenna; logistics for establishing and maintaining slave stations in remote areas were difficult and expensive; setups and calibrations were time-consuming procedures that often delayed the start of survey operations; equipment malfunctions or atmospheric disturbances necessitated regular reference checks; and effective ranges were often limited, with frequent overnight suspensions of survey operations due to skywave interference.

Most of these drawbacks were eliminated with the introduction of rho-rho Loran-C as a primary positioning system following tests in 1971-72 (Grant, 1973). Rho-rho positioning is again a triangulation technique based on measured transmission times from two or more shore stations to the ship. Where it differs from Decca Lambda is in the use of a precise shipboard clock to maintain synchronization between shore transmitters and the shipboard receiver. This clock tends to drift, but drift rates can be derived through an analysis of positions obtained from the U.S. Navy Navigation Satellite System (NNSS). Initially, this analysis was performed manually, and it consisted basically of a series of comparisons between Loran-C and NNSS fixes.

By 1976, enough experience had been gained with this procedure to consider automating it. Within two years, specialists of the BIO Navigation Group produced an integrated system – BIONAV – that combined input from a variety of navigation sensors to yield the best possible fix (Fig. 20.5). BIONAV is now used routinely on all multiparameter surveys, and has also become popular with oceanographers at BIO, who use it for nonmapping purposes (Wells and Grant, 1981; Grant and Wells, 1982).

As a computer-controlled system, BIONAV stores fixes in digital form and can produce ship's tracks in real time on an attached plotter. In practice, however, fixes are still plotted manually by hydrographic watchkeepers who try to keep the ship on a pre-defined track, and who must exercise considerable care in calling for course and speed adjustments that have minimal effect on underway gravity measurements.

With the combined input of NNSS and the North Atlantic Loran-C chain, it is estimated that BIONAV can yield ship's positions to an accuracy of ±200 m or better anywhere in most parts of the offshore area extending from the Bay of Fundy to Hudson Strait (Fig. 20.6). However, from the northern part of the Labrador Sea through Davis Strait and into Baffin Bay, positioning accuracy is drastically reduced by factors that affect Loran-C performance: weak signals, skywave interference, and excessive landpath.

Satisfactory Loran-C coverage can be extended by the use of auxiliary transmitter stations installed temporarily at selected locations along the coast. In 1980 and 1981, Davis Strait was mapped with the aid of Accufix transmitters located at Saglek Bay and on Brevoort Island. This approach yielded good results, but the expense and difficulty of establishing and maintaining these remote Loran-C stations were reminiscent of Decca Lambda problems in the early days. Moreover, the rigours of the northern climate took their toll: in 1980, the Davis Strait survey had to be cut short when the transmitter tower at Saglek collapsed on account of icing.

Short of establishing a string of expensive and vulnerable Accufix transmitters along the coast of Baffin Island, it is not clear yet how to achieve accurate positioning for surveys in Baffin Bay. It was thought at one time that the U.S. 'Navstar' Global Positioning System (GPS) might eventually provide a navigational capability in this region, but full deployment is not expected until later in the decade. More importantly, it appears that non-military users may be denied access to the precise GPS code that is required for the calculation of accurate fixes.

Survey Instrumentation

Most survey instrumentation is commercially available. Echo sounding equipment is usually provided by DFO, with DEMR responsible for geophysical devices.

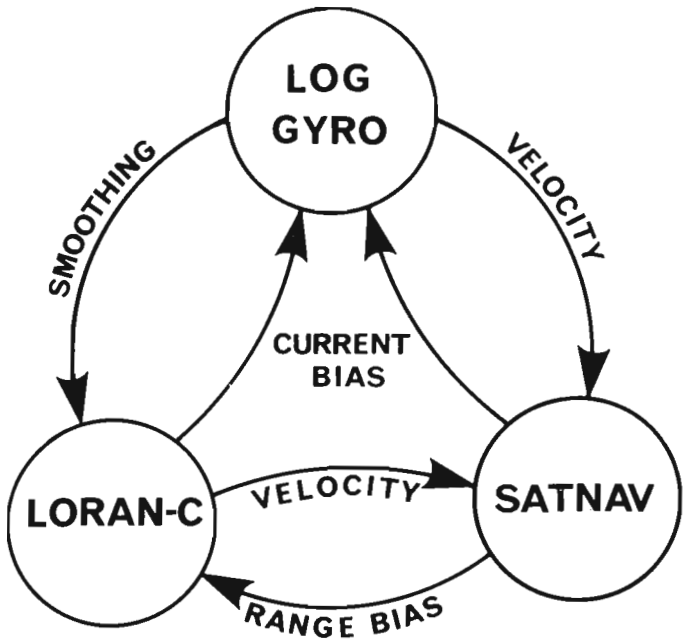

Figure 20.5. *Interactions between the three major components of the Bedford Institute of Oceanography integrated Navigation System (BIONAV): log and gyrocompass, which provide continuous course and speed; Loran-C, which provides continuous positions by radio-triangulation; and satellite navigation, which provides periodic "absolute" positions that are used to correct for clock drift in the Loran receiver (from Grant and Wells, 1982).*

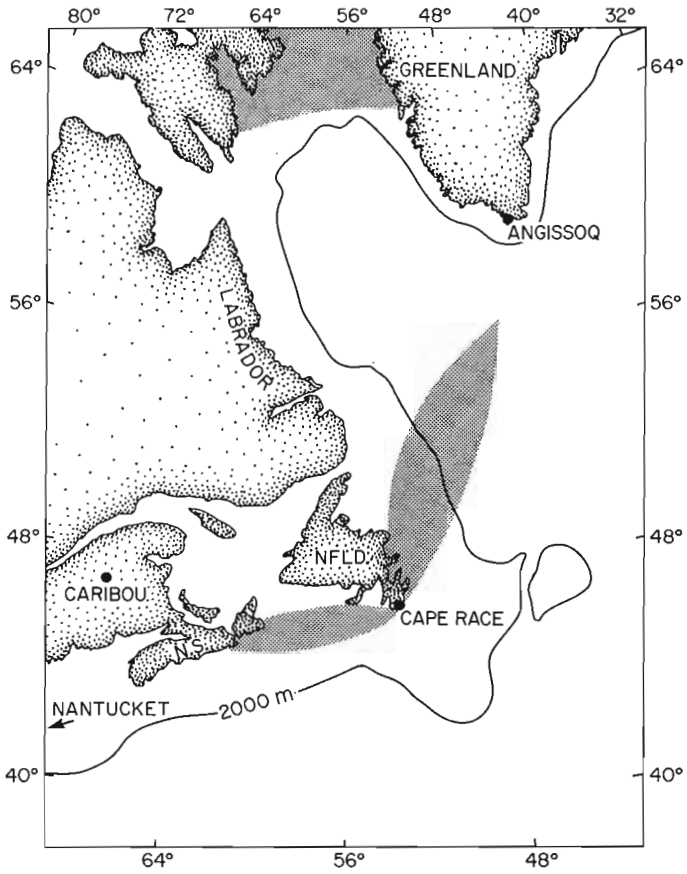

Figure 20.6. *Locations of Loran-C stations that are available for multiparameter survey operations in the Canadian east coast offshore. (Not shown is the station in Sandur, Iceland.) The shaded areas indicate where Loran-C signals are too weak for mapping operations, or where estimated positioning errors in the rho-rho mode exceed 200 m at the 68% confidence level. These constraints apply to the use of BIONAV in this region (adapted from Grant, 1973).*

Water depth is normally measured with a 12kHz hull – or ram-mounted transducer connected typically to a Raytheon transceiver and recorder. Total magnetic field is measured with a Varian, Barringer, or Geometrics proton precession magnetometer connected to a sensor towed some 200 m astern of the ship.

Gravity data have for the most part been collected with Graf-Askania type GSS-2 sea gravimeters, while LaCoste and Romberg devices have been used on some surveys.

Sediment thickness is generally mapped with the aid of a simple reflection system consisting of Bolt airgun, a single-channel hydrophone streamer, and a mix of associated electronics that have been built or bought. Hull-mounted or towed 3.5 kHz sounding systems have been operated on a trial basis on some surveys, to evaluate their potential for systematic mapping of shallow sediments. Sidescan sonar and the Huntec Deep Tow System have also been deployed on occasion.

Shipboard Data Logging and Processing

The general flow of data through current field acquisition and processing stages is shown in the upper part of Figure 20.7.

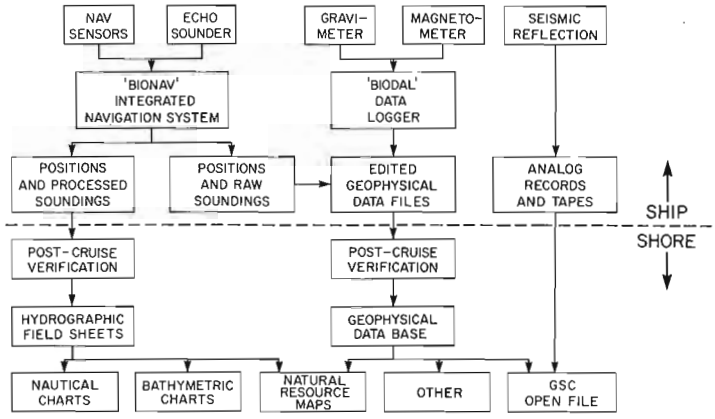

Figure 20.7. *Generalized diagram showing the flow of multiparameter survey data aboard ship and ashore.*

The primary digital data logger is BIODAL – a hard-wired apparatus developed and constructed at BIO several years ago. Its main purpose nowadays is the recording of magnetometer and gravimeter data onto 9-track tape. BIODAL does have the capability of logging some types of navigational information (radio-positioning co-ordinates, log and gyro), but this function has been made obsolete by the development and introduction of BIONAV.

Bathymetric data are not automatically logged in computer-readable form, because of difficulties in the real-time digitizing of deep-sea soundings. Instead, the sounding display is scaled manually, and the readings are entered through the BIONAV keyboard for merging with the navigational data.

All basic survey data i.e. water depth, total magnetic field, and gravimeter output, are displayed and saved as strip chart records. Auxiliary seismic data are also displayed and saved on strip chart records, in addition to being recorded in analog form on magnetic tape.

Aboard ship, the bathymetric and potential field data are processed on a minicomputer. The processing serves three purposes: initial quality control, data display for verification and survey planning, and creation of digital files for archiving and further processing ashore.

For hydrographic purposes, bathymetric data are corrected for sound velocity, transducer depth, and tide where appropriate. This is in keeping with the requirement to produce accurate charts for navigation and for the precise representation of seafloor topography.

Processing of potential field data at this stage consists of: conversion of gravimeter output to milligals, with correction for the Eotvos effect; derivation of magnetic anomalies with reference to the International Geomagnetic Reference Field; and merging with raw bathymetric data. Corrections for gravimeter drift and magnetic diurnal variation are only applied during post-cruise processing.

Processing output for both bathymetric and potential field data consists of listings, profile plots, track plots, postings, and digital files on magnetic tape or disc.

Post-Processing and Disposition of Data

When a survey cruise is over, data are brought ashore for final processing and merging with previously collected data. As outlined in the lower part of Figure 20.7, bathymetric and geophysical data are handled separately.

Hydrographic data are further verified for accuracy, and then are machine plotted to create final field sheets. These sheets are the primary input for the production of a variety of navigation and bathymetric charts. (Navigation charts are intended principally for mariners concerned with the plotting of routes and the safety of passage; bathymetric charts are intended for those interested in seafloor topography, such as fishermen, mining and oil companies, dredging contractors, pipeline and cablelaying enginners, etc.)

Geophysical data are turned over to AGC personnel for similar verification, followed by entry to a computer-based archival/retrieval system. Data can then be extracted in a variety of forms, depending on the use to which it will be put, be it in-house scientific interpretation of public release: contour maps, profile plots, digital files, etc.

In reports on scientific investigations the data most often appear as part of regional compilation maps (e.g. Haworth and MacIntyre, 1975; Srivastava, 1978; Keen and Hyndman, 1979; Fournier, 1980). Data released directly to the public may appear in several different forms. The most formal route for publication is the Natural Resource Map (NRM) series, which covers the oceanic areas adjacent to Canada. These 1:250 000 contour maps are published by the Geoscience Mapping Unit of the Canadian Hydrographic Service; they portray bathymetry, Bouguer gravity anomaly, and magnetic anomaly (Canadian Hydrographic Service, 1981). Preliminary contour maps are periodically released through the GSC Open File (see Table 20.2). Depending on the density of survey lines, these preliminary maps may or may not conform to the NRM format and scale.

Generally, data that have been made public in the form of contour maps are also released in the form of digital files on magnetic tape, so that users may apply their own processing techniques.

Figures 20.8 and 20.9 outline the geographical areas for which geophysical data have been published as Natural Resource Maps or released through GSC Open File, respectively. Clearly, not all survey results have been released (compare with Fig. 20.1). The biggest problem area is the Labrador Sea gravity data, which consist of numerous sets of data collected over a long period of time on different datums. A major effort is underway to resolve the inconsistencies between different surveys through careful review and adjustment of all the data.

Present and Future Developments

Related developments could impact the multiparameter mapping project in a number of ways.

The first development is the recent acquisition of a digital sea gravimeter know as the KSS-30. Designed and constructed in Germany by Bodenseewerk Geosystems, this device uses an embedded microprocessor to control the operation of its sensor and stabilized platform. With navigation input, the device also performs a real time conversion of sensor output to Eotvos corrected gravity. This substantially reduces the shipboard data processing workload. Capable of measuring gravity accurately during ship maneuvers and rigorous sea conditions, the KSS-30 should increase our data collection capabilities on smaller (and therefore less costly) vessels and in ice-infested waters.

The KSS-30 procurement has prompted further development in two related areas: navigation and data logging. In the open ocean, achievement of the ultimate accuracy of the KSS-30 will require improved methods for measuring ship's course and speed; new technologies may be necessary to upgrade our present capabilities. Microprocessor advances now offer the possibility of cheap and compact data loggers that not only monitor instrument

Table 20.2

Geological Survey of Canada Open Files of Geophysical Data Collected on Multiparameter Survey Cruise

Open File	Year	Area	Type of Data	Digital Form	Contour Maps
183	1973	Gulf of Maine Orpheus Basin Gulf of St. Lawrence Grand Banks	raw bathymetry gravity magnetics	X	
248	1975	Northeast Newfoundland Shelf	raw bathymetry gravity magnetics	X	
391	1976	South Labrador Sea	raw bathymetry gravity magnetics	X	
525	1978	South Labrador Sea	gravity magnetics		X
607	1979	Saglek Bank	raw bathymetry gravity magnetics	X	
750	1981	Scotian Margin	raw bathymetry gravity magnetics	X	X
850	1982	Labrador Sea	magnetics	X	X

performance and undertake real time calculations, but which allow operators to interact with their data. Work is proceeding on the development of such an intelligent device that interfaces with the KSS-30 and other instruments.

Major efforts have gone into the development of software packages to handle large quantities of geophysical survey data at sea and ashore. A suite of programs known collectively as SHIPAC has recently been completed for use in BIO's shipboard Hewlett-Packard 1000 minicomputers. These routines represent a substantial streamlining of older data processing procedures. A data base package known as GEOFFREY has also been assembled recently, for execution of BIO's shore-based Control Data Corporation mainframe. GEOFFREY accepts cruise data sets for merging and permanent archiving. When fully implemented, this package will facilitate the extraction of data on a time- or location-dependent basis for scientists and mapmakers alike.

Methods for constructing publication-quality contour maps for the Natural Resource Map series have been undergoing continuous improvement. Potential field contours for early editions in 1970 and 1971 were manually drawn by an AGC geophysicist. In 1972, a mounting backlog of unpublished survey data made it necessary to undertake this task by computer, and for six years it was contracted out to Calgary-based data processing firms. This activity contributed to the development of in-house expertise in the computer contouring process (Haworth, 1974).

When BIO acquired a large mainframe in 1978, it became feasible to attempt computer contouring in-house. A series of investigations and refinements relating mainly to the CalComp General-Purpose Contouring Package (GPCP) led to the institution of procedures for the routine production of good-quality maps (Hunter et al., 1982). The use of in-house facilities not only assures reasonably fast production; it also permits a high degree of control in the manipulative processes necessary for the construction of acceptable maps.

As a follow-up to the activity described in the previous paragraph, procedures are now being implemented for the computer production of colour separations required for the multi-colour printing of gravity and magnetic data in the Natural Resource Map series. These separations are currently done by hand in a time-consuming process that requires a skilled cartographic draftsman. We plan to exploit available technology that will allow us to submit data from a work station in Dartmouth, Nova Scotia for camera-ready output on a colour plotter in the GSC Headquarters in Ottawa. This is expected to reduce substantially the time elapsed between data collection and data publication.

A more difficult challenge arises from a recent legislation which provides for more timely release of industrial survey results. Most of this information has been collected by offshore exploration firms on behalf of oil companies. This very large commercial data base could bolster and complement our own data holdings at a fraction of the cost and time of acquiring it ourselves. However, there are major problems to get the data in a form that we can easily use, so we are anticipating only moderate progress in this direction for the foreseeable future.

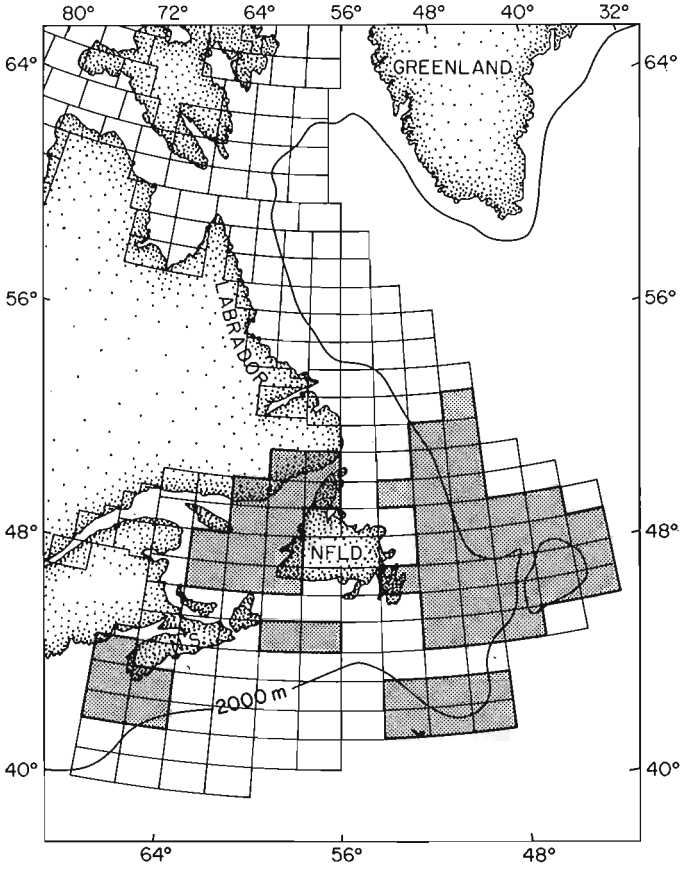

Figure 20.8. Arrangement of Natural Resource Maps off the Canadian east coast. Shaded areas indicate where geophysical data have been published (adapted from Canadian Hydrographic Service, 1981).

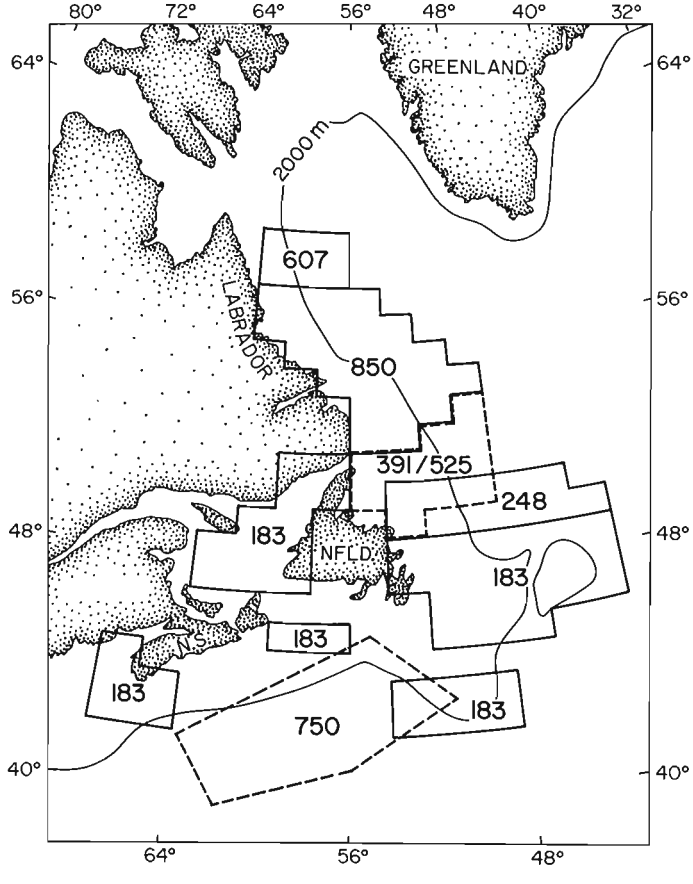

Figure 20.9. Areas covered by multiparameter survey data released through GSC Open File in digital or map form. Individual Open Files are described in greater detail in Table 20.2.

Law of the Sea and Territorial Limits

Further incentive for offshore multiparameter mapping has been provided by the Draft Convention on the Law of the Sea. Article 76 of the Convention contains a definition of the "continental shelf" of a coastal state which, for purposes of the Convention, also encompasses the continental slope and rise. The seaward limits of this "continental shelf", and hence of the coastal state, are specified by geological and morphological parameters, e.g. thickness of sedimentary rocks and change in seafloor gradient.

The full implications of this Article have yet to unfold, and will probably require the efforts of a generation or so of maritime jurists to unravel. It is clear also that a lot of detailed mapping work will be necessary to justify territorial claims and to resolve contentious areas. Due in part to the DFO-EMR multiparameter mapping project, some of this work has been done. Moreover, we are in good position to start the assessment of what needs to be done next, and how.

Acknowledgments

Keh-Gong Shih and Darrell Beaver assisted in the compilation of cruise and survey statistics.

References

Canadian Hydrographic Service
1981: Catalogue of geoscientific publications; Department of Fisheries and Oceans, Ottawa.

Fournier, K.
1980: Interactive graphics for retrieval, display, and editing of marine gravity data; in Frontiers in Data Storage, Retrieval and Display: Proceedings of a marine geology and geophysics data workshop November 5-7, 1980, Boulder, Colorado, ed. A.M. Hittelman and R.L. Larson.

Grant, S.T.
1973: Rho-rho Loran-C combined with satellite navigation for offshore surveys; International Hydrographic Review, v. 50, p. 35-54.

Grant, S.T. and Wells, D.E.
1982: Interactions among integrated navigation system components; International Association of Geodesy Symposium on Marine Geodesy, Tokyo.

Haworth, R.T.
1974: Gravity and magnetic Natural Resource Maps (1972) Offshore Eastern Canada – philosophy and technique in preparation by computer; International Hydrographic Review, v. 51, p. 131-155.

Haworth, R.T. and MacIntyre, J.B.
1975: The gravity and magnetic field of Atlantic Offshore Canada; Canadian Hydrographic Service, Marine Sciences Paper 16/Geological Survey of Canada, Paper 75-9.

Hunter, C., Shih, K.G., and Macnab, R.
1982: A compilation of marine magnetometer data from the Southwest Labrador Sea; Geological Survey of Canada, Open File 850.

Keen, C.E. and Hyndman, R.D.
1979: Geophysical review of the continental margins of eastern and western Canada; Canadian Journal of Earth Sciences, v. 16, p. 712-747.

Srivastava, S.P.
1978: Evolution of the Labrador Sea and its bearing on the early evolution of the North Atlantic; Royal Astronomical Society, Geophysical Journal, v. 52, p. 313-357.

Wells, D.E. and Grant, S.T.
1981: An adaptable integrated navigation system: BIONAV; Proceedings of Colloquium III on Petroleum Mapping and Surveys in the 80's, The Canadian Petroleum Association, Banff, Alberta.

21.

COMPUTER CONTOURING OF MARINE SURVEY DATA: CHOOSING THE BEST TECHNIQUE FOR GRIDDING INPUT DATA

Project 730081

K.G. Shih and R.F. Macnab
Atlantic Geoscience Centre, Dartmouth

Shih, K.G. and Macnab, R.F., Computer contouring of marine survey data: choosing the best technique for gridding input data; in Current Research, Part A, Geological Survey of Canada, Paper 83-1A, p. 173-178, 1983.

Abstract

Computer contouring procedures usually require prior gridding of input data to produce a uniform matrix of point values that describe the surface to be contoured. The choice of gridding procedure can have a profound effect on the final contour map, depending on the gridding parameters specified, as well as on the nature and distribution of the original data.

This is especially noticeable when working with data sets collected on marine surveys. Measurements in this case are distributed in a highly non-uniform manner, e.g. they are closely spaced along parallel ship's tracks which are themselves widely spaced.

In connection with the production of contour maps portraying large marine data sets, we have recently completed a series of experiments with different gridding techniques, and have devised some rules of thumb to guide us in the selection of the 'best' method

Introduction

It is common practice to construct geophysical contour maps by computer, especially when dealing with large sets of data in digital form. The technique is relatively straightforward when data points are well distributed throughout an area of interest, and when distances between points are less than the dimensions of the features that one wants to portray. It is an altogether different matter, however, when data points are sparse, or their distribution is non-uniform.

A particular case of non-uniform distribution is a data set collected on a regional marine survey: at one-minute collection intervals, data points are typically spaced 200 to 500 m apart along parallel ship's tracks, while the tracks themselves may be separated by 20 to 40 km. Stated differently, the along-track data density is two to five points per kilometre, while the cross-track density is one point every 20 to 40 km. In the absence of cross tracks, the information on which to base the construction of contour maps is thus concentrated in a series of parallel lines that divide the study area into strips. The problem then becomes one of overcoming the disparity in along- and cross-track data densities in order to identify and to connect similar features across the strips that contain no information. (This assumes, of course, that the features are continuous from track to track, as is the case for magnetic lineations). In most cases, this involves the use of a gridding procedure to create a matrix of intermediate data points in the 'blank' area. As it turns out, there are a number of gridding procedures, and selection of the most appropriate one is crucial to the success or failure of the subsequent contour map in portraying the data realistically.

Computer contouring of marine survey data has been used as a production technique at AGC for over ten years now (Haworth, 1974). In recent years, the acquisition of a more capable computer facility (a CDC Cyber 170) has allowed us to pursue this activity extensively and on an in-house basis.

One of the benefits of in-house processing is the greater degree of direct control that it affords, with increased opportunities for trial and experimentation. While preparing contour maps of two large data sets for public release recently (Shih et al., 1981; Hunter et al., 1982) we undertook a series of such experiments to determine what were the effects of various gridding procedures on the final contour maps, and to attempt to formulate some guidelines for the selection of the 'best' approach.

The General-Purpose Contouring Package

The contouring software used in all these tests was GPCP-II: the Cal-Comp General-Purpose Contouring Package II (California Computer Products, Inc., 1973). This is a well-documented and widely-used package that is marketed in a number of versions for different computers. The results of our investigations should therefore apply in other installations where GPCP is available.

GPCP features a gridding capability; at the user's option, the package accepts randomly-spaced data for gridding prior to the construction of contours, or it accepts regularly spaced data that has already been gridded by a separate program. We used both options in our tests.

GPCP offers a choice of two gridding methods: the weighted mean and the polynomial fit. The weighted mean method entails a radial search around each grid point for the nearest n data points (n is selectable by the user), which are referred to as "neighborhood points". The data values at the neighborhood points are weighted according to their distances from the grid point, and summed to obtain an average value which is assigned to the location of the grid point. The polynomial fit consists of fitting an n^{th} degree polynomial (maximum n = 10) to the entire set of input data, followed by evaluation of the polynomial at the grid points.

The GPCP manual does not divulge specifics of the software that actually carries out either gridding procedure.

The Effect of Pre-gridding and Decimating Input Data

A map area with moderately dense survey coverage can typically contain some 20 000 data points. Before attempting to grid and contour, it is necessary to reduce the number of data points for two reasons. The first is computer memory limitations: in our installation, for instance, a maximum of 3600 input points appears to be about the limit for efficient GPCP computation.

The second reason for decimating input data arises whenever the gridding procedure involves a search for neighborhood points, and when the interval between original data points is small compared to the spacing between survey tracks: the effective interval between data points has to be increased to force the search algorithm to encompass points on adjacent tracks. This will reduce, if not eliminate altogether, a possible bias introduced by having all the

selected points located on one track only. (This would be less of a problem if the search method incorporated a form of azimuthal control that forced it to seek neighborhood points in a 360° sweep.)

We used one of two methods to decimate input data. The simpler method consisted of selecting data points at fixed intervals of two, five, ten, or twenty minutes, depending on the reduction factor desired. The second method entailed a form of pre-gridding, in which the study area was divided into a number of "cells". For each cell, an average data value was then calculated from all the data points residing in that cell; the position of the average data value was assigned either to the cell mid-point, or to a "mean" location derived by averaging the co-ordinates of all the cell data points.

The use of different decimation techniques yields different sets of values for input to the gridding procedures, and so should be expected to affect the final contour maps. Of course, further variation can be introduced in the process by changing the decimation parameter in one or the other technique, i.e. by selecting a longer or shorter time interval between data points, or by altering the size of the pre-gridding cell.

Other Gridding Methods

We experimented with a number of gridding methods additional to those available in GPCP: minimum curvature, triangulation, weighted average of closest points, polynomial fit, and local surface fitting.

The minimum curvature method produces a grid of values that define the smoothest surface passing through a number of control points (Briggs, 1974; Swain, 1976).

The triangulation method divides the study area into triangular cells having data points as vertices. A fifth-degree polynomial evaluates grid points within each cell (Akima, 1978; IMSL, 1980).

The weighted average of closest points and the polynomial fit methods are similar to GPCP techniques described above, but for comparison purposes, we decided to experiment with methods that are described in the literature (Falconer, 1971; Kuester and Mize, 1973, p. 205-217).

The local surface method is a variant of the GPCP polynomial fit; instead of attempting to fit a single polynomial surface to the entire input data set, the method fits a series of polynomial surfaces to small regions of the study area, and so derives grid values in a piecewise fashion (Braile, 1978).

A Simple Comparison

For a simple illustration of the effects of different gridding techniques, we applied several to the problem of contouring the surface of a hypothetical dome shaped like a spherical segment.

If the gridding and contouring are performed correctly, the final contour lines should look like concentric circles. As shown in Figure 21.1A, this is indeed the case with data that has been gridded by the polynomial (GPCP and non-GPCP) or the triangulation method. Figure 21.1B shows the sort of contour distortion typically produced when data have been gridded by the local surface, the minimum curvature, or the weighted average (GPCP and non-GPCP) method.

In this example, the surface of the dome was described by 24 data points that were distributed more or less evenly throughout the plot area. More data points would not have improved the contours of Figure 21.1A, but would no doubt have made a difference in Figure 21.1B.

A point worth mentioning here is that edge effects were avoided in this and in all subsequent contour plots by enlarging the input data set to include additional information about the data field surrounding the plot area.

Comparisons Using a Simulated Data Field with Lineations

Marine magnetic fields are often characterized by strong patterns of lineations. To determine how various gridding methods coped with this arrangement of data, we simulated a magnetic field with a simple corrugated surface. This was sampled in a series of points distributed along straight, parallel lines in a technique analogous to actual measurements at sea. Several gridding methods were then used to prepare the data for contouring.

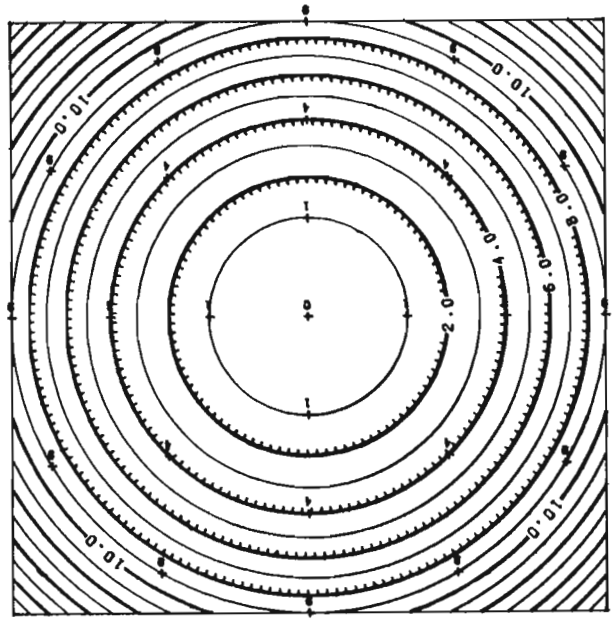

A. Data points gridded by polynomial and triangular methods.

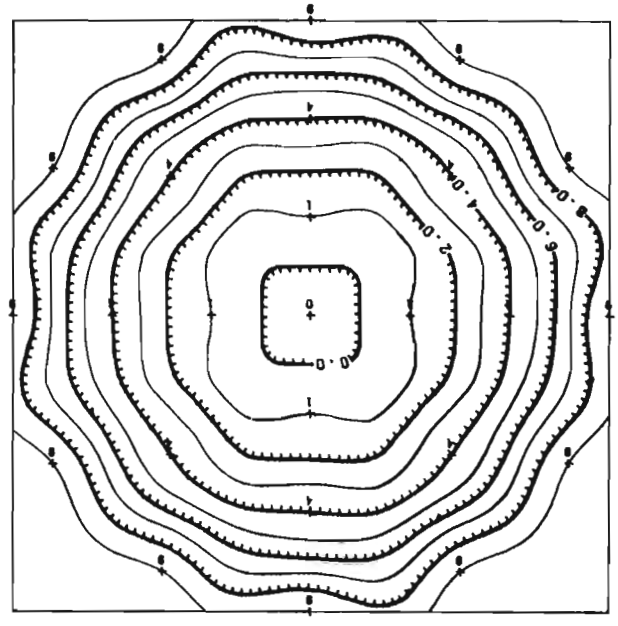

B. Typical contours for data points gridded by local surface, minimum curvature, and weighted average methods.

Figure 21.1. *Contours of a spherical dome. Contour interval is 1.*

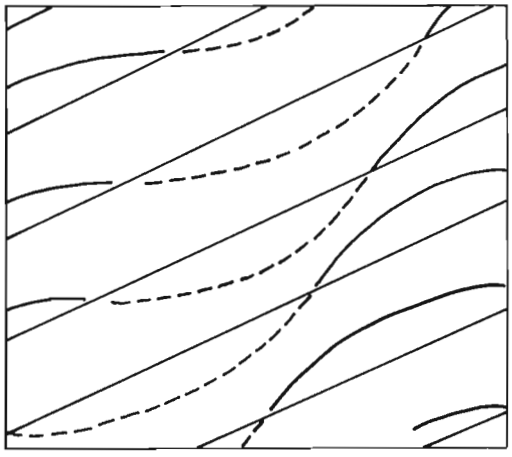

Figure 21.2

Contours of data field with lineation, simulated by corrugated surface. The ratio of the simulated track spacing to interval between data points is 20 to 3. Data gridded over a 30 by 30 matrix. Contour interval is 25. Data gridding performed by the following methods:

A. Triangular

B. GPCP weighted

C. Minimum curvature

D. GPCP polynomial.

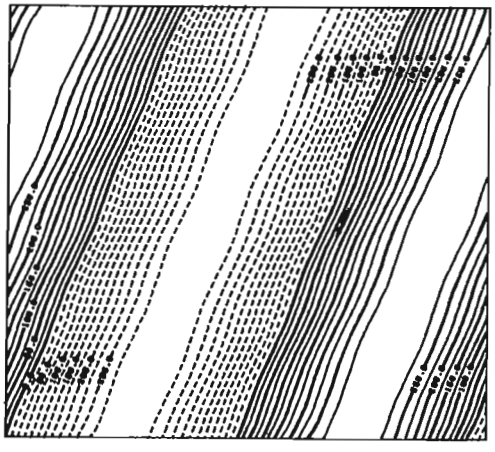

(A)

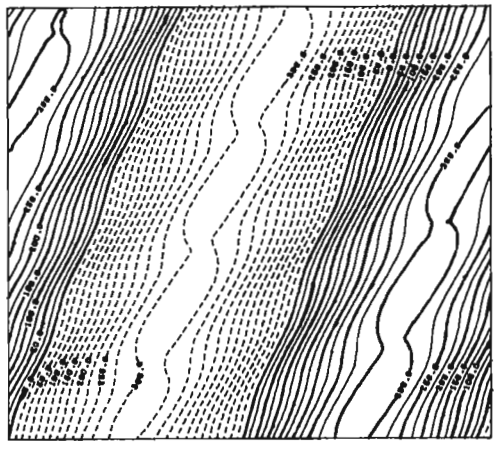

(B)

(C)

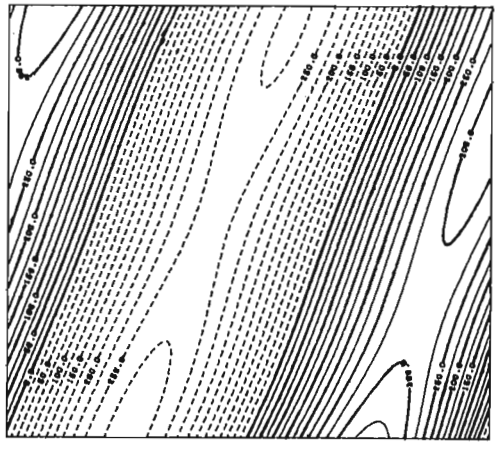

(D)

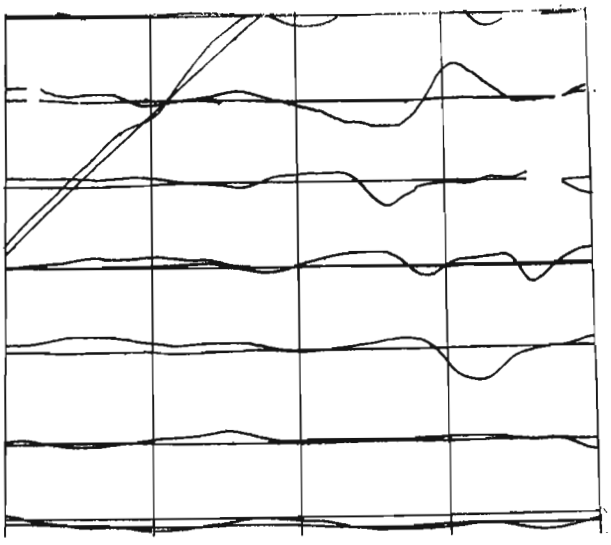

Figure 21.3

Contours of magnetic anomalies over the area bounded by 54N-55N and 48W-50W. Data gridded over a 30 by 30 matrix. Contour interval is 50 gammas.

A. 20-minute interval data. Gridded by triangular method

B. 20-minute interval data. Weighted by GPCP method

C. 20-minute interval data. Gridded by minimum curvature method

D. All data points pre-gridded and then weighted by GPCP method.

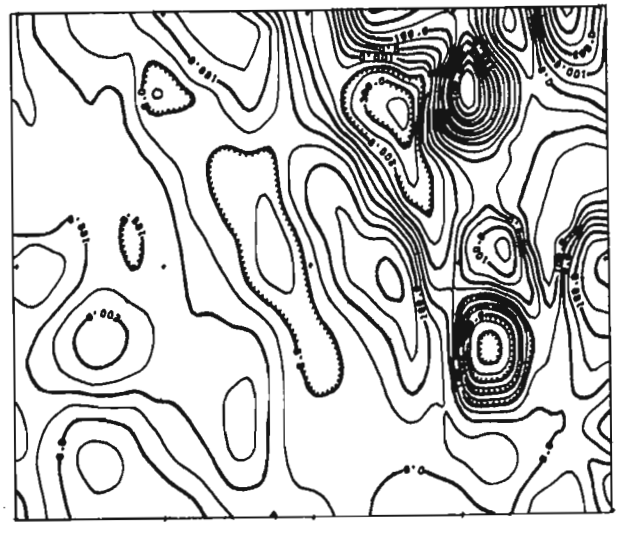

(A)

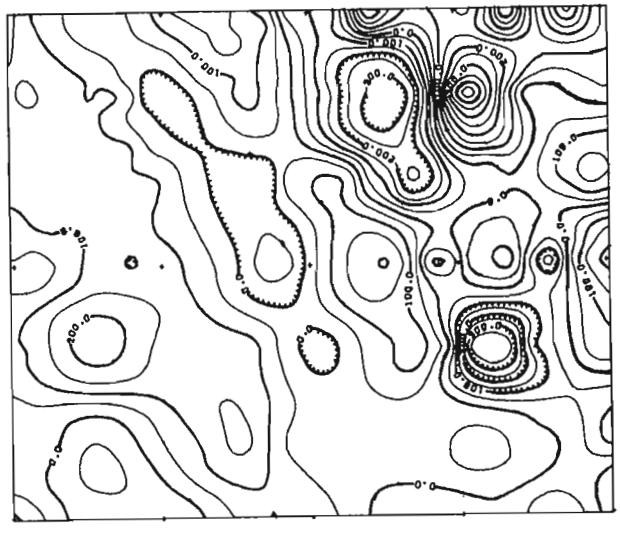

(B)

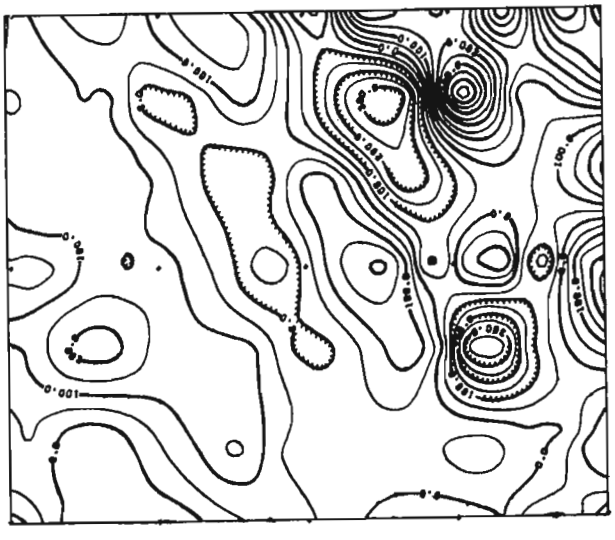

(C)

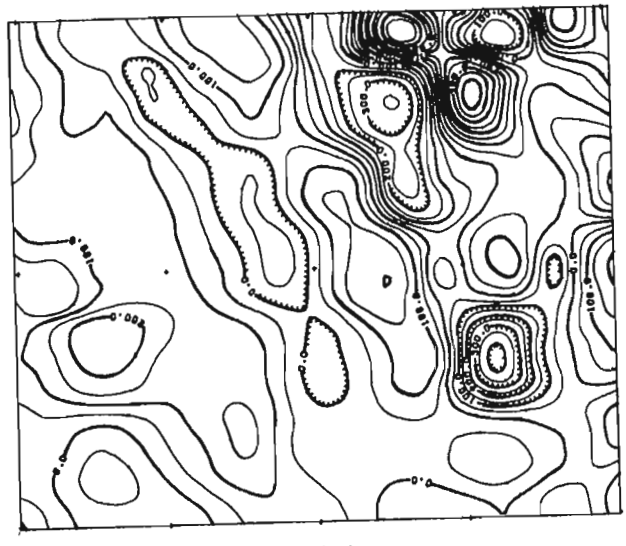

(D)

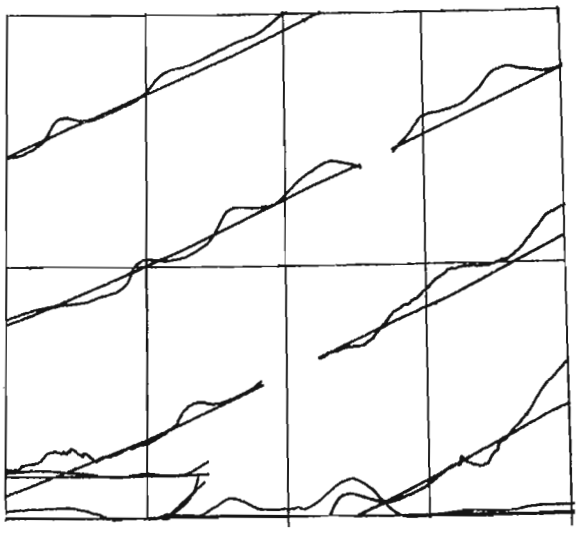

Figure 21.4

Contours of magnetic anomalies over the area bounded by 56N-57N and 52W-54W. Data gridded over a 30 by 30 matrix. Contour interval is 50 gammas.

A. 20-minute interval data. Gridded by triangular method

B. 20-minute interval data. Weighted by GPCP method

C. 20-minute interval data. Gridded by minimum curvature method

D. All data points pre-gridded and then weighted by GPCP method.

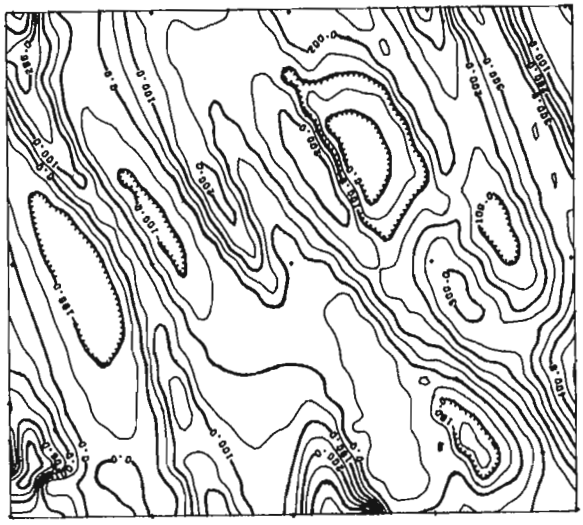

(A)

(B)

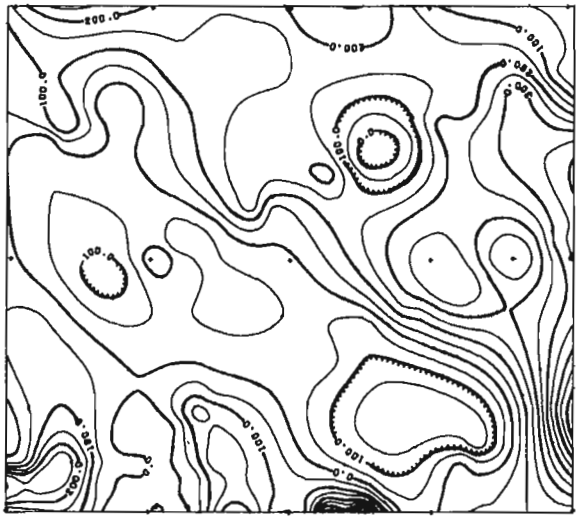

(C)

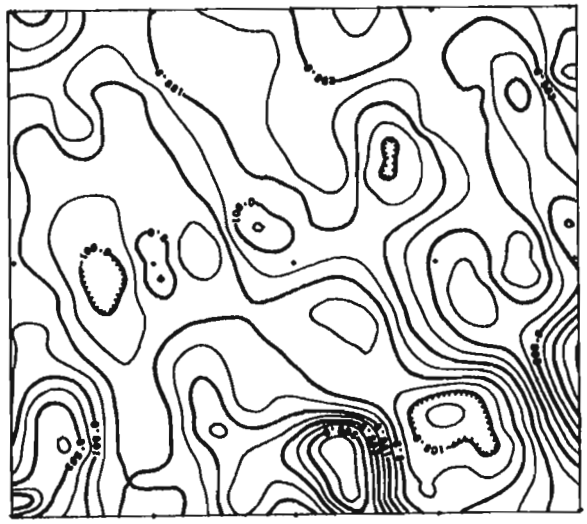

(D)

Figure 21.2 compares the outcome of four tests. With the given gridding parameters, all four methods were successful at portraying the positive and negative banding of the simulated field. The triangulation method came closest to replicating the straight contour lines that one would expect to see.

Comparison Studies with Real Data

Experiments were carried out with a number of real data sets. The contours for only two sets – one with 20-km track spacing, the other with 40-km spacing – are presented here because they are typical. Both sets consist of magnetic anomaly values in different parts of the Labrador Sea, with each set occupying a map area measuring one degree of latitude in the N-S direction, and two degrees of longitude in the E-W direction.

Figure 21.3 illustrates the 20-km data. With the given parameters, all the tested gridding methods gave similar results. Individually, the maps exhibit small differences, but generally all compare well with an existing hand-drawn contour map (Srivastava, 1979).

As shown in Figure 21.4, the contour maps produced from the 40-km data all contained artifacts: data gridded by the triangulation method displayed a pronounced trend perpendicular to the ship's tracks, while that gridded by other methods featured along-track 'puddles'. Clearly, automatic processes don't work well with this combination of track spacing and gridding parameters.

Conclusion

There are many options and approaches to the gridding of data for contouring purposes. The choice of the 'best' method can be very much a function of the nature and distribution of the data, and of the features that one wishes to bring out in the final contour plot. Rather than blindly select any gridding method, it behooves one to try several, in order to determine which technique yields the most accurate and realistic portrayal of the data.

From the results of our investigations to date, we have formulated the following rules of thumb to guide us in the selection of gridding methods for our contouring applications:

1. When the track spacing is greater than 20 km, no method is likely to give really satisfactory results. However, if one is determined to use automatic procedures, the best that one could hope to do is to select data points at intervals of 4 to 10 km, and to grid by the triangulation method.
2. When the track spacing is 10-20 km, satisfactory results are usually achievable with data points 2 to 5 km apart, and gridding by any of the methods described above.
3. When the track spacing is less than 10 km, data points selected 1 to 2.5 km apart and gridding with any of the above methods should yield a reasonable plot. If data points are very numerous in the plot area due to proximity of the tracks (2 to 5 km), pre-gridding may have to be considered.

With further experimentation, we expect to be able to refine these rules of thumb. We also plan to investigate other gridding procedures as well as some different contouring packages, to see if they are more suited to our kinds of data.

References

Akima, H.
1978: A method of bivariate interpolation and smooth surface fitting for irregularly distributed data points; ACM Transactions on Mathematical Software, v. 4, 148-159.

Braile, L.W.
1978: Comparisons of four random to grid methods; Computers and Geosciences, v. 4, 341-349.

Briggs, I.C.
1974: Machine contouring using minimum curvature; Geophysics, v. 39, 39-48.

California Computer Products, Inc.
1973: GPCP-II: A general purpose contouring program; Anaheim, California.

Falconer, K.J.
1971: A general purpose algorithm for contouring over scattered data points; National Physical Laboratory, Division of Numerical Analysis and Computing, Report NAC6.

Haworth, R.T.
1974: Gravity and magnetic Natural Resource Maps (1972) Offshore Eastern Canada – philosophy and technique in preparation by computer; International Hydrographic Review, v. 51, 131-155.

Hunter, C., Shih, K.G., and Macnab, R.
1982: A compilation of marine magnetometer data from the southwest Labrador Sea; Geological Survey of Canada Open File 850.

IMSL
1980: IMSL Library Reference Manual; IMSL, Inc. v. 2, IQHSCV-1.

Kuester, J.L. and Mize, J.H.
1973: Optimization Techniques with FORTRAN; McGraw-Hill, New York, 500 p.

Shih, K.G., Macnab, R., and Halliday, D.
1981: Multiparameter survey data from the Scotian Margin; Geological Survey of Canada, Open File 750.

Srivastava, S.P.
1979: Marine gravity and magnetic anomalies map of the Labrador Sea; Geological Survey of Canada, Open File 627.

Swain, C.J.
1976: A FORTRAN IV program for interpolating irregularly spaced data using the difference equations for minimum curvature; Computers & Geosciences, v. 1, 231-240.

22. HUMBER ARM ALLOCHTHON AT SOUTH ARM, BONNE BAY, WEST NEWFOUNDLAND

EMR Research Agreement 152-4-82

Louise Quinn [1] and Harold Williams [1]
Precambrian Geology Division

Quinn, L. and Williams, H., Humber Arm Allochthon at South Arm, Bonne Bay, west Newfoundland; in Current Research, Part A, Geological Survey of Canada, Paper 83-1A, p. 179-182, 1983.

Abstract

Correlatives of the Humber Arm Supergroup are represented in lower structural slices of the Humber Arm Allochthon at South Arm, Bonne Bay. The Bay of Islands and Little Port complexes occur in higher structural slices, and a chaotic zone with mountain-size blocks of igneous and metamorphic rocks borders the east side of the Table Mountain ophiolite slice.

The South Arm segment of the Humber Arm allochthon has relatively intact older sedimentary units to the east and chaotic younger sedimentary units to the west. Assembly of the allochthon involved the emplacement of higher igneous slices above the youngest uppermost parts of the Humber Arm Supergroup, with concomitant major mélange formation.

Introduction

Mapping of the Pasadena area (12 H/4) was completed in 1982 and investigations at South Arm, Bonne Bay were conducted by the first author as part of an M.Sc. thesis project. It is planned to continue mapping in the Lomond area (12 H/5) during 1983 in an attempt to cover the entire Humber Arm Allochthon (Williams, 1973; Schillereff and Williams, 1979; Williams and Godfrey, 1980; Williams, 1981; Williams, et al., 1982). The present report is concerned only with the geology of the Bonne Bay area.

The Bonne Bay area was mapped by Troelsen (1947) as part of a Ph.D. study, and also by Baird (1960) as part of the reconnaissance mapping of the Sandy Lake (12 H), west half, area. The ultramafic rocks of Table Mountain were mapped by Smith (1958), and parts of the area were mapped by Brinex during the mid 1950s.

The Bonne Bay area has rugged terrain that is heavily tree covered except for the barren ground developed upon higher parts of the Little Port Complex, and the bare flat topography characterizing the Table Mountain ophiolite slice. Much of the mapping was conducted along streams, many of which are steep with precipitous waterfalls toward their headwaters. Woods roads are useful in some places and a helicopter was used briefly to inspect the highest peaks east of Table Mountain. The area is accessible by gravel road from Wiltondale, which in turn is connected to the Trans Canada Highway at Deer Lake by a paved highway.

Acknowledgments

The authors acknowledge the able field assistance of Christine Furlong and Alex Pittman, and the many favours extended by Ella Manuel and Lisa Sorensen. We extend special thanks to Viking Helicopters, Newfoundland Limited, for their field support, and for providing 5 hours of free flying time as a scholarship to one of us (L.Q.).

General Geology

Rocks of the Bonne Bay area (Fig. 22.1) are part of the Humber Arm Allochthon, which is bordered to the east by autochthonous Ordovician rocks of the West Newfoundland carbonate terrane. At South Arm, lower structural slices of the allochthon are made up of sedimentary rocks that are correlatives of the Cambrian-Ordovician Humber Arm Supergroup (Stevens, 1965, 1970; Williams, 1975). Higher structural slices are represented by Cambrian-Ordovician ophiolitic rocks of the Little Port Complex and the Bay of Islands Complex. A chaotic zone of sedimentary rocks along the west side of Bonne Bay has mountain-size blocks of pillow lava and pillow breccia, and huge blocks of gabbro, amphibolite and serpentinite. Another mountain-size block of volcanic breccia and associated mafic dykes occurs on the east side of South Arm at the contact between units 3 and 5 (Fig. 22.1).

Autochthonous Rocks (Units 1 and 2)

Thickly bedded fossilferous grey limestones occur to the east of Gadds Harbour and along the Glenburnie-Wiltondale road just east of Barters Brook. These represent the top of the west Newfoundland carbonate sequence and they are typical of the Table Head and St. George groups (unit 1).

At Gadds Harbour, the limestones are overlain stratigraphically by thin- to medium-bedded sandstones and shales with crossbedding and grading (unit 2). These clastic beds are identical to the Goose Tickle autochthonous clastics beneath the Hare Bay Allochthon of the St. Anthony area (Cooper, 1937). The Gadds Point clastics are followed southwestward and structurally upward by a chaotic zone approximately 70 m wide (2b). It contains brecciated limestone blocks in a shale matrix at Gadds Point and internally disrupted black shale units farther southwest. Across a narrow exposure gap the chaotic rocks are followed southwestward by intact coarse greywackes (unit 3) of the Humber Arm Allochthon.

On the road at Barters Brook, rocks of unit 2 include limestone breccia, grey to green and black argillites, and argillites with buff silty laminae and local sandy beds (2a). The contact with carbonates of unit 1 farther east is unexposed, but extreme shearing in limestone breccias of unit 2 suggests faulting and a tectonic contact. Possibly the clastic rocks in this area are part of the Humber Arm Allochthon.

Humber Arm Allochthon (Units 3 to 10)

Sedimentary Rocks of Lower Structural Slices (Units 3 to 6)

Four units are recognized among sedimentary rocks of the Humber Arm Allochthon at Bonne Bay and these can be correlated lithologically with the five formations of the Humber Arm Supergroup in its type area at Humber Arm (Stevens, 1970). Formations of the allochthon in its type

[1] Department of Earth Sciences, Memorial University of Newfoundland, St. John's, Newfoundland, A1B 3X5

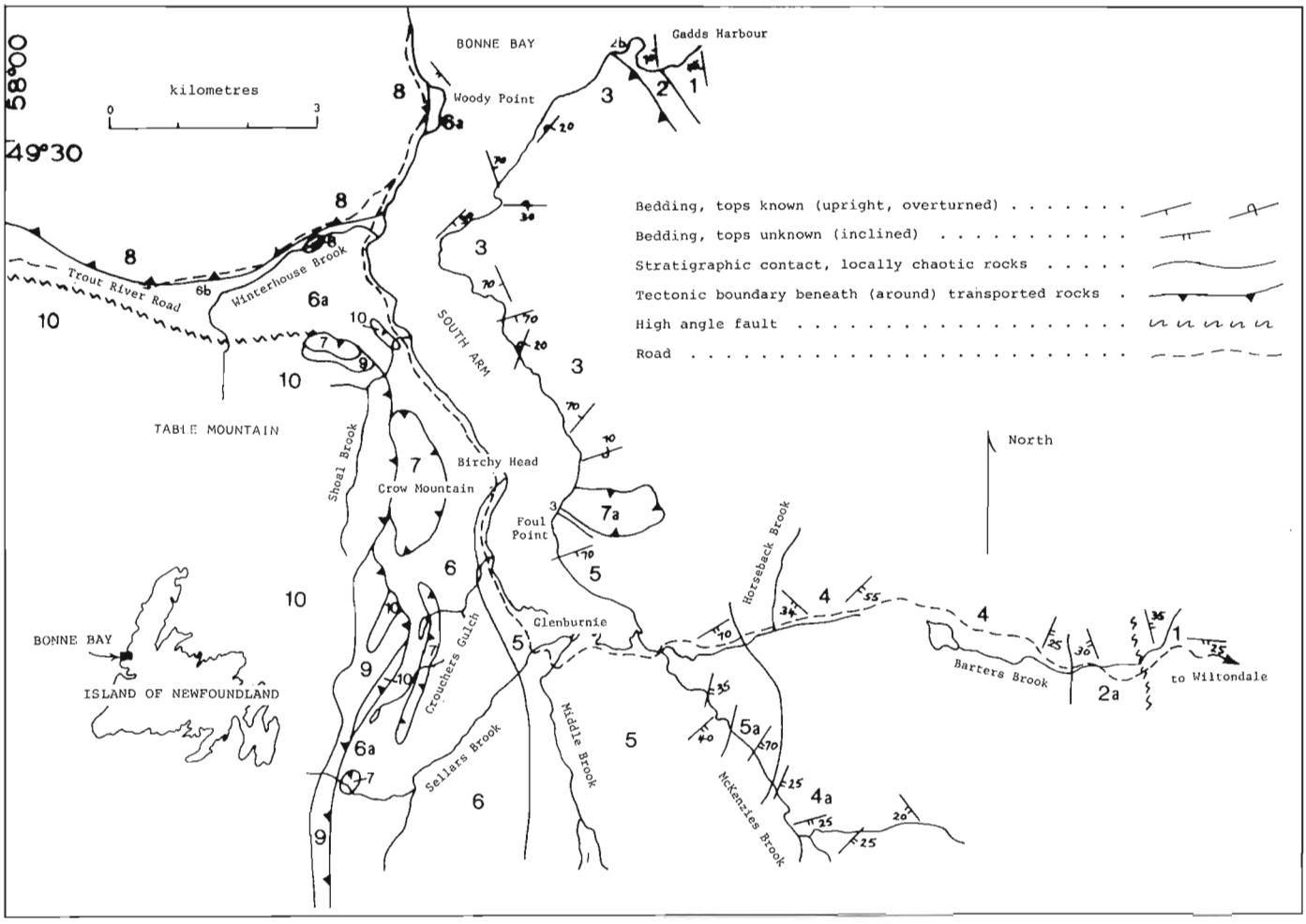

HUMBER ARM ALLOCHTHON

IGNEOUS AND METAMORPHIC ROCKS - HIGHER STRUCTURAL SLICES AND MOUNTAIN-SIZE OLISTOLITHS

LOWER ORDOVICIAN AND CAMBRIAN (?)

10 Bay of Islands Complex (9-10)
Mainly harzburgite, serpentinized ultramafic rocks and serpentinite.

9 Amphibolite, greenschist and quartz-feldspar gneiss

8 Little Port Complex (10)
Gabbro, amphibolite, mafic dykes and pillow lavas

7 Pillow lavas, mafic volcanic breccias and associated dykes, minor sedimentary rocks; 7a, pillow breccia and associated dykes

SEDIMENTARY ROCKS - LOWER STRUCTURAL SLICES

LOWER ORDOVICIAN TO CAMBRIAN AND LATE PRECAMBRIAN (?)

Humber Arm Supergroup (3-6)

6 Blow Me Down Brook Formation (Lower Ordovician)
Grey to green and pale pink-weathering greywacke, red and green shale and minor micaceous red sandstone; 6a, chaotic with sedimentary and igneous blocks; 6b, mainy black and green shales with blocks of greywacke, quartzite, limy siltstone and gabbro

5 Cooks Brook and Middle Arm Point Formations (Middle Cambrian to Lower Ordovician)
Thin bedded grey shales with interbeds of buff dolomitic siltstone and grey limestone; 5a, dark grey to green argillite with chaotic mixtures of buff-weathering limy siltstone and greywacke

4 Irishtown Formation (Lower to Middle Cambrian)
Dark grey to black shale with prominent thick quartzite units and conglomerate units; 4a, includes thin bedded limestones and siltstones of possible Cooks Brook affinity

3 Summerside Formation (Lower Cambrian to Late Precambrian)
Thick bedded greywacke, arkosic greywacke and conglomerate

AUTOCHTHONOUS ROCKS

MIDDLE ORDOVICIAN

2 Greywacke and shale; 2a, limestone breccias and shales, possibly allochthonous; 2b, chaotic shales at base of Humber Arm Allochthon

LOWER AND MIDDLE ORDOVICIAN

1 Table Head and St. George Groups
Mainly thick bedded limestones and dolomites, minor red and grey shales

Figure 22.1. *General geology of South Arm, Bonne Bay, area.*

area, from oldest to youngest are as follows: Summerside (late Precambrian to Cambrian), Irishtown (Lower to Middle Cambrian), Cooks Brook (Middle Cambrian to Lower Ordovician), Middle Arm Point (Lower Ordovician) and Blow Me Down Brook (Lower Ordovician).

Summerside Formation (Unit 3)

A continuous coastal section of greywackes on the east side of South Arm is correlated with the Summerside Formation of the Humber Arm Supergroup. The rocks directly overlie the authochthonous section at Gadds Point but they are absent in the roadside section above the autochthon to the south. At Foul Point, the contact between unit 3 greywackes to the north and sedimentary rocks of unit 5 to the south is interpreted as tectonic because of the occurrence of a possible volcanic block (7a) at the contact, the presence of chaotic rocks to the south of the volcanics, and the absence of unit 4.

The greywackes are thickly bedded with some beds exceeding 2 m. Grading is common and pebbly zones mark the base of most beds. Cobble to boulder conglomerates form thin local units, and a 5 m red shale unit is also present in the section. Clasts are mainly white to grey and blue quartz, pink feldspar, dark grey shale, and less commonly red chert and granite.

Dip reversals are common and inverted beds occur in homoclinal sections, implying complex internal structures.

Irishtown Formation (Unit 4)

A dark shale sequence with prominent white quartzite and conglomerate units between Horseback Brook and Barters Brook on the Glenburnie-Wiltondale road is correlated with the Irishtown Formation of the Humber Arm Supergroup. Relationships with adjacent units are unknown, but the western contact with unit 5 may be stratigraphic. The distinctive quartzite-conglomerate beds of unit 4 are not represented southward along McKenzies Brook, suggesting structural truncation of units 3 and 4 against the autochthon to the east.

Dark shales with thin buff-weathering limy layers and slightly thicker quartz-rich beds outcrop extensively in the roadside section. The shales exhibit small scale cross lamination in places, with local ripple marks and tubular marking on some bedding surfaces. Quartzites are thickly bedded with local ripple marks, cross lamination and channel structures. The rocks contain well sorted grains that are also well rounded.

Conglomerate units are poorly bedded with well rounded cobbles and boulders up to 45 cm diameter. A distinctive feature of the conglomerates is the occurrence of circular shale pockets up to one metre in diameter that contain rounded cobbles and boulders. Quartzites and limestones form the commonest boulders with sparse foliated metamorphic rock fragments and local dark shale clasts. Some of the limestone boulders are fossiliferous and one example contains button algae, which are distinctive of Lower Cambrian carbonates of western Newfoundland (Schuchert and Dunbar, 1934; Williams et al., 1982). Fossiliferous limestone boulder conglomerates like those of unit 4 are probable equivalents of fossiliferous limestone boulder conglomerates of the Irishtown Formation at McIvers of Humber Arm (Stevens, 1965; Williams, 1973).

Deformation in unit 4 is locally intense and some conglomerate beds appear as isolated exposures surrounded by strongly foliated shales.

A sequence of quartzites, shales and limy siltstones in McKenzies Brook (4a) may be an Irishtown equivalent, but relationships to unit 4 and strata to the west are unknown.

Cooks Brook and Middle Arm Point Formations (Unit 5)

Thinly bedded limestones and shales, buff-weathering limy siltstones and dark grey to black and green shales are correlated with the combined Cooks Brook and Middle Arm Point formations of Humber Arm. The rocks are best exposed south of Birchy Head along the west side of South Arm. They also occur south of Foul Point and in stream sections of Crouchers Gulch, Middle Brook, Sellars Brook and McKenzies Brook. Proportions of typical lithologies vary from place to place making further subdivision and sharper definition difficult. Beds are everywhere tightly folded and locally internally broken to chaotic. A contact between units 5 and 6 is well exposed at Birchy Head but the rocks there are chaotic suggesting a tectonic contact.

In Middle Brook and McKenzies Brook, quartzose sandstones occur as interbeds and disturbed blocks in thinly bedded shales. Also in McKenzies Brook a chaotic unit of disturbed dark grey and green argillite (5a) has buff-weathering blocks of limy siltstone, and greywacke blocks up to 3 m diameter.

Blow Me Down Brook Formation (Unit 6)

Thickly bedded greywackes with red and green shale units between Winterhouse Brook and Birchy Head are assigned to the Blow Me Down Brook Formation. Similar rocks are exposed in Winterhouse Brook, Sellars Brook and Crouchers Gulch. The rocks are grey to green and weather buff to pale pink. They consist of quartz, feldspar, shale fragments and detrital muscovite. Chaotic zones (6a) are common, especially near contacts with higher structural slices of igneous and metamorphic rocks.

A mélange zone (6b) is exposed in Winterhouse Brook and outcrops as a thin zone along the southern contact of the Little Port Complex. Blocks up to 3 m diameter consisting mainly of greywacke, quartzose sandstone, and limy siltstone are surrounded by black, red and green shale. A large outcrop of gabbro in Winterhouse Brook is interpreted as a 500 m diameter block, since contacts with surrounding sediments are sharp and lack features of intrusion. The gabbro resembles the nearby Little Port Complex and it contains pods of massive sulphide (pyrrhotite-pentlandite). A large serpentinite exposure at the mouth of Shoal Brook is also interpreted as a block. Other chaotic rocks are exposed north of Woody Point.

Igneous and Metamorphic Rocks of Higher Structural Slices (Units 7 to 10)

Discrete Volcanic Megablocks (Unit 7)

Several large volcanic blocks, three of which are one to two kilometres long, form conspicuous hills to the west of South Arm. These are mainly mafic pillow lavas and volcanic breccias with associated mafic dykes. Contacts are poorly exposed, except in Crouchers Gulch where a steep cliff of volcanic rocks is in close proximity to chaotic Blow Me Down Brook sediments.

Large mountain-size volcanic blocks such as the above are common all along the eastern margins of the Bay of Islands ophiolite massifs. A comparable situation to that of South Arm is represented along the east margin of the Blow

Me Down massif at Serpentine Lake (Williams and Godfrey, 1980; Godfrey, 1982) and farther southward along the east margin and at the southern end of the Lewis Hills massif (Schillereff and Williams, 1979; Schillereff, 1980; Williams, 1981).

Little Port Complex (Unit 8)

The Little Port Complex forms a structural slice above allochthonous sedimentary rocks in the northern part of the area. It consists of gabbro, amphibolite, mafic dykes and pillow lavas, plagiogranite and felsic volcanic rocks. A distinctive feature of the complex is the widespread brecciation of all lithologies.

The Little Port Complex is juxtaposed with red shales of unit 6 along the Trout River Road. The contact is tectonic with sheared and slickensided shales stuck to steep surfaces of mafic volcanic rocks, or locally commingled with the volcanic rocks. A similar steep contact between resistant igneous rocks and chaotic black and green shales is exposed in a tributary to Winterhouse Brook.

Bay of Islands Complex (Units 9 and 10)

Ultramafic rocks of the Bay of Islands Complex occur in the western part of the area at Table Mountain. The rocks are brownish weathering harzburgite and serpentinite that are essentially bare of vegetation. The base of the ophiolite slice is not exposed but a high angle tectonic contact between ultramafic rocks (10) and sediments (6) occurs in Winterhouse Brook. The contact is marked by a resistant 2 m wall of rodingite and a 20 m wide zone of serpentinite. The serpentinite is locally chaotic with randomly distributed harzburgite blocks.

A narrow dynamothermal aureole of mainly greenschist and amphibolite follows the east margin of the Table Mountain ophiolite from Upper Trout River Pond 8 km northward into the map area. The aureole terminates south of Crow Mountain where it is three times its normal width compared to occurrences farther south. A lense of ultramafic rocks occurs within the aureole amphibolites just south of Crow Mountain and a thin band of serpentinized ultramafic rocks occurs along the east side of the aureole west of Crouchers Gulch. This anomalous distribution of ultramafic rocks and aureole lithologies, and the excessive width of the aureole, either implies structural repetition of lithic units 9 and 10, or indicates dismemberment and juxtapositioning of blocks of ultramafic and aureole lithologies.

Summary

Easterly parts of the Humber Arm Allochthon at Bonne Bay consists of relatively intact older stratigraphic units of the Humber Arm Supergroup compared to more chaotic and younger sedimentary units to the west. The higher igneous slices of the Little Port Complex and Bay of Islands Complex directly overlie the chaotic younger sedimentary rocks. This implies that assembly of the allochthon involved the emplacement of higher igneous slices above the youngest and stratigraphically uppermost parts of the Humber Arm Supergroup. The presence of extensive chaotic mixtures toward the west implies major disruption and mélange formation concomitant with this phase of assembly of the allochthon.

References

Baird, D.M.
1960: Sandy Lake (west half) Newfoundland, Geological Survey of Canada, Map 47-1959.

Cooper, J.R.
1937: Geology and Mineral Deposits of the Hare Bay area; Newfoundland Department of Natural Resources, Bulletin No. 9, 36 p.

Godfrey, S.C.
1982: Rock groups, structural slices and deformation in the Humber Arm Allochthon at Serpentine Lake, western Newfoundland; unpublished M.Sc. thesis, Memorial University of Newfoundland, 182 p.

Schillereff, H.S.
1980: Relationships among rock groups within and beneath the Humber Arm Allochthon at Fox Island River, western Newfoundland; unpublished M.Sc. thesis, Memorial University of Newfoundland, 166 p.

Schillereff, H.S. and Williams, H.
1979: Geology of Stephenville map area, Newfoundland; in Current Research, Part A, Geological Survey of Canada, Paper 79-1A, p. 327-332.

Schuchert, C. and Dunbar, C.O.
1934: Stratigraphy of western Newfoundland; Geological Society of America, Memoir 1, 123 p.

Smith, C.H.
1958: Bay of Islands igneous complex, western Newfoundland; Geological Survey of Canada, Memoir 290, 132 p.

Stevens, R.K.
1965: Geology of the Humber Arm Area, west Newfoundland; unpublished M.Sc. thesis, Memorial University of Newfoundland.

1970: Cambro-Ordovician flysch sedimentation and tectonics in west Newfoundland and their possible bearing on a proto-Atlantic Ocean; in Flysch Sedimentology in North America, ed. J. Lajoie, Geological Association of Canada, Special Paper No. 7, p. 165-177.

Troelsen, J.C.
1947: Stratigraphy and structure of the Bonne Bay-Trout River area; unpublished Ph.D. thesis, Yale University.

Williams, H.
1973: Bay of Islands map-area, Newfoundland; Geological Survey of Canada, Paper 72-34, 7 p.

1975: Structural succession, nomenclature, and interpretation of transported rocks in western Newfoundland; Canadian Journal of Earth Sciences, v. 12, p. 1874-1894.

1981: Geological map of Stephenville map area, north half, southwestern Newfoundland; Geological Survey of Canada, Open File 726.

Williams, H. and Godfrey, S.C.
1980: Geology of Stephenville map area, Newfoundland; in Current Research, Part A, Geological Survey of Canada, Paper 80-1A, p. 217-221.

Williams, H., Gillespie, R.T., and Knapp, D.A.
1982: Geology of Pasadena map area, Newfoundland; in Current Research, Part A, Geological Survey of Canada, Paper 82-1A, p. 281-288.

23.

THE SEDIMENTOLOGY OF THE LOWER MORIEN GROUP NEAR PORT MORIEN, NOVA SCOTIA [1]

Contract 1583338

S. Dilles and B.R. Rust [2]

Dilles, S. and Rust, B.R., The sedimentology of the lower Morien Group near Port Morien, Nova Scotia; in Current Research, Part A, Geological Survey of Canada, Paper 83-1A, p. 183-186, 1983.

Also in Mineral Resources Division, Report of Activities, 1982, Nova Scotia Department of Mines and Energy, Report 83-1, 1983.

Abstract

The lower Morien Group (Westphalian C age) is an alluvial succession comprising two facies associations. The sandstone facies association occurs in the lower part of the succession and outcrops in the southern part of the study area. It is dominated by trough cross-stratified sandstone in fining-upward sequences with erosional bases; coal seams and mudstone units are rare. It is attributed to deposition on a distal sandy braidplain.

The alternating facies association is characterized by an alternation of fining-upward sandstone and coal-bearing mudstone sequences, the latter comprising one half to one third of the succession. The association is attributed to deposition by a meandering alluvial system, in which compaction of extensive muddy floodplain deposits maintained high water tables, and permitted accumulation of thick peat units.

Introduction

The Pennsylvanian Morien Group in the Sydney Basin of Cape Breton Island, Nova Scotia was divided into three zones by Bell (1938). These zones, recognized on the basis of their megaflora, were mapped across the eastern part of the basin by Hayes et al. (1938) and extended to the west by Bell and Goranson (1938). The two lower zones, the **Linopteris obliqua** and **Lonchopteris** zones are distinct from the upper, **Ptychocarpus unitus** zone by the presence of economic coal seams in the latter. According to Barss and Hacquebard (1967), the three megafloral zones correspond to distinct spore assemblages (Table 23.1).

This report is part of a large project which aims to establish lithostratigraphic subdivisions for the Morien Group throughout the Sydney Basin, and examine its sedimentology in detail. The report is based on the study of coastal sections, drill core and drillhole data from the lower two zones (the lower Morien Group) for the northeast coast of Cape Breton Island between Bateston (east end of Bateston Fault) and Cap Percé (Fig. 23.1). About 10 per cent of the coastal section is inaccessible even at low tide. These sections were studied by close-up reconnaissance from a boat, and by analysis of photographs. Over 150 rock samples were collected, including 80 for petrographic analysis, 30 for X-ray diffraction and 25 submitted to M.S. Barss, Atlantic Geoscience Centre, Geological Survey of Canada, for spore analysis. A 332 m core from the study area was logged, as were pertinent sections of two other cores from the area. As far as possible, the core data will be correlated with the coastal sections.

Structure

Hayes et al. (1938) mapped the structure of this area as a series of simple east-west folds, with a major east-west fault at the southern margin of the Morien Group outcrop (the Bateston Fault). The folds are locally asymmetric, notably the Cap Percé anticline and the Port Morien syncline (located 2 km to the southeast), whose northern limb dips up to 45 degrees, but whose southern limb dips at about 10 degrees.

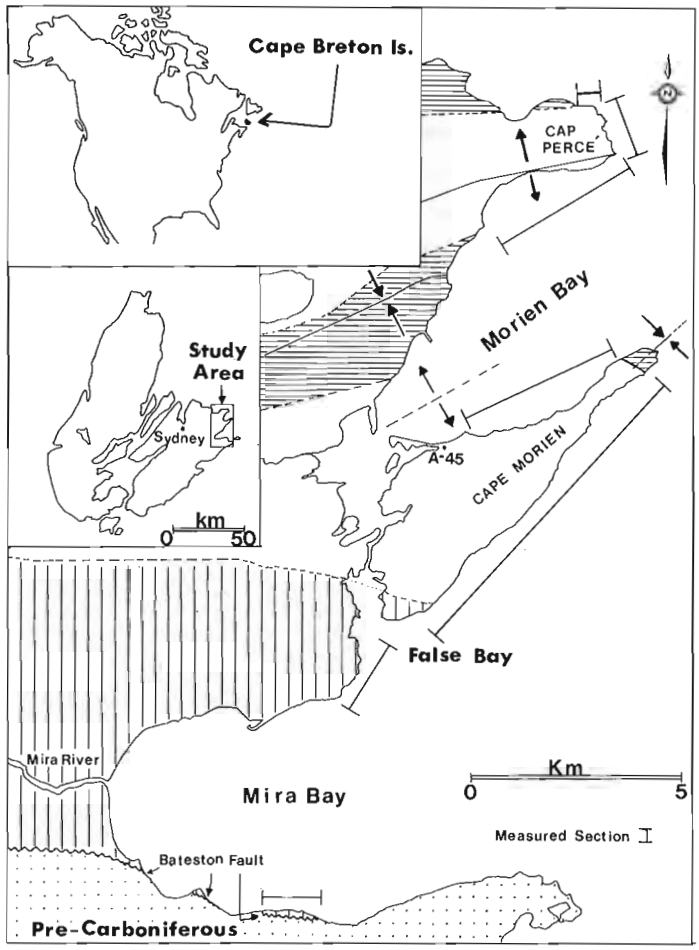

Figure 23.1. *Location map for eastern part of Sydney Basin. Horizontal ruling:* ***Pytchocarpus unitus*** *zone of Hayes et al. (1938); blank:* ***Linopteris obliqua*** *zone; vertical ruling:* ***Lonchopteris*** *zone. A-45 locates borehole from which core was measured.*

[1] Contribution to Canada-Nova Scotia Co-operative Mineral Program 1981-84. Project carried by Nova Scotia Department of Mines and Energy and by Geological Survey of Canada.

[2] Department of Geology, University of Ottawa, Ottawa, Ontario K1N 6N5 and Ottawa-Carleton Centre for Geoscience Studies.

Offshore drilling and geophysical work over the last decade have shown that the structure of the area is more complex, with several faults in Morien Bay (Hacquebard, in press). Another, previously unrecognized feature is the fact that the strike of strata on either side of Cape Morien indicates that the headland coincides with the axis of an eastward-plunging syncline. This necessitates the presence of an anticline in the southern part of Morien Bay. Apart from this complication, and some minor faults, the coastal sections are remarkable for their lack of tectonic disruption.

Stratigraphy

A summary of previous and existing stratigraphic nomenclature for the Morien Group in the Sydney Basin is given in Table 23.1. As discussed later, the lower part of the succession on the east coast, that extending south of False Bay is characterized by a sandstone-rich facies association. To the north of False Bay the strata comprise a facies association in which subequal sandstone and mudrocks alternate, commonly in erosionally-based, fining upward sequences.

The outcrop at Bateston is isolated from the main Morien Group outcrop by an extensive unexposed area. It is steeply dipping and partly overturned due to proximity to the Bateston Fault. The succession is predominantly sandstone, and its assignment to the lower part of the Morien Group by Hayes et al. (1938) seems appropriate.

The boundary between the middle (**Linopteris obliqua**) and the upper (**Ptychocarpus unitus**) zones of Hayes et al. (1938) was delineated at the base of the Spencer Seam, equivalent to the Emery Seam of the northern outcrops. This can also be regarded as a lithostratigraphic boundary, for it marks the lowest horizon of the more abundant economic coal seams in the upper part of the Morien Group. However, the east coast section discussed here does not reveal any significant difference between the clastic successions above and below the Spencer-Emery Seam. In any case, proper identification of lithostratigraphic units must await the completion of data analysis from the whole of the Sydney Basin.

Table 23.1

Table of stratigraphic units within the Morien Group (formerly Series) of Cape Breton Island, Nova Scotia

	Age	Robb 1876	Hayes, Bell and Goranson 1938	Barss and Hacquebard 1967
PENNSYLVANIAN	West-phalian D	Productive Coal Measures	**Ptychocarpus unitus** zone	**Thymospora** zone C
	West-phalian C	Millstone Grit	**Linopteris obliqua** zone	**Torispora** zone B
			Lonchopteris zone	**Vestispora** zone A

Facies Descriptions

The principal facies of the Morien Group in the Port Morien (located at south end of Morien Bay) area are as follows (after Miall, 1978):

Facies Gm. Massive to crudely stratified polymictic clast-supported conglomerate. Clasts are well rounded; quartz is the most abundant clast type. The facies occurs as thin lag deposits at some channel bases.

Facies Se. Erosional scours with intraclasts in a sandstone matrix are present at most channel bases. The sandstone is medium grained to granule-bearing; the intraclasts are commonly grey to tan coloured siderite nodules 0.5 to 2 cm in diameter. Less abundant are mudstone intraclasts, but carbonized plant fragments are common.

Facies St. Trough cross-stratified sandstone is the most abundant facies, forming the bulk of the channel deposits. The sandstone varies from fine to coarse grained, but is predominantly medium or fine. Troughs range in thickness from 3 to 70 cm, but are mostly between 10 and 25 cm thick.

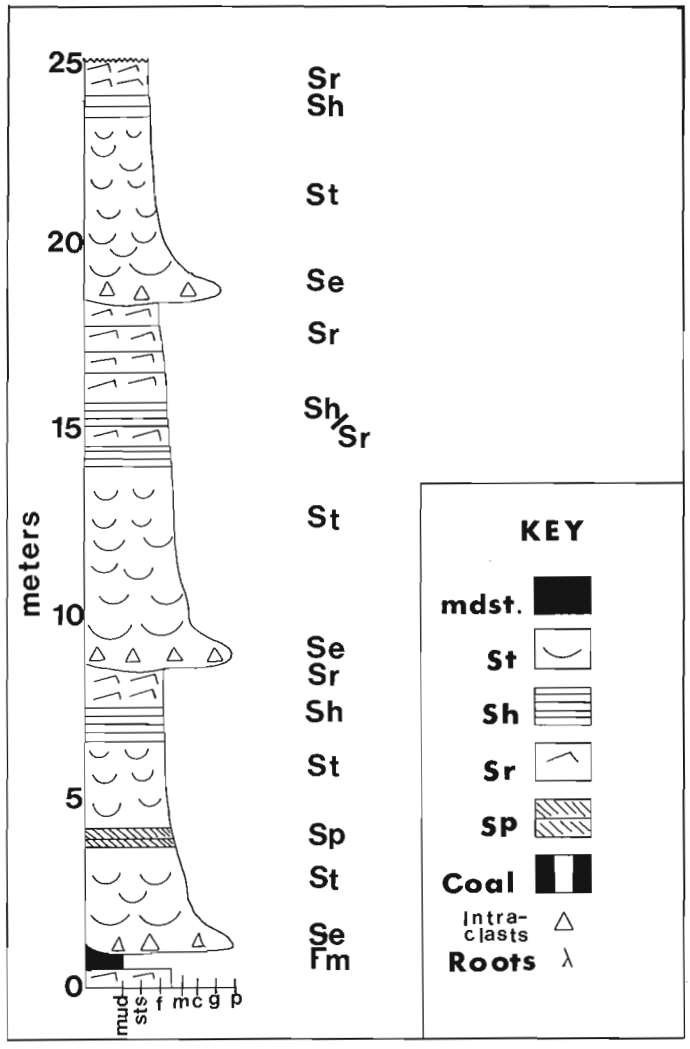

Figure 23.2. *Composite section of sandstone facies assemblage south of False Bay.*

Facies Sr. Ripple cross-laminated fine grained sandstone occurs towards the top of many channel-fill sequences (commonly interstratified with facies Sh), as well as in levee and crevasse-splay deposits. Ripples vary up to 3 cm in height. Some wavy-laminated fine sandstones are probably Sr units that have been deformed by compaction of interlayered thin mudstone units.

Facies Sh. Horizontally stratified fine grained sandstone commonly occurs interstratified with facies Sr in the upper parts of channel sequences. This facies is characterized by primary current lineation.

Facies Sp. Planar/tabular cross-stratified sandstone is a relatively uncommon facies. Sandstone grade varies from fine to coarse grained, and set thickness varies from 5 to 50 cm.

Facies Fl. This facies includes interlaminated fine grained sandstone, siltstone, and mudstone. The mudstone is commonly red to grey, with green mottles which commonly are tubular or spherical, resulting from differential reduction in relation to plant fragments or roots.

Facies Fm. This facies consists of massive red to grey mudstone, siltstone and silty fine sandstone. It contains desiccation cracks and rare raindrop imprints. Some units of this facies display a pattern of deep (up to 0.7 m) interconnected cracks, which may be a pedogenic feature.

Facies Fr. This facies consists of massive fine grained deposits with rootlets, interpreted as seat earths, even if no coal overlies them. The facies is common, although it does not form a large part of the succession.

Facies C. Coal recurs throughout the succession, in beds varying from less than 1 cm to 2 m in thickness. It commonly underlies channel sandstones.

Facies Associations

Two facies associations have been observed, one of which is sandstone-dominated, the other in which sandstone and mudrocks occur in approximately equal proportion. There is no faunal or sedimentological evidence for marine incursion in either association, and the repetition of paleosols, rooted horizons, raindrop imprints, mudcracks, and coals indicates terrestrial deposition.

The sandstone facies association is present in the 140 m succession south of False Bay, and at Bateston. The associated facies, in order of decreasing abundance are Se, St and Sr-Sh, with minor amounts of Sp and rare Fl-Fm, Fr and C. Figure 23.2 is a typical measured section from this facies association. It shows poorly defined upward-fining sequences, in which an erosion surface (Se) is overlain by trough cross-stratified sandstone (St) and minor fine grained facies. The succession resembles facies association S_{II} of Rust (1978), and is interpreted as the deposit of a distal braided fluvial system. A modern analogue is the South Saskatchewan River described by Cant (1978), although the lateral extent of the Morien Group indicates that it was deposited on a braidplain. Locally, the plain probably showed transition to a meandering channel pattern.

To the north of False Bay the assemblage contains a significantly higher proportion of mudrocks (Fig. 23.3). Facies St, Sh, Sr and Fl-Fm are dominant, with minor amounts of facies Se, Sp, Fr and C. Sequences within the succession are generally clearly differentiated into channel or overbank deposits. Facies St is dominant in channel sequences, within which it is commonly interspersed with facies Sh, and fines upward to Sr. Facies Sr also occurs in levee sequences, characterized by upright tree trunks, and in crevasse-splay sequences. Facies Sh is also present in levee and crevasse-splay sequences, together with the Fm-Fl combination. The latter is the dominant facies of overbank sequences away from levee and crevasse-splay sandstones. Lesser amounts of seatearth and coal are also found in overbank sequences, commonly close to or immediately beneath the succeeding channel sandstone.

The facies association described above is attributed to deposition by an alluvial system dominated by meandering channels. Channel accretion by lateral migration is confirmed by the presence of lateral accretion surfaces in several of the channel sequences.

Approximately 300 paleocurrent readings were recorded from facies St, Sr and Sh in the Morien Group of the Port Morien area. Figure 23.4 shows the data for trough cross-strata, because these are considered to be the most reliable of the paleocurrent indicators present. The mean orientation is towards the north (019°) with a vector magnitude of 83 per cent. The crossbed data indicte that paleoflow from the south or southwest was maintained throughout deposition of the Morien Group in this area. A similar picture is emerging for the whole of the Sydney Basin, although analysis is not yet complete.

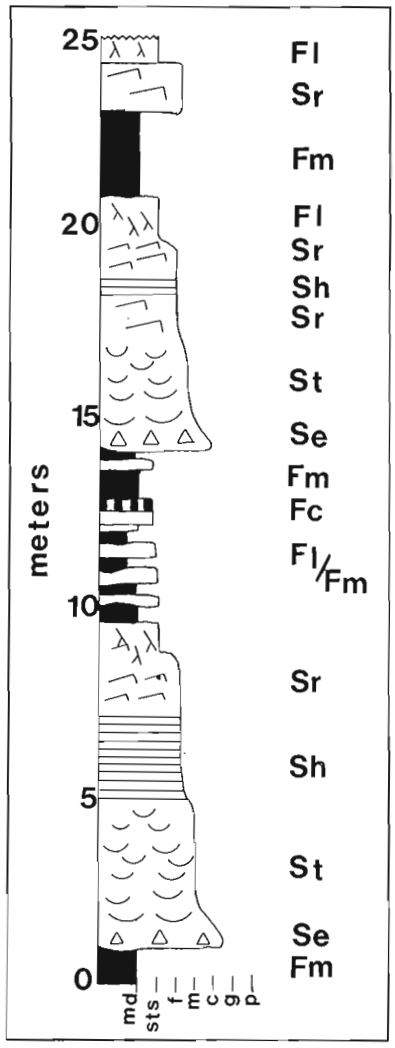

Figure 23.3. Composite section of alternating facies assemblage north of False Bay.

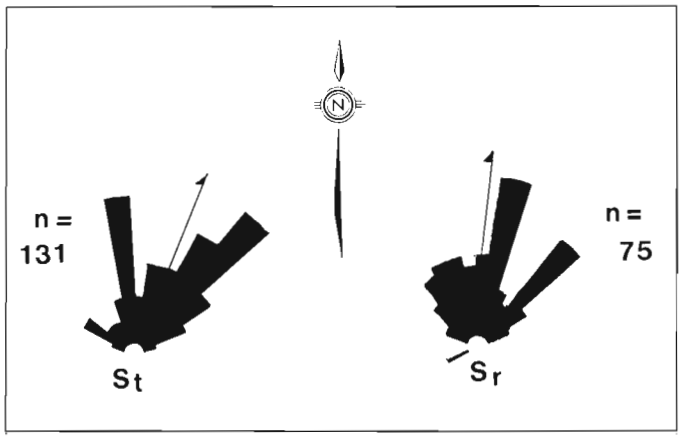

Figure 23.4. Paleocurrent data from east coast sections between Cap Percé and Mira River based on trough cross-strata (facies St) and ripple cross-lamination (facies Sr). Arrows indicate mean vector azimuth, n indicates number of observations.

The Morien Group succession at the eastern margin of the Sydney Basin shows an upward change from a distal sandy braidplain to an alluvial plain with fewer, larger, high-sinuosity channels. As this change took place, there was a significant increase in the proportion of the alluvial plain on which fine grained sediment accumulated. The thickness of fine grained sequences also increased. As a result, local compaction of sediment became an increasingly important factor in the evolution of the basin, superimposed on continuing regional subsidence. Compaction produced depressions on the floodplain in which plant material accumulated, in some cases to the extent that thick, widespread peat was formed. At the present time it is not clear why the conditions for peat accumulation became more frequent and lasted longer during late Morien times, in contrast to the apparently similar preceding environment. However, it is expected that integration of data from all parts of the Sydney Basin will aid in answering this question.

Further Work

The large amount of data collected during 1982 has not yet been fully analyzed. The remaining tasks are:

1. completion of stratigraphic sections: coast and boreholes;
2. correlation of coastal and borehole sections throughout the area and into the rest of the Sydney Basin; and
3. petrographic and XRD analysis of lithological specimens. In addition to better description of facies types, this analysis will be used to investigate diagenetic history.

References

Barss, M.S. and Hacquebard, P.A.
1967: Age and stratigraphy of the Pictou Group in the Maritime Provinces as revealed by fossil spores; Geological Association of Canada, Special Paper 4: p. 267-282.

Bell, W.A.
1938: Fossil flora of the Sydney coalfield, Nova Scotia; Geological Survey of Canada, Memoir 215, 334 p.

Bell, W.A. and Goranson, E.A.
1938: Sydney Sheet, East Half, Nova Scotia; Department of Mines and Resources, Canada, Map 361A.

Cant, D.J.
1978: Development of a facies model for sandy braided river sedimentation: Comparison of the South Saskatchewan River and the Battery Point Formation; in Fluvial Sedimentology, editor A.D. Miall; Canadian Society of Petroleum Geologists, Memoir 5, p. 627-639.

Hacquebard, P.A.
Geologic development and economic evaluation of the Sydney Coal Basin, Nova Scotia; Compte Rendu, Carboniferous Congress, Urbana, Illinois. (in press)

Hayes, O.A., Bell, W.A., and Goranson, E.A.
1938: Glace Bay Sheet, Nova Scotia; Department of Mines and Resources, Canada, Map 362A.

Miall, A.D.
1978: Lithofacies types and vertical profile models in braided river deposits: a summary; in Fluvial Sedimentology, editor A.D. Miall; Canadian Society of Petroleum Geologists, Memoir 5, p. 597-604.

Robb, C.
1876: Report on explorations and surveys in Cape Breton, Nova Scotia; in Report of Progress for 1874-75; Geological Survey of Canada, p. 166-266.

Rust, B.R.
1978: Depositional models for braided alluvium; in Fluvial Sedimentology, editor A.D. Miall, Canadian Society of Petroleum Geologists, Memoir 5, p. 605-625.

24. LES POLIS GLACIAIRES AU TÉMISCAMINGUE: UNE CHRONOLOGIE RELATIVE

Projet 770030

J.J. Veillette
Division de la science des terrains

Veillette, J.J.; Les polis glaciaires au Témiscamingue: une chronologie relative; dans Recherches en cours, partie A, Commission géologique du Canada, Etude 83-1A, p. 187-196, 1983.

Résumé

Des mesures de marques d'écoulement glaciaire levées à 602 endroits sur le substratum rocheux d'une région de plus de 8 200 km², centrée sur le lac Témiscamingue permettent de proposer qu'au moins 3 directions d'écoulement différentes, autant par leurs caractéristiques propres que par l'âge de leur mise en place, ont affecté la région. Une direction ancienne ouest-sud-ouest, une direction intermédiaire sud-ouest, et des écoulements plus récents vers le sud et le sud-est ont été déduites des mesures de terrain. La présence de 2 tills superposés, la dispersion d'indicateurs lithologiques et la distribution de moraines et d'eskers confirment ces directions. La synthèse de ces données est à la base d'un nouveau modèle de déglaciation proposé pour la région.

Une analyse des mesures d'orientation de marques et de microformes du poli glaciaire, surtout des stries, relevés à 602 endroits à l'intérieur d'une région centrée sur le lac Témiscamingue, permet de proposer une chronologie relative pour les principaux écoulements glaciaires de la région. Des données sur la stratigraphie des sédiments meubles (till), sur la distribution des principales moraines et de certaines accumulations fluvioglaciaires de même que sur la distribution d'indicateurs lithologiques sont présentées de façon très sommaire comme complément à l'étude des polis glaciaires. Ces derniers aspects feront l'objet d'études ultérieures plus complètes. La plupart des données de terrain sur la partie ontarienne de la région ont été acquises pendant l'été 1982. Du côté québécois, les observations remontent aux étés 1978 et 1981.

La région étudiée et le pourquoi de la méthode choisie

D'une superficie d'environ 8 200 km² la région comprend un peu plus de 9 feuillets au 1:50 000 et englobe la totalité des rives du lac Témiscamingue tant du côté québécois qu'ontarien (fig. 24.1). La plaine de Cobalt, les hautes terres de l'Abitibi et les hautes terres laurentidiennes constituent les grandes zones physiographiques (Bostock, 1970). Le substratum rocheux, presqu'exclusivement d'origine précambrienne, est aussi subdivisé en trois provinces géologiques: Grenville, Supérieure et du Sud. La province du Sud, caractérisée ici surtout par des roches aphébiennes couvre une importante superficie de la région. On y trouve le diabase de Nipissing de part et d'autre du lambeau de roche paléozoïque au nord-ouest du lac Témiscamingue, les quartzites de la formation de Lorrain et les conglomérats de la formation de Gowganda du groupe de Cobalt, et, dans une moindre mesure, les granites et granodiorites archéens. De même, des granodiorites et gneiss archéens constituent les roches principales de la province Supérieure. Enfin les gneiss à hornblende et à biotite de l'Archéen occupent la plus grande partie de la province de Grenville au sud-est.

Un élément particulier de la géologie locale est la présence d'un lambeau de roches paléozoïques, les seules dans un rayon de 225 km. Lovell et Caine (1970) ont désigné du nom de "Temiskaming Rift Valley" un système de failles orientées NW-SE (fig. 24.1) dont la partie intérieure, centrée sur le lac Témiscamingue et sont extension vers le nord-ouest, est un grabben dans lequel les roches paléozoïques auraient été protégées de l'érosion. À part le lambeau principal au nord-ouest du lac, on trouve des petites parcelles dans le voisinage de Haileybury et à quelques endroits du côté québécois. Ces roches, d'âge dévonien et silurien, constituées de calcaire, de dolomies, de grès, de shales et de siltstones, donc lithologiquement très différentes des roches précambriennes avoisinantes, font d'excellents indicateurs d'écoulement glaciaire. Il est possible que du côté québécois l'épaisse couverture de sédiments lacustres masque d'autres sub-affleurements de ces roches.

À l'exception d'une bande au sud de la carte, la cartographie préliminaire des sédiments superficiels à l'échelle du 1:50 000 est maintenant complète. La répartition de ces travaux, faits par la Commission géologique du Canada et par la Commission géologique de l'Ontario apparait sur la figure 24.1. La région fait partie de la petite enclave argileuse du nord-est ontarien et du nord-ouest québécois et occupe une partie importante du bassin du lac proglaciaire Barlow (Wilson, 1979). Les eaux de ce lac ont atteint une altitude de 365 m dans la portion centrale-nord du territoire et au moins 275 m dans la partie sud-est. Au sud-ouest, aux environs du lac Témagami, il est probable que les eaux du lac proglaciaire Algonquin aient inondé les bassins ouverts aux eaux proglaciaires à moins d'environ 305 m d'altitude. Avec environ 80% du territoire situé à moins de 300 m d'altitude ces transgressions glaciolacustres ont probablement eu comme résultat de détruire, masquer ou tout au moins de modifier considérablement de nombreuses macroformes morainiques, fluvioglaciaires ou encore celles résultant de l'abrasion glaciaire. À cause de ces contraintes une étude basée uniquement sur l'examen des formes de terrain à partir de photographies aériennes et même de levés sur le terrain, aussi minutieux que soit ce travail, ne suffirait pas à dégager l'orientation et la direction de l'écoulement glaciaire de façon nette. C'est pourquoi une attention toute particulière a dû être accordée aux microformes de l'écoulement glaciaire. Lamarche (1971, 1974) a démontré le bien fondé de cette méthode pour élucider un problème impliquant plus d'une seule direction d'écoulement glaciaire.

Les travaux antérieurs

Les travaux géologiques où l'on rapporte des mesures de polis glaciaires relevées à divers endroits du territoire sont assez nombreux mais nul d'entre eux n'avait comme but spécifique un inventaire complet et systématique de ces microformes. Jusqu'à maintenant une vision intégrée des différentes manifestations de la déglaciation du Témiscamingue n'était pas possible, faute d'une bonne compréhension de la chronologie relative des différents écoulements glaciaires. C'est à Barlow (1899) que revient le mérite d'avoir dressé les premières listes de mesures de stries, d'avoir reconnu plus d'une direction d'écoulement glaciaire et finalement d'avoir suggéré un retrait plus tardif

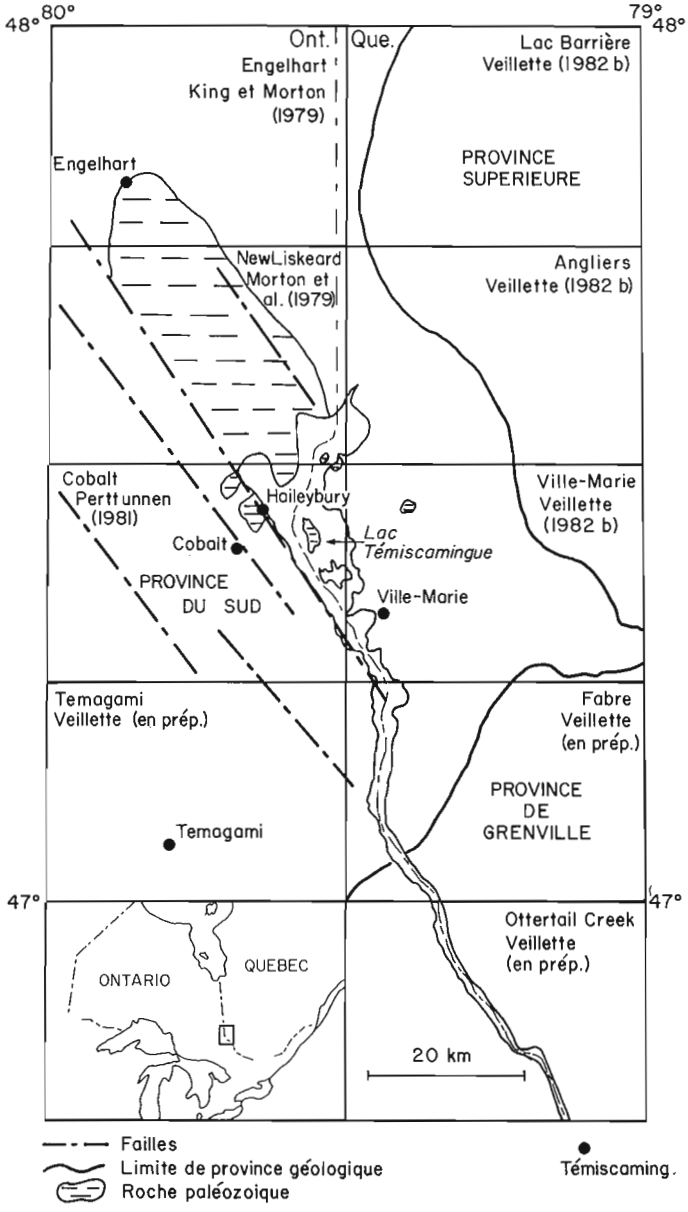

Figure 24.1. *Localisation de la région étudiée. La carte montre les limites des provinces structurales du Précambrien, les grandes failles, et la distribution des sédiments paléozoïques. Les 9 feuillets au 1:50 000 qui constituent la région sont indiqués, de même que l'auteur ou les auteurs de chacune des cartes des sédiments de surface, leur année de publication ou le stage des travaux en cours.*

des glaces dans l'auge du lac Témiscamingue. A. Murry avait, dès 1846, rapporté des mesures de stries dans la partie nord du lac Témiscamingue, mais ses observations étaient limitées aux rives immédiates du lac (Geological Survey of Canada, 1863). Sabourin (1957) montrait sur sa carte glaciaire de l'époque des stries vers le sud-est dans l'axe du lac Témiscamingue. Plus tard Thomson (1965), au cours de campagnes de cartographie de la roche en place à l'extrémité nord-ouest du lac Témiscamingue, notait des stries indiquant un fléchissement du sud-est vers l'est de l'écoulement glaciaire. Boissonneau (1968) a rapporté aussi quelques stries à divers endroits à l'intérieur de la région. Lovell et Caine (1970) ont établi une compilation sommaire de stries mais ont semblé rattacher celles-ci uniquement à des phénomènes d'avancées des glaciers localement influencés par la topographie.

Parmi les travaux plus récents ayant comme objectif immédiat une meilleure connaissance de la géologie du Quaternaire il est surprenant de noter le peu d'attention accordé aux polis glaciaires. Vincent (1971) a relevé quelques stries à l'est du lac Témiscamingue dans la région de Ville-Marie au cours d'une campagne de cartographie des sédiments superficiels dans ce secteur. Morton et al. (1979), King et Morton (1979), qui ont dressé les cartes des sédiments superficiels de New Liskeard et d'Engelhart pour le compte de la Commission géologique de l'Ontario ont à peu près totalement ignoré les marques d'écoulement glaciaire de ces régions. Perttunnen (1981) a, par contre, présenté un relevé adéquat des marques d'écoulement glaciaire de la carte de Cobalt et a reconnu la présence d'écoulements d'âges différents aux environs de Cobalt. Veillette (1982 a et b et sous presse) a présenté des données sur l'écoulement glaciaire du côté québécois du lac Témiscamingue montrant la présence d'au moins deux directions principales d'écoulement dans les cartes du lac Barrière, d'Angliers et de Ville-Marie. Enfin des travaux récents sur les polis glaciaires menés pour fins d'exploration minière (J. Brunet, 1982, Monopros Ltd., comm. pers.) confirment la complexité de l'écoulement glaciaire à l'est de la partie nord du lac Témiscamingue et appuient les directions d'écoulement que nous avons proposées pour ce secteur.

La méthode de terrain

Seuls les sites montrant de façon nette et distincte, des stries, cannelures, ou des queues-de-rat ont été cartographiés. De même un effort particulier a été fait pour ne retenir que les mesures obtenues sur des surfaces lisses et planes ou légèrement inclinées, afin d'éviter les irrégularités d'écoulement dues à la morphologie de l'affleurement. Il n'a pas toujours été possible d'observer des marques ou microformes indiquant une direction d'écoulement certaine à chacun des sites portés sur la carte. À défaut de queue-de-rat, de tête-de-clou, ou de "chattermarks" les faces de débitage et la morphologie générale de l'affleurement ont servi à déterminer les directions d'écoulement. Dans certains secteurs où les microformes indicatrices de direction étaient rares cette lacune a été parfois partiellement compensée par un plus grand nombre de mesures à faible distance les unes des autres.

Plusieurs sites qui ne montrent que des formes profilées et altérées souvent avec des axes longitudinaux plus ou moins nets ont été décrits et même des mesures d'orientation y ont été levées, ceci dans des régions où de bons exemples de microformes sont rares. Toutefois, ces mesures n'ont pas été cartographiées et ne servent pas à définir les écoulements glaciaires.

Il a donc fallu, à cause de ces critères de sélection s'abstenir de cartographier des mesures à de nombreux sites présentant des orientations semblables à celles des sites choisis. Cette discrimination dans les données de terrain ne peut que donner plus de poids à l'analyse.

En général, dépendant de la lithologie, seulement un affleurement ou une zone d'affleurements sur trois visités rencontraient les critères énumérés plus haut. Malgré ces restrictions, des mesures d'orientation et de direction furent levées à 602 sites. Pour des raisons d'échelle et parce que plusieurs de ces mesures sont répétitives, environ 40% des sites n'apparaissent pas sur la fig. 24.2.

Les principales directions d'écoulement glaciaire

Sans tenir compte de la chronologie relative des écoulements, l'examen rapide de la figure 24.2 révèle trois directions d'écoulement principales: une vers l'est-sud-est, une autre vers le sud et une vers l'ouest-sud-ouest. En fait les nombreux exemples de stries entrecroisées et

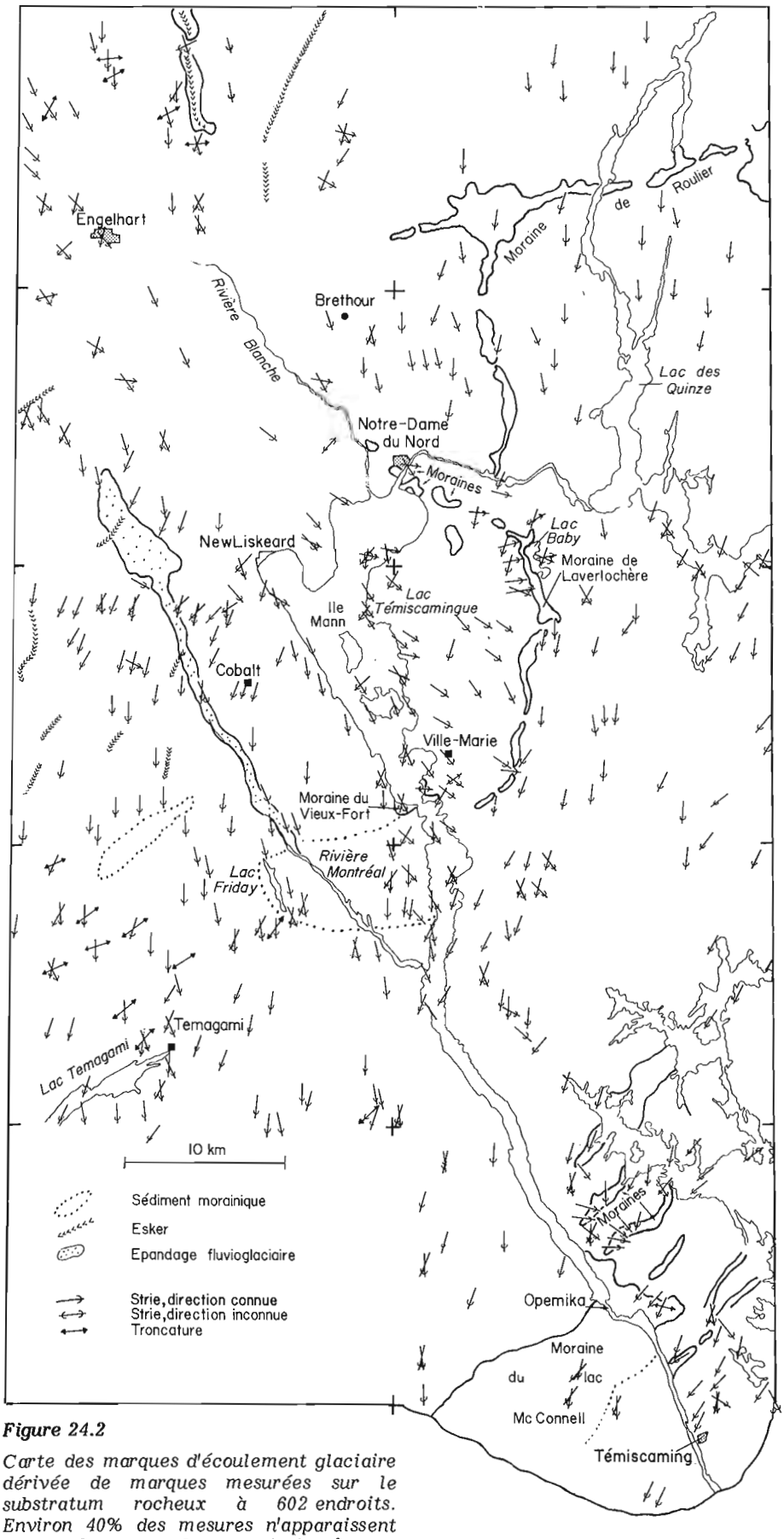

Figure 24.2

Carte des marques d'écoulement glaciaire dérivée de marques mesurées sur le substratum rocheux à 602 endroits. Environ 40% des mesures n'apparaissent pas sur la carte. Les principales formes de terrain, moraines et eskers, sont indiquées.

d'affleurements tronqués et façonnés laissent entrevoir la possibilité de 5 directions d'écoulement différentes dans le temps.

L'écoulement le plus ancien

Les preuves d'un écoulement ancien, ouest-sud-ouest, se rencontrent dans les régions d'Engelhart et de Témagami (partie ouest). Les affleurements montrant de 2 à 3 surfaces planes polies et tronquées, avec la surface marquée par le dernier mouvement glaciaire mieux striée et plus polie que les autres surfaces, sont nombreux. En étudiant d'abord des affleurements fraîchement dégagés de leur couverture de sédiments meubles comme on en trouve dans les fonds de gravières, le long des chemins forestiers, fossés, etc. ..., il a été possible de mesurer l'orientation de plans tronqués et en certains cas de stries entrecroisées dans des situations qui laissaient peu de doute quant à la chronologie relative des écoulements glaciaires responsables de leur modelé. À partir de l'identification de ces affleurements – types bien conservés et non altérés, il a été plus facile de repérer et d'analyser les sites où ces relations étaient moins évidentes (fig. 24.3A, 24.3B). Dans certains cas ce façonnement a été tellement prononcé que des affleurements de grandes dimensions et considérablement altérés montrent encore une dissymétrie évidente, et des axes de troncature bien préservés.

L'aptitude des affleurements à retenir les marques d'écoulement glaciaire est influencée par la lithologie. Les granites, quartzites, argilites et conglomérats de la région se prêtent bien au façonnement par les glaces tandis que les gneiss, paragneiss, basaltes ou diabases s'y prêtent moins bien. Malgré ceci, des surfaces tronquées bien dévelopées ont été observées sur presque tous les types de roches de la région.

La granodiorite et le monzonite quartzique du batholite à l'ouest du village d'Engelhart portent plusieurs surfaces tronquées, bien que les stries y soient parfois mal préservées. Dans cette région, 8 sites portant chacun de 2 à 3 directions d'écoulement glaciaire avec l'une d'elle associée à un mouvement ancien ouest-sud-ouest, furent choisis pour tenter d'établir un azimuth moyen pour ce mouvement. L'orientation des axes de troncature varie de 215° à 275°, avec une valeur médiane de 240° et à deux endroits les surfaces anciennes sont striées: l'une à 236° et l'autre à 240°. Tous les affleurements montrent des stries "fraîches" vers le sud-est.

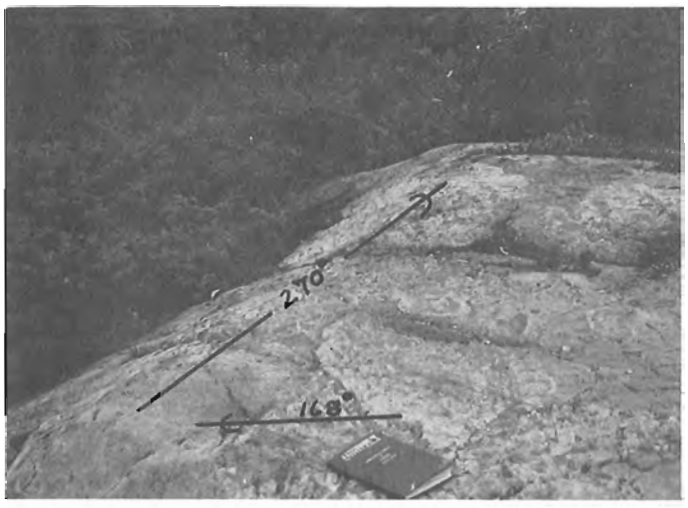

Figure 24.3A. *Affleurement altéré de conglomérat de Gowganda, région d'Engelhart. Trois écoulements ont marqué la roche: le plus ancien selon un azimuth de 270°, une direction intermédiaire à 215° et une dernière à 168°. La direction à 215° n'apparait pas sur la photo. Photographie CGC 203506-U.*

Figure 24.3B. *Affleurement altéré montrant des plans tronqués, région d'Engelhart, l'axe de troncature principal est orienté à 230°. Photographie CGC 203506-P.*

Un secteur de la partie ouest de la carte de Témagami comprend aussi plusieurs affleurements qui montrent 2 ou 3 surfaces tronquées, associées à des directions d'écoulement glaciaire différentes. Douze sites montrent un mouvement ancien avec des azimuth entre 210° et 261° et une valeur médiane de 230°. On les retrouve aux environs des lacs Jackpine, Anima-Nipissing et Thieving Bear. Plusieurs de ces surfaces anciennes ont aussi préservé des stries, généralement à l'intérieur de larges cannelures sur le flanc situé à l'aval d'un écoulement glaciaire plus récent. Dans ce secteur la direction 230° est généralement recoupée par un mouvement plus jeune vers 180° et 190°. Le granite local semble favoriser le développement de ces surfaces façonnées (fig. 24.4).

À quelques autres endroits isolés du territoire délimité par la figure 24.2, on observe des troncatures dont l'orientation ouest-sud-ouest des axes s'apparente à celles des secteurs de Témagami et d'Engelhart. Avec les données actuelles il n'est pas possible de déterminer si ces directions préférentielles relèvent d'un unique écoulement ancien ouest-sud-ouest qui aurait affecté l'ensemble de la région, ou si elles résultent de phénomènes purement locaux. La possibilité d'un écoulement ancien n'ayant laissé de traces que localement ne peut être rejetée.

Figure 24.4. *Affleurement de granite au nord-ouest de Témagami, avec troncature orientée à 246° et un mouvement glaciaire à 190°. Photographie CGC 203506-I.*

L'écoulement d'âge intermédiaire

L'écoulement glaciaire qui occupe l'éventail de direction de 180° à 210° est celui qui a laissé de plus de traces. C'est aussi le mouvement glaciaire le mieux documenté de la région. Il semble être responsable de la majeure partie du transport des débris glaciaires. La fosse tectonique du lac Témiscamingue, même avec sa rive ouest très escarpée, n'a probablement pas constitué une entrave importante au mouvement des glaces de cet écoulement intermédiaire. De part et d'autre du lac, on retrouve la même direction sud-sud-ouest.

Cet écoulement est étroitement lié au dernier écoulement sud-sud-est ayant marqué la région. Aux abords immédiats du lac et dans la fosse tectonique se prolongeant de New Liskeard au-delà de Engelhart vers le nord-ouest, la majorité des affleurements qui ont bien survécu à l'altération chimique portent les marques de ces deux écoulements. Ces surfaces tronquées et striées laissent peu de toute, étant donné la constance des orientations qu'elles exhibent, quant à la direction des écoulements responsables de leur morphologie (fig. 24.5A, 24.5B, 24.5C).

L'orientation de cette direction d'âge intermédiaire est difficile à distinguer de celle liée à l'écoulement occupant l'extrémité nord-est de la région. L'écoulement dans ce secteur a une forte composante sud et ne correspond pas à la direction sud-sud-ouest observée ailleurs. Un relevé plus détaillé des polis glaciaires dans ce secteur pourrait peut-être apporter certains éclaircissements.

Figure 24.5. *Exemples de stries entrecroisées et de surfaces tronquées impliquant l'écoulement d'âge intermédiaire et un écoulement plus récent.*

A. Roche métavolcanique à l'ouest d'Engelhart montrant une direction d'écoulement à 188° recoupée par un mouvement à 139°. Des stries orientées à 188° ont été protégées sur la paroi à l'aval de la direction 139°. Photographie CGC 203506 -U.

B. Roche métavolcanique au sud-est de Brethour, carte de New Liskeard portant une large cannelure et des stries à 200° recoupées par des stries à 170°. Photographie CGC 203506-T.

C. Quartzite de la formation de Lorrain à l'est de Fabre portant une surface striée à 210°, tronquée par une surface sriée à 166°. Photographie CGC 203506-N.

Les écoulements plus récents

Les preuves de ces écoulements sont abondantes partout aux abords du lac Témiscamingue et dans la fosse tectonique au nord-ouest du lac. Les directions de 140° et 170° dominent mais localement sur la rive est du lac Témiscamingue et jusqu'aux environs du lac Baby les sites montrant des directions de 85° à 140° sont nombreux (fig. 24.2). Ces écoulements, vers l'est-sud-est recoupent l'écoulement d'âge intermédiaire partout jusqu'au niveau du rétrécissement d'Opémika. À l'ouest du lac Témiscamingue aux environs de Cobalt et au nord de la rivière Montréal, on trouve par endroits des stries de 215° à 225° recoupant le mouvement d'âge intermédiaire de 180° à 200°. Perttunnen (1981) a elle aussi noté cet écoulement sud-ouest plus récent recoupant un écoulement vers le sud dans ce secteur.

Les marques d'un écoulement vers l'est s'arrêtent brusquement au niveau de la moraine de Laverlochère (fig. 24.2). À l'est de cette moraine l'écoulement régional sud-sud-ouest domine nettement. Ailleurs dans la région, la vallée de la rivière Montréal a favorisé un écoulement est-sud-est lors de la déglaciation finale, de même qu'aux environs de Témagami. À cet endroit un dernier écoulement à 150° tronque des queues-de-rat orientées à 184° (fig. 24.6A, 24.6B). On distingue plusieurs autres sites dans la région de Témagami portant des stries entrecroisées ayant des directions de 180° à 200° (mouvement ancien) et de 150°-175° (dernier écoulement).

Sur la carte de Ottertail Creek, des stries entrecroisées indiquent des réajustements d'écoulement de la masse glaciaire lors de son retrait. Toutefois, les mesures ne sont pas assez nombreuses pour proposer des directions d'écoulement précises. Il semble qu'un écoulement sud-sud-ouest (180°-190°) soit recoupé par endroits par un écoulement sud-ouest (200°-228°).

Les données géomorphologiques

L'épisode de déglaciation le plus récent, c'est-à-dire le retrait vers le nord-ouest, bien que très bien représenté dans les marques des polis glaciaires, a laissé peu de traces dans les formes de terrain morainique et fluvioglaciaires. Ceci peut s'expliquer si l'on suppose que plusieurs de ces formes de terrain sont probablement masquées par les fortes épaisseurs de sédiments glaciolacustres qui comblent les dépressions structurales, notamment, la fosse tectonique au nord-ouest du lac Témiscamingue. Des sondages ont démontré la présence de 30 à 40 m de sable et gravier sous jusqu'à 75 m d'argile à plusieurs endroits dans cette fosse tectonique (Kenney et Balins, 1975). Prenant à témoin le relief local de moins de 30 m de la plupart des accumulations fluvio-glaciaires et morainiques de la région, de telles épaisseurs de sédiments lacustres suffiraient à les masquer complètement.

A. *Cannelure orientée à 184° avec de nombreuses queues-de-rat, dues aux phénocrystaux plus résistants à l'abrasion que la roche encaissante. L'écoulement secondaire à 150° a laissé des stries nettes des deux côtés de la cannelure, mais très peu à l'intérieur de celle-ci. Photographie CGC 203407-L.*

B. *Des queues-de-rat à 180° sont légèrement asymétriques, vue en plan, ceci est dû à l'abrasion résultant du dernier écoulement à 150°. De fines stries à 150° sont visibles sur les "queues". Photographie CGC 203506-5.*

Figure 24.6. *Stries entrecroisées dans des andésites, village de Témagami*

Mais d'autres formes de terrain ne sont pas totalement enfouies. C'est le cas de la moraine de Laverlochère. Recouverte de sédiments glaciolacustres par endroits, elle n'en est pas moins continue et facilement identifiable sur photographies aériennes. Elle marque l'étendue maximale du dernier lobe à se retirer de la partie nord du lac Témiscamingue (fig. 24.2). Du côté ontarien, certaines accumulations morainiques dans le voisinage de la rivière Montréal, de même que celles de la carte de Cobalt (fig. 24.2) sont probablement associées à la retraite vers le nord-est du dernier culot de glace à bloquer la partie nord du lac Témiscamingue. Les moraines concentriques à la partie nord du lac à Notre-Dame-du-Nord et à Judge représentent sans doute une phase de récession de la moraine de Laverlochère. Les moraines barrant le lac au Vieux-Fort, à Opémika et, d'après les données bathymétriques (Kenney et Balins, 1975), à plusieurs autres endroits du lac Témiscamingue, témoignent d'un retrait des glaces plus ou moins, à angle droit au lac Témiscamingue. Enfin, les orientations de courts segments d'esker cartographiés par Morton et al. (1979) dans la région de New Liskeard et par Perttunnen (1981) dans celle de Cobalt indiquent un dernier retrait vers le nord-est dans ce secteur. Ceci est conforme au modèle de déglaciation présenté plus loin.

Les indicateurs lithologiques et la stratigraphie des tills

La classification de granules provenant d'une cueillette systématique d'échantillons de till faite pendant l'été 1982 dans la région délimitée par les cartes de Cobalt, de Témagami, de New Liskeard, d'Engelhart et d'Ottertail Creek indique une direction de transport dominante légèrement à l'ouest du sud, et ainsi compatible avec l'écoulement sud-ouest d'âge intermédiaire, pour les roches paléozoïques provenant du grabben du lac Témiscamingue. Les derniers écoulements vers le sud et le sud-est eux, ne se traduisent pas par des déplacements considérables de débris glaciaires. Mais à 2 km au sud de Ville-Marie et à l'est du lac Témiscamingue, on trouve un bloc erratique de calcaire paléozoïque de plus d'un mètre de diamètre perché sur du quartzite de la formation de Lorrain. De même, un till riche en calcaire paléozoïque repose sur le quartzite à plus de 1 km à l'est du lac au niveau de Ville-Marie. Ces distances de transport sont minimales puisque l'on ne connaît pas la nature du substratum rocheux dans le bassin même du lac. Elles confirment, par contre, un dernier écoulement des glaces vers l'est et le sud-est dans ce secteur. Une analyse détaillée de la teneur en carbonates des tills, maintenant en cours, viendra plus tard préciser la limite de ce dernier écoulement vers l'est et le sud-est.

La présence, dans une coupe de la vallée du ruisseau Milberta au nord de New Liskeard de deux couches de till superposées, constitue à date la meilleure preuve stratigraphique d'écoulements glaciaires d'âges différents dans la région. La surface de contact des deux tills est déformée et possiblement tronquée, mais il ne sont pas séparés par d'autres sédiments.

À quelques mètres de cette coupe, le socle dégagé de son couvert de sédiments meubles par l'érosion fluviatile, montre une surface d'environ 1 000 m^2 de roche polie et striée. Cet affleurement est l'un des plus spectaculaires de la région. On y distingue très clairement un mouvement ancien marqué surtout par des cannelures orientées à 190°, recoupé par un dernier mouvement vers 160° caractérisé par des nombreuses stries fines, têtes de clou, chattermarks et broutures (fig. 24.7). Il est probable que les deux tills correspondent dans le même ordre chronologique aux deux directions d'écoulement.

À environ 8 km d'Engelhart, à l'est de la rivière Blanche, une excavation de bâtiment visitée en juillet 1982 montrait une coupe de 2 m de varves sur 10 cm de gravier fin et de sable recouvrant 0,50 m de till sur la roche en place. Ce till présente des caractéristiques très semblables au till inférieur de la coupe de Milberta Creek. La roche exposée au

Figure 24.7. *Affleurement du diabase de Nipissing fraîchement dégagé dans la vallée du ruisseau Milberta, carte de New Liskeard. L'écoulement à 190° a laissé de nombreuses et distinctes cannelures recoupées par des stries fines du dernier écoulement à 160°. Photographie CGC 203506-Z.*

fond de l'excavation montrait des stries et des cannelures bien conservées à 206° et à 178° et des stries à 160°, ce dernier mouvement recoupant les deux autres. Il s'agit probablement d'un till associé à l'écoulement plus ancien à 206° et appartenant au même épisode glaciaire que le till inférieur du ruisseau de Milberta.

Enfin Perttunnen (1981) rapporte un till de 1 à 2 m d'épaisseur recouvrant le till régional dans la région de Cobalt. Les hautes falaises de till sur la rive ouest du lac, face à l'île Mann, montrent de bonnes coupes de ce till.

Comme les tills du ruisseau Milberta ceux de Cobalt ne sont pas séparés par d'autres sédiments. Perttunnen a suggéré que le till supérieur est dérivé du till régional. Il est probable qu'il est associé au dernier écoulement vers le sud-ouest décrit auparavant dans la région de Cobalt.

Chronologie relative des écoulements glaciaires du Témiscamingue

Un projet en cours en coopération avec P. Richard (université de Montréal) visant d'une part à établir un cadre palynostratigraphique suivant la déglaciation et d'autre part la chronologie en valeur absolue (^{14}C) de la déglaciation viendra probablement plus tard ajouter aux données présentées ici. Néanmoins les observations acquises à ce jour, surtout celles sur les polis glaciaires, permettent de présenter un ordre chronologique de déglaciation. La chronologie relative de divers épisodes de l'englaciation et de la déglaciation ayant affecté la région apparait à la figure 24.8.

Les plus anciens écoulements 1 et 2, particulièrement le 2, ont fortement marqué le paysage. C'est à l'écoulement n^{o} 2 que sont dues les roches moutonnées de grandes dimensions, les cannelures importantes et autres formes profilées du substratum rocheux. Dans le voisinage du barrage Lower Notch sur la rivière Montréal, des travaux de construction au début des années 70 ont nécessité l'extraction de forts volumes de till. La plupart des bancs d'emprunt sont sur le côté aval de gros drumlins là où le till atteint par endroits plusieurs mètres d'épaisseur.

La roche en place dégagée, constituant le plancher de ces excavations, ne porte que des stries conformes à l'écoulement n^{o} 2, (axe des drumlins à 190°-200°). Par contre dans le voisinage immédiat de ces bancs d'emprunt des affleurements qui n'ont jamais été masqués par de grandes épaisseurs de till portent de nombreuses stries reliées à l'écoulement n^{o} 3 vers le sud-est. C'est aussi à l'écoulement n^{o} 2 que l'on doit attribuer le gros du transport des débris glaciaires dans la région étudiée, ceci même là où les marques de l'écoulement n^{o} 3 sont nombreuses. Il est intéressant de comparer cette situation à celle de la région de Cadillac-Val d'Or où Kish et al. (1979) lors de campagnes d'échantillonnage du till de fond ont déduit un transport vers le sud-ouest des constituents du till alors que les stries à la surface indiquent une direction d'écoulement sud-est.

L'écoulement n^{o} 3 bien que très bien représenté par des stries fines et nettes, et même par de grandes surfaces striées aux abords du lac Témiscamingue et au nord-ouest du lac n'en demeure pas moins secondaire. Son influence sur le modelé du terrain n'est discernable que dans les microformes. De même cet écoulement n'a apparemment déplacé que très peu de matériaux glaciaires et ceci sur probablement des distances relativement courtes. Mais tel que décrit auparavant, il existe tout de même des preuves de terrain autres que les stries qui indiquent des directions de transport vers le sud-est. Enfin, l'écoulement n^{o} 4 est possiblement contemporain du 3 ou plus jeune. Des datations au radiocarbone à l'est de la région laissent croire que ce secteur aurait été parmi les derniers endroits à être déglacié. L'étude de l'écoulement glaciaire est moins poussée dans ce secteur que dans le reste de la région.

La chronologie relative de l'écoulement glaciaire du Témiscamingue, mal connu jusqu'à maintenant, exige à la lumière de ces nouvelles données une réinterprétation de la déglaciation locale. On doit reconnaître qu'un dernier écoulement vers le sud-est conduit à des configurations de marge glaciaire incompatibles avec celles des modèles théoriques de Prest (1970) et Vincent et Hardy (1979). Card et al. (1973, p. 49) rapportent pour la région de Maple Mountain, immédiatement à l'ouest de la nôtre, une situation semblable à celle du Témiscamingue, "...there is evidence in the form of glacial striae for ice movement in two directions. In the north and west, glacial striae are oriented south to S20E whereas in the southeast, striae strike mainly S20W. Locally, in the south-central part of the area, the two sets of striae occur together, with the southwest set apparently older than the north-south set". Encore ici, l'ancienneté de la direction sud-ouest est observée. Il est intéressant de considérer la possibilité d'un ou de plusieurs écoulements anciens vers le sud-ouest ayant affectés de grandes superficies du nord-est ontarien et nord-ouest québécois. Mais sur cet aspect, les données disponibles à ce jour ne permettent pas de dépasser le stage de l'hypothèse.

Un modèle de déglaciation pour le Témiscamingue

La synthèse des données présentées nous emmène au modèle suivant: d'abord une ouverture initiale des glaces vers le nord-est ou moins dans l'axe de la moraine d'Harricana (Veillette, 1982b) avec pénétration des eaux glaciolacustres. Cette ouverture se serait faite en travers du lac Témiscamingue (fig. 24.9) et aurait créé un passage pour un plan d'eau possiblement associé à une extension nord-est du lac Algonquin.

Ensuite, la transgression lacustre se serait poursuivie vers le nord-est le long d'un couloir qui aurait scindé le glacier laissant au nord une mase plus ou moins centrée dans la fosse tectonique du lac Témiscamingue et au sud, une autre masse venant de l'intérieur du Québec et rattachée à l'inlandsis (fig. 24.10). Cette dernière aurait ainsi barré le

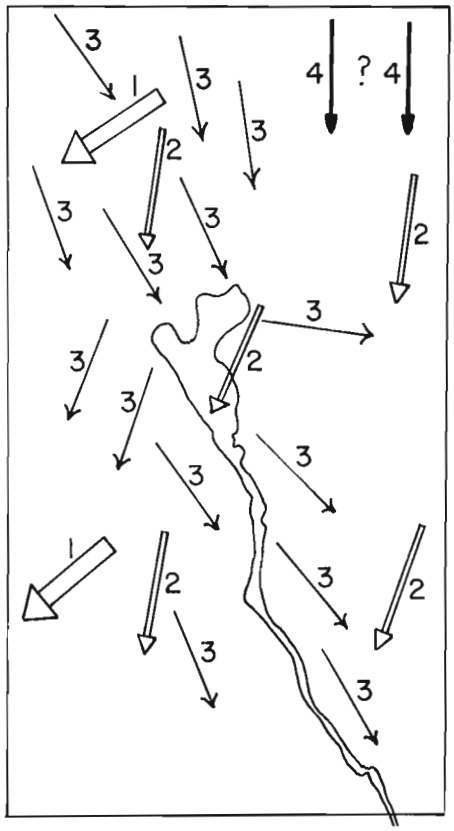

Figure 24.8. Chronologie relative des écoulements glaciaires du Témiscamingue. Les directions d'écoulement 1 et 2 sont possiblement reliées, l'écoulement 2 a probablement couvert toute la région. L'écoulement 3 recoupe les deux autres. L'écoulement 4 est possiblement contemporain de l'écoulement 3.

Figure 24.10. Prolongement des eaux proglaciaires vers le nord-est et début du lac Barlow avec deux entités glaciaires l'une au nord, l'autre au sud de l'ouverture initiale du glacier.

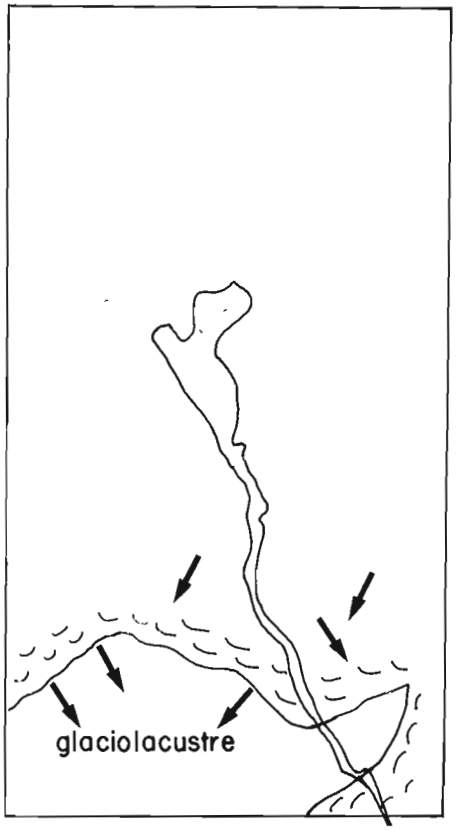

Figure 24.9. Pénétration des eaux du lac proglaciaire Algonquin vers le nord-est dans l'axe de la moraine d'Harricana.

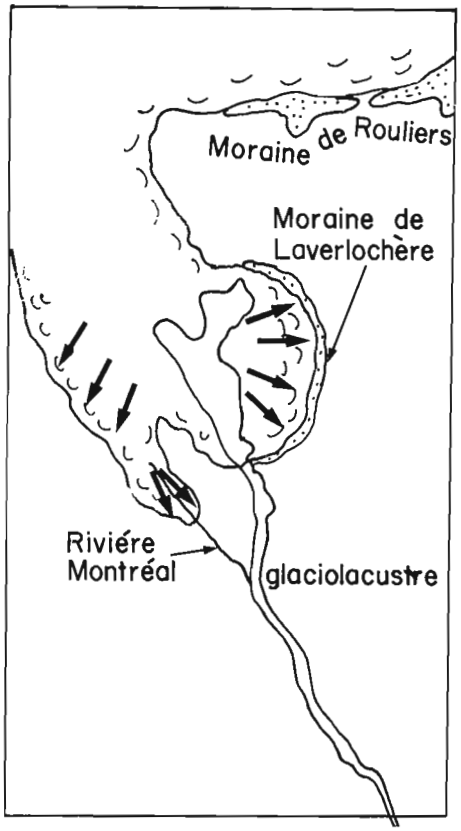

Figure 24.11. Langue glaciaire en retrait centrée sur la fosse tectonique du lac Témiscamingue.

lac Témiscamingue ravivant, du moins partiellement, l'hypothèse du barrage de glace de Wilson (1919). Cette hypothèse est supportée par l'analyse des stries entre le village de Témiscaming et le rétrécissement d'Opémika. Entre ces deux localités, des marques d'écoulement indiquent un seul mouvement vers le sud-ouest (210°) et l'on n'observe pas la complexité d'écoulement qui est présente au nord du rétrécissement d'Opémika.

Avec le recul des glaces vers le nord, la fosse tectonique du lac Témiscamingue serait devenu le point d'attache d'une langue du glacier se retirant vers le nord-ouest (fig. 24.11). Vers la toute fin de la déglaciation, cette langue de glace a possiblement été séparée du glacier principal pour devenir un culot résiduel créant ainsi l'écoulement plus ou moins radial responsable des stries orientées vers l'est et le nord-est et vers le sud et le sud-est à l'est du lac Témiscamingue, et vers le sud-ouest, dans la région de Cobalt; de même pour les eskers dirigés vers l'ouest-sud-ouest dans les régions de Cobalt et de New Liskeard. Un culot de glace semblable, mais de plus faibles dimensions aurait occupé la dépression de la rivière Montréal et laissé les stries orientées vers le sud-est qui sont depuis longtemps connues dans ce secteur.

Les implications de ce mode de déglaciation sur la distribution des sédiments superficiels et la prospection minière

Il est probable que le retrait rapide des glaciers au contact de grandes étendues d'eau proglaciaire ne se soit pas fait en maintenant une marge glaciaire plutôt régulière comme l'indiquent la plupart des modèles de déglaciation. Au contraire, il semble plus raisonnable de concevoir une marge glaciaire très irrégulière influencée par les importantes contraintes de la topographie, par les variations de profondeur des eaux proglaciaires et échancrée par les baies de vêlage et autres phénomènes associés à la fonte d'un glacier en contact avec un fort volume d'eau de fonte. Des travaux de cartographie de sédiments meubles que nous avons menés à l'est de la région décrite ici montrent que l'écoulement glaciaire dans le voisinage des grands eskers au moment de la déglaciation était très complexe et la plupart du temps différent de l'écoulement plus uniforme qui l'a précédé. Ceci est démontré clairement dans la région de Belleterre sous l'influence du retrait de la moraine d'Harricana, (l'esker d'Harricana?) (Veillette, 1982a). Cette situation donne fréquemment naissance à plus d'une génération de stries. Il convient, donc, afin de reconstituer le plus fidèlement possible une marge glaciaire en retrait de relever le plus grand nombre possible de stries et autres marques permettant d'établir les étapes du retrait. Cette technique comme l'a auparavent démontré Lamarche (1971, 1974) dans le sud-est du Québec, peu s'avérer précieuse à une meilleure connaissance des dernières phases de la déglaciation d'une région.

Les différents écoulements glaciaires du Témiscamingue ne résultent, en fait, que des ajustements d'écoulement des glaces en réponse à des modifications de la géométrie de la marge glaciaire. Ces changements de direction se réflètent à leur tour par des changements de provenance des matériaux glaciaires pouvant ainsi créer de sérieuses difficultés pour l'interprétation des données géochimiques des tills. L'absence de sédiments d'origine non glaciaire entre les tills décrits auparavant pourrait indiquer que ces changements de direction se sont faits sous la masse glaciaire.

Comme le dernier écoulement sud-est ne semble avoir affecté que la partie supérieure des sédiments meubles il est plus prudent d'échantilloner le till de fond près du substratum rocheux que le till des couches supérieures, afin de déterminer l'axe de transport dominant. D'un autre côté, il faut connaître les "déviations" locales dans les directions d'écoulement à l'intérieur de la région aussi bien que les directions régionales, afin de pouvoir évaluer leur influence respective sur le transport des matériaux glaciaires.

Bibliographie

Barlow, A.E.
1899: Geology and Natural Resources of the Area included by Nipissing and Temiscaming Map-sheet Comprising portions of the District of Nipissing, Ontario, and of the County of Pontiac, Quebec, Report of the Geological Survey of Canda, No. 672, p. 18-287.

Boissonneau, A.N.
1968: Glacial history of northeastern Ontario, II. The Timiskaming-Algoma area, Canadian Journal of Earth Sciences, v. 5, p. 97-109.

Bostock, H.S.
1970: Physiographic Regions of Canada; in Geology and Economic Minerals of Canada, ed. R.J.W. Douglas; Geological Survey of Canda, Economic Geology Report No. 1, Map 1254A.

Card, K.D., McIlwaine, W.H., et Meyn, H.D.
1973: Geology of the Maple Mountain area, District of Timiskaming, Nipissing and Sudbury; Ontario Division of Mines, Ministry of Natural Resources, Geological Report 106, 133 p.

Geological Survey of Canada
1863: Report of progress from its commencement to 1863; Geological Survey of Canada, 983 p., preface by W.E. Logan.

Kenney, T.C. et Balins, J.K.
1975: Bathymetric survey of Lake Temiskaming; University of Toronto, Department of Civil Engineering, Publication 75-11, ISSN 0316-7968, 20 p.

King, R.C.F. et Norton, J.D.
1979: Quaternary Geology of the Engelhart Area, District of Temiskaming; Ontario Geological Survey, Preliminary Map P2292, Geological series, scale 1:50 000.

Kish, L., LaSalle, P., et Szoghy, I.M.
1979: Rb, Sr, Y, Zr, Nb, Mo dans les tills de base de l'Abitibi, Min. Rich. Nat. Qué, dossier public 662, 8 p.

Lamarche, R.Y.
1971: Northward moving ice in the Thetford Mines area of southern Quebec; American Journal of Science, v. 271, p. 383-388.

1974: Southeastward, northward, and westward ice movement in the Asbestos area of southern Quebec; Geological Society of America Bulletin, v. 85, p. 465-470.

Lovell, H.L. et Caine, T.W.
1970: Lake Timiskaming rift valley; Ontario Department of Mines, MP39, 16 p.

Morton, J.W., King, R.C.F., et Kalin, N.W.
1979: Quaternary geology of the New Liskeard area, District of Temiskaming; Ontario Geological Survey Preliminary Map 2291, Geological series, scale 1:50 000.

Perttunnen, M.
1981: Quaternary geology of the Cobalt area, northern Ontario, District of Timiskaming; rapport non publié préparé pour la Commission géologique de l'Ontario, 48 p., accompagne la carte préliminaire des formations superficielles de Cobalt, 1:50 000, 31M/5.

Prest, V.K.
1970: Quaternary geology of Canada; in Geology and Economic Minerals of Canada, ed. R.J.W. Douglas; Geological Survey of Canada, Economic Geology Report No. 1, p. 676-764.

Sabourin, R.J.E.
1957: Glacial Map of Quebec; Québec, université Laval, Département de géologie et minéralogie, contribution n° 128.

Thomson, R.
1965: Geology of Casey and Harris Townships, District of Temiskaming; Ontario Department of Mines, Geological Report No. 36, 77 p.

Veillette, J.J.
1982a: Géologie des formations superficielles: cartes d'Angliers 31M/6, de Ville-Marie 31M/10, et du lac Simard 31M/11. Commission géologique du Canada, dossier public n° 871.

Veillette, J.J. (suite)
1982b: Écoulements glaciaires à l'ouest de la moraine d'Harricana au Québec; Commission géologique du Canada, dossier public n° 841.

– Déglaciation de la vallée supérieure de l'Outaouais: le lac Barlow et la partie sud du lac Ojibway: Géographie physique et Quaternaire. (sous presse)

Vincent, J.S.
1971: Le Quaternaire des cantons de Guigues, Baby, Duhamel et Laverlochère, comté de Témiscamingue, Québec, thèse de maîtrise, Département de géographie, université d'Ottawa, 146 p.

Vincent, J.S. et Hardy, L.
1979: The evolution of glacial Lakes Barlow and Ojibway, Quebec and Ontario; Geological Survey of Canada, Bulletin 316, 18 p.

Wilson, M.E.
1919: Le comté de Témiscaming, Province de Québec; Commission géologique du Canada, Mémoire 103, série géologique n° 86, 177 p.

25.

SURFICIAL GEOLOGY OF THE WESTERN PART OF CUMBERLAND COUNTY, NOVA SCOTIA[1]

Project 820019

R.R. Stea[2]
Nova Scotia Department of Mines and Energy

Stea, R.R., Surficial geology of the western part of Cumberland County, Nova Scotia; in Current Research, Part A, Geological Survey of Canada, Paper 83-1A, p. 197-202, 1983.

Also in Mineral Resources Division, Report of Activities, 1982, Nova Scotia Department of Mines and Energy, Report 83-1, 1983.

Abstract

Surficial materials of the western part of Cumberland County, Nova Scotia were mapped in the summer of 1982. New information was gained on the glacial history of the region. At Joggins, three tills were confirmed and studied in detail. An early eastward ice flow is indicated by 'old' striae and the lowest till at Joggins. Major south to southwest ice flows created the upper two tills at Joggins and produced, upon recession, large areas of stratified drift including stagnation moraine and outwash deltas. Emerged marine features along the coast of Chignecto Bay decrease in elevation from 37 m at Squally Point to 15 m at Joggins. The oldest, eastward flow may be Early Wisconsian in age; the later pulses of south- to southwest-flowing ice are probably Middle to Late Wisconsinan in age.

Introduction

Mapping of surficial deposits in northern Nova Scotia is part of a project that also involves trace-element analysis of till. This project is part of the Canada-Nova Scotia Cooperative Mineral Program 1981-84. It follows a program of surficial mapping and till geochemistry that was initiated by Canada Department of Regional Economic Expansion and Nova Scotia Department of Mines in 1977 covering southern Nova Scotia on the Meguma terrane (Stea and Fowler, 1979, 1981; Stea, 1982a; Stea and O'Reilly, 1982). The aim of this project is to provide a similar data base on the nature and extent of surficial materials and the effects of glaciation, in order to aid mineral exploration, environmental assessment, and industrial construction.

The area covered by this report lies between latitudes 45°15'N and 45°50'N and longitudes 64°20'W and 65°00'W, that is, west of Parrsboro and is a summary of field work carried out during the 1982 season.

Acknowledgments

I am grateful to Phillip Finck for his able assistance in the field, to W.H. Poole for his support of this field project, and to D.R. Grant (GSC) for photogeological terrain interpretation, consultation, and critical reading.

Physiography and General Geology

The study area consists of two distinct physiographic regions: the Cumberland-Pictou lowland (Goldthwait, 1924) and the Cobequid Highlands. The lowland area is predominately underlain by sedimentary rocks of the Cumberland Group (Late Carboniferous). The highland region which rims the southern and southwestern coast of the peninsula (Fig. 25.1) is formed by metasedimentary volcanic and igneous rocks of Hadrynian, Devono-Carboniferous, and Early Carboniferous age that are segregated into numerous fault blocks and bounded on the south by the Minas Geofracture (Donohoe and Wallace, 1978; Keppie, 1982).

Previous Work

Previous mapping done in the area has been of varying scale and purpose. Chalmers (1895) and Wickenden (1941) mapped the northern portion of the area. Swift and Borns (1967) and Wightman (1980) produced maps of the glaciofluvial and glaciomarine sediments on the Minas Basin shore. MacNeill (1956) and soil survey scientists (Nowland and MacDougall, 1973) produced maps of the area dealing with aspects of surficial geology.

Concomitant with the previous mapping was the development of glaciation concepts for the region. Chalmers (1895) noted two main sets of striations in the region, an earlier set trending eastward and later sets trending southward and southwestward. He attributed the eastward trending set to ice flowing eastward from New Brunswick which he called the Northumberland Glacier. Later southward and southwestward sets were attributed to a more or less separate ice mass centred on the isthmus of Chignecto, which he termed the Chignecto Glacier. Goldthwait (1924) dismissed the evidence for chronologically separate local ice masses and explained divergent striae in terms of a lobation of Laurentide ice which he called the 'Acadian Bay Lobe'. In recent years, Prest and Grant (1969) returned to the local ice concept. They stated: "It appears that the development of local ice in some parts of the region was sufficiently early and extensive to hold off the Laurentide ice flood or, at least, to direct it along defined channels." Grant (1977) further developed this model of restricted ice cover and depicted the limit of Late Wisconsinan glaciers. In his reconstruction the western Cobequid Highlands remained essentially ice-free during this period. An alternative viewpoint was put forward by Wightman (1980) in his study of pebble lithology of the outwash deltas of the north shore of the Minas Basin. He concluded that at some time in the Late Wisconsinan, ice did cross part of the Cobequid Highlands.

The mapping of surficial deposits and ice flow features, and the detailed study of important stratigraphic sections which are the main aims of this project shed some new light on the nature and timing of glaciation in the region.

Surficial Units

Glacially Scoured Bedrock

Areas along the Chignecto Bay coast of the study area are characterized by exposed bedrock with a discontinuous veneer of till and boulders. The topography is controlled by bedrock with strike ridges formed by relatively resistant sandstone units. The till is generally thin (<1 m), loose and rich in clasts consisting primarily of the adjacent bedrock.

---

[1] Contribution to Canada-Nova Scotia Co-operative Mineral Program 1981-84. Project carried by Geological Survey of Canada and Nova Scotia Department of Mines and Energy.

[2] Nova Scotia Department of Mines and Energy, P.O. Box 1087, Halifax, Nova Scotia, B3J 2X1.

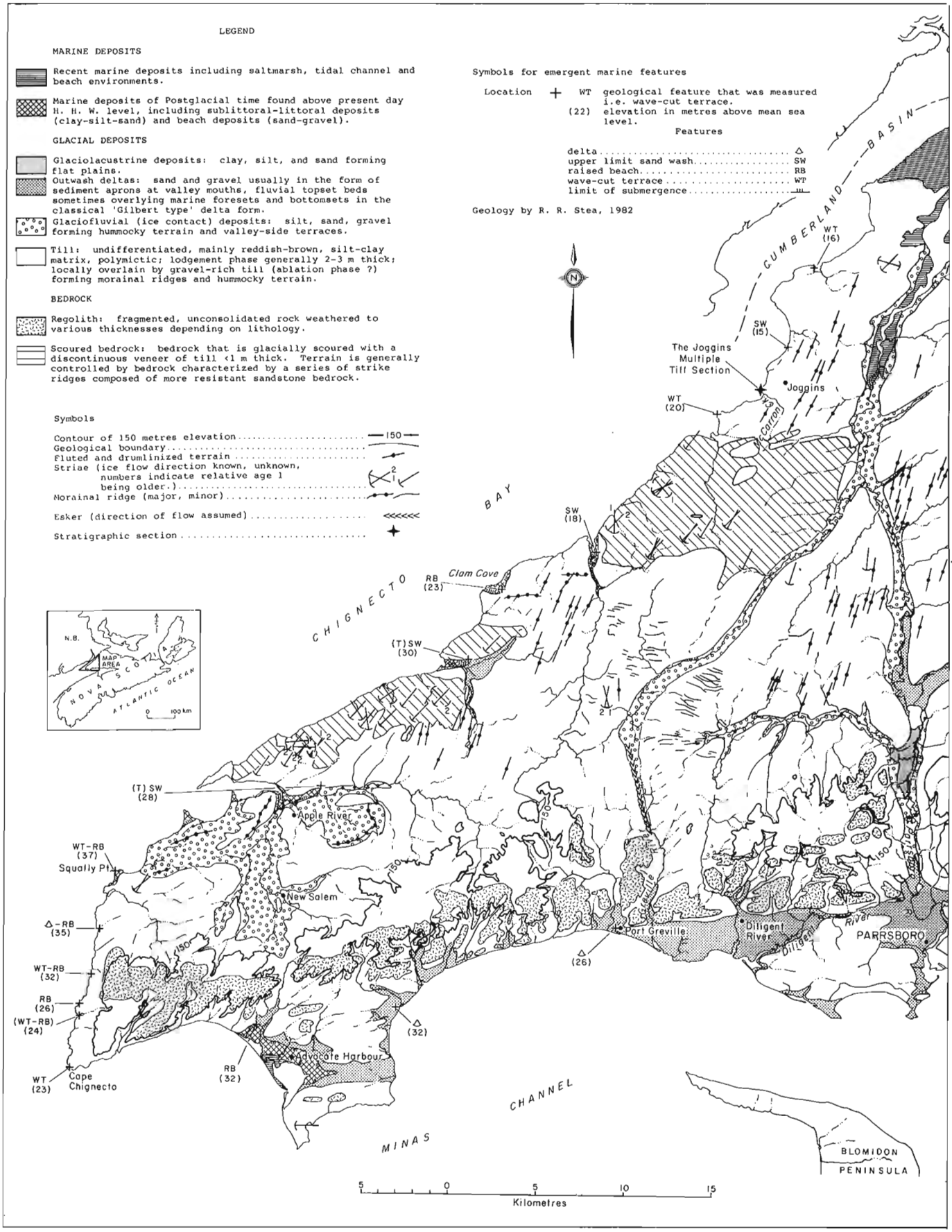

Figure 25.1. *Surficial geology of the western part of Cumberland County, Nova Scotia. (based in part on photogeological interpretation by D.R. Grant)*

The surface of many of the exposures was scoured by glaciers that moved generally southwestward. Pebbles in the sandstone matrix reveal 'pressure shadows', or miniature crag-and-tail (Fig. 25.2). Many surfaces exhibit crossing striations with younger southwest-trending sets curving to conform to local topographic trends. Preserved on the lee side of some outcrops are relatively more weathered, more degraded striations that are oriented eastward and southeastward.

Regolith

The surface material of large areas in the Cobequid Highlands is bedrock that has been fragmented, disintegrated and altered to varying degrees in situ (Fig. 25.1). Mechanical and chemical weathering is implied. Hence, there is little or no evidence of glacial scouring in these regions. Till generally pinches out up-slope against the friable rock and overlies it in some areas of the highlands. Bedrock lithology is evidently the controlling factor in the depth and intensity of rock weathering. Metamorphosed, steeply dipping shales north of Advocate Harbour have been disrupted and disaggregated to depths of 10 m below the surface while foliated granites at Cape Chignecto are broken for only 2-5 m. The age and genesis of this material is problematic, but it must predate the overlying till.

Till

The Joggins Till Section

At the mouth of McCarron Brook, north of Joggins, shore cliffs reveal three till units with a total thickness of 20 m. The section was first described by Wickenden (1941).

Figure 25.2. *Pressure shadows or miniature crag-and-tail features on the down-glacier or lee side of quartzite pebbles embedded in a sandstone matrix near Apple River, Nova Scotia. The inferred azimuth of ice flow is 210°.*

Prest et al. (1972, p. 37) noted that from bottom to top the three tills are distinctly reddish, grey and yellowish and attributed them all to fluctuations of the south- and southwest-flowing ice. This author's observations on the section are summarized in Figure 25.3.

The lowest till (Unit I) is characterized by reddish hues and a higher percentage of allochthonous clasts, particularly chloritized, foliated granitic clasts. Their provenance is uncertain but is likely to be New Brunswick. The fabric trends northeast at the bottom of the section and changes to almost east at the top. The till overlies a bedrock surface whose striae are oriented 110-290 degrees and are thus aligned with the till fabric. Unit Ic, below its contact with unit II, shows signs of alteration. This may represent a period of subaerial weathering before deposition of the overlying till.

The upper tills (Units II and III) are characterized by a predominance of sedimentary clasts, mainly sandstone, limestone, and coal, and by a northeast trending fabric. Unit III is differentiated from Unit II by a weathered appearance and numerous sand partings along fissility planes.

Surface Till Sheet

Till covers a major part of Cumberland County north of the Cobequid Highlands. The most prevalent type is a reddish brown, mud-rich till composed chiefly of sandstone clasts. It is generally 2-5 m thick and overlies bedrock surfaces inscribed with southwest-trending striae. A gravel-rich till phase is also present locally, and is associated with hummocky and ribbed moraine areas. In the Joggins area the surface till has a more greyish cast and is calcareous, presumably because of incorporated local grey limestones, carbonaceous shales and coaly beds.

Glaciofluvial Sediments

Ice-contact Stratified Drift

Large bodies of ice-contact stratified drift in the form of kames, kame terraces and eskers occur in the region (Fig. 25.1), notably in the Apple River area, and in the valleys of River Hebert, Kelley and Parrsboro rivers. Spectacular kame terraces (Fig. 25.4) are found along Parrsboro River, associated with a recessional end moraine (Wightman, 1980). These deposits show rapid changes in grain sizes between beds and in some cases have intercalated flow tills (Nielsen, 1976, p. 47). The deposits can reach up to 30 m in thickness.

The Apple River area is also characterized by ice contact deposits and moraines. D.R. Grant (personal communication, 1982) interprets this broad zone of ice-frontal deposits to mark a major glacier marginal stand, perhaps the stadial limit.

Outwash and Outwash Deltas

South of the mouth of the Greville, Diligent and Parrsboro rivers are flat plains, locally dissected, pitted, and terraced, composed of horizontal beds of gravelly sand. This unit has been termed the Saints Rest Member and is interpreted as outwash (Swift and Borns, 1967; Wightman, 1980). Where shoreline exposure reveals stratigraphy, the Saints Rest Member is found to overlie marine foreset and bottomset beds termed the Advocate Harbour Member (Swift and Borns, 1967) in the classic 'Gilbert delta' form (Wightman, 1980).

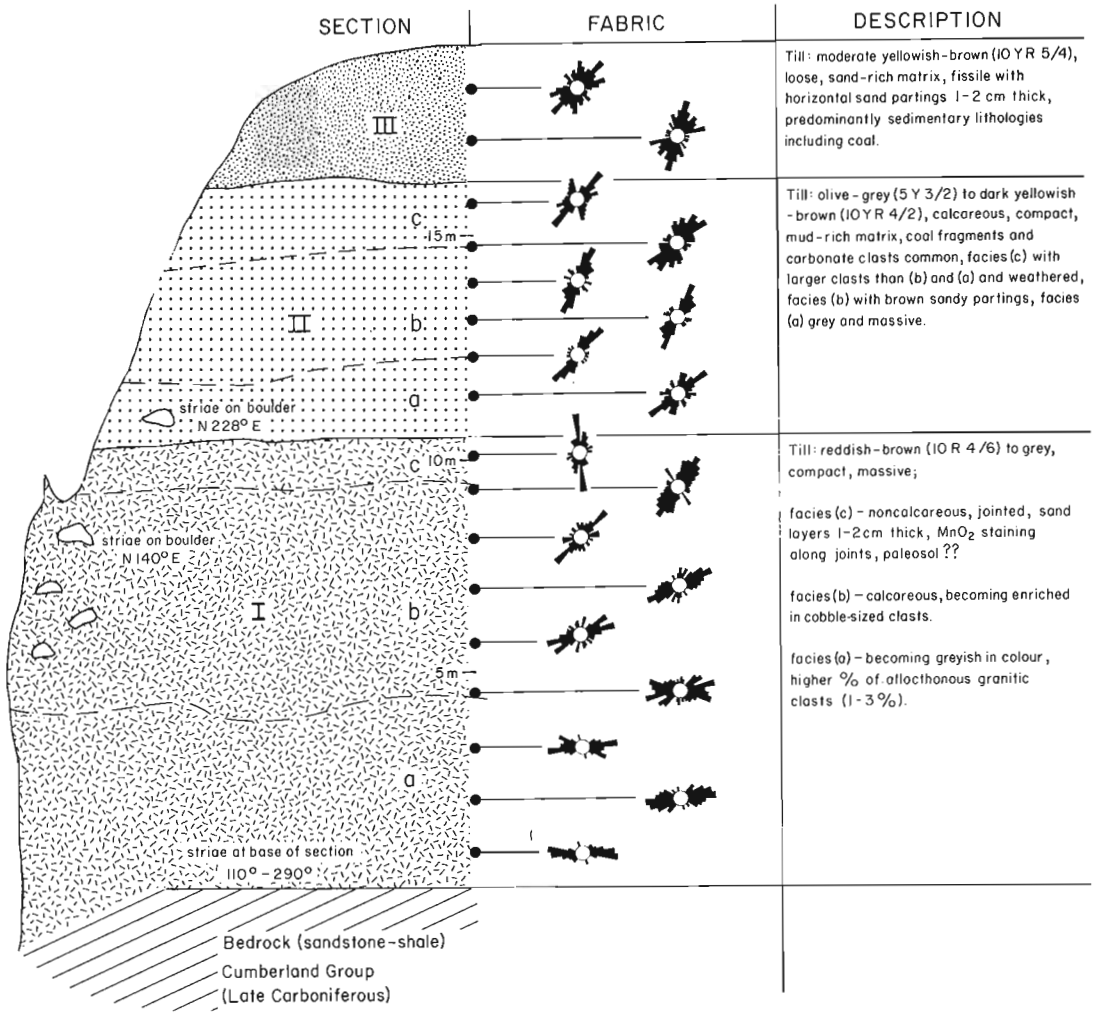

Figure 25.3. *Analysis of the multiple till section at Joggins, Cumberland County, Nova Scotia.*

Figure 25.4. *A kame terrace flanking the Parrsboro River valley, Nova Scotia.*

Marine Sediments

Emerged Marine Featues

At Advocate Harbour, the Saints Rest Member occurs inland from marine shoreline deposits (Swift and Borns, 1967). Raised strandlines occur in this area. The highest strandline west of Advocate Harbour was measured at 32 m above mean sea level. The outwash deltas and raised marine features along the southern coast are discussed in detail by Wightman (1980). D.R. Grant (personal communication, 1982) notes that the kettled marine outwash terrace at Diligent River and the ice-contact scarps that back the terrace at the mouths of Wards Brook and Fox River to the west point to a highly digitate ice mass confined to the valleys while the bulk of the marine terrace was constructed.

Along the coast from Cape Chignecto to Squally Point (Fig. 25.1) is a discontinuous wave-cut terrace in bedrock. At Squally Point this terrace has superimposed littoral-type deposits which attain an elevation of 37 m above m.s.l. (Fig. 25.5). The terrace elevation apparently decreases from Squally Point to Cape Chignecto (23 m above m.s.l.), but it may actually be a complex of several successive levels.

Along the Chignecto Bay coast, raised marine deposits are best exposed at Clam Cove where gullying along a logging road reveals a transition from unaltered till, a beach berm with rounded stones, to upper shoreface marine sands.

Figure 25.5. *A wave-planed surface on bedrock at Squally Point, veneered with beach deposits that reach 37 m above m.s.l.*

The height of the emerged strandline is 23 m above mean sea level. The elevation of emerged marine features decreases along the coast of Chignecto Bay from an elevation of 37 m above m.s.l. at Squally Point to 15 m at Joggins (Fig. 25.1).

Glacial History and Correlations

The oldest striae in the region trend east and southeast. The lowest till at Joggins overlies striated bedrock and has a fabric concordant with this trend. The chloritized hornblende-bearing, foliated granitic erratics in this till suggest a New Brunswick provenance. This movement appears to have been due east in an initial stage, then later southeastward. For this reason it is correlated with the East Milford Till of the Carboniferous lowlands of central Nova Scotia to the south, which was also deposited by southeast-flowing ice. It overlies peat beds of interstadial and interglacial rank (Stea and Hemsworth, 1979; Stea, 1982b). Chalmers (1895) invoked the New Brunswick-centred 'Northumberland Glacier' to explain these trends, while in New Brunswick this event is termed the "Caledonia Phase" by Rampton and Paradis (1981, p. 13), who give it a Wisconsinan age because striations related to it are inscribed on a wave-planed rock bench which is elsewhere assigned a Sangamon age by Grant (1980).

The silt and sand between Units I and II at Joggins (Wickenden, 1941, p. 144) and the altered Unit Ic may attest to a period of ice withdrawal, subaerial exposure and climatic amelioration before the deposition of Unit II.

Striae and fluting in the region indicate a major intermediate period of south-southwest flow (Fig. 25.1). Rampton and Paradis (1981) termed this south-southwest flow the 'Chignecto Phase'. Inland, these ice flow features appear to swing to a more southward direction (Fig. 25.1). This suggests ice radiating from a centre lying to the north of the map area. Till Unit II at Joggins contains abundant coal derived from the northeast and has a strong northeast-trending fabric implying that it was deposited by this flow. Unit III may represent a late fluctuation in this flow, or a melt-out phase of Unit II. Younger southwest-oriented striae along the Chignecto Bay coast point to an ice lobe in the bay induced by late-stage drawdown.

The 'Chignecto Phase' probably postdates the Early Wisconsinan but since it has not yet been dated directly its age can only be spectulated to be Middle-Late Wisconsinan. There is some evidence that ice on the Cobequid Highlands to the east of the study area reactivated and flowed northward subsequent to this phase (Prest et al., 1972, p. 39). Rampton and Paradis (1981) describe two iceflow phases after the Chignecto Phase. Stea (1982b) postulated two Late Wisconsinan till-forming events in central Nova Scotia.

The deltas along the Minas Basin Shore, though not dated directly, are assigned a Late Wisconsinan age because they belong to the same general phase of submergence in Bay of Fundy which farther west has been dated between 13 000 and 14 000 years B.P. Wightman (1980) suggested that the deltas were formed during recession of glaciers that had crossed Cobequid Highlands whereas Grant (1977) associated them with the limit of Late Wisconsinan northern ice which he placed on the north flank of the highlands. The question remains unresolved because this study can adduce no evidence bearing on the extent of ice during any of the three phases.

In Minas Basin the configuration of marine limit, and hence its interpretation, is controversial. The elevation of the upper reach of the paleoshore was taken by Swift and Borns (1967) and by Wightman (1980) to be the contact between the foreset beds (the Advocate Harbour Member) and the topset, supposedly fluvial beds (the Saints Rest Member). Prest (1970), on the other hand, considered the topset beds to be littoral and thus argued for greater, more extensive submergence. Both however show a decline of the paleoshore eastward up Minas Basin. This is attributed to a tapering of the effective ice load toward the southeast by Wightman and Cooke (1978) and by Grant (1980), whereas Prest (1970, p. 710) invoked an ice lobe retreating eastward in the basin.

In Chignecto Bay, also, the pattern of marine limit, specifically its decrease up the bay (Fig. 25.1) is incongruous with the ice load model. Since the axis of the bay is parallel to the general trend of isobases and hence to the contours of ice load as inferred from the overall direction of glacier recession to the northwest, there should be little or no differential uplift along its length. The irregular decline in marine limit therefore points to a last-stage ice lobe lying north of Squally Point which delayed marine incursion and thus led to successively lower marine limits. Moreover, the decline of marine limit also southward from its maximum reach at Squally Point, where the Apple River end-moraine belt terminates, may represent the normal proglacial slope of the stable water plane associated with that inferred ice-marginal stand.

References

Chalmers, R.
1895: Report on the surface geology of eastern New Brunswick, northwestern Nova Scotia and a portion of Prince Edward Island; Geological Survey of Canada, Annual Report, v. 1, no. 7, pt. M.

Donohoe, H.V. and Wallace, P.I.
1978: Preliminary map of the Cobequid Highlands; Nova Scotia Department of Mines, Map 78-1.

Grant, D.R.
1977: Glacial style and ice limits, the Quaternary stratigraphic record, and changes of land and ocean level in the Atlantic Provinces, Canada; Geographie Physique et Quaternaire, v. 31, no. 3-4, p. 247-260.

1980: Quaternary sea-level change in Atlantic Canada as an indication of crustal delevelling; in Earth Rheology, Isostasy and Eustasy, ed. N.A. Morner; John Wiley and Sons, p. 201-214.

Goldthwait, J.W.
1924: Physiography of Nova Scotia; Geological Survey of Canada, Memoir 140, 179 p.

Keppie, J.D.
1982: The Minas Geofracture; in Major structural zones and faults of the northern Appalachians, ed. P. St-Julien and J. Béland; Geological Association of Canada, Special Paper 24, p. 264-278.

MacNeill, R.H.
1956: Surficial geology maps of Nova Scotia, 1:50 000; unpublished manuscript, Nova Scotia Research Foundation, Dartmouth, Nova Scotia.

Nielsen, E.
1976: The composition and origin of Wisconsinan tills in mainland Nova Scotia; unpublished Ph.D. thesis, Dalhousie University, Halifax, Nova Scotia.

Nowland, J.L. and MacDougall, J.I.
1973: Soils of Cumberland County, Nova Scotia; Nova Scotia Soil Survey, Report No. 17, 133 p.

Prest, V.K.
1970: Quaternary geology of Canada; in Geology and Economic Minerals of Canada, ed. R.J.W. Douglas; Geological Survey of Canada, Economic Geology Report No. 1, p. 676-764.

Prest, V.K. and Grant, D.R.
1969: Retreat of the last ice sheet from the Maritime Provinces, Gulf of St. Lawrence region; Geological Survey of Canada, Paper 69-33, 15 p.

Prest, V.K., Grant, D.R., Borns, H.W., Brookes, I.A., MacNeill, R.H., and Ogden, J.G.
1972: Quaternary geology, geomorphology and hydrology of the Atlantic Provinces; 24th International Geological Congress, Guidebook A61-C61, 79 p.

Rampton, V.N. and Paradis, S.
1981: Quaternary geology of the Amherst map area (21 H), New Brunswick; New Brunswick Department of Natural Resources, Map Report 81-3, 36 p.

Stea, R.R.
1982a: Pleistocene geology and till geochemistry of south central Nova Scotia (Sheet 6); Nova Scotia Department of Mines and Energy, Map 82-1.

1982b: The properties, correlation and interpretation of Pleistocene sediments in central Nova Scotia; unpublished M.Sc. thesis, Dalhousie University, Halifax, Nova Scotia.

Stea, R.R. and Fowler, J.H.
1979: Minor and trace element variations in Wisconsinan tills, Eastern Shore region, Nova Scotia; Nova Scotia Department of Mines and Energy, Paper 79-4, 30 p.

1981: Pleistocene geology and till geochemistry of central Nova Scotia; Nova Scotia Department of Mines and Energy, Map 81-1.

Stea, R.R. and Hemsworth, D.
1979: Pleistocene stratigraphy of the Miller Creek section, Hants County, Nova Scotia; Nova Scotia Department of Mines and Energy, Paper 79-5.

Stea, R.R. and O'Reilly, G.A.
1982: Till geochemistry of the Meguma terrane in Nova Scotia and its metallogenic implications; in Prospecting in areas of glaciated terrain, 1982, ed. P.H. Davenport; Canadian Institute of Mining and Metallurgy, p. 82-104.

Swift, D.J.P. and Borns, H.W., Jr.
1967: A raised fluviomarine outwash terrace, north shore of the Minas Basin, Nova Scotia; Journal of Geology, v. 75, no. 6, p. 693-710.

Wickenden, R.T.D.
1941: Glacial deposits of part of northern Nova Scotia; Transactions of the Royal Society of Canada, Section 4, p. 143-149.

Wightman, D.M.
1980: Late Pleistocene glaciofluvial and glaciomarine sediments on the north side of the Minas Basin, Nova Scotia; unpublished Ph.D. thesis, Dalhousie University, Halifax, Nova Scotia.

Wightman, D.M. and Cooke, H.B.S.
1978: Postglacial emergence in Atlantic Canada; Geoscience Canada, v. 5, p. 61-65.

26.

STRATIGRAPHY AND STRUCTURE OF THE WESTERN MARGIN OF THE NORTHERN SELKIRK MOUNTAINS: DOWNIE CREEK MAP AREA, BRITISH COLUMBIA

EMR Contract 04SB.23254-2-0239

Richard L. Brown, Larry S. Lane, John F. Psutka, and Peter B. Read[1]
Cordilleran Geology Division, Vancouver

Brown, R.L., Lane, L.S., Psutka, J.F., and Read, P.B., Stratigraphy and structure of the western margin of the northern Selkirk Mountains: Downie Creek map area, British Columbia; in Current Research, Part A, Geological Survey of Canada, Paper 83-1A, p. 203-206, 1983.

Abstract

Goldstream slice of the Selkirk allochthon has been mapped northwestward from Carnes Creek to Standard Peak. Complexly deformed strata of the Cambrian Marsh Adams, Mohican and Badshot formations, and Index and Jowett formations of the Lardeau Group of presumed early Paleozoic age comprise the slice. The distribution of map units within the northwesterly trending, northeasterly dipping Goldstream slice is the result of two macroscopic phases of tight to isoclinal folding and subsequent faulting that have cut the slice into several fault-bounded domains. Within the map area, the domains from east to west are: Carnes, Kelly, Roseberry and Holdich. In Carnes domain, superposition of second-phase folds on inverted stratigraphy has produced synformal anticlines and antiformal synclines. In Kelly domain and the eastern margin of Roseberry domain refolding of macroscopic first-phase isoclines by non-coaxial second-phase folds has developed type 2 interference patterns that give rise to both normal and inverted stratigraphy. The central and eastern parts of the Roseberry domain are dominated by macroscopic first-phase isoclines with normal stratigraphy. In Holdich domain, the presumed upper Index Formation dips northeasterly and underlies Jowett Formation in the hanging wall of the Columbia River fault zone.

Metavolcanic rocks and phyllite of the upper Index Formation host the Standard copper-zinc deposit.

Introduction

The Goldstream slice of the Selkirk allochthon lies in the hanging wall of the Columbia River fault zone (Fig. 26.1; Read and Brown, 1981). Structural complexity of the slice, which arises from two phases of isoclinal folding and subsequent faulting, has obscured stratigraphic relationships. According to various workers, the slice includes rocks of the Hadrynian Horsethief Creek Group, Lower Cambrian Hamill Group and Badshot Formation, and presumed lower Paleozoic Lardeau Group. Wheeler's geological mapping at 1 inch to 4 miles (1965) showed that of the Hamill Group, Badshot Formation, and Lardeau Group in the Carnes Peak area southwest of upper Downie Creek, only the Lardeau and Badshot extend northward to Goldstream River. Brown et al. (1977) and Höy (1979) studied part of the same region from Standard Peak northward to the Goldstream River and tentatively correlated map units with Horsethief Creek Group and Hamill Group. Lane (1977) mapped the slice from Standard Peak northward to Downie Creek, and suggested that map scale folds are second-phase structures that have been superimposed on the inverted limb of a first-phase nappe. Read and Brown (1979) found a zone of inverted stratigraphy in the Carnes Peak area, but were uncertain whether the inversion was due to phase one folding or refolding of phase one by phase two folds. Northeast of Downie Creek in the Mount Anstey area, both phase one and phase two isoclinal folds exist, but the stratigraphy is not inverted.

Two weeks were devoted to further unravelling of the stratigraphy and structure of that part of the Goldstream slice lying within map area 82M/8. Working at a scale of 1:25 000, mapping was started from fossiliferous Badshot Formation lying within rocks of known stratigraphic position in the vicinity of Roseberry Mountain (Fig. 26.2) and proceeded northwestward to rocks of uncertain stratigraphic correlation.

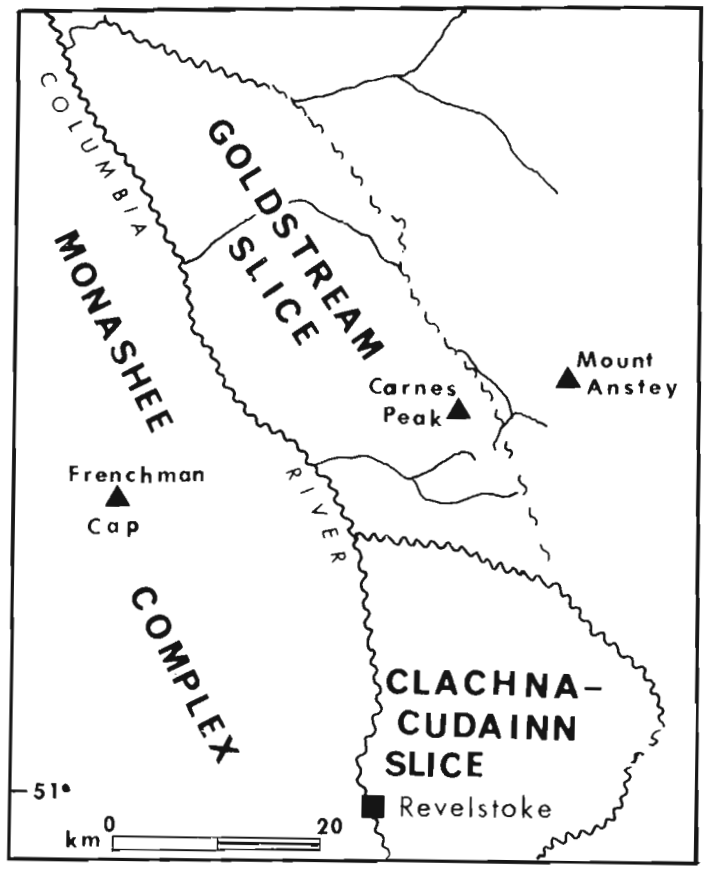

Figure 26.1. *Location and setting of Downie Creek map area.*

[1] Geotex Consultants Limited, 1200-100 West Pender Street, Vancouver, B.C.

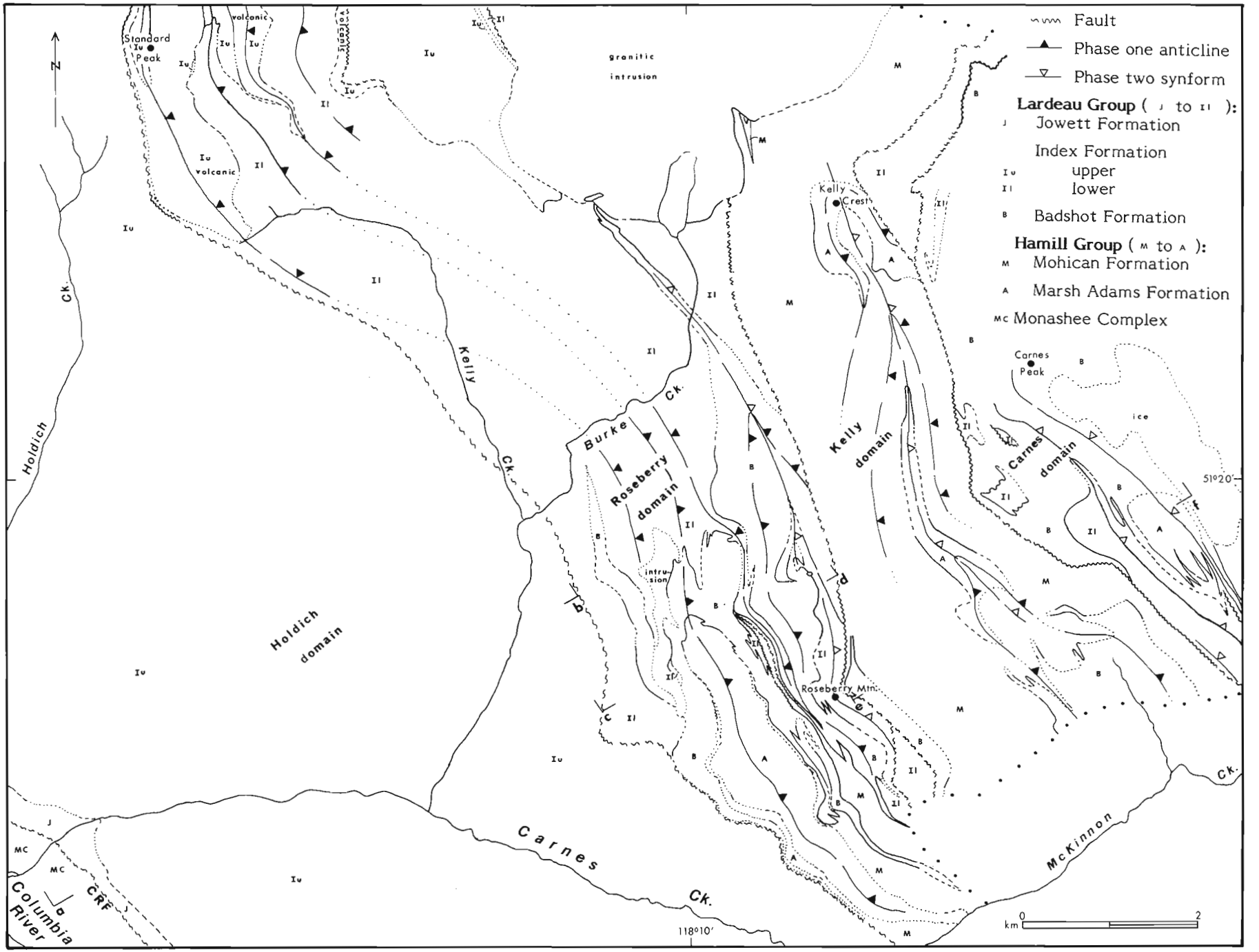

Figure 26.2. *Simplified structural and stratigraphic map. CRF = Columbia River fault zone.*

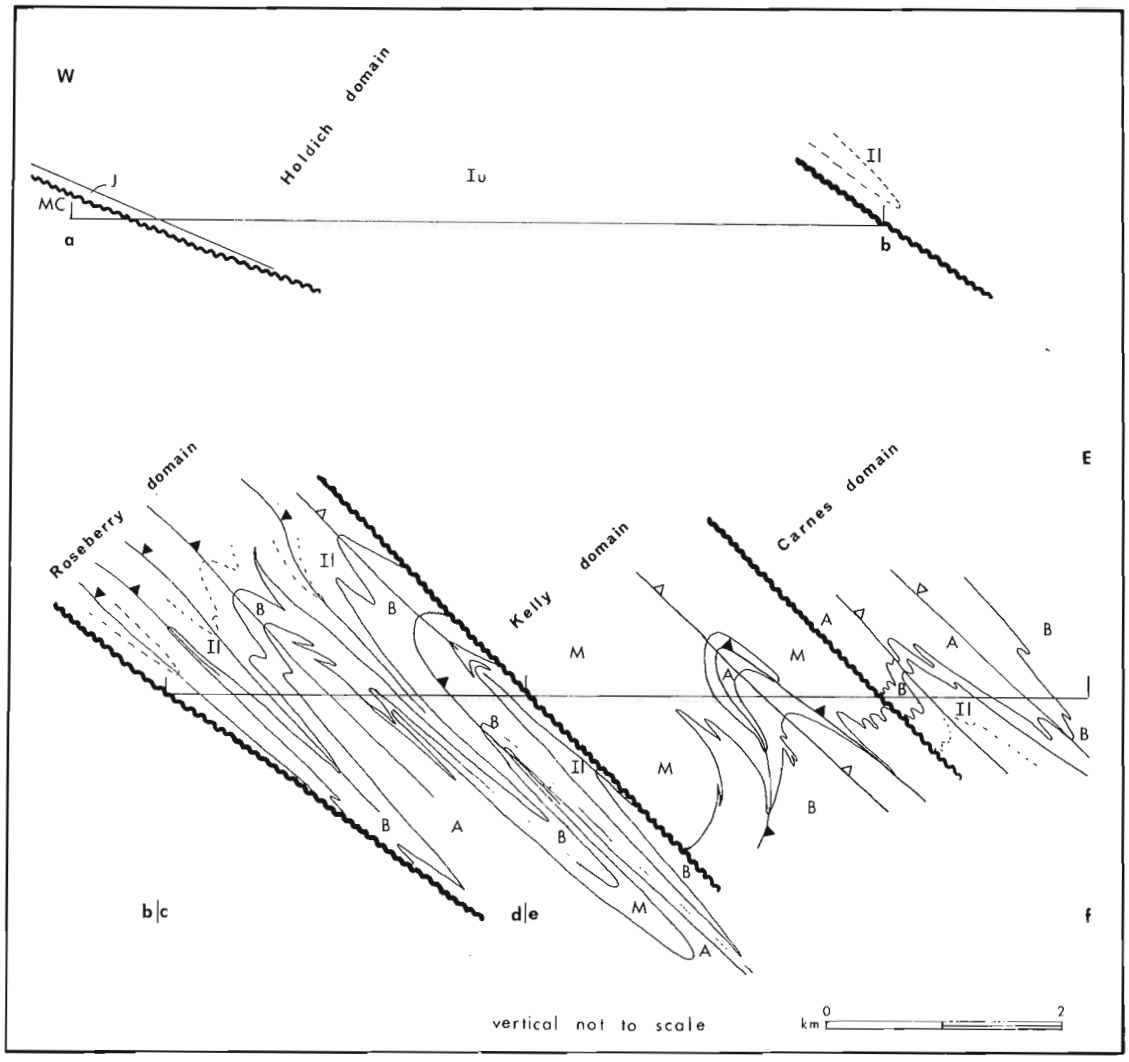

Figure 26.3. *Structural cross section. True dips of stratigraphic and structural boundaries have been drawn to scale, but projection above and below the section is diagrammatic. Section lines located and units described in Figure 26.2.*

Stratigraphy

Archaeocyathid-bearing, grey limestone of the Badshot Formation (fossils, located by Read in 1978 on the peak of Roseberry Mountain) extends southeastward to McKinnon Creek and northwestward across the headwaters of Burke Creek where it is truncated by a granitic pluton. The underlying Hamill Group consists of light green calcareous phyllite of the Mohican Formation underlain, in turn, by phyllitic quartzite of the Marsh Adams Formation. The lower part of the Index Formation, overlying the Badshot Formation, comprises grey phyllite except in the Carnes Peak area where it is accompanied by a local basal conglomerate. Near Standard Peak, grey phyllite underlies basic volcanic flows and local tuffs of the upper Index Formation. East of Standard Peak grey and green siliceous phyllite and phyllitic limestone structurally, and probably stratigraphically, overlie the basic volcanic rocks. West of Standard Peak green siliceous phyllite and phyllitic quartzite lie faulted against grey phyllite of the lower Index Formation. To the west along the lower slopes of the Columbia River valley are dark green tuffaceous volcanic rocks (with thin white dolomitic limestone) which are lithologically similar to the Jowett Formation of the Lardeau Group. Because the green siliceous phyllite and phyllitic quartzite structurally underlie the metavolcanic rocks, they probably belong to the upper Index Formation rather than the Broadview Formation.

Structure

Southeast of Burke Creek the distribution of stratigraphic boundaries results from the interference between two phases of non-coaxial isoclinal folding and subsequent faulting (Fig. 26.2). Repetition of stratigraphic units along axial surface traces and generation of Type 2 (Ramsay, 1967, p. 525) interference patterns implies an initially high angle between phase one and phase two hinge lines, as in the Mount Anstey area to the east. Early faulting is related to limb attenuation during folding, but significant faulting later than folding has disrupted the fold geometry.

North-northwesterly striking and easterly dipping, late faults truncate northwesterly trending folds and cut Goldstream slice into fault-bounded domains which are 2 to 6 km wide. From east to west these are Carnes, Kelly, Roseberry and Holdich domains. In Carnes domain, second-phase folding obliterated evidence of earlier deformation, produced synformal anticlines and antiformal synclines, and inverted the intensely deformed rocks (Fig. 26.3).

Southeast of Carnes Peak, the core of a second-phase antiform exposes grey phyllite of the lower Index Formation structurally under the older Badshot limestone, and a second-phase synform has a core of siliceous phyllite of the Marsh Adams Formation structurally over the younger Badshot limestone (Fig. 26.2, 26.3). A steep northeasterly dipping fault sets Carnes domain against Kelly domain on the southwest. A northwesterly plunging second-phase antiform dominates the structure of Kelly domain. Northwestward along the trace of the axial plane of the antiform, Mohican, then Marsh Adams, and a repetition of the two formations all structurally overlie the Badshot Formation. The inverted and then normal stratigraphic order along the trace of the second-phase axial surface probably arises from a series of non-coaxial first-phase folds deformed about a second-phase antiform (Fig. 26.2, 26.3). A moderate northeasterly dipping fault separates Roseberry domain from Kelly domain. Northwest of Roseberry Mountain a major second-phase antiform deforms a first-phase fold with a core of Badshot limestone surrounded by grey phyllite of the lower Index Formation (Fig. 26.2, 26.3). Second-phase folding decreases in intensity west of Roseberry Mountain and isoclinal first-phase folds with sheared and attenuated limbs are preserved as antiformal anticlines and synformal synclines with a northwest trend and northeasterly dipping axial surface. Holdich domain lies between moderately to gently northeasterly dipping faults. Within the domain rocks form a northeasterly dipping panel structurally bottomed by the Jowett Formation. To the southwest, the Columbia River fault zone separates the Goldstream slice of Selkirk allochthon from the early Proterozoic rocks of Monashee Complex.

Discussion

Detailed mapping between Carnes Creek and Standard Peak confirmed that the area is underlain by Marsh Adams and Mohican formations of the Hamill Group, Badshot Formation, and Index and Jowett formations of the Lardeau Group. The complex distribution of these units involving inversion, repetition, and omission is the result of interference of two phases of non-coaxial isoclinal folding and subsequent faulting. Superposition of second-phase folds on previously inverted stratigraphy as proposed by Lane (1977) and considered by Read and Brown (1979) only partly accounts for the structural geometry of the Carnes Peak area. Instead second-phase, westerly verging isoclines have refolded first-phase easterly verging folds of the same order resulting in some areas of inverted stratigraphy and others of normal stratigraphy. The presence of larger first-phase folds (nappes) remains conjectural.

The Columbia River fault was active in Middle to Late Jurassic when major dip-slip displacement brought younger hanging wall rocks from the west onto pre-Windermere rocks of the Monashee Complex. Minor motion occurred along this fault during Tertiary reactivation (Read and Brown, 1981). The age and sense of displacement of faults that bound domains in the Goldstream slice are unknown. Because the same formations are found in the fault-bounded domains, motion on the faults is probably relatively minor.

The Standard copper-zinc property (see Hoy, 1979, for location and geology) lies within rocks that have been of uncertain correlation; our results place the deposit in basic metavolcanic rocks and phyllite of the upper Index Formation.

References

Brown, R.L., Höy, T., and Lane, L.
1977: Geology of the Goldstream River – Downie Creek area, Southeastern British Columbia; B.C. Ministry of Energy, Mines and Petroleum Resources, Preliminary Map 25.

Höy, T.
1979: Geology of the Goldstream area; British Columbia Ministry of Energy, Mines and Petroleum Resources, Bulletin 71.

Lane, L.S.
1977: Structure and stratigraphy. Goldstream River – Downie Creek area, Selkirk Mountains, British Columbia; M.Sc. thesis, Carleton University, Ottawa, Ont. 140 p.

Read, P.B. and Brown, R.L.
1979: Inverted stratigraphy and structures, Downie Creek, British Columbia; in Current Research, Part A, Geological Survey of Canada, Paper 79-1A, p. 33-34.

1981: Columbia River fault zone: southeastern margin of the Shuswap and Monashee complexes, southern British Columbia; Canadian Journal of Earth Sciences, v. 18, p. 1127-1145.

Ramsay, J.
1967: Folding and fracturing of rocks; McGraw Hill, New York, 568 p.

Wheeler, J.O.
1965: Big Bend map-area, British Columbia; Geological Survey of Canada, Paper 64-32.

27.

MULTIPARAMETER GEOPHYSICAL SURVEYS OFF THE WEST COAST OF CANADA: 1973-1982

Project 800010

R.G. Currie, R.V. Cooper[1], R.P. Riddihough[2], and D.A. Seemann[2]
Cordilleran Geology Division, Patricia Bay

Currie, R.G., Cooper, R.V., Riddihough, R.P., and Seemann, D.A., Multiparameter geophysical surveys off the west coast of Canada: 1973-1982; in Current Research, Part A, Geological Survey of Canada, Paper 83-1A, p. 207-212, 1983.

Abstract

Systematic marine geophysical surveys off the west coast of Canada have almost completed coverage out to the 200 nautical mile limit. Magnetic, gravity, bathymetric and seismic data are all available through a series of published maps and open files at various scales.

Introduction

The Pacific Geoscience Centre, in conjunction with the Canadian Hydrographic Service, the Gravity Division of Earth Physics Branch in Ottawa, and the Geological Survey of Canada in Vancouver, has, since 1973, conducted a series of multiparameter marine geophysical surveys off Canada's west coast (Fig. 27.1). The survey platform for all work has been **CSS Parizeau**, a 65 m oceanographic research vessel. The surveys have been conducted on lines running normal to the coast with a spacing of 5 km on the continental shelf and 10 km in deeper water and with an absolute accuracy of ± 200 m. The parameters measured consistently have been bathymetry (12 kHz), gravity and magnetic fields. As equipment has improved, single channel reflection profiling has been conducted on a reconnaissance line spacing of 30-40 km, and some 3.5 kHz sounding records have also been obtained. At all times, only measurements that can be made with the ship under way have been included in the program.

Systematic regional measurements of gravity, magnetic field and bathymetry have been completed out to a distance of 100 nautical miles from the Canadian west coast. Approximately half of a further program to survey to 200 nautical miles has been completed over the last three years. All navigation, magnetic and gravity field measurements plus a large proportion of bathymetric soundings are recorded in digital form and available through computer files. All the surveys have been merged and adjusted through cross-over

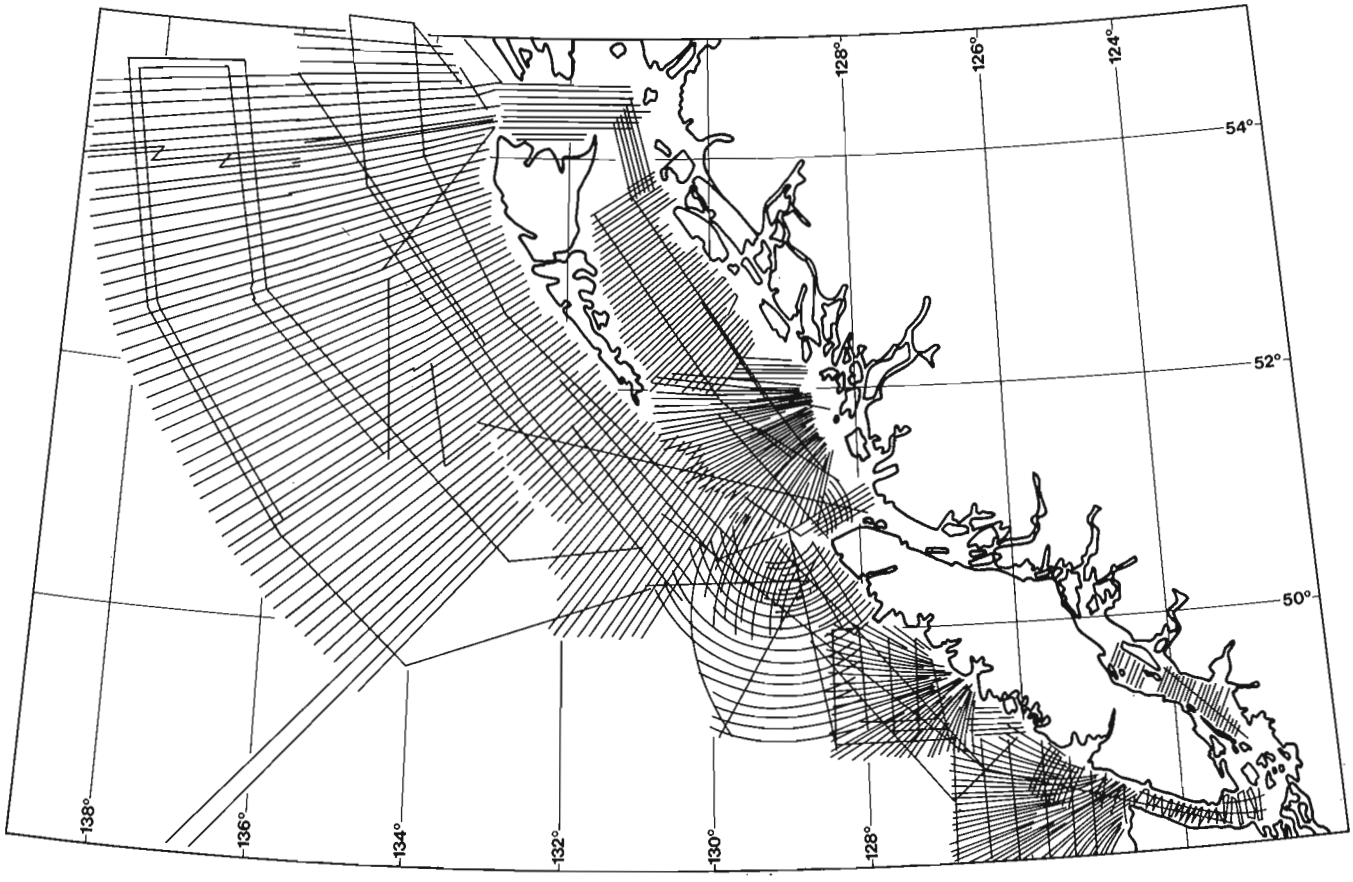

Figure 27.1. *Track chart of west coast multiparameter surveys to 1982.*

[1] Gravity, Geothermics and Geodynamics Division, Earth Physics Branch, Ottawa, Ont. K1A 0Y3.
[2] Pacific Geophysics Division, Earth Physics Branch, Pacific Geoscience Centre, Box 6000, Sidney, B.C. V8L 4B2.

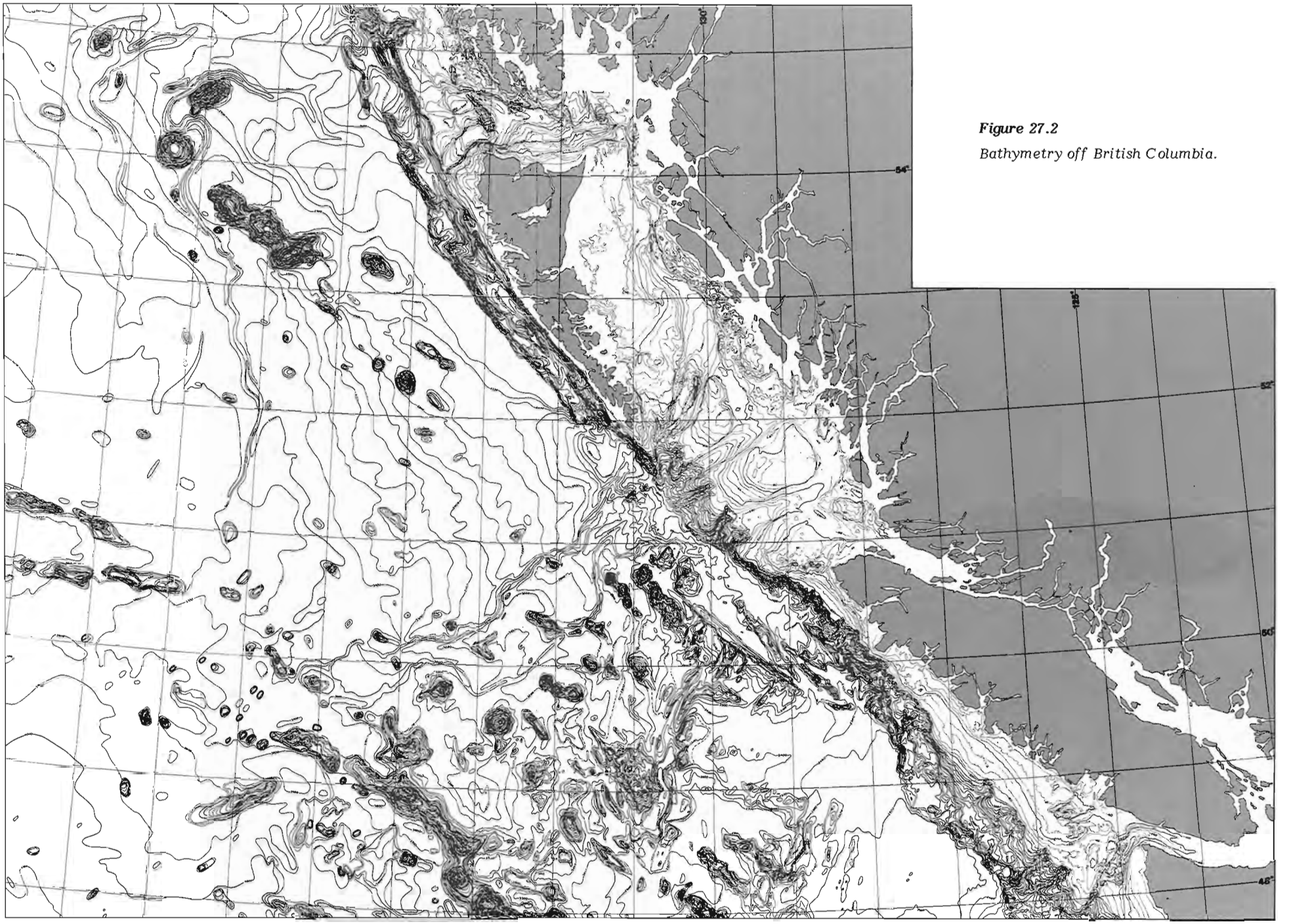

Figure 27.2

Bathymetry off British Columbia.

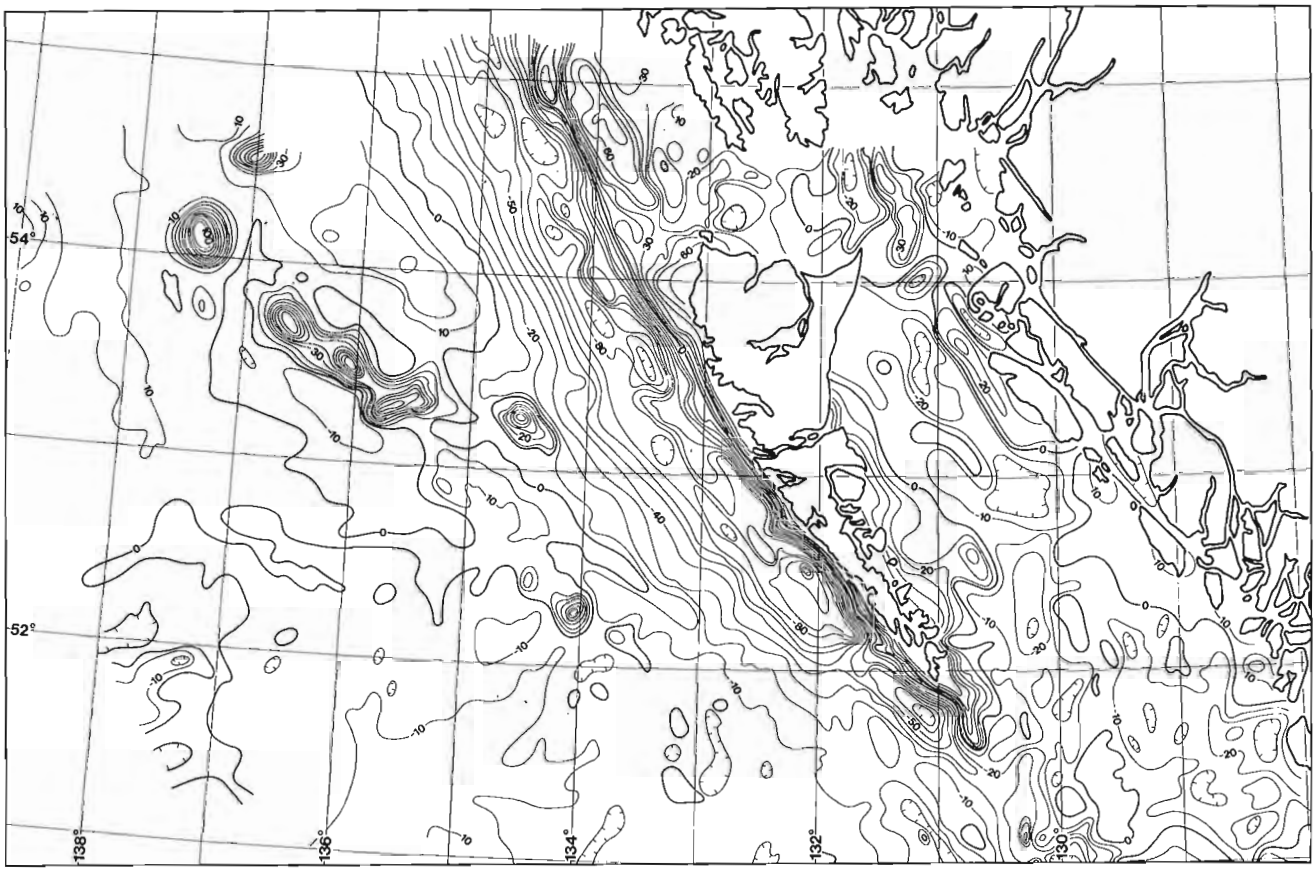

Figure 27.3. *Free-air gravity anomaly (relative to IGSN 71, GRF 67) off British Columbia; NW. Contour interval 10 mgals.*

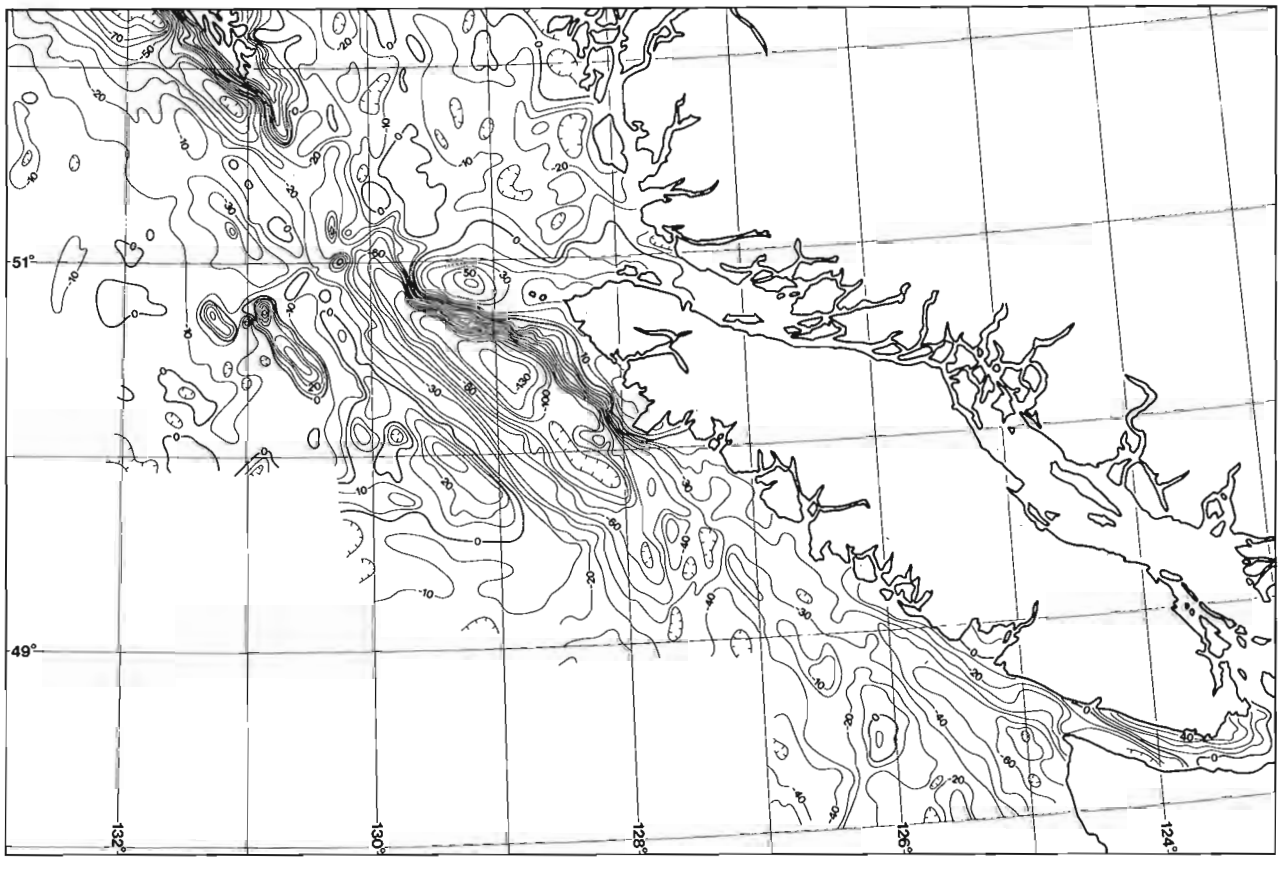

Figure 27.4. *Free-air gravity anomaly (relative to IGSN 71, GRF 67) off British Columbia; SE. Contour interval 10 mgals.*

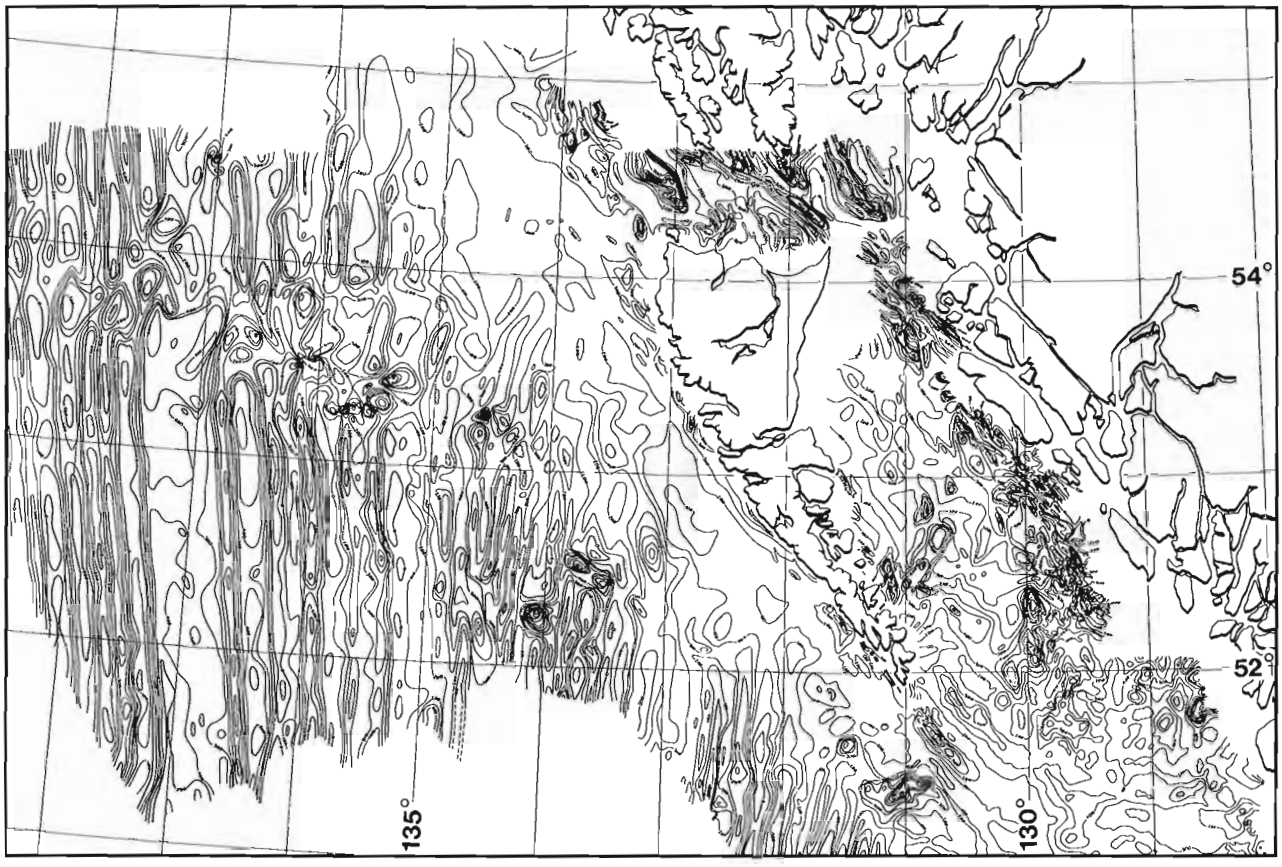

Figure 27.5. *Total field magnetic anomaly (relative to IGRF) off British Columbia; NW. Contour interval 100 nT.*

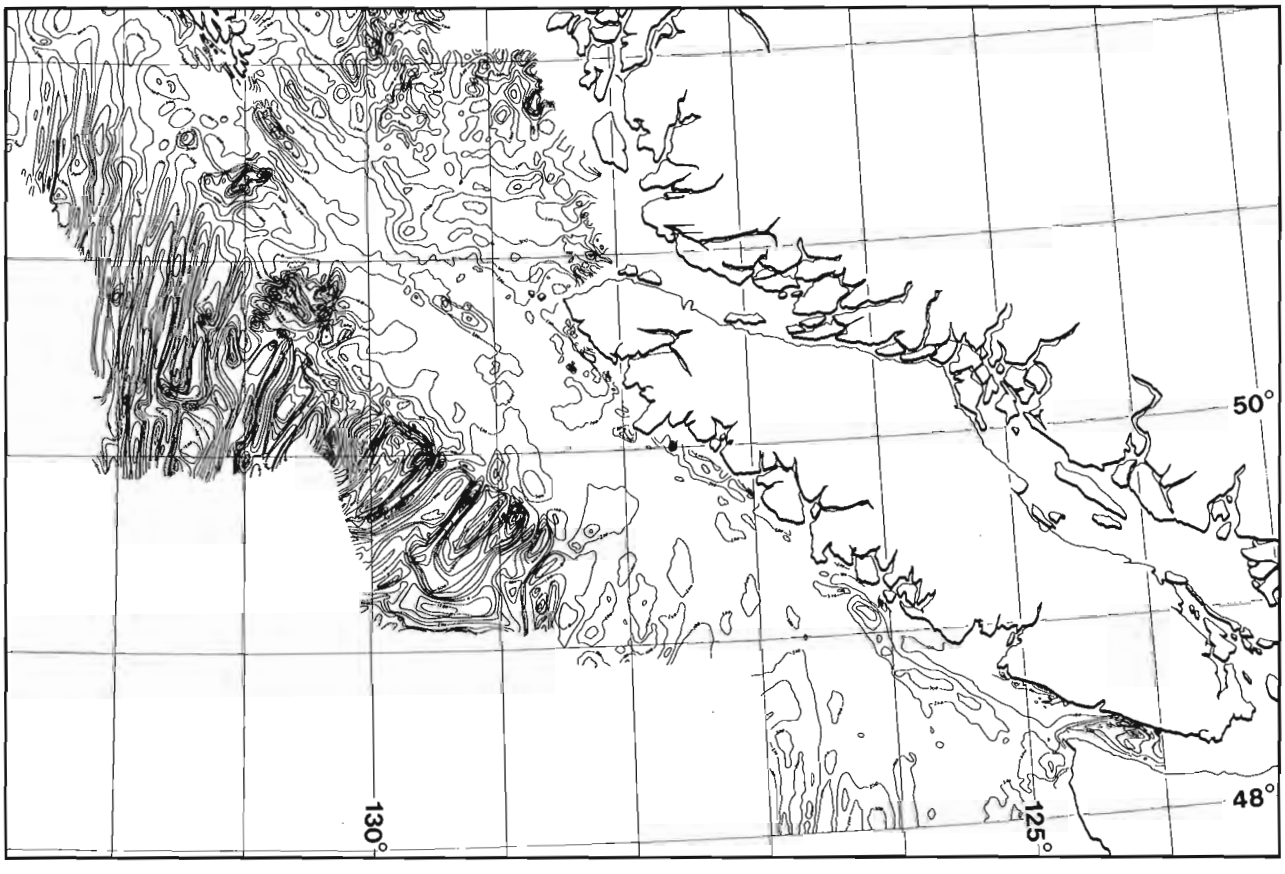

Figure 27.6. *Total field magnetic anomaly (relative to IGRF) off British Columbia; SE. Contour interval 100 nT.*

analysis, gravity base ties, instrument calibration, regional field removal and magnetic diurnal corrections to form a uniform data set of the highest standards.

The data have been made available throughout the program (usually within a year of the survey) on an Open File or manuscript basis. Much of it has been issued as Natural Resource Charts at 1:250 000, as Open File maps, or as Hydrographic plotting sheets at 1:500 000 or 1:250 000. A selection of reflection seismic data was released in an unique open file compilation of profiles optically reduced to uniform horizontal and vertical scales corresponding to distance and time respectively (Davis and Seemann, 1981). The gravity data up to 1980 are included in the recently published Gravity Map of Canada (Earth Physics Branch, 1982). A full list of data sources is included as an Appendix to this report.

The information gathered by this regional program provides a foundation for further geoscience investigations as well as mineral and energy exploration on the western margin. The gravity field forms an integral and critical part of the information necessary for inertial guidance and navigation necessary under the North American Defence system.

Bathymetry

Figure 27.2 shows a compilation of all bathymetric data to 1982 (D.A. Seemann, 1982). The majority of soundings have been reduced with a constant velocity of 1463 m/sec. Contours are at 20 m intervals on the shelf, 100 m elsewhere.

Amongst the most notable features shown in this recent compilation are: (i) the complex and yet strongly lineated structure of the marine terrace off the Queen Charlotte Islands; (ii) the size and distribution of the seamounts forming the southeastern end of the Kodiak-Bowie seamount chain; and (iii) two major sea channels running south from Dixon Entrance towards the abyssal plain.

Gravity

The free-air gravity data, contoured in Figures 27.3 and 27.4, were obtained with dynamic La Coste and Romberg gravimeters S56, S41 or SL1. Surveys were initiated in Victoria or Sidney with intermediate gravity bases ties at Port Hardy, Tasu or Prince Rupert, as appropriate. The final accuracy is estimated at ±2 mgal. The data are available in digital, plotted or contoured map form through the Open Files listed in the Appendix.

Notable features of the gravity map are the series of linear gravity lows and steep gradients which occur along the continental slope and rise. In particular, the marine terrace off the Queen Charlotte Islands is characterized by an approximately -100 mgal free-air low (Fig. 27.3). The largest anomaly is located over the Winona Basin off the northern tip of Vancouver Island where the free-air values reach -130 mgal.

Magnetics

A compilation of total field magnetic data (Currie et al., 1982) is shown in Figures 27.5 and 27.6. Data were obtained with a Barringer OM 104 proton precession magnetometer and have been corrected for diurnal variations and reduced to IGRF.

The north-south magnetic lineations of the oceanic crust are clearly visible well beyond Anomaly 6 (20 MaBP) in the northwest of the survey area. The amplitude of oceanic anomalies increases towards the modern spreading centres off Vancouver Island and Queen Charlotte Sound. On the shelf, Hecate Strait and Dixon Entrance are characterized by high gradient, high amplitude anomalies produced by shallow, heterogeneous sources.

Future Programs

The present program and rate of coverage is expected to continue until all areas within 200 nautical miles of the coast are covered to the same standard and spacing. It is estimated that this will be completed in 1984 or 1985 at which time proposals to extend the surveys beyond 200 nautical miles will be assessed.

References

Currie, R.G., Seemann, D.A., and Riddihough, R.P.
1982: Total field magnetic anomaly offshore British Columbia; Geological Survey of Canada, Open File 828.

Davis, E.E. and Seemann, D.A.
1981: A compilation of seismic reflection profiles across the continental margin of western Canada; Geological Survey of Canada, Open File 751.

Earth Physics Branch
1982: Gravity Map of Canada; Earth Physics Branch, Energy, Mines and Resources Gravity Map Series 80-1.

Seemann, D.A.
1982: Bathymetry off the coast of British Columbia; Earth Physics Branch, Open File 82-25.

APPENDIX

Bathymetric Data

Natural Resource Charts

15783, 15785, 15787, 15789, 15792, 15794, 15796, 15798, 15890*, 19304, 19306, 19308*, 19316, 19318, 19400, 19410 (printed, coloured, 100 m contours, 10 m on shelf. 1:250 000 Transverse Mercator) (* in press).

Source: 1.

Open Files	(Geological Survey of Canada)
OF 301/1975	Western Canadian Margin 1:1 000 000 Lambert Conf.
OF 550/1980	Winona Basin 1:250 000 Trans. Merc.
OF 684/1980	Dixon Entrance 1:250 000 Trans. Merc.

- the above are reproduced as black line prints.

Source: 3.

Open Files	(Earth Physics Branch)
OF 82-25	Bathymetry off the coast of British Columbia 1:1 000 000, Lambert Conf.

Source: (contact D.A. Seemann, Pacific Geoscience Centre).

Gravity Data

Natural Resource Charts

15783, 15796*, 15798*, 19308*, 19400* (printed, coloured, 10 mgal Bouguer anomaly contours, 1:250 000 Transverse Mercator) (* in press).

Source: 1.

Open Files	(Earth Physics Branch)
76-1	Queen Charlotte Sound 1:250 000 Trans. Merc.
76-2	La Perouse Bank 1:250 000 Trans. Merc.
77-1	Nootka Sound 1:250 000 Trans Merc.
77-2	Brooks Peninsula 1:250 000 Trans. Merc.
82-15	British Columbia Coast 1:1 000 000 Lambert Conf.

- the above are available as either contoured Bouguer or free air anomaly maps reproduced as black line prints. In addition, all data up to 1980 may be obtained at any scale or projection at the users request. Copies of the data files are available on magnetic tape.

Source: 4.

Magnetic Data

Natural Resource Charts

15783, 15785, 15796, 15798*, 19308*, 19318*, 19400*, 19410 (printed, coloured, anomaly and total field, contour interval 50 nT, 1:250 000 Transverse Mercator) (* in press).

Source: 1.

Magnetic Data (cont.)

Open Files	(Geological Survey of Canada)
OF 392/1976	S. Vancouver Island 1:500 000 Trans. Merc.
OF 393/1976	Queen Charlotte Sound 1:500 000 Trans. Merc.
OF 622/1979	N. Vancouver Island 1:500 000 Trans. Merc.
OF 724/1981	Vancouver Island 1:1 000 000 Lambert Conf.
OF 828/1982	Total Field Magnetic Anomaly Offshore British Columbia 1:1 000 000 Lambert Conf.

- the above are contoured anomaly maps reproduced as black line prints.

Source: 3.

Seismic Data (Single channel reflection)

Open Files	(Geological Survey of Canada)
OF 83/1972	CSP data off Tofino Basin
OF 154/1973	CSP data off northwestern British Columbia
OF 394/1976	CSP data from Strait of Georgia

- the original data on 19" wide dry paper were photographed onto 105 mm Micro-master negatives and can be reproduced at any desired scale. A track plot and navigation listing are also included.

Source: 2. Open files are available for viewing at Geological Survey libraries. Paper reproductions may be obtained at user's expense.

OF 751/1981 – A compilation of seismic reflection profiles across the Continental Margin of Western Canada.

- the original profiles have been photographically processed so that the vertical and horizontal scales are the same, then stacked and displayed as sections. The file contains prints of each of the six sections plus detailed navigation plots.

Source: 3.

Source addresses:

1. Chart Sales & Distribution,
   Institute of Ocean Sciences,
   P.O. Box 6000, 9860 West Saanich Road,
   Sidney, B.C., V8L 4B2

2. Vancal Reproduction Group
   1180 West Hastings St.
   Vancouver, B.C., V6E 1B4

3. Geological Survey of Canada,
   Information Service, 6th Floor,
   100 West Pender Street,
   Vancouver, B.C., V6B 1R8

4. Data Centre,
   Gravity, Geothermics and Geodynamics Division,
   Earth Physics Branch, Dept. EMR,
   Ottawa, Ontario, K1A 0Y3

28.

PERMAFROST MAPPING OVER A DRAINED LAKE BY ELECTROMAGNETIC INDUCTION METHODS

Project 810003

Ajit K. Sinha and L.E. Stephens
Resource Geophysics and Geochemistry Division

Sinha, A.K., and Stephens, L.E., Permafrost mapping over a drained lake by electromagnetic induction methods; in Current Research, Part A, Geological Survey of Canada, Paper 83-1A, p. 213-220, 1983.

Abstract

A field investigation using two portable electromagnetic induction systems was carried out over a frozen drained lake basin at Illisarvik, 60 km west of Tuktoyaktuk, N.W.T., to map the growth of permafrost beneath the lake. The two instruments, with depth sounding capabilities of from 6 m to 60 m were used in a 300 x 600 m grid with readings taken every 25 m. Contour maps of measured apparent conductivity values, obtained for different coil separations and coil attitudes, indicated the presence and extent of permafrost and unfrozen material at different locations in the grid.

The field data were also interpreted quantitatively along three lines 50 m apart to determine the thickness of the frozen upper layer. The interpretation indicates that the thickness of the permafrost varies from 11 to 23 m in the central part of the lake with greater values toward the shoreline. These values of permafrost thickness agree well with results from thermal measurements in several boreholes in the area.

Introduction

In the Richards Island region of Northwest Territories, lakes cover up to 40 per cent of the total land mass and natural lake drainage has been going on for thousands of years. In 1973, J.R. Mackay of University of British Columbia proposed that a lake, which he named Illisarvik[1], be drained in order to study the process of permafrost formation. Illisarvik Lake was 60 km west of Tuktoyaktuk, N.W.T. in the Mackenzie Delta and measured approximately 300 by 600 m with a maximum water depth of 4.7 m. In permafrost areas of the arctic, the material beneath deep lakes and rivers is normally unfrozen because of the thermal influence of water cover. Removal of the water subjects the thawed lake bottom to mean annual temperatures below 0°C thus beginning the process of permafrost formation.

Predrainage geological and geophysical studies were carried out during the spring of 1978 to determine the composition and thickness of thawed sediments. Hydraulic drilling (Judge et al., 1976; MacAulay et al., 1977) provided lithological information at various spots and also holes for the insertion of multithermistor cables for thermal studies (Judge et al., 1981). At that time 32 m of lake bottom sediments consisting chiefly of sand interspersed with clay and about 5 m of organic material at the top were found to be unfrozen. It was reported later (Burgess et al., 1982) that by 1980, the sediments had frozen down to a depth of 5 to 6 m. D.C. Schlumberger soundings were also carried out over the frozen lake in 1978 by Scott (1980). The two soundings at right angles to each other have a common centre 30 m south and 10 m west of the grid origin on the lake (Fig. 28.1). The soundings indicated the presence of a moderately resistive material (35 ohm-m) in the top 15 m underlain by lower resistivity material (5 ohm-m) down to a depth of about 35 m, where the resistivity increased sharply. It was obvious, however, that to determine the nature of the sediments at greater depths, the electrode separations would have to be expanded greatly, but this would bring in enough lateral inhomogeneity to render one dimensional interpretation of the sounding data invalid. It was therefore decided to use an electromagnetic induction technique since in such systems larger depth penetration may be achieved by decreasing the frequency while keeping the coil separation constant. Induction methods also avoid the problem of contact resistance in frozen terrain which hinders direct current techniques. The energy in induction methods is induced into the ground without making physical contact.

The lake was drained in August 1978. Since then several investigators have carried out studies on the growth of permafrost over the lake basin mainly by thermal and seismic techniques. The bathymetry map of the lake before drainage (Fig. 28.1) shows a depression with a maximum depth of 4.7 m centred at 25 m west and 75 m south of the centre of the grid. All geophysical studies carried out at this site relate to this metric grid.

Laboratory studies have shown that a decrease in temperature below 0°C leads to a rather sharp increase in the electrical resistivities for most geological material. Hence permafrost or permanently frozen materials exhibit sharply higher electrical resistivities than the corresponding values in their thawed stage. Figure 28.2 (from Hoekstra and McNeill, 1973) illustrates the sharp change in resistivity values with temperature for four types of geological material when the temperature is lowered below 0°C. When the temperature gets low enough, even clay which normally has rather low resistivities behaves like a highly resistive material. This property is what the electrical techniques use for the detection of frozen materials and discrimination from adjacent thawed material.

A field investigation was carried out during the spring of 1981 over the lake basin to test the capabilities of two electromagnetic induction systems for mapping the growth of permafrost from the surface. The two instruments are battery powered portable EM systems with depth penetration capabilities to 60 m below the surface. The purpose of this survey was to cover the entire grid area shown in Figure 28.1 with the two systems and make a comparative study of the accuracy and usefulness of the systems both in a qualitative and quantitative sense. It was felt that this type of survey repeated every two or three years might establish a rate of permafrost growth beneath the lake bottom. Such information should be useful for studying the growth of permafrost under natural conditions.

[1] An Innuit word meaning "A place of learning".

Electromagnetic Resistivity Survey

Equipment

The two instruments used for the survey, EM-31 and EM-34-3, are direct reading terrain conductivity meters built by Geonics Ltd. EM-31 is a one man instrument capable of measuring ground conductivity to a depth of 6 m (Fig. 28.3). The transmitter and the receiver coils are horizontal coplanar and are mounted at the ends of a rigid fibreglass boom which may be dismantled when not in use. The coil separation and frequency of operation are 3.7 m and 9.8 kHz respectively. Ground conductivity values in mmho/m can be read directly from a meter with this instrument. Its light weight (9 kg) makes the system useful for rapid reconnaissance surveys with one operator.

EM-34-3 is a two-man unit (Fig. 28.4) similar to EM-31. The transmitter and the receiver coils are connected by a reference cable. Three coil separations of 10, 20 and 40 m may be used, the frequencies of operation being 6.4, 1.6 and 0.4 kHz for the three separations, respectively. The system may be used in two modes: horizontal coplanar (vertical dipole) or vertical coplanar (horizontal dipole) and the system's depth of investigation varies from 7.5 m to 60 m. The instrument, described earlier by Sinha (1980), therefore produces six apparent conductivity values at each station (three separations in two modes of operation) which may be inverted in terms of the conductivity and thickness of a layered ground.

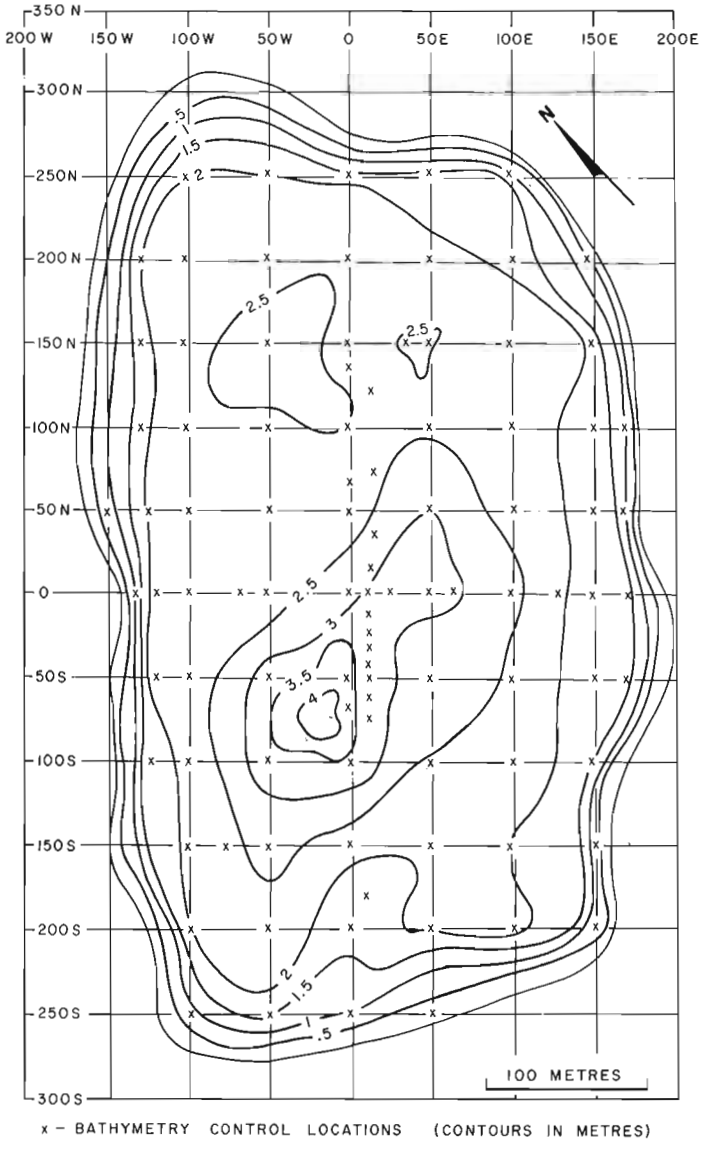

Figure 28.1. Bathymetry map over Illisarvik lake showing sounding control positions.

Theory

The theory for the computation of electromagnetic fields from oscillating magnetic dipoles over a homogeneous and a layered earth has been available for some time (Wait, 1951; Wait and Campbell, 1953; Sinha and Bhattacharya, 1966). The mutual coupling ratio (Z/Z_o) or the ratio of the secondary to the primary magnetic fields (H_s/H_p) for the case of vertical and magnetic dipoles over a homogeneous earth may be written as:

$$(Z/Z_o)_v = (H_s/H_p)_v = \frac{2}{\gamma^2 s^2}\left[9-(9+9\gamma s+4\gamma^2 s^2+\gamma^3 s^3)\exp(-\gamma s)\right] \quad (1)$$

$$(Z/Z_o)_h = (H_s/H_p)_h = \frac{2}{\gamma^2 s^2}\left[(\gamma^2 s^2-3)+(3+3\gamma s+\gamma^2 s^2)\exp(-\gamma s)\right] \quad (2)$$

where the subscripts v and h indicate vertical and horizontal dipoles and γ is the propagation constant of the medium $= \sqrt{i\omega\mu\sigma}$

where ω = angular frequence $= 2\pi f$

f = frequency in Hz

μ = magnetic permeability of the medium in Henry/m

s = separation between the transmitter and receiver coil in m

σ = conductivity of the medium in Siemens (mhos)

$i = \sqrt{-1}$, the imaginary operator.

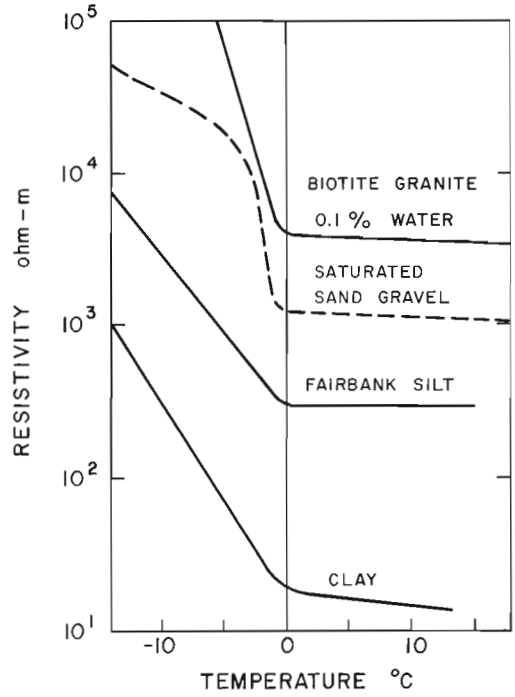

Figure 28.2. Variation of the resistivity of different geological materials with temperature (from Hoekstra and McNeill, 1973).

Figure 28.3. *Schematic representation of the Geonics EM-31 system.*

The parameter γs may be rewritten as:

$$\gamma s = \sqrt{2i}\, s/\delta = \sqrt{2i}\, B \qquad (3)$$

where $\delta = (2/\omega\mu\sigma)^{\frac{1}{2}}$ is the skin depth in metres, i.e. the depth where an incident plane wave would be reduced to 1/e or 37% of its value at the surface.

Now, if parameter $B = s/\delta$ is much smaller than 1, then equations (1) and (2) can be simplified to

$$\left(\frac{H_s}{H_p}\right)_v \approx \left(\frac{H_s}{H_p}\right)_h \approx \frac{iB^2}{2} \simeq \frac{i\omega\mu\sigma s^2}{4} \qquad (4)$$

Hence the secondary magnetic field has only a quadrature component proportional to the conductivity of the medium. Thus, when $B << 1$, i.e. when operating at low induction number, a measurement of the secondary magnetic field yields a value for the conductivity of the medium since they are linearly related. This condition prevails for both EM-31 and EM-34-3 systems in most situations. If, however, the ground is very conductive, resulting in a small δ and a large B, the linear relation shown in equation (4) is no longer valid. It may be shown that only when ground conductivity exceeds 50 mmho/m (resistivity of 20 ohm-m), the errors become significant.

For an n-layered ground, the apparent conductivity σ_a measured by the systems for values of $B << 1$ may be written as (McNeill, 1980a)

$$\sigma_a = \sum_{i=1}^{n} (\sigma_i - \sigma_{i-1})\, R(z_{i-1}) \qquad (5)$$

where the function $R(z_1)$, $R(z_2)$, etc. are evaluated at interface depths z_1, z_2, etc. from the surface. The conductivity of air (σ_0), is taken to be zero and $R(z_0) = 1$. The function R(z), called the cumulative response by McNeill (1980a) is a function of the depth z to a particular layer and indicates the contribution to the apparent conductivity from that particular depth to infinity. Since this function is known for both horizontal and vertical magnetic dipole systems, one can, for modelling purposes, compute the apparent conductivity over a multilayer earth if the conductivities and depths to different layers are known. Figure 28.5 illustrates the variation of $R_v(z)$ and $R_H(z)$ (for vertical and horizontal dipoles, respectively) against the parameter z/s. It should be noted that the cumulative response $R_v(z)$ is about twice the magnitude of $R_H(z)$ for $z/s > 1$. In other words, the vertical dipole mode has approximately twice the effective depth of exploration as the horizontal dipole mode. Hence, the apparent conductivities measured with the horizontal coplanar system (vertical dipole) will in general be different from those measured with the vertical coplanar (horizontal dipole) system at any point over a multilayer ground.

Field data from EM-31 can be quantitatively inverted for the case of a two-layer ground by taking measurements at several heights above the ground. However, this is somewhat inconvenient from the operator's point of view and the measured apparent conductivities do not change significantly with height unless the conductivity contrast is large. The EM-34-3 system produces six apparent conductivity values at each point with three separations and two modes of operation. It is relatively easy to invert these values in terms of the parameters of a two-layer ground. If the ground is more complex, one may try to model the response of a multilayer ground as given by equation (5) and modify the ground parameters until a good match is obtained with the field data. The interpretation procedure has been outlined by McNeill (1980b).

Survey Method

Geonics EM-31. The EM-31 system is carried by means of a strap hung from the operator's shoulder so that the system is horizontal at waist level (Fig. 28.3). The operator may record the reading at up to three elevation levels and may also rotate the system by 90° along a horizontal axis so that it behaves like a vertical coplanar system. At Illisarvik, readings were taken at waist level at 25 m intervals along survey lines running E-W, with a line spacing of 25 m. An area 150 m by 150 m over the residual pond, centred approximately at 20W, 75S was surveyed every 10 m along east-west lines 25 m apart. Figure 28.6 shows the plot of apparent conductivity in mmho/m over the survey area.

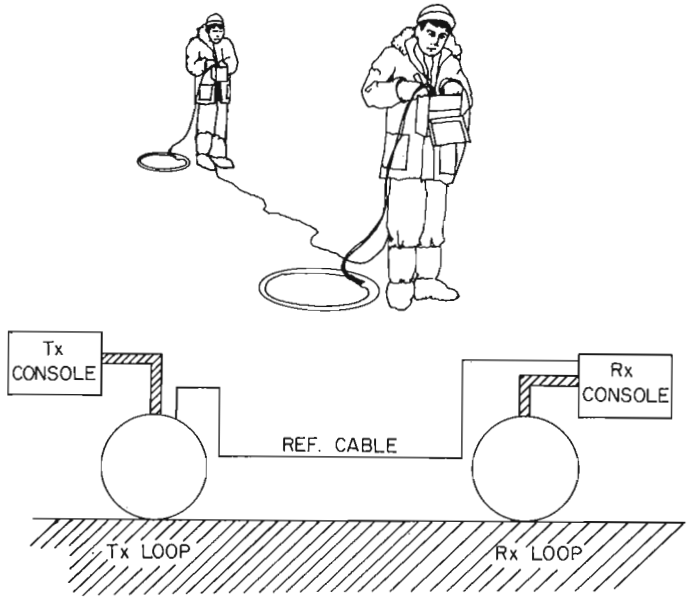

Figure 28.4. *Illustration of the Geonics EM-34-3 system in the horizontal and vertical modes.*

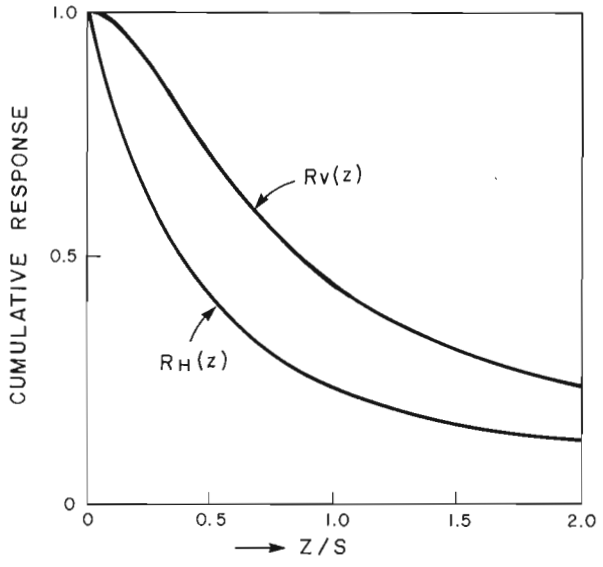

Figure 28.5. *Plot of the cumulative responses with depth for vertical and horizontal dipoles (after McNeill, 1980a).*

Geonics EM-34-3. This unit required two operators who normally took a total of six readings at each station using three coil separations and two modes of operation. Readings were taken every 25 m along east-west lines 50 m apart (Fig. 28.1). Over the residual pond, station spacings were 10 m along east-west lines 25 m apart. However, in this case only 10 and 20 m separations were used. Figures 28.7 and 28.8 illustrate the variation of apparent conductivity in mmho/m for the horizontal and vertical dipoles, respectively, with a coil separation of 10 m. There is a striking similarity between these two diagrams and the bathymetry map shown in Figure 28.1 (This is discussed in detail in the next section). Figures 28.9-28.12 illustrate the plots of apparent conductivities with coil separations of 20 and 40 m and for the horizontal and the vertical dipole configurations. All seven conductivity plots show a high near the centre of the lake and lower values toward the shoreline. However, as the coil separations increase (resulting in larger depth penetrations) the apparent conductivities increase in magnitude indicating the presence of more conductive material at greater depths.

Qualitative Interpretation of Data

The basic electromagnetic response at Illisarvik Lake is a broad elliptical anomaly bounded by the lake shoreline and becoming more pronounced towards the lake centre. The permafrost surrounding the lake has predictably low conductivity values. The maxima in the apparent conductivity plots generally coincide with the location of the depression at the bottom of the lake (residual pond) which was not drained (see Figure 28.1). The presence of residual water lying in the depression insulated the underlying unfrozen material; this material shows up as a conductivity high on all plots. In fact, there is some indication that there may be two ponds (Fig. 28.10) instead of one. The increasing intensity of the conductivity anomaly towards the lake centre is possibly caused by a thinning of the frozen ground beneath the pond.

In the two years after Illisarvik Lake was drained, the talik has frozen to a depth of 7 m below the surface (Judge et al., 1981). The conductivity of permafrost around the lake margins is imparted by significant interstitial water within the permafrost, even though the temperature is below 0°C. Anderson et al. (1973) presented evidence indicating the presence of unfrozen water in permafrost to temperatures as low as -15°C. There is also some evidence that the conductivity of permafrost materials may be frequency dependent and that mechanisms other than ionic conduction may become significantly in certain situations (Olhoeft, 1975).

As coil separations increase from 3.7 m for the EM-31 to 40 m for the EM-34-3 in the vertical dipole mode, greater depths are probed by the systems. The peak conductivity anomaly associated with the residual pond correspondingly increases from 20.8 mmho/m for EM-31 to 72.5 mmho/m for the vertical dipole mode of EM-34-3 with a coil separation of 40 m. The location of the peak shifts eastward from 10W, 100S in Figure 28.6 to 10E, 75S in Figure 28.12, as the effects of more conductive features at greater depths become more prominent.

Superimposed on the broad elliptical anomaly are perturbations caused by minor structures beneath the lake. An unexpected extension of the Illisarvik Lake anomaly was followed across the low ridge toward the east side of the lake near 250E, 50S. J.R. Mackay (personal communication, 1981) suggested that Illisarvik Lake had previously drained at this location into an adjoining lake, now naturally drained. The cessation of flowing water would have permitted permafrost to form under the ridge and a subsequent residual higher temperature or interstitial saline solutions under the ridge could cause the conductivity anomaly. An ancient drainage pathway under the ridge could also explain the presence of the weak conductive feature to the east.

Quantitative Interpretation of Data

The qualitative interpretation gives an indication of the location and extent of conductive talik in the survey area. If repeated over a period of several years such results would also indicate the relative growth of permafrost in different zones of the drained lake basin. However, qualitative results do not indicate the thickness of the permafrost or the conductivities of the different zones. This type of information is expected from quantitative interpretation of EM-34-3 data. Such interpretation could also be carried out with the EM-31 results if data were collected at several elevations. Because of the difficulty of taking readings at fixed elevations, the EM-31 was used more as a reconnaissance tool and no attempts were made to interpret EM-31 results quantitatively.

Over 250 stations were occupied by the EM-34-3 system. While quantitative interpretation of the data over the whole survey area is still in progress, this paper illustrates the results over three lines, namely, 50N, 100N and 150N. For a two-layer medium, the results may be interpreted using data sets for the vertical dipole, horizontal dipole or a combination of both. From a preliminary interpretation of the data, it was noted that the data sets from the vertical dipole were more noisy presumably because of the difficulty of keeping the two coils in the same horizontal plane over undulating terrain, and the ground is more complex than a simple two-layered case. In fact, it has 3 or more electrically distinct layers which make unique interpretation difficult. It is, however, possible to consider the ground as two-layered, with two or more layers combining to form an equivalent layer with one conductivity. Sartorelli and French (1982) have indicated that such an approach is valid over permafrost covered terrain in Yukon and Alaska.

Figure 28.13 illustrates the variation of apparent conductivity in mmho/m along the three lines for a coil separation of 20 m using both horizontal and vertical dipole modes. The conductivities are low near the eastern and western edges of the lake and have maxima near the centre. The conductivities for the vertical dipole mode are, in general, higher than those for the horizontal dipole, thereby indicating the presence of more conductive material at depth. On line 150N, however, at location 25W, the conductivity is higher for the horizontal dipole mode. This could be explained if

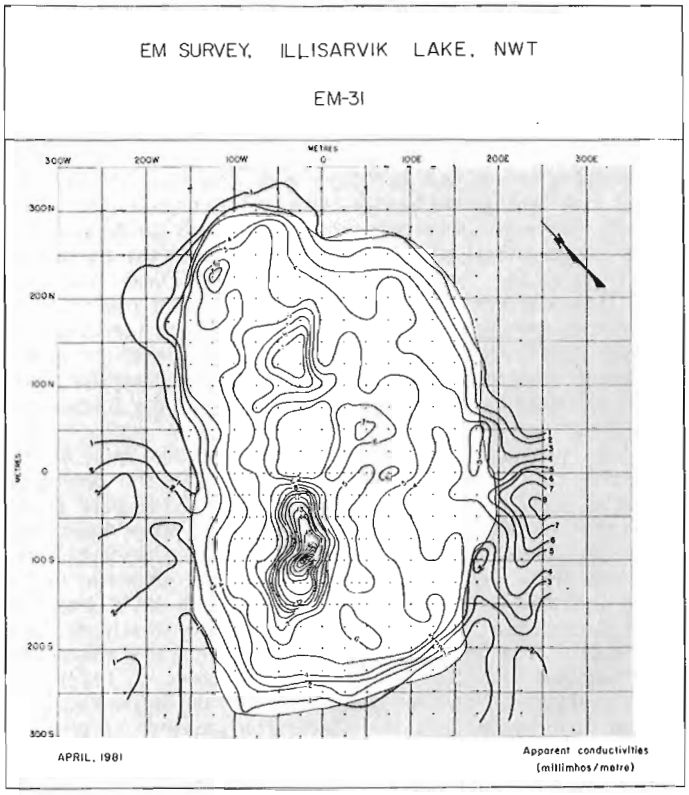

Figure 28.6. *Contoured representation of the apparent conductivity in mmho/m over the lake bed with Geonics EM-31.*

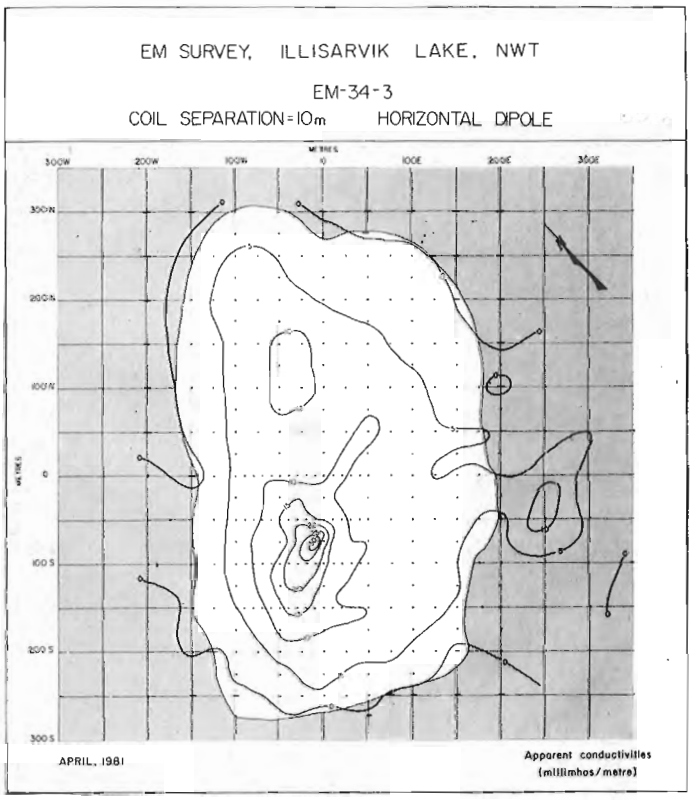

Figure 28.7. *Contours of the apparent conductivity in mmho/m over the lake with Geonics EM-34-3 in the horizontal dipole mode with 10 m coil separation.*

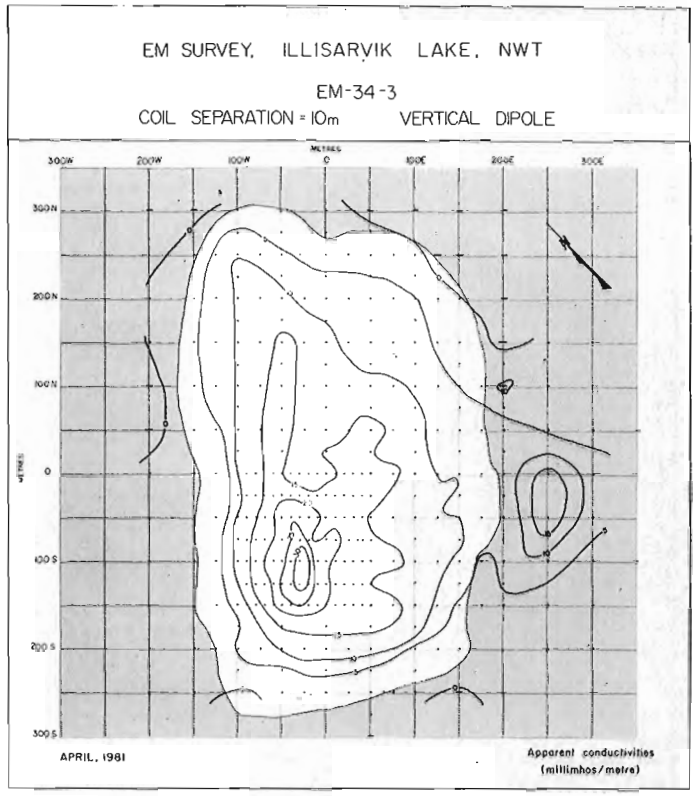

Figure 28.8. *Contours of the apparent conductivity in mmho/m with Geonics EM-34-3 in the vertical dipole mode with 10 m coil separation.*

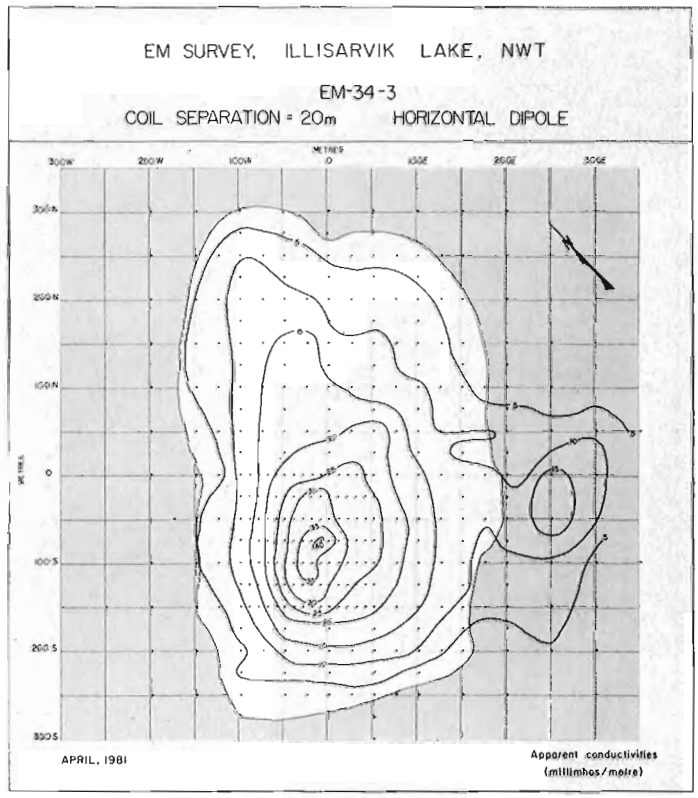

Figure 28.9. *Contours of the apparent conductivity in mmho/m over the lake with Geonics EM-34-3 in the horizontal dipole mode with 20 m coil separation.*

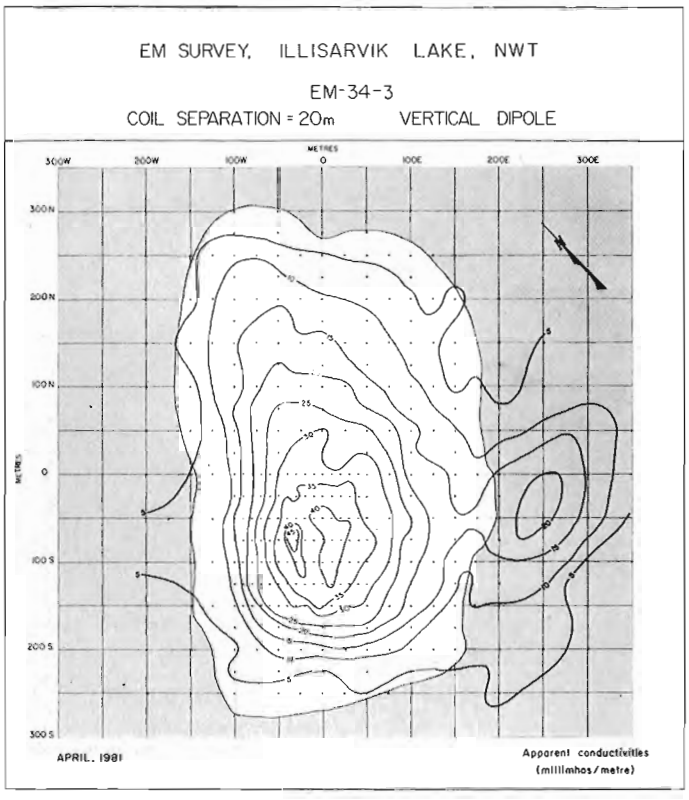

Figure 28.10. *Contours of apparent conductivity in mmho/m over the lake with Geonics EM-34-3 in the vertical dipole mode with 20 m coil separation.*

there were another resistive layer (permafrost) at a depth which, while not influencing the horizontal dipole results, might reduce the apparent conductivity values for the vertical dipole results because of the greater penetration achieved in the vertical dipole mode.

The horizontal dipole data over the three lines were interpreted assuming a two-layer ground with a resistive top layer (ice and permafrost) and a conductive bottom layer (talik). The significant parameter, the depth to the unfrozen (high conductivity) layer, has been plotted for the three lines in Figure 28.14. The resistivity of the top layer was very high (low conductivity) for all stations. At a few stations, mostly toward the edge of the lake, the observed data did not fit the two-layer model. These areas are shown by dashed lines and question marks. Near the former shoreline, even when the data satisfied the two-layer model, the fit between the field and model results was generally poor. These stations produced large values for the thickness of the resistive layer which, although possible from the geological point of view, may be in error because of the poor match with the theoretical model. Results from all three lines point to a maximum thickness of the top resistive layer between 25E and 50E. Reasonably uniform thickness between 11 and 23 m prevail at all other positions between 100W and 75E. The interpreted thickness of 18 m of the resistive layer (permafrost) at 00E on line 50N compares favourably with thermal data (A. Taylor, personal communication, 1982) from a borehole at 00E, 68.6N which indicated the thickness of the frozen layer to be 13.7 m. Data from another borehole at 00E, 132N indicated that the ground was frozen down to a depth of 16.7 m in September 1980 but had frozen to the bottom of the hole (28 m) by April 1981 which agrees well with our interpreted depths at locations 00E, 100N and 00E, 150N.

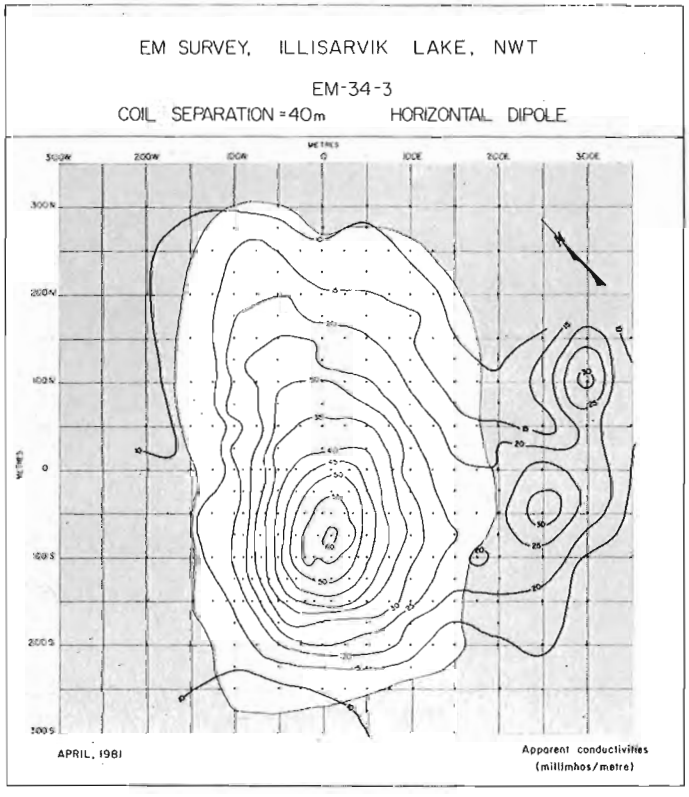

Figure 28.11. *Contours of apparent conductivity in mmho/m over the lake with Geonics EM-34-3 in the horizontal dipole mode with 40 m coil separation.*

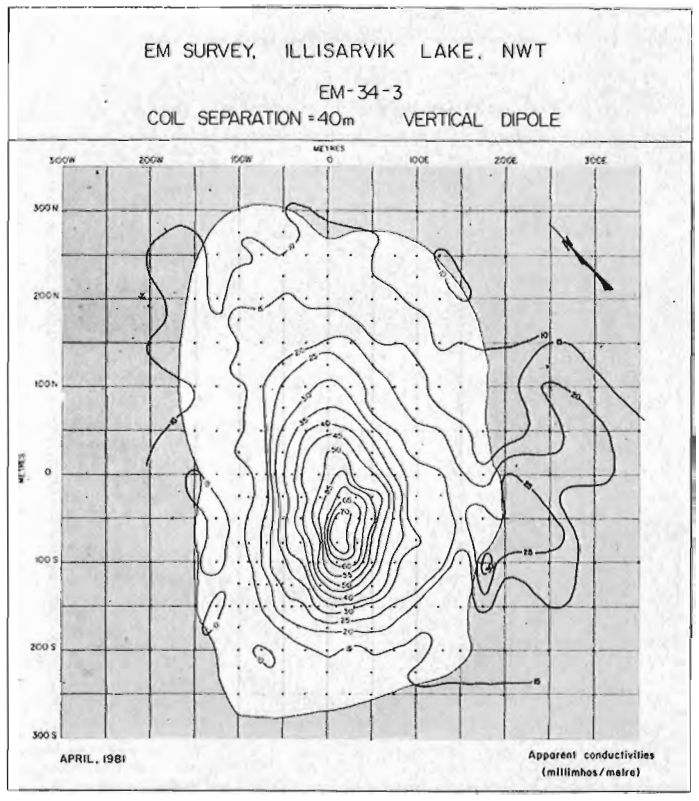

Figure 28.12. *Contours of apparent conductivity in mmho/m over the lake with Geonics EM-34-3 in the vertical dipole mode with 40 m coil separation.*

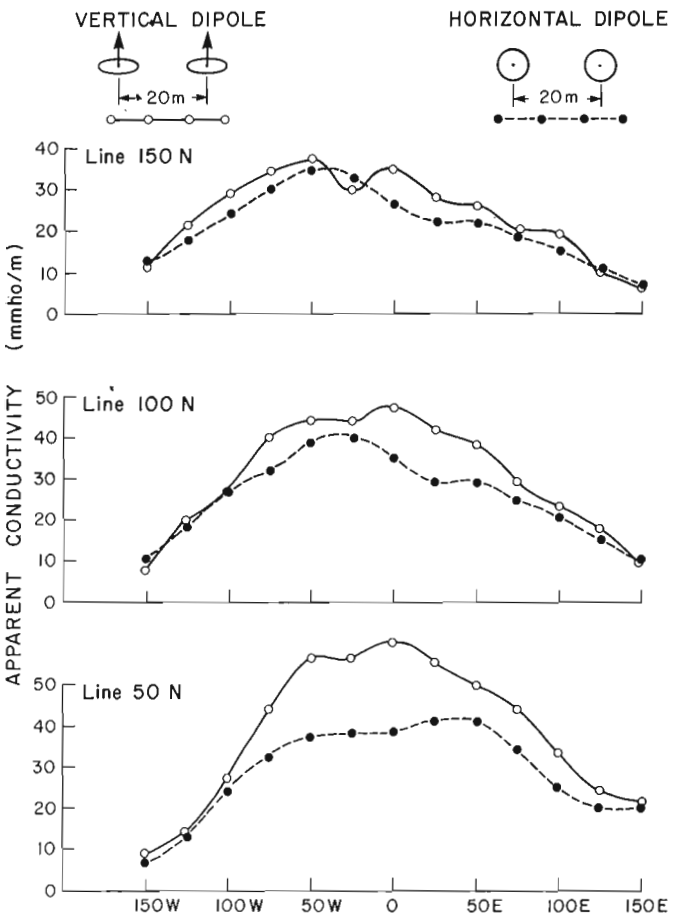

Figure 28.13. Plot of apparent conductivities along three lines for vertical and horizontal dipole modes for a coil separation of 20 m.

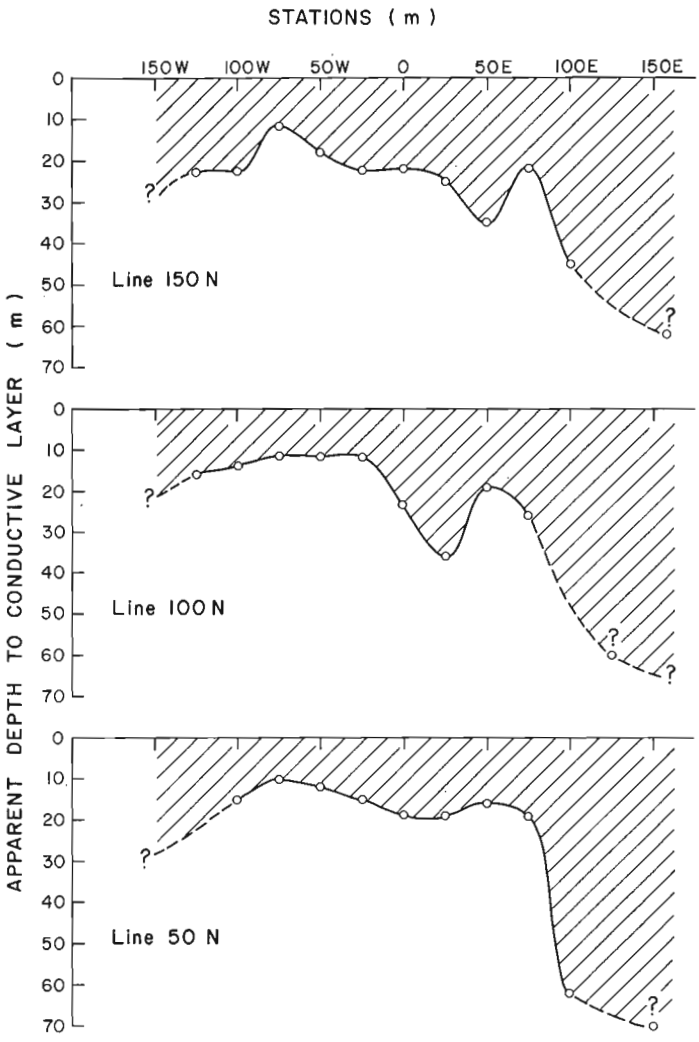

Figure 28.14. Plot of the apparent depths to the conductive layer in metres along three lines over the lake using horizontal dipole data.

Conclusions

This paper describes an application of two portable electromagnetic induction systems, EM-31 and EM-34-3 for shallow mapping of permafrost over a drained lake basin at Illisarvik, 60 km west of Tuktoyaktuk, N.W.T., in the Richards Island area. The interpreted permafrost thickness values of 11 to 23 m over three lines are in good agreement with borehole thermal data. The advantages of using EM induction systems over D.C. sounding techniques in permafrost mapping are: (a) the elimination of the necessity to make electrical contacts with the frozen ground which permits use in winter months, and (b) better lateral resolution for comparable depth penetration resulting from reduced noise due to lateral inhomogeneities. Furthermore, the induction systems are logistically efficient; the whole Illisarvik area was covered in about a week.

Electrically, the ground at Illisarvik is not two-layered, but has several distinct layers which should be considered in the final interpretation. Unfortunately, little lithological information is available for the area. More extensive lithological mapping using drillhole information is required for a more satisfactory and reliable interpretation of electromagnetic data. Studies of the temperature and frequency dependance of the conductivity of frozen materials should be carried out with a view to distinguishing clay materials from talik since both appear as good conductors in electromagnetic induction surveys. It is hoped that this area will be resurveyed periodically to monitor the growth of permafrost in the area and to examine the amplitude of the conductivity anomaly near the centre of the lake.

Acknowledgments

J.A. Hunter initially suggested the field studies and helped with field planning and with many discussions about the Illisarvik geology. Ian Rae participated in the field work in 1981 and carried out preliminary analysis of the data. Logistical support for field operations was provided by the Polar Continental Shelf Project, Tuktoyaktuk.

References

Anderson, D.M., Tice, A.R., and McKim, H.L.
1973: The unfrozen water content and the apparent specific heat loss capacity of frozen soils; in Proceedings of 2nd International Conference on Permafrost, Yaktusk, p. 289-294.

Burgess, M., Judge, A., Taylor, A., and Allen, V.
1982: Ground temperature studies of permafrost growth at a drained lake site, Mackenzie Delta; in Proceedings, 4th Canadian Permafrost Conference, p. 3-11.

Hoekstra, P. and McNeill, J.D.
1973: Electromagnetic probing of permafrost; in Proceedings of 2nd International Conference on Permafrost, Yaktusk, p. 517-526.

Judge, A.S., Burgess, M.M., Taylor, A., and Allen, V.
1981: Geothermal investigations at Illisarvik Drained Lake Site; Geothermal Services of Canada, Earth Physics Branch, Internal report 81-7, 15 p.

Judge, A.S., MacAulay, H.A., and Hunter, J.A.
1976: An application of hydraulic jet drilling techniques to mapping of sub-seabottom permafrost; in Report of Activities, Part C, Geological Survey of Canada, Paper 76-1C, p. 75-78.

MacAulay, H.A., Judge, A.S., Hunter, J.A., Allen, V., Gagné, R.M., Burgess, M.M., Neave, K.G., and Collyer, J.
1977: A study of sub-seabottom permafrost in the Beaufort Sea – Mackenzie Delta by hydraulic drilling methods; Geological Survey of Canada, Open File 472, Earth Physics Branch, Open File No. 77-3.

McNeill, J.D.
1980a: Electromagnetic terrain conductivity measurement at low induction numbers; Geonics Ltd., Technical Note TN-6, 15 p.

1980b: EM-34-3 Survey Interpretation Techniques; Geonics Ltd., Technical Note TN-8, 7 p.

Olhoeft, G.R.
1975: The electrical properties of permafrost; Ph.D. thesis, University of Toronto, 172 p.

Sartorelli, A.N. and French, R.B.
1982: Electromagnetic induction methods for mapping permafrost along northern pipeline corridors; Proceedings, 4th Canadian Permafrost Conference, p. 283-295.

Scott, W.J.
1980: D.C. soundings at Illisarvik Lake prior to drainage; Proceedings of a Symposium on Permafrost Geophysics (No. 5), Technical Memorandum No. 128, N.R.C., p. 21-25.

Sinha, A.K.
1980: Electromagnetic resistivity mapping of the area around Alfred, Ontario, with Geonics EM-34 system; in Current Research, Part A, Geological Survey of Canada, Paper 80-1A, p. 293-300.

Sinha, A.K. and Bhattacharya, P.K.
1966: Vertical magnetic dipole buried inside a homogeneous earth; Radio Science, v. 1 (new ser.), no. 3, p. 379-395.

Wait, J.R.
1951: The magnetic dipole over the horizontally stratified earth; Canadian Journal of Physics, v. 29, p. 577-592.

Wait, J.R. and Campbell, L.L.
1953: The fields of an oscillating magnetic dipole immersed in a semi-infinite conducting medium; Journal of Geophysical Research, v. 8, no. 2, p. 167-178.

29.

STRATIGRAPHY, STRUCTURE AND METAMORPHISM IN THE SIFTON RANGES, CASSIAR MOUNTAINS, NORTHERN BRITISH COLUMBIA

Project 700047

C.A. Evenchick[1]
Cordilleran Geology Division

Evenchick, C.A., Stratigraphy, structure and metamorphism in the Sifton Ranges, Cassiar Mountains, northern British Columbia; in Current Research, Part A, Geological Survey of Canada, Paper 83-1A, p. 221-224, 1983.

Abstract

The Sifton Ranges are underlain by two stratigraphic assemblages separated by the Sifton fault. The assemblage west of the Sifton fault comprises strata of the Ingenika, Atan, and Kechika groups, ranging in age from late Proterozoic to Ordovician. The assemblage east of Sifton fault comprises an unique assemblage of schist, mylonitic quartzite, amphibolite, marble, orthogneiss and paragneiss.

In the footwall (west) of the Sifton fault are recumbently folded greenschist to amphibolite facies metasediments refolded by upright folds. In the hanging wall is a tectonic melange of highly strained retrograde and amphibolite facies rocks with mylonitic textures preserved locally up to 6 km east of the fault trace. The structurally lowest unit in the hanging wall is basement gneiss dated at 1.84 Ga.

Introduction

Two months in each of the 1981 and 1982 field seasons were devoted to mapping in the Sifton Ranges, an area bounding the west side of the Northern Rocky Mountain Trench (Fig. 29.1). Field studies confirmed the presence of two stratigraphic assemblages separated by the gently dipping Sifton fault (Gabrielse et al., 1977) and revealed their differences in stratigraphy, structural style and metamorphic grade. West of Sifton fault are rocks of the upper Proterozoic Ingenika Group, the Lower Cambrian Atan Group, and the Cambro-Ordovician Kechika Group. East of the Sifton fault the hanging wall rocks are probably Precambrian, but are not easily correlated with other strata in the northern Omineca Crystalline Belt.

Excellent and cheerful assistance was provided by Lisel Currie of Queen's University.

West of Sifton Fault

West of Sifton fault are two successions of metasediments separated by steep north-northwest trending faults in the valley of Spinel Lake (see Fig. 29.2). The two successions differ in metamorphic grade and in detailed stratigraphy, but both contain quartzofeldspathic grit and pebble conglomerate characteristic of the Ingenika Group.

West of Spinel Lake, formations of the Ingenika, Atan and Kechika groups are recognized. The lithologies of the Ingenika Group include a distinctive quartzofeldspathic grit (Swannell Formation), chlorite schist and marble members (Tsaydiz Formation?), pure marble 15-20 m thick (Espee Formation), and in the upper part, laminated quartzitic siltstone and schist and marble of the Stelkuz Formation. These formations are significantly thinner than those sections measured elsewhere in the Cassiar and Omineca Mountains (Mansy and Gabrielse, 1978). The Atan Group is also relatively thin, consisting of 1-5 m of quartzite overlain by 10-15 m of limestone and dolomite. The Kechika Group comprises grey and green phyllite finely interlayered with carbonate. In the Ingenika Group foliations are generally parallel with bedding and rare isoclinal folds are refolded by kink folds. The highest grade rocks contain the mineral assemblage quartz + chlorite + biotite + muscovite ± garnet and occur generally in the area underlain by the Swannell Formation. These rocks are separated from the main part of the Sifton Ranges by dextral(?) transcurrent faults in a zone of north-northeast trending lamprophyre dykes and north-northwest trending shear zones, both of which form conspicuous lineaments in the Spinel Valley and where this zone crosses ridges to the northwest.

East of Spinel Lake the dominant lithologies of the footwall assemblage are pelitic schist, marble, calc-silicate rock, quartzite, quartz-feldspar pebble conglomerate and grit, and paragneiss (see legend, Fig. 29.2). A distinctive succession of pure marble (10-15 m, unit 9), calc-silicate marble and calc-silicate rock (15-25 m), and pelitic schist (>20 m) is an excellent structural marker. Unit 7 is dominated by conspicuous rusty weathering orthoquartzite with beds to 40 cm thick (Fig. 29.3). Pelitic schist, tremolite marble and hornblende garnet biotite schist are also present.

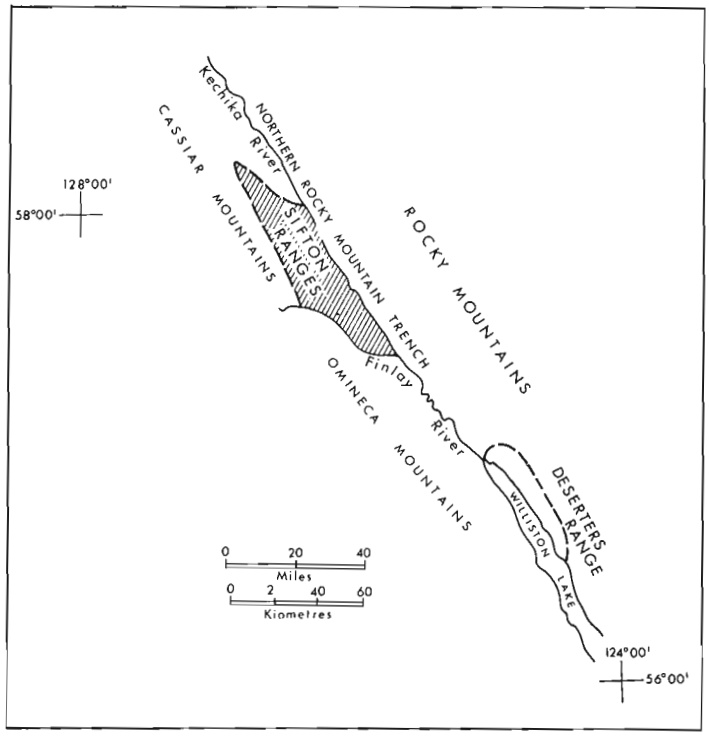

Figure 29.1. *Location map.*

[1] Department of Geological Sciences, Queen's University, Kingston, Ontario

Rocks of the footwall have a strong foliation subparallel with bedding and both are tightly folded into gently north-northwest plunging, recumbent to steeply inclined folds which give the footwall the appearance of a gently north-northwest plunging antiform (Fig. 29.2, 29.4, 29.5). No stratigraphic tops were recognized. The highest grade rocks are in the core of the antiform where the mineral assemblage in pelitic schists is quartz + garnet + muscovite + biotite ± sillimanite. On the flanks of the antiform the assemblage is quartz + garnet + muscovite + biotite ± staurolite.

East of Sifton Fault

The hanging wall of the Sifton fault may be divided into four units that are gently dipping north of latitude 57°45' (Fig. 29.6) but steeply dipping farther south. The westernmost (unit 12) is dominated by retrograde quartz-chlorite-muscovite (± garnet) schist with two strong foliations imparting a wavy appearance to the schist. Quartzofeldspathic augen mylonite is also present. To the east is unit 13, which consists of quartzitic mylonite, ultramylonite, pelitic schist with wavy foliation, amphibolite, and tremolite marble (Fig. 29.7). Quartz-lenticle biotite schist with wavy foliation is common. The quartz lenses are warped, in many places tightly folded, and locally form sheath folds. Tremolite marble members provide the only structural markers in the hanging wall assemblage. Structurally overlying this unit is unit 14, dominated by amphibolite with a strong mineral lineation and foliation and by quartzite with a strong lineation. The

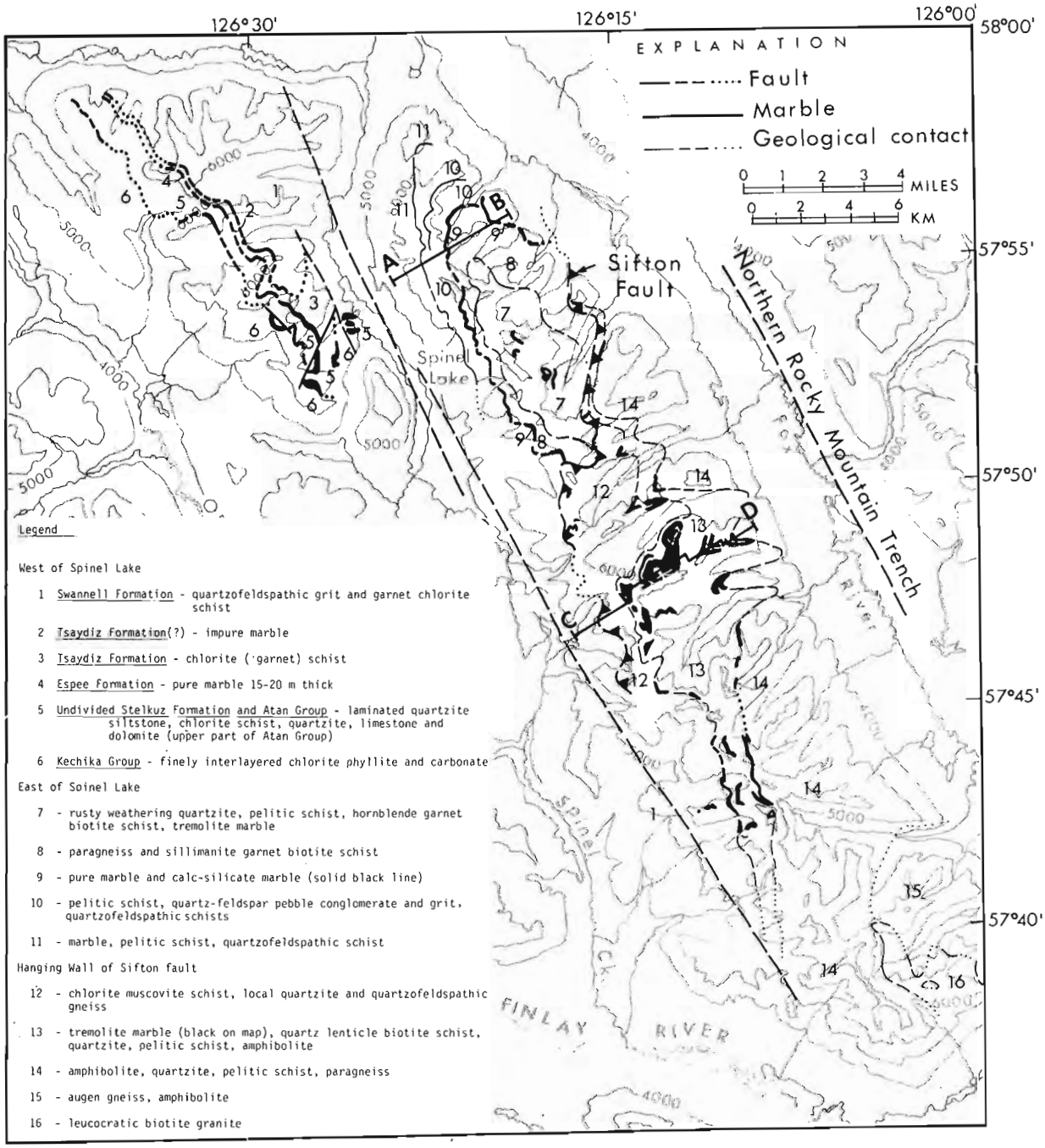

Figure 29.2. *Geological map of Sifton Ranges.*

Figure 29.3. *Isoclinal folds in quartzite of unit 7.*

lineations have a consistant gentle north to north-northwest plunge. Both amphibolite and quartzite occur as lenses, 1-10 m thick, bounded by faults. The primary relations of quartzite and amphibolite are unknown due to intense dislocation along shear zones subparallel with the layering. This degree of disruption is in sharp contrast with the relative continuity of members of the footwall assemblage. The abundance of feldspar in some of the quartzite south of latitude 57°42' suggests that at least some of the quartzites of unit 14 are clastic sediments rather than chert. Augen paragneiss and feldspathic quartzite are present locally south of latitude 57°45'.

At the south end of the range mesocratic granitoid basement gneiss (unit 15, Fig. 29.8) has boudins of amphibolite. A U-Pb model age on zircons from the gneiss is

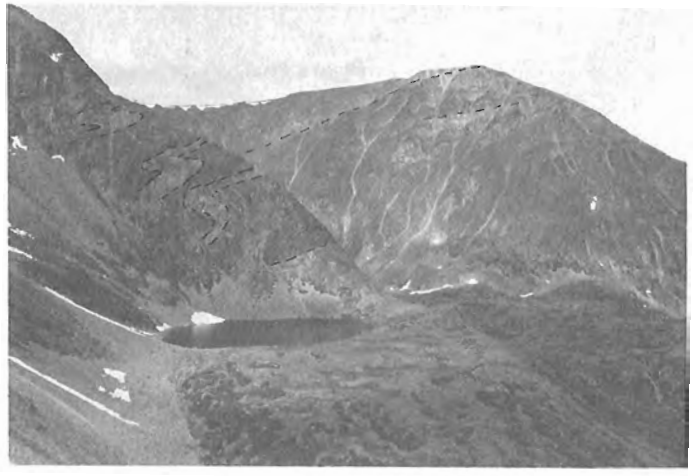

Figure 29.4. *View north-northwest from core of antiform at lat. 57°55'N to structures in unit 10.*

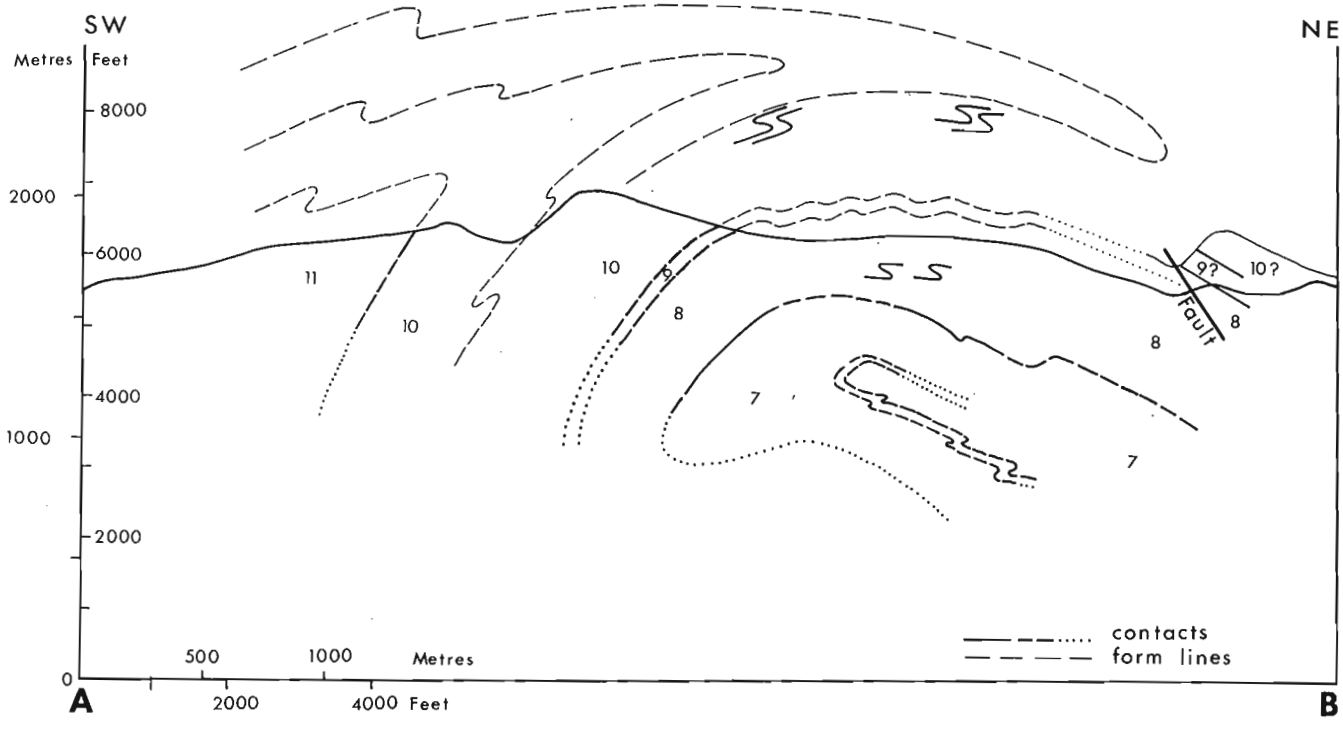

Figure 29.5. *Cross-section AB in footwall rocks of Sifton fault.*

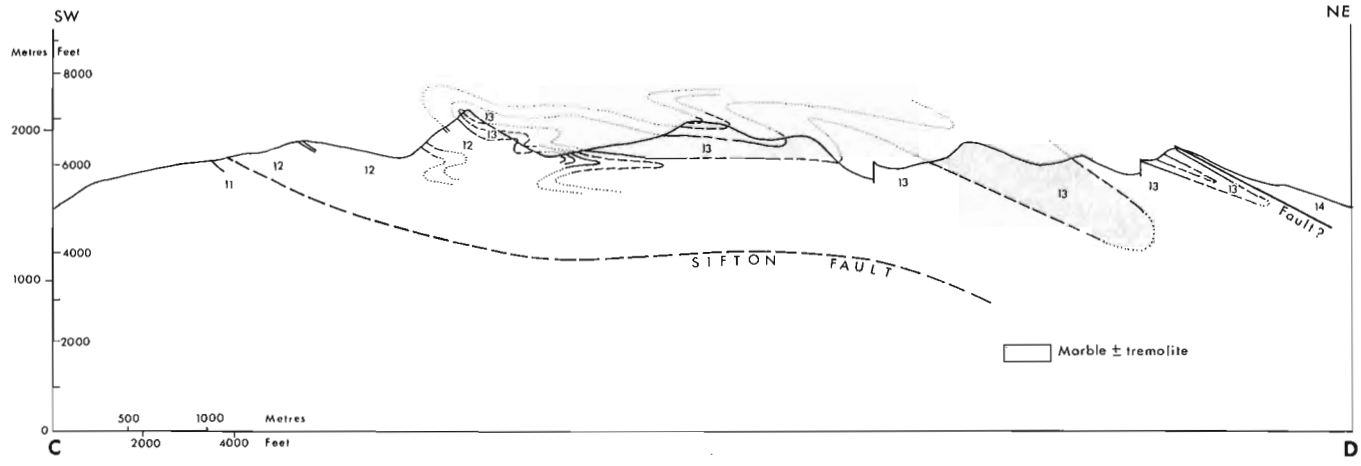

Figure 29.6. *Cross-section CD in hanging wall rocks of Sifton fault.*

Figure 29.7. *Amphibolite and schist (dark) in tight recumbent folds within marble of unit 13.*

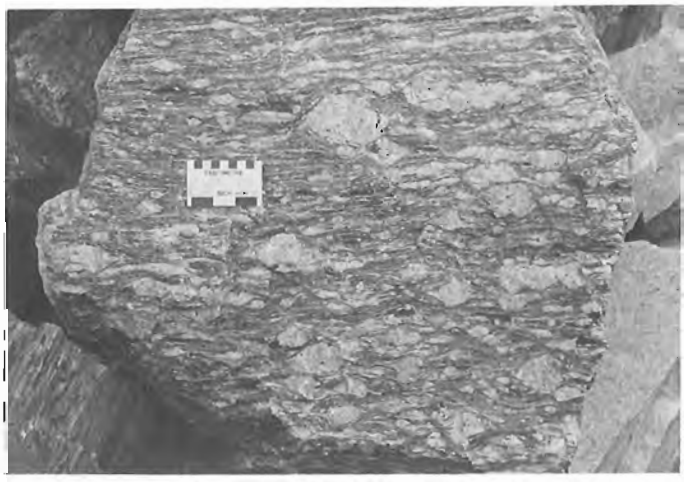

Figure 29.8. *Boulder of granitoid augen gneiss in southern Sifton Ranges.*

1.84 Ga (R. Parrish, pers. comm. 1982). Both basement gneiss and the quartzite of unit 14 have been intruded by undeformed leucocratic biotite granite with a K-Ar model age on biotite of 41.6 ± 2.2 Ma (Wanless et al., 1979). Units of the hanging wall are probably bounded by faults subparallel with the foliation, with the exception of the granite which clearly crosscuts layering in units 14 and 15, and appears to truncate the contact of units 14 and 15.

The mineral assemblage in pelitic rocks north of latitude 56°47' is quartz + chlorite (probably retrograde) + muscovite + biotite ± garnet. South of latitude 57°47' staurolite is present with this assemblage in units 13 and 14, and one locality of kyanite is in unit 14 at latitude 57°47'. At latitude 57°42' rare pelitic layers may have the assemblage quartz + garnet + biotite + potassium feldspar ± kyanite ± sillimanite.

Sifton Fault

Regionally, the Sifton fault can be recognized as separating two distinctly different assemblages of rock. However, where retrograde chlorite muscovite schist of unit 12 truncates retrograde schist of the footwall the position of the Sifton fault is difficult to locate. North of latitude 57°50' the footwall schists have not undergone thorough retrograde metamorphism and sillimanite in the footwall rocks distinguishes them from hanging wall rocks. South of latitude 57°50' the footwall rocks are lower grade and lack sillimanite, invalidating this criterion. Amphibolite is restricted to the hanging wall assemblage, but its usefulness in tracing the fault is minimal because of its rarity in unit 12. Movement on the Sifton fault was post-metamorphic but occurred prior to upright folding which folded both footwall and hanging wall rocks.

References

Gabrielse, H., Dodds, C.J., and Mansy, J.L.
1977: Operation Finlay, British Columbia; in Current Research, Part A, Geological Survey of Canada, Paper 77-1A, p. 243-246.

Mansy, J.L. and Gabrielse, H.
1978: Stratigraphy, terminology and correlation of Upper Proterozoic rocks in Omineca and Cassiar Mountains, North-central British Columbia; Geological Survey of Canada, Paper 77-19.

Wanless, R.K., Stevens, R.D., Lachance, G.R., and Delabio, R.N.
1979: Age determinations and geological studies, K-Ar isotopic ages, Report 14, Geological Survey of Canada, Paper 79-2, p. 10.

30. THRUST FAULTS IN THE ANVIL RANGE AND A NEW LOOK AT THE ANVIL RANGE GROUP, SOUTH-CENTRAL YUKON TERRITORY

Project 820015

S.P. Gordey
Cordilleran Geology Division, Vancouver

Gordey, S.P., Thrust faults in the Anvil Range and a new look at the Anvil Range Group, south-central Yukon Territory; in Current Research, Part A, Geological Survey of Canada, Paper 83-1A, p. 225-227, 1983.

Abstract

The Anvil Range Group, as formerly mapped, is shown to include two lithologically and chemically similar, but tectonically and stratigraphically distinct volcanic suites, one of upper Paleozoic age and the other of Cambro-Ordovician age. A consequence is the recognition of a subhorizontal thrust fault at least 18 km long and with 9 km of overlap, and the realization that hroizontal shortening in Anvil Range and along strike is much greater than earlier suspected.

Introduction

In 1982 a project to refine geological mapping of Sheldon Lake (105 J) and Tay River (105 K) map areas at 1:250 000 scale was begun by the Geological Survey of Canada. Three weeks of the field season was spent mapping the northeast flank of the Anvil Range in Tay River map area to test suspicions (D.J. Tempelman-Kluit, pers. comm., 1982; G. Jilsen, pers. comm., 1982) that the Anvil Range Group, an extensive assemblage of basic volcanics, chert, serpentinite, and limestone, thought to be upper Paleozoic, may include strata of widely different age and tectonic significance. Re-interpretation of the Anvil Range Group presented here is based on mapping beyond the boundaries of Tempelman-Kluit (1972) and a critical new fossil locality.

Regional Setting

Paleozoic strata of the Anvil Range represent the most westerly offshelf facies preserved in the northern Cordillera. Those in the lower Paleozoic consist predominantly of fine grained, variably calcareous clastic rocks, chert, and volcanics. Their transition to shallower carbonate facies equivalents is some 200 km to the east in the Mackenzie Mountains. Devono-Mississippian sediments include chert, limestone, and coarse and fine clastics characterized by chert detritus. Although apparent differences in structural complexity and metamorphism at different stratigraphic levels may reflect early tectonism (Templeman-Kluit, 1972), deformation of regional extent did not occur until the Early Cretaceous with the northeastward folding and imbrication of autochthonous stratigraphy and the synchronous obduction above those sediments of mylonite, ophiolite, and granite allochthons (Tempelman-Kluit, 1979). Intrusion of mid-Cretaceous plutons followed. Late Cretaceous-Tertiary, dextral strike-slip along Tintina Fault, which borders the Anvil Range to the southwest, amounted to 450 km (Tempelman-Kluit, 1979).

Stratigraphy

Anvil Range stratigraphy in Tay River map areas was first mapped by Roddick and Green (1961) during reconnaissance geological mapping. It has been described more recently in detail by Tempelman-Kluit (1972) and briefly by Gondi (1972) and Jennings et al. (1980) who outlined the setting of the important zinc-lead orebodies of the Faro district. A geological sketch map of the area of present concern is shown in Figure 30.1.

The oldest fossiliferous strata are blue-black weathering, black, locally graptolitic slate and chert (about 130 m; unit 5, Fig. 30.1). Graptolite collections range in age from Early Ordovician (Arenigian – basal Llanvirnian; see following section) to Early Silurian (Tempelman-Kluit, 1972). This unit is overlain by grey weathering, medium grained, massive to thick bedded orthoquartzite (40 m+; unit 6) and limestone and dolostone (0-30 m; unit 7). The carbonate is dated by conodonts as late Middle Devonian (Tempelman-Kluit, 1972). An unconformity may occur at the base of the quartzite because near peak 6671 ft. strata are found between the graptolitic slate and quartzite that are not found elsewhere (see unit 5 in legend for Fig. 30.1), including orange to brown weathering, wispy-laminated, pyritic mudstone (10-80 m+) and brown to blue-black weathering, grey to black slate (100 m+). To the south (southwest margin of Fig. 30.1) the quartzite may directly overlie Cambro-Ordovician volcanics (unit 3), with the graptolitic slate (unit 5) being thin or absent. Devono-Mississippian grey slate, chert, greywacke, chert-pebble conglomerate, and limestone (500? m+; unit 8) are in thrust-fault contact with older units.

Immediately and conformably underlying the graptolitic slate in part of northeast Anvil Range is a thick succession (400 m+; unit 4) of dark grey to black weathering, light grey to black, siliceous argillite, siltstone, and minor chert, containing rare flows(?) of amygdaloidal basalt (unit 4a). Although the unit is well laminated it lacks other bedding. Its base was seen only in the aureole of a pluton where laminated hornfels rests sharply above muscovite-biotite-quartz schist and calc-silicate. The laminated unit can be traced beneath graptolitic slate to the southwest where laterally a thick succession (500 m+; unit 3) of basic volcanic tuff and pillow basalt is found in the same stratigraphic position. The volcanic succession overlies grey, lustrous, locally tuffaceous muscovite phyllite (1350? m; unit 2) containing pods of andesitic greenstone and chloritic tuff (unit 2a) (Tempelman-Kluit, 1972), which in turn overlie laminated skarn and schist, with local amphibolite (600? m; unit 1) (Tempelman-Kluit, 1972). The thick volcanics of unit 3 represent a culmination of volcanic activity weakly manifested in the underlying strata.

On the basis of regional correlation (see following section) and an upper stratigraphic limit provided by the graptolitic slate, the volcanics and underlying phyllite (units 1? and 2, Fig. 30.1), including the orebodies of the Faro district, are considered to be Late Cambrian-Early Ordovician.

The lithological and chemical similarity of the Cambro-Ordovician volcanics to those on the southwest side of the Anvil Range that were dated by fossils as upper Paleozoic led to their earlier mis-correlation (Tempelman-Kluit, 1972). Recognition that the volcanics comprise two different suites explains why associated red and green chert, serpentinite, and massive carbonate on the southwest side of the range (Templeman-Kluit, 1972) does not occur with the volcanics on the northeast side (see Fig. 30.1).

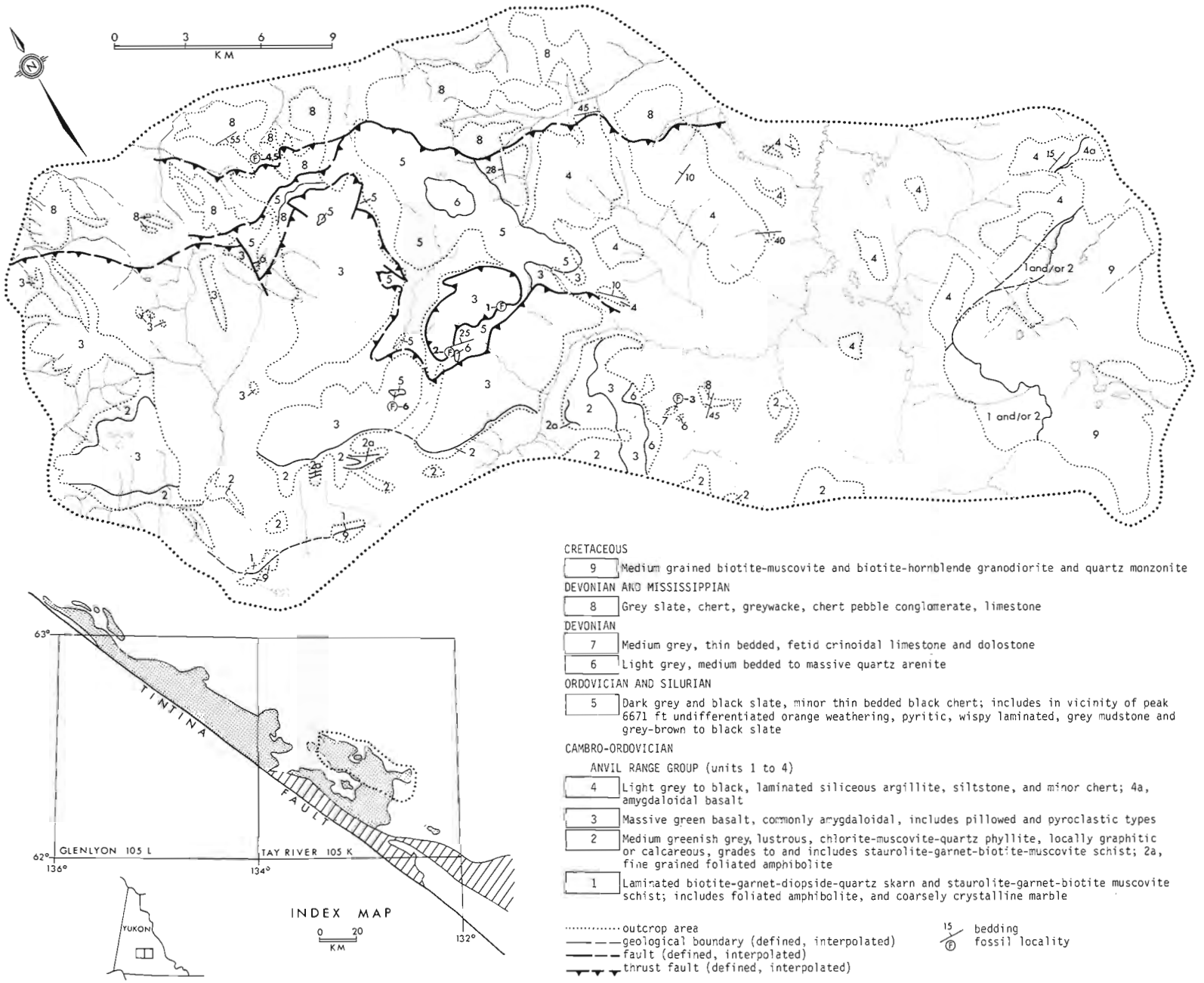

Figure 30.1. *Geological sketch map of northeast Anvil Range, south-central Yukon (in large part, from Tempelman-Kluit (1972) with modification and re-interpretation). The index map shows the regional distribution of parauthochthonous Cambro-Ordovician Anvil Range Group (dotted) and formerly included allochthonous upper Paleozoic volcanics and associated rocks of the Anvil Allochthon (hachured). Fossil locality F-6 described in text, for others see Tempelman-Kluit (1972).*

Structure

Cambro-Ordovician volcanics in the northeast Anvil Range are preserved in the hanging wall of an extensive subhorizontal thrust sheet (Fig. 30.1). In various places the sheet overlies Ordovician-Silurian black slate, Devonian quartzite, and Devono-Mississippian sandstone and shale; a relationship previously interpreted as unconformable (Templeman-Kluit, 1972). The thrust sheet itself in at least two localities contains black slate similar to that in the footwall. At one locality 10 m stratigraphically (?) above the volcanics, a single graptolite (**Tetragraptus** sp.), of Arenigian to basal Llanvirnian age (G.S.C. locality C-107902; B.S. Norford, pers. comm., 1982) was found, which proves an older-over-younger thrust relationship. The thrust sheet has a measured overlap (northeast-southwest) of 9 km and a minimum strike length (northwest-southeast) of 18 km. Detachment probably occurred in the incompetent phyllite immediately below the compenent volcanic rocks. A second thrust fault, at least 22 km long, is exposed to the northeast and brought Cambro-Ordovician laminated argillite and siltstone against strata as young as Mississippian. At its northwest end, a northern splay repeats local stratigraphy recognized within unit 8.

Terminology

Campbell (1967, p. 58) originally defined the Anvil Range Group in Glenlyon map area (105 L) as characterized by "grey and greenish grey andesitic and dioritic rocks, and dark grey argillite, slate and phyllite". By regional correlation and scant stratigraphic evidence he concurred with Roddick and Green (1961) who guessed that similar strata in Tay River map area are upper Paleozoic. Campbell's description clearly corresponds to strata shown here (units 1?, 2-4, Fig. 30.1) to be Cambro-Ordovician. The upper Paleozoic volcanics, chert, serpentinite, and carbonate on the southwest side of the Anvil Range should be excluded from the Anvil Range Group because they comprise an assemblage distinct from those rocks originally included in the group by Campbell (1967). Rather, they form part of the Anvil Allochthon ophiolitic suite thrust over the western edge of the Cordilleran miogeocline in the Mesozoic (Tempelman-Kluit, 1979) (see Fig. 30.1).

Regional Implications

A late Cambrian-Early Ordovician age for the volcanics of the northeastern Anvil Range and the underlying phyllite agrees with what is known of the geology in adjacent regions. In northern British Columbia the Kechika Group of Cambro-Ordovician age (Gabrielse, 1963; Cecile and Norford, 1979) consists of limestone and calcareous and noncalcareous phyllite containing local, small to large, greenstone bodies. In the Pelly Mountains of the south-central Yukon Cambro-Ordovician phyllite contains much tuffaceous material, and local thick piles of basic flows occur within the phyllite and beneath Ordovician graptolitic slate (Gordey, 1981; Tempelman-Kluit et al., 1976).

Details of the distribution of Anvil Range Group volcanics with respect to those in the upper Paleozoic Anvil Allochthon (Fig. 30.1) are not well known in the Anvil Range; and if the two suites have anywhere been structurally juxtaposed without their associated lithologies, distinguishing them might be difficult. The upper Paleozoic assemblage in the southwest Anvil Range is of the same age and has many lithologies in common with the Sylvester Allochthon in northern British Columbia (Gabrielse, 1963; Gabrielse and Mansy, 1980; Gordey, 1982).

The recognition of important thrust faults in the Anvil Range implies a similar structural style will be recognized along strike, and that horizontal shortening in the region may be considerable. Campbell's (1967) impression in Glenlyon map area that the Anvil Range Group rests unconformably on Devon-Mississippian strata, may be explained as a thrust relationship.

References

Campbell, R.B.
1967: Reconnaissance geology of Glenlyon map area, Yukon Teritory (105 L); Geological Survey of Canada, Memoir 352, 92 p.

Cecile, M.P. and Norford, B.S.
1979: Basin to platform transition, lower Paleozoic strata of Ware and Trutch map areas, northeastern British Columbia; in Current Research, Part A, Geological Survey of Canada, Paper 79-1A, p. 219-226.

Gabrielse, H.
1963: McDame map area, British Columbia; Geological Survey of Canada, Memoir 319, 138 p.

Gabrielse, H. and Mansy, J.L.
1980: Structural style in northeastern Cry Lake map area, north-central British Columbia; in Current Research, Part A, Geological Survey of Canada, Paper 80-1A, p. 33-35.

Gondi, J.
1972: Geology of the Anvil Mine; XXIV International Geological Congress, Guidebook, Field Excursion A24-C24, p. 20-24.

Gordey, S.P.
1981: Stratigraphy, structure and tectonic evolution of southern Pelly Mountains in the Indigo Lake area, Yukon Territory; Geological Survey of Canada, Bulletin 318, 44 p.

Gordey, S.P., Gabrielse, H., and Orchard, M.J.
1982: Stratigraphy and structure of Sylvester Allochthon, southwest McDame map area, northern British Columbia; in Current Research, Part B, Geological Survey of Canada, Paper 82-1B, p. 101-106.

Jennings, D.S., Jilson, G.A., and Pigage, L.C.
1980: Anvil Range stratigraphy, south-central Yukon Territory; Geological Association of Canada, Cordilleran Section, Programme and Abstracts, p. 16-17.

Roddick, J.A. and Green, L.H.
1961: Tay River map area, Yukon Territory; Geological Survey of Canada, Map 13-1961.

Tempelman-Kluit, D.J.
1972: Geology and origin of the Faro, Vangorda, and Swim concordant zinc-lead deposits, central Yukon Territory; Geological Survey of Canada, Bulletin 208, 73 p.

1979: Transported cataclasite, ophiolite and granodiorite in Yukon: evidence of arc-continent collision; Geological Survey of Canada, Paper 79-14, 27 p.

Tempelman-Kluit, D.J., Gordey, S.P., and Read, B.C.
1976: Stratigraphic and structural studies in the Pelly Mountains, Yukon Territory; in Report of Activities, Part A, Geological Survey of Canada, Paper 76-1A, p. 97-106.

31. STRATIGRAPHIC AND STRUCTURAL RELATIONS OF THE MILFORD, KASLO AND SLOCAN GROUPS, ROSEBERRY QUADRANGLE, LARDEAU MAP AREA, BRITISH COLUMBIA

Project 790041

David W. Klepacki[1]
Cordilleran Geology Division

Klepacki, D.W., Stratigraphic and structural relations of the Milford, Kaslo and Slocan groups, Roseberry Quadrangle, Lardeau map area, British Columbia; in Current Research, Part A, Geological Survey of Canada, Paper 83-1A, p. 229-233, 1983.

Abstract

In Roseberry Quadrangle lower Paleozoic grit and schist of Lardeau Group are overlain with angular unconformity by Upper Mississippian sediments and subordinate volcanics of Milford Group. Kaslo Group, of uncertain late Paleozoic-early Mesozoic age, comprises andesitic pyroxene-plagioclase porphyry volcanics, volcaniclastics, and cherty tuff underlain partly by serpentinized ultramafic rocks and partly by siliceous argillite similar to that at the top of Milford Group. Kaslo Group is overlain disconformably by Slocan Group, composed of basal greenstone conglomerate, which partly interfingers with uppermost Kaslo volcanics, overlain by Upper Triassic phyllite and limestone.

The siliceous argillite unit and younger rocks are deformed into the northeasterly inclined, southeast-plunging Mount Dryden Anticline which folds a thrust fault that repeats much of Kaslo stratigraphy. The northeast limb abuts a west-facing panel of Milford and Lardeau rocks across the steeply west-dipping Mount Schroeder normal fault.

Correlations across Mount Schroeder fault suggest that the volcanics and cherty tuff of Milford Group represent a tongue of Kaslo volcanics. Accordingly, at this latitude, the eastern elements of western Cordilleran accreted terranes, which include Kaslo and Slocan groups, were apparently deposited near Milford and Lardeau groups. The latter, in turn, accumulated probably not far from the ancient margin of North America.

Introduction

Volcanic and related rocks of the Carboniferous to Triassic Kaslo Group in Roseberry Quadrangle (82K/13) in central Kootenay Arc of southeastern British Columbia form part of the Eastern Assemblage of Monger et al. (1982) (Fig. 31.1, 31.2). The belt forms the eastern edge of a collage of foreign terranes, represented in the map area by the Upper Triassic Slocan Group, accreted to the ancient margin of North America which apparently included the Carboniferous Milford Group. The purpose of the project is to determine the nature of the Kaslo Group and its relations to the underlying sediments and subordinate volcanics of the Milford Group and to the overlying calcareous flysch of the Slocan Group. Thus the focus is on the boundary zone between the leading edge of the accreted terranes of the western Cordillera and rocks linked to ancient North America.

The Milford, Kaslo, and Slocan groups were originally defined by Cairnes (1934) who mapped in the southeastern part of the present map area. Local work related to structure and mineral deposits in the Slocan and Kaslo Groups was done respectively by Hedley (1945) and Maconachie (1940). Fyles (1967) mapped units in the Ainsworth area which are on strike with those mapped in this study. Ross and Kellerhalls (1968) presented a structural interpretation which includes the southeastern portion of the project area. Read and Wheeler (1976) mapped the project area on a regional scale, and recognized a belt of Slocan Group strata previously included in the Milford Group.

The principal results of field work in 1982 (Fig. 31.3) are:

1. Kaslo Group may be lithologically correlated across the Mount Schroeder fault with the upper part of the Milford Group, suggesting no great displacement along this fault.
2. Much of the stratigraphy of the Kaslo Group is repeated by eastward thrusting in which the overriding plate is floored by serpentinized ultramafic rocks.

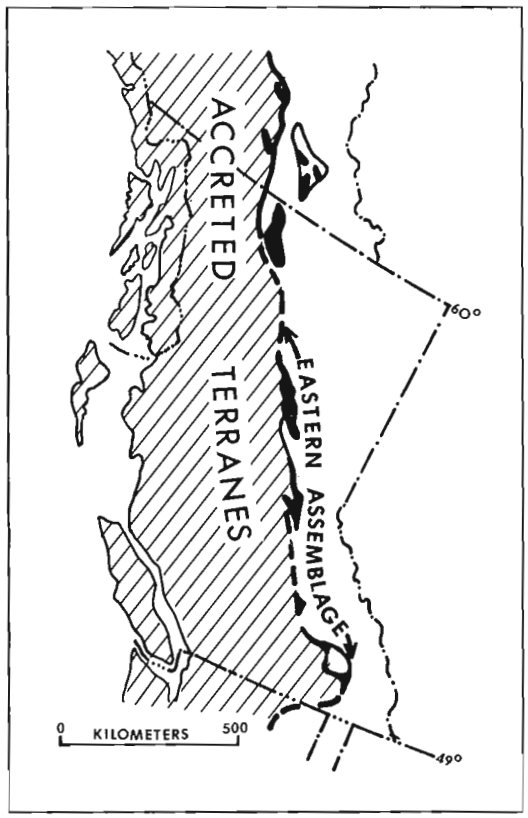

Figure 31.1. *Distribution of Eastern Assemblage. From Monger et al., 1982.*

[1] Department of Earth and Planetary Sciences, Massachusetts Institute of Technology, Cambridge, MA, U.S.A. 02139.

3. Slocan Group lies disconformably on Kaslo Group.
4. Preliminary data suggests that Milford, Kaslo and Slocan groups represent the telescoping of a partly oceanic volcanic arc against the late Paleozoic-early Mesozoic margin of North America.

Acknowledgment

The author is grateful for the enthusiastic assistance of Keenon Jang.

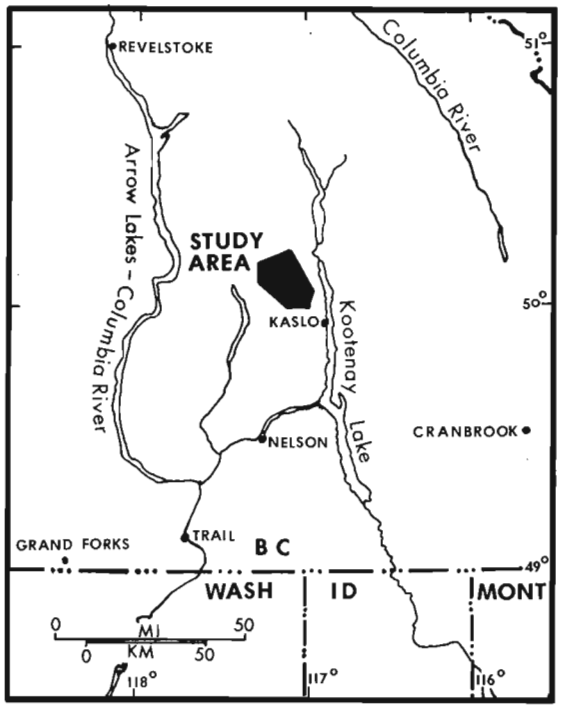

Figure 31.2. Location of study area.

Stratigraphy

The stratigraphy presented here elaborates on that of Read and Wheeler (1976). Fossil data from the 1982 field season are not yet available.

Lardeau Group, Broadview Formation

The oldest and structurally lowest rocks in the study area are those of the lower Paleozoic Broadview Formation comprising quartzo-feldspathic grit and rusty weathering silvery phyllite and schist interbedded on a scale of centimetres to tens of metres. Quartz and quartz-feldspar veinlets and pods are characteristic of these rocks but are absent in younger units. The primary foliation in the Broadview Formation is at an angle to the slaty cleavage and bedding in the overlying Milford Group where these units are in unfaulted contact east of Mount Schroeder.

Milford Group, Limestone Unit

Unconformably overlying the Broadview Formation is a 100-200 m-thick unit of limestone. Dominantly light grey and bedded, the unit is locally fossiliferous, containing horizons of crinoidal fragments and rare gastropod and pelecypod fossils and fragments. Bedding is defined by pelitic and arenaceous laminae. The basal 10-20 m of the unit are dark grey pyritic limestone and calcareous slate, locally containing pods of quartz pebble conglomerate. This unit has yielded Upper Mississippian (Chesterian) conodonts (M.J. Orchard, personal communication).

Milford Group, Sandstone/Phyllite Unit

Overlying the limestone is a 100-300 m-thick unit of interbedded light grey to pink sandstone and grey slate and phyllite. Sandstone layers vary from centimetres to metres in thickness, sandstone predominating in the thicker units. The sandstone is commonly horizontally laminated, with rare planar crossbeds and scour structures. Two crossbed localities indicate sediment transport from east to west.

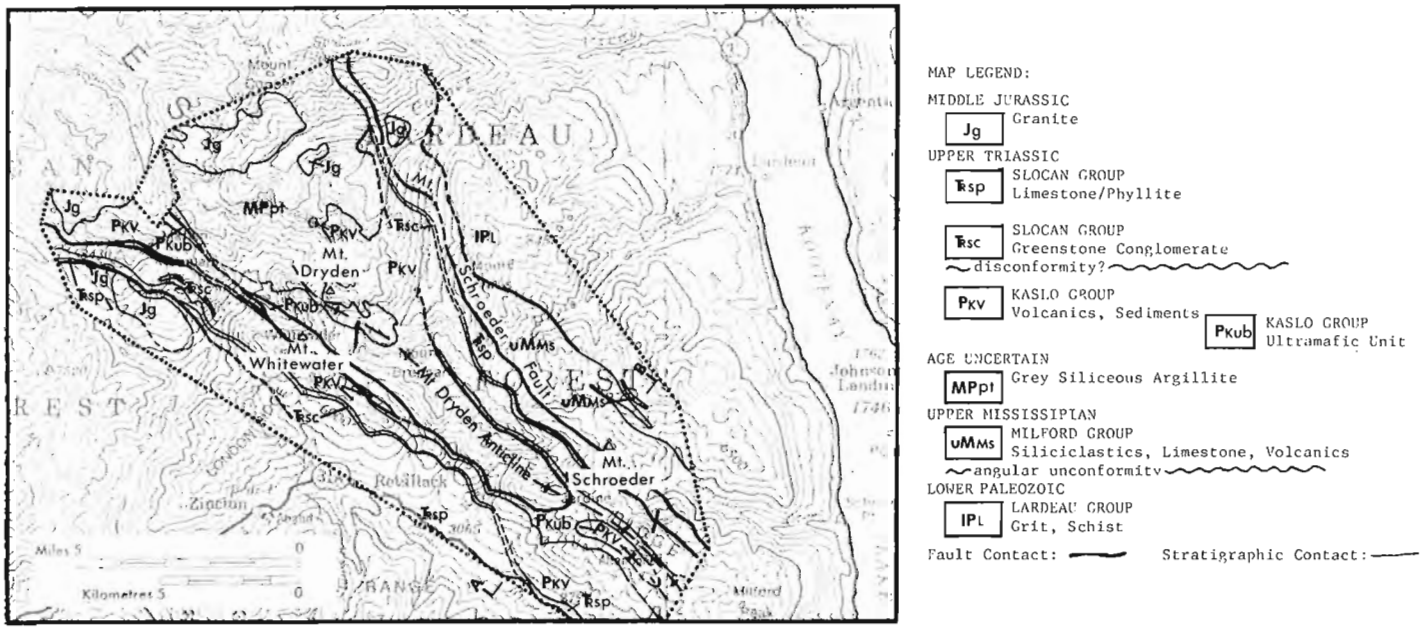

Figure 31.3. Generalized geological map of the eastern portion of the Roseberry Sheet from work of the 1982 field season. Section A-B shows location of Figure 31.4. The contour interval is 500 feet.

Milford Group, Cherty Tuff Unit

Grey and light green laminated chert and grey phyllite are interbedded with wacke and arkosic arenite near the top of the sandstone/phyllite unit and in the space of a few metres grade upwards into predominantly chert that defines the base of the cherty tuff unit. Although the rock is mostly silica, rare feldspars and an overlying volcanic unit suggest a volcanic related protolith for this unit. The cherty tuff is finely laminated (1-2 mm) siliceous rock, commonly light green or maroon, and locally white. This unit has also yielded Chesterian conodonts.

Figure 31.4a. *Pyroxene-plagioclase porphyry pillow lavas typical of Kaslo Group greenstone.*

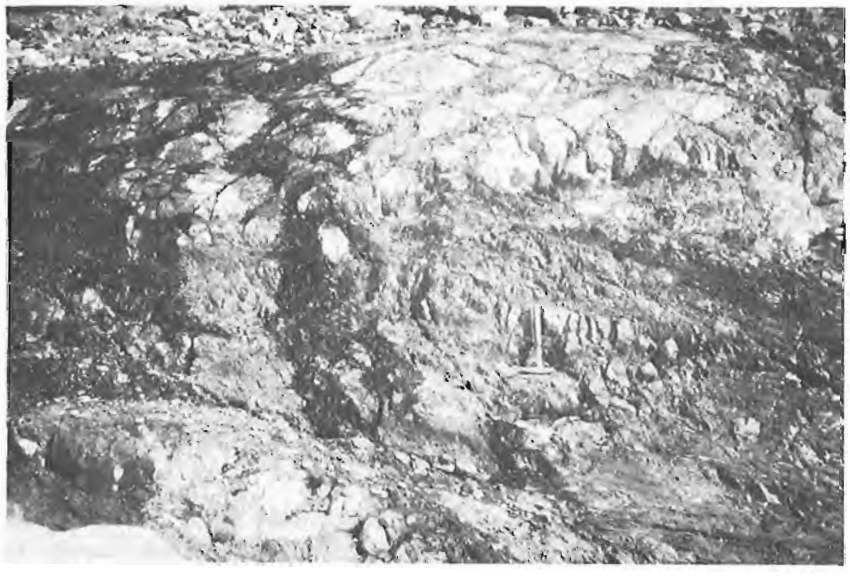

Figure 31.4b. *Serpentinite breccia of the Kaslo Group Ultramafic Unit exposed at the headwaters of Whitewater Creek southeast of Whitewater Mountain.*

Milford Group, Phyllitic Greenstone Unit

Green cherty tuff is intercalated with a phyllitic greenstone unit 20-40 m thick. The greenstone is mostly fragmental, containing clasts of greenstone, chert, andesitic volcanic rock, pillow breccia, and serpentinite. This unit is well exposed on Mount Schroeder.

Milford Group, Grey Siliceous Argillite Unit

Bedded dark grey siliceous argillite with light grey bands 1-2 cm thick locally overlies the greenstone. It includes some white cherty tuff layers which, together with the general siliceous nature of the unit, helps to distinguish this unit from the tectonically juxtaposed calcareous Slocan Group. The Grey Siliceous Argillite Unit is well exposed on the ridge 2 km northwest of Mount Schroeder.

Also included in this unit is a bedded siliceous grey argillite that underlies the Kaslo Group but which has not been traced into the main belt of Milford Group rocks. This tentative correlation is based on the siliceous character of the argillite and the resemblance to the grey siliceous argillite found locally on top of the Phyllitic Greenstone Unit.

Kaslo Group, Lower Plate Units

The Kaslo Group can be divided into two sequences, a para-autochthonous lower plate sequence and an allochthonous upper plate sequence. From stratigraphically lowest to highest, the lower plate sequence is: Lower Greenstone Unit, Lower Cherty Tuff Unit, Middle Greenstone Unit, Upper Cherty Tuff Unit, and Upper Greenstone Unit. The greenstone units are composed of pyroxene-plagioclase andesite porphyry pillow lavas, flows, pillow breccia, and tuffaceous greenstone (Fig. 31.4a). The greenstone units also contain lenses of greywacke, volcanic conglomerate, and cherty tuff with layers of green phyllite. The cherty tuff units comprise light green and white laminated chert in which the laminae are defined by colour banding or green to grey phyllite layers. Locally, siliceous layers contain feldspars, which, together with gradational boundaries into tuffaceous layers, suggest a volcanic origin for this rock type.

Kaslo Group, Upper Plate Units

A layer of serpentinite breccia, talc schist, or talc-chlorite schist defines the base of the upper plate (Fig. 31.4b). Where exposed, the lower boundary of this ultramafic unit is faulted. Depositionally overlying the ultramafic unit is a discontinuous horizon, 10-20 m thick, of volcaniclastic conglomerate and wacke with clasts of serpentinite, volcanic rock, and diorite. Serpentinite clasts are particularly common immediately above the ultramafic layer (Fig. 31.4c). The volcaniclastic unit and ultramafic rock is overlain, in turn, by a 200-600 m thick sequence of pyroxene-plagioclase porphyry flows and pillow lava with rare, thin layers of lithic wacke.

Figure 31.4c. *Dark lens-shaped serpentinite clasts in volcanic conglomerate and lithic wacke immediately overlying the Kaslo Group Ultramafic Unit.*

Slocan Group, Greenstone Conglomerate Unit

Greenstone conglomerate as much as 150 m thick defines the base of the Slocan Group. This conglomerate is composed mostly of greenstone and plagioclase-porphyry clasts in a green to grey phyllitic matrix. Southeast and northwest of Whitewater Mountain the unit is pyritic and rusty weathering, with beds and clasts of grey limestone. Locally, the contact between the greenstone conglomerate and underlying greenstone or fragmental greenstone is difficult to define. About 5 km northwest of Whitewater Mountain, lenses of pyritic greenstone conglomerate occur in the uppermost section of Kaslo Group greenstone, and andesitic pillow lavas are present in the conglomerate.

Slocan Group, Limestone/Phyllite Unit

The youngest sedimentary rocks in the study area are a thick (greater than 1500 m) sequence of interbedded grey limestone and dark grey phyllite with minor light grey to pinkish sandstone. The limestone beds have yielded Upper Triassic (Karnian to Norian) conodonts, shell and crinoid fragments, and cephalopods. Sedimentary structures, observed only in sandstone layers, include slump folds, convolute lamination and planar crossbeds. Two localities, 2 km southeast of Whitewater Mountain and at an elevation of 1305 m, 2.5 km east-northeast of Retallack, show cross-bedding with current directions from the west. The transition from greenstone conglomerate to grey phyllite or light grey limestone is gradational over a 1-5 m interval.

Intrusive Rocks

Three major types of intrusive rocks occur in the study area: synvolcanic dioritic rocks, syntectonic dioritic rocks, post-folding granitic and felsic rocks. Synvolcanic rocks are medium grained, brecciated pyroxene-plagioclase porphyry and light grey, commonly glomerophyric hornblende-pyroxene porphyry. Dykes of synvolcanic rocks are common in the Grey Siliceous Argillite which underlies the Kaslo Group. Syntectonic diorites are weakly foliated, medium- to coarse-grained equigranular diorite and coarse grained hornblende-pyroxene-plagioclase porphyry dykes which cut foliation but are folded by second generation folds. Post-folding granitic rocks are medium grained biotite granite, leucogranite dykes and grey to white feldspar porphyry and felsite dykes. Granitic rocks commonly have small (3-4 cm) inclusions of biotite-chlorite schist and are porphyritic in the interior of the intrusive bodies.

Structure

Stratigraphic facing directions were determined from pillow tops, graded bedding, scour structures and settling features. Foliation in the Lardeau Group is truncated by the unconformity at the base of the Milford Group, thus some folds in the Lardeau Group predate the first generation folds in overlying rocks. Grey Siliceous Argillite Unit and the Kaslo and Slocan groups form the large first generation Mount Dryden Anticline which is steeply inclined to the northeast, plunges southeast at 15 degrees, and is separated from the Milford Group to the east by the Mount Schroeder fault (Fig. 31.3, 31.5). This fold deforms a thrust fault at the base of the ultramafic unit which cuts bedding at a low angle and repeats much of the Kaslo Group. Continuation of the fault northeast of Mount Dryden into Slocan Group is uncertain. Large first-phase folds in the Milford Group are upright and easterly verging in view of west limbs that are longer than east limbs. The phyllitic foliation and slaty cleavage in the area are axial-planar to minor folds and the large Mount Dryden Anticline. This foliation is deformed about southeast-plunging, asymmetric major and minor folds which have a reversed N-shape profile when viewed toward the northwest. These second generation folds are best developed in phyllite of the Slocan and Milford Groups. Northeast-trending high-angle faults have minor (30 m or less) normal and/or left-lateral displacement. Northwest-trending high-angle faults have a complex history indicated by superposed slickensides. Locally, however, slickensides, minor folds, and offset of granitic bodies indicate left-lateral and normal components of net slip. Mount Schroeder fault, separating Milford and Slocan Groups, has significant normal displacement. Age relationships between northeast- and northwest-trending faults are uncertain.

Correlation

Several new stratigraphic correlations result from interpretation of this field season's data (Fig. 31.7). Correlation of the greenstone at the top of the Milford Group with Kaslo Group greenstone is based on identical greenstone

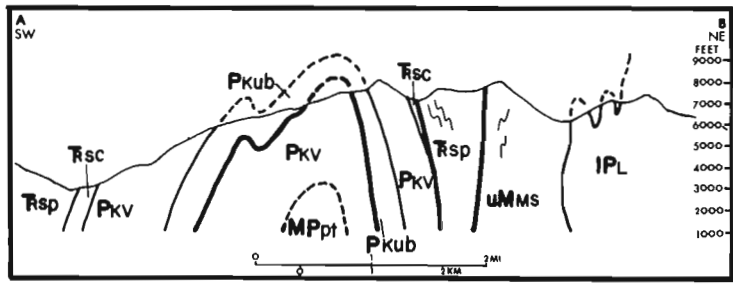

Figure 31.5. *Generalized structure section across the southeastern part of the map area illustrating the Mount Dryden Anticline, and vergence change across the fault separating Slocan Group from Milford Group. Map symbols as in Figure 31.3.*

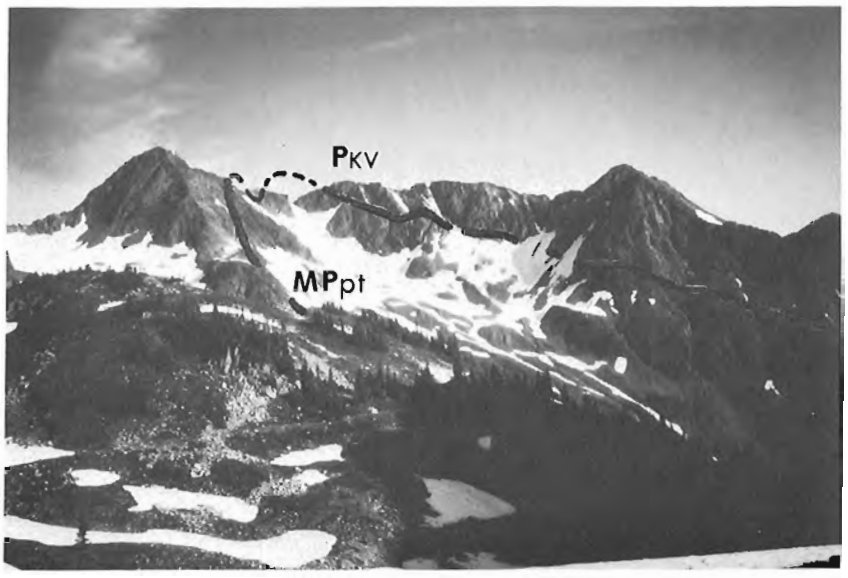

Figure 31.6. *Mount Dryden viewed from the southeast, illustrating the major anticline with Kaslo Group folded over Grey Siliceous Argillite.*

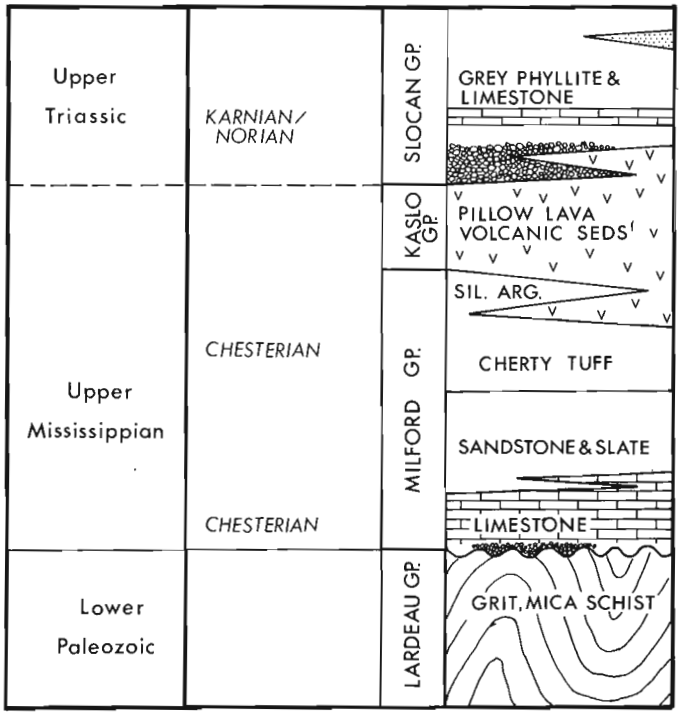

Figure 31.7. *Diagram of stratigraphic relationships resulting from lithologic correlations in the study area.*

lithologies and the common presence of cherty tuff and serpentinite clasts. Correlation of the Grey Siliceous Argillite unit beneath the Kaslo Group with the Milford Group is based on the sedimentary and siliceous character of the rocks similar to that of the upper sequences of the Milford Group. Correlation of the eastern belt of Upper Triassic rocks with Slocan Group is based on the presence of pyritic greenstone conglomerate at the base of the sequence, identical interbedded grey phyllite and light grey limestone, and similar **Gondolella** conodont forms in both belts (M.J. Orchard, pers. comm.). Grouping of the post-folding granitic bodies into the Kuskanax or Nelson Suites is uncertain.

Paleogeography

The correlations outlined above lead to a geologic history and paleogeographic interpretation to test with future mapping and geologic data. The Milford Group rests unconformably on deformed "basement" of Lardeau Group, and consists of a lower carbonate and clastic sequence on a west-facing continental margin. Sediments apparently were derived from the east. Andesitic volcanism was initiated in Late Mississippian time partly on siliciclastics of the Milford Group and partly on oceanic crust to the west. Some volcanics and distal silica-rich volcanic facies were deposited within the upper part of the Milford Group. Andesitic volcanism may have continued into Late Triassic time when erosion led to deposition of greenstone conglomerate. Subsidence of the volcanic terrane was followed in the Late Triassic by deposition of mud and limestone. Sparse paleocurrent data and facies changes (Cairnes, 1934) suggest a westerly source for some of the Slocan Group clastics. The basin occupied by these sediments must have been marginal to North America but was bounded by a volcanic arc to the west. This basin was telescoped by Middle Jurassic time, placing a plate of Slocan Group-Kaslo Group-oceanic crust on top of another comprising the Kaslo Group-Milford Group-Lardeau Group.

If the Lardeau Group is attached to North America, this model requires the Eastern Assemblage and the Slocan Group sediments also to be attached to North America, and telescoped in the Columbian Orogeny.

References

Cairnes, C.E.
1934: Slocan Mining Camp, British Columbia; Geological Survey of Canada Memoir 173, 137 p.

Fyles, J.T.
1967: Geology of the Ainsworth-Kaslo area, British Columbia; British Columbia Department of Mines and Petroleum Resources, Bulletin 53, 125 p.

Hedley, M.S.
1945: Geology of the Whitewater and Lucky Jim mine areas; British Columbia Department of Mines, Bulletin 22, 54 p.

Maconachie, R.J.
1940: Lode Gold Deposits, Upper Lemon Creek Area and Lyle Creek-Whitewater Creek Area, Kootenay District; British Columbia Department of Mines, Bulletin 7, 50 p.

Monger, J.W.H., Price, R.A., and Tempelman-Kluit, D.J.
1982: Tectonic accretion and the origin of the two major metamorphic and plutonic welts in the Canadian Cordillera; Geology, v. 10, p. 70-75.

Read, P.B. and Wheeler, J.O.
1976: Geology, Lardeau west-half, British Columbia; Geological Survey of Canada, Open File 432.

Ross, J.V. and Kellerhalls, P.
1968: Evolution of the Slocan Syncline in south-central British Columbia; Canadian Journal of Earth Sciences, v. 5, p. 851-872.

32. STRATIGRAPHY AND STRUCTURAL IMPLICATIONS OF CENTRAL KOOTENAY ARC ROCKS, SOUTHEASTERN BRITISH COLUMBIA

Project 790030

Alain D. Leclair[1]
Cordilleran Geology Division

Leclair, A.D., Stratigraphy and structural implications of central Kootenay Arc rocks, southeastern British Columbia; in Current Research, Part A, Geological Survey of Canada, Paper 83-1A, p. 235-240, 1983.

Abstract

In the central segment of the Kootenay Arc structural zone polydeformed and metamorphosed strata ranging in age from late Proterozoic (Helikian) to Mesozoic form an essentially west-facing homocline. This stratigraphic succession decreases drastically in thickness northward along its trend as a result of faulting and tectonic attenuation. A major west-dipping "thrust" fault juxtaposes a complexly folded and faulted sequence of strata of Hadrynian to Triassic age over an unbroken stratigraphic section extending from the upper Purcell Supergroup (Helikian) to the upper Hamill Group (Lower Cambrian). South and east of this "thrust" fault the west-facing homocline displays a "fan structure" as it becomes progressively overturned to the west at high stratigraphic and structural levels. In the hanging wall of the "thrust" fault tight to isoclinal folds (F_1 and F_2), which are the dominant structures, form a tectonically attenuated zone with lenticular granitoid masses. In the same zone obscure strike faults extending southward from the Ainsworth-Kaslo area played an important role in reducing the stratigraphic thickness of the Kootenay Arc rocks. The Purcell Trench, which truncates rocks of the Bayonne Batholith, shows an apparent right-lateral displacement of approximately 25 km along Kootenay Lake.

Introduction

The Kootenay Arc is a north-trending arcuate structural zone of regionally metamorphosed and polydeformed strata of late Proterozoic to Middle Jurassic age (Hedley, 1955). Its particular tectonic setting, at the boundary of the North American rocks of the Cordilleran miogeocline and the allochthonous eugeoclinal terranes to the west (Price, 1981; Archibald et al., in press), along with its economic potential for gold, silver, lead, zinc, tungsten and molybdenum deposits (Fyles and Hewlett, 1959; Fyles, 1967, 1970; Höy, 1980) make it one of the most interesting and important tectonic features of the southern Canadian Cordillera.

The present study, initiated in 1981 as part of a 1:250 000 scale mapping project in the Nelson (82F, east half) map area, focuses on the stratigraphic, structural and metamorphic complexities of the central segment of the Kootenay Arc structural zone (Fig. 32.1) and their relationships with previous geological findings by Rice (1941), Fyles and Hewlett (1959), Little (1960), Fyles (1967), Lis and Price (1976), Glover and Price (1976), Glover (1978), and Höy (1974, 1980) in neighbouring regions. During 1982 geological mapping was concentrated in the southwestern part of the Crawford Bay map area (82F/10) with additional work in the Boswell map area (82F/7).

Previous work in 1981 in the central Kootenay Arc (Leclair, 1982) established that stratigraphic units of the upper Purcell Supergroup, the Windermere Supergroup and the lower Cambrian Hamill Group form a moderate to steep west-facing homocline which at high structural levels becomes progressively overturned to the west. The stratigraphic succession is truncated to the north and northwest by a major "thrust" fault which juxtaposes an assemblage of rocks of strikingly different structural and metamorphic character against the Monk Formation. The results also revealed evidence for right-lateral displacement along the segment of the Purcell Trench occupied by Kootenay Lake.

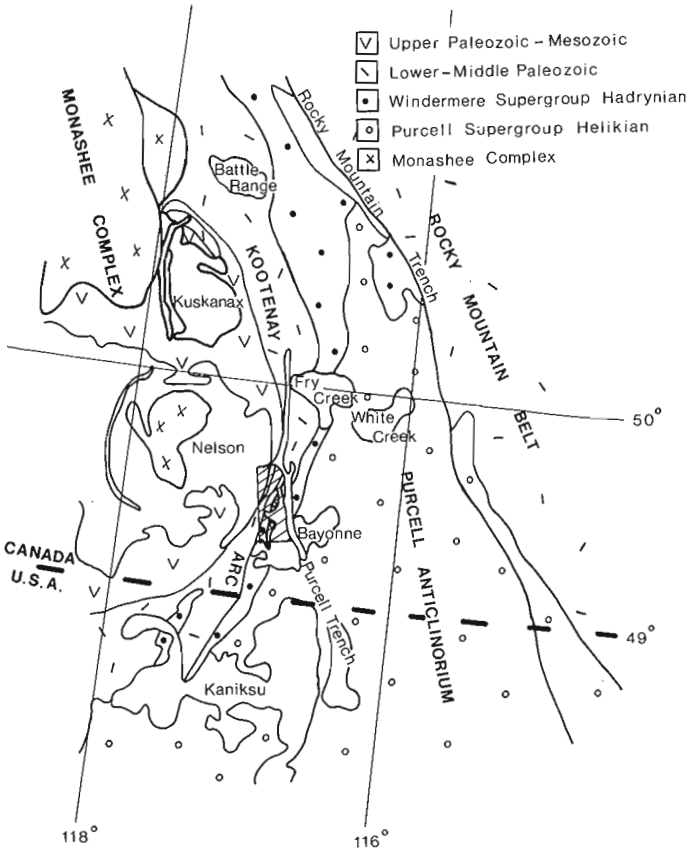

Figure 32.1. *Generalized geological map showing the location of the project area (stippled) in the tectonic framework of the southeastern Canadian Cordillera.*

[1] Department of Geological Sciences, Queen's University, Kingston, Ontario.

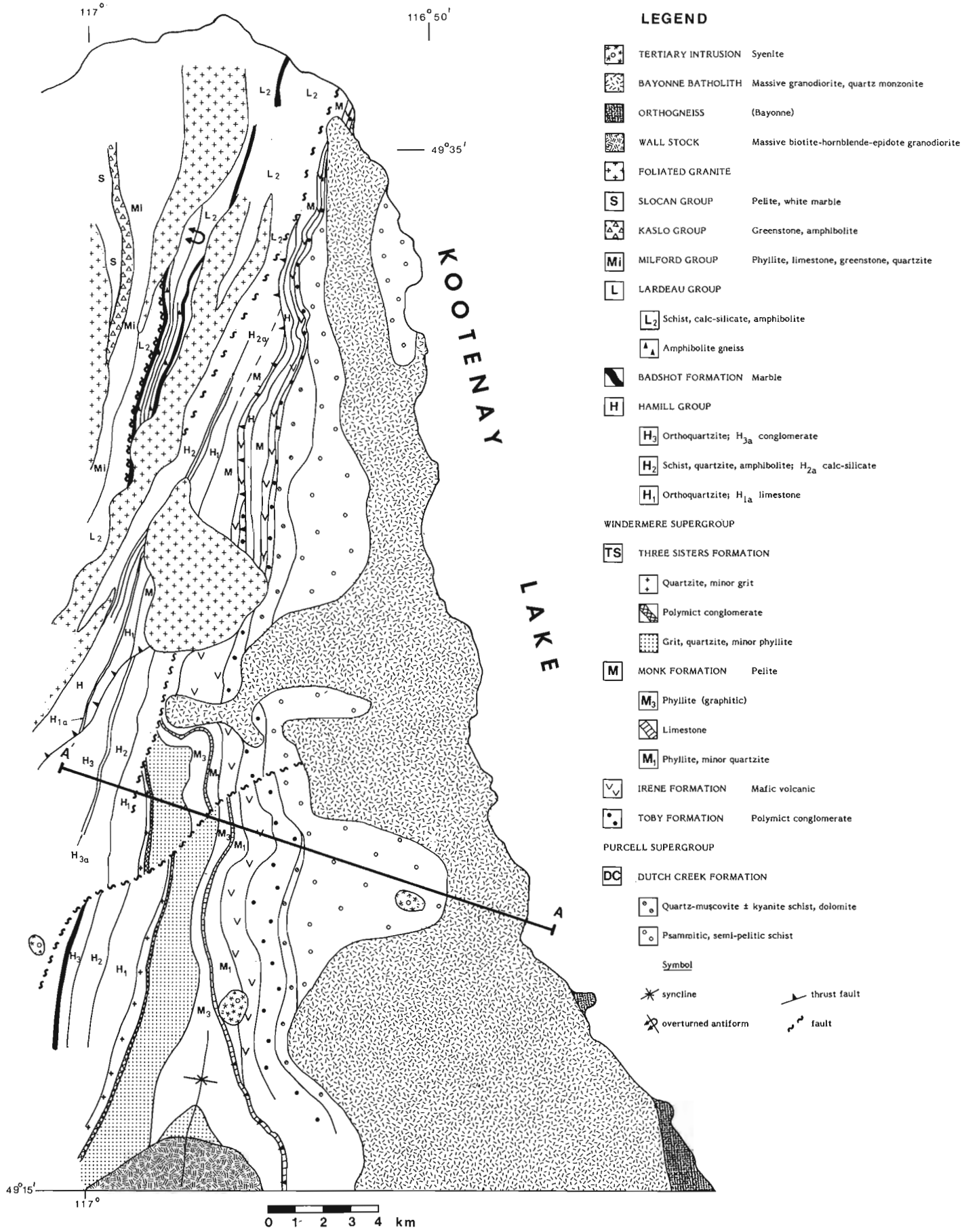

Figure 32.2. *Geological map of the central segment of the Kootenay Arc structural zone along the western edge of the Nelson (east half, 82F) sheet.*

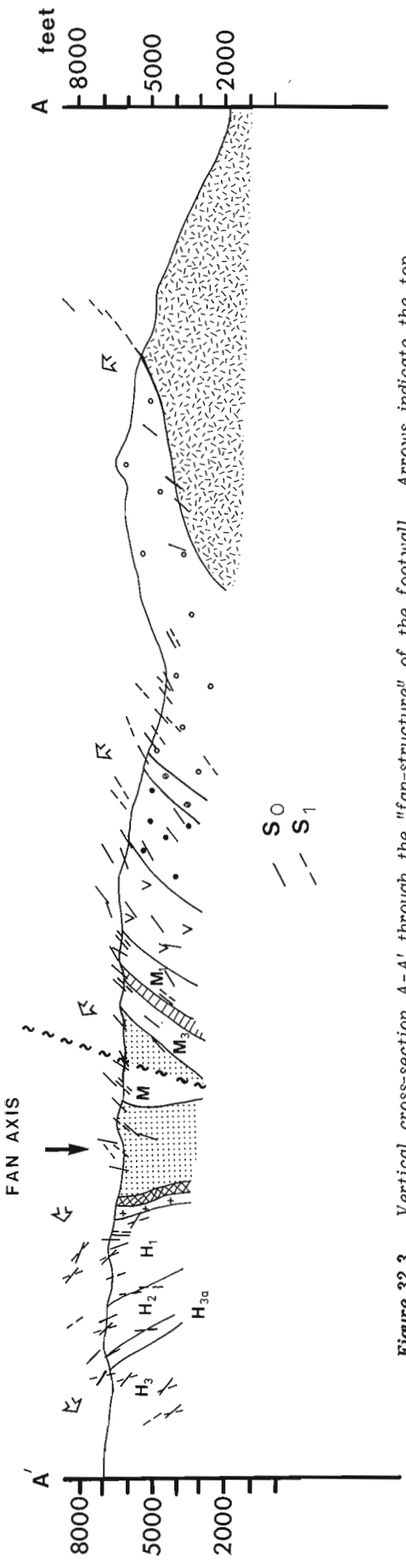

Figure 32.3. *Vertical cross-section A-A' through the "fan-structure" of the footwall. Arrows indicate the top direction of the stratigraphic succession. Description of stratigraphic units and location of cross-section are in Figure 32.2.*

Stratigraphy

The upper Proterozoic (Windermere) to Mesozoic strata of the Kootenay Arc form an estimated aggregate thickness of 20 km (Price, 1981). In the moderate west-dipping stratigraphic sequence of the northern half of the study area (Fig. 32.2) these strata form a width of less than 10 km from the base of the Windermere Supergroup to the Slocan Group. The missing stratigraphic thickness is highly suggestive of considerable tectonic thinning and faulting.

The following description of the stratigraphic units supplements an earlier one (Leclair, 1982), and unravels the stratigraphy of the "undivided Paleozoic rocks" (Little, 1960) that occur in fault contact with the Monk Formation and the Hamill Group in the northwestern part of the area.

Upper Purcell Supergroup (Helikian)

The units of the upper Purcell sequence which are intruded by the Bayonne Batholith are the stratigraphic equivalent of the Dutch Creek Formation. At the north end of the Bayonne Batholith the thick lower unit of thinly interlayered psammitic and semipelitic schists is exposed along the lakeshore. The upper Dutch Creek unit, comprising white quartz-muscovite ± kyanite schist with minor quartzite and dolomite bands, is locally truncated by the unconformity marking the base of the overlying Windermere Supergroup.

Windermere Supergroup (Hadrynian)

The Windermere Supergroup, made up of the polymict conglomerate of the Toby Formation, the mafic volcanic rocks of the Irene Formation, the pelite and limestone of the Monk Formation and the grit, quartzite and conglomerate of the Three Sisters, forms a north-trending belt that markedly decreases in width northward. In the northern half of the map area, the aggregate thickness of the stratigraphic units of the Toby, Irene and Monk formations is less than 1 km and the Three Sisters Formation is absent. At the locus of this disappearance of Windermere strata the Lower Cambrian quartzite of the Hamill Group is in fault contact with the Irene and Monk formations. Syndepositional block-faulting during the late Proterozoic, as proposed by Lis and Price (1976), may explain the rapid disappearance of the stratigraphic units of the Three Sisters Formation along strike.

Lower Cambrian Hamill Group

The subdivisions of the Hamill Group proposed by Hoy (1980) for the dominantly quartzite and schist sequence directly above the Windermere Supergroup are adopted for stratigraphic counterparts in this study area.

The base of the Hamill Group, immediately overlying the Monk Formation, is a unit of pure white, pink or green orthoquartzite with minor argillite and schist interlayers. It contains a narrow horizon of buff dolomite and limestone that vanishes northward. A rusty weathered unit (H_2) of quartz-muscovite-biotite schist, quartzite and meta-siltstone with minor amphibolite overlies the basal quartzites of unit H_1. Near its base it is characterized by a discontinuous band, approximately 20 m thick, of calc-silicate schist and brownish marble. The upper part of the Hamill Group (H_3 and H_4) is truncated by granitic intrusions which may be satellites of the Nelson Batholith.

Lower Cambrian Badshot Formation

The Badshot Formation is a very distinctive unit, 5 to 40 m thick, of pure white calcite and dolomite marble and calc-silicate containing tremolite, phlogopite and/or diopside.

It marks the transition from the predominant quartzite of the Hamill Group to the carbonate and schist of the Lardeau Group and is the most reliable marker horizon for deciphering the structure of the Kootenay Arc (Brown et al., 1981). In the map area, it is either at the contact of strongly foliated granitoid rocks or in fault contact with schist, amphibolite and calc-silicate of the Lardeau Group. Its absence along parts of the Hamill-Lardeau Group contact infers the presence of obscure faults more or less parallel with the regional trend.

Lower Paleozoic Lardeau Group

The Lardeau Group rocks of the area have been grouped into two stratigraphic units based on their lithological similarities (with minor facies change) to the L_2 and L_3 units of Höy (1980). The lower unit is composed of dark amphibolite schist and gneiss with minor quartz-muscovite-biotite schist. The rest of the Lardeau Group is represented by green diopside-bearing calc-silicate gneiss and amphibolite layers and boudins with minor quartzite, quartz-muscovite-biotite schist and white calcite marble bands.

Mississippian Milford Group

Throughout the Kootenay Arc the Milford Group is separated from the underlying Lardeau Group by an unconformity across which stratigraphic and structural evidence indicate a difference of one phase of folding (Brown et al., 1981). In the map area the small angular difference in trend between the strata of the Milford Group and older rocks suggests that this tectono-stratigraphic break corresponds to a strike fault. The magnitude and direction of displacement along this fault is not known.

The Milford Group has been divided into three distinct mappable units. The lower part consists essentially of dark grey to black phyllite and schist and blue grey laminated limestone with minor quartzite and greenstone. It is overlain by a thin middle unit of greenstone and amphibolite. The upper part consists of thinly bedded grey to light grey quartzite and chert intercalated with greenstone and amphibolite which implies that the sediments of the Milford Group partly overlapped the volcanic rocks of the Kaslo Group.

Pennsylvanian-Triassic Kaslo Group

The Kaslo Group is less than 0.5 km thick and consists of dark green greenstone and amphibolite containing slivers of siliceous garnet-bearing schist and minor metagreywacke.

Upper Triassic Slocan Group

The Slocan Group, exposed along the western boundary of the Nelson east half map area, structurally overlies the Kaslo Group to the east and is intruded by strongly foliated granitoid rocks of the Nelson Batholith to the west. It consists of pelitic schist intercalated with white calcite marble, weathered calc-silicate schist and pure to slightly micaceous quartzite.

Structure

The project area is near the central part of the Kootenay Arc structural zone where sedimentary and volcanic rocks of late Proterozoic to Mesozoic age form the thinnest segment of the arc. In the northern half of the area faulting and tectonic thinning significantly reduced the thickness of these strata.

Three distinct faults or sets of faults are recognized. The most prominent, trending north-northeast across the area, is a major "thrust" fault that separates rocks of contrasting structural style. The second is a set of obscure strike faults extending southward from the Ainsworth-Kaslo area of Fyles (1967). The third caused a major displacement along the Purcell Trench.

Major "Thrust" Fault

A major west-dipping "thrust" fault juxtaposes the Windermere Supergroup (hanging wall) over the Hamill Group (footwall). Northward it progressively truncates the stratigraphic succession from the lower part of the Windermere Supergroup to the Hamill Group. It resembles the West Bernard fault described by Höy (1980) as it separates a right-side-up panel of upper Proterozoic to Lower Cambrian rocks to the south and east from a tightly folded and possibly up-side-down sequence to the west. However, more evidence is required to confirm the structure and the connection between these two thrust faults.

Footwall Structures. South and east of the "thrust" fault an unbroken stratigraphic sequence from upper Proterozoic to Lower Cambrian forms a west-facing homocline which becomes progressively overturned to the west and tightly folded at high stratigraphic and structural levels. Bedding (S_0) together with a well-developed pervasive foliation (S_1) display a "fan structure" with axis of rotation near the Precambrian-Cambrian boundary (Fig. 32.3). East of the fan axis the S_1 fabric is associated with east-verging tight to isoclinal mesoscopic F_1 folds having subhorizontal axes. West of the fan axis the same fabric is associated with upright to slightly overturned, isoclinal F_1 folds of large amplitude (i.e., Laib syncline and Sheep Creek anticline). In the eastern part of the area a weak and moderately west-dipping crenulation cleavage (S_2), which produced a gently northwest-plunging lineation (L_2) on S_0 and S_1 surfaces, is probably responsible for the development of the "fan structure".

Hanging Wall Structures. West of the "thrust" fault the style of deformation changes dramatically from the simple "fan structure" of the footwall. There, a very tightly folded sequence of strata, ranging from Hadrynian to Mesozoic, forms a tectonically conformable succession along with elongate granitoid intrusions. This area of strongly deformed rocks is a tectonically attenuated zone. Tight to isoclinal west-dipping folds (F_1 and/or F_2) with axes mainly plunging gently to the southwest are the dominant structures. These folds are affected by gentle warps that seem to have an open N-shape when viewed from the south.

Ainsworth-Kaslo Type Faults

In the tectonically attenuated zone the stratigraphic section is incomplete and many units are thinner than their counterparts elsewhere in the Kootenay Arc. For example, the total thickness of quartzites and schists in the Hamill Group is less than 1.5 km and the marble unit of the Badshot Formation is absent from its position below the Lardeau Group. Obscure strike-slip faults more or less parallel to the main foliation are inferred to truncate the stratigraphic succession. Two faults of this type are shown on Figure 32.2. In this segment of the Kootenay Arc, a post-metamorphic, west-side-up, dip-slip component along these faults is consistent with the juxtaposition of high grade metamorphic rocks to the west with lower grade ones to the east.

These faults are probably southern extensions of the northerly trending strike faults inferred by Fyles (1967) in the Ainsworth-Kaslo area.

Purcell Trench

The Purcell Trench, defined as a north-south topographic depression extending more than 650 km from northern Idaho to the Rocky Mountain Trench, displays an apparent right-lateral displacement of approximately 25 km along Kootenay Lake (Fig. 32.4). This movement is considered a late event in the tectonic evolution of the Kootenay Arc because of its accentuated topographic expression. Moreover, it separates higher grade metamorphic rocks to the west from the lower grade rocks to the east and truncates rocks of the Bayonne Batholith.

Discussion

The tectonically attenuated zone of the northern half of the map area may be viewed as the highly deformed and faulted remnants of what was once a continuous stratigraphic section. It is obvious that rocks of this zone have been affected by a more pronounced east-west shortening than their footwall counterparts to the south. Isolated granitoid intrusions, which occur as long thin slivers, are deformed along with the country rocks into a very tightly folded west-dipping sequence.

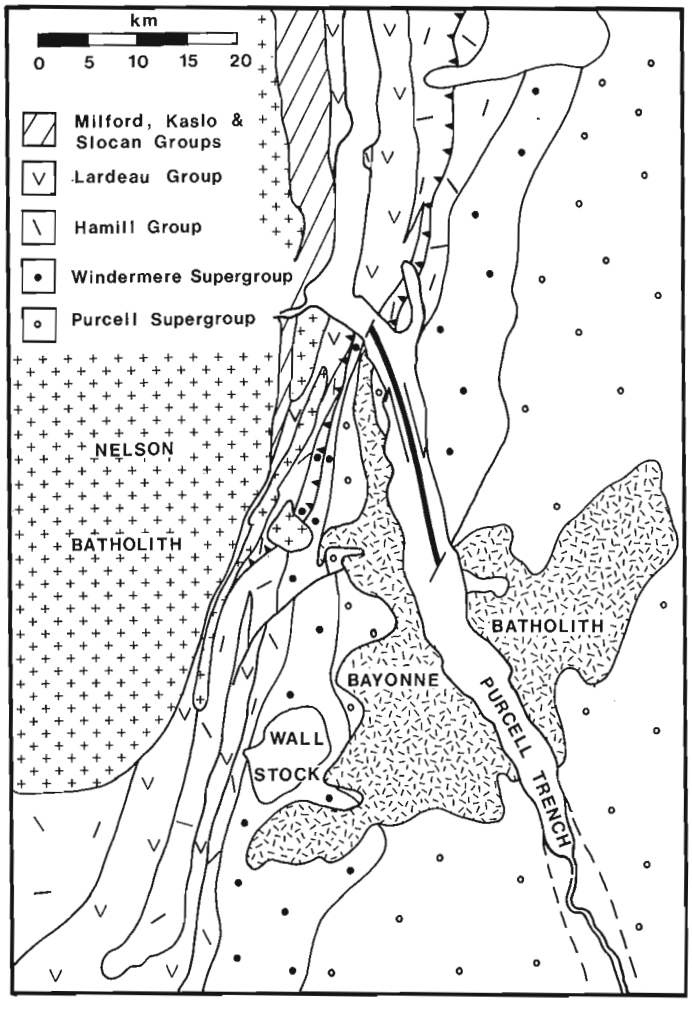

Figure 32.4. *Geological map compiled from Rice (1941), Fyles and Hewlett (1959), Little (1960), Fyles (1967), Glover (1978), Hoy (1980) and work of the writer to portray the apparent right lateral displacement along the Purcell Trench and the northward thinning of the stratigraphic units between the Bayonne and Nelson batholiths.*

The recognition of obscure strike faults, which depends on detailed mapping over a relatively long distance along strike, warrants consideration in future models for the tectonic evolution of the Kootenay Arc. These faults are thought to be associated with the bending of the late Proterozoic to Mesozoic strata into a convex eastward belt, forming the curvature of the Kootenay Arc. This is substantiated by the apparent restriction of these faults to the central segment of the Kootenay Arc where the stratigraphic thickness of late Proterozoic to Mesozoic strata is considerably less than elsewhere along the arc.

Acknowledgments

The writer greatly benefited from the geological and logistical expertise of J.E. Reesor of the Geological Survey of Canada. Andrew Arthur, Geoff Freeze, Bruce Krutow (all from University of British Columbia) and Lisel Currie (Queen's University) provided excellent assistance and great humour. I am grateful to Dr. J.T. Fyles, the expert on the geology of the Kootenay Arc, who shed light on some stratigraphic and structural complexities in the area during a visit in late June. Dugald Carmichael (Queen's University) significantly contributed to the mapping and recognition of the Lardeau stratigraphy along the lakeshore, during a 2-day visit in early August. Discussions with David Klepacki (Massachusetts Institute of Technology) on several occasions over the summer greatly improved my knowledge of the overall structure of the Kootenay Arc. Rolf Ganong and Doug Williams (both of Okanagan Helicopters Ltd.) provided safe transportation. J.A. Roddick and John Reesor revised the report and suggested improvements.

References

Archibald, D.A., Glover, J.K., Price, R.A., Farrar, E., and Carmichael, D.M.
– Geochronology and tectonic implications of magmatism and metamorphism; southern Kootenay Arc and neighbouring regions, south-eastern British Columbia: Part I; Jurassic to Mid-Cretaceous; Canadian Journal of Earth Sciences. (in press)

Brown, R.L., Fyles, J.T., Glover, J.K., Höy, T., Okulitch, A.V., Petro, V.A., and Read, P.B.
1981: Southern Cordillera cross-section – Cranbrook to Kamloops; in Calgary '81, Field Guides to Geology and Mineral Deposits, eds. R.L. Thompson and D.G. Cook; Geological Association of Canada, p. 335-372.

Fyles, J.T.
1967: Geology of the Ainsworth-Kaslo area; British Columbia Department of Mines, Bulletin 53, 125 p.

1970: Geological setting of the lead-zinc deposits in the Kootenay Lake and Salmo areas of British Columbia; Washington Division of Mines, Bulletin 61, p. 43-53.

Fyles, J.T. and Hewlett, C.G.
1959: Stratigraphy and structure of the Salmo lead-zinc area; British Columbia Department of Mines, Bulletin 41, 162 p.

Glover, J.K.
1978: Geology of the Summit Creek map-area, southern Kootenay Arc, British Columbia; unpublished Ph.D. thesis, Queen's University, Kingston, Ontario, 143 p.

Glover, J.K. and Price, R.A.
1976: Stratigraphy and structure of the Windermere Supergroup, southern Kootenay Arc, British Columbia; in Report of Activities, Part B, Geological Survey of Canada, Paper 76-1B, p. 21-23.

Hedley, M.S.
1955: Lead-zinc deposits of the Kootenay Arc; Western Miner, v. 28, p. 31-35.

Höy, T.
1974: Structure and metamorphism of Kootenay Arc rocks around Riondel, British Columbia; unpublished Ph.D. thesis, Queen's University, Kingston, Ontario, 201 p.

1980: Geology of the Riondel area, central Kootenay Arc, southeastern British Columbia; British Columbia Ministry of Energy, Mines and Petroleum Resources, Bulletin 73, 89 p.

Leclair, A.D.
1982: Preliminary results on the stratigraphy, structure and metamorphism of central Kootenay Arc rocks, southeastern British Columbia; in Current Research, Part A, Geological Survey of Canada, Paper 82-1A, p. 45-49.

Lis, M.G. and Price, R.A.
1976: Large-scale block faulting during deposition of the Windermere Supergroup (Hadrynian) in southeastern British Columbia; in Report of Activities, Part A, Geological Survey of Canada, Paper 76-1A, p. 135-136.

Little, H.W.
1960: Nelson map area, west half, British Columbia; Geological Survey of Canada, Memoir 308, 205 p.

Price, R.A.
1981: The Cordilleran foreland thrust and fold belt in the southern Canadian Rocky Mountains; in Thrust and Nappe Tectonics, eds. N.J. Price and K. MacClay, Geological Society of London, Special Publication 9, p. 427-448.

Rice, H.M.A.
1941: Nelson map area, east half, British Columbia; Geological Survey of Canada, Memoir 228, 86 p.

33.

COASTAL SEDIMENTS OF THE STRAIT OF JUAN DE FUCA: IMPLICATIONS FOR OIL SPILLS

Project 780027

Patrick McLaren
Cordilleran Geology Division, Patricia Bay

McLaren, P., Coastal sediments of the Strait of Juan de Fuca: implications for oil spills; in Current Research, Part A, Geological Survey of Canada, Paper 83-1A, p. 241-244, 1983.

Abstract

The Strait of Juan de Fuca is a high-risk area for an oil spill. Shoreline sediment and geomorphic studies suggest that oil in the coastal zone will tend to move from west to east and/or will be eroded from the beach into the offshore where trajectory models indicate westward movement into the open Pacific Ocean. If necessary, cleanup operations should proceed from west to east to minimize the probability of recontamination. In most cases, however, cleanup should be unnecessary because the sediments are highly mobile and undergoing net erosion which will result in rapid self-cleaning. Sediment removal could drastically increase erosion rates and should be discouraged. Only about 19 per cent of the coast has a high physical sensitivity with respect to probable long term contamination. These environments occur in areas where intertidal flats are wide and in lagoons that commonly contain marshland. Sediment trends indicate that the lagoons are not being infilled by sediment from the littoral drift system. It is probable, therefore, that dispersed oil will not remain in the lagoon to become incorporated into the bottom sediments, and that dispersing an oil slick offshore will ensure an uncontaminated lagoon.

Introduction

About 250 tankers per year enter the Strait of Juan de Fuca from Alaska and elsewhere. This amount may almost double depending on the acceptance of future oil transportation proposals (Wolferstan, 1981). According to the Oceanographic Institute of Washington (1978) a tanker casualty (i.e. a collision, ramming, grounding etc.) occurred on an average once every 4-5 days between 1969 and 1976. Wolferstan concluded that the risk for a major oil spill capable of contaminating vulnerable and highly valued portions of the southern British Columbia coast is "relatively high".

Several studies based on drift card observations and spill trajectory modelling indicate that an oil spill confined to the Strait of Juan de Fuca will tend to move seaward despite strong prevailing westerly winds (Bureau of Land Management, 1979; Pashinski and Charnell, 1979; Ages, 1978). This study, based on the sediments found at the shoreline along 121 km of the strait (Fig. 33.1) is designed to enhance the previous modelling assuming oil has reached the coastal zone.

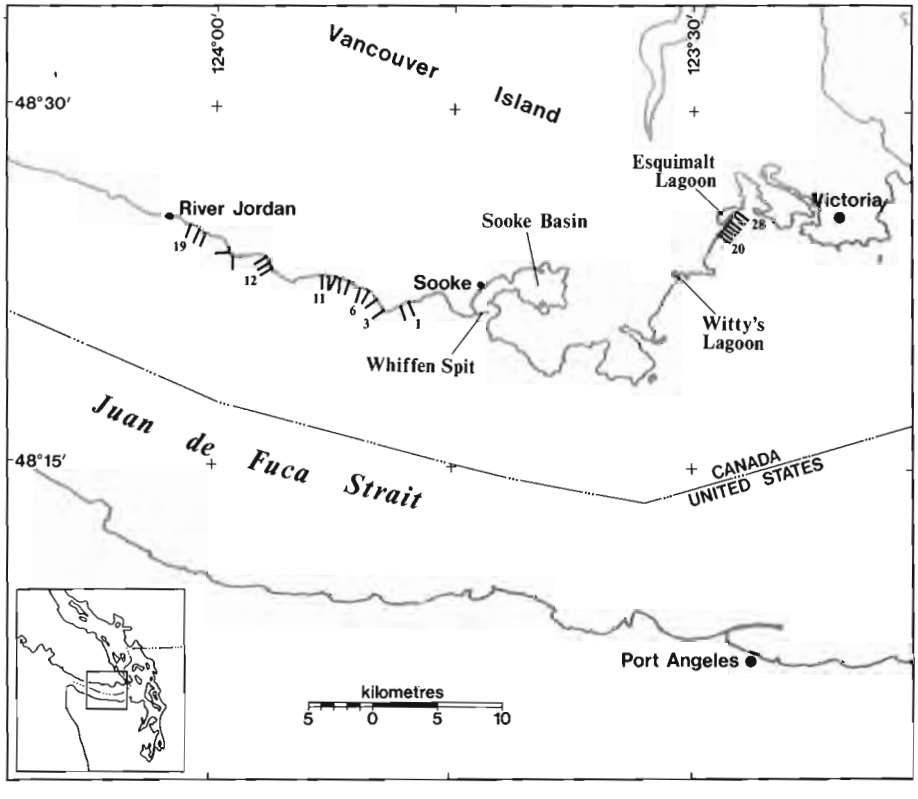

Figure 33.1. *Location of study area and beach sample sites.*

Coastal Morphology

Most of the coastal region under study comprises bedrock (65%) consisting principally of Tertiary augite gabbro and basalt and lesser amounts of Upper Tertiary sandstone, shale and conglomerates. The backshore, generally tree covered, slopes at about 10° although frequently there is a rock bluff at the shoreline less than 20 m high suggesting erosion (Fig. 33.2).

The remaining 35 per cent of the shore is constructed in unconsolidated Quaternary sediments consisting of till or glacial-fluvial deposits. At several localities unconsolidated sediments form steep eroding bluffs up to 50 m high which are sources for much of the shoreline sediments (Fig. 33.3). Well developed spits at the entrance to Sooke Basin, (Whiffen Spit), Witty's Lagoon and Esquimalt Lagoon immeditely east of eroding bluffs point to an eastward littoral drift (Fig. 33.4).

Beaches are present on 69 per cent of the coast, small pocket beaches (Fig. 33.5) trapped in the innumerable indentations of the rocky shoreline being the most common (40%). Elsewhere, particularly on unconsolidated coast, they are continuous (Fig. 33.6). Only 26 per cent of the shore contains intertidal flat deposits of any significance. These may be up to 500 m across but average about 30 m.

Figure 33.2. *Rock shoreline formed in Tertiary basalt (PSC 1).*

Figure 33.5. *Small pocket beaches (PSC 3).*

Figure 33.3. *Unconsolidated eroding bluff immediately west of Whiffen Spit (PSC 8).*

Figure 33.6. *Continuous beach formed on a low unconsolidated shoreline (PSC 5).*

Figure 33.4. *Whiffen Spit at the entrance to Sooke Basin (PSC 9).*

Small creeks draining the relatively low mountainous terrain (elevations up to 700 m) are common but do not appear to provide significant amounts of coastal sediment. One notable exception is the Sooke River which terminates in a delta of about 2 km^2 within the confines of Sooke Basin. Two other relatively large streams, Jordan River and Muir Creek, enter the open strait. Although deltas have not formed, particularly wide intertidal flats surround their mouths.

Sedimentology

Sediment samples collected from locations 1 to 19 (Fig. 33.1) show that gravel is the principal component of the upper beach whereas sand becomes dominant on the lower beach face and intertidal-flat deposits (Table 33.1). Source-deposit relationships (McLaren, 1981b) among all beach-face samples suggest that there is a continuum of sand transport from west to east. Of 80 possible trends 65 are eastward and exhibit predominantly Case IIIB sedimentation (i.e., beach-face sediments generally become coarser, better sorted and more positively skewed in the direction of transport).

Table 33.1

Summary of Grain Size Statistics

Environment	% Gravel	% Sand	% Mud	Mean (ϕ)	Sorting (ϕ)	Skewness (ϕ)	No. of Samples
storm berm	66 ± 33	34 ± 33		-1.92 ± 1.19	1.87 ± .75	.12 ± 1.16	5
berm	73 ± 16	27 ± 16		-1.97 ± .60	1.85 ± .82	.30 ± .50	5
upper beach face	71 ± 18	29 ± 18		-1.92 ± .97	2.00 ± .73	.47 ± .69	14
lower beach face	54 ± 25	45 ± 25		-.88 ± 1.48	2.19 ± .45	-1.0 ± .93	14
intertidal flat	23 ± 27	75 ± 27		1.25 ± 1.79	1.78 ± .92	-.48 ± 1.50	16
shelf	19 ± 30	63 ± 30	18 ± 30	1.85 ± 2.52	2.00 ± 1.04	1.58 ± 1.26	37

Relationships among the beach sub-environments strongly suggest a predominant offshore movement from berm to intertidal deposits. In 16 profiles containing sufficient samples to establish trends, 13 indicated an offshore direction of transport, 2 were onshore and one was ambiguous. The dominant offshore movement is further supported in a comparison of all beach sediments with 37 offshore samples near Jordan River. In 654 possible source-deposit relationships 63 per cent suggest movement of sand-size material onto the shelf to water depths generally less than 30 m. Among the offshore samples themselves sediment trends signify east and northeast as the favoured transport direction.

In summary, sediment trends demonstrate that eroding Quaternary deposits are the chief source for coastal sediments. Although there may not be a well defined winter-summer beach sedimentation cycle (Harper, 1980) in the Strait of Juan de Fuca, beach sediments are eroded onto the shelf and transported back to the beach with a net eastward drift. Net erosion is occurring and beaches are maintained by a continual supply of eroding Quaternary sediments.

Implications for Oil Spills

The coastal sediments are characterized by large percentages of gravel with a sandy matrix (Table 33.1). Such beaches, because of their high porosity, are able to retain large quantities of oil even after extensive cleanup operations (Long et al., 1981). This apparent seriousness of long term pollution potential is mitigated by high sediment mobility and net erosion both of which will result in rapid self cleaning. In most cases, cleanup of beaches should be discouraged as any sediment removal could drastically increase erosion rates, particularly at localities where eroding bluffs are presently supplying coastal sediments. However, formation of an asphalt could have undesirable consequences; beaches to the east would quickly become sediment starved with a resultant increase in erosion. All effort should be made to break up such a pavement if conditions favour its formation.

If cleanup is desirable, sediment trends suggest that there is a greater probability of recontamination from the west rather than from the east. Cleanup should proceed, therefore, from west to east.

At several localities, spits shelter lagoon environments known to be highly sensitive to the effects of an oil spill. A sediment-trend analysis from localities 20-28 (Fig. 33.1) clearly shows that fine sediments within Equimalt Lagoon have not been derived from the eroding till bluffs and beach system. Because dispersed oil is likely to follow similar transport routes to suspended sediment, oil that has been dispersed in the offshore before reaching the lagoon will probably not remain within the lagoon or become incorporated into the bottom sediments. Offshore dispersal of oil to protect the lagoons is therefore recommended (McLaren, 1981a).

Table 33.2

Physical Sensitivity Summary

Physical Sensitivity Category (PSC)	Per cent of coast	Description
1	20	Moderately sloping rock coast; no beach or intertidal flat sediments.
2	25	Moderately sloping rock coast containing less than 20 per cent gravel and sand beaches.
3	10	Moderately sloping rock coast with 20 to 80 per cent pocket beaches or less than 20 per cent intertidal flat sediments.
4	5	Moderately sloping rock coast with 20 to 80 per cent continuous gravel beaches.
5	9	Low sloping unconsolidated coast with continuous beaches.
6	9	Moderately sloping rock or unconsolidated coast with few beaches and a continuous intertidal flat.
7	2	Moderately sloping rock coast; 20 to 80 per cent gravel pocket beaches and continuous intertidal flat deposits.
8	9	Unconsolidated coast, continuous beach and intertidal flat.
9	7	Low sloping, unconsolidated coast with particularly wide intertidal flats.
10	3	Low sloping, unconsolidated coast with continuous beaches and particularly wide intertidal flats.

Physical Sensitivity

Physical sensitivity, defined as a relative measure of the seriousness of oil pollution in a particular environment with respect to the probable dispersal of oil, residence time and cleanup difficulties, is assessed by a combination of the morphology and sedimentology of the coast (McLaren, 1980).

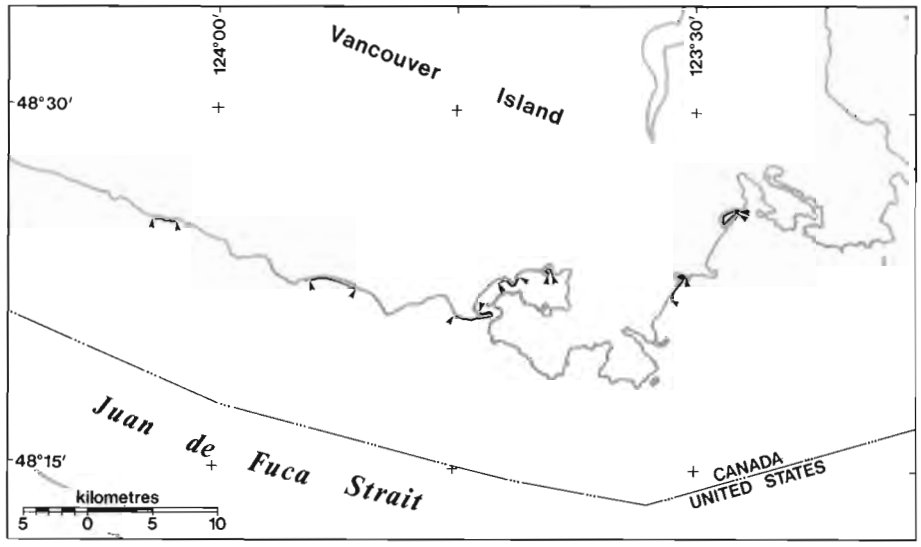

Figure 33.7. *Shorelines with physical sensitivity categories 8 to 10.*

In general physical sensitivity increases as the amount of both beach and intertidal deposits increase (Table 33.2). In the Strait of Juan de Fuca, the majority of the coast may be considered as having low physical sensitivity as 55 per cent of the shore is represented by the first three physical sensitivity categories. Shorelines in categories 8, 9 and 10 have the highest physical sensitivity and every effort should be made to protect these environments from an encroaching spill (Fig. 33.7).

These most sensitive environments comprise 19 per cent of the coast and are located where intertidal flats are especially wide, such as at the mouths of the larger rivers or inside the lagoons. The latter may be protected by booming; however, because the probability that dispersed oil will have little effect on the coastal sediments the use of dispersants for shoreline protection appears to be a reasonable alternative. Furthermore, oil remaining outside the coastal zone has a high probability of being carried westwards towards the open ocean.

Summary

i) Oil in the coastal zone is more likely to move eastwards resulting in potential recontamination problems from west to east. This is contrary to the westward movement of oil farther offshore as predicted by drift card studies and trajectory models.

ii) Most of the shoreline is undergoing net erosion indicating cleanup of beaches should be discouraged because self-cleaning will be rapid and sediment removal will increase erosion problems.

iii) If conditions favour the formation of an asphalt pavement, care should be taken to destroy it. Its presence will result in depletion of beach material and increased erosion to the east of its formation.

iv) Lagoons are particularly sensitive environments; dispersal of oil prior to shoreline impact will have little detrimental effect in these environments.

Acknowledgments

The writer is indebted to R. Currie for developing computer programs to determine source-deposit relationships rapidly and to analyze the morphological elements of the coastal description. T. Mullin, K. Conway and J. Truscott carried out all sediment analyses.

References

Ages, A.
1978: Oil spill modelling in British Columbia; in Oil Spill modelling, Proceedings of a workshop held in Toronto, Canada, Nov. 7-8, 1978, Institute of Environmental Sciences, University of Toronto, Publication No. EE-12.

Bureau of Land Management
1979: Environment statement crude oil transportation systems.

Harper, J.
1980: Seasonal changes in beach morphology along the B.C. coast; The Canadian Coastal Conference, 1980, National Research Council of Canada, Burlington, Ontario, p. 136-150.

Long, B.F.N., Vandermeulen, J.H., and Abern, T.P.
1981: The evolution of stranded oil within sandy beaches; Proceedings of the 1981 Oil Spill Conference (Prevention, Behaviour, Control Cleanup), American Petroleum Institute No. 4334, p. 519-524.

McLaren, P.
1980: The coastal morphology and sedimentology of Labrador: a study of shoreline sensitivity to a potential oil spill; Geological Survey of Canada, Paper 79-28, 41 p.

1981a: Coastal geology and oil spills; Episodes, v. 1981, p. 3-8.

1981b: An interpretation of trends in grain size measures; Journal of Sedimentary Petrology, v. 51, p. 611-624.

Oceanographic Institute of Washington
1978: Oil spill risk analysis; Seattle, Washington.

Pashinski, D.J. and Charnell, R.L.
1979: Recovery record for surface drift cards released in the Puget Sound – Strait of Juan de Fuca system during calendar years 1976-1977; NOAA Technical Memo ERL PMEL-14, Washington, D.C.

Wolferstan, W.H.
1981: Oil tanker traffic: assessing the risks for the southern coast of British Columbia; Province of British Columbia, Ministry of the Environment, APD Bulletin 9, 82 p.

34.

STRUCTURAL TRANSITION AND STRATIGRAPHY IN THE CARIBOO MOUNTAINS, BRITISH COLUMBIA

EMR Research Agreement 207-4-82

Donald C. Murphy and C.J. Rees[1]
Cordilleran Geology Division, Vancouver

Murphy, D.C. and Rees, C.J., Structural transition and stratigraphy in the Cariboo Mountains, British Columbia; in Current Research, Part A, Geological Survey of Canada, Paper 83-1A, p. 245-252, 1983.

Abstract

A structural sequence has been established in low grade metasediments of the Proterozoic Kaza Group and Isaac Formation in the area between Castle Creek and Raush River, southern Cariboo Mountains. Two phases of folding (D1 and D2) developed prior to the metamorphic peak and two postmetamorphic phases (D3 and D4) have been superimposed. Di folds which are tight and inclined, plunge northwestwardly and verge to the northeast. D2 folds are also northwestwardly trending and plunging, tight, and inclined, but are southwestwardly verging. D3 folds are gentle and open, northwestwardly trending, warps of earlier structures. D4 crenulations trend to the northeast and appear to be associated with northeast trending domains (of equal plunge) of early structure.

The structural sequence is the same as that determined for the higher grade Kaza Group rocks of the Premier Range; however, the geometry of equivalent phases of folding is different. Along the trace of the Premier Anticlinorium, first and second phase folds change from reclined and isoclinal structures in the Premier Range, to tight and slightly inclined north of Raush River, and, then to steeply inclined and even more open north of Castle Creek. Third phase folds vary from diffuse upright warps in the Premier Range to even more gentle warps north of Raush River and are practically absent near Castle Creek. Fourth phase structures remain unchanged from southwest to northwest. This transition appears to be accomplished continuously although low-angle shear zones have been observed.

The contact of the Kaza Group with the overlying Isaac Formation is unfaulted. Outer mid-fan or depositional lobe turbidites of the upper Kaza Group which contain increasing amounts of carbonate and shale clasts towards the contact and a decreasing ratio of sand to shale and limestone beds, imply offlap of shelf facies (Isaac Formation) over the outer mid-fan portion of the Kaza turbidite fan.

Introduction

In the Cariboo Mountains east central British Columbia (Fig. 34.1, 34.2), metasediments of the Proterozoic Kaza and Cariboo groups exhibit a variation in structural style that roughly corresponds with variations in metamorphic grade (Campbell, 1968; Campbell et al., 1973). In 1981, a three year project to investigate this variation in structural style was initiated by the first author as a doctoral thesis at Carleton University, under the supervision of Richard L. Brown. The study is focused on the structural transition from open to isoclinal folds along the trace of the Premier Anticlinorium, a regional scale antiform that is best exposed in the Premier Range of the southern Cariboo Mountains (Campbell, 1968). The 1981 field season was spent unravelling fold geometry in the Premier Range where metasediments range in metamorphic grade from garnet to kyanite-staurolite zone. Two phases of tight to isoclinal folding developed before the regional peak of metamorphism, and two phases of postmetamorphic, open and upright folding have been superimposed. The Premier Anticlinorium is an upright third phase warp of the axial surfaces of isoclinal first and second phase folds (Murphy and Journeay, 1982).

Only upright folds have been observed by Campbell et al. (1973) along the trace of the Premier Anticlinorium near Castle Creek (Fig. 34.2). Thus, a major change in structural style has occurred between Castle Creek and the Premier Range. Two months of the 1982 field season were spent in the area between Raush River and Castle Creek, mapping folds on a 1:50 000 scale base and analyzing fold data in the hopes of determining the relationship between Premier Range isoclinal folds and Castle Creek upright folds. Of particular interest are the following questions:

1. Does the sequence of deformation and metamorphism established in higher grade rocks in the Premier Range apply to the low grade (chlorite to garnet zone) rocks as well?

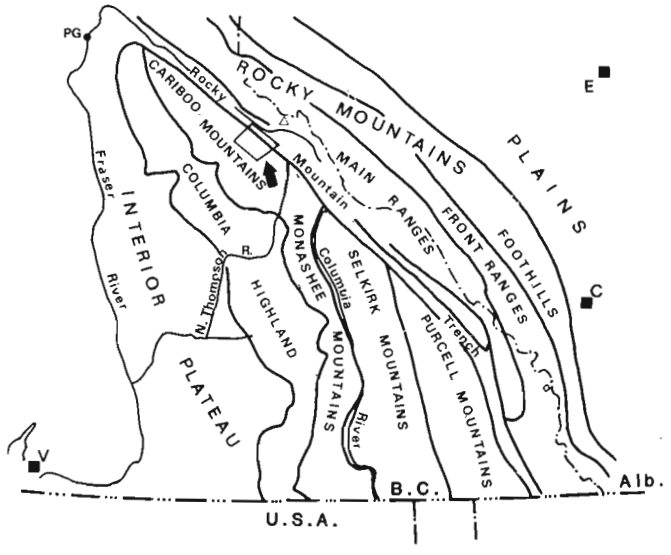

Figure 34.1. *Physiographic subdivisions of British Columbia (from Campbell, 1973). The location of Figure 34.2 is indicated by the dark arrow.*

[1] Department of Geology, Carleton University, Ottawa, Ontario K1S 5B6

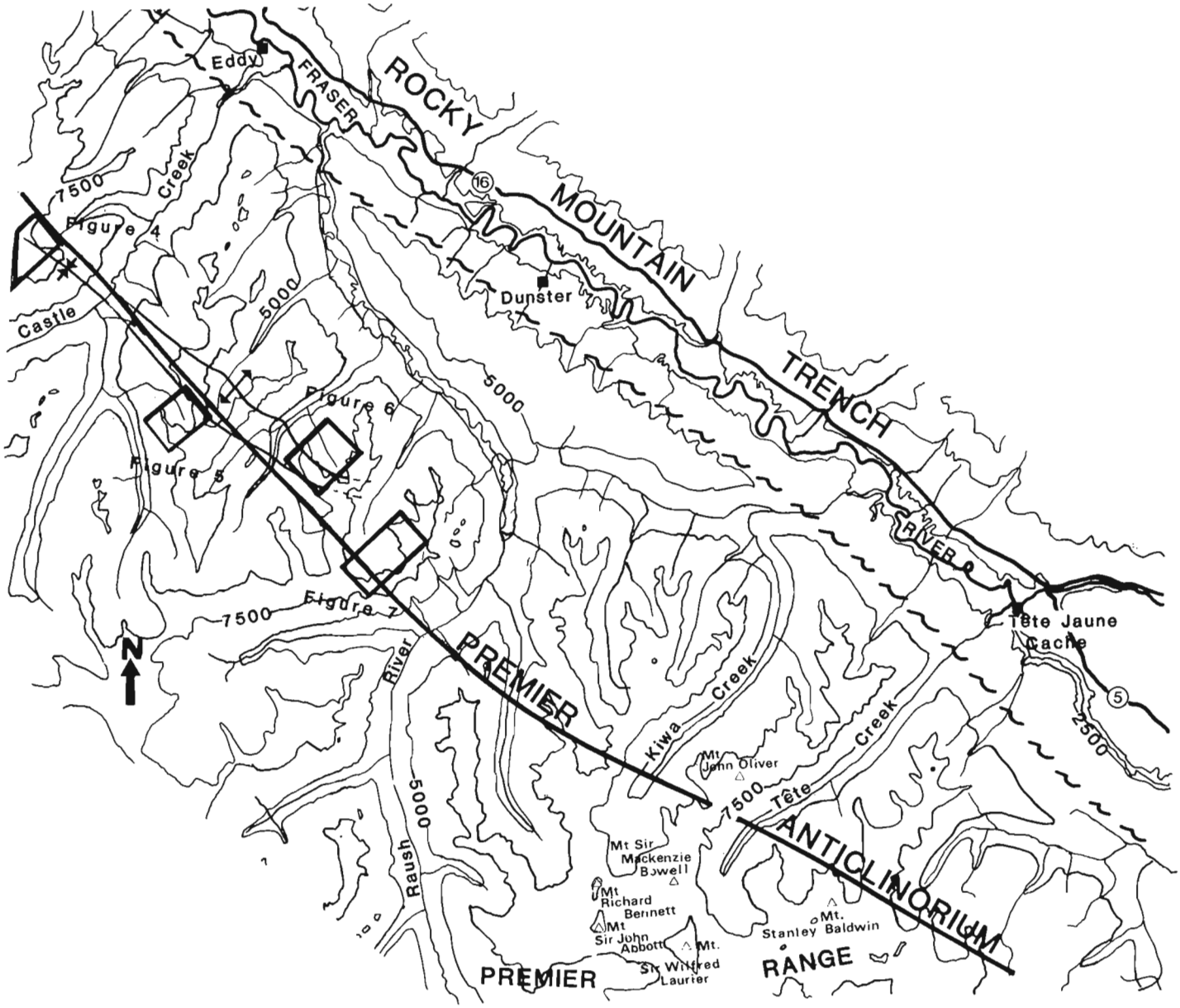

Figure 34.2. *Location map for the Southern Cariboo Mountains between Castle Creek and the Premier Range. Trace of Premier Anticlinorium from Campbell (1968) and Campbell et al. (1973). The locations of Figures 34.4a, 34.5a, 34.6a and 34.7a are shown.*

2. If so, where do the upright folds near Castle Creek fit into that sequence?
3. Is the transition between upright and recumbent folds continuous or interrupted by discontinuities?
4. What is the nature of the Premier Anticlinorium at higher structural levels?

Stratigraphy

The area between Raush River and Castle Creek is underlain by feldspathic, locally calcareous and pebbly metasandstones, shales and rare marbles of the Proterozoic Kaza Group. The position of these rocks in the upper portion of the Kaza Group is confirmed by their stratigraphic transition into shales and marbles of the overlying Proterozoic Isaac Formation (Fig. 34.3). This relationship is well exposed north of Castle Creek (Fig. 34.4a, b).

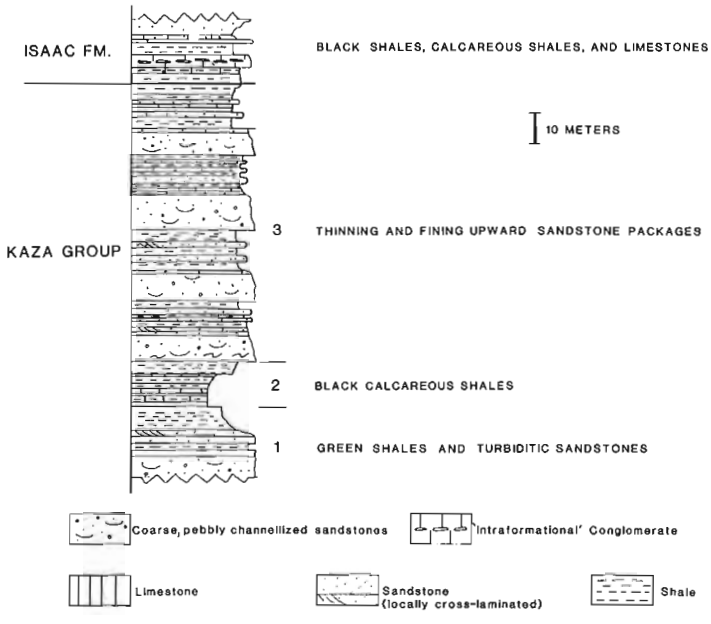

Figure 34.3. *Stratigraphy of the upper Kaza Group.*

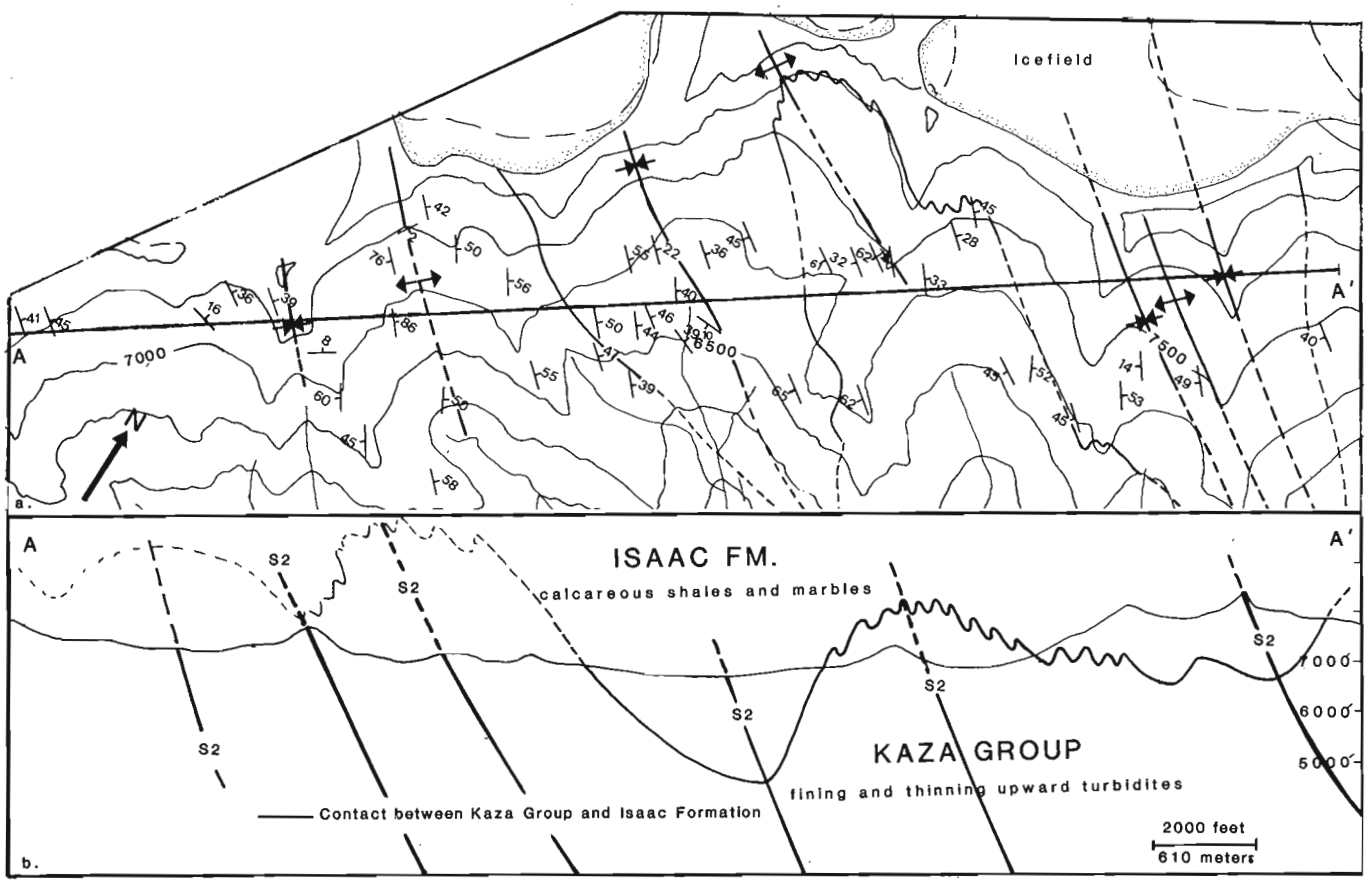

Figure 34.4. *Map (a) and cross-section (b) illustrating folding north of Castle Creek. The change in geometry of the second phase syncline that folds the Kaza-Isaac contact into its lowest structural position is illustrated in Figures 34.5 and 34.6.*

Figure 34.3 is a composite stratigraphic column of the upper portion of the Kaza Group compiled from exposures near Castle Creek. Only the upper portion of the Kaza Group displays sufficient lithologic diversity to permit subdivision into mappable units. Elsewhere, the Kaza Group consists of homogeneously interbedded grey metasandstones and grey to red-grey and green metashales without distinctive marker horizons.

The upper Kaza Group has been subdivided into three mappable units: (1) green sandstones and shales; (2) a 10-15 m-thick black shale; and, (3) thinning and fining upward packages of grey quartzofeldspathic sandstones and shales which are transitional with the shales, marbles and rare sandstones of the basal Isaac Formation.

Unit 1

Distinctive green sandstones and shales are the lowest observed map unit in the upper Kaza Group. The bottom of this unit was not observed. The green colour of these sandstones contrasts sharply with the greyish hues of more typical muscovite-bearing Kaza sandstones of equivalent metamorphic grade and appears to be due to a high percentage of chlorite. The presence of chlorite and ubiquitous coarse pyrite porphyroblasts implies a more mafic bulk composition than other Kaza sandstones.

Sandstones display prominent graded beds and thin contorted or crosslaminated beds arranged in variably complete Bouma cycles. Thin, flaggy, finer grained sandstones with ABCE or ACE Bouma cycles are more common than coarser grained, channellized sandstones.

The bedding characteristics and sedimentary structures described above support the interpretation that these beds are turbidites. The large percentage of thin, finer grained beds with more complete Bouma cycles indicates a setting on outer mid-fan or depositional lobe portions of the fan. The more mafic bulk composition of this portion of the section suggests a contribution from a different source than that of the typical grey quartzofeldspathic, muscovite-bearing sandstones.

Unit 2

The uppermost green sandstones fine and thin upward into a persistent 10-15 m-thick black, graphitic, pyritic, calcareous shale and shaly marble unit. A quiet basinal setting may be inferred for this unit from the persistence and finely laminar character of its bedding. Local varve-like laminations may be interbedded distal turbidites and normal hemipelagic deposits.

Unit 3

Directly overlying this black shale unit are thinning and fining upward packages of greyish, quartzofeldspathic, locally pebbly and calcareous turbidites. Directly above the contact are tan to brown, crumbly-weathering, calcareous sandstones. Within individual coarse grained beds of sandstone a crude layering of calcareous and less calcareous sandstone is disharmonically folded by second phase folds, a characteristic unique to this porton of the Kaza.

The basal calcareous sandstone package fines upward into a 5 m-thick grey-green calcareous shale above which mainly quartzofeldspathic sandstones are found. These are characterized by ABCE, ACE, and occasionally complete Bouma sequences, high sand/shale ratio, and a fine grain size relative to other Kaza turbidites, suggesting an outer mid-fan setting. The top of the Kaza Group is placed at a persistent grey shale separating the thinning and fining upward cycles of the Kaza from the basal Isaac Formation.

Isaac Formation

The Isaac Formation consists of metashale, shaly marble and a thickening upward package of coarse calcareous quartzofeldspathic metasandstone which occur about 10 m above the base of the formation and represent the last influx of turbiditic clastics. The transition from the dominantly turbiditic clastic sequences of the Kaza Group into the metamorphosed shales and limestones of the Isaac Formation is interpreted as the progradation (offlap) of calcareous outer shelf deposits outward over mid-fan portions of the Kaza turbidite fan complex. Although the Isaac Formation was not examined in detail, a shelf setting is inferred from the presence of oolitic clasts in an 'intraformational' conglomerate found about 5 m above the base of the formation, and the increasing percentage of carbonate ahd shale clasts in Kaza sandstones directly underlying the contact with the Isaac Formation. This change in clast composition suggests that the change in environment to the nonturbiditic setting of the Isaac Formation was felt first in the source area for Kaza turbidites, before the actual overlap of Isaac Formation over the Kaza turbidite fan proper. Thus, overlap came from a more proximal or shelf direction. A more radical change in basin dynamics would be necessary for the site of basinal deposition to become the source area of time equivalent, more proximal deposits, just prior to the onlap of the more basinal facies.

Structural Geometry

As in the Premier Range (Murphy and Journeay, 1982), rocks of the Kaza Group and Isaac Formation between Castle Creek and Raush River exhibit structural fabrics indicating polyphase deformation. In this region, however, only one phase of deformation (D2) produced significant regional scale structures resulting in what appears to be a fairly simple structural geometry.

A structural sequence similar to that found in the Premier Range has been found in the Castle Creek-Raush River area. Two phases of northwesterly trending and plunging folds (D1 and D2) developed prior to the metamorphic peak followed by two phases of upright folding, one with a very weak northwest trending axial planar fabric (D3) and the latest (D4) with a stronger northeast trending fabric. Additionally, local pre-D3 low angle shear zones have been observed.

First phase (D1) structures

First phase deformation throughout most of this area is evidenced by a weak foliation (S1) which is inclined to bedding and is folded by later folds. Mesoscopic D1 folds are rare but were observed near section C-C' (Fig. 34.6b). These northwest trending folds are tight, but not isoclinal. It is likely that these folds are the largest scale D1 structures in this area; younging criteria are consistently right-way up between Raush River and Castle Creek, precluding the presence of regional scale folds that would invert the stratigraphy. The asymmetry of macroscopic folds and the orientation of S1 with respect to bedding indicate that D1 folds verge to the east.

Second phase (D2) structures

Second phase folds are the most prominent in the area. They consist of northwest trending, westwardly verging regional scale folds of both bedding and first phase axial surfaces. At low to medium grades of regional metamorphism where S1 is characterized by parallel orientation of coarser grained phyllosilicates, a D2 axial planar foliation (S2) lies in the axial plane of crenulations of S1. At low and very low metamorphic grades, S2 is a

strongly refracting, spaced and curviplanar 'fracture' or solution cleavage. A prominent northwest trending lineation (L2) is the result of intersection of S2 with bedding. Elongation of clasts parallel to L2 indicates that extension has occurred parallel to second phase fold axes. S2 and L2 are overgrown by porphyroblasts (chlorite and white mica at the lowest metamorphic grades; garnet at higher grade). This relationship defines the upper limit of D2 deformation as the peak of regional metamorphism.

Individual axial surface traces of first order, second phase folds have been traced southward in the hope of determining their relationship to recumbent and isoclinal, second phase folds in the Premier Range (Fig. 34.4-34.6). Folds were traced as far south as the line of section C-C' in Figure 34.6b where they were lost in complex interference with first phase structures. These structures changed in geometry from northwest to southeast, which implies continuous transition into the recumbent and isoclinal structures of the Premier Range. This change in geometry involves a change in both orientation of axial surface and fold tightness.

Figures 34.4-34.6 and 34.8 illustrate the change in orientation of second phase axial surfaces from a steeply inclined position near Castle Creek to a more shallowly inclined to recumbent position near the line of section C-C'. Dips of axial planes average 75° close to Castle Creek and decrease to around 45° in the vicinity of section C-C'.

Fold tightness is a difficult characteristic to measure but it may be estimated by the angle between bedding and the axial planar cleavage. Figures 34.8e-h show the average angle between bedding and cleavage on limbs of second phase folds. It may be seen that the angle decreases nonsystematically from left to right in Figure 34.8, or from northwest to southeast.

Due to complex interference of first and second phase folds near the line of section C-C' (Fig. 34.6b), it has not been possible to trace individual folds farther to the southeast. Mapping to the southeast (Fig. 34.7a, b), however, has defined a zone of upright stratigraphy with anomalously low fold density. Mesoscopic first and second phase folds are rare and regional scale folds appear to be totally absent. Bedding is crosscut by two fabrics, an eastwardly verging (foliation dips more steeply to the west than bedding) foliation (S1) and a westwardly verging (axial surfaces of crenulations dip more steeply to the east than bedding) crenulation of S1 (S2). Upright third phase folds that fold S1 and S2 are present in this zone.

This anomalous zone is an apparent discontinuity in the transition from inclined to more recumbent second phase axial surfaces, which has been continuous up to this point. The discontinuity may only be apparent, however, because further decrease in the angle between S2 and bedding does occur in this zone, coinciding with continued overturning of the axial surface to an almost recumbent position.

Third phase (D3) structures

Phase one and two structures are broadly warped around generally upright, northwest trending, phase three, axial surfaces (Fig. 34.3, 34.4, 34.9). However, unlike third phase structures in the Premier Range which are associated with a consistently oriented axial planar crenulation cleavage, third phase structures at the higher structural levels north of Raush River do not have a distinct population of higher order crenulations (Fig. 34.9). Crenulation of S1 and S2 occurs locally but these crenulations neither define a consistently oriented population nor link with lower order third phase folds. Poles to S2 show some spread in their orientations (Fig. 34.8), but cleavage refraction rather than interference with third phase structures accounts for most of

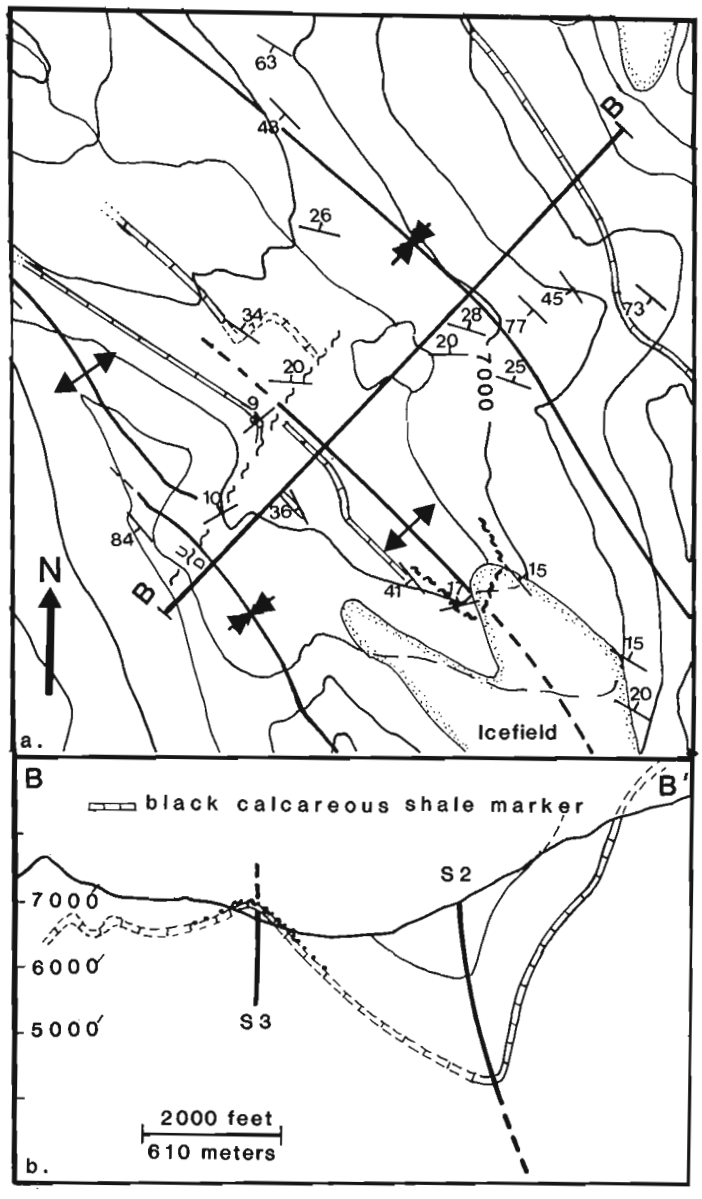

Figure 34.5. Map (a) and cross-section (b) illustrating the folding in an area 6 km southwest of the line of section A-A' (Fig. 34.4). Second phase folds are still steeply inclined.

this spread. Regional and local third phase strain may not have been of sufficient magnitude to produce a strongly oriented mesoscopic fabric.

The Premier Anticlinorium, a large scale, third phase antiform which exposes the lowest structural levels in the Premier Range, loses its identity as a third phase structure north of Raush River, becoming indistinct among large overturned to inclined second phase structures. The trace of the third phase structure intersects the trace of a major second phase anticline which continues to expose the lowest structural levels to the northwest; hence the trace of the anticlinorium may be continued to the northwest as a second phase structure (Fig. 34.2).

Fourth phase structures

Fourth phase structures consist of northeast trending high angle crenulations of first and second phase fabrics (Fig. 34.9). Because of the high angle between the northeast trend of the later structures and the northwest trend of the

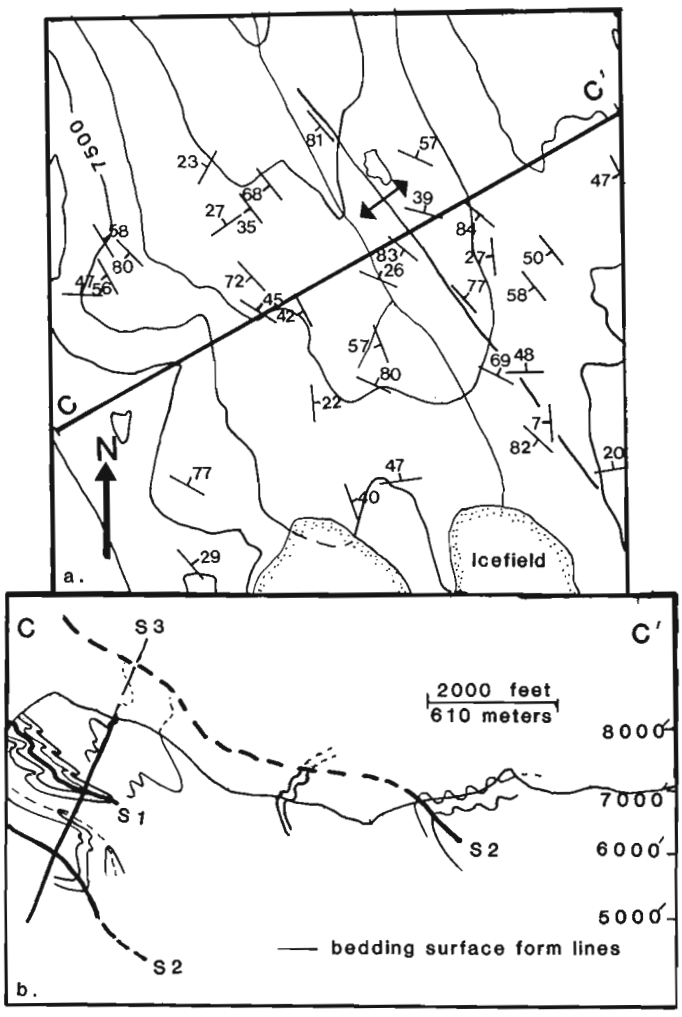

Figure 34.6. *Map (a) and cross-section (b) illustrating folding in an area 10 km southeast of the line of cross-section B-B' (Fig. 34.5). Second phase folds are in a less steeply inclined position. Interference with both first and third phase structures is displayed in the southwestern end of the cross-section.*

early structures, the most notable result of fourth phase deformation is a variation in the magnitude to the northwest plunge of early structures. Although no lower order fourth phase folds have been mapped, the cumulative regional effect of phase four deformation has been to divide the southern Cariboo Mountains into northeast trending domains of similarly plunging first and second phase structures.

Low angle shear zones

A low angle shear zone of unknown significance was observed in the vicinity of Section B-B' in Figure 34.5. The shear zone is warped around a third phase anticline, and is therefore pre-phase three deformation. The geometry of deformation of quartz-calcite veins within the shear zone suggests weatward translation of hanging wall with respect to footwall, and implies kinship with westwardly verging second phase folds. Where observed, the shear zone is localized to a distinct black calcareous shale horizon. As this horizon does not always contain a shear zone, it is likely that the shear zone cuts across stratigraphy. However, the same stratigraphy appears beneath the calcareous marble where sheared as well as where unsheared, which suggests only limited movement.

Discussion

Nature of infrastructure/suprastructure transition

The geometry of first, second, and third phase folds in the Cariboo Mountains undergoes a transition between the Premier Range and Castle Creek. First phase folds, which are isoclinal in the Premier Range, appear to change through tight to open structures based on the presence of an observable angle between bedding and S1. First phase folds decrease in magnitude until macroscopic and possibly mesoscopic folds are absent north of section C-C'. Second phase folds change from tight and isoclinal with subhorizontal to shallowly (<30°) dipping axial planes, to less tight folds with more steeply dipping axial planes in the vicinity of section C-C', and ultimately become steeply (>60°) dipping axial planes north of Castle Creek. Third phase folds appear to die out northwestward from broad warps in the Premier Range into even more diffuse structures with very low structural relief near Castle Creek. In the case of second phase structures, the continuity of this transition is well exposed between the ridge north of Castle Creek southeastward to the line of section C-C'; south of this line, further work is required to prove continuity.

The transition from upright to recumbent structures as suggested for the early folds in the Cariboo Mountains is a common feature in orogenic belts. Isolating the factors that control this transition in the Cariboo Mountains is the subject of work in progress and a few preliminary conclusions have been drawn:

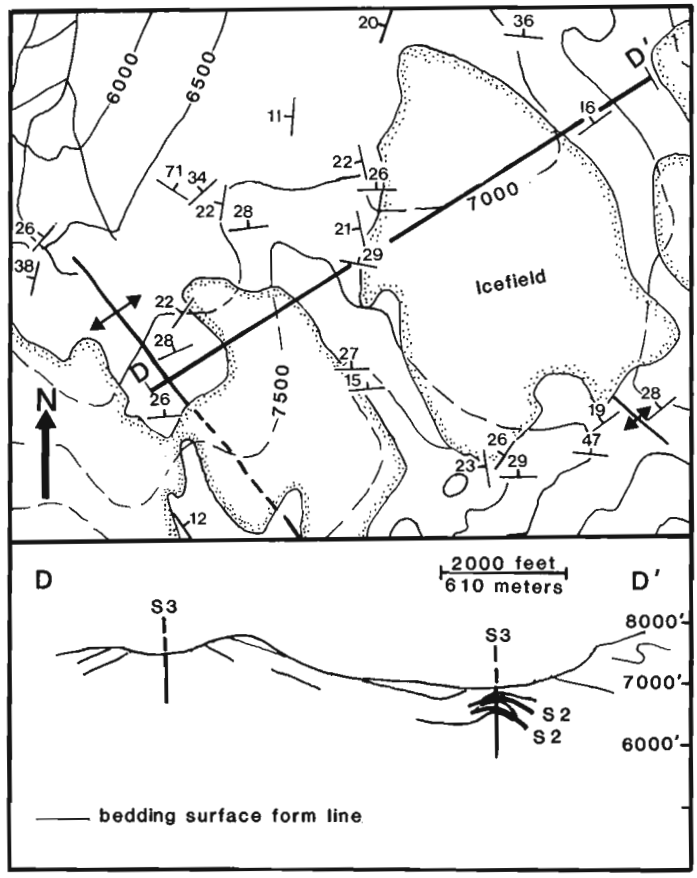

Figure 34.7. *Map (a) and cross-section (b) illustrating the paucity of folds in the zone north of Raush River but south of the line of section C-C'.*

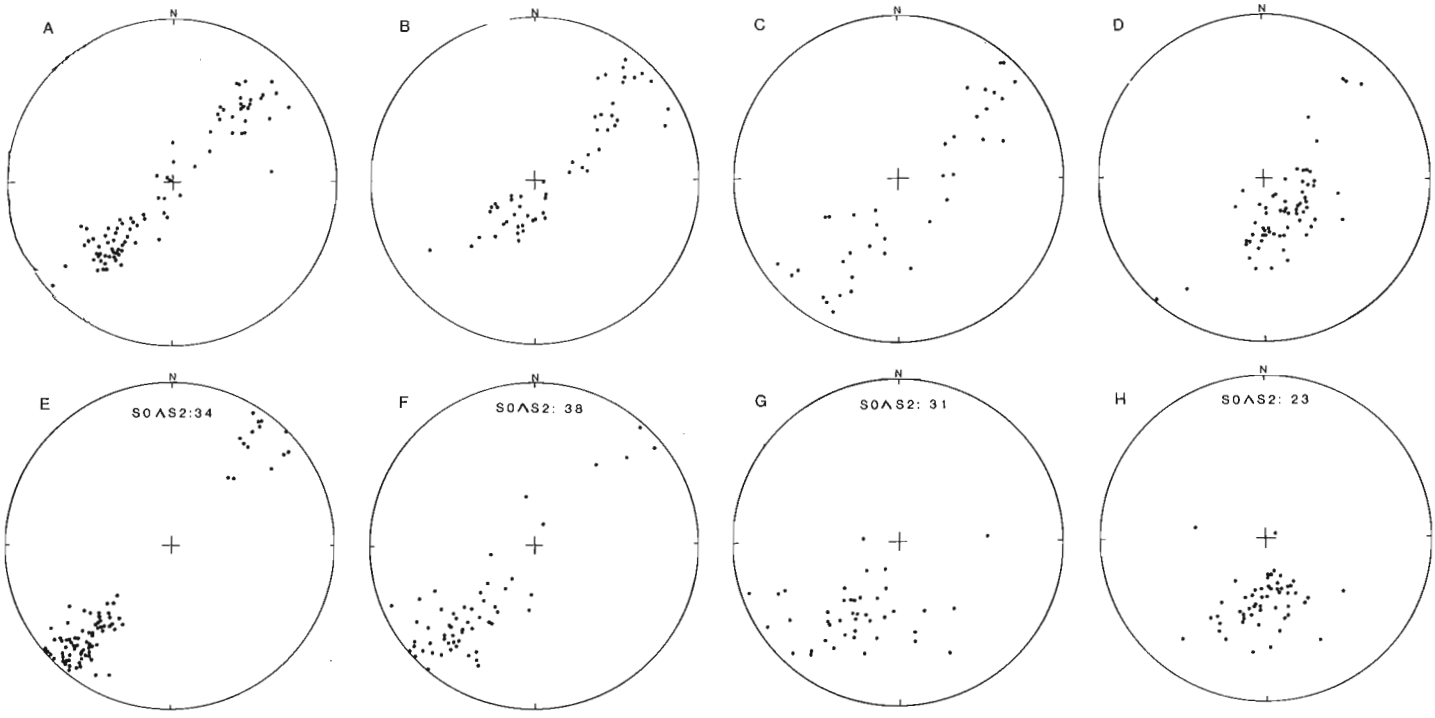

Figure 34.8. *Equal area stereonet compilations of poles to bedding A through D and poles to S2 from four areas (Fig. 34.4-34.7) illustrating the change in orientation and shape of major second phase structures.*

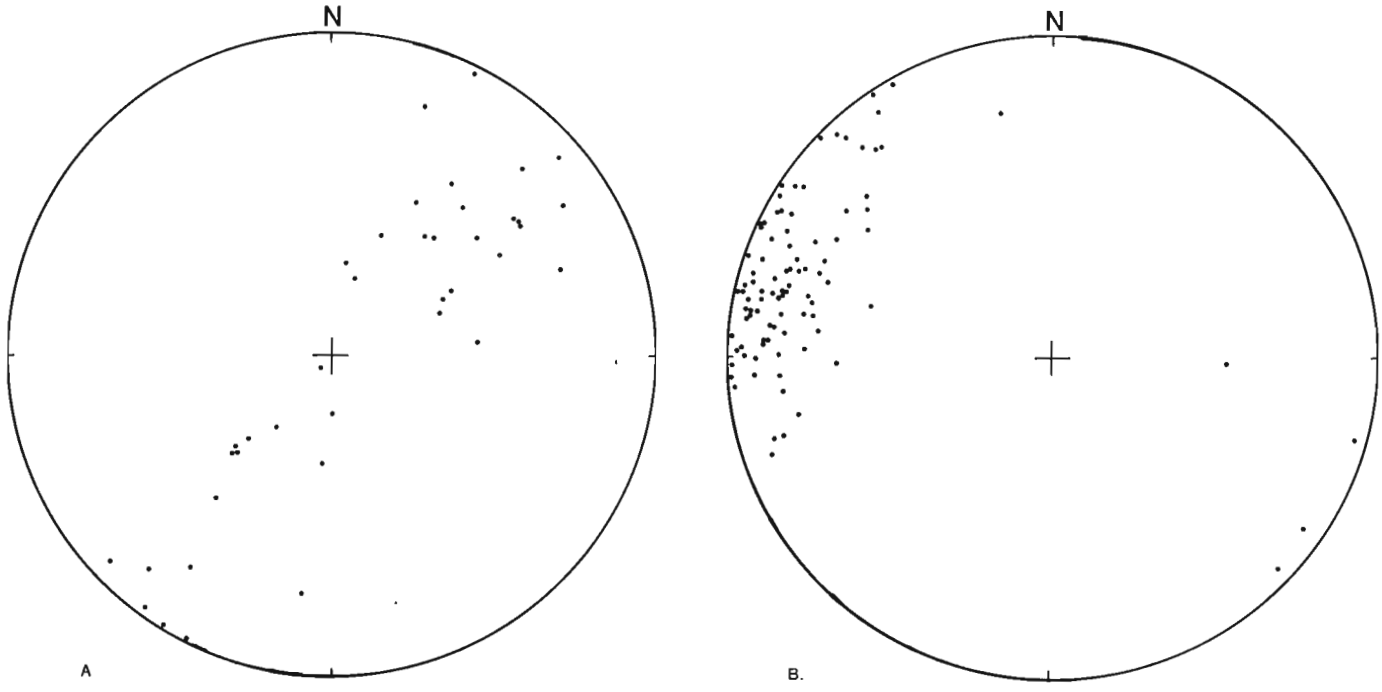

Figure 34.9. *Equal area stereonet plots of poles to S3(a) and poles to S4 from all measurements between Raush River and Castle Creek.*

1. The steepening of axial surfaces probably does not result from interference with younger structures. Third phase folds of second phase axial surfaces at higher structural levels cause flattening of the axial surface rather than steepening (C-C'). Steepening of early axial surfaces by third phase interference occurs in the Premier Range but it is likely that second phase folds were recumbent prior to third phase deformation. Thus, the tendency for third phase folds is to steepen the axial planes of isoclinal folds at deeper structural levels and flatten the axial planes of the more open folds at higher structural levels; refolding has worked against the observed overall transition from recumbent isoclinal folds at deeper structural levels to more upright and open folds at higher structural levels.

2. Gradients in simple shear strain have been known to produce variably oriented folds. Sanderson (1980) correlated decreasing dip of axial plane and interlimb angle with an increase in simple shear strain in a chevron and box folded terrane in the Variscan fold belt of southwest England. Progressive simple shear within ductile shear zones produces recumbent structures at high strains and upright structures at lower strains (Cobbold and Quinquis, 1980).

   However, in the absence of regional marker horizons, it is difficult to estimate the nature and magnitude of the strain accommodated by regional polyphase folding. A model of progressive simple shear may not necessarily be applicable in the Cariboo Mountains; more information about the relationship between oppositely verging first and second phase folds is necessary to better define the state of strain.

3. The correlation of fold geometry with metamorphic grade is only approximate. For example, garnet-zone rocks are isoclinally folded in the Premier Range and more openly folded south of section C-C'. The transition in fold geometry does not appear to occur in the presence of a distinct metamorphic transition. Metamorphism in the Cariboo Mountains outlasted second phase deformation and continuing prograde metamorphism after the termination of second phase deformation may have obliterated a distinct metamorphic of rheological gradient.

4. The presence of low angle shear zones both north and south of Raush River presents the possibility that the main transition between isoclinally and more openly folded rock is not completely continuous, however, the data from the shear zone near section B-B' suggest only small movements have occurred on shear zones, minimizing their role in the overall transition.

Conclusions

1. The stratigraphic transition between the Kaza Group and the overlying Isaac Formation of the Cariboo Group records the offlap of shelf facies (Isaac Formation) onto outer mid-fan turbidites of the Kaza Group.

2. The same sequence of deformation and metamorphism exists in both suprastructural- and infrastructural-level rocks in the Cariboo Mountains: two phases of early (pre-metamorphic peak) folds, followed by two sets of upright, postmetamorphic crenulations with only weakly developed regional scale structures.

3. The geometry of deformation for individual structural phases changes between suprastructural and infra-structural levels. First phase folds at higher structural levels appear to be more open than first phase folds at deeper levels. At the highest structural levels, only a weak foliation remains as evidence of first phase deformation. Second phase folds at high structural levels are more open and upright than second phase folds at deeper levels. Third phase folds vary from broad warps at infrastructural levels to even more diffuse structures without a well developed mesoscopic fabric at higher levels.

4. This transition in fold geometry appears to be continuous, without detachment between infrastructure and suprastructure. However, the significance of low angle shear zones has yet to be fully evaluated.

5. The Premier Anticlinorium may be traced northward out of the Premier Range where it continues to expose the lowest structural levels. It loses its identity as a third phase structure, however, when it intersects the trace of a second phase anticline and continues to the northwest as a second phase structure.

6. First phase folds verge eastwardly and second phase folds verge westwardly.

Acknowledgments

This report was greatly improved through discussions with Richard L. Brown and J. Murray Journeay. The authors' understanding of Cariboo geology continues to be enhanced by the advice of Richard Campbell of the Geological Survey of Canada. Expediting services during the field season were provided by Maryanne Snowden of Cariboo Lodge, a Canadian Mountain Holidays Helicopter Skiing and Hiking operation. I thank Maryanne for providing the service and also Cariboo Lodge Manager, Ernst Buehler, for permitting the use of Cariboo Lodge facilities and staff for this purpose.

References

Berthe, D. and Brun, J.P.
1980: Evolution of folds during progressive shear in South Armaricain Shear Zone, France; Journal of Structural Geology, v. 2, p. 127-133.

Campbell, R.B.
1968: Canoe River, British Columbia; Geological Survey of Canada, Map 15-1967.

1973: Structural cross-section and tectonic model of the Southeastern Canadian Cordillera; Canadian Journal of Earth Sciences, v. 10, p. 1607-1620.

Campbell, R.B., Mountjoy, E.W., and Young, F.G.
1973: Geology of McBridge map area, British Columbia; Geological Survey of Canada, Paper 72-35, 104 p.

Cobbold, P.R. and Quinquis, H.
1980: Development of sheath folds in shear regimes; Journal of Structural Geology, v. 2, no. 1/2, p. 119-126.

Murphy, D.C. and Journeay, M.
1982: Structural style in the Premier Range, Cariboo Mountains, Southern British Columbia: preliminary results; in Current Research, Part A, Geological Survey of Canada, Paper 82-1A, p. 289-292.

Sanderson, D.J.
1980: The transition from upright to recumbent folding in the Variscan fold belt of southwest England: a model based on the kinematics of simple shear; Journal of Structural Geology, v. 1, no. 3, p. 171-180.

35. COMPUTER PROGRAMS TO ESTIMATE WAVE GENERATED ORBITAL VELOCITIES AND THRESHOLD EROSION VELOCITIES

Project 800010

R.A. Pickrill[1] and R.G. Currie
Cordilleran Geology Division, Patrica Bay

Pickrill, R.A. and Currie, R.G., Computer programs to estimate wave generated orbital velocities and threshold erosion velocities; in Current Research, Part A, Geological Survey of Canada, Paper 83-1A, p. 253-261, 1983.

Abstract

Marine geologists are frequently confronted with the problem of estimating the velocity field at the seafloor and assessing the mobility of the surface sediments. Under wind waves, orbital velocities are a product of the water depth, wave height and wave period. The threshold velocity, when sediment begins to move, is a function of grain density, grain size and wave period. Published empirical formulae have been used to write two Fortran programs to calculate orbital and threshold velocities for a range of controlling conditions. From the tables produced by these programs the stability of the surface sediments can be assessed and the wave conditions capable of moving sediment identified.

Introduction

On the continental margins, sediment is transported by currents, which can be considered unidirectional, and by oscillatory orbital flow under waves. In recent years there has been increasing demand for information on the velocity field near the bed and the velocities required to initiate sediment transport. The marine geologist is frequently confronted with the problem of measuring the near-bed currents and from these inferring the environment of deposition and texture of the deposits, or alternatively inferring the processes of sediment transport and deposition from the sediments. Under unidirectional flows, site-specific studies usually have to be carried out to measure near-bed velocities. Once the velocity field is known any one of a number of well established threshold erosion curves (e.g. Sundborg, 1967) can be used to compare the threshold required to initiate sediment transport with measured near-bed velocities and thereby established the probable stability of the deposit.

The measurement of oscillatory orbital velocities under waves is extremely difficult. Until recently, the rapid reversals in flow direction have been faster than the response time of most mechanical current meters. One approach has been to monitor sediment transport directly at the seafloor using sophisticated instrument packages incorporating current meters, wave recorders, underwater television cameras and sediment traps. Unfortunately, most marine geologists do not have access to this sort of equipment. If the wave climate is known, however, empirical wave theory can be used to predict both the orbital velocities under the waves and the threshold erosion velocities required to set sediment in motion. Computation of both orbital and threshold velocities for a range of water depths, wave heights and periods, and grain sizes and densities is a time consuming process unless computers are used.

Komar and Miller (1974) published a computer program that, for a given combination of grain diameter (D) and density (ρ_s), calculated the orbital velocity (U_m) required for threshold at a specific wave period and then printed incremented combinations of wave height (H) and water depth (h) which would give that threshold orbital velocity for sediment motion. While this program has proved extremely useful we found the output restrictive. Their program has been supplemented by the two programs presented here. ORBIT which produces a table of orbital velocities for a specified wave period over a range of wave heights and water depths and THRESH which produces a table of threshold erosion velocities for a specified grain density and grain diameter over a range of wave periods. All possible combinations of threshold and orbital velocities can be compared when these two sets of tables are constructed with parameters appropriate to the wave climate and sediment types of the study area.

Orbital velocities under waves

Orbital velocities (U_m) at the seafloor may be calculated using the Airy linear wave equation*:

$$U_m = \frac{\pi H}{T \sinh(2\pi h/L)} \quad (1)$$

or its extension, Stokes equation to the second order:

$$U_s = U_m + C(3\pi^2 H^2)/4L^2 (\sinh(2\pi h/L))^4 \quad (2)$$

where C is the phase velocity and H, T and L are the wave height, wave period and wavelength and h is the water depth. Stokes equation (2) has been used when:

$$H/L \geq 0.0625 \tanh(2\pi h/L) \quad (3)$$

that is, when the wave height increases, higher order terms must be considered (Komar, 1976, p. 61). The wavelength equation for Airy and Stokes waves has the general form:

$$L = T^2(g/2\pi) \tanh(2\pi h/L) \quad (4)$$

where g is the acceleration of gravity. To simplify the analyses, three depth ranges are specified when calculating the wavelength:

a. Deep water (L_∞): in this case

$h/L \to \infty$, $\tanh(2\pi h/L) \to 1$

so that equation (4) becomes

$$L_\infty = T^2(g/2\pi) \quad (5)$$

and wavelength is independent of water depth.

As water depth decreases, waves begin to 'feel bottom' and wavelengths are shortened. Deep water has been arbitrarily defined by engineers and geologists as depths exceeding approximately half the deep water wavelength ($h/L = 0.5$). Komar (1976, p. 42) pointed out that this limit is much

[1] Present address: New Zealand Oceanographic Institute, P.O. Box 12-346, Wellington, New Zealand.

* All equations from Komar (1976) unless otherwise specified.

too stringent as the error in equation (5) is only 0.37% when h/L = 0.5 and that at h/L = 0.25 (the cut-off used in this study) the error is only 5%, which is acceptable for most applications.

b. Shallow water (L_S): in this case

$h/L \to 0$, $\tanh(2\pi h/L) \to 2\pi h/L$

so that equation (4) yields

$$L_S = T(gh)^{\frac{1}{2}} \quad (6)$$

This relationship is valid to within 5% (Komar, 1976) in depths where h/L is less than 0.05.

c. Intermediate water (L_I): in depth range h/L=0.05 to h/L=0.25, wavelength is best approximated by a relationship derived by Eckart (1955):

$$L_I = L_\infty [\tanh(2\pi h/L_\infty)]^{\frac{1}{2}} \quad (7)$$

Program ORBIT uses equations (1) or (2) and (5) to (7) to calculate orbital velocities. Three input parameters are required to run the program:

1. the range of wave periods (T1, T2) and the incremental period step (DT) in seconds;
2. the range of wave heights (WHM1, WHM2) and the incremental height step (DWHM) in metres; and
3. the range of water depths (WDM1, WDM2) and the incremental depth step (DWDM) in metres.

The program (Appendix 1) produces a series of tables of orbital velocities for each wave period as a function of wave height and water depth. Orbital velocities are calculated for the specified range of wave heights and water depths or until: 1. all orbital velocities at a depth are less than 5 cm s^{-1}; or 2. limiting conditions of wave generation are reached: (a) the wave steepness ratio (H/L) exceeds 0.142 tanh (2πh/L) and the wave becomes unstable and breaks; or (b) the wave height/water depth ratio (H/h) exceeds 0.78 and the wave crest collapses and breaks. Regions where these limiting conditions are exceeded are indicated by a zero velocity in the output.

Shallow water regions where neither Airy sinusoidal nor Stokes trochoidal waves are reasonable approximations are flagged by a negative velocity. This indicates that a wave can exist with the specified parameters of wave length, period, wave height and water depth but that it cannot be accurately described by the equations used in program ORBIT. The cut off chosen:

$$HL^2/h^3 \leq 32\pi^2/3 \quad (8)$$

is that given by Komar (1976, p. 62). Solitary or cnoidal wave theory should be applied in this area.

In the example (Appendix 1) a wave period of 6 seconds is specified, wave heights are increased in 0.5 m increments to 10 m while water depth is incremented by 1 m. Tabulation stops at a depth of 46 m where velocities are below 5 cm s^{-1}. At wave heights greater than 7.5 m maximum wave steepness is exceeded, while at shallow depths (<6 m) wave breaking stops the tabulation. Reasonable velocities cannot be calculated for a wave height of 0.5 m in 1 m of water or a wave height of 1.5 m in 2 m of water.

Threshold of sediment motion

Under waves, sediment entrainment occurs at the bed when orbital velocities exceed the threshold velocity of sediment motion. From a synthesis of experimental data, Komar and Miller (1973, 1974) have shown the boundary layer at the threshold is laminar for size fractions equal to or finer than medium sand (0.5 mm) and turbulent for coarser fractions. The threshold for laminar flow can best be represented by:

$$\phi_t = \frac{\rho U_m^2}{(\rho_s - \rho)gD} = 0.21 (d_o/D)^{\frac{1}{2}} \quad (9)$$

where U_m is the near-bed orbital velocity (equation 1) and d_o is the near-bed orbital diameter of the wave motion, ρ is the density of water, and ρ_s and D are respectively the density and diameter of the sediment grains.

For coarser sediments (>0.5 mm) the near bottom flow is turbulent and the threshold velocities is best represented by the equation:

$$\phi_t = \frac{\rho U_m^2}{(\rho_s - \rho)gD} = 0.463 \pi (d_o/D)^{\frac{1}{4}} \quad (10)$$

Since $d_o = U_m T/\pi$ equations (9) and (10) can be solved for threshold velocity. These velocities are calculated by program THRESH for a specified grain density for a range of grain sizes and wave periods. The input parameters required to run the program are:

1. the grain density in g cm^{-3} (DEN);
2. the range of wave periods (T1, T2) and the incremental period step (DT) in seconds;
3. the number of grain diameters being entered (NSIZES); and
4. the grain diameter in millimetres (GS).

A listing of program THRESH and a sample of the output are included in Appendix 2. A grain density of 2.65 g cm^{-3} has been used. Threshold velocities are tabulated for a wave period range of 3 to 20 seconds in 1 second increments and grain sizes (in mm) chosen in 0.5 phi increments in the sand to granule range (4 to -2 phi) and 2 phi increments for coarse gravels.

Using the orbital velocity tables it is a simple procedure to define the velocity field near the bed for a known wave climate in any depth of water, while the threshold tables show velocities required to initiate sediment transport. By comparing the velocities in these two sets of tables, estimates can be made of the stability of a sediment at the seafloor and the velocities and wave conditions required to move the sediment.

Acknowledgments

Research for this paper was carried out when one of the authors (R.A.P.) held a NSERC Visiting Fellowship. The manuscript was improved by comments from J. Luternauer and R.E. Thomson.

References

Eckart, C.
1952: The propagation of waves from deep to shallow water; in Gravity Waves, National Bureau of Standards Circular no. 521, p. 165-73.

Komar, P.D.
1976: Beach Processes and Sedimentation; Prentice-Hall, Englewood, New Jersey, 429 p.

Komar, P.D. and Miller, M.C.
1973: The threshold of sediment movement under oscillatory water waves; Journal of Sedimentary Petrology, v. 43, p. 1101-1110.

1974: On the comparison between the threshold of sediment motion under waves and unidirectional currents with a discussion of the practical evaluation of the threshold, Journal of Sedimentary Petrology, v. 45, p. 362-367.

Sundborg, A.
1967: Some aspects on fluvial sediments and fluvial morphology; Geografiska Annaler, v. 49A, p. 333-343.

Appendix 1

```
@FTN,CS THRESH.D
FTN 8R1  *10/20/82-13:53(4,)
      1.    C
      2.    C******************  PROGRAM ORBIT ********************************
      3.    C
      4.    C            PROGRAM TO CALCULATE ORBITAL  VELOCITY UNDER WAVE
      5.    C             AS A FUNCTION OF WAVE HEIGHT AND WATER DEPTH
      6.    C
      7.    C
      8.    C               VARIABLES USED
      9.    C
     10.    C         UM     ORBITAL VELOCITY        CM/SEC
     11.    C         WHM    WAVE HEIGHT             METRES
     12.    C         WH     WAVE HEIGHT             CM
     13.    C         WDM    WATER DEPTH             METRES
     14.    C         WD     WATER DEPTH             CM
     15.    C         GRAV   GRAVITATIONAL CONSTANT CM/SEC2
     16.    C         T      WAVE PERIOD             SECONDS
     17.    C
     18.    C
     19.    C*************************************************************************
     20.    C
     21.           DIMENSION UM(20),PWH(20),PWD(500),WH(20),WD(500)
     22.    C
     23.           GRAV=981.0
     24.           PI=3.14159
     25.           PI2=2.0*PI
     26.           AFLAG=-0.1
     27.    C
     28.    5      WRITE(6,100)
     29.    100    FORMAT(1H1,'INPUT WAVE PERIOD (SEC) START,STOP AND INCREMENT')
     30.    C
     31.    C       INPUT WAVE PERIODS (SEC) START,STOP AND INCREMENT
     32.    C
     33.           READ(5,*,END=999) T1,T2,DT
     34.           T=T1
     35.    C
     36.           WRITE(6,101)
     37.    101    FORMAT(5X,' INPUT WAVE HT (M) START,STOP AND INCREMENT')
     38.    C
     39.    C       INPUT WAVE HEIGHTS IN METRES AND CONVERT TO CM
     40.    C
     41.           READ(5,*,END=999)WHM1,WHM2,DWHM
     42.           WH1=WHM1*100.0
     43.           WH2=WHM2*100.0
     44.           DWH=DWHM*100.0
     45.    C
     46.           PWH(1)=WHM1
     47.           JLIM=1
     48.           WH(1)=WH1
     49.           WRITE(6,102)
     50.    102    FORMAT(5X,' INPUT WATER DEPTH (M) START,STOP AND INCREMENT')
     51.    C
     52.    C       INPUT WATER DEPTHS IN METRES AND CONVERT TO CM
     53.    C
     54.           READ(5,*,END=999)WDM1,WDM2,DWDM
     55.           WD1=WDM1*100.0
     56.           WD2=WDM2*100.0
     57.           DWD=DWDM*100.0
     58.    C
     59.           NDEPTH=INT((WD2-WD1)/DWD) + 1
     60.           WD(1)=WD1
     61.           PWD(1)=WDM1
     62.    C
     63.           DO 10 I=2,NDEPTH
  1  64.           WD(I)=WD(I-1) + DWD
  1  65.    10     PWD(I)=WD(I)*0.01
  1  66.    C
     67.    12     CONTINUE
     68.    C
```

Appendix 1 (cont.)

```
      69.    C       CALCULATE THE DEEP WATER WAVELENGTH  (WLD)
      70.    C
      71.           WLD=156.13*T*T
      72.    C
      73.    C       CALCULATE WAVE HEIGHTS (ACROSS PAGE)
      74.    C
      75.    15     CONTINUE
      76.           PWH(1)=PWH(JLIM)
      77.           WH(1)=WH(JLIM)
      78.           DO 16 J=2,20
1     79.           WH(J)=WH(J-1)+DWH
1     80.           PWH(J)=WH(J)*0.01
1     81.           IF(WH(J).GE.WH2) GO TO 17
1     82.    16     CONTINUE
      83.           J=20
      84.    17     JLIM=J
      85.    C
      86.           WRITE(6,103) T
      87.    103    FORMAT(1H1,' WAVE GENERATED ORBITAL VELOCITIES (CM/SEC) ',
      88.          $1X,'FOR WAVE PERIOD OF',F5.1,' SECONDS ',/)
      89.           WRITE(6,104)(PWH(J),J=1,JLIM)
      90.    104    FORMAT(1X,'WAVE HT  M',20F6.1,/)
      91.           WRITE(6,105)
      92.    105    FORMAT(1X,'DEPTH  M')
      93.    C
      94.    C       LOOP FOR MULTIPLE WATER DEPTHS
      95.    C
      96.           IREC=1
      97.           DO 80 I=1,NDEPTH
1     98.           IF(WD(I).EQ.0.0) GO TO 80
1     99.           IF(MOD(IREC,50).NE.0) GO TO 20
1    100.           WRITE(6,103) T
1    101.           WRITE(6,104)(PWH(J),J=1,JLIM)
1    102.           WRITE(6,105)
1    103.    20     CONTINUE
1    104.    C
1    105.    C       CALCULATE SHALLOW WATER WAVELENGTH (WLS)
1    106.    C
1    107.           WLS=T*SQRT(GRAV*WD(I))
1    108.    C
1    109.    C       CALCULATE WAVELENGTH FOR INTERMEDIATE WATER DEPTH  (WLM)
1    110.    C
1    111.           WLM=WLD*SQRT(TANH(PI2*WD(I)/WLD))
1    112.    C
1    113.    C       TEST TO SELECT APPROPRIATE WAVELENGTH EQUATION
1    114.    C
1    115.           TEST=WD(I)/WLD
1    116.           IF(TEST.GT.0.25) WL=WLD
1    117.           IF(TEST.LE.0.25.AND.TEST.GE.0.05) WL=WLM
1    118.           IF(TEST.LT.0.05) WL=WLS
1    119.    C
1    120.    C       INCREMENT WAVE HEIGHTS
1    121.    C
1    122.           TOT=0
1    123.           DO 72 J=1,JLIM
1    124.    C
2    125.           IF(WH(J).EQ.0.0) GO TO 70
2    126.    C
2    127.    C       WAVE BREAKING TEST
2    128.    C
2    129.           BREAK=WH(J)/WD(I)
2    130.           IF(BREAK.GE.0.78) GO TO 70
2    131.    C
2    132.    C       OVERSTEEP TEST
2    133.    C
2    134.           STEEP=WH(J)/WL
2    135.           ATEST=TANH(PI2*WD(I)/WL)
2    136.           OSTEST=0.142*ATEST
2    137.           IF(STEEP.GE.OSTEST) GO TO 70
2    138.    C
```

Appendix 1 (cont.)

```
2       139.    C       CALCULATE ORBITAL VELOCITY
2       140.    C
2       141.            UM(J)=PI*WH(J)/(T*SINH(PI2*WD(I)/WL))
2       142.    C
2       143.    C            CHECK TO SEE IF STOKES WAVE EQUATION SHOULD BE APPLIED
2       144.    C
2       145.            SKTEST=0.0625*ATEST
2       146.            IF(STEEP.GE.SKTEST) THEN
3       147.              COR=0.75*PI*P1*WH(J)*WH(J)
3       148.              B=SINH(PI2*WD(I)/WL)
3       149.              COR=COR/(B*B*B*B*WL*WL)
3       150.              C=(GRAV*T/PI2)*(TANH(PI2*WD(I)/WL))
3       151.              UM(J)=UM(J)+C*COR
3       152.            ELSE
3       153.            ENDIF
2       154.    70      TOT=TOT+UM(J)
2       155.    C
2       156.    C         URSELL TEST : CHECK APPLICABILITY OF LINEAR OR STOKES THEORY
2       157.    C
2       158.            URSELL=WH(J)*WL*WL/(WD(I)*WD(I)*WD(I))
2       159.            IF(URSELL.GE.105.3) UM(J)=AFLAG
2       160.            IF(BREAK.GE.0.78) UM(J)=0.0
2       161.            IF(STEEP.GE.OSTEST) UM(J)=0.0
2       162.    72      CONTINUE
1       163.            IF(TOT.LE.0.00001) GO TO 78
1       164.    C
1       165.    C       OUTPUT
1       166.    C
1       167.            WRITE(6,106)PWD(I),(UM(J),J=1,JLIM)
1       168.            IREC=IREC+1
1       169.    106     FORMAT(1X,F9.2,1X,20F6.1)
1       170.    C
1       171.    C       SEE IF ALL VELOCITIES < 5.0 CM/SEC IF SO, FINISHED
1       172.    C
1       173.            IFLAG=0
1       174.            DO 75 J=1,JLIM
2       175.    75      IF(UM(J).GT.5.0.OR.UM(J).EQ.AFLAG) IFLAG=1
2       176.    C
2       177.    C       NULL ARRAY
2       178.    C
1       179.    78      CONTINUE
1       180.            DO 76 J=1,JLIM
2       181.    76      UM(J)=0.0
2       182.    C
1       183.            IF(TOT.LE.0.00001) GO TO 80
1       184.            IF(IFLAG.LT.1) GO TO 90
1       185.    C
1       186.    80      CONTINUE
1       187.    C
1       188.    C       MORE WAVE HEIGHTS ??
1       189.    C
        190.    90      IF(WH(JLIM).LT.WH2) GO TO 15
        191.    C
        192.    C       MORE PERIODS ?
        193.    C
        194.            T=T+DT
        195.            IF(T.GT.T2) GO TO 999
        196.    C
        197.    C       RESET WAVE HEIGHTS TO CALCULATE FOR NEXT PERIOD
        198.    C
        199.            JLIM=1
        200.            WH(1)=WH1
        201.            PWH(1)=WHM1
        202.    C
        203.    C
        204.            GO TO 12
        205.    C
        206.    C       FINISHED
        207.    C
        208.    999     WRITE(6,200)
        209.    200     FORMAT(1H1,' END OF JOB ')
        210.            STOP
        211.            END
```

Appendix 1 (cont.)

WAVE GENERATED ORBITAL VELOCITIES (CM/SEC) FOR WAVE PERIOD OF 6.0 SECONDS

WAVE HT M	.5	1.0	1.5	2.0	2.5	3.0	3.5	4.0	4.5	5.0	5.5	6.0	6.5	7.0	7.5	8.0	8.5	9.0	9.5	10.0
DEPTH M																				
1.00	-.1	.0	.0	.0	.0	.0	.0	.0	.0	.0	.0	.0	.0	.0	.0	.0	.0	.0	.0	.0
2.00	53.4	181.3	-.1	.0	.0	.0	.0	.0	.0	.0	.0	.0	.0	.0	.0	.0	.0	.0	.0	.0
3.00	41.9	83.8	178.9	262.2	.0	.0	.0	.0	.0	.0	.0	.0	.0	.0	.0	.0	.0	.0	.0	.0
4.00	35.1	70.1	127.9	180.6	238.3	301.1	.0	.0	.0	.0	.0	.0	.0	.0	.0	.0	.0	.0	.0	.0
5.00	30.2	60.3	90.5	140.7	182.1	226.0	272.4	.0	.0	.0	.0	.0	.0	.0	.0	.0	.0	.0	.0	.0
6.00	26.4	52.7	79.1	116.3	148.8	182.6	217.8	254.3	.0	.0	.0	.0	.0	.0	.0	.0	.0	.0	.0	.0
7.00	23.3	46.5	69.8	93.0	126.1	153.6	181.9	211.1	241.0	.0	.0	.0	.0	.0	.0	.0	.0	.0	.0	.0
8.00	20.6	41.3	61.9	82.6	109.1	132.3	156.0	180.1	204.8	229.9	.0	.0	.0	.0	.0	.0	.0	.0	.0	.0
9.00	18.4	36.8	55.2	73.6	92.0	115.6	135.9	156.4	177.3	198.4	219.8	.0	.0	.0	.0	.0	.0	.0	.0	.0
10.00	16.4	32.9	49.3	65.8	82.2	101.9	119.5	137.3	155.3	173.5	191.8	210.3	.0	.0	.0	.0	.0	.0	.0	.0
11.00	14.7	29.4	44.2	58.9	73.6	90.4	105.9	121.4	137.1	152.9	168.8	184.9	.0	.0	.0	.0	.0	.0	.0	.0
12.00	13.2	26.4	39.6	52.8	66.0	80.5	94.1	107.9	121.7	135.6	149.5	163.6	177.7	.0	.0	.0	.0	.0	.0	.0
13.00	11.8	23.7	35.5	47.3	59.2	71.0	84.0	96.1	108.4	120.6	133.0	145.3	157.7	.0	.0	.0	.0	.0	.0	.0
14.00	10.6	21.2	31.8	42.4	53.1	63.7	75.0	85.8	96.7	107.6	118.5	129.5	140.5	151.5	.0	.0	.0	.0	.0	.0
15.00	10.1	20.3	30.4	40.6	50.7	60.9	71.6	81.9	92.2	102.6	113.0	123.4	133.8	144.3	.0	.0	.0	.0	.0	.0
16.00	9.0	18.0	27.0	36.0	45.0	54.0	63.4	72.5	81.6	90.8	99.9	109.1	118.3	127.5	136.7	.0	.0	.0	.0	.0
17.00	8.0	16.0	24.0	32.0	40.0	48.0	56.3	64.4	72.4	80.5	88.6	96.8	104.9	113.0	121.1	.0	.0	.0	.0	.0
18.00	7.1	14.3	21.4	28.5	35.6	42.8	50.0	57.2	64.4	71.6	78.8	86.0	93.2	100.4	107.6	.0	.0	.0	.0	.0
19.00	6.4	12.7	19.1	25.4	31.8	38.1	44.5	50.9	57.3	63.7	70.1	76.5	82.9	89.3	95.7	.0	.0	.0	.0	.0
20.00	5.7	11.3	17.0	22.7	28.3	34.0	39.7	45.4	51.1	56.7	62.4	68.1	73.8	79.5	85.2	.0	.0	.0	.0	.0
21.00	5.1	10.1	15.2	20.2	25.3	30.3	35.4	40.5	45.5	50.6	55.7	60.7	65.8	70.9	75.9	.0	.0	.0	.0	.0
22.00	4.5	9.0	13.5	18.0	22.5	27.1	31.6	36.1	40.6	45.1	49.7	54.2	58.7	63.2	67.7	.0	.0	.0	.0	.0
23.00	4.0	8.1	12.1	16.1	20.1	24.2	28.2	32.2	36.3	40.3	44.3	48.4	52.4	56.4	60.5	.0	.0	.0	.0	.0
24.00	3.6	7.2	10.8	14.4	18.0	21.6	25.2	28.8	32.4	36.0	39.6	43.2	46.8	50.4	54.0	.0	.0	.0	.0	.0
25.00	3.2	6.4	9.6	12.9	16.1	19.3	22.5	25.7	28.9	32.1	35.4	38.6	41.8	45.0	48.2	.0	.0	.0	.0	.0
26.00	2.9	5.7	8.6	11.5	14.4	17.2	20.1	23.0	25.8	28.7	31.6	34.5	37.3	40.2	43.1	.0	.0	.0	.0	.0
27.00	2.6	5.1	7.7	10.3	12.8	15.4	18.0	20.5	23.1	25.7	28.2	30.8	33.4	35.9	38.5	.0	.0	.0	.0	.0
28.00	2.3	4.6	6.9	9.2	11.5	13.8	16.1	18.3	20.6	22.9	25.2	27.5	29.8	32.1	34.4	.0	.0	.0	.0	.0
29.00	2.1	4.1	6.2	8.2	10.3	12.3	14.4	16.4	18.5	20.5	22.6	24.6	26.7	28.7	30.8	.0	.0	.0	.0	.0
30.00	1.8	3.7	5.5	7.3	9.2	11.0	12.8	14.7	16.5	18.3	20.2	22.0	23.8	25.7	27.5	.0	.0	.0	.0	.0
31.00	1.6	3.3	4.9	6.6	8.2	9.8	11.5	13.1	14.7	16.4	18.0	19.7	21.3	22.9	24.6	.0	.0	.0	.0	.0
32.00	1.5	2.9	4.4	5.9	7.3	8.8	10.3	11.7	13.2	14.6	16.1	17.6	19.0	20.5	22.0	.0	.0	.0	.0	.0
33.00	1.3	2.6	3.9	5.2	6.5	7.9	9.2	10.5	11.8	13.1	14.4	15.7	17.0	18.3	19.6	.0	.0	.0	.0	.0
34.00	1.2	2.3	3.5	4.7	5.9	7.0	8.2	9.4	10.5	11.7	12.9	14.1	15.2	16.4	17.6	.0	.0	.0	.0	.0
35.00	1.0	2.1	3.1	4.2	5.2	6.3	7.3	8.4	9.4	10.5	11.5	12.6	13.6	14.7	15.7	.0	.0	.0	.0	.0
36.00	.9	1.9	2.8	3.7	4.7	5.6	6.6	7.5	8.4	9.4	10.3	11.2	12.2	13.1	14.0	.0	.0	.0	.0	.0
37.00	.8	1.7	2.5	3.3	4.2	5.0	5.9	6.7	7.5	8.4	9.2	10.0	10.9	11.7	12.6	.0	.0	.0	.0	.0
38.00	.7	1.5	2.2	3.0	3.7	4.5	5.2	6.0	6.7	7.5	8.2	9.0	9.7	10.5	11.2	.0	.0	.0	.0	.0
39.00	.7	1.3	2.0	2.7	3.3	4.0	4.7	5.4	6.0	6.7	7.4	8.0	8.7	9.4	10.0	.0	.0	.0	.0	.0
40.00	.6	1.2	1.8	2.4	3.0	3.6	4.2	4.8	5.4	6.0	6.6	7.2	7.8	8.4	9.0	.0	.0	.0	.0	.0
41.00	.5	1.1	1.6	2.1	2.7	3.2	3.7	4.3	4.8	5.4	5.9	6.4	7.0	7.5	8.0	.0	.0	.0	.0	.0
42.00	.5	1.0	1.4	1.9	2.4	2.9	3.4	3.8	4.3	4.8	5.3	5.7	6.2	6.7	7.2	.0	.0	.0	.0	.0
43.00	.4	.9	1.3	1.7	2.1	2.6	3.0	3.4	3.9	4.3	4.7	5.1	5.6	6.0	6.4	.0	.0	.0	.0	.0
44.00	.4	.8	1.1	1.5	1.9	2.3	2.7	3.1	3.4	3.8	4.2	4.6	5.0	5.4	5.7	.0	.0	.0	.0	.0
45.00	.3	.7	1.0	1.4	1.7	2.1	2.4	2.7	3.1	3.4	3.8	4.1	4.4	4.8	5.1	.0	.0	.0	.0	.0
46.00	.3	.6	.9	1.2	1.5	1.8	2.1	2.4	2.8	3.1	3.4	3.7	4.0	4.3	4.6	.0	.0	.0	.0	.0

```
)FTN,CS THRESH.T
=TN 8R1  *09/16/82-11:53(22,)
      1.    C
      2.    C************************PROGRAM THRESH*********************************
      3.    C
      4.    C         TO CALCULATE THRESHOLD VELOCITIES FOR A GRAIN
      5.    C         OF SPECIFIED DENSITY AS A FUNCTION OF WAVE PERIOD
      6.    C         AND GRAIN SIZES (DIAMETERS)
      7.    C
      8.    C                     VARIABLES USED
      9.    C      UM     CRITICAL EROSIONAL VELOCITY    CM/SEC
     10.    C      GRAV   GRAVITATIONAL CONSTANT         CM/SEC2
     11.    C      RHOW   DENSITY OF FLUID               G/CM3
     12.    C      DEN    DENSITY OF GRAIN               G/CM3
     13.    C      T      WAVE PERIOD                    SECONDS
     14.    C      GS     GRAIN DIAMETER                 MILLIMETRES
     15.    C
     16.    C*************************************************************************
     17.    C
     18.    C
     19.    C
     20.          DIMENSION UM(19),PHI(100),PERIOD(19),GS(100)
     21.    C
     22.          PI=3.141593
     23.          CON=1.0/ALOG(2.0)
     24.          RHOW=1.03
     25.          GRAV=981.0
     26.    C
     27.    C      INPUT GRAIN DENSITY (G/CM3)
     28.    C
     29.          WRITE(6,100)
     30.    100   FORMAT(1H1,'  INPUT GRAIN DENSITY (G/CM3) ')
     31.          READ(5,*,END=999) DEN
     32.    C
     33.    C      INPUT WAVE PERIOD (SEC) START,END AND INCREMENT
     34.    C
     35.          WRITE(6,101)
     36.    101   FORMAT(1X,' INPUT START PERIOD,END AND INCREMENT (SEC)_')
     37.          READ(5,*,END=999) T1,T2,DT
     38.    C
     39.          JLIM=1
     40.          PERIOD(1)=T1
     41.    C
     42.          WRITE(6,108)
     43.    108   FORMAT(1X,' INPUT NUMBER OF SIZES TO BE EVALUATED')
     44.          WRITE(6,109)
     45.    109   FORMAT(1X,' THEN ENTER GRAIN DIAMETER (MM) ONE PER CARD')
     46.    C
     47.    C      INPUT NUMBER OF SIZES TO BE EVALUATED
     48.    C
     49.          READ(5,*,END=999) NSIZES
     50.          IF(NSIZES.LE.100) GO TO 14
     51.          WRITE(6,106) NSIZES
     52.    106   FORMAT(10X,' SPECIFIED MORE THAN 100 SIZES ',I4)
     53.          GO TO 999
     54.    14    CONTINUE
     55.    C
     56.    C      INPUT GRAIN DIAMETER (MM)  AND CONVERT TO PHI
     57.    C
     58.          DO 15 I=1,NSIZES
  1  59.          READ(5,*,END=999)GS(I)
  1  60.    15    PHI(I)=-ALOG(GS(I))*CON
  1  61.    C
     62.    5     WRITE(6,102)DEN
     63.    102   FORMAT(1H1,' THRESHOLD EROSIONAL VELOCITIES (CM/SEC) FOR',
     64.         $1X,'GRAIN DENSITY OF',F5.2,' G/CM3',/)
     65.          PERIOD(1)=PERIOD(JLIM)
     66.          DO 10 I=2,19
  1  67.          PERIOD(I)=PERIOD(I-1)+DT
  1  68.          IF(PERIOD(I).GE.T2) GO TO 11
```

Appendix 2 (cont.)

```
1        69.    10     CONTINUE
         70.           I=19
         71.    11     JLIM=I
         72.           WRITE(6,103)(PERIOD(I),I=1,JLIM)
         73.    103    FORMAT(1X,' PERIOD  (SEC)',F5.1,18F6.1/)
         74.           WRITE(6,107)
         75.    107    FORMAT(1X,'DIAMETER  PHI')
         76.           WRITE(6,110)
         77.    110    FORMAT(3X,'(MM)')
         78.    C
         79.    C       DO IN LOOPS OF 19 FOR PAGE WIDTH AND 50 FOR PAGE LENGTH
         80.    C
         81.           DO 80 I=1,NSIZES
1        82.           IF((MOD(I,50)).NE.0) GO TO 19
1        83.           WRITE(6,102) DEN
1        84.           WRITE(6,103)(PERIOD(K),K=1,JLIM)
1        85.           WRITE(6,107)
1        86.           WRITE(6,110)
1        87.    C
1        88.    C       USE EQUATION APPROPRIATE TO GRAIN SIZE I.E. < OR > 0.5 MM
1        89.    C
1        90.    19     IF(GS(I).LT.0.5) GO TO 50
1        91.           A=0.463*PI
1        92.           B=0.25
1        93.           GO TO 70
1        94.    50     A=0.21
1        95.           B=0.50
1        96.    70     PWR=1.0/(2.0-B)
1        97.    C
1        98.    C       CONVERT GRAIN DIAMETER TO CM TO MAINTAIN UNITS
1        99.    C
1       100.           GSCM=GS(I)/10.0
1       101.           FAC=(A*(DEN-RHOW)*GRAV/(RHOW*PI**B))**PWR
1       102.           FAC1=FAC*GSCM**((1.0-B)*PWR)
1       103.    C
1       104.    C       CALC THRESHOLD VELOCITIES FOR THE RANGE OF PERIODS SPECIFIED
1       105.    C
1       106.           DO 90 J=1,JLIM
2       107.    90     UM(J)=FAC1*PERIOD(J)**(B*PWR)
2       108.    C
1       109.           WRITE(6,104)GS(I),PHI(I),(UM(J),J=1,JLIM)
1       110.    104    FORMAT(1X,F8.4,F5.1,19F6.1)
1       111.    80     CONTINUE
1       112.    C
        113.           IF(PERIOD(JLIM).GE.T2) GO TO 999
        114.           GO TO 5
        115.    C
        116.    C       END OF JOB
        117.    C
        118.    999    WRITE(6,200)
        119.    200    FORMAT(1H1,' END OF JOB ')
        120.           STOP
        121.           END
```

Appendix 2 (cont.)

THRESHOLD EROSIONAL VELOCITIES (CM/SEC) FOR GRAIN DENSITY OF 2.65 G/CM3

PERIOD (SEC)		3.0	4.0	5.0	6.0	7.0	8.0	9.0	10.0	11.0	12.0	13.0	14.0	15.0	16.0	17.0	18.0	19.0	20.0
DIAMETER (MM)	PHI																		
.0625	4.0	8.6	9.4	10.1	10.8	11.3	11.9	12.3	12.8	13.2	13.6	14.0	14.3	14.6	15.0	15.3	15.5	15.8	16.1
.0883	3.5	9.6	10.6	11.4	12.1	12.7	13.3	13.8	14.3	14.8	15.2	15.7	16.0	16.4	16.8	17.1	17.4	17.8	18.1
.1250	3.0	10.8	11.9	12.8	13.6	14.3	15.0	15.5	16.1	16.6	17.1	17.6	18.0	18.4	18.8	19.2	19.6	19.9	20.3
.1768	2.5	12.1	13.3	14.3	15.2	16.1	16.8	17.5	18.1	18.7	19.2	19.7	20.2	20.7	21.1	21.6	22.0	22.4	22.8
.2500	2.0	13.6	15.0	16.1	17.1	18.0	18.8	19.6	20.3	20.9	21.6	22.1	22.7	23.2	23.7	24.2	24.7	25.1	25.6
.3536	1.5	15.2	16.8	18.1	19.2	20.2	21.1	22.0	22.8	23.5	24.2	24.9	25.5	26.1	26.6	27.2	27.7	28.2	28.7
.5000	1.0	22.6	23.6	24.3	25.0	25.5	26.0	26.5	26.9	27.2	27.6	27.9	28.2	28.5	28.7	29.0	29.2	29.4	29.7
.7071	.5	26.2	27.3	28.2	29.0	29.6	30.2	30.7	31.2	31.6	32.0	32.4	32.7	33.0	33.3	33.6	33.9	34.2	34.4
1.0000	.0	30.4	31.7	32.7	33.6	34.4	35.0	35.6	36.2	36.7	37.1	37.5	37.9	38.3	38.7	39.0	39.3	39.6	39.9
1.4142	-.5	35.3	36.8	38.0	39.0	39.9	40.6	41.3	41.9	42.5	43.1	43.5	44.0	44.4	44.9	45.2	45.6	46.0	46.3
2.0000	-1.0	41.0	42.7	44.1	45.2	46.2	47.1	47.9	48.7	49.3	49.9	50.5	51.1	51.6	52.0	52.5	52.9	53.3	53.7
2.8300	-1.5	47.5	49.5	51.1	52.5	53.7	54.7	55.6	56.5	57.2	58.0	58.6	59.2	59.8	60.4	60.9	61.4	61.9	62.3
4.0000	-2.0	55.1	57.5	59.3	60.9	62.2	63.4	64.5	65.5	66.4	67.2	68.0	68.7	69.4	70.0	70.7	71.2	71.8	72.3
16.0000	-4.0	99.9	104.1	107.5	110.3	112.7	114.9	116.9	118.6	120.3	121.8	123.2	124.5	125.7	126.9	128.0	129.0	130.0	131.0
64.0000	-6.0	180.9	188.5	194.6	199.8	204.2	208.2	211.7	214.9	217.8	220.6	223.1	225.5	227.7	229.8	231.8	233.7	235.5	237.3
256.0000	-8.0	327.8	341.5	352.6	361.9	369.9	377.1	383.5	389.3	394.6	399.6	404.2	408.5	412.5	416.3	419.9	423.4	426.7	429.8

36. # RECONNAISSANCE MAPPING OF THE SOUTHERN CAPE BRETON HIGHLANDS – A PRELIMINARY REPORT

R.A. Jamieson [1] and D. Craw [1]
Atlantic Geoscience Centre, Dartmouth

Jamieson, R.A. and Craw, D., Reconnaissance mapping of the southern Cape Breton Highlands – a preliminary report; in Current Research, Part A, Geological Survey of Canada, Paper 83-1A, p. 263-268, 1983.

Abstract

A preliminary 1:250 000 map of the Cape Breton Highlands has been compiled on the basis of new field work in the southern Highlands and re-evaluation of existing maps. The main features include a metavolcanic-metasedimentary complex extending along the western Highlands, which is gradational into a gneiss complex, a major Precambrian intrusive diorite complex, and a belt of Acadian intrusions in the central Highlands. The ages of many units are unknown but some new dates and new evidence concerning relative ages are presented.

Introduction

The Cape Breton Highlands occupy a central position in the Canadian Appalachian belt, but the geology of the Highlands is poorly known. Even the most recent geological compilations show much of the area as undifferentiated gneiss (e.g. Keppie, 1979). Detailed mapping in 1979-1982 in the Crowdis Mountain – Middle River area (Jamieson, 1981; Jamieson and Doucet, 1983) and in the Cheticamp River area in 1982 by D. Craw, combined with reconnaissance work along the extensive Nova Scotia Forest Industries road network in 1980-1982 form the basis for a 1:50 000 compilation of the geology of the southern Cape Breton Highlands now in preparation. On the basis of this work and brief examination of other sections in the Highlands, recent studies by MacNabb et al. (1976), Macdonald and Smith (1980), Barr and Macdonald (1982), and Blanchard (1982), and existing compilations (Keppie, 1979), a preliminary 1:250 000 map of the Cape Breton Highlands has been compiled (Fig. 36.1). This map shows the distribution of the main units of the southern Highlands, and tentative correlations of these units with others to the north and east. Absolute and even relative ages of many units are unknown, but on the basis of field work and available Rb-Sr data, it is now possible to make some generalizations. The purpose of this paper is to summarize our results, to comment on their regional significance, and to point out problems for which more data are required.

Acknowledgments

The authors gratefully acknowledge the financial support of the Geological Survey of Canada through EMR Research Agreements awarded to RAJ in 1980-1982. DC was supported in part by a Killam Post-Doctoral Fellowship and a Research Development grant from Dalhousie University. The co-operation of Nova Scotia Forest Industries in providing access to their private road network is greatly appreciated. L. More, D. Conrod, and K. Craw provided invaluable field assistance, and we have benefited greatly from discussions with G.C. Milligan, S. Barr, A.S. Macdonald, K.L. Currie, and many others.

Late Precambrian Rocks

Several suites of supracrustal rocks and their metamorphic equivalents can be distinguished for which a late Precambrian age seems likely, although absolute ages are unknown. These units may be chronological equivalents and may correlate with gneissic rocks outside the study area. These rocks are intruded by ultrabasic to granitic rocks of various ages.

George River Group Metasedimentary Rocks

This unit, defined in south-central Cape Breton as a sequence of quartzites, marbles, schists and minor metavolcanic rocks (e.g. Milligan, 1970), can be traced in a belt running down the eastern side of the Highlands from Wreck Cove to Christopher McLeod Brook. Since this corresponds approximately to the eastern limit of the area investigated by the authors, the distribution of George River rocks shown in Figure 36.1 is taken mainly from Milligan (1970) and Keppie (1979). Within the study area, the main rock type is strongly foliated white to buff metaquartzite associated with pelitic and calcareous schists. In Figure 36.1, many areas shown on existing maps as George River Group have been reassigned to other units on the basis of our recent work. This reflects a long-standing problem with terminology in the Cape Breton Highlands, where it has been customary to equate all metasedimentary schists and gneisses with the George River Group whether or not a basis for correlation exists. In our opinion, local names should be used until equivalence among these units is demonstrated.

Unnamed Meta-Igneous and Metasedimentary Complex (Unit 2)

In the study area, meta-igneous and metasedimentary rocks underlie the Crowdis Mountain – Gold Brook area (Jamieson and Doucet, 1983) and the Rocky Brook – Cheticamp River area. The rock types include pelitic, semi-pelitic, and minor psammitic phyllites and schists, prominent in the Cheticamp River and Gold Brook areas, metabasite (locally intrusive) in the Campbell Brook, Cheticamp River, and Middle River areas, and rhyolite and felsic tuffs in the Crowdis Mountain and Rocky Brook areas. The rocks have undergone polyphase deformation and metamorphism, characterized by the growth of biotite, chloritoid, garnet, hornblende, staurolite, and kyanite porphyroblasts over an early phyllitic foliation. With increasing metamorphic grade and structural complexity, the rocks pass into the paragneisses and amphibolites of unit 3. The transition appears to be structurally telescoped but gradational in well exposed sections along Cheticamp River and Middle River. Local mineralization has been exploited on a small scale in the Dauphinee Brook and Gold Brook areas (Milligan, 1970; Chatterjee, 1982). Similar lithologies with similar structural and metamorphic histories are observed in the Cape North area (Money Point Group of Macdonald and Smith, 1980), the Jumping Brook – Trout Brook area (Currie, 1975, and pers. comm., 1982, although a definite structural break between schists and gneisses has been reported there), and the Mabou Highlands (Barr and Macdonald, pers. comm., 1982); these rocks are included with unit 2 on Figure 36.1.

[1] Department of Geology, Dalhousie University, Halifax, Nova Scotia, B3H 3J5.

LEGEND

UNKNOWN AGE

13. Miscellaneous granitic to dioritic rocks.

CARBONIFEROUS

12. Undifferentiated younger sedimentary rocks, including Windsor Group.
11. Horton Group and its Lower Mississippian equivalents.

DEVONIAN – CARBONIFEROUS

10. Undeformed granitic rocks, locally associated with gabbro and diorite.
9. Fisset Brook Formation and its equivalents.

LOWER PALEOZOIC (CAMBRIAN – SILURIAN)

8. Unfoliated granitic rocks.

LATE PRECAMBRIAN

7. Foliated granitic rocks.
6. Variable deformed dioritic and gabbroic rocks, including minor ultramafic rocks.
5. Anorthosite.
4. Undivided gneisses, possibly equivalent to or older than unit 3.
3. Gneiss complex, high grade equivalent of unit 2.

   3a – paragneiss

   3b – orthogneiss
2. Unnamed meta-igneous and meta-sedimentary complex.
1. George River Group metasedimentary rocks.

Figure 36.1. *Geology of the Cape Breton Highlands modified after Keppie (1979). Heavy lines represent fault boundaries. Study area is outlined. Geology in the study area is after Jamieson and Doucet (this volume), Jamieson (unpublished data), Craw (in prep.), Blanchard (1982), and Barr and Macdonald (1982). Dates are new data obtained by Jamieson at Memorial University. Boundaries outside the study area are simplified after Keppie (1979) but some units have been reassigned on the basis of new work.*

Gneiss Complex, High Grade Equivalent of Unit 2 (Unit 3)

Much of the central Cape Breton Highlands is occupied by a complex of paragneiss, amphibolite, and granodioritic orthogneiss. In the study area, it is exposed in the eastern Cheticamp River – Leblanc Brook area, along woods roads south of Cape Breton Highlands National Park, and in the area north of Middle River. The most widespread lithology is a biotite-rich paragneiss, locally containing garnet, kyanite, and rare sillimanite, and cut by variably deformed pegmatites. Garnet amphibolite is locally common. The paragneisses are locally intruded by granodioritic orthogneiss north of Campbell's Lake. This unit is almost certainly continuous with the Pleasant Bay gneiss complex to the north (Currie, 1975, and pers. comm. 1982). It probably correlates with orthogneisses common in the Neil's Harbour area, and may be equivalent to some or all of the undivided gneisses discussed below.

Undivided Gneisses, Equivalent to or Older than Unit 3 (Unit 4)

Gneissic rocks not investigated in detail by the authors or described in other recent published reports have been grouped together as a single undivided unit. Many of these rocks may be equivalent to unit 3, but an interesting exception is the Kelly's Mountain gneiss complex located northeast of Baddeck. This complex has given a metamorphic age of 701 ± 66 Ma by Rb-Sr (Olszewski et al., 1981) and is characterized by a low pressure metamorphic assemblage that contrasts markedly with the medium-pressure assemblages of the central Highlands (Jamieson, 1982). Kelly' Mountain has been interpreted as "basement" by Keppie (1979), but given the ambiguity inherent in this term and the lack of clearly exposed contact relationships, it has been included with the undivided gneisses in this paper.

Anorthosite (Unit 5)

Anorthosite pods and fault-bounded slivers occurring north of the Grande Anse River have been described by several authors (e.g. Jenness, 1966; Macdonald and Smith, 1979; Mitchell, 1979). The anorthosite is generally highly brecciated and altered, and in one locality is associated with granulite facies rocks. It does not occur in the southern Highlands and its regional significance, if any, remains obscure.

Variable Deformed Dioritic and Gabbroic Rocks (Unit 6)

Small diorite and gabbro plutons, and larger gabbro-diorite-tonalite complexes, are common in the Cape Breton Highlands. In the study area, a variable deformed mafic-intermediate complex, referred to informally as the Beddeck Lakes complex (Jamieson and Doucet, 1983), intrudes quartzite along its eastern margin and is faulted against metavolcanic rocks in the southwest. A preliminary Rb-Sr whole rock date of 750 ± 65 Ma represents the probable age of intrusion (Jamieson, unpublished data); further work is in progress to improve this result. The complex ranges from hornblende to tonalite and granodiorite in composition, with diorite dominating. The relationship between the diorite and the gneisses of unit 3 is unclear. Locally, zones of amphibolite within the gneisses resemble the more deformed varieties of the diorite. The relationship of the Baddeck Lakes diorite complex to other major diorite plutons, notably that west of Ingonish, has not been investigated, but they are shown as equivalent on Figure 36.1.

Foliated Granitic Rocks (Unit 7)

In the central Highlands, deformed granitic rocks, including syenogranite with K-feldspar augen, medium grained leucogranite, and foliated aplite, are common. Similar rocks also occur as small lenses within the gneiss terranes. The degree of deformation can be highly variable; the rocks range from mylonitic along the southern extension of the Aspy Fault to essentially undeformed. Local preservation of igneous textures and lack of compositional layering suggest that these rocks are younger than the orthogneisses of unit 3. Hadrynian granitic rocks shown by Keppie (1979) have been included with this unit in Figure 36.1. It is probable that some of the "gneisses" of unit 4 are actually younger deformed granitic intrusions.

Lower Paleozoic (Cambrian – Silurian) Rocks

Cambrian to Silurian stratified rocks do not appear to be present in the Cape Breton Highlands, in contrast to southeastern Cape Breton. Some rocks of unknown age, particularly the metavolcanics and metasediments of unit 2, may be lower Paleozoic rather than Precambrian (e.g. K.L. Currie, pers. comm.). This would be consistent with the recent recognition of high grade lower Paleozoic rocks in southwestern Newfoundland (e.g. Chorlton, 1980). Unfortunately, neither the age of deposition nor the age of metamorphism has been determined for this sequence. Lower Paleozoic granitic plutons occur in several localities.

Unfoliated Granitic Rocks (Unit 8)

Unfoliated Cambrian granitic rocks have been reported from the Kelly's Mountain, St. Ann's, and Cheticamp areas (Cormier, 1972; Barr et al., 1979; Keppie, 1979). An undeformed syenogranite that intrudes the Kelly's Mountain gneiss complex has been dated at 553 ± 25 Ma (Cormier, 1972). The Cheticamp pluton, which outcrops in a narrow belt from Corney Brook to the Northeast Margaree River (Fig. 36.1), is an undeformed monzogranite that is muscovite-bearing in the south (Barr and Macdonald, 1982). A Rb-Sr date of 530 ± 44 Ma reported by Cormier (1972) for this pluton now appears to have been based on several unrelated samples and should be disregarded (Barr, pers. comm., 1982). Although its age is unknown, the Cheticamp pluton must be pre-late Devonian, since it is unconformably overlain by the Fisset Brook Formation (unit 9; see below), and a lower Paleozoic, rather than Precambrian, age is suggested by its lack of foliation. East of the study area, the Cape Smokey pluton has been dated at 447 ± 37 Ma (Cormier, 1972).

Devonian – Carboniferous

Devonian to lower Carboniferous rocks in the Cape Breton Highlands include both the uppermost Devonian Fisset Brook Formation and its equivalents, and Devonian and Carboniferous plutonic rocks. These rocks are generally undeformed except along local faults and shear zones. As more radiometric dates become available, it appears that "Acadian" and younger plutonic rocks are more widespread in the Highlands than previously recognized.

Fisset Brook Formation and its Equivalents (Unit 9)

The Fisset Brook Formation, defined by Mackasey (1963), consists of upper Devonian mafic and felsic volcanic rocks and associated redbeds that extend in two narrow belts from the Cheticamp River to the Northeast Margaree River (Fig. 36.1). The western section has yielded latest Devonian to earliest Carboniferous spores and has been dated at 376 ± 12 Ma (Cormier and Kelley, 1964). The eastern section contains well preserved Upper Devonian plant fossils (Archaeopteris **sp. cf. jacksonii**; Forbes, pers. comm., 1982). Bimodal volcanic rocks in the Lake Ainslie area to the south (Creed, 1968) and the Lowland Cove area to the north (Smith and Macdonald, 1981) have also been included with the Fisset Brook Formation. A small volcanic complex at

MacMillan Mountain, dated at 384 ± 10 Ma (Jamieson and Doucet, 1983) and a single basalt flow within lower Carboniferous conglomerates on the North Baddeck River (More, 1982) are possible equivalents. Volcanic rocks in the St. Ann's, Mabou, and Creignish Hills have also been correlated with the Fisset Brook Formation (Keppie, 1979), but little work has been done in these areas. The volcanic rocks appear to be somewhat diachronous, with differences in lithological, geochemical, and petrological characteristics from place to place (Blanchard, 1982). The bimodal volcanism is generally interpreted as related to the rifting that immediately preceded Carboniferous molasse sedimentation in Cape Breton (e.g. Blanchard, 1982).

Undeformed Granitic Rocks, Locally Associated with Gabbro and Diorite (Unit 10)

Two Devonian ages have recently been obtained for plutons previously thought to be late Precambrian (Jamieson, unpublished data). These are the early Devonian West Branch North River pluton (401 ± 13 Ma) that occupies the central part of the study area (Jamieson and Doucet, 1983), and the late Devonian Margaree granite (365 ± 46 Ma) that extends from Northeast Margaree River to Aspy River (Currie, 1975, and pers. comm., 1982). The West Branch North River pluton is a hornblende-biotite monzogranite with rare aplite, which is locally weakly foliated and is cut by mylonite near its eastern margin. The Margaree pluton is generally a megacrystic hornblende-biotite monzogranite, locally with rapakivi texture, which is totally undeformed except where cut by faults near the upper reaches of the Northeast Margaree River. In the southern part of the study area, a diorite-microgranite complex separates the older metavolcanic rocks of the Crowdis Mountain area from the younger MacMillan Mountain volcanics (Jamieson and Doucet, 1983). Its age is unknown, but it clearly intrudes the older metavolcanics and it may be subvolcanic to the MacMillan Mountain rocks. The presence of hybrid textures, abundant intrusion breccia, and local mutually intrusive contacts suggest that the mafic and felsic rocks were closely associated in space and time.

Along the Cheticamp River, two medium grained leucogranite plutons informally termed the Salmon Pool granite (Currie, pers. comm., 1982) cut the metavolcanic-metasedimentary complex. The granite intrudes but is spatially associated with an undeformed fine- to medium-grained melagabbro. Currie (1973, and pers. comm., 1982) shows this granite cutting the Margaree pluton in the upper reaches of the Margaree River, which implies a latest Devonian to Carboniferous age.

Outside the study area, a Devonian granite occurs at White Point in the northeastern Highlands (403 ± 22 Ma; Barr et al., 1979; Keppie, 1979) and a Carboniferous date has been obtained from a pluton near Cape North (Keppie, 1979; Macdonald and Smith, 1980). Many of these granites lie along a radiometric anomaly reported by Chatterjee (1982) which probably reflects a concentration of "Acadian" intrusions.

Carboniferous

Carboniferous sedimentary rocks flank the Cape Breton Highlands on all sides. These rocks have been studied locally where they contain gypsum deposits or coal horizons, although in many areas their stratigraphy and structure are poorly known. No attempt has been made to map these rocks in detail, and Figure 36.1 shows only the distribution of Lower Mississippian and younger Carboniferous sediments as given by Keppie (1979).

Horton Group and its Lower Mississippian Equivalents (Unit 11)

Lower Mississippian conglomerate, arkose, micaceous fine sandstones, and shales of the Horton Group and its equivalents flank most of the Cape Breton Highlands (Fig. 36.1). Contacts with older rocks are commonly steep faults or, more rarely, thrusts (Currie, 1977). Locally, these rocks unconformably overlie the older rocks, and they may conformably overlie or be interbedded with Fisset Brook lithologies in some places (Mackasey, 1963). The sediments vary greatly in lithological and stratigraphic characteristics from place to place, and range from essentially flat lying in the southern part of the study area to strongly deformed along the western side of the Highlands near Cheticamp.

Undifferentiated Younger Sedimentary Rocks, Including the Windsor Group (Unit 12)

Post-Horton Carboniferous sedimentary rocks including Grantmire, Windsor, Mabou, and Riversdale lithologies outcrops around the Cape Breton Highlands. These sedimentary rocks have not been separated in Figure 36.1; the reader is referred to Keppie (1979) for a recent compilation.

Unknown Age

Miscellaneous Granitic to Dioritic Rocks (Unit 13)

Various plutonic rocks of unknown age, ranging from diorite to granite and syenite, are noted on current maps of Nova Scotia (Keppie, 1979). Within the study area, they have been included with the late Precambrian, lower Paleozoic, or Devonian-Carboniferous groups on the basis of our work. Outside the study area no attempt has been made to reassign these rocks to any particular unit.

Structure, Metamorphism, and Plutonism

Most of the crystalline rocks of the southern Cape Breton Highlands have undergone deformation and metamorphism, ranging from polyphase folding and high grade metamorphism in the gneiss complexes, to late faulting and associated retrograde effects evident along the western Highland front. Several distinct episodes of diorite and granite intrusion have also been documented. A detailed discussion is beyond the scope of this paper, but a few general points can be made based on the detailed work we have done in the Middle River and Cheticamp areas.

1. Metamorphic grade and structural complexity increase from west to east in the Cheticamp area, south to north in the Middle River area, and east to west in the Wreck Cove and Cape North areas. This appears to be a structurally telescoped gradational increase.
2. The predominant north-south to northeast-southwest structural trend evident on all maps of the Cape Breton Highlands is a long-lived, fundamental tectonic feature. It is reflected in foliation trends, patterns of faulting, shear zones, elongation of plutonic complexes, and the Devonian volcanic belts. This trend is at a high angle to the mainly east-west trends of nearby southern Newfoundland and mainland Nova Scotia.
3. Intrusive activity from late Precambrian to Carboniferous times was concentrated east of the Aspy Fault. Only one major lower Paleozoic granite (the Cheticamp pluton), a few smaller plutons of unknown age, and some orthogneiss occur on the western side of the Highlands. Pre-Devonian intrusive rocks are largely lacking in the central Highlands, whereas "Acadian" intrusive activity was concentrated in the eastern and central Highlands.

4. Faulting is common and complex throughout the Highlands. The Aspy Fault is a major structure that extends from Cape North to the Margaree Valley. Mylonites, higher-level cataclasites, and pseudotachylite along this fault zone suggest that it was a long-lived structure, active possibly from late Precambrian and certainly into lower Carboniferous times. Elsewhere, major steep faults bound most of the eastern and western Highlands. Moderately to steeply dipping reverse faults are locally important, but shallow thrust faulting does not appear to be of regional significance (cf. Currie, 1977). An east-west trending fault shown along the Cheticamp River valley on recent maps of Nova Scotia (e.g. Keppie, 1979) does not exist. Late shear zones are important in the southern Highlands near Middle River (Jamieson and Doucet, 1983), where they may account for the swing of the foliation from north-south to east-west.

Discussion

This work, as yet at a reconnaissance level, raises many questions about the tectonic evolution of northwestern Cape Breton and its setting within the Canadian Appalachians. For example, what is the age of the metavolcanic-metasedimentary complex of the western Highlands, and what is its relationship to the George River Group and other Avalonian rocks? There is some evidence from a few scattered outcrops that "George River" lithologies occur within the gneisses of the central Highlands. If so, since the metavolcanic and metasedimentary rocks also grade into the gneiss complex, determination of the structure of the gneisses and their age of metamorphism becomes very important. The 750 Ma Baddeck Lakes diorite complex intrudes the George River Group and appears to have been deformed with the gneisses along its eastern margin. Since the age of this diorite is remarkably similar to that of the Burin Group tholeiitic intrusive and volcanic rocks of southeastern Newfoundland (Strong et al., 1978; and D.F. Strong, pers. comm., 1982), further detailed study of the eastern Highlands diorites is of local and regional importance. The concentration of high grade metamorphic and intrusive rocks in the eastern and central Highlands, with lower grade rocks in the west and south, requires some explanation. The presence or absence of "basement" rocks in the Cape Breton Highlands remains a contentious problem. We have seen no evidence for pre-existing crystalline basement in the study area, but large parts of the central Highlands have not been mapped in detail. The very complex structural relationships between the crystalline rocks and the Carboniferous sediments along the western margin of the Highlands need to be studied in detail from both a structural and stratigraphic point of view, since they have important implications for the evolution of the Magdalen basin and the history of the "Maritime Disturbance" in northern Nova Scotia.

These and other interesting problems are a long way from being solved; we are now just finding out what questions to ask. This paper has pointed out the need for further study, particularly detailed mapping geochronological work in selected areas.

References

Barr, S.M. and Macdonald, A.S.
1982: Geology, petrology, and mineralization of the Cheticamp pluton, northwestern Cape Breton Island, Nova Scotia; GAC-MAC Program with Abstracts, v. 7, p. 38.

Barr, S.M., O'Reilly, G.A., and O'Beirne, A.M.
1979: Geochemistry of granitoid plutons of Cape Breton Island; in Nova Scotia Department of Mines and Energy, Report 79-1, p. 109-141.

Blanchard, M.C.
1982: Geochemistry and petrogenesis of the Fisset Brook Formation, western Cape Breton Island, Nova Scotia, unpublished M.Sc. thesis, Dalhousie University, 225 p.

Chatterjee, A.K.
1982: Precambrian metallotects and metallogenic evolution in Cape Breton Island. Abstract, Nato Advanced Study Institute, "Regional Trends in the Geology of the Appalachian – Hercynian – Caledonian – Mauritanide Oogen", Fredericton, N.B.

Chorlton, L.B.
1980: Geology of the LaPoile River area (110/16), Newfoundland, Newfoundland Department of Mines and Energy, Report 80-3, 86 p.

Cormier, R.F.
1972: Radiometric ages of granitic rocks, Cape Breton Island, Nova Scotia; Canadian Journal of Earth Sciences, v. 9, p. 1074-1085.

Cormier, R.F. and Kelley, D.M.
1964: Absolute age of the Fisset Brook Formation and the Devonian-Mississippian boundary, Cape Breton Island, Nova Scotia, Canadian Journal of Earth Sciences, v. 1, p. 159-166.

Creed, R.M.
1968: Barite-fluorite mineralization at Lake Ainslie, Inverness Co., N.S.; unpublished M.Sc. thesis, Dalhousie University, 158 p.

Currie, K.L.
1975: Studies of granitoid rocks in the Canadian Appalachians; in Report of Activities, Part A, Geological Survey of Canada Paper 75-1A, p. 265-268.

1977: A note on post-Mississippian thrust faulting in northwestern Cape Breton Island; Canadian Journal of Earth Sciences, v. 14, p. 2937-2941.

Jamieson, R.A.
1981: The geology of the Crowdis Mountain volcanics, southern Cape Breton Highlands; in Current Research, Part A, Geological Survey of Canada Paper 81-1C, p. 77-81.

Jamieson, R.A.
1982: The petrology of cordierite gneisses, Kelly's Mountain, Nova Scotia; GAC-MAC Program with Abstracts, v. 7, p. 57.

Jamieson, R.A. and Doucet, P.
1983: The Middle River – Crowdis Mountain area, southern Cape Breton Highlands; in Current Research, Part A, Geological Survey of Canada Paper 83-1A, Report 37.

Jenness, S.E.
1966: The anorthosite of northern Cape Breton Island, Nova Scotia; a petrological enigma; Geological Survey of Canada Paper 66-21.

Kelley, D.M. and Mackasey, W.O.
1965: Basal Mississippian volcanic rocks in Cape Breton Island, N.S.; Geological Survey of Canada Paper 64-34, 10 p.

Keppie, J.D.
1979: Geological map of the province of Nova Scotia; Nova Scotia Department of Mines and Energy.

Macdonald, A.S. and Smith, P.K.
1979: Red River anorthosite complex; in Nova Scotia Department of Mines and Energy, Report 79-1, p. 103-104.

1980: Geology of Cape North area, Northern Cape Breton Island, Nova Scotia; Nova Scotia Department of Mines and Energy, Paper 80-1, 60 p.

Macnabb, B.E., Fowler, J.H., and Covert, T.G.N.
1976: Geology, geochemistry, and mineral occurrences of the Northeast Margaree River drainage basin in parts of Inverness and Victoria Countries, Cape Breton, Nova Scotia, Nova Scotia Department of Mines and Energy, Paper 76-4, 30 p.

Mackasey, W.O.
1963: Petrography and stratigraphy of a Lower Mississippian pre-Horton volcanic succession in northwest Cape Breton Island, unpublished M.Sc. thesis, Carleton University.

Milligan, G.C.
1970: Geology of the George River Series, Cape Breton; Nova Scotia Department of Mines, Memoir 7, 111 p.

Mitchell, P.L.
1979: A study of the rare earth element geochemistry and mineral chemistry of the anorthosites and related rocks near Pleasant Bay, Cape Breton Island, Nova Scotia, unpublished B.Sc. thesis, Dalhousie University.

More, E.B.
1982: The stratigraphy and structure of a section of the Horton Group along the North Baddeck River, Victoria County, Cape Breton Island, unpublished B.Sc. thesis, Dalhousie University.

Olszewski, W.J., Gaudette, H.E., Keppie, J.D., and Donohoe, H.V.
1981: Rb-Sr whole rock age of the Kelly's Mountain basement complex, Cape Breton Island, Geological Society of America, Abstracts with Programs, v. 13, p. 169.

Smith, P.K. and Macdonald, A.S.
1981: The Fisset Brook Formation at Lowland Cove, Inverness County, Nova Scotia. Nova Scotia Department of Mines and Energy, Paper 81-1, 18 p.

Strong, D.F., O'Brien, S.J., Taylor, S.W., Strong, P.G., and Wilton, D.H.
1978: Aborted Proterozoic rifting in eastern Newfoundland; Canadian Journal of Earth Sciences, v. 15, p. 117-131.

37. THE MIDDLE RIVER – CROWDIS MOUNTAIN AREA, SOUTHERN CAPE BRETON HIGHLANDS

R.A. Jamieson[1] and P. Doucet[1]
Atlantic Geoscience Centre, Dartmouth

Jamieson, R.A. and Doucet, P., The Middle River – Crowdis Mountain area, southern Cape Breton Highlands; in Current Research, Part A, Geological Survey of Canada, Paper 83-1A, p. 269-275, 1983.

Abstract

A detailed field study of the Middle River – Crowdis Mountain area of the southern Cape Breton Highlands has been completed, and a few new radiometric dates are available for this area. The major units include a metavolcanic-metasedimentary complex of probable late Precambrian age, a gneiss complex gradational into the lower grade rocks, a 750 Ma dioritic intrusive complex, various younger granitic rocks including a 401 Ma monzogranite, and a 384 Ma volcanic complex overlain by the Horton Group. These rocks are cut by various dykes, late shear zones, and faults. The bearing of this study on the regional geology of the Cape Breton Highlands is discussed.

Introduction

The Middle River – Crowdis Mountain area of the southern Cape Breton Highlands was interpreted as sedimentary, volcanic, and metamorphic rocks of the George River Series by Milligan (1970), and appears on the recently compiled geological map of Nova Scotia as Proterozoic volcanic and sedimentary rocks, Hadrynian granites, and undivided Proterozoic George River Group gneisses (Keppie, 1979). In 1979, detailed work was begun in the area to determine a basis for correlation with southeastern Cape Breton. On the basis of this work, Jamieson (1981) identified distinct sequences of volcanic and volcaniclastic rocks in the Crowdis Mountain area, high grade metamorphic rocks in the Middle River area, and deformed granitic rocks in the Egypt Highlands area. In 1981 the field study of the Crowdis Mountain area was completed, and in 1982 a more detailed study of the metamorphic rocks of the Middle River area was also completed.

The results of the field work and preliminary petrological and geochronological studies indicate a more complex tectonic history than was previously imagined. It is now clear that there are two distinct volcanic sequences, a younger, southern one (MacMillan Mountain) that is probably related to the Fisset Brook Formation of western Cape Breton, and an older northern one (Crowdis Mountain) of unknown age and tectonic affinity. These are separated by an intrusive complex and by a shear zone in which there has been a component of southward thrusting. In addition, it appears that the older volcanic complex grades into the higher grade rocks of the Middle River area.

The following discussion treats each major unit separately before discussing the overall structural and metamorphic geology, probable ages, and regional significance of the rocks.

Acknowledgments

The authors are grateful for the financial support given to this project by the Geological Survey of Canada through a research fellowship to RAJ in 1979, and EMR Research Agreements in 1980-82. Support has also come from NSERC Operating Grant A-7365 awarded to RAJ in 1980-82, and a Dalhousie Graduate Fellowship awarded to PD in 1981-82. Nova Scotia Forest Industries kindly provided access to their extensive road network, as well as base maps showing new roads. RAJ is greatly indebted to B. Fryer, P. Davis, and D. Press for the use of the geochemistry and geochronology labs at Memorial University. G. Tessier, L. More, K. Johnston, and D. Conrod provided able field assistance, and we have had valuable discussions with G.C. Milligan, K. Currie, S. Barr, A. Macdonald, and many others in the course of this work.

Northern (Crowdis Mountain) Volcanic Unit

The area between Sarach Brook, the North Baddeck River, and Muskrat Brook is underlain by a complex but poorly exposed sequence of variably deformed volcanic and volcaniclastic rocks (unit 1, Fig. 37.1), bounded by shear zones and intruded by granitic to dioritic rocks of various ages.

The best preserved volcanic rocks occur near the eastern edge of the area, where they are faulted against foliated tonalites of the Baddeck Lakes unit. They consist mainly of pyroclastic rocks and epiclastic volcanogenic sediments, with crystal-lithic tuff predominating. Some fine grained tuffs preserve primary laminations but no facing directions could be determined. Crystals and crystal fragments of euhedral plagioclase and doubly terminated, partially embayed quartz are characteristic. Common lithic fragments include spherulitic rhyolite, microlitic volcanics, and siltstone. Farther west, south of Sarach Brook, a deformed, flow-banded, spherulitic rhyolite is associated with the pyroclastic rocks. In at least one locality a dioritic sill occurs within with the volcanic sequence. Very similar pyroclastic rocks occurring in the upper part of Second Gold Brook suggest that the northern volcanic unit is gradational into the Middle River metamorphic complex.

Virtually all the rocks have undergone some degree of metamorphism and deformation. In the northern part of the unit, garnet occurs in some of the crystal-lithic tuffs, and metamorphic hornblende occurs in the diorite sill and mafic tuffs. The unit is cut by narrow east-west trending mylonites that appear to swing into a major northeast-southwest trending shear zone running parallel to Sarach Brook. Within the volcanic rocks strain is highly heterogeneous, and the transition from mildly foliated pyroclastics to mylonite can occur over a few metres. In general, the rocks display a northeasterly to easterly trending, steeply dipping foliation which is only weakly developed in more resistant rocks like rhyolite, and is difficult to distinguish from primary flattening in welded tuff.

Four types of intrusive rocks cut the northern volcanic unit – the pink, north-south trending syenogranite that also intrudes the Middle River metamorphic complex, the West Branch North River hornblende-biotite monzogranite, small plugs of a diorite-microgranite complex which is fully developed farther south, and late diabase and rhyolite dykes. These intrusive rocks will be discussed in more detail below.

Middle River Unit

The area bounded by Gold Brook in the south, Middle River in the east, Lake O'Law in the west, and Fielding Road in the north is underlain by a complex of metamorphic rocks.

[1] Department of Geology, Dalhousie University, Halifax, Nova Scotia, B3H 3J5

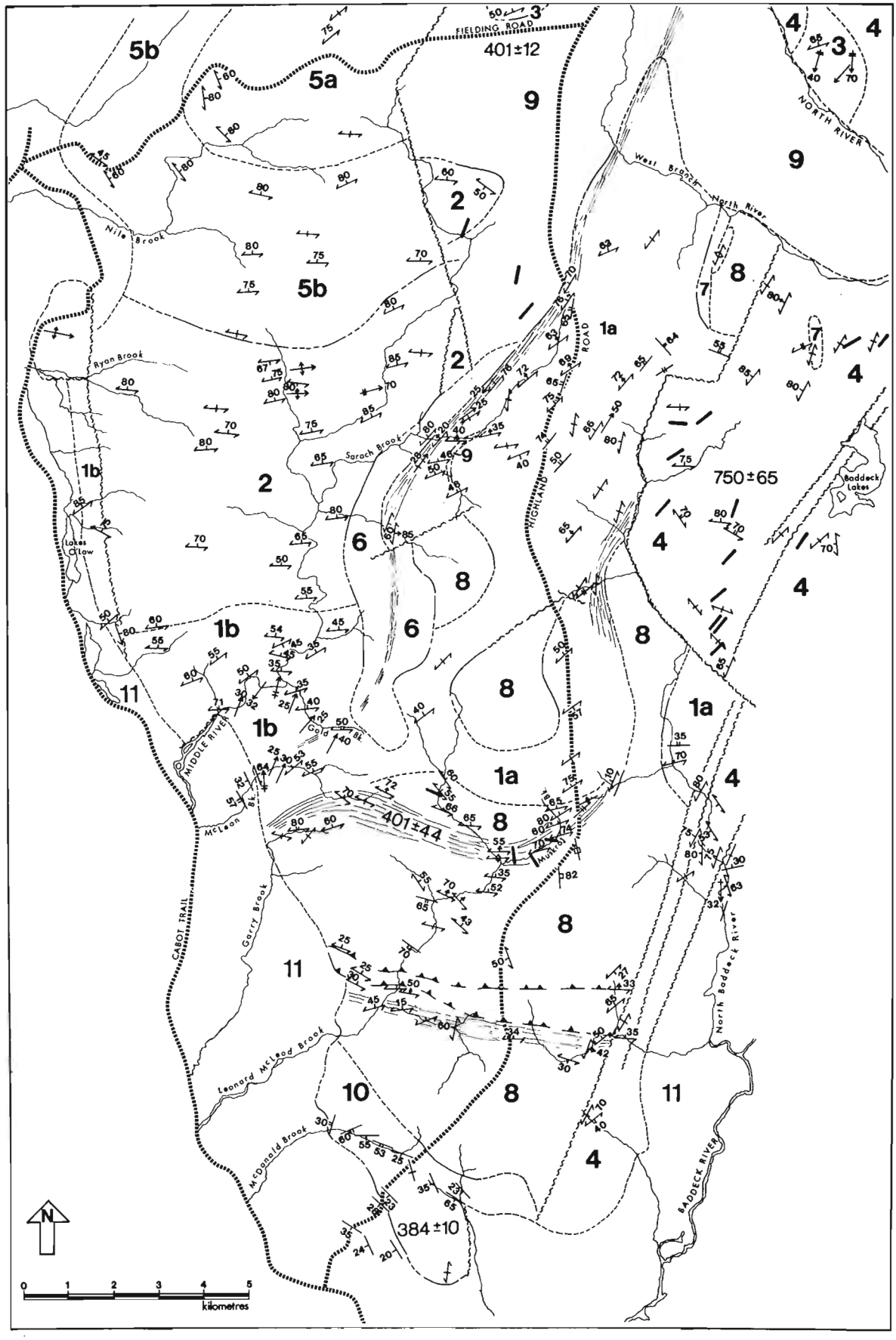

Figure 37.1. *Geology of the Middle River – Crowdis Mountain area, southern Cape Breton Highlands. Dates refer to new work done by R.A. Jamieson at Memorial University.*

LEGEND

CARBONIFEROUS

11. Horton Group

DEVONIAN

10. Southern (MacMillan Mountain) volcanic unit
9. West Branch North River monzogranite

DEVONIAN OR EARLIER

8. Leonard McLeod Brook diorite-microgranite complex
7. Diabase dykes and small intrusions
6. Bothan Brook syenogranite

LATE PRECAMBRIAN (?)

5. Egypt Highlands unit – 5a, coarse grained foliated granitic rocks; 5b, fine grained foliated granitic rocks
4. Baddeck Lakes diorite-gabbro complex
3. Undivided gneisses, possibly equivalent to or older than unit 2
2. Middle River unit paragneiss and amphibolite, high grade equivalent of unit 1
1. Northern (Crowdis Mountain) volcanic unit – 1a, mainly felsic metavolcanic and pyroclastic rocks; 1b, mainly metasedimentary and interlayered metabasic rocks

Symbols

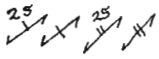

foliation – inclined, vertical, first, second

bedding – inclined, vertical, tops unknown


fault – vertical, thrust

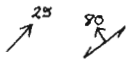

lineation – oblique, downdip

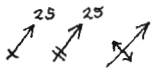

fold axis – first, second, major antiform

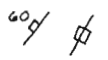

joint – inclined, vertical


mafic dyke


shear zone


geological contact – observed, approximate

These can be divided into two major assemblages, informally referred to here as the Middle River unit (unit 2) and the Egypt Highland unit (unit 5). These rocks are cut by granites and dykes and are faulted against lower grade metavolcanic rocks and Carboniferous sediments to the west.

The Middle River unit in the southern part of the area comprises low to medium grade metasedimentary rocks with local thin metabasite horizons. Fine grained, dark green to brown, quartz-biotite-muscovite phyllites and schists occur in the vicinity of Second Gold Brook, whereas medium grained, dark brown, quartz-biotite-oligoclase-muscovite gneisses dominate to the north (Fig. 37.1). Fine- to medium-grained, dark green metabasites composed of hornblende, quartz, and minor intermediate plagioclase make up the remainder of the Middle River unit. Contacts between these units are sharp and parallel to the foliation. A thin, east-west trending marble horizon is located in the biotite gneiss along Middle River north of Sarach Brook. Marble also outcrops locally along Middle River near Second Gold Brook, and in the upper part of Fionnar Brook. Near the northern end of Second Gold Brook and in scattered outcrops along Middle River a distinctive metaconglomerate is found which contains elongated clasts of quartzite, siltstone, and volcanic rocks in a fine grained phyllitic matrix.

The Egypt Highland unit is made up of schistose to gneissic granitic rocks. They are commonly foliated but appear to grade into less deformed granite at the northern edge of the area near Fielding Road. Two main types can be distinguished – a fine grained, pale pink, K-feldspar-quartz-oligoclase-biotite schist, and a coarser grained, dark red, K-feldspar-quartz-oligoclase gneiss with distinctive K-feldspar augen. Contacts between these two types are gradational. The Egypt Highland unit is cut by numerous zones of very fine grained micaceous schist that may be small shear zones.

Near the junction of Fielding and Highland roads is a black and white monzogranite to granodiorite containing disseminated K-feldspar crystals in a medium- to coarse-grained matrix of plagioclase, biotite, and quartz. This is informally termed the West Branch North River monzogranite (unit 9) and appears to be in fault contact, at least locally, with the Egypt Highland unit. Northeast-southwest trending diabase and rare rhyolite dykes cut all rock types. The Middle River unit is intruded on the east by a north-south trending, salmon pink, medium grained syenogranite.

The structural complexity of the Middle River area is more evident in the south where early structures are preserved, although the metamorphic grade increases to the north. Mesoscopic F_1 folds are found locally in biotite gneiss where strong lithological layering occurs. The dominant planar element, S_2, is a strongly developed micaceous foliation, ranging from a phyllitic schistosity in the south to a gneissic foliation in the north. Both the Middle River and Egypt Highland units strike east-west and dip moderately to steeply north to northwest. In the north the foliation swings to the northwest in the west and to the northeast in the east, forming a concentric structure focused on the least deformed granite. Mesoscopic F_2 folds and kinks are best developed in the biotite gneiss. A well developed northeast trending lineation (L_2) is defined by elongated clasts in the metaconglomerate. A large F_3 fold plunges moderately to the north along Middle River near Second Gold Brook. A very fine crenulation cleavage (S_3) and intersection lineation (L_3) are observed in the same area. No sedimentary facing directions have been detected in the area. Late faults, joints, and dykes trend north-south to northeast-southwest, across the structural grain.

The metamorphic grade increases rapidly from chlorite zone phyllites in the south to staurolite and kyanite schists and garnet amphibolites in the central part of the region. Two episodes of mineral growth have been identified, the first associated with the main fabric (S_2), the second represented by chlorite, chloritoid, biotite, and hornblende porphyroblasts cutting across this fabric near Gold Brook. Multiple episodes of mineral growth have not yet been identified in the higher grade rocks. Retrograde metamorphism, locally associated with shear zones, is common in all units. The concentration of pegmatite veins and pockets also increases toward the north as the granites are approached.

Baddeck Lakes Unit

Between the North Baddeck River and the Baddeck (Bell) Lakes is a complex of foliated diorite, tonalite, and amphibolite (unit 4) and amphibolitic and metasedimentary gneisses (unit 3) cut by a major northeast trending mafic dyke swarm. The rocks are well exposed along logging roads, but so far have been mapped on a reconnaissance level only. The unit is fault bounded on the west against mildly deformed volcaniclastic rocks of the Crowdis Mountain volcanic unit; its eastern limit is unknown. The metamorphic grade is similar to that of the Middle River metamorphic complex, but the rocks have a totally different character and structural style. It therefore seems unlikely that this unit is related to any others in the region; its possible relationship to other rocks in the Cape Breton Highlands is discussed by Jamieson and Craw (1983). Some of the mafic dykes cutting the Baddeck Lakes unit also cut the adjacent volcanic rocks, indicating a post-faulting age of dyke injection.

Southern (MacMillan Mountain) Volcanic Unit

The southernmost part of the study area, in the vicinity of MacMillan Mountain, is underlain by undeformed felsic and mafic volcanic, pyroclastic, and related sedimentary rocks (unit 10) that are well exposed on Harris and MacDonald brooks and in gravel pits along Highland Road. The rocks dip and face gently to the southwest, and are overlain by conglomerates and coarse arkosic sandstones of the Horton Group. The exposure is not good enough to establish an internal stratigraphy, particularly since there are rapid lateral and vertical changes that may reflect an original complex interfingering of flows, pyroclastic deposits, and sediments. The rocks are undeformed except for fracturing, which locally can be very intense, and range from mildly altered (minor chlorite, some oxidation), to intensely altered (abundant chlorite, sericite, and hematite).

The rock types include rhyolites, mafic to intermediate flows, lithic pyroclastic and epiclastic rocks, sandstones, siltstones, and local conglomerates, with a diorite-microgranite intrusive complex bounding the volcanic rocks on the north. The rhyolites are fine grained, with minor alkali feldspar phenocrysts, rarely spherulitic or flow banded, and completely devitrified. The concentration of massive rhyolite near MacMillan Mountain suggests that this was once a volcanic centre. The mafic flows are poorly exposed and generally highly altered, and contain sparse plagioclase phenocrysts in a trachytic matrix of plagioclase microlites and interstitial oxide. Clinopyroxene is virtually absent, suggesting that these rocks may be andesitic or trachytic in composition. The mafic flows are locally amygdaloidal. Owing to poorly exposed contacts it is possible that some of the rocks mapped as rhyolitic and mafic flows are in fact sills or dykes.

The pyroclastic rocks interbedded with these flows are highly variable in texture and composition, ranging from crystal-lithic tuffs composed primarily of pumice and trachytic volcanic fragments and feldspar crystals, to epiclastic rocks consisting primarily of lithic volcanic, tuff, and siltstone fragments. An accretionary lapilli tuff, implying subaerial eruption, has been identified in one locality, and two occurrences of welded, spherulitic, rhyolitic tuff have been found.

The sedimentary rocks associated with these volcanics are mainly sandstones with abundant quartz and feldspar clasts and minor volcanic fragments, generally subangular and closely packed. Interbedded with the rhyolite at MacMillan Mountain are maroon siltstone, green volcanogenic sandstone, and a conglomerate containing abundant tabular clasts of maroon siltstone and rounded vein quartz and jasper pebbles in a highly arkosic matrix with some volcanic quartz.

These sediments are clearly distinguishable from the overlying, buff-coloured, coarse arkose with pockets of conglomerate that is interpreted as part of the Horton Group (unit 11). The younger rocks contain abundant rounded granitic clasts, microcline crystals, and fragments of vein quartz, schist, and highly altered volcanics. The degree of rounding of the clasts and the variety of lithologies represented argue for a more distal source; there is surprisingly little local debris. The Horton sediments are broadly conformable with the volcanic rocks at MacMillan Mountain, but show significant variation in attitude elsewhere. This and the always distinct nature of the transition suggest that the volcanic rocks are significantly older than the Horton Group sediments, which overlie them unconformably to disconformably.

On the North Baddeck River, a sequence of grey, thinly bedded sandstones and siltstones overlying red arkose and conglomerate probably represents the Strathlorne Formation of the Horton Group (More, 1982). This sequence is faulted against steeply dipping to overturned red micaceous sandstones with coarse conglomerate lenses that contain a single amygdaloidal basalt flow. Neither the basalt nor its associated sediments resembles the volcanic rocks at MacMillan Mountain, but the rocks are similar in many respects to the Fisset Brook Formation of western Cape Breton.

Intrusive Rocks

The southern Highlands area is intruded by a variety of mafic to felsic rocks of different ages. The foliated tonalites of the Baddeck Lakes area and the deformed syenogranites, augen gneisses, and granitic schists of the Egypt Highlands unit are probably the oldest, but their relative ages are unknown. However, the granitic rocks of the Egypt Highlands area must predate the deformation of the Middle River unit, since they are deformed with it.

A distinctive north-south trending syenogranite (unit 6) occupies the central part of the study area. It intrudes the Middle River metamorphic complex on the west, and the northern volcanic unit on the south near Boundary Line Road. It is a medium grained, equigranular, salmon pink and white, quartz and K-feldspar rich rock that is nearly free of mafic minerals. It is deformed by the Sarach Brook mylonite along its northwestern margin, and is probably offset by it in its central part. It is referred to informally here as the Bothan Brook syenogranite.

In the north of the area, near the junction of Fielding and Highland roads, a hornblende-biotite granodiorite to monzogranite (unit 9), informally referred to as the West Branch North River monzogranite, intrudes all other lithologies. It ranges from weakly foliated to undeformed, and from black and white, medium grained granodiorite through pink, black, and white monzogranite, to grey aplite, and is generally equigranular. Its relationship to the Sarach Brook mylonite is unclear and will be discussed further below.

The most common intrusive rocks of the area are diorites and microgranites that underlie most of the area between Harris Brook and Muskrat Brook, and are well exposed along Leonard McLeod Brook (unit 8). They also occur as distinct plugs intruding the older volcanic rocks farther north. Commonly, thin veinlets of microgranite are found cutting the diorite, but locally the two lithologies are mutually intrusive. Intrusion breccia of diorite in microgranite is common, particularly in streams on the west side of the North Baddeck River. An apparently hybrid rock, containing green hornblende crystals and hornblende-plagioclase aggregates in a pink granitic matrix, is very common. It is therefore concluded that the diorites and microgranites are essentially contemporaneous, and they are referred to informally as the Leonard McLeod Brook complex. These rocks are essentially undeformed north of Boundary Line Road, although they are invariably altered. Between Gillis Brook and Boundary Line Road, however, the rocks are mildly to intensely foliated, becoming virtually unrecognizable in places, particularly within the Muskrat Brook mylonite zone. South of Gillis Brook the rocks are again virtually undeformed, and their close association with the younger volcanic rocks suggests that they may represent a subvolcanic intrusive complex.

Various types of late dykes (unit 7) cut the region. These include the hornblende-rich, locally porphyritic dyke swarm of the Baddeck Lakes area that also cuts the eastern part of the Crowdis Mountain Brook volcanic unit, and a few large alkaline diabase dykes that occur in several widely separated localities. Locally, silicic, spherulitic rhyolite dykes occur; one of these clearly cuts mylonite on Sarach Brook.

Structure and Metamorphism

Except for the amphibolite facies rocks of the Baddeck Lakes and Middle River units noted above, the metamorphic grade throughout the region does not exceed the greenschist facies. There is a tendency for the grade to increase towards the north. This is particularly evident in the Middle River sequence, which grades from lower greenschist facies assemblages in the Gold Brook area to amphibolite facies schists and gneisses containing garnet, staurolite, kyanite, and rare sillimanite over a distance of a few kilometres. South and east of this area, the grade increases from chlorite schists in the south to garnet and hornblende-bearing rocks in the north near Sarach Brook.

The structural geology of the area is complex, and owing to the poor exposure may never be unravelled. The dominant structures are two shear zones – the northeast-southwest trending Sarach Brook mylonite in the north, and the east-west trending Muskrat Brook mylonite in the central part of the region. These are superimposed on the main east-west trending, north dipping foliation that characterizes both the Middle River metamorphic complex and the northern volcanic unit.

Just north of Gillis Brook, a moderately north-dipping fault cuts the Leonard McLeod Brook diorite-microgranite complex. Immediately beneath the fault the intrusive rocks are strongly foliated and folded. The fault, which can be traced as far east as MacRae Brook, is interpreted as a southward-directed thrust. Between the Gillis Brook fault and the Muskrat Brook shear zone diorite, microgranite, and rare metavolcanic rocks are heterogeneously deformed, ranging from weakly foliated to mylonitic. The strain increases rapidly as the Muskrat Brook mylonite is approached. The shear zone itself consists of nearly vertical felsic schists and phyllites with boudins of volcanic and pyroclastic rocks as well as diorite and microgranite. Much of the zone consists of nondescript, very fine grained, well foliated, compositionally banded to homogeneous schist and phyllite, commonly with a down-dip or steeply plunging lineation. Macroscopically and microscopically it conforms to the present usage of the term "mylonite" (e.g. Bell and Etheridge, 1973), and characteristically displays rapid strain gradients, intrafolial isoclinal folds with steeply plunging axes, and inclusions of somewhat less deformed, protoliths. It trends east-west and probably extends into Garry Brook and the upper reaches of McLean Brook which both consist largely of felsic to mafic mylonite. In the eastern part of the zone there is a swing to the northeast, and it may become parallel to the Sarach Brook mylonite zone. It deforms both the diorite-microgranite complex and the northern volcanic unit, and thus postdates both. There is clear textural evidence that the north side of the zone has moved up relative to the south, but evidence concerning relative lateral displacement is still ambiguous.

The Sarach Brook mylonite zone extends in a northeasterly direction from Bothan Brook along Sarach Brook and continues for some distance towards the north. It affects both the Bothan Brook syenogranite and the northern volcanic unit. Smaller shear zones trending east-west within the volcanics appear to swing into the main zone. Northwards it disappears in an area of granitic rocks but owing to the poor exposure it is not clear whether or not these rocks intrude the mylonite. In this vicinity the mylonite is cut by some quartz-K-feldspar veins but the relationship of these veins, if any, to the granite is unclear. In the south, the mylonite also disappears in an area of virtually no outcrop that coincides with a sudden widening of the Bothan Brook syenogranite. Since on Sarach Brook the mylonite clearly deforms this granite, and since the granite is altered near the area where the mylonite disappears, it is likely that the mylonite cuts through the granite at this point, and that the widening of the granite results from structural repetition. It may re-emerge in the Gold Brook area, where small shear zones are present, but nothing on the scale of the Sarach Brook mylonite has been found there.

The Sarach Brook mylonite resembles the Muskrat Brook mylonite in many respects, since it consists predominantly of deformed pyroclastic rocks. Drawn out ash fragments define a prominent down-dip lineation that locally plunges obliquely across the dip and rarely has a shallow plunge. Most of the rocks are fine grained felsic schists and phyllites, but some very well banded mylonites occur. Deformed granite can be distinguished from deformed pyroclastics only by the presence of large K-feldspar porphyroclasts, which can resemble elongated, pink ash fragments. In the vicinity of Bothan Brook and South Sarach Brook a strongly deformed, flow banded rhyolite is preserved, which presumably has been more resistant to the strain than the less competent surrounding pyroclastic rocks. No deformed microgranite or diorite has been recognized within the Sarach Brook mylonite zone, but it is cut in one locality by a spherulitic, undeformed rhyolite dyke.

This mylonite involves a component of sinistral shear, with the volcanics moving north relative to the granite and metamorphic rocks, but the down-dip lineation implies a major component of vertical displacement. This is unlikely to have developed from simple shear alone, and a component of flattening may also be involved (cf. Bell, 1981). It is also possible that both this zone and the Muskrat Brook mylonite originated as shallow structures but have been steepened since their formation.

The relation of the Sarach Brook mylonite to the Muskrat Brook mylonite is unclear. The Sarach Brook mylonite does not deform the diorite-microgranite suite, and if the rhyolite dyke that cuts it is related to the microgranites, then the Sarach Brook mylonite must be older.

On the other hand, there is no conclusive evidence that the dyke is related to the microgranites, and no cross-cutting relation between the two zones has yet been identified.

Age of Rocks

Absolute ages for most of the rocks in the Middle River – Crowdis Mountain area are lacking. No fossils have yet been discovered in any of the pre-Carboniferous rocks. Rb-Sr dates were obtained at Memorial University in 1981 and 1982 for the MacMillan Mountain rhyolites (383.6 ± 10 Ma), the West Branch North River monzogranite (401.3 ± 12.9 Ma), the Baddeck Lakes diorites (750 ± 65 Ma), and the Muskrat Brook shear zone (401 ± 44 Ma). Preliminary work on the Leonard McLeod Brook diorite-microgranite complex and the Sarach Brook mylonite gave poor results, owing to analytical difficulties, the alteration of some samples, and probable incomplete homogenization of Rb and Sr in the mylonites. Further Rb-Sr work, combined with $^{40}Ar/^{39}Ar$ and zircon dates, is planned in order to improve the date for the diorite and the mylonites, and to determine the age of the high grade metamorphism in the Baddeck Lakes and Middle River areas.

Owing to poor exposure, critical cross-cutting relations cannot always be determined. However, based on the known absolute and relative ages of the various units, the following sequence of events is suggested:

1. The Middle River metamorphic complex grades north into granite and south into greenschist facies metasediments and volcaniclastic rocks. The age of metamorphism is unknown. However, volcaniclastic rocks at the southern end of Gold Brook resemble the Crowdis Mountain volcanic sequence. The metaconglomerate near the mouth of Gold Brook contains metavolcanic clasts, and it is conceivable that the metasediments of the Gold Brook area originally overlay or were interbedded with the Crowdis Mountain volcanics. Since the Middle River complex represents a continuous sequence in which metamorphic grade increases rapidly northwards, this implies that the metamorphism postdated the deposition of the northern volcanic unit. If the relative northward displacement of the volcanics along the Sarach Brook mylonite zone is taken into account, the original sequence would have consisted of a volcanic and volcaniclastic complex grading vertically or laterally into a predominantly sedimentary sequence.
2. The Baddeck Lakes diorite – gneiss complex is faulted against all other rocks in the study area. Its relative age is therefore unknown, but reconnaissance studies farther north suggest that it intrudes gneisses which may be equivalent to the Middle River unit. A Rb-Sr whole rock isochron age of 750 ± 65 Ma was obtained for this unit; this is a preliminary age only and probably represents the age of intrusion. This date is the oldest yet obtained from the Cape Breton Highlands, and implies that the northern volcanic rocks unit and its metamorphic equivalents are older than 750 Ma.
3. The Bothan Brook syenogranite cuts the Middle River metamorphic complex and the northern volcanic unit. It is deformed by the Sarach Brook mylonite. In many respects it resembles Cambrian granites elsewhere in northern Cape Breton, but this is unlikely to be proven either by radiometric work, given the highly altered state of the rocks, or by geochemical comparisons, given the lack of geochemical "fingerprints" for these granites.
4. The diorites and microgranites are probably contemporaneous and cogenetic both north and south of the Muskrat Brook shear zone. They intrude the northern volcanic unit and are cut by the Muskrat Brook shear zone which has been dated at 401 ± 44 Ma. These rocks may have originated as subvolcanic intrusions related to the younger volcanic rocks.
5. The West Branch North River monzogranite, dated at 401.3 ± 12.9 Ma (early Devonian), intrudes the northern volcanic complex, and is possibly cut by the Sarach Brook shear zone.
6. The Muskrat Brook mylonite zone, which cuts the Leonard McLeod Brook diorite-microgranite complex, has been dated by Rb-Sr at 401 ± 44 Ma. The Sarach Brook mylonite zone must postdate the Bothan Brook syenogranite and the West Branch North River monzogranite which has been dated at 401 ± 13 Ma. Although cross-cutting relationships between the two shear zones have not been established, the Sarach Brook shear zone may be younger than, or contemporaneous with, the Muskrat Brook shear zone.
7. The MacMillan Mountain volcanics are the youngest rocks studied in detail. At 384 ± 10 Ma, they are middle Devonian and comparable to the Fisset Brook Formation of western Cape Breton (376 ± 12 Ma near Cheticamp, 370 ± 20 Ma near Lake Ainslie; Cormier and Kelley, 1964). These volcanics are unconformably to disconformably overlain by Lower Carboniferous Horton Group sediments, which in one locality on the North Baddeck River contain a single basalt flow (More, 1982).

Regional Significance

There are few areas in the Cape Breton Highlands that have been studied in enough detail to warrant close comparison with the Middle River – Crowdis Mountain area. It is clear that the rocks should not be included with the George River Group, partly because the incautious use of this term should be discouraged, and partly because there are obviously rocks of totally different character and probably different ages present. A few points of similarity with other areas in Cape Breton are worth noting (see also Jamieson and Craw, 1983).

The Middle River metamorphic complex resembles the sequences described by Macdonald and Smith (1980) in the Cape North area, and by Currie (personal communication, 1982) for the Jumping Brook area. Macdonald and Smith (1980) described a sequence of metatuffs, metasediments, and biotite schists and gneisses with lit-par-lit injection features which resemble the rocks north and west of Middle River and which also contain chloritoid, kyanite, and marble horizons. The authors tentatively interpreted the rocks as equivalent to the late Precambrian George River and Fourchu groups. On the other hand, Currie has interpreted a broadly similar assemblage north of Cheticamp as probably lower Paleozoic. Obviously until at least one of the three complexes is dated, further speculation is unwarranted.

The West Branch North River monzogranite, dated at 401.3 ± 12.9 Ma, is almost exactly the same age as the White Point pluton of the northeastern Cape Breton Highlands (403 ± 22 Ma; reported by Keppie, 1979). It resembles in chemistry and mineralogy, although not in texture, the Margaree granite (Currie, personal communication, 1982) of the central Cape Breton Highlands. This is an undeformed megacrystic granite, locally with a rapakivi texture, from which a preliminary whole rock Rb-Sr date of 365 ± 46 Ma has been obtained. These new dates suggest that there may be more "Acadian" granitic rocks in the central Highlands than has previously been recognized.

The volcanic rocks at MacMillan Mountain are middle Devonian and probably originated in the same tectonic setting as the Fisset Brook Formation. There are some notable differences, particularly in the type of associated sediments and abundance of pyroclastic deposits (Blanchard, 1982). The single flow and associated sediments on the North Baddeck River more closely resemble Fisset Brook lithologies. It seems likely, therefore, that the younger volcanics are tectonically similar to, but somewhat older than, the type Fisset Brook Formation.

Once the age relations have been worked out, and combined with further analysis of the lithologies, petrology, and structure, a tectonic model might be developed for the area. At the moment, except for the youngest rocks, which appear to conform to the pattern of middle Devonian to lower Carboniferous postorogenic volcanism throughout the eastern Appalachians, any such model would be entirely speculative.

References

Bell, T.H.
1981: Foliation development – the contribution, geometry, and significance of progressive, bulk, inhomogeneous shortening; Tectonophysics, v. 75, p. 273-296.

Bell, T.H. and Etheridge, M.A.
1973: Microstructure of mylonites and their descriptive terminology; Lithos, v. 6, p. 337-348.

Blanchard, M.C.
1982: Geochemistry and petrogenesis of the Fisset Brook Formation, western Cape Breton Island, Nova Scotia; unpublished M.Sc. thesis, Dalhousie University, 225 p.

Cormier, R.F. and Kelley, D.M.
1964: Absolute age of the Fisset Brook Formation and the Devonian-Mississippian boundary, Cape Breton Island, Nova Scotia; Canadian Journal of Earth Sciences, v. 1, p. 159-166.

Jamieson, R.A.
1981: The geology of the Crowdis Mountain volcanics, southern Cape Breton Highlands; in Current Research, Part C, Geological Survey of Canada, Paper 81-1C, p. 77-81.

Jamieson, R.A. and Craw, D.
1983: Reconnaissance mapping of the southern Cape Breton Highlands – a preliminary report; in Current Research, Part A, Geological Survey of Canada, Paper 83-1A, report 36.

Keppie, J.D.
1979: Geological map of the province of Nova Scotia; Nova Scotia Department of Mines and Energy.

Macdonald, A.S. and Smith, P.K.
1980: Geology of Cape North area, northern Cape Breton Island, Nova Scotia; Nova Scotia Department of Mines and Energy, Paper 80-1, 60 p.

Milligan, G.C.
1970: Geology of the George River Series, Cape Breton; Nova Scotia Department of Mines, Memoir 7, 111 p.

More, E.B.
1982: The stratigraphy and structure of a section of the Horton Group along the North Baddeck River, Victoria County, Cape Breton Island; unpublished B.Sc. thesis, Dalhousie University.

38. RECOGNITION OF URANIUM CONCENTRATION PROCESSES IN GRANITES AND RELATED ROCKS USING AIRBORNE RADIOMETRIC MEASUREMENTS

Projects 760045, 760047

Y.T. Maurice and B.W. Charbonneau
Resource Geophysics and Geochemistry Division

Maurice, Y.T. and Charbonneau, B.W., Recognition of uranium concentration processes in granites and related rocks using airborne radiometric measurements; in Current Research, Part A, Geological Survey of Canada, Paper 83-1A, p. 277-284, 1983.

Abstract

A method of recognizing granites and related rocks, which have been subjected to magmatic or post-magmatic radioelement concentration processes, is described. The technique utilizes the eU and eTh signatures of the rocks and their ratio from airborne radiometric profiles. Examples are given for unmineralized granites (north of Elliot Lake, Ontario), granites that have undergone postmagmatic remobilization of their uranium (Fury and Hecla Strait, NWT) and differentiated plutons which contain concentrations of radioelements in the late differentiates (Blachford Lake complex, NWT) and South Mountain Batholith, Nova Scotia.

Introduction

About 20 per cent of Canada's landmass (2 000 000 km^2) has been surveyed by airborne radiometric methods under the auspices of the Uranium Reconnaissance Program (Darnley et al., 1975). These surveys made use of a high sensitivity gamma ray spectrometer with 50 L of sodium iodide detectors. Measurements for eU, eTh and K were made along lines 5 km apart with an aircraft flying at about 120 m above the ground. To date, most of the surveys have been carried out in the Canadian Precambrian Shield and in the Appalachian regions of Nova Scotia, New Brunswick and Prince Edward Island.

The results show that granites and related rocks often produce strong radiometric responses. On a contoured eU map of the areas surveyed (Fig. 38.1) the regions shown to contain in excess of 2 ppm eU generally correspond to granitic rocks. Significantly enriched granite bodies, containing in the order of 8-12 ppm U, (2 to 3 times normal) produce airborne radiometric anomalies in the order 3-4 ppm eU (Charbonneau, 1982).

Close examination of airborne radiometric profiles over anomalously radioactive granites gives an indication of whether or not the radioelements have been concentrated as a result of magmatic or postmagmatic processes and thus permits speculation on their potential for hosting mineralization of one type or another.

To illustrate this, four anomalously radioactive granites were examined; one is devoid of mineralization whereas the others were affected by different uranium concentration processes during their magmatic or postmagmatic history. The location of these granites is shown in Figure 38.1: a) the granites north of Elliot Lake, Ontario; b) the granites north of Fury and Hecla Strait, Baffin Island; c) the Blachford Lake intrusive complex, N.W.T.; and d) the South Mountain Batholith, Nova Scotia.

Elliot Lake

The Elliot Lake area is well known for its conglomeratic ores composed of detrital unraninite and brannerite in pyritiferous Huronian quartz-pebble conglomerates. To the north of these conglomerates, an older granite mass, more radioactive than normal granites, contains on average 8 ppm U and 37 ppm Th (about twice normal) in stable accessory minerals including thorite, allanite, zircon, monazite, and sphene (Fig. 38.2) (Charbonneau, 1982).

At the present erosion level, these granites are not known to contain any uranium mineralization. Because of their high radioactivity and their proximity to the conglomeratic ores, they have been regarded as a possible source of the uranium in the conglomerates. However, the batholith exposed at the present erosion level is probably quite different from the source granite because the major radioactive constituents of the conglomerates, uraninite and brannerite, are not found in the granite presently exposed. The source of the uranium in the conglomerates may have been a different phase of this granite, rich in radioactive pegmatites or veins, now completely eroded.

A radiometric profile across the Elliot Lake area (Fig. 38.3) shows the ore deposits in the conglomerates as intense anomalies which in fact correspond to the mine dumps. The granite is shown by the increase in potassium. Note that uranium and thorium vary sympathetically over the entire batholith resulting in a flat U/Th ratio.

A radiometric signature such as this, where U and Th vary sympathetically over the entire batholith producing a constant U/Th ratio is believed to indicate that uranium and thorium have not separated to any significant degree as a result of magmatic or postmagmatic processes. Whether the U/Th ratio is high or low will depend on the ratio of the original magma. In these granites, U and Th are tied in stable accessory minerals in a nonlabile form. As a result, one would not expect such granites to be mineralized.

Fury and Hecla Strait

At Fury and Hecla Strait there are two strong radiometric anomalies caused by two granite masses which are probably connected at depth (Fig. 38.4) (Maurice, 1982). The granite is typically calc-alkaline containing on the average 8 ppm U and 84 ppm Th (similar in U content to the Elliot Lake granite). The radioactive accessory minerals are also similar to those at Elliot Lake with allanite and thorite constituting the main phases with some zircon and sphene. At Fury and Hecla, however, the allanites and the thorites are invariably altered, suggesting that they have lost at least part of their uranium content.

A profile across the anomaly (Fig. 38.5) shows a uniform Th distribution, interrupted here and there by fresh water lakes and a thickening till cover on the north side. Th varies sympathetically with potassium indicating that Th is uniformly distributed over the entire batholith.

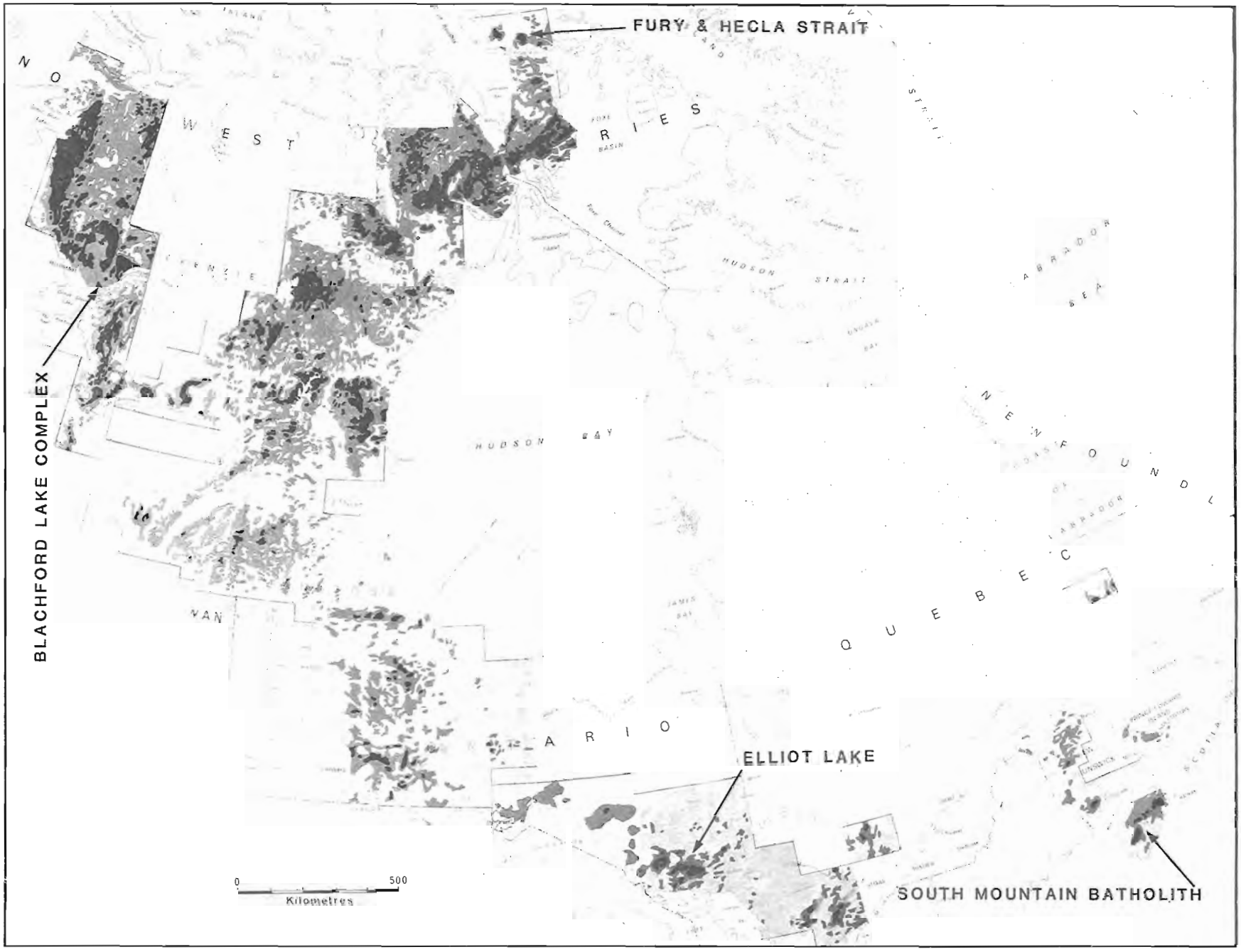

Figure 38.1. *Uranium distribution in Canada from airborne radiometric surveys flown along lines 5 km apart. Light shading: 0 to 1 ppm eU; medium shading: 1 to 2 ppm eU; dark shading: over 2 ppm eU. The four areas discussed in this paper are indicated.*

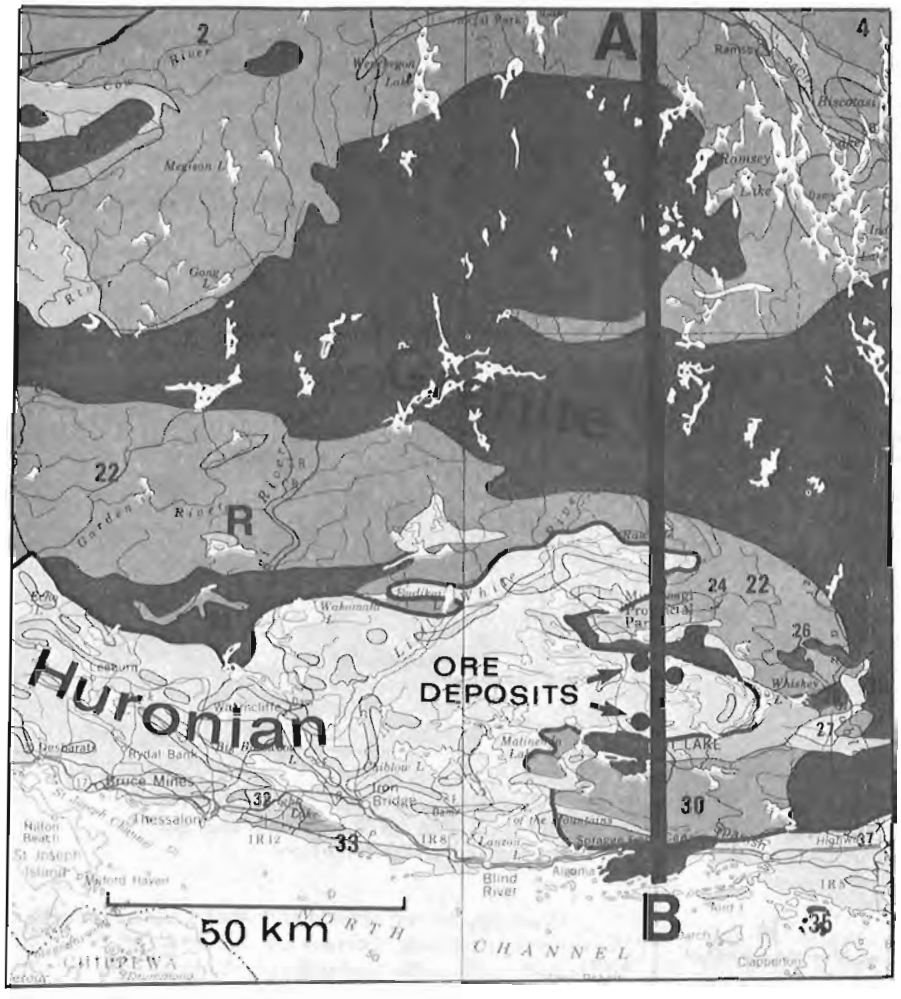

Figure 38.2

General geology of the Elliot Lake area. Granites are shown in dark tone. Note location of conglomeratic ore deposits and profile A-B (Fig. 38.3).

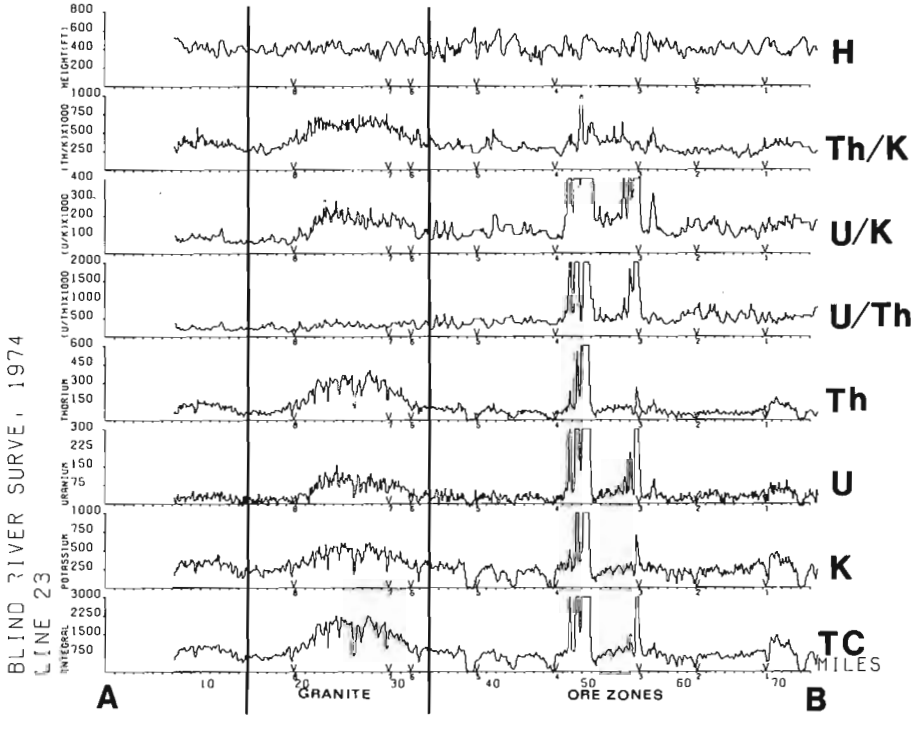

Figure 38.3. *Radiometric profile along line A-B (Fig. 38.2). TC = total count; H = height.*

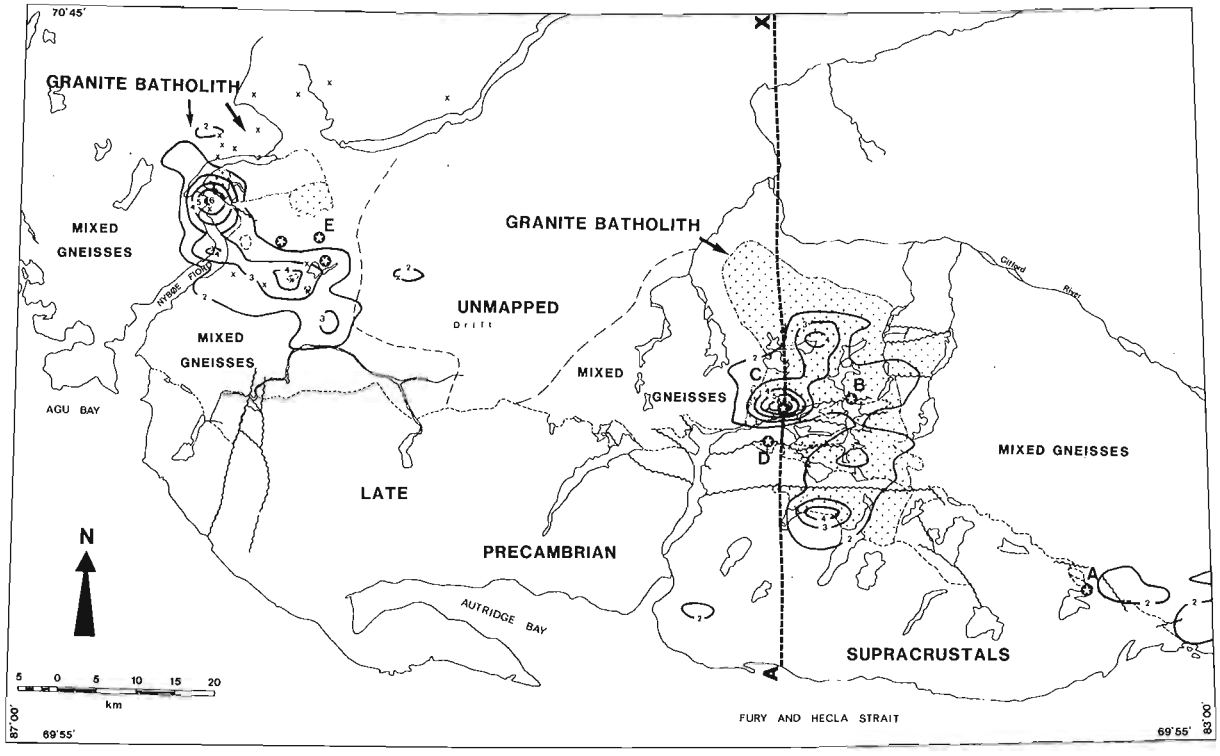

Figure 38.4. General geology of Fury and Hecla Strait area after Chandler et al. (1980) showing radiometric anomalies (contoured in ppm eU) and location of profile A-X (Fig. 38.5). The Xs near the western anomaly indicate isolated granite outcrops. Stars indicate uranium mineralization.

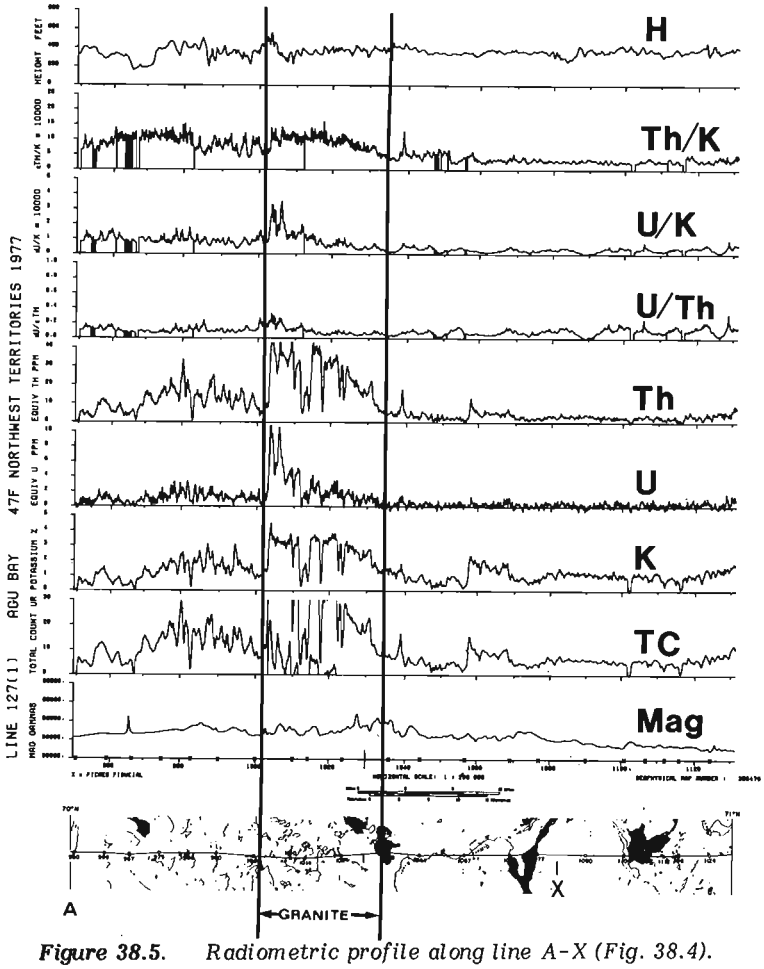

Figure 38.5. Radiometric profile along line A-X (Fig. 38.4).

Uranium, on the other hand, shows a sharp increase in a much narrower portion of the granite producing U/Th and U/K ratio anomalies. Examination of thin sections has indicated that in the more uraniferous parts of the granite, postmagmatic addition of uranium took place (Maurice, 1982). In these areas, uranium is found in microfractures, along grain boundaries and adsorbed onto sericite and biotite. None of the major elements shows similar variation to uranium ruling out the possibility that uranium enrichment is due to magmatic differentation. Uranium is thought to have been removed from the bulk of the granite mass and concentrated in certain parts of the batholith as a result of supergene or hydrothermal processes.

At Fury and Hecla Strait, this situation is particularly interesting. The age of the granite is uncertain but the uranium enrichment occurs near an unconformity which is about the same age as the Athabasca unconformity where uranium deposits are also thought to originate from uranium remobilization from a granitic source rock, followed by concentration in suitable traps (Darnley, 1982). At Fury and Hecla Strait, vein type mineralization, very low in thorium, has been found at localities B, C, and D shown in Figure 38.4.

Blachford Lake Complex

Another mechanism for concentrating uranium in magmatic processes is differentiation. This is seen at the 2150 Ma old Blachford lake igneous complex (Fig. 38.6) which constitutes a differentiated series ranging in composition from gabbro and diorite to peralkaline granite and syenite (Davidson, 1982). The magma that produced this differentiated series probably did not contain high radioelement concentrations. The various rock types range from less than 1 ppm U and less

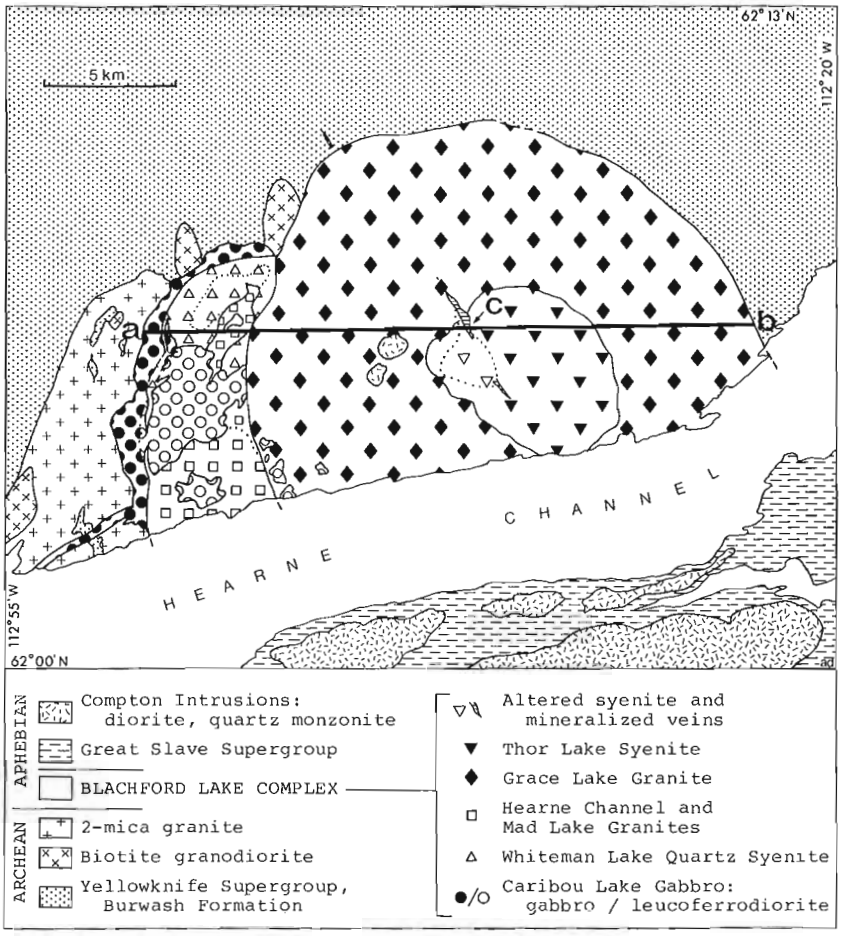

Figure 38.6

General geology of Blachford Lake complex from Davidson (1982) and location of profile a-b (Fig. 38.7).

than 5 ppm Th in the gabbroic and dioritic rocks to 5-6 ppm U and about 30 ppm Th in the aluminous granites. However, both U and Th along with Nb, Ta, F, Be, REE, Rb, and Zr are concentrated in a small body of albitic syenite which, along with localized soda metasomatism and mineralization, is thought to represent the last phase of differentiation (Davidson, 1982). A profile across the complex (Fig. 38.7) shows a sharp anomaly in both the eU and eTh channels and a low U/Th ratio over the most differentiated portion of the complex.

Magmatic differentiation will result in an increase in U and Th towards the more differentiated rocks. Whether this produces a U/Th ratio anomaly or not depends on the proportion of U and Th in the original magma and the degree of U and Th fractionation in the different magmatic phases.

Pegmatites, which are the end product of crystallization of magma, also tend to concentrate radioelements sometimes to very high levels, resulting in anomalous levels of both eU and eTh on radiometric profiles.

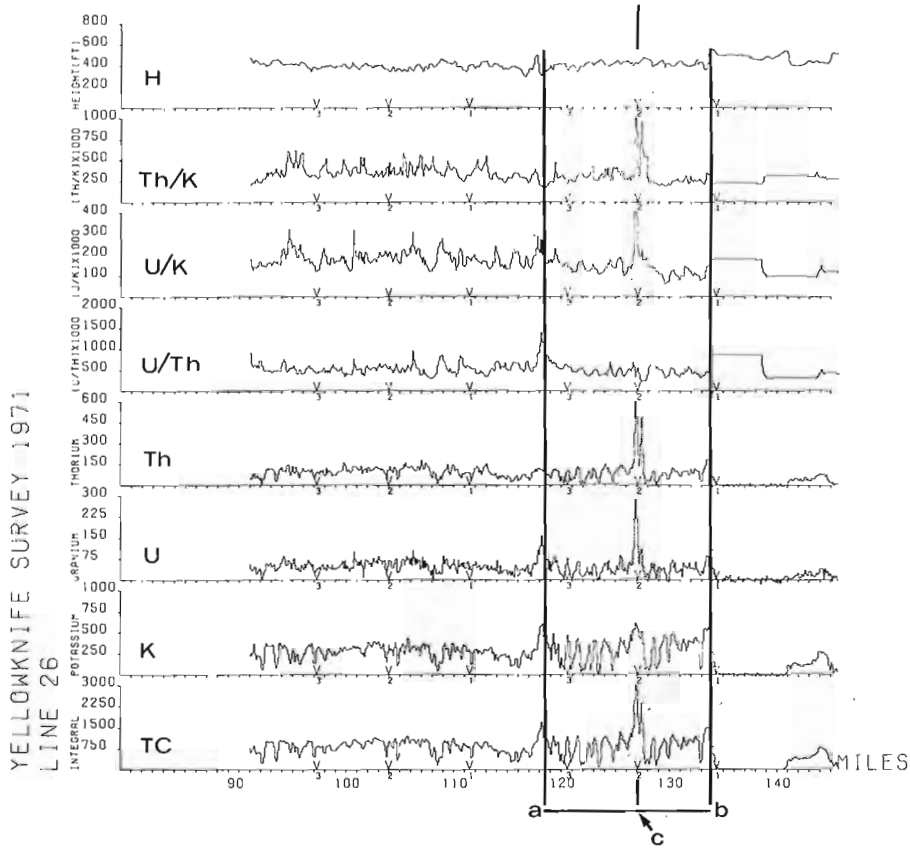

Figure 38.7. *Radiometric profile along line a-b (Fig. 38.6).*

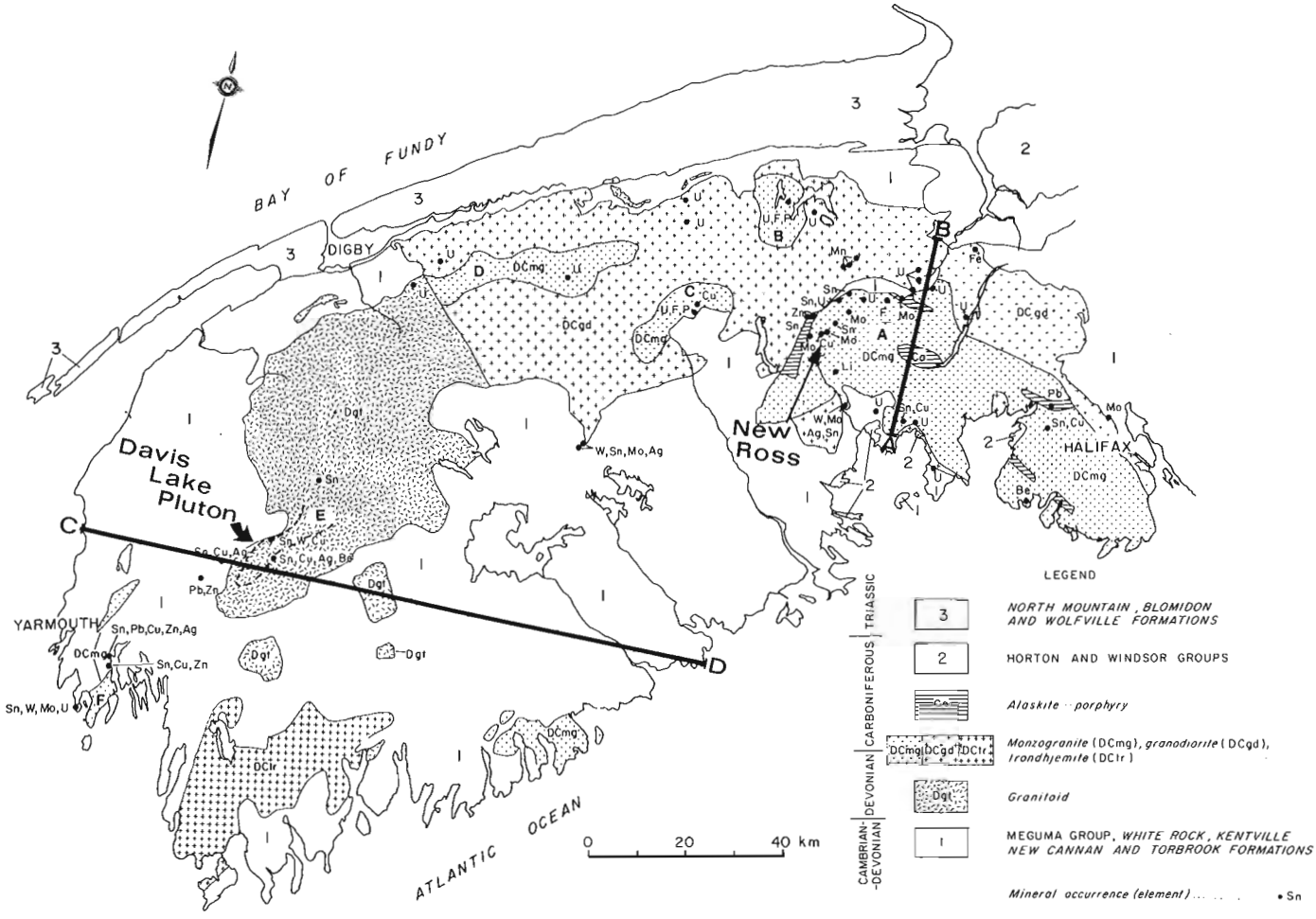

Figure 38.8. *Geology of southwest Nova Scotia from Chatterjee and Muecke (1982) showing location of profiles A-B and C-D (Fig. 38.9, 38.10).*

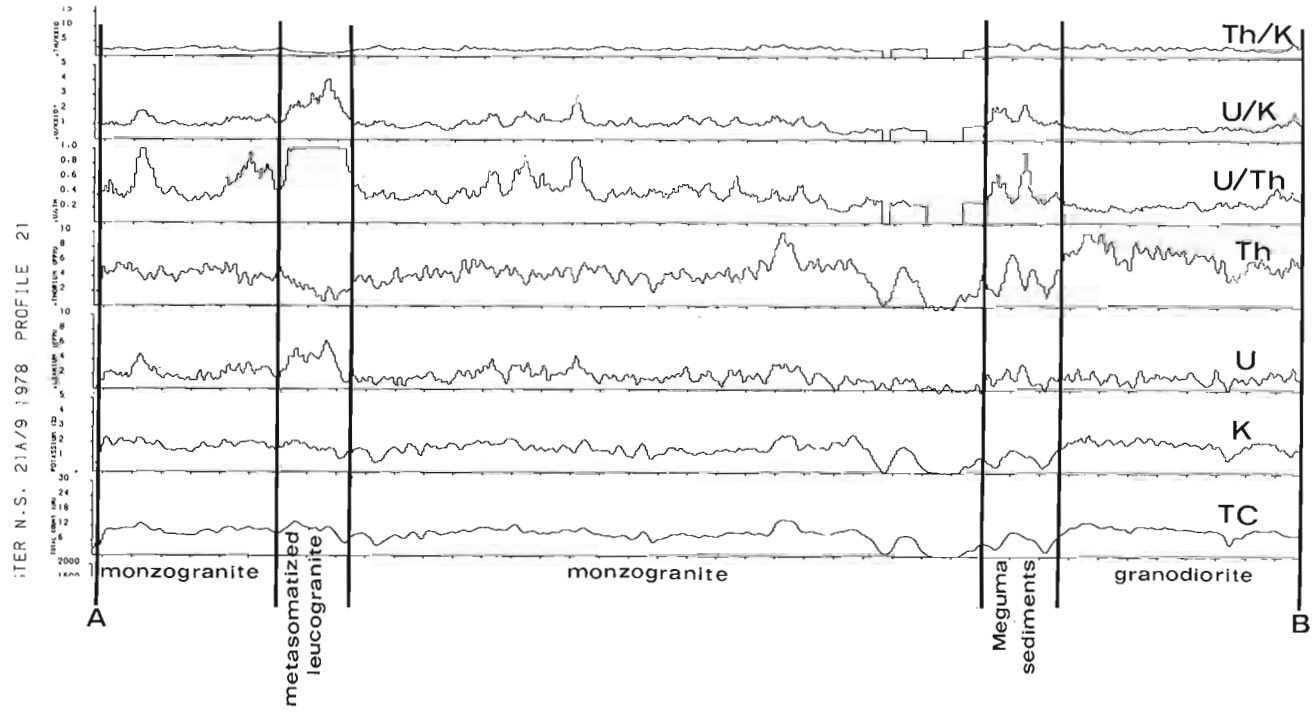

Figure 38.9. *Radiometric profile along line A-B (Fig. 38.8).*

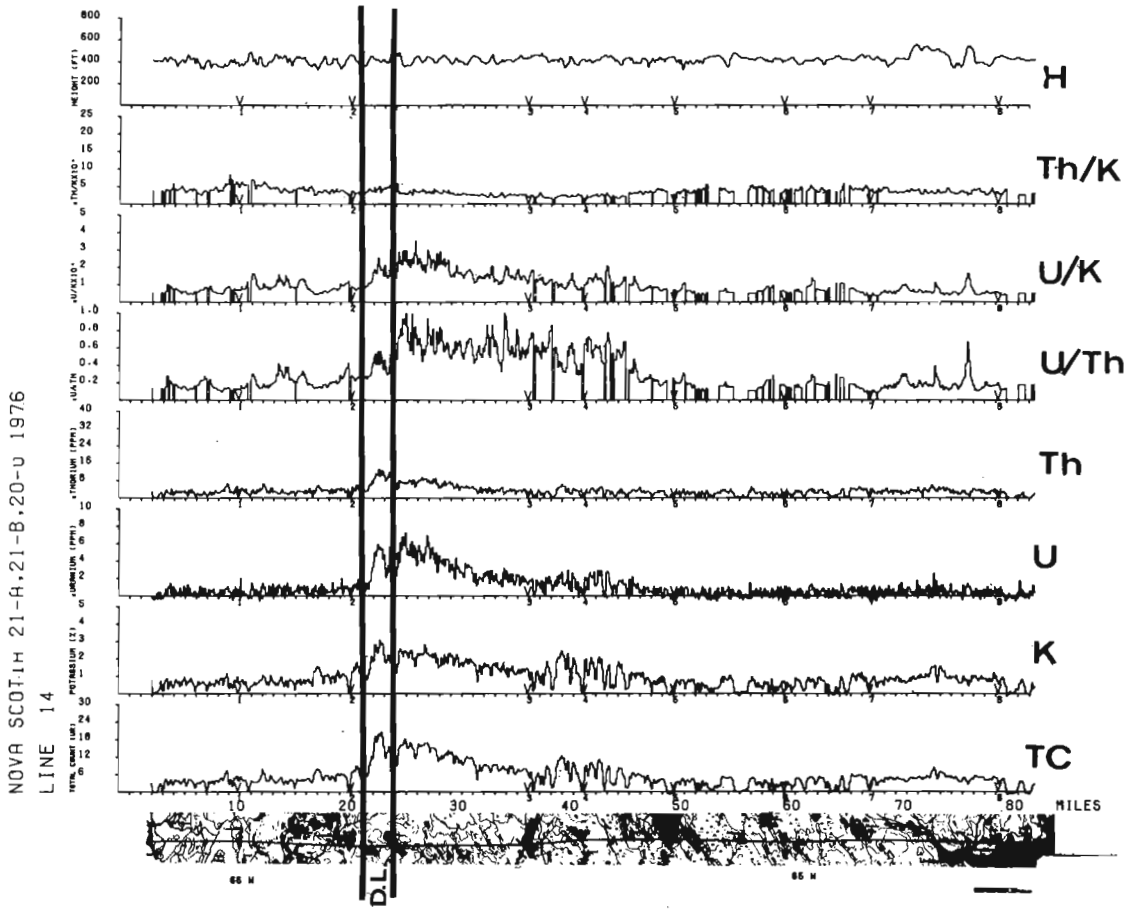

Figure 38.10. *Radiometric profile along line C-D (Fig. 38.8). DL = Davis Lake Pluton.*

Table 38.1

Summary of radioelement behaviour in the four plutons investigated in this study.

RADIOELEMENT CONCENTRATION PROCESSES	EXAMPLES	RADIOELEMENT BEHAVIOUR (DETECTABLE ON AIRBORNE PROFILES)
unmineralized	Elliot Lake, Ont.	Th = uniform over entire batholith U = follows Th over entire batholith U/Th= uniformily low or high depending on original ratio in the magma
post-magmatic remobilization and concentration	Fury and Hecla, N.W.T.	Th = uniform over entire batholith U = increases in certain parts of batholith U/Th= increases with U; generally low elsewhere
magmatic differentiation including pegmatites	Blachford Lake, N.W.T. Davis Lake, N.S.	Th = increases over the more differentiated phases U = follows Th U/Th= variable depending on original ratio in the magma and degree of fractionation in the different magmatic phases
	New Ross, N.S.	Th = decreases U = increases U/Th= increases sharply

South Mountain Batholith

Figure 38.8 shows the geology of the South Mountain Batholith of late Devonian-early Carboniferous age. The main mass of the batholith consists of granodiorite into which are intruded smaller bodies of biotite-muscovite monzogranite, leucocratic monzogranite, dykes and irregular bodies of aplite and pegmatite. According to Chatterjee and Muecke (1982) these rocks form a cogenetic suite derived from magmatic differentiation. It appears that the more differentiated rocks were affected by a late fluid phase towards the end of the crystallization of the batholith generating what Chatterjee and Muecke (1982) called a paraintrusive suite of biotite leucogranite, argillized and sericitized granites, albitites, and various types of greisens. During this evolution, two different trends have developed in the concentration of the radioelements.

In the New Ross area, where U-Sn mineralization occurs in the paraintrusive rocks, Chatterjee and Muecke (1982) have shown from surface and drill core samples, that uranium increases with differentiation while thorium decreases.

This trend is visible on the airborne radiometric profile shown in Figure 38.9. Across the New Ross area (profile A-B, Fig. 38.8) the profile shows a sharp drop in thorium with increasing uranium in the metasomatized leucogranites, with sharp increase in the U/Th ratio. Note also that the granodiorite is slightly higher in thorium than the more differentiated monzogranite. This decrease in thorium with increasing differentiation is unusual, although M. Cuney (personal communication, 1982) found similar situations in France.

In another part of the batholith, in the Davis Lake pluton (Fig. 38.8), the normal differentiation trend, with both U and Th increasing with differentiation, is apparent. This area contains an important deposit of Sn-W but no known U occurrences.

The airborne profile shown in Figure 38.10, representing line C-D on Figure 38.8, confirms these observations. Note an increase in the U/Th ratio suggesting that, unlike the Blachford Lake case, there was proportionally more U than Th in the original magma.

Muecke and Chatterjee (1982) have speculated that the partitioning of U from Th as seen in the New Ross area may be more favourable for the occurrence of U-Sn mineralization than the more normal differentiation trend as seen in the Davis Lake area.

Summary

The behaviour of radioelements, as detected on airborne radiometric profiles, for the four plutons investigated in this study is summarized in Table 38.1. This constitutes a first attempt to recognize and classify radioactive granites on the basis of airborne radiometric signatures and the method has yet to be tested against other cases both in Canada and abroad. It will surely undergo many modifications. One future addition will be to incorporate gravity and magnetics as well as multielement geochemical data obtained from regional lake and stream sediment and water surveys which are available for large parts of Canada.

References

Chandler, F.W., Charbonneau, B.W., Ciesielski, A., Maurice, Y.T., and White, S.
1980: Geological studies of the late Precambrian supracrustal rocks and underlying granitic basement, Fury and Hecla Strait area, Baffin Island, District of Franklin; in Current Research, Part A, Geological Survey of Canada, Paper 80-1A, p. 125-132.

Charbonneau, B.W.
1982: Radiometric study of three radioactive granites in the Canadian Shield: Elliot Lake, Ontario; Fort Smith, and Fury and Hecla, N.W.T.; in Uranium in Granites, ed. Y.T. Maurice; Geological Survey of Canada, Paper 81-23, p. 91-99.

Chatterjee, A.K. and Muecke, G.K.
1982: Geochemistry and the distribution of uranium and thorium in the granitoid rocks of the South Mountain Batholith, Nova Scotia: Some genetic and exploration implications; in Uranium in Granites, ed. Y.T. Maurice; Geological Survey of Canada, Paper 81-23, p. 11-17.

Darnley, A.G.
1982: 'Hot' granites: some general remarks; in Uranium in Granites, ed. Y.T. Maurice; Geological Survey of Canada, Paper 81-23, p. 1-10.

Darnley, A.G., Cameron, E.M., and Richardson, K.A.
1975: The Federal-Provincial Uranium Reconnaissance programs; in Uranium Exploration 1975; Geological Survey of Canada, Paper 75-26, p. 49-68.

Davidson, A.
1982: Petrochemistry of the Blachford Lake complex near Yellowknife, Northwest Territories; in Uranium in Granites, ed. Y.T. Maurice; Geological Survey of Canada, Paper 81-23, p. 71-79.

Maurice, Y.T.
1982: Uraniferous granites and associated mineralization in the Fury and Hecla Strait area, Baffin Island, N.W.T.; in Uranium in Granites, ed. Y.T. Maurice; Geological Survey of Canada, Paper 81-23, p. 101-113.

Muecke, G.K. and Chatterjee, A.K.
1982: Lithogeochemistry as an indicator of uranium and tin mineralization, South Mountain Batholith, Nova Scotia, Canada; 9th International Geochemical Exploration Symposium, Saskatoon (abstract), p. 65-68, May 12-14.

39.

GEOLOGY OF THE D'ESPOIR BROOK MAP AREA AND PART OF THE FACHEUX BAY MAP AREA, SOUTH-CENTRAL NEWFOUNDLAND[1]

Project 820026

W.L. Dickson[2] and S.L. Tomlin[3]
Newfoundland Department of Mines and Energy

Dickson, W.L. and Tomlin, S.L., Geology of the D'Espoir Brook map area and part of the Facheux Bay map area, south-central Newfoundland; in Current Research, Part A, Geological Survey of Canada, Paper 83-1A, p. 285-290, 1983.

Also in Current Research, ed. R.V. Gibbons, Newfoundland Department of Mines and Energy, Mineral Development Division, Report 83-1, 1983.

Abstract

The D'Espoir Brook map area, in south-central Newfoundland, is dominated by the Silurian North Bay Granite which has intruded a variety of gneissic, metasedimentary and foliated granitoid rocks which range in age from possibly Late Precambrian to Ordovician. Possible Precambrian basement rocks consist of strongly foliated tonalitic and granodioritic biotite ± muscovite gneiss and migmatite which form large screens (up to 2 km^2) within the granitoid terrane. Middle Ordovician metasedimentary rocks of the Baie d'Espoir Group outcrop along the northern and southern margins of the map area and consist of polydeformed and highly metamorphosed biotite-garnet psammites and semi-pelites with minor staurolite-bearing schist. Near the northern margin of the map area, an elongate belt of strongly deformed granitoids has intruded the Baie d'Espoir Group. The North Bay Granite, which has been radiometrically dated at 430 and 427 Ma, cuts all the other major units in the area. The North Bay Granite consists of four major rock types: medium grained, equigranular, biotite ± muscovite granodiorite; medium grained, porphyritic, biotite granite; medium grained, equigranular, biotite ± muscovite granite; and coarse grained, coarsely porphyritic, biotite granite. All units of the North Bay Granite have been variably deformed during the later deformation events of the metasediments. The deformation of the metasediments and North Bay Granite is considered to be Acadian. The North Bay Granite has been intruded by a few massive diabase and microsyenite dykes. No significant metallic mineral occurrences were found. Four large quartz veins (one of which has been assessed at over 1.22 x 10^{6}t) have some potential as a source of silica.

Introduction

Location and Access

The D'Espoir Brook map area is located in south-central Newfoundland between 47°45'N and 48°N and longitudes 56°W and 56°30'W. Facheux Bay map area (11P/9) is located immediately to the south (Fig. 39.1). The town of St. Albans is located about 10 km east of D'Espoir Brook map area. Access to the northeast corner of the map area is gained by the Upper Salmon River hydro-electric project access road.

North Bay, East Bay and Facheux Bay provide access to Facheux Bay map area and the southern part of D'Espoir Brook map area. These fjords, however, are bounded by high, steep cliffs which prevent access to the plateau. Most of the study area was mapped from the helicopter-placed fly camps and by canoe and foot traverses from the road.

Exposure is excellent in the southern and eastern parts of the map area, and along the ridge to the west of D'Espoir Lake. In the remaining areas exposure is poor and much of this area was surveyed by helicopter.

Previous Work

Jewell (1939) mapped the North Bay and East Bay area as part of a survey of the Bay d'Espoir area and introduced the term North Bay Granite. The only other major work carried out in the map area was by Williams (1971) who mapped at 1:250 000 scale and defined the main lithological units. Colman-Sadd (1974, 1980) and Colman-Sadd and Swinden (1981) have briefly described a few aspects of the geology in the North Bay and Facheux Bay areas and postulated that a Late Precambrian gneissic basement is present, mainly as large screens, within the North Bay Granite.

Butler (1973) and Butler and Greene (1976) carried out a detailed geochemical assessment of a large quartz vein near the northern edge of the map area to determine the potential of the vein as a source of silica.

The D'Espoir Brook and Facheux Bay map areas formed part of a reconnaissance lake sediment geochemical survey carried out by Butler and Davenport (1978), Davenport and Butler (1981) and Davenport (1982) to assess the mineral potential of south-central Newfoundland. Only tungsten gave a significant anomaly within D'Espoir Brook map area (Davenport, 1982).

The adjacent map area to the east (1M/13) was mapped by Colman-Sadd (1976). The area to the south (11P/9) was mapped by Blackwood (1983) and part of the map area to the north (12A/1E) was mapped by Colman-Sadd (1983). The map area to the west (11P/15) will be mapped during 1983.

General Geology

The rocks of the D'Espoir Brook map area can be divided into four main units as follows:

Strongly deformed paragneiss, tonalitic gneiss and migmatitic granite and granodiorite which occur as large screens and underlie sizeable areas within the North Bay Granite. These gneisses are concentrated in the east-central and eastern parts of the map area and along the northern margin of the North Bay Granite. Colman-Sadd (1974) has termed some of these deformed rocks the Little Passage Gneisses. The structural complexity of the gneisses compared to the Baie D'Espoir Group led Colman-Sadd (1974, 1976) to suggest that the gneisses were possibly Precambrian.

---

[1] Contribution to Canada-Newfoundland co-operative mineral program 1982-84. Project carried by Geological Survey of Canada and Newfoundland Department of Mines and Energy.

[2] Newfoundland Department of Mines and Energy, Mineral Development Division, P.O. Box 4750, St. John's, Newfoundland, A1C 5T7.

[3] 78A Carter's Hill, St. John's, Newfoundland, A1C 4C2.

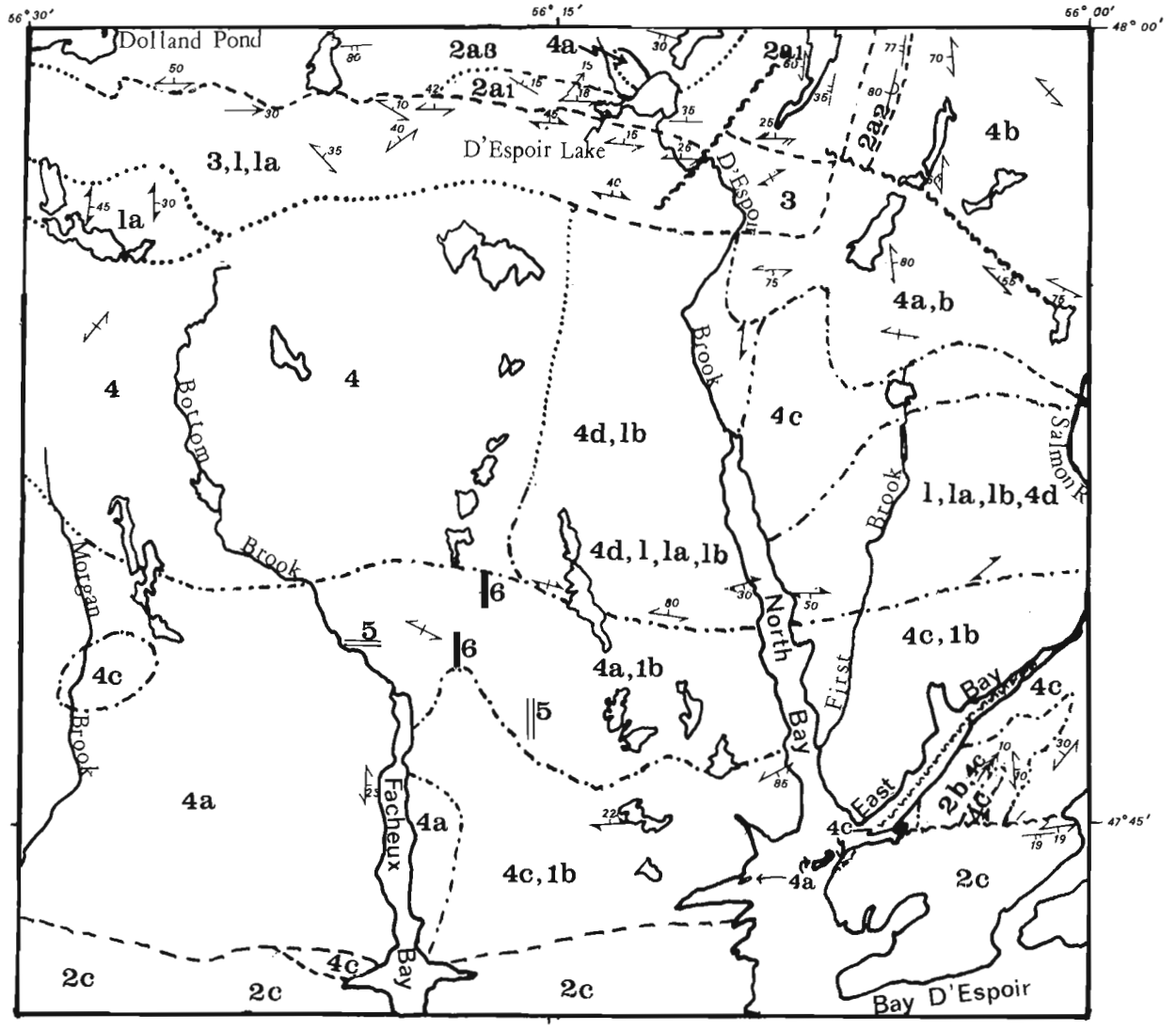

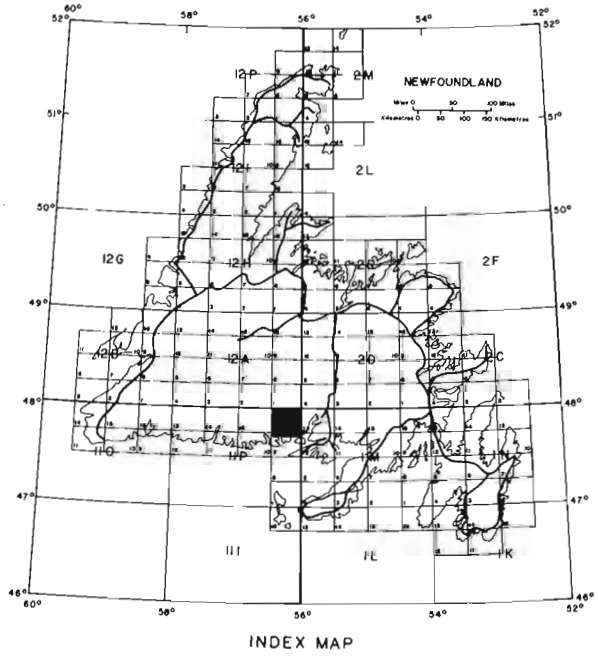

miles
kilometers
Scale 0 5
0 5

SYMBOLS

- gneissic layering or foliation
- bedding (top known/overturned/unknown)
- cleavage (first / second)
- plunge of fold
- dyke – diabase
- dyke – syenite
- fault
- geological contact (approximate / gradational / assumed)

Figure 39.1. *Geology of D'Espoir Brook map area (11/P16) and part of Facheux Bay (11/P9), Southern Newfoundland.*

Variably deformed and metamorphosed metasediments of the Salmon River Dam Formation and the Riches Island Formation which form part of the Ordovician Baie d'Espoir Group.

Strongly deformed granitic gneiss, foliated granite and leucogranite which are located along the northern margin of the North Bay Granite.

The North Bay Granite consisting of a variety of granitoids that range in composition from biotite granodiorite to garnet-muscovite leucogranite. The granitoids also vary in degree of deformation from locally strongly schistose granitoids in the northeast of the map area to weakly deformed or massive in the remainder of the map area.

Rb-Sr (whole rock) age dates from the eastern end of the North Bay Granite (east of the map area) have been determined by Elias (1981) who obtained Rb-Sr (whole rock) ages of 430 ± 4 Ma and 427 ± 11 Ma. These dates indicate a Silurian age for the North Bay Granite.

LEGEND FOR FIGURE 39.1

CARBONIFEROUS ?

6 Massive, fine grained, diabase dykes.

DEVONIAN ?

5 Massive, fine grained, leucocratic biotite-hornblende microsyenite dykes.

SILURIAN

4 North Bay Granite:

4a, Massive, medium grained, porphyritic biotite granite;

4b, medium to coarse grained, porphyritic biotite granite;

4c, medium grained, equigranular to slightly porphyritic biotite ± muscovite granodiorite;

4d, massive, medium grained, equigranular biotite ± muscovite granite.

3 Strongly foliated, equigranular to porphyritic biotite-muscovite and biotite granite, and garnet-muscovite leucogranite.

ORDOVICIAN

2 Baie d'Espoir Group:

2a, Salmon River Dam Formation;

2a1, Thin to medium bedded, grey sandstones, calcareous sandstones; minor limestone;

2a2, thin bedded black, rusty pelites and semi-pelites;

2a3, strongly deformed and metamorphosed equivalent of 2a1-upper greenschist facies;

2b, Riches Island Formation: Interbedded pelites, semi-pelites and psammites. Variably metamorphosed from lower greenschist to upper amphibolite facies;

2c, Undivided Baie d'Espoir Group: Includes metasediments, metavolcanics, migmatites, and minor granitic dykes from the North Bay Granite.

PRECAMBRIAN ?

1 Strongly foliated orthogneiss and paragneiss.

1a, banded, pink, medium grained, biotite granodioritic migmatite;

1b, strongly schistose, semi-pelites, psammites, amphibolites, orthoquartzites.

The area has been substantially modified by glacial action. The central part of the map area is covered by a thick blanket of till, which contains well rounded boulders up to 3 m in diameter. Ultramafic boulders were found throughout the map area and indicate a minimum transportation of 40 km from the nearest known source of ultramafics. Several southerly trending eskers occur in northern part of the map area; the largest is 5 km in length. Glacial striae and stoss and lee surfaces indicate a southerly direction of ice movement.

Description of units

Precambrian?, strongly foliated, orthogneiss and paragneiss - Unit 1

A variety of strongly deformed and metamorphosed granitoid and metasedimentary rocks occur throughout the North Bay Granite in the study area. Two main areas of these rocks can be defined. One area, to the south and west of D'Espoir Lake within unit 3, contains strongly banded, biotite granodiorite gneiss which occurs as abundant large xenoliths in the strongly foliated granitoids. The other area is located south of D'Espoir Lake, within units 3 and 4, and consists of several square kilometres of granodioritic gneiss which is cut by numerous thin pegmatite dykes and massive granodiorite dykes (subunit 4c). On the east side of North Bay, the gneiss is tonalitic and locally garnetiferous and has a well developed vertical L-S fabric. No metasedimentary xenoliths were found in the orthogneiss.

Subunit 1a consists of a pink, medium grained, biotite granodiorite with an abundance of slightly contorted, well-aligned, discontinuous layers of biotite, up to 6 cm long and 1 to 3 mm thick. The granodiorite matrix has a weak foliation which is parallel to the aligned biotite layers. The rock is possibly an injection gneiss or migmatite. This rock type is best exposed on the west side of North Bay and near the northwest corner of D'Espoir Brook map area.

Subunit 1b is tentatively included within unit 1. The rock types include strongly schistose amphibolite facies semi-pelites, psammites, amphibolites, and orthoquatzites, which are locally migmatized. Biotite psammite, the most common rock type within subunit 1b, occurs as screens which range in length from a few centimetres to about 100 m. Sillimanite-bearing, biotite-rich semi-pelite also forms a few screens. The southern portion of the North Bay Granite, mainly within subunit 4c, contains an abundance of metasedimentary screens. Throughout the map area, the screens contain a strong tectonic foliation which is commonly folded. The main deformation of the screens clearly predates their incorporation into the North Bay Granite. In areas where the granite contains a tectonic fabric, this fabric can also be traced into the sedimentary screens at an angle to the main fabric in the metasediments.

Colman-Sadd (1974, 1976, 1980) has included the metasediments, which are spatially associated with the orthogneisses (unit 1), within a Precambrian basement terrane. However, the strong similarity in grade of metamorphism, degree and style of deformation, and lithology of these metasediments with those of the Riches Island Formation to the south indicates that the paragneiss may be Ordovician rather than Precambrian in age (see Blackwood, 1983).

Ordovician Baie d'Espoir Group - Unit 2

This unit was not examined in detail within map area 11P/9 in this project. Blackwood (1983) mapped this unit in 11P/9 and has described it as pelitic, semi-pelitic and psammitic schists, with concordant, leucogranite veins and migmatites, which are probably Ordovician in age. The unit is cut by the North Bay Granite in map area 11P/9.

Ordovician Salmon River Dam Formation - Unit 2a. The Salmon River Dam Formation (unit 2a), within the map area, is located along the northern margin of the North Bay Granite and unit 3 and forms the lower part of the Baie d'Espoir Group (Colman-Sadd, 1976). In the lesser deformed areas of the formation (subunit 2a1), the rocks consist of thin to medium and parallel bedded, grey sandstones and calcareous sandstones, with poorly developed parallel laminations, graded beds, local flame structures and convolute laminations. Most beds are massive. One isolated thick, massive bed of limestone also occurs at the southern edge of the subunit, close to the contact with unit 3, southwest of D'Espoir Lake. Subunit 2a2, conformably overlies subunit 2a1 and consists of thinly bedded, and strongly cleaved, rusty siltstones and sandstones with locally well developed parallel laminations. Subunit 2a3 is probably a higher grade metamorphic equivalent of subunit 2a1. It is also more intensely deformed with tight isoclinal folds, transposed bedding, and commonly contains two strong schistosities. Subunit 2a3 also contains minor metatuff. Granitoid veins and dykes are common within subunit 2a3, and these are also strongly deformed.

The Salmon River Dam Formation, within the map area, can be divided into two structural units. To the west of D'Espoir Lake, the Salmon River Dam Formation bedding and cleavage generally have a strong easterly trend. S_1 is generally parallel to S_0, and near the contact with unit 3 bedding dips gently to the north at about 15° A second step cleavage, axial planar to open folds, trends towards the northeast. To the east of D'Espoir Lake, the metasediments have a northerly trend with a steep S_1 cleavage parallel to S_0. S_2 transposes S_1 and has an easterly trend. Lack of exposure has obscured the intermediate area but from an aerial photo interpretation there appears to be a gradual change in structural orientation which indicates the presence of a major gently plunging northerly trending synform.

West of D'Espoir Lake, within subunit 2a1, a tight isoclinal fold occurs within a thinly bedded unit. The axial plane is subparallel to bedding and the fold axis plunges gently to the northeast. This is probably an F_1 fold and indicates that subunit 2a1 has been recumbently folded.

Ordovician Riches Island Formation - Subunit 2b. To the southeast of East Bay (within map area 11P/16), a sequence of interbedded pelites, semi-pelites, and orthoquartzites (subunit 2b), which have been polydeformed and invaded by thick granite dykes (subunit 4c), is tentatively assigned to the Ordovician Riches Island Formation of Colman-Sadd (1976). The sequence is dominated by highly metamorphosed biotite-muscovite schists which locally contain garnet and staurolite. Interbedded with the schists is a sequence of strongly cleaved orthoquartzites which is concentrated in a northeasterly trending belt in the centre of the area.

To the south of the easterly trending fault near the southeast corner of map area 11P/16, the Riches Island Formation consists of thin to medium bedded, black pelites which structurally underlie a thick sequence of psammites found mainly within map area 11P/9.

The Riches Island Formation is polydeformed with two main tectonic fabrics and two readily apparent fold generations. S_1 is a gently dipping schistosity, which is subparallel to bedding and is also axial planar to F_1 folds. The fold axes of the F_1 folds plunge to the northeast at a low angle. The S_1 schistosity is folded by F_2 and forms upright to slightly overturned folds with a moderate to steeply dipping axial planar cleavage. The F_2 folds also plunge to the northeast at a low angle.

Granite and pegmatite dykes are abundant throughout the Riches Island Formation and have been deformed during the second deformation of the metasediments.

Undivided foliated granites and granodiorites - Unit 3

Unit 3 consists of a variety of strongly foliated, mainly leucocratic granites which range in composition and texture from medium grained, equigranular, biotite granite and porphyritic biotite granite to equigranular muscovite-garnet granite and pegmatite.

Southeast of Dolland Pond, medium grained, biotite-muscovite granite intrudes metasediments of the Ordovician Salmon River Dam Formation. Southeast of D'Espoir Lake, the leucogranite contains small xenoliths of grey psammite which are clearly derived from the Salmon River Dam Formation to the north. The contact is otherwise unexposed and is generally marked by a pronounced break in slope from the granite to the metasediments. Tonalitic gneiss (unit 1) commonly occurs as screens in unit 3, particularly south of D'Espoir Lake and 6 km east-southeast of Dolland Pond. Unit 3 is cut by weakly foliated biotite granodiorite dykes similar to subunits 4c and 4d.

The generally poor exposure of unit 3 and the presence of a great variety of granites has prevented a meaningful subdivision of the various varieties of foliated granite.

The granites of unit 3 are strongly deformed, with a well developed foliation defined by aligned mica and flattened quartz and feldspar. Locally, a second fabric or folding of the first fabric may be found. The first fabric generally dips gently to the north. In the vicinity of D'Espoir Lake, the granites are more intensely deformed than the adjacent metasediments. It is possible that the metasediments and the granites in the D'Espoir Lake area are in fault contact.

North Bay Granite - Unit 4

The North Bay Granite has been subdivided into four subunits (4a-4d) based on rock type and texture. Contacts are generally gradational and only subunit 4c has a clear intrusive relationship with the other subunits. Dykes of subunit 4c have intruded subunits 4a and 4b. The contacts between the other units are considered to be gradational as grain size, colour, proportion of muscovite and the proportion of phenocrysts may vary over distances of about 1 km. Granitoid dykes from the other units are generally absent.

The undivided area of the North Bay Granite (unit 4 on Fig. 39.1) is an area of very poor exposure with a number of varieties of granite. The widely scattered outcrops prevent a meaningful subdivision of this area.

Massive, medium grained, porphyritic, biotite granite - Subunit 4a. Subunit 4a is mainly located in the southern, southwestern and eastern parts of the map area. The dominant rock type is pink to white, porphyritic biotite granite with 10 to 20% phenocrysts of alkali feldspar, 1 to 2 cm in length, in an equigranular matrix of quartz, plagioclase, alkali feldspar and biotite and rare muscovite. In the southwest corner of the map area, the granite contains a prominent but weak fabric defined by poorly aligned biotite and phenocrysts of alkali feldspar.

Immediately to the north of First Brook, subunit 4a contains a relatively high proportion of garnets (approximately 1%), which range in diameter from less than 1 mm to over 1 cm. The large garnets are highly shattered and are slightly altered. Inclusions of quartz are commonly present in the large garnets. The granite also contains minor muscovite. Screens of schist are also locally abundant in this area.

Dykes of grey, equigranular, biotite granodiorite, similar to subunit 4c, cut subunit 4a. These are particularly prominent along North Bay. However, the contacts between th main bodies of subunits 4a and 4c are apparently gradational over 1 km.

Small pegmatite dykes, which locally contain muscovite, are common throughout subunit 4a. Two microsyenite dykes (unit 5) and two diabase dykes (unit 6) also cut subunit 4a.

Medium- to coarse-grained, porphyritic, biotite granite - Subunit 4b. Subunit 4b is located in the northeast corner of the map area and mainly consists of coarse grained, highly porphyritic, biotite granite which generally contains a weak foliation and/or alignment of potassium feldspar phenocrysts. The unit is cut by a southeast trending fault along which the granite is strongly foliated.

Contacts with the metasediments to the west are not exposed and granite dykes were not found to cut the country rock metasediments. However, screens of strongly schistose biotite psammite and semi-pelite, with minor limestone occur along the fault trace within the granite and these are cut by granite dykes. The contact with subunit 4c is difficult to define. Dykes of subunit 4c cut subunit 4b but no sharp contact was found between the subunits. Towards the southern limit of subunit 4b, in the northeast corner of the map area, the granite becomes finer grained and the size of the phenocrysts is smaller. However, the change is so gradual that in this area subunit 4a is probably equivalent to subunit 4b. Along Salmon River, subunit 4b also occurs as screens in subunit 4c.

The granite consists of essential quartz, microcline, plagioclase and biotite. Muscovite is rarely present. In subunit 4b, phenocrysts range in length from 2 cm to over 10 cm, with an average of 6 cm.

The fabric in the weakly foliated granite is generally defined by the orientation of phenocrysts and a weak parallel alignment of biotite and slightly flattened quartz. The strongly deformed granite along the fault has a mylonitic fabric which dips to the northeast at about 60°. This fabric decreases in intensity to the south over 2 km.

Medium grained, equigranular to slightly porphyritic, biotite ± muscovite granodiorite - Subunit 4c. Subunit 4c is mainly located in the southeastern half of the map area. The dominant rock type is grey, massive to weakly foliated, medium grained, equigranular, biotite granodiorite which locally contains up to 1% muscovite. Screens of migmatite, schist, and granitic gneiss are common, particularly near the entrance to North Bay and East Bay. Some screens are over 100 m in length and, on the cliffs at North Bay, large screens are completely surrounded by granodiorite. Williams (1971) has described this area of abundant screens as a zone of intrusion breccia.

Fine grained, biotite granodiorite dykes and thin pegmatite dykes are common throughout the subunit. Well developed, parallel, alternating biotite-rich and biotite-poor layers, 2 to 3 mm wide, occur in a few outcrops of generally massive granodiorite and are possibly a result of flow foliation.

The granodiorite contains a weakly developed, steeply dipping, easterly trending, tectonic fabric which is defined by poorly aligned biotite.

Minor beryl mineralization occurs in a thin granite pegmatite vein north of East Bay. Pegmatite and quartz veins are particularly abundant south of East Bay, in the vicinity of the contact with the Riches Island Formation.

Massive, medium grained, equigranular, biotite ± muscovite granite - Subunit 4d. This unit is predominately a buff, massive, medium grained, equigranular, biotite granite, which locally contains less than 1% muscovite. The granite locally contains a weak tectonic fabric defined by aligned mica.

West of North Bay, the central part of the unit contains a large proportion of foliated granite, gneiss and migmatite screens. Pegmatite dykes and locally garnetiferous granite veins occur throughout the unit. Quartz veins and segregations are common in the screens but are rare within the granite.

Microsyenite dykes - Unit 5

Massive, fine grained, leucocratic, biotite-hornblende microsyenite dykes were found north and east of Facheux Bay and cut subunit 4a of the North Bay Granite. North of Facheux Bay, the microsyenite forms thin anastomosing veins which cut pegmatites and aplites. Northeast of Facheux Bay, a 10 m wide, northerly trending dyke underlies a prominent northerly trending lineament. This dyke can be traced for over 300 m. These dykes may be related to the Devonian Cape La Hune "Granite" which is described as a syenite by Williams (1971).

Diabase dykes - Unit 6

Two diabase dykes cut subunit 4a of the North Bay Granite, northeast of Facheux Bay. The dykes are 15 cm and 30 cm to 1 m wide respectively. The dykes trend about 180° and are fresh, massive and fine grained, with well developed, chilled margins. Similar dykes occur throughout the Gander Zone and have been considered to be Carboniferous in age (Jayasinghe and Berger, 1976).

Mineralization

Trace amounts of pyrite were found at scattered localities in the North Bay Granite. At one locality, west of Facheux Bay tourmaline associated with the pyrite, occurs along a joint surface. However, an examination of the area failed to reveal further mineralization.

Pyrite-rich pelites occur within the Riches Island Formation in fault contact with the granite. Two generations of pyrite can be determined. Highly flattened pyrite occurs along cleavage planes and euhedral pyrite forms veins on joint surfaces in the pelites. The pelites possibly have some potential for copper mineralization.

A small outcrop of highly silicified, rusty gossan occurs close to the contact between the Salmon River Dam Formation and the unit 3 granitoids (Williams, 1971). Apart from pyrite, no metallic mineralization was found, although Williams (1971) speculated on the possibility of molybdenite mineralization.

Large quartz veins occur along the contact between unit 3 and the Salmon River Dam Formation and cut both units. The largest vein is 12 km west of D'Espoir Lake and cuts the metasediments. Another vein cuts strongly foliated granite 10 km west of D'Espoir Lake, close to the contact with the metasediments. Two smaller veins are located close to the contact between unit 3 and the Salmon River Dam Formation, south of D'Espoir Lake. The largest vein is 600 m in length and up to 100 m in width; the smallest of the major veins is aout 50 m wide and 100 m in length.

Butler (1973) and Butler and Greene (1976) have described and geochemically sampled and largest vein, 12 km east of D'Espoir Lake, and assessed a silica content of 1.22×10^6t. The average analysis of the vein is 97.1% SiO_2, 1.9% Al_2O_3 and 0.5% Fe_2O_3.

The two veins south of D'Espoir Lake are similar to the largest quartz vein west of D'Espoir Lake and probably have a similar chemistry but the vein 10 km west of D'Espoir Lake contains abundant screens of granite and, therefore, has little potential as a source of silica.

Davenport (1982) reported anomalous tungsten values in lake sediment samples taken from the northeast corner of the map area and also southeast of East Bay. A careful examination of the granitoids in these areas did not uncover any wolframite mineralization or alteration. The anomaly in the northwest corner of the map area is within an area of migmatitic granodiorite gneiss (subunit 1a), close to the contact with units 3 and 4. The East Bay anomaly lies within an area of high grade metasediments, biotite-muscovite granite and garnet-tourmaline pegmatite which are cut by numeorus small quartz veins.

Geochemistry

Samples of granitoid rocks were collected from 260 sites using a 2 km grid system from the North Bay Granite in map areas 11P/15, 11P/9 and 12A/1. These samples will be analyzed for major elements and about 20 trace elements including Sn, W, F, Mo, Li and U and will be reported in the final report of this project.

Summary and Conclusions

The Ordovician metasedimentary rocks of the Baie d'Espoir Group have reached the amphibolite facies of metamorphism and have a complex structural history which mainly predates the North Bay Granite. Small recumbent folds and gently dipping cleavage and schistosity indicate that the major folds in these units are also recumbent and verge to the southeast. The gently dipping schistostiy in the strongly foliated granites of unit 3 may also be related to the recumbent folds or possibly to thrusting.

The gneissic granitoids (unit 1) may be older than the Ordovician metasediments and could be basement rocks. Most of the high grade paragneisses are probably Ordovician. However, the situation is still not clear. Samples of the gneissic granitoids have been collected for age dating and may clarify the relationships.

The North Bay Granite is a composite body with a wide variety of granitoids. The granite was syntectonically intruded into the Baie d'Espoir Group, as both contain similarly oriented cleavages. Screens of metasediment are abundant in the granite along a 1 to 2 km wide belt along the southern contact. The latest fabric in the screens is also found in the granite.

A few minor pyrite occurrences occur within the North Bay Granite. However, no other metallic mineralization or any significant alteration of the granite was found. Sizeable quartz veins in the north of the map area have some potential as a source of silica.

Acknowledgments

The efficient and conscientious field assistance of Paul Delaney and Barry Wheaton is greatly appreciated. The co-operation of S.P. Colman-Sadd and R.F. Blackwood throughout the field work was assisted greatly in this project. Sealand Helicopters Ltd., at St. Albans, provided an efficient service. James Barrett, Sydney Parsons and Wayne Ryder of the Newfoundland Department of Mines and Energy provided excellent logistical support. The manuscript has benefitted from critical reading by C.F. O'Driscoll and R.F. Blackwood.

References

Blackwood, R.F.
1983: Geology of the Facheux Bay (11P/9) area, Newfoundland; in Current Research, Editor R.V. Gibbons, Newfoundland Department of Mines and Energy, Mineral Development Division, Report 83-1.

Butler, A.J.
1973: Jocko Pond quartz vein; Newfoundland Department of Mines and Energy, Mineral Development Division, Unpublished report, 9 p.

Butler, A.J. and Davenport, P.H.
1978: A lake sediment geochemical survey of the Meelpaeg Lake area, Central Newfoundland; Newfoundland Department of Mines and Energy, Mineral Development Division, Open File Nfld. 986, St. John's.

Butler, A.J. and Greene, B.A.
1976: Silica resources of Newfoundland; Newfoundland Department of Mines and Energy, Mineral Development Division, Report 76-2, 68 p.

Colman-Sadd, S.P.
1974: The geologic development of the Bay d'Espoir area, southeastern Newfoundland; Unpublished Ph.D. thesis, Memorial University of Newfoundland, 172 p.

1976: Geology of the St. Alban's map area, Newfoundland (1M/13); Newfoundland Department of Mines and Energy, Mineral Development Division, Report 76-4, 19 p.

1980: Geoloy of south-central Newfoundland and the evolution of the eastern margin of Iapetus; American Journal of Science, v. 280, p. 991-1017.

1983: Geology of the east half of the Cold Spring Pond map area (12A/1), Newfoundland; in Current Research, Editor R.V. Gibbons, Newfoundland Department of Mines and Energy, Mineral Development Division, Report 83-1.

Colman-Sadd, S.P. and Swinden, H.S.
1981: Geology and mineral potential of south-central Newfoundland; Newfoundland Department of Mines and Energy, Mineral Development Division, Report 81-5, 84 p.

Davenport, P.H.
1982: Tungsten in lake sediment over granitoids in south-central Newfoundland; Newfoundland Department of Mines and Energy, Mineral Development Division Open File Nfld. 1302, St. John's.

Davenport, P.H. and Butler, A.J.
1981: Fluorine distribution in lake sediment in the Meelpaeg Lake area, Central Newfoundland; Newfoundland Department of Mines and Energy, Mineral Development Division, Open File 1222.

Elias, P.
1981: Geochemistry and petrology of granitoid rocks of the Gander Zone, Bay d'Espoir area, Newfoundland; Unpublished M.Sc. thesis, Memorial University of Newfoundland, 271 p.

Jayasinghe, N.R. and Berger, A.R.
1976: On the plutonic evolution of the Wesleyville area, Bonavista Bay, Newfoundland; Canadian Journal of Earth Sciences, v. 13, p. 1560-1570.

Jewell, W.B.
1939: Geology and mineral deposits of the Baie d'Espoir area; Newfoundland Geological Survey, Bulletin 17, 29 p.

Williams, H.
1971: Burgeo (east half), Newfoundland; Geological Survey of Canada, Map 1196A, with descriptive notes.

40. PRELIMINARY REPORT ON THE GEOLOGY NORTH OF UPPER LAKE MELVILLE, LABRADOR [1]

Project 820030
Contract 1583302

Philippe Erdmer [2]

Erdmer, P., Preliminary report on the geology north of upper Lake Melville, Labrador; in Current Research, Part A, Geological Survey of Canada, Paper 83-1A, p. 291-296, 1983.

Also in Current Research, ed. R.V. Gibbons, Newfoundland Department of Mines and Energy, Mineral Development Division, Report 83-1, 1983.

Abstract

Mapping at 1:100 000 scale of 3500 km² of the eastern Grenville Province suggests that Aphebian or earlier(?) granitic and tonalitic gneiss complexes, that include supracrustal remnants and metagranitoid rocks, are the oldest rocks of the area. The gneiss complexes were intruded by a late Hudsonian or early Paleohelikian granite pluton, as well as by Paleohelikian anorthositic rocks and later(?) plutons of granite to syenite. A southeast dipping mylonite zone that was probably the locus of thrust faulting coincides with the margin of a half graben filled with Hadrynian(?) conglomerate. Several uranium showings are associated with diatexite developed in parts of the granitic gneiss complex. Strain resulting from the Grenvillian Orogeny is either relatively weak or strongly heterogeneous.

Introduction

This report covers approximately 3500 km² of the eastern Grenville Province north of Lake Melville, mapped at 1:100 000 scale during the 1982 field season. It includes NTS 1:50 000 map areas 13F/16, 13G/13, 13G/14 and part of 13J/3 (Figure 40.1).

Eade (1962) and Stevenson (1967, 1970), as a result of reconnaissance mapping of various parts of the area, reported mostly tonalitic and granitic gneiss, commonly with a steeply dipping fabric, intruded by weakly deformed monzonite to granite bodies. Stevenson inferred that the rocks were of Helikian or Aphebian age, or both, and were all affected by the Grenvillian orogeny. Absolute age data remain unavailable. A half graben of Hadrynian (?) arkose and conglomerate (Double Mer Formation) was recognized along the shore of Lake Melville.

Recent systematic mapping of the adjoining areas has been carried out at 1:100 000 scale by Gower (1980), Gower et al. (1981; 1982a, b), Ryan et al. (1981) and Ryan (1982), and at 1:250 000 scale by Emslie (1976; personal communication, 1982). Approximately 200 km² of the present map area between Double Mer and Lake Melville, where several uranium showings occur, were mapped at 1:50 000 scale by Bailey (1980).

The area was selected because it provides a link between mapping by Gower et al. (1981) in the east and by Ryan et al. (1981) in the west, and because it contains recently reported uranium-bearing units.

Setting and General Geology

The area lies approximately 100 km south of the Grenville Front, as defined by Gower et al. (1980), within an east-trending belt of Helikian or earlier(?) dominantly tonalite and granodiorite gneiss with supracrustal remnants, that extends through much of western and central Labrador. This belt separates rocks of an extensive, composite granitic batholith to the north, in which individual plutons have yielded ages from 1700-1650 Ma to 1450-1350 Ma (Wardle et al., 1982), from rocks of the Mealy Mountains anorthositic complex (dated at 1640 Ma, Emslie, 1982) to the south (Fig. 40.1). Small half graben filled with Hadrynian or later(?) conglomerate and sandstone are developed in the gneiss belt.

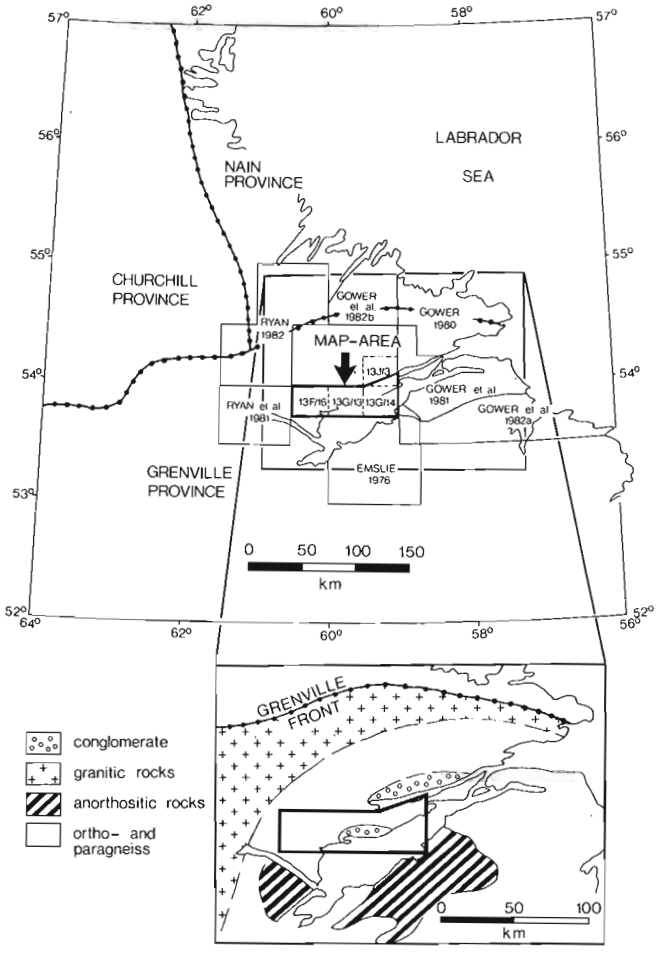

Figure 40.1. *Location and setting of the map area. Regional geology is simplified from sources shown.*

[1] Contribution to Canada-Newfoundland co-operative mineral program 1982-84. Project carried by Geological Survey of Canada.

[2] c/o Newfoundland Department of Mines and Energy, Mineral Development Division, P.O. Box 4750, St. John's, Newfoundland, A1C 5T7.

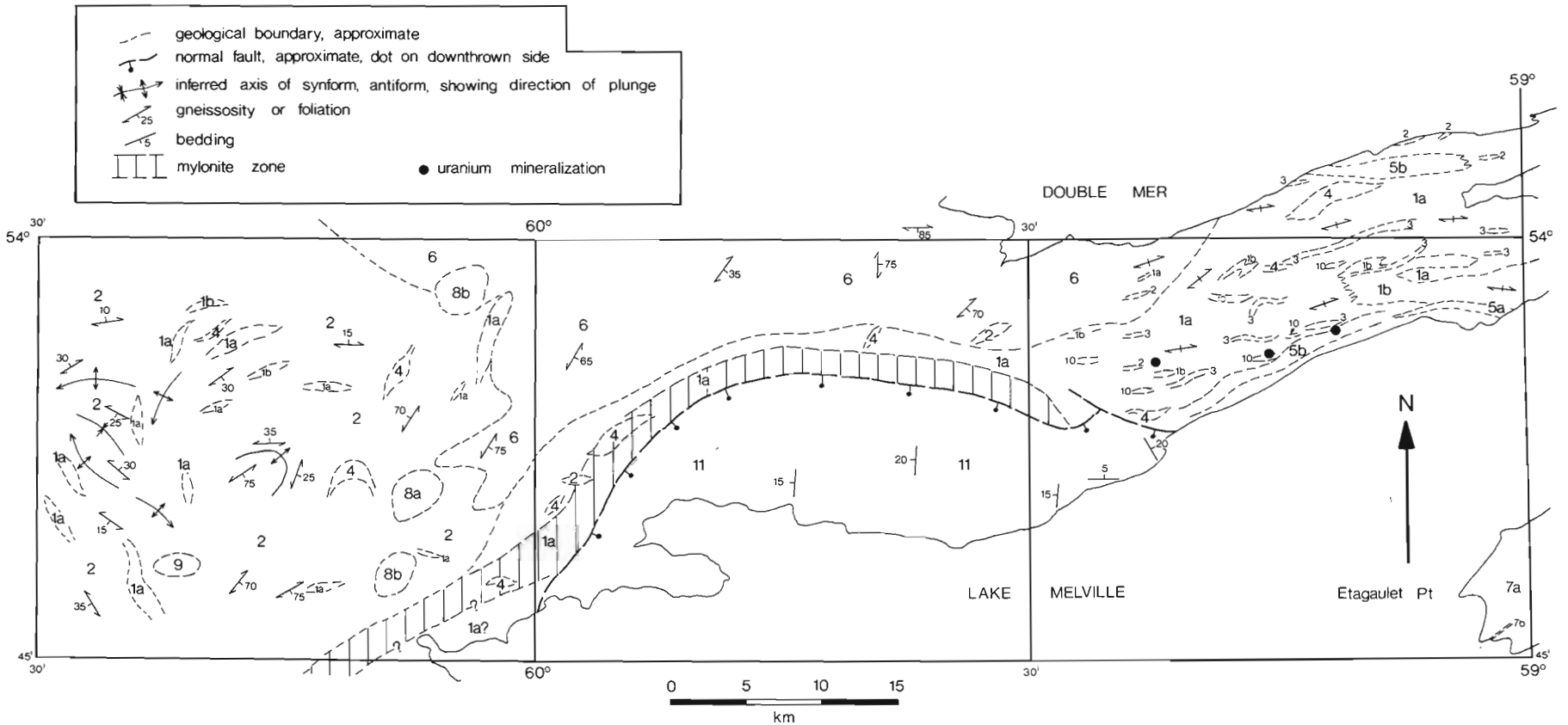

LEGEND

HADRYNIAN

11. **Double Mer Formation:** *Red arkose and polymictic, clast-supported conglomerate.*

HELIKIAN OR EARLIER

10. *Coarse grained, massive, equigranular, white-weathering quartzofeldspathic diatexite.*

9. *Coarse grained, massive metagabbro and hornblendite.*

8. a. *Pink, coarse grained, massive to weakly foliated biotite syenite to quartz syenite.*
   b. *Massive, buff, coarse grained biotite quartz monzonite to granite.*

7. **Mealy Mountains Intrusive Suite (Paleohelikian)**
   a. *Coarse grained, massive, dark gray leuconorite and anorthosite.*
   b. *Fine grained diabase.*

6. *Coarse grained, pink-to-buff granite; massive to strongly foliated.*

5. a. *Coarse grained, pink, megacrystic (K-spar) biotite granodiorite; weakly foliated.*
   b. *Coarse grained, gray augen (K-spar) biotite granite; moderately foliated.*

4. *Medium grained, dark, hornblende dioritic to quartz dioritic gneiss.*

3. *Medium grained amphibolite, micaceous amphibolite and amphibolite gneiss.*

APHEBIAN OR EARLIER (?)

2. *Medium grained, gray (black and white) biotite tonalite to granodiorite gneiss; well banded, migmatitic.*

1. a. *Pink-to-red-to-buff, medium to coarse grained, well banded biotite granitic gneiss; commonly migmatitic and with amphibolite enclaves.*
   b. *Salmon-to-cream colored, fine grained aplitic gneiss to microgranite; with amphibolite enclaves; migmatitic in places.*

Figure 40.2. *Generalized geology of the area north of upper Lake Melville.*

Because of extensive forest cover, and drift in low lying areas, exposure in the map area is generally poor, and contacts are not visible. Exceptions are the shoreline and some ridge tops at the eastern extremity of the area, where exposure is excellent.

About two-thirds of the area (Fig. 40.2) are underlain by well layered and strongly folded, partially interlayered granitic gneiss in the east and tonalitic gneiss in the west. As both gneiss units contain interbanded amphibolite, hornblende dioritic gneiss, and granodiorite in various amounts, they constitute gneiss complexes rather than homogeneous units on the scale of the map.

A biotite granite pluton is inferred to intrude both gneiss complexes in the northern portion of the area. It is weakly foliated when compared with the intruded gneiss, which suggests either that Grenvillian deformation was relatively weak in the area, or that strain was heterogenous.

Three small, pre-Grenvillian, almost unstrained plutons of quartz monzonite to granite appear to truncate the foliation in the surrounding gneiss.

A gently southeast-dipping mylonite zone, at least 50 km long and 5 km wide (apparent map width), developed across the gneiss complexes, coincides in part with the northern boundary of the downfaulted block of Double Mer sedimentary rocks, but its formation predated the block faulting.

Map Units

Unit 1 includes granitic and aplitic gneiss. Subunit 1a is a pink to reddish to buff, medium- to coarse-grained, well banded biotite granitic gneiss. It is commonly migmatitic, and includes abundant layers and lenses of amphibolite; where extensive, the amphibolite is differentiated on the map as unit 3. Some amphibolite layers are conformably interbanded and others are crosscutting; thus, it is clear that at least two (and possibly more) protoliths exist. From these characteristics, the amphibolite bodies are interpreted as being in large part relict dykes. Pegmatite veins and dykes truncate the gneissosity and are themselves folded. A sliver of garnetiferous rock composed of coarse grained micaceous amphibolite and fine grained, well layered quartzofeldspathic gneiss interlayered over a few metres, thought to be of supracrustal origin, occurs within the gneiss complex on the shore of Double Mer. It is included in the western exposure of unit 2 on the map. Subunit 1b is a salmon to cream, fine grained aplitic gneiss to microgranite. Rock types intermediate between subunit 1a and 1b "end members" constitute most of the granitic gneiss complex. It appears that units 1 and 2 contain rocks of differing protolith (i.e. metagranitoid, metasediment, mafic dykes, etc.). They may also contain rocks of more than one age, and are likely to have had a prolonged deformation history which includes both Hudsonian and Grenvillian components. Unit 1 is correlated with parts of the granodiorite gneiss terrane to the east (unit 5 of Gower et al., 1981), and is interpreted as an early granitic terrane of pre-Grenvillian age.

Unit 2 is a medium grained, grey or black and white, strongly banded, migmatized biotite tonalitic to granodioritic gneiss. It commonly contains minor garnet, epidote and muscovite. In contrast to unit 1, amphibolite is rare. Enclaves of granitic gneiss, from 1 to 100 m across strike, that are interlayered in unit 2, are included in unit 1 on the map because of broad lithological similarity. However, these enclaves could also be of sedimentary origin, as suggested by the fine grained sillimanite and kyanite tentatively identified in two outcrops, near the eastern and western boundaries of 13F/16 map area; they may be equivalent to distinctive aluminosilicate-bearing gneiss mapped farther west (unit 2 of Ryan et al., 1981). The tonalite gneiss of unit 2 is correlated with similar rocks to the west, for which Ryan et al. (1981; units 1 and 13) propose an Aphebian or earlier age. The relative ages of units 1 and 2 are unknown. On the basis of interdigitation with unit 1, unit 2 is interpreted to be of Helikian or earlier age. Its protolith may have been mostly tonalite or granodiorite, or it may have been sedimentary strata.

Unit 3 includes medium grained amphibolite, amphibolite gneiss and micaceous amphibolite. Both early, partially digested layers and lensoid heterogeneous boudins with nebulitic margins, and later, more homogeneous cross-cutting, but folded, dykes can be recognized in the eastern part of the area; similar features characterize the map-scale bodies. Protoliths of unit 3 are considered to be mafic dykes of Aphebian to Grenvillian age.

Unit 4 is dark, dense, medium grained hornblende (and minor pyroxene) dioritic to quartz dioritic gneiss, commonly garnetiferous. It occurs as small, isolated lenses interleaved with units 1 and 2, and is gradational in part to unit 3 (amphibolite). Its age relative to units 1, 2 and 3 is unclear; it may be Aphebian or younger. The unit could represent diorite intrusions into the "basement gneiss" of units 1 and 2, or it may itself be part of the basement complex.

Unit 5 includes distinctive, coarse grained augen (K-feldspar) foliated granitoid rocks and augen gneiss. It is divided into subunit 5a, a pink megacrystic biotite granodiorite that is only moderately foliated, and subunit 5b, a grey augen biotite granite gneiss with a strong foliation. A few nearly rectiplanar crosscutting pegmatite dykes occur near the centre of the orthogneiss bodies; amphibolite layers are rare, and confined mostly to the margins. Unit 5 is interleaved with units 1 and 2, and has sharp contacts. The bodies may be intrusions of Paleohelikian age, emplaced into the older gneiss terrane, and foliated before or during the Grenvillian Orogeny. They are correlated with elongate megacrystic granodiorite bodies occurring to the east (unit 6 of Gower et al., 1981).

Unit 6 comprises coarse grained, pink to buff biotite granite. It occurs as a pluton at least 50 km across in an east-west direction. It is nearly massive in its centre but is strongly foliated at its margins, where it is difficult to distinguish from its gneissic host because of strong boundary deformation. Garnet occurs sparingly in many outcrops. Amphibolite does not occur in the unit. Pending radiometric dating, unit 6 is correlated with granite plutons of similar character occurring to the north (Benedict Mountains Suite, Gower, 1981), that have yielded Paleohelikian K-Ar and Rb-Sr ages (Gower, personal communication, 1982).

Unit 7 is exposed on the south shore of Lake Melville. Subunit 7a comprises dark grey, massive, coarse grained leuconorite and anorthosite. It is part of the Mealy Mountains complex of Paleohelikian age (Emslie, 1982). A small, rectiplanar northeast-striking diabase dyke (subunit 7b) intrudes the anorthosite near Etagaulet Point; it is correlated with the olivine diabase dyke swarm mapped by Emslie (1976), of Elsonian age (Emslie, 1370 Ma age determination, unpublished data; Gittins, 1972).

Unit 8 occurs as three intrusive bodies, each less than 3 km across, that appear to truncate the regional foliation sharply. Subunit 8a is pink, coarse grained, massive to weakly foliated biotite syenite to quartz syenite; subunit 8b is massive, buff, coarse grained biotite quartz monzonite to granite. The northern body of unit 8b contains garnet; in both bodies, quartz is characteristically dark grey to brown. From their generally massive and discordant character, the bodies of unit 8 are interpreted to be of Elsonian or younger age, and show evidence of only weak Grenvillian deformation.

Unit 9 comprises coarse grained, massive metagabbro and hornblendite occurring as a small intrusive body, about 2 km across, that appears to truncate the regional foliation sharply in surrounding rocks of unit 2. Based on this apparent

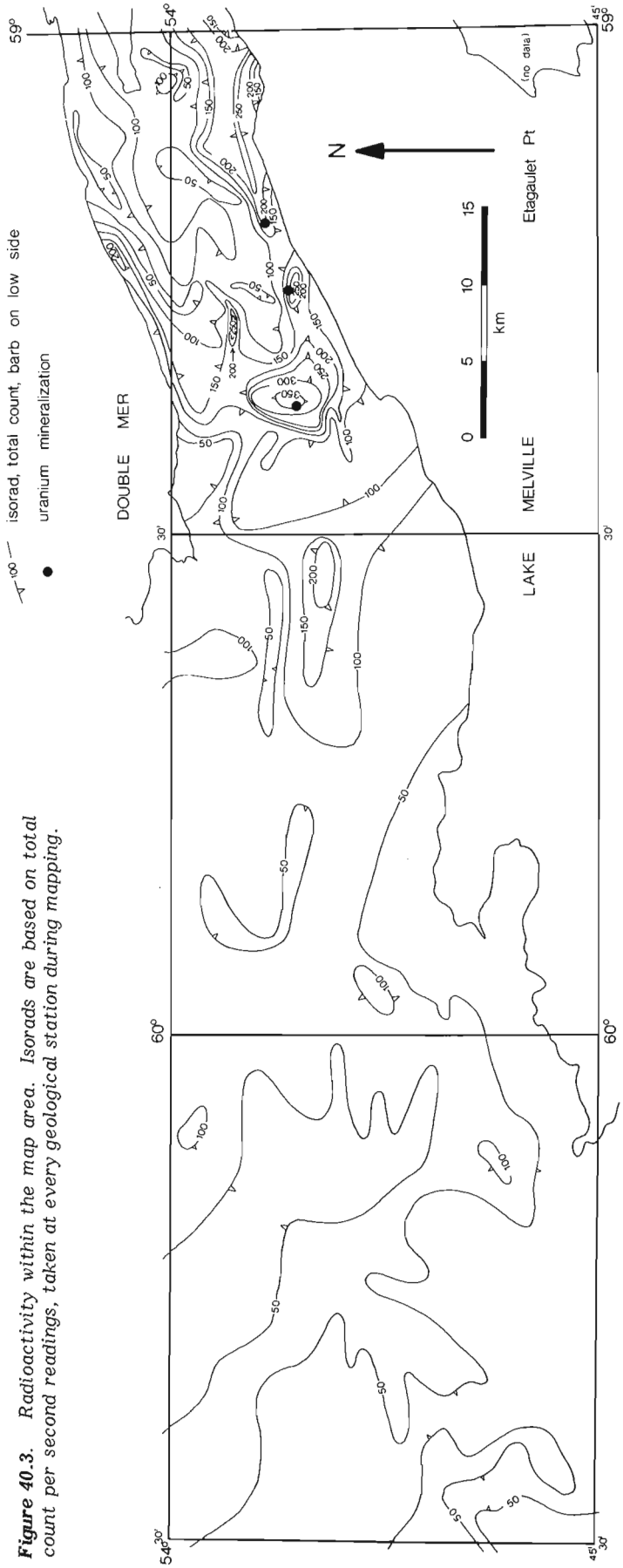

Figure 40.3. *Radioactivity within the map area. Isorads are based on total count per second readings, taken at every geological station during mapping.*

regional truncation and on the low strain in the rocks, unit 9 may be of the same age as unit 8, assuming that strain was homogeneous in this part of the area.

Unit 10 occurs as elongate, discontinuous, lensoid bodies interbanded within unit 1. It comprises chalky white weathering, equigranular, coarse grained, leucocratic quartzofeldspathic rock of migmatitic origin. The largest masses are differentiated on the map, but almost every outcrop of unit 1 in the region where bodies of unit 10 are shown on the map includes amounts of partial melt substantially higher than elsewhere in the area (over 50% is common). These nearly homogeneous masses of diatexite invariably have radioactivity above regional background levels; three uranium showings are known in the area (see below). Gower (personal communication, 1982) identified sillimanite in a thin section of a sample of the unit, cut from drill core obtained by Northgate Exploration Ltd. at the central uranium showing (see Fig. 40.3). Sillimanite-bearing paragneiss has been mapped by Gower et al. (1981) on strike to the east, across Lake Melville, where it is also associated with uranium mineralization; the paragneiss is thought by Gower (personal communication, 1982) to be derived from a pre-Hudsonian protolith. This suggests that the diatexite in the present area may have developed in part from Aphebian or earlier metasedimentary rocks, assuming that strain was heterogeneous in this part of the area. The unit is assumed to be of Neohelikian or Grenvillian age.

Unit 11 is the Double Mer Formation (Kindle, 1924). It is a succession of reddish brown arkosic sandstone and clast-supported polymictic conglomerate of post-Grenvillian age. It occurs as a nearly homoclinal, gently west-dipping sequence, in a lowland bounded on the north by a scarp up to 200 m high. Samples of sandstone from five localities were processed for palynomorphs, but proved to be barren of recognizable microfossils (E. Erdmer, personal communication, 1982). The unit is suspected to be of Hadrynian age.

Structure

The dominant fabric element of units 1 and 2 is a marked gneissosity. In outcrops of unit 1 on the Double Mer Peninsula, this fabric is commonly affected by contorted, irregular, tight folds ranging from 10 cm to over 10 m in amplitude. Highly distorted, local superimposed folding patterns are present in outcrops where the folding is less extreme. Although this folding somewhat obscures regional trends, an east-northeast vertical grain is dominant. In unit 2, open vertical folds inferred on the map suggest an interference pattern of domes and basins, elongated in a northwesterly direction near the western boundary of the area. This style of deformation was recognized farther west by Ryan et al. (1981).

The amphibolite and dioritic gneiss of units 3 and 4 have a foliation parallel to their contacts, and are structurally concordant.

The homogeneity of units 5a and 5b and the fact that the type of surrounding rocks varies suggest that the megacrystic granodiorite and granite are structurally younger, although now nearly structurally concordant.

Notwithstanding its foliated margins, the large pluton of unit 6 is regionally apparently discordant relative to the intruded gneiss. The intrusive rocks of units 8 and 9 are clearly crosscutting from map patterns, and only weakly foliated near their margins.

The mylonite zone in the western half of the area is characterized by strong, shallowly southeast- to south-plunging rodding and mullion structure, flattened and drawn out quartz and feldspar grains visible in hand specimen, and

comminuted micas resulting from cataclasis. These features are overprinted by another deformation recorded in epidote coated fractures, chloritic, very fine grained, sheared friable rock and hematite veining. A tentative interpretation is that these later, brittle features resulted from normal faulting at shallow depth associated with, or postdating the deposition of the Double Mer sediments, and that the mylonite was developed previously from "basement" gneiss at considerable depth. The mylonite outlines a zone of high strain interpreted as the trace of a (pre-?) Grenvillian, shallowly southeast-dipping fault that was reactivated by normal faulting.

To the west of the map area, Ryan et al. (1981) recognized a gently southeast-dipping mylonite zone associated with a thrust fault, whose strike extension matches the trace of the present mylonite zone. This suggests continuity of the structure; it is thus likely that mylonite is also associated with thrust faulting north of lake Melville.

Metamorphism

With the exception of the Double Mer Formation, all units in the map area, including the mylonite, are recrystallized. A sugary, friable texture characterizes many of the quartzofeldspathic rocks.

A partial melt phase, in the form of small lenses and strips of quartzofeldspathic material a few centimetres wide, is developed between the folia of most rocks of units 1 and 2. Kyanite and sillimanite have been tentatively identified in slivers of inferred supracrustal gneiss included in unit 2. Unit 1 contains the assemblage quartz-K-feldspar-plagioclase-biotite-hornblende-garnet. The tonalite gneiss of unit 2 contains the assemblage quartz-plagioclase-biotite-muscovite-garnet-epidote; a coarse grained, equigranular rock containing the assemblage quartz-garnet-clinopyroxene-plagioclase is interbanded in unit 2 near the centre of 13F/16 map area. Sillimanite, biotite, quartz and K-feldspar occur in at least one outcrop of diatexite (unit 10); this places the rock above the muscovite "breakdown" curve (with quartz), in the stability field of sillimanite, which implies a minimum temperature of 620°C, and pressure greater than 200 MPa (equilibrium curves after Holdaway, 1971, and Helgeson et al., 1978).

Chlorite, and/or sericite are present in many outcrops as retrograde minerals.

This evidence suggests that metamorphic grade in the crystalline rocks is at upper amphibolite facies, with some retrograde overprinting in the greenschist facies.

Economic Potential

No new surface occurrences of economic minerals were found and, with the exception of uranium in unit 10, the region has attracted little exploration interest.

Recent work by McConnell (1979) determined the presence of anomalous uranium concentrations in lake sediments; uranium mineralization, showing as a yellow uranophane(?) stain on outcrop surfaces, occurs in three localities. Uraninite has been identified as the primary uranium mineral (Kerswill and McConnell, 1982). Northgate Exploration Ltd. carried out exploratory trenching and drilling at the central showing in 1979.

A scintillometer survey carried out during the present mapping reveals that regional radioactivity peaks in the general area of known showings (Fig. 40.3). Although they occur over a wide area, higher total counts are low in absolute terms (a few hundred counts per second); this suggests that mildly uraniferous partial melt (unit 10) is the major source of radioactivity. As this unit occurs over a relatively extensive area, and several other positive anomalies occur, it is possible that additional uranium concentrations exist. On the basis of the occurrence of unit 10 and higher radioactivity, prospective mineralization sites may be located a few kilometres north and east of the known showings, within areas bounded by the 250 counts per second isorads on Figure 40.3.

Summary

The geological infrastructure of the area appears to include the following elements. Two compositionally distinct, heterogeneous, highly deformed gneiss complexes, of possible Aphebian or earlier age, contain remnants of inferred supracrustal origin, whose age is unclear but may be close to that of the gneiss, and younger(?) metaplutonic rocks. The complexes were intruded by a late Hudsonian or early Paleohelikian granite pluton, as well as by Paleohelikian anorthositic rocks and by structurally late plutons of granite to syenite. Northwesterly directed thrusting may be of Grenvillian or Neohelikian age, as inferred by Ryan et al. (1981) for the area to the west. The thrust fault zone was reactivated as a normal fault during or following deposition of the postorogenic Double Mer sediments.

The broad, open folds and shallowly dipping foliation that characterize the western part of the area suggest that the latest deformation was relatively weak; this is in contrast to the marked east-northeast vertical grain in the east, where strain is considerably higher. This suggests either that deformation during the Grenvillian Orogeny was inhomogeneous, or that it was very weak and was superimposed on a heterogeneously (previously) deformed area.

Acknowledgments

Glenn Bursey, Chris Pinsent, Tony Power (Memorial University) and Mark Wilson (Carleton University) were competent field assistants. E.W. and E.J. Tuttle (Newfoundland Department of Mines and Energy) provided expediting help, often well beyond normal working hours.

Charles Gower (Newfoundland Department of Mines and Energy) organized a visit to the neighbouring parts of his field area at the beginning of the season. Charles Gower, Richard Wardle and Rex Gibbons (Newfoundland Department of Mines and Energy) critically read this report and suggested many improvements.

References

Bailey, D.G.
1980: The geology of the Double Mer-Lake Melville area, Labrador; in Report of Activities for 1979, ed. C.F. O'Driscoll and R.V. Gibbons, Newfoundland Department of Mines and Energy, Report 80-1, p. 154-160.

Eade, K.E.
1962: Geology, Battle Harbour-Cartwright; Geological Survey of Canada, Map 22-1962.

Emslie, R.F.
1976: Mealy Mountains complex, Grenville Province, southern Labrador; in Report of Activities, Part A, Geological Survey of Canada, Paper 76-1A, p. 165-170.

1982: Estimation of intensive paleovariables and timing of Proterozoic events in the Mealy Mountains, Labrador; in Grenville Workshop, 1982, program with abstracts, p. 4.

Gittins, J.
1972: A note on the age of basaltic dikes in the Mealy Mountains, Labrador, Canada; Canadian Journal of Earth Sciences, v. 9, p. 1337-1338.

Gower, C.F.
1980: Geology of the Benedict Mountains and surrounding areas (13J (east) and 13I); in Report of Activities for 1979, ed. C.F. O'Driscoll and R.V. Gibbons, Newfoundland Department of Mines and Energy, Report 80-1, p. 182-191.

1981: The geology of the Benedict Mountains, Labrador (13/J northeast and 13/I northwest); Newfoundland Department of Mines and Energy, Report 81-3.

Gower, C.F., Ryan, A.B., Bailey, D.G., and Thomas, A.
1980: The position of the Grenville Front in eastern and central Labrador; Canadian Journal of Earth Sciences, v. 17, p. 784-788.

Gower, C.F., Noel, N., and Gillespie, R.T.
1981: The geology of the Rigolet region, Labrador; in Current Research for 1980, ed. C.F. O'Driscoll and R.V. Gibbons, Newfoundland Department of Mines and Energy, Report 81-1, p. 121-129.

Gower, C.F., Owen, V., and Finn, G.
1982a: The geology of the Cartwright region, Labrador; in Current Research for 1981, ed. C.F. O'Driscoll and R.V. Gibbons, Newfoundland Department of Mines and Energy, Report 82-1, p. 122-130.

Gower, C.F., Flanagan, M.J., Kerr, A., and Bailey, D.G.
1982b: Geology of the Kaipokok Bay-Big River area, Central Mineral Belt, Labrador, Newfoundland Department of Mines and Energy, Report 82-7.

Helgeson, H.C., Delany, J.M., Nesbitt, H.W., and Bird, D.K.
1978: Summary and critique of the thermodynamic properties of rock-forming minerals; American Journal of Science, v. 278A.

Holdaway, M.J.
1971: Stability of andalusite and the aluminum silicate phase diagram; American Journal of Science, v. 271, p. 97-131.

Kerswill, J.A. and McConnell, J.W.
1982: Geochemistry and geology of some uraniferous granites in Labrador; in Uranium in Granites, ed. Y.T. Maurice; Geological Survey of Canada, Paper 81-23, p. 171-172.

Kindle, E.M.
1924: Geography and geology of Lake Melville district, Labrador Peninsula; Geological Survey of Canada, Memoir 141.

McConnell, J.W.
1979: Geochemical follow-up studies in Labrador; in Report of Activities for 1978, ed. C.F. O'Driscoll and R.V. Gibbons, Newfoundland Department of Mines and Energy Report 79-1, p. 159-162.

Stevenson, I.M.
1967: Goose Bay map-area (13F); Geological Survey of Canada, Paper 67-33.

1970: Rigolet and Groswater Bay map-area, Newfoundland (Labrador); Geological Survey of Canada, Paper 69-48.

Ryan, B.
1982: Geology of the Central Mineral Belt, Labrador; Newfoundland Department of Mines and Energy, Maps 82-3 and 82-4.

Ryan, B., Neale, T., and McGuire, J.
1981: The geology of the Grand Lake area, Labrador, 13F/10, 11, 14, 15; in Current Research for 1980, ed. C.F. O'Driscoll and R.V. Gibbons, Newfoundland Department of Mines and Energy, Report 81-1, p. 103-110.

Wardle, R.J. and staff, Labrador Section
1982: The Trans-Labrador Batholith; a major pre-Grenvillian feature of the eastern Grenville Province; in Grenville Workshop, 1982, program with abstracts, p. 11.

41.

THE ARCHEAN-PROTEROZOIC BOUNDARY IN THE SAGLEK FIORD AREA, LABRADOR: REPORT 1[1]

Project 820028

A.B. Ryan[2], Y. Martineau[2], D. Bridgwater[3], L. Schiøtte[3], and J. Lewry[4]
Newfoundland Department of Mines and Energy

Ryan, A.B., Martineau, Y., Bridgwater, D., Schiøtte, L., and Lewry, J., The Archean-Proterozoic boundary in the Saglek Fiord area, Labrador: report 1; in Current Research, Part A, Geological Survey of Canada, Paper 83-1A, p. 297-304, 1983.

Also in Current Research, ed. R.V. Gibbons, Newfoundland Department of Mines and Energy, Mineral Development Division, Report 83-1, 1983.

Abstract

The Aphebian Ramah Group in northern Labrador occupies the boundary zone between gneisses of the Archean (Kenoran deformed) Nain Province and gneisses of the lower Proterozoic (Hudsonian deformed) Churchill Province. The Nain Province displays few effects of lower Proterozoic thermotectonism, and the major lithological components identified by previous workers in the eastern Archean block are recognized throughout the area. The Ramah Group unconformably overlies the Archean complex; eastward transgression of the Hudsonian orogenic front has resulted in increased deformation and metamorphism of the Ramah southward from Saglek Fiord, and major thrust interleaving of basement and cover has occurred. Gneisses of the Churchill Province west of the Ramah Group are granulite facies rocks with mylonitic fabrics. Magnetite iron formation, graphite and copper sulphides occur in the area.

Introduction

The 1982 field season was the first of a two year project funded by the Federal Mineral Program in Newfoundland to examine the Nain-Churchill boundary zone in northern Labrador. The program involves 1:50 000 and 1:100 000 scale mapping of NTS sheets 14 L/2, 3, 4, 5, 6 and 7 (Fig. 41.1). The region lies within the southern part of the Torngat Mountains, where topography and exposure are ideal for documenting the character of the structural province boundary.

Ryan and Martineau were responsible for regional mapping. Associated participants Bridgwater and Schiøtte concentrated on specific problems in the Archean block arising from earlier mapping; Lewry examined part of the Ramah Group and its contact with adjacent gneisses.

Geological Setting

The survey area (Fig. 41.1) straddles the contact between the Nain Province in the east, an Archean block containing 3.6 Ga to 2.5 Ga gneisses and last deformed during the Kenoran Orogeny, and the Churchill Province in the west, an Aphebian mobile belt incorporating reworked Archean rocks and lower Proterozoic supracrustals last deformed during the Hudsonian Orogeny (Taylor, 1971). The Ramah Group, a variably deformed and metamorphosed Aphebian supracrustal sequence, occupies the central part of the map area, and records the easternmost influence of major Hudsonian thermotectonism.

Previous Work

The earliest geological studies in the region were those of Bell (1884), Daly (1902), Delebarre (1902), Coleman (1921) and Odell (1938). Geological mapping along the coastal strip was carried out by Christie (1952) and Douglas (1953). Major geological elements were defined only after regional scale mapping in the late 1960s and early 1970s (Taylor, 1969, 1970, 1971, 1979; Morgan, 1972, 1973, 1975).

In 1974 and 1975, a joint Geological Survey of Canada – Memorial University of Newfoundland party carried out detailed investigations of the geology of the eastern Archean block in the Saglek area (Bridgwater et al., 1975). This study defined and informally named major rock units, and established a relative age sequence of rocks and events involved in development of the complex. A concurrent Rb-Sr isotope study (Hurst et al., 1975) identified pre-3.6 Ga components. It was established that the geological evolution of the Saglek area was similar to that of the Godthaabsfjord area of West Greenland (McGregor, 1973). Collerson and coworkers, between 1976 and 1978, continued detailed work on several aspects of the Archean complex of eastern Saglek Fiord, and further refined the chronology (cf. Collerson et al., 1976; Bridgwater and Collerson, 1976; Bridgwater et al., 1978; Collerson and Bridgwater, 1979; Kerr, 1980; Collerson et al., 1982).

Present Study

The current project involves geological mapping and economic mineral evaluation of the area west of that investigated in detail during the earlier GSC-MUN program, with particular emphasis on establishing the effects of the Hudsonian Orogeny on the Aphebian Ramah Group and its Archean basement along the eastern orogenic front. This report focuses on the Proterozoic rocks, and only salient features of Archean rocks not affected by penetrative Hudsonian deformation are documented here.

Nain Province

The Archean complex of the Nain Province comprises predominantly quartzofeldspathic gneisses, derived from intrusive protoliths interlayered with subordinate belts of supracrustal rocks derived from sedimentary and volcanic successions. The detailed work of Bridgwater et al. (1975) and by Collerson and his colleagues showed that the Archean block could be divided across the Handy fault into a largely amphibolite facies terrane in the east, and a largely granulite

---

[1] Contribution to Canada-Newfoundland co-operative mineral program 1982-84. Project carried by Geological Survey of Canada and Newfoundland Department of Mines and Energy.

[2] Newfoundland Department of Mines and Energy, Mineral Development Division, P.O. Box 4750, St. John's, Newfoundland, A1C 5T7.
[3] Geologisk Museum, Øster Voldgade 5-7, 1350 København, Denmark.
[4] Presently at Department of Earth Sciences; Memorial University of Newfoundland, St. John's, Newfoundland.

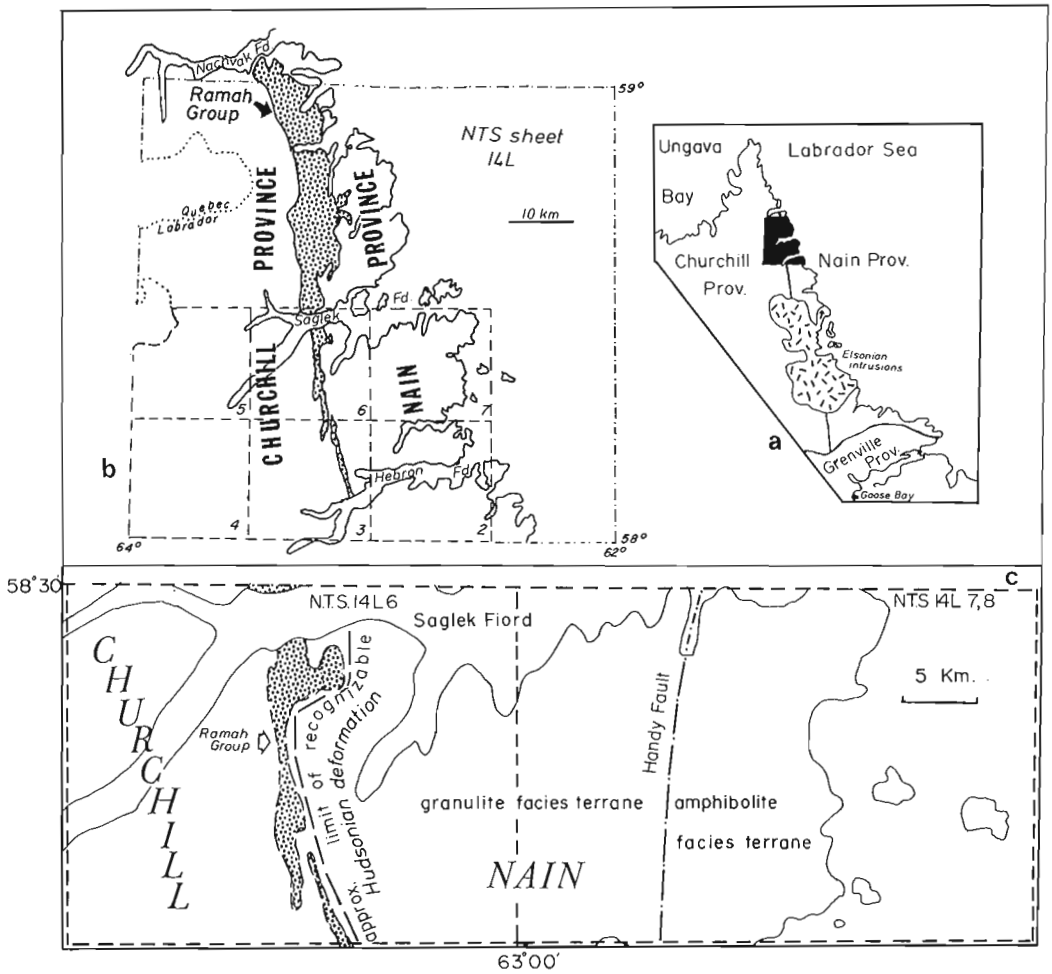

Figure 41.1

a. Sketch map showing the portion of Labrador covered by NTS sheet 14 L.

b. Outline of 14 L showing six 1:50 000 sheets to be covered during project.

c. Generalized subdivisions of regional geology in area of 1982 survey; in part after Bridgwater et al. (1975).

facies terrane in the west (Fig. 41.1, 41.2). Major rock units can be correlated on both sides of the fault, and the two terranes are interpreted to represent different structural levels of the same crustal components. Details of rock types are given by previous workers and only a generalized summary of chronology of the major stratigraphic units (Fig. 41.2) is presented here.

The earliest components are small (1-10 m^2 in area) rafts and belts (2 x 0.1 km) of basic intrusive and extrusive rocks, magnetite iron formation, calc-silicate rock and pelitic gneiss, known collectively as the Nulliak assemblage (Collerson and Bridgwater, 1979). These occur within a multiphase orthogneiss group (Uivak gneisses) comprising a grey migmatitic tonalitic to quartz monzonitic member (Uivak I) and a younger iron rich porphyritic (augen) granodioritic to dioritic member (Uivak II; Bridgwater et al., 1975). The Univak I suite was deformed and migmatized prior to the emplacment of the Uivak II augen gneiss. A major deformational and metamorphic/metasomatic event occurred circa 3.6 Ga which isotopically homogenized all rocks within the complex. This was followed by intrusion of a basic dyke swarm (Saglek dykes), and accumulation of a series of sedimentary, volcanic and basic intrusive rocks known as the Upernavik supracrustals (Bridgwater et al., 1975). Tectonic interleaving of the Uivak gneisses and Saglek dykes (Plate 41.1a) with the Upernavik supracrustals occurred circa 3.0 Ga giving rise to a regionally layered complex of paragneiss and orthogneiss. The complex was remobilized circa 2.8 Ga and the early orthogneisses were transformed into a heterogeneous suite ranging from Uivak gneiss with a local in situ irregular melt component, to lit-par-lit migmatites, to nebulites in which nearly all earlier features of the precursor are destroyed. The Upernavik supracrustal rocks were disrupted locally and injected by sheets of the mobilizate. Hurst et al. (1975) referred to these rocks as "undifferentiated gneisses". Recently Kerr (1980) and Collerson et al. (1982) have referred to this younger group of gneisses west of the Handy fault as the Kiyuktok gneisses. The reworking event appears to have been coeval with the granulite facies metamorphism, the effects of which have locally been nearly completely masked by later retrogression in the western block. Similar reworked gneisses in the southern part of the eastern (amphibolite facies) block, also showing evidence of having developed during a granulite grade event and having suffered subsequent retrogression, were earlier termed Iterungnek gneisses by Ryan (1977). These gneisses imply that rocks from deeper crustal levels are exposed to the south in the area east of the Handy fault.

In addition to the major lithostratigraphic units mentioned above, there are several types and generations of granitoid rocks.

The injection of regional diabase dyke swarms circa 2.3 Ga is the last major recognized event to affect the Archean complex prior to Aphebian erosion, uplift, and deposition of the Ramah Group. The dykes are conspicuous and abundant in the eastern half of the Nain Province in the study area, but become less abundant westward.

This year's mapping has shown that major rock units identified in the eastern Saglek Fiord area can be traced south and west within the Archean block (Fig. 41.2). Minor rafts and larger coherent belts of the Nulliak and Upernavik associations extend to the limits of the study area. One such belt of grey quartzite (interpreted as recrystallized chert),

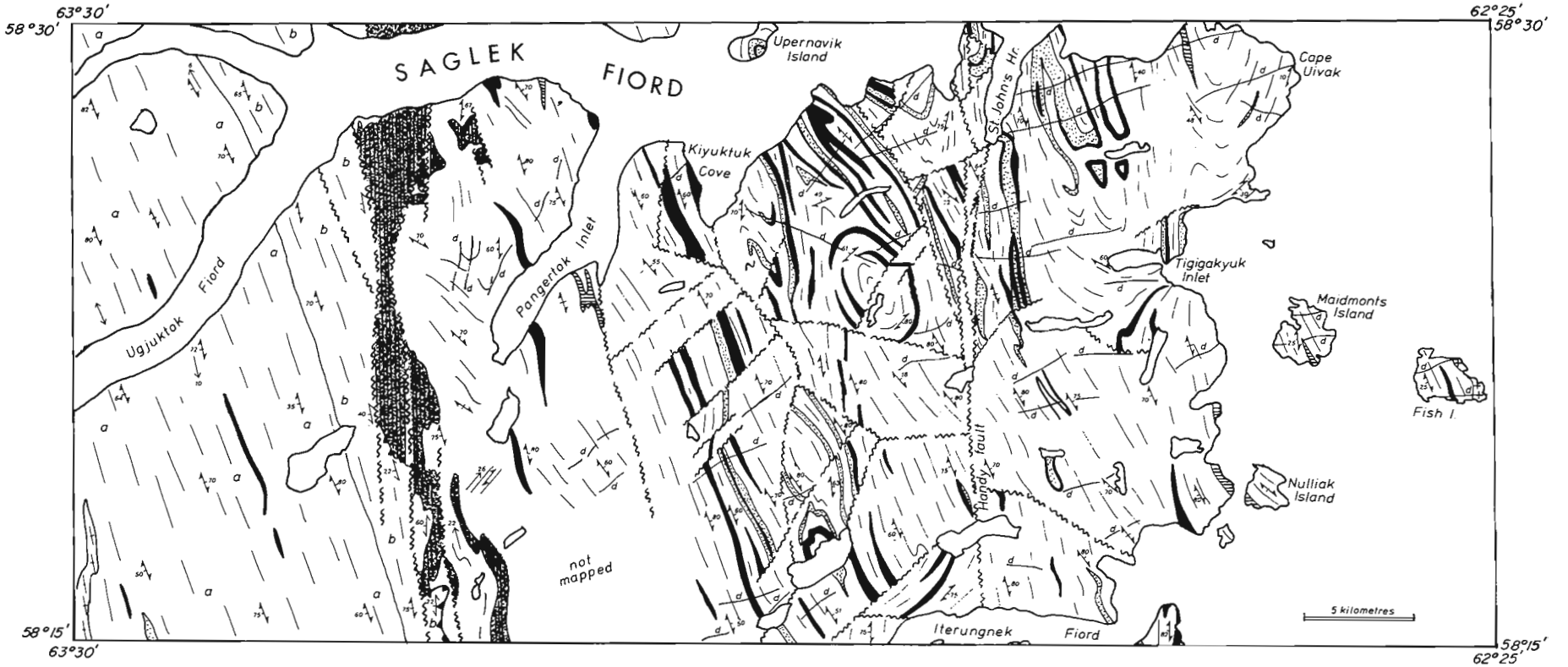

LEGEND

CHURCHILL PROVINCE

Aphebian

Ramah Group: *Quartzite, dolostone/marble, black slate/pelitic schist.*

Archean and/or Aphebian

Quartz-feldspar-garnet-graphite gneiss; mafic and ultramafic granulite (black); garnet-sillimanite gneiss (dots); foliated granite (crosses).

Quartzofeldspathic and mafic granulite, mylonitized and retrogressed locally.

NAIN PROVINCE

Archean-Aphebian

Diabase dikes (many omitted for clarity).

Archean

Granite.

Upernavik Supracrustals: *Metasedimentary rocks (dots), metavolcanic and mafic/ultramafic intrusive rocks (black).*

Quartzofeldspathic Gneiss: *Uivak gneiss and its reworked and migmatized derivatives.*

Nulliak Assemblage: *Metasedimentary and mafic/ultramafic rocks.*

SYMBOLS

Geological boundary

Fault

Thrust

Trend of gneissic layering

Gneissosity: inclined, vertical, dip unknown

Mylonitic foliation: inclined

Lineation: inclined, horizontal

Figure 41.2. *Generalized lithological map for the area south of Saglek Fiord. The St. John's Harbour – Cape Uivak area and the coastal strip and off-shore islands between Tigigakyuk Inlet and Nulliak Island compiled from Collerson and Bridgwater (1979); area directly east of Kiyuktuk Cove after Kerr (1980).*

magnetite iron formation and calc-silicate rock of the Nulliak assemblage at Pangertok Inlet is one of the largest pre-Uivak supracrustal remnants found in this area. The belt of migmatites east of St. John's Harbour (not distinguished on Fig. 41.2), originally defined by Bridgwater et al. (1975), is more extensive to the south, and the granitic component forms discrete homogeneous masses and sheets in this area. In addition, we have found that the gneisses east of the Handy fault especially in the Iterungnek Fiord area show more widespread effects of the 2.8 Ma granulite facies event than previously recognized. Retrogression caused by intrusion of younger granites has destroyed nearly all vestiges of this high grade overprint. Much of the western granulite facies block comprises Kiyuktok gneisses, but zones of unreworked granulite facies Uivak gneisses also occur, particularly in the south. This granulite terrane is characterized by conspicuous, white weathering, late kinematic granite sheets (generally less than 0.5 km wide) parallel to the regional lithological layering.

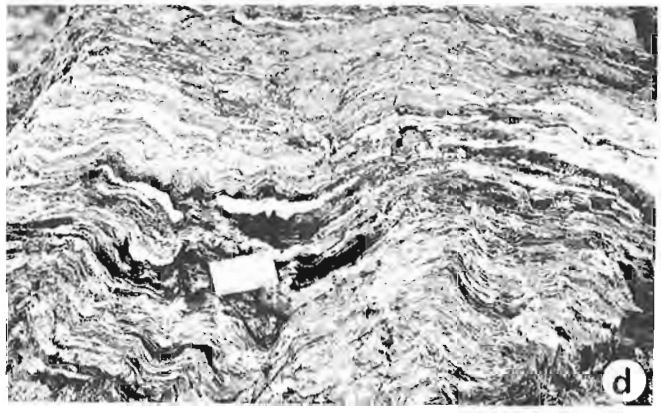

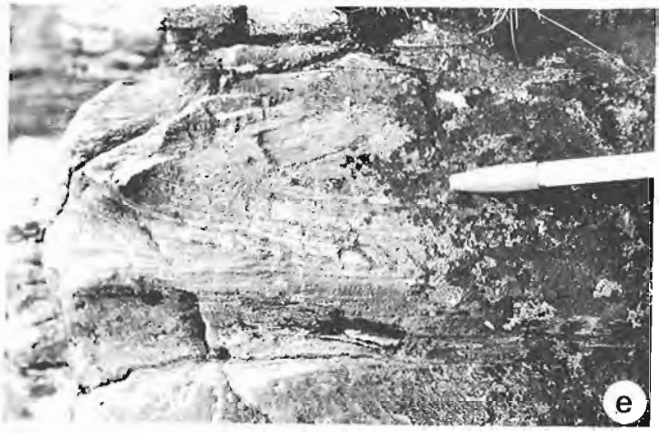

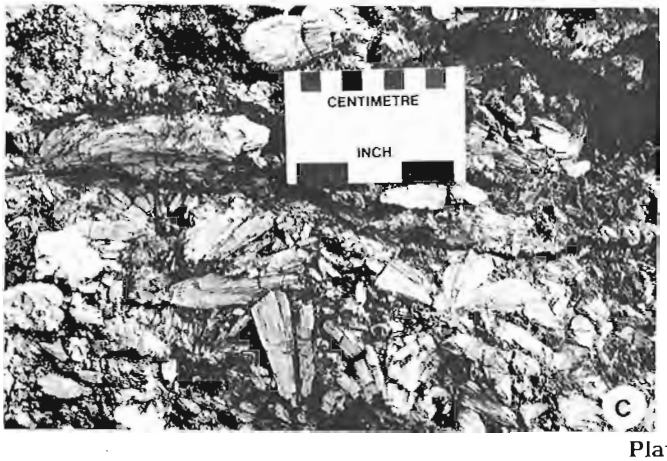

Plate 41.1

a. Migmatized Uivak gneiss and Saglek dykes, Maidmonts Island

b. Subhorizontal Ramah Group (Rowsell Harbour Formation) in unconformable contact with Archean gneiss, south shore of Saglek Fiord. Unconformity occurs at base of white quartzite unit in centre of photograph. Cliff face is approximately 300 m high

c. Radiating tremolite aggregates in marble, western margin of Ramah Group at Saglek Fiord

d. Refoliated gneiss adjacent to the Ramah Group, south of Pangertok Inlet

e. Isoclinal folds in Ramah Group quartzite, south of Pangertok Inlet

f. Quartz-feldspar-garnet-graphite gneiss, Ugjuktok Fiord.

Churchill Province

The Churchill Province is defined by the presence of rock types, isotopic ages, metamorphism, and structures resulting from the Hudsonian Orogeny. Its eastern boundary in northern Labrador was defined by Morgan (1975) as the eastern limit of the folded Aphebian Ramah Group. This definition is retained here, although present work indicates a Hudsonian thermotectonic overprint in the Archean foreland several kilometres east of the Ramah Group (Fig. 41.1c). Thus, in the study area, the Churchill Province comprises the Ramah Group, bounded to the west by granulite facies quartzofeldspathic gneiss and quartz-feldspar-garnet-graphite gneiss. The Ramah Group is affected by increasing deformation to the south and west; the western gneisses are typified by a north- to northwest-trending mylonitic fabric.

Hudsonian Effects in the Archean Foreland

Many faults and shear zones in the Archean block, including the Handy fault may in part be related to Hudsonian deformation (cf. Bridgwater et al., 1975). More obvious, however, are the effects which the Hudsonian tectonic overprint has had on the basement up to several kilometres east of the Ramah Group. The best markers of this are the late Archean diabase dykes which are converted into massive or foliated amphibolite near the more pronounced deformational front defined by the Ramah Group. In the vicinity of the latter south of Pangertok Inlet, both dykes and planar features in the basement gneisses are commonly rotated into parallelism with the sheared basement-cover contact. The extent of Hudsonian meta-morphic overprint on the structurally unreworked Archean gneisses where dykes are absent is ill-defined but much of the retrogression in the terrane immediately east of the Ramah Group may be of Proterozoic age.

Hudsonian effects on the Ramah Group

The Aphebian Ramah Group (Morgan, 1972, 1973, 1975; Knight, 1973) is best preserved north of Saglek Fiord, in a northerly-trending, doubly plunging synclinal belt up to 16 km wide, extending approximately 90 km from Saglek Fiord to Nachvak Fiord (Fig. 41.1b). Six formations are recognized in the Group (Knight and Morgan, 1977, 1981; Table 41.1). In this region the eastern boundary of the fold belt is little disturbed, and the group rests with profound unconformity on peneplaned Archean gneisses. The western boundary is faulted and overthrust, and metamorphic grade reaches amphibolite facies. Morgan (1975) recognized that the Ramah Group extended south of Saglek Fiord through the present study area as a narrower, increasingly tectonized and metamorphosed belt; he was able to trace it 35 km southward to Hebron.

In the north of the study area, along the south shore of Saglek Fiord (Fig. 41.3), the group comprises interbedded white and maroon quartzite, pelite and dolostone of the Rowsell Harbour and Reddick Bight formations, overlain by black slate of the Nullataktok Formation. Several diabase sills are present, one of which, in the Nullataktok Formation, is the highest stratigraphic unit preserved. The sequence is folded into open anticlines and tighter synclines. In the east it is autochthonous and lies unconformably on basement (Plate 41.1b). In the west it is fault-bounded and is in sheared contact with underlying Archean gneiss. Vertical and lateral changes in metamorphic grade are apparent along the fiord wall. Pelite of the Nullataktok Formation is represented by black slate at 600 m elevation, whereas pelite of the Rowsell Harbour Formation at sea level is muscovite-andalusite schist containing kyanite in quartz-feldspar segregations. Similarly, brown dolostone interbedded with quartzite at the top of the Reddick Bight Formation in the east is transformed to spectacular pale green tremolite marble in the west (Plate 41.1c).

Table 41.1

Summary of stratigraphy of the Ramah Group (from Knight and Morgan, 1981)

RAMAH GROUP Maximum measured thickness 1702 m	Cameron Brook Formation		200 m +	Greywacke – sandstones and mudstones.
	Typhoon Peak Formation		85-130 m	Slates; some sandstone and limestone.
	Warspite Formation		165 m	Dolomitic breccias and sandstones; dololutites; some limestone and calcareous mudstone; argillite, mudstone.
	Nullataktok Formation		595 m	Varicoloured mudstones and shales; graphitic pyritiferous; chert; pyrrhotite-pyrite unit; calcareous and dolomitic mudstones.
	Reddick Bight Formation		53-143 m	Black quartzite; grey muddy sandstone; sandstone-siltstone laminites; yellow weathering dolomite unit.
	Rowsell Harbour Formation 251-470 m	Upper White Quartzite Member	46-267 m	White quartzite; some conglomerate; interbedded shale and mudstone.
		Phyllite Member	15-44 m	Laminated purple mudstone and very fine grained sandstone.
		Purple Quartzite and Mudstone Member	75-157 m	Pink quartzite; alternating units of purple quartzite and purple mudstone; grey sandstone and shale.
		Volcanic Member	0-9 m	Altered tholeiitic basalt flow.
		Lower White Quartzite Member	31-97 m	Granitic wash; pebble conglomerate; white quartzite with heavy mineral laminae; white quartzite; pebbly, coarse grained sandstone.

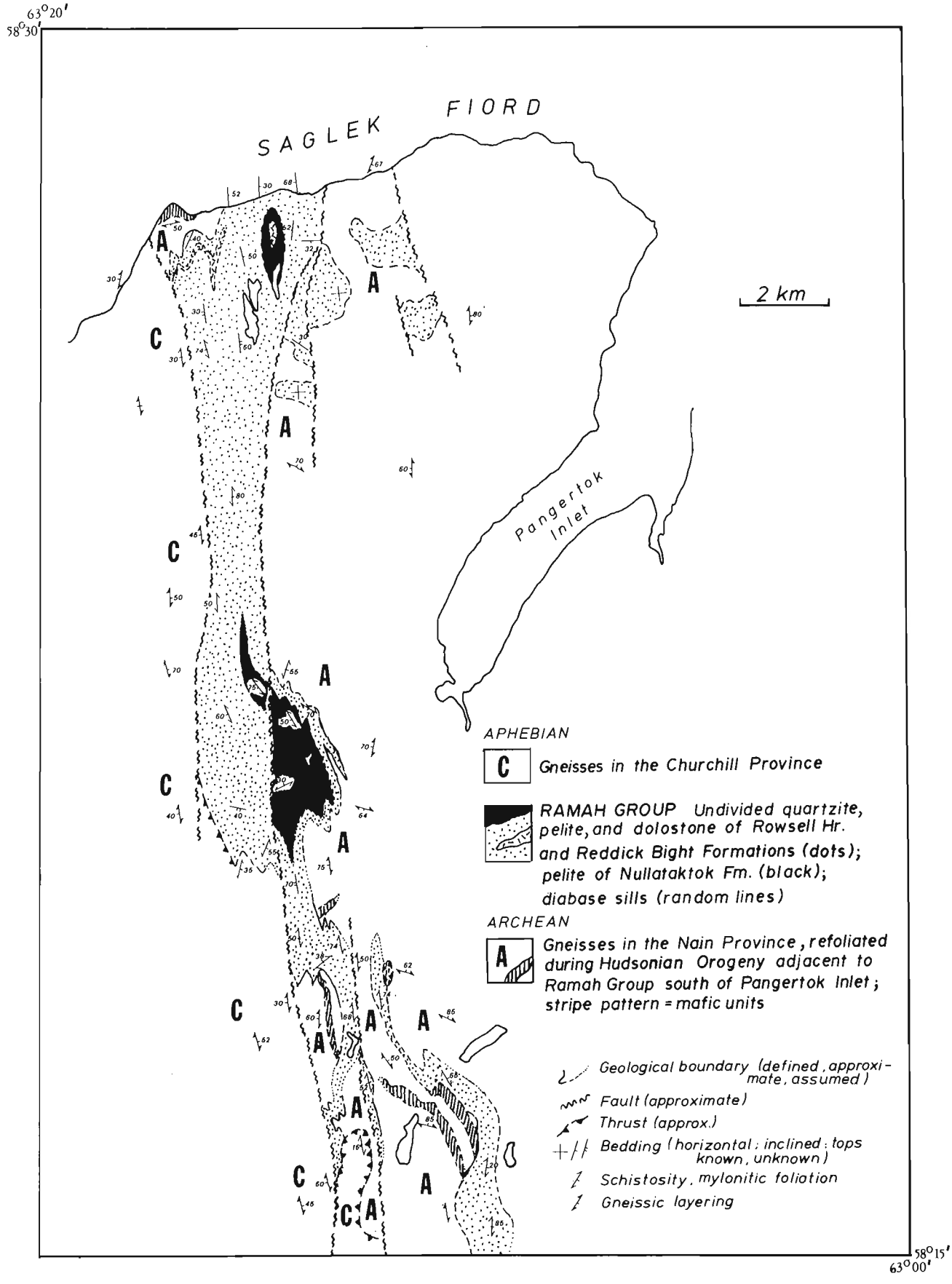

Figure 41.3. *Distribution of the Ramah Group in the map-area south of Saglek Fiord.*

Southward from Saglek Fiord, the Ramah Group narrows markedly in outcrop width, becomes entirely bounded by tectonic junctions, and is increasingly tightly folded and metamorphosed. Approximately 10 km south of the fiord it splits into two or more narrow belts, generally less than 1 km in width. Just north of this bifurcation, an extensive zone of black muscovite schist is thought to represent Nullataktok Formation; the quartzite sequence to the east is tectonically thinned, and the eastern contact is a décollement surface of basement-cover detachment. The western margin in this part of the belt varies from a steep reverse fault to a low angle westward-dipping thrust which has transported refoliated granulite facies gneisses over the Ramah Group.

Still farther south, the narrow belts of Ramah Group are entirely of white quartzite, muscovite schist and minor calc-silicate rocks (Rowsell Harbour Formation?). The configuration of the belts is a function both of thrust interleaving with basement and multiple folding. All contacts are tectonic; on both margins of the belts, recognizable Ramah Group is separated from basement gneisses by a zone of tectonic schist, phyllonite, and mylonite derived both from cover and basement (Plate 41.1d). Structural data indicate that early deformation involved thrust slice intercalation of mylonitically refoliated basement coeval with development of recumbent isoclinal folding and axial planar schistosity within the cover (Plate 41.1e). Both F_1 folds and basement slices are refolded by open to tight upright F_2 folds, and S_1 axial plane fabrics are crenulated. Further, post-F_2, thrusting is evident along the southern periphery of the area where a subhorizontal sheet of quartzofeldspathic and mafic gneiss overrides and truncates upright F_2 folds in the Ramah Group.

Gneisses of the Churchill Province

The zone immediately west of the Ramah Group comprises dark green to grey weathering, slightly retrogressed granulite facies quartzofeldspathic and subordinate mafic gneisses. These rocks commonly possess a mylonitic fabric, and pseudotachylyte vein networks related to later faulting occur locally. It is unclear at present whether the granulite facies parageneses are Archean or Proterozoic in age. Morgan (1975) interpreted numerous discordant amphibolites in this unit north of Saglek Fiord as metamorphic equivalents of the late Archean dykes east of the Ramah Group. If this is so, then the character of the gneisses probably results from an Archean granulite event, overprinted by a Hudsonian amphibolite facies metamorphism.

The westernmost part of the map area comprises a rather uniform, white weathering, quartz-feldspar-garnet-graphite gneiss (Plate 41.1f) of uncertain derivation. Mesoscopically the gneiss has an apparently medium grained granitoid texture, with local coarse pegmatoid zones; however, mineral subdomains are polycrystalline and the rock in fact has a blastomylonitic fabric. Locally, lenticular grey quartz subdomains parallelling this fabric are slightly oblique to the compositional layering. A pronounced mineral rodding plunging gently (2-10°) north and south is evident throughout the unit. Two phases of garnet growth, predating and postdating the main tectonic fabric, are evident.

The contact of the white granitoid gneiss with granulite gneisses to the east is largely modified by faulting, but locally the contact is marked by a zone in which thin (1 m or less) sheets of the quartz-feldspar-garnet-graphite gneiss occur within the granulites with an apparently intrusive relationship. Subordinate metasedimentary and mafic granulite rafts occurring locally within the granitoid gneiss also display small-scale intrusion by white granitoid neosome.

Morgan (1975) interpreted the western leucocratic granitoid gneiss as paragneiss. However, the inclusion of discrete paleosomal metasedimentary rafts, contact relations with the granulite gneisses to the east, rather uniform character over large areas, and apparent coarse grained premylonitic relict granitoid textures suggest that this unit is predominantly magmatic in origin. Mineralogically it resembles granitoid segregations and intrusive bodies found in granulite facies paragneisses in the Archean block to the east. It is, therefore, suggested that this unit is a diatexite representing an advanced stage of anatexis of metasediments under granulite facies conditions. However, the age of the metasedimentary paleosome and extent of migration of the mobile mass is unknown.

Economic Geology

The Archean layered quartzite-magnetite iron formation documented by exploration companies in the 1950s and 1960s (Brinex, 1960; Schlobohm, 1958) has a limited distribution. The best zones are found on the southeast shore of Pangertok Inlet on Saglek Fiord where a belt of calc-silicate rocks and grey quartzite (recrystallized chert?) of the Nulliak assemblage locally contains 1-3 m bands of quartzite with 70-80 per cent magnetite. Several other iron formations occur in this area, but none appear economically viable.

A graphite occurrence described from the white granitoid gneiss of inner Saglek Fiord by H.S. MacLean (in Douglas, 1953) could not be located. However, coarse graphite, with a similar mode of occurrence to that described from the prospect, has been observed by us in this part of the survey area.

A scintillometer ("total count" BGS-1L) survey proved unrewarding, with 4000 cps from gneisses at Pangertok Inlet being the highest reading recorded. This is only 8-10 times normal background for this area.

Minor sulphide mineralization occurs on the south wall of Saglek Fiord, where a gabbro sill has intruded black slate of the Nullataktok Formation of the Ramah Group. The slate locally contains 2-5 per cent disseminated pyrite, pyrrhotite and chalcopyrite. A scintillometer survey of the Ramah/basement contact did not reveal any anomalous radioactivity.

Summary

The major Archean rock units identified by earlier mapping in the Nain Province of the Saglek area have been traced southward and westward. The Hudsonian front swings eastward south of Saglek Fiord, transgressing the Ramah Group and giving rise to a complex zone of southward-increasing deformation and metamorphism, but the extent of Hudsonian overprint on the Archean terrane of the Nain Province has not been fully defined. The area has several small mineral occurrences.

Acknowledgments

The assistance of Dan Lee, Bob Voutier, Tim Froude and Janet Russell contributed to the success of the field season. Helicopter services were provided by Codiac Helicopters of Moncton, New Brunswick. The staff of Petro-Canada Ltd. at Saglek and St. John's are thanked for continued co-operation throughout the summer. The Tuttles in Goose Bay expedited, and provided logistical support. This paper was improved by critical review by C. Gower, P. Erdmer, and R. Wardle.

References

Bell, R.
1884: Observations on the geology, mineralogy, zoology and botany of the Labrador coast, Hudson Strait and Bay; Geological Survey of Canada, Report of Progress 1882-85.

Bridgwater, D. and Collerson, K.D.
1976: The major petrological and geochemical characters of the 3600 m.y. Uivak gneisses from Labrador; Contributions to Mineralogy and Petrology, v. 54, p. 43-59.

Bridgwater, D., Collerson, K.D., Hurst, R.W., and Jesseau, C.W.
1975: Field characters of the early Precambrian rocks from Saglek, coast of Labrador; in Report of Activities, Part A, Geological Survey of Canada, Paper 75-1A, p. 287-296.

Bridgwater, D., Collerson, K.D., and Myers, J.S.
1978: The development of the Archean gneiss complex of the North Atlantic region; in Evolution of the Earth's Crust, ed. D.H. Tarling; London Academic Press, p. 19-69.

Brinex
1960: Field investigation of the Saglek Bay area; unpublished report on file with Mineral Development Division, Newfoundland Department of Mines and Energy, St. John's.

Christie, A.M.
1952: Geology of the northern coast of Labrador, from Grenfell Sound to Port Manvers, Newfoundland; Geological Survey of Canada, Paper 52-22.

Coleman, A.P.
1921: Northeastern part of Labrador and New Quebec; Geological Survey of Canada, Memoir 124.

Collerson, K.D. and Bridgwater, D.
1979: Metamorphic development of early Archean tonalitic and trondhjemitic gneisses; Saglek area, Labrador; in Trondhjemites, Dacites and Related Rocks, ed. F. Barker; Elsevier, p. 205-273.

Collerson, K.D., Jesseau, C.W., and Bridgwater, D.
1976: Crustal development of the Archean gneiss complex: eastern Labrador; in The Early History of the Earth, ed. B.F. Windley; John Wiley and Sons, Ltd., p. 237-253.

Collerson, K.D., Kerr, A., Vocke, R.D., and Hanson, G.N.
1982: Reworking of sialic crust as represented in late Archean-age gneisses, northern Labrador; Geology, v. 10, p. 202-208.

Daly, R.A.
1902: The geology of the northeast coast of Labrador; Bulletin of Harvard University Museum of Comparative Zoology, v. 38, Geological Series, v. 5, p. 205-270.

Delebarre, E.C.
1902: Report of the Brown-Harvard expedition to Nachvak, Labrador, in the year 1900; Geological Society of Philadelphia, Bulletin, v. 3, p. 65-212.

Douglas, G.V.
1953: Notes on localities visited on the Labrador coast in 1946 and 1947; Geological Survey of Canada, Paper 53-1.

Hurst, R.W., Bridgwater, D., Collerson, K.D., and Wetherill, G.W.
1975: 3,600 m.y. Rb-Sr ages from early Archean gneisses from Saglek Bay, Labrador; Earth and Planetary Science Letters, v. 27, p. 393-403.

Kerr, A.
1980: Late Archean igneous, metamorphic and structural evolution of the Nain Province at Saglek, Labrador; unpublished M.Sc. thesis, Memorial University of Newfoundland, St. John's.

Knight, I.
1973: The Ramah Group between Nachvak Fiord and Bears Gut, Labrador; in Report of Activities, Part A, Geological Survey of Canada Paper 73-1A, p. 156-161.

Knight, I. and Morgan, W.C.
1977: Stratigraphic subdivision of the Ramah Group, northern Labrador; Geological Survey of Canada, Paper 77-15.

1981: The Aphebian Ramah Group, northern Labrador; in Proterozoic Basins of Canada, ed. F.H.A. Campbell; Geological Survey of Canada, Paper 81-10, p. 313-330.

McGregor, V.R.
1973: The early Precambrian gneisses of the Godthaab district, West Greenland; Philosophical Transactions of the Royal Society of London, v. A273, p. 343-358.

Morgan, W.C.
1972: Ramah Group and Proterozoic-Archean relationships in northern Labrador; in Report of Activities, Part A, Geological Survey of Canada, Paper 72-1A, p. 125-128.

1973: Ramah Group and the contact between Archean and Proterozoic in north Labrador; in Report of Activities, Part A, Geological Survey of Canada, Paper 73-1A, p. 162.

1975: Geology of the Precambrian Ramah Group and basement rocks in the Nachvak Fiord – Saglek Fiord area, north Labrador; Geological Survey of Canada, Paper 74-54.

Odell, N.E.
1938: The geology and physiography of northernmost Labrador; in Northernmost Labrador Mapped From the Air, ed. A. Forbes; American Geographical Society Special Publication 22, p. 187-215.

Ryan, A.B.
1977: Progressive structural reworking of the Uivak gneisses, Jerusalem Harbour, northern Labrador; unpublished M.S. thesis, Memorial University of Newfoundland, St. John's.

Schlobohm, S.F.
1958: Pangertok Inlet-Saglek Fiord discovery area, Labrador; unpublished Brinex report on file with Mineral Development Division, Newfoundland Department of Mines and Energy, St. John's.

Taylor, F.C.
1969: Reconnaissance geology of a part of the Precambrian Shield, northeastern Quebec and northern Labrador; Geological Survey of Canada, Paper 68-43.

1970: Reconnaissance geology of a part of the Precambrian Shield: northeastern Quebec and northern Labrador, Part 2, Geological Survey of Canada, Paper 70-24.

1971: A revision of Precambrian structural provinces in northeastern Quebec and northern Labrador; Canadian Journal of Earth Sciences, v. 8, p. 579-584.

1979: Reconnaissance geology of a part of the Precambrian Shield, northeastern Quebec, northern Labrador and Northwest Territories; Geological Survey of Canada, Memoir 393.

42.

GEOLOGY OF THE WINOKAPAU LAKE AREA, GRENVILLE PROVINCE, CENTRAL LABRADOR[1]

Project 820036

A. Thomas[2] and D. Wood[3]
Newfoundland Department of Mines and Energy

Thomas, A. and Wood, D., Geology of the Winokapau Lake area, Grenville Province, central Labrador; in Current Research, Part A, Geological Survey of Canada, Paper 83-1A, p. 305-312, 1983.

Also in Current Research, ed. R.V. Gibbons, Newfoundland Department of Mines and Energy, Mineral Development Division, Report 83-1, 1983.

Abstract

Precambrian crystalline rocks within the northern part of the Grenville Structural Province southeast of Churchill Falls, Labrador, constitute a mixed granitoid-gneiss terrane. A range of hills is underlain by granulite facies quartzofeldspathic paragneiss containing the mineral assemblage hypersthene, sillimanite, quartz and feldspar. Lowlands contain amphibolite facies quartzofeldspathic paragneiss, orthogneiss and deformed porphyritic granite characterized by the assemblage biotite, sillimanite, muscovite, garnet, quartz and feldspar.

Although extensively tectonized during the Grenvillian Orogeny, paragneiss within the area is tentatively correlated with equivalent rocks in and around the Red Wine Mountains massif to the north which have been deformed and metamorphosed during the Paleohelikian sub-era. Orthogneiss is correlated with granitoid rocks of known Paleohelikian age. The protolith of both amphibolite and granulite grade paragneiss may be as old as Aphebian, and probably had its origin in eugeosynclinal facies greywackes and pelitic sandstones of the Hudsonian orogen in western Labrador.

Introduction

Geological studies in Labrador have to date been focused mainly on Aphebian to Paleohelikian sedimentary-volcanic successions of the Labrador Trough and the Central Mineral Belt. By comparison, relatively little has been done on the huge expanse of gneissic and granitoid rocks belonging to the Grenville Structural Province in southern Labrador. This is due to several factors such as lack of exposure, geological complexity, difficulty in access and the resultant logistical problems which arise such as increased cost of field operations. Most previous programs in the Grenville Province have been large scale, regional geological reconnaissance surveys carried out by the Geological Survey of Canada (Eade, 1952, 1962; Wynne-Edwards, 1960; Stevenson, 1967a, b, 1968, 1969, 1970; Jackson, 1974) at 1:500 000, 1:250 000 or 1:125 000 scale. In addition, Brinex has carried out mapping in selected areas of the Grenville Province ranging in scale up to 1:250 000.

In 1978, with the aid of a Federal-Provincial funding agreement to help offset the high cost of field work, the Newfoundland Department of Mines and Energy began a systematic approach aimed at mapping at 1:100 000 scale, a strip at least 2 NTS map sheets deep along the entire Grenville Front Zone from the Labrador Trough in the west to the coast in the east. In central Labrador, this was done originally with the idea of following previously mapped units, some of which had either proven or potential mineralization, from the Central Mineral Belt, south into the Grenville Province in order to define more clearly the nature of the Grenville Front Zone in this part of Canada. The area mapped between 1978 and 1981 is shown in Figure 42.1. Summaries of this work can be found in Thomas and Hibbs (1980), Thomas (1980, 1981), Thomas et al. (1981) and Jackson and Finn (1982). The study of Emslie et al. (1978) was initiated prior to that of the Newfoundland Department of Mines and Energy, and data from this study have since been incorporated.

In 1982 it was decided to extend the mapping south-westward into the Grenville Province (Fig. 42.1) due to some interesting results from the 1978-1981 study. Specifically, it was discovered that gneissic rocks thought originally to have been Grenvillian in age, were older; Rb-Sr isochron ages of

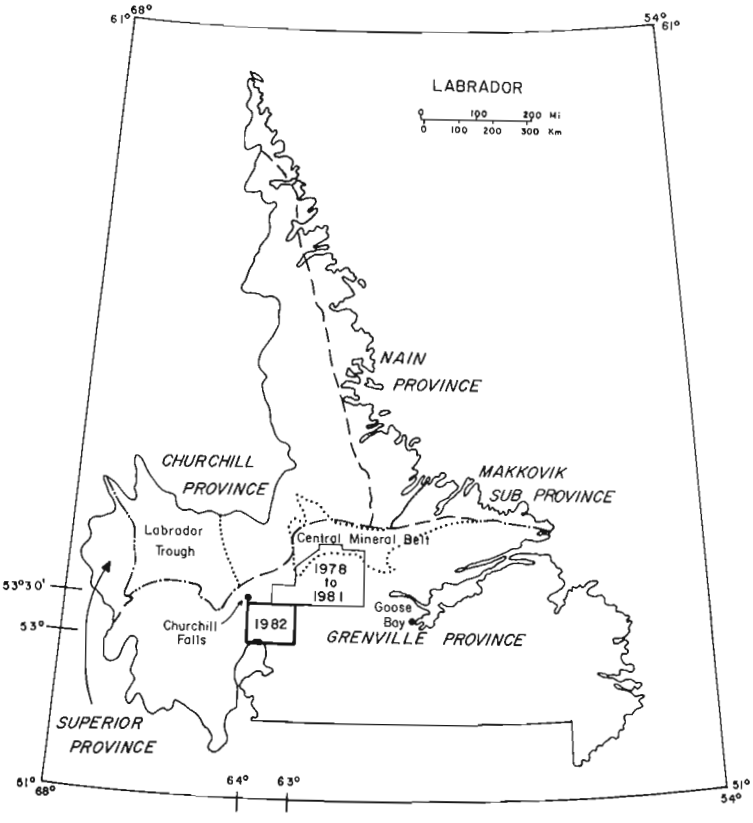

Figure 42.1. *Location of present and previous map areas in central Labrador (structural province divisions after Taylor, 1971).*

[1] Contribution to Canada-Newfoundland co-operative mineral program 1982-84. Project carried by Geological Survey of Canada and Newfoundland Department of Mines and Energy.

[2] Newfoundland Department of Mines and Energy, Mineral Development Division, P.O. Box 4750, St. John's, Newfoundland, A1C 5T7.

[3] Present address, Department of Geology, University of British Columbia, Vancouver, B.C.

1660 ± 37, 1661 ± 88 and 1666 ± 28 Ma were obtained by Fryer (in Thomas, 1981, and personal communication, 1982). This prompted a renewed search for polydeformed gneisses which would yield Grenvillian ages. The 1982 map area is located southeast of Churchill Falls and encompasses NTS 1:50 000 sheets 13E/3, 4, 5 and 6 (Fig. 42.1). Access is primarily by helicopter from Churchill Falls or by road from the Trans-Labrador Highway.

Regional Setting

Regional metamorphic grades and structural trends of rocks in Labrador are shown in Figures 42.2 and 42.3 respectively. The boundaries of the five structural provinces in Labrador (after Taylor, 1971) appear on Figure 42.1 along with those of the Labrador Trough and Central Mineral Belt. The dashed line representing the limit of the Grenville Province indicates the approximate northern extent of recognizable Grenvillian structural deformation. This does not preclude the presence south of this line of rocks exhibiting evidence of older orogenic events.

The Winokapau Lake area encompasses a mixed granitoid, paragneiss terrane metamorphosed primarily to amphibolite and granulite facies (Fig. 42.2). It is located along the southwestern edge of a larger block of crystalline rocks to the east and northeast, the Red Wine Mountains massif, consisting mainly of amphibolite and granulite grade paragneiss intruded by a suite of noritic and charnockitic rocks (see Emslie et al., 1978; Thomas et al., 1981). This block has been thrust northwards over a body of deformed granitoids (termed North Pole Brook Intrusive Suite by Thomas and Hibbs, 1980) of Paleohelikian age. These granitoids are in turn thrust over subgreenschist to greenschist grade sedimentary and volcanic supracrustal rocks belonging to the Nelhelikian Seal Lake Group. To the north of the Winokapau Lake area, a boggy lowland terrane contains scattered exposures of North Pole Brook Suite

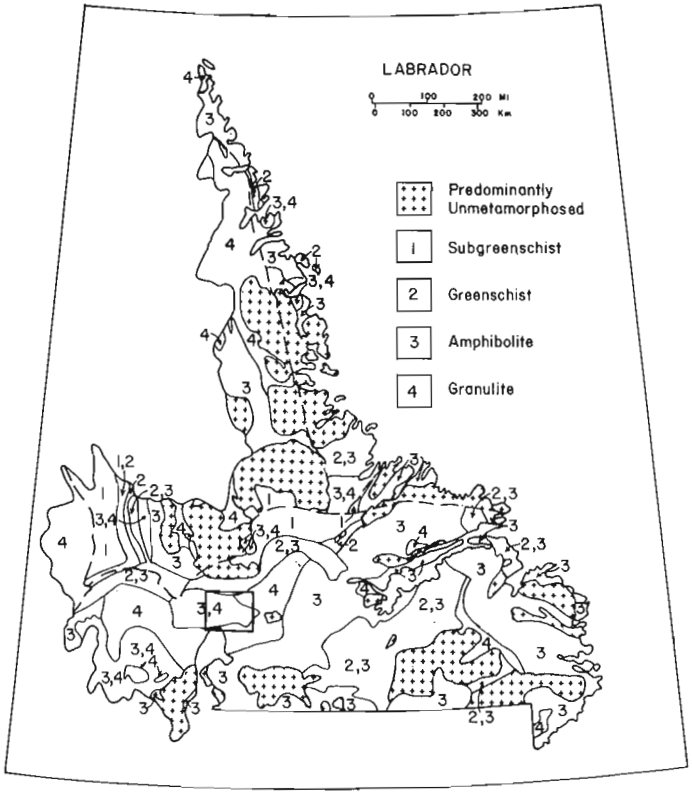

Figure 42.2. Regional metamorphic grades of rocks in Labrador (modified from Fraser and Heywood, 1978).

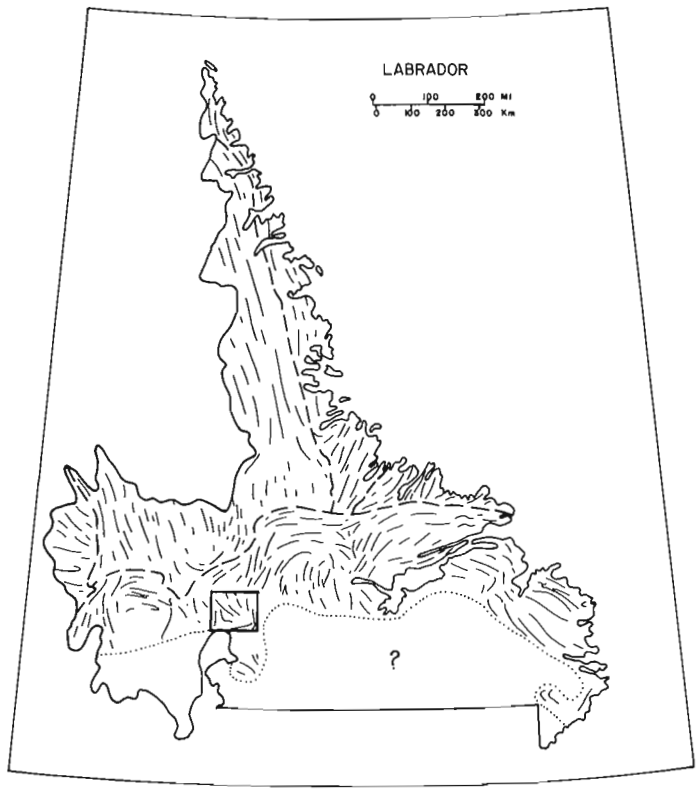

Figure 42.3. Generalized map illustrating regional structural trends in Labrador.

granitoid rocks and older paragneiss. West of the area, the granitoid gneiss terrane continues into the region presently being investigated by Nunn and Christopher (1983). With the exception of granitoids belonging to the North Pole Brook Intrusive Suite, rocks in the region are polydeformed and polymetamorphosed. The entire area has been affected to some degree by the Grenvillian Orogeny, but abundant evidence exists, especially in granitoids and gneiss to the north, of an earlier, presumably late Hudsonian, orogenic event (Thomas, 1981).

General Geology of the Winokapau Lake Area

Although structurally and metamorphically complex, there is little lithological variation of rocks within the map area. Eight units were defined (Fig. 42.4), with two of them, quartzofeldspathic paragneiss and granodioritic to granitic orthogneiss, constituting approximately 80 per cent of exposed bedrock. A range of hills in the northeastern and southern segments of the area is underlain by granulite grade paragneiss (unit 1a), tentatively correlated with the Hope Lake gneiss of Emslie et al. (1978), Thomas (1981) and Thomas et al. (1981). The northeastern hills are actually a physical extension of the Red Wine Mountains massif in which granulite grade paragneiss was first recognized by Emslie et al. (1978). Till or sand covered lowland terrane in the northern, south-central and southeastern parts of the area is dominated by poorly exposed amphibolite grade paragneiss (unit 1b), similar in lithological character and style of deformation to Disappointment Lake gneiss of Thomas (1981) and Thomas et al. (1981) to the northeast. Although granulite and amphibolite grade paragneisses in the vicinity of Winokapau Lake are mineralogically distinct from one another, they exhibit lithological and compositional similarities. It is, therefore, presently assumed that the two are metamorphic variants of the same unit.

Orthogneiss (unit 4b) is poorly to moderately well exposed, primarily in a 16 km wide band passing diagonally from northwest to southeast, through the central part of the area. Porphyritic granite to granodiorite protolith (unit 4a) is identifiable in places within this band. A small body of orthogneiss is also exposed near the northeastern corner of the area. Granodiorite to quartz diorite (unit 5), recrystallized and foliated but with a recognizable relict igneous texture, occurs in the north-central part of the area. It is correlated with less deformed granodiorite to the north, belonging to the North Pole Brook Intrusive Suite of Thomas (1981) and Thomas et al. (1981). Three small, recrystallized and foliated quartz dioritic to dioritic bodies (unit 6) of unknown age and origin are present within the gneisses south of the Churchill River. In addition, a small, plutonic body of foliated to massive granite (unit 8) occurs just south of Winokapau Lake in the southeastern part of the area. Its predominantly massive nature suggests that the body is a late syn- to post-kinematic intrusion associated with the Grenvillian Orogeny.

Gabbronorite, gabbro, diabase and parts of a charnockitic suite more widely exposed to the northeast of the map area (see Emslie et al., 1978), constitute the remaining lithologies. Folded bodies of norite (unit 2) are confined to granulite grade paragneiss in the southern hills. Paleohelikian Shabogamo gabbro and gabbronorite (unit 7) occur as deformed sills and bodies within the amphibolite grade paragneiss and orthogneiss; two late syntectonic diabase dykes of unknown affinity cut orthogneiss and paragneiss near the eastern boundary of the area. The charnockitic rocks (unit 3) are minor in occurrence, confined to several small outcrops north of the west end of Winokapau Lake and in the central part of the southern granulite paragneiss.

All rocks within the Winokapau Lake area have been extensively deformed during the Grenvillian Orogeny, but at least some of the earlier folds and possibly faults are probably pre-Grenvillian. No radiometric age data are presently available on rocks of the Winokapau Lake area, but geological relationships between units and tentative correlations with less tectonized equivalent rocks to the north and northeast, suggest a Paleohelikian or earlier age protolith for the gneisses. They most probably originated within a eugeosynclinal succession of greywackes, sandstones and mudstones similar to that exposed along the western margin of the Labrador Trough.

Paragneiss (unit 1)

Granulite grade paragneiss (unit 1a) is rusty pink to buff, fine- to medium-grained, dense and extremely resistant to weathering. It is banded, with prismatic to fibrous sillimanite, fine grained hypersthene, magnetite and minor biotite confined to mafic layers which pinch and swell, imparting an anastomosed appearance to the rock. Mafic bands vary in width up to 2 cm and commonly contain lenticular clots of densely packed aggregates of fibrolitic sillimanite, pyroxene and magnetite. Ubiquitous fine grained magnetite within these bands results in the granulite paragneiss having a unique, intense aeromagnetic "signature". The anomaly patterns reflect bedrock structural trends and can be used to delineate the limits of the gneiss in drift covered areas. Felsic bands consist of very dense, fine- to medium-grained granoblastic polygonal aggregates of quartz, K-feldspar and plagioclase. These bands are tightly folded, also pinch and swell, and may be up to 5 cm wide. Black pseudotachylyte lenticles and discontinuous layers up to 1 cm wide are commonly found parallel or subparallel to mafic bands; pseudotachylyte veinlets in the same size range also crosscut felsic bands. Abundant evidence of partial melting is present in the granulite paragneiss. Both layer parallel and crosscutting quartz-feldspar sweats are common, as are localized zones of incipient melting within felsic bands. This melting took place under dry conditions at high temperatures as evidenced by subhedral to euhedral hypersthene crystals up to 1 cm long within some of the sweats.

Granulite grade paragneiss is highly deformed with tight isoclinal, chevron and hook folds well developed on a centimetre scale. Shear and cataclastic zones occur locally near faults and along the contact with amphibolite grade paragneiss in the lowlands. The polydeformed nature, high metamorphic grade and predominance of a quartz, feldspar, sillimanite assemblage suggest that granulite paragneiss is derived from an old sedimentary protolith.

Buff-white to pink, amphibolite grade paragneiss (unit 1b) is similar in lithology to granulite grade paragneiss, consisting of quartz, K-feldspar, plagioclase, sillimanite, biotite, muscovite, garnet and magnetite-ilmenite. Hornblende is present in local amphibolite layers within the quartzofeldspathic gneiss and metamorphic differentiation is well developed with mafic minerals segregated into bands up to 0.5 cm wide, separated by 2-3 cm wide quartz-feldspar bands.

Unlike granulite grade paragneiss, amphibolite paragneiss is less dense and more fissile due to its richness in biotite and muscovite. Strong linear and planar fabrics are developed respectively within and parallel or subparallel to the gneissic banding. Sillimanite may be prismatic or fibrolitic and tends to form radiating clusters along the contact between mafic and quartzofeldspathic bands. Lenticular fibrolite clots are also common within the mafic bands as are euhedral to subhedral garnet porphyroblasts which overgrow the foliation. Granoblastic polygonal texture predominates within the quartz-feldspar bands and is in most places medium- to coarse-grained. At least three generations of pegmatite sweats indicate that partial melting was an ongoing process during formation of the paragneiss. Early melt bands, parallel to the gneissic banding, are abundant throughout the amphibolite paragneiss terrane and commonly result in a migmatitic structure. These bands are ptygmatically folded and cut by a later set of veinlets which are also deformed. The most recent sweats are associated with deformed, coarse grained tourmaline pegmatite dykes; together with these dykes, they crosscut all previous structures, melt bands and veinlets.

Amphibolite grade paragneiss is highly tectonized, exhibiting complex minor fold patterns including mushroom and dome and basin structures. The structural style, mineralogy and overall lithology of this unit compares favourably with that of the Disappointment Lake gneiss of Thomas (1981) dated by B. Fryer (personal communication, 1982) by Rb-Sr at 1666 ± 88 Ma. Although amphibolite grade paragneiss around Winokapau Lake has undergone a more complex deformational history, it is tentatively correlated with Disappointment Lake gneiss to the northeast.

Gabbronorite (unit 2)

Bodies of noritic to gabbroic composition intrude granulite grade paragneiss in the south. They consist of plagioclase, hypersthene, diopside, magnetite, and minor biotite and hornblende. Igneous textures are preserved in the centres of the bodies whereas the margins are recrystallized to granoblastic polygonal aggregates. Sharp, intrusive, chilled marginal contacts of gabbronorite against granulite gneiss are well exposed. These rocks are similar in composition and intrusive style to gabbronoritic rocks to the northeast, described by Emslie et al. (1978) and Thomas et al. (1981).

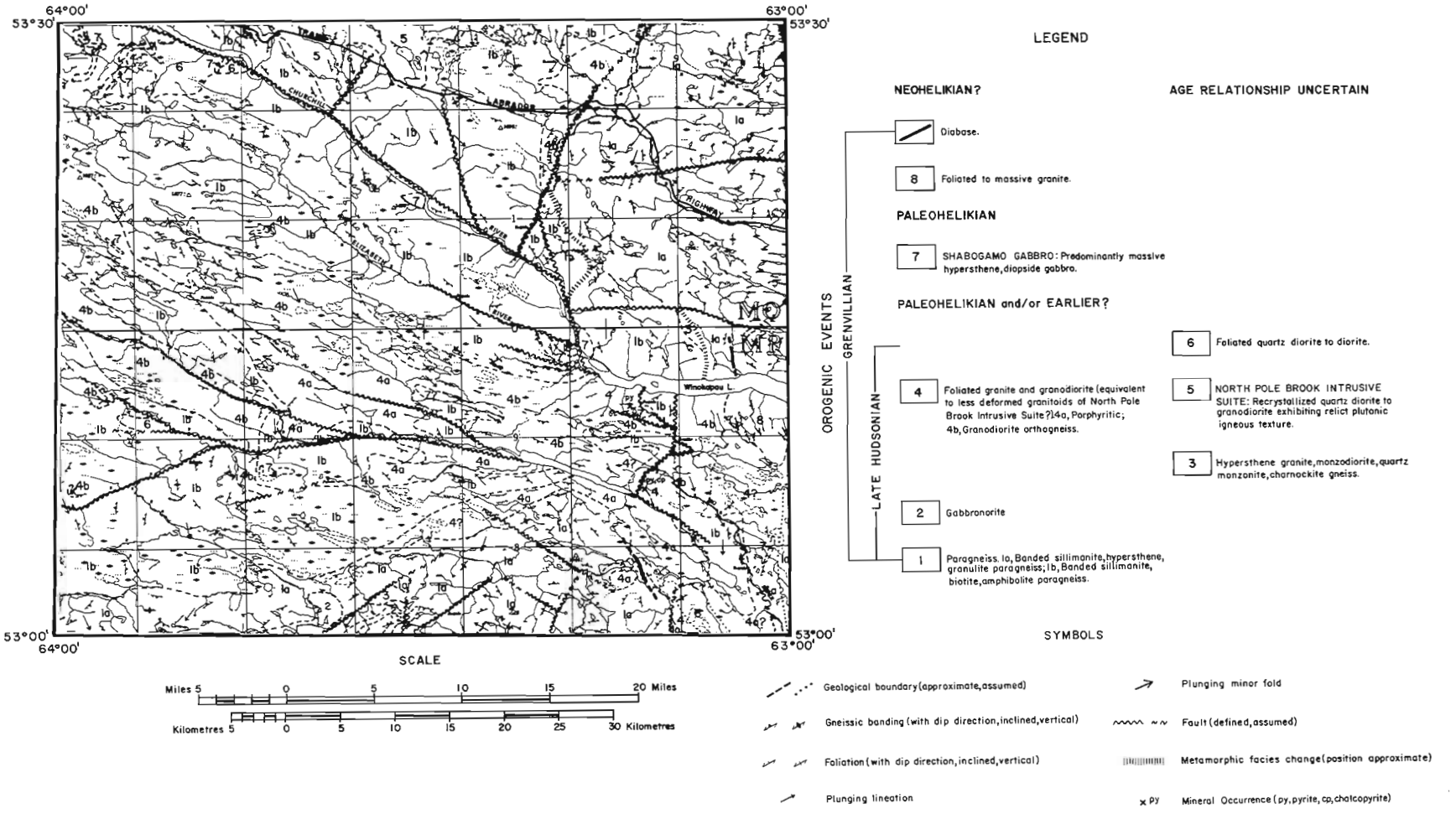

Figure 42.4. *Geology of the Winokapau Lake area, central Labrador.*

Hypersthene Granitoids (unit 3)

Several outcrops define a small body of hypersthene-bearing granite-granodiorite north of Winokapau Lake. A body of similar size also occurs in the central part of the granulite paragneiss. Quartz, K-feldspar, plagioclase, hypersthene and minor biotite are the main constituents. The body north of Winokapau Lake is highly deformed with a cataclastic texture. It is fault bounded on the north and its eastern margin runs close to a presumed metamorphic facies change from amphibolite to granulite grade. The southern body is approximately rectangular, bounded on two sides by faults and on the remaining two sides forming an intrusive contact within host gneiss.

Foliated Granite and Orthogneiss (unit 4)

The metamorphosed granitoid rocks are divided into two main subunits. Porphyritic granite to granodiorite (unit 4a) is most common in the central and southeastern parts of the area. It consists of abundant megacrysts of microcline up to 2 cm set in a medium grained groundmass of quartz, plagioclase, orthoclase, biotite and hornblende. A variety of metamorphic and structural characteristics are displayed. Porphyritic granite-granodiorite may be moderately to strongly foliated, lineated or banded. Where lineated, primary igneous texture is preserved on outcrop faces normal to the plunge of the lineation, and megacrysts are attenuated on faces parallel to the lineation. With increased deformation and metamorphism, total recrystallization takes place resulting in formation of orthogneiss (unit 4b). The mineralogy remains the same except for the addition of euhedral garnets up to several millimetres in size. Igneous texture is completely altered to coarse, granoblastic polygonal texture although megacrysts remain as lenticular augen. With extreme deformation, the megacrysts are strung out to form quartzofeldspathic bands. Since intense deformation is widespread throughout the area and low strain zones are present only locally in fold noses, banded or augen orthogneiss predominates over its megacrystic protolith.

No contacts between paragneiss of unit 1 and rocks of unit 4 were observed, but sillimanite-bearing paragneiss xenoliths are present within porphyritic granodiorite and orthogneiss in the adjoining map area (see Nunn and Christopher, 1983). Indications are that the granitoids intruded the paragneiss terrane prior to at least the last major period of deformation.

North Pole Brook Intrusive Suite (unit 5)

Quartz diorite to granodiorite, present in the northern part of the area, exhibits relict equigranular igneous texture and is much less deformed than the orthogneiss. It consists of quartz, K-feldspar, biotite, hornblende and magnetite. Although strongly foliated in the map area, it can be traced northwards into almost undeformed equivalents, which have been collectively termed North Pole Brook Intrusive Suite by Thomas and Hibbs (1980). This unit is intrusive into older polydeformed amphibolite grade paragneiss north of the Churchill River, but could not be traced south of the river into orthogneiss which is thought to represent its higher grade equivalent.

Foliated Quartz Diorite to Diorite (unit 6)

Confined to three small bodies south of the Churchill River and Winokapau Lake, quartz diorite-diorite consists of quartz, K-feldspar, plagioclase, hornblende, minor biotite and magnetite. The rock is dark green, almost black on weathered and fresh surfaces, and in places approaches gabbroic composition. No contacts were observed, but the bodies probably represent younger intrusives within the amphibolite grade paragneiss.

Shabogamo Gabbro (unit 7)

Gabbro is present within the amphibolite grade paragneiss terrane as narrow, elliptical bodies, probably representing disjointed and boudinaged sills. Although the bodies are metamorphosed, relict igneous textures are preserved within their centres; corona textures are present locally. Orthopyroxene, clinopyroxene, abundant magnetite-ilmenite and plagioclase are the main constituents. The bodies tend to be extremely coarse grained in their centres, and fine grained and recrystallized along their margins. They intrude amphibolite grade paragneiss and orthogneiss and are correlated with the Shabogamo Intrusive Suite, widely exposed throughout western Labrador.

Foliated to Massive Granite (unit 8)

This is the least tectonized rock in the area and is thought to be quite young. Granite characterized by coarse, equigranular grain size and plutonic, igneous texture occurs in a small body south of Winokapau Lake. It consists of quartz, orthoclase, plagioclase and biotite with minor magnetite or ilmenite. Xenoliths of mafic to quartzofeldspathic paragneiss are abundant within the granite which is bleached along the xenolith contacts. The body has intruded a previously deformed gneiss terrane and may have had its origin in the partial melt fraction derived during the metamorphism of those same gneisses.

Structure

No major regional structures were observed due to a combination of poor exposure, especially along contacts between different rock types, and lack of continuous passive marker horizons within individual units. Therefore, all fold closures and axes are inferred from variations in trends of gneissic banding, foliation and approximated contacts between contrasting rock types. Figure 42.5 shows the major structural elements within the Winokapau Lake map area. It is emphasized that the structural inferences made are preliminary and have to undergo more rigorous testing by the data which have not yet been fully compiled. Four major periods of deformation are postulated, with evidence for four phases of folding and as many faulting events. Figure 42.6 pictorially illustrates a possible theoretical structural interpretation for rocks within the map area.

The first period of deformation resulted in the creation of a well developed gneissic and primary melt banding. The banding has a moderate to steep dip and is parallel to F_1 isoclinal fold axes about which it has been folded by D_1. The original trend of these axes has been changed by later deformations, but may have been east-west. During D_2, F_1 isoclinal structures were folded about closed to tight northwest-southeast F_2 fold axes. A second melt banding consisting of quartz-feldspar veinlets which crosscut the primary gneissic banding also formed at this time. Under the effects of D_3, F_1 and F_2 regional structures were deformed about east-trending F_3 fold axes into isoclinal mushroom and dome and basin fold patterns. The D_2 melt banding was ptygmatically folded and a third system of crosscutting partial melt veinlets formed, as well as associated tourmaline pegmatite dykes.

Stretched augen, mineral elongation and mineral streaking define a consistent pattern of strongly developed lineations (Fig. 42.7) presently thought to be associated with F_3 structures within the amphibolite grade paragneiss and orthogneiss. The lineations plunge at an angle of approximately 40° on a bearing of 155° and indicate a probable northwesterly transport direction for bulk rock movement during D_3. The trend of these lineations is strikingly similar to those within the Red Wine Mountains massif to the northeast (see Emslie et al., 1978, Fig. 27.3).

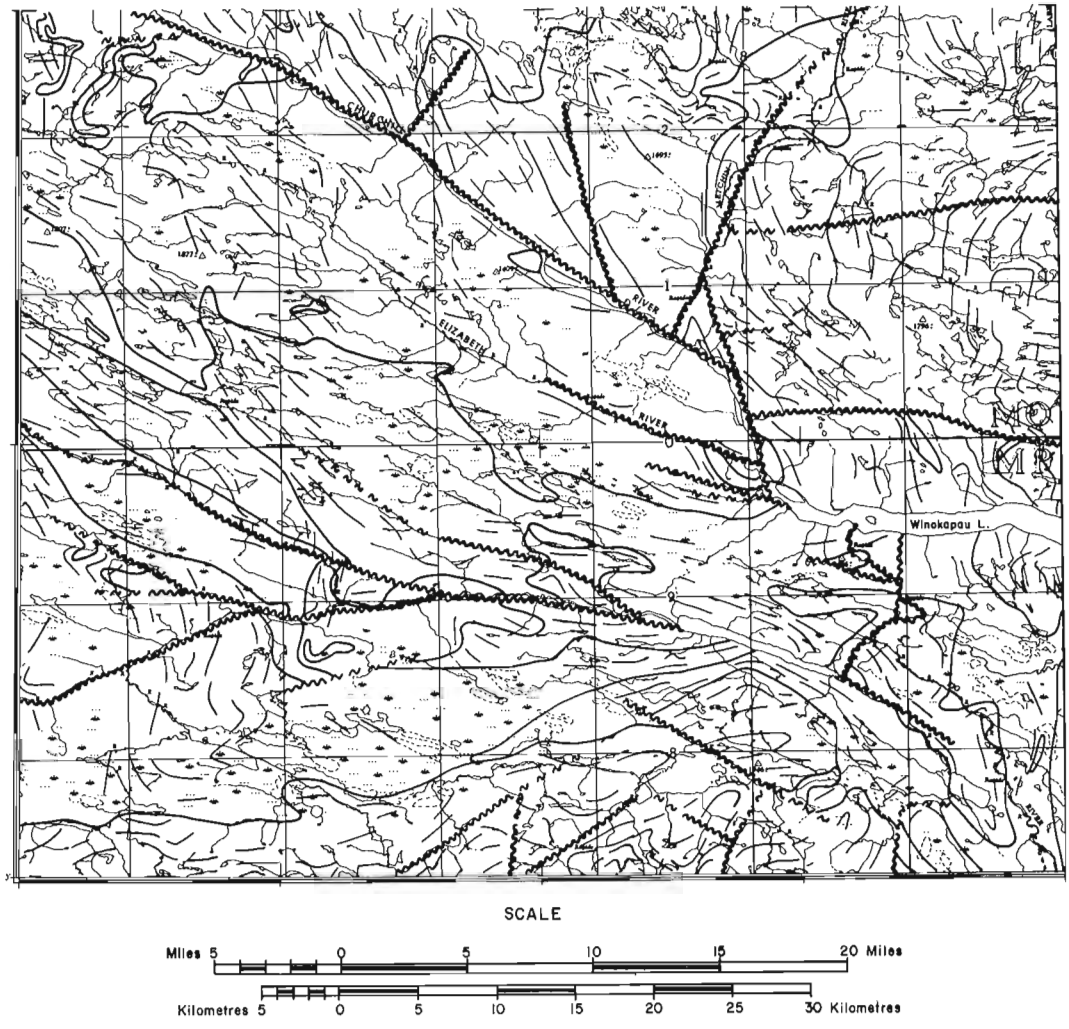

Figure 42.5. *Structural grain in the Winokapau Lake area, based on trends of gneissic banding and foliation.*

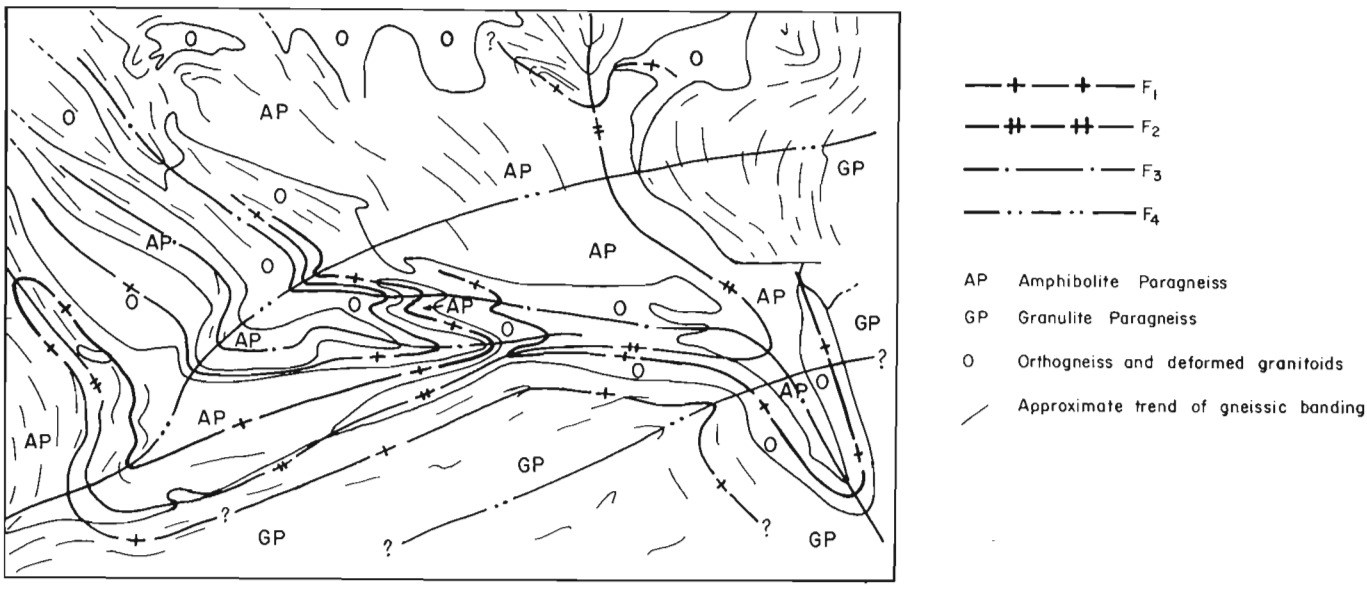

Figure 42.6. *Pictorial diagram (not to scale and neglecting effects of faulting) illustrating possible structural interpretation of rocks around Winokapau Lake.*

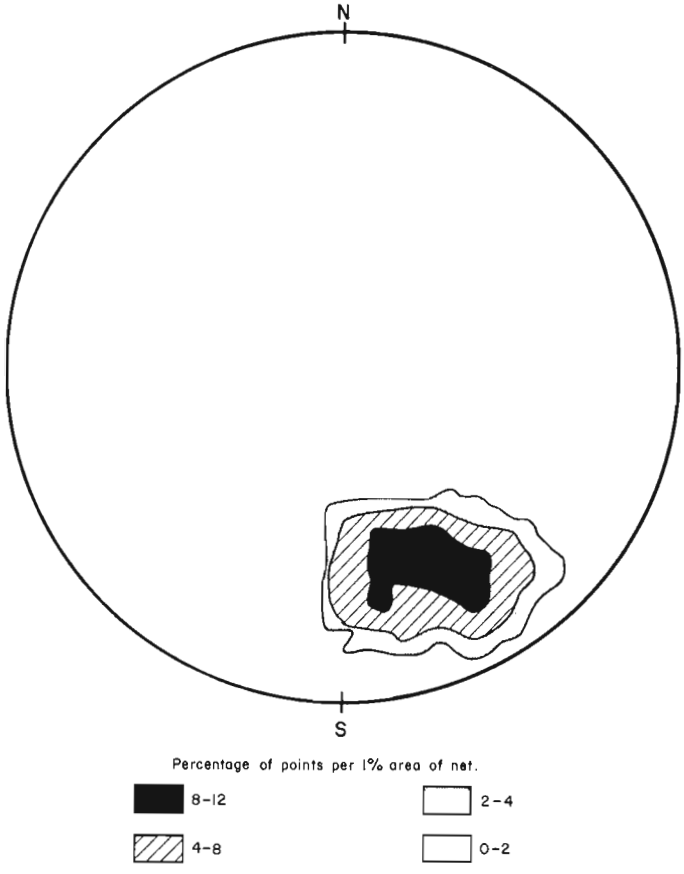

Figure 42.7. *Contoured lower hemisphere stereographic plot of lineations from the amphibolite paragneiss, orthogneiss and granitoids (based on 56 data points).*

The most recent deformation (D_4) has resulted in open folding of all previous structures about east-northeast-trending F_4 fold axes. This has caused F_3 fold structures to open up and F_2 fold structures simultaneously to become more attenuated. The D_3 melt veinlets have been strongly deformed whereas the associated pegmatite dykes were more gently deformed into open minor folds.

In Figure 42.6, structures have been tentatively extended from the amphibolite grade paragneiss and orthogneiss into the granulite grade paragneiss terrane. In the adjoining area to the west, there is limited evidence to suggest that the granulite gneiss constitutes a separate structural block which acted as a buttress against some of the deformation within the amphibolite grade rocks. If this turns out also to be the case in the Winokapau Lake area, the above structural extension may be invalid.

No attempt is made to correlate faults within the map area with deformation events responsible for folding. All faults are based on one or more of the following criteria: (1) presence of fault breccia; (2) shear and/or mylonite zones; (3) slickensided surfaces associated with shearing; (4) mismatch of lithological units across lineaments; (5) scarps associated with shearing and lineaments; (6) well defined lineaments alone.

The earliest generation faults are found within the granulite grade paragneiss. In the eastern granulite terrane, east-west faults have a poorly documented but apparent sinistral component to their movement. In the southern granulite terrane, a conjugate set of northeast and southwest faults are associated with intense mylonitization and shearing.

Second generation northeast- to north-trending faults terminate the east-west faults in the eastern granulite terrane, and at least one is an extremely deep-seated reverse fault. It separates granulite grade paragneiss from the lower grade rocks to the west, and is continuous north of the map area with the major fault that defines the Red Wine Mountains granulite massif. It has also been folded during D_3 and cut by Shabogamo gabbro. In addition, sometime during its history, the fault underwent ductile movement during a high grade metamorphic event. Evidence for this is the presence of syntectonic sillimanite, having a preferred orientation within the plane of the fault.

A single fault running south from the west end of Winokapau Lake constitutes evidence for third generation faulting.

The numerous fourth and last generation faults are reflected in the northwest- to west-trending drainage pattern. They are fundamental structures along which preglacial and postglacial erosion has taken place to produce spectacular deep gorges. These gorges normally contain abundant glaciofluvial deposits and it is obvious that the fourth generation faults have influenced the orientation of postglacial spillways and more recently regenerated drainage. Erosion along one of these faults has created the Churchill River gorge through which the entire runoff of the Smallwood Reservoir (formerly Michikamau Lake) catchment area flows. The fourth generation faults terminate or impart a sizeable left lateral offset component to second generation faults, and the Churchill River fault which continues through Winokapau Lake terminates the third generation fault.

First and second generation faults are thought to be extremely old structures which may date back to the Hudsonian Orogeny. The previously mentioned, deep seated reverse fault is probably an ancient structure which has been reactivated several times, the last being during the Grenvillian Orogeny. Third and fourth generation faults are most likely Grenvillian in age and may incorporate significant reverse movement as well as repeated cycles of activation.

Metamorphism

The metamorphic grade of rocks within the Winokapau Lake area varies from amphibolite in the northwest to granulite in the south and east. The division between amphibolite grade and granulite grade rocks is for the most part abrupt. In the east, it runs partly along the reverse fault which juxtaposes rocks of the two facies, and in part constitutes a metamorphic transition. In the south, the nature of the division is unknown. There is no evidence to indicate a gradual increase in metamorphic grade from north to south throughout the area.

Granitoid rocks in the northern and northwestern part of the area exhibit static recrystallization textures and incipient melt zones resulting from a single amphibolite grade metamorphic event. The stable mineral assemblage present is plagioclase, quartz, biotite and hornblende. Paragneiss in contact with these granitoids has been metamorphosed at least once to amphibolite grade. A prograde plagioclase, K-feldspar, quartz, biotite, sillimanite, garnet assemblage is overprinted by retrograde muscovite. Plates up to 1 cm can be found within and discordant to the foliation, but the retrogression is patchy and muscovite-free zones are common.

Both paragneiss and orthogneiss in the central part of the map area have been metamorphosed to amphibolite grade, at least once by the same event which affected granitoids in the northern part of the area. Plagioclase, K-feldspar, quartz, biotite, sillimanite, garnet and muscovite are present in paragneiss; plagioclase, K-feldspar, quartz,

biotite, hornblende and garnet in orthogneiss. The development of muscovite is patchy within the central paragneiss terrane, but much more voluminous than in the north and northwest.

Granulite grade paragneiss and gabbronorite in the south and east, chiefly have the assemblages plagioclase, K-feldspar, quartz, hypersthene, sillimanite, minor biotite, and plagioclase, hypersthene, diopside, magnetite-ilmenite respectively. Sapphirine was also tentatively identified. Temperature, total pressure and water pressure constraints on these rocks, require formation near the base of the crust; therefore it is probable that granulite and amphibolite grade paragneisses are respectively deeper and shallower crustal level equivalents of the same unit.

Discussion

Granitoids and orthogneiss are tentatively correlated with less deformed, lower grade equivalent rocks belonging to the North Pole Brook Intrusive Suite, which yield a Rb-Sr isochron cooling age of 1654 ± 22 Ma (Fryer in Thomas, 1981). The amphibolite grade event recorded in both granitoids and orthogneiss at Winokapau Lake must therefore be younger and is probably Grenvillian.

Amphibolite grade paragneiss is correlated with equivalent grade Disappointment Lake gneiss, which is intruded by North Pole Brook granitoids (Thomas, 1981) and was determined by Fryer (personal communication, 1982) to have a preliminary Rb-Sr age of 1666 ± 28 Ma. If this correlation is valid, paragneiss at Winokapau Lake must have been deformed and metamorphosed to amphibolite grade at least twice; once during the Hudsonian Orogeny or an early Paleohelikian event, and again during the presumed Grenvillian event recorded in the granitoids and orthogneiss. The development of three generations of melt-banding within the paragneiss also suggests a history of more than one metamorphic event.

Granulite grade paragneiss is correlated with Hope Lake gneiss (see Emslie et al., 1978; Thomas, 1981; Thomas et al., 1981) which gives a preliminary Rb-Sr error-chron age of 1675 Ma (Emslie in Thomas, 1981). The granulite grade paragneiss at Winokapau Lake has probably experienced a similar metamorphic history to that of the amphibolite grade paragneiss, but due to the anhydrous condition of the rocks no evidence of lower grade metamorphic events remains.

Therefore, although all rocks within the Winokapau Lake area have undergone amphibolite facies metamorphism during the Grenvillian Orogeny, it is possible that granulite grade and in part amphibolite grade events recorded in the paragneiss terrane may be as old as late Hudsonian. At present no thin sections have been examined and the identification of specific assemblages and textures which might enable the separation of earlier and later metamorphic events awaits further work.

Acknowledgments

We thank Lakeland Helicopters Limited and helicopter pilots W. Muise and A. Vandrie. T. Brace, J. Hayes and D. King provided field assistance. The manuscript was critically reviewed by D. Wardle and B. Ryan of the Newfoundland Department of Mines and Energy.

References

Eade, K.E.
1952: Unknown River (Ossokmanuan Lake, east half), Labrador, Newfoundland; Geological Survey of Canada, Paper 52-9.

1962: Battle Harbour – Cartwright, Newfoundland; Geological Survey of Canada, Map 22-1962.

Emslie, R.F., Hulbert, L.J., Brett, C.P., and Garson, D.F.
1978: Geology of the Red Wine Mountains, Labrador: the Ptarmigan Complex; in Current Research, Part A, Geological Survey of Canada, Paper 78-1A, p. 129-134.

Fraser, J.A. and Heywood, W.W., ed.
1978: Metamorphism in the Canadian Shield; Geological Survey of Canada, Paper 78-10.

Jackson, G.D.
1974: Opocopa Lake (east half), Quebec-Newfoundland; Geological Survey of Canada, Map 1417A.

Jackson, V. and Finn, G.
1982: Geology, petrography and petrochemistry of granulite rocks from Wilson Lake, Labrador (13E/7); Newfoundland Department of Mines and Energy, Mineral Development Division, Open File Report Lab. 13E/7 (40).

Nunn, G.A.G. and Christopher, A.
1983: Geology of the Atikonak River area, Grenville Province, western Labrador; in Current Research, Part A, Geological Survey of Canada, Paper 83-1A, report 51.

Stevenson, I.M.
1967a: Minipi Lake, Newfoundland; Geological Survey of Canada, Map 6-1967.

1967b: Goose Bay map area, Labrador; Geological Survey of Canada, Paper 67-33.

1968: Geology of Lac Joseph map area, Newfoundland and Quebec; Geological Survey of Canada, Paper 67-62.

1969: Lac Brûlé and Winokapau Lake map areas, Newfoundland and Quebec; Geological Survey of Canada, Paper 67-69.

1970: Rigolet and Groswater Bay map areas, Newfoundland (Labrador); Geological Survey of Canada, Paper 69-48.

Taylor, F.C.
1971: A revision of Precambrian structural provinces in northeastern Quebec and northern Labrador; Canadian Journal of Earth Sciences, v. 8, p. 579-584.

Thomas, A.
1980: A summary of geology and data collected during 1978 in the Red Wine Lake – Letitia Lake area, central Labrador; Newfoundland Department of Mines and Energy, Mineral Development Division, Open File Report Lab. 13L (56).

1981: Geology along the southwestern margin of the Central Mineral Belt, Labrador; Newfoundland Department of Mines and Energy, Mineral Development Division, Preliminary Report 81-4.

Thomas, A. and Hibbs, D.
1980: Geology of the southwestern margin of the Central Mineral Belt, Labrador; in Current Research, ed. C.F. O'Driscoll and R.V. Gibbons, Newfoundland Department of Mines and Energy, Mineral Development Division, Report 80-1, p. 166-176.

Thomas, A., Jackson, V., and Finn, G.
1981: Geology of the Red Wine Mountains area, central Labrador (13E/9, 10, 11, 15, 16; 13F/12, 13); Newfoundland Department of Mines and Energy, Mineral Development Division, Open File Report Lab. (573).

Wynne-Edwards, H.R.
1960: Michikamau Lake (west half), Newfoundland; Geological Survey of Canada, Map 2-1960.

43.

THE MACLEAN EXTENSION OREBODY, BUCHANS, NEWFOUNDLAND[1]

Contract 08GR.23233-2-0500

W.P. Binney[2], J.G. Thurlow[3], and E.A. Swanson[4]
Economic Geology Division

Binney, W.P., Thurlow, J.G., and Swanson, E.A., The MacLean Extension orebody, Buchans, Newfoundland; in Current Research, Part A, Geological Survey of Canada, Paper 83-1A, p. 313-319, 1983.

Also in Current Research, ed. R.V. Gibbons, Newfoundland Department of Mines and Energy, Mineral Development Division, Report 83-1, 1983.

Abstract

About 53 per cent of the ore mined to date at Buchans, Newfoundland has been from transported volcanogenic massive sulphide deposits. A detailed sedimentological investigation is in progress to determine the source, transport mechanism and deposit lithologies for the MacLean and MacLean Extension orebodies. This report describes briefly lithological and sedimentological features of the MacLean Extension orebody. Two ore units occur in a sequence of felsic pyroclastic rocks of the Lucky Strike Ore Horizon Sequence. Three lithological units: sulphide matrix ore, polylithic breccia-conglomerate and arenaceous conglomerate are distinguished in the lower ore unit. The upper ore unit is exposed at one location in the MacLean Extension workings. Here two sedimentary cycles have been identified. Sedimentological work to date supports the concept of ore emplacement by subaqueous sedimentary gravity flows with deposition in channels. Several individual flows have been recognized based on their distinctive lithologies.

Introduction

From 1928 to 1978, the volcanogenic massive sulphide deposits of the Buchans camp yielded 15 813 000 tonnes of ore with an average grade of 14.62% Zn, 7.60% Pb, 1.34% Cu, 114.77 g Ag/t and 1.34 g Au/t (Thurlow and Swanson, 1981). About 53 per cent of this total was transported ore[5] from the Lucky Strike North, Two Level, Rothermere, MacLean, Oriental #2 and Old Buchans Conglomerate ore deposits (Fig. 43.1). The economically most significant transported ore has been the Rothermere and MacLean orebodies. The MacLean Extension orebody, currently under development in

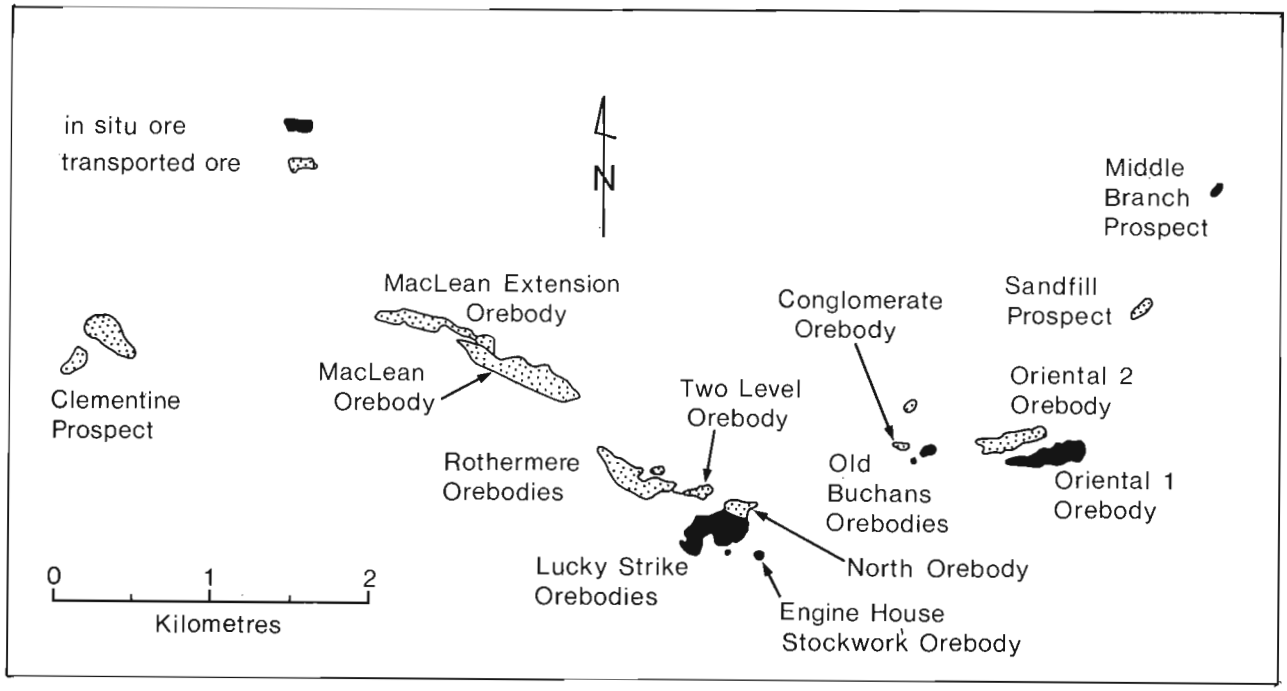

Figure 43.1. *Distribution of orebodies and ore types at Buchans, Newfoundland projected to surface. After Thurlow and Swanson (1981) with MacLean Extension orebody added.*

[1] Contribution to Canada-Newfoundland co-operative mineral program 1982-84. Project carried by Geological Survey of Canada.

[2] P.O. Box 1152, Truro, Nova Scotia B2N 5H1
[3] Abitibi-Price Inc., Buchans, Newfoundland A0H 1G0
[4] ASARCO Incorporated, Buchans, Newfoundland A0H 1G0

[5] Transported orebodies are elongate-tabular accumulations composed of discrete high grade sulphide fragments and occurring in paleotopographic depressions at and near the same stratigraphic horizon as the major in situ orebodies (Thurlow and Swanson, 1981).

September 1982, is the most northwesterly deposit on the Rothermere-MacLean trend and contains 339 400 tonnes of ore with an average grade of 10.22% Zn, 5.90% Pb, 1.42% Cu, 88.02 g Ag/t and 0.72 g Au/t.

The present study, undertaken by Binney, is an extension of an ongoing study by Thurlow, Swanson and other company personnel. The study emphasizes the nature, origin and exploration guides for transported ore and will be concentrated on the MacLean and MacLean Extension orebodies. This report outlines some stratigraphic and sedimentological relationships of the MacLean Extension orebody.

Acknowledgments

W.P. Binney would like to thank the staff of ASARCO and Abitibi-Price for their generous assistance throughout this study.

R.V. Kirkham and W.H. Poole reviewed the manuscript and made many useful comments.

Geological Setting

The following descriptions of lithology, structure and sedimentological relationships apply only to the MacLean Extension orebody. These are based on observations in underground workings and diamond drill core. For general descriptions of the transported ores of the Buchans camp see Thurlow and Swanson (1981), Walker and Barbour (1981) and Calhoun and Hutchinson (1981).

The mineralization is contained within the Lucky Strike Ore Horizon Sequence, a group of predominantly felsic pyroclastic rocks with interbedded flows, breccias and volcaniclastic sedimentary rocks. The Lucky Strike Ore Horizon Sequence conformably overlies the Intermediate Footwall, a complex assemblage of altered volcanic and volcaniclastic rocks (Thurlow and Swanson, 1981).

Only those portions of the Lucky Strike Ore Horizon Sequence that contain transported sulphides and/or barite have been examined in detail. The lateral distribution of two ore-bearing units in the MacLean Extension orebody is shown in Figure 43.2 and as a schematic idealized cross-section in Figure 43.3. The MacLean Extension orebody adjoins the MacLean deposit but the contact relationships are obscured by faults and a diabase dyke.

The lower ore unit conformably overlies green dacitic tuffaceous rocks along an irregular contact. Mineralization occurs as clasts of sphalerite-galena, sphalerite-galena-chalcopyrite and barite in a matrix which consists of varying proportions of lithic detritus, galena, sphalerite and barite. Overlying the lower ore unit is a sequence of felsic pyroclastic rocks including volcanic breccias.

The upper ore unit, known in mine terminology as the "#4 baritic zone", conformably overlies these felsic pyroclastic rocks. The ore beds within the upper unit are notable for their high content of barite in addition to galena, sphalerite and small lithic fragments. Felsic pyroclastic rocks of the Lucky Strike Ore Horizon Sequence form the hangingwall of the MacLean Extension orebody.

Both major and minor faults occur in the MacLean Extension orebody. A major thrust fault defines the southern margin of the orebody. Thrust and normal faults with small displacements cut the ore beds at numerous locations. Offsets on these faults range from a few centimetres to tens of metres. Felsite and diabase dykes also cut the ore beds, but in most areas little offset of the ore exists across the dykes.

The Lower Ore Unit

The lower ore unit ranges in thickness from 0 to greater than 15 m. Within the unit a virtual continuum exists from high grade sphalerite and galena containing scattered lithic clasts, through sphalerite and galena blocks and lithic

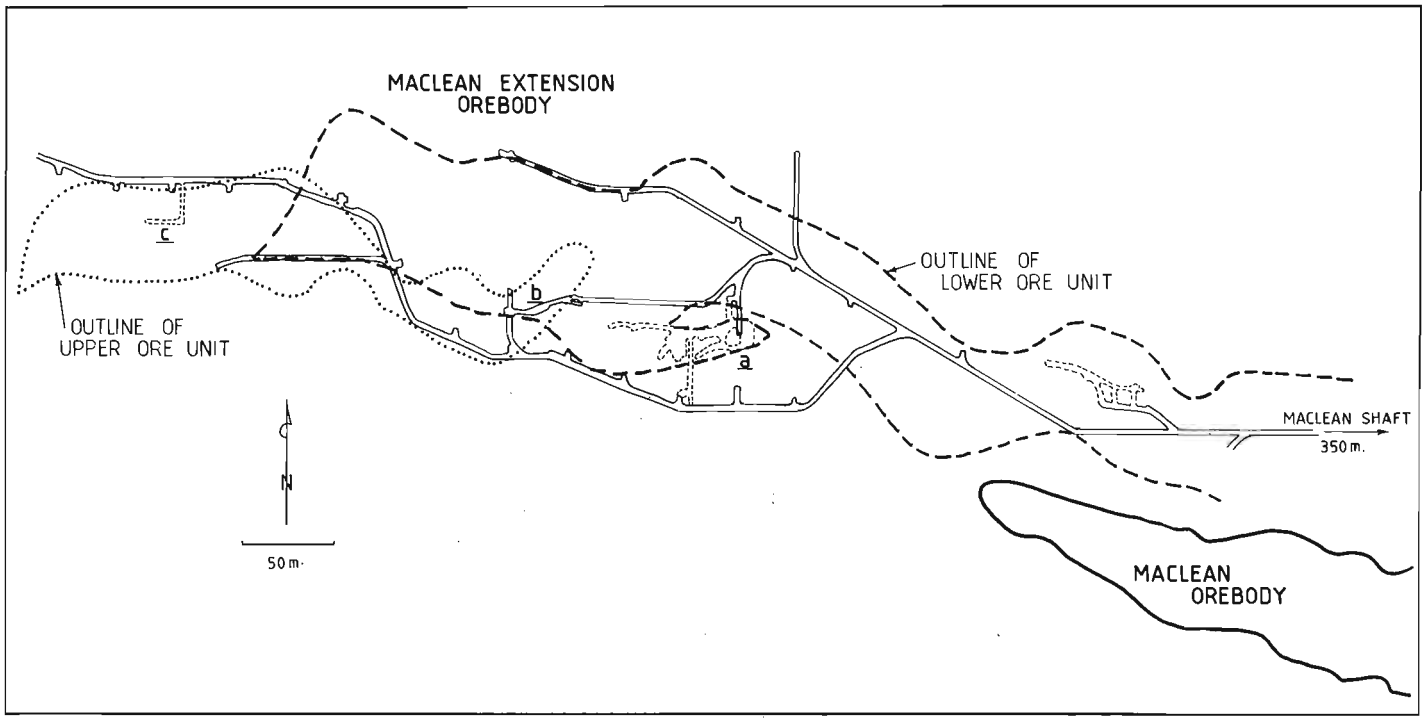

Figure 43.2. Vertical projection of the ore-bearing units of the MacLean Extension orebody to the 20 level, MacLean Shaft. Letters are locations referred to in text.

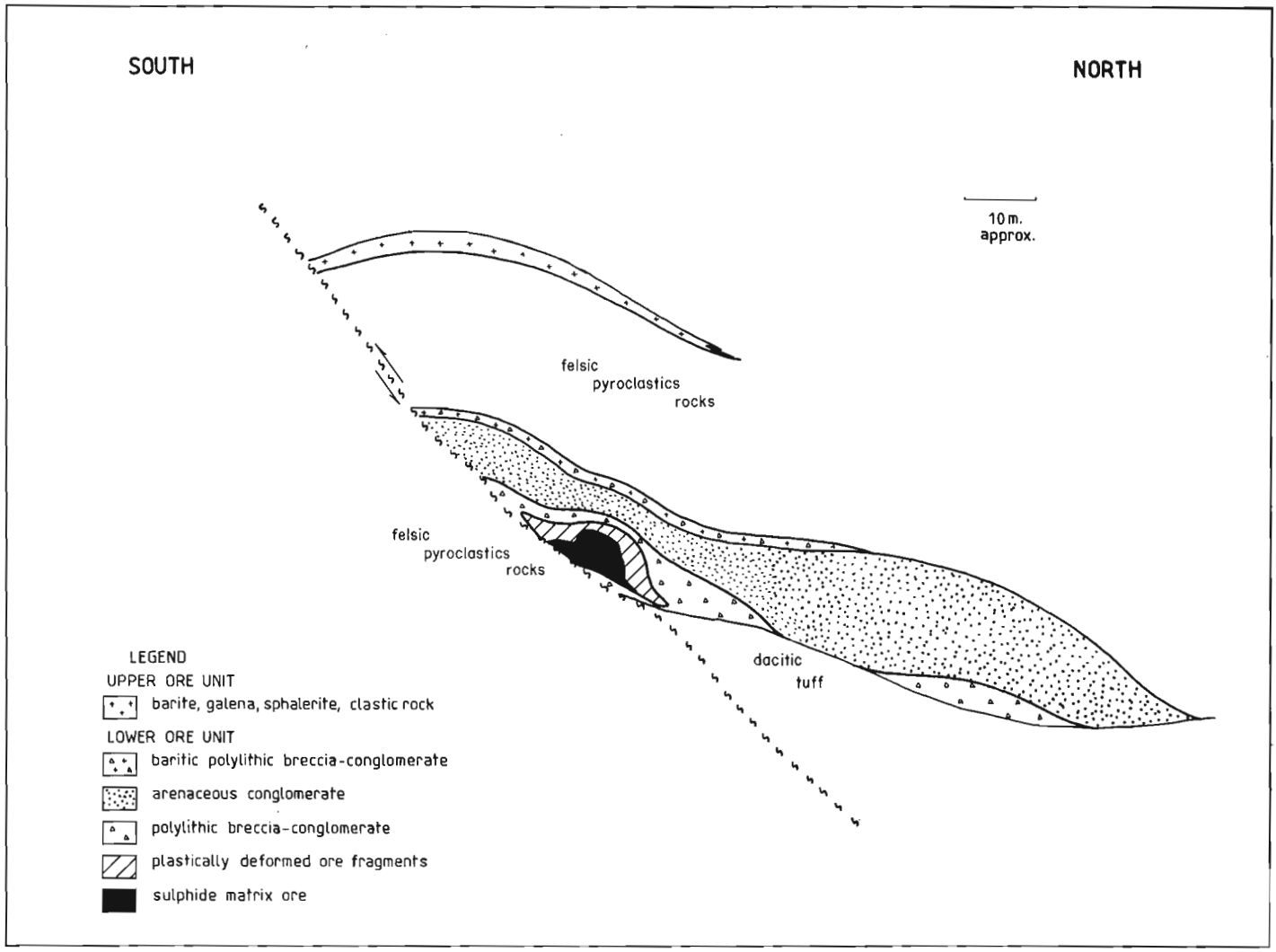

Figure 43.3. *Schematic north-south cross-section of the MacLean Extension orebody showing some generalized lithological units.*

fragments in a clastic matrix, to arenaceous conglomerate with minor pebble-size detritus including rare sphalerite and galena clasts.

Three lithological units have been defined that are believed to be fundamental divisions within this continuum. The divisions are based on the nature and distribution of the sulphide and lithic components of the rock without reference to the grade of the ore. Several intermediate lithologies are of local significance and by adding modifiers to the basic units most beds in the lower ore unit can be described accurately. The three main lithological units will be referred to as sulphide matrix ore, polylithic breccia-conglomerate and arenaceous conglomerate.

Sulphide matrix ore consists of a fine grained matrix of sphalerite, galena and locally barite with a minor amount of admixed lithic detritus. Within the matrix are subangular to subrounded clasts including siltstone, rhyolite, altered Intermediate Footwall, pyritic stockwork and barite (Fig. 43.4). All these clast types occur in the Intermediate Footwall or at the base of the Lucky Strike Ore Horizon Sequence in the vicinity of the Lucky Strike ore deposit or along the Rothermere-MacLean trend, the current suggested source and transport channel for the ore (Walker and Barbour, 1981). The clasts rarely exceed 15 cm in length and comprise less than 15 per cent of the unit. To date no sorting has been indicated by measurement of clast size and type for all clasts more than 1 cm in length in areas 0.5 m wide by the accessible height of the bed (generally 1-3 m). Segregation of clasts into distinct beds within the sulphide matrix ore has been noted.

Sulphide matrix ore occurs in a discontinuous bed at, or near, the base of the lower ore unit. Ore grades in this bed range from 15 to 40 per cent combined zinc and lead. In a sublevel of 20 level (a on Fig. 43.2) thin, laterally continuous layers of chalcopyrite in the matrix define planar zones in the rock. The bed of sulphide matrix ore changes thickness rapidly. Presently available exposures and drill core information suggest that the sulphide matrix ore grades into polylithic breccia-conglomerate with a change in the mode of occurrence of sphalerite and galena from the matrix to distinct clasts of ore.

Polylithic breccia-conglomerate comprises the broad central part of the lithological continuum between sulphide matrix ore and arenaceous conglomerate. It is distinguished from the sulphide matrix ore by its arenaceous matrix and from the arenaceous conglomerate by the number, size and variety of clasts. Breccia-conglomerate is the term chosen to describe this unit due to the angularity of a majority of

Figure 43.4. *High grade sulphide matrix ore with some lithic clasts at location a, Figure 2. Rock bolt is 12.6 cm across.*

the clasts. However, polylithic breccia-conglomerate contains subangular to subrounded clasts which include siltstone, rhyolite, altered Intermediate Footwall, stockwork pyrite, mafic volcanic rocks, felsic tuff, jasper, sphalerite-galena-chacopyrite and barite. In addition, sphalerite-galena fragments are common and granitic boulders are present in local concentrations. The granitic boulders, although larger than most other clasts, are subrounded to rounded. They are also the only clast type not recognized in situ in the Intermediate Footwall or the Lucky Strike Ore Horizon Sequence. For further information on granitic clasts the reader should refer to Stewart (1983). The size range of the clasts in the breccia-conglomerate is considerable with large boulders (up to 4.5 by 2.4 by 1.8 m, minimum measurements) in a sand-size matrix. In typical polylithic breccia-conglomerate the clasts range from 1 to 30 cm long and comprise from 15 to 50 per cent of the rock.

Polylithic breccia-conglomerate occurs overlying, underlying and adjacent to sulphide matrix ore, as isolated beds at the base of the lower ore unit, within the arenaceous conglomerate and at the top of the lower ore unit (Fig. 43.3). In the latter case, barite fragments are concentrated in a polylithic breccia-conglomerate. In marginal parts of the lower ore unit this baritic polylithic breccia-conglomerate rests directly on the footwall dacitic tuff and is overlain by felsic pyroclastic rocks.

The relationship between the sulphide matrix ore and polylithic breccia-conglomerate has been documented in several areas of the MacLean Extension workings. Along a drift at location b (Fig. 43.2) sphalerite-galena-barite sulphide matrix ore with less than 5 per cent lithic fragments overlies dacitic tuff or a thin polylithic breccia-conglomerate bed. Above and adjacent to the sulphide matrix ore are large blocks of sphalerite-galena, and sphalerite-galena-chalcopyrite in a clastic matrix (Fig.43. 5). The ore clasts are typically tabular with length-to-width ratios from 3 to 10. They exhibit draping and plastic deformation over and against adjacent lithic detritus (pebbles, cobbles and boulders). Ore clasts are less abundant and matrix more abundant farther away from the sulphide matrix ore, and some granitic clasts are present. The granitic clasts tend to be large (20 to 50 cm in diameter) and are concentrated in a

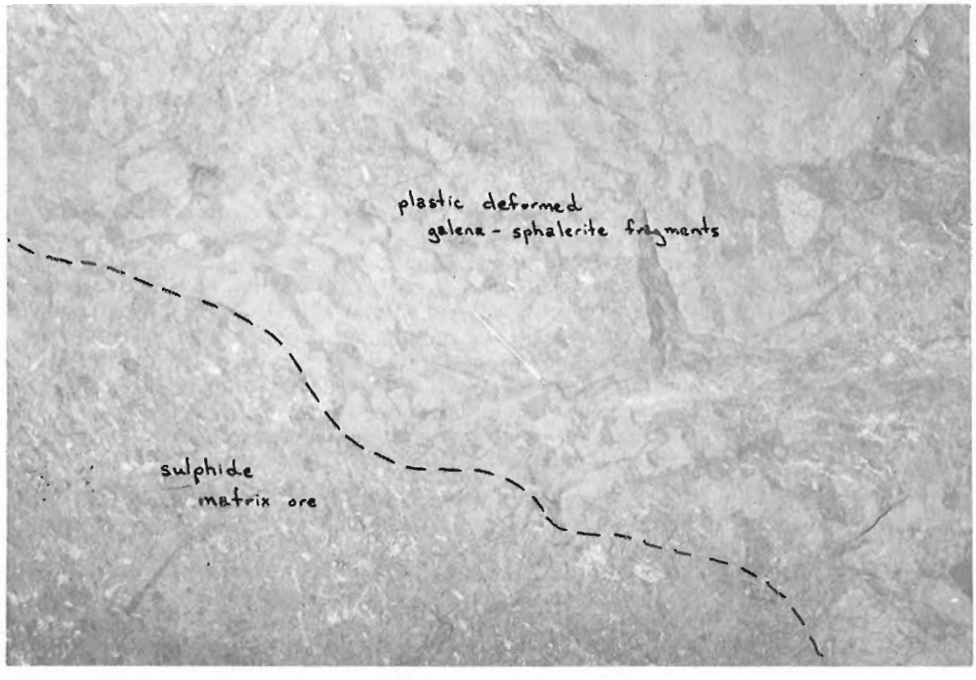

Figure 43.5

Contact of sulphide matrix ore and plastically deformed galena-sphalerite fragments in a matrix of lithic detritus at location b, Figure 2.

distinct stratigraphic unit. This unit is succeeded by a typical polylithic breccia-conglomerate with a wide range of clast lithologies and sizes. The complete sequence is observed in a strike length of 15 m.

A separate lithological unit, arenaceous conglomerate, occurs also in the lower ore unit of the MacLean Extension orebody. This unit has a wide lateral distribution judging from drill intersections but has been found only in one location in the underground workings. The rock consists of an arenaceous matrix with less than 10 per cent subangular to subrounded clasts. Rhyolite and granite comprise two thirds of all the clasts. Other types include siltstone, altered Intermediate Footwall, mafic volcanic rocks, sphalerite-galena and sphalerite-galena-chalcopyrite. Where examined underground, the arenaceous conglomerate overlies footwall dacitic tuffaceous rocks and is overlain by polylithic breccia-conglomerate, but in drill core this unit can be seen to overlie polylithic breccia-conglomerate as well.

The Upper Ore Unit

The upper ore unit is separated from the lower ore unit in the MacLean Extension orebody by 30 to 50 m of felsic pyroclastic rocks (Fig. 43.3). An excellent exposure, undisturbed by faults, exists in a drift above 20 level (location c in Fig. 43.2). Details of the geology of the south wall of this drift are shown in Figure 43.6. Notable features of the exposure are cyclic units of barite-rich transported ore and graded beds of sandy sedimentary rocks at the top of the ore layers.

At the base of the exposure, massive, yellow-green felsic tuff is conformably, but irregularly, overlain by a bed containing single barite crystal clasts (up to 5 cm long) in a matrix of barite, galena, sphalerite and minor lithic detritus. Other clast types include siltstone, rhyolite, altered Intermediate Footwall and basalt. Granitic clasts are absent. This massive bed grades upward into about 10 cm of sandy lithic detritus and barite. Above the sandy bed, and gradational with it, is a thin bed of felsic tuffaceous rock. The combined thickness of the sandy and tuffaceous beds ranges from 5 to 50 cm at location c.

A second cycle consisting of a barite-galena-sphalerite-rich basal portion overlain by arenaceous, polylithic pebble conglomerate grading upward into sandy and tuffaceous rocks rests on the basal graded unit.

The baritic beds contain cobbles and boulders of galena-sphalerite exceeding 30 cm in length as well as other large blocks of siltstone, rhyolite and basalt. These occur in localized areas associated with the barite-rich ore beds and in places have penetrated the fine grained top of the first cycle (Fig. 43.7).

Origin of the Ore Sequence

Earlier work on the genesis of the transported ores by Walker and Barbour (1981) and Calhoun and Hutchinson (1981) was restricted to diamond drill core and a limited number of ore exposures remaining in the MacLean orebody. The MacLean Extension orebody is presently being developed for mining and consequently contains some excellent exposures.

This is an ongoing study but preliminary results indicate several features bearing on the transport and deposition of the ore beds. Thurlow (1977) suggested that the transported ores of the Buchans camp represent deposits from subaqueous sedimentary gravity flows initiated by explosive volcanic eruption or local earthquake. The size and angularity of the clasts, in addition to the types and diversity of lithologies represented by the clasts, all support this hypothesis.

Sedimentary gravity flows can be divided into four main types based on the sediment support mechanisms. These types are turbidity currents, fluidized sediment flow, grain flow and debris flow (Middleton and Hampton, 1976). Each type of flow has specific depositional features.

Within the MacLean Extension orebody, and especially the lower ore unit, a range of depositional features have been observed that suggest complex channel filling from several

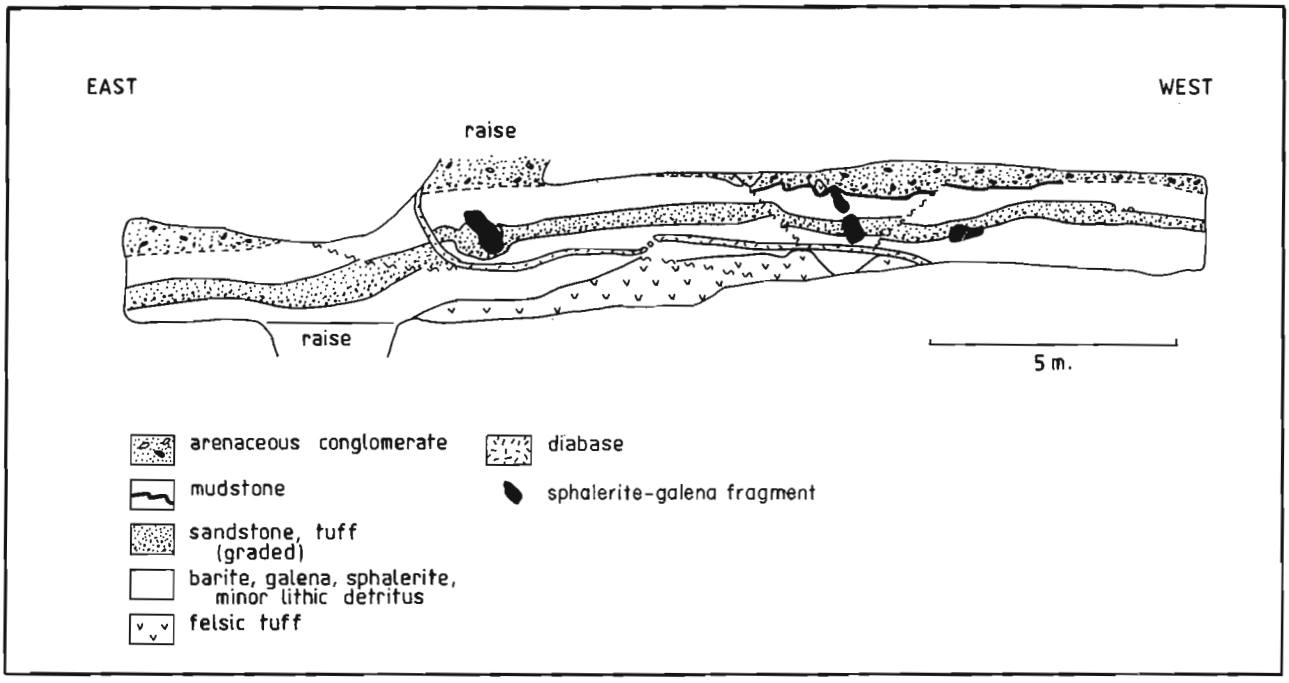

Figure 43.6. *Subdivisions of the upper ore unit along the south wall of drift, above 20 level, location c, Figure 2.*

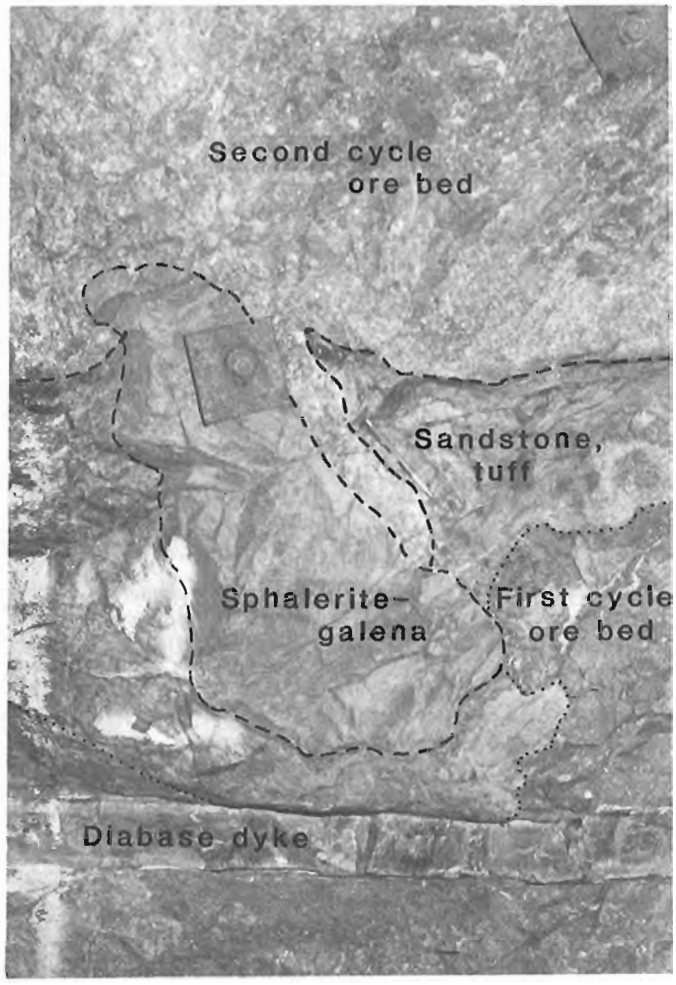

Figure 43.7. *Galena-sphalerite block penetrating the top of the first cycle ore bed of the upper ore unit at location c, Figure 2. Rock bolt is 12.6 cm across.*

episodes and types of sedimentary gravity flows. Individual flows can be separated by their distinct clast lithologies. The most obvious example is the baritic polylithic breccia-conglomerate which is at the top of the lower ore unit in many areas. Underlying the baritic polylithic breccia-conglomerate is a polylithic breccia-conglomerate bed with a distinctive high content of granitic fragments. Both beds are localized, probably in topographic depressions which existed at the time of emplacement.

With the exception of the above beds, most of the lower ore unit is a sequence of beds grading from sulphide matrix ore to coarse sphalerite-galena blocks in a lithic matrix, to sphalerite-galena-bearing polylithic breccia-conglomerate, and to arenaceous conglomerate with few lithic clasts and only rare sphalerite-galena clasts. There is an overall sorting of dense, sulphide-rich material toward the base of the lower ore unit.

The contacts between massive sulphide matrix ore and polylithic breccia-conglomerate beds are quite steep suggesting a subaqueous debris flow with matrix strength as the transport mechanism for some high density, sphalerite-galena-rich material (Middleton and Hampton, 1976). Turbidity currents can account for graded units within arenaceous conglomerate beds.

Several beds were selected for clast counts in the MacLean Extension workings. Modifications were made to Walker's (1975) method to typify grading. Rather than vertical traverse lines, an area was chosen 0.5 m wide through the entire thickness of the bed. Within this area the length and width of all clasts over 1 cm long were recorded, as well as clast type and height in the bed. The length of galena, sphalerite, chalcopyrite and barite clasts was corrected to allow for their greater density. This was done by multiplying clast length by clast density divided by a density of 2.8 gm per cm^3. A plot of clast height in the bed versus length is presented in Figure 43.8 for a polylithic breccia-conglomerate bed that contains granitic clasts. Inverse grading in the lower part of the bed is succeeded by a disorganized to normally graded top. This sequence, duplicated by clast measurements in the bed at a second location, suggests proximal deposition from a high-sediment-concentration turbidity current (Walker, 1975).

The supply of lithic and sulphide detritus to the basin, although intermittent, was not interrupted by long periods of quiescence. This is suggested by the massive nature of the lower ore unit and the recognition of several separate flow deposits. The sedimentary gravity flows would have the capacity to erode any thin intervening pyroclastic units.

The upper ore unit reflects a change in the depositional history. Two discrete cycles of ore deposition are separated by a thin bed of sandy and tuffaceous rocks. The transport mechanism, although similar to that of the lower ore unit, appears to have a greater component of turbulent flow.

Summary and Exploration Guides

The MacLean Extension orebody contains two main ore units, both comprising distinct and interrelated lithologies. The lower ore unit is characterized by pebble and boulder size ore and lithic clasts in a matrix which is predominantly sandy lithic material with the exception of the economically important sulphide matrix ore. In this ore the matrix is galena and sphalerite with or without barite. The upper ore unit is of different character with at least two distinct cycles of deposition. At the base of each cycle is a bed of galena, sphalerite, barite and fine grained lithic detritus.

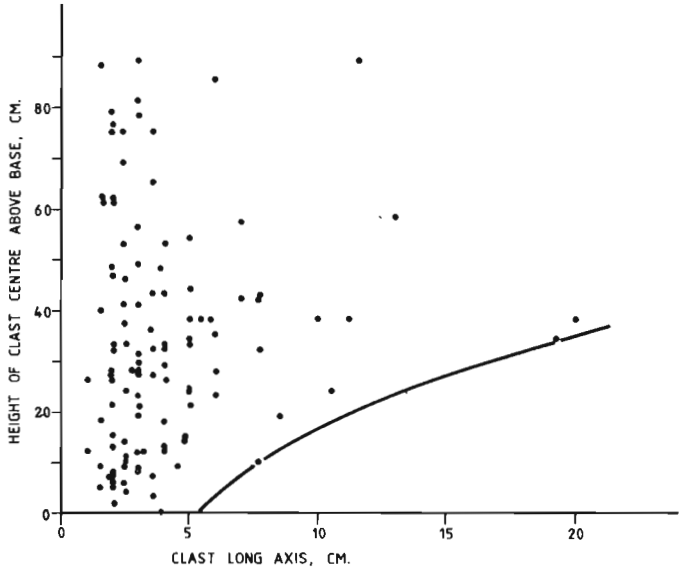

Figure 43.8. *Plot of height of clast centre above base of bed versus corrected clast long axis (cm) for a polylithic breccia-conglomerate bed in the lower ore unit, MacLean Extension workings. The lower 35 cm of the bed is inversely graded. Curve is limit of largest clast.*

Preliminary sedimentological work indicates that the ore-bearing beds are products of subaqueous sedimentary gravity flows. A few clast orientations determined in the MacLean orebody support previous interpretations that the ores were transported down the Rothermere-MacLean channel and could have been derived from the vicinity of the Lucky Strike in situ deposits. Thin, low grade arenaceous conglomerate units, widespread in diamond drill holes, can be traced laterally into thicker and denser gravity flow deposits containing high grade sulphide ores.

References

Calhoun, T.A. and Hutchinson, R.W.
1981: Determination of flow direction and source of fragmental sulphides, Clementine deposit, Buchans, Newfoundland; in The Buchans Orebodies: Fifty Years of Geology and Mining, eds. E.A. Swanson, D.F. Strong, and J.G. Thurlow; Geological Association of Canada, Special Paper 22, p. 187-204.

Middleton, G.V. and Hampton, M.A.
1976: Subaqueous sediment transport and deposition by sedimentary gravity flows; in Marine Sediment Transport and Environmental Management, eds. D.J. Stanley, and D.J.P. Swift; John Wiley & Sons, p. 197-218.

Stewart, P.W.
1983: Granitoid clasts in boulder breccias of MacLean Extension orebody, Buchans, Newfoundland; in Current Research, Part A, Geological Survey of Canada, Paper 83-1A, report 44.

Thurlow, J.G.
1977: Occurrence, origin and significance of mechanically transported sulphide ores at Buchans, Newfoundland (abstract); in Volcanic Processes In Ore Genesis; Geological Society of London, Special Publication, no. 7, p. 127.

Thurlow, J.G. and Swanson, E.A.
1981: Geology and ore deposits of the Buchans area, central Newfoundland; in The Buchans Orebodies: Fifty Years of Geology and Mining, eds. E.A. Swanson, D.F. Strong, and J.G. Thurlow; Geological Association of Canada, Special Paper 22, p. 113-142.

Walker, P.N. and Barbour, D.M.
1981: Geology of the Buchans ore breccias; in The Buchans Orebodies: Fifty Years of Geology and Mining, eds. E.A. Swanson, D.F. Strong, and J.G. Thurlow; Geological Association of Canada, Special Paper 22, p. 161-185.

Walker, R.G.
1975: Generalized facies models for resedimented conglomerates of turbidite association; Geological Society of America, Bulletin, v. 86, p. 737-748.

GRANITOID CLASTS IN BOULDER BRECCIAS OF MACLEAN EXTENSION OREBODY, BUCHANS, NEWFOUNDLAND[1]

Contract 1583327

Peter W. Stewart[2]
Economic Geology Division

Stewart, P.W., Granitoid clasts in boulder breccias of MacLean Extension orebody, Buchans, Newfoundland; in Current Research, Part A, Geological Survey of Canada, Paper 83-1A, p. 321-324, 1983.

Also in Current Research, ed. R.V. Gibbons, Newfoundland Department of Mines and Energy, Mineral Development Division, Report 83-1, 1983.

Abstract

Approximately fifty per cent of the Buchans massive sulphide orebodies mined to date occurred in subaqueous breccia-conglomerate beds within an Ordovician-Silurian volcanic island-arc sequence, the Buchans Group. Amongst the diverse lithic clasts in these beds are rounded, subspherical granitoid pebbles, cobbles and boulders. An intrusive body to the southwest of the mine area, the Feeder Granodiorite, is lithologically similar to some of the granitoid clasts and has been interpreted to be comagmatic with some of the Buchans Group volcanic rocks. Twelve types of granitoid clasts were recognized based on megascopic characteristics but this number will probably be reduced after laboratory investigations have been completed.

Introduction

The volcanogenic sulphide ore deposits at Buchans occur as three types: stockwork ore, in situ ore and transported ore (Thurlow, 1981a; Thurlow and Swanson, 1981). The transported ore forms a series of sulphide-bearing breccia-conglomerate beds with diverse lithic clasts, including granitoids (i.e. plutonic rocks of felsic to intermediate composition) within an Ordovician-Silurian sequence of subaqueous volcanic, volcaniclastic and sedimentary rocks. The source of these granitoid clasts has been enigmatic. An intrusive body of small surface area (approximately 1.5 km^2), the Feeder Granodiorite, outcrops 12 km southwest of Buchans. It has been interpreted to be comagmatic with Buchans Group volcanics and the possible source of the granitoid clasts (Thurlow, 1981b). A description of the central volcanic belt is given in Kean et al. (1981).

It is the intent of this study to determine the petrological character, geochemistry, and age of the granitoid clasts and of the Feeder Granodiorite and shed light on the relationship of the Feeder Granodiorite to the Buchans Group and the included granitoid clasts, and in turn on the provenance and derivation of the clasts.

Acknowledgments

The author is grateful for co-operation and help at Buchans from J.G. Thurlow, E.A. Swanson, W.P. Binney and the staff of ASARCO and Abitibi-Price.

D.F. Strong, W.H. Poole and R.V. Kirkham made many useful suggestions to improve the manuscript.

Underground Observations

The transported orebodies consist of a sequence of breccias and conglomerates which are considered to show characteristics of sediment gravity flow deposits (Walker and Barbour, 1981; Binney et al., 1983). Detailed examination of those units which are relatively rich in granitoid clasts indicates that most granitoid-rich units overlie and flank the sulphide-rich breccias. Granitoid clasts, however, are found in other units not intimately associated with the sulphide-rich breccias. These granitoid clasts are typically smaller (pebble-sized) than the typical cobble-sized granitoid clasts found with the ore. Rare granitoid clasts have been found in almost all Buchans Group formations, although nowhere in significant numbers or volume as compared to the ore horizon (J.G. Thurlow, personal communication, 1982).

The nature of the granitoid clasts varies appreciably in hand specimen. A tentative field classification based on colour, grain size, presence or absence of quartz phenocrysts and mafic mineral content indicate twelve clast types (Table 44.1).

The average granitoid clast size as determined within several exposures of granitoid-bearing (arenaceous) breccia-conglomerate (see Table 44.2) on 20 level, MacLean Extension orebody, is 6.4 by 4.1 cm. The long dimensions of granitoid clasts range from 1 cm to more than 50 cm. Where intimately associated with the transported massive sulphide ore (e.g. 20-5 sublevel, 20-13 drift), average clast size is of the order of 16.5 by 10 cm and granitoid clasts comprise approximately 4 per cent by volume. In more arenaceous units, granitoid clasts average 4.2 by 2.0 cm and constitute 1 per cent of the rock. Rare granitoid clasts have been observed in tuffaceous rocks, both overlying and underlying the ore horizon. These clasts average 7.5 by 6.0 cm and comprise much less than 1 per cent.

Granitoid clasts are subrounded to well rounded and typically subspherical, although many are oval and elongate. They are consistently better rounded than other clast types in the breccia-conglomerate units.

Surface Observations

The Feeder Granodiorite is an irregularly shaped body of approximately 1.5 km^2 occurring in upper Wiley's River area (Fig. 44.1). Along its southern and western exposures the granodiorite can be seen in contact with rocks presumed to be part of the Topsails complex (Taylor et al., 1980). At the Feeder Granodiorite-Topsails contacts, Topsails granite shows a weakly developed chilled margin against the Feeder Granodiorite. Brick-red, fine grained, equigranular dykes, macroscopically similar to the Topsails granite cut Feeder Granodiorite. The granodiorite and the Topsails granite are both cut by diabasic dykes. No exposures of the contact between Feeder Granodiorite and Buchans Group rocks were found. No definite evidence of cross-cutting relationships between diabasic and granitic dykes was observed.

---

[1] Contribution to Canada-Newfoundland co-operative mineral program 1982-1984. Project carried by Geological Survey of Canada.

[2] Department of Earth Sciences, Memorial University of Newfoundland, St. John's, Newfoundland A1B 3X5.

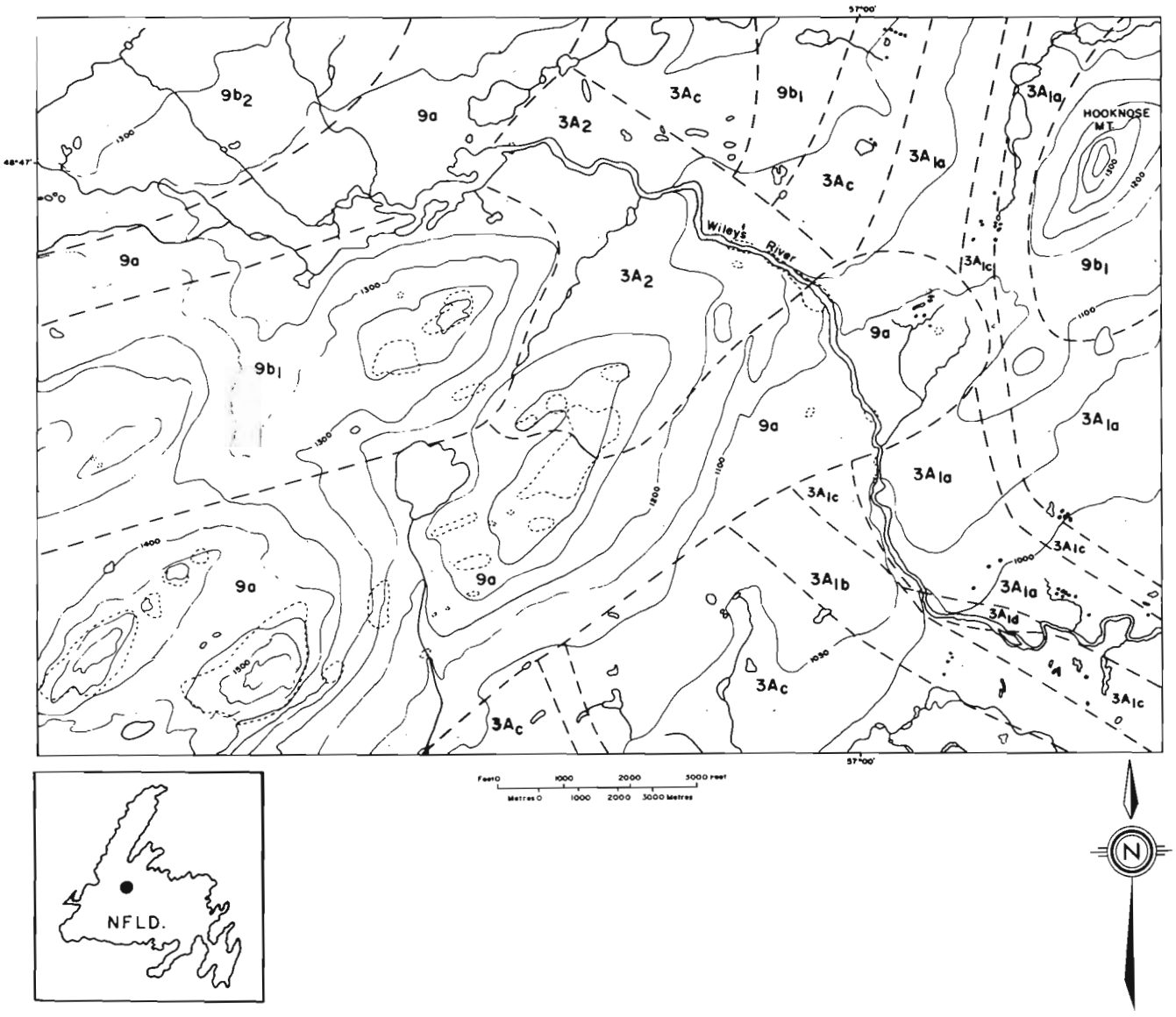

LEGEND

SILURIAN AND DEVONIAN

TOPSAILS GRANITE

9a	Alkali Feldspar granite: fine to medium grained, brick red granite
$9b_1$ | $9b_2$	Mafic Intrusives (associated with Topsails Granite): fine to coarse grained diabase ($9b_1$) and gabbro ($9b_2$).

ORDOVICIAN-SILURIAN

BUCHANS GROUP

$3A_a$ | $3A_c$	Footwall Arkose: $3A_a$, lithic arkose; $3A_c$, basaltic lava, pillow lava, pillow breccia.
$3A_{1a}$ | $3A_{1b}$ | $3A_{1c}$ | $3A_{1d}$	Wiley's Prominent Quartz Sequence: Stratigraphic volcanic equivalent of 3A; characterized by quartz crystals commonly exceeding 1 cm in diameter; $3A_{1a}$, rhyolite flows and tuffs; $3A_{1b}$, dacitic pyroclastics; $3A_{1c}$, basaltic lavas, pillow lavas; $3A_{1d}$, tuffaceous siltstone.
$3A_2$	Feeder Granodiorite: whitish-brown, medium grained biotite granodiorite, with coarse grained quartz phenocrysts.

SYMBOLS

Geological boundary (defined, assumed)

Outcrop boundary (examined)

Elevations in feet above mean sea level

Approximate magnetic declination: 28° W

Formation numbers taken from and geology modified from "Geological Map of Buchans Area, Newfoundland," by Thurlow and Swanson, 1982.

Figure 44.1. Geological map of upper Wiley's River area, Buchans, Newfoundland.

The Feeder Granodiorite is a whitish brown rock, which becomes increasingly reddish toward the contact with the Topsails granite in Wiley's River area. The granodiorite is medium grained with abundant coarse grained quartz phenocrysts. Quartz crystals are generally rounded (5-10 mm average diameter), clear, locally appear as aggregates of crystals rather than true individual phenocrysts, and comprise 25-30 per cent of the rock by volume. The predominant feldspar is plagioclase, comprising 55-65 per cent of the rock, that is subhedral (locally euhedral), white and frequently darkened red-brown (by hematite). Fine grained clots of subhedral biotite crystals constitute 5 per cent. A fine grained pink-brown mineral (potash feldspar?) occurs interstitially to the quartz phenocrysts and the plagioclase (plus biotite) masses, and comprises 5 per cent of the rock.

The Topsails granite in this area is brick-red, ranges from fine- to medium-grained and is consistently equigranular. All feldspars are medium to dark red and comprise 65 per cent of the rock. Quartz crystals are clear, 1-3 mm across and form 30 per cent of the rock and biotite 5 per cent. The granite is miarolitic, especially near the contact with Feeder Granodiorite. The cavities are typically 1 mm in diameter, although near the contact they are 3-5 mm and partly filled with variable amounts of quartz,

Table 44.1

Field Classification of Granitoid Clasts

Clast type	Dominant colour, groundmass	Grain size	Phenocryst type	Mafic mineral content	Distinguishing features
1	strong-moderate brown-red	f.-m.g.	qtz. (c.g.)	variable; f.-m.g., generally distinct	colour strong brown-red; f.-m. grain size; presence of qtz. phenocrysts
2	strong-moderate brown-red	f.g.	equigranular	f.-m.g., distinct, variable	colour, strong-mod. brown-red; f. grain size; absence of qtz. phenocrysts
3	black & white with light browns, occasionally greenish or greyish	m.-c.g.	rare qtz. (c.g.)	m.-c.g.; distinct and indistinct in different clasts	coarse grain size; equigranular; spotted colour (black and white)
4	moderate-light brown (weak red)	m.g., rarely f.g.	qtz. (c.g.); rock may be m.g. & equi-granular	variable; distinct & indistinct	qtz. phenocrysts; lighter red colour than type 1, otherwise the same, includes medium grained equigranular equivalents
5	light brown-pink darkened with mafic minerals in some	f.-m.g.	equigranular	generally distinct except when very abundant & f.g.	absence of qtz. phenocrysts; same colour as type 4, or even less pink (or red)
6	variable, light green with white & light brown	f.-m.g.	qtz. (m.-c.g.) rare m.g. plag.	generally indistinct variable	presence of qtz. phenocrysts; large amount of qtz. present; absence of brown & especially red colours except in isolated crystals
7	grey-white, rarely very light brown	f.g. (rarely m.g.)	equigranular	typically indis-tinct, content varies from 0-20%	white and/or grey colour; commonly with pyrite
8	greenish-yellow with occasional red tinges	f.-m.g.	qtz. (m.g.)	indistinct	vague crystal boundaries, with the exception of qtz. phenocrysts; most likely a volcanic rock
9	dark-moderate greenish with specks of white (plag.), red (K-feldspar) and qtz.	f.g.	equigranular; rare m.g.	abundant, distinct, prob-ably amphibole	dark, spotted appearance; fine grained; seen only in siltstone breccia
10	dark green with grey & light brown	f.g.	K-feldspar & plag. (m.g.) rare qtz. (smaller)	abundant (to 40%) distinct	similar to type 9 but with abundant plag. phenocrysts – only one sample seen
11	strong brown-red with white	f.-m.g.	qtz. (m.g.)	few to 5%, distinct	very abundant qtz; brown-red colour
12	variable; a mixture of whites, greens and weak browns	m.-c.g.	equigranular	unaltered, 10-15%	large grain size; equigranular; greenish plag. crystals (?)

Table 44.2

Classification – MacLean Extension Orebody
(modified after E.A. Swanson, personal communication, 1982)

Ore Horizon Sequence in MacLean Extension area	Upper Baritic Ore-Bearing member (without granitoid clasts)	Baritic unit
		Tuffaceous or breccia unit
		Baritic unit
	Felsic Pyroclastic member	Strongly lithic beds with isolated sulphide clasts; occasional polylithic breccia bed with minor granitoid clasts
	Lower Ore-Bearing member (Generally gradational from high grade at bottom to low grade arenaceous granitoid-bearing breccia-conglomerate. The top baritic bed seems distinct).	Baritic low grade polylithic ore breccia
		Granitoid-bearing breccia-conglomerate with arenaceous matrix. Beds of arenaceous wacke within unit
		Granitoid-bearing ore breccia-conglomerate; low grade with some arenaceous matrix
		Polylithic ore breccia; matrix becomes increasingly arenaceous towards top
		Mainly massive sulphide, in part streaky with minor lithic material
Intermediate Footwall Formation		Interbedded and altered mafic to felsic flows, pyroclastic rocks and volcanic breccias, related tuffaceous pyritic siltstone and wacke

specular hematite, fluorite and a silvery grey unidentified mica. At the contact, the granite shows a weakly developed graphic texture.

Summary

Granitoid clasts within the Buchans Group breccia-conglomerate beds and pyroclastic units comprise several lithologic types. Those clasts with coarse grained quartz phenocrysts (to 1 cm) in a brown-red groundmass are megascopically similar to the Feeder Granodiorite in the Wiley's River area.

The relationship of the Feeder Granodiorite to the Buchans Group remains unknown. Topsails granite has a chilled margin against the Feeder Granodiorite. Brick-red granitic dykes of presumed Topsails affiliation cut the Feeder Granodiorite. Both intrusive bodies are cut by diabasic dykes.

References

Binney, W.P., Thurlow, J.G., and Swanson, E.A.
1983: The MacLean Extension orebody, Buchans, Newfoundland; in Current Research, Part A, Geological Survey of Canada, Paper 83-1A.

Kean, B.F., Dean, P.L., and Strong, D.F.
1981: Regional geology of the central volcanic belt of Newfoundland: in The Buchans Orebodies: Fifty Years of Geology and Mining, eds. E.A. Swanson, D.F. Strong, and J.G. Thurlow; Geological Association of Canada, Special Paper 22, p. 65-78.

Taylor, R.P., Strong, D.F., and Kean, B.F.
1980: The Topsails igneous complex: Silurian-Devonian peralkaline magmatism in western Newfoundland; Canadian Journal of Earth Sciences, v. 17, p. 425-439.

Thurlow, J.G.
1981a: Geology, ore deposits and applied rock geochemistry of the Buchans Group, Newfoundland; unpublished Ph.D. thesis, Memorial University of Newfoundland, 305 p.

1981b: The Buchans Group: its stratigraphic and structural setting; in The Buchans Orebodies: Fifty Years of Geology and Mining, eds. E.A. Swanson, D.F. Strong, and J.G. Thurlow; Geological Association of Canada, Special Paper 22, p. 79-90.

Thurlow, J.G. and Swanson, E.A.
1981: Geology and ore deposits of the Buchans area, central Newfoundland: in The Buchans Orebodies: Fifty Years of Geology and Mining, eds. E.A. Swanson, D.F. Strong, and J.G. Thurlow; Geological Association of Canada, Special Paper 22, p. 113-142.

Walker, P.N. and Barbour, D.M.
1981: Geology of the Buchans ore horizon breccias: in The Buchans Orebodies: Fifty Years of Geology and Mining, eds. E.A. Swanson, D.F. Strong, and J.G. Thurlow, Geological Association of Canada, Special Paper 22, p. 161-186.

45.

THE CIRCUM-UNGAVA BELT OF EASTERN HUDSON BAY: GEOLOGY OF THE CAPE SMITH REGION

Project 780012

W.R.A. Baragar,
Precambrian Geology Division

Baragar, W.R.A., The Circum-Ungava belt of eastern Hudson Bay: geology of the Cape Smith region; in Current Research, Part A, Geological Survey of Canada, Paper 83-1A, p. 325-328, 1983.

Abstract

Volcanic rocks of the late Aphebian Circum-Ungava Belt in the Cape Smith region of northern Quebec-Northwest Territories can be grouped stratigraphically into upper komatiitic and lower tholeiitic suites. The komatiitic rocks are divisible into mappable units based in part on Mg content manifested in the physical appearance of the lavas. Thus high- and low-Mg lavas have distinctive physical characteristics that serve to distinguish them, whereas those of medium-Mg lavas are mixed. Systematic sampling across komatiitic assemblages on Smith Island and the Ottawa Islands indicates a bimodal distribution of MgO contents with modal peaks at 8-9 and 16-17% and supports subdivision of the lavas at 10 and 16% MgO into high-, medium-, and low-Mg categories. The TiO_2 content, with a unimodal peak at 0.6-0.65%, shows the underlying coherence of the suite.

Layered flows formed of cumulate and noncumulate zones appear to be thickened lenses of massive lava and are most abundant in the high-Mg lava unit. The Hudson's Bay Layered Flow, mapped in detail, may show the mode of formation. It appears to have thickened from the massive top of a normal flow as the result of successive damming action by pillow buildup and resulting overspills. The cumulate layer eventually formed by flowage paralleling the barrier. One of the layered flows contains spinifex texture which appears in its upper part in random growth and in multiple layers of parallel growth.

Introduction

Detailed mapping of volcanic rocks of the Aphebian Circum-Ungava Belt in eastern Hudson Bay begun in 1979 with work on the Belcher, Sleeper, and Ottawa Islands and continued last year with further work in the Ottawa Islands and Cape Smith was finished this past summer with completion of mapping in the Cape Smith region. Reports of the earlier work are contained in previous issues of Current Research (Baragar and Lamontagne, 1980; Baragar and Piché, 1982). Results for the Cape Smith region obtained in the past two summers are incorporated in the preliminary map of Figure 45.1, which combines the geology in three adjoining map areas (NTS 35 D/16E – Knight Harbour, 35 D/9 W and 16 W – Smith Island, 35 D/10 E and 15 E – Smith Island).

General Geology

The region is underlain by a northeasterly-striking volcanic succession which generally dips steeply towards and faces northwesterly. If no repetition by faulting were assumed, its thickness exposed in the map area would exceed 8000 m. However, one obvious décollement present in the eastern part of the area is probably indicative of other strike faults as yet unrecognized. Moreover, several transverse faults shown on the map appear to spring from and to pass into bedding planes as if they were bedding faults stepping from one stratigraphic level to another. Hence, at least some repetition of the sequence seems likely.

The succession is divisible stratigraphically into two major petrochemical groupings; komatiitic in its upper and tholeiitic in its lower part. These can generally be separated on the basis of field characteristics but there is some overlap in appearances and consequently uncertainty in the placing of the stratigraphic boundary between the groupings. The Massive Low-Mg Lavas of the mainland and those of the Low-Mg Lavas present on the south side of Babs Bay are placed in the komatiitic suite but could well be part of the tholeiitic suite. These same petrochemical groupings in similar stratigraphic relationship to one another are recognized throughout much of the Cape Smith belt east of the present map area (Baragar and Scoates, 1981; Hynes and Francis, 1982).

The Komatiitic Suite

Lithology

The komatiitic suite is subdivided into a number of physically distinctive members as shown on the map of Figure 45.1. These have been described (Baragar and Piché, 1981) and need only a brief review here. The major part of the sequence is represented by the high-, medium-, and low-Mg lavas designated as such on the basis of experience with previously analysed lavas from the Ottawa Islands. Analyses of lavas collected from Smith Island last year generally confirm the subdivisions made on this basis. Low-Mg lavas tend to be thick (± 100 m), pillowed and massive flows marked by smoothly rounded, thick-rimmed, commonly variolitic pillows. The rocks are typically grey weathering and have inter- and intra-pillow cavities filled with quartz. High-Mg flows, on the other hand, are generally thin (3-50 m) and typically contain brownish weathering, thin-rimmed, and rather irregular and polygonally jointed pillows. Quartz filling is absent from cavities. In both types, pillows generally form the basal, and massive lava the upper part of individual flows. Medium-Mg lavas tend to be intermediate in their characteristics. Onion skin pillowed lavas are a distinctive variety of the low-Mg lavas marked by very thick (3-10 cm), scaley rims and are almost invariably variolitic. Layered flows are generally, but not necessarily, a variant of the high-Mg lavas and they represent fractionation in situ of massive lava, either the massive upper part of a pillowed to massive flow or of a totally massive flow. Most simply they comprise an olivine cumulate layer in the lower part of the massive unit overlain by olivine-depleted and more or less feldspathic lava in the upper part. Commonly, the upper zone contains a family of veinlets of pegmatoid aspect subparallel to the upper flow margin. A rare variety of layered flow contains spinifex texture in its upper part.

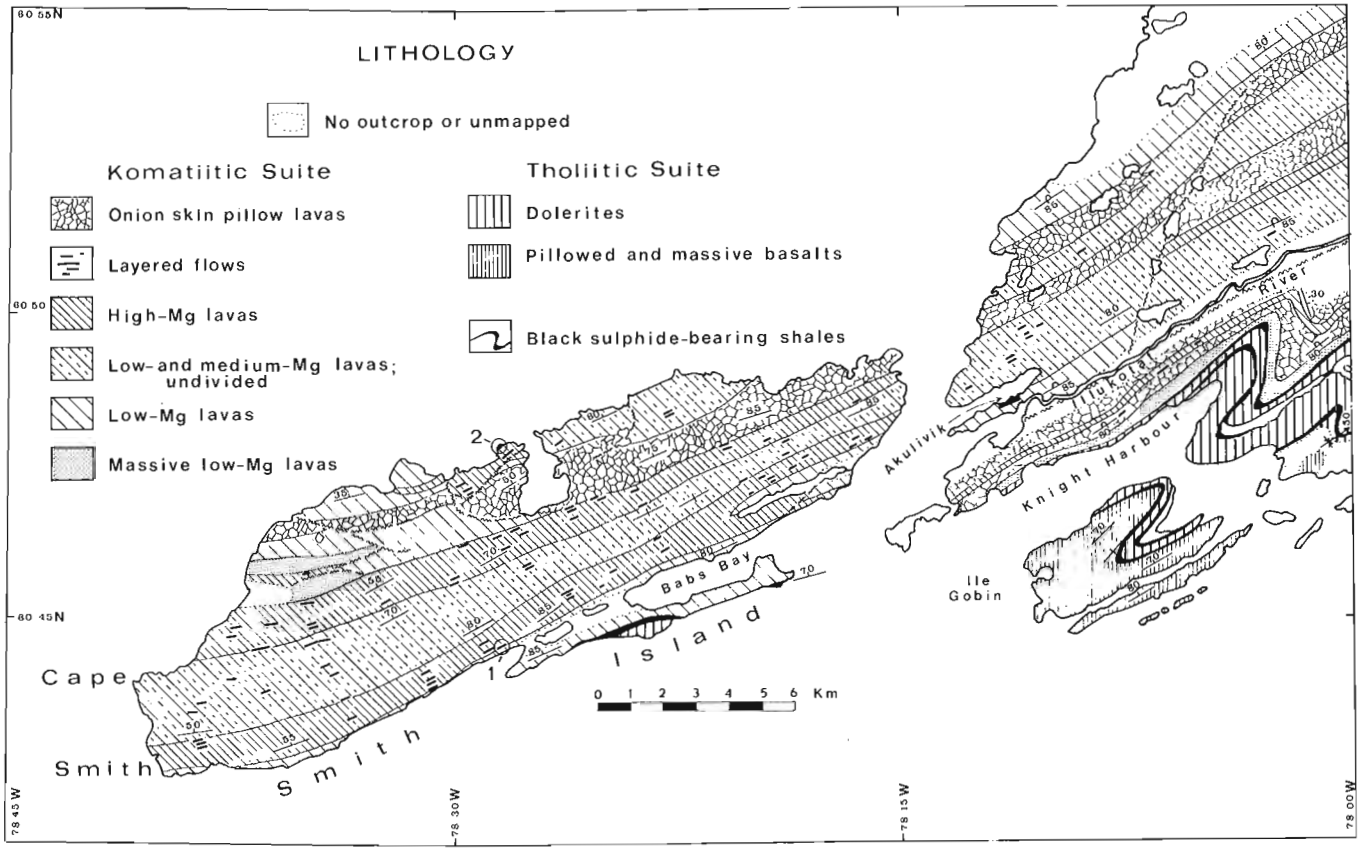

Figure 45.1. *Geological map of Cape Smith region. Locations shown for Hudson's Bay Layered flow (1) and spinifex-textured flow (2).*

Massive low-Mg Lavas was not one of the subdivisions used in last year's report and warrants a little fuller description. On the northwest side of Smith Island it appears at two levels as a thick, massive flow believed to be repeated by faulting. It is about 250 m thick and for the most part has the aspect of a feldspathic dolerite, but fines upward through about one-third of its thickness and is capped by a 30-40 m thickness of flow top breccia. The flow is continuous for several kilometres along strike and appears to be faulted off at its eastern end. On the mainland north of Knight Harbour, rocks designated in this category comprise several massive flows with remarkable strike continuity that mark out a distinctive band on the air photographs. They are probably not correlative with the massive flow just described from Smith Island. They are typically dark mafic flows with brownish weathering surfaces and a small but persistent content of finely disseminated pyrrhotite. The major flow is about 150 m thick but several others are 25 to 50 m thick, and near the base of the unit is a succession of thin (5-20 m) pillowed to massive flows of similar appearance. Discontinuous hyaloclastite layers and black shale beds, neither more than a few centimetres thick, are present at some of the flow contacts. It is questionable if this unit should be classed with the komatiitic suite, as has been done in Figure 45.1, or with the tholeiitic rocks that immediately underlie it. Analyses are not yet available and the black shale interlayers may suggest that it belongs with the tholeiitic lavas which farther east are typically interbedded with shaley sediments.

Composition

The chemical analyses of samples collected systematically across the komatiitic assemblage of Smith Island and the Ottawa Islands in previous years can be used to demonstrate the major characteristics of the komatiitic suite. In Figure 45.2 are shown frequency distribution diagrams for analyses of MgO and TiO_2, the oxides of prime importance in identification of the komatiitic suite. Note that MgO tends to be bimodal with peaks at 8-9 per cent and 16-17 per cent, whereas TiO_2 is essentially unimodal with a peak value at 0.6-0.65 per cent. This is consistent with field observations where high- and low-Mg lavas each form distinctive, readily recognizable types, but lavas with intermediate characteristics may be highly variable in their appearance. On the basis of the diagram it would seem reasonable to subdivide low-, medium-, and high-Mg lavas at MgO compositions of 10 and 16 per cent. The low TiO_2 content is characteristic of komatiitic rocks in general. Thus, the nearly unimodal distribution of the analyses at well below 1 per cent is evidence of the underlying unity of the suite despite the variability of the MgO content and is justification for the grouping used here. Analyses forming the minor peak at between 1.1 and 1.2 per cent TiO_2 are from the low-Mg lavas on the south side of Babs Bay which, as previously mentioned, are of questionable affinity.

Distribution

Most of the high-Mg lavas are confined to two parallel strips that run the length of Smith Island and flank its medial ridge. The core of the ridge is formed of a complexly interlayered mixture of mostly medium- and low-Mg lavas. On the mainland these continue as a subdued ridge but little high-Mg lava is evident. The layered flows are most abundantly distributed along the strips of high-Mg lavas. Few appear to have great strike length and many are very stubby lenses such as the one described later in this report. On the northwestern side of Smith Island, underlying lowlands north of the medial ridge and continuing onto the mainland, are

lavas of predominantly low-Mg types, including the distinctive onion skin pillow lavas. The latter are also present on the south side of the Illukotat River, where they are interlayered with a remarkably continuous belt of high-Mg lavas. The distribution of these various lavas does not seem to show much systematic relationship to the stratigraphy.

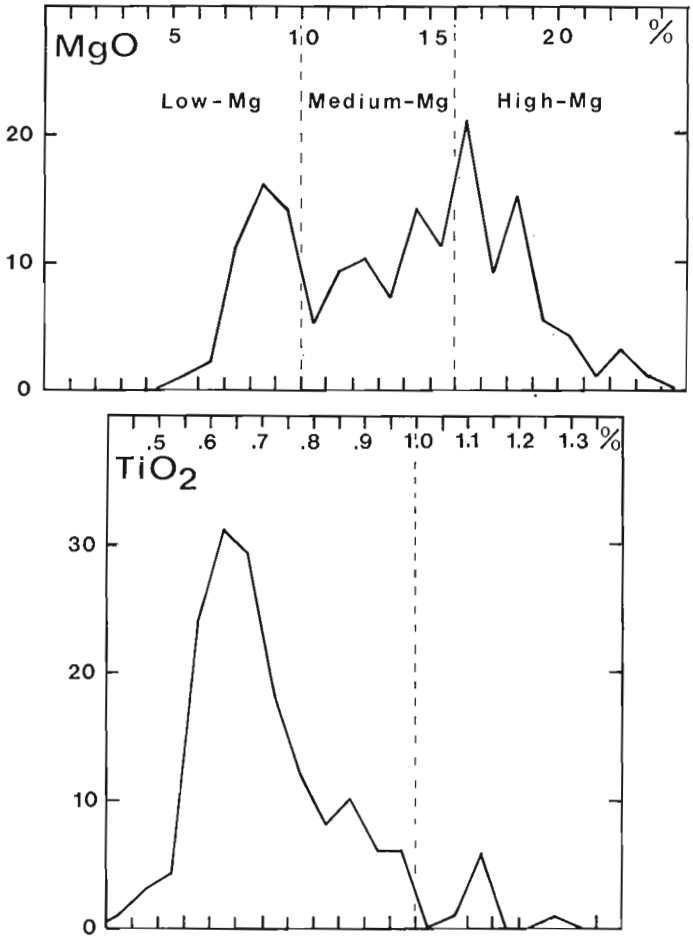

Figure 45.2. Frequency distribution diagram of analyses of MgO and TiO_2 for the komatiitic suite on the Ottawa Islands and Smith Island. Suggested division shown for low-Mg, medium-Mg, and high-Mg flows.

Tholeiitic Suite

Rocks designated as the tholeiitic suite include the dolerite sills and the pillowed and massive basalts of Knight Harbour and Ile Gobin. The pillowed lavas are green weathering, smoothly rounded and thick-rimmed, with none of the characteristics of the komatiitic lavas. Although not yet analyzed, they resemble tholeiitic lavas farther east in the Cape Smith belt with which they appear to be roughly stratigraphic equivalents and are similarly interlayered with black carbonaceous shales and siltstones. In places, the shales are highly pyrrhotized. In last year's report volcanic rocks on the north side of Knight Harbour were classed as part of the tholeiitic suite. With further work this summer it is evident that most belong to the komatiitic suite, although there is some doubt regarding the massive low-Mg lavas mentioned previously.

Hudson's Bay Layered Flow

The Hudson's Bay Layered Flow, named for the site of the old Hudson's Bay Company post on the coastline below it, is located on Figure 45.1. A detailed map of the fractionated part of the flow is given in Figure 45.3. It comprises the following elements: a pillowed base of unknown thickness, and a swollen, massive top consisting of an olivine cumulate zone suspended near its floor, an overlying olivine-depleted region with pegmatitic-like veinlets in its upper part subparallel to the roof, and a polygonally jointed top capped in part by a hyaloclastite breccia zone. The lower contact of much of the thickened massive zone is along a quartz-filled shear zone, but on both the west and east sides of the area mapped the underlying pillows can be seen to branch into the massive top, and therefore are established as a lower part of the flow itself. The olivine-depleted lava overlying the cumulate zone is white weathering dolerite that fines upward to grey aphanitic basalt. The veins appear to be leucocratic segregations from the dolerite, generally with a platy texture, and are most commonly 2 to 5 cm thick. One, however, is 60 to 70 cm thick, comprises platy, randomly oriented plagioclase and pyroxene, commonly 2 to 3 cm in length, and is penetrated by downward oriented pyroxenes as much as 15 to 20 cm long. This vein has some of the aspects of spinifex-textured zones observed elsewhere in layered flows. Interestingly, the breccia flow top, which can be as much as 3 m thick, is present only over the thickened part of the flow. Westward it thins to a typical pahoehoe flow top and eastward it gives way to pillows that appear to spring directly from the upper part of the flow.

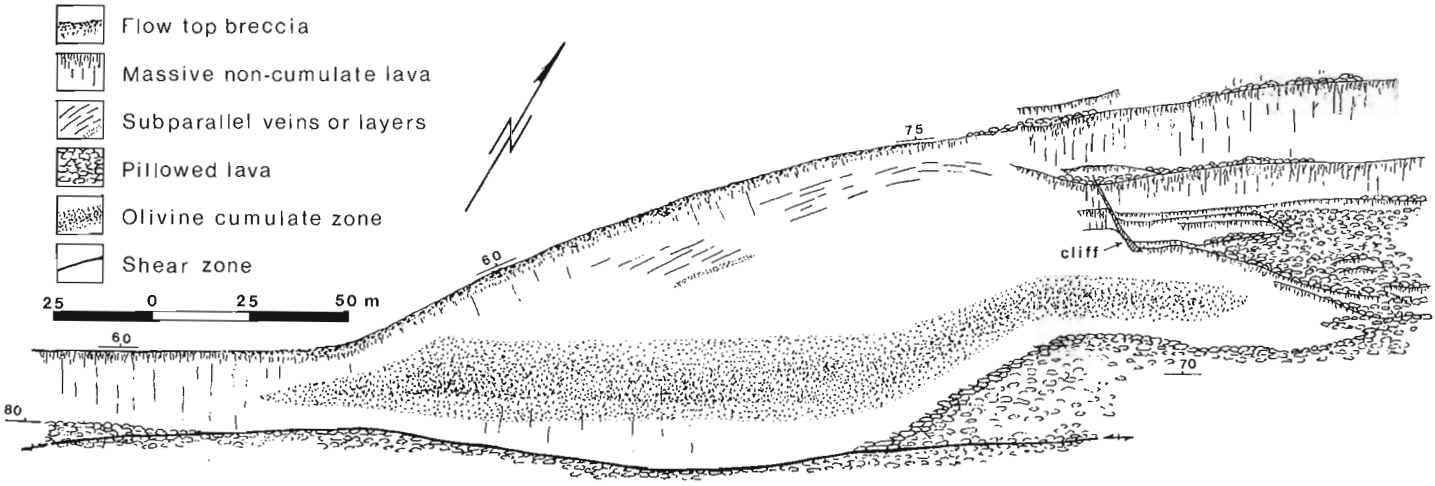

Figure 45.3. Detailed map of Hudson's Bay Layered Flow.

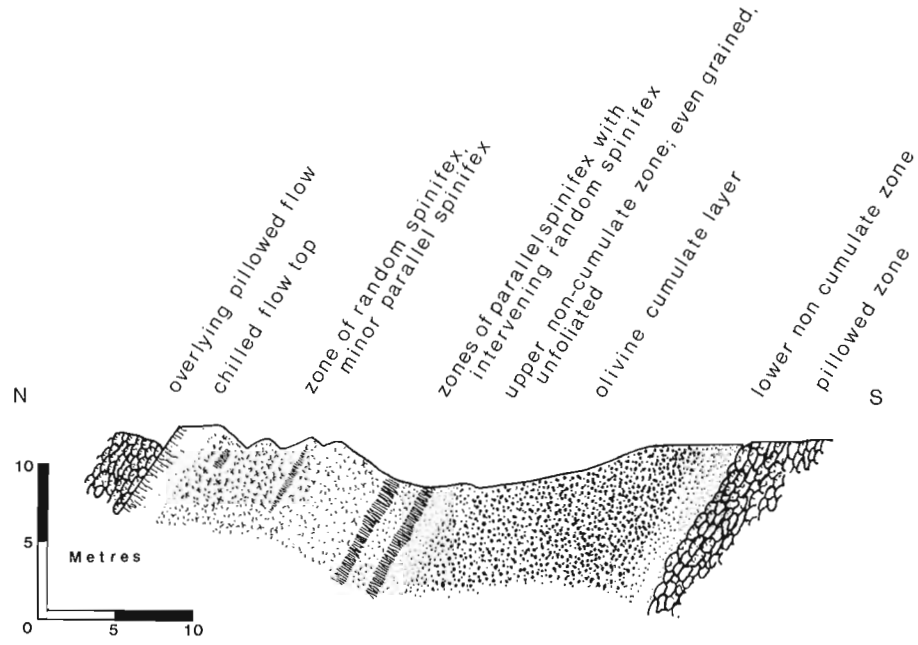

Figure 45.4. *Profile through a spinifex-textured layered flow on the north of coast of Smith Island.*

The mechanics of forming the layered flow can probably be interpreted from the following observations. The flow swells eastward from the massive top of a flow of normal thickness (20-25 m). Farther east it passes directly into pillow lavas in its lower part and into a succcession of thin, massive and partly pillowed flows in its upper part. The olivine cumulate zone follows the contour of the base of the massive part of the flow and pinches out in the constricted parts at its ends. The following explanation may account for these features. A flow moving from west to east thickens behind a barrier of pillows of its own making and eventually spills over to form the extended prong of the thickened magma chamber shown on the map. Subsequent influxes of magma lead to a succession of spills that give rise to the series of thin flows into which the main body of the layered flow passes. Each adds to the height of the barrier with consequent thickening of the main body. This and the effect of the periodic spills result in continual agitation at the top of the expanding magma chamber, thus creating the thick breccia flow top over the active region. At some time during the building of the barrier, the direction of the drainage is likely to change and the direction of flow to become parallel with the barrier. This could account for the configuration of the olivine cumulate layer. As a flow-suspended cumulate it would tend to position itself at a constant distance above the floor of the conduit and thereby assume its configuration.

Spinifex-textured Flow

Only one of the numerous layered flows examined in the map area has well-developed spinifex texture. Its location is shown in Figure 45.1 and a profile across the flow based on a field sketch is given in Figure 45.4. Like most of the layered flows, the fractionated part is the upper massive part of a combined pillowed-massive flow and is about 35 m thick. It comprises an olivine cumulate layer forming the lower half of the flow and a spinifex-textured zone the upper half. Most of the latter consists of randomly oriented spinifex, with individual crystals ranging from about 1 to 3 or 4 cm long, but two prominent layers of parallel spinifex growth occur near the base of the zone and minor layers or lenses were observed within it. The major layers appear to be pyroxene spinifex and crystal lengths range from 30 to 75 cm. It was not possible to judge in the field what proportion of the random spinifex would have been olivine but it may have been substantial.

This flow differs considerably from the spinifex-textured flows previously described from the Ottawa Islands (Baragar and Lamontagne, 1980; Baragar and Piché, 1982; Arndt, 1982). It contains multiple layers of long-fibre, parallel spinifex growth and it lacks a foliated zone (B_1 zone of Pyke et al., 1973) just above the olivine cumulate layer.

Acknowledgments

I am very pleased to acknowledge the competent and cheerful help I received during the summer from my assistants Lyn MacIntyre and Marc Baragar, who were largely responsible for making the summer rewarding and enjoyable. I am also grateful to the citizens of Akulivik who were most helpful in every way, and especially to the Mayor, Tania Qinuayuak, and General Manager, Eli Aullaluk, who undertook to keep us in radio contact with the village and extended us many courtesies.

References

Arndt, N.T.
1982: Proterozoic spinifex-textured basalts of Gilmour Island, Hudson Bay; in Current Research, Part A, Geological Survey of Canada, Paper 82-1A, p. 137-142.

Baragar, W.R.A. and Lamontagne, C.
1980: The Circum-Ungava Belt in eastern Hudson Bay: The Geology of Sleeper Islands and parts of the Ottawa and Belcher Islands; in Current Research, Part A, Geological Survey of Canada, Paper 80-1A, p. 89-94.

Baragar, W.R.A. and Piché, M.
1982: The Circum-Ungava Belt in eastern Hudson Bay: The Geology of the Ottawa Islands and Cape Smith region; in Current Research, Part A, Geological Survey of Canada, Paper 82-1A, p. 11-15.

Baragar, W.R.A. and Scoates, R.F.J.
1981: The Circum-Superior Belt: A Proterozoic Plate Margin? in Kroner, A., ed., Precambrian Plate Tectonics, Elsevier Scientific Publishing Co., p. 297-330.

Hynes, A. and Francis, D.M.
1982: A transect of the early Proterozoic Cape Smith fold belt, New Quebec; Tectonophysics, v. 88, p. 23-59.

Pyke, D.R., Naldrett, A.J., and Eckstrand, O.R.
1973: Archean ultramafic flows in Munro Township, Ontario; Geological Society of America Bulletin, v. 84, p. 955-978.

46.

GEOLOGY AND U-Pb GEOCHRONOLOGY OF PARTS OF THE LEITH PENINSULA AND RIVIÈRE GRANDIN MAP AREAS, DISTRICT OF MACKENZIE

Project 820009

R.S. Hildebrand, S.A. Bowring[1], M.E. Steer[2], and W.R. Van Schmus[1]
Precambrian Geology Division

Hildebrand, R.S., Bowring, S.A., Steer, M.E., and Van Schmus, W.R., Geology and U-Pb geochronology of parts of the Leith Peninsula and Rivière Grandin map areas, District of Mackenzie; in Current Research, Part A, Geological Survey of Canada, Paper 83-1A, p. 329-342, 1983.

Abstract

This report describes the geology of parts of the Hottah Terrane and Great Bear Magmatic Zone, Wopmay Orogen, which were mapped during the 1982 field season. On Leith Ridge the Hottah Terrane comprises schists, orthogneiss, and foliated granitoid plutons. One of the deformed plutons is 1902 ± 4 Ma. These rocks are cut by plutons of the Great Bear batholith. At Hottah Lake, rocks of the Hottah Terrane include metasedimentary and metavolcanic rocks plus a variety of deformed plutons, one of which is 1914 ± 2 Ma. Unconformably overlying the Hottah Terrane in the Hottah Lake area is a varied and complex sequence of sedimentary rocks, subaerial siliceous to mafic lava flows, ash-flow tuff, and pillow basalts – all intruded by mafic sills. The Hottah Terrane and its cover sequence were later intruded by granitoid plutons of the Great Bear batholith. Regional geological and geochronological considerations suggest that the Hottah Terrane is allochthonous with respect to the Coronation margin and was accreted about 1900-1890 Ma.

Introduction

This paper reports the results of 1982 field work and U-Pb zircon chronology done in parts of the Rivière Grandin (86E) and Leith Peninsula (86D) map areas. The two map sheets span the western boundary of the Canadian Shield (Fig. 46.1) and include flat lying lower Paleozoic rocks, Proterozoic clastic and carbonate rocks of Hornby Bay Group, and early Proterozoic rocks belonging to two tectono-stratigraphic zones of Wopmay Orogen: the Great Bear Magmatic Zone and the Hottah Terrane.

The early Proterozoic rocks of the Rivière Grandin sheet and those in the southeastern part of the Leith Peninsula sheet were mapped at 1:250 000 scale by McGlynn (1975, 1979), who discovered a deformed and metamorphosed basement complex unconformably beneath rocks of the Great Bear Magmatic Zone in the Hottah Lake area (Fig. 46.1). Additional exposures of pre-Great Bear rocks were subsequently found by Hildebrand (1981, 1982) in the Conjuror Bay area (Fig. 46.1) who designated all deformed rocks in the basement complex as the Hottah Terrane (Hildebrand, 1981).

Recent tectonic models for the development of Wopmay Orogen have inferred that the Hottah Terrane is allochthonous with respect to the Coronation margin (Hoffman and St-Onge, 1981; Hildebrand, 1981; Hoffman et al., 1982). They suggested that the terrane may have been a volcanic arc or microcontinent beneath which the leading edge of Coronation margin was subducted. Since much of the Hottah Terrane remained unmapped, the models could not be tested and our understanding of the true nature and significance of the Hottah Terrane with respect to the rest of Wopmay Orogen remained enigmatic. The current project was undertaken to identify and characterize rocks of the Hottah Terrane, to establish the spatial and temporal relationships of their metamorphism and deformation with respect to the rest of Wopmay Orogen, and to continue Hildebrand's earlier investigations (1981, 1982, in press) into the oldest and westernmost rocks of the Great Bear Magmatic Zone.

Field work, from late May to early September, was carried out by ground-based 1:16 000 scale and 1:50 000 scale geological mapping. Work during the first six weeks of the

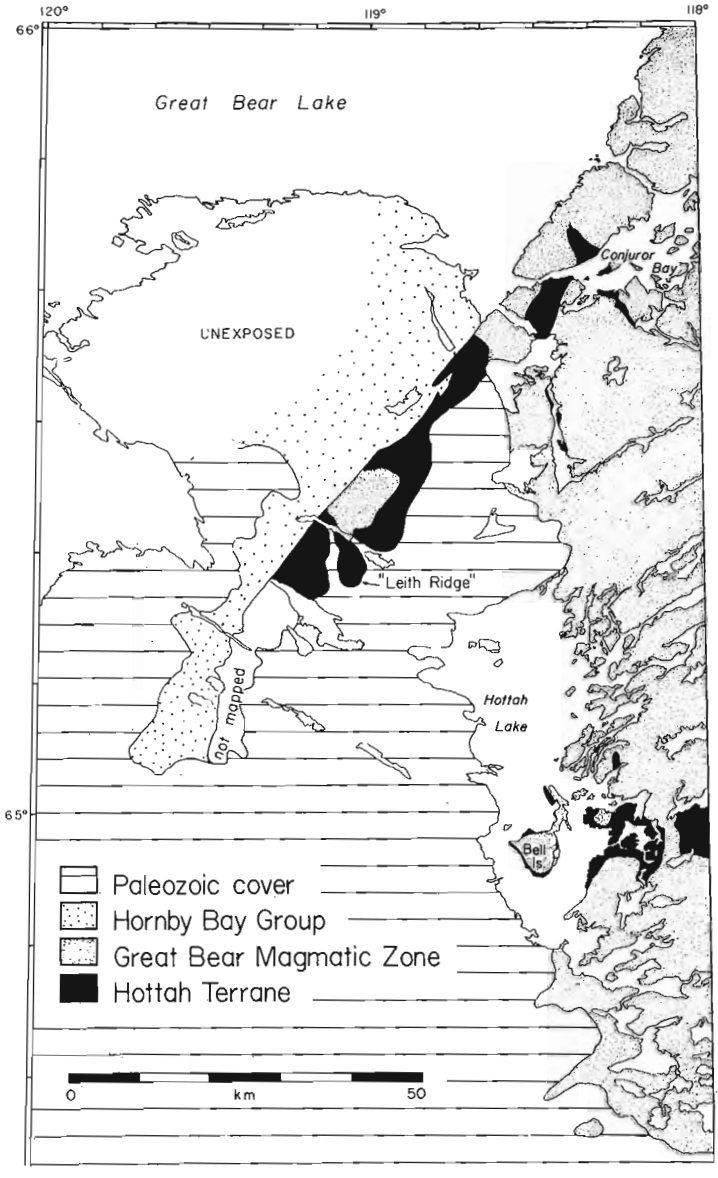

Figure 46.1. *Sketch map showing major tectono-stratigraphic units of the project area and location of major geographical features mentioned in text.*

[1] Department of Geology, University of Kansas, Lawrence, Kansas, 66045 U.S.A.

[2] Department of Earth Sciences, Memorial University of Newfoundland, St John's, Newfoundland, A1B 3X5.

Table 46.1

Analytical data for zircons from Hottah Terrane

Sample Fraction	Concentration[1] U(ppm)	Pb(ppm)	Observed Pb Isotopic Ratios[2] 204/206	207/206	208/206	Calculated Isotopic Ratios[3] 206Pb*/238U	207Pb*/235U	207Pb*/206Pb* age (Ma)
RSH 82-2								
A′	219.6	80.8	0.001101	0.130314	0.16825	0.3276	5.2165	0.11548 (1888)
A	262.3	100.5	0.002168	0.144381	0.21363	0.3174	5.0407	0.11517 (1882)
B	287.6	99.2	0.000882	0.126100	0.16436	0.3072	4.8380	0.11420 (1867)
C	282.9	93.1	0.000670	0.122721	0.15531	0.2970	4.6558	0.11368 (1859)
VS 79-104								
A(+200)	457.7	154.7	0.000209	0.118792	0.11944	0.3165	5.0607	0.11598 (1895)
C(200-270)	613.9	188.6	0.000483	0.120651	0.13358	0.2828	4.4508	0.11414 (1866)
C(+200)	644.5	182.4	0.000361	0.117768	0.12425	0.2636	4.1026	0.11289 (1847)
E(-270)	734.0	195.4	0.000320	0.116175	0.13123	0.2470	3.8089	0.11185 (1830)

[1]Corrected for blank.
[2]Uncorrected for blank.
[3]Corrected for blank, non-radiogenic Pb.
*Radiogenic Pb.

field season focused on the northern half of Leith Ridge (Fig. 46.1), while the remaining eight weeks were spent in the Hottah Lake area (Fig. 46.1).

U-Pb analyses were done at University of Kansas using an automated 22.5 cm radius, single-filament mass spectrometer. Zircon analyses (Table 46.1) followed the general method of Krogh (1973). Analytical blanks range from 0.6 to 1.2 nanograms total Pb. Corrections for non-radiogenic Pb were made using model Pb compositions of Stacey and Kramers (1975). All data reduction and age calculations were done using the constants recommended by Steiger and Jaeger (1977). Concordia intercept ages were derived using a York (1966) least-squares fit for the discordia lines and calculating the intercept ages from the mean slope and the ± 1 sigma slope. Uncertainties are reported at the 1 sigma uncertainty level.

Acknowledgments

We were capably assisted in the field by Wanda Sheldrick and Monzo Spethmann and are all grateful for the high-quality, efficient expediting of Winifred Bowler and Martin Irving (DIAND). Discussions in the field with M.R. St-Onge and M.E. Bickford were especially beneficial. S. Hanmer and M.R. St-Onge critically read the manuscript. Geochronological work was supported by NSF grants 79-19544 and 81-18234 to W.R. Van Schmus.

Leith Ridge

Leith Ridge, named by Balkwill (1971), is a topographically high-standing ridge of early Proterozoic rocks about 5 km wide and nearly 75 km long. It is a continuation of the rugged, deeply incised eastern shoreline of Great Bear Lake. The ridge is flanked on the southeast by swampy lowlands underlain by very poorly exposed, flat-lying lower Paleozoic rocks. The northwestern side of the ridge (Fig. 46.2), and likely the entire eastern shoreline of Great Bear Lake, is bounded by northeast-trending, northwest side down, normal faults which place Hornby Bay Group sedimentary rocks against older Proterozoic rocks.

Hottah Terrane

The oldest rocks of Leith Ridge are deformed rocks of the Hottah Terrane (units a-d; Fig. 46.2). Age relations between units a,b,c and d are unknown and their order on the figure legend is purely arbitrary.

Unit a is a mixed unit of quartz-plagioclase-biotite ± muscovite schists (sedimentary protolith), with minor garnet amphibolite, intimately intruded by sheets, dykes, and irregularly-shaped bodies of undeformed to slightly foliated granitoid rocks. The maximum phase assemblage is quartz-plagioclase-biotite+sillimanite+granitic melt. The first appearances of sillimanite and granitic melt were mapped in the field. Original compositional layering in the schists has been completely transposed and primary sedimentary structures obliterated. The transposed fabric is isoclinally folded with shallowly plunging axes and vertical to gently inclined axial planes. Granitic pods are isoclinally folded and the trace of the first appearance of granitic melt in the schists is also tightly folded.

Orthogneiss of dioritic, quartz dioritic, quartz monzonitic, and granitic compositions make up the bulk of unit c and parts of unit b. Hornblende and biotite are the dominant ferromagnesium minerals. Virtually all the rocks of unit c are L/S tectonites with shallowly plunging lineations and steep to gently inclined planar fabrics. In general the planar element dominates, but locally only a lineation defined by stretched crystals is present. Local zones of gabbro and clinopyroxenite also occur within this unit and are only slightly deformed. Contacts between all rock types parallel the planar fabric and may be tectonic.

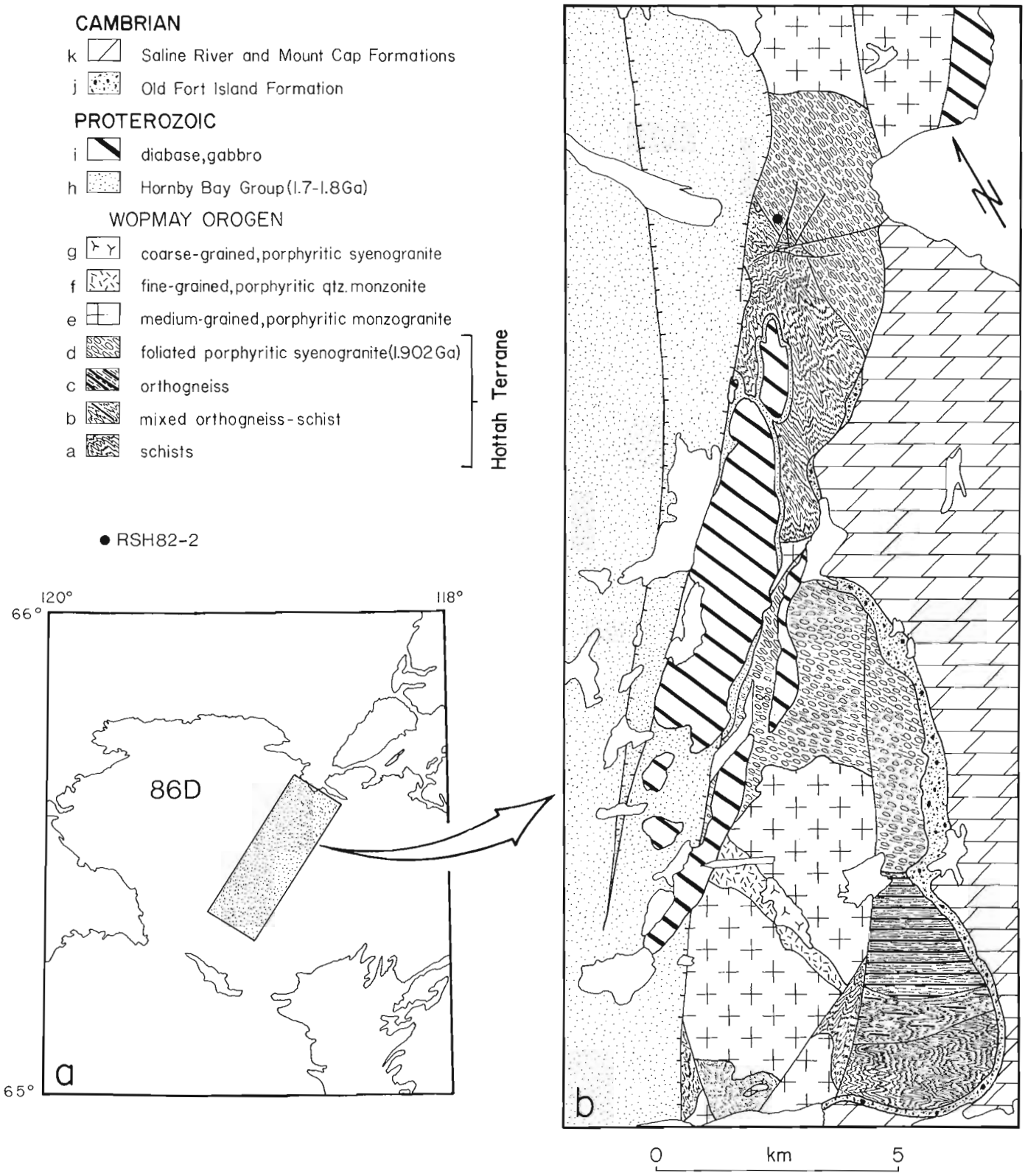

a. Sketch map of Leith Peninsula (86D) map area showing that part of Leith Ridge mapped during the 1982 field season.

b. Geological sketch map showing distribution of major map units.

Figure 46.2

A peculiar rock, probably best termed a lenticular or flaser-like gneiss, occurs as lenses 3-4 m thick and 40-50 m long in the northern part of this map unit. The gneiss is a plagioclase-quartz-potassium-feldspar-biotite rock in which the biotite forms lenses 2-3 cm long and less than 1 cm thick. The lenticular nature of this rock was probably generated by isoclinal folding and extreme flattening of a rock containing alternating quartzofeldspathic and biotite bands. Sillimanite, perhaps pseudomorphing kyanite, forms sparse, blocky porphyroblasts 1 cm across.

The planar fabric of rocks included in unit c is transposed by ductile shear zones of dominantly sinistral sense (Fig. 46.3). They commonly trend east-west.

All of the above rocks are intruded by undeformed aplite dykes. Crosscutting relationships, visible in some outcrops, indicate at least three generations of these intrusions and there does not appear to be any spatial relationship between the shear zones and dykes.

Coarse grained, foliated porphyritic biotite syenogranite (unit d) is the most common lithology of the Hottah Terrane on Leith Ridge (Fig. 46.2) and similar rocks occur in the Conjuror Bay area (Hildebrand, 1982). The granite is variably deformed, ranging from virtually undeformed to strongly mylonitic. Most typically the unit is an L/S tectonite with the planar fabric defined by biotite and the lineation by stretched potassium feldspar megacrysts. The lineation is gently plunging, while the foliation is steep to gently inclined. A deformed sample of this unit was collected for U-Pb zircon geochronology during the 1982 field season and has yielded an age of 1902 ± 4 Ma (Fig. 46.4). This is interpreted as the emplacement age.

Figure 46.3. *Sinistral, ductile shear zones in orthogneiss of Hottah Terrane cut by fine grained biotite granite. GSC 203695-N*

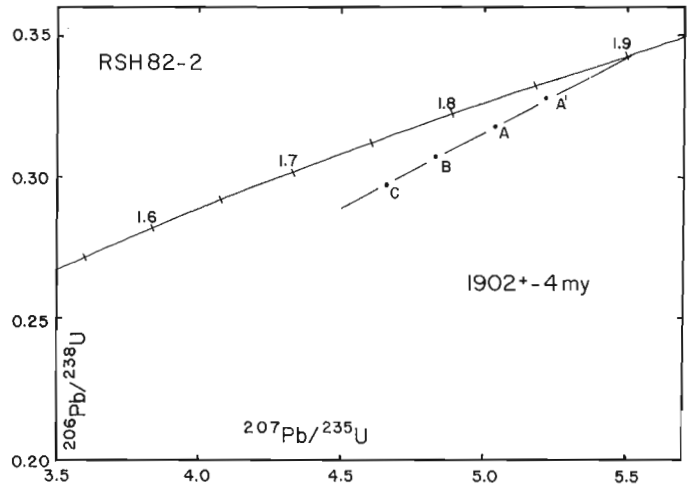

Figure 46.4. *Concordia diagram for deformed syenogranite of Leith Ridge.*

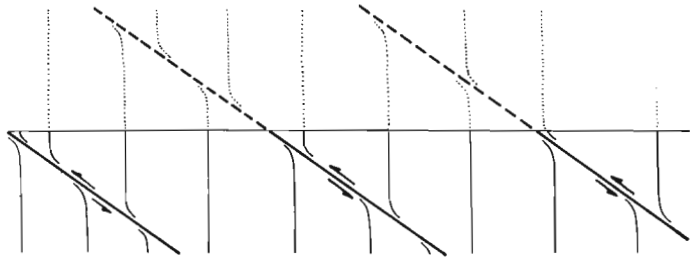

Figure 46.5. *Diagramatic cross-section showing relationship of foliations and contacts on Leith Ridge.*

The contacts of units a through d generally dip less than 40 degrees and are zones of intense mylonitization. For example, the foliated porphyritic syenogranite (unit d) becomes progressively deformed to a mylonitic gneiss over 3 or 4 m as the contact with the schists (unit a) is approached. Planar fabrics in both units shallow into the plane of the contacts and are almost always concordant to the same. Within the mylonitic zones mineral lineations lie within the plane of the foliation and are nearly orthogonal to the strike of the foliation. A schematic cross-section of relations at the contacts is shown in Figure 46.5. Rotation of the foliations into the shear zones indicates that the structurally higher blocks have moved over the lower blocks. Therefore the shear zones are tentatively interpreted as ductile thrust zones.

An interesting feature of the tectonites occurring on Leith Ridge is the abrupt change in strike of foliations across younger, nearly vertical, faults of unknown displacement (Fig. 46.2). As mineral lineations and/or fold axes are nearly horizontal in each block it is difficult to attribute the rotations to movement along the younger faults by dip-slip, reverse-slip, or strike-slip displacement. Rotations therefore occurred prior to the generation of the faults, possibly during a younger collisional event, which is suggested by paired gravity anomalies to the west (Hoffman et al., 1982).

Great Bear Magmatic Zone

Rocks of the Hottah Terrane on Leith Ridge are intruded by plutons similar to plutons of the Great Bear Magmatic Zone. The most common are bodies of grey-weathering, medium grained, hornblende-biotite syenogranite to monzogranite containing pink phenocrysts of potassium

feldspar to 4 cm. They have sharp contacts with their wall rocks, and often contain numerous xenoliths. The northernmost pluton shown on Figure 46.2 is cut by myriads of aplite and pegmatite sheets. The mapped contact dips shallowly to the north, suggesting that it is the lower contact of the body.

The two large bodies exposed near the south end of the mapped area (Fig. 46.2) are similar in composition yet are probably two different plutons. Potassium feldspar phenocrysts in the northern body are generally much smaller than those in the southern one and those in the northern body often contain abundant inclusions of quartz, plagioclase and biotite while those in the southern body do not. The southern body contains few enclaves while they are especially numerous in the northern body. In fact, the more northerly of the two bodies has a marginal zone about 200 m wide containing abundant enclaves of schist and gneiss with foliations that are still parallel to the regional fabric of the Hottah Terrane. This suggests that the enclaves are roof pendants, and that the two granites are indeed two separate bodies, the southern one of which intruded to a higher structural level than the northern.

The thin strip of fine grained, hornblende-biotite quartz monzonite (unit f) also contains abundant enclaves of country rocks, most of which also have a fabric parallel to the regional trend. This body is compositionally very diverse, with irregular zones of varying dimensions which contain blue quartz, perhaps xenocrystic, subhedral to euhedral crystals of plagioclase up to 1 cm long, and potassium feldspar crystals to 2 cm. Contacts with both large bodies of granite are sharp and nearly vertical. In places along the contact potassium feldspar phenocrysts protrude from the granites and appear to be in the process of being plucked.

Both the northern granite and the quartz monzonite are intruded by a coarse grained, hornblende-biotite, potassium feldspar porphyritic syenogranite (unit g). This pluton is virtually xenolith-free, weathers pinkish red, and has sharp external contacts.

Other Rocks

Sedimentary rocks of Hornby Bay Group (unit h) occur mostly in west-side down fault blocks along the western side of Leith Ridge but locally sit unconformably upon older rocks on the ridge itself (Fig. 46.2). Doubtless they once covered the entire ridge but were eroded away, except where protected by gabbro sills.

Much of the Hornby Bay Group within the area of Figure 46.2 is a fine grained, mature quartz arenite which weathers white, or where cemented by hematite, red. It is mostly crossbedded with both planar and trough sets, but stratigraphically lower parts tend to be planar bedded with rippled surfaces. Paleocurrent measurements (>200) indicate that sediment transport was toward the west-southwest.

Most beds of the Hornby Bay Group strike northeast-southwest and dip less than 10 degrees to the northwest but in gaps between normal faults bedding strikes northwest-southeast and dips close to vertical. Where the Hornby Bay Group sits on older rocks, weathering of the basement is limited to within 10 or 15 m of the unconformity. A more comprehensive treatment of the Hornby Bay Group is presented in Kierens et al. (1981). The reader is referred to that paper for further details.

Two swarms of diabase occur within the area but are not shown on Figure 46.2. The oldest are east-west trending diabase dykes which cut rocks of the Hottah Terrane and the younger granitoids. They are part of a regional swarm of east-west trending dykes mapped by Hildebrand (1981, 1982, in press) all along the eastern shore of Great Bear Lake and termed Cleaver Diabase by Hoffman (1982). They are not known to cut the Hornby Bay Group and are considerably altered. The second set of diabase dykes trend north-south, weather recessively, and are found in the north end of the map area where they intrude rocks of the Hornby Bay Group. Similar north-south trending dykes occur farther east in the Great Bear Magmatic Zone where they are mapped by Hoffman (1978) in the Sloan River map area and McGlynn (unpublished) in the Calder River map area.

Gabbro sheets (unit i) which dip gently northwestward intrude both the Hornby Bay Group and the older Proterozoic rocks. There are two sheets at different structural levels. The lower sheet appears to be a continuation of the Gunbarrel Gabbro (Hildebrand, 1982).

Map units j and k are lower Paleozoic sedimentary rocks of the Old Fort Island and Saline River-Mount Cap formations. They are generally poorly exposed and because they are outside the realm of this project the reader is referred to Balkwill (1971) for detailed descriptions of those units. It is, however, worth mentioning that the Old Fort Island Formation contains, at its base adjacent to Leith Ridge, abundant feldspar fragments probably derived from the early Proterozoic granitoid rocks.

Of particular interest to geologists working on Quaternary problems is the occurrence of spectacular sets of raised beaches up to 215 m above the present level of Great Bear Lake. The beaches are comprised of local debris and are cobbly to bouldery, except in protected paleobays, where they are composed of sand.

Hottah Lake Area

Most of the area in the Hottah Lake region mapped during the 1982 field season is shown on Figure 46.6. The oldest rocks of the belt are rocks of the Hottah Terrane. They are overlain unconformably by a varied sequence of subaerial to submarine volcanic and sedimentary rocks (McTavish Supergroup). Granitoid plutons of the Great Bear batholith intrude both the basement and the volcano-sedimentary sequence.

Hottah Terrane

Rocks of the Hottah Terrane in this area are diverse and include metamorphosed sedimentary and volcanic rocks plus a wide spectrum of intrusive rocks. The highest grade of metamorphism attained in the rocks was amphibolite facies but locally they show retrogression to greenschist facies. Age and structural relations between many units within the terrane are unknown due to extremely heterogeneous strain, intrusion by younger granitoid rocks of the Great Bear batholith, folding, and at least two generations of younger faults. In addition, many exposures occur on the hundreds of islands in Hottah Lake, thus critical contacts are often under water.

Isoclinally-folded and sheared metasedimentary rocks in which bedding has been completely transposed occur on Bell Island and a few small islands to the east. These rocks are fine grained assemblages of plagioclase-biotite-amphibole-quartz and chlorites. They were intruded prior to folding by swarms of granitoid sills and dykes which have compositions ranging from alkali feldspar granite to quartz diorite. Many of the granitoids are protomylonitic and a few are ultramylonitic. Fold axes are generally gently plunging and foliations, parallel to the nearly vertical limbs of isoclinal folds, strike about 300 degrees on the east side of the island and nearly north-south on the southern part. Most of the folds have been completely disrupted, probably due to extreme elongation after their formation. The fabric in the mylonitic rocks is parallel on horizontal surfaces to the disrupted limbs of folds. One of the deformed granitoids, a strongly flattened granodiorite, was collected by RSH, SAB, and WRVS during the summer of 1979. It yielded zircons, considered to be magmatic, dated at 1914 ± 2 Ma (Fig. 46.7).

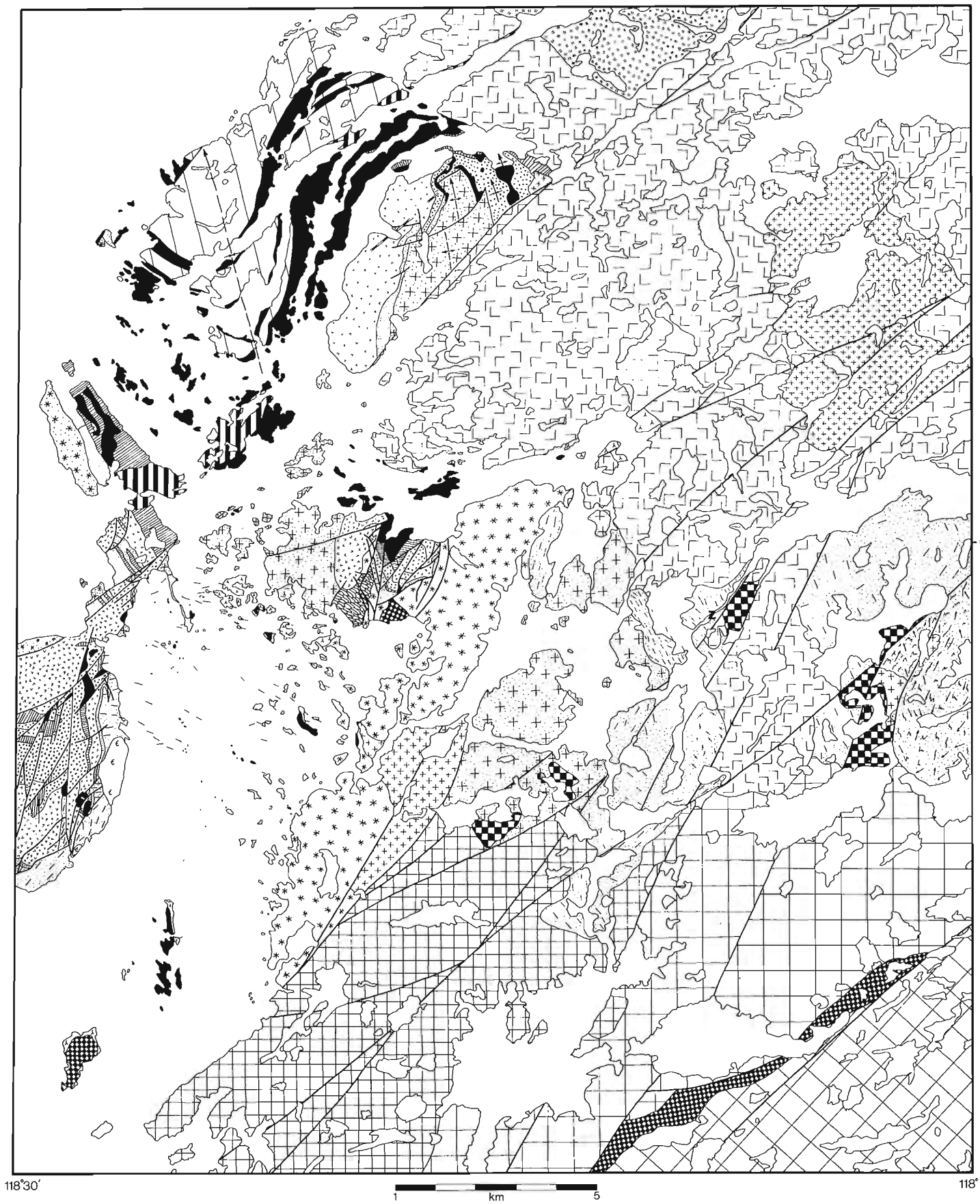

Figure 46.6. *Generalized geological map of the Hottah Lake area mapped during 1982.*

LEGEND FOR FIGURE 46.6

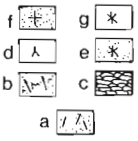

Hottah Terrane:

(a) metasedimentary rocks, mylonitic granitoids, gabbro, minor gneiss;

(b) dioritic gneiss;

(c) pillow basalt, breccia;

(d) fine-grained diorite, quartz diorite, agmatite;

(e) biotite-hornblende granodiorite;

(f) leucocratic monzogranite and granodiorite;

(g) biotite-hornblende granodiorite and quartz diorite;

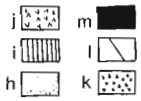

McTavish Supergroup:

(h) sandstone, conglomerate, lithic tuff, basaltic lava flows;

(i) basalt, sandstone;

(j) siliceous lava flows;

(k) ash-flow tuff;

(l) pillow basalt, gabbro, diabase;

(m) gabbro, diabase, microgabbro, minor pillow basalt;

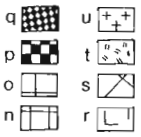

Great Bear Batholith:

(n) porphyritic biotite granite;

(o) biotite granite;

(p) quartz diorite, quartz monzodiorite, diorite;

(q) hypabyssal porphyries;

(r) Zebulon granodiorite;

(s) biotite granite-alkali feldspar granite;

(t) biotite-hornblende quartz monzonite;

(u) fine-grained biotite granite;

Younger rocks:

(v) gabbro, diabase;

(w) Old Fort Island Formation;

Z = Zebulon River (geographic locality)

Agmatite-like rocks occur on many islands east of Bell Island. They comprise blocks of fine grained diorite and medium- to coarse-grained gabbro surrounded by fine- to medium-grained quartz diorite. Some of the gabbroic blocks contain clots of clinopyroxene 15 cm in diameter. These rocks range from slightly flattened (Fig. 46.8) to intensely flattened (Fig. 46.9), with steep foliations trending close to 300 degrees. The transition between the two strain states is remarkably abrupt, often occurring over one metre or less, and usually exhibits material continuity. The gabbro blocks, being more competent than the diorities, are often angular or slightly necked, while adjacent diorite blocks are strongly flattened (Fig. 46.10). Locally, ultramylonitic zones are found in these rocks (Fig. 46.11). Their trend parallels that of the regional foliation.

Numerous bodies of medium- to coarse-grained granodiorite-monzogranite cut the agmatite-like rocks. Their deformation (Fig. 46.12) is similar to that of their host rocks.

All of the above were intruded by numerous dykes and sills of fine- to medium-grained biotite granite and alkali feldspar granite. Many of the intrusions lie within the foliation or are perpendicular to it. They are undeformed to weakly foliated.

A large body of coarse grained, leucocratic monzogranite occurs on Bell Island beneath the unconformity, on many islands northeast of there, and on the mainland east of Hottah Lake. It is usually undeformed or at most only weakly foliated.

On the mainland east of Bell Island and on a few islands to the south, deformed pillow basalts were found. In a few places they are only slightly flattened, but elsewhere they are ribbon-like in cross-section and are 1 or 2 cm thick by 3 to 4 m long. Minor deformed breccia is associated with the lavas.

A belt of metasedimentary rocks, mostly quartzites, occurs on the peninsula that juts out into the large bay east of Hottah Lake. They are strongly flattened and boudinaged. A few scattered outcrops of pelitic schist with tiny melt pods (1-2 cm) occur just north of Zebulon River. There are two sets of folds and a later crenulation cleavage present in these rocks. The crenulation cleavage trends close to north-south and dips 40-50 degrees to the west. The enveloping surfaces of the second generation folds trend about 300 degrees.

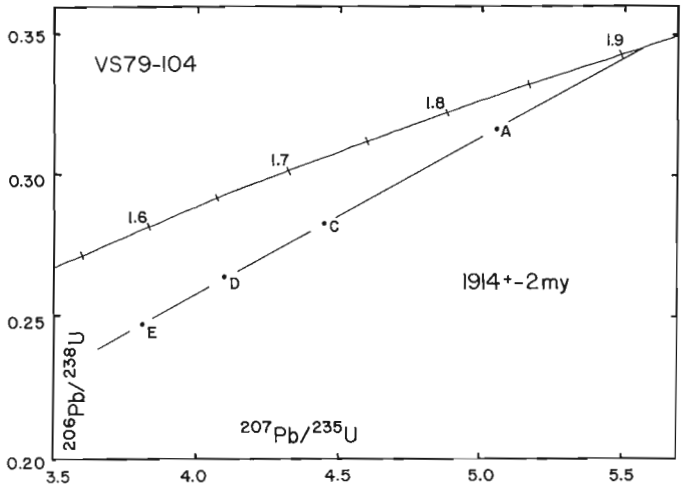

Figure 46.7. *Concordia diagram for deformed granodiorite, Bell Island.*

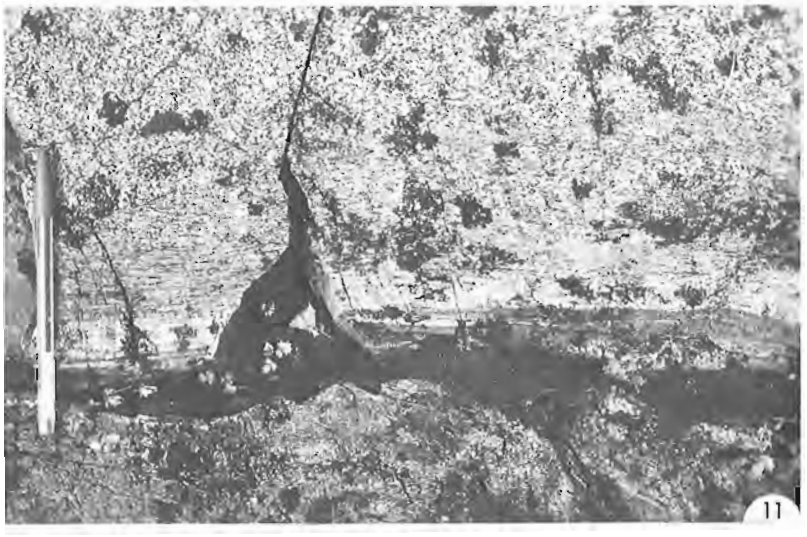

Figure 46.8. *Slightly deformed, agmatite-like rock comprising diorite blocks surrounded by quartz diorite. Pen in lower right for scale. GSC 203695-R*

Figure 46.9. *Strongly-deformed equivalent of rock shown in Figure 46.8. Pen in top centre for scale. GSC 203695-U*

Figure 46.10. *Diorite and gabbro blocks showing pinch-and-swell structure related to competence contrast. GSC 203695-Q*

Figure 46.11. *Transition from undeformed gabbro (top) to ultramylonite (bottom). GSC 203695-O*

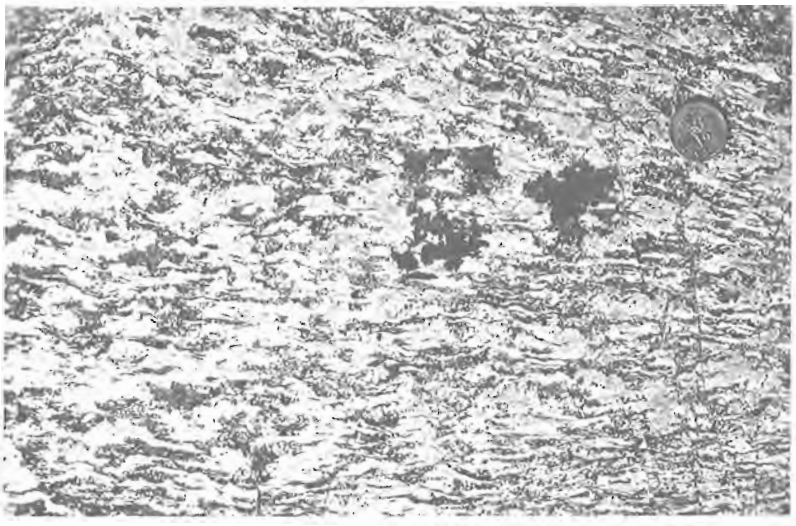

Figure 46.12

Typical texture of flattened granodiorite-monzogranite. GSC 203695-M

Figure 46.13

Unconformity between steeply-foliated granitoid rocks of the Hottah Terrane and pebbly, arkosic sandstone, eastern Bell Island. GSC 203695-V

A unit of dioritic L tectonite occurs in the extreme western part of the mapped area. It is intimately intruded by younger undeformed granitoid rocks of the Great Bear batholith.

A large area of medium grained, biotite-hornblende granodiorite to quartz diorite, usually undeformed or only weakly foliated, occurs on the eastern side of Hottah Lake where it is unconformably overlain by supracrustal rocks. Another undeformed, medium grained biotite-hornblende granodiorite was found along the northwestern side of Bell Island. Relationships with the supracrustal rocks are unclear, but this pluton may also be part of the basement complex.

McTavish Supergroup

Unconformably overlying the Hottah Terrane in the Hottah Lake area is a varied sequence of sedimentary rocks, subaerial mafic to siliceous lava flows and breccias, ash-flow tuffs, and pillow basalts. The unconformity is well exposed at numerous localities and exposures on Bell Island are superb (Fig. 46.13). There, highly strained metasedimentary and intrusive rocks with a near vertical foliation are overlain by a shallowly dipping, cobbly to pebbly, granular arkose that reaches its maximum thickness of about 100 m on the western side of the island. The unit thins rapidly to the east and northeast, where it is generally less than 10 m thick and commonly absent. The arkose is poorly bedded near its base and fines upward to well bedded, fine grained arkosic sandstone. The lower part of the unit contains abundant pebbles and cobbles of basement lithologies and undeformed volcanic fragments ranging from subangular to rounded. Locally, there are lenses and 0.5 m thick planar beds holding angular quartz fragments to 20 cm. In general, the lower part of the unit is massive with sparse trough crosslamination, while the upper, fine grained part of the section is ubiquitously trough-crossbedded with westward directed paleocurrents.

On western and northern Bell Island the sandstone contains several subaerial basaltic lava flows, probably filling paleovalleys, and minor lenses of lithic tuff. The sandstone is interpreted to record deposition in a fluvial environment, probably an alluvial fan complex, with a westward paleoslope.

Overlying the sandstone is a complex sequence of thinly bedded pyroclastic flows and a variety of siliceous lava flows. On eastern Bell Island several siliceous flows are underlain by yellowish green weathering tuff, typically one or two metres thick, containing dark green to black vitreous rock fragments and pink to orange felsophyric volcanic rock fragments. The tuffs are inversely graded with respect to size of lithic fragments. The overlying lava flows, at this locality, are

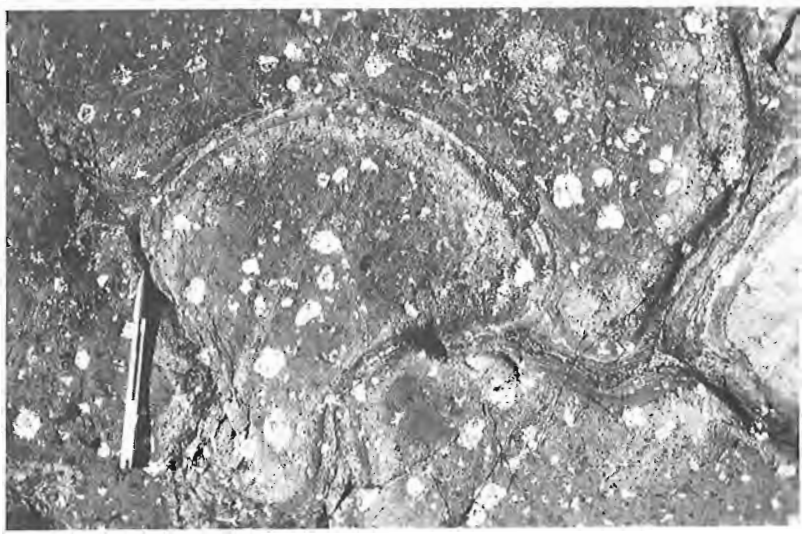

Figure 46.14

Plagioclase glomeroporphyritic pillow basalts. GSC 203695-T

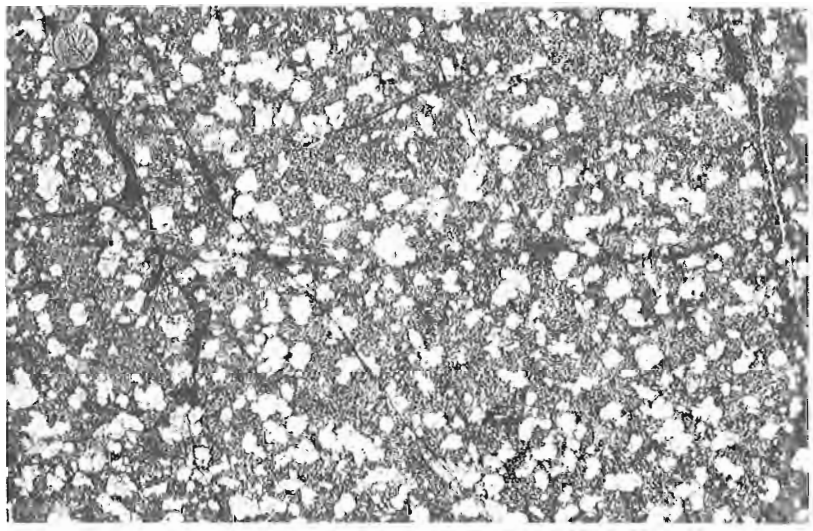

Figure 46.15

Plagioclase glomeroporphyritic gabbro sill, northeast Bell Island. GSC 203695-K

best termed block flows as they are almost entirely fragmental, consisting of 90 per cent red weathering, aphanitic volcanic fragments up to 1 m in diameter and 10 per cent yellowish green tuff-like fragmental material. In the matrix there is a continuous gradation from microscopic particles to fragments which can be considered small blocks. The larger blocks are often flow-banded and/or spherulitic. These lavas are similar to Tertiary rhyolite flows seen east of Death Valley, California by the senior author and described by Haefner (1969). A thick, strongly flow-banded, flow folded, and partially brecciated lava complex occurring just above the arkose on northern Bell Island may be a more proximal facies of this pile of lavas.

Another type of siliceous lava occurring above the arkose-basalt sequence contains abundant silica amygdules, many of which are stretched and outline flow folds. These lavas weather reddish brown. Other siliceous lava flows, which occur at the same stratigraphic horizon northeast of Bell Island, contain peculiar spherical to semi-spherical bodies which appear similar to rounded cobbles in outcrop. They range in size from 5 cm to 0.5 m and in places overlap one another. Locally, flow banding can be traced directly through the bodies. The spherical bodies are clearly not spherulites as they do not have a spherulitic texture. Their origin is, however, problematic. Identical bodies were found in Tertiary siliceous lavas by Bowring (1980) in the Datil-Mogollon volcanic field of New Mexico.

Locally on Bell Island an interval of basaltic lava flows overlies the siliceous lavas and in turn are overlain by a simple cooling unit of ash-flow tuff up to 75 m thick. The tuff weathers reddish orange and contains less than 10 per cent broken crystals of plagioclase-potassium feldspar, quartz, and ferromagnesium minerals. Near the top and bottom it is strongly eutaxitic, with flattened pumice to 6 cm. In places on Bell Island a discontinuous lithic-rich ash-flow tuff containing less than 5 per cent shattered plagioclase phenocrysts fills paleovalleys cut into the underlying tuff. This tuff is overlain either by another amygdaloidal, siliceous lava flow or by an amygdaloidal basalt flow with well developed columnar jointing.

On central Bell Island the next highest unit in the sequence is a quartz-phyric, brick-red weathering lava that is mostly massive, but occasionally flow-banded. The lava is at least 100 m thick, commonly columnar-jointed, and may be part of a dome complex. Elsewhere this lava is absent from the sequence and the ash-flow tuffs are overlain by subaerial basaltic lava flows, volcanogenic sandstones of mafic composition, or by mature quartz arenite.

The above units are, in turn, overlain by a thick sequence of amygdaloidal pillow basalts. The pile is probably at least 1 km thick but contains numerous mafic sills which make thickness estimates unreliable. The pillow basalts are of three main types: aphyric, plagioclase porphyritic, or

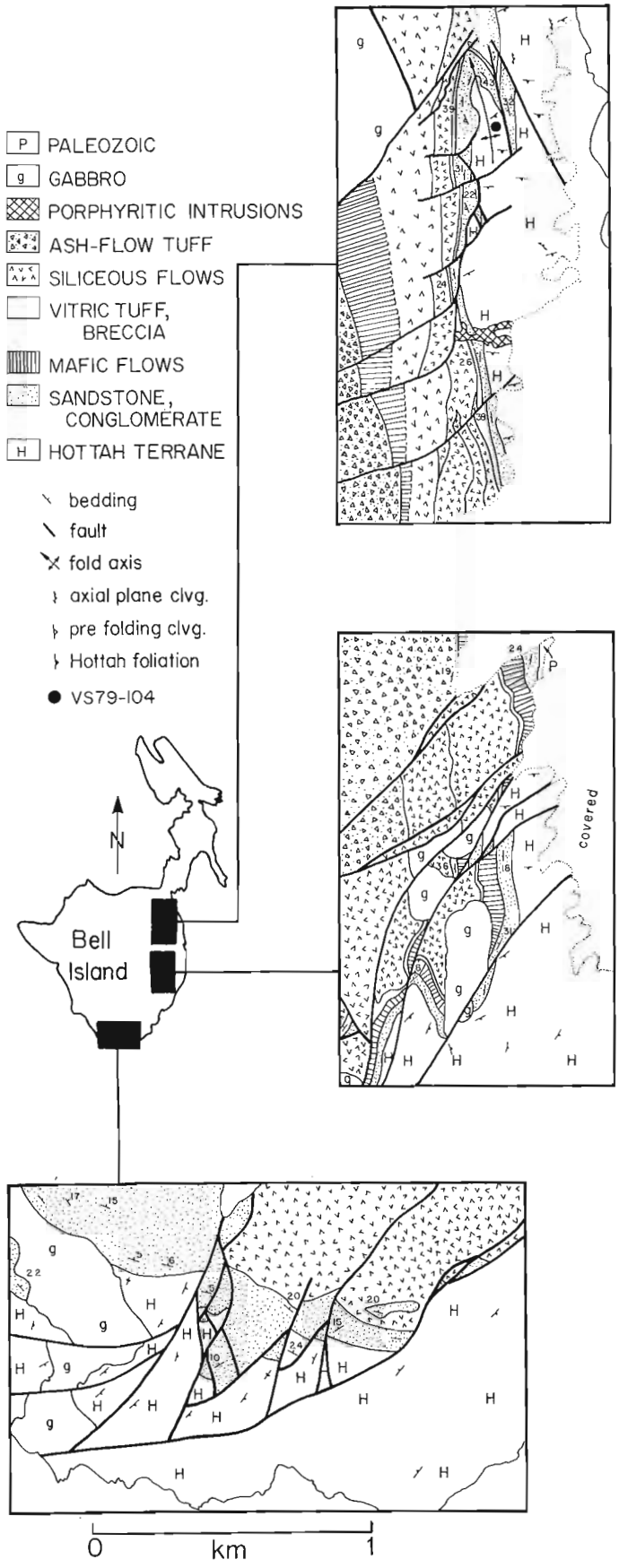

Figure 46.16. *Detailed sketch maps of geology on eastern and southern Bell Island showing complexity of structure and facies.*

plagioclase glomeroporphyritic (Fig. 46.14), which form mappable, wedge-shaped to planar units at 1:16 000 scale. Many of the pillows have round hollow cores partially filled with silica and epidote. In places the cavities are lenticular in cross-section. Spectacular 3-dimensional exposures of these lavas, showing the typical branching bulbous form, occur along the western shoreline of the largest island north of Bell Island.

Plagioclase glomeroporphyritic intrusions of ophitic to subophitic gabbro and diabase (Fig. 46.15) are very common throughout the area and cut all rocks except granitoids of the Great Bear batholith. Where they intrude rocks of the Hottah Terrane they most commonly form dykes, but where they intrude supracrustal rocks of the McTavish Supergroup they form sills. The glomeroporphyritic clots are typically 1-2 cm in diameter, normally consist of 2-5 intensely fractured and saussuritized plagioclase crystals, and commonly make up to 60 per cent of the rock. In a few places fist-size clots are common and in one locale northeast of Bell Island a football-shaped clot 20 cm long was found.

Locally a weakly developed mineralogical banding occurs in the groundmass and in areas rich in glomeroporphyritic clots there are typically irregular to planar zones in which there are no clots. One large sill, which occurs at the base of the thick pile of pillow basalts, contains oikocrysts of pyroxene up to 3 cm across in its lower half while the upper half contains clots of plagioclase. This sill has a fine grained upper border phase several tens of metres thick which contains sparse silica filled cavities up to 15 cm in diameter.

The occurrence of identical plagioclase clots in both the sills and the pillow basalts suggests that the two are comagmatic. Therefore, the intrusions may have been the magma chambers from which the pillow basalts were erupted.

Similar sills, also cutting a thick pillow basalt pile, occur in the Conjuror Bay area where they are unconformably overlain by rocks of the LaBine Group (Hildebrand, 1982). If the pillow basalts and sills in the Conjuror Bay and Hottah Lake areas are the same age, as suggested by Hoffman and McGlynn (1977), then the thick pre-basalt sequence of lava flows and sedimentary rocks of the Hottah Lake area are older than the LaBine Group and are the oldest known supracrustal rocks of the Great Bear Magmatic Zone.

Great Bear Batholith

The Zebulon granodiorite is the largest body of granitic rock mapped during the field season. It is typically a medium grained biotite-hornblende granodiorite and is distinctive in that it nearly always contains euhedral prisms of hornblende up to 1 cm long. Virtually every outcrop contains fist-sized, rounded xenoliths of partly digested country rock.

The contact of the pluton with its wall rocks is irregular on nearly every scale. A narrow aureole of contact metamorphism appears to range up to hornblende hornfels facies. Locally, spectacular intrusion breccias (Fig. 46.17) occur at the contact. In the Zebulon river area, where the pluton intrudes rocks of the Hottah Terrane, there are marginal zones rich in quartz, up to 1 cm across, and biotite. In these areas the pluton is clogged with xenoliths in varying states of assimilation.

An oval-shaped pluton of fine grained equigranular biotite monzogranite intrudes the Zebulon granodiorite. The monzogranite weathers a fleshy pink colour. The contact with the granodiorite is sharp and no border phase was evident in the field but locally, within 20 m of the contact, sheets of the monzogranite cut the granodiorite.

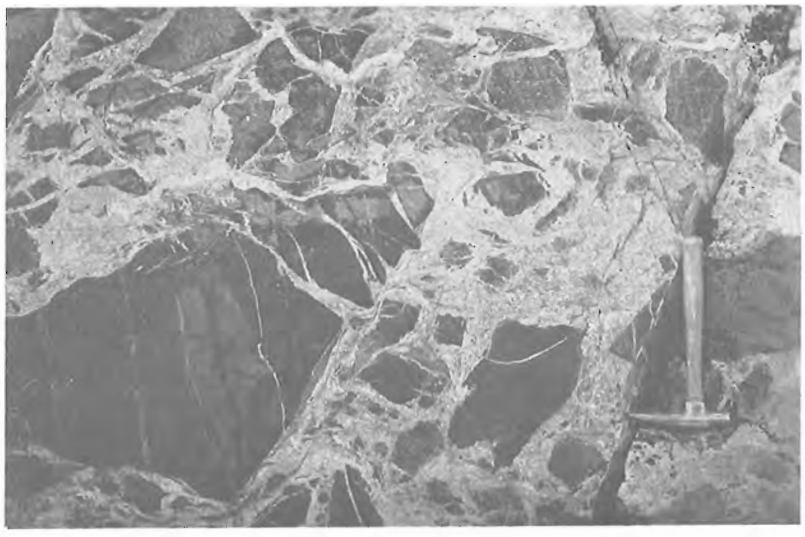

Figure 46.17. *Intrusion breccia at contact of Zebulon granodiorite. GSC 203695-S*

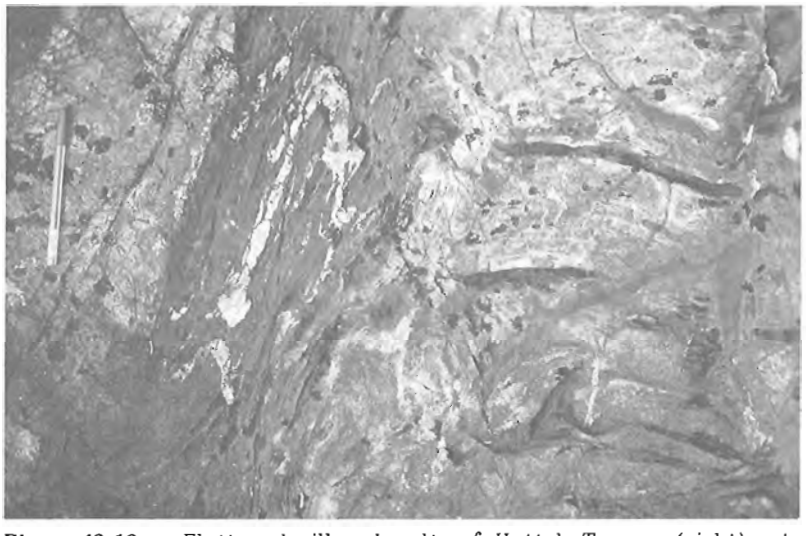

Figure 46.18. *Flattened pillow basalts of Hottah Terrane (right) cut by post-Great Bear folding shear zone (left). GSC 203695-L*

At the north end of the mapped area a fine grained, biotite-hornblende quartz monzonite intrudes the Zebulon granodiorite. This pluton is an even grained and massive rock which weathers pink. The extent of this body is unknown as only the southern contact was mapped during 1982.

Other intrusive bodies of the Great Bear batholith found in the southern part of the mapped area (Fig. 46.6) were described by McGlynn (1979) and will not be discussed here.

Structure

The structure of the supracrustal rocks in the area is complex and reflects a long history of tectonism. The oldest known tectonic event appears to have been a period of extension, probably active prior to, and during extrusion of the thick pile of pillow basalts since the faults cut the lower part of the volcanic pile but are themselves cut by the glomeroporphyritic gabbro sills. These relations are best seen in the extreme northern part of the mapped area.

Tuffaceous units within the sequence record the next deformational event which is the development of a low-angle cleavage that dips to the west at 30-40 degrees with respect to horizontal bedding planes. This suggests a component of bedding parallel simple shear, top side over bottom. The basement, the cleavage, and all of the supracrustal rocks were folded about gently-plunging axes that trend approximately north-south. These folds, part of the regional set which affects most of the Great Bear Zone, are rather broad, open folds with second order folds on their limbs (Fig. 46.6, 46.16). A second cleavage, nearly vertical and trending north-south, is well developed in lithologies such as tuffs, and protomylonitic granites, and is thought to be axial planar to the north-south folds.

A broad north-south zone of ductile shear zones trending 320 degrees to 40 degrees which postdate the folding but predate most granitoid intrusions of the Great Bear batholith cuts both the supracrustal and basement rocks along the east side of Hottah Lake (Fig. 46.18). The zones are steep dipping, less than 1 m wide, and are spaced several metres to tens of metres apart. They may form a conjugate set as both dextral and sinistral zones occur.

A swarm of northeast-trending, right-lateral transcurrent faults (Fig. 46.5) typical of those found throughout the entire Great Bear Magmatic Zone postdates emplacement of the granitoid rocks. On Bell Island they appear to be splaying into north-south faults with vertical displacement. Because the transcurrent faults were not found on Leith Ridge, the western boundary of the fault system may lie between Hottah Lake and Leith Ridge.

Many of the strike-slip faults east of Hottah Lake were apparently reactivated, probably as dip-slip faults at a later date, perhaps during deposition of the Hornby Bay Group. Numerous normal faults with limited displacement not necessarily of the same age as the above, are found where stratigraphy is well developed (Fig. 46.6, 46.16) and doubtless many more exist throughout the area. Their age relations to the transcurrent faults is unclear at present.

Younger Rocks

North-south trending, altered diabase dykes and northeast-trending gabbro sheets cut the faults. The sheets are relatively fresh and display well-developed columnar jointing. They are probably part of a regional swarm found on Leith Peninsula (i.e. Gunbarrel Gabbro), in the Calder River map area (McGlynn, unpublished), and the Hardisty Lake map area (Fraser, 1967).

Nearly flat lying lower Cambrian sandstone and conglomerate of the Old Fort Island Formation unconformably overlie the early Proterozoic rocks on eastern Bell Island. This unit ranges from massively-bedded conglomerate containing 90 per cent rounded cobbles and pebbles of the underlying basement to fine grained, crossbedded quartz arenite. Rocks of this unit are weakly indurated.

Tectonic Implications

One of the principal objectives of the study was to understand the relationship of the Hottah Terrane to the rest of Wopmay Orogen. Possibilities include the following: (1) the Hottah Terrane represents part of the Coronation margin, which is the west-facing sedimentary wedge overlying the Slave Craton; (2) it represents a fragment torn from the Slave Craton during initial rifting; (3) the terrane represents an arc beneath which the Coronation margin was subducted; (4) it is a block of unknown provenance which collided with the margin; or (5) some combination of the above.

The emplacement of granitoid intrusions in the Hottah Terrane at about 1914 Ma and 1900 Ma appears inconsistent with the terrane being part of the Coronation margin because the age of initial rift volcanism in the margin is bracketed between 2010 Ma and 1900 Ma (Bowring and Van Schmus, 1982) and it is unlikely that voluminous high-K granitic magmatism was taking place adjacent to, and oceanward of, a newly rifted and actively subsiding continental margin. If the age of rifting is close to the minimum age of 1900 Ma then the Hottah Terrane must be either a continental fragment torn from the Slave Craton or a block of unknown provenance. To date there is no indication of the existence of Archean basement in the terrane and therefore a model in which the Hottah Terrane is allochthonous with respect to the Slave Craton and of unknown provenance is favoured. Only if the age of initial rift volcanism is older than 1914 Ma could the Hottah Terrane represent part of an arc complex beneath which the Coronation margin was subducted. Even so, it would still be allochthonous with respect to the margin.

If the Hottah Terrane is allochthonous with respect to the Coronation margin and was accreted to it then the ages of deformation in both zones should be roughly synchronous. Deformation in the Hottah Terrane must, at least in part, postdate 1902 ± 4 Ma, the age of the youngest known deformed pluton in the terrane, and predate magmatism of the Great Bear Magmatic Zone which probably initiated at about 1875 Ma (Bowring and Van Schmus, 1982). Metamorphic isograds, postdate the major pulse of eastward vergent thrusting in the rise-prism sequence of Coronation margin (Hoffman et al., 1980) and are considered to be related to the Hepburn plutonic suite (St-Onge and Carmichael, 1979) whose mean age is 1885 Ma (Bowring and Van Schmus, 1982). This indicates that the age of deformation in the Coronation margin occurred between 1900 Ma, the U-Pb zircon age of porphyries that intrude the initial rift sequence but predate thrusting, and 1890 Ma - 1880 Ma, the age of the Hepburn intrusive suite. Thus, the age of deformation in both the Coronation margin and the Hottah Terrane is roughly synchronous. This is consistent with a model in which the Hottah Terrane was accreted to the Coronation margin between about 1900 Ma and 1890 Ma.

References

Balkwill, H.R.
1971: Reconnaissance Geology, southern Great Bear Plain, District of Mackenzie; Geological Survey of Canada, Paper 71-11, 47 p.

Bowring, S.A.
1980: The geology of the west-central Magdalena Mountains, Socorro County, New Mexico; unpublished M.Sc. thesis, New Mexico Institute of Mining and Technology, Socorro, New Mexico, 127 p.

Bowring, S.A. and Van Schmus, W.R.
1982: Age and Duration of Igneous events, Wopmay Orogen, Northwest Territories, Canada; in Abstracts with Programs, Geological Society of America, v. 14, no. 7, p. 449.

Fraser, J.A.
1967: Geology of the Hardisty Lake map area (west half); Geological Survey of Canada, Map 1224A.

Haefner, R.
1969: Emplacement and cooling history of a rhyolite lava flow and related tuff at Deadman Pass, near Death Valley, California; unpublished M.Sc. thesis, The Pennsylvania State University, University Park, Pennsylvania, 82 p.

Hildebrand, R.S.
1981: Early Proterozoic LaBine Group of Wopmay Orogen: Remnant of a continental volcanic arc developed during oblique convergence; in Proterozoic Basins of Canada, F.H.A. Campbell, editor; Geological Survey of Canada, Paper 81-10, p. 133-156.

1982: A continental arc of early Proterozoic age at Great Bear Lake, Northwest Territories; unpublished Ph.D. dissertation, Memorial University of Newfoundland, St. John's, Newfoundland, 237 p.

– Geology of the Echo Bay-MacAlpine Channel area, District of Mackenzie; Geological Survey of Canada Map, 1546A. (in press)

Hoffman, P.F.
1978: Geology of the Sloan River map-area (86K), District of Mackenzie; Geological Survey of Canada, Open File Map 535.

1982: The Northern Internides of Wopmay Orogen; Geological Survey of Canada, Open File Map 882.

Hoffman, P.F. and McGlynn, J.C.
1977: Great Bear Batholith: A volcano-plutonic depression; in Volcanic Regimes in Canada, W.R.A. Baragar, L.L. Coleman, and J.M. Hall, editors; Geological Association of Canada, Special Paper 16, p. 170-192.

Hoffman, P.F. and St-Onge, M.R.
1981: Contemporaneous thrusting and conjugate transcurrent faulting during the second collision in Wopmay Orogen: implications for the subsurface structure of post-orogenic outliers; in Current Research, Part A, Geological Survey of Canada, Paper 81-1A, p. 251-257.

Hoffman, P.F., McGrath, P.H., Bowring, S.A., and Van Schmus, W.R.
1982: Plate tectonic model for Wopmay Orogen consistent with zircon chronology, gravity and magnetic anomalies east of Mackenzie Mtns; Canadian Geophysical Union, Annual Meeting 1982.

Hoffman, P.F., St-Onge, M.R., Easton, R.M., Grotzinger, J., and Schulze, D.L.
1980: Syntectonic plutonism in north-central Wopmay Orogen (early Proterozoic), Hepburn Lake Map Area, District of Mackenzie; in Current Research, Part A, Geological Survey of Canada, Paper 80-1A, p. 171-177.

Keirens, C., Ross, G.M., Donaldson, J.A., and Geldsetzer, H.J.
1981: Tectonism and depositional history of the Helikian Hornby Bay and Dismal Lakes groups, District of Mackenzie; in Proterozoic Basins of Canada, F.H.A. Campbell, editor; Geological Survey of Canada, Paper 81-10, p. 157-182.

Krogh, T.E.
1973: A low-contamination method for hydrothermal decomposition of zircon and extraction of U and Pb for isotopic age determinations; Geochimica et Cosmochimica Acta, v. 37, p. 485-494.

McGlynn, J.C.
1975: Geology of the Calder River map area (86F), District of Mackenzie; in Report of Activities, Part A, Geological Survey of Canada, Paper 75-1A, p. 339-341.

1979: Geology of the Precambrian rocks of the Rivière Grandin and in part of the Marian River map areas, District of Mackenzie; in Current Research, Part A, Geological Survey of Canada, Paper 79-1A, p. 127-131.

St-Onge, M.R. and Carmichael, D.M.
1979: Metamorphic conditions, northern Wopmay Orogen, N.W.T.; in Programs with Abstracts, Geological Association of Canada, v. 4, p. 81.

Stacey, J.S. and Kramers, J.D.
1975: Approximation of terrestial lead isotope evolution by a two stage model; Earth and Planetary Science Letters, v. 26, p. 207-221.

Steiger, R.H. and Jaeger, E.
1977: Subcommission on geochronology: Convention on the use of decay constants in geo- and cosmochronology; Earth and Planetary Science Letters, v. 36, p. 359-362.

York, D.
1966: Least-squares fitting of a straight line; Canadian Journal of Physics, v. 44, p. 1079-1086.

47. ONE ASPECT OF THE DRAINAGE PROBLEM IN BIOGEOCHEMICAL PROSPECTING

Project 810005

P.A. Egginton
Terrain Sciences Division

Egginton, P.A., One aspect of the drainage problem in biogeochemical prospecting; in Current Research, Part A, Geological Survey of Canada, Paper 83-1A, p. 343-346, 1983.

Abstract

Relatively small (10-100 m^2), topographically depressed areas are common on the Canadian Shield. These areas may 'puddle' with surface runoff for periods of several weeks during the early spring but by early summer all or most visible evidence of the inundation has disappeared. Experimental data are presented which indicate that significant increases in the availability of readily reduced elements may occur in shield soils as a result of short-term flooding. The concentration of these micronutrients is also significantly increased in ***Picea glauca*** *growing on flooded soils.*

Introduction

The two major requirements for successful biogeochemical prospecting are that the plant species selected for use accumulate the elements that are sought and that in a spatial sense the concentrations in the plants mirror changes that occur in the soil or underlying bedrock. More than twenty variables affect the accumulation of micronutrients by vegetation and compound the problem. Fortunately most have a relatively minor effect; however, variability introduced by local drainage conditions may be fairly significant (Brooks, 1966, p. 109).

One of the most common drainage-related problems is the introduction of quantities of extraneous elements into an area by seepage. Mobile elements are leached from topographic highs and carried in seepage waters to topographic lows where they may be concentrated in quantities that far exceed the concentrations naturally available in the soil or the underlying bedrock. Waterlogging is another aspect of the drainage problem. Continued waterlogging produces distinctive soil horizons resulting from the oxidation-reduction process. Waterlogging may significantly alter the availability of micronutrients to plants (Ponnamperuma, 1972). Typically known areas of seasonal ponding of long duration (waterlogging) and areas of known seepage are avoided in biogeochemical surveys.

In the course of investigating the biogeochemical expression of a dispersal train near Hopetown, Ontario, many minor (10-100 m^2) topographically depressed areas were observed to 'puddle' with water for periods of several weeks during the early spring melt. This condition is common over much of the Canadian Shield. By mid to late summer visual evidence of this brief period of flooding has disappeared. This report presents some preliminary results of experimental work on the effect of the duration of puddling on soil chemistry and on the concentration of elements in **Picea glauca** (white spruce) growing in soil derived from shield rocks.

Acknowledgments

The author gratefully acknowledges the many useful suggestions made by and discussions with R.N.W. DiLabio (Geological Survey of Canada); A. Rencz (Canada Centre for Remote Sensing); J. Ross and S. Nelson (Department of Agriculture). R.N.W. DiLabio and J.A. Heginbottom reviewed the manuscript and provided many useful comments.

Methodology

In an attempt to isolate 'puddling' from the many other variables that affect soil and tree chemistry, an experimental program using potted trees was developed. Bulk surface samples were obtained from three varied locations on a metalliferous dispersal train located near Hopetown, Ontario, some 80 km west of Ottawa. The dispersal train and site are described in some detail elsewhere (DiLabio et al., in press). A 10 m^2 area at each site was stripped of vegetation and the upper 20 cm of the soil collected. Each bulk sample was mixed by shovel in an effort to obtain a uniform potting medium. One thousand, three year old, white spruce were potted in 10" (25 cm) plastic pots using these soils. The pots were kept in an outdoor plot on the Central Experimental Farm, Ottawa, for the 1981 growing season to ensure root development throughout the potting medium prior to experimentation in 1982.

In early spring 1982, the pots were moved into a polyhouse (a framed structure covered by polyethylene sheeting). The pots were numbered and randomly divided into groups. Commencing April 1982, each group was flooded for a different length of time from 0 days up to a maximum of 21 days. Distilled water, well water, or well water containing various additional concentrations of Ca and Mg was used to flood the pots. Flood waters covered the soil surface, i.e., only the tree roots remained below the surface of the water (Fig. 47.1).

Surface or near-surface soil samples were obtained at various times during the flood period by suction using a 20 cm^3 syringe with the tip removed. New growth, including both twigs and needles, was sampled in early August 1982 at the conclusion of the experiment.

The pots, when removed from the pools, were watered as needed to ensure sustained tree growth throughout the duration of the experiment. Fertilizers and insecticides were not used on the trees at any time.

Analysis

Soil

Micronutrients exist in the soil in a variety of states. The total concentration of a particular element in a soil many remain constant over time. The quantity in a given state may change, however, in response to an external stimulus such as puddling. The availability of a micronutrient to a plant is dependent upon its state. Most researchers agree that the availability of the trace elements in a soil can best be evaluated by extractants that remove only a portion

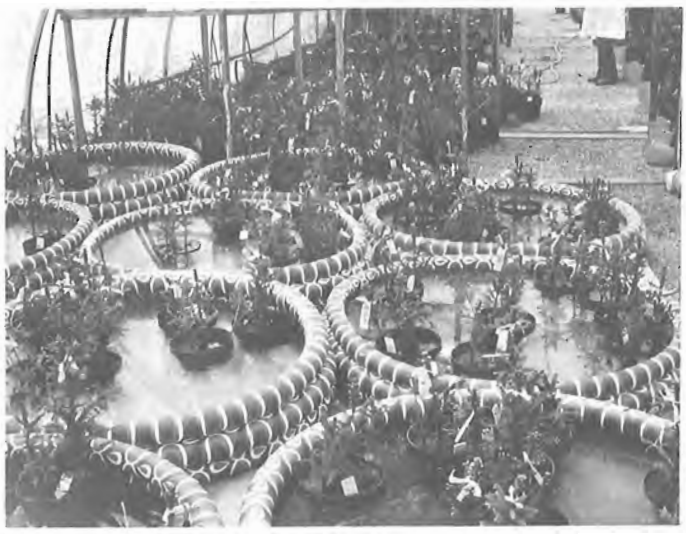

Figure 47.1. *Vinyl pools and white spruce used in individual puddling experiments, Ottawa, Ontario.*

of the total nutrient. Lindsay and Norvell (1969) developed a micronutrient soil test procedure using DPTA (diethylenetriaminepentaacetic acid) as the extractant. The concentration of DPTA-extractable elements (Zn, Fe, Cu, Mn) in a soil is thought to be representative of the concentrations that are readily available for plant uptake (Follet and Lindsay, 1971). This extraction technique was adopted.

DPTA-Extraction. The procedure used was similar to, but modified from that outlined by Soltanpour et al. (1976). Relatively small soil samples (<10 g) were collected and air dried. The dried soil was gently crushed with a mortar and pestle; 5 g of soil passing a 1 mm mesh was mixed with 10 mL of DPTA and shaken for two hours. The sediment was then removed by filtration through a No. 42 Whatman filter. Aliquots were analyzed for various elements by Atomic Absorption Spectrophotometry (AAS).

Total Nutrients. Total concentration of the selected elements in the soil was determined prior to experimentation. Soil samples (50 g) were freeze dried. The clay fraction was separated from the bulk sample by centrifugation and then digested in either an HNO_3-HCl solution (for Mn, Zn, Ni, Cu) or an HF-HNO_3-$HClO_4$-HCl solution (for Al and Fe). Aliquots were analyzed for various elements by AAS.

Vegetation

New growth, both needles and twigs, was cut from growing trees. Approximately 4 g of each sample was ashed at 450°C in a muffle furnace. The ash was then digested in an HNO_3-HCl mixture and analysis was done by AAS.

Considerable effort was expended to ensure that all sample preparation and analysis were internally consistent. The precision of the various analyses is thought to be ±10%.

Results

Soil Chemistry

Selected data are presented here. Table 47.1 shows total concentrations of various elements and Figure 47.2 gives concentrations of DPTA-extractable elements for a soil flooded with well water. Only a small proportion of the total

Table 47.1

Total concentration of various elements in soils used for flooding experiments

	Mn (ppm)	Zn (ppm)	Cu (ppm)	Ni (ppm)	Fe %	Al %
Soil 1	5200	266	29.0	20.0	7.60	6.56
Soil 2	2555	1160	18.0	9.0	5.76	6.36
Soil 3	1450	1750	30.0	15.0	7.04	7.18

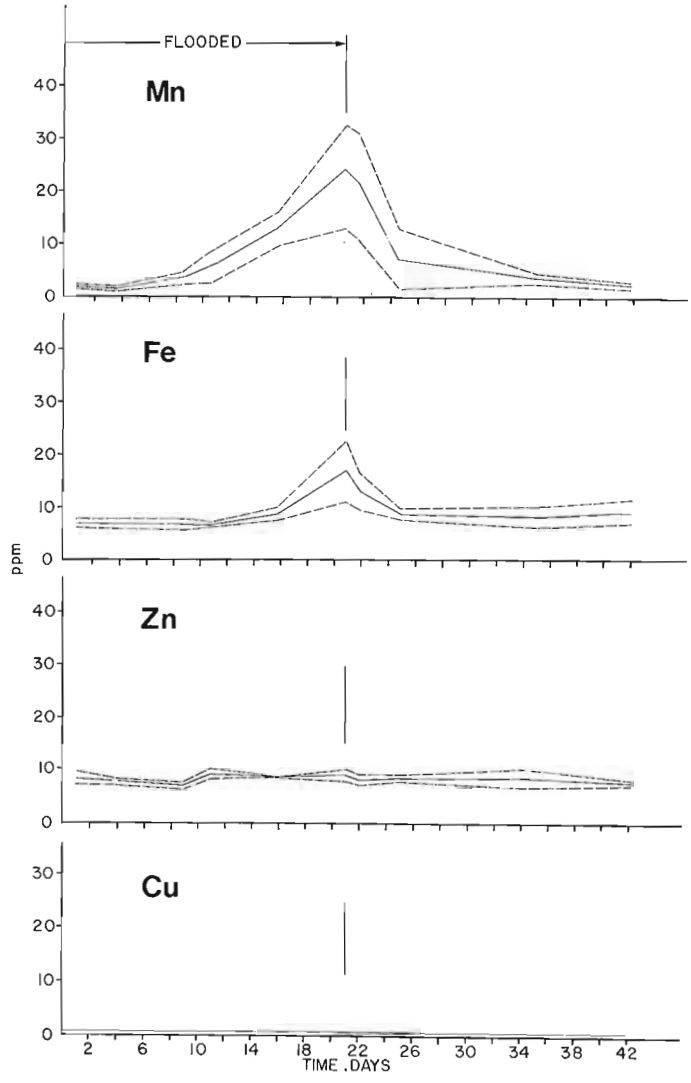

Figure 47.2. *DPTA-extractable Mn, Fe, Zn, and Cu from soil 2 after various intervals of time. The flooding commenced on day 0 and terminated after 21 days. The mean values and 1 standard deviation are shown (n = 4 or 5).*

element concentration in the soil (<4%) is actually available to plants: compare, for example, values in Table 47.1 with values at the commencement of flooding in Figure 47.2.

DPTA-extractable Mn is particularly responsive to flooding. Mean values rose from 2 ppm at the commencement of flooding to 12 ppm after 16 days, reaching a value of 24 ppm after 21 days – the maximum flood length in this experiment. Concentrations then dropped rapidly to pre-flood levels when the soils were drained. DPTA-extractable Fe showed a much less marked response to flooding although concentrations were increased by more than 200% above pre-flood levels (Fig. 47.2). DPTA-extractable Zn and Cu did not increase as a result of 21 days of flooding (Fig. 47.2).

Vegetation Chemistry

Batches of pots were flooded for different periods of time – 1, 4, 16, and 21 days – and then were removed from the pools and allowed to drain. The trees were allowed to grow over the summer; new shoots of white spruce from the respective batches were then sampled at the conclusion of the experiment in August. Element concentrations in the new growth are given for trees growing in soil 1, flooded with well water (Fig. 47.3). The longer the trees were flooded the higher the concentration of Mn and Fe in the new growth (Fig. 47.3). Trees flooded for 21 days had Mn values 1800 ppm compared to 800 ppm for unflooded controls; Fe values were 2200 and 1100 ppm, respectively. Zn values did not fluctuate in a determinate manner with flood length (Fig. 47.3).

Discussion

Short-duration floods (<21 days) can cause a short-lived change in the availability of at least some elements in soils from the Hopetown area. In the experiments reported here, after 21 days of flooding the availability of Mn increased by 1200% while Fe availability increased by 200% above pre-flood values.

The change in availability is, for the most part, a result of reduction reactions. Results similar to those reported here were obtained using distilled water as the flooding medium; elevated levels do not result from the influx of readily available micronutrients in the flood water.

A variety of electrochemical changes occur when a soil is submerged, including (1) an increase of pH in acid soil or a decrease in pH in alkaline soils, (2) a decrease in redox potential, (3) changes in specific conductance and ionic strength, (4) drastic shifts in mineral equilibria, (5) changes in cation and anion exchange reactions, and (6) sorption and desorption of ions (Ponnamperuma, 1972).

When a soil is inundated, oxygen diffusion into the soil drops by three or four orders of magnitude. Aerobic micro-organisms consume the remaining oxygen and die or become dormant. Anaerobes then multiply and use oxidized soil components as electron acceptors. Reduction of these components proceeds along the following thermodynamic sequence: nitrates, manganic compounds, ferric compounds, organic acids, sulphates, and sulphides (Ponnamperuna, 1965, 1972; Sanchez, 1976). In the Hopetown soils, reduction resulting from short-term flooding apparently does not progress beyond the manganic and ferric compounds. Certainly the quantity of DPTA-extractable Mn and Fe was still increasing at the conclusion of 21 days of flooding. On the other hand, Zn and Cu availability was not significantly altered by 21 days of flooding.

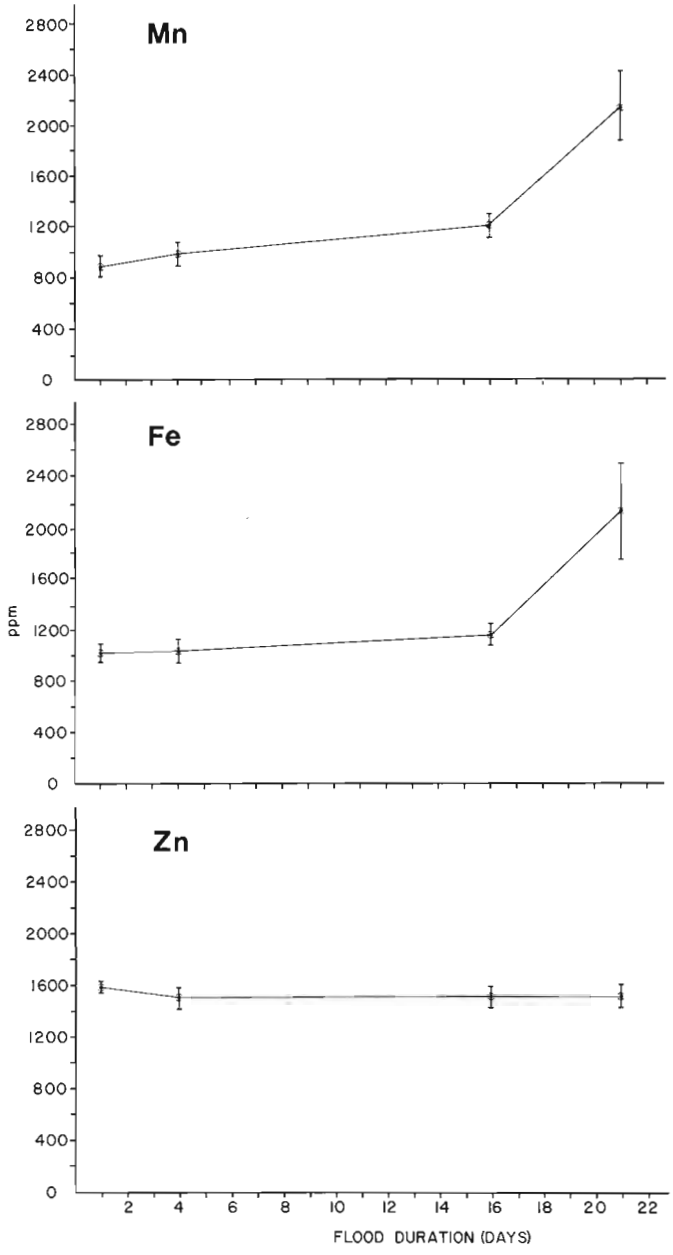

Figure 47.3. *Total element concentration (Mn, Fe, and Zn) in new growth of white spruce growing in a soil flooded for various periods of time (1, 4, 16, 21 days). The flooding occurred in April 1982, and the vegetation sampling was carried out August 1982. The mean values and 1 standard deviation are shown (n = 5 to 12).*

Mn and Fe are more soluble in a reduced form and therefore are generally more available to most plants. It is interesting that in these experiments elevated levels of Mn and Fe were maintained in the soils for only a short duration (Fig. 47.2) and for a short part of the total growing season (<10%). In spite of this, a substantial increase in the concentration of Mn and Fe (230% and 200%) still occurs in white spruce growing in a soil flooded for 21 days (Fig. 47.3).

Given the shape of the concentration – flood duration curves for white spruce, substantially higher concentrations of Mn and Fe may be obtained if the puddling is maintained for longer than the 21 days maximum used in this study.

Both Mn and Fe levels were increasing at better than 200 ppm/day after 16 days of flooding (Fig. 47.3). On the other hand, even shorter duration puddling may be sufficient to cause a significant increase in the micronutrient content of the vegetation (Fig. 47.3).

Summary and Conclusions

Short-duration flooding or puddling is common during early spring on soils in the Canadian Shield. By late summer, areas that puddle may be extremely difficult to identify. The concentration of Mn and Fe in both the soil and in plant tissue may be significantly elevated at puddled sites relative to well drained sites. The elevated levels may reflect the relative availability of the micronutrients rather than a real difference in the total concentrations of the element in the soil or the underlying bedrock. In the tests reported here, Zn and Cu availability were not affected by short-duration flooding.

Given the limited and preliminary nature of the data presented here, any conclusions are at best speculative; however, the implications of the flooding experiments are clear. In biogeochemical surveys in the Canadian Shield, particularly for readily reduced elements, it would be prudent to limit sampling to well drained slopes and to avoid all topographically depressed areas which are suspected sites of puddling. A variety of electrochemical changes occur when a soil is submerged, and vegetation growing on sites that puddle may have significantly different concentrations of elements compared to the same vegetation growing on adjacent well drained sites.

References

Brooks, R.R.
1966: Geobotany and Biogeochemistry in Mineral Exploration; Harper and Row, New York, 290 p.

DiLabio, R.N.W., Rencz, A.N., and Egginton, P.A.
– Biogeochemical expression of a classic dispersal train of metalliferous till near Hopetown, Ontario; Canadian Journal of Earth Sciences. (in press)

Follet, R.H. and Lindsay, W.L.
1971: Changes in DPTA-extractable zinc, iron, manganese, and copper in soils following fertilization; Soil Science Society of America Proceedings, v. 35, p. 600-603.

Lindsay, W.L. and Norvell, W.A.
1969: A micronutrient soil test for Zn, Fe, Mn, Cu; Agronomy Abstracts, American Society of Agronomy, p. 84.

Ponnamperuma, F.N.
1965: Dynamic aspects of flooded soils and the nutrition of the rice plant; in The Mineral Nutrition of the Rice Plant; International Research Institute, John Hopkins Press, Baltimore, p. 295-328.

1972: The chemistry of submerged soils; in Advances in Agronomy, Academic Press, New York, v. 25, p. 29-96.

Sanchez, P.A.
1976: Properties and Management of Soils in the Tropics; John Wiley and Sons, New York, p. 413-477.

Soltanpour, P.N., Khan, A., and Lindsay, W.L.
1976: Factors effecting DPTA-extractable Al, Fe, Mn and Cu from soils; Soil Science and Plant Analysis, v. 7, no. 9, p. 797-821.

48.

A STUDY OF THE HEAVY MINERAL DISTRIBUTION IN THE BOTTOM SEDIMENTS OF HUDSON BAY

Project 690095

Penny J. Henderson
Terrain Sciences Division

Henderson, P.J., A study of the heavy mineral distribution in the bottom sediments of Hudson Bay; in Current Research, Part A, Geological Survey of Canada, Paper 83-1A, p. 347-351, 1983.

Abstract

A preliminary study of the heavy mineral composition of bottom sediment samples from Hudson Bay considered the distribution patterns of siderite, hematite, augite, and pyrite. The distribution patterns indicate that 1) bottom sediments are, at least in part, derived from Quaternary glacial sediments transported by glacial and fluvial processes and ice rafting, and modified by marine currents; 2) siderite concentration is related to both submarine and subaerial exposures of the Devonian Stooping River and Kwataboahegan formations; 3) based on hematite and augite dispersal trains, ice flow directions in the northwestern part of Hudson Bay are in an easterly direction and, in the southeastern part, are in a westerly direction; and 4) pyrite is not a useful indicator mineral within Hudson Bay because of its chemical instability.

Introduction

A preliminary study of the heavy mineral composition of bottom sediment samples from Hudson Bay was initiated in an attempt to determine the provenance of the material and possible late Quaternary glacial flow directions through the distribution patterns of certain trace minerals. The study included 28 grab samples and 21 subsamples from 13 cores collected in Hudson Bay in 1974 by B.V. Sanford and C.F.M. Lewis (Fig. 48.1).

Methods

All samples were wet and dry sieved to obtain the 0.063 to 0.250 mm size fraction and separated into light and heavy fractions using methylene iodide (specific gravity 3.3). Magnetic minerals were removed from the heavy fraction using a hand magnet. Heavy mineral grains were mounted in araldite on glass slides and were identified and counted (400 points per sample) using a binocular microscope in order to determine the percentage of all minerals in each sample.

Bedrock Geology

The bedrock underlying Hudson Bay consists of the remnants of a Paleozoic sedimentary basin unconformably overlying Archean and Proterozoic basement (Fig. 48.2). Part of the Paleozoic sequence of Ordovician, Silurian, and Devonian carbonates and evaporites with minor clastics occurs on the mainland along the southwest coast of the bay (Norris and Sandford, 1969).

Archean rocks of the Churchill and Superior structural provinces outcrop on the western and eastern coasts of the bay, respectively. The western region, north of Churchill, is composed of granitic gneiss, migmatite, and highly metamorphosed volcanic and sedimentary rocks. Granitic gneiss and granulite facies metamorphic rocks of the Superior Province are exposed along the eastern coast of the bay (McGlynn, 1970).

Proterozoic volcanic and sedimentary rocks and iron formations of the Belcher Island and Cape Smith Fold belts are exposed on the Belcher and Ottawa Islands and underlie the eastern part of the bay. The Sutton inlier on Cape Henrietta Maria is a continuation of the Belcher Fold Belt and unconformably overlies the Archean basement (Donaldson, 1970).

Previous Work

Initial studies of the composition of bottom sediments of Hudson Bay were carried out by Pelletier (1969) who concluded that ice rafting and marine currents were the main agents of sediment transport. When the fraction of the sediment that was assumed to be the ice rafted material was removed from the analyses, the resulting dispersal pattern could be related to fluvial sources modified by marine currents within the bay. Sedimentation through ice rafting was limited to shallow, nearshore areas and contributed little to sediment distribution in the central bay.

Bayliss et al. (1970), using X-ray diffraction techniques on bulk samples of the same material, reported on the distribution of quartz, feldspar, carbonate, and clay minerals. They corroborated Pelletier's conclusions, indicating that mineral distribution in the bay was dependent upon the mineralogy of the exposed adjacent shoreline and did not reflect underlying bedrock lithology.

Mineral Distribution in Sediments

Results from the present study show variations in all mineral groups but the most striking occur in the distribution of siderite, hematite, pyrite, and augite. These minerals could also be identified consistently. To minimize the problem of mineral instability, grab sample material from close to the sediment-water interface was used, where possible, with the hope that the postdepositional physical-chemical conditions would be reasonably similar at each sample location. When surface material was not available, the uppermost available section of core was used.

Siderite

Siderite occurs as honey brown, single, elongate crystals, crystal aggregates, and irregular spherulitic masses. It is generally clear but may contain dark brown inclusions. At location L-1 (Fig. 48.1), the siderite is dark brown and appears dusty, which may indicate alteration to goethite.

Siderite occurs in the Devonian limestones of the Stooping River and Kwataboahegan formations as fracture and cavity fillings (Sanford and Norris, 1975). These formations outcrop on the southwestern shore of the bay between the mouths of Nelson and Severn rivers and extend under the bay in an annular outcrop pattern following the

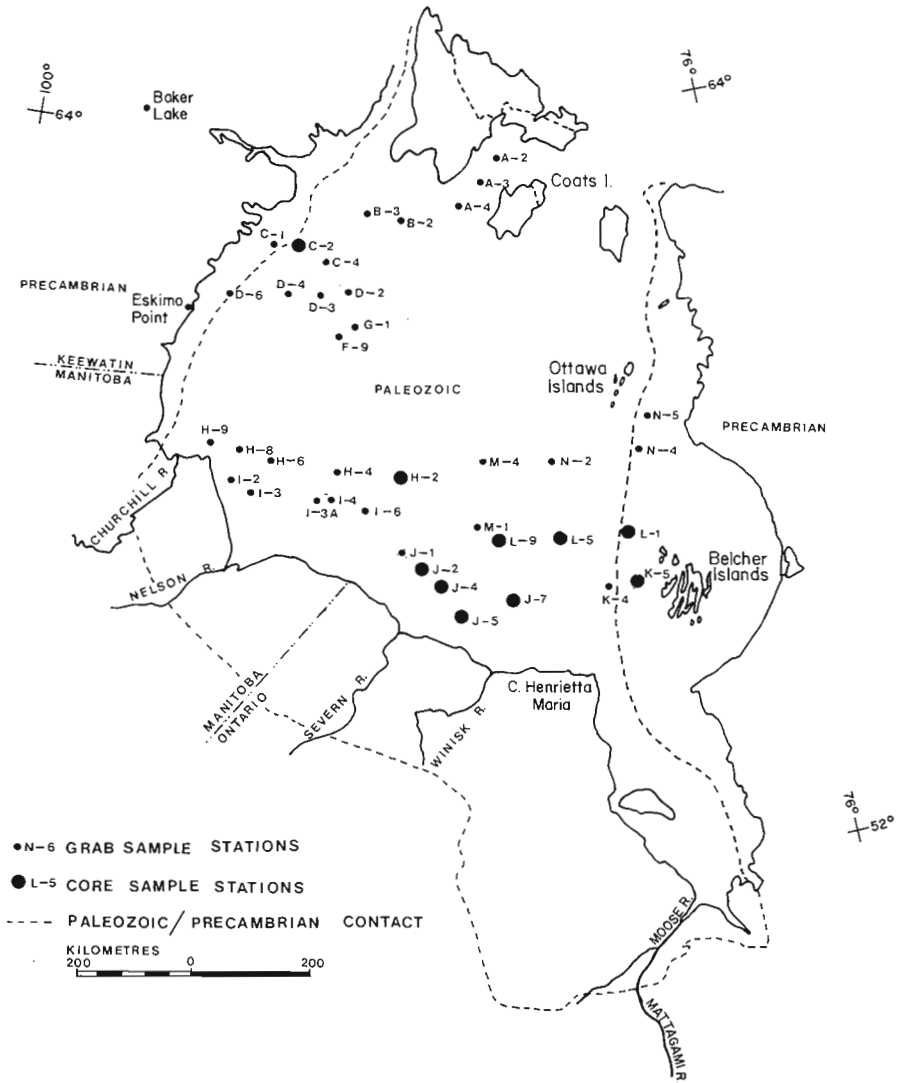

Figure 48.1. *Sample location map, Hudson Bay, Canada. Sample numbers are those of B.V. Sanford and C.F.M. Lewis. Paleozoic-Precambrian contact after Sanford et al. (1979).*

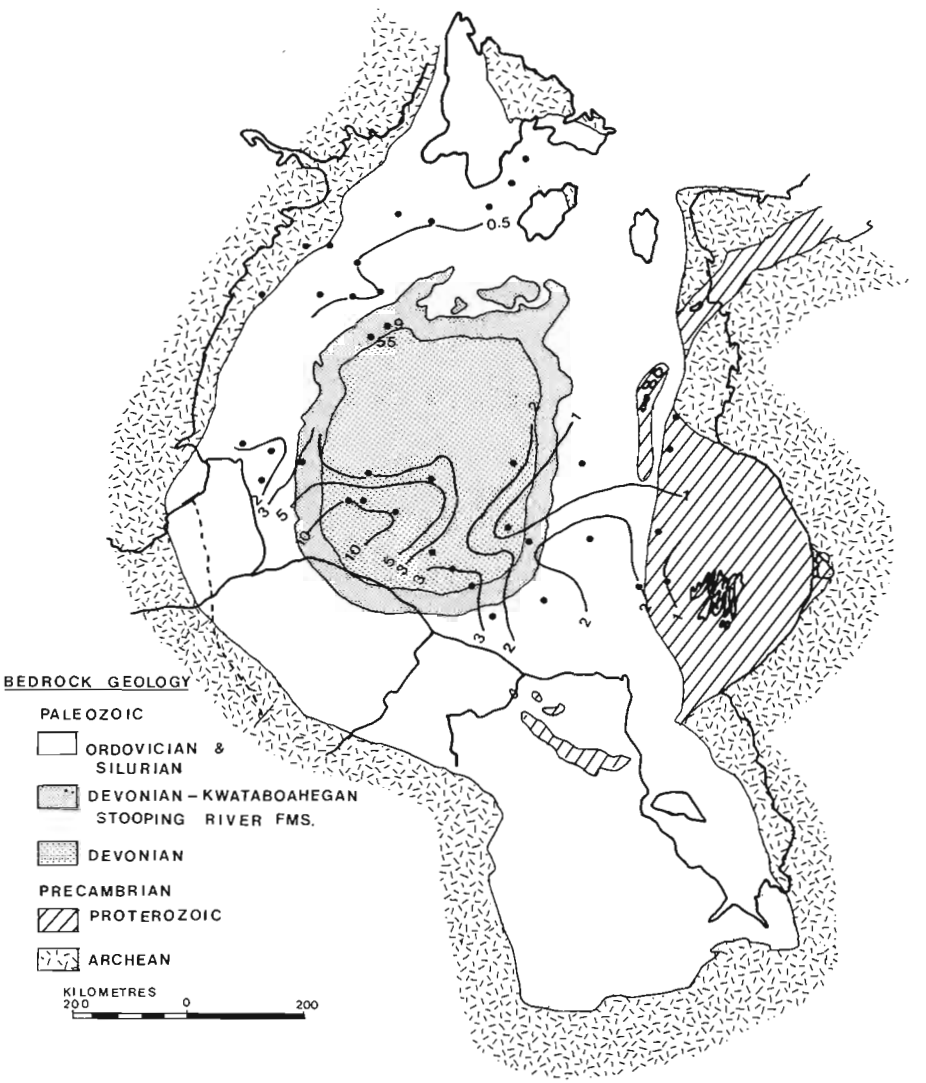

Figure 48.2. *Geology of Hudson Bay showing the distribution of siderite in the bottom sediments. Isopleths represent percentage siderite counted. Numbers next to sample stations indicate percentage found at that particular station. Geology after Sanford et al. (1979). The dashed line on the western shore of the bay represents that part of the proposed Polar Gas pipeline route that Shilts (1980a) reported as having high siderite concentrations in the tills.*

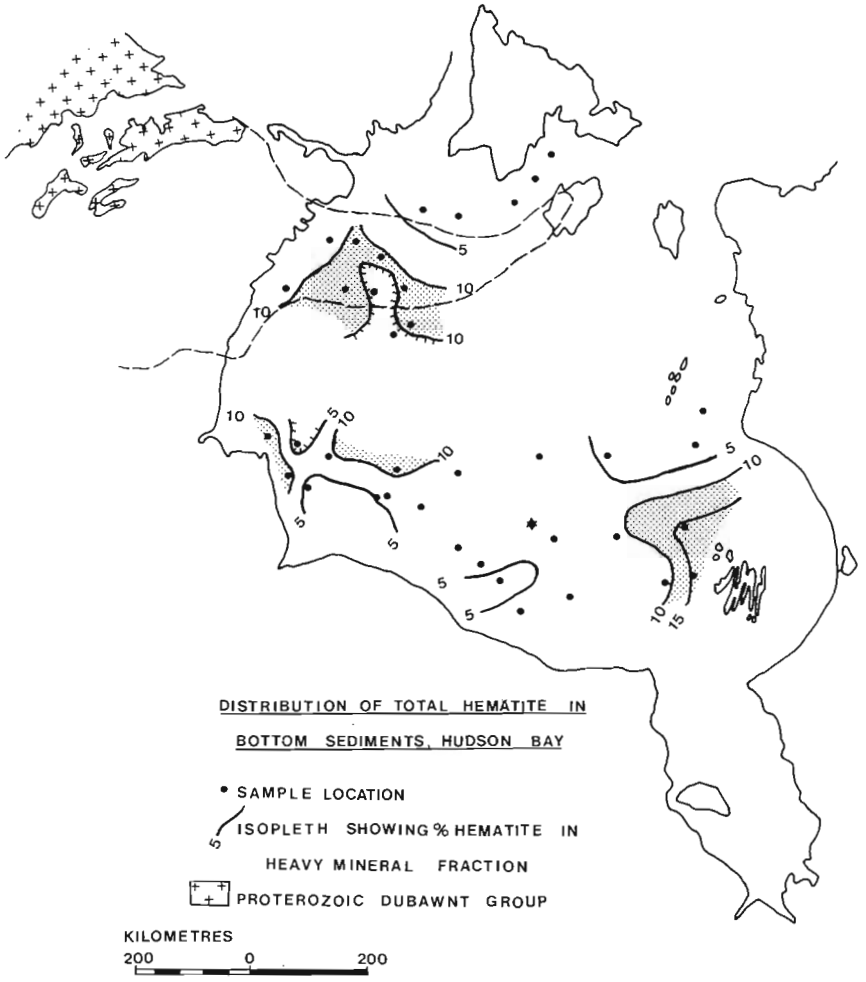

Figure 48.3. Distribution of hematite in bottom sediments of Hudson Bay. Stippled areas indicate greater than 10% hematite. Star denotes sample location which represents anomalous value at M-1 (35%). Dashed line extending from Proterozoic Dubawnt outcrops represents dispersal train of Dubawnt lithic granules from till or till-like sediment (Shilts, 1980b).

Figure 48.4. Distribution of augite in bottom sediments of Hudson Bay. All unlabelled locations outside the contoured area have no recorded augite.

configuration of the Hudson Bay basin (Fig. 48.2). Siderite also occurs in the cherty and carbonate facies of the Proterozoic iron formations of the Belcher Islands (Jackson, 1960).

Shilts (1980a) reported high siderite values from heavy mineral separates in till collected from drillholes along the proposed Polar Gas pipeline route in the region between the Ontario-Manitoba border and the Churchill area on the west coast of Hudson Bay (Fig. 48.2). The distribution suggested a dispersal train extending southwestwardly from the Devonian formations in Hudson Bay. Skinner (1973) reported siderite in the tills of the Moose River Basin south of Hudson Bay and concluded that the mineral was reworked Devonian siderite derived from limestones similar to those at Grand Rapids on Mattagami River (Bennett et al., 1967). Up to four per cent siderite has been counted in heavy mineral suites from till on Coats Island (D. Paré, personal communication, 1982).

Siderite in fluvial sediments from Severn River estuary is described by Adshead (in press).

Results of this study show that siderite distribution in Hudson Bay sediments (Fig. 48.2) is influenced primarily by the outcropping of the two Devonian formations within the bay. In the northwestern portion of the bay, high siderite values of about 9 and 55 per cent at locations G-1 and F-9, respectively, occur directly over the Stooping River and Kwataboahegan formations. Because there is no other known source for the mineral in this area, it is concluded that this siderite must be derived from the erosion of these formations within the bay. Therefore, the bottom sediment in the bay is, at least partly, the result of erosion and redeposition of bedrock material, possibly during glaciation. The bottom of the bay has not been exposed subaerially since the Tertiary (Pelletier, 1969).

High siderite concentrations in the southwestern part of the bay appear to be due primarily to erosion and redeposition of the mineral from subaerial coastal exposures of Stooping River and Kwataboahegan formations and secondly to the fluvial input of sediment reworked from glacial tills exposed along Nelson and Severn rivers.

Slightly elevated percentages of siderite west of the Belcher Islands could represent material transported from known iron formations (Jackson, 1960). Except for location L-1, however, all siderite in the bay appears similar under the binocular microscope and a similar provenance for the mineral seems likely. The concentration in the area of the Belcher Islands, therefore, may be the result of ice-rafted, nearshore Paleozoic-derived material being moved by the general counter-clockwise current movements in Hudson Bay (Pelletier, 1969).

Because of the occurrence of siderite in till beyond the bay, and the limited nature of the distribution in close association with the Devonian formations in the bay, the mineral is believed to be reworked from these rocks or from tills derived from these rocks and, consequently, is not authigenic in origin.

Hematite

Hematite occurs in four forms in the samples: 1) steel-grey, rounded and subrounded to angular grains, 2) dark grey, specular and granular hematite, 3) brick-red, angular grains, and 4) botryoidal and framboidal brick-red hematite.

Total hematite contents in excess of 10% occur in the northwest portion of the bay east of Eskimo Point, at the mouth of Churchill River, and in a dispersal train extending westerly from the Belcher Islands (Fig. 48.3). The sample from M-1 in the central part of the bay is unique in that it contained more than 35% bright-red framboidal hematite, as well as high pyrite and goethite values. The goethite appears to be an overgrowth on the hematite grains. Only a few grains of this framboidal hematite were noted at any other site. The results for site M-1 are unexplained at present.

The provenance of the hematite would appear to be the Precambrian terrane adjacent to the bay. Red lithic granules of the Dubawnt Group outcropping near Baker Lake have been traced into the bay (Shilts et al., 1979) and across the northern part of the bay as far as Coats Island (Shilts, 1980b, Fig. 48.3). Rounded, steel-grey, sand-sized hematite grains similar to grains in the bay sediments, have been observed in sedimentary rocks of the Dubawnt Group (W.W. Shilts, personal communication, 1980). In the northwestern part of the bay, near the source area, the proportion of steel-grey hematite to total hematite present in the heavy mineral fraction is higher than in the south.

The distribution of hematite in the southeastern portion of the bay suggests a dispersal train extending westerly from its source – the hematite-bearing iron formations on and around the Belcher Islands (Jackson, 1960). The direction of this trend is opposite to present day marine currents and may, therefore, reflect Quaternary ice movements.

High hematite values in the southwestern portion of the bay near the mouth of Churchill River may represent extensions of the Belcher Islands or Dubawnt dispersal trains and the reworking of the resulting till by fluvial processes. Dubawnt material in this area may also be present due to the effects of ice rafting and the general southerly trending marine currents. Because of the variety of hematite present in the samples, it is difficult to distinguish the provenance of the material without a thorough examination of the possible source material.

Pyrite

Pyrite occurs as cubic crystals and as irregular, angular to subrounded grains and botryoidal masses. Pyritized fossil foraminifera are present in some samples.

Pyrite generally represents less than 1% of the heavy minerals in the surface sediment grab samples although samples from sites D-3, D-4, M-1, M-4, and K-4 (Fig. 48.1) contain somewhat more. On the other hand, the pyrite content of the subsurface core material is consistently greater than 1% of the heavy mineral suite, suggesting that pyrite is not preserved near the sediment-water interface.

Pyrite has an irregular distribution pattern. The concentration of the mineral at any one point is more an indication of the postdepositional chemical environment rather than its original abundance. In addition, some of the pyrite may be authigenic. Therefore, the distribution pattern is not thought to be a clear expression of clastic transport agents.

Augite

Khaki brown augite (electron probe identification by M. Bonardi) occurs on the eastern side of the bay near the Belcher Islands with a distinct distribution pattern decreasing towards the west (Fig. 48.4). Assuming the source area of this pyroxene is the mafic basalts of the Belcher Islands (Jackson, 1960), the trend could be indicative of Quaternary ice flow directions, because, like the hematite pattern, it suggests transport opposite to the general direction of present current flow and pack ice movement in the bay.

Summary and Conclusions

1. Siderite concentration is related to present day submarine and subaerial outcrop patterns of siderite-bearing Paleozoic formations. The presence of siderite in the northern part of Hudson Bay, where no source area other

than the Devonian formations is present, is strong evidence that glacial erosion of the underlying bedrock contributed to the mineralogy of the bottom sediments in the bay.

2. High concentrations of hematite and augite can be related to source areas in adjacent Precambrian terranes. Near the Belcher Islands, the abundance trends oppose the present day current directions, suggesting that glacial erosion and transport played important roles in the dispersal of these minerals. The glacial movement was in a westerly direction.

   In the northern part of the bay, hematite and siderite distributions indicate Quaternary glacial transport in an easterly direction.

3. Due to its instability, pyrite is not useful as an indicator mineral in this study.

Acknowledgments

The project was suggested and supervised by W.W. Shilts. Special thanks to B.R. Pelletier and R.N.W. DiLabio for critical reviews of the manuscript. The author also wishes to thank the following for discussions, suggestions, and other assistance: J.A. Fraser, G.D. Jackson, W.R.A. Baragar, J.B. Henderson, D. Paré, and J.D. Adshead.

References

Adshead, J.D.
– Hudson Bay river sediments and regional glaciation. Part I, Iron and carbonate dispersal trains southwest of Hudson and James Bays; Canadian Journal of Earth Sciences. (in press)

Bayliss, P., Levinson, A.A., and Klovan, J.L.
1970: Mineralogy of bottom sediments, Hudson Bay, Canada; Bulletin of Canadian Petroleum Geologists, v. 18, no. 4, p. 469-473.

Bennett, G., Brown, D.D., George, P.T., and Leahy, E.J.
1967: Operation Kapuskasing; Ontario Department of Mines, Miscellaneous Paper No. 10.

Donaldson, J.A.
1970: Geology of the Canadian Shield, Cape Smith and Belcher Island Fold Belt; in Geology and Economic Minerals of Canada, ed. R.J.W. Douglas; Geological Survey of Canada, Economic Geology Report No. 1, p. 104-107.

Jackson, G.D.
1960: Belcher Islands, Northwest Territories; Geological Survey of Canada, Paper 60-20.

McGlynn, J.C.
1970: Geology of the Canadian Shield, Superior and Churchill Provinces; in Geology and Economic Minerals of Canada, ed. R.J.W. Douglas; Geological Survey of Canada, Economic Geology Report No. 1, p. 58, 100.

Norris, A.W. and Sanford, B.V.
1969: Paleozoic and Mesozoic geology of the Hudson Bay Lowlands; in Earth Science Symposium on Hudson Bay, ed. P.J. Hood; Geological Survey of Canada, Paper 68-53, p. 169-205.

Pelletier, B.R.
1969: Submarine physiography, bottom sediments and models of sediment transport; in Earth Science Symposium on Hudson Bay, ed. P.J. Hood; Geological Survey of Canada, Paper 68-53, p. 100-136.

Sanford, B.V. and Norris, A.W.
1975: Devonian stratigraphy of the Hudson Platform; Geological Survey of Canada, Memoir 379.

Sanford, B.V., Grant, A.C., Wade, J.A., and Barss, M.S.
1979: Geology of Eastern Canada and adjacent areas; Geological Survey of Canada, Map 1401A.

Shilts, W.W.
1980a: Geochemical profile of till from Longlac, Ontario to Somerset Island; Canadian Mining and Metallurgical Bulletin, v. 73, p. 85-94.

1980b: Flow patterns in the central North American Ice Sheet; Nature, v. 286, no. 5770, p. 213-218.

Shilts, W.W., Cunningham, C.M., and Kaszycki, C.A.
1979: Keewatin Ice Sheet – Re-evaluation of the traditional concept of the Laurentide Ice Sheet; Geology, v. 7, p. 537-541.

Skinner, R.G.
1973: Quaternary stratigraphy of the Moose River Basin, Ontario; Geological Survey of Canada, Bulletin 225, 77 p.

49. # A PRELIMINARY REPORT ON DRIFT PROSPECTING STUDIES IN LABRADOR [1]

Project 820039

R.A. Klassen
Terrain Sciences Division

Klassen, R.A., A preliminary report on drift prospecting studies in Labrador; in Current Research, Part A, Geological Survey of Canada, Paper 83-1A, p. 353-355, 1983.

Also in Current Research, ed. R.V. Gibbons; Newfoundland Department of Mines and Energy, Mineral Development Division, Report 83-1, 1983.

Abstract

A study of glacial history and till geochemistry was begun in east-central Labrador during 1982. Field observations, chiefly of striae trends, indicate that regional directions of ice movement were eastward to southeastward in the southern part of the area, and northeastward in the northern part. Erratics of sedimentary rock derived from bedrock located west of the study area can be a significant component of glacial sediments.

Introduction

During 1982, the Geological Survey of Canada began a study of Quaternary geology in east-central Labrador that is designed to identify directions of ice movement, regional variation in till composition, and geochemical properties of till. This work is intended to provide a basis for future mineral exploration using glacial deposits in Labrador. This report is a preliminary account of field operations and observations; no laboratory results are presently available. Observations of ice flow direction and lithology of erratic clasts presented here provide a basis for determining the provenance of glacial dispersal trains, and for understanding variations in till composition.

Acknowledgments

The excellent field assistance of Mr. C. Lyall and Mr. A. Michelin is gratefully acknowledged. Mr. A.J. Willy, Brinco geologist, provided much geological information and contributed significantly to the success of field operations. Field logistics for the project, including aircraft support, were generously provided by Brinco Mining Ltd.

Location and Geology

The area studied is located in east-central Labrador and includes the west half of Rigolet (13J) and east half of Snegamook Lake (13K) map areas (Fig. 49.1). It occupies parts of the Nain and Grenville structural geological provinces and is underlain by Aphebian acidic intrusive and metamorphic rocks, Helikian and Aphebian sedimentary and volcanic rocks of Aillik and Croteau groups, Aphebian and older metamorphic rocks of quartzo-feldspathic lithologies, and Helikian and Aphebian metamorphic equivalents of Labrador Trough rocks and Seal and Croteau groups (Greene, 1974, Fig. 5). Uranium occurrences are known at various locations within the area, and include the Michelin deposit (Gandhi, 1978).

Previous Work

Few published Quaternary studies have been directly concerned with the area of Labrador described here. Surficial materials have been mapped at 1:250 000 scale by Fulton et al. (1980a, b). A brief report on ice flow directions in the central part of the study area has been given by Vanderveer (1982).

Methods

During August 1982, a field program of Quaternary geological mapping and till sampling was carried out in the study area using helicopter support. Base camp was located at 'Melody Lake', about 70 km southwest of the community of Makkovik (Fig. 49.1). During reconnaissance mapping flights, till samples were collected systematically at a density of about one per 10-20 km^2. Coverage of the entire area, however, was not uniform. Near known trains of mineralized boulders and sites of bedrock mineralization, sample density was increased to about one per 1-2 km^2. At this higher density it was more difficult to locate suitable landing sites and further decrease in spacing between samples was not practical. Near one boulder train, samples were collected at spacings of 75-250 m on foot traverses oriented perpendicular to directions of regional ice flow.

Pits were dug in till to depths of 40-100 cm, and samples were collected from the least oxidized soil horizon near the pit base. In all cases an attempt was made to sample below the zone of obvious iron staining, although commonly either bedrock or large clasts restricted sampling to the oxidized zone. Where soils were well developed, or where sample sites were located near known mineralization, multiple samples were collected from each pit and identified with regard to depth of burial and position within the weathering sequence. In all, 225 samples were collected.

Where possible, measurements of striation orientations and examination of lithologies of erratic clasts were made at the collection sites. In general, observations of this kind were best made in exposed locations where vegetation did not obscure outcrops and boulders.

Results and Discussion

Direction of Movement

Within the study area glacial striae vary in orientation from about southeast to northeast (Fig. 49.1) and are similar to patterns of ice flow outlined by Prest et al. (1968). Based on the streamlined shape of outcrops, ice flow had an eastward component and no evidence of westward movement was observed. Most measurements were made on hilltops, and the striae are thought to be the product of regional ice movement. They are, for the most part, aligned with the long axes of topographic ridges, suggesting a relation between landform and ice flow direction. At some locations,

[1] Contribution to Canada-Newfoundland co-operative mineral program 1982-84. Project carried by Geological Survey of Canada.

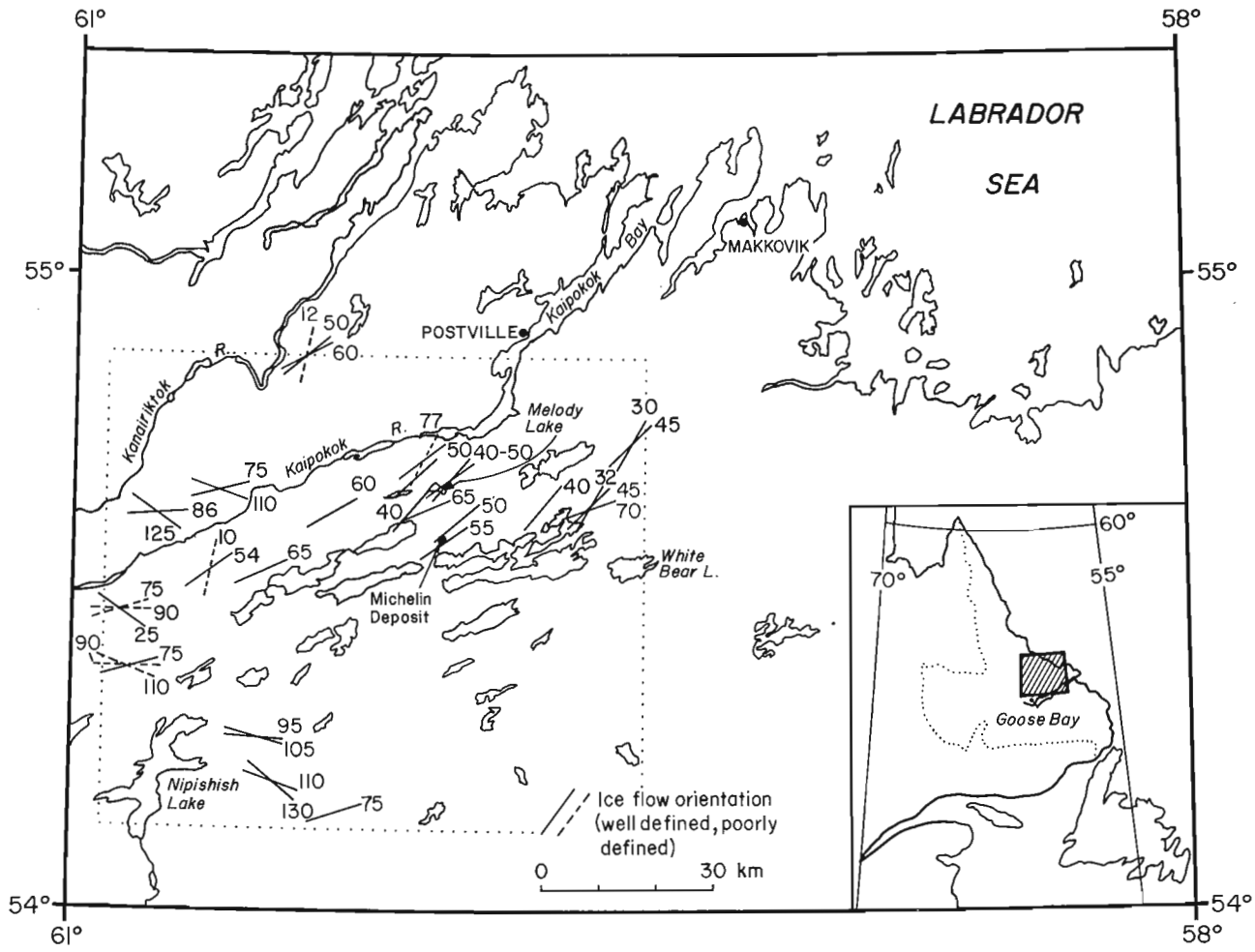

Figure 49.1. *Ice flow trends within the study area (outlined), based chiefly on glacial striae. Regional movement is thought to be generally eastward, based on streamlined bedrock landforms. Numbers indicate orientation in degrees east of north; magnetic declination N32°W assumed throughout the study area.*

however, for example in the area of Melody Lake, striae were oriented obliquely to the trend of valleys and ridges, and obliquely to directions of ice flow indicated by ribbed moraine deposits which trend across valley floors. There, the ribbed moraine may have been formed later than the striae on neighbouring hilltops, during a phase of ice flow that was controlled topographically.

Several striae orientations were commonly observed at each site, with one set being more common and better developed than all others. If the best developed sets are contemporaneous and formed during the same phase of flow, the data indicate collectively that ice entered the area from the west and northwest, and moved easterly to southeasterly across the southern part of the area, and northeasterly across the northern part. Ice in the northern part moved towards the valley of Kaipokok River and Kaipokok Bay, and these low-lying areas were likely main pathways of ice movement to the outer coast.

Other striae, which are presumed to be older because they are fewer in number and do not occur in the glacial polish of outcrops, indicate a west-east trend of ice movement. At two sites poorly developed striae of possible glacial origin trended nearly north-south, although directions of ice movement during that phase of ice flow are not known; this trend was also shown by a single measurement made by Vanderveer (1982, Fig. 2).

Lithologies of Erratics

At many sites, erratics of distinctive appearance were found, some of which are not known to have bedrock sources within the study area. The types of erratics identified most easily include red and pink quartzite, red arkose, mudstone, and polymictic conglomerate; of these, the quartzites were found throughout the study area, the others were seen chiefly in the northwestern part. The erratics of red quartzite are most likely derived from Helikian sedimentary formations lying west of the study area, possibly the Red Quartzite Formation of the Seal Group. They are up to ten per cent by weight of the 4-6 mm size fraction of till samples, and they demonstrate that till of the study area can have a significant component of far-travelled (>50 km) debris. The other sedimentary erratics, mentioned above, are most likely derived from sedimentary rocks of the Croteau Group that outcrops near the headwaters of Kaipokok River.

Conclusions

This study is currently at a preliminary stage and conclusions presented here are based chiefly on field observations. The main conclusions are:

1. During the last regional glaciation ice moved into the study area from the west and northwest. Flow directions were generally towards the east and southeast in the southern part, and towards the northeast in the northern part of the study area. In some areas later ice flow may have been channelled topographically within valleys, based on orientations of ribbed moraine.
2. Erratics derived from bedrock sources located west of the study area include sedimentary rocks such as red quartzite, and this far-travelled (>50 km) debris can constitute significant proportions of till.

References

Fulton, R.J., Hodgson, D.A., Mining, G.V., and Thomas, R.D.
1980a: Surficial materials, Rigolet, Labrador; Geological Survey of Canada, Map 26-1979, scale 1:250 000.

Fulton, R.J., Hodgson, D.A., and Mining, G.V.
1980b: Surficial materials, Snegamook Lake, Labrador; Geological Survey of Canada, Map 29-1979, scale 1:250 000.

Gandhi, S.S.
1978: Geological setting and genetic aspects of uranium occurrences in the Kaipokok Bay-Big River area, Labrador; Economic Geology, v. 73, no. 8, p. 1492-1522.

Greene, B.A.
1974: An outline of the geology of Labrador; Information Circular No. 15, Department of Mines and Energy, Newfoundland, 64 p.

Prest, V.K., Grant, D.R., and Rampton, V.N.
1968: Glacial map of Canada; Geological Survey of Canada, Map 1253A, 1:5 000 000.

Vanderveer, D.G.
1982: Reconnaissance glacial mapping in the Melody Lake – Anna Lake area, Labrador; in Current Research, Report 82-1, ed. C.F. O'Driscoll and R.V. Gibbons; Department of Mines and Energy, Newfoundland and Labrador, p. 235-236.

TAXA IN LAKE SEDIMENTS OF THE DISTRICT OF KEEWATIN

Project 750074

R.A. Klassen, J.V. Matthews, Jr., and L.K. Philips[1]
Terrain Sciences Division

Klassen, R.A., Matthews, J.V., Jr., and Philips, L.K., Taxa in lake sediments of the District of Keewatin; in Current Research, Part A, Geological Survey of Canada, Paper 83-1A, p. 357-361, 1983.

Abstract

Sediments in cores from six lakes lying below the limit of postglacial marine inundation in the District of Keewatin were examined for stratigraphic variation in types of taxa. Taxa indicate a change from marine to freshwater environments in lake basins associated with 'silt' and 'gel' sediments, respectively. During marine deposition shoreline may not have been far distant.

Introduction

As part of a study of lakes and lake sediments in the District of Keewatin, NWT during 1976 and 1977, sediment cores were collected from six lakes that were situated between the treeline and Baker Lake (Fig. 50.1). The cores form a record of geological and limnological evolution of their lake basins during the postglacial period. To investigate the macrofossil content of these sediments and the nature of stratigraphic changes, core samples were examined during 1982 and identifications made of their organic components.

Acknowledgments

R.A. Klassen collected the cores and provided geological information concerning them. J.V. Matthews, Jr. and L.K. Philips examined the core sediments and identified taxa; Matthews provided environmental interpretations of them.

Previous Work

Little has been published concerning biogenic materials in lake sediments of the eastern District of Keewatin. Collections of benthos, phytoplankton, and zooplankton from Baker Lake and lower Thelon River have been made as part of the environmental studies program of the Polar Gas Corporation (McLeod et al., 1976). A core from Yandle lake (Edwards, 1978) has yielded a diatom succession that demonstrates a major change in depositional environment from marine/brackish water to freshwater conditions. Geologically, these two environments were associated with massive to laminated silty clay and sand and with 'gel', respectively (Shilts et al., 1976). Diatom frustules and fragments of tests have been found to be significant components of modern freshwater sediments of that lake (Adshead, 1978).

Methods

Sediment cores were collected by SCUBA divers using clear plastic tubes, which were about 6.5 cm inside diameter and 2 m in length. The tubes were pushed vertically into the sediments, the upper end was then capped prior to tube removal, and the lower end capped as the tube with core was pulled free of the sediments. In order to minimize disturbance, core tubes were cut along their long axis and the sediments then split equally into the tube half-sections. Sediments were sampled in 2 cm-wide increments spaced at 10 cm intervals, or wherever evidence of either physical or chemical change was clearly evident, and then were freeze-dried. In this study, samples chosen for examination were from the freshwater ('gel') and marine/brackish water ('silt') sedimentary units in each lake. They were selected with regard to their stratigraphic position and represented the top and base of the gel unit and the top and cored base of the silt.

Re-hydrated samples, most of which consisted of approximately 10 cm^3 of sediment, were examined with the use of a binocular microscope and the macrofossils separated with the use of a fine-point brush prior to identification. No attempt was made to quantify the relative abundance of the various identified fossils.

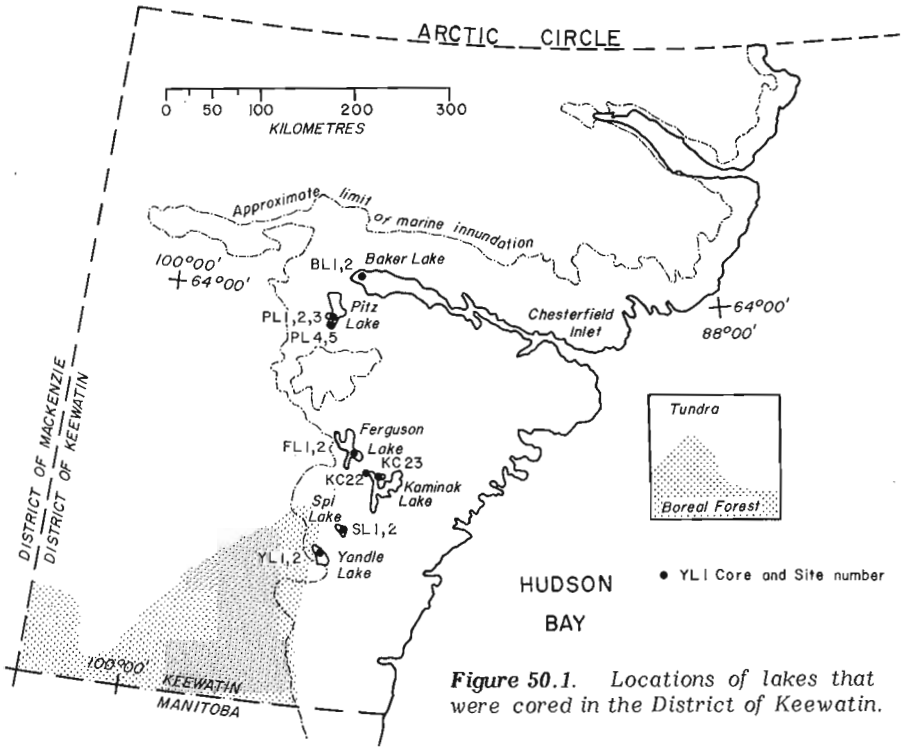

Figure 50.1. *Locations of lakes that were cored in the District of Keewatin.*

Results

Geology of Sediment Cores

The lakes that were cored vary greatly in area, ranging between 800 and 160 000 ha, and their surface elevations are between 2 and 114 m a.s.l. (Table 50.1). In that area of the District of

[1] Carleton University, Department of Biology

Table 50.1

Summary of lake, sediment core, and radiocarbon data

Lake	Area (ha)	Surface Elevation (m a.s.l.)	Core Number	Core Length (cm)	Collection Depth (m)	Radiocarbon Date	Comments
BAKER	160 000	2-3	BL-1	100	20		Lake bottom elevation is presently below sea level.
			BL-2	126	20		
PITZ	25 000	63	PL1	<20	5		Cores PL2 and 3 collected near centre of lake at its southern end. Cores PL4 and 5 collected 300 m from inflow stream at southern shore.
			PL2	96	11		
			PL3	108	11		
			PL4	116	18		
			PL5	130	18		
FERGUSON	10 000	114	FL1	202	9		
			FL2	185	9		
KAMINAK	37 000	53	KC22	196	~15		
			KC23	146	~25	1000 ± 120 (GSC-2696) 2370 ± 120 (GSC-2688)	Both dated samples are based on laminae of detrital organic material. Coring site was remote from inflow streams. Laminae were at 12-14 cm (GSC-2676) and102-104 cm (GSC-2688) below the sediment surface.
SPI	800	67	SL1	108	8		
			SL2	114	8		
YANDLE	1900	110	YL1	252	8	5080 ± 170 (GSC-2634)	Age is based on fine grained organic material collected at the base of gel in cores YL1 and YL2, combined.
			YL2	194	8		

Keewatin, marine limit varies regionally between 127 and 177 m a.s.l.; consequently, all lake basins have been inundated by the postglacial Tyrrell Sea.

Most cores examined were bi-partite in that they were commonly composed of an upper 'gel', which is thought to have been formed in freshwater, and a lower 'silt', which is thought to have been formed in either marine or brackish water. 'Gel' is a term that is used here to describe a grey-green, loose sediment that is, stratigraphically, the uppermost sediment in all cores. More detailed description of gel in Yandle Lake has been given by Shilts et al. (1976). Gel would be equivalent in a general sense to gyttja. Gels had high contents of water and organic carbon (<2 to 10 wt.%) compared with silts (<2 wt.%) and were characterized typically by precipitates of iron and manganese in their upper portions. These sediments were fine grained and composed of silt-sized minerogenic debris, chiefly quartz and feldspar, and of biogenic debris including siliceous tests of diatoms, testate rhizopods (Difflugiidae), and fecal pellets. Gels generally became firmer downwards, indicating lower water contents, and in one core graded into relatively inorganic silts. Laminations within gel were seen to be caused by mineral detritus, chemical precipitates, and detrital organic carbon. Radiographs of cores showed that some of the gel units were also finely laminated, with laminae between <0.5 to 2 mm thick. The origins of these laminae are not known.

In contrast, the underlying silts were firmer and contained less organic carbon (<2 wt.%). Structurally, silts varied from being massive (e.g., Yandle, Spi lakes) to finely laminated (e.g., Pitz, Ferguson lakes).

Radiocarbon Age Determinations

Three radiocarbon determinations provide an estimate of the age of gel and sedimentation rates (Table 50.1). Gel from the base of Yandle Lake cores was estimated to have formed about 5080 ± 170 years ago (GSC-2634), and this is a minimum estimate of the onset of freshwater deposition in that lake basin. Laminae of detrial organic matter from about 13 cm below the sediment-water interface from Kaminak Lake were dated at 1000 ± 120 years B.P. (GSC-2696), and from 103 cm depth at 2370 ± 120 years B.P. (GSC-2688). Based on these dates, estimates of annual sediment accumulation rates vary between about 0.08 and 0.7 mm/year.

Fossils

The taxa identified in the sediments from the various lakes are listed in Table 50.2. The samples from each lake are identified as to whether they come from the gel or silt zones. In some cases samples of equivalent stratigraphic position from several cores in the same lake were combined. The following are comments on specific taxa.

Testate Protozoa: Difflugiidae are rhizopods that commonly have tests made up of small sand grains. They are abundant in both bog and lake sediments (Frey, 1964) and have been found in lakes well north of treeline (Holmquist, 1975). Due to their small size and glassy colour, difflugid tests are likely to be underrepresented in the samples discussed here; nevertheless, it is probably significant that with the exception of one Ferguson Lake sample, difflugid tests occurred only in the gel portion of the cores.

Table 50.2

Fossils in lake cores from the District of Keewatin

	LAKES SAMPLED																			
	Spi				Ferguson				Baker		Kaminak				Yandle				Pitz Cores 2-3				Pitz Cores 4-5			
	TG	BG	TS	BS	TG	BG	TS	BS	TG	BG	TG	BG	TS	BS	TG	BG	TS	BS	TG	BG	TS	BS	TG	BG	TS	BS
PLANTS																										
Fungal Sclerotia										+	+		+						+	+						
Algae																										
Characeae																										
Chara or **Nitella** sp.							+				+		+			+		+								
Bryophytes		+		+		+		+		+	+	+	+	+	?		+	+	?	+		+	+		+	+
Angiosperms																										
Gramineae																							+			
Cyperaceae																										
Carex sp.											+												+			
Kobresia sp.											+															
Juncaceae																										
Luzula sp.																			?							
Salicaceae																										
Salix sp.											+												+			
Betulaceae																										
Alnus crispa Ait (Pursh)											+												+			
Alnus incana (L.) Moench											?															
Betula glandulosa type			+						+		+		+	+						+			+		+	
Caryophyllaceae																							+			
Cruciferae		+							+																	
Rosaceae																										
Dryas sp.																									+	
Dryas integrifolia Vahl.			+																							
Potentilla sp.					+																					
Ericaceae																										
Cassiope sp.																			+							
Andromeda polifolia L.											+															
ANIMALS																										
Protozoa (Rhizopoda)																										
Difflugiidae	+	+					+				+				+				+	+						
Coelenterata (Hydrozoa)			+	+				+										+			+		?			+
Turbellaria	+	+	+	+	+	+	+		+		+	+	+		+	+	+	+	+	+	+	+	+	+	+	
Bryozoa																										
Cristatella mucedo C.		+	+								+					+		+								
Plumatella sp.		+														+										
Fredericella typ.	+	+			+		+		+		+	+	+		+	+	+	+	+	+	+		+	+	+	
Annelida																										
Oligochaeta							?						?								?				?	
Hirudinea					+						+	+													+	
Arthropoda																										
Insecta																										
Homoptera																										
Psyllidae							+																			
Coleoptera																										
Dytiscidae																										
Colymbetes sp.												+														
Staphylinidae																										
Omalinae												+							+							
Arpedium sp.																							+			
Stenus sp.	+																									
Aleocharinae																			+							
Trichoptera	+				+		+		+			+	+	+	+		+		+		+	+	+			
Diptera																										
Chironomidae	+	+	+		+		+	+	+		+	+	+		+	+	+	+	+	+	+	+	+	+	+	
Hymenoptera																			+							
Symphyta																							+			
Ichneumonoidea									+																	
Crustacea																										
Cladocera																										
Daphnia sp.		?			?		?		?		+		+	?	+	+		+	+	+	+		+	+		
cf. Bosminidae	+				+		+		+		+	+	+	+				+	+	+	+			+		
Notostraca																										
Lepiduris sp.		+			+	+			?		+	+	+	+	+	+			+	+	+		+	+		
Ostracoda									+			+				+							+			
Arachnida																										
Acari																										
Oribatei	+																+									
Platynothris sp.							+																			
Ameronothris sp.			?																							
Araneae											+															

TB = top of gel zone, BG = bottom of gel (stratigraphic), TS = top of silt, BS = bottom of silt (cored);
? signifies fossil too poorly preserved for positive determination.

NOTE: In some cases the listed fossils come from more than one core and more than one location in the lake basin.
See Fig. 50.1 for location of the lakes.

Turbellaria: By far the most abundant fossils in the core samples were small chitinous spheres with a large opening at one end. A few bore a relatively long stalk. Such objects are likely to be cocoons of various types of non-parasitic flatworms. The stalked forms are similar to the Holmquist (1967) illustrations of the cocoons of **Gyratrix.** Turbellarian cocoons, particularly those of the larger triclad flatworms, are probably more commonly found in lake sediments than the literature indicates (Frey, 1964). Although little is known about the northern flatworm fauna, Holmquist's (1967) work in Alaska and the Yukon shows that they occur today in lakes located well beyond treeline.

Hydrozoa: The coelenterate class Hydrozoa includes the solitary freshwater hydras as well as colonial forms. Most of the latter possess chitinous supporting structures that may be preserved as fossils. All of the colonial forms, except the genus **Cordylophora,** are marine, and **Cordylophora** commonly occurs in brackish water. Holmquist's (1975) survey of lakes from Alaska and northwestern Canada (including some that have an intermittent connection to the sea) lists no records of colonial Hydrozoa. The chitinous tubes of the colonial Hydrozoa have been found as fossils in various types of marine sediments (Prest et al., 1976; Mott et al., 1981; J.V. Matthews, Jr., unpublished GSC Fossil Arthropod reports 82-3, 82-15, 82-16). The hydrozoan fragments reported do not appear to represent **Cordylophora;** hence they probably indicate marine conditions. With the possible exception of a single poorly preserved fragment from Pitz lake, all of the ones listed in Table 50.2 come from the silt portion of the cores.

Tadpole shrimp (Notostraca): Mandibles of tadpole shrimp **Lepiduris** are common in Pleistocene and Holocene sediments from arctic and subarctic areas (Frey, 1964). Although they cannot be identified to species on the basis of their mandibles, most of the northern fossils probably represent **Lepiduris arcticus** (Pallas), the only northern species. Tadpole shrimp usually inhabit temporary, freshwater ponds, but **L. arcticus** is also known to occur in large lakes where it may be an important food for salmonid fish (Longhurst, 1955). The specimens from Kaminak Lake are unusual in that they comprise a broader spectrum of anatomical elements than is usually seen, and even include eggs.

Midges (Chironomidae): Head capsules of chironomid larvae ranked second in abundance to turbellaria cocoons in most of the samples. Many of the specimens could probably be identified by an expert on chironomids, and if so they potentially provide the best source of paleoecological and paleolimnological evidence. Most of the samples contained other dipteran fragments, some of which are undoubtedly from adult Chironomidae.

Bryozoa: Statoblasts of freshwater bryozoa often occur in Holocene and Pleistocene contexts, and like **Lepiduris** mandibles, often in sediments that are not lacustrine. A major distinction of the samples from the lakes discussed here is that statoblasts of **Cristatella mucedo** are rare compared to other types. The most abundant statoblasts were the **Fredericella** type. They probably represent the common species **F. sultana** (Blumenbach). Holmquist, in her 1975 study of lakes in Alaska and the Yukon, found **Fredericella** to be more abundant than **Cristatella,** but its distinctive statoblasts were rare.

Discussion and Conclusions

Despite the small size of the samples and the paucity of identified fossils, Table 50.2 displays some trends that may be of stratigraphic and/or paleoecological significance.

The hydrozoan fossils are presumed to be from a marine species; therefore, it is interesting that all of the hydrozoan fragments, except one questionable specimen, come from the silt portion of the cores. In contrast, freshwater fossils, such as leech cocoons (Hirudinea) and difflugid tests, were confined largely to the gel zone of the cores. As noted above, diatoms from Yandle Lake show that there the silts are marine and the gels freshwater (Edwards, 1978); according to the fossils described here, this may be the case for the other lakes as well. However, the silts also contain freshwater fossils and as well some terrestrial types; therefore, if the silts are marine, shoreline could not have been located far from the coring sites.

The shoreline problem represents another characteristic of the samples. Ordinarily, even very small samples from ponds or small lakes contain fossils of **Carex, Potamogeton,** and other emergent or aquatic macrophytes. The insect fragments in such samples invariably represent dytiscid beetles (the only one in these samples was a piece of an elytron attached to a caddis-fly case), water-boatman, and other nearshore taxa. In the samples discussed here, on the other hand, the non-bryoid plant fossils included mostly seeds of terrestrial plants such as **Betula** and **Alnus.** The lakes from which these samples came are large. Their present shorelines are ice scoured in spring and probably were similarly disrupted in the past. Consequently, the lakes may not have supported large tracts of shoreline communities. It is also possible that the core samples come from sites too far from shore to include shoreline taxa, yet not so distant as to preclude occurrence of plant fragments blown out onto the frozen lake during the winter. Both **Betula** and **Alnus** have seeds adapted for such dispersal. Many of the other fossils in the assemblages are the type that readily float. Thus, except for fossils of Turbellaria, Chironomidae, and **Lepiduris,** which are all bottom dwellers, the fossils in the samples are probably allochthonous.

The samples from Pitz Lake cores 4 and 5 were collected directly off the mouth of a large inflowing stream, and this may seem an appropriate explanation for the abundance of terrestrial plants in that core compared to Pitz Lake cores 2 and 3, which came from a site more than 1 km from shore.

Clearly these samples raise more questions than they answer. Their greatest value is that they provide a direction for future research. For example, future studies must involve larger samples and enlist the help of experts on specific groups, such as the Chironomidae. Furthermore, the study of macrofossils should be conducted in conjunction with analyses of microfossils, such as pollen and diatoms. In order to determine the spatial distribution of organics within the lakes today, future coring programs should include collection and study of modern lake sediments, preferably in the form of samples collected in transects from shoreline to deep water (cf. Birks, 1972). Finally, the organics from such cores must be viewed within the geological context (historical and lithological) of the lakes.

References

Adshead, J.D.
1978: Diatomaceous arctic lake sediments; in Current Research, Part A, Geological Survey of Canada, Paper 78-1A, p. 475-480.

Birks, H.H.
1972: Modern macrofossil assemblages in lake sediments in Minnesota; in Quaternary Plant Ecology, ed. H.J.B. Birks and R.G. West; John Wiley and Sons, New York, p. 173-189.

Edwards, T.W.D.
1978: Post-glacial diatom stratigraphy of a lake basin of the eastern arctic shield; in Current Research, Part A, Geological Survey of Canada, Paper 78-1A, p. 403-407.

Frey, D.G.
1964: Remains of animals in Quaternary lake and bog sediments and their interpretation; Archiv für Hydrobiologie: Ergenbnisse der Limnologie, v. 2, p. 1-114.

Holmquist, C.
1967: Turbellaria of northern Alaska and northwestern Canada; Internationale Revue der Gesamten Hydrobiologie, v. 52, p. 123-139.

1975: Lakes of northern Alaska and nordwestern Canada and their invertebrate fauna; Zoologische Jahrbücher, v. 102, p. 333-484.

Longhurst, A.R.
1955: A review of the Notostraca; Bulletin of the British Museum (Natural History), Zoology, v. 3, p. 1-57.

McLeod, C.L., Wieke, P.J., and Mokr, R.A.
1976: An examination of aquatic ecosystems in the Baker Lake-lower Thelon River, N.W.T., area in relation to proposed polar gas pipeline development; unpublished report by Renewable Resources Consulting Services Ltd. to Polar Gas Corporation, Toronto, 268 p.

Mott, R.J., Anderson, T.W., and Matthews, J.V., Jr.
1981: Late-glacial paleoenvironments of sites bordering the Champlain Sea based on pollen and macrofossil evidence; in Quaternary Paleoclimate, ed. W.C. Mahaney; Geoabstracts. p. 129-171.

Prest, V.K., Terasmae, J., Matthews, J.V., Jr., and Lichti-Federovich, S.
1976: Late Quaternary history of Magdalen Islands, Quebec; Marine Sediments, v. 12, p. 39-59.

Shilts, W.W., Dean, W.E., and Klassen, R.A.
1976: Physical, chemical and stratigraphic aspects of sedimentation in lake basins of the eastern arctic shield; in Report of Activities, Part A, Geological Survey of Canada, Paper 76-1A, p. 245-254.

51. GEOLOGY OF THE ATIKONAK RIVER AREA, GRENVILLE PROVINCE, WESTERN LABRADOR [1]

Project 820029

G.A.G. Nunn [2] and A. Christopher [3]
Newfoundland Department of Mines and Energy

Nunn, G.A.G. and Christopher, A., Geology of the Atikonak River area, Grenville Province, western Labrador; in Current Research, Part A, Geological Survey of Canada, Paper 83-1A, p. 363-370, 1983.

Abstract

The map area lies within the Grenville Province immediately southwest of Churchill Falls in western Labrador. An area of paragneiss within the Grenville Province is correlated with similar supracrustal rocks of Aphebian age to the west. Posttectonic intrusion by granitoid and gabbroid rocks, tentatively correlated with the Paleohelikian North Pole Brook Intrusive Suite and the Shabogamo Intrusive Suite respectively, indicate that initial deformation of the paragneiss was Hudsonian or early Paleohelikian. A zone which might contain the approximate continuation of the Hudsonian front in the Grenville Province is suggested.

Introduction

This report presents the results of the first part of a two year co-operative program between the Geological Survey of Canada and the Newfoundland Department of Mines and Energy. The aim of the project is to elucidate the stratigraphy and tectonic evolution of the Atikonak River area in western Labrador. The project area includes NTS map areas 23H/1, 2, 7 and 8 (Fig. 51.1). These were mapped at 1:100 000 scale using helicopter support.

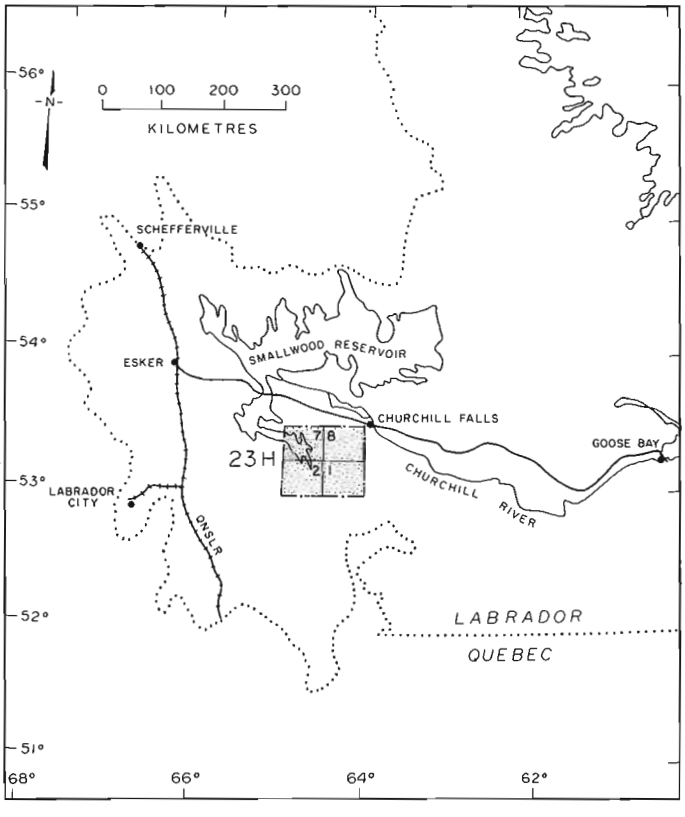

Figure 51.1. *Location map of the Atikonak River area, western Labrador.*

The physiography of the area is dominated by Ossokmanuan Lake, a flooded area that forms part of the Smallwood Reservoir. No correction for flooding has been made to the map. Access to the western part of the area is from Ossokmanuan Lake, the Atikonak River or a road from Churchill Falls to the power transmission line. Access to the remainder of the area is by helicopter.

Previous Work

Earlier work in the area comprises reconnaissance mapping by Eade (1952) at 1:126 720 scale, and Wardle (1982). Eade described an older complex of granitic paragneiss, gabbroic gneiss, amphibolite and garnet-, biotite-, and chlorite-bearing schist, intruded by younger, undeformed gabbro. Greene (1972, 1974) divided the granitic paragneisses into those with assumed Aphebian or older parentage in the west and those of supposed Helikian origins in the east. Smyth and Green (1976) positioned the northern boundary of the Grenville Province in the area giving it a lobate form separating the two gneissic groups of Greene (1972) within the Grenville Province from a re-entrant underlain by undeformed gabbro that was excluded from the Grenville Province.

Wardle (1982) noted that both western and eastern lobes were apparently the same assemblage of polydeformed and migmatized sillimanite-bearing paragneiss that was subsequently intruded by pre- and late-tectonic granitoid plutonic rocks. Wardle (1982) interpreted the gabbroic gneisses of Eade (1952) as deformed equivalents of the younger gabbro and considered that the whole area lay within the Grenville Province.

General Geology

The map area (Fig. 51.2) is divided into two metamorphic terranes that coincide with peneplain levels at 875 m and 680 m. The upper peneplain is underlain by granulite facies rocks, the lower one by amphibolite facies rocks. Locally a mylonite has been mapped at the contact between the two facies and the boundary is assumed to be a thrust fault.

Unit 1 (Fig. 51.2) is composed of strongly migmatized sillimanite-bearing paragneiss at granulite and upper amphibolite facies and is the oldest lithology recognized in the map area. Retrogression is of only minor significance and occurred late during the Grenvillian Orogeny. Neither Wardle (1982) nor the writers find sufficient reason to separate the amphibolite and garnet-, biotite- or chlorite-bearing schist unit of Eade (1952) although amphibolite (metagabbro of unit 3) and biotite-garnet paragneiss (unit 1) are minor lithologies near Ossokmanuan Lake.

---

[1] Contribution to Canada-Newfoundland co-operative mineral program 1982-84. Project carried by Geological Survey of Canada.

[2] Newfoundland Department of Mines and Energy, Mineral Development Division, P.O. Box 4750, St. John's, Newfoundland, A1C 5T7.

[3] 83 Kathryn Crescent, North Bay, Ontario, P1B 8P5.

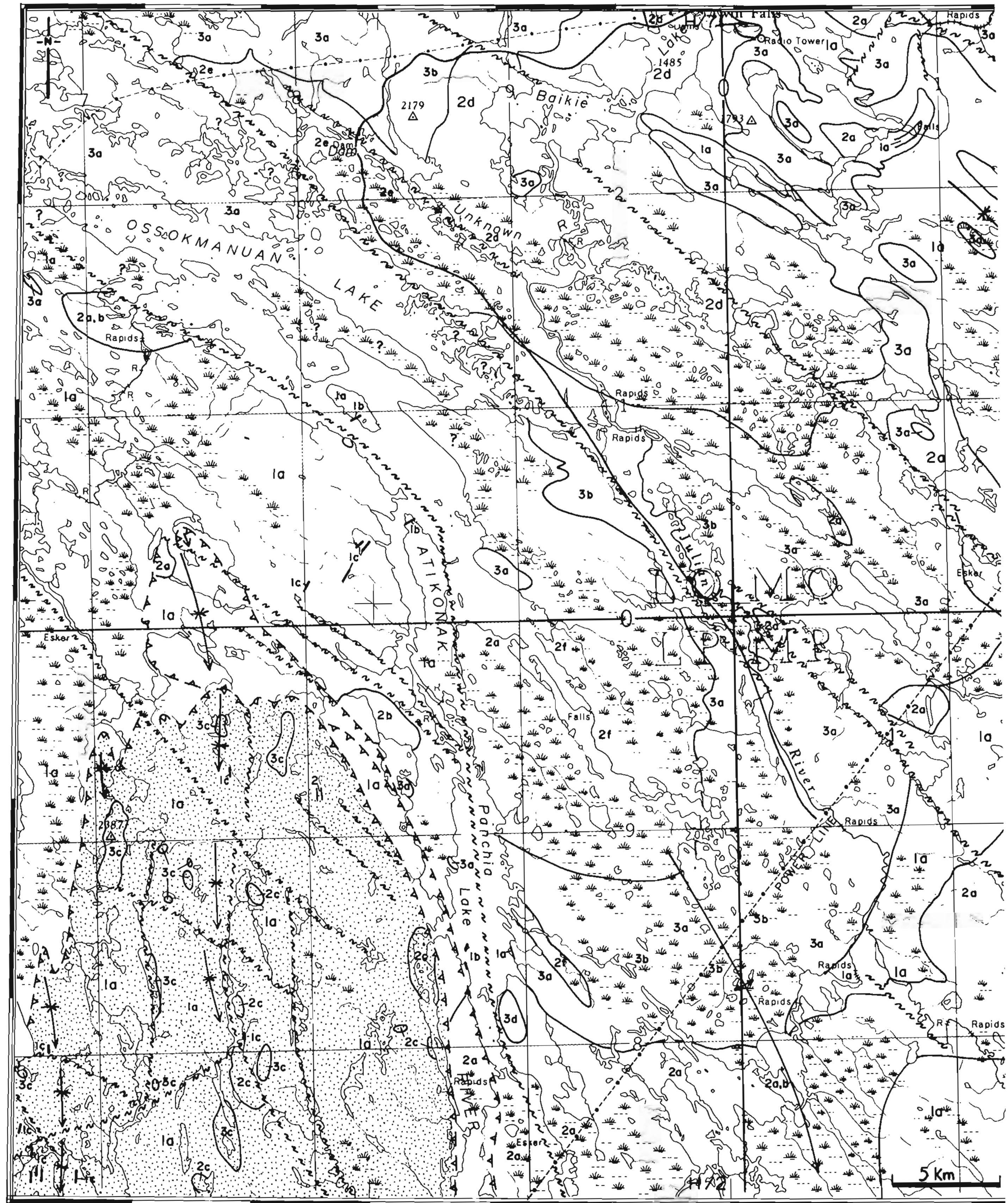
N
Twin Falls
Baikie Lake
Radio Tower
Unknown R.
OSSOKMANUAN LAKE
ATIKONAK
Panchia Lake
Julian
Rapids
Falls
Esker
Dam
River
POWER LINE
2179
1485
793
2087
5 Km
65°00'
45'
30'

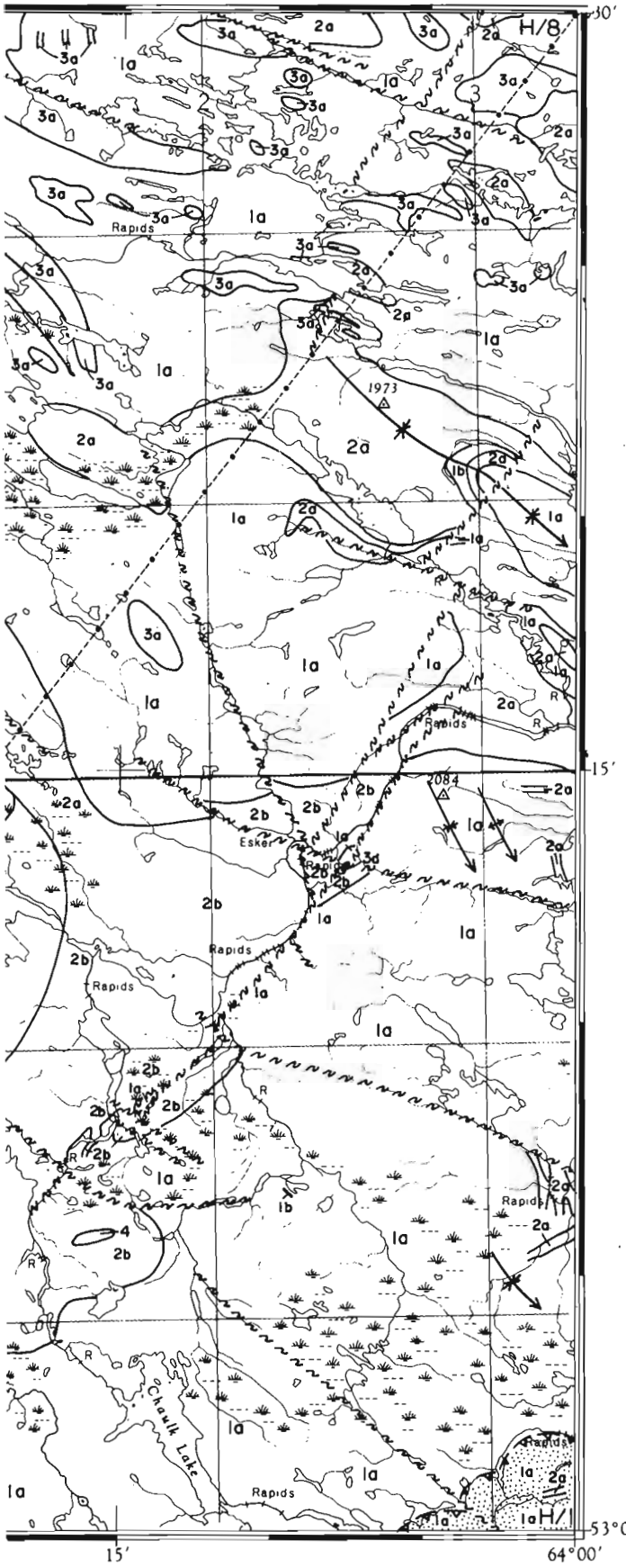

LEGEND

NEOHELIKIAN ?

Unit 4. White, very coarse grained muscovite granite.

PALEOHELIKIAN ?

Unit 3. **Shabogamo Intrusive Suite?:**

- 3a Fine- to coarse grained, intergranular textured gabbro and leucogabbro and their amphibolite facies metamorphosed equivalents, commonly with coronas; minor pegmatite;
- 3b fine- to coarse-grained, layered gabbroic rocks and their amphibolite facies metamorphosed equivalents;
- 3c fine- to medium-grained, equigranular, granulite facies leucogabbro with minor gabbro, ultramafic rock and anorthosite; minor intergranular textured gabbro and fine grained dykes.

Unit 2. **Orthogneiss and foliated granitoid rocks:** Possible equivalents of the North Pole Brook Intrusive Suite (Thomas and Hibbs, 1980).

- 2a grey, fine- to medium-grained, static textured, granodioritic and tonalitic rocks, variably migmatized ranging from homogeneous to lit-par-lit layered, granite or trondhjemite leucosomes;
- 2b grey, megacrystic granodiorite, groundmass fine-to medium-grained, static textured; coarse porphyritic to fine porphyroblastic microcline megacrysts;
- 2c buff, medium- to coarse-grained, strongly foliated, microcline porphyritic, quartz monzonite;
- 2d grey, medium grained, sphene-rich, microcline porphyritic, quartz monzonite; moderately to strongly foliated and migmatized;
- 2e pink, fine-to medium-grained, granite layered, granodioritic gneiss; very strongly migmatized;
- 2f pink, fine- to medium-grained, statically recrystallized, biotite granite and aplite, rarely weakly migmatitic.

APHEBIAN

Unit 1. **Paragneiss.**

- 1a pink, granite migmatite banded; either strongly foliated sillimanite + opaque oxide ± minor biotite restite or statically recrystallized sillimanite + biotite + garnet restite;
- 1b thin, discontinuous quartzite, and subarkosic and arkosic arenite;
- 1c fine grained, pyroxene-bearing basic gneiss, probably supracrustal with minor dykes;
- 1d fine grained, pyroxene-bearing metabasic rocks in amphibolite facies areas.

SYMBOLS

- Geological contact (assumed)
- Thrust, teeth on upthrust block (assumed)
- Fault and major photo lineaments (assumed)
- Fold axis – GD_4; anticline, syncline (assumed)
- Granulite facies
- ? Uncertain, dominantly drift covered areas

Figure 51.2. Generalized solid geology of the Atikonak River area.

Unit 1 has been intruded by a plutonic suite (unit 2) consisting of granitoid rocks ranging in composition from diorite to granite.

Unit 3 consists of a variety of gabbroic rocks including rocks correlated with the Paleohelikian Shabogamo Intrusive Suite, a major intrusive feature of the northern Grenville Province in western Labrador.

Unit 4 comprises late syntectonic to posttectonic granite dykes (not shown on the map) and a small, very coarse grained body of muscovite granite. Widespread development of late Grenvillian intrusions was not found during this study. Several minor units previously considered Grenvillian (Wardle, 1982) are thought to be a part of unit 2.

No age dates are available for rocks within the map area.

Unit 1: Supracrustal Gneisses

Unit 1 is composed of paragneiss, and minor metabasic supracrustal rocks which are mostly confined to the southwestern portion of the map area. Bulk compositional variation within the paragneiss is rare suggesting a homogeneous protolith.

Migmatitic paragneiss (unit 1a). The paragneiss includes pinkish brown and grey banded rocks in which partial melting has produced a location fabric[1] of alternating layers of granitic melt and aluminous restite, and several generations of crosscutting migmatitic granite veins. Layering representing the initial melt is pink to brown weathering, several millimetres to one centimetre thick and forms the most regular banding. It is composed of fine- to medium-grained quartz + feldspar ± biotite ± opaque oxides ± garnet ± sillimanite. The restite occurs as 0.5-3 mm thick, white to grey foliae composed of either sillimanite + biotite + magnetite ± garnet, or sillimanite + opaque oxides ± a fine grained biotite selvage. Paragneiss with biotite-rich restite occurs only in northern and northeastern parts of the area. Kyanite has been recorded from the northern margin of the area (Wardle, 1982). Later generations of migmatitic veins are pink, medium grained, 1-2 cm thick and consist of microcline + quartz + plagioclase + biotite ± magnetite ± garnet. Wherever this later migmatization is well developed the restite is more prominent. Crosscutting dykes composed of biotite or two-mica granite are also present.

In places the rock forms an inhomogeneous diatexite with patches of restite within areas of coalesced melt. Gradations occur between the isotropic granitoid-looking migmatite and the layered migmatitic gneiss. The gradational rocks usually contain palimpsest structures and the areas of coalesced melt appear to have remained in situ. However, nebulitic, sheet-like examples of the diatexite indicate local mobility as dykes.

Homogeneous sedimentary layers (unit 1b). Locally, homogeneous, nonmigmatitic layers occur intercalated with the main paragneiss. They consist of quartz + feldspar ± biotite ± opaque oxides and appear to have been derived from arkosic to quartz arenites. Thin layered quartzites are also present and commonly occur as trains of boudins or as thin layers associated with amphibolite. A thick, folded quartzite layer is present in the east of map area H/8.

Metabasic rocks (unit 1c). Basic gneiss is interlayered with the paragneiss in the western part of map area H/2, and includes a few layers, several tens of metres thick, and abundant thinner, less continuous layers, enclaves, and trains of boudins. The thicker layers are net-veined or sheeted by granitoid material. The basic gneiss consists of plagioclase + orthopyroxene + diopside + hornblende; a quartz-rich segregation layering is common. In the eastern part of the area the metabasic rocks (amphibolite) are much less abundant than in the southwest. The intimate intercalation of the basic gneiss with paragneiss, including quartzite, appears primary and indicates that the metabasic rocks are probably of volcanic origin.

Other thinner, boudinaged metabasic layers, which locally preserve relict porphyritic texture and fine grained margins, are derived from mafic dykes.

The age of unit 1 has not been determined directly. However, the paragneiss is contiguous with lithologically similar rocks that extend over 100 km to the west into the Wabush area (T. Rivers, personal communication, 1982). There, Rivers (1980) has interpreted them to be the deformed and metamorphosed equivalents to Aphebian greywackes and shales of the Labrador Trough. Rb-Sr dates in the same area have indicated a Grenvillian age of metamorphism of this sequence. The paragneiss extends to the northeast into the area of the Red Wine Mountains where it has yielded circa 1660 Ma ages of metamorphism (B. Fryer, personal communication, 1982). At present it is uncertain whether the paragneisses in the Ossokomanuan area were formed by Grenvillian, Paleohelikian or Hudsonian events. In all probability they are polyorogenic.

Unit 2: Orthogneiss and Foliated Granitoid Rocks

This unit comprises a variety of predominantly granodioritic to quartz mozonitic lithologies that are intrusive into unit 1.

Migmatitic granodiorite and tonalite (unit 2a). In the east, northeastern and central parts of the map area grey, fine- to medium-grained, hornblende-biotite granodiorite and tonalite occur. Homogeneous, and randomly to lit-par-lit migmatized types are present.

Central megacrystic granodiorite (unit 2b). This unit consists mostly of homogeneous, foliated, megacrystic granodiorite with euhedral to rounded K-feldspar megacrysts up to 5 cm long. The unit is rarely gneissic. Relict megacryst cores are grey to purple, contain primary biotite and plagioclase inclusions, and have been partly polygonized during posttectonic recrystallization. The megacrysts are thought to be of primary origin. Partial melting was rare but, where present, apparently did not affect the megacrysts, despite experimental predictions to the contrary (Wyllie et al., 1976).

The unit also contains a finer megacrystic facies characterized by 0.5-1 cm diameter, ragged, microline crystals that appear to represent porphyroblasts developed in originally equigranular granodiorite. Both facies contain nonmegacrystic rocks with which there are no sharp contacts.

Dykes of coarse augen granodiorite are intrusive into paragneiss of unit 1, and the megacrystic granodiorite also contains inclusions of paragneiss.

Megacrystic quartz monzonite (unit 2c). This unit occurs in the southwestern part of the area and is composed of strongly foliated, megacrystic, quartz monzonite. The medium grained groundmass contains biotite and probably orthopyroxene. One body contains xenoliths of folded migmatitic paragneiss.

[1] Distribution of fabric elements in (3D) layers.

Sphene-rich, megacrystic quartz monzonite and gneissic equivalents (unit 2d). Foliated, megacrystic, biotite-hornblende-quartz monzonite is characteristic of the area north of Baikie Lake. Relict K-feldspar is common and sphene is an abundant accessory mineral. Migmatization was confined to a few discordant veins commonly following the locus of small shear zones. To the east, west and south the granitoid rocks become progressively deformed and recrystallized. K-feldspar is replaced by elliptical aggregates of microcline, and evidence of late migmatization, consisting of discordant quartzofeldspathic veins with large poikilitic hornblende grains, is more abundant. Further deformation induced attenuation of the feldspathic aggregates, imparting a banded appearance to the rock that is enhanced by concordant veins of anatectic granite and aplite. Discordant, migmatitic veins with poikilitic hornblende are also present but sphene was not observed. Diorite inclusions are rare.

Pink, granite banded orthogneiss (unit 2e). A strongly banded orthogneiss consisting of a pale grey, granodioritic paleosome and pink, granitic, migmatitic layering outcrops between Baikie Lake and Ossokmanuan Lake. The granitic layers range from centimetre-wide veins to metre-thick dykes and dominate the lithology. Both granite and granodiorite contain hornblende, biotite and epidote; the epidote appears stable and is located at plagioclase-hornblende grain boundaries.

Pink granite (unit 2f). Pink, biotite-bearing aplite and fine grained granite occur at the southern end of Ossokmanuan Lake. These contain a vague migmatite banding defined by slightly coarser aplitic phases.

Correlation of unit 2. The rocks around Baikie Lake (unit 2d) are the southerly continuation of the granitoid gneisses (unit 9) of Wardle and Britton (1981). The remainder of unit 2 is similar to other members (units 6, 7 and 8) of the granitoid plutonic lithologies of Wardle and Britton (1981) which pass north into weakly deformed plutonic rocks apparently intruded circa 1650-1700 Ma (C. Brooks, personal communication, 1982). Unit 2 as a whole also has features indicating possible correlations with the North Pole Brook Intrusive Suite (Thomas and Hibbs, 1980) in the Red Wine Mountains to the northeast, and the Michikamau plutonic suite (Nunn, 1981; Nunn and Noel, 1982) around Michikamau Lake to the north. The North Pole Brook Intrusive Suite has yielded Rb-Sr ages of around 1650 Ma (B. Fryer, personal communication, 1982). We draw attention to the textural and lithological similarities between this suite and unit 2, and tentatively suggest an equivalent age for unit 2.

Unit 3: Shabogamo Intrusive Suite

The gabbroic rocks in the map area are divisible into three main types: subophitic to intergranular textured gabbro and leucogabbro, layered varieties, and equigranular leucogabbro. In most parts of the area gabbro has generally been emplaced into low structural levels.

Intergranular textured gabbro (unit 3a). The intergranular textures vary from fine- to coarse-grained and consist of randomly orientated plagioclase laths, with a groundmass of pyroxene and magnetite. Olivine was recorded by Wardle (1982). Pegmatitic patches with intergranular textures are common and grade into the normal gabbro. The pegmatites generally preserve primary gabbro mineralogy as purple plagioclase laths, up to 20 cm long, intergrown with shiny, grey pyroxene (?bronzite). In the finer grained rocks the primary mineralogy is preserved only in eastern parts of map area H/7; elsewhere corona textures or alteration to an amphibolite facies mineralogy prevail. Several mineralogical variations occur in the coronas:

i) Amorphous brown core (altered olivine?) ± pale fibrous zone (orthopyroxene or termolite?) + deep green fibrous zone of actinolite + garnet + plagioclase.

ii) Matt black, uncleaved, mafic mineral (uralite?) ± garnet + white, granular plagioclase ± relict, green, saussuritized plagioclase cores.

iii) ± relict orthopyroxene + green hornblende and/or biotite + garnet + plagioclase.

The first two types may have developed in response either to igneous re-equilibration or to metamorphism. They occur only in areas where primary textures are well preserved. The third type is a metamorphic corona.

Layered gabbros (unit 3b). Layered gabbro is not as abundant as the unlayered unit. The layering results from variations in mineral proportions and grain size heterogeneities. Layered gabbro is exposed in the body west of Baikie Lake where composition ranges from gabbro to leucogabbro with minor anorthositic layers. Mineralogical grading, inclusions of underlying layers, and igneous lamination are present and primary mineralogy and corona types (i) and (ii) are common. Compositional layering also occurs in gabbro bodies in the southeast of area H/7 and farther south in the area of the power line. Most of these gabbros are strongly deformed and metamorphosed and pyroxene is pseudomorphed by hornblende or is left as relicts rimmed by biotite. Garnet occurs as coronas or is disseminated within recrystallized plagioclase.

Equigranular leucogabbro (unit 3c). Almost all of unit 3 in the southwestern area is equigranular leucogabbro. The unit is dominated by fine grained, two-pyroxene leucogabbro with minor hornblende; the main ferromagnesian minerals being orthopyroxene and diopside. Clinopyroxene or hornblende occur as rare coronas round orthopyroxene, and garnet is a rare accessory. The leucogabbros are mostly homogeneous, lacking any layering, contain coarser grained sweats, and are weakly foliated with a polygonal texture. They are cut by finer grained dykes of similar composition and also contain a few coarse grained, gabbroic to ultramafic patches net-veined by anorthositic material. The leucogabbro may be unrelated to the intergranular and layered gabbros.

Two-pyroxene metagabbro (unit 3d). Two bodies containing metamorphic mineral assemblages of plagioclase + orthopyroxene ± diopside ± hornblende ± biotite occur in the south and east of the area. The surrounding paragneiss, orthogneiss and gabbro, however, contain amphibolite facies assemblages.

Contacts between unit 3 and other units have not been observed and the relative ages of units 2 and 3 are not known. The intergranular textured gabbro west of Baikie Lake is continuous to the west with gabbro of the Shabogamo Intrusive Suite (Rivers, 1982). Textural comparison with this suite (cf. Fahrig, 1967; Rivers, 1980; Wardle and Britton, 1981) also indicates that a preliminary correlation can be made with the remainder of unit 3. The Shabogamo Intrusive Suite has been dated at 1375 ± 60 Ma (Brooks et al., 1981) to the northwest of this area.

Unit 4: Alkali-Feldspar Granite

This unit, a white weathering, very coarse grained, alkali-feldspar granite, occurs in the southeast of the area. The granite contains abundant muscovite, magnetite and

Table 51.1

Summary of chronology incorporating structural and metamorphic events

UNIT	EVENTS	FOLDING, FAULTING	FABRICS	MIGMATIZATION	METAMORPHIC GRADE
1	*Deposition*				
	Basic dykes				
	HD_1	–	HS_1, *Location fabric in (1a, c)*	HM_1, *major*	*Au +*
	HD_2	HF_2, *rare insoclines in (1a)*	–		*A +*
	Basic dykes				
2	*Intrusion*	*relative ages unknown*			
3	*Intrusion*				
	GD_1	GF_1, *isocline(s?) in (3b)*	GS_1, *Location fabric weak in (2b, f) variable in (2a, d), strong in (2e)*	GM_1, *possible range in (1)*	*A +*
	GD_2 - *early*	GF_2, *tight to isoclinal in (1, 2), thin shear zones in (3)*	GS_2, *major, mineral and shape fabrics in (1, 2, 3)*	GM_2, *minor + late to post -tectonic sweats*	*Au north* / *G south*
	- *late*	*Thrusting, possible range or regeneration*	*Mylonite*		*Au*
	GD_3, *possible range*	*Thin shear zones in (2)*	GS_3, *diorite in (2d) only*	GM_3, *possible range in shear zones only*	*A*
	Basic dykes?				
	GD_4	GF_4, *open to tight, regional map scale*	–	–	
4	*Intrusion*			*2-mica and muscovite-bearing granite dykes*	*A*
	D	*Faulting*			*Gs*

Numbers in parentheses refer to legend and text.
A, amphibolite; Au, upper amphibolite facies; G, granulite facies; Gs, greenschist facies; + denotes "or higher"; north and south are regional designations referring to the two metamorphic terrains (see text).

minor biotite and a small xenolith of folded paragneiss restite. Although this rock could be a part of unit 2, we suggest, because of primary igneous textures and a lack of deformation, that it could be the end product of Grenvillian migmatization: an "S-type" granite.

Related late and posttectonic granite dykes and milky quartz veins are present throughout the area but are not represented on the map. The dykes are commonly graphic and muscovite ± biotite-bearing. Both the dykes and the quartz veins have alteration halos in the adjacent paragneiss in which muscovite has partly or wholly replaced restite foliae for distances of up to 2.5 m from the contacts. Unit 4 dykes intrude all other units.

Structure and Metamorphism

Table 51.1 summarizes the structural amd metamorphic history of the area. Pre-Grenvillian deformation is assumed to be Hudsonian (HD) but conceivably could be early Paleohelikian in age. All units were strongly deformed and metamorphosed in the Grenville Orogeny (GD).

The earliest structure recognized in the area is the migmatitic layering that is pervasive throughout most of unit 1. It occurs as layers of granitic melt in the paragneiss (unit 1a) and as a quartz segregation layering in the basic gneiss (unit 1c). The layering formed during the first deformation HD_1 which occurred at upper amphibolite or higher metamorphic grade. Relict HD_1 prismatic sillimanite forms dense lineated mats parallel to the restite foliae.

Rare examples of isoclinal folds of the layering formed during HD_2. They predate the intrusion of basic dykes and K-feldspar megacrystic granitoid rocks in the southwest.

The deformation sequence is divided by the emplacement of units 2 and 3 which are taken to represent markers between Grenvillian and older deformation.

GD_1 is represented by isoclinal folding of layered gabbro in unit 3 and by variable degrees of migmatization in unit 2. Crosscutting migmatitic veins in unit 1 were probably developed at this time.

The metamorphic facies attained during the HD_2 and GD_1 events are unknown because there are no surviving index minerals that may be confidently assigned to either of these events. However, two metabasic bodies (unit 3d) in the south and east of the map area contain orthopyroxene + diopside assemblages indicating that metamorphism during GD_1 may have peaked in the lower granulite facies.

GD_2 structures represent a major structural reworking throughout the area. Concordant and crosscutting migmatitic veins of HD_1 and GD_1 generation in both the paragneiss and the orthogneiss units were tightly to isoclinally folded during GD_2 with the development of a strong axial planar mineral foliation in most lithologies. Syntectonic axial plane-parallel migmatization was minor but this fabric was greatly enhanced by the intense transposition of the pre-existing location fabrics. Fold mullions, augen gneisses and a strong shape and mineral rodding indicate an extensional strain regime. Lineations generally plunge south-southeast at moderate angles.

The gabbroic rocks of units 3a and 3b responded inhomogeneously to the GD_2 deformation. The foliation of these units is composed of strongly deformed shape aggregates of plagioclase, hornblende and garnet and cuts across GD_1 folds. Foliated gabbro of unit 3a contains augen of relatively undeformed gabbro. Some augen and the large body west of Baikie Lake are deformed only in discrete, narrow shear zones which contain an amphibolite facies mineralogy.

The southwestern metamorphic terrane is characterized by a more intense development of the structures during GD_2 compared to the remainder of the map area. The migmatitic layering has a consistent approximately north-trending strike and steep dip, and the fabric in the paragneiss is commonly porphyroclastic or submylonitic in texture. The lineation pitches moderately to steeply to the south on the foliation. GD_2 deformation in unit 3c was more homogeneous and resulted in a penetrative granulite facies mineral fabric.

The GD_2 deformation was accompanied by a pervasive mineral recrystallization. This occurred at granulite facies grade in the southwestern and southeastern parts of the area, where it represented peak metamorphism, and is characterized by mineral assemblages containing sillimanite ± biotite in the paragneiss, and orthopyroxene ± diopside ± hornblende ± biotite ± garnet in the orthogneiss (units 2 and 3). Throughout the remainder of the area upper amphibolite facies conditions prevailed and characteristic

index mineral assemblages consist of combinations of sillimanite, biotite, hornblende and garnet. Sillimanite-bearing paragneiss developed fine grained biotite selvages at restite and melt contacts in both granulite and amphibolite facies terranes.

The eastern boundary between the granulite facies uplands and the enveloping amphibolite facies in map area H/2 is a mylonite zone dipping moderately to the west. The remainder of the contact is unexposed. The mylonite is glassy and structurally conformable with the GD_2 foliation and lineation on either side of the zone. Within the granulite facies terrane the foliation is disposed into a map scale synform indicating that the mylonite originated as a deep level ductile thrust along which granulite facies supracrustals were translated northwards over their amphibolite facies equivalents. Although the structural conformity of the mylonite with the GD_2 structures indicates a coeval relationship between the two, the thrusting must postdate the peak metamorphic conditions associated with the formation of the structures (Table 51.1). The mylonite zone is parallel to other high strain zones in the area, both to the east and west. These zones are usually porphyroclastic and less glassy than the example described above.

Post-GD_2 static recrystallization has partly to completely annealed pre-existing fabrics. Coarse grained random needles of sillimanite sporadically overprint the restite foliae in paragneiss of the southern part of the area. Hydration accompanied the recrystallization in the northern areas and the paragneiss is characterized by posttectonic garnet and mimetic textured sillimanite and biotite.

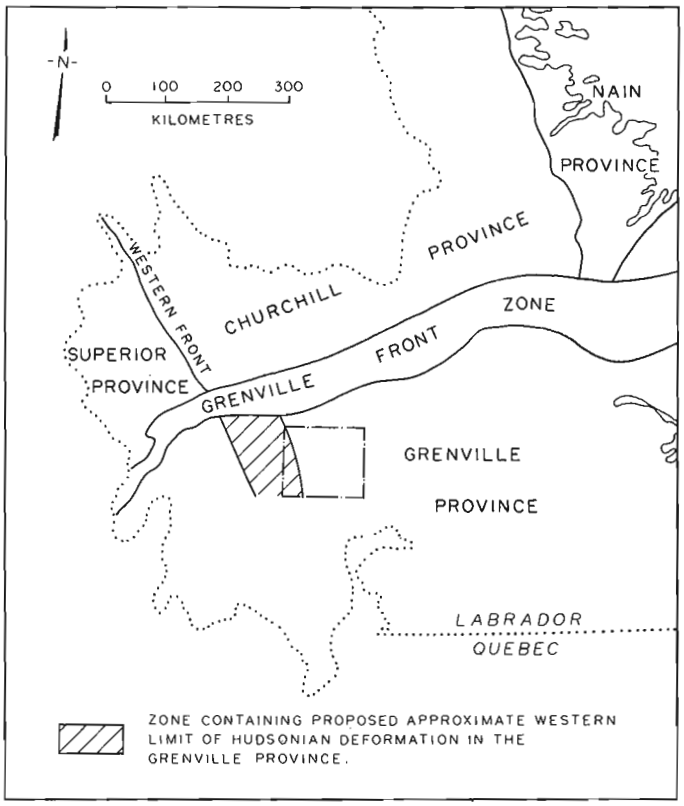

Figure 51.3. *Proposed zone containing the possible extension of the western Hudsonian Front south of the Grenville Front Zone. Province boundaries modified from Stockwell (1961) and Smyth and Greene (1976); Grenville Front Zone modified from Gower et al. (1980) and other work of the Newfoundland Department of Mines and Energy.*

The GD_2 foliation is deflected in shear zones (GD_3) in some of the unit 2 orthogneiss. The shear zones are variable in orientation and may form the locus of late migmatite veins. The veins contain equant quartz and feldspar and coarse grained, poikilitic hornblende.

The map pattern is controlled by regional scale folds (GD_4) that are generally moderate to open. Fold axes fan from north-trending in the southwest to northwest-trending in the northeast. A weak fracture cleavage may be developed in the quartzofeldspathic minerals in GD_4 fold hinges. GD_4 and GD_2 are commonly coaxial but there is no known new mineral growth associated with the later deformation. A retrogressive appearance to some foliation surfaces in the Atikonak River area indicates continuing motion in the thrust zones or reactivation during GD_4.

Muscovite occurs throughout the amphibolite facies area in localized patches or associated with faults and unit 4 pegmatite dykes and quartz veins. The muscovite is always a replacement mineral growing randomly both within and across the restite foliae and in the adjacent melts, and appears to be the result of late retrogression.

Many brittle structures transect the area and postdate GD_4. Two fault systems, in particular, trending approximately 020° and 100°-200°, control the gorge system of the Churchill River (A. Thomas, personal communication, 1982) and its tributaries in the north of the map area. The 100°-120° set has a transcurrent, dominantly sinistral, sense of displacement and appears to be the younger of the two.

Discussion

The metamorphic fabrics in the Helikian granitoid and gabbroic rocks of units 2 and 3 respectively, clearly indicate that the area has been thoroughly affected by high grade, Grenvillian, dynamothermal metamorphism. The strong similarity of fabrics in these units to those in the paragneiss would initially suggest that both formed during the same event. However, several key outcrops suggest that the primary layering developed at different times. Megacrystic granitoid rocks of unit 2, which elsewhere have been migmatized and subsequently further deformed, include paragneiss xenoliths with a melt layering that was clearly folded prior to incorporation. Similar features were described by Wardle (1982) for granitoid rocks south of the area. Some of the paragneiss has, therefore, been deformed by early events prior to the emplacement of orthogneiss and gabbro and is polyorogenic in origin.

Assuming the correlation of unit 2 with the North Pole Brook Intrusive Suite (ca. 1650 Ma) and of unit 3 with the Shabogomo Intrusive Suite (ca. 1375 Ma) the tectonic events recorded in the paragneiss inclusions represent the Hudsonian or an early Paleohelikian orogeny. The Paleohelikian has not yet been shown to be a time of gneiss-forming deformation in central Labrador and the Hudsonian Orogeny is thought to be a more likely cause of early deformation in the paragneiss. The structural boundary between the Churchill and Superior provinces outside of the Grenville Province (Fig. 51.3) is located to the northwest of the map area. The continuation of this boundary, the Hudsonian Front, although probably offset to the east by structural telescoping in the Grenville Front Zone, must still pass to the west of most of the map area (Fig. 51.3).

A similar polyorogenic sequence has been documented affecting gneisses in the Red Wine Mountains (Thomas, Jackson and Finn, 1981) and is suspected in the granulite facies terrane contiguous with the southeastern part of the map area (A. Thomas, personal communication, 1982).

However, a detailed isotopic dating study is needed to confirm the presence of Hudsonian tectonites within this area of the Grenville Province.

Acknowledgments

The project is funded by the Federal Department of Energy, Mines and Resources, as a part of the Federal Mineral Program in Newfoundland, through the Director General's Office at the Geological Survey of Canada. We thank Lakeland Helicopters of North Bay, Ontario, for excellent service, T. van Nostrand, J. Blagdon and D. Taylor for field assistance, and A. Thomas and T. Rivers for fruitful discussion. Special thanks are given to the Churchill Falls (Labrador) Corporation Limited and to the people of Churchill Falls for their assistance and friendship throughout the summer. The manuscript was reviewed by C.F. Gower and R.J. Wardle.

References

Brooks, G., Wardle, R.J., and Rivers, T.
1981: Geology and geochronology of Helikian magmatism, western Labrador; Canadian Journal of Earth Sciences, v. 18, p. 1211-1277.

Eade, K.E.
1952: Preliminary map: Unknown River (Ossokmanuan Lake east half), Labrador, Newfoundland; Geological Survey of Canada, Paper 52-9.

Fahrig, W.F.
1967: Shabogamo Lake map-area, Newfoundland-Labrador and Quebec; Geological Survey of Canada, Memoir 354, 23 p.

Gower, C.F., Ryan, A.B., Bailey, D.G., and Thomas, A.
1980: The position of the Grenville Front in eastern and central Labrador; Canadian Journal of Earth Sciences, v. 17, p. 784-788.

Greene, B.A.
1972: Geological map of Labrador, 1:1,000,000; Newfoundland Department of Mines, Agriculture and Resources, Mineral Resources Division.

1974: An outline of the geology of Labrador; Newfoundland Department of Mines and Energy, Mineral Development Division, Information Circular no. 15, 64 p.

Nunn, G.A.G.
1981: Regional geology of the Michikamau Lake map area, central Labrador; in Current Research, Newfoundland Department of Mines and Energy, Report 81-1, p. 138-148.

Nunn, G.A.G. and Noel, N.
1982: Regional geology east of Michikamau Lake, central Labrador; in Current Research, Newfoundland Department of Mines and Energy, Report 82-1, p. 149-167.

Rivers, T.
1980: Revised stratigraphic nomenclature for Aphebian and other rock units, southern Labrador Trough, Grenville Province; Canadian Journal of Earth Sciences, v. 17, p. 668-670.

1982: Preliminary report on the geology of the Gabbro Lake and McKay River map areas (23H/11 and 23H/12), Labrador; Newfoundland Department of Mines and Energy, Report 82-2, 27 p.

Smyth, W.R. and Greene, B.A.
1976: Isotopic age map of Labrador; Newfoundland Department of Mines and Energy, Mineral Development Division, Map 764.

Stockwell, C.H.
1961: Structural provinces, orogenies, and time classification of rocks of the Canadian Precambrian Shield; in Geological Survey of Canada, Paper 61-17, p. 108-118.

Thomas, A. and Hibbs, D.
1980: Geology of the southwestern margin of the Central Mineral Belt; in Current Research, Newfoundland Department of Mines and Energy, Report 80-1, p. 166-181.

Thomas, A., Jackson, V., and Finn, G.
1981: Geology of the Red Wine Mountains and surrounding area, central Labrador; in Current Research, Newfoundland Department of Mines and Energy, Report 81-1, p. 111-120.

Wardle, R.J.
1982: Geology of the Churchill Falls Region; in Current Research, Newfoundland Department of Mines and Energy, Report 82-1, p. 131-148.

Wardle, R.J. and Britton, J.M.
1981: The geology of the Churchill Falls area, Labrador; in Current Research, Newfoundland Department of Mines and Energy, Report 81-1, p. 130-137.

Wyllie, P.J., Huang, W.H., Stern, C.R., and Maaloe, S.
1976: Granitic magmas: possible and impossible sources, water contents and crystallization sequences; Canadian Journal of Earth Sciences, v. 13, p. 1007-1019.

52.

LATE GLACIAL AND POSTGLACIAL MACROFOSSILS FROM THE OTTAWA-ST. LAWRENCE LOWLANDS, ONTARIO AND QUEBEC

Project 740068

Cyril G. Rodrigues[1] and S.H. Richard
Terrain Sciences Division

Rodrigues, C.G. and Richard, S.H., Late glacial and postglacial macrofossils from the Ottawa-St. Lawrence Lowlands, Ontario and Quebec; in Current Research, Part A, Geological Survey of Canada, Paper 83-1A, p. 371-379, 1983.

Abstract

Seven marine macrofaunal associations and one freshwater macrofaunal association are present in late glacial and postglacial sediments west of 74°W in the Ottawa-St. Lawrence Lowlands. Consistent patterns in the succession of associations have been recognized. The successions are related to the changing physical and chemical properties of the bottom water and variations in the substrate. The ***Macoma balthica*** *association characterizes deposits of the early Champlain Sea episode in the study area. Between 11 600 and 10 500 years, the* ***Hiatella arctica, Macoma balthica, Mytilus edulis, Portlandia arctica,*** *and* ***Balanus hameri*** *associations inhabited different parts of the western Champlain Sea basin. Postglacial deposits from the interval 10 300 to 10 000 years contain the* ***Hiatella arctica, Macoma balthica, Mya arenaria, Mya truncata, Mytilus edulis, Portlandia arctica,*** *and* ***Lampsilis*** *associations. The occurrence of marine and freshwater macrofaunal associations in Ottawa valley during the late Champlain Sea episode is probably related to the presence of Lake Algonquin water which formed a freshwater surface layer underlain by marine Champlain Sea water in the deeper parts of the basin.*

Introduction

With the exception of a single paper by Wagner (1970), the invertebrate macrofossils in the western Champlain Sea basin have not been the subject of intensive investigation since the work of Goldring (1922). This report discusses the distribution and significance of some macrofossils that are found in late glacial and postglacial sediments west of 74°W. The locations of sites discussed herein are shown in Figure 52.1.

Acknowledgments

Financial support to C.G. Rodrigues for this study has come from the Natural Sciences and Engineering Research Council of Canada Operating Grant A8012.

Distribution of Selected Macrofaunal Species

Barnacles, bryozoans, gastropods, pelecypods, and sponges are present in late glacial and postglacial sediments of the western Champlain Sea basin. Pelecypods are the most abundant macrofossil group in the area and are commonly the only taxon comprising the assemblages. Eight species are considered to be important in the interpretation of depositional environments and chronology of the sediments in the area. The distribution of the species is summarized below.

Balanus hameri (Ascanius) occurs most commonly in ridges of coarse grained sediment at Twin Elm, South Gloucester, Rivière-Beaudette, and Beaver Crossing. The species is most abundant at the base of fossiliferous strata which are exposed in gravel and sand pits in the ridges.

Hiatella arctica (Linné) and **Macoma balthica** (Linné) are the most common species in the western Champlain Sea basin. They are found in coarse and fine grained sediments and are commonly the dominant species of the macrofaunal assemblages. The average size of specimens of both species and the thickness of valves of **H. arctica** from different populations are highly variable. Shell beds with sandy and muddy matrix, 30-60 cm thick, consisting mainly of **H. arctica** were observed in the Cornwall, Kemptville, and Wakefield areas. **Macoma calcarea** (Gmelin) is not as common as **M. balthica.** The former species is most abundant in the Alexandria area in sand, clayey sand, and clay.

Mya arenaria (Linné) is present in the Alexandria, Cornwall, Huntingdon, Lachute, and Vaudreuil areas in cobble to boulder gravel, cobbly to bouldery sandy mud, sand, and muddy sand. The species occurs in Fort Covington Till – map unit 2 of Gwyn and Lohse (1973) and map unit 1 of Terasmae (1965) – in the Alexandria and Cornwall areas, respectively. **Mya arenaria** was not observed west of Lochiel (45°22'45"N, 74°37'30"W) in the Alexandria area, and west of Sandfield Mills (45°08'50"N, 74°46'45"W) in the Cornwall area. **Mya truncata** (Linné) s.l. is present in the Russell, Huntingdon, Lachute, and Vaudreuil areas in pebbly muddy sand, sand, and muddy sand. In the Russell area, the species was observed at one locality about 0.5 km northwest of Bearbrook (45°23'35"N, 75°20'12"W), which is the farthest west reported occurrence of **M. truncata.**

Mytilus edulis Linné occurs in coarse and fine grained sediments throughout the study area. Assemblages consisting of large numbers of specimens of the species were observed in sand and gravel in the Winchester, Alexandria, and Lachute areas. **Portlandia arctica** (Gray) is widely distributed in the western Champlain Sea basin. The species is most abundant in clay, which at some sites directly overlies Precambrian or Paleozoic rocks, and is rare in coarser grained sediments. In the Kemptville area **P. arctica** occurs in pebbly clay and clay beds at the base of fossiliferous strata in sand and gravel ridges.

Macrofaunal Associations

Macrofaunal assemblages from late glacial and postglacial sediments in the Ottawa-St. Lawrence Lowlands west of 74°W are commonly characterized by one dominant species. Thus, assemblages can be arranged into groups based on the dominant species and readily identified in the field. Each group is herein termed an association and is named after the dominant species of the assemblages comprising the association. Seven marine associations have been recognized: **Hiatella arctica, Macoma balthica, Mya arenaria,**

[1] Department of Geology, University of Windsor, Windsor, Ontario N9B 3P4

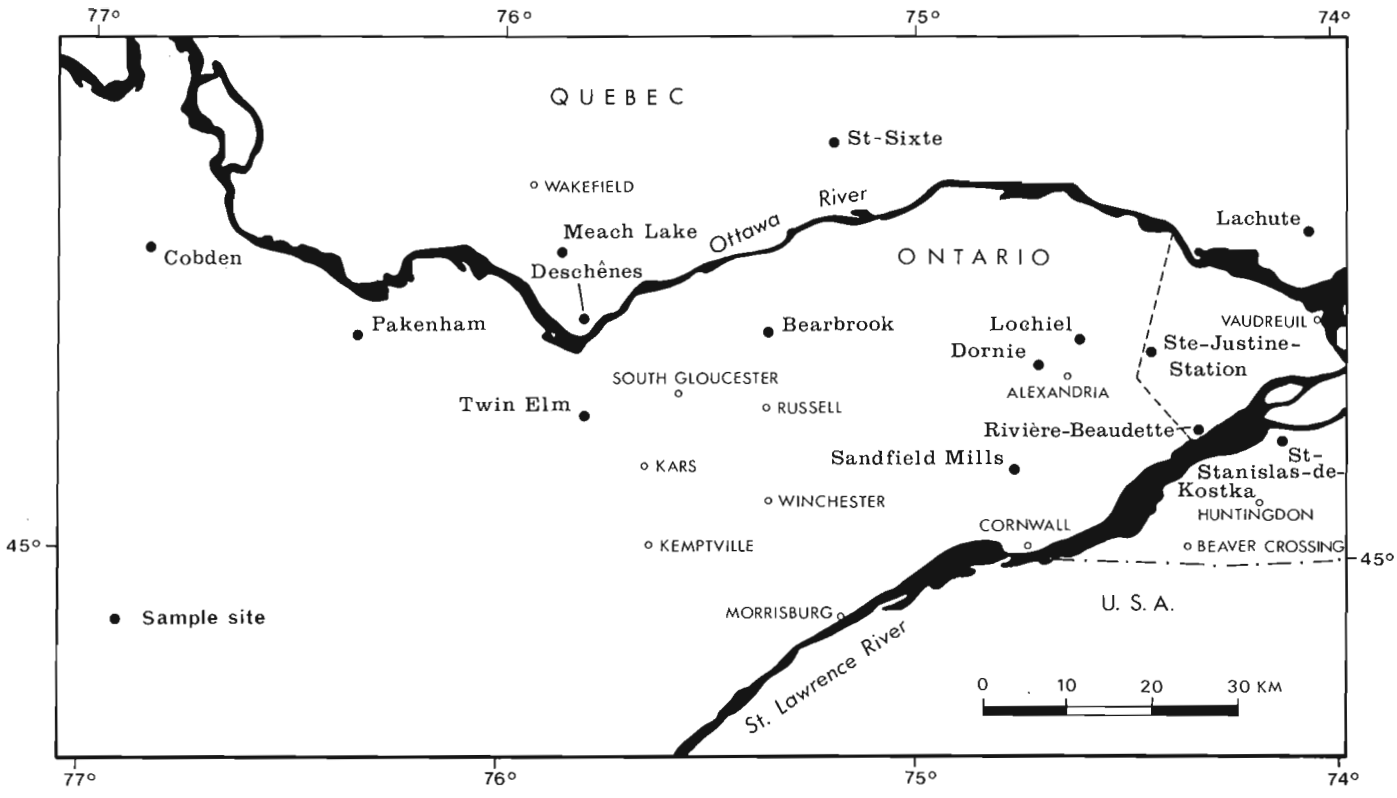

Figure 52.1. *Location map of Ottawa-St. Lawrence Lowlands showing some sites discussed. Open circles represent cities and towns.*

Table 52.1

Presence of taxa in macrofaunal associations from Champlain Sea deposits in Ontario and Quebec west of 74°W

Taxon	Association*						
	1	2	3	4	5	6	7
Balanus hameri (Ascanius)	X	X				X	X
Balanus spp.	X	X		X	X	X	X
Astarte montagui (Dillwyn) s.l.	X			X			X
Hiatella arctica (Linné)	X	X	X	X	X	X	X
Macoma balthica (Linné)	X	X	X	X	X	X	
Macoma calcarea (Gmelin)	X	X				X	
Mya arenaria (Linné)	X	X	X				
Mya truncata (Linné) s.l.	X			X			
Mytilus edulis Linné	X	X	X	X	X	X	
Nuculanid pelecypods	X					X	X
Portlandia arctica (Gray)	X	X				X	X
Cylichna alba Brown	X					X	X
Lepeta caeca (Müller)							X
Natacid gastropods	X			X		X	X
Neptunea despecta tornata (Gould)	X					X	
Tethya logani Dawson	X	X	X			X	
Cheilostome bryozoan						X	

*Associations:

1. **Hiatella arctica**
2. **Macoma balthica**
3. **Mya arenaria**
4. **Mya truncata**
5. **Mytilus edulis**
6. **Portlandia arctica**
7. **Balanus hameri**

Table 52.2

Macrofaunal associations that occur in the map units of Richard (1982a-e)

Unit	Description of Map Unit	Associations
5a	Nearshore sediments: gravel, sand, and boulders, generally well sorted; nature of sediment controlled by underlying material	**Hiatella arctica, Macoma balthica, Mya arenaria,** and **Mytilus edulis**
5b	Fine to medium grained sand, calcareous; nearshore sand generally occurs as a sheet or as bars or spits associated with glaciofluvial material	**Macoma balthica** and **Mya arenaria**
4	Deltaic and estuarine deposits: medium to fine grained sand	**Macoma balthica, Mya arenaria,** and **Lampsilis**
3	Offshore marine deposits: massive blue-grey clay, silty clay, and silt, calcareous	**Macoma balthica** and **Portlandia arctica**
2	Ice-contact stratified drift: gravel and sand, poorly to well sorted and bedded, mainly coarse to medium grained with numerous cobbles, boulders, and lenses of till	**Balanus hameri, Hiatella arctica,** and **Portlandia arctica**
1	Till: grey to brown sandy and silty compact diamicton, calcareous in places	**Hiatella arctica** and **Portlandia arctica**

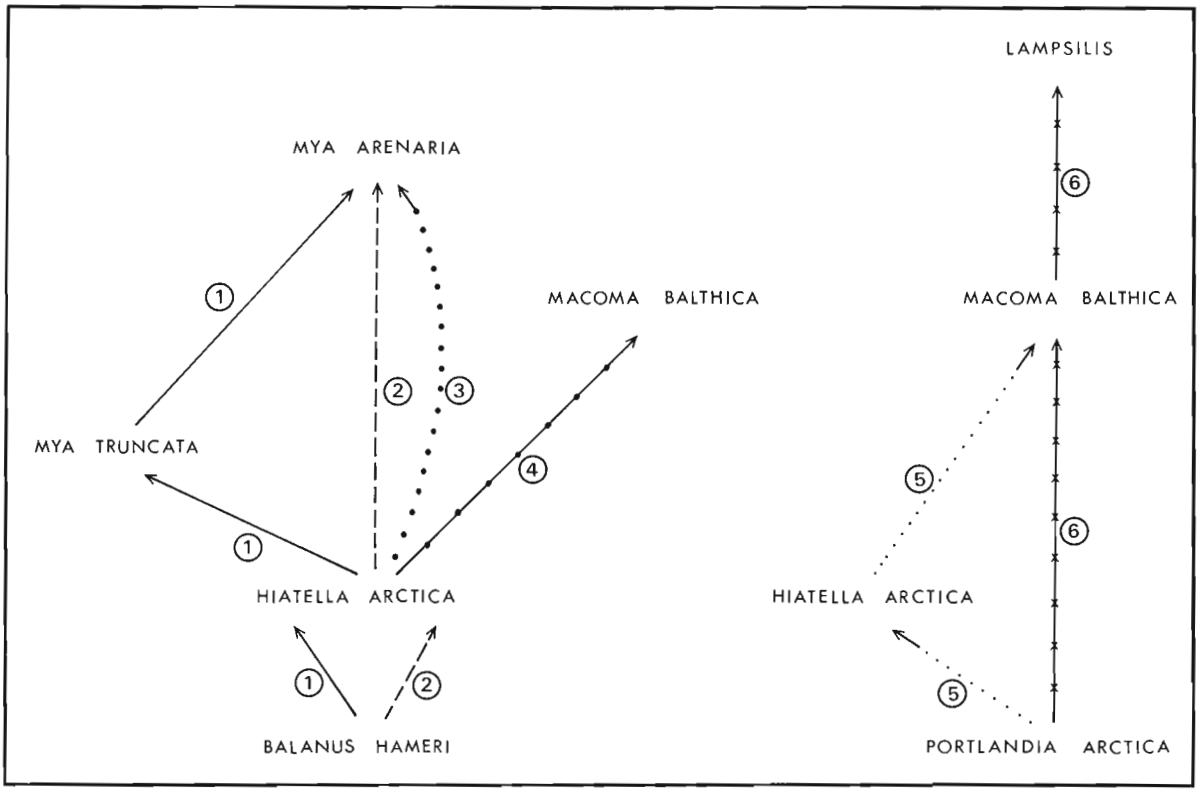

Figure 52.2. Successions of macrofaunal associations in late glacial and postglacial deposits of Ontario and Quebec west of 74° W.

Mya truncata, Mytilus edulis, Portlandia arctica, and **Balanus hameri.** The pelecypod associations are comparable to the communities that were described from the postglacial deposits of Quebec by Hillaire-Marcel (1977, 1980). Some of the taxa occurring in the associations are listed in Table 52.1. The accompanying taxa are not present at each locality; for example, **Astarte montagui** (Dillwyn) s.l., **Macoma calcarea,** and **Neptunea despecta tornata** (Gould) are only present in the **Hiatella arctica** association at some localities. The presence or absence of the accompanying taxa can be used to subdivide the associations into sub-associations. It is anticipated that the number of accompanying species and their occurrences in the associations will increase with further sampling. The occurrences of the associations in the map units of Richard (1982a-e) for the Morrisburg, Kemptville, Winchester, Huntingdon, and Vaudreuil areas are listed in Table 52.2.

The associations replace each other in some sections exposed in gravel pits, ditches, and roadcuts. Six successions have been recognized (Table 52.3, Fig. 52.2). The **Balanus hameri** or **Portlandia arctica** or **Hiatella arctica** association is found at the base of the sections, and the **Macoma balthica** or **Mya arenaria** association occurs at the top of the sections. In a roadside ditch about 1 km northwest of Saint-Stanislas-de-Kostka, Beauharnois County, Quebec, the marine associations are replaced by the freshwater **Lampsilis** association. The faunal successions are related to shoaling of the Champlain Sea. As the sea shoals the temperature of the bottom water increases, the salinity decreases, and the nature of the substrate may vary; therefore, the faunal successions are indicative, in part, of changes in the temperature and salinity of the water on the seafloor. The **Balanus hameri** and **Portlandia arctica** associations occur in deeper, cooler, and more saline water and are replaced by the **Macoma balthica** or **Mya arenaria** association in shallower water which has higher temperature and lower salinity. The variations in the temperature and salinity characteristics of the sea through time at a single site are similar to vertical temperature and salinity variations observed in modern nearshore and offshore marine environments.

Table 52.3

Successions of macrofaunal associations in late glacial and postglacial deposits of Ontario and Quebec west of 74°W

	Succession					
Association	1	2	3	4	5	6
Lampsilis						X
Mya arenaria	X	X	X			
Macoma balthica				X	X	X
Mya truncata	X					
Hiatella arctica	X	X	X	X	X	
Balanus hameri/	X	X				
Portlandia arctica					X	X

Comparable changes in the abundant species of the microfaunal assemblages accompany the macrofaunal successions. For example, the **Balanus hameri** through **Mya arenaria** succession (No. 2) was observed in a gravel pit about 2 km south of Rivière-Beaudette, Soulanges County, Quebec; the macrofossils which are present in the associations are listed in Table 52.4. The abundant species of the foraminiferal assemblages obtained from five samples at different levels of the section are given in Table 52.5. A **Astrononion gallowayi** Loeblich and Tappan, **Cassidulina reniforme** Nørvang, **Cibicides lobatulus** (Walker and Jacob), and **Islandiella norcrossi** (Cushman) dominant assemblage from the level of the **Balanus hameri** association is replaced in the interval of the **Hiatella arctica** association by assemblages in which **Elphidium clavatum** Cushman, **Eoeponidella** sp., and **Protelphidium orbiculare** (Brady) are abundant. Near the top of the section at the level of the **Mya arenaria** association, **Elphidium albiumbilicatum** (Weiss), **E. clavatum,** and **P. orbiculare** are the abundant species. In general, the number of specimens and the number of taxa per assemblage decrease from the lower to the upper part of the section. The changes in the abundant species, number of specimens, and number of taxa of the foraminiferal assemblages are related to increasing temperature and decreasing salinity of the bottom water.

Temporal Distribution of Macrofaunal Associations

Radiocarbon dates for marine shells from Champlain Sea deposits west of 74°W range from 12 800 ± 200 years (GSC-1859, Richard, 1974) to 9910 ± 150 years (BGS-258, Sharpe, 1979). Richard (1978) pointed out that the oldest dates were obtained from shells of **Macoma balthica.**

Table 52.4

Macrofaunal associations and taxa observed in a section in the Rivière-Beaudette ridge, Soulanges County, Quebec

Association	Sample Number	Balanus hameri (Ascanius)	Balanus sp.	Hiatella arctica (Linné)	Macoma balthica (Linné)	Mya arenaria (Linné)	Mya truncata (Linné)s.l.	Mytilus edulis Linné
Mya arenaria	3-E				X	X		X
Hiatella arctica	3-D		X	X	X	X		X
	3-C-1		X	X	X		X	X
	3-C		X	X				
Balanus hameri	3-B	X		X				

Table 52.5

Per cent abundance of dominant foraminiferal species in samples from a section in the Rivière-Beaudette ridge, Soulanges County, Quebec

Macrofaunal Association	**Balanus hameri**	**Hiatella arctica**			**Mya arenaria**
Sample Number	3-B	3-C	3-C-1	3-D	3-E
Astrononion gallowayi Loeblich and Tappan	44.3	0.3	0.2	0.2	
[1]**Cassidulina reniforme** Nørvang	19.7	0.2		0.2	
Cibicides lobatulus (Walker and Jacob)	10.7	0.4			
Elphidium albiumbilicatum (Weiss)				22.9	77.4
Elphidium asklundi Brotzen	1.0	24.2	2.3	0.7	2.1
[2]**Elphidium clavatum** Cushman	2.1	23.6	13.5	40.8	6.8
Elphidium subarcticum Cushman	2.0	11.6	6.3		
Eoeponidella sp.	0.8	10.9	31.9	3.1	
Islandiella helenae Feyling-Hanssen and Buzas	4.1		0.2	0.2	0.5
Islandiella norcrossi (Cushman)	7.0	0.1			
Protelphidium orbiculare (Brady)	1.1	22.4	44.9	27.0	13.2
Number of specimens	1080	1852	876	681	190
Number of taxa	25	27	11	13	5
Weight of sediment processed (g)	29.2	26.6	27.1	29.2	26.5

[1] **Cassidulina crassa** d'Orbigny of Cronin (1979)
[2] **Elphidium excavatum** (Terquem) forma **clavata** Cushman of Cronin (1979)

Similarly, in Champlain valley, New York, the older dates are from shells of **M. balthica** (Table 52.6). At the Clayton, White Lake, and Val-des-Bois sites **M. balthica** characterizes the monospecific macrofaunal assemblages. Also, **M. balthica** is the dominant species or one of the dominant species at the sites in Champlain valley (Cronin, 1979, Appendix, p. 812). The oldest date (12 000 ± 200 years) for marine shells from the St. Lawrence Lowlands, New York, was reported by Kirkland and Coates (1977). Except for the comment "from Champlain Sea clay in downtown Massena (Locality 21)", no data regarding the material used for dating, elevation of the site, and laboratory reference number for the date were given. The youngest date for populations of **Macoma balthica** from the study area is 10 000 ± 320 years (GSC-1553, Lowdon and Blake, 1973) for shells from a beach deposit near Russell, Ontario. Thus, the range for the **Macoma balthica** association west of 74°W is 12 800 ± 200 to 10 000 ± 320 years.

There are no dates from shells of **Portlandia arctica** west of 74°W; however, an approximate range can be inferred from the occurrence of the species at or in the vicinity of sites from which radiocarbon dates have been obtained on other species. At the Saint-Sixte site about 1.5 km northeast of Saint-Sixte, Papineau County, Quebec, the **Portlandia arctica** association is replaced by the **Macoma balthica** association in a clay unit exposed in the bank of Rivière Saint-Sixte. Shells of **Macoma balthica** from the level of the **Macoma balthica** association yielded a date of 11 500 ± 200 years (GSC-2863, Lowdon and Blake, 1980); this date gives an approximate maximum age for the **Portlandia arctica** association. Clay containing **Portlandia arctica** occurs at low elevations throughout the study area. The clays are commonly overlain by nonmarine deposits. At one locality about 1 km northwest of Saint-Stanislas-de-Kostka, Quebec, the **Portlandia arctica** association is replaced by the **Macoma balthica** association in a clay unit. The sand overlying the clay contains **Lampsilis** sp. The age of the freshwater

Table 52.6

Radiocarbon dates for some populations of **Macoma balthica** (Linné) from Champlain Sea deposits in Ontario and Quebec west of 74°W and in Champlain valley, New York

Laboratory Number	Date (years BP)	Elevation (m a.s.l.)	Locality	Reference
GSC-1859	12 800 ± 200	168	Clayton, Lanark County, Ontario	Richard, 1974
GSC-2151	12 800 ± 100 (Outer fraction)	168	Clayton, Lanark County, Ontario	Richard, 1978
	12 700 ± 100 (Inner fraction)			
*GSC-3110	12 100 ± 100 (Outer fraction)	170-171	White Lake, Renfrew County, Ontario	Richard, unpublished
	12 200 ± 100 (Middle fraction)			
	12 100 ± 100 (Inner fraction)			
GSC-1013	11 800 ± 210	103	Maitland, Grenville County, Ontario	Lowdon and Blake, 1970
GSC-1646	12 200 ± 160	192	Cantley, Gatineau County, Quebec	Lowdon and Blake, 1973
GSC-1772	11 900 ± 160	176	Martindale, Gatineau County, Quebec	Lowdon and Blake, 1973
GSC-2769	11 800 ± 100	182	Val-des-Bois, Papineau County, Quebec	Lowdon and Blake, 1980
GSC-2338	11 900 ± 120	101	Peru, New York	Lowdon and Blake, 1979
GSC-2366	11 800 ± 100	96	Plattsburg, New York	Lowdon and Blake, 1979
QC-200	11 665 ± 175	95	Plattsburg, New York	Cronin, 1977

* The shells were collected from a raised beach about 1.5 km east of White Lake, Ontario (45°21'15"N, 76°28'25"W).

Lampsilis shells should be comparable to the 9750 ± 180 years date (GSC-2414, Lowdon and Blake, 1979) for **Lampsilis** shells from a site about 3.5 km southeast of Saint-Stanislas-de-Kostka. An age of about 10 000 years is anticipated for the **Portlandia arctica** association from the site northwest of Saint-Stanislas-de-Kostka. Thus, the range of the **Portlandia arctica** association west of 74°W appears to be approximately 11 500 to 10 000 years.

A date of 11 600 ± 150 years (GSC-842, Lowdon and Blake, 1970) from a site near Meach Lake, Gatineau Park, Quebec and one of 9910 ± 150 years (BGS-258, Sharpe, 1979) from the Dornie site, near Alexandria, give the approximate range of the **Hiatella arctica** association. Radiocarbon dates for populations of **Mya arenaria** are from the Lachute area, Quebec, and range from 10 500 ± 270 years (QU-50, Hillaire-Marcel, 1974) to 9950 ± 185 years (Gif-2107, Hillaire-Marcel, 1974). Only one date is available for the **Mya truncata** association; the date 10 300 ± 100 years (GSC-2261, Lowdon and Blake, 1979), was obtained for shells from a site about 3.2 km southwest of Sainte-Justine-Station, Vaudreuil County, Quebec. A date of 11 370 ± 300 years (QU-51, Hillaire-Marcel, 1974) is the only one available for shells of **Mytilus edulis**, and none have been published for **Balanus hameri** west of 74°W. At one site in the Lachute area, the **Mytilus edulis** association overlies the **Mya truncata** association. Thus, the range of the **Mytilus edulis** association in the eastern part of the study area appears to be approximately 11 370 to 10 300 years.

One date is available for the **Lampsilis** association in southwest Quebec. Shells of **Lampsilis siliquoidea** from a drainage ditch about 3.5 km southeast of Saint-Stanislas-de-Kostka yielded a date of 9750 ± 150 years (GSC-2414, Lowdon and Blake, 1979). The **Lampsilis** association was observed near Bourget, Russell County; Vankleek Hill, Prescott County; and Cornwall, Glengarry County, Ontario. Dates of 10 200 ± 90 years (GSC-1968, Lowdon and Blake, 1976) and 10 300 ± 90 years (GSC-3235, Lowdon and Blake, 1981) were reported for shells of **Lampsilis** from the Bourget and Vankleek Hill sites, respectively. Thus, the range of the **Lampsilis** association in the study area is 10 300 ± 90 to 9750 ± 150 years.

The stratigraphic ranges of some of the marine macrofaunal associations and the freshwater **Lampsilis** association are shown in Figure 52.3. The first association to inhabit the study area was the **Macoma balthica** association. Between 11 600 and 10 500 years the **Hiatella arctica, Macoma balthica,** and **Portlandia arctica** associations colonized different parts of the Champlain Sea west of 74°W. Postglacial sediments from the interval 10 300 to 10 000 years contain the marine **Hiatella arctica, Macoma balthica, Mya arenaria,** and **Portlandia arctica** associations, and the freshwater **Lampsilis** association.

Proposed Phases of the Champlain Sea and Post Champlain Sea Episodes

Elson and Elson (1959) proposed the **Hiatella** and **Mya** phases for the Champlain Sea episode and the **Lampsilis** Lake for the post-Champlain Sea freshwater episode based on observations around Montreal, Quebec. The phases are named after the abundant macrofossils comprising the assemblages. Elson (1969a, b) reported that the earlier deep water **Hiatella** (=**Hiatella arctica**) phase lasted from about 11 800 to between 10 800 and 10 600 years. The **Hiatella arctica** association, i.e., assemblages in which **Hiatella arctica** are abundant, ranges from about 11 600 to 9910 years west of 74°W. The **Macoma balthica, Mytilus edulis, Portlandia arctica,** and **Balanus hameri** associations were also present in different parts of the sea during the proposed

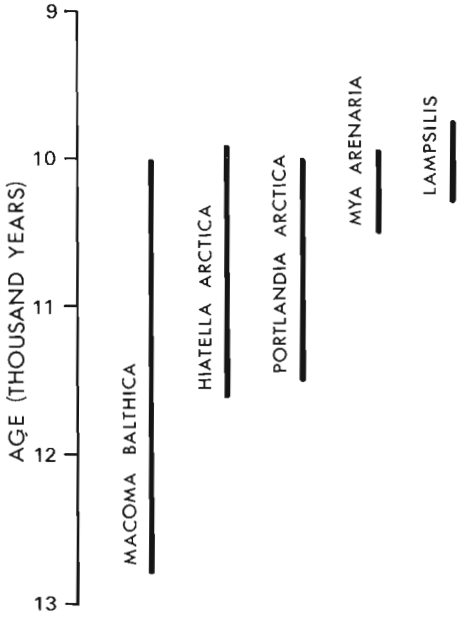

Figure 52.3. *Stratigraphic distribution of some marine and freshwater macrofaunal associations in late glacial and postglacial deposits of Ontario and Quebec west of 74°W.*

Hiatella phase. The presence of more than one macrofaunal association during a particular interval of the marine episode is related to lateral and bathymetric variations in the physical and chemical properties of the bottom water and/or the substrate. Therefore, **Hiatella arctica** dominant assemblages are not characteristic of a particular interval of the Champlain Sea episode. Hillaire-Marcel (1980) reached a similar conclusion.

The shallow water **Mya** phase of Elson and Elson (1959) lasted from 10 870 ± 100 years (GRO-2031, Elson, 1969b) to 9950 ± 185 years (Gif-2107, Hillaire-Marcel, 1974). No radiocarbon dates are available for shells of **Mya arenaria** from Champlain Sea deposits in southern Ontario; the species was not observed west of approximately 74°47'W. Radiocarbon dates within the range of the **Mya** phase have been reported for sites west of 74°47'W. For example, Mott (1968) reported a date of 10 800 ± 150 years (GSC-570) for marine algae from a sand pit near Twin Elm, Carleton County, Ontario. Whale bones found in blue clay with **Macoma balthica** about 6 km northeast of Pakenham, Ontario yielded a date of 10 400 ± 80 years (GSC-2418, Lowdon and Blake, 1979). A date of 10 100 ± 130 years (GSC-2189, Lowdon and Blake, 1979) was obtained from shells of **Hiatella arctica** which were collected about 3.2 km north of Deschênes, Gatineau County, Quebec. Thus, during the late **Mya** phase, the characteristic species **Mya arenaria** was not present throughout the Champlain Sea. The presence of cold surface water west of 74°47'W during the interval 10 800 to 10 500 years may have prevented the westerly migration of the species.

Elson (1969a, b) postulated that the freshwater **Lampsilis** Lake succeeded the marine **Mya** phase in southwestern Quebec ca. 10 000 years ago. Two radiocarbon dates have been published for freshwater shells from southwestern Quebec: 9750 ± 150 years (GSC-2414) and 9730 ± 140 years (GSC-1796, LaSalle et al., 1977) for shells from Saint-Stanislas-de-Kostka and Quebec City areas, respectively. Freshwater shells from postglacial deposits in Ottawa valley yielded dates of 10 300 ± 90 years (GSC-3235) and 10 200 ± 90 years (GSC-1968) from the Vankleek Hill and Bourget sites, respectively. The Ottawa valley dates overlap with dates for marine shells from the Deschênes and Dornie sites and are older than the dates from southwestern Quebec. The difference between the dates for freshwater shells from Ottawa valley and southwestern Quebec and the overlap between dates for marine and freshwater shells from Ottawa valley are of particular significance.

Terasmae and Hughes (1960) postulated that Lake Algonquin water drained through the North Bay outlet between 11 000 and 10 000 years ago. Karrow et al. (1975) and Catto et al. (1982) estimated that the North Bay outlet opened about 10 500 to 10 400 years ago. Barnett and Clarke (1980) pointed out that large freshwater shells were observed in a small delta about 13.5 km southeast of Cobden, Renfrew County, Ontario, at an elevation of 122 m. The presence of freshwater shells near Cobden is consistent with the proposed Georgian Bay-Lake Nipissing-Petawawa drainage route for water from Lake Algonquin. Therefore, freshwater was present in Ottawa valley during the late part of the Champlain Sea episode. The mixing of Lake Algonquin water and marine Champlain Sea water would result eventually in the presence of freshwater at shallow depths. Over the deeper parts of the sea the freshwater would form a surface layer underlain by marine Champlain Sea water. Thus, during the late stages of the Champlain Sea episode macrofaunal assemblages characterized by freshwater and marine species should be present at different depths of the sea in Ottawa valley. The overlap between dates for freshwater and marine shells supports the postulated salinity stratification of the water in Ottawa valley during the late Champlain Sea episode.

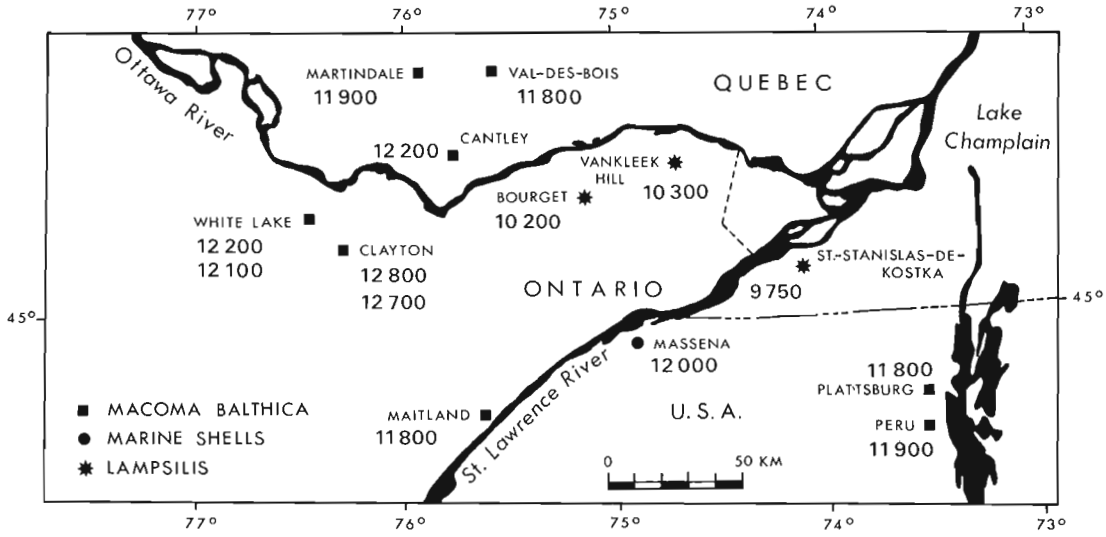

Figure 52.4. *Sites from which radiocarbon dates have been obtained for marine shells of the early Champlain Sea episode and for freshwater shells in the Ottawa-St. Lawrence Lowlands.*

The distribution of the freshwater shells and the published radiocarbon dates for the shells presented above indicate that the appearance of freshwater macrofossils was diachronous in Ottawa valley and southwestern Quebec. Freshwater macrofossils appear to have arrived later in southwestern Quebec compared to Ottawa valley. The sites from which radiocarbon dates have been obtained for freshwater shells and for marine shells from the early Champlain Sea episode in the Ottawa-St. Lawrence Lowlands west of 74°W are shown in Figure 52.4.

Summary and Conclusions

Molluscs are the most common macrofossils in late glacial and postglacial deposits of Ontario and Quebec west of 74°W. **Hiatella arctica, Macoma balthica, Mytilus edulis,** and **Portlandia arctica** are widely distributed in the study area whereas **Mya arenaria** and **M. truncata** s.l. are not as widely distributed. **Mya arenaria** was not observed west of approximately 74°47'W. The farthest west occurrence of **M. truncata** is about 0.5 km northwest of Bearbrook (45°23'35"N, 75°20'12"W). **Macoma calcarea** is most abundant in the Alexandria area. The barnacle **Balanus hameri** is most abundant at the base of fossiliferous strata in ridges at Twin Elm, South Gloucester, Rivière-Beaudette, and Beaver Crossing. **Lampsilis** spp. are present in the sediments overlying marine Champlain Sea deposits.

Seven marine macrofaunal associations and one freshwater macrofaunal association are recognized for the Champlain Sea and post-Champlain Sea episodes in the study area. Each association is named after the dominant species of the assemblages comprising the association. The marine associations replace each other in some sections. At one site marine associations are replaced by the freshwater **Lampsilis** association. The **Balanus hameri** or **Portlandia arctica** or **Hiatella arctica** association occurs at the base of the marine sequences and is replaced by the **Macoma balthica** or **Mya arenaria** association at the top of the sequences. Six successions of the macrofaunal associations have been recognized. The successions are related to increasing temperature and decreasing salinity of the bottom water and variations in the substrate. Comparable changes in the foraminiferal assemblages accompany the macrofaunal successions.

The published radiocarbon dates indicate that the **Macoma balthica** association is common in the marine deposits of the early part of the Champlain Sea episode in the study area and in Champlain valley, New York. The **Hiatella arctica, Macoma balthica, Mytilus edulis,** and **Portlandia arctica** associations inhabited different parts of the western Champlain Sea basin between 11 600 and 10 000 years approximately. The **Mya arenaria** association colonized the eastern part of the study area from about 10 500 years to the end of the marine episode. Only one date, 10 300 ± 100 (GSC-2261), is available for the **Mya truncata** association and no dates have been published for the **Balanus hameri** association west of 74°W. Thus, more than one macrofaunal association occurred in different parts of the western Champlain Sea basin after 11 600 years approximately. The presence of more than one macrofaunal association in different parts of the sea in a particular interval is related to lateral and bathymetric variations in the physical and chemical properties of the bottom water and/or the substrate. Radiocarbon dates for macrofossils from selected sites are required to define precisely the stratigraphic ranges of the macrofaunal associations in the western Champlain Sea basin.

Radiocarbon dates for freshwater shells from sites near Vankleek Hill and Bourget overlap with dates for marine shells from sites near Deschênes and Dornie in Ottawa valley. The presence of freshwater shells in Ottawa valley during the late Champlain Sea episode appears to be related to discharge of water from Lake Algonquin through the North Bay outlet beginning 10 500 to 10 400 years ago. Over the deeper parts of the sea, the freshwater from Lake Algonquin would form a surface layer underlain by marine Champlain Sea water. Therefore, during the late Champlain Sea episode freshwater and marine macrofaunal associations were present at different depths of the sea in Ottawa valley.

References

Barnett, P.J. and Clarke, W.S.
1980: Quaternary geology of the Cobden area, Renfrew County; Ontario Geological Survey Preliminary Map P. 2366, Geological Series, scale 1:50 000.

Catto, N.R., Patterson, R.J., and Gorman, W.A.
1982: The late Quaternary geology of the Chalk River region, Ontario and Quebec; Canadian Journal of Earth Sciences, v. 19, no. 7, p. 1218-1231.

Cronin, T.M.
1977: Late Wisconsin marine environments of the Champlain Valley (New York, Quebec); Quaternary Research, v. 7, no. 2, p. 238-253.

1979: Late Pleistocene benthic foraminifers from the St. Lawrence Lowlands; Journal of Paleontology, v. 53, no. 4, p. 781-814.

Elson, J.A.
1969a: Radiocarbon dates, **Mya arenaria** phase of the Champlain Sea; Canadian Journal of Earth Sciences, v. 6, no. 3, p. 367-372.

1969b: Late Quaternary marine submergence of Quebec; Revue de géographie de Montréal, v. XXIII, no. 3, p. 247-258.

Elson, J.A. and Elson, J.B.
1959: Phases of the Champlain Sea indicated by littoral molluscs (Abstract); Geological Society of America Bulletin, v. 70, p. 1596.

Goldring, W.
1922: The Champlain Sea; evidence of its decreasing salinity southward as shown by the fauna; New York State Museum Bulletin, no. 239-240, p. 153-187.

Gwyn, Q.H.J. and Lohse, H.
1973: Quaternary geology of the Alexandria area, southern Ontario; Ontario Division of Mines, Preliminary Map P. 906, Geological Series, scale 1:50 000.

Hillaire-Marcel, C.
1974: La déglaciation au nord-ouest de Montréal: données radiochronologiques et faits stratigraphiques; Revue de géographie de Montréal, vol. XXVIII, n° 4, p. 407-417.

1977: Les isotopes du carbone et de l'oxygène dans les mers post-glaciaires du Québec; Géographie physique et Quaternaire, vol. XXXI, n° 1-2, p. 81-106.

1980: Les faunes des mers post-glaciaires du Québec: quelques considérations paléoécologiques; Géographie physique et Quaternaire, vol. XXXIV, n° 1, p. 3-59.

Karrow, P.F., Anderson, T.W., Clarke, A.H., Delorme, L.D., and Skreenivasa, M.R.
1975: Stratigraphy, paleontology, and age of Lake Algonquin sediments in southwestern Ontario; Quaternary Research, v. 5, no. 1, p. 49-87.

Kirkland, J.T. and Coates, D.R.
1977: The Champlain Sea and Quaternary deposits in the St. Lawrence Lowland, New York; in Amerinds and their Paleoenvironments in Northeastern North America, ed. W.S. Newman and B. Salwen; Annals of the New York Academy of Sciences, v. 288, pt. IX, p. 498-507.

LaSalle, P., Martineau, G., and Chauvin, L.
1977: Morphology, stratigraphy, and deglaciation in Beauce-Notre-Dame Mountains-Laurentide Park area; Ministère des richesses naturelles, Québec, DPV-516, 74 p.

Lowdon, J.A. and Blake, W., Jr.
1970: Geological Survey of Canada radiocarbon dates IX; Radiocarbon, v. 12, p. 46-86.

1973: Geological Survey of Canada radiocarbon dates XIII; Geological Survey of Canada, Paper 73-7, 61 p.

1976: Geological Survey of Canada radiocarbon dates XVI; Geological Survey of Canada, Paper 76-7, 21 p.

1979: Geological Survey of Canada radiocarbon dates XIX; Geological Survey of Canada, Paper 79-7, 58 p.

1980: Geological Survey of Canada radiocarbon dates XX; Geological Survey of Canada, Paper 80-7, 28 p.

1981: Geological Survey of Canada radiocarbon dates XXI; Geological Survey of Canada, Paper 81-7, 22 p.

Mott, R.J.
1968: A radiocarbon-dated marine algal bed of the Champlain Sea episode near Ottawa, Ontario; Canadian Journal of Earth Sciences, v. 5, no. 2, p. 319-324.

Richard, S.H.
1974: Surficial geology mapping: Ottawa-Hull area (parts of 31 F, G); in Report of Activities, Part B, Geological Survey of Canada, Paper 74-1B, p. 218-219.

1978: Age of Champlain Sea and "Lampsilis Lake" episode in the Ottawa – St. Lawrence Lowlands; in Current Research, Part C, Geological Survey of Canada, Paper 78-1C, p. 23-28.

1982a: Surficial geology, Morrisburg, Ontario – New York; Geological Survey of Canada, Map 1493A.

1982b: Surficial geology, Kemptville, Ontario; Geological Survey of Canada, Map 1492A.

1982c: Surficial geology, Winchester, Ontario; Geological Survey of Canada, Map 1491A.

1982d: Surficial geology, Huntingdon, Quebec – Ontario; Geological Survey of Canada, Map 1489A.

1982e: Surficial geology, Vaudreuil, Quebec – Ontario; Geological Survey of Canada, Map 1488A.

Sharpe, D.R.
1979: Quaternary geology of the Merrickville area, southern Ontario; Ontario Geological Survey, Report 180, 54 p.

Terasmae, J.
1965: Surficial geology of the Cornwall and St. Lawrence seaway project areas, Ontario; Geological Survey of Canada, Bulletin 121, 54 p.

Terasmae, J. and Hughes, O.L.
1960: Glacial retreat in the North Bay area, Ontario; Science, v. 131, p. 1444-1446.

Wagner, F.J.E.
1970: Faunas of the Pleistocene Champlain Sea; Geological Survey of Canada, Bulletin 181, 104 p.

53.

BIOCLIMATIC ZONATION IN A HIGH ARCTIC REGION: CENTRAL QUEEN ELIZABETH ISLANDS

Project 760058

S.A. Edlund
Terrain Sciences Division

Edlund, S.A., Bioclimatic zonation in a High Arctic region: central Queen Elizabeth Islands; in Current Research, Part A, Geological Survey of Canada, Paper 83-1A, p. 381-390, 1983.

Abstract

The central Queen Elizabeth Islands in the High Arctic are subdivided into four bioclimatic zones based on plant community life-forms, species diversity within plant communities, total number of species, and the presence and abundance of a variety of indicator species such as woody plants, marsh emergents, sedges, vascular cryptogams, legumes, and Compositae. These zones, which cross lithologic boundaries, establish a 'mini-treeline' north of which no woody species occur (prostrate dwarf shrubs such as arctic willow and mountain avens) and a 'mini-forest zone' in which dwarf shrubs are the major vascular plant component. This bioclimatic zonation occurs on latitudinal, altitudinal, and local scales. It appears likely that the mean daily July temperature for the limit of vascular plants is a little above 2.5°C, for woody plants ('mini-treeline') is between 3° and 3.5°C and for the 'mini-forest zone', is between 3.5° and 4°C.

Introduction

Little is known of detailed climatic variations in the broad region of the Canadian High Arctic (the region north of 74°N). Five permanent weather stations, all located near sea level, were established in this region after World War II (Fig. 53.1). Little short- or long-term weather data are available for vast areas between these stations and for areas away from the coast (Maxwell, 1980).

During a decade of fieldwork in the Arctic Islands involving the study of plant communities – their composition and relationships to surficial materials – I have observed vegetation patterns that cross lithological boundaries and seem to reflect climatic zones within the High Arctic. This report summarizes these patterns for the central Queen Elizabeth Islands between 90° and 114°W (Fig. 53.1) and parts of adjacent eastern islands.

The better understanding of the coincidence of climate and vegetation boundaries will help in the more accurate interpretation of paleobotanical samples and of paleoclimates. This knowledge also may be used to extrapolate climatic data into regions where few weather statistics are available and has implications for the delineation of critical wildlife habitats, especially for herbivores dependent on dwarf shrubs and sedges.

Previous Work

Polunin (1951) subdivided the Canadian Arctic into three major regions, based primarily on extent of vegetation cover: (1) Low Arctic, the region immediately north of treeline, with continuous vegetation on all landforms; (2) Mid Arctic, where vegetation is less continuous, with bare areas common on the tops of hills and windswept plateaus; and (3) High Arctic, the region in the far North, with continuous vegetation confined to sheltered, well watered locations such as lower slopes and valley bottoms. The Queen Elizabeth Islands lie within this High Arctic zone.

Babb and Bliss (1974) have subdivided the High Arctic into four broad categories: (1) polar desert areas of very sparse vegetation; (2) polar semi-desert having continuous vegetation only locally; (3) diverse terrain, with greater potential for tundra or sedge moss meadows; and (4) sedge-moss meadows, with nearly continuous vegetation, found mainly in lowlands. These categories primarily reflect availability of moisture. Aleksandrova (1970, 1980) included the Canadian Arctic in her circumpolar classification of vegetation, which is also based on continuity of vegetation but also takes account of degrees of floristic diversity. The central Queen Elizabeth Islands lie within her polar desert and semi-desert zones.

Young (1971) divided the High Arctic into two floristic zones based on degrees of impoverishment of the vascular flora: zone 1 is a region of extreme improverishment, with generally less than 50-75 species of which most are circumpolar, an absence of vascular cryptogams, and a lack of closed communities; zone 2 has a slightly richer flora (75 to 125 species) and a few vascular cryptogams.

Beschel (1970) subdivided the vegetation of the mountainous eastern Queen Elizabeth Islands (Axel Heiberg, Ellesmere, and Devon islands) into five categories based on species diversity and community complexity: (1) polar desert, (2) **Luzula** steppe, (3) **Dryas** tundra, (4) **Cassiope** tundra, and (5) polar steppe. The criteria for this zonation, however, were not published. He showed that for this region, changes in elevation influenced the zonation of vegetation to a greater degree than did changes in latitude and documented zones of unusually rich vegetation, atypical of High Arctic communities. Beschel (1969) also listed total number of vascular plant species for each island of the Canadian Arctic, thereby showing the variation between islands.

In all these classifications, the central Queen Elizabeth Islands region is one of extreme improverishment of vegetation.

Relationships Between Vegetation and Surficial Materials

Although my work confirms the regional impoverishment of vegetation in the central Queen Elizabeth Islands, it also indicates a greater variety of plant communities exists than previous regional classifications have recognized. During fieldwork it became apparent that some surficial materials, commonly certain types of weathered bedrock, do not readily support plant growth regardless of moisture regime or degree of shelter. Examples are areas of strongly alkaline bedrock (pH 8.0-8.6), including certain facies of limestone, dolomite, and gypsum; white quartzose sandstones which lack plant nutrients and may be prone to eolian processes; strongly acidic shales (pH 3); and extremely saline marine sediments.

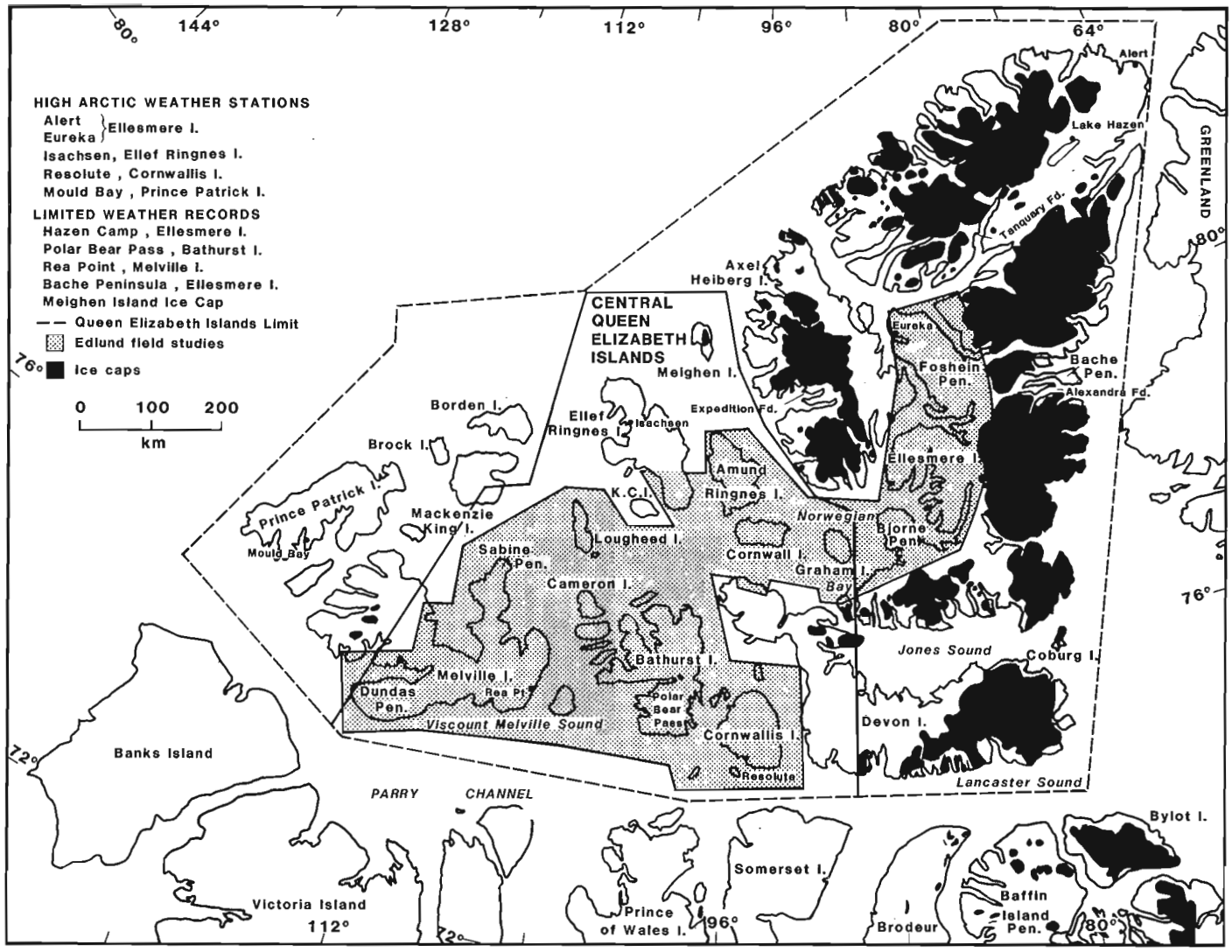

Figure 53.1. Queen Elizabeth Islands, showing study area, the location of weather stations, field areas covered, and the extent of ice cover.

All other types of bedrock and surficial deposits, other than those listed above, are consistently vegetated but the plant communities vary with substrate texture, chemistry, and moisture availability. Calciphilic communities occur on weakly to moderately calcareous material; certain graminoid species are most common on silts and clays; and **Luzula** (rush)-based communities occur on noncalcareous sandy silt and sand (Barnett et al., 1975; Hodgson and Edlund, 1975, 1978; Edlund, 1980, 1982a, b). Variation in type of surficial material does not, however, account for all the differences seen within plant communities in the Queen Elizabeth Islands.

Bioclimatic Zonation

For each type of material that supports vegetation, a suite of plant communities occurs, reflecting the changes in moisture regime (wet, mesic, or xeric). For each type of moisture regime on a given substrate, the vascular plant component of plant communities in the High Arctic forms a continuum in which floristic diversity and per cent cover decreases and the importance of the dwarf shrub life-form diminishes, until it is replaced by an entirely herbaceous life-form. These trends of increasing impoverishment cross lithological boundaries.

These continua may be divided into four zones, in each of which the community life-form is constant for each moisture regime, even though the individual species composition varies for different substrates. Emphasis is placed on changes in the vascular plant flora, for these changes are most readily detected. Identification of similar trends for lichens and bryophytes has not yet been attempted.

Criteria for Bioclimatic Zonation

The vegetation of the central Queen Elizabeth Islands is subdivided into four zones based on: the presence and abundance of woody species, the presence and diversity of Cyperaceae (sedges and cottongrasses), the types of emergent marsh species, the presence and types of vascular cryptogams (ferns, horsetails, and club mosses), the diversity of halophytic (salt tolerant) communities, and the total number of vascular species. Certain herbaceous species are used as zonal indicators.

The presence and abundance of woody species are the easiest recognized zonal characteristics. In the High Arctic, the only woody species are dwarf shrubs such as prostrate willows (**Salix arctica** and in a few places **S. polaris**), mountain avens (**Dryas integrifolia**), arctic heather (**Cassiope tetragona**), and bilberry (**Vaccinium uliginosum**) (Porsild, 1964; Porsild and Cody, 1980).

The presence of vascular cryptogams was used by Young (1971) to help distinguish his zone 2 from zone 1; he also used the total number of vascular species to help define his boundaries. Aleksandrova (1970, 1980) found variation of halophytic and marsh species useful in defining her zones. These criteria have been useful in my zonation as well; vascular cryptogams and diversity of marsh and halophytic species help define zones 3 and 4 (Table 53.2).

The diagnostic characteristics of each bioclimatic zone are described, starting with the zone of least diversity (zone 1) and progressing to the zone of greatest diversity and abundance (zone 4). This is summarized in Table 53.1 and the distribution of selected species by zones is shown in Table 53.2.

Zone 1

Zone 1 represents the most impoverished flora in the High Arctic. Permanent snowbeds are common in ravines and gullies and on the upper parts of some long, steep slopes where redistribution of winter snow creates thick drifts. Much of the terrain is unvegetated; vascular plant species total less than 35 species and are entirely herbaceous. Where vegetation occurs, total cover of vascular species is generally less than 5% and in many areas is as low as 1 or 2%.

Xeric sites, where vegetated, generally have less than 5% vascular plant cover, and rarely is there a cryptogamic lower stratum although scattered mosses and lichens may be present. Within this herbaceous vegetation, dominance varies with the different substrates: purple saxifrage (**Saxifraga oppositifolia**) is common on weakly to moderately calcareous materials; woodrush (**Luzula** species) is common on weakly acidic sand and sandy silt; and grasses such as **Alopecurus alpinus** and **Puccinellia** are common on silt and clay. In places no dominance is detected in the herbaceous layer; **Papaver**, Saxifrages, and grasses are present in about the same amounts.

Mesic sites have a higher per cent total plant cover (50-75%) than xeric sites due to a thin lower stratum of soil lichens (including **Polyblastia** species) and bryophytes. Nevertheless, as indicated above, the cover of vascular plants rarely exceeds 5%. Vascular species dominance is commonly similar to that found on more xeric areas.

Wet sites, if vegetated, are dominated by grass species (**Alopercurus alpinus** and to a lesser extent **Dupontia Fisheri**). The lower stratum, which is composed of bryophytes and soil lichens, is commonly broken (50-75%) but locally may be continuous.

Dwarf shrubs, sedges, vascular cryptogams, legumes, and Compositae do not occur in this zone, nor do exclusively emergent marsh species. Halophytic communities are generally absent; where present they consist of scattered tufts of **Puccinellia phryganodes**, which rarely flower, and the sporadic **Cochlearia officinalis**.

Zone 2

Vascular plant diversity increases to between 35 and 60 species in zone 2 and cover may reach 10%, although much of the landscape still appears unvegetated. Permanent snowbeds are less common and extensive. Dwarf shrubs (**Salix arctica** and **Dryas integrifolia**) and the sedges **Carex aquatilis** and **Eriophorum Scheuchzeri** (cottongrass), may occur locally but do not form major components of the plant communities.

Table 53.1

Change in life form, per cent vascular plant cover, and floristic diversity for the major moisture regimes within the bioclimatic zones, Queen Elizabeth Islands

Bioclimatic Zone	Total no. vascular species	Moisture Regime: Wetlands	% cover vascular	% cover total	Mesic	% cover vascular	% cover total	Xeric	% cover vascular	% cover total
1	less than 35	bryophytic mat	<1	<75	patina of soil lichens and bryophytes	<1	<75	scattered lichens	<1	<5
		graminoid-moss meadow	1-5	50-100	herb-patina tundra	1-5		herb barrens	1-5	<5
2	35-60	graminoid-sedge moss meadow	1-10	75-100	herb-patina tundra with scattered dwarf shrubs	5-10	<75	herb barrens	1-10	<10
3	60-100	sedge-moss meadow	5-15	75-100	dwarf shrub herb-patina tundra	5-25	<90	dwarf shrub-herb barrens	5-15	<20
4	greater than 100	sedge-moss wet meadow (local willow)	10-25	75-100	dwarf shrub-patina tundra	15-50	<90	dwarf shrub barrens	5-25	<30

Table 53.2

Distribution of some vascular species by bioclimatic zone, High Arctic Islands

	Bioclimatic Zone			
	4	3	2	1
Woody species				
Salix arctica	*	*	l	-
Salix polaris ssp. **pseudopolaris**	r	-	-	-
Dryas integrifolia	*	*	l	-
Cassiope tetragona	l	r	-	-
Vaccinium uliginosum	r	-	-	-
Major wetland species				
Alopecurus alpinus	*	*	*	*
Arctagrostis latifolia	*	l	-	-
Dupontia Fisheri	*	*	*	l
Hierochloe pauciflora	l	-	-	-
Carex aquatilis var. **stans**	*	*	l	-
Carex membranacea	r	-	-	-
Eriophorum angustifolium	l	-	-	-
Eriophorum triste	*	*	l	-
Eriophorum vaginatum	r	-	-	-
Emergent marsh species				
Arctophila fulva	*	-	-	-
Pleuropogon Sabinei	*	*	l	-
Caltha palustris	*	-	-	-
Ranunculus hyperboreus	*	*	-	-
Ranunculus Gmelini	l	-	-	-
Halophytic species				
Puccinellia phryganodes	*	*	l	r
Stellaria humifusa	*	l	-	-
Senecio congestus	l	-	-	-
Vascular cryptogams				
Cystopteris fragilis	l	-	-	-
Dryopteris fragrans	l	-	-	-
Woodsia glabella	l	-	-	-
Equisetum arvense	l	-	-	-
Lycopodium Selago	l	-	-	-
Tundra species and unusual colonizers of disturbed areas				
Agropyron latiglume	l	r	-	-
Deschampsia brevifolia	*	l	-	-
Hierochloe alpinus	l	-	-	-
Trisetum spicatum	l	r	-	-
Melandrium affine	l	r	-	-
Melandrium apetalum	*	l	r	-
Melandrium triflorum	l	-	-	-
Ranunculus pedatifidus	l	-	-	-
Erysimum Pallasii	l	-	-	-
Lesquerella arctica	l	-	-	-
Chrysosplenium tetrandrum	l	-	-	-
Saxifraga Hirculus	*	l	r	-
Geum Rossii	*	-	-	-
Potentilla pulchella	l	-	-	-
Potentilla rubricaulis	l	-	-	-
Potentilla Vahliana	*	r	-	-
Astragalus alpinus	l	-	-	-
Oxytropis arctobia	l	-	-	-
Oxytropis Maydelliana	*	-	-	-
Epilobium latifolium	l	r	-	-
Androcaceae septentrionalis	l	-	-	-
Armeria maritima	r	-	-	-
Polemonium borealis	r	-	-	-
Pedicularis arctica	*	l	-	-
Pedicularis capitata	l	r	-	-
Pedicularis hirsuta	l	-	-	-
Pedicularis sudetica	l	-	-	-
Campanula uniflora	r	-	-	-
Arnica alpina	l	r	-	-
Crepis nana	r	-	-	-
Erigeron compositus	l	-	-	-
Erigeron eriocephalis	l	-	-	-
Petasites frigidus	l	r	-	-
Taraxacum hyparcticum	l	r	-	-
Taraxacum lacerum	r	-	-	-
Taraxacum phymatocarpum	l	r	-	-

r = rare; l = local; * = common; - = absent

Xeric and mesic sites have a herbaceous flora similar to that of comparable sites in zone 1, although the per cent cover and diversity of herbs are greater. A component (less than 2% cover) of small dwarf shrubs, consisting of **Salix** and **Dryas**, distinguishes this zone from zone 1.

In the wetlands grasses are dominant, but sedges and cottongrass occur at some sites. The only emergent marsh species, semaphore grass (**Pleuropogon Sabinei**), grows at the edges of some ponds and lakes.

As in zone 1, halophytic communities consist of **Puccinellia phryganodes** and **Cochlearia** but these species are somewhat more common here and occur sporadically on coastal sediments. A number of typical arctic species are absent from the flora of zone 2, most notably arctic heather, bilberry, numerous sedge and cottongrass species, vascular cryptogams, and many forbs and grasses.

Zone 3

The vascular flora of zone 3 consists of between 60 and 100 species. Continuous vegetation is more common than in zones 1 and 2 although it is generally restricted to lower slopes, valley bottoms, and areas adjacent to ponds and lakes. This zone is readily distinguished by the prevalence of dwarf shrubs on xeric and mesic sites. Persistent snowbeds are less common.

Xeric sites are vegetated by dwarf willow (**Salix arctica**) and mountain avens (**Dryas integrifolia**), the latter being confined to weakly to moderately calcareous materials. Total vegetation cover reaches 15% (locally 25%), with herbaceous species (usually herbs found on similar materials as in zones 1 and 2) reaching only 5% cover; however, herbs may be more common locally. As in zones 1 and 2, a lower stratum is generally absent, although mosses may occur beneath and adjacent to dwarf shrub branches.

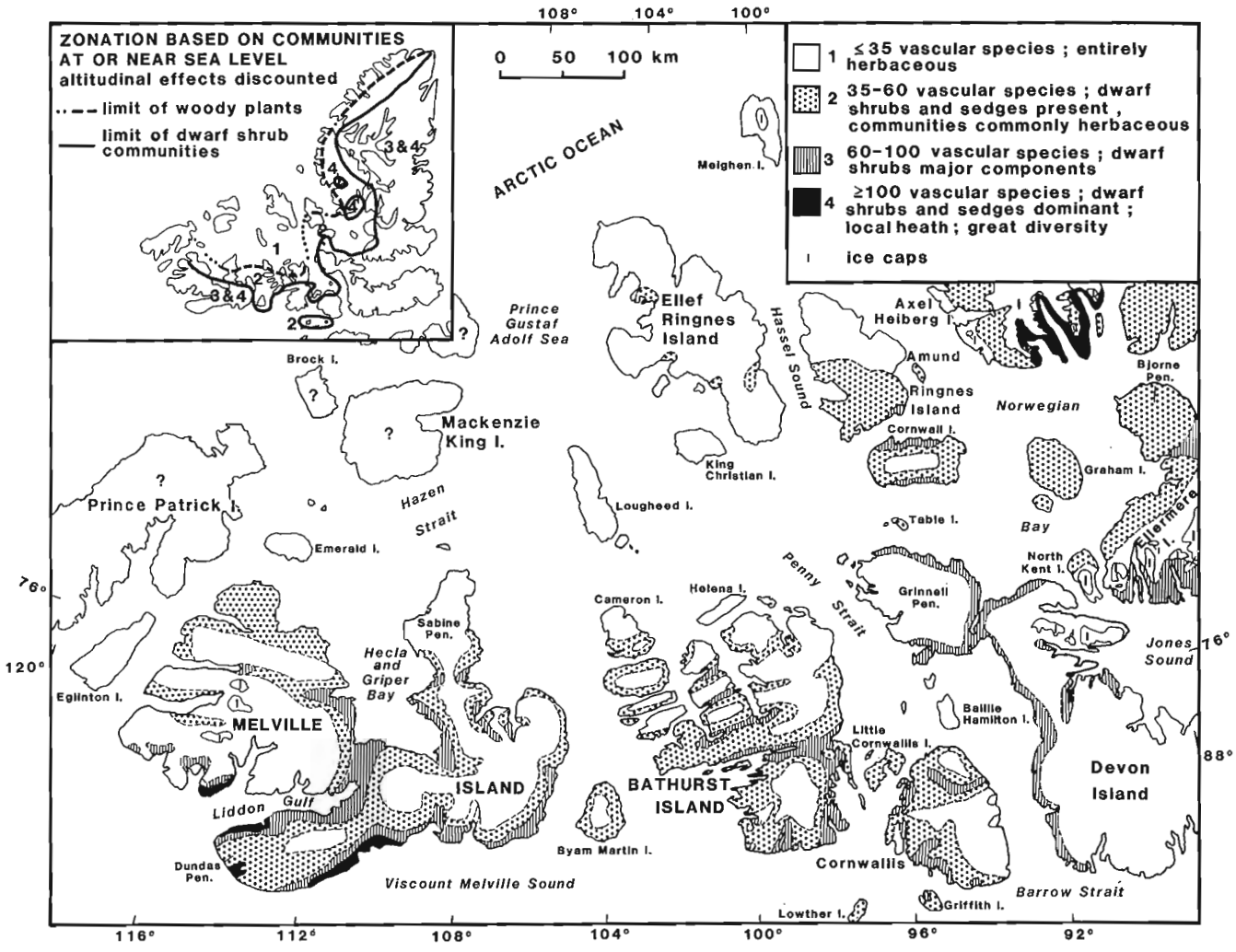

Figure 53.2. Bioclimatic zonation of the central Queen Elizabeth Islands and vicinity.

On mesic sites total vascular plant cover reaches 25% and, as on xeric areas, willow and mountain avens are dominant, with herbs as significant associates. A lower stratum may be present and is similar to that described for zone 1. Arctic heather may occur locally in sheltered locations, generally on noncalcareous materials.

Carex aquatilis and **Eriophorum** species are the major components of wetland communities, although grass species are common associates as well. Marsh emergents include the grass **Pleuropogon Sabinei** and, in places, **Ranunculus hyperboreus.** A continuous lower stratum of bryophytes, especially **Drepanocladus** species, occurs on wetlands.

Halophytic communities, consisting of **Puccinellia phryganodes** turf and some mats of **Stellaria humifusa,** occur on many undisturbed coastal sediments. Vascular cryptogams, including the club moss **Lycopodium Selago** and horsetails (**Equisetum arvense** and **E. vaginatum**), occur locally on sandy materials.

Zone 4

At least 100 vascular plant species are found in zone 4 which has the richest vegetation in the High Arctic. Vegetation is commonly continuous on mid to lower slopes and in valley bottoms on all materials capable of supporting vegetation. Persistent snowbeds rarely last through mid August.

Xeric sites have vegetation similar to that of zone 3; however vascular plant cover commonly reaches 25%, because of an increase in dwarf shrub cover.

Mesic sites are also dominated by dwarf shrubs, as in zone 3, with up to 50% vascular plant cover. In some areas a thin patina, with bryophytes in cracks and depressions, makes the vegetation cover nearly continuous (50-75%). Local thickets of arctic heather occur in sheltered locations on noncalcareous materials. Legumes, **Geum Rossii,** Compositae, and Cyperaceae (e.g., **Carex, Kobresia,** and **Eriophorum**) are common.

Wetlands include a variety of sedges and grasses, with cover up to 25%, and a continuous bryophytic lower stratum. Willow may occur locally on some raised moss hummocks. Marsh emergents include **Caltha palustris, Arctophila fulva, Ranunculus Gmelini,** as well as those emergents found in zone 3.

Halophytic communities are similar to those of zone 3; in some sheltered lagoons, **Senecio congestus** occurs. Vascular cryptogams are more common and diverse than in zone 3; ferns occur in some areas but generally are rare. Herbs are diverse and many species common to low and mid arctic tundra communities make rare appearances in this zone (Table 53.2), generally in specialized niches such as stablized eolian deposits and recently deposited alluvium.

Table 53.3

Selected climatological data from weather stations in the Queen Elizabeth Islands, 1948-1970[1]

Location (cf. Fig. 53.1)	Average length of melt season (days)[2]	Days of frost[3]	Mean daily temperature °C		
			July	Maximum, July	Annual
Resolute, Cornwallis Island	96	321	4.3	6.9	-16.4
Eureka, Ellesmere Island	100	299	5.5	8.5	-19.4
Isachsen, Ellef Ringnes Island	86	338	3.3	5.7	-19.0
Mould Bay, Prince Patrick Island	-	332	3.7	6.2	-17.8
Alert, Ellesmere Island	92	336	3.9	6.9	-18.0
Rea Point, Melville Island	-	-	4.7	7.4	-17.4
Polar Bear Pass, Bathurst Island (summers, 1971-76)[4]	-	-	4.4	7.1	-
Bache Peninsula, Ellesmere Island (1930-33)[4]	-	-	5.0	8.9	-15.6
Meighen Island Ice Cap (1960-62; 1968-70)[4]	-	-	0.6	-	-

[1]Atmospheric Environment Service, 1975

[2]Days with daily maximum temperature above 0°C

[3]Days with daily minimum temperature of 0°C or lower

[4]Maxwell, 1980

Regional Distribution of Vegetation Zones

Figure 53.2 shows the four bioclimatic zones in the central Queen Elizabeth Islands. The regional picture shows only a weak correlation of the zones with latitude; on the other hand, a strong correlation exists with elevation, as revealed by the prevalence of zone 1 vegetation in the central (higher) parts of the more southern islands. Furthermore, this zonation also occurs at an extremely local level downslope from snowbeds. This latitudinal, altitudinal, and local bioclimatic zonation is discussed below and some comparisons are made with vegetation of the eastern Queen Elizabeth Islands.

Altitudinal Zonation

Bioclimatic zonation shows strong altitudinal control. On Dundas Peninsula, Melville Island, where all four zones occur, zone 4 occurs locally at elevations of less than 50 m a.s.l.; zone 3 from near sea level to 75 m; zone 2, which covers much of the plateau, up to 150 m; and zone 1 occupies the highest, most continental part of the peninsula (Fig. 53.2). Similar altitudinal differences occur in the rest of the central Queen Elizabeth Islands, although the elevation of the zone boundaries varies from island to island. The plateaus and highlands above 150 m of the more southerly islands invariably have zone 1 vegetation. In the northern part of the region, zone 1 vegetation occurs at 50 m or less, and on some islands, such as Lougheed (Edlund, 1980) and northern Amund Ringnes (Hodgson and Edlund, 1978), zone 1 vegetation exists at sea level. Floristic data on King Christian Island (less than 35 vascular species, no woody plants collected) (Bell and Bliss, 1977) and Meighen Island (Kuc, 1970) confirm that these islands also lie entirely within zone 1.

Beschel's (1970) zonation of the eastern Queen Elizabeth Islands shows similar increasing depauperization with increasing elevation. He speculated that the altitudinal limit for vascular plants on these islands occurs roughly at 400 m near the coast and a bit higher inland. His zones of greatest impoverishment occur along the western fringe of Axel Heiberg Island and northwestern Ellesmere Island. This area is near the eastern boundary for my zone 1 in the north-central Queen Elizabeth Islands (see inset Fig. 53.2).

Latitudinal Zonation

When vegetation near sea level is compared on an inter-island and regional basis (to eliminate an altitudinal bias) there is a weak trend towards latitudinal zonation in the central Queen Elizabeth Islands. The richest vegetation, zones 3 and 4, occurs in the southern parts of Melville, Bathurst, Cornwallis, and Cornwall islands and is confined to coastal and lowland areas (Fig. 53.2). Zone 2 is common in the east-central region, around Norwegian Bay near Graham Island, and on Melville Island, Bathurst, and the Cornwallis islands. Zone 1 dominates the northwestern islands of the region, including northern Amund Ringnes, most of Ellef Ringnes (Savile, 1961), Meighen, northern Sabine Peninsula of Melville Island, Lougheed, northernmost Bathurst, and Cameron.

The broad latitudinal trend does not occur in the eastern Queen Elizabeth Islands, however, where zone 3 and 4 vegetation occurs as far north as the northeastern tip of Ellesmere Island. Young (1971) and Beschel (1970) noted this pattern as well. Zonation runs at right angles to latitudinal trends and parallels the north-south trending mountains. Arctic heather thickets are reported at Expedition Fiord and southern Axel Heiberg Island (Beschel, 1970); Waterston and Waterston (1972) and Parker and Ross (1976) reported zone 3 and 4 vegetation on eastern Axel Heiberg Island and Fosheim Peninsula, Ellesmere Island. Zone 3 vegetation occurs even farther north on Ellesmere, at Tanquary Fiord (Brassard and Beschel, 1968), Van Hauen Pass (Brassard and Longton, 1970), and Lake Hazen (Powell, 1961; Savile, 1964; England et al., 1981), and zone 4 vegetation at Alexandra Fiord on eastern Ellesmere Island (Svoboda and Freedman, 1980).

In the central Queen Elizabeth Islands, only parts of southern Melville Island have zone 4 vegetation. The fact that it and the eastern High Arctic islands fall mostly within zones 3 and 4 helps to explain the presence of disjunctive distribution of species such as **Lycopodium Selago, Cystopteris fragilis, Dryopteris fragrans, Hierochloe alpina, Trisetum spicatum, Geum Rossii, Androsaceae septentrionalis,** and **Chrysosplenium tetrandrum,** all of which in the High Arctic occur only in the northeastern Queen Elizabeth Islands and southwestern Melville Island.

Local Zonation

Detailed plant community studies show that vegetation downslope from persistent snowbeds on Cornwallis, Bathurst, and Melville islands exhibit the same trends as the regional bioclimatic zonation. The areas farthest downslope from the snowbed, which still receive abundant meltwater, have the richest flora, whereas vegetation immediately downslope from the snowbed is extremely impoverished, consisting of bryophytes, lichens, and only a few herbs, even though the materials are as wet as those below. The plant communities grade sharply from great diversity to great poverty, for example, from a willow-sedge-dominated community to a sparse grass community. This rapid change in diversity, which can represent a transition from zone 4 to zone 1 in a short distance, probably reflects the length of time various parts of the slope are snowfree, i.e., length of growing season. This snowbed zonation is described in detail for the calciphilic vegetation of Cornwallis Island (Edlund, in press). In regions characterized by zone 4 vegetation, all four bioclimatic zones may be present downslope from major snowbeds. Farther north of course only those zones more impoverished than the regional vegetation occur in these local anomalous positions.

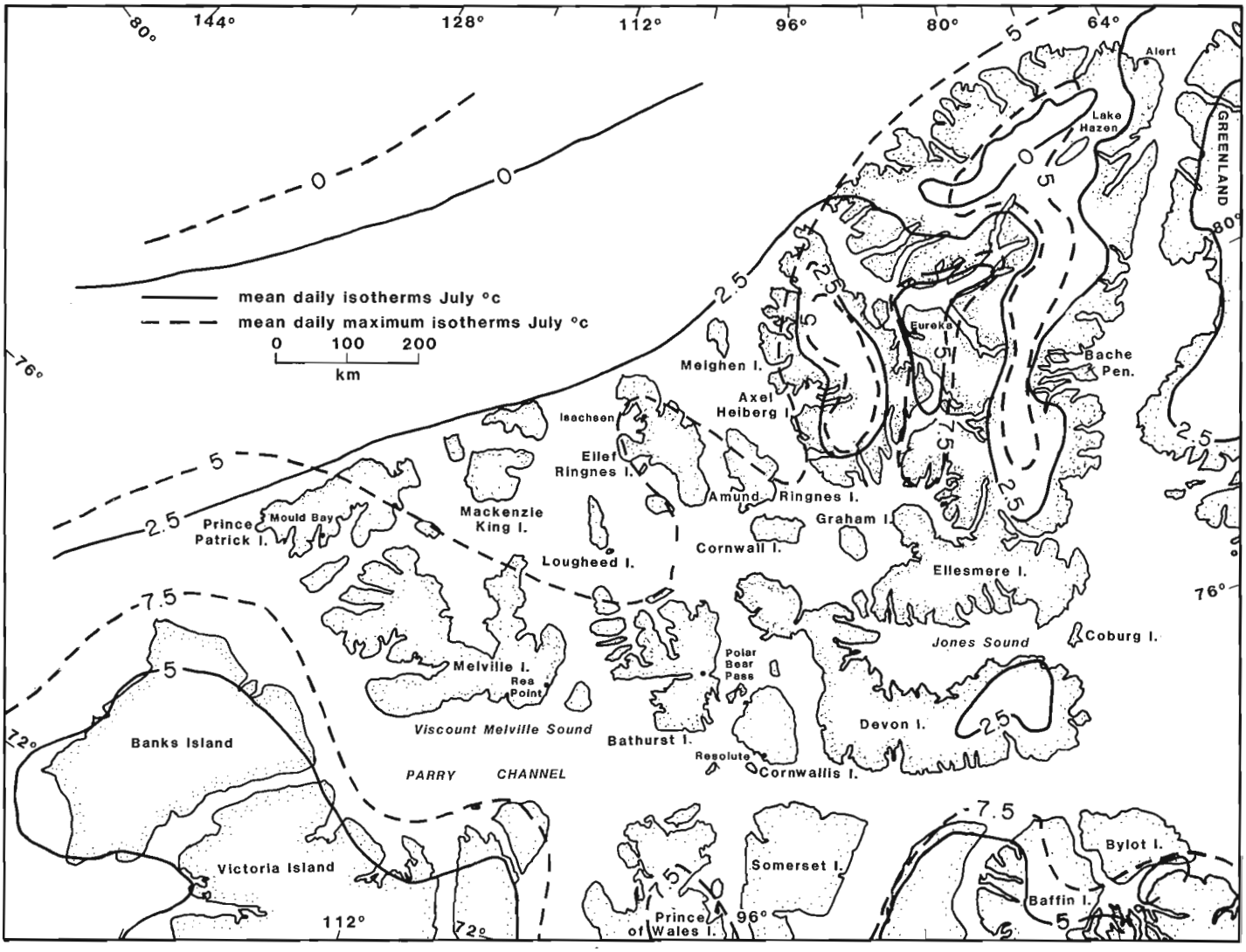

Figure 53.3. Selected isotherms of possible significance to floristic zonation.

Discussion

Climatic Controls

The climatic controls that influence the bioclimatic zonation are not yet understood. Bliss (1974) suggested that moisture availability or desiccation by wind is a major controlling factor; but since annual precipitation is lower in the eastern Queen Elizabeth Islands, where zones 3 and 4 predominate, than in the central region (Maxwell, 1980), moisture availability is probably not the major climatic control of zonation. The sparse climatic data available for the Arctic Islands (Maxwell, 1980) do reveal regional climatic trends that parallel those of the vegetation. For example, the eastern Queen Elizabeth Islands, where zones 3 and 4 prevail, are warmer and have longer growing seasons than the central and northwestern Queen Elizabeth Islands, even though mean temperatures are low (see data for Eureka, Table 53.3).

The reversed L-shaped patterns of circumpolar vegetation zones in the Arctic Islands (see inset, Fig. 53.2) as shown by this study, as well as by Young (1971) and Aleksandrova (1970, 1980), also match other climatic parameters mapped by Maxwell (1980), such as persistence of snow, mean daily summer maximum and mean annual temperatures, and thawing degree-days.

Vegetation downslope from snowbeds in an environment in which moisture is available throughout the growing season shows definite zonal stratification similar to regional zonation, which suggests that moisture availability is not the limiting factor, at least not at wet and mesic sites. The controlling factor is probably best expressed in growing degree-days or the length of the growing season on a local scale. In the High Arctic, where summer lasts for less than 2.5 months, the persistence of regional snow cover a week or two longer in spring and its reappearance a week or two earlier in August would curtail the growing season in a fashion similar to that of local, persistent snowbeds, which sequentially expose the surface as their margins retreat.

The limit of dwarf shrubs – the boundary between zone 1, which is entirely herbaceous, and zone 2, which has scattered dwarf shrubs – forms a 'mini-treeline' that delimits the northernmost extent of woody plants in northern Canada. Zones 3 and 4, where dwarf shrubs are the dominant vascular plant component, form what is here called a 'mini-forest zone'.

Such analogies, particularly the one to regional treeline, are appropriate in this treeless environment, for treeline (northernmost limit of the tree life-form), and the limit of the northern boreal forest (where trees are the dominant plants) are biological boundaries long observed to coincide either directly or indirectly with various isotherms.

Köppen (1936) showed that the northern limit of trees roughly corresponded with the 10°C mean July isotherm; Nordenskjöld (in Nordenskjöld and Mecking, 1928) suggested that for the northern hemisphere, the mean July 10°C isotherm does coincide closely with the limit of tree growth in continental climates but is less accurate in maritime environments; Bird (1967) showed similarities between the -7°C mean annual isotherm and treeline.

Other isotherms have been suggested as significant boundaries within the polar regions. Nordenskjöld and Mecking (1928) proposed that the mean July 5°C isotherm coincides with the limit of bushes (erect and semi-erect shrubs), the southern limit of high arctic vegetation, and the northern limit of continuous vegetation. As this isotherm falls to the south of the central Queen Elizabeth Islands, it cannot be applied to the study area. However the 5°C isotherm does occur in a pocket around Eureka, Ellesmere Island (Fig. 53.3) and no bushes have been observed.

In the High Arctic, zone 1 corresponds to the zone of coolest temperatures and the shortest growing season. Only herbs tolerate this severe climate. Woody plants, sedges, and herbs, more typical of the Low and Mid Arctic regions, appear to require the longest growing seasons, for they grow in those parts of the Queen Elizabeth Islands with the warmest summer temperatures. Thus it seems likely that the vegetation zones coincide with thermal balance rather than moisture.

Possible Congruency of Vegetation with Isotherms

Although climatic data are limited for the region, it is still possible to speculate on possible thermal constraints on vascular plants. These comparisons are extremely speculative and physiological control is not likely to be as simplistic as isothermal control (Larsen, 1974; Wardle, 1974); however, these are offered as suggestions as to areas where future multidisciplinary investigations may be beneficial.

Figure 53.3 shows the mean daily and mean maximum daily isotherms for July, the warmest month (cf. Table 53.3). The 0°C isotherm, which marks the limit of plant growth because it approximates the zone in which the ground is permanently frozen, lies to the north and west of the Queen Elizabeth Islands except in the vicinity of the ice caps on Ellesmere Island. Even the 2.5°C isotherm lies to the north and west of most islands, except in the vicinity of ice caps. The 5°C isotherm lies south of Parry Channel, except for the Eureka area (Ellesmere Island), which is an oasis of warmth. The islands that form the northern rim of the Queen Elizabeth Islands all have a vascular plant component to their plant communities (Porsild, 1964). Thus the limit of vascular plants seems to coincide with an mean daily isotherm (July) marginally greater than 2.5°C. Areas with no vascular plants occur only in the mountainous regions of Axel Heiberg and Ellesmere islands, close to present day ice caps and permanent snowfields (Beschel, 1970), in highlands of northern Bathurst and Melville islands, and locally near the base of persistent snowbeds.

The only weather station close to the 'mini-treeline' is Isachsen, Ellef Ringnes Island, which has a mean daily temperature for July of 3.3°C, and sporadic willow growing in sheltered locations (Savile, 1961). The other stations with long term weather data – Resolute, Alert, Rea Point, and Polar Bear Pass – all have dwarf shrub dominated communities in the vicinity, and all have mean daily (July) temperatures of 3.9°C or greater (Table 53.3). The sites lie well within the limit of woody growth. The mean daily (July) isotherm coincident with dwarf shrub survival ('mini-treeline') seems to be one of less than 4°C, perhaps between 3 and 3.5°C; the isotherm coincident with the 'mini-forest' line is less than 4°C but greater than 3.5°C.

The richest vegetation, in areas of the Queen Elizabeth Islands that have weather statistics, occurs at Eureka and Bache Peninsula, Ellesmere Island, both of which have a mean daily July temperatures greater than 5°C. While Nordenskjöld (Nordenskjöld and Mecking, 1928) suggested that the 5°C isotherm is coincident with the limit of erect shrub growth, this hypothesis cannot be tested in the Queen Elizabeth Islands because the woody species that have a potential for erect growth (**Salix alexensis, S. lanata, S. cordifolia,** and **S. niphoclada**) do not occur in the area (Porsild and Cody, 1980).

The isotherms possibly coincident with vascular plant growth, the 'mini-treeline' and the 'mini-forest' line fall within a narrow range of mean daily July temperatures of greater than 2.5°C and less than 4°C. This suggests that a small change in mean summer temperature, a fraction of a degree, could have major effects on plant community composition.

Summary

The islands of the High Arctic can be divided into four vegetation zones which cross lithological boundaries. These zones may eventually be helpful in the prediction of high arctic climate in more detail than is possible from the limited number of meteorological stations presently operating in the region. These zones are based on vascular plant physiognomy and floristics, e.g. the presence, diversity, and abundance of woody species, Cyperaceae, emergent marsh species, vascular cryptogams, halophytic species, and a number of indicator species, as well as comparisons of the total number of vascular species present.

Zone 1 represents the region with the most depauperate flora; its vascular flora is entirely herbaceous, and the total number of species is generally less than 35. Zone 2, having between 35 and 60 vascular species, is also primarily herbaceous but includes small amounts of dwarf shrubs. The boundary between zones 1 and 2 may be regarded as a 'mini-treeline' within the Canadian High Arctic. Zone 3, having 60 to 100 vascular species and a major component of dwarf shrubs and Cyperaceae, comprises a 'mini-forest zone' together with zone 4. Zone 4, which has the richest and most diverse flora, occurs only on southwestern Melville Island in the central High Arctic but is more common in the eastern Queen Elizabeth Islands.

This bioclimatic zonation, based on vegetation patterns, is roughly correlated with regional climatic trends and as such may have predictive value. Present data indicate that the mean daily July temperature for the limit of vascular plant growth is a little above 2.5°C, for woody plants is 3°-3.5°C, and for dwarf shrub communities, is 3.5°-4°C.

The 'mini-treeline' and the 'mini-forest zone' are also biological markers that nonbotanists can easily identify and hence may assist in further refining of vegetation zone boundaries.

Acknowledgments

This work was greatly assisted over the years by logistical support from Polar Continental Shelf Project, and by field officers of Terrain Sciences Division, particularly D.A. Hodgson, D.M. Barnett, J-S. Vincent, and M.F. Nixon, who contributed numerous botanical observations from sites I did not visit, and provided base camps from which to operate. J.V. Matthews, Jr. critically reviewed the manuscript. Much appreciation is given to all.

References

Aleksandrova, V.
1970: The vegetation of the tundra zones in the USSR and data about its productivity; in Proceedings, Conference on Productivity and Conservation in Northern Circumpolar Lands, ed. W.A. Fuller and P.G. Kevan, Edmonton, Alberta, 1969; International Union for the Conservation of Nature and Natural Resources, Morges, Switzerland, p. 93-114.

1980: The Arctic and Antarctic: Their Division into Geobotanical Areas (translated by D. Love); Cambridge University Press, England, 247 p.

Atmospheric Environment Service
1975: Canadian Normals, Volume 1-SI, Temperature, 1941-1970; Environment Canada, Downsview, Ontario.

Babb, T.A. and Bliss, L.C.
1974: Susceptibility of environmental impact in the Queen Elizabeth Islands; Arctic, v. 27, no. 3, p. 234-237.

Barnett, D.M., Edlund, S.A., Dredge, L.A., Thomas, D.C., and Prevett, L.S.
1975: Terrain classification and evaluation, Melville Island, N.W.T.; Geological Survey of Canada, Open File 252, scale 1:125 000.

Bell, K.L. and Bliss, L.C.
1977: Overwinter phenology of plants in a polar semi-desert; Arctic, v. 30, no. 2, p. 118-121.

Beschel, R.E.
1969: Floristic relations of the Nearctic Islands (translated by Canada, Secretary of State); Botanicheski Zhurnal, v. 54, p. 872-891.

1970: The diversity of tundra vegetation; in Proceedings, Conference on Productivity and Conservation in Northern Circumpolar Lands, ed. W.A. Fuller and P.G. Kevan, Edmonton, Alberta, 1969; International Union for Conservation of Nature and Natural Resources, Morges, Switzerland, p. 85-92.

Bird, J.B.
1967: The Physiography of Arctic Canada, with Special Reference to the Area South of Peary Channel; Johns Hopkins Press, Baltimore, Maryland, 336 p.

Brassard, G.R. and Beschel, R.E.
1968: The vascular flora of Tanquary Fiord, northern Ellesmere Island, N.W.T.; Canadian Field-Naturalist, v. 82, p. 103-113.

Brassard, G.R. and Longton, R.G.
1970: The flora and vegetation of Van Hauen Pass, northwestern Ellesmere Island; Canadian Field-Naturalist, v. 84, p. 357-364.

Edlund, S.A.
1980: Vegetation of Lougheed Island, District of Franklin; in Current Research, Part A, Geological Survey of Canada, Paper 80-1A, p. 29-333.

1982a: Vegetation of Melville Island, District of Franklin, N.W.T.; Geological Survey of Canada, Open File 852, scale 1:250 000.

1982b: Vegetation of the Cornwallis Island area, District of Franklin, N.W.T.; Geological Survey of Canada, Open File 857, scale 1:250 000.

– Vegetation of Cornwallis and adjacent islands, District of Franklin: Relationships between vegetation and surficial materials; Geological Survey of Canada. (in press)

England, J., Kershaw, L., LaFarge-England, C., and Bednarski, J.
1981: Northern Ellesmere Island, a natural resource inventory; Report submitted to Parks Canada, Environment Canada, Ottawa, 237 p.

Hodgson, D.A. and Edlund, S.A.
1975: Surficial materials and biophysical regions, eastern Queen Elizabeth Islands, Part 1; Geological Survey of Canada, Open File 265, scale 1:125 000.

1978: Surficial materials and vegetation, Amund Ringnes and Cornwallis islands, District of Franklin; Geological Survey of Canada, Open File 541, scale 1:125 000.

Köppen, W.
1936: Das geographische system der klimate; in Handbuch der Klimatologie, Volume 1, ed. W. Koppen and R. Seiger, Borntrager, Berlin, 44 p.

Kuc, M.
1970: Vascular plants from some localities in the western and northern parts of the Canadian Arctic Archipelago; Canadian Journal of Botany, v. 48, no. 11, p. 1931-1938.

Larsen, J.A.
1974: Ecology of the northern continental forest border; in Arctic and Alpine Environments, ed. J.D. Ives and R.G. Barry; Methune, England, p. 341-369.

Maxwell, J.B.
1980: The climate of the Canadian Arctic Islands and adjacent waters, Volume 1; Environment Canada, Climatological Studies No. 30, 531 p.

Nordenskjöld, O. and Mecking, L.
1928: The Geography of the Polar Regions; American Geographical Society Special Publication, no. 8, 359 p.

Parker, G.R. and Ross, R.K.
1976: Summer habitat use by muskoxen (**Ovibos moschatus**) and Peary caribou (**Rangifer tarandus pearyi**) in the Canadian Arctic; Polarforschung, v. 46, p. 12-25.

Polunin, N.
1951: The real Arctic: suggestions for its delimitation, subdivision and characterization; Journal of Ecology, v. 39, p. 308-315.

Porsild, A.E.
1964: Illustrated flora of the Canadian Arctic Archipelago; National Museum of Canada, Bulletin 146, 218 p.

Porsild, A.E. and Cody, W.J.
1980: Vascular Plants of the Continental Northwest Territories; National Museums of Canada, Ottawa, 667 p.

Powell, J.M.
1961: The vegetation and microclimate of the Lake Hazen area, northern Ellesmere Island, N.W.T.; Operation Hazen Report 14, Defence Research Board, Ottawa, 12 p.

Savile, D.B.O.
1961: The botany of the northwestern Queen Elizabeth Islands; Canadian Journal of Botany, v. 39, p. 909-942.

1964: General ecology and vascular plants of the Hazen Camp area; Arctic, v. 17, no. 4, p. 237-258.

Svoboda, J. and Freedman, W. (ed.)
1980: Ecology of a High Arctic Lowland oasis, Alexandra Fjord (78°53'N, 75°65'W), Ellesmere Island, N.W.T., Canada; November 1980 Progress Report, Department of Botany, University of Toronto, and Dalhousie University, Halifax, 109 p.

Wardle, P.
1974: Alpine timberline; in Arctic and Alpine Environments, ed. J.D. Ives and R.G. Barry; Methune, London, p. 371-402.

Waterston, G. and Waterston, I.
1972: Report on wildlife, vegetation, and environmental values in the Queen Elizabeth Islands, Ellesmere and part of Axel Heiberg, June 28-August 15, 1972; report to Canadian Wildlife Service, Ottawa, 54 p.

Young, S.B.
1971: Vascular flora of St. Lawrence Island, with special reference to floristic zonation in the arctic regions; Contributions from The Gray Herbarium of Harvard University No. 201, p. 11-115.

PRELIMINARY STUDIES ON GAMMA RAY SPECTRAL LOGGING IN EXPLORATION FOR GOLD

Project 740085

C.J. Mwenifumbo, T.I. Urbancic[1], and P.G. Killeen
Resource Geophysics and Geochemistry Division

Mwenifumbo, C.J., Urbancic, T.I., and Killeen, P.G., Preliminary studies on gamma ray spectral logging in exploration for gold; in Current Research, Part A, Geological Survey of Canada, Paper 83-1A, p. 391-397, 1983.

Abstract

Several studies have indicated that the distribution of the naturally occurring radioelements (K, U, Th) can serve as a useful guide to gold deposits. This is because most gold deposits are characterized by wall rock alterations (adularization and sericitization) in which potassium, including the radioactive isotope K-40 is considerably enriched. Theoretically it should be possible to outline areas enriched in potassium by gamma ray spectrometry. Preliminary investigations have been conducted to observe and confirm this gold-potassium correlation and evaluate its usefulness in gold exploration. The distribution of the naturally occurring radioactive elements (K, U, Th) has been determined by gamma ray spectral logging in several boreholes intersecting gold mineralization in the Larder Lake area of Ontario. The orebodies in this area are of two types. The carbonate orebodies consist of irregular lenses of quartz stockworks lying within highly altered and brecciated carbonatized ultramafic rocks. The flow-type orebodies consist of pyritized and silicified zones lying within altered volcanic flows and tuffs. The present work was conducted in the flow-type orebodies. Most gold in this type of orebody is associated with pyrite mineralization. Preliminary gamma ray spectral logging data indicate that, in the Larder Lake area there is not always a definite correlation between high gold values and an increase in potassium content. In some boreholes gold mineralization can be correlated with massive pyritization as well as an increase in potassium content. Logging of boreholes in the quartz-carbonate stockworks seems to indicate that low potassium content is associated with the high gold content. In addition, to complicate matters, in some boreholes gold is found in zones without massive pyritization and without an increase in potassium. It is therefore likely that the distribution of the radioactive element K-40 can only be used as a guide in localizing zones with high gold content if additional information is available (e.g. pyrite content, and rock type). Ratios of the radioelements (Th/K, U/K, U/Th), which have sometimes been used as indicators of halos around certain types of deposits, could not be computed due to poor counting statistics in the U and Th spectral windows.

Introduction

In a conventional geophysical exploration program one tends to use techniques that will directly detect the physical properties of the target being sought. This direct approach is not applicable in gold exploration. Gold is present in its deposits in such small amounts that it is difficult to detect any changes in the physical properties of the host rock due to its presence. As a result, geophysical techniques have not been used in the direct detection of the element. Many types of gold deposits, particularly those in volcanic rocks and intrusive rocks are characterized by hydrothermal alteration zones which possess measurable physical properties. One important type of alteration is potassium metasomatism. This includes adularization where there is an increase in potassium feldspar (adularia) and also sericitization, where there is an increase in muscovite. In potassium metasomatism there is an increase in the element potassium which includes the radioactive isotope potassium-40. The second major type of alteration is pyritization. Pyrite is the second most abundant mineral associated with gold deposits, being exceeded only by quartz. The third type of alteration that is of geophysical significance is silicification.

It is theoretically possible to use gamma ray spectrometric methods to outline zones enriched in potassium and to use Induced Polarization (IP) and resistivity to outline areas of pyritization and silicification. The present study focuses on the possibility of using gamma ray spectrometry to outline zones of potassium alteration which may be related to gold mineralization.

Few surveys involving the use of gamma ray spectrometers have been carried out with the aim of prospecting for gold deposits in North America (Gross, 1952; Tihor and Crocket, 1975; Thomson, 1980). However, there have been a number of reports from Russia on the use of airborne and ground gamma ray spectrometric surveys in the search for gold. Ostrovskiy et al. (1970) and Portnov et al. (1971) reported on the use of airborne gamma ray spectrometric methods in mapping zones of potassium alteration which are associated with gold occurrences. Other studies on the use of gamma ray spectral methods as a technique for gold exploration have been reported by Blyumentsev et al. (1974), Balykin et al. (1973), Krendelev et al. (1976), and Fel'dman et al. (1975). In general they all found a strong association between gold mineralization and potassium alteration zones.

An attempt was made to determine the distribution of the radioactive elements, potassium, uranium and thorium by gamma ray spectral logging of several boreholes intersecting gold mineralization at the Kerr-Addison property in the Larder Lake area of Ontario. The object of the investigation was to evaluate any correlation between gold and concentrations of these elements, particularly potassium.

Geology and Type of Mineralization

The major rock types that host the gold in the Larder Lake area are Precambrian mafic volcanic rocks and associated volcanogenic sediments belonging to the

[1] Department of Geology, University of Toronto

Timiskaming and Larder Lake groups. The two main types of gold orebodies are the carbonate associated type and the flow-type. The carbonate type consists of irregular lenses of quartz-carbonate stockwork lying within highly altered and brecciated ultramafic rocks and related to the Larder Lake fault zone while the flow-type orebodies lie within hydrothermally altered volcanic flows and tuffs. The data presented in this report were collected in flow-type orebodies. Gold in this environment occurs in scattered sulphide bodies which replace either flows, flow breccia or tuffs and also in the quartz-carbonate stockworks within the flows. Sulphide mineralization comprises pyrite, pyrrhotite and minor amounts of chalcopyrite. The type of potassic alteration in these Precambrian volcanic rocks takes the form of sericitization (Boyle, 1979; Downes, 1981).

Field Equipment

The boreholes were logged with the Geological Survey of Canada (GSC) research and development borehole spectral logging system which has been described by Bristow (1979). This full spectral digital recording system is based on a NOVA minicomputer. Data were recorded every second (normal sample time at a logging speed of 3 m/minute) on nine-track magnetic tape in 256 channels covering a gamma ray energy range from approximately 0.2 MeV to 3.0 MeV. Gamma ray counts in ten selected energy windows in the spectrum were also accumulated and recorded on tape. The four standard windows used in the data analysis include the potassium window centred on the potassium-40 gamma ray peak at 1.46 meV, the uranium window centred on the 1.76 MeV gamma ray emissions of bismuth-214 in the uranium decay series, and the thorium window centred on the 2.62 MeV gamma ray peak from thallium-208 in the thorium decay series. The fourth window, the total count window, covers a wide energy range between 0.4 MeV to 3.0 MeV and is used to monitor the overall levels of radioactivity. Logs of any selected energy windows in the spectrum, are displayed on a multipen chart recorder during the data acquisition. The acquisition of the complete spectra makes it possible to re-window the data in subsequent processing to produce new logs for any desired energy region. The scintillation detector that was used in the present work was a 32 x 125 mm cesium iodide (CsI(Na)) detector.

Calibration of the Gamma Ray Spectral Logging System

In order to accurately determine the radioelement concentrations from the observed gamma ray spectral data, it is essential that the logging equipment be properly calibrated. Spectral logs must be

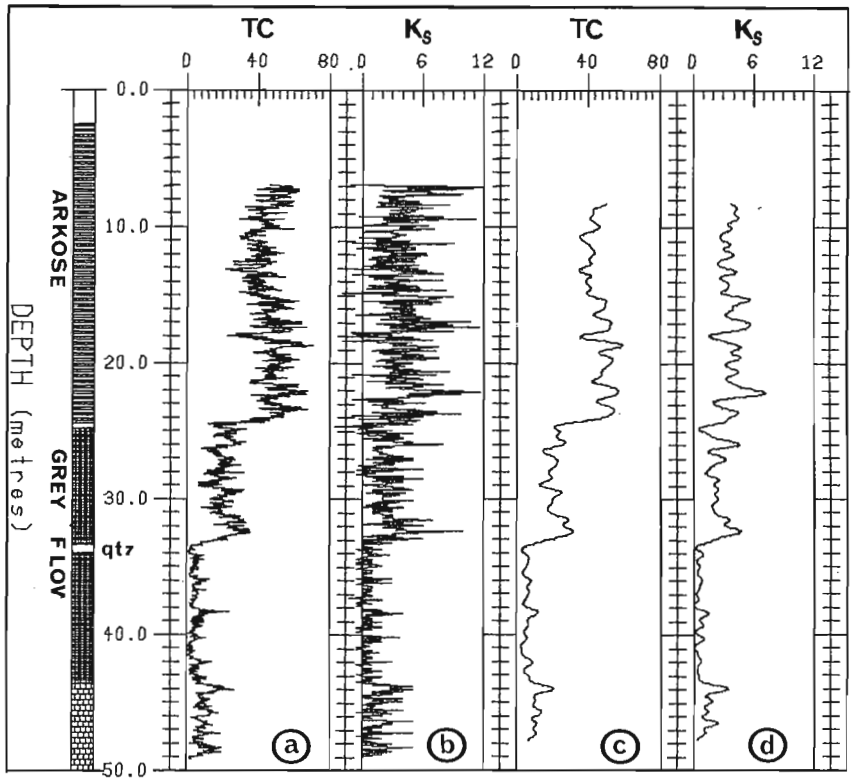

Figure 54.1. Total count (TC) and stripped K logs recorded in borehole BL-80-47 with a 32 mm x 125 mm CsI(Na) detector, logging veolocity v = 3 m/minute and a sample time of 1 second. Unsmoothed logs are shown in Figures 54.1a-b. Figures 54.1c-d show logs after the application of a 15-point least-squares smoothing operator. Gamma ray intensities are in counts per sample time (in this case counts per second).

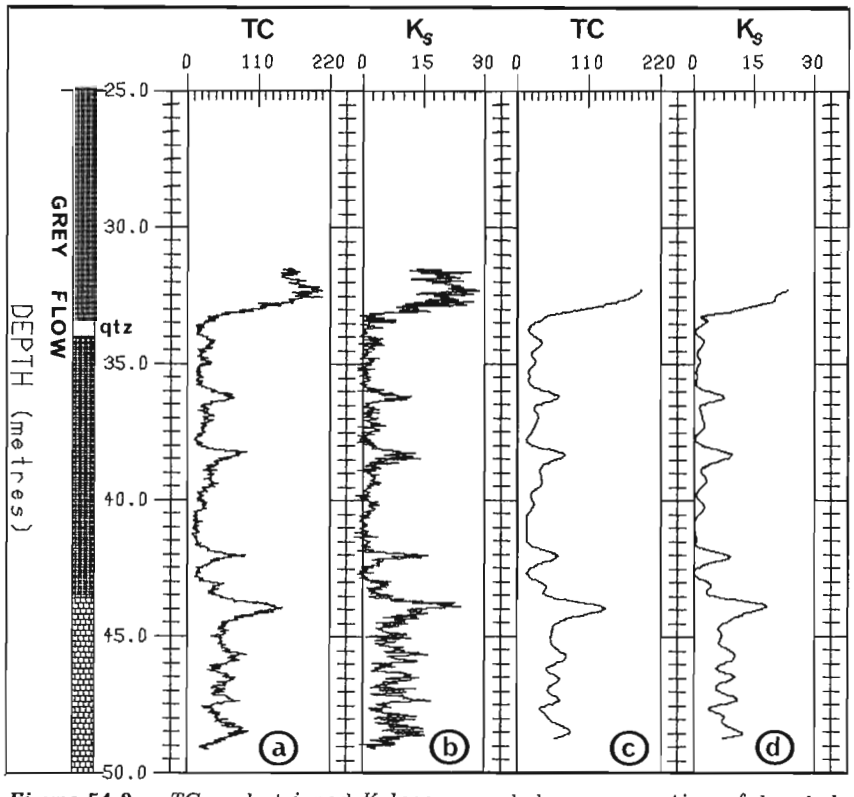

Figure 54.2. TC and stripped K logs recorded over a section of borehole BL-80-47 with a 32 mm x 125 mm CsI(Na) detector, a slow logging velocity v = 0.3 m/minute and a sample time of 6 seconds. Raw TC and unsmoothed stripped K logs are shown in Figure 54.2a-b. Figures 54.2c-d show logs after the application of a 15-point least-squares smoothing operator. Gamma ray intensities are in counts per sample time (i.e. counts per 6 seconds).

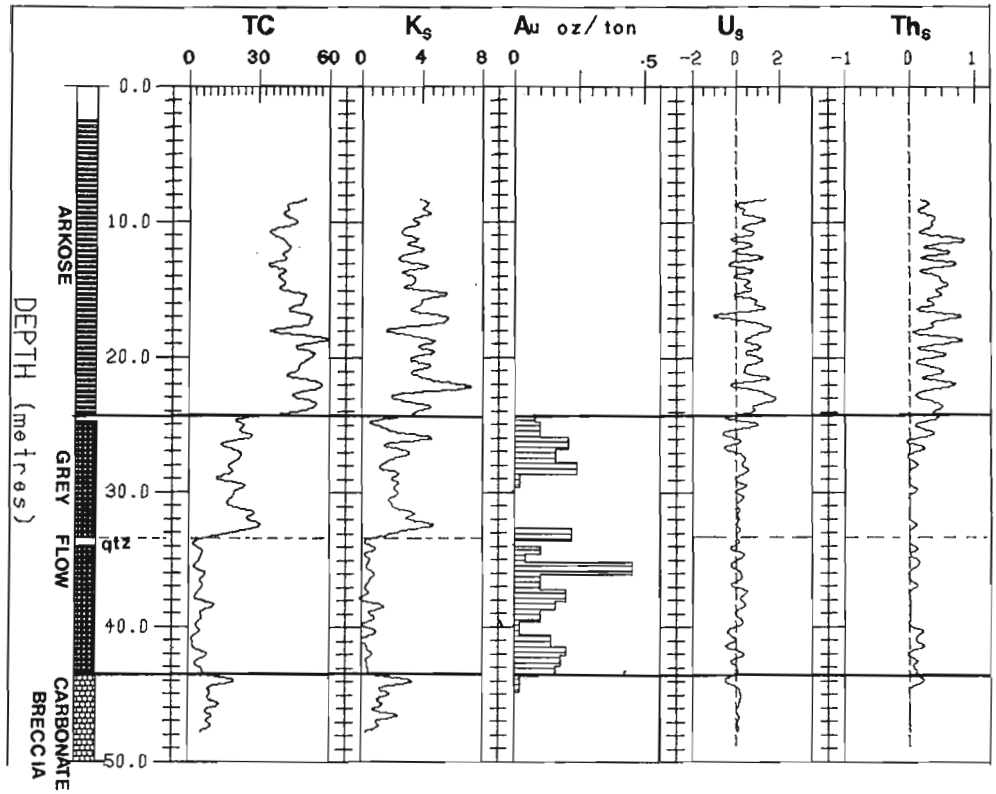

Figure 54.3. TC, stripped K, U and Th logs recorded in borehole BL-80-47 using a 32 mm x 125 mm CsI(Na) detector, logging velocity v = 3 m/minute and a sample time of 1 second. A 15-point smooth has been applied to the logs. Gamma ray intensities are in counts per sample time. Also shown is the gold assay log.

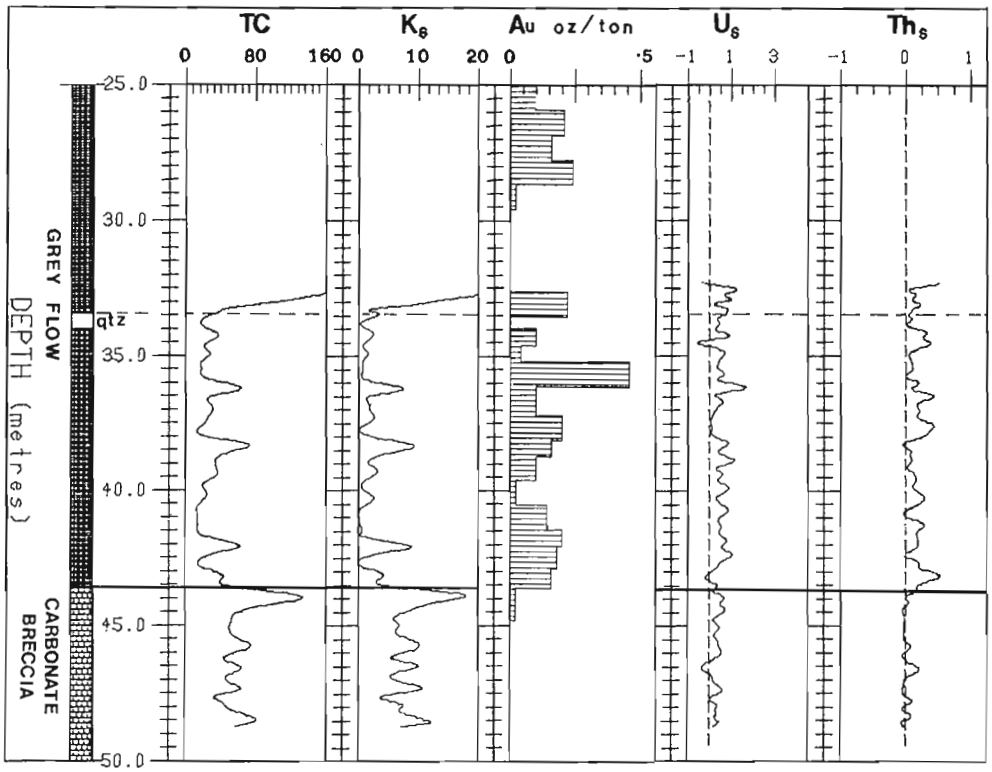

Figure 54.4. TC, stripped K, U and Th logs recorded over a section of borehole BL-80-47 using a 32 mm x 125 mm CsI(Na) detector, a slow logging velocity v = 0.3 m/minute and a sample time of 6 seconds. A 15-point smooth has been applied to the logs. Gamma ray intensities are in counts per sample time. Also shown is the gold assay log.

corrected for interference of gamma rays originating from different radioelements. Ambiguities may arise in the interpretation of spectral data if the data are not corrected. For example, a high concentration of thorium, will cause anomalously high count rates to be observed in both the potassium and the uranium window as well as the thorium window. Some gamma rays originating from the thorium decay series will be counted in the uranium and potassium windows. This is partly due to the gamma rays scattering and being degraded in energy as they pass through the source rock and the detector, and partly due to the low energy gamma rays from the many daughter radioelements in the thorium decay series. The stripping ratios, to correct for this, are determined from measurements made in model boreholes such as those constructed in Ottawa (Killeen and Conaway, 1978). The model holes contain zones of known concentrations of potassium, uranium and thorium. The other calibration factors that are also determined from model holes are called sensitivities. These are used for deriving the concentrations of the radioelements from the observed and corrected gamma ray intensities. The logging system was calibrated in the Ottawa model boreholes before the field trip.

Data Processing

Due to the random nature of the gamma rays being emitted by the radioactive elements at any particular moment, the accumulated counts acquired during gamma ray logging, are subject to high frequency noise due to Poisson counting statistics. For a given detector, the statistical noise on the measured signal is dependent on the level of radioactivity and the counting time. Gamma ray logs obtained in areas of low radioactivity exhibit a large amount of statistical noise, compared to areas of high radioactivity. Also the process of stripping tends to amplify the noise. Consequently a low-pass or smoothing filter must be applied to the raw gamma ray logs to reduce the high frequency noise. All logs presented in this report have been smoothed with a quadratic least-squares smoothing operator (Savitzky and Golay, 1964; Madden, 1978). The gamma ray intensities are given in counts per sample time. Due to the low count rates and hence poor counting statistics in the U and Th windows, the count rates in these windows can effectively average out to zero and

therefore sometimes show negative values after stripping. In addition, the stripped count rates have not been converted to radioelement concentrations in this investigation because the logs must first be deconvolved (Conaway and Killeen, 1978). The poor counting statistics in these windows makes this difficult because deconvolution amplifies the high frequency noise component. In the present study the evaluation of any correlation between the radioelement distribution and gold occurrences based on stripped potassium window count rates, is valid even though the logs have not been deconvolved.

Figure 54.1 illustrates a gamma ray log before and after smoothing. The log was obtained in borehole BL-80-47 using a 32 mm x 125 mm CsI(Na) detector, logging velocity v = 3 m/minute (5 cm/second) and a counting time Δt = 1 second (sample length Δz = 5 cm). Figures 54.1a and b are raw total count (TC) and unsmoothed stripped potassium (K) logs, respectively. Both these logs show the high frequency statistical noise resulting from the short counting time. A 15-point quadratic least-squares smoothing operator was applied to the data and the results are shown in Figure 54.1c and d for the TC and stripped K, respectively. After smoothing it is easy to locate areas with anomalous radioactivity. One way to improve the counting statistics in gamma ray logging is to increase the counting time. If the logging speed is decreased accordingly, there will be no loss of spatial resolution. Figure 54.2 is an example of a gamma ray log obtained over a section of borehole BL-80-47 (31.5-49 m) using a 32 mm x 125 mm CsI(Na) detector, logging velocity v = 0.3m/minute (0.5 cm/second) and counting time Δt = 6 seconds (Δz = 3 cm). It can be seen that there is a significant improvement in the signal to noise ratio with the longer counting time (compare the logs in Fig. 54.1a and b to Fig. 54.2a and b). However there is still considerable statistical scatter in the data. The smoothed logs after applying a 15-point least-square filter operator are shown in Figures 54.2c and d. There is a definite improvement in the log without significant deterioration of the signal.

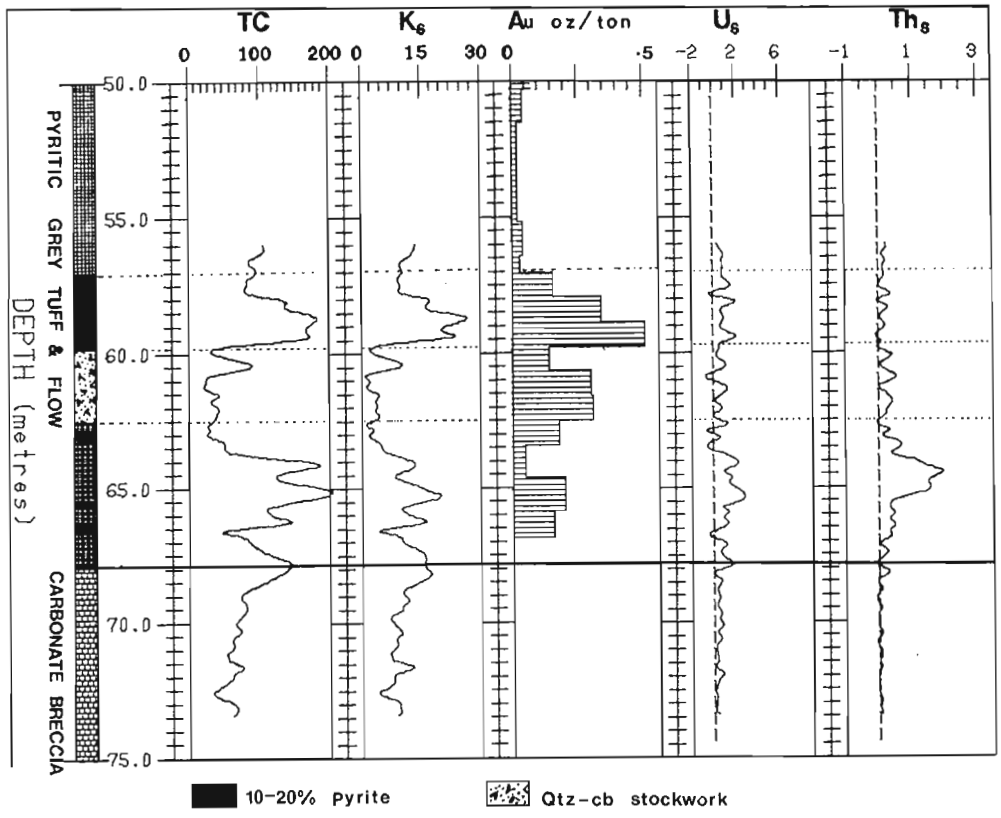

Figure 54.5. TC, stripped K, U and Th logs recorded in borehole BL-80-25 using a 32 mm x 125 mm CsI(Na) detector, logging velocity v = 3 m/minute and a sample time of 1 second. A 15-point smooth has been applied to the logs. Gamma ray intensities are in counts per sample time. Also shown is the gold assay log.

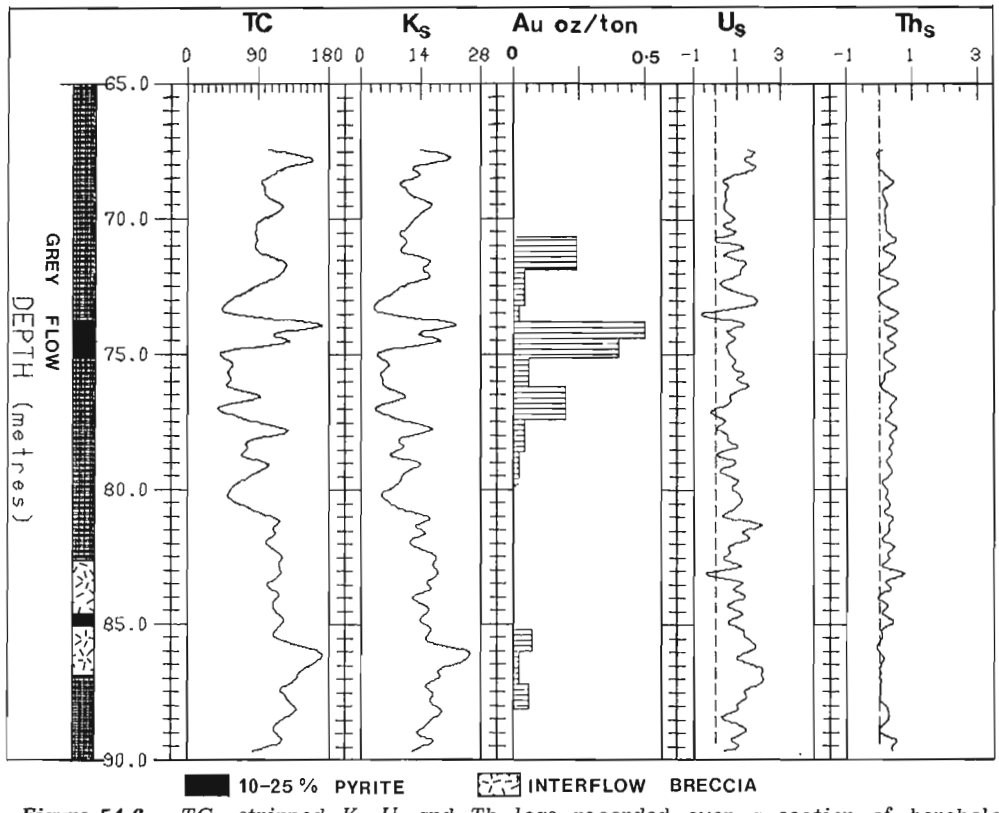

Figure 54.6. TC, stripped K, U and Th logs recorded over a section of borehole BL-80-25 using a 32 mm x 125 mm CsI(Na) detector, a slow logging velocity v = 0.3 m/minute and a sample time of 6 seconds. A 15-point smooth has been applied to the logs. Gamma ray intensities are in counts per sample time. Also shown is the gold assay log.

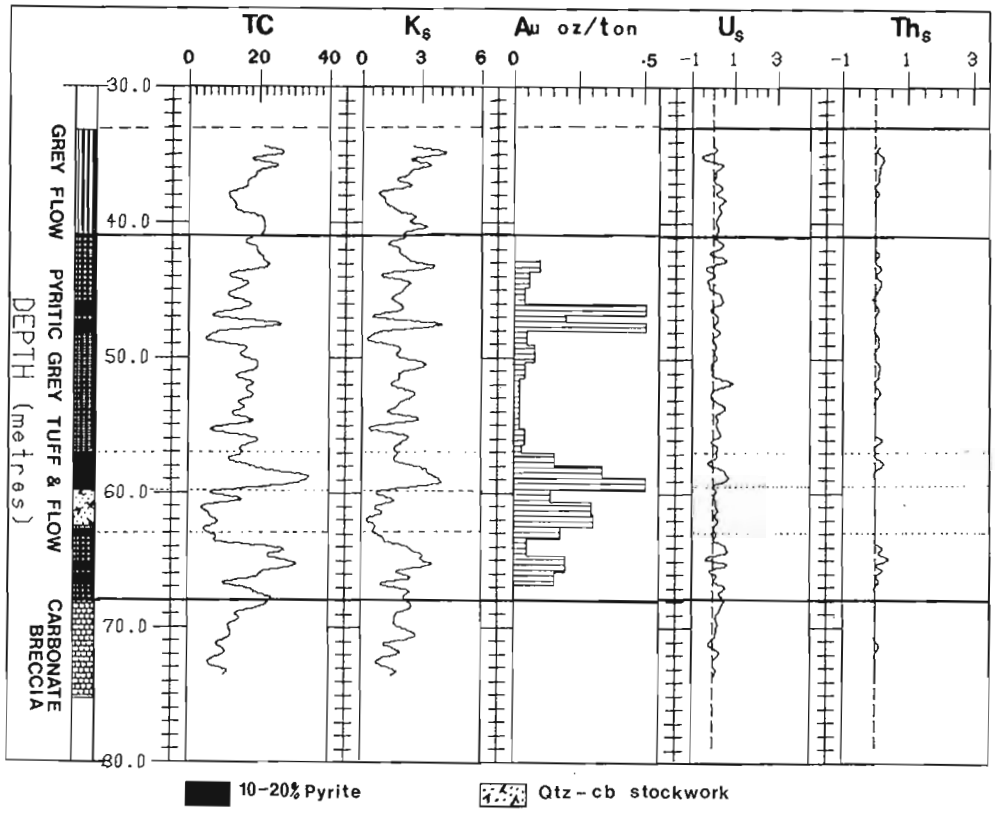

Figure 54.7. TC, stripped K, U and Th logs recorded in borehole BL-80-40 using a 32 mm x 125 mm CsI(Na) detector, a slow logging velocity v = 0.3 m/minute and a sample time of 6 seconds. A 15-point smooth has been applied to the logs. Gamma ray intensities are in counts per sample time. Also shown is the gold assay log.

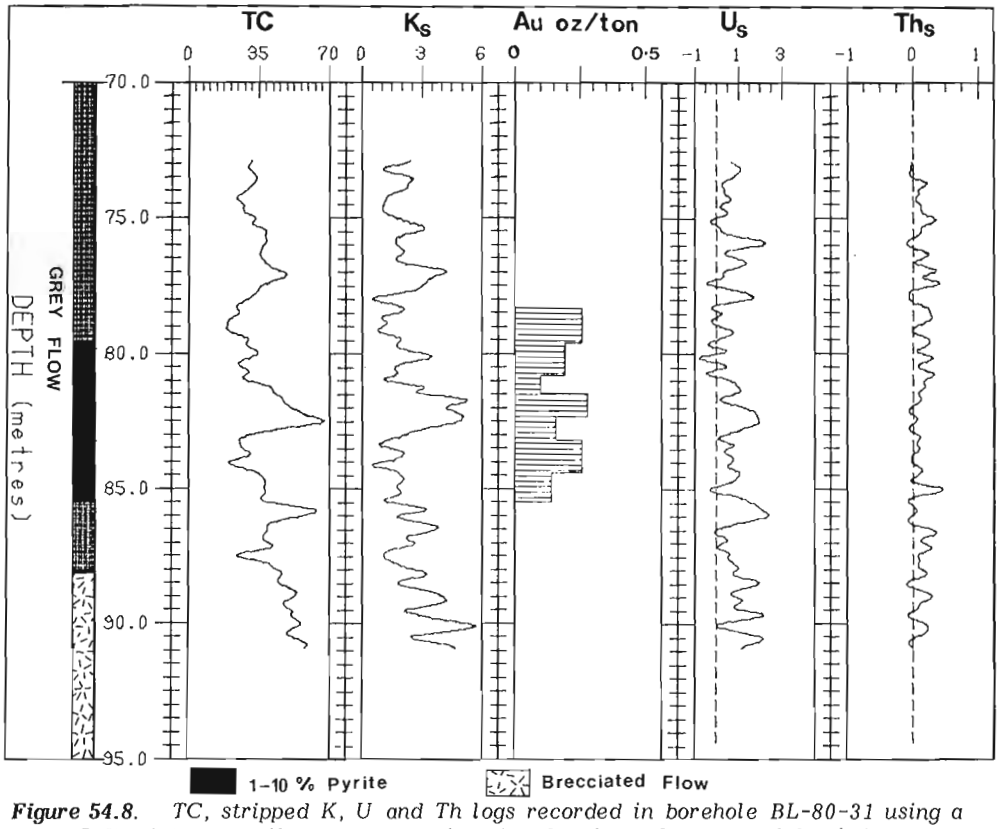

Figure 54.8. TC, stripped K, U and Th logs recorded in borehole BL-80-31 using a small CsI(Na) detector (25 mm x 76 mm), a slow logging velocity v = 0.3 m/minute and a sample time of 6 seconds. A 15-point smooth has been applied to the logs. Gamma ray intensities are in counts per sample time. Also shown is the gold assay log.

Field Results and Discussions

Six boreholes intersecting gold mineralization were logged at the Barber-Larder Lake property of Kerr Addison Mines. For each of these boreholes, general geological logs and gold assay data were available. The boreholes intersected three major rocks units: 1) A greywacke and/or arkosic unit; 2) middle unit composed of lava flows, breccias and tuffs; 3) and a lower unit composed of green carbonate breccia (fuchsite-bearing car-bonatized ultramafic volcanics). The favorable ore-bearing horizons lie within the lava flows and breccias. The boreholes were first logged using a logging speed of 3 m/minute and sampling time of one second. This is considered to be the "normal" logging speed which is adequate for uranium exploration but because of the low radioelement concentrations observed in the area (and hence low count rates), a slower logging speed of 0.3 m/minute with a sampling interval of 6 seconds was used in selected zones. The logs obtained with a logging speed of 3 m/minute had very poor counting statistics in the K, U and Th windows. Some information on the distribution of K, U and Th, however, could be extracted from these logs. Major lithologic contacts, where there was a significant change in the radioelement concentrations, could be easily outlined.

One of the major problems in attempting to correlate potassium increases and gold occurrences is that of relating depths obtained from borehole logging to those obtained from the brief core log records as documented by the core logger. The nature of drilling and recovering core is highly prone to errors regarding exact depths and locating intersections precisely. Cable stretching also introduces some errors in depth measurements from borehole logging data. In this study there could be discrepancies of up to 1 m in depths obtained from borehole logging and core logs. In the present report the depths from borehole logging have been adjusted so that the contact between the greywacke (or arkose) and the volcanic rocks is matched with the marked change in radioactivity at this contact (see Fig. 54.3). For precise correlation one needs to examine the core in greater detail to determine where and what type of mineralogical changes of geophysical significance exist.

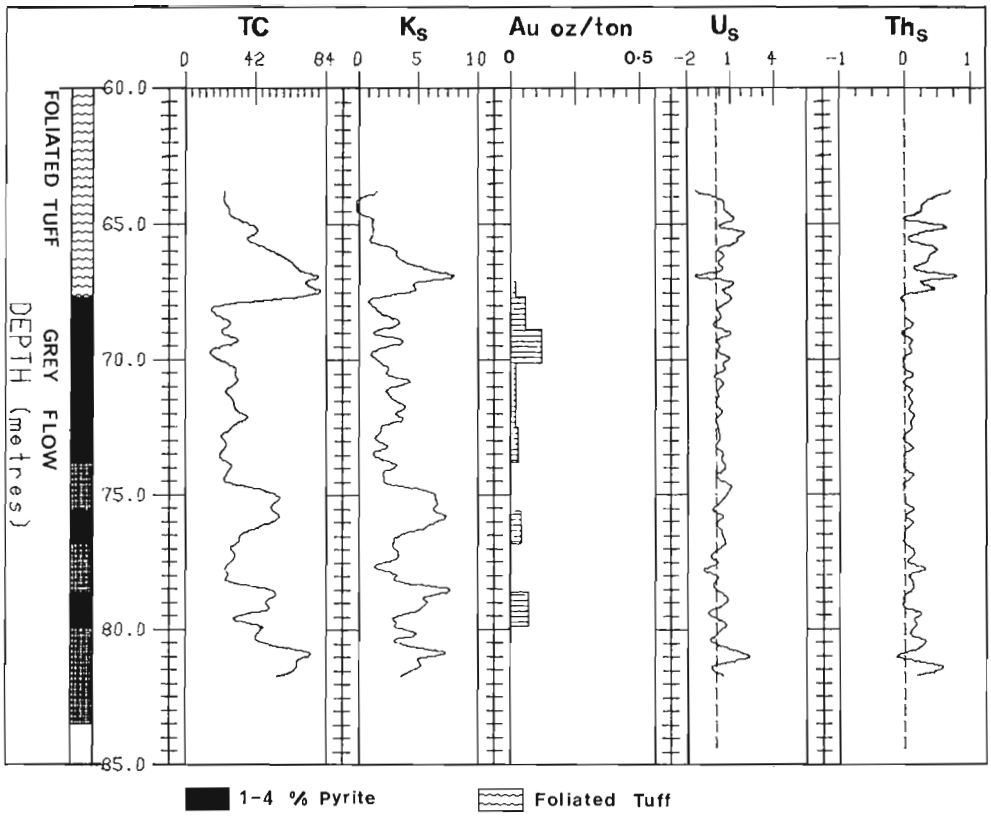

Figure 54.9

TC, stripped K, U and Th logs recorded in borehole BL-80-30 using a small CsI(Na) detector (25 mm x 76 mm), a slow logging velocity v = 0.3 m/minute and a sample time of 6 seconds. A 15-point smooth has been applied to the logs. Gamma ray intensities are in counts per sample time. Also shown is the gold assay log.

Figure 54.3 shows gamma ray logs of the total count, (TC), stripped K, U and Th, and gold assay values along borehole BL-80-47. The borehole was logged with a logging velocity v = 3 m/minute and counting time Δt = 1 second. The geological log shows an arkose rock unit, volcanic flow unit and the green carbonate breccia unit. The boundaries between these rock units are clearly indicated on the TC log. The TC and stripped K logs indicate two levels of radioactivity within the volcanic flow unit. This suggests that there are two distinct flow units of different mineralogical composition, separated by a quartz vein. The upper unit has somewhat higher potassium content than the lower unit. Uranium and thorium are negligible in the lava flows and in the green carbonate breccias. In the upper volcanic flow unit we see gold occurring at depths of 25 to 29 m and at 33 m. There is not a prominent corresponding increase in potassium content at these depths. The lower volcanic flow unit has very low count rates. The section from 32 m to 50 m was relogged at a slower logging speed of 0.3 m/minute and the data are shown in Figure 54.4. On the average, the low count rate volcanic flow unit contains gold of ore grade. The peaks of higher-than-average potassium content of 36.2, 38.5 and 42 m, show no corresponding increase in gold.

Figure 54.5 shows gamma ray logs of TC, stripped K, U and Th, and the gold assay log obtained from borehole BL-80-25. The borehole was logged at 3 m/minute with a sample time Δt = 1 second. There are three volcanic units: the grey volcanic flow unit, the pyritic tuffs and flow unit, and the carbonate breccia. Again we see that there is virtually no uranium or thorium within the volcanics and carbonates. Within the pyritic tuffs and flows there are massive sulphide zones containing from 15 to 20 per cent pyrite (shown in solid shading), and a quartz-carbonate stockwork zone. The stripped K log and the gold assays indicate that there is a positive correlation between potassium count rates and gold content at depths of 46 to 49 m, 57 to 60 m and at 64 to 67 m. The quartz-carbonate stockwork between 60 and 63 m, however, shows a negative correlation between concentrations of potassium and gold assay values. High gold values are associated with low potassium count rates. Another log was obtained at a slower logging speed of 0.3 m/minute over a depth range between 52 to 75 m (Fig. 54.6). This log confirms the fairly low potassium count rates observed within the quartz-carbonate stockwork. Thus silicified units with a high gold-bearing potential seem to be depleted in potassium. The stripped Th log shows a thorium anomaly at 64.0 to 65.5 m. This anomaly cannot be correlated with either the stripped K or the gold assay log.

Figure 54.7 shows the gamma ray logs and the gold assay log obtained in borehole BL-80-40. The borehole was logged at 0.3 m/minute with counting time of 6 seconds. The ore zone at 73.75 to 75 m seems to correlate well with an increase in the potassium content and the massive pyritized zone (25 per cent pyrite). However, the high gold content (0.2-0.25 ounce of Au per ton) at 70.6 to 72 m and 76.1 to 77.5 m does not show any corresponding increase in potassium.

Gamma ray spectral logs and the gold assay log of borehole BL-80-31 are shown in Figure 54.8. This section of the borehole was logged with a 25 mm x 76 mm CsI(Na) detector, logging velocity v = 0.3 m/minute and a sample time of 6 seconds. Pyritization is rare in this massive, brecciated grey flow unit except between 75.5 to 85.5 m. Here there is 1 to 10 per cent disseminated pyrite. The ore is found within the pyritized zone. There is no overall increase in potassium content within the ore zone except around 82 m. Figure 54.9 shows gamma ray logs obtained in borehole BL-80-30 using a 25 mm x 76 mm CsI(Na) detector, logging velocity v = 0.3 m/minute and a sample time of 6 seconds. This borehole does not intersect ore. There are, however, zones of higher-than-average potassium content.

The above spectral logs indicate that, in the flow-type orebodies in the Larder Lake area, there is not always a definite correlation between gold mineralization and an increase in potassium concentrations due to hydrothermal alteration. This is not surprising, for to presuppose that there is always a correlation between an increase in potassium and high gold content would imply a very simple genetic history of the gold mineralization within the volcanic flows. Gold mineralization in the Larder Lake area seems to have a complex history. Several stages of gold mineralization are known to have taken place (Jensen, 1980). Gold ores that are related to hydrothermal alterations are likely to be associated with increases in potassium content.

Conclusions

From these preliminary data the following tentative conclusions may be drawn:

1. Gamma ray spectral logging may be used to outline areas of higher than normal potassium concentration which may be associated with gold;
2. There is a positive correlation between high gold values and high potassium content in the pyritized volcanic flows and tuffs; and
3. Quartz-carbonate stockwork within the flows and tuffs have low potassium content but are associated with high gold content.

A detailed analysis of the correlation between potassic alteration zones and gold occurrences is in progress. More boreholes are scheduled to be logged in the near future. These boreholes will include those that intersect ore and those that are barren. Because of the low count rates observed in the area, larger detectors and slower logging speeds will be used. It is possible that zones low in potassium but which are favourable ore-bearing horizons may be outlined by an IP/resistivity log. The silicified zones should show higher resistivities and lower IP effect (rare or fairly low percentage of sulphides) than nonsilicified zones. IP/resistivity logging will be conducted to complement the gamma ray spectral logging data.

Acknowledgments

We would like to thank Kerr Addison Mines Limited and in particular D.M. Hendrick, Chief Geologist-Exploration, for permission to carry out this work on their property. They also kindly made available to us the geological logs and the gold assay data and gave us permission to present this data.

References

Balykin, P.A., Borob'yev, V.I., and Krendelev, F.P.
1973: Gamma-spectrometric measurements of Clarkes of radioactive elements in gold deposits of the schist zone; Doklady Akademii Nauk SSSR, v. 209, no. 1, p. 189-191.

Blyumentsev, A.M., Khrust, A.R., and Chepizhnaya, E.A.
1974: Radioactive elements as indicators of gold in effusives; Yad. Geol, p. 187-197 (Chemical Abstracts, v. 83, 100886a).

Boyle, R.W.
1979: The geochemistry of gold and its deposits; Geological Survey of Canada, Bulletin 280.

Bristow, Q.
1979: Airborne and vehicle mounted geophysical data acquisition system controlled by NOVA mini-computers; in Proceedings of the 6th Annual Data Generals User's Group Meeting, New Orleans.

Conaway, J.G. and Killeen, P.G.
1978: Quantitative uranium determinations from gamma-ray logs by application of digital time series analysis; Geophysics, v. 43, p. 1204-1221.

Downes, M.J.
1981: Structural and stratigraphic aspects of gold mineralization in the Larder Lake area, Ontario; in (Genesis of Archean, Volcanic Hosted Gold Deposits, editors E.G. Pye and R.G. Roberts), Ontario Geological Survey, Miscellaneous Paper 97, p. 66-69.

Fel'dman, A.A., Slepnev, P.V., and Kul'kov, B.N.
1975: Use of gamma spectrometry in prospecting for gold ore deposits near the surface; Razved. Okhr. Nedr., no. 10, p. 59-60. (Chemical Abstracts, v. 84, 138431g).

Gross, W.H.
1952: Radioactivity as a guide to ore; Economic Geology, v. 47, p. 722-742.

Jensen, L.S.
1980: Gold mineralization in the Kirkland Lake-Larder Lake areas; Ontario Geological Survey, Miscellaneous Paper 97, p. 59-64.

Killeen, P.G. and Conaway, J.G.
1978: New facilities for calibrating gamma-ray spectrometric logging and surface exploration equipment; Canadian Mining and Metallurgical Bulletin, v. 71, no. 793, p. 84-87.

Krendelev, F.P., Mironov, A.G., and Gofman, A.M.
1976: Gamma spectrometry applied to contouring ore zones in the Trans Baikal Region; Geologiya Geofizika, v. 17, no. 8, p. 67-75.

Madden, H.H.
1978: Comments on the Savitzky-Golay convolution method for least-squares fit smoothing and differentiation of digital data; Analytical Chemistry, v. 50, no. 9, p. 1383-1386.

Ostrovskiy, E.Y., Portnov, A.M., and Drabkin, I.Y.
1970: Aerogamma spectrometric prospecting for perisurficial deposits of gold in effusives; Int. Geol. Rev., v. 14, no. 7, p. 688-691.

Portnov, A.M., Ostrovskiy, E.Y., and Kolotov, B.A.
1971: Prospecting for near-surface gold-silver deposits by aerial gamma-spectrometric and hydrogeochemical methods; Razved, Okhr. Nedr., v. 37, no. 11, p. 13-16. (Chemical Abstracts, v. 76, 61759v).

Savitzky, A. and Golay, J.E.
1964: Smoothing and differentiation of data by simplified least squares procedures; Analytical Chemistry, v. 36, p. 1627-1638.

Thomson, I.
1980: Gamma ray mapping of alteration zones associated with gold-bearing horizons: orientation studies at the Kerr Addison Mine, Virginiatown, District of Timiskaming; Ontario Geological Survey, Miscellaneous Paper 96, p. 145-149.

Tihor, L.A. and Crocket, J.H.
1975: Gold distribution and gamma-ray spectrometry in the Kirkland Lake-Larder Lake gold camp; in Report of Activities, Geological Survey of Canada, Paper 75-1A, p. 355-357.

55.

LITHOLOGICAL SUITES AS GLACIAL 'TRACERS', EASTERN ELLESMERE ISLAND, ARCTIC ARCHIPELAGO

Project 750063

R.L. Christie
Institute of Sedimentary and Petroleum Geology, Calgary

Christie, R.L., Lithological suites as glacial 'tracers', eastern Ellesmere Island, Arctic Archipelago; in Current Research, Part A, Geological Survey of Canada, Paper 83-1A, p. 399-402, 1983.

Abstract

Morainic debris in the Cape Herschel area contains distinctive lithological suites, the distribution of which can be mapped. It appears that glacial ice from Kane Basin overrode the eastern capes of Ellesmere Island and that eastward-flowing glaciers of the island were deflected southward. The combined ice flows formed a large glacier that emptied southward through Smith Sound into northern Baffin Bay.

Introduction

Field studies of Pleistocene and Holocene features of the Smith Sound region have been carried out by W. Blake, Jr., of the Geological Survey of Canada, since 1977 (Blake, 1977, 1978, 1981). The field work has been based at the Cape Herschel station of the "North Water Project", established in 1973 by the late F. Müller (Müller et al., 1975). The author accepted an invitation to join Blake's field party during the spring of 1982 to study glacial erratic material in the Cape Herschel region; it was expected that at least some of the rock types in the glacially transported debris would be sufficiently distinctive to allow the assignment of 'probable source areas' to them. It was, indeed, soon apparent during field work that at least two contrasting 'suites' of debris can be identified. Mapping of the lithological composition of glacial debris in this region may allow the determination of the courses and limits of former glacial ice flows.

Lithological Suites

The morainic material in the Cape Herschel region is dominated, in most places, by angular and subangular debris from the local bedrock: mainly granitoid gneiss of various hues. This debris represents the exposed Precambrian crystalline 'basement' of the area and is of no diagnostic use at localities on or very near the outcrop. The granitoid debris at such localities will not be considered further here.

The non-granitoid debris contains a wide variety of rocks, mainly of sedimentary origin but including a few igneous rocks. The fragments of sedimentary rock are generally recognizable as representatives of the upper Precambrian and lower Paleozoic formations that are widely exposed in the Flagler Bay – Bache Peninsula region (noted by Blake, 1977, p. 114). The igneous rocks mainly resemble the diabase dykes or sills that are known to intrude both the Precambrian sedimentary rocks and probably derive from beds of the Precambrian Thule Group, which outcrops in the region. Dark grey, green-grey weathering impure limestone or limy greywacke fragments occur at certain places near sea level; outcrops of this distinctive rock are not known in the Bache Peninsula region and the debris may be exotic, transported by floating ice rather than by glacial ice streams.

Two lithological suites can be defined for the Cape Herschel region. 1. A suite, here named the 'Cape Suite', characterized by the presence of a variety of sedimentary rocks probably derived from both the lower Paleozoic beds of the region and the Precambrian Thule Group. 2. A suite, here called the 'Inland Suite', that represents the lower Paleozoic formations of the region and in which Thule Group rocks appear to be absent.

Cape Suite

The non-granitoid debris of the Cape Suite comprises, in addition to representatives of lower Paleozoic sedimentary formations (described later under 'Inland Suite'), an assortment of distinctive rocks that includes[1]:

1. White, fine grained quartzite with a pinkish cast.
2. Intraformational conglomerate: round red carbonate clasts in a lighter-coloured matrix; weathering reddish to purplish white.
3. Dark red shaly quartzite.
4. Platy, fine grained white sandstone with ripple marks; weathering yellow to white.
5. Pink, yellow, green and white weathering, domal-banded algal rock.
6. Light green ooidal-fragmental rock with white calcite matrix; weathering with a scoriaceous surface.
7. Green and red slaty shale.
8. Maroon slaty shale.
9. Oncolitic dolomite; weathering light green.
10. Dolomite with quartz and chert grains; weathering greenish grey.
11. Purple sandstone, poorly sorted but with well rounded grains and pink feldspar grains.
12. Dark, green-black, fine- to medium-grained diabase; weathering dark yellow-brown to green-brown.
13. Dark green-grey volcanic rock with green amygdules (mineral not identified).
14. Dark purplish volcanic? rock with green mineral patches (mineral not identified).

Rocks similar or identical to those listed above have been observed in the Rensselaer Bay Formation of the Thule Group (Christie, 1967; Dawes, 1976; Peel et al., 1982). Beds of this unit are well exposed in the south-coastal cliffs of Bache Peninsula (Christie, 1967).

Inland Suite

The Inland Suite of glacial erratic debris contains variable amounts (rare to abundant) of sedimentary rock that can be ascribed to the lower Paleozoic formations of the region. The older (Rensselaer Bay Formation) rocks of the Cape Suite are not represented, although a few specimens

[1] The descriptions listed here are based on field notes. Limestone and dolomite were differentiated in the field by means of dilute HCl.

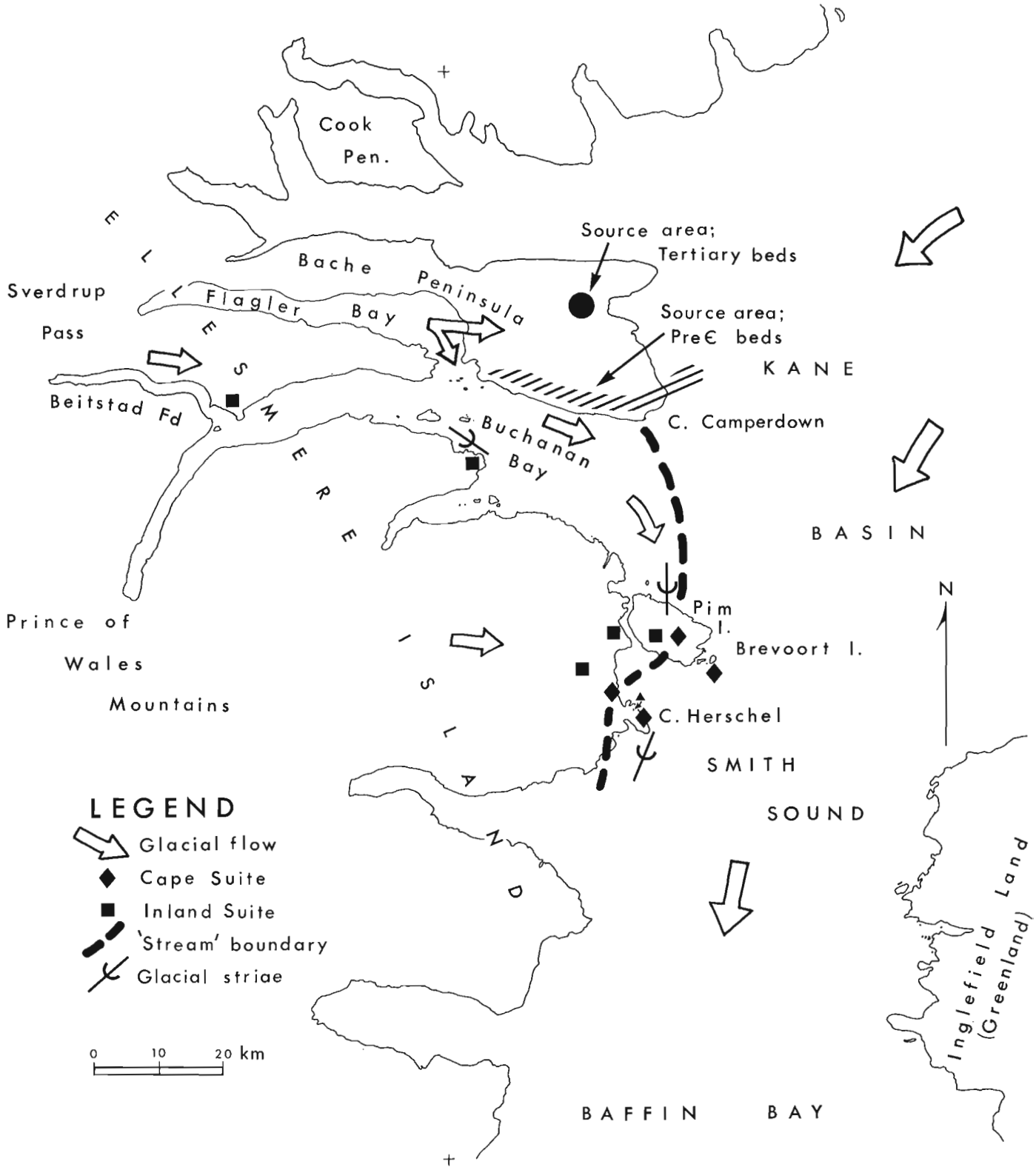

Figure 55.1. *Distribution of lithological suites in glacial debris, and some source areas, Cape Herschel region, Ellesmere Island.*

were found that may be assigned to the older unit. A partial list (based on field descriptions) of rocks typical of the Inland Suite follows:

1. Light violet-grey to grey, very fine grained limestone; weathering pale brown.
2. Grey, fine- to medium-grained limestone; weathering grey-black.
3. Grey, fine grained sandy limestone; weathering greenish grey.
4. Very pale yellow-white, medium crystalline dolomite; weathering orange.
5. Fine grained, grey limestone intraformational conglomerate with scattered round quartz grains; weathering green-grey.
6. Light grey to grey, fine grained dolomite with domal laminae; weathering pale yellow to pale green.
7. Light grey to grey-yellow, medium crystalline dolomite that breaks into flat plates; weathering pale yellow.
8. Grey, very fine grained limestone with dark grey partings and a silty? pattern standing out on weathered surface; weathering pale brown.
9. Grey, medium crystalline oolitic limestone with medium sized rounded quartz grains; weathering green-grey.
10. Dark grey, medium grained sandstone; weathering dark grey.

The suite of rocks listed above clearly represents the Cambrian to Ordovician formations of the Flagler Bay region (see Christie, 1967). The Cambrian and younger units are exposed over almost all of Bache Peninsula and over much of Knud Peninsula (south of Flagler Bay), and scattered outliers of these rocks occur in the rugged mountains south of the line of Beitstad Fiord and Buchanan Bay (Christie, 1962; Frisch et al., 1978).

Some confirmation of the usefulness of lithological suites as tracers for erratic trains became available from a reconnaissance visit by W. Blake, Jr., to Cook Peninsula, north of Bache Peninsula. A collection of glacial debris (the site was not visited by the writer) contained a suite of rocks markedly different from either the Cape or the Inland Suite. Sedimentary rocks exposed to the northwest, in the probable source area, are known to contrast with those of the Bache Peninsula region (Trettin, 1978, 1979).

Glacial Flow in the Cape Herschel Region

Glacial erratic 'trains' can be mapped in east-central Ellesmere Island, it appears, from the distribution of rock types in the surficial debris. The Cape Suite, described above, is here taken to be such an erratic train; rocks of the Inland Suite, although also present with the Cape Suite, can also be considered as a train. The distinctive lithological characteristics of the erratic trains, and of the probable source area of eastern Bache Peninsula, allow some tentative conclusions on the flow of ice in former glacial times.

Bache Peninsula and Other Source Areas

The lithologically distinctive beds of the Precambrian Rensselaer Bay Formation of Bache Peninsula and Inglefield Lands, with the limited areal extent of the unit (Fig. 55.1), make this formation useful in tracing glacial streams. The Paleozoic rocks, in contrast, are very widely distributed in outcrop and are more or less ubiquitous in the morainic debris of the coasts. Of very limited, almost 'point' distribution, are the Tertiary Eureka Sound beds of eastern Bache Peninsula (Christie, 1967, Map 1188A). This distinctive unit might be expected to provide good tracer debris, but the weakly lithified beds probably produced few large erratic fragments and the fragments almost certainly were short-lived, rapidly broken down to unrecognizable fines.

The Rensselaer Bay Formation, in addition to its outcrops on land as noted, must also form submarine outcrops in southwestern Kane Basin. This submarine source area may now be mantled by glacial and marine deposits.

Glacial Ice Flow

The source area for the Cape Suite probably lay along the south coast of Bache Peninsula or in southern Kane Basin, or in both places. A line extended northward from the western limit of the Cape Suite to the south-coastal outcrop area resembles or suggests a medial moraine trending southward from Cape Camperdown (Fig. 55.1). Such a moraine (or boundary between ice flows) would, presumably, lie between ice flowing southeastward through Buchanan Bay and ice flowing southward in southwestern Kane Basin. A polynya that can be seen off Cape Camperdown may be evidence of shallow water due to such a moraine ridge.

The delineation of the ice flow boundary in Figure 55.1 is based on data from rather few points and is therefore tentative and subject to modification. A question arises concerning the reason for an apparent westward bulge of the boundary near Cape Herschel. A possible explanation is that Pim Island may have acted as a barrier, behind which Kane Basin ice pushed westward at some stage.

Field confirmation of a southward flow of ice from Bache Peninsula to Cape Herschel was found in a small col atop the cape: fragments of brown sandy shale with black, carbonaceous markings. These fragments probably derive from the Eureka Sound beds of the peninsula. It is here suggested that Flagler Bay ice at some stage overrode the broad head of Bache Peninsula and swept Tertiary rock debris eastward onto south-flowing Kane Basin ice. Such a flow direction was earlier suggested (Christie, 1967, p. 7) to account for red granite erratics and 'old' shell debris on the uplands of eastern Bache Peninsula.

The probable Eureka Sound erratic debris was found, however, at about the local limit of marine submergence (somewhat above 100 m, W. Blake, Jr., personal communication) and the possibility that it was floated into place by sea ice must also be considered.

The hypothesis of a southwestward flowing Kane Basin ice stream meeting an eastward-flowing Ellesmere Island stream and the two combining to flow southwestward through Smith Sound has some interesting corollaries:

a. Greenland and Ellesmere Island glacial ice met, probably during a 'young' (just prior to deglaciation about 9000 years B.P., Blake, 1981) glacial stage.
b. The glacial junction crossed Pim Island and Cape Herschel so that the Kane Basin stream must have dominated. The filling of Kane Basin by glacial ice and the deflection southward of Ellesmere Island ice was earlier deduced by Blake (1977, p. 114) from the directions of glacial striae on Pim Island and Cape Herschel.

The southward flow of glacier ice through Smith Sound and the modification of an older, now drowned, drainage system was proposed by Pelletier (1966) from a study of submarine topography.

The domination of Kane Basin ice over that from south of Bache Peninsula could be expected for the following reasons. Firstly, Kane Basin is a large (over 200 km in length) inland sea into which the enormous Humboldt Glacier empties and, during glacial times, glaciers from a large area

of Ellesmere Island north of Bache Peninsula must also have flowed into the basin. Secondly, the greater 'cryodynamic head' available to Kane Basin ice, with much of its large drainage basin lying at the high elevations of interior Greenland, could be expected to result in Kane Basin ice overwhelming the ice flow from the relatively small area of the Prince of Wales Mountains and Sverdrup Pass.

The question of the age of the glaciation that produced the prominent and fresh-appearing glacial features of the Cape Herschel region is under active study (Blake, 1977, 1981).

Postglacial Drift

A distinctive rock type was noted among erratic debris at low elevations: dark green-grey weathering, medium grained, limy greywacke or impure arenaceous limestone. This rock was observed in beach deposits at the Cape Herschel camp and on Brevoort Island, always in small amounts and occasionally as large (about 20 cm) slabs. Beds of this rock type are found in the Silurian and younger Imina Formation, a unit exposed east of Cañon Fiord (Trettin, 1978, 1979) and on Judge Daly Promontory (Christie, 1974; Kerr, 1976), parts of Ellesmere Island northwest and north, respectively, of Bache Peninsula. The debris may have been carried southward along Nares Strait by floating ice in postglacial times. Sea ice drifts southward in the strait today (Ito and Müller, 1982).

It would also be reasonable to suppose that some debris from east of Cañon Fiord could be carried into Kane Basin by glacial ice flowing through such channels as Princess Marie Bay or Dobbin Bay (north and northeast of Bache Peninsula). Glaciers in these channels lie to the south of the 'drowned watershed' of Pelletier (1966) and would tend to join south-flowing ice.

Conclusions

The mapping of lithological suites in the glacial debris of east-central Ellesmere Island can be useful in determining the glacial history of the region. The distribution of the suites of erratics and the directions of striae in the Cape Herschel area can be accounted for by supposing that two major ice flows were present, one flowing eastward from the Prince of Wales Mountains and Sverdrup Pass region, and the other southwestward from Kane Basin. The southward deflection of the Ellesmere Island ice suggested by Blake is confirmed by the glacial erratic trains, and the boundary between the two glacial ice flows at some stage lay along the east coast of Ellesmere Island. The combined ice evidently moved southward through Smith Sound into northern Baffin Bay.

Acknowledgments

The author expresses his gratitude to W. Blake, Jr., for providing excellent and agreeable logistic support for the field work and thanks Louise Légère for able and cheerful assistance.

References

Blake, W., Jr.
1977: Glacial sculpture along the east-central coast of Ellesmere Island, Arctic Archipelago; in Current Research, Part C, Geological Survey of Canada, Paper 77-1C, p. 107-115.

1978: Coring of Holocene pond sediments at Cape Herschel, Ellesmere Island, Arctic Archipelago; in Current Research, Part C, Geological Survey of Canada, Paper 78-1C, p. 119-122.

Blake, W., Jr. (cont.)
1981: Lake sediment coring along Smith Sound, Ellesmere Island and Greenland; in Current Research, Part A, Geological Survey of Canada, Paper 81-1A, p. 191-200.

Christie, R.L.
1962: Geology, Alexandra Fiord, Ellesmere Island, District of Franklin; Geological Survey of Canada, Map 9-1962 (map with marginal notes).

1967: Bache Peninsula, Ellesmere Island, Arctic Archipelago; Geological Survey of Canada, Memoir 347.

1974: Northeastern Ellesmere Island: Lake Hazen region and Judge Daly Promontory; in Current Research, Part A, Geological Survey of Canada, Paper 74-1A, p. 297-299.

Dawes, P.R.
1976: Precambrian to Tertiary of northern Greenland; in Geology of Greenland, ed. A. Escher and W.S. Watt; Geological Survey of Greenland, Copenhagen, p. 249-303.

Frisch, T., Morgan, W.C., and Dunning, G.R.
1978: Reconnaissance geology of the Precambrian Shield on Ellesmere and Coburg Islands, Canadian Arctic Archipelago; in Current Research, Part A, Geological Survey of Canada, Paper 78-1A, p. 135-138.

Ito, H. and Müller, F.
1982: Ice movement through Smith Sound in northern Baffin Bay, Canada, observed in satellite imagery; Journal of Glaciology, v. 28, p. 129-143.

Kerr, J.Wm.
1976: Stratigraphy of central and eastern Ellesmere Island, Arctic Canada, III. Upper Ordovician (Richmondian), Silurian and Devonian; Geological Survey of Canada, Bulletin 260.

Müller, F., Blatter, H., and Kappenberger, G.
1975: Temperature measurement of ice and water surfaces in the North Water area using an airborne radiation thermometer; Journal of Glaciology, v. 15, p. 241-250.

Peel, J.S., Dawes, P.R., Collinson, J.D., and Christie, R.L.
1982: Proterozoic – basal Cambrian stratigraphy across Nares Strait; correlation between Inglefield Land and Bache Peninsula; in Nares Strait and the Drift of Greenland: a Conflict in Plate Tectonics, ed. P.R. Dawes, and J.W. Kerr; Meddelelser on Grønland, Geoscience v. 8, p. 105-115.

Pelletier, B.R.
1966: Development of submarine physiography in the Canadian Arctic and its relation to crustal movement; in Continental Drift, ed. G.D. Garland; Royal Society of Canada, Special Publication no. 9, University of Toronto Press, Toronto, p. 77-101.

Trettin, H.P.
1978: Devonian stratigraphy west-central Ellesmere Island, Arctic Archipelago; Geological Survey of Canada, Bulletin 302.

1979: Middle Ordovician to Lower Devonian deep-water succession at southeastern margin of Hazen Trough, Cañon Fiord, Ellesmere Island; Geological Survey of Canada, Bulletin 272.

56. GEOLOGY OF THE DEEP ROSE LAKE MAP AREA, DISTRICT OF KEEWATIN

Project 820007

Subhas Tella, K.E. Ashton[1], D.L. Thompson[2], and A.R. Miller[3]
Precambrian Geology Division

Tella, S., Ashton, K.E., Thompson, D.L., and Miller, A.R., Geology of the Deep Rose Lake map area, District of Keewatin; in Current Research, Part A, Geological Survey of Canada, Paper 83-1A, p. 403-409, 1983.

Abstract

The area is underlain by a deformed and metamorphosed Archean and/or Aphebian granitoid and migmatitic gneiss terrane that is basement to Aphebian supracrustal rocks of the Amer group, and Helikian continental clastic rocks of the Thelon Formation. Deformed and diagenetically altered Amer group strata are made up of two dominantly clastic sequences (orthoquartzite and feldspathic sandstone) separated by transitional lithologies that host stratabound uranium mineralization. The lower sequence is affected by northeast- to east-trending thrust faults that show north-northwesterly tectonic transport. Porphyritic granite and related rocks intrude the basement complex and the Amer group, and are unconformably overlain by the Thelon Formation. Northwest-trending diabase and gabbro dykes related to the Mackenzie swarm record the youngest intrusive activity in the region.

Northeast- and northwest-trending shear zones and faults, some characterized by cataclastic to mylonitic textures, transect the region on all scales and affect both basement and supracrustals. The Amer mylonite zone, a regionally penetrative shear zone, records at least two periods of displacements of undetermined magnitude. The latest movements on this zone are marked by dextral offsets.

Introduction

Bedrock mapping in the southeast half of the Deep Rose Lake map area (NTS 66 G), at a scale of 1:250 000, was completed during the 1982 field season. Mapping in the remaining portion of the area is scheduled for completion in 1983. This report summarizes preliminary results of the mapping. A.R. Miller spent two weeks in the area as part of a regional study of uranium and phosphate occurrences, concentrating on Amer group and Thelon Formation lithologies. J.T. Krol, Carleton University, is currently studying the petrology and structural history of the Amer mylonite zone, as part of a B.Sc. thesis. J.C. Roddick, Geochronology Section GSC, spent one week collecting samples for U-Pb and Rb-Sr dating. M. Best, University of Ottawa, measured several stratigraphic sections at selected localities within the Amer group and in the Thelon Formation. Detailed accounts of the stratigraphy and structure of the Amer group will be reported in a later communication.

Previous Work

The map area is part of a region mapped by Wright (1955, 1967), at a scale of one inch to eight miles. Parts of 66 G/1 and G/2 were mapped in detail by Knox (1980) as part of a M.Sc. thesis project. Bedrock mapping and other topical studies (stratigraphy and structure) in the adjoining area to the east (Amer Lake map area, NTS 66 H), were carried out by several workers (Annesley, 1981a,b; Ashton, 1981, 1982; Barrett et al., 1978; Heywood, 1977; Patterson, 1980a, b, 1981; Patterson and Barrett, 1979; Tella and Heywood, 1978; Tippett and Heywood, 1978). Mapping is in progress in areas to the northeast and to the south (Frisch and Patterson, 1983; LeCheminant and Ashton, 1983).

Acknowledgments

We thank M. Best, J.R. Kenwood, J.T. Krol, our field assistants, Angela Dunn, cook, and Gordon Collett and Rob Pritchard, pilots, for their excellent support during the summer. Boris and Liz Kotelewitz, Baker Lake, provided expediting services. We also thank to A.N. LeCheminant and T. Frisch for their co-operation and assistance.

General Geology

The distribution of rock units in the Deep Rose Lake area is shown in Figure 56.1. Archean and/or Aphebian foliated granitoid rocks, migmatite, and minor paragneiss and gabbro are widely exposed in the northwestern and northern portions between Sand Lake and the northeast boundary of the Deep Rose Lake map sheet, and to a lesser extent in the southeast corner of the area (Fig. 56.1).

Deformed and unmetamorphosed supracrustal rocks of the Amer group (probable Aphebian), mostly exposed as scattered outcrops in the central and southeastern portions of the map sheet, define a broad, west-southwest-trending synclinorium. Undeformed Helikian continental clastic rocks of the Thelon Formation overlie the basement granitoids and the supracrustal rocks unconformably. Massive granitic and related rocks record post-Amer group and pre-Thelon Formation igneous activity.

Basement Complex (Units 1 to 3) - Archean and/or Aphebian

Fine- to medium-grained, greenish-grey, deformed metasediments composed of chlorite schist, phyllite, and wacke (unit 1) occur in the southeast corner of the map area as a narrow lens within an augenitic granitoid (unit 3A). They appear to be the oldest metasedimentary rocks recognized in the area.

[1] Department of Geological Sciences, Queen's University, Kingston, Ontario K7M 5X1
[2] Department of Geological Sciences, McMaster University, Hamilton, Ontario L8S 4M1
[3] Economic Geology Division

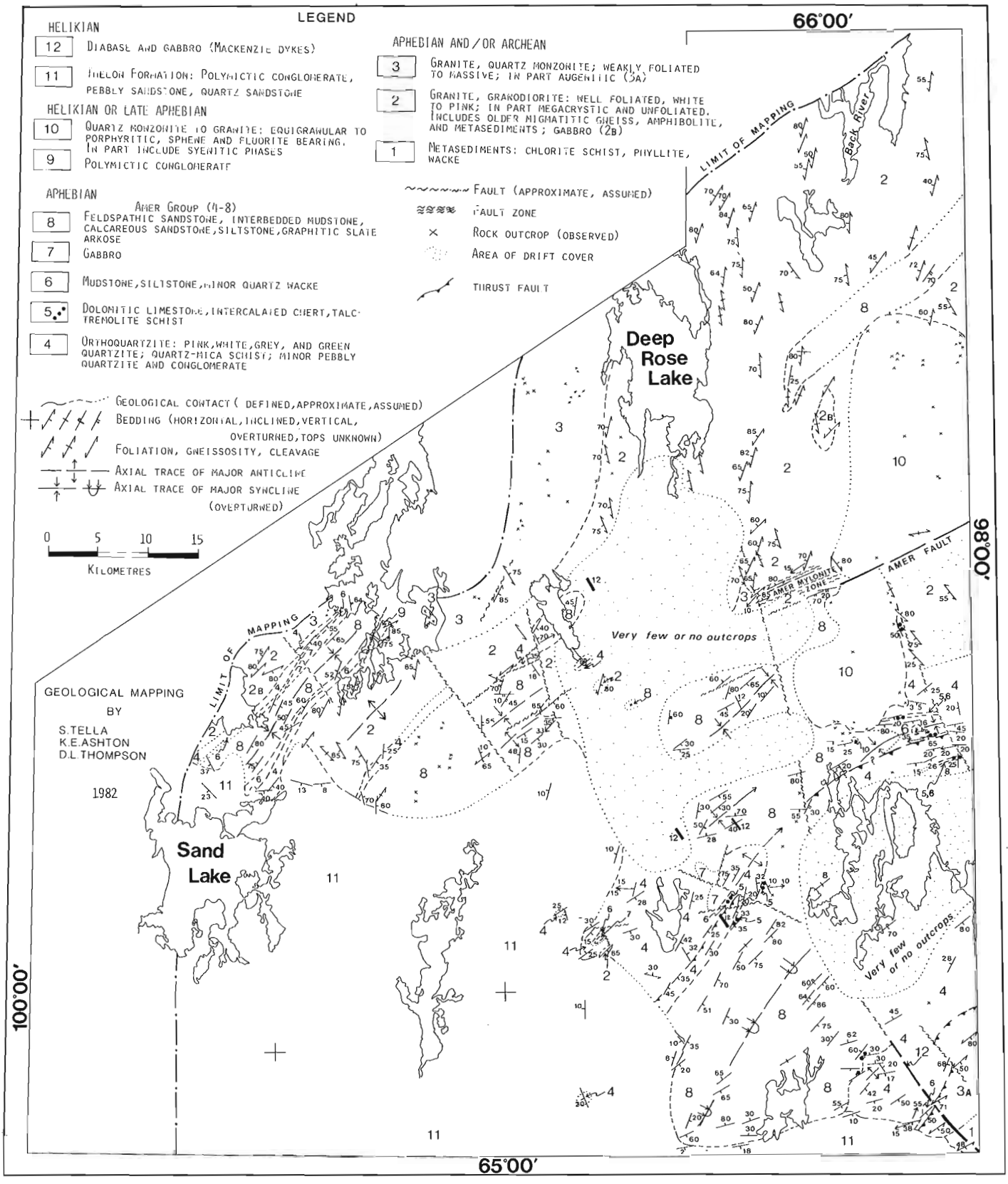

Figure 56.1. *Geological sketch map showing the distribution of major rock units in part of the Deep Rose Lake map area (NTS 66 G).*

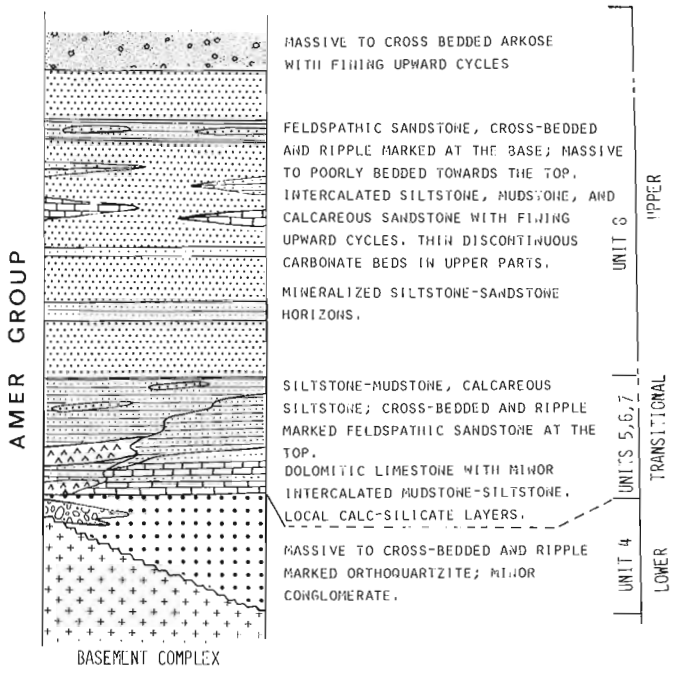

Figure 56.2. *Schematic stratigraphic section of the Amer Group. No stratigraphic thicknesses are implied.*

Unit 2 is a mixed unit consisting of well foliated, augenitic, granitoid metaplutonic rocks, migmatite, and rare paragneiss. The metaplutonic rocks contain quartz+K-feldspar+plagioclase+amphibole+biotite ± opaques. Although these rocks are fairly homogeneous on a regional scale, local compositional and structural heterogeneities are common. Relative proportions of K-feldspar and plagioclase are variable, and the mafic constituents (10-20%) are altered to chlorite. North- to north-northeast-trending and steeply dipping (65-90°W) foliation is the most penetrative planar fabric element in these granitoid rocks. Locally preserved, massive to porphyritic (megacrystic K-feldspar) texture in more highly deformed portions (Fig. 56.3), together with inclusions of deformed amphibolite (Fig. 56.4), suggest an igneous origin.

Migmatitic rocks occur within, and proximal to, the Amer mylonite zone (Fig. 56.1). There the lithology is variable and the structure more complex as a result of mylonitization. Mesoscopic folds in migmatitic gneiss are upright, tight isoclines that plunge shallowly (10-15°) towards the southwest. Minor gabbroic bodies (unit 2B) are sporadically distributed throughout the granitoid gneiss terrane. The weakly deformed to massive and less altered character of these bodies suggests that they postdate the gneiss unit. Thinly banded, complexly deformed biotite-chlorite paragneiss occurs in several localities within unit 2.

The rocks described above are cut by light grey to pink, coarse grained, muscovite-biotite granite and pegmatite dykes. The presence of both deformed and undeformed granitic dykes indicates more than one period of emplacement. Some pegmatitic fractions may represent locally generated partial melt. The regional metamorphic grade appears to be within the middle- to upper-amphibolite facies. In most places amphibole is partially altered to chlorite that may record retrogressive effects. Euhedral to subhedral garnet occurs in mafic clots together with biotite.

Several isolated outcrops of syenite porphyry (dykes?) are present (Fig. 56.5). The porphyry contains coarse grained, green feldspar phenocrysts in a fine grained to aphanitic, pink to green matrix, and shows no signs of deformation or alteration, except in the vicinity of shear zones.

Unit 3 is a homogeneous, massive, coarse grained, pink, porphyritic (K-feldspar) granite. Zoning in (6-8 cm long) feldspars is common, and biotite and amphibole make up less than 5% of the rock. Mafic minerals are completely absent in some localities. Penetrative shear fabric is locally developed proximal to minor faults. Contact relationships with unit 2 are uncertain but the massive, homogeneous and relatively undeformed character of unit 3 suggests that it postdates unit 2. Augenitic granitoid (unit 3A), exposed in the southeast corner of the map area (Fig. 56.1), is lithologically similar to unit 3 and appears temporally related to it.

Amer Group (Units 4 to 8) - Aphebian

Deformed and diagenetically altered sedimentary and igneous rocks (Hurwitz Group of Wright, 1955) cover most of the southeastern portion of the map area and are scattered throughout the region northeast of Sand Lake. The rocks define a broad west-southwest-trending synclinorium that extends eastward into the Amer Lake map area. The term 'Amer Group' was informally applied to these rocks in the Amer Lake area (Heywood, 1977; Tippett and Heywood, 1978; Knox, 1980; Patterson, 1981) and is retained here to include rocks that are in lithological and structural continuity with those of the Amer Lake area. The Amer group is considered to be of probable Aphebian age (Heywood, 1977; Tippett and Heywood, 1978; Patterson, 1981). Geochronological studies are currently in progress in Deep Rose Lake area.

A schematic stratigraphic section of the Amer group in Deep Rose Lake area is shown in Figure 56.2. The group predominantly consists of two clastic sequences – a lower white orthoquartzite (unit 4) and an upper, interbedded sequence of feldspathic sandstone, siltstone and mudstone, and arkose (unit 8). The two are separated by a transitional sequence that includes thin, discontinuous dolomitic limestone (unit 5) at the base and intercalated mudstone-siltstone (unit 6) at the top. Minor gabbroic rocks (unit 7), interpreted as sills, occur stratigraphically above the mudstone-siltstone (unit 6) in the southeastern part of the area, and above the orthoquartzite (unit 4) northeast of Sand Lake. The lower orthoquartzite sequence is generally massive, but in places is thin to thick bedded. Colour commonly ranges from pink, to white, grey or green in vertical sections. The constituent sugary to glassy quartz grains average 0.5 to 1 mm in size. Pebbly interbeds and minor intercalated impure (feldspathic) sandstone are locally present. Primary structures such as bedding, crossbedding, and ripple marks (Fig. 56.6) are well preserved in most places. 20 km northeast of Sand Lake (Fig. 56.1), a thinly bedded, ripple marked, white orthoquartzite with basal pebble conglomerate layers rests unconformably on the basement. Altered lithic feldspar clasts are locally present in the conglomerate beds. Following detailed stratigraphic studies in 66 G/1 and 2, Knox (1980) estimated a minimum thickness of 1280 m for the quartzite unit. Recent work indicates a facies change to the northwest where the quartzite becomes thinner and is commonly blue-grey to black. Minor graphitic zones within quartzite are present 20 km northeast of Sand Lake. The buff to yellow weathering dolomitic limestone (unit 5) contains cherty zones and calc-silicate layers. Interbeds of pyrite- and magnetite-bearing wackes are intercalated with grey to black mudstone-siltstone, red phyllite, and chloritic schists (unit 6). In general the dolomite unit is recessive, and outcrops are scattered along linear belts. Calc-silicate layers (talc-tremolite schists) are well developed near gabbro sills, indicating contact metamorphic effects. The upper

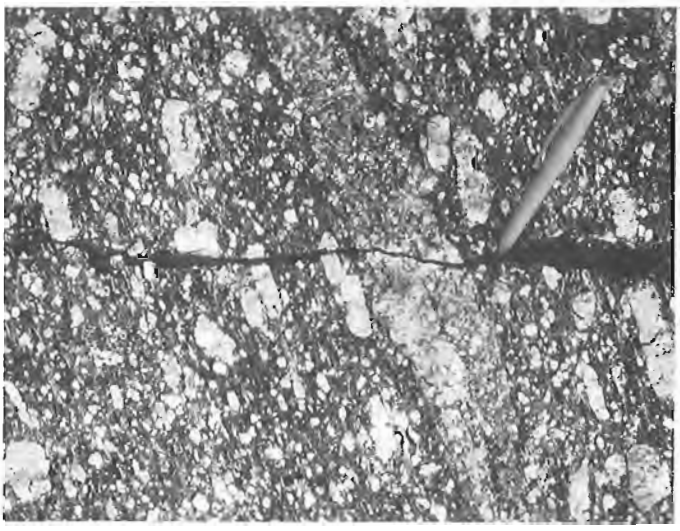

Figure 56.3. *Deformed equivalent of porphyritic granodiorite (unit 2). Note strong alignment of K-feldspar crystals. (GSC 203944-B)*

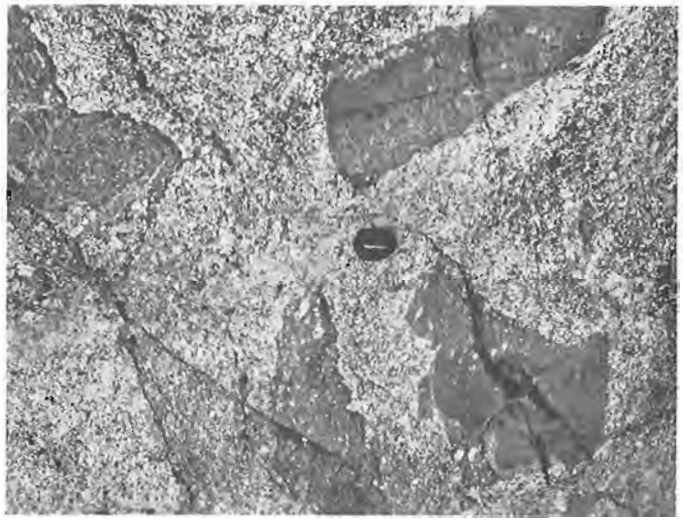

Figure 56.4. *Amphibolite inclusions in granitoid gneiss of unit 2. (GSC 203944)*

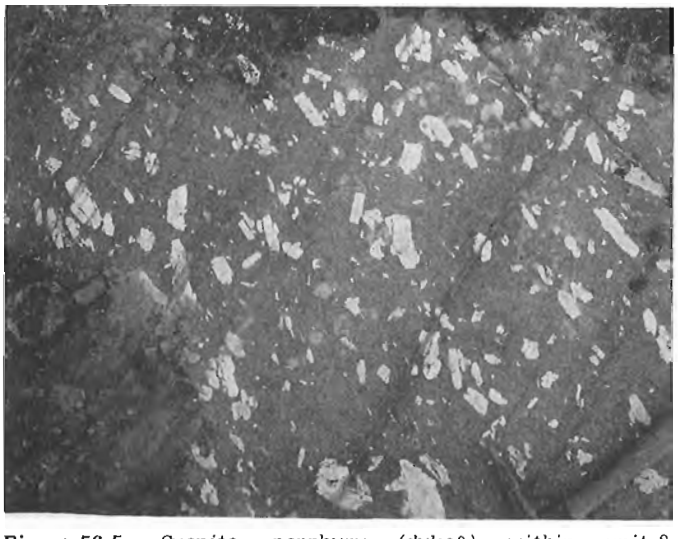

Figure 56.5. *Syenite porphyry (dyke?) within unit 2. (GSC 203944-A)*

Figure 56.6. *Asymmetrical ripple marks in orthoquartzite (unit 4), Amer group. (GSC 203944-J)*

Figure 56.7. *Subrounded to well rounded granodiorite clasts in polymictic conglomerate (unit 9). (GSC 203944-K)*

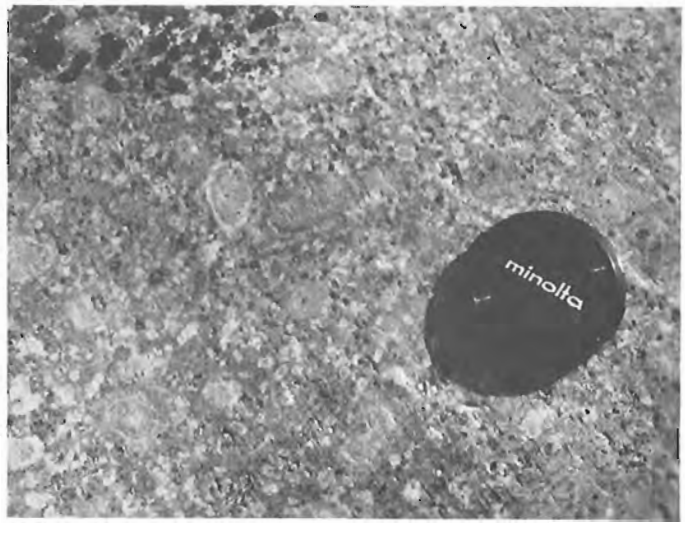

Figure 56.8. *Porphyritic granite (unit 10) showing zoned K-feldspar phenocrysts. (GSC 203944-L)*

parts of the transitional lithologies are mineralized with uranium. Knox (1980) estimated a total thickness of 1110 m for units 5 and 6, and divided the upper unit (unit 8), consisting of mixed clastic rocks, into four informal subunits in parts of 66 G/1 and 2. They are, from bottom to top, feldspathic sandstone, siltstone, upper feldspathic sandstone, and arkose. Thickness was estimated to be 4835 m. Poor outcrop distribution and complex structural relationships preclude such a subdivision in areas to the north and northwest.

The Amer group is moderately to intensely folded and faulted. A series of west- and southwest-trending, moderate to tight anticlines and synclines define a broad synclinorium. Mesoscopic folds plunge at shallow to moderate angles (10°-35°) to the west and southwest, but local reversals to the northeast and east are common. The Amer group strata are affected by east- to northeast-trending thrust faults, and north-northwest-verging overturned folds that show north-northwesterly tectonic transport. Several northwest-trending normal and reverse faults affect the Amer group and the basement, exposing systematically lower stratigraphic units to the southwest. The fault traces are commonly marked by lineaments. Where not drift covered, the boundary of the Amer group with the basement rocks is marked by high angle faults, mylonite zones, and rarely, by unconformable relationships. Approximately 15 km north-northeast of Sand Lake, the supracrustal rocks unconformably overlie unit 2.

Post-Amer Group Sediments (Unit 9)

Approximately 20-25 km northeast of Sand Lake, a coarse grained, polymictic, pebble to boulder conglomerate (Fig. 56.1, 56.7) unconformably overlies the basement complex and is in apparent fault contact with the Amer group. Over 90 per cent of the clasts are made up of granodiorite to granite, the remainder being represented by vein quartz, and rare white orthoquartzite and lithic feldspar grains. The majority of the clasts are aligned in a locally developed shear-induced planar fabric. They are well rounded and lack internal fabric, suggesting a proximal source of massive granitoid. Although the stratigraphic and structural position with respect to the Amer group is uncertain, clasts of orthoquartzite lithologically similar to unit 4 suggests a post-Amer group age for the unit.

Late Intrusive Rocks (Units 10 and 12)

Massive, equigranular to porphyritic, sphene- and fluorite-bearing, hornblende granite (unit 10, Fig. 56.1, 56.8) occupies most of the east-central part of the Deep Rose Lake map area. Quartz monzonite to syenite fractions, presumably related to the main plutonic mass, are present in the southern portions. This granite clearly intrudes the Amer group and older rocks, as evidenced by the presence of abundant inclusions of dolomitic limestone and feldspathic sandstone (units 5 and 8) along the southern and eastern margins of the pluton. A shear-induced foliation is present in the vicinity of Amer fault.

Northwest-trending, medium- to coarse-grained diabase and gabbro dykes (unit 12) related to the Mackenzie swarm cut the basement complex and the cover rocks.

Thelon Formation (Unit 11)

The Thelon Formation, consisting of flat lying to gently dipping (10-15°), light grey-to pink, grey weathering, pebble to boulder conglomerate and gritty sandstone, overlies the basement complex and the Amer group unconformably. These rocks cover most of the southwestern part of the map area. General characteristics of the Thelon Formation in adjacent areas to the south have been described by Donaldson (1965, 1969), and Tella and Thompson (1983). In Deep Rose Lake area, immature to mature, poor to well sorted, pebble to boulder conglomerate occurs at the base. Clasts include angular to rounded, white, grey, and pink orthoquartzite, vein quartz, and rare mudstone (Fig. 56.9, 56.10). Pink, gritty, feldspathic sandstone with fining upward cycles is interbedded with conglomerate. Primary structures include large-scale trough and planar crossbedding, and channel features. Regolith zones that show red hematitic and clay-rich weathering profiles and rare chlorite alteration zones are locally well developed on granitoid basement and on the Amer group rocks at the base of the Thelon Formation.

Figure 56.9. *Boulder conglomerate, Thelon Formation (unit 11) containing angular to rounded clasts of white and grey orthoquartzite (unit 4). The conglomerate is locally developed near a paleoweathering surface of the Amer group quartzite. (GSC 203944-N)*

Figure 56.10. *Polymictic, well rounded, pebble conglomerate at the base of the Thelon Formation (unit 11). Clast compositions are predominantly white, grey, and pink quartzite, and rare red mudstone. (GSC 203944-M)*

Figure 56.11. *Mylonitic layering cut by late fractures and epidote veins. Locally generated pseudotachylyte (PT) zones are present. (GSC 203944-C)*

Faults and Shear Zones

Northeast-trending shear zones, as well as northeast- and northwest-trending faults that are characterized by mylonitic and cataclastic rocks, transect the area on all scales. Low- to high-angle thrust faults affect the Amer group strata and parts of the basement complex (unit 3A). The Amer mylonite zone (Fig. 56.11) and Amer fault (Fig. 56.1) represent short segments of the regionally pervasive, northeast-trending, McDonald-Amer-Meadowbank Fault System (Heywood and Schau, 1978). Southwest continuation of the Amer mylonite zone is somewhat obscured by heavily drift-covered areas and post-mylonite intrusions. The zone, which is truncated and offset by northwesterly faults, is coincident with a pronounced aeromagnetic anomaly (Geological Survey of Canada, 1974a, b). Preliminary analysis of structural data indicates that at least two periods of movement took place along the Amer mylonite zone. Mesoscopic fracture patterns associated with the Amer fault record late dextral displacements of undetermined magnitude. The latest movements postdate the emplacement of porphyritic granite (unit 10). The structural history of the Amer mylonite zone is consistent with that described in the Amer Lake map area (Tella and Heywood, 1978).

Economic Geology

Stratabound and stratiform uranium mineralization is present within drab fine clastic units situated near the boundary of the transitional and upper units of the Amer group. Mineralization is similar mineralogically and stratigraphically to radioactive strata to the northeast in the Amer Lake map area (Curtis and Miller, 1980). Mineralization within black to green-black interbedded siltstone-feldspathic sandstone is localized along silt-sand interfaces or within sandy beds. Pitchblende, uranium-titanium phases, magnetite and disseminated iron and copper-iron sulphides occupy interclastic volumes. Uraniferous zones are underlain by intercalated medium grained, calcareous, feldspathic sandstone and sandy carbonate.

Uranium-phosphorus mineralization was noted in fluorapatite impregnated zones at the base of the Thelon Formation and veins within the basement complex (Miller, 1983).

No mineralization of economic significance was noted within the basement. Minor amounts of pyrite, chalcopyrite, and specularite are sporadically distributed in granitoid gneisses, especially within minor shear zones.

References

Annesley, I.R.
1981a: Field characteristics, petrology, and geochemistry of the Amer Lake ultramafic metavolcanics, District of Keewatin; in Current Research, Part A, Geological Survey of Canada, Paper 81-1A, p. 275-279.

1981b: A field, petrographic and chemical investigation of the Amer Lake mafic and ultramafic komatiites and associated mafic volcanic rocks; unpublished M.Sc. thesis, University of Windsor, 159 p.

Ashton, K.E.
1981: Preliminary report on Geological Studies of the "Woodburn Lake Group" northwest of Tehek Lake, District of Keewatin; in Current Research, Part A, Geological Survey of Canada, Paper 81-1A, p. 269-274.

1982: Further geological studies of the "Woodburn Lake Group" northwest of Tehek Lake, District of Keewatin; in Current Research, Part A, Geological Survey of Canada, Paper 82-1A, p. 151-157.

Barrett, K.R., Laporte, P.J., and Schaub, G.
1978: Preliminary geology map of Amer Lake, 66H/7, Department of Indian Affairs and Northern Development, Economic Geology Section, 1978-1.

Curtis, L. and Miller, A.R.
1980: Uranium geology in the Amer-Dubawnt-Yathkyed-Baker Lakes region, Keewatin District, N.W.T., Canada; in Uranium in the Pine Creek Geosyncline, International Atomic Energy Agency, Vienna, 1980, p. 595-616.

Donaldson, J.A.
1965: The Dubawnt Group, Districts of Keewatin and Mackenzie; Geological Survey of Canada, Paper 64-20.

1969: Descriptive notes (with particular reference to the Late Proterozoic Dubawnt Group) to accompany a geological map of central Thelon Plain, Districts of Keewatin and Mackenzie (65M, NW1/2, 66B,C,D, 75P, E1/2, 76A, E1/2). Report and P.S. Map 16-1968.

Frisch, T. and Patterson, J.G.
1983: Preliminary account of the geology of the Montresor River area, District of Keewatin; in Current Research, Part A, Geological Survey of Canada, Paper 83-1A.

Geological Survey of Canada
1974a: Amer Lake; Geophysical Series (Aeromagnetic) Map 7869G.

1974b: Deep Rose Lake; Geophysical Series (Aeromagnetic) Map 7870G.

Heywood, W.W.
1977: Geology of the Amer Lake map-area, District of Keewatin; in Report of Activities, Part A, Geological Survey of Canada, Paper 77-1A, p. 409-410.

Heywood, W.W. and Schau, M.
1978: A subdivision of the northern Churchill Structural Province; in Current Research, Part A, Geological Survey of Canada, Paper 78-1A, p. 139-142.

Knox, A.W.
1980: The geology and mineralization of the Aphebian Amer Group, southwest of Amer Lake, District of Keewatin, N.W.T.; unpublished M.Sc. thesis, University of Calgary, p. 207.

LeCheminant, A.N. and Ashton, K.E.
1983: Geology of Aberdeen Lake map area, District of Keewatin: preliminary report; in Current Research, Part A, Geological Survey of Canada, Paper 83-1A.

Miller, A.R.
1983: Progress Report: Uranium-Phosphorus association in the Helikian Thelon Formation and Sub-Thelon saprolite, central District of Keewatin; in Current Research, Part A, Geological Survey of Canada, Paper 83-1A.

Patterson, J.G.
1980a: Petrographic study of rocks from the Amer Lake area, District of Keewatin; Department of Indian Affairs and Northern Development, Economic Geology Section, 1980-1.

1980b: Preliminary geology map, eastern end of the Amer belt; Department of Indian affairs and Northern Development, Economic Geology Section, 1980-9.

Patterson, J.G. (cont.)
1981: Amer Lake: An Aphebian fold and thrust complex; unpublished M.Sc. thesis, University of Calgary, 105 p.

Patterson, J.G. and Barrett, K.
1979: Preliminary Geological Map of the Amer Lake Area (66H/7, 10); Department of Indian Affairs and Northern Development, Economic Geology Section, 1979-12.

Tella, S. and Heywood, W.W.
1978: The structural history of the Amer mylonite zone, Churchill Structural Province, District of Keewatin; in Current Research, Part C, Geological Survey of Canada, Paper 78-1C, p. 79-88.

Tella, S. and Thompson, D.L.
1983: Basement Thelon relationships north of Aberdeen Lake (66B/16); in Current Research, Part A, Geological Survey of Canada, Paper 83-1A.

Tippett, C.R. and Heywood, W.W.
1978: Stratigraphy and structure of the northern Amer group (Aphebian), Churchill Structural Province, District of Keewatin, N.W.T.; in Current Research, Part B, Geological Survey of Canada, Paper 78-1B.

Wright, G.M.
1955: Geological notes on central District of Keewatin; Geological Survey of Canada, Paper 55-17.

1967: Geology of the southeastern barren grounds, parts of the Districts of Mackenzie and Keewatin (Operation Keewatin, Baker, Thelon); Geological Survey of Canada, Memoir 350.

57.

NONLINEAR ELASTIC CHARACTERISTICS OF GRANITE ROCK SAMPLES FROM LAC DU BONNET BATHOLITH[1]

Project 810043

A. Annor[2] and T.J. Katsube
Resource Geophysics and Geochemistry Division

Annor, A. and Katsube, T.J., Nonlinear elastic characteristics of granite rock samples from Lac du Bonnet Batholith; in Current Research, Part A, Geological Survey of Canada, Paper 83-1A, p. 411-416, 1983.

Abstract

Rocks exhibit a nonlinear elastic behavior at low stresses. This is due to the presence of pores and microfractures in the rock. This phenomenon has been studied in the past by a number of investigators. An attempt is being made to utilize this phenomenon in characterizing rocks in terms of the effect that stress has on changes in pore structure and, therefore, radionuclide migration. This is being accomplished by polynomial regression of the nonlinear stress-strain curves and the development of nonlinear elastic parameters.

Introduction

Micropores along grain-boundaries, within grains or across grains constitute the network of ion and radionuclide transport paths in crystalline rocks (Katsube, 1981; Wadden and Katsube, 1982; Katsube et al., 1982b). Long term effects such as glacier activities, or short term effects such as construction of large subsurface cavities can change the pattern of subsurface stress distribution in rocks in the Canadian Shield that might be used to store high level nuclear fuel waste.

The stress-strain relationship of materials is generally considered linear and governed by Young's modulus. For rocks at low stresses, however, the relationship is nonlinear (Walsh, 1965a, b; Brace, 1965) as shown in Figure 57.1. Adams and Williamson (1923) suggested that this nonlinear behavior is due to cracks and cavities in the rock. Walsh (1965a, b) studied the effect of cracks on the compressibility of rocks under both uniaxial and hydrostatic pressure. He showed that nonlinear behaviour in the initial stages of the uniaxial stress-strain curve is due to the presence of cracks. An increase in axial stress closes some cracks and rocks become stiffer as the linear portion of the stress-strain curve is reached. He also indicated that in certain cases where pores consist of narrow cracks, their porosity could be determined from hydrostatic compressibility measurements. Brace (1965) confirmed this finding through experimental studies on Westerly granite samples and utilized a graphical technique developed by Walsh (1965a) for evaluating "crack porosity" from stress-strain curves. This "crack porosity" relates to the porosity of the cracks that become closed under stress. This is accomplished by projecting the linear portion of the stress-strain curve to the zero pressure intercept on the strain axis (Fig. 57.1).

It is obvious from these studies that a change in applied stress could affect the aperture of certain pores and, therefore, change the characteristics of ion or radionuclide transport paths. Katsube (1981) showed an example of permeability decreasing to less than a tenth of its original value by doubling the hydrostatic pressure on a granite sample (see permeability of rock sample under confined and unconfined pressure at 700-800 m depth in Fig. 57.2). It is imperative to determine the extent that pores close at any given stress in the nonlinear region of elasticity, and how the effect of stress on pore closure varies within the rock mass. Methods to represent the nonlinear elasticity of rocks are being developed. This paper introduces a set of nonlinear elastic parameters which can be used to characterize the rock mass in terms of its nonlinear behavior and which may eventually be used to determine the pore closure at any given stress.

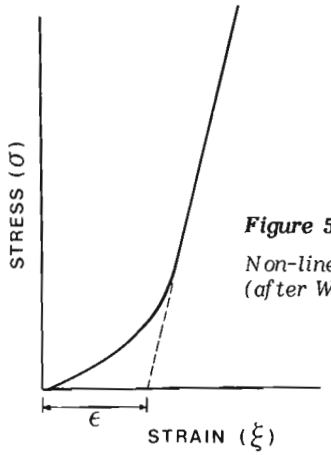

Figure 57.1

Non-linear stress-strain curve of rocks (after Walsh 1965a).

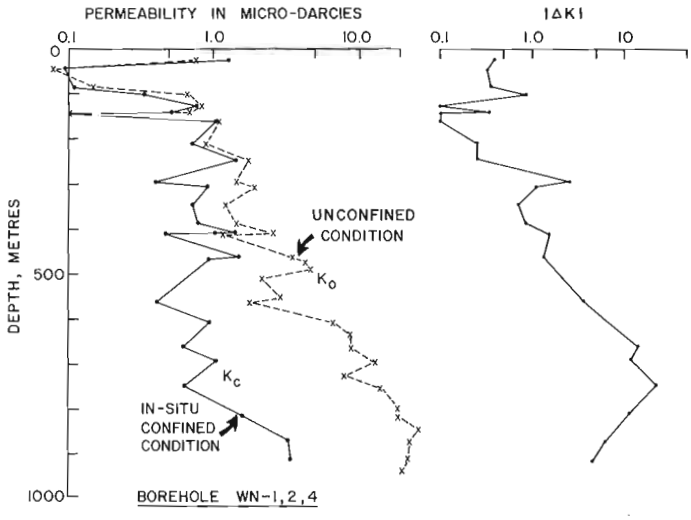

Figure 57.2. *Permeability under in-situ confined pressure (k_c) and unconfined pressure (k_o) down borehole WN-1,2,4 in Lac du Bonnet batholith (after Katsube, 1981).*

[1] Work done for Atomic Energy of Canada Limited as part of the Nuclear Fuel Waste Management Program

[2] Canada Centre for Mineral and Energy Technology

Theory

As one of the parameters to represent micropore closure, we adopt "crack porosity (ε)" that was introduced by Walsh (1965a) and Brace (1965). The linear part of the stress-strain curve in Figure 57.1 is expressed by

$$\sigma = E(\xi - \varepsilon) \quad (1)$$

where σ = stress (MPa) ξ = strain E = elastic modulus (MPa).

The theoretical basis for crack closure with pressure has been dealt with extensively in papers by Walsh (1965a, b), Brace (1965), Walsh and Grosenbaugh (1979). Walsh (1965a) determined the pressure required to close elliptical cracks under hydrostatic compression. Expressed mathematically,

$$P_c = \frac{\pi E \alpha}{4(1-\gamma^2)} \quad (2)$$

where P_c = Pressure (MPa) α = Aspect ratio (length/width) γ = Poisson's ratio

Walsh and Grosenbaugh (1979) found that the compressibility (β) of a material with continuous fractures with rough surfaces is dependent upon the fracture surface topography parameter Ah/V:

$$(\beta - \beta_s)^{-1} = (\beta_o - \beta_s)^{-1} + P(V/Ah) \quad (3)$$

where β_s = compressibility of matrix material,
β_o = effective compressibility when no asperities are in contact,
P = pressure
A/V = total apparent surface area per unit volume
h = standard deviation of height distribution of the asperities.

Elements that affect the nonlinear and linear portions of the stress-strain curves are described in equations (1)-(3). It is now of interest to determine the strain at any given pressure from the actual stress-strain measurements. To do this, we consider the relationship between the stress (σ) and strain (ξ) to be,

$$\xi = f(\sigma) \quad (4)$$

where $f(\sigma)$ = function of stress.

Then determine the coefficients for the following polynomial equation, by use of polynomial regression analysis.

$$f(\sigma) = a_0 + a_1\sigma + a_2\sigma^2 + a_3\sigma^3 + a_4\sigma^4 + a_5\sigma^5 \quad (5)$$

where $a_0 \ldots a_5$ = coefficients

Experimental Procedure

Samples

Core specimens (diameter = 4.5 cm, length = 10 cm) used for the investigation originated from depths ranging between 24.0 and 461.0 m from boreholes WN1 and WN2 in the Lac du Bonnet batholith in Manitoba. The sample population consisted of fourteen granite and two tonalite specimens. There were no fractures visible in the specimens.

The granite specimens were generally homogeneous, pinkish coloured and massive. They were composed of about 45-60% pink subhedral potassium feldspar, 25-40% quartz, 20-25% white zoned euhedral plagioclase, 5-10% biotite and traces of chlorite. Quartz is interstitial to the potassium feldspar and formed an irregular mosaic. The two tonalite specimens contained 50% of white, oblong-shaped plagioclase phenocrysts (0.5 to 1.5 cm long), outlined by clots of hornblende (up to 1.8 cm long) plus minor biotite. Quartz constitutes about 15% of the rock and is interstitial to plagioclase (Chernis, 1979).

Sample Preparation

Cylindrical test specimens with an average length to diameter ratio of about 2.2 were used for the measurements. Samples were cut slightly larger than their final dimensions using a diamond saw and water as a coolant. Sample ends were then ground parallel to each other to within 0.03 mm, and at right angles to the longitudinal axis using hardened steel jigs and a lapping wheel. To carry out elastic deformation measurements, strain gauges oriented to measure axial and transverse strain were centred equidistant from the two ends of the specimen with gauges of similar orientation located on the opposite side of the specimen. The axial and transverse gauges were connected in series to form single active-gauges which were used in half bridge configurations for strain measurements. The gauges used were of the BLH Electronics Co. SR-4, FAE series (Gyenge and Herget, 1977).

Equipment and Measurement Procedure

Equipment used to measure axial and transverse specimen deformation under applied axial load, consisted of two Phillips PR9302 strain bridges and a Mosley Autograph 2FRA X-Y recorder. The bridges were used in a half-bridge configuration. Axial and transverse strain gauges were used to provide voltage analog outputs of the axial and transverse strains produced in the samples by axial loading. These analogs were used to drive independently the two Y-axes plotters of the 2FRA X-Y recorder. Axial and transverse stress-strain curves were obtained in this manner for each specimen tested (Annor and Geller, 1979). These curves were used to determine Young's modulus and Poisson's ratio (Annor et al., 1979). Typical axial and circumferential stress-strain curves reproduced from recorder output are provided in Figure 57.3.

Data Analysis and Results

The total crack porosity (ε) for each sample was determined by projecting the linear portion of the axial stress-strain curve to the zero pressure intercept on the strain axis (Fig. 57.1, 57.3). The elastic modulus was determined from the linear portion of the curve. The stress co-ordinate at the point of tangency was assumed to represent the total axial stress (P_o) required for pore closure. The regression analysis package available for a Hewlett Packard H.P. 85 portable mini-computer was used for polynomial regression of the experimental data, and to determine the coefficients in equation (5). A fifth order polynomial was used for the regression analysis. The correlation coefficient values for the regression are in the order of 0.97-0.99. The results are compiled in Table 57.1.

Discussion

Some typical stress-strain curves are shown in Figure 57.4. The sample numbers indicate the depth in the borehole (Table 57.1). It seems that these curves generally tend to shift to the right as depth increases. This is probably due to a larger stress release with depth. It is interesting to note that some curves rise more rapidly than others (Fig. 57.5). The stress-strain curves can be divided into two sections, and are labelled as 'primary' and 'secondary' portions of the stress-strain curves.

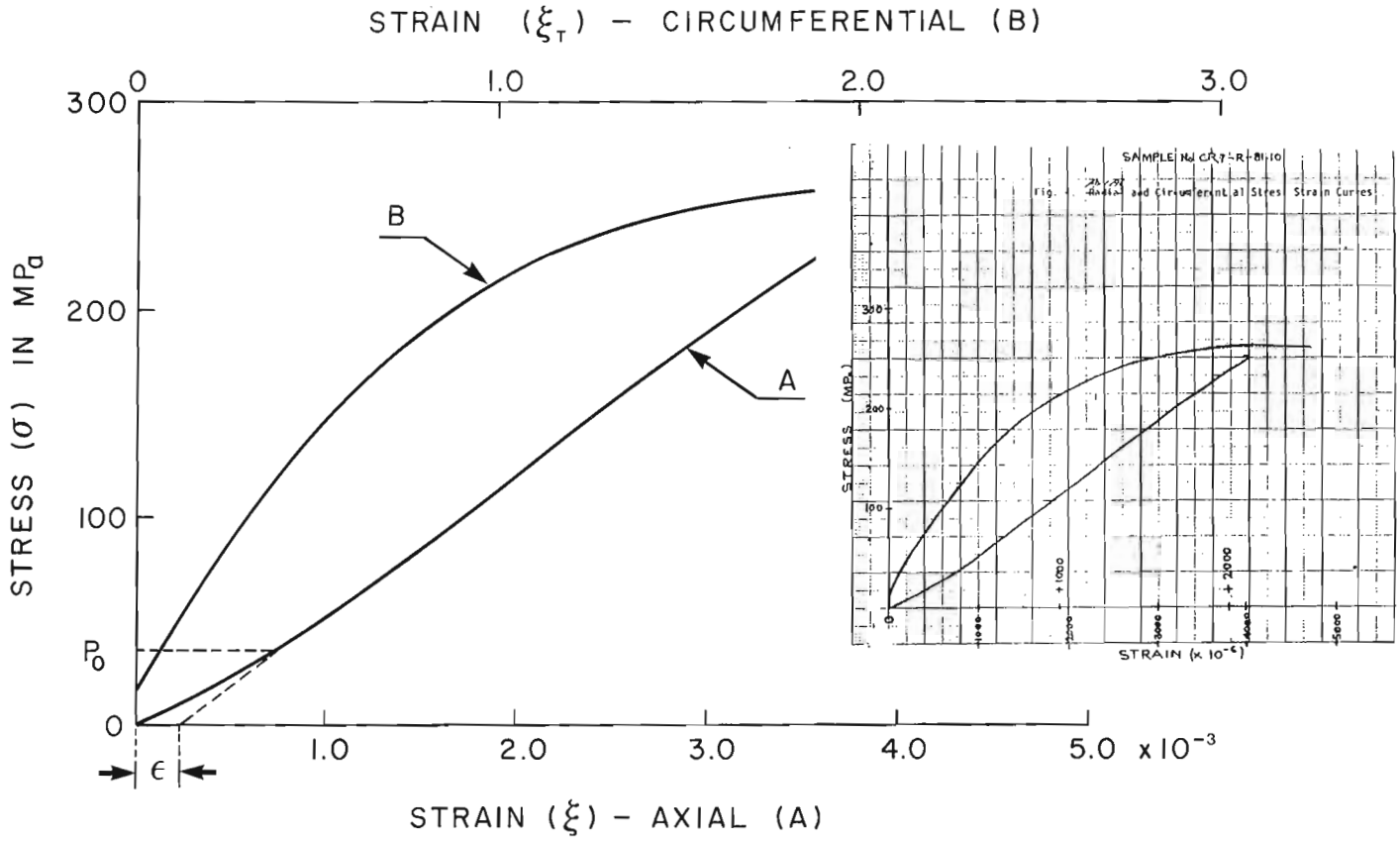

Figure 57.3. *Stress-strain curves representing analog traces of actual measurements (inserted diagram).*

Table 57.1

Mechanical properties and values for the coefficient of the polynomial equation

Sample	Depth H	Crack Porosity ϵ	Point of Tangency P_o	Elastic Modulus E	Coefficients* a_0	a_1	a_2	a_3	a_4	Correlation Coefficient
WN2 -24	24.75	.016	3.6	7.0E4	5.0E-6	3.6E-5	-1.86E-6	7.3E-8	-2.6E-9	.998
-55	55.45	.008	14.3	7.4E4	0	4.2E-5	-2.4E-6	8.2E-8	0	.996
-85	85.40	.004	14.3	7.3E4	0	2.4E-5	-5.6E-7	1.8E-8	0	.999
-98	98.50	.008	14.3	6.9E4	-4.2E-7	1.83E-5	-9.8E-8	9.2E-9	0	.999
-124	124.70	.012	3.5	6.9E4	4.2E-6	3.5E-5	-1.37E-6	4.6E-8	0	.996
WN1 -138	138.60	.021	14.3	6.9E4	6.4E-5	4.8E-5	-2.9E-6	1.19E-7	-2.6E-9	.974
WN2 -145	145.85	.028	14.3	7.1E4	8.3E-5	5.1E-5	-2.9E-6	1.28E-7	-2.6E-9	.992
WN1 -160	160.90	.017	14.3	6.6E4	4.2E-5	3.5E-5	-1.80E-6	8.2E-8	-2.6E-9	.996
-224	224.00	.016	7.1	7.2E4	4.2E-5	3.1E-5	-1.01E-6	3.7E-8	0	.996
-246	246.00	.019	14.3	7.1E4	4.2E-5	3.5E-5	-9.8E-7	2.7E-8	0	.992
-294	294.50	.020	21.4	7.1E4	4.4E-5	4.4E-5	-2.6E-6	1.10E-7	-2.6E-9	.992
-303	303.50	.012	14.3	6.7E4	1.3E-6	3.0E-5	-2.9E-7	-2.7E-8	2.6E-9	.996
-345	345.50	.024	14.3	7.0E4	4.3E-5	4.3E-5	-2.1E-6	6.4E-8	0	.994
-384	384.80	.020	7.1	6.9E4	4.8E-5	4.2E-5	-1.83E-6	6.4E-8	0	.992
-410	410.70	.028	28.4	7.3E4	6.3E-5	4.2E-5	-1.76E-6	5.5E-8	0	.994
-460	460.60	.036	28.4	6.4E4	-7.1E-6	4.7E-5	-1.34E-6	2.7E-8	0	.991
(Units)	(M)	(%)	(MPa)	(MPa)		$(MPa)^{-1}$	$(MPa)^{-2}$	$(MPa)^{-3}$	$(MPa)^{-4}$	

* a_5 = 9 For all Samples

The strain (ξ) for various pressures is calculated for all the samples by inserting the values for the coefficients listed in Table 57.1 into equation (5). Some of the results are shown in Table 57.2 and Figure 57.6. The strain for a given stress varies with depth to a great extent, but generally shows a slight increase with depth. It is interesting to note that the sharp increases and decreases in strain are related to open fractures with large dips and to zones containing veins (Fig. 57.7).

The strain at several overburden stresses (σ_V) has also been calculated using equation (5). The results are shown in Table 57.2 and Figure 57.8. The overburden stress (σ_V) is calculated by,

$$\sigma_V = \rho g z \qquad (6)$$

where σ_V = overburden stress (kPa)
ρ = density ($kg\ m^{-3}$)
g = acceleration due to gravity ($m\ s^{-2}$)
z = depth (m)

These results are also listed in Table 57.2. The trends in Figure 57.8 are similar to those in Figure 57.6, except that the increase of strain with depth is greater. This is because the stress-strain curves generally shift to the right due to greater stress release (Fig. 57.5) for samples from greater depths and because the secondary portion of the curve is more dependent on the effect of depth, whereas the primary portion is more dependent on local geological features such as veins and fractures.

The anomalous minimums that appear at depths of about 85, 303 and 460 m on the strain versus depth curves (Fig. 57.6, 57.8) gradually disappear as overburden stresses are increased. This implies that the mechanism that causes the primary portion of the stress-strain curve to enhance itself is not active at higher stresses. Because pores and microfractures are the cause of the nonlinear elastic behaviour of the rock, this may suggest that the pores in these regions show greater stiffness compared to the other regions.

The increase of strain with depth at constant stresses (Fig. 57.6, 57.7) is due to larger stress release with depth. According to Katsube et al. (1982a) this stress release is reflected in the porosity of the rocks which show greater available porosity with depth. The same study also suggests that as the stress release increases, a larger portion of the available porosity becomes connecting porosity.

Though it may be generally accepted that the existence of pores are the cause of the nonlinear elasticity (Brace, 1965; Walsh, 1965a, b; Katsube et al., 1982a), the precise mechanism involved is unclear at this stage. This study indicates that there could be two different categories of mechanisms that govern the nonlinearity. This is due to

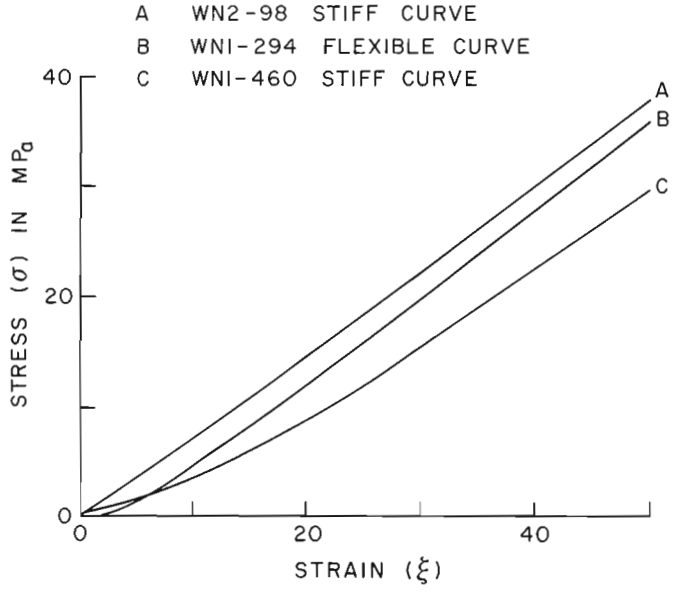

Figure 57.4. *Some typical stress-strain curves for samples from Lac du Bonnet batholith.*

Table 57.2

Strain at various stresses

Sample	$\xi(\sigma)$ σ=1.0	(σ: MPa) 1.4	2.0	5.0	10.	$\xi(\sigma_V)$ σ_V	$0.5\sigma_V$	$1.0\sigma_V$	$2.0\sigma_V$
WN2 -24	4.9E-5	5.4E-5	8.8E-5	1.74E-4	2.3E-4	.56	1.78E-5	3.0E-5	5.4E-5
-55	5.2E-5	5.5E-5	9.7E-5	2.0E-4	3.4E-4	1.26	3.4E-5	6.5E-5	1.18E-4
-85	3.1E-5	3.2E-5	6.0E-5	1.39E-4	2.6E-4	1.93	3.0E-5	5.8E-5	1.10E-4
-98	2.4E-5	2.4E-5	4.8E-5	1.20E-4	2.5E-4	2.23	2.7E-5	5.4E-5	1.07E-4
-124	4.8E-5	5.0E-5	8.8E-5	1.89E-4	3.4E-4	2.82	6.5E-5	1.18E-4	2.1E-4
WN1 -138	1.2E-4	1.20E-4	1.71E-4	2.8E-4	3.8E-4	3.13	1.50E-4	2.2E-4	3.2E-4
WN2 -145	1.42E-4	1.42E-4	2.0E-4	3.2E-4	4.5E-4	3.30	1.78E-4	2.6E-4	3.7E-4
WN1 -160	6.3E-5	8.5E-5	1.21E-4	2.1E-4	2.9E-4	3.64	1.15E-4	1.74E-4	2.6E-4
-224	7.9E-5	8.1E-5	1.15E-4	2.1E-4	3.6E-4	5.06	1.34E-4	2.1E-4	3.6E-4
-246	8.6E-5	8.3E-5	1.28E-4	2.4E-4	4.0E-4	5.56	1.60E-4	2.6E-4	4.4E-4
-294	9.6E-5	9.4E-5	1.42E-4	2.5E-4	3.4E-4	6.66	1.93E-4	2.9E-4	3.6E-4
-303	4.0E-5	4.0E-5	7.8E-5	1.82E-4	3.6E-4	6.86	1.29E-4	2.4E-4	5.8E-4
-345	9.5E-5	9.5E-5	1.42E-4	2.5E-4	3.9E-4	7.81	2.2E-4	3.3E-4	6.2E-4
-384	9.9E-5	9.9E-5	1.42E-4	3.6E-4	4.3E-4	8.70	2.4E-4	3.8E-4	8.6E-4
-410	1.13E-4	1.13E-4	1.61E-4	2.8E-4	4.4E-4	9.29	2.7E-4	4.1E-4	8.9E-4
-460	5.4E-5	1.10E-4	2.6E-4	4.5E-4	4.5E-4	10.41	2.7E-4	4.6E-4	8.7E-4
(Units)						(MPa)			

σ_V: Overburden Stress

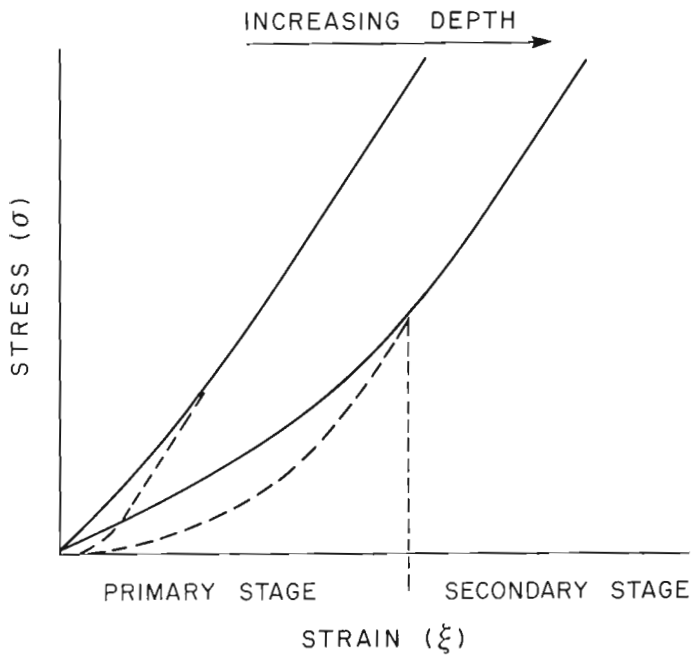

Figure 57.5. Illustration of stress-strain curve characteristics. Solid line traces the rapidly rising curve; the broken line traces the slowly rising curve.

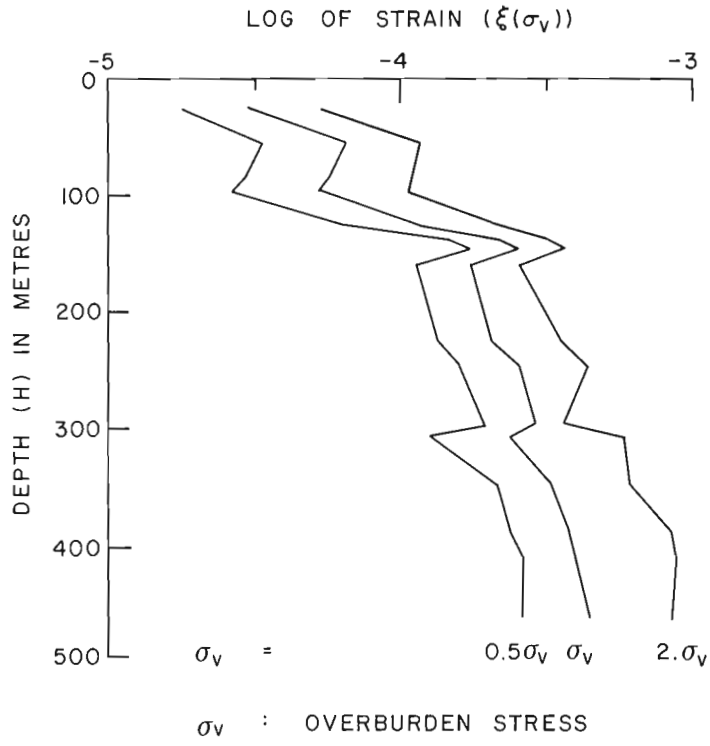

Figure 57.7. Strain (ξ) variation with depth and its relationship with geological features (after Katsube et al., 1982a). Shaded areas a and b represent zones affected by fractures with large dip angles, and zones affected by veins, respectively. Broken lines indicate zones without data.

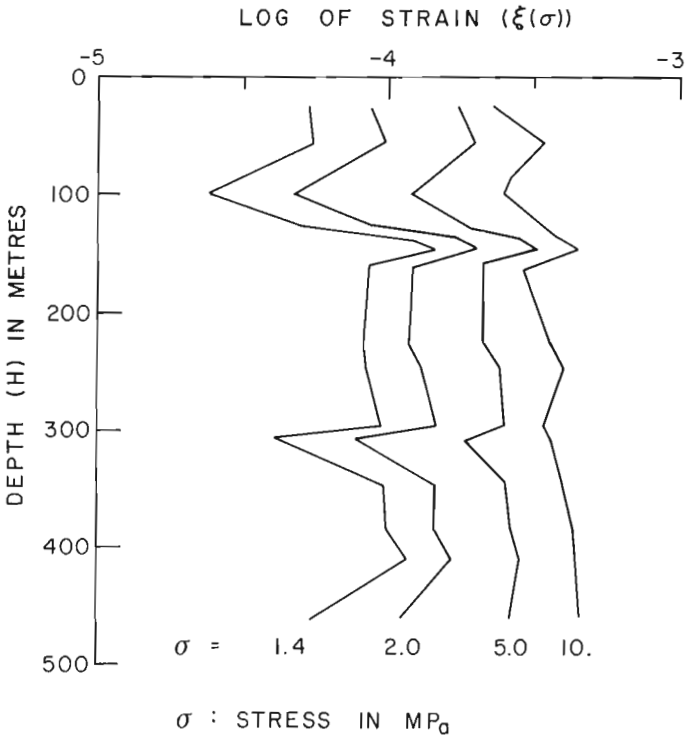

Figure 57.6. Strain (ξ) variation with depth for different stresses in borehole (WN-1) in the Lac du Bonnet batholith.

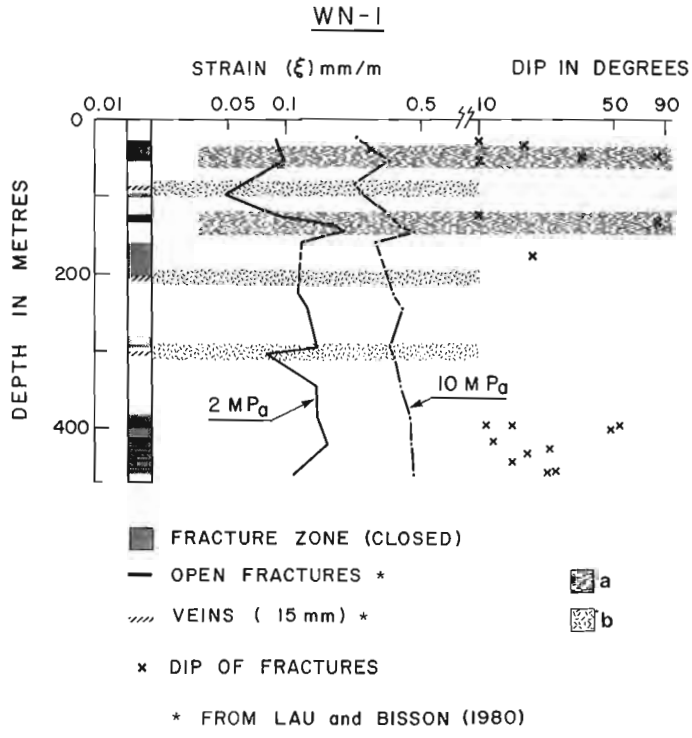

Figure 57.8. Strain (ξ) variation with depth for different overburden stresses (σ_v) down borehole (WN-1) in Lac du Bonnet batholith.

the fact that the nonlinear curve can be divided into two portions. However, regardless of the existence of these uncertainties, the strain determined at different stresses reveals the effects that certain geological features have on nonlinearity, and which obviously are relevant to pore structure (Katsube et al., 1982a). Any effect on pore structure implies possible change in aperture of connecting pores. Therefore, these parameters (strain determined at different stresses) may be used to characterize the rock mass in a way that is significant with respect to radionuclide migration.

Conclusions

Polynomial regression is used to determine the nonlinear parameters, which essentially, are strain at different stresses. Although the precise mechanisms involved in relating pore structure to the nonlinearity are not yet clear, these parameters reveal interesting characteristics which appear to be significant, in both the geological and depth effect on pore structure and which possibly will eventually be linked to radionuclide migration characteristics of the rocks. This study suggests that the nonlinear part of the stress-strain curve can be divided into two portions, and that the mechanisms involved may fall into two separate categories. The results obtained to date indicate that the application of nonlinear tests on a wider variety of rock types could reveal further information relevant to pore structure characteristics.

Acknowledgments

The authors wish to acknowledge the contributions of J.B. Percival (Atomic Energy of Canada Limited) for her suggestions and critical review of the manuscript. C. Huang (AECL) for his critical review of the manuscript. The authors also express thanks to J.P. Hume (AECL) and A.G. Darnley (GSC) for reviewing of the manuscript, and to G.E. Larocque (Canada Centre for Mineral and Energy Technology) for his general guidance in this study.

References

Adams, L.H. and Williamson, E.D.
1923: The compressibility of minerals and rocks at high pressure; Journal of Franklin Institute, v. 195, p. 475-529.

Annor, A., Larocque, G.E., and Chernis, P.
1979: Uniaxial compression tests, Brazilian tensile tests and dilatational velocity measurements on rock specimens from Pinawa and Chalk River; CANMET Laboratory Report MRP/MRL 79-60 (TR).

Annor, A. and Geller, L.
1979: Dilatational velocity, Young's modulus, Poisson's ratio, uniaxial compressive strength and Brazilian tensile strength for WN1 and WN2 samples; CANMET-Mining Research Laboratories. Technical Data 303410-M01/78.

Brace, W.F.
1965: Some new measurements of linear compressibility of rocks, Journal of Geophysical Research, v. 70(2), p. 391-398.

Chernis, P.J.
1979: Petrographical analysis of borehole samples (Label-P specimens) from WN-1, WN-2, CR-6 and CR-7; GSC Electrical Rock Property Laboratory Technical Report 7879-T5 (Available from T.J. Katsube (GSC).

Gyenge, M. and Herget, G.
1977: Pit Slope Manual Supplement 3-2; Laboratory Tests for Design Parameters; CANMET Report 77-26, 74 p.

Katsube, T.J.
1981: Pore structure and pore parameters that control the radionuclide transport in crystalline rocks; Proceedings of the Technical Program International Powder and Bulk Solid Handling and Processing, Rosemont, Ill., May 12-14, p. 393-409.

Katsube, T.J., Annor, A., Hume, J.P., Kamineni, D.C., and Percival, J.B.
1982a: Effect of stress and alteration on pore structure and radionuclide transport; Geological Association of Canada-Mineralogical Association of Canada Joint Annual Meeting, Winnipeg, May 17-19. Abstract.

Katsube, T.J., Percival, J.B., and Hume, J.P.
1982b: Contribution of pore structure to the isolation capacity of crystalline rocks; Proceedings of the Nuclear Fuel Waste 12th Information Meeting, University of Waterloo, Jan. 27-28, Atomic Energy of Canada Limited, Technical Record-200.

Lau, J.S.O. and Bisson, J.G.
1980: A preliminary report on borehole WN-1 television survey; Atomic Energy of Canada Limited, Technical Record TR 115-8.

Wadden, M.M. and Katsube, T.J.
1981: Radionuclide diffusion in crystalline rocks; Chemical Geology, v. 36, p. 191-214.

Walsh , J.B.
1965a: The effect of cracks on the compressibility of rock; Journal of Geophysical Research, v. 70(2), p. 381-389.

1965b: The effect of cracks on the uniaxial elastic compression of rocks; Journal of Geophysical Research, v. 70(2), p. 399-411.

Walsh, J.B. and Grosenbaugh, M.A.
1979: A new model for analyzing the effect of fractures on compressibility; Journal of Geophysical Research, v. 84 (B7), p. 3532-3536.

58. EVIDENCE OF SEAFLOOR INSTABILITY IN THE SOUTH-CENTRAL STRAIT OF GEORGIA, BRITISH COLUMBIA: A PRELIMINARY COMPILATION

Projects 820017 and 740062

T.S. Hamilton [1] and J.L. Luternauer [1]
Cordilleran Geology Division, Vancouver

Hamilton, T.S. and Luternauer, J.L., Evidence of seafloor instability in the south-central Strait of Georgia, British Columbia: a preliminary compilation; in Current Research, Part A, Geological Survey of Canada, Paper 83-1A, p. 417-421, 1983.

Abstract

Geophysical profiles (1700 km) in the Strait of Georgia reveal widespread distribution of features suggesting seafloor instability including faults, slumps, slides, and submarine valleys.

Introduction

A geophysical survey was conducted in the Strait of Georgia (Fig. 58.1-58.4) during the period 15-29 February, 1982 on board the **CSS Vector**. This survey constituted the first stage of a new program of the Geological Survey of Canada to define the regional geology, stratigraphy and tectonic character of the Georgia Depression. In addition to elucidating the Cenozoic history, the findings can help guide industrial development and environmental control of the area.

The marine geophysical survey (Fig. 58.3) consisted of: single-channel seismic profiles (CSP), 3.5 kHz high-resolution profiles and total field magnetometer data. A total of 1700 km of survey lines were run across the strait on a 2 km spacing with a pair of connecting tie lines along the strait.

The single-channel seismic system consisted of an array of 2 airguns (Bolt, 16.5 and 82 cc) towed immediately below the surface and an 18 m hydrophone array consisting of 50 elements (Aquadyne AQ-1) with a 36 cm spacing towed 33 m astern of the guns. The hydrophone array had a built-in pre-amp with a gain of 100 in the range from 22Hz to 100 kHz. Data were displayed on an EPC graphic recorder (0-1 s full scale, half wave-rectified, variable-density plot) with filter settings of 70 and 480 Hz. The 3.5 kHz system consisted of an array of hull-mounted transducers with the data displayed on another EPC graphic recorder (0.25 s full scale). Navigational fixes were taken from the West Coast Canadian 5990 Loran C chain at 5 minute intervals and recorded on a portable hydrographic data logger (PHAS 8800), with periodic radar fixes. The magnetic survey consisted of a Barringer OM-104 proton precession instrument towed 180 m astern and recorded on the PHAS system. Ship speed during the survey varied from 3 to 6 knots; this information together with course changes, wind and noise conditions were noted in a handwritten log.

Analyses of the data resulted in the interpretation of the seismic stratigraphy of the CSP records and the examination of the shallowest part of the section for features that can be mapped. The information from the CSP profiles has been combined with field evidence derived from investigations of Fraser Delta sedimentation (Luternauer, 1975, 1976a,b, 1977, 1980; and Luternauer et al., in press; Luternauer and Finn, in press). Shallow and surface features indicative of instability on the present surface of the seafloor include submarine valleys, slides, slumps, sand waves and fault scarps (Fig. 58.5)

Geological Setting

The Strait of Georgia is one of a series of structural depressions extending from northern California to Hecate Strait (Fig. 58.1) that have subsided intermittently since Late Cretaceous time (Muller, 1977; Roddick et al., 1979; Mathews et al., 1970; Mathews, 1971). This subsidence may be linked to the underthrusting of oceanic lithosphere beneath Vancouver Island (Atwater, 1970; Riddihough and Hyndman, 1976; Riddihough, 1977; Rogers, 1979). Upper Cretaceous and Tertiary rocks which accumulated in this depression dip basinwards from the margins and underlie both Pleistocene glacial and interglacial deposits from which much of the present marine basin has been sculpted, and postglacial deposits including the Fraser Delta (Fig. 58.2, 58.4, 58.5) (Luternauer et al., in press).

Review of Recent Seismicity

No major earthquakes (i.e. those having magnitudes greater than 5.0) have occurred within the strait during historical times and recorded earthquakes (Milne et al., 1978) do not appear to lie along fault lines previously mapped within the strait (Roddick et al., 1979; Tipper et al., 1981). Areas adjacent to the strait have, however, experienced major earthquakes (Milne et al., 1978). The closest, and most intense of those occurred on June 23, 1946 and was associated with suspected movement along the Beaufort Range Fault (Slawson and Savage, 1979) in central Vancouver Island. It had an epicentre 20-30 km south of Campbell River (Fig. 58.1) and a magnitude of 7.2 ± 0.1 (Rogers and Hasegawa, 1978).

The capability of recording and locating low magnitude earthquakes in this area has been in place since 1951. Since that time the region between southern Texada Island and the middle of the Gulf Islands (Fig. 58.4) has been comparatively aseismic (Milne et al., 1978; Rogers, 1982). The only

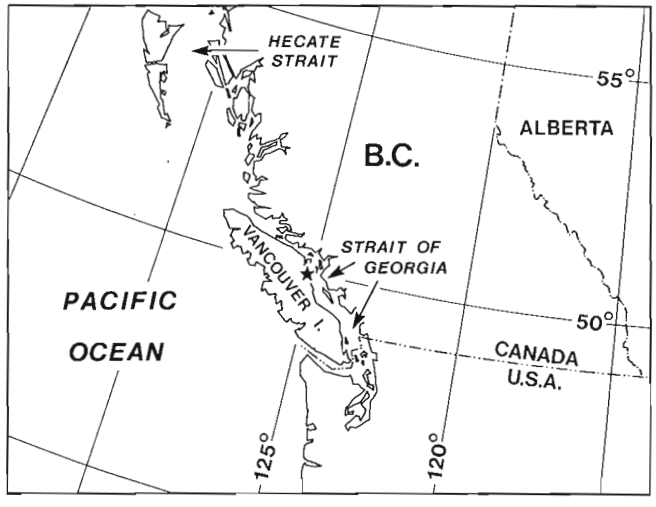

Figure 58.1. *Geographic setting of the Strait of Georgia. Asterisk indicates location of Campbell River.*

[1] Pacific Geoscience Centre, Sidney, B.C.

significant earthquake in the Strait of Georgia was the magnitude 4.9 event on November 30, 1975 with a series of small aftershocks continuing into 1976. The most likely interpretation from the fault plane solution is thrust faulting across an east-west fault (Rogers, 1979). The epicentre position coincides (within error) with a young east-west fault scarp which extends from the Fraser Ridge westward into Ballenas Basin (Fig. 58.2, 58.4, 58.5) (Luternauer et al., in press).

The existence of recent seafloor scarps and fault offsets on the Fraser Delta, along the eastern margin of the Gulf Islands and along the floor of the Ballenas Basin is somewhat problematical in light of the low incidence of seismicity. Faulting on the delta may be due to soft-sediment compaction, variable compaction due to different sediment thicknesses and underlying topography, and listric slumping or mass wasting. Faulting along the Gulf Islands side of the strait could be rootless, down basin movement of blocks of Tertiary and Cretaceous rocks which had been unloaded and oversteepened on the basinward side by Pleistocene erosion. Another nontectonic explanation for the young faulting could be a rebound response to deglaciation. Mörner (1982) observed similar paleoseismic indicators in the Fennoscandian shield including extensively faulted, 'glacifluvial' deltas and eskers, and 'deformational tills'. This type of explanation for faults in the Strait of Georgia cannot, at present, be dismissed. A further consideration is that during the last 30 years the seismic climate of the strait has been atypically quiescent and may not reflect earlier postglacial levels of energy release.

Discussion

Channels, Trenches, Canyons and Other Submarine Valleys

Sea valleys and/or canyons on the foreslope of the Fraser Delta have symmetrical or asymmetrical cross-sectional profiles and have developed off present or former distributary mouths; likely in response to failure of oversteepened deposits at a channel mouth, intermittent sliding of gully-bottom sediments and flushing action of tidal currents (Luternauer, 1980; Luternauer and Finn, in press). A major valley (on the north side of Fraser Ridge) and the channels within the tractive-transfer corridor (Luternauer et al., in press; Fig. 58.2, 58.4) have low, symmetrical cross-sectional profiles and are generally consequent to local slump traces or faults. Channels and submarine canyons along the Gulf Islands and margins of Ballenas Basin have asymmetrical profiles and are developed alongshore, parallel to Cretaceous or Tertiary bedrock ridges or parallel to steeply walled banks consisting of Pleistocene sediments (Luternauer et al., in press). Where an asymmetrical channel parallels a ridge or bank the difference in channel slopes can be explained by differential erosion. Channel cross-sectional profiles also are asymmetrical where a channel is perched on a ledge and one of the sides is fault controlled. In neither of the above two circumstances is asymmetry imposed by the regional slope.

Slumps and Slides

Smaller scale, apparent slumps having asymmetrical profiles are abundant on the Fraser Delta slope and at the margins of banks. Larger slumps are evident at the base of the delta slope and in perched, sediment-covered ledges along the margins of the strait. In the region of the foreslope hills (Tiffin et al., 1971; Fig. 58.2, 58.4, 58.5), a series of disharmonic undulating reflectors extended down through the entire postglacial succession suggesting that slumping locally has been a recurring phenomenon (Luternauer and Finn, in press). Although some of these folds may have been generated by mass wasting, the shallow regional slopes may require alternate explanations for their origin, such as soft sediment postdepositional deformation due to loading, compaction and/or faulting.

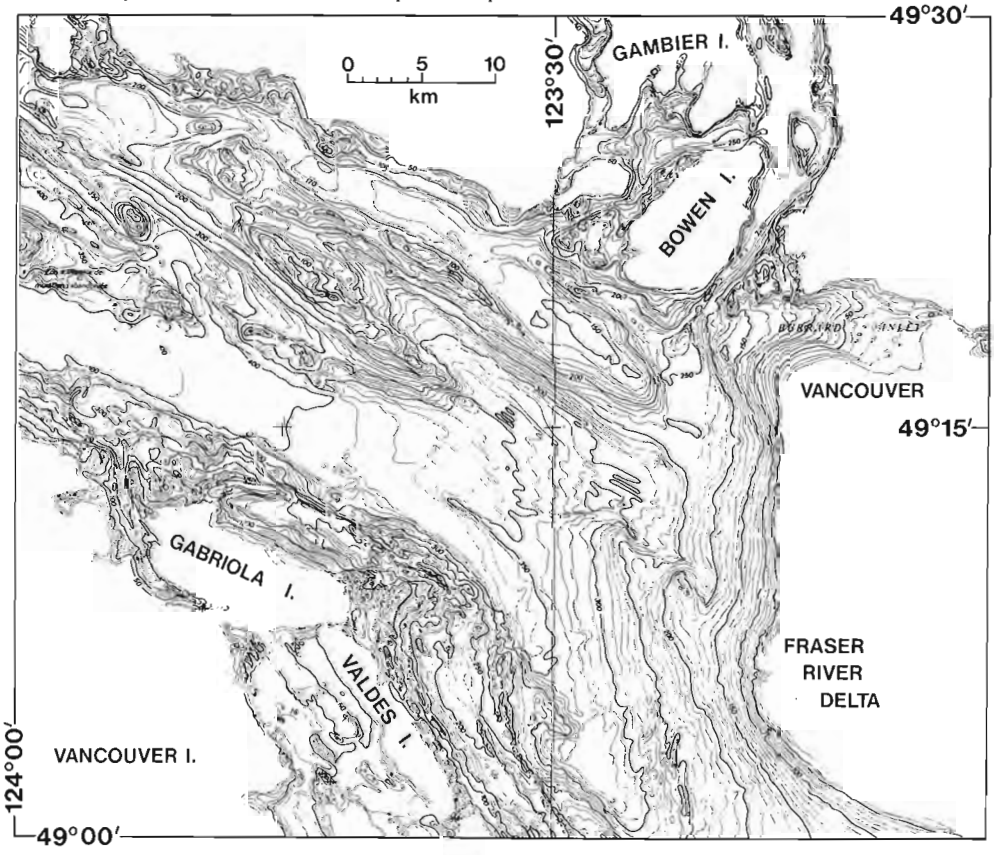

Figure 58.2. Bathymetry of the Strait of Georgia.

A comparison of the bottom trace on the February 1982 geophysical data with a 1968 Canadian Hydrographic Survey has been made for the region of the foreslope hills. An apparent shift in bottom morphology at a water depth of 225 to 325 m, may have resulted from erosion, deposition and slumping during the intervening 14 years.

Submarine landslides occur at the base of eroded slopes along banks. Their wedge-shaped or talus cone form in cross-section often has considerable relief and variation in slope on the upper surface. They are commonly separated from their parent slope indicating subsequent sag or erosion. Acoustically, the most easily recognized slides rest on the typical upper postglacial (Luternauer et al., in press) "seafloor" reflection signature. The slides have a more disturbed or chaotic structure compared to the subjacent upper postglacial (UPG) unit. The slides also show a higher impendance contrast than their adjacent Pleistocene source, or the sediments that they overlie. Older slides, now buried by UPG sediments can be recognized in many of the subbottom records.

Sand Waves

Hydraulic bedforms have been observed (Luternauer et al., 1978; Luternauer, 1980; Luternauer and Finn, in press) on the sand blanketed slopes of Roberts Bank on the Fraser River Delta. These features gradually increase in size from small ripples, a few centimetres across near the main channel, to large asymmetrical sand waves 2-3 m high and approximately 30 m long on the southernmost part of the slope. They are generated primarily by flood-tidal currents which scour the seabed to a water depth in excess of 100 m. Evidence suggests that the most intensely mobilized part of the slope surface is gradually retreating.

Faults

Recognition of relatively young faulting on the acoustic records (CSP and 3.5 kHz) depends on finding changes in bathymetry (either depth or slope rate), offset in subbottom reflectors of distinctive character, abrupt changes in the thickness of the soft sediments, diffraction limbs and acoustic shadow zones. Due to the lack of a gain-recovery system, the faults on the CSP records can only be traced to depths of about 100 m (0.13 s two-way time).

Faults along the Gulf Islands side of the strait are both normal and reverse with as many as 14 distinctive blocks or fault slivers across a typical 4 km profile section. The shallow faults cut the young UPG sediments and are related to offset in Tertiary and Cretaceous bedock. This Gulf Islands fault zone overlies a major crustal fault which is visible on the deeper multifold reflection profiles kindly donated by Pan Canadian Petroleum Limited and the profiles presented by Edwards and Aud (1969). This major fault strikes parallel to the Gulf Island chain, intersecting the seafloor of the strait along the toe of the Gulf Islands submarine ridge system, dipping northeastwards at 75° to 85° with extension to depth of several kilometres (5 seconds two-way travel time).

Faulting along the lower slope of the Fraser Delta and central Strait of Georgia includes normal, reverse and listric styles. The normal faults commonly exhibit uphill facing (anti-slope) scarps. Reverse faulting is steep and associated with normal faulting. Both normal and reverse faults commonly occur in the UPG sediments where they drape ridges consisting of Pleistocene sediments and Tertiary bedrock. These high-angle faults commonly exhibit growth-fault character, with offsets decreasing upsection. Some associated faults do not intersect the

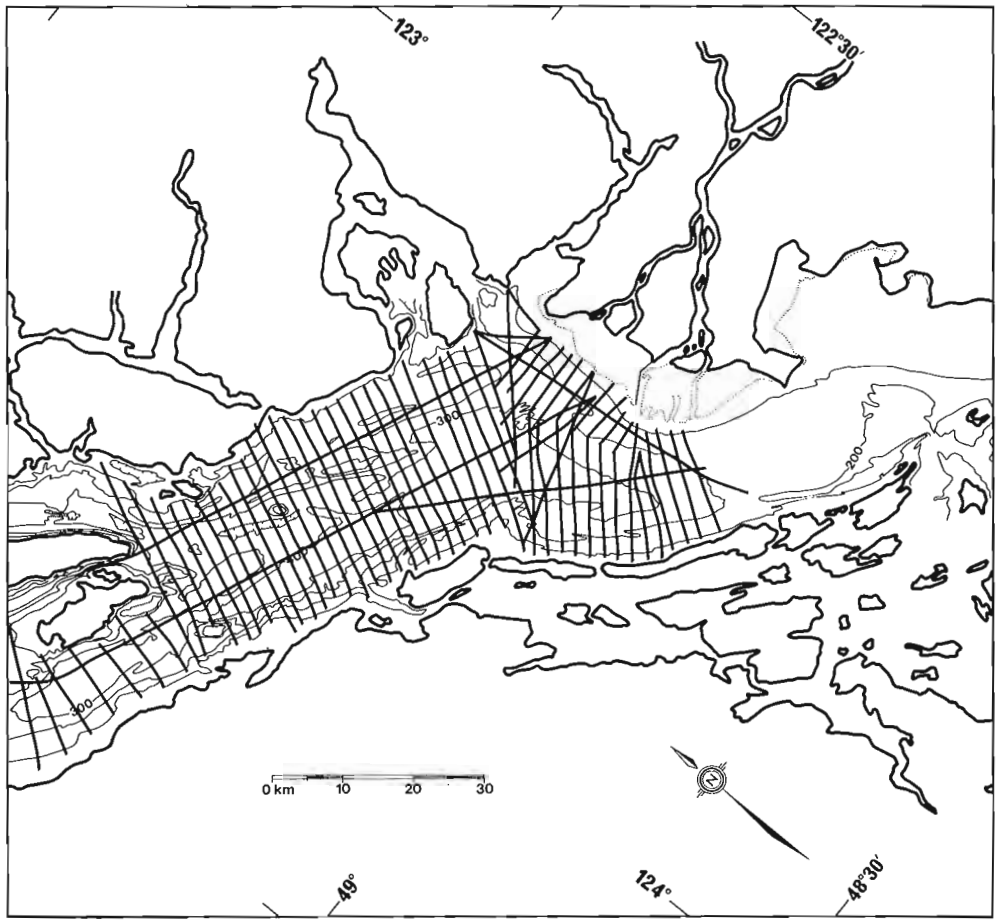

Figure 58.3. Geophysical survey (February 1982) trackline locations.

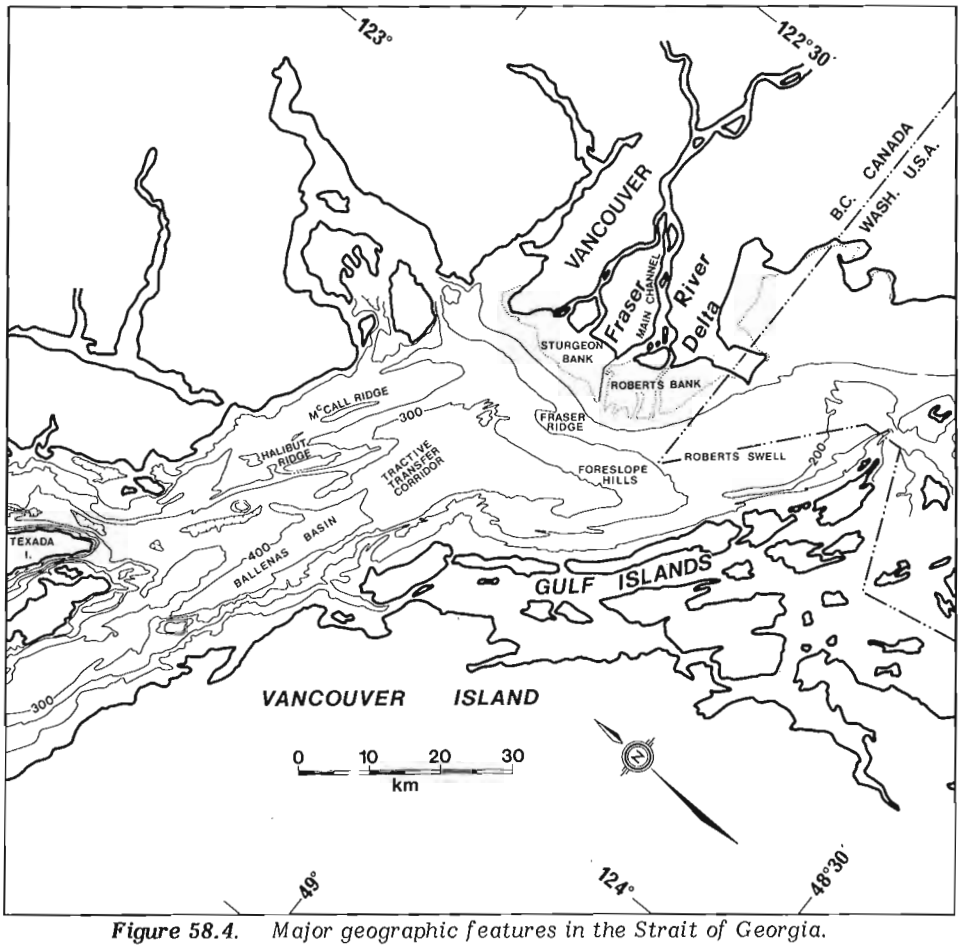

Figure 58.4. Major geographic features in the Strait of Georgia.

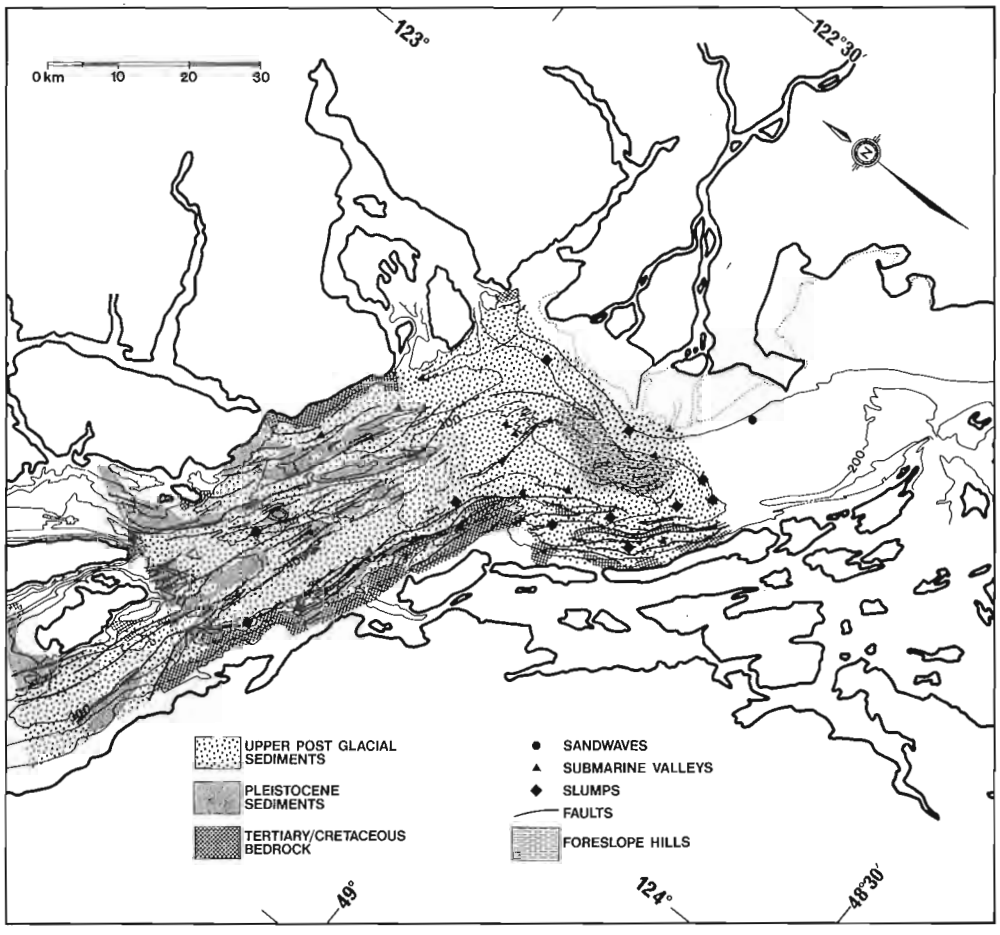

Figure 58.5. *Quaternary geology of the Strait of Georgia.*

present seafloor but are covered by drape and monoclined flexure, indicating that the rate of faulting may have been decreasing during postglacial time. Listric faults are restricted to the basinward side of buried ridges consisting of Pleistocene and Tertiary materials. They dominantly have anti-slope scarps and sole-out down basin within the upper 20 m, as seen in the rapid lateral-thickness changes of the uppermost sedimentary package.

Faulting in Ballenas Basin is usually restricted to the basin margins and abrupt breaks in slope. Perched basins, commonly fault-bounded, preserve remnants of lower postglacial sediments (Luternauer et al., in press). On the floor of Ballenas Basin fault-bounded, uplifted blocks of UPG sediment may represent mud diapirs.

Faulting in the banks and ridges (Halibut and McCall ridges; Fig. 58.4) in the strait can extend to the present seafloor but more commonly is draped and covered by UPG sediments and fades up section. Both normal and reverse faults are observed but their occurrence is greater in the subbottom than on the seafloor indicating a reduction of this type of activity since deglaciation.

Conclusions

Geophysical and geological investigations indicate that the seafloor of the Strait of Georgia has been prone to faulting, mass movements, tractive flows, and tidal erosion. Although no means are available as yet to ascertain the frequency and/or periodicity of such events the present investigation identified the apparently dominant destabilizing mechanisms in the different areas of the south-central Strait of Georgia.

References

Atwater, T.
1970: Implications of plate tectonics for the Cenozoic tectonic evolution of western North America; Geological Society of America, Bulletin, v. 81, p. 3513-3536.

Edwards, R.C. and Aud, B.W.
1969: Marine Vibroseis Report of the 1969 Seismic Survey of the Strait of Georgia for Texaco Exploration Company by Olympic Geophysical Company; unpublished Assessment Report, No. 1529 (1) and (2) Petroleum Research Branch, Government of British Columbia.

Luternauer, J.L.
1975: Fraser Delta sedimentation, Vancouver, B.C.; in Report of Activities, Part B, Geological Survey of Canada, Paper 75-1B, p. 171-172.

1976a: Fraser Delta sedimentation, Vancouver, B.C.; in Report of Activities, Part A, Geological Survey of Canada, Paper 76-1A, p. 213-219.

1976b: Fraser Delta sedimentation, Vancouver, B.C.; in Report of Activities, Part B; Geological Survey of Canada, Paper 76-1B, p. 169-171.

1977: Fraser Delta sedimentation, Vancouver, B.C.; in Report of Activities, Part A, Geological Survey of Canada, Paper 77-1A, p. 65-72.

1980: Genesis of morphologic features on the western delta front of the Fraser River, B.C. – status of knowledge; in The Coastlines of Canada, ed. S.B. McCann; Geological Survey of Canada, Paper 80-10, p. 381-396.

Luternauer, J.L. and Finn, W.D.L.
– Stability of the Fraser River Delta front; Canadian Geotechnical Journal (in press).

Luternauer, J.L., Clague, J.J., Pharo, C.H., McGee, T.M., and Linden, R.H.
– Late Quaternary geological evolution of the Strait of Georgia; Canadian Journal of Fisheries and Aquatic Sciences (in press).

Luternauer, J.L., Swan, D., and Linden, R.H.
1978: Sand waves on the southeastern slope of Roberts Bank, Fraser River Delta, B.C.; in Current Research, Part A, Geological Survey of Canada, Paper 78-1A, p. 351-356.

Mathews, W.H.
1971: Geology of Vancouver area of British Columbia; 24th International Geological Congress, Guidebook, Field Excursion 405-C05, 47 p.

Mathews, W.H., Fyles, J.G., and Nasmith, H.W.
1970: Postglacial crustal movements in southwestern British Columbia and adjacent Washington State; Canadian Journal of Earth Sciences, v. 7, p. 690-702.

Milne, W.G., Rogers, G.C., Riddihough, R.P., McMechen, G.A., and Hyndman, R.D.
1978: Seismicity of western Canada; Canadian Journal of Earth Sciences, v. 5, p. 1170-1193.

Mörner, N.A.
1982: Paleoseismicity Fennoscandian Records; EOS (Transactions of the American Geophysical Union), v. 63, p. 583.

Muller, J.E.
1977: Evolution of the Pacific margin, Vancouver Island, and adjacent regions; Canadian Journal of Earth Sciences, v. 14, p. 2062-2085.

Riddihough, R.P.
1977: Gravity and structure of an active margin – British Columbia and Washington; Canadian Journal of Earth Sciences, v. 16, p. 350-363.

Riddihough, R.P. and Hyndman, R.D.
1976: Canada's active western margin: the case for subduction; Geoscience Canada, v. 3, p. 269-278.

Roddick, J.A., Muller, J.E., and Okulitch, V.A.
1979: Fraser River, British Columbia – Washington; 1:1000 000 Geological Atlas Sheet 92, Geological Survey of Canada, Map 1386A.

Rogers, G.C.
1979: Earthquake fault plane solutions near Vancouver Island; Canadian Journal of Earth Sciences, v. 16, p. 523-531.

1982: Some comments on the seismicity of the northern Puget Sound – southern Vancouver Island region; in Earthquake Hazards of the Puget Sound Region Washington State, ed. J.C. Yount; United States Geological Survey, Open File Report, 21 p.

Rogers, G.C. and Hasegawa, H.S.
1978: A second look at the British Columbia earthquake of June 23, 1946; The Seismological Society of America, Bulletin, v. 68, p. 653-675.

Slawson, W.F. and Savage, J.C.
1979: Geodetic deformation associated with the 1946 Vancouver Island, Canada earthquake; The Seismological Society of America, Bulletin, v. 69, p. 1487-1496.

Tiffin, D.L., Murray, J.W., Mayers, I.R., and Garrison, R.E.
1971: Structure and origin of foreslope hills, Fraser Delta, British Columbia; Canadian Petroleum Geology, Bulletin, v. 19, p. 589-600.

Tipper, H.W., Woodsworth, G.J., and Gabrielse, H.
1981: Tectonic assemblage map of the Canadian Cordillera and adjacent parts of the United States of America; Geological Survey of Canada, Map 1505A.

59.

MOUNT HARPER COMPLEX, YUKON; EARLY PALEOZOIC VOLCANISM AT THE MARGIN OF THE MACKENZIE PLATFORM

Project 800022

C.F. Roots[1]
Cordilleran Geology Division, Vancouver

Roots, C.F., Mount Harper complex, Yukon; early Paleozoic volcanism at the margin of the Mackenzie Platform; in Current Research, Part A, Geological Survey of Canada, Paper 83-1A, p. 423-427, 1983.

Abstract

The Mount Harper complex in the Ogilvie Mountains consists of 105 km² of undeformed volcanic rocks lying between two thick dolostone units of late Proterozoic and early Paleozoic age. Volcanic stratigraphy indicates three periods of mafic volcanism separated by two effusions of intermediate and felsic composition.

Pillowed and massive lava flows comprise more than two thirds of the volcanic pile; subaerially deposited rocks form less than one tenth. Most breccias were formed by fracturing and shattering of crystalline flows, with pyroclastic and laharic deposits locally present. Quartz-phyric lavas, ignimbrite and felsic breccias occur near the top of the pile. Pebbly mudstone and volcarenite are locally intercalated with the volcanic rocks.

Three fault sets affect the complex. Block faulting at the edge of the platform may have caused conglomerate deposition and initiated volcanism. Northwest-striking sets appear related to dyke swarms and structural adjustments late in the volcanic history. Other faults are associated with the regional Mesozoic compressional regime.

Trace sulphide occurrences were found in the mafic volcanic rocks.

Introduction

The Mount Harper volcanic complex is located in the southwestern Ogilvie Mountains, 100 km northwest of Dawson, Yukon. It is an unique occurrence within the 'shelf assemblage' (Thompson and Roots, 1982) and represents prolonged cyclic volcanism at the margin of the Mackenzie Platform, separating the deposition of massive dolostone units.

This study of the volcanic complex supplements regional investigations (Green, 1972; and Thompson and Roots, 1982) by furthering the understanding of the role of volcanism in the geological evolution of the region. Work in the 1982 season involved 1:25 000 scale mapping of the Mount Harper complex (8 km by 16 km), measurement of stratigraphic sections, and systematic sampling for chemical analyses. This report outlines the general stratigraphy in the area, and presents preliminary conclusions on its volcanic history.

Stratigraphy

Sedimentary rocks adjacent to the volcanic complex (Fig. 59.1) include four older (phyllite, laminated siltstone, dark grey dolostone and boulder conglomerate) and three younger units (epiclastic sediments, sugary white dolostone and Road River Formation). The unit descriptions given below add specific detail to some of the regional units outlined in Thompson and Roots (1982). Their ages remain uncertain, but preliminary assessments of fossil collections suggest that the sediments were deposited between latest Proterozoic to early Ordovician time.

Pre-volcanic Units

Phyllite (Unit 3) occurs southeast of Mount Harper surrounded by dolostone and conglomerate. It is bounded to the north by a vertical fault, and is largely confined to lower elevations along the Fifteenmile River. The phyllite is formed from grey and brown chloritic mudstone and siltstone and shows a pervasive cleavage not present in the overlying units.

Green and brown laminated siltstone is exposed as crumbling cliffs along Coal Creek valley south of Mount Harper. Thin, rhythmically bedded siltstone and mudstone that show normal grading and flame structures (0.5 cm scale) form a section about 135 m thick.

This unit disconformably overlies phyllite, and is capped by dark grey dolostone. It appears to be limited in extent, and could be a local facies equivalent of black clastic marker (Unit 7).

Dark grey and light grey cryptalgal laminated dolostone (Units 8a and 8b?), extensively exposed in the southern Ogilvie Mountains, appear within the southward-tilted succession north of Mount Harper, and again as a flat-lying unit on the south side of the volcanic complex. The two occurrences have similar rock types and the same stratigraphic position, but are separated by an east-striking fault and volcanic rocks. In the north part, two lithologic members are distinguished. A crudely bedded, dark grey siliceous dolostone, about 200 m thick, predominates. It locally contains silicified pisolitic horizons, sandy layers and pods of intraformational breccia. A light, smooth-weathering, layered dolostone forms irregular deposits up to 252 m thick near the top of the darker member. It is characterized by ubiquitous fan-shaped stacks (10-150 cm across) of white laminations that are probably algal structures. The flat-lying part of the unit most closely resembles the dark grey member. Thick, nodular beds consist of fine grained, dark grey to black calcareous dolostone and locally show silicified algal structures.

The lower contact of the tilted dark grey member is obscure where it overlies the 'craggy dolomite' (Unit 6). The flat-lying member overlies the green and brown siltstone unit south of Mount Harper. These members were shown as belonging to Units 8a and 8b by Thompson and Roots (1982) but this correlation may have been premature.

Dolostone boulder conglomerate (Unit 9) underlies the north side of the volcanic complex (5-50 m thick) and becomes very thick (400 m) east of Mount Harper.

[1] Department of Geology, Carleton University, Ottawa, K1S 5B6
Publication No. 02-82, Ottawa-Carleton Centre for Geoscience Studies.

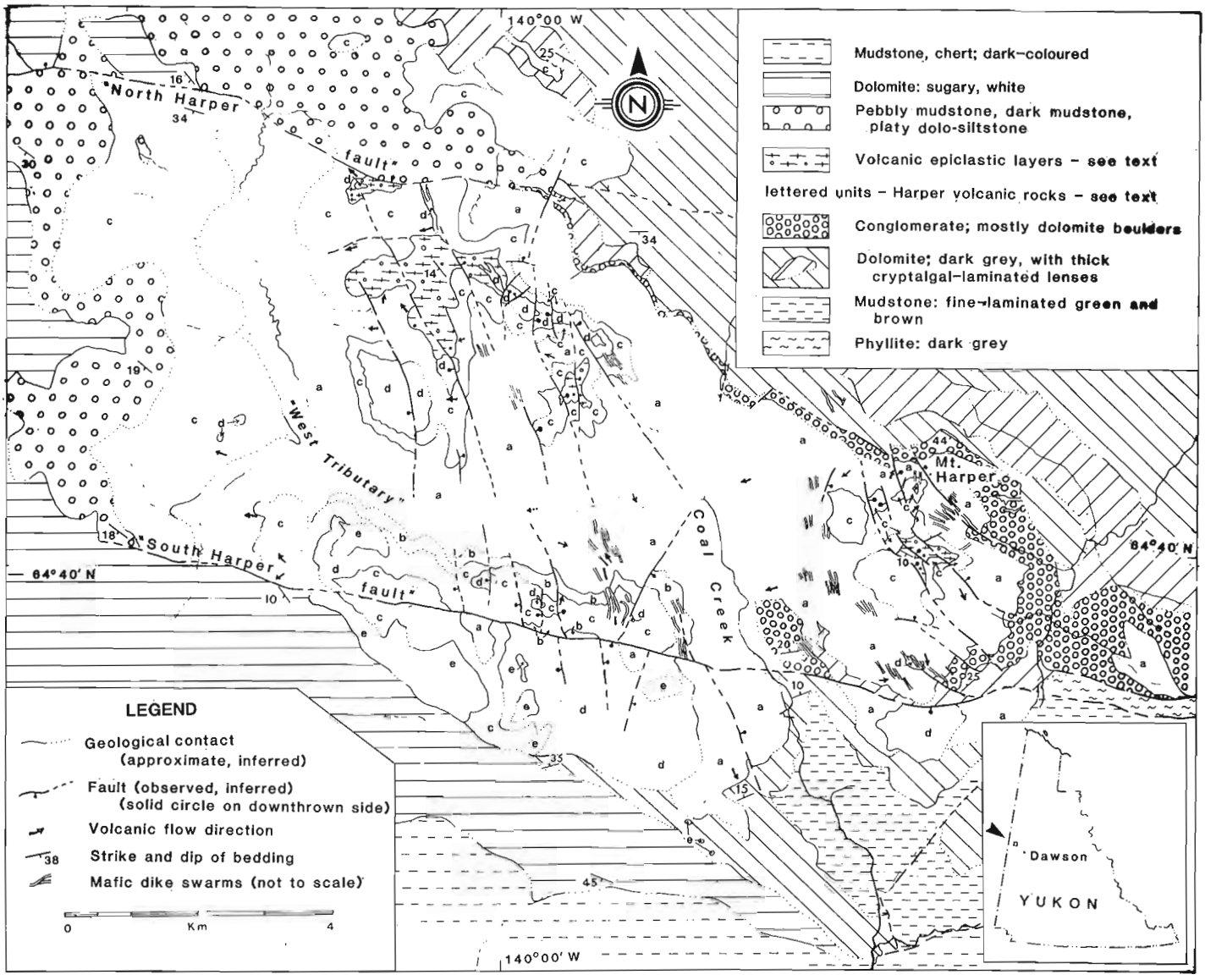

1) *Harper Ridge,*
2) *West Harper,*
3) *Southwest Harper.*

Figure 59.1. *Geology of the Mount Harper volcanic complex.*

The conglomerate comprises lenticular horizons 2 to 10 m thick, with variably sorted, well rounded pebbles, cobbles and boulders up to 2 m across. Dolostone derived from older units constitutes most of the clasts, but quartzite of various colours, jasper and chalcedony are present. North of Mount Harper, diamictite (resembling Unit 9a) with cross-stratified quartz-sand horizons, indicating paleocurrents towards the north and northeast, and slump-fold structures occur in mudstone laminations beneath the basal lava flows. In places the conglomerate contains channel fillings marked by angular dolostone blocks at the base.

At the northwest end of the complex, the boulder conglomerate is overlain by similarly weathering paraconglomerate (pebbly mudstone). Because the latter contains 5-35 per cent mafic volcanic clasts, and locally overlies middle members of the complex, it is grouped with the younger epiclastic unit.

Mount Harper Volcanic Complex (Unit 10)

Volcanic rocks are uncommon in the shelf assemblage, and are best exposed around Mount Harper (1875 m). This complex is the eroded remnant of an edifice more than 1200 m thick. It is exposed in three mountainous areas, separated by Coal Creek and its major western tributary (Fig. 59.1). As correlation across these streams is difficult, the complex is divided for purposes of description into three subareas (Table 59.1).

The volcanic complex is exposed in a central 'horst', with its longitudinal margins downdropped by the North and South Harper faults (Fig. 59.1). High cliffs along the north side reveal that part of the original edifice has been removed. In addition, the western and southwestern extension of the volcanic rocks is buried beneath overlying units.

Table 59.1

General stratigraphy of the Mount Harper volcanic complex, outlined by subareas. Maximum thicknesses are shown in brackets.

MEMBER	LITHOLOGY	SUBAREAS of the MOUNT HARPER VOLCANIC COMPLEX			DEPOSITIONAL ENVIRONMENT (water depth, local relief)
		Harper Ridge	West Harper	Southwest Harper	
Overlying units		(not present)	conformably overlain by pebbly mudstone, platy dolomite, mudstone to west, northwest	onlapped (?) by crystalline dolostone to south	shallow to moderate water depth; gently rolling bottom topography with eroding scarps
E	blue-black mafic flows and breccias	(not present)	(not present)	lavas 2-20 m thick; local breccia flows and pillow lavas (150 m)	moderate water depth, possibly emergent locally; irregular thicknesses due to lava 'ponding'
Epiclastic sediments		grey mudstone, some layers with felsic cobbles; dolostone horizons; basal maroon pebbly mudstone (70 m)	maroon siltstone and mudstone with rare mafic clasts (25 m)	(not present)	shallow subaqueous basins, possibly beaches locally; erosion of probably emergent volcanic edifice
D	ii) felsic lavas, ignimbrites and breccias i) col. jointed, dark intermediate flows	ii-quartz phyric lavas 5-30 m thick (270 m)	i-northwest-striking dike swarms; ridges capped by massive flows (180 m)	ii-feldspar +/- quartz phyric lavas, ignimbrites and block breccias (50 m) i-dark, tabular flows	local subaerial activity, probably related to northwest striking faults; overlies gently sloping terrain
Epiclastic sediments		(not present)	platy dolostone, laminated tuffs and maroon/grey mudstone with dolostone and mafic cobbles (150 m)	(not present)	shallow subaqueous basins, mass flows from west, north probably emergent volcanic, uplifted dolostone terrain
C	iv) cobble breccias iii) oxidized tephra ii) hyaloclastic breccia i) green mafic flows	iii-oxidized cinder (cored bombs common) deposits (240 m) ii-pillow and sheeted lavas (250 m)	iv- extensive breccia flows (70 m) ii-broken-lava breccia deposits (70 m) i-dome-shaped pillows (30 m)	iv-breccia flows with rounded mafic cobbles (50 m) ii-broken-lava and pillow breccias with hyaloclastite (30 m)	shallow water, with emergent cone to east; lavas progressively fragmented and reworked to west and south
B	dark, spherulitic lava flows	(not present)	(not present)	col. jointed, 1.5-5 m thick tabular flows (150 m)	water depth unknown; uniform topographic relief
A	ii) vesicular mafic flows, hematite-altered breccias i) grey-green pillow (elongate, tubular) flows	ii-broken-pillow breccia deposits (125 m) i-basal pillows form layers 50-80 m thick (200 m)	ii-broken-lava and flow-top breccias (150 m) i-pillow accumation tapers westward (225 m)	ii-broken-lava breccias (150 m) i-pillow lava pile with clay-altered ash intercalations (185 m)	moderate water depth, shallowing upward; pillow lavas form shield-like mound up to 10 km across
Underlying units		conformable over maroon diamictite and dolostone cobble conglomerate	disconformable over cobble-boulder conglomerate and cryptalgal dolostone	disconformable over dark grey dolostone	volcanic flows overran coelesced subaqueous alluvial fans and uplifted dolostone beds

Three mafic and two interspersed felsic to intermediate volcanic members can be distinguished (Table 59.1). Physical volcanic features indicate that early deposits were entirely subaqueous, but later an emergent cone was formed (members 'c' and 'd'). It is probable that subaerially erupted products were eventually deposited underwater. Intercalated sediments indicate erosion of adjacent volcanic and dolostone terrane. Subsequent intermediate and felsic volcanism opened multiple vents and was related to subsidence faulting throughout the complex. The final effusions consisted of massive, probably ponded lava flows, vesicular pillows and subaqueous breccias.

Mafic Volcanic Rocks

The common deposit types in mafic members ('a', 'c' and 'e') are pillowed, massive and columnar jointed lavas, with two types of subaqueous breccia deposits. The 'c' member is most diverse, with scoriaceous oxidized lavas, cinder and pyroclastic beds with a few cored bombs. Great thicknesses of hyaloclastic and epiclastic breccias form cliff bands near the top of West and Southwest Harper subareas.

The morphology of pillows and their deposits vary among flow units. Fluid lavas of member 'a' form elongated, tightly packed pillows in massive mounds or 'banks' 50-100 m thick. These pillows contain scattered or concentric zones of tiny vesicles. Those of the 'c' member have radiating vesicles (0.5 cm across), form dome-shaped structures (1-2 m high) and are loosely packed. Mattress-shaped pillows in member 'e' have evenly distributed vesicles and are clustered in irregular pods. These differences probably represent decreasing fluidity of the lavas accompanying exsolution.

Subaqueously deposited breccias are related to crumbling and shattering of lavas (cobble breccias) and the mass wasting of exposed highlands or unstable underwater deposits (lahars). Cobble breccias consist of equidimensional fragments of vesicular or dense lava, generally in a chloritic, fine debris- and shard-filled matrix. Their sharp, straight fragment edges and lack of comminution imply internal fracturing of the lavas. Transition from completely brecciated lava flows, through increasing disaggregation, size reduction and winnowing, was observed in member 'a' near Mount Harper, and along a 5 km length of member 'c' on the Southwest Harper ridge. Within this continuum, several transitional breccia types between lavas and epiclastic deposits can be recognized. An extensive silicified hyaloclastite layer 5-80 m thick may have been caused by shattering lava as it entered the water. Laharic breccias are most common in the western part of the complex. They commonly contain well rounded cobbles (mafic and locally dolostone) that are widely spaced in a fine, clay-like matrix; mudstone laminations show slump folds indicating westward transport.

Intermediate and Felsic Volcanic Rocks

These are distinguished by reddish weathering hues and quartz phenocrysts. Light grey, tabular flows 1.5 to 6 m thick with abundant millimetre-scale spherulites constitute member 'b', exposed only in Southwest Harper subarea. Member 'd' has two parts. A lower, darker rock, forms separated rubble-covered mounds of columnar-jointed flows or domes and is overlain by light grey, feldspar- and/or quartz-phyric lava flows with welded pyroclastic flow deposits. Flows of the upper part are extensively exposed on the down-dropped side of the South Harper Fault. Varying phenocryst proportions may imply different flows and their extent suggests multiple source areas.

Epiclastic Intercalations

A layered succession of pebbly siltstone, with volcarenite and mudstone, caps broad ridges in the West Harper and Mount Harper subareas. Subrounded, polymodal clasts were derived from subjacent mafic volcanic members and dolostone units beneath the complex. Both volcanic and dolostone pebbles occur as dropstones in finely laminated mudstone. Epiclastic sediments did not completely cover the complex because they are absent farther south and are in places covered by members 'd' and possibly 'e'. These beds record an erosional history of the volcanic edifice, and indicate that older platform dolostone was uplifted and probably eroded to the north of the complex.

Post-volcanic Units

A mixed sedimentary assemblage ('epiclastic unit') is exposed around the western end of the volcanic complex. The unit contains four members, which in ascending order are: cobbly sandstone and mudstone, platy dolostone with local chaotic breccia lenses, dark siltstone and grit, and black, fissile mudstone. They individually range greatly in thickness and together measure from 200 m thick in the south to over 600 m in the north. The epiclastic unit disconformably overlies the dark grey dolostone and lower volcanic rocks, although in places it grades from laharic breccias of member 'c'.

Although the basal contact is not exposed, at the northwest end of the complex the pebbly mudstone facies appears to grade upward from dolostone boulder conglomerate by increasing sand and silt content. Clasts are smaller, less rounded and predominantly derived from older carbonate rocks, although 5 to 10 per cent mafic volcanic pebbles are locally present. Within younger beds of thin, evenly laminated dolostone are pods of angular blocks of massive dolostone, quartzite and concretions in an unsorted and loosely packed framework.

Light grey, sugary dolostone underlies most of the area west of the volcanic complex. The unit is conformable over the epiclastic synvolcanic sediments and overlaps the lavas of member 'e' at the southwest corner of the volcanic complex. Its average thickness is estimated to be 250 m. Like the lower dolostone units, this carbonate is massive to crudely bedded, patchily silicified, and has a complex distribution of finely layered, nodular bedded, conglomeratic and breccia facies. Lacking distinctive markings, its light grey weathering and clean, white, medium crystalline texture are notable at most localities, and uncommon in other units.

Archeocyathids found 20 km west of Mount Harper (R.I. Thompson, personal communication, 1982) indicate late Early Cambrian age (Fritz, personal communication, 1982).

Road River Formation (Unit III) consisting of dark, fine clastic sediments and chert, underlie subdued, thickly vegetated slopes and valleys south of the older 'shelf assemblage' rocks. Folded beds of brown siltstone and black argillite contain thin grey limestone and lenticular quartzite horizons. Black and grey chert appears to be a single marker horizon 3-30 m thick. Sausseritized mafic volcanic rocks (Unit II) are locally present above and below the chert.

Graptolite and Lingulid faunas were collected by Green (1972, p. 50; Early Ordovician) and by the writer in 1982 from the base of the Road River formation in the Shell Creek area. This lower contact which is the locus of a variety of structural relations, has been known as the 'Dawson Fault'. The nature of this boundary will be described later.

Structural History

Tectonic instability predated volcanism on the continental shelf. In sedimentary units older than the complex, widespread unconformities, block faulting and conglomerate indicate an environment with high relief and changing depositional regimes. The thick carbonate units are internally complex, with sand wedges, chaotic breccias and irregular bedding. The spatial distribution of faults and unconformities with respect to conglomerate and volcanic rocks imply possible association between them.

Faults that predate the volcanic complex cut the phyllite, dark grey dolostone and conglomerate, but did not affect the younger volcanic rocks. Such a fault, located east of Mount Harper, strikes west into the mountain. It marks the southern extent in the area of the dolostone boulder conglomerate. Phyllite on the south side is disconformably overlain by dark grey dolostone, where several stratigraphic units present elsewhere beneath this dolostone unit are absent. The disconformity implies uplift of the phyllite and possible erosion before deposition of the dolostone.

Conglomerate, on the north side of the fault, overlies the dolostone disconformably and reaches a maximum thickness of 400 m. To the northwest, where it is exposed along the base of the volcanic complex, the unit thins to 5-50 m. That the uplift block immediately south of the fault may have been a local source area for the boulders is indicated by northward-directed paleocurrents in sandstone horizons within the conglomerate near Mount Harper. Although the westward extension of the fault is buried beneath the volcanic complex, continued north-side-down offset in the older units is indicated, and no conglomerate is known on the south side.

Dykes along the trace of such faults may have extruded pillowed flows that formed the subaqueous 'shield' at the base of the volcanic complex (member 'a'). In time the accumulating pile overstepped dolostone scarps and filled depressions in the conglomerate unit. Increased vesicularity and oxidized rims on breccia fragments suggest decreasing water depths. An interval of glassy flows of volcanic member 'b' spread in uniform layers across relatively smooth slopes of the volcanic edifice. Shallow water depths may have caused pyroclastic activity. An emergent cone was built and its subaqueous flanks were probably broadened by the increased production of fragmental rocks by erosion, shattering of lavas at the water's edge, and oversteepened subaqueous deposits (all facies of member 'c'). Periodic subsidence was also probable, because dolostone cobbles present in epiclastic intercalations were locally supplied from higher terrain underlain by prevolcanic units.

A second stage of volcanism, marked by felsic lavas, pyroclastic flows, and probably synvolcanic faulting, is revealed in the western and southern parts of the complex.

Reddish weathering dyke swarms that cut volcanic members 'a', 'b' and 'c' strike northwest. Dark flows of member 'd' are compositionally similar to the dykes, and separate occurrences are dotted along faults parallel to the swarms. These faults are shown by offsets of the tabular, reddish weathering flows and faint lineaments on aerial photographs. Vertical movement on the faults ranges up to 70 m, although the sense of movement is inconsistent. Their continuity is implied by the occurrence of several small centres with basal flows compositionally similar to the lower member 'd' about 12 km northwest of the west margin of the volcanic complex. Ignimbrite exposures within the complex are also situated on fault traces. Arching or subsidence along the northwest-striking fault set appears to have influenced the second stage of volcanism at the complex.

In contrast to sedimentary units in the Mount Harper area that dip moderately southward, much of the volcanic complex is flat lying. Only the northeast and southwest edges are tilted to conform with the regional dip. The North and South Harper faults, which cut the younger sugary dolostone and down-drop the northwest and southeast margins of the complex, must have occurred after the volcanism. They may have alleviated local strain around the thick volcanic pile during the Mesozoic compression regime that affected the southern Ogilvie Mountains.

The 'Dawson Fault' zone is poorly exposed south of the Mount Harper volcanic complex. Its relative age (older or younger than the volcanism) remains unclear. No movement is indicated in some places but elsewhere along the strike of the boundary units the rocks are highly deformed. Near the southwest corner of the volcanic complex, the zone appears to be a depositional contact between sugary dolostone and the overlying Road River shales. In valleys south of Mount Harper, shale, phyllite and siltstone are sheared along surfaces dipping vertically or steeply northward. Farther east the 'Dawson Fault' zone is marked by volcanic rocks and dykes (Unit II).

Mineralization

The volcanic rocks near Mount Harper show rare traces of base metal mineralization. Pyrite and chalcopyrite specks are scattered throughout the upper amygdaloidal flows of member 'a', and secondary copper minerals occur in several shear zones through member 'c' in Southwest Harper subarea. Several thin quartz veins south of Mount Harper contain traces of sulphides.

Mafic lava flows in the Mount Harper complex, particularly the upper part of member 'a', contain amygdaloidal pink, orange and grey agate, but most are too fractured for collector's items.

Acknowledgments

This study is part of the Ogilvie Mountains Project. I am grateful to J.M. Moore, Jr., B.S. Brock and R.I. Thompson for their editing of the manuscript.

References

Green, L.H.
1972: Geology of Nash Creek, Larsen Creek and Dawson map-areas, Yukon Territory; Geological Survey of Canada, Memoir 364.

Thompson, R.I. and Roots, C.F.
1982: Ogilvie Mountains Project, Yukon; part A: a new regional mapping program; in Current Research, Part A, Scientific and Technical Notes, Geological Survey of Canada, Paper 82-1A, p. 403-411.

60.

THE EXTERNIDES OF WOPMAY OROGEN, POINT LAKE AND KIKERK LAKE MAP AREAS, DISTRICT OF MACKENZIE

Project 810021

P.F. Hoffman, Rein Tirrul, and J.P. Grotzinger[1]
Precambrian Geology Division

Hoffman, P.F., Tirrul, R., and Grotzinger, J.P., The externides of Wopmay Orogen, Point Lake and Kikerk Lake map areas, District of Mackenzie; in Current Research, Part A, Geological Survey of Canada, Paper 83-1A, p. 429-435, 1983.

Abstract

Some results of recent field work are briefly discussed as they pertain to the following topics: (1) north-south stratigraphic continuity of the Precambrian continental-terrace wedge, (2) stromatolite elongation, paleowind direction and global polarity during deposition of the Rocknest dolomite shelf, (3) evidence for primary aragonitic mineralogy of the Rocknest Formation, (4) attempted quantitative paleobathymetry of the upper continental slope, (5) eastward migration of foredeep flysch, (6) nature of basement involvement in Asiak Fold-Thrust Belt, (7) relation of thrusting to the foredeep molasse, (8) mysterious basement-involved cross folding of regional extent, (9) normal faults associated with late transcurrent faulting, and (10) the first reported minor lead-zinc vein mineralization in Rocknest dolomite. Future field work is outlined.

Introduction

The externides of Wopmay Orogen include the Asiak Fold-Thrust Belt and the autochthonous basins located between the frontal thrusts and cratonic basement of the Slave Province (Fig. 60.1). In 1981, a three-year project was initiated to study the externides in the Point Lake (86H), Takijuq Lake (86I), Kikerk Lake (86P) and Coppermine (86O) map areas, with special emphasis on the stratigraphy and structure of the Epworth Group (Odjick and Rocknest formations). This group constitutes the remnants of an immature, west-facing, continental terrace of Atlantic type that onlaps the Archean basement. It underlies the Recluse Group, which consists of orogenic flysch and other sediments deposited in a foredeep that migrated eastward in front of the evolving fold-thrust belt and which ultimately was incorporated partly within it. This deformation may be related to collision of the "Coronation Margin" with a microcontinent (Hoffman, 1980), possibly the Hottah Terrane (Hildebrand et al., 1983), and attempted subduction of the margin beneath it.

In 1982, field work was concentrated near the ends of the fold-thrust belt, specifically east of the Carousel basement massif in the south and around the intersection of Kikerk Thrust and the Tree River Fold Belt in the north (Fig. 60.1). This report summarizes some of the more significant findings, including the discovery of rare galena-sphalerite veins in dolomite of the Rocknest Formation.

Original Continuity of the Continental Margin

A striking feature of Wopmay Orogen is the virtual absence of externides in the south half (south of 65°25'N latitude) of the orogen. Is this due simply to deeper erosion in the south and consequent removal of the thin-skinned externides, or does it reflect an original change in character of the continental margin? For example, a drastic thinning of the marginal sedimentary prism would be expected in passing from an embayment to a promontory of a continent, or from a rifted to a sheared segment of its margin.

Any original change in character along the continental margin should be reflected by north-south variation in stratigraphy or facies of the Epworth Group in the north half of the orogen. No such variation is apparent. The basic three-fold subdivision of the shelf-facies Odjick Formation persists the length of the belt (i.e. lower member mainly laminated argillite, middle member stacked coarsening-upward cycles of semipelite and quartzite, upper member semipelite with numerous ferruginous and intraclastic dolomite beds transitional into the overlying Rocknest Formation). Although a snow-white quartzite and megacrystic mafic sills and flows in the lower member are seen only at the south end, mainly in the autochthonous mantle of Carousel Massif, no autochthonous strata are exposed on strike to the north.

North-south correlations in the Rocknest Formation are even more impressive. Not only do its ten members persist virtually unchanged along strike, but many individual shale-dolomite cycles (Hoffman, 1975), 2-5 m thick, do so as well. In Member 4, for example, all seventeen cycles present appear to correlate from one end of the belt to the other, a distance of 215 km. Thus, there is no evidence of change in the original character of the margin from north to south. An explanation for the absence of externides in the south half of the orogen must therefore be sought in deeper erosion or a thinner Recluse Group in the south.

Stromatolite Elongation, Paleowinds and Global Polarity

Strongly elongate stromatolites in the Rocknest Formation are consistently oriented northeast-southwest, both at the shelf edge and throughout all of the externides. Even after tectonic rotations related to the late conjugate transcurrent faults are removed, the elongation remains quite oblique to the shelf edge, which is surprising. Locally, especially in the Tree River Fold Belt, the elongation may be enhanced by penetrative tectonic strain, but this cannot be true in most places because ooids and other stromatolites are generally very weakly strained. The most plausible explanation may be that the elongation parallels the prevailing paleowind direction.

There are no paleomagnetic data for the Rocknest Formation itself, but paleolatitudes for the central Rocknest shelf area before and after Rocknest deposition can be deduced from paleopoles obtained by Evans and Hoye (1981) for rocks correlative with the Odjick Formation (Western River Formation) and lower Recluse Group (Akaitcho River and Mara formations). The resulting paleolatitudes are 10 degrees in Odjick time and 16-17 degrees in early Recluse time. The Rocknest Formation was probably also deposited within the low-latitude belt of trade winds (10-30 degrees), consistent with the paleowind hypothesis.

[1] Department of Geological Sciences,
Virginia Polytech Institute and State University,
Blacksburg, VA 24061.

The paleomagnetic measurements are ambiguous as to polarity and this has led to controversy in tectonic interpretation of the data (e.g. Cavanaugh and Seyfert, 1977; Irving and McGlynn, 1979). The ambiguity can be resolved if the paleowind hypothesis is correct because the low-latitude trade winds blow from the northeast in the northern hemisphere and southeast in the southern hemisphere. As all paleopoles for the Coronation Supergroup and its correlatives project near South America (Irving and McGlynn, 1979; Evans and Hoye, 1981), trade winds would have blown from the southwest (present day co-ordinates), consistent with the observed stromatolite orientation, if the Rocknest shelf were in the northern hemisphere but from the southeast (present day co-ordinates) if the shelf was antipodean.

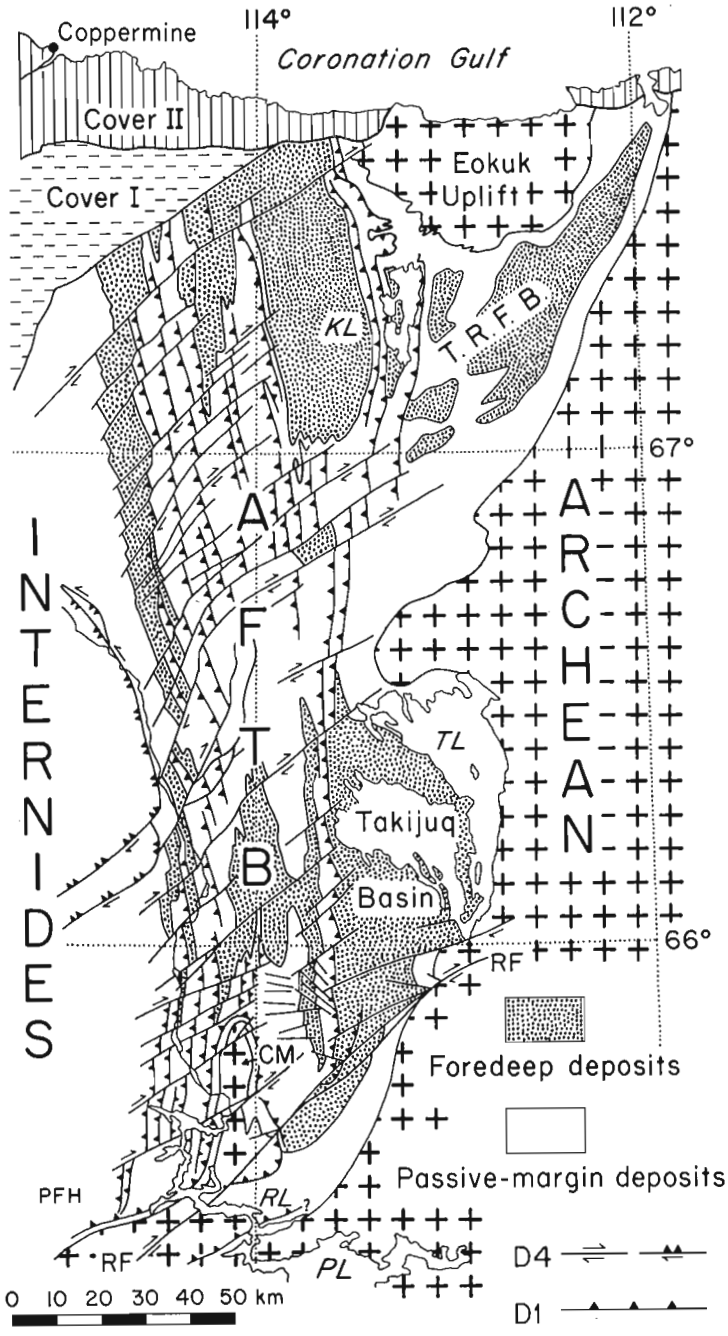

Figure 60.1. *The externides of Wopmay Orogen. AFTB, Asiak Fold-Thrust Belt; TRFB, Tree River Fold Belt; CM, Carousel Massif; RF, Redrock Fault; KL, Kikerk Lake; TL, Takijuq Lake; RL, Redrock Lake; PL, Point Lake.*

The prevalence of onshore not offshore winds is also consistent with the notably starved fore-slope facies of the Rocknest Formation. Irving and McGlynn's (1979) treatment of the Coronation paleopoles as north poles is therefore supported.

Evidence that some Rocknest Dolomite was Originally Aragonite

Aragonite is the dominant carbonate mineral precipitated in modern oceans but the abundance of dolomite in the Precambrian with well preserved primary features, the Rocknest Formation for example (Hoffman, 1973, Fig. 6c), has prompted renewed interest in the possibility of primary Precambrian dolomite (Tucker, 1982). Aragonite, being metastable under near-surface conditions, is inevitably replaced during diagenesis and it is generally too fine grained to leave recognizable pseudomorphs. An exception is the coarsely crystalline botryoidal aragonite cement found in active Holocene reefs (Ginsburg and James, 1976) and recognized as pseudomorphs in some older Phanerozoic reefs and associated facies (e.g. Assereto and Kendall, 1977, Fig. 19).

Well preserved silica pseudomorphs of botryoidal aragonite (Fig. 60.2) associated with tepee structures were found in peri-reefal facies near the Rocknest shelf edge (Grotzinger and Read, in press). They occur in a muddy, locally cryptalgalaminated facies that overlies crossbedded ooid and intraclast grainstone (dolomitized back-reef sands), which in turn overlies and occurs landward of a stromatolite boundstone reef facies that forms a 1 km thick rim to the carbonate continental shelf.

The silica pseudomorphs show that the aragonite botryoids grew downwards into cavities from the undersides of tepees. They are up to 3 cm in diameter and form discontinuous sheets. Where unsilicified, the botryoids are only faintly visible as poorly defined radiating fibrous structures in medium anhedral dolomite (0.2 to 0.8 mm crystals) and may be outlined by patchy chalcedony. However, well silicified botryoids have clearly defined, radiating needle fibres that project downwards from growth points on the undersides of tepees. The botryoids have smoothly curved undersides and the fibres appear to have been orthorhombic. Silicified botryoids consist of chalcedony, growing inward from the fibre margins (outlined by dolomite euhedra) in small radiating masses (up to 0.5 mm) that pass toward the interior of fibres into a coarser (0.2-0.4 mm) anhedral mosaic of quartz.

Other features in the Rocknest Formation indicative of primary aragonite are silicified ooids with well developed concentric coatings, and tufa-like cryptalgalaminites that contain square-tipped needle fibres outlined by mud drapes (microbially precipitated aragonite tufas?). There may be no need, therefore, to account for primary Precambrian dolomite by invoking differences in seawater chemistry (Tucker, 1982) but the problem of secondary dolomitization without destruction of primary features remains.

Quantitative Paleobathymetry of the Upper Continental Slope

A continuous syncline of Recluse Group flysch, 165 km in length and 2-10 km in width, occurs just west of the Rocknest shelf edge (Fig. 60.1). The fold is segmented by late transcurrent faults and plunges gently to the north. Numerous turbidite beds can be observed to close around the fold hinge, assuring that the hinge is not faulted. The fold invariably has contrasting facies of Rocknest Formation on its two limbs. The west limb has a starved sequence of slope-facies dolomite rhythmites and rhythmite breccias, whereas the east limb has thicker, more proximal, slope-facies rhythmite that interfingers with reefal shelf-edge facies.

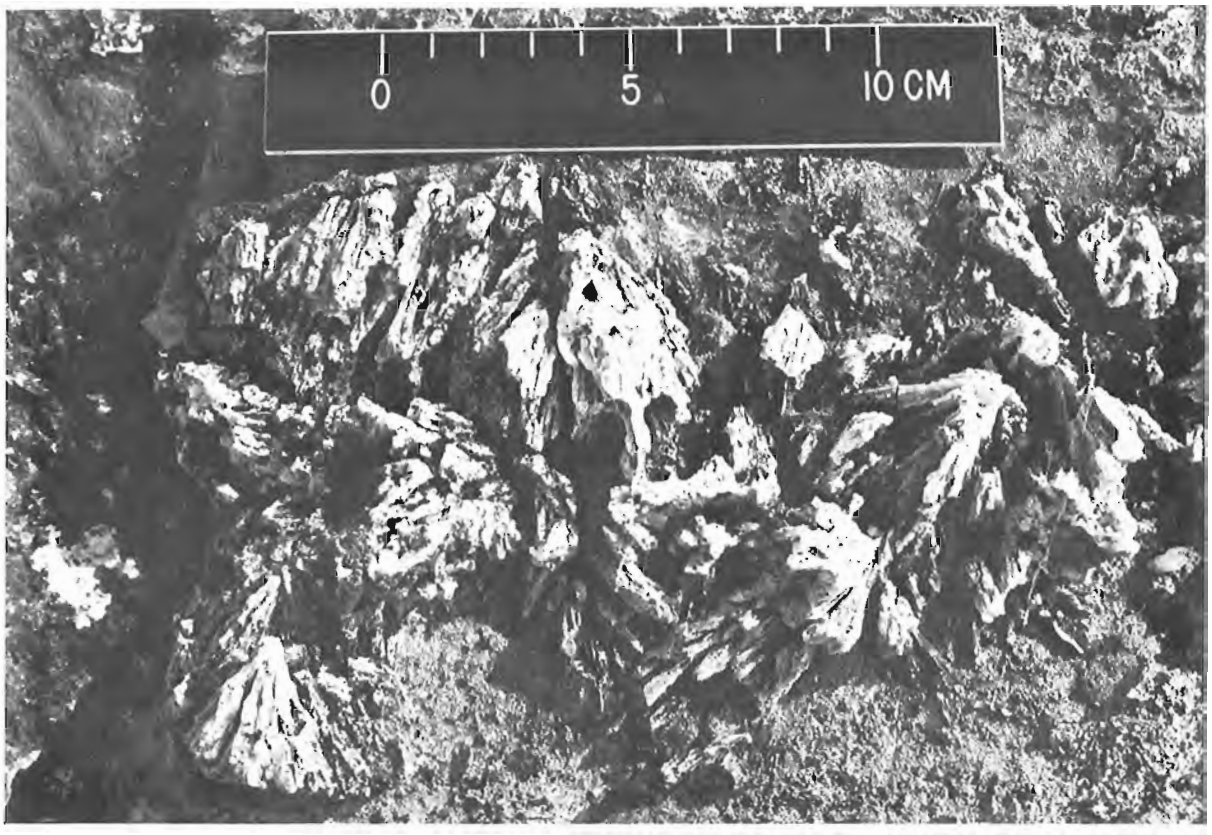

Figure 60.2. *Silicified aragonite botryoids in proximal back-reef facies of Rocknest Formation. The fibres radiate stratigraphically downwards.*

The Recluse Group turbidites onlap the Rocknest continental slope, a relationship that can be seen on air photographs (NAPL No. A14234-90) of the southern closure of the Recluse Group syncline.

If it is assumed that the turbidites, which were deposited by axially-flowing currents, approximate the horizontal in an east-west section, then the difference in decompacted thickness of Recluse Group strata between the two limbs should equal the paleobathymetric relief at the end of Rocknest deposition plus the effect of regional flexure during Recluse sedimentation. By further considering the difference in Rocknest thickness across the fold, the increase in relief from the beginning to the end of Rocknest deposition can be obtained. The values for paleobathymetric relief can be converted to paleobathymetric slopes by unfolding the syncline, utilizing surface dips and down-plunge projections, to determine the original horizontal distance between the measured sections.

This was done near the south end of the syncline, where the Rocknest comprises 230 m of slope facies on the west limb and 660 m of shelf edge facies on the east limb. The difference in decompacted thickness of the Recluse Group, measured from the top of the Rocknest Formation to a marker bed in the core of the fold is 590 m, of which 430 m (the change in Rocknest thickness) can be related to constructional aggradation of the Rocknest shelf edge. Note that because the measured sections converge toward the upper marker bed and thereby minimize the difference in Recluse Group thickness, and because the method used for unfolding maximizes the original horizontal separation, the paleoslopes reported here are minimum values. The average slopes obtained are 7 degrees for the top of the Rocknest Formation and 2 degrees for its base. Regional flexure cannot have exceeded 2 degrees or a reversed Odjick paleoslope would be implied in defiance of known facies relations. Therefore, the original paleoslopes are estimated to have averaged less than 2 degrees at the end of Odjick deposition, increasing to at least 5-7 degrees at the end of Rocknest time. These values compare well with average inclinations of 1-1.5 degrees for clastic slopes and 4-10 degrees (locally steeper) for carbonate slopes on modern Atlantic-type continental margins. It should be possible to make similar measurements elsewhere along the syncline.

Eastward Migration of Foredeep Flysch

Implicit in the interpretation of the Recluse Group as a foredeep deposit is the eastward migration of flysch deposition in front of the evolving foreland fold-thrust belt (Hoffman, 1973). Such diachroneity is difficult to prove in the absence of biostratigraphy, but by establishing a basin-wide stratigraphy for the hemipelagic "background" sediments between turbidites, evidence for eastward migration has now been obtained.

At the base of the Recluse Group throughout the externides is a westward tapering wedge of dark semipelite and craton-derived quartz siltite (Tree River Formation) with a few beds containing glauconite and/or ferruginous dolomite. The top of this unit is invariably below the flysch. The three succeeding units all intertongue westward into gritty feldspathic-lithic greywacke flysch (Asiak Formation). The lowest unit is a flat-laminated, noncalcareous pelite (Fontano Formation) that tapers and becomes increasingly graphitic and sulphidic westward. It passes upward rather sharply into

a less fissile, more resistant pelite characterized by abundant calcareous concretions 2-5 cm in diameter (Kikerk Formation). This unit is overlain, above a thin transitional interval, by a remarkable unit, about 0.5 km thick, consisting of millimetre-scale limestone-argillite rhythmite (Cowles Lake Formation). These three stratigraphic units can be recognized even in sections composed dominantly of greywacke. The same sequence occurs all along the externides and in correlative sequences as far as 500 km away in Athapuscow Aulacogen (Kahochella and basinal Pethei groups: Hoffman, 1968). Basically, the sequence records stepwise increases in rate of deepwater calcium carbonate precipitation, probably due to increases in temperature or evaporation of the basin. The unit boundaries are therefore treated as approximate time planes against which the first appearance of flysch can be calibrated. As predicted in the dynamic foredeep model, the generally abrupt onset of coarse grained greywacke deposition occurs in the Fontano Formation in the west half of the fold-thrust belt, in the Kikerk Formation in the east half of the belt, and in the Cowles Lake Formation on the autochthon.

Carousel Massif and the Nature of Basement Involvement in Asiak Fold-Thrust Belt

Carousel Massif is a unique, basement-cored, anticlinal structure within Asiak Fold-Thrust Belt (Fig. 60.1). It is here that the nature and timing of basement involvement in the deformation can be most directly ascertained. Fraser (1974) established the gross anticlinal form of the structure and recently a major décollement, located high in the lower member of the Odjick Formation, has been shown to wrap around the plunging north end of the massif (St-Onge et al., 1982, 1983). The tightly folded and thrusted panel above the décollement contrasts with the broad, simple folds of the footwall strata, which conform to the basement unconformity.

St-Onge et al. (1982) suggest that the décollement might be the sole fault for thrusts exposed to the east and our observations support this view. The décollement appears to continue down the east flank of the anticline and to merge, in the plunging syncline south of Redrock (transcurrent) Fault, with the main frontal thrust (Fig. 60.1), which places Odjick Formation quartzite above rocks as young as Cowles Lake Formation. It seems probable that the main phase of décollement folding and thrusting did not involve basement, but that the entire overthrust complex and the underlying autochthon were subsequently folded to produce Carousel anticline. This structural sequence is similar to that documented around Hepburn Batholith in the internides of the same fold-thrust belt (Hoffman et al., 1980). There, the peak of thermal metamorphism, coincident with batholith emplacement, separates an earlier phase of thrusting from a later phase of upright folding similar in scale to Carousel Massif. It is currently assumed that thrusting and later folding are two phases of the same collision event (D1 of Hoffman, 1982). The folding of Carousel Massif certainly predates the Tree River (D2) cross folding (see below) and also the D4 transcurrent faulting.

There remains the possibility of a relatively minor blind thrust having developed beneath Carousel Massif during folding. There is a fault emerging from the basement at longitude 114 degrees on Redrock Lake and apparently dying out within the Odjick Formation, but whether it is a thrust or a late transcurrent fault must be investigated further in the field. If a thrust, Carousel Massif would be only parautochthonous with respect to Slave Craton.

Relation of Thrusting to the Takiyuak Molasse

The relation of thrusting to the Takiyuak Formation, a nonmarine, lithic-feldspathic sandstone and minor conglomerate that disconformably overlies the Cowles Lake Formation in Takijuq Basin, has been problematic. Fraser (1974) shows the main frontal thrust cutting the Cowles Lake Formation but not in contact with the Takiyuak Formation. We have recognized a smaller thrust, exposed 1-4 km east of the main frontal thrust, that extends for 17 km north of the main strand of Redrock Fault (Fig. 60.1). This thrust, also west dipping, places greywacke-rich Kikerk and Cowles Lake formations over typical red crossbedded sandstone of the Takiyuak Formation. Therefore, the possibility that the Takiyuak molasse, and its correlatives the Tochatwi Formation in Athapuscow Aulacogen (Hoffman, 1968, 1969) and the Amagok Formation in Kilohigok Basin (Campbell and Cecile, 1981), might postdate D1 thrusting has been eliminated.

Transverse (D2) Folding of Regional Extent but Unknown Origin

The Tree River Fold Belt (Fig. 60.1) is a spectacular system of east-northeast-trending folds forming a broad synclinorium exposing Archean basement uplifts on its flanks and Kikerk Formation (Recluse Group) in its centre. So far, our mapping of these folds is limited to the south margin of Eokuk Uplift and the area of intersection of Tree River folds with the front of Asiak Fold-Thrust Belt around Kikerk Lake. In addition, a number of important features elsewhere in the orogen and beyond have come into focus as probable effects of this deformation (D2 of Hoffman, 1982), for which no obvious cause is apparent.

The fold belt is extremely well exposed due to a myriad of perpendicular diabase dykes that have been plucked out by Quaternary glaciation where they transect the Rocknest Formation, exposing hundreds of deep roadcut-like cross-sections. The folds are characteristically disharmonic, open, upright or steeply inclined, and approximately parallel. No significant thrusting has been found. Asymmetry is imposed by a penetrative cleavage that evidently formed just prior to folding. When unfolded, the cleavage dips uniformly to the north-northwest, perpendicular to subsequent folds, at an angle of less than 20 degrees. Due to flexural shear during folding, the angle between bedding and cleavage was diminished on north-dipping limbs and increased on south-dipping ones, but only in the tightest fold hinges does the characteristic pre-fold cleavage give way to a stronger axial plane cleavage. The apparent absence of thrusting and of any significant décollement within the sedimentary cover is consistent with the observed involvement of basement in the folding, which occurs on all scales from metres to kilometres. Eokuk Uplift (Fig. 60.1) is merely a major structural culmination in the Tree River Fold Belt.

The Tree River Fold Belt intersects the frontal D1 folds and thrusts around Kikerk Lake. Detailed mapping demonstrates conclusively that the D1 thrusts are folded by and therefore older than the Tree River (D2) folds, as noted earlier by Hoffman (1970). Several thrusts were first folded by D1 folds, which parallel the thrust traces, before being refolded by the transverse Tree River folds. The Tree River folds are cut by D4 transcurrent faults.

The effects of Tree River deformation are less coherent within Asiak Fold-Thrust Belt than to the east, where bedding remained relatively undisturbed until the onset of Tree River folding. Nevertheless, there are numerous 0.5 km-scale cross folds and areas of transecting cleavage that parallel the Tree River folds after rotations associated with conjugate transcurrent faulting (D4) are restored.

The major culminations and saddles in the externides as a whole, evidenced by the configuration of the basement contact and the distribution of foredeep deposits (Fig. 60.1), can now be considered as due to large scale cross folding of D2 (Tree River) age. The previously mysterious transverse arch in Crustal Block B (Hoffman and St-Onge, 1981; St-Onge, in press) of the internides may be an extension, somewhat disrupted by transcurrent faults, of the transverse arch (culmination) north of Takijuq Lake. An even higher arch at the south end of the externides exposes the Scotstoun and Acasta basement-cored anticlines in the internides southwest of Carousel Massif (St-Onge et al., 1983). These transverse D2 structures do not obviously affect the Great Bear Magmatic Zone and are tentatively assumed to be older.

Looking even farther afield, the open syncline of Kilohigok Basin strata between Contwoyto Lake and Bathurst Inlet also parallels the Tree River Fold Belt, as do the great nappes in Athapuscow Aulacogen (Hoffman et al., 1977; Hoffman, 1981). The nappes postdate the Tochatwi molasse, correlative with the Takiyuak molasse (see above), and predate the Compton Laccoliths, which are coeval with Great Bear magmatism (Bowring and Van Schmus, 1982). This is consistent with the age relations of Tree River deformation in Wopmay Orogen. The nappes, like the folds south of Eokuk Uplift, involve basement and are overturned toward Slave Craton. The cause of this extensive northwest-southeast oriented compression is not known but is probably a collision somewhere, possibly in southeastern Churchill Province (Lewry, 1981; Lewry et al., in press) or, equally possible, to the north under the Arctic Platform.

Normal Faults Associated with D4 Transcurrent Faulting

There is a broad region centred northeast of Carousel Massif where the regional pattern of late transcurrent faults (D4), dominated by northeast-trending right-slip faults, breaks down and is replaced by a fault array of less regular trends. Specifically:

1. the right slip faults assume a more easterly orientation and commonly show evidence for dip-slip movement.
2. There is at least one domain dominated by northwest-trending left-slip faults, having up to 1 km separation.
3. There are numerous normal faults, with east-west trends and up to 250 m demonstrated slip, especially along the boundaries between right-slip and left-slip domains. Measured fault dips vary from 40 to 75 degrees, usually to the south.

Approximate contemporaneity of the faults is indicated by the fact that normal faults locally appear to merge with right lateral faults, and because there is no clear evidence that one fault set consistently offsets the other. Also, a single set of inferred principal planes of stress or strain accommodates the orientation of all fault sets. Thus the aggregate fault geometry in this region is interpreted as having arisen from a single three dimensional deformational phase involving east-west shortening, north-south extension, and (modest) vertical shortening. Although the study of general, three dimensional brittle strain is as yet in infancy, the fault orientations observed here are crudely compatible with the experimental work of Aydin and Reches (1982).

Localization of normal faulting in this region may in part be related to compatibility problems along boundaries between right-slip and left-slip domains, or to space problems where the right-slip fault system dies out toward the autochthon. However, domain boundary problems are elsewhere accommodated by faults with reverse slip (Hoffman and St-Onge, 1981), indicating some more fundamental control.

Lead-zinc Vein Mineralization in the Rocknest Dolomite

The discovery of several minor galena-sphalerite showings during the past season indicates that the Rocknest Formation, although not conspicuously mineralized, is not barren. Northwest of Carousel Massif (65°57'N, 114°16'W), an array of about six veins, 1-40 cm wide and exposed along a strike length of 50 m, contain quartz, galena, sphalerite and minor chalcopyrite. Massive sphalerite-galena occurs in pods up to 40 cm thick and 70 cm long. The veins cut Rocknest Member 5 along the west limb of an outcrop scale D1 syncline. They strike southwest (220 degrees), with a nearly constant 50 degree northwest dip, irrespective of the bedding of the host rock, suggesting that they postdate at least some D1 structures. The mineralization clearly predates D4, because the veins are offset by numerous mesoscopic left-lateral faults.

At a second locality north of Kikerk Lake (67°28'N, 113°23'W) a non-intersecting vein set trending 350 to 005 degrees displays the same mineralogy. Individual veins are up to 2 cm wide with a 0.3 to 1.0 m spacing. They occur in Rocknest Member 10, on the footwall of Kikerk Thrust, but do not extend into the Odjick pelite on the hanging wall. It is not clear whether this observation has mechanical or temporal significance. Two other Pb-Zn indications in the same region were also found within Rocknest Member 10.

From crosscutting relations and from their trend, it is clear that the veins predate D4 transcurrent faulting. More precise dating at this time is speculative. They may be extensional fracture fillings related to D1 (buckling stresses), or perhaps D2 folding.

Although the veins are economically uninteresting in themselves, they could be indicative of more significant concentrations of cryptic, finely disseminated mineralization for which we have not searched. The occurrence in the Rocknest Formation of a distinct reefal shelf-edge facies with primary porosity, of a down-slope shale-out, and of sand sheets and organic-rich tidal-flat facies that interfinger with evaporitic (salt-casted) lagoonal muds across a shelf, 210 km in strike length and at least 160 km in restored width, that was subsequently sealed by black shale, could present some interesting situations for potential mineralization. By establishing in detail the sedimentological anatomy and dynamics of the Rocknest shelf, this project could provide the basis for some enlightened exploration.

Future Work

For 1983, the final year scheduled for field work, study of the Rocknest Formation will concentrate firstly on the shelf edge and adjacent facies zones, and secondly on east-west changes in character of the well developed Rocknest cycles (Hoffman, 1975), especially along the Tree River Fold Belt, which appears to hold the key to understanding the dynamics of cycle generation. Priorities for structural work will be to fill in the two remaining gaps, west of Takijuq Lake and south of Kikerk Lake, in the frontal part of Asiak Fold-Thrust Belt to establish the strike lengths of individual thrusts, and to complete the work begun in the Tree River Fold Belt.

Acknowledgments

Jean David, Mark Daynecka, Greg Eiché, Karen Pelletier and Janien Schwarz made an outstanding team of field assistants. René Brulé was a skillful and reliable helicopter engineer-pilot. Winn Bowler and Martin Irving provided superior expediting, and we thank the staff of the Geology Office in Yellowknife for practical support. Spare parts from Joe's Garage were much appreciated. Adrian Camfield, Dan Krenz, M.E. Bickford and J. Fred Read visited, stimulated and encouraged us in the field.

Tirrul's work on the structure of the externides will form the basis of a Ph.D. thesis to be submitted to University of California at Santa Barbara. Grotzinger's study of the Rocknest Formation will likewise constitute a Ph.D. thesis for submission to Virginia Tech. His work has been supported by a Geological Society of America Grant 2992-82, and a Grant-in-Aid of Research from the Scientific Research Society of Sigma Xi.

References

Assereto, R.L.A.M. and Kendall, C.G.St.C
1977: Nature, origin and classification of peritidal tepee structures and related breccias; Sedimentology, v. 24, p. 153-210.

Aydin, A. and Reches, Z.
1982: Number and orientation of fault sets in the field and in experiments; Geology, v. 10, p. 107-112.

Bowring, S.A. and Van Schmus, W.R.
1982: Age and duration of igneous events, Wopmay Orogen, Northwest Territories, Canada; in Abstracts with Programs, v. 14, Geological Society of America, p. 449.

Campbell, F.H.A. and Cecile, M.P.
1981: Evolution of the Early Proterozoic Kilohigok Basin, Bathurst Inlet – Victoria Island, Northwest Territories; in Proterozoic Basins of Canada, ed. F.H.A. Campbell; Geological Survey of Canada, Paper 81-10, p. 103-131.

Cavanaugh, M.D. and Seyfert, C.K.
1977: Apparent polar wander paths and the joining of the Superior and Slave Provinces during early Proterozoic time; Geology, v. 5, p. 207-211.

Evans, M.E. and Hoye, G.S.
1981: Paleomagnetic results from the lower Proterozoic rocks of Great Slave Lake and Bathurst Inlet areas, Northwest Territories; in Proterozoic Basins of Canada, ed. F.H.A. Campbell; Geological Survey of Canada, Paper 81-10, p. 191-202.

Fraser, J.A.
1974: The Epworth Group, Rocknest Lake area, District of Mackenzie; Geological Survey of Canada, Paper 73-39, 23 p., and Map 1384A.

Ginsburg, R.N. and James, N.P.
1976: Submarine botryoidal aragonite in Holocene reef limestones, Belize; Geology, v. 4, p. 431-436.

Grotzinger, J.P. and Read, J.F.
– Silica pseudomorphs of aragonite botryoids in tepee structures of 1.9 B.Y. rimmed shelf, Rocknest Formation, Wopmay Orogen, N.W.T., Canada; in Abstracts for Annual Meetings, Society of Economic Paleontologists and Mineralogists, American Association of Petroleum Geologists Bulletin. (in press)

Hildebrand, R.S., Bowring, S.A., Steer, M.E., and Van Schmus, W.R.
1983: Geology and U-Pb geochronology of parts of the Leith Peninsula and Rivière Grandin map areas, District of Mackenzie; in Current Research, Part A, Geological Survey of Canada, Paper 83-1A, report 46.

Hoffman, P.F.
1968: Stratigraphy of the Great Slave Supergroup (Aphebian), east arm of Great Slave Lake, District of Mackenzie; Geological Survey of Canada, Paper 68-42, 92 p.

Hoffman, P.F. (cont.)
1969: Proterozoic paleocurrents and depositional history of the East Arm fold belt, Great Slave Lake, Northwest Territories; Canadian Journal of Earth Sciences, v. 6, p. 441-462.

1970: Study of the Epworth Group, Coppermine River area, District of Mackenzie; in Report of Activities, Part A, Geological Survey of Canada, Paper 70-1A, p. 144-149.

1973: Evolution of an early Proterozoic continental margin: the Coronation geosyncline and associated aulacogens of the northwestern Canadian Shield; Royal Society of London, Philosophical Transactions, Series A, v. 273, p. 547-581.

1975: Shoaling-upward shale-to-dolomite cycles in the Rocknest Formation, Northwest Territories, Canada; in Tidal Deposits, ed. R.N. Ginsburg; Springer-Verlag, New York, p. 257-265.

1980: Wopmay Orogen: a Wilson cycle of early Proterozoic age in the northwest of the Canadian Shield; in The Continental Crust and Its Mineral Resources, ed. D.W. Strangway; Geological Association of Canada, Special Paper 20, p. 523-549.

1981: Autopsy of Athapuscow Aulacogen: a failed arm affected by three collisions; in Proterozoic Basins of Canada, ed. F.H.A. Campbell; Geological Survey of Canada, Paper 81-10, p. 97-102.

1982: The northern internides of Wopmay Orogen (Sloan River, Hepburn Lake and part of Coppermine map areas, N.W.T.); Geological Survey of Canada, Open File 832, Map with marginal notes (1:250 000 scale).

Hoffman, P.F. and St-Onge, M.R.
1981: Contemporaneous thrusting and conjugate transcurrent faulting during the second collision in Wopmay Orogen; implications for the subsurface structure of post-orogenic outliers; in Current Research, Part A, Geological Survey of Canada, Paper 81-1A, p. 251-257.

Hoffman, P.F., Bell, I.R., Hildebrand, R.S., and Thorstad, L.
1977: Geology of the Athapuscow Aulacogen, East Arm of Great Slave Lake, District of Mackenzie; in Current Research, Part A, Geological Survey of Canada, Paper 77-1A, p. 117-129.

Hoffman, P.F., St-Onge, M.R., Easton, R.M., Grotzinger, J.P., and Schulze, D.E.
1980: Syntectonic plutonism in north-central Wopmay Orogen (early Proterozoic), Hepburn Lake map area, District of Mackenzie; in Current Research, Part A, Geological Survey of Canada, Paper 80-1A, p. 171-177.

Irving, E. and McGlynn, J.C.
1979: Paleomagnetism in the Coronation Geosyncline and arrangement of continents in the middle Proterozoic; Royal Astronomical Society, Geophysical Journal, v. 58, p. 309-336.

Lewry, J.F.
1981: Lower Proterozoic arc-microcontinent collisional tectonics in the western Churchill Province; Nature, v. 294, no. 5836, p. 69-72.

Lewry, J.F., Sibbald, T.I.I., and Schledewitz, D.C.P.
– Variation in character of Archean basement in the western Churchill Province and its significance; in Archean Supracrustal Sequences, Geological Association of Canada, Special Paper. (in press)

St-Onge, M.R.
– Geothermometry and geobarometry in pelitic rocks of north-central Wopmay Orogen (Early Proterozoic), Northwest Territories, Canada; Geological Society of America, Bulletin. (in press)

St-Onge, M.R., King, J.E., and Lalonde, A.E.
1982: Geology of the central Wopmay Orogen (Early Proterozoic), Bear Province, District of Mackenzie: Redrock Lake and the eastern portion of Calder River map areas; in Current Research, Part A, Geological Survey of Canada, Paper 82-1A, p. 99-108.

St-Onge, M.R., Lalonde, A.E., and King, J.E.
1983: Geology of the central Wopmay Orogen (Early Proterozoic), Bear Province, and of the western Archean Slave Province, District of Mackenzie: Redrock Lake and the eastern portion of Calder River map areas; in Current Research, Part A, Geological Survey of Canada, Paper 83-1A, report 18.

Tucker, M.E.
1982: Precambrian dolomites: petrographic and isotopic evidence that they differ from Phanerozoic dolomites; Geology, v. 10, p. 7-12.

61.

GEOLOGY OF ABERDEEN LAKE MAP AREA, DISTRICT OF KEEWATIN: PRELIMINARY REPORT

Project 820004

A.N. LeCheminant, K.E. Ashton[1], J. Chiarenzelli[2], J.A. Donaldson[2], M.A. Best[3], S. Tella, and D.L. Thompson
Precambrian Geology Division

LeCheminant, A.N., Ashton, K.E., Chiarenzelli, J., Donaldson, J.A., Best, M.A., Tella, S., and Thompson, D.L., Geology of Aberdeen Lake map area, District of Keewatin: preliminary report; in Current Research, Part A, Geological Survey of Canada, Paper 83-1A, p. 437-448, 1983.

Abstract

Early Proterozoic and Archean basement rocks underlie undeformed Dubawnt Group successions in the Aberdeen Lake map area. Migmatitic, granitic and granodioritic gneisses characterize a large lithostructural domain in central and southeastern parts of the map area. The domain is interpreted as Archean basement that has been mildly affected by Aphebian remobilization and cataclasis. Northeast of Aberdeen Lake similar rocks underlie a small, wedge-shaped area bounded by faults and shear zones that displace Thelon Formation cover. The major northeast-trending bounding fault is a reactivated ductile deformation zone in the basement.

The basement domain west of Marjorie Lake is made up of north-northeast-trending units of deformed potassic intrusive rocks. The easternmost unit is a complex tectonic zone that appears to have been the locus of early Proterozoic cataclastic deformation accompanied by greenschist facies retrogression. Orthoquartzite-bearing sequences within the domain are in tectonic contact with adjacent mylonitic rocks. Megacrystic gneissic granite and augen gneiss are the most widespread rocks in the western domain.

An east-northeasterly-trending metasedimentary belt of uncertain age underlies Thelon Formation strata south of Aberdeen Lake. The belt is dominated by metagreywacke with minor schist, quartzite and banded iron formation. Large plutons of fluorite-bearing granite and smaller bodies of younger syenite intrude the metasedimentary rocks and the Archean gneiss domain to the south. All of these units are cut by syenite and biotite lamprophyre dykes.

Extensive weathering preceded deposition of the Pitz and Thelon formations. The first period of extensive weathering followed deposition of Kunwak Formation braidplain sediments and preceded deposition of Pitz Formation fluvial and aeolian sandstones and associated rhyolitic lavas and pyroclastics. Minor episodes of weathering occurred during pauses in volcanism and a second major period of weathering affected uppermost Pitz Formation flows. Thelon Formation strata display upward trends of increasing compositional maturity. Synsedimentary faults are recognized in the lowermost fluvial sediments. Upper units include sandstones of probable aeolian origin.

Introduction

Sedimentary and volcanic successions of the Dubawnt Group underlie almost two-thirds of the Aberdeen Lake (66B) map area (Wright, 1967; Donaldson, 1969). Dubawnt Group successions are primarily flat-lying to gently northwest-dipping rhyolitic volcanic rocks and interflow sedimentary rocks (Pitz Formation) with overlying conglomerates and quartz arenites (Thelon Formation). Pre-Dubawnt Group basement extends across the southern part of the map area (Fig. 61.1) and also is exposed in a fault-bounded, wedge-shaped area north of Aberdeen Lake in 66B/16.

This paper outlines the geology of the southern half of the Aberdeen Lake map area based on 1:250 000 mapping initiated during the 1982 field season. It is augmented by a discussion of pre-Thelon Formation regoliths and Thelon Formation depositional environments by J. Chiarenzelli, J.A. Donaldson and M. Best, and by a study of basement-Thelon Formation relationships in 66B/16 by Subhas Tella and D.L. Thompson. Investigation of the sub-Thelon regolith constitutes part of J. Chiarenzelli's M.Sc. study at Carleton University. In addition, M. Best and D. Mainville measured detailed stratigraphic sections and resampled the Ordovician shelf carbonate outlier north of Aberdeen Lake (Donaldson, 1969; Bolton and Nowlan, 1979). Samples have been turned over to T.E. Bolton for assessment of the fossil assemblage.

Acknowledgments

We thank Danielle Mainville, A.R. Miller, Iori Miller, J.C. Roddick and Rob Scammell for their enthusiastic field assistance and mapping contributions. Reliable, cheerful transportation was provided by Rob Pritchard and Gord Collett of Les Hélicoptères Verreault. We are grateful to Anaconda Canada Exploration, Ltd., Vancouver, B.C. and Cominco Ltd., Toronto, Ontario for permission to examine and sample drill core on site in the Aberdeen Lake area. J.A. Donaldson and J. Chiarenzelli received logistical support from the Geological Survey of Canada. Additional field and laboratory support for their work has been provided by the Geology Office, DIAND and by NSERC operating grant A5536.

ABERDEEN LAKE MAP AREA (S½)

A.N. LeCheminant and K.E. Ashton

Archean and Aphebian Basement Complex

The pre-Dubawnt Group basement south of Aberdeen Lake has been subdivided into three lithological packages: (1) a central and southeastern domain of granitoid gneisses with minor supracrustal remnants; (2) a western domain of deformed potassic intrusive rocks and north-northeasterly trending cataclastic gneisses; and (3) the Aberdeen Lake belt, an east-northeasterly trending metasedimentary sequence dominated by greywacke with

[1] Queen's University, Kingston, Ontario.
[2] Carleton University, Ottawa, Ontario.
[3] University of Ottawa, Ottawa, Ontario.

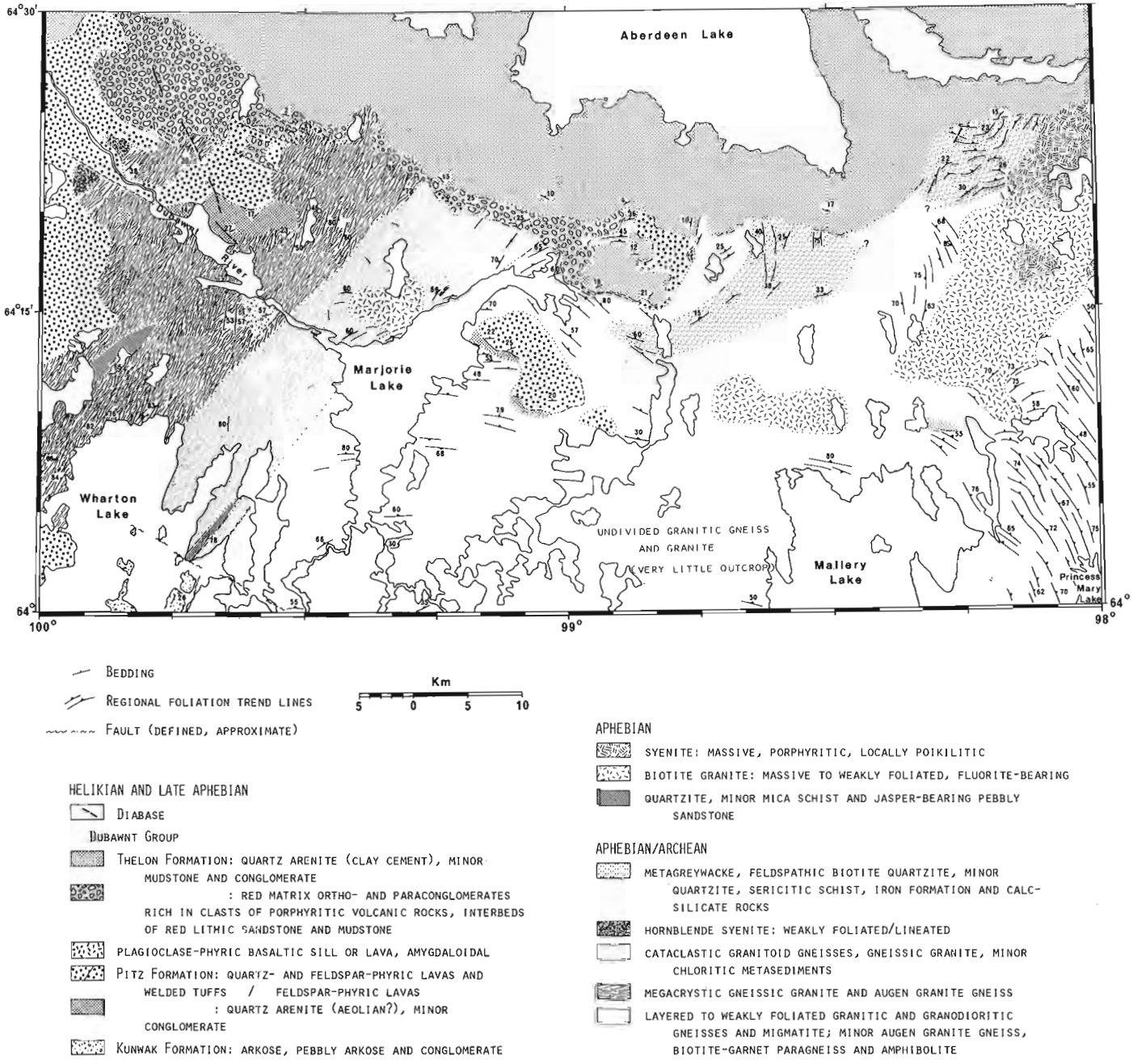

Figure 61.1. *Geological sketch map of the south half of the Aberdeen Lake map area (66B).*

minor quartzite, sericitic schist and iron formation. The first two domains are northern extensions of the contiguous central and Pukiq domains in the Tebesjuak Lake map area (LeCheminant et al., 1981).

Intrusive into the metasedimentary belt and the central gneiss domain are large plutons of fluorite-bearing granite with smaller bodies of younger syenite. All of these units are cut by syenite and biotite lamprophyre dykes.

Central and Southeastern Domain

Layered to weakly foliated migmatitic, granitic and granodioritic gneisses characterize this large domain, which extends to the south and southeast (LeCheminant et al., 1979, 1981). A major north-northeasterly trending cataclastic zone bounds the domain on the west (Fig. 61.1). To the north, gneisses are in contact with lower grade metasedimentary rocks of the Aberdeen Lake belt or overlain by Dubawnt Group strata.

The central and southeastern domain is interpreted as Archean basement that has been mildly affected by Aphebian remobilization and cataclasis. Migmatitic, grey, layered, biotite-hornblende granodiorite gneiss and pink to white, nebulitic, biotite granite gneiss are the dominant lithologies. Granoblastic textures are typical of most rocks in the domain except north and west of Marjorie Lake where local units of cataclastic potash feldspar augen gneiss are found. The dominant hornblende-biotite-quartz-feldspar assemblage and extensive migmatite suggest regional middle to upper amphibolite facies metamorphism. In most areas the gneisses

are crosscut by 5-30 per cent of centimetre- to metre-scale bands, pods and dykes of white to pink granitic pegmatite and/or medium grained granite.

Regional foliation trends swing from north-northwesterly near Princess Mary Lake to westerly between Mallery and Marjorie lakes (Fig. 61.1). Dips are moderate to steep northeasterly to northerly. First phase biotite-hornblende foliation is parallel to compositional layering. Second phase tight to isoclinal folding is seen as locally abundant intrafolial minor folds, most with a biotite axial planar foliation. Variations in the regional foliation trend outline third phase broad, open folds.

East of Mallery Lake metasedimentary and metavolcanic remnants occur as well layered units within the migmatitic rocks. Paragneisses are medium grained, grey to pink, psammitic rocks exhibiting good, centimetre-scale compositional layering. They contain 5-10 per cent biotite, up to 1 per cent magnetite and trace allanite. Interlayered with the biotite gneisses are grey, medium grained biotite-hornblende-plagioclase gneisses and rare, green diopside-bearing gneisses. Minor rusty horizons, 1-3 cm thick contain traces of pyrite, pyrrhotite and chalcopyrite. Metasedimentary rocks also occur on the southeast side of Marjorie Lake. Here, thin units of lean oxide facies iron formation containing abundant quartz and garnet are associated with garnet-biotite-hornblende-plagioclase-quartz paragneiss.

A small body of deformed mafic rocks, ranging from metagabbros and metadiorites to tonalitic gneisses, is exposed along the edge of the map area just north of Princess Mary Lake. The dark green to black, medium grained gabbroic rocks are massive to well lineated. They grade into more leucocratic gneissic diorites containing 20-25 per cent hornblende and minor biotite. White, tonalitic gneisses outline the margins of the mafic complex.

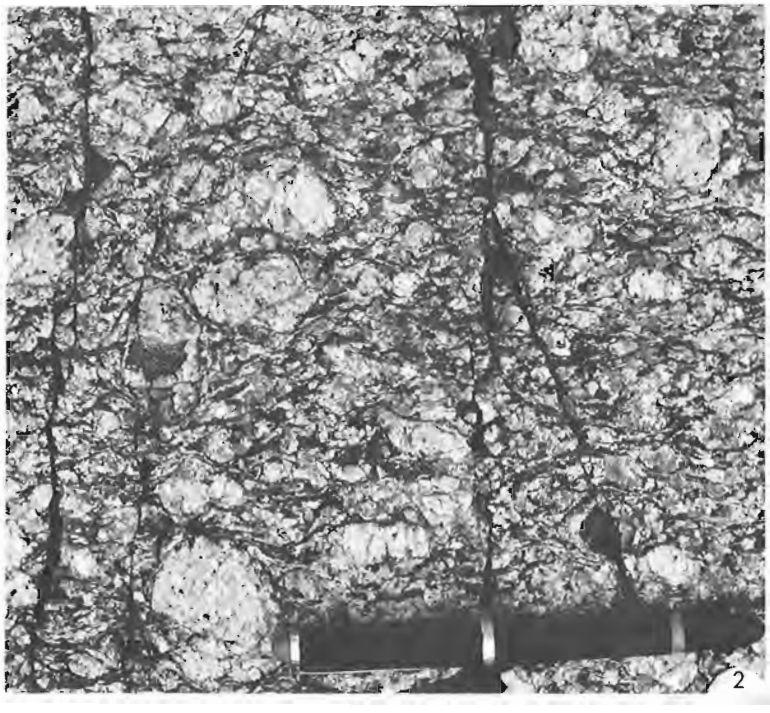

Figure 61.2. *Megacrystic gneissic granite, Wharton Lake. Potash feldspar megacrysts to 8 cm characterize this large homogeneous unit in the western domain. GSC 203601-M*

Bedrock in the region between Mallery and Marjorie lakes is poorly exposed and mapping is incomplete. The few known outcrops are of migmatitic, granitic gneiss and massive, leucocratic granite. These two units have not been separated in Figure 61.1 pending additional mapping in 1983.

Western Domain

The western domain is made up of three north-northeast-trending units of variably deformed potassic intrusive rocks, two of which contain narrow belts of orthoquartzite (Fig. 61.1). The poorly exposed eastern unit is a complex tectonic zone 8-10 km wide which truncates regional structural trends in the adjacent central domain. The unit contains a heterogeneous mixture of retrograded central domain gneisses, gneissic granite, fine grained mylonitic augen gneisses and chlorite schist. This tectonic zone appears to have been the locus of early Proterozoic movements that superimposed north-northeasterly cataclastic zones and younger faults on earlier structures. The deformation was accompanied by greenschist facies retrogression.

Two orthoquartzite belts within the eastern unit are in tectonic contact with adjacent mylonite and mylonite gneiss. The southern belt trends at 040° with vertical to steep southeast dips. It can be traced for 6 km and comprises 300-350 m of white to pink orthoquartzite with one interbedded, boudinaged, 10-20 m wide unit of crenulated mica schist. The exposure north of Marjorie Lake is a tectonic sliver of orthoquartzite less than 100 m wide. Just north of the Dubawnt River and northwest of Marjorie Lake a small body of medium grained, red, leucocratic granite cuts mylonitic gneiss. Biotite within the granite is chloritized and the granite is cut by numerous quartz stockworks.

A distinctive and homogeneous unit of megacrystic gneissic granite and augen granite gneiss underlies the region west of the tectonic zone (Figs. 61.1 and 61.2). Similar large bodies of deformed granite to quartz monzonite are known to the south and southwest (LeCheminant et al., 1981; Tella et al., 1981) and in the Deep Rose Lake map area to the north (Tella et al., 1983). Locally the gneissic granite is cut by narrow cataclastic zones. Potash feldspar megacrysts up to 8 cm are deformed into smaller augen set in a fine grained crushed matrix. The new foliation is at a low angle to the early biotite-hornblende foliation (Fig. 61.3). The deformed granite body is at least 10 km wide and extends 45 km from Wharton Lake to north of the Dubawnt River.

A northeast-trending, steeply southeast-dipping orthoquartzite-bearing sequence exposed northwest of Wharton Lake is probably in tectonic contact with the megacrystic granite. The succession is a ridge-forming unit that is exposed for 4 km. It comprises almost 1 km of white to pink, massive to well bedded orthoquartzite overlain by thin units (30-50 m) of pebbly subarkosic sandstone. Flattened pebbles within the sandstone include jasper, hematitic iron formation, quartzite and a quartz-eye-bearing red volcanic(?) rock. The same succession is exposed along strike to the southwest in 66C/1 just 1 km west of the map boundary. LeCheminant et al. (1981) report an identical sequence to the south in 65O/13 where it was tentatively correlated with the Aphebian Hurwitz or Amer groups on the basis of lithology.

North and northwest of the orthoquartzite belt the western domain is poorly exposed, with only a few outcrops of augen granite gneiss and mylonitic gneiss visible through Pitz and Thelon formation cover. The westernmost unit of the domain is a deformed

Figure 61.3

Narrow mylonite to protomylonite zones within megacrystic gneissic granite. Potash feldspar megacrysts are deformed into smaller augen set in a fine grained matrix. Note late-stage brittle fractures. GSC 203601-R

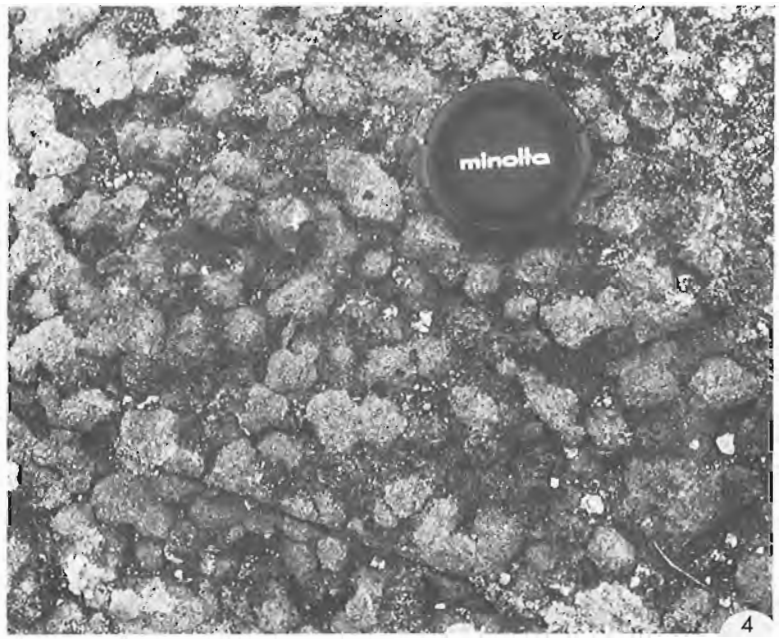

Figure 61.4

Knobbly weathering poikilitic mafic syenite. 1-3 cm oikocrysts of potash feldspar enclose clinopyroxene, biotite, sphene and apatite. Lens cap is 6.2 cm in diameter. GSC 203601-Z

intrusive complex of weakly foliated and lineated hornblende syenite cut by a network of pink, leucocratic, quartz syenite to granite dykes and veins. Syenite is exposed on both sides of the Dubawnt River underlying Pitz Formation lavas. The intrusive rocks have a radiometric response up to five times higher than mylonitic augen gneiss to the southeast, and exposures are coincident with a northeast-trending aeromagnetic high that extends under Dubawnt Group cover.

Three minor occurrences of epigenetic fracture-controlled uranium mineralization were located during 1982 mapping in the western domain (472000E, 7118400N; 476100E, 7134960N; and 480140E, 7122640N). In all cases, the pitchblende and/or anomalous radioactivity was confined to discontinuous, narrow chlorite-carbonate seams and fractures. These features are part of multiple fracture and joint sets resulting from late brittle deformation in eastern parts of the domain.

Aberdeen Lake Belt

An east-northeasterly trending metasedimentary belt, up to 8 km wide, extends 45 km from the southeast arm of Aberdeen Lake almost to Marjorie Lake (Fig. 61.1). Rocks of the belt are unconformably overlain by Thelon Formation strata to the north and are intruded by a granite-syenite complex to the east.

The metasedimentary sequence is dominated by greywacke, primarily psammitic, with only minor pelitic layers. Intercalated with the wackes are chlorite-sericite schists, lean banded iron formation (sulphide and oxide facies), feldspathic quartzite and minor white orthoquartzite. Many of these units are sulphide-bearing with abundant pyrite and minor chalcopyrite. Metavolcanic rocks are represented by a few outcrops of fine grained amphibolite and thin laminated mafic schist. Primary features other than compositional layering are not preserved.

Biotite foliation parallel to compositional layering has consistent shallow, northerly to westerly dips. The foliation outlines open folds with northwesterly trending axes. A few examples of a second biotite foliation at a low angle to the layering – parallel foliation suggest the sequence may contain tight to subisoclinal folds. However, no minor folds were observed and outcrop is insufficient to resolve any earlier fold patterns or the complete stratigraphic sequence. Structural trends in central domain gneisses are truncated by the metasedimentary rocks near the east end of the belt, but they are conformable with gneisses near Marjorie Lake. Contacts are not exposed.

Metamorphic grade is upper greenschist to lower amphibolite. Biotite-garnet-muscovite assemblages in pelitic layers are largely retrograded to greenschist facies chlorite-sericite-epidote mineralogy. Many exposures in the northern part of the belt show weathering effects related to the overlying Thelon Formation unconformity. White orthoquartzites contain specularite-quartz veined breccia zones and metagreywackes are converted to kaolinite-hematite-quartz assemblages that still preserve most textural characteristics of the rocks.

The Aberdeen Lake belt is lithologically similar to clastic sequences exposed along strike to the east-northeast. Donaldson (1966a) assigned a sequence containing an upper, thick orthoquartzite unit in the Schultz Lake area to the Lower Proterozoic Hurwitz Group. The basal part of this sequence comprises upper greenschist-lower amphibolite grade immature clastic rocks identical to the wackes of the Aberdeen Lake belt (A.R. Miller, personal communication, 1982). Farther to the east packages of greywacke-dominated metasedimentary rocks without thick orthoquartzite units are mapped as Archean and/or Lower Proterozoic by Donaldson (1966a). The eastern continuation of these rocks in the Baker Lake area has been informally named the Ketyet River group by Schau et al. (1982) who speculate that they project along strike to join with the Archean Prince Albert Group. Adequate correlation and dating of these metasediments awaits more detailed mapping in the Schultz Lake area.

Intrusive Rocks

Large plutons of medium- to coarse-grained fluorite-bearing biotite granite and smaller bodies of syenite underlie more than 350 km^2 between Mallery Lake and the southeast arm of Aberdeen Lake (Fig. 61.1). Rocks of the syenitic suite invariably intrude the granites. In some cases intrusive relationships are obscured by local remelting of granite along contacts to produce fluorite-rich aplitic granite dykes that backvein the syenites. An aeromagnetic high outlines the granite bodies southeast of Aberdeen Lake. Local highs within the anomaly discriminate several of the more mafic syenite plugs.

Granites from central parts of the plutons are typically massive and equigranular. However, near contacts with surrounding gneisses weakly foliated and/or porphyritic granites are common. Contacts are generally discordant although large gneissic rafts and xenoliths can retain foliations consistent with regional trends. Deep purple fluorite is a ubiquitous accessory. Other accessory minerals include sphene, iron oxides, allanite, apatite and zircon. Fracture-coating and alteration assemblages involve quartz, chlorite, epidote, calcite, sericite, hematite and leucoxene. Aplite and pegmatite dykes, some with minor molybdenite and galena, cut gneisses adjacent to granite plutons.

The syenitic suite displays a remarkable range in composition, texture and contained xenoliths. The most spectacular rock is a greenish to pinkish grey, knobbly weathering poikilitic syenite containing oikocrysts of potash feldspar (Fig. 61.4) and titanian garnet (melanite). Enclosed minerals are pale green clinopyroxene (20 per cent) with up to 10 per cent biotite and abundant accessory sphene and apatite. More typical syenites are medium-to coarse-grained subporphyritic to porphyritic rocks containing all minerals noted above, except garnet. In addition, most contain hornblende and sodic plagioclase with minor accessory fluorite and iron oxides. Potash feldspar laths display weak parallel alignment adjacent to contact zones. Compositions range from leucocratic alkali feldspar syenites to mafic-rich syenites and rare syenodiorite.

Rimmed mafic xenoliths, sparsely scattered throughout many of the syenites, range in composition from biotite pyroxenite to amphibolite. Xenoliths are typically 1-5 cm in diameter, however, a few reach up to tens of centimetres. Local concentrations of xenoliths make up as much as 30 per cent of some zones. Biotite pyroxenite xenoliths are probably cumulates derived from disaggregation of wall rocks produced by earlier pulses of similar magma. A few are essentially clusters of biotite and clinopyroxene xenocrysts surrounded by a thin biotite-rich rim. As many as four concentric zones make up complex rims that surround amphibole-rich xenoliths. The rims show randomly oriented and radial intergrowths of various proportions of bladed amphibole, biotite, clinopyroxene, sphene and potash feldspar. Cores are amphibole-rich and a few preserve a foliation parallel to xenolith elongations. The cores were probably mafic gneisses or amphibolites derived from country rock.

The fluorite granite and syenitic suite, along with surrounding gneisses and metasediments, are cut by syenite and biotite lamprophyre (minette) dykes. The abundance of these fresh, undeformed dykes increases towards the southeast corner of the map area where intersecting swarms and multiple intrusive relationships are commonly observed. The lamprophyre dykes are identical in all respects to those related to Christopher Island Formation alkaline volcanism in the Baker Lake Basin to the south (LeCheminant et al., 1979). Intrusive contacts of lamprophyres with fluorite granite plutons near Aberdeen Lake suggest these plutons predate Christopher Island Formation magmatic activity. The plutons are therefore older than epizonal fluorite granites that cut Dubawnt Group strata to the south (LeCheminant et al., 1981). A 160 km^2 pluton of biotite granite west of Tebesjuak Lake (LeCheminant et al., 1981, p. 125) could be the same age as the Aberdeen Lake plutons.

Dubawnt Group

Kunwak Formation

An east-dipping succession of Kunwak Formation red arkose and orthoconglomerate is exposed along the eastern shores of Wharton Lake and on islands in the lake (Fig. 61.1). Strata consist of fine- to coarse-grained arkose interbedded with polymictic orthoconglomerate. Clasts are predominantly cataclastic granitoid gneiss with subordinate vein quartz and quartzite. Sedimentary structures include trough crossbeds, channel scours, graded beds, current ripple marks and primary current lineations. The suggested depositional environment is proximal to distal braidplain. The succession is the northern continuation of the Wharton Basin (LeCheminant et al., 1981). Strata are tilted into, and partly cover, the major northeasterly trending fault zone that separates the central and western gneiss domains. To the north the succession is truncated by a west-northwest fault.

A second arkosic redbed unit interpreted as Kunwak Formation occurs west of Marjorie Lake and south of the Dubawnt River. The poorly exposed rocks comprise gneiss

pebble orthoconglomerate and fine- to medium-grained carbonate-cemented arkose and red siltstone. This isolated sequence is faulted against cataclastic augen gneiss of the western domain.

Pitz Formation

Porphyritic lavas and intercalated quartz-rich epiclastic and pyroclastic rocks of the Pitz Formation are well exposed on the hills east and north of Marjorie Lake and along the western boundary of the map area (Fig. 61.1). Sedimentary successions east and west of Marjorie Lake that underlie porphyritic flows are distinguished in Figure 61.1 as a separate map unit of the Pitz Formation. Sequences, up to 150 m thick, are made up of a thin, basal, clay-cemented orthoconglomerate overlain by fine- to medium-grained, well-sorted quartz arenite. The strata overlie a regolith developed on deeply weathered granitoid gneiss. Basal beds contain hematized and clay-altered clasts of gneiss with subordinate vein quartz and pink quartzite. Overlying sandstones are characterized by large scale wedge-planar crossbedding (Fig. 61.5).

East of Marjorie Lake the sandstone unit is overlain concordantly by red-brown rhyolitic flows that are intercalated with red tuffaceous sandstones, siltstones and conglomerates. The abundantly porphyritic flows include both lavas and welded crystal lithic tuffs. Flows contain 10-20 per cent quartz eyes up to 5 mm across and up to 30 per cent ovoid, in places rimmed, feldspar phenocrysts up to 3 cm. Individual flows range up to 30 m thick, with both upper and lower flow contacts displaying intense kaolinization.

Pitz Formation flows west of Marjorie Lake are predominantly red, maroon and dark red-brown feldspar-phyric lavas that contain only rare small (1-2 mm) quartz eyes. Mafic phenocrysts, replaced by iron oxides, are sparsely scattered throughout the matrix or form clots within feldspar phenocrysts. Skeletal, sieve-textured feldspar phenocrysts, with or without thin continuous feldspar rims, are locally common within darker flows. These textures indicate periods of instability between phenocrysts and the enclosing magma (Hibbard, 1981; Lofgren, 1981). Unfortunately, investigation of the state of disequilibrium in the phenocrysts of these lavas is severely hampered by the effects of weathering episodes that occurred before deposition of the overlying sandstones and conglomerates of the Thelon Formation.

Flows northeast of Marjorie Lake are sparsely potash feldsparphyric to aphyric. Rubbly weathering outcrops display the irregular closely spaced joint sets that are characteristic of these maroon to red-brown lavas. To the east of the Pitz Formation lavas a low ridge of columnar jointed amygdaloidal basalt overlies weathered granitoid gneiss. The basaltic lava or sill contains up to 25 per cent euhedral calcic plagioclase phenocrysts (Fig. 61.6). Basaltic magmatism apparently occurred before deposition of the Thelon Formation. Calcite-specularite veins in the basalt are similar to those associated elsewhere with sub-Thelon Formation weathering.

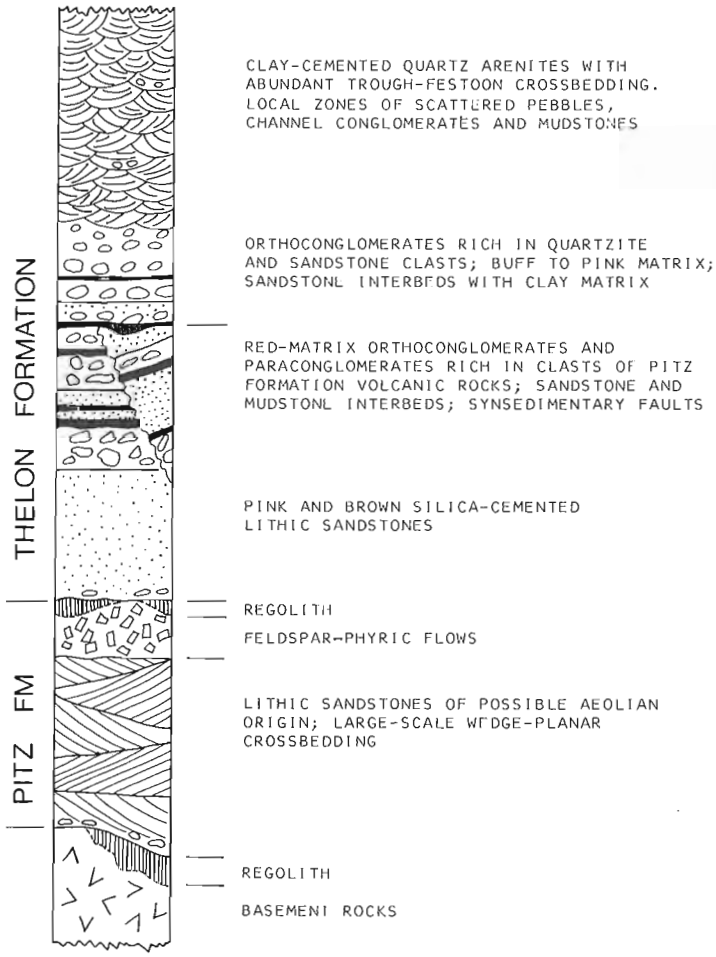

Figure 61.5. *Generalized stratigraphic section of the Pitz and Thelon formations based on observations in the Marjorie Hills.*

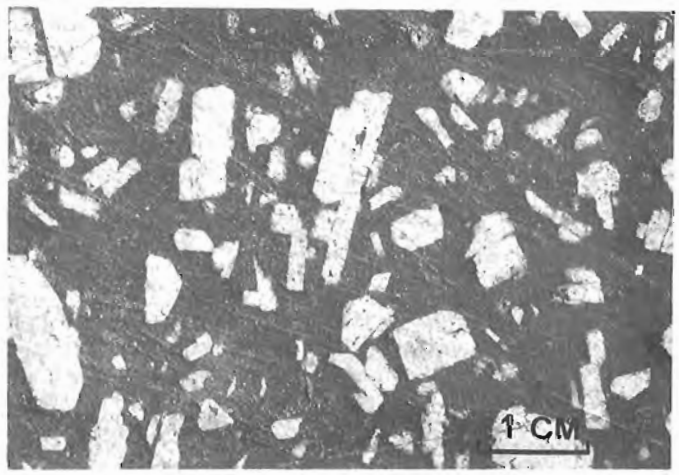

Figure 61.6. *Euhedral plagioclase phenocrysts in amygdaloidal basalt northeast of Marjorie Lake. GSC 203601-N*

SEDIMENTOLOGY AND STRATIGRAPHY OF THE THELON FORMATION AND THE SUB-THELON REGOLITH

J. Chiarenzelli, J.A. Donaldson, and M.A. Best

Distinctive red-matrix conglomerates, noted during previous regional mapping (Donaldson, 1966b), together with associated sandstones, siltstones and mudstones, can be distinguished as a separate map unit at the base of the Thelon Formation in the Aberdeen Lake map area (Fig. 61.1 and and 61.5). Most of these sedimentary rocks contain abundant clasts of Pitz Formation volcanic rocks (predominantly feldsparphyric). The content of clasts such as vein quartz, gneiss, granite, quartzite and iron formation rarely exceeds 30 per cent of the conglomerate framework. These sediments are inferred to have been deposited in a continental setting during a period of active tectonism. Framework-supported conglomerates of this map unit (Fig. 61.7) show characteristics of deposition in fluvial channels (cut-and-fill structures, well sorted lenses, and imbrication of tabular clasts). Associated lithic sandstones (with both planar lamination and trough crossbedding in sets up to 1 m) and mudstones (with abundant desiccation cracks and derived mudflake conglomerates) probably represent braidplain/overbank and playa deposits, respectively. Unsorted matrix-supported conglomerates that contain angular blocks of mudstone up to 2 m long are interpreted as debris-flow deposits (Fig. 61.8). Frameworks of these paraconglomerates generally are characterized by isotropic fabrics; their matrix typically consists of poorly sorted red to mauve sandstone and mudstone.

The succeeding Thelon map unit (Fig. 61.1 and 61.5) in most places overlies the lowermost unit abruptly but in apparent conformity. In places, however, the transition appears to be gradational, whereas in one well exposed area, the contact is clearly unconformable, with at least 600 m of section truncated along a near horizontal erosional unconformity beneath which the lowermost sequence is inclined as much as 45°. These relationships indicate synsedimentary faulting, and thus the lowermost unit is here retained as a subdivision of the Thelon Formation. Lithological similarity of this unit to interflow sedimentary rocks of the Pitz Formation poses difficulties for mapping isolated outcrops. Stratigraphic reassignment therefore may be appropriate, but a decision on such revision is postponed until completion of detailed mapping in areas west of Aberdeen Lake.

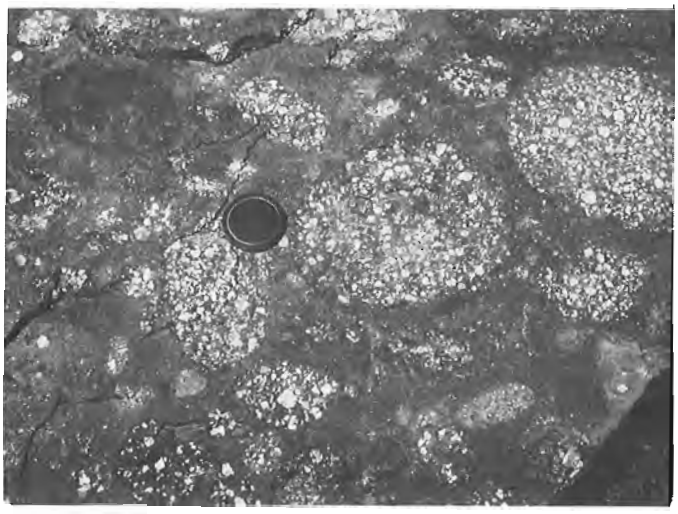

Figure 61.7. *Basal unit of the Thelon Formation: intact framework red-matrix conglomerate containing abundant porphyritic volcanic clasts derived from the Pitz Formation. GSC 203601-O*

Unlike the lower unit, the overlying sediments appear to lack debris flows. The conglomerates are characterized by intact frameworks, sandy interbeds, good sorting, and imbrication. Clasts of Pitz Formation volcanic rocks are abundant only in the lowermost few metres above the contact. More characteristic are well rounded clasts of white quartzite, vein quartz, silcrete, red and brown lithic sandstone and a few clasts similar to the underlying conglomerate. Clasts rarely exceed 25 cm in diameter (Fig. 61.9).

Whereas the lowermost unit is generally silica-cemented and therefore well indurated, much of the overlying unit contains interstitial clay, and tends to be less indurated. Buff, pale pink, grey and cream prevail, in contrast to the deep red, mauve and brown characteristic of the underlying unit. Sandstone beds increase in abundance up-section, where the conglomerates give way to pebbly sandstones with only rare conglomerate-filled channels. The sandstones almost everywhere are characterized by trough crossbedding in sets up to several metres thick. Individual troughs commonly are up to 5 m wide, and some can be

Figure 61.8. *Basal unit of the Thelon Formation: debris flow showing matrix-supported angular to subangular clasts. Clipboard is 33 cm long. GSC 203601-T.*

Figure 61.9. *Upper unit of the Thelon Formation: framework-supported conglomerate containing abundant well rounded clasts of vein quartz, quartzite and red sandstone (dark grey in photograph). GSC 203601-P*

traced up to 100 m along trough axes. Fining-up cycles can be observed in well exposed successions of trough sets, and also within some individual crossbeds. In comparison to paleocurrent data for the lower unit, which reflect predominant northward transport (Fig. 61.10c), paleocurrents for the upper unit of the Thelon Formation show wide dispersion about a westward-directed trend (Fig. 61.10b).

Field evidence from the central and northern parts of Aberdeen Lake (66B) and Schultz Lake (66A) map areas suggests that at least two periods of extensive weathering occurred before deposition of the Thelon Formation. Mapping, supplemented by a study of drill core, has shown that Aphebian and possibly some Archean basement rocks were affected by an early episode of weathering, creating a regolith with a thickness that locally exceeds 50 m. In some areas, fresh basement paleohighs have a relief above regolith-filled paleovalleys of greater than 200 m.

The second major episode of weathering affected the uppermost lavas and pyroclastic rocks of the Pitz Formation, producing a regolith up to 25 m thick. Minor episodes of weathering also appear to have occurred during pauses in volcanism, creating thin altered zones within the Pitz Formation.

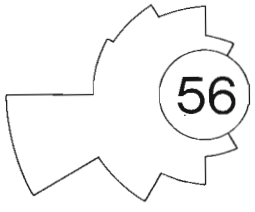

a. Data for probable aeolian sandstones, northwest corner of Schultz Lake map area (66A).

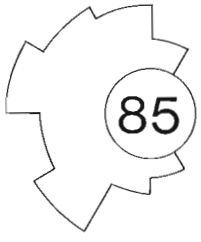

b. Data for upper unit of Thelon Formation, based on measurements between Marjorie Lake and the east end of Aberdeen Lake.

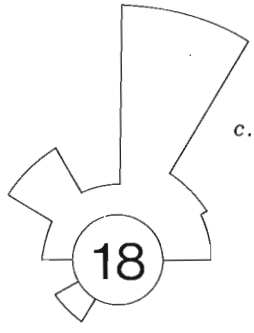

c. Data for lower unit of Thelon Formation, based on measurements north of Marjorie Lake.

Figure 61.10. *Rose diagrams of paleocurrent measurements: 30° intervals; number of readings indicated in centre.*

The two principal regoliths record similar processes of chemical weathering, hematization, kaolinization and silicification. Paleosols are poorly preserved, being best exposed in outcrops where silcrete caps the regolith (Fig. 61.11).

An area underlain by sandstones of probable aeolian origin (first observed by J.A. Donaldson during earlier regional mapping in 1965) was briefly visited. This area, in the northwestern part of Schultz Lake (66A) map area, displays overlapping sets of arcuate crossbeds up to 5 m thick, with inclinations commonly in the range of 35°-40°. Foreset inclinations record inferred paleowinds with a

Figure 61.11. *Silcrete developed on regolith derived from biotite paragneiss. Quartz stringers accentuate original foliation and cross cutting fractures; dark areas consist mainly of quartz, clay and hematite intergrowths that mimic primary textures. Field of view in foreground is 3 m wide. GSC 203601-X*

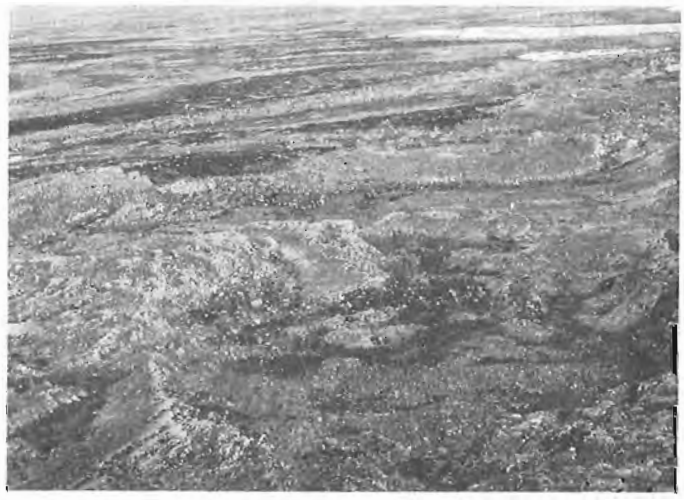

Figure 61.12. *Aerial view, looking northward, of probable barchan dunes in the Thelon Formation, northwest corner of Schultz Lake map area (66A). The two prominent megasets of arcuate crossbedding are more than 100 m wide. GSC 119610*

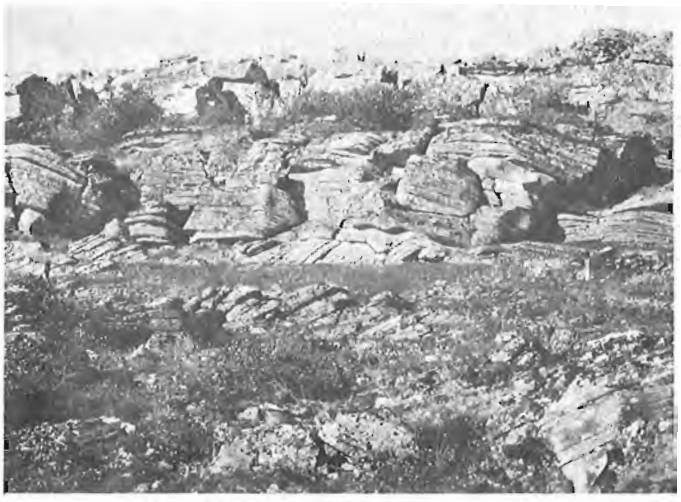

Figure 61.13. *Wedge-planar crossbedding in possible aeolian sandstones, basal unit of the Pitz Formation east of Marjorie Lake. Northwest-inclined crossbeds in foreground are truncated by a set of northeast-inclined crossbeds near the base of scarp. A porphyritic rhyolite flow (not visible in this view) caps the sandstone scarp which is about 6 m high. GSC 203943-A*

distinct mode to the west-southwest (Fig. 61.10a). Some individual arcuate crosslaminations can be traced for more than 100 m (Fig. 61.12). The sandstones, all fine to very fine grained, are extremely well indurated. This occurrence is tentatively interpreted as an exhumed near-horizontal section through a field of barchan dunes.

A second occurrence of possible aeolian sandstones is exposed beneath a rhyolite flow of the Pitz Formation near the north end of Marjorie Lake (Fig. 61.1). These sandstones are fine grained, moderately well-sorted lithic arenites which form overlapping sets of crossbeds at least 9 m thick (Fig. 61.13). Because these sandstones are exposed only in vertical section, their full geometry cannot be established. However, like the occurrence previously described, foreset inclinations up to 40° have been recorded.

Recent detailed mapping of the Hornby Bay Group (Kerans et al., 1981) has demonstrated upward trends of increasing compositional maturity and generally decreasing tectonic activity during deposition of these predominantly fluvial siliciclastic sediments. In addition, aeolian origin has been documented for some of the Hornby Bay sandstones (Ross and Donaldson, 1982). Data presented here for the Thelon Formation demonstrate similar depositional environments and tectonic history.

BASEMENT-THELON FORMATION RELATIONSHIPS NORTH OF ABERDEEN LAKE (66B/16)

Subhas Tella and D.L. Thompson (Project 820007)

Introduction

Part of the northeast corner of the Aberdeen Lake map area is underlain by an Archean and/or Aphebian polydeformed and regionally metamorphosed granitoid gneiss complex that is basement to continental clastic rocks of the Thelon Formation. This preliminary report summarizes results of field mapping (1:50 000 scale) undertaken during the latter part of June, 1982. Emphasis was placed primarily on study of faults and shear zones in the map area to outline their distribution and to understand their tectonic history. These investigations are the initial phase of a regional study of shear zones in the Churchill Province. Figure 61.14 is a geological sketch map showing the distribution of faults and minor shear zones.

Archean and/or Aphebian Basement Complex

The basement complex (units 1-3; Fig. 61.14), widely exposed in the southern and eastern parts of the map area, is similar to central and southeastern domain gneisses south of Aberdeen Lake. Unit 1 is a mixed unit consisting of well foliated, medium- to coarse-grained, layered, banded or nebulitic, hornblende-biotite orthogneiss (Fig. 61.15) of granodiorite composition, and porphyroblastic (potash feldspar) augen gneiss. The augen gneiss, containing subhedral pink feldspar crystals, is of quartz monzonite composition. Locally preserved porphyritic texture indicates an igneous protolith for the augen gneiss.

Migmatite banding is locally present. Quartz-feldspar-biotite paragneiss lenses and amphibolite inclusions occur sporadically within the layered gneiss.

The layered and augenitic quartzofeldspathic gneiss sequence has been injected and disrupted by light pink to white weathering, medium- to coarse-grained biotite granite/granodiorite intrusions. In the south-central part of the area (Fig. 61.14), folded and irregular gneiss fragments appear to be "floating" in a granitoid matrix (unit 2, Fig. 61.14, 61.16) in which the proportion of injected material may reach as high as 70-80 per cent by volume, but is typically in the order of 20-40 per cent. The degree of injection decreases to the west and to the east. In several well exposed outcrops (unit 2) complex agmatitic to arteritic structures are present (Fig. 61.17). Abundant pegmatite sheets, dykes, and veins, presumably related to the medium grained, equigranular, massive to weakly foliated granite/granodiorite (unit 3), intrude units 1 and 2 at several localities.

Field relations and structural data indicate that the basement complex has undergone at least two periods of deformation and an event of regional metamorphism. North to northeast-trending regional foliation, the most penetrative planar fabric element, represents a syntectonic metamorphic fabric. Two sets of mesoscopic fold structures have been identified. One set, characterized by upright, open to tight fold geometry, trends north-northwest and commonly plunges either to north-northwest or to the south-southeast at shallow to moderate angles (20°-45°). The second set of mesoscopic upright, open folds plunges to the west and west-southwest at moderate angles (40°-50°). The regional metamorphic grade in the basement complex appears to be within the upper amphibolite facies, and the mineral assemblages have been partially retrograded to chlorite-epidote-bearing assemblages. The deformation and metamorphism in units 1 and 2 predate the emplacement and

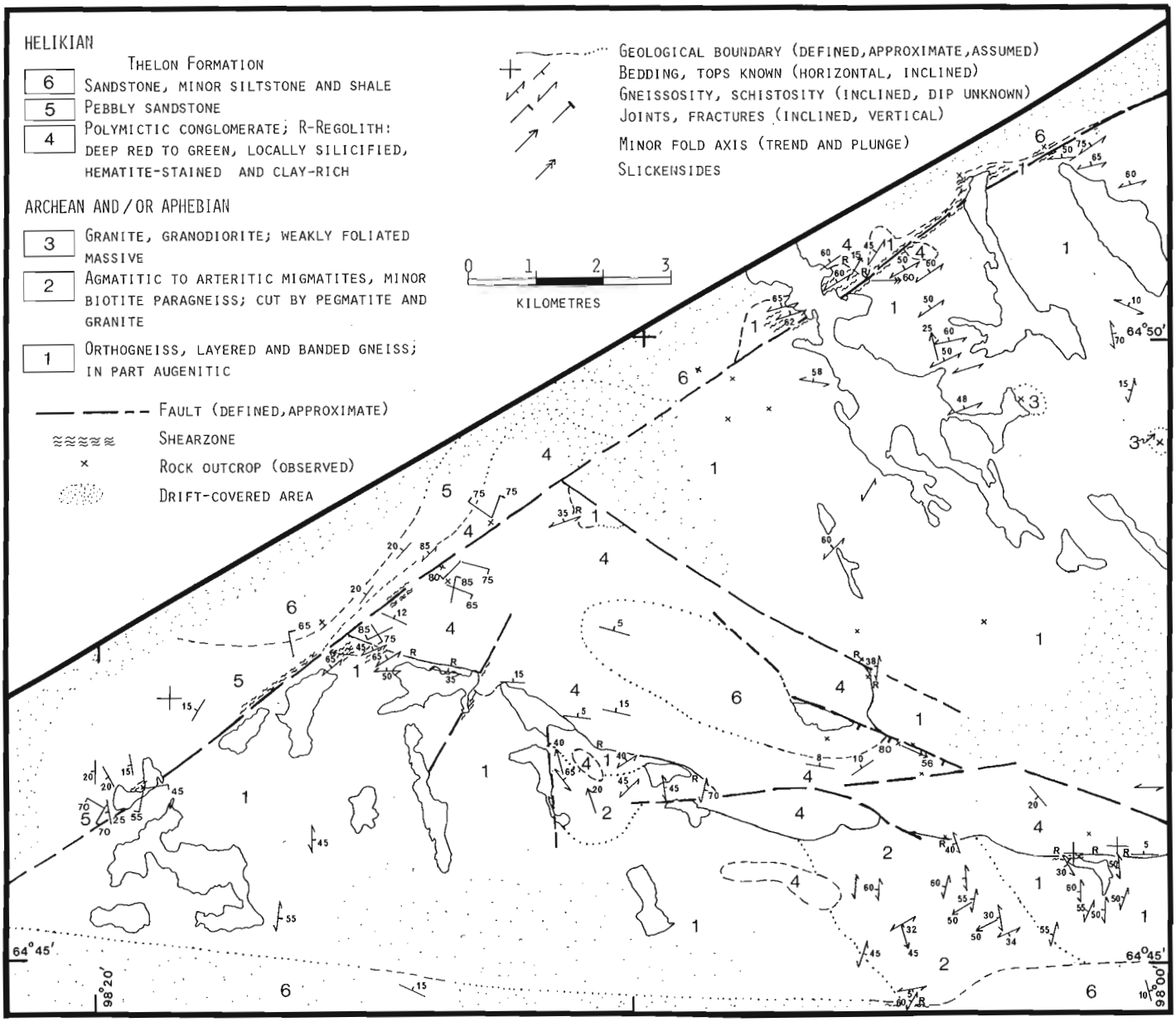

Figure 61.14. *Geological sketch map of part of the northeast corner of the Aberdeen Lake map area showing the distribution of faults and minor shear zones.*

injection of equigranular granite/granodiorite (unit 3). The presence of a weak foliation in unit 3, suggests a later syn- to post-emplacement deformational event. At one locality, specks of molybdenite (1-3 mm in size) occur in thin (0.5-1.0 cm) quartz-filled fractures in a fine grained quartzofeldspathic gneiss (unit 1).

Thelon Formation

The Thelon Formation (units 4-6), consisting of flat lying to gently dipping (10-15°), light grey to buff-pink, grey weathering, cobble to boulder orthoconglomerate, pebbly sandstone, sandstone and mudstone, unconformably overlies or is in fault contact with the basement complex in 66B/16. The lithological character of the Thelon Formation elsewhere has been described by Donaldson (1965, 1969) and Chiarenzelli et al. (this report). Immature, cobble to boulder conglomerate (unit 4) with red silty matrix occurs at the base. Clasts include subangular to rounded white, grey, and buff quartzites, mud chips, vein quartz, hematitic iron formation, and rare, maroon quartz-feldspar porphyry clasts. A well developed regolith (R, Fig. 61.14) is locally preserved at the base of the conglomerate (see Fig. 61.18). Red hematitic weathering profiles, clay-rich and chlorite-rich zones are common. Regolith zones are crosscut by fine quartz stringers and veins, and at some localities they contain small, angular, breccia fragments. The latter are interpreted as faulted regolith zones. Pebbly sandstone and sandstone (units 5 and 6) are buff, grey, white, or pink. Well rounded ellipsoidal to spherical clasts are predominantly vein quartz, white quartzite, and rare mud chips. The fine- to medium-grained sandstone is friable to well indurated with clay and silica cement. Primary structures include large scale trough and planar crossbedding, channel features, and asymmetric and symmetric ripple marks. Intercalated mudstone layers within the sandstone are characterized by desiccation features.

Figure 61.15. *Hornblende-biotite orthogneiss (unit 2, Fig. 61.14) showing mafic and felsic layers and segregations. GSC 203944-H*

Figure 61.17. *Agmatitic to arteritic structures in the basement complex. GSC 203944-P*

Figure 61.16. *Folded mafic and gneiss fragments in a pink granitoid matrix (unit 2, Fig. 61.14). GSC 203944-G*

Figure 61.18. *Regolith at the base of Thelon Formation conglomerate. Field of view is 1 m high. GSC 203944-F*

Unconformity related uranium mineralization was noted at several localities in phosphate impregnated zones at the base of the Thelon Formation, and less frequently at higher stratigraphic levels. U-P association in the Thelon Formation currently is being studied by Miller (1983).

Faults and Shear Zones

The basement complex and cover rocks are transected by four major sets of faults and associated shear zones (Fig. 61.14). The major northeast-trending fault in the northern part of the area is a zone of ductile and brittle deformation that is characterized by mylonitic to cataclastic rocks. Preliminary analysis of structures indicates that the ductile deformation along the fault predates deposition of the Thelon Formation. Subsequent movements displaced the Thelon Formation and are characterized by brittle deformation structures. East-, northwest-, and north-trending faults and minor shear zones that displace the basement and the Thelon Formation are also well represented in the region. Basement granitoid rocks proximal to the faults show a variety of protomylonitic to mylonitic textures. The latest movements on some of these structures appear to be normal oblique-slip, as is evidenced by rare, well developed slickensides, and pebble elongation direction on fracture surfaces. Structural and petrographic data currently are being analyzed to determine the detailed tectonic history of the fault zones.

References

Bolton, T.E. and Nowlan, G.S.
1979: A Late Ordovician fossil assemblage from an outlier north of Aberdeen Lake, District of Keewatin; in Contributions to Canadian Paleontology, Geological Survey of Canada, Bulletin 321, p. 1-26.

Donaldson, J.A.
1965: The Dubawnt Group, Districts of Keewatin and Mackenzie; Geological Survey of Canada, Paper 64-20.

1966a: Geology, Schultz Lake, District of Keewatin; Geological Survey of Canada, Map 7-1966.

1966b: Study of the Dubawnt Group; in Report of Activities, Geological Survey of Canada, Paper 66-1, p. 22.

1969: Descriptive notes (with particular reference to the Late Proterozoic Dubawnt Group) to accompany a geological map of central Thelon Plain, Districts of Keewatin and Mackenzie (65M, NW1/2, 66B,C,D, 75P,E1/2, 76A,E1/2). Report and P.S. Map 16-1968; Geological Survey of Canada, Paper 68-49.

Hibbard, M.J.
1981: The magma mixing origin of mantled feldspars; Contributions to Mineralogy and Petrology, v. 76, p. 158-170.

Kerans, C., Ross, G.M., Donaldson, J.A., and Geldsetzer, H.J.
1981: Tectonism and depositional history of the Helikian Hornby Bay and Dismal Lakes groups, District of Mackenzie; in Proterozoic Basins of Canada, ed. F.H.A. Campbell; Geological Survey of Canada, Paper 81-10, p. 157-182.

LeCheminant, A.N., Leatherbarrow, R.W., and Miller, A.R.
1979: Thirty Mile Lake (65P, W1/2) map-area, District of Mackenzie; in Current Research, Part B, Geological Survey of Canada, Paper 79-1B, p. 319-327.

LeCheminant, A.N., Iannelli, T.R., Zaitlin, B., and Miller, A.R.
1981: Geology of Tebesjuak Lake map area, District of Keewatin: A progress report; in Current Research, Part B, Geological Survey of Canada, Paper 81-1B, p. 113-128.

Lofgren, G.E.
1981: Experimental duplication of plagioclase sieve and overgrowth textures; Geological Society of America, Abstracts with Programs 1981, v. 13(7), p. 498.

Miller, A.R.
1983: A progress report: uranium-phosphorus association in the Helikian Thelon Formation and Sub-Thelon saprolite, central District of Keewatin; in Current Research, Part A, Geological Survey of Canada, Paper 83-1A, report 62.

Ross, G.M. and Donaldson, J.A.
1982: The Bigbear Erg: a Proterozoic aeolian sand sea in the Hornby Bay Group, Northwest Territories, Canada; Eleventh International Congress on Sedimentology, Abstracts, p. 68.

Schau, M., Tremblay, F., and Christopher, A.
1982: Geology of Baker Lake map area, District of Keewatin: a progress report; in Current Research, Part A, Geological Survey of Canada, Paper 82-1A, p. 143-150.

Tella, S., Eade, K.E., Miller, A.R., and Lamontagne, C.G.
1981: Geology of the west half of the Kamilukuak Lake map area, District of Keewatin; a part of the Churchill Structural Province; in Current Research, Part A, Geological Survey of Canada, Paper 81-1A, p. 231-240.

Tella, S., Ashton, K.E., Thompson, D.L., and Miller, A.R.
1983: Geology of the Deep Rose Lake map area, District of Keewatin, N.W.T.; in Current Research, Part A, Geological Survey of Canada, Paper 83-1A, report 56.

Wright, G.M.
1967: Geology of the southeastern barren grounds, parts of the Districts of Mackenzie and Keewatin; Geological Survey of Canada, Memoir 350.

62.

A PROGRESS REPORT: URANIUM-PHOSPHOROUS ASSOCIATION IN THE HELIKIAN THELON FORMATION AND SUB-THELON SAPROLITE, CENTRAL DISTRICT OF KEEWATIN

Project 810024

A.R. Miller
Economic Geology Division

Miller, A.R., A progress report: uranium-phosphorous association in the Helikian Thelon Formation and sub-Thelon saprolite, central District of Keewatin; in Current Research, Part A, Geological Survey of Canada, Paper 83-1A, p. 449-456, 1983.

Abstract

Phosphate-cemented uranium-bearing lithologies in the Helikian Thelon Formation occur predominantly in the basal fluvial clastics but also as vein systems in the sub-Thelon saprolitic basement complex. Fluorapatite, with or without goyazite, illite and hematite are the principal mineralizing phases. Variable but anomalous concentrations of B, Ba, Li, Rb and Sr in phosphate-cemented sediments are similar to elements enriched during evaporation of modern saline lakes. Phosphate in the Thelon Formation may have been generated in continental, ephemeral, saline lakes but migrated into strata lateral to or vertically below the site of origin. One isotopic age date suggests a minimum age for phosphate cementation at ~1660 Ma.

Introduction

This paper is intended as a progress report to document the setting, mineralogy, petrography, geochemistry and possible sedimentary environment that generated phosphate-bearing units associated with the Thelon Basin, central District of Keewatin, Northwest Territories. This project was initiated with the purpose of examining the trace element contents of phosphatic units to see if phosphatic horizons may be pathfinders for unconformity-type uranium mineralization.

Phosphate-bearing sedimentary rocks are present throughout the rock record in strata as old as 2200 Ma. However the principal phosphogenic provinces occur within Phanerozoic sedimentary rocks of marine origin. Christie (1979, 1980) on the basis of the paleolatitude positions of numerous marine to continental Proterozoic basins has suggested that the distribution of phosphate-bearing strata may be more widespread than presently recognized.

Acknowledgments

The writer is thankful to Urangesellschaft Canada Ltd., BP Canada, Gulf Minerals Canada Ltd., Westmin Resources Ltd., S.E.R.U. Nucléaire (Canada) Ltd., Taiga Consultants Ltd., Marline Oil Ltd. and Andaconda for supplying some of the rock specimens for this study. Discussions with H.E. Dunsmore (G.S.C.) were of great benefit.

Thelon Basin – General Geology

Helicopter reconnaissance operations in the mid-1950s (Wright, 1955, 1957, 1967) outlined the distribution of Dubawnt Group rocks in the central barren grounds, north and northwest of a line from the eastern end of Baker Lake to Yathkyed and Kamilukuak lakes. Donaldson (1965, 1966, 1969) outlined the sedimentology and stratigraphy of the Dubawnt Group and termed the upper conglomerate-sandstone sequence the Thelon Formation. The region covered by this formation, lying principally northwest of a line through Schultz, Aberbeen, Dubawnt and Sid lakes, was termed the Thelon Basin (Douglas, 1973). Cecile (1973) extended the subdivision of the Thelon Formation into four facies based on petrographic-mineralogical criteria derived from regionally distributed rock specimens.

Thelon sediments lie unconformably upon a diverse basement complex that includes Archean tonalitic to granitic gneisses, Aphebian meta-psammites to meta-pelites of the Amer Group and interpreted equivalents, and late Aphebian-early Paleohelikian continental sediments and volcanics of the lower Dubawnt Group. Basement lithologies beneath and adjacent to the erosional edges of the Thelon Formation display intense hematitization with accompanying clay crystallization. These units, composed essentially of quartz-hematite-kandite group clays, are termed saprolite. Preserved saprolitic thicknesses vary with lithology from tens of centimetres on Aphebian orthoquartzite to approximately 60 m where developed on Archean gneisses and Aphebian psammitic to pelitic metasediments.

Sedimentological studies of the Thelon Basin by Donaldson (1969) and Cecile (1973) have shown that the basin is divisible into four facies which in general reflect the present erosional form of the basin. Conglomerate, though present at higher stratigraphic positions, dominates the lithologies near the base of the Thelon Formation. Coarse clastic rocks grade upward into lithic pebbly arkose to medium grained subarkose. Sedimentary features such as varying clast size, the proportion of matrix, planar and trough stratification and fining upward sequences suggest the basal units were deposited under continental alluvial fan – braided fluvial conditions. Clast lithologies vary depending upon the local provenance and can be locally characterized by banded iron formation, orthoquartzite or Pitz rhyolite. However, white meta-orthoquartzite cobbles to pebbles abruptly dominate the lithic component of the sediments above the basal coarse clastics.

Quartz arenite to feldspathic arenite comprise more than 90 per cent of the sandstones of the basin and characterize the lithologies of the upper three facies. Variations in grain size, diagenetic cements, quartz, clay, chlorite and muscovite and sedimentary structures have been interpreted as braided fluvial to nearshore marine depositional environments (Donaldson, 1969; Cecile, 1973).

Donaldson (1969) recognized that near the top of the formation multicoloured siltstones and mudstones are intercalated with sandstones. These fine clastic sediments are overlain by oolitic and stromatolitic dolostone and siliceous dolostone. These upper units of the Thelon Formation indicate nearshore marine conditions. Subaerial basalt is associated with the upper sandstone-dolostone but the stratigraphic relationships of the basalt to these units is uncertain.

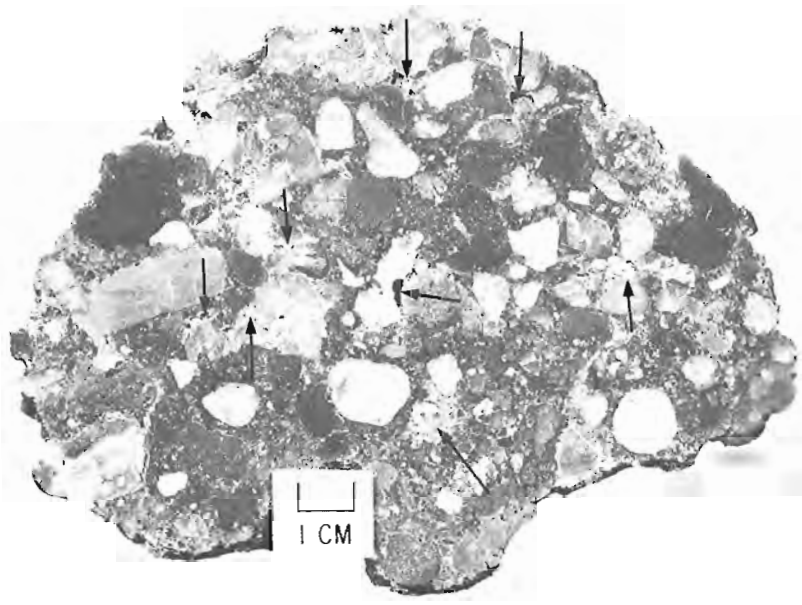

Figure 62.1. Polished slab of pebbly conglomerate near the base of the Thelon Formation. Black arrows mark cavities in the matrix partially lined or completely filled by fluorapatite + illite + hematite (specularite). GSC 203345-S

Figure 62.3. Trench through white to buff pebbly arkose-coarse lithic arkose. Dark areas outlined by black lines contain phosphate + clay + iron oxide cements (P). Phosphate cement discordant to bedding marked by arrows. GSC 203592-S

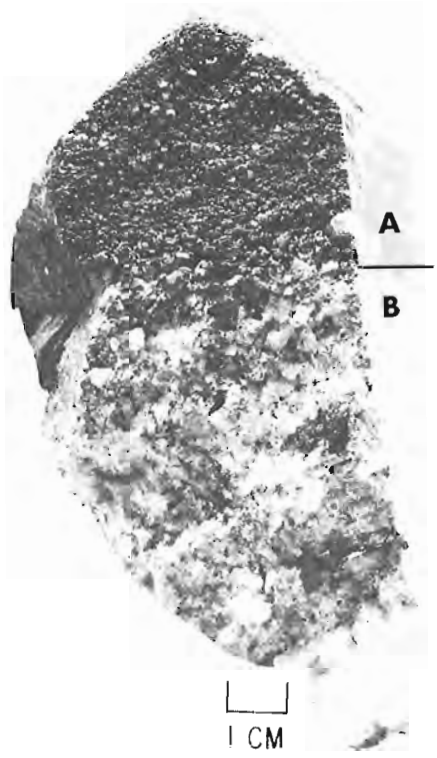

Figure 62.2. Weathered surface of partially phosphate cemented lithic arkose near the base of the Thelon Formation. Note the microrelief of the dark phosphate cemented portion (A) compared to the light coloured quartz cemented portion (B). GSC 203345-T

Field Recognition of Phosphate-Bearing Units

There are several visual features that distinguish the presence of phosphate minerals in addition to anomalous radioactivity. Thelon Formation sediments have undergone numerous periods of diagenetic alteration involving silicification, authigenic phyllosilicate crystallization and iron removal from rocks that were most probably redbeds. Typical hues range from white to buff. In contrast phosphate-bearing strata are typically a light flesh pink to deep red colour resulting from the addition of hematite which accompanies phosphate cements. Hematite is present as an ultra fine-grained cement throughout the matrix as well as mantling framework clasts, or as finely bladed specularite occupying or lining voids between framework clasts. Ultra fine-grained aggregates of chalk white or hematite-stained clay commonly indicate the presence of phosphate-bearing minerals. Voids developed between framework clasts by diagenetic alteration can be partially occupied by clay (Figure 62.1) or by intergrowths of inwardly terminated crystals of specularite, colourless to pale yellow fluorapatite, and clay.

Weathered surfaces of phosphate- and silica-cemented lithologies are distinctive. Phosphate bearing lithologies display considerable microrelief, due to weathering of the soluble and soft cements in contrast to the rather smooth weathering surfaces of quartz cemented units (Figure 62.2).

Pervasive hematitization throughout the saprolitic profile does not permit recognition of phosphate-bearing saprolite based on colour criteria. However disseminated or vein filling specularite, vein filling white clay, bleaching and radioactivity indicate phosphate-bearing saprolite.

Distribution of Phosphatic Thelon Sediments

Phosphate-bearing sediments were recognized during regional and detailed mapping in NTS map areas 66A,B and G and from regionally distributed samples throughout the Thelon Basin. Phosphate cements are not restricted to any particular lithology but have been recognized in pebbly conglomerate, pebbly arkose, coarse to fine-grained lithic arkose, subarkose and quartz arenite. Basal fluvial clastics ranging from pebbly conglomerate to arkose are the most common phosphate-cemented lithologies in the Thelon Formation. When present in the basal sediments, structurally controlled phosphate can be expected at various levels in the saprolitic profile. Phosphate cemented sediments can display small geoid like cavities occupied by phosphate crystals and associated cements. These cavities are interpreted to result from a secondary porosity possibly related to diagenesis in the Thelon sediments.

Phosphate-bearing strata appear stratabound even though discontinuous and podiform in distribution. On the outcrop scale hematite-phosphate cemented zones are often discordant to bedding, a feature most evident when hematitic phosphate cements white to buff coloured coarse grained basal clastics (Figure 62.3).

Phosphate Mineralogy and Associated Phases

X-ray identification of phases cementing clastic sediments were determined by single crystal powder patterns or from diffraction traces of whole rock powders. The latter traces were obtained from powder smears on glass slides. Fluorapatite [$Ca_5(PO_4)_3$ F] is the most ubiquitous phosphate phase present in the Thelon sediments and saprolite. Goyazite [$SrAl_3(PO_4)_2(OH)_5 \cdot H_2O$] is present in clay-rich units. Both phosphates are intimately intergrown with ultra fine grained sooty hematite, specularite and ultra fine grained illite. Rare violet to Prussian blue acicular grains of baricite [$Mg,Fe^{+2})_3(PO_4)_2 \cdot 8H_2O$] may occur as a cement in fine clastic sediments or as fracture coatings in Thelon sediments and the saprolite.

Petrography of Phosphate-Bearing Units

Before describing the petrographic features characterizing phosphate-bearing units within the Thelon Basin rocks, diagenetic alteration of non-phosphatic Thelon strata is described because these features may control the distribution of phosphate cements. Marked variations in compositional and textural maturity of Thelon sediments depend upon provenance, stratigraphic position and subsequent diagenesis. Lithic arenite and arkose situated near the basal paleosurface display angular to subrounded framework clasts compared to the textural maturity of unimodal equant framework grains within quartz arenites higher in the basin. Variations in the proportion of matrix exist in each of these lithologies; however, all non-phosphatic lithologies display similar cements which vary in amount depending on lithology.

Silica of different textural forms is the commonest cement throughout the Thelon Formation. Textural variations of quartz include: i) optically continuous rims mantling framework grains; ii) fine crystallites filling former interframework voids or iii) ultra fine-grained crystalline mosaics. Varying proportions of quartz cement are accompanied by a variety of diagenetic phyllosilicates. These phyllosilicates comprise kandite group clays; kaolinite nacrite, dickite, muscovite and minor alumina-rich dioctahedral chlorite (Cecile, 1973; Miller, unpublished data).

Trace quantities of relict hematite cement present as very thin rims situated at the interface between framework clasts and later diagenetic quartz overgrowths are recognized in white to buff Thelon clastics. The position of this early iron oxide cement suggests that portions of the Thelon Formation were once redbeds.

In addition to these diagenetic cements, textures indicative of replacement of framework clasts have been recognized in arkosic to arenaceous lithologies. Feldspar clasts or components of lithic clasts were replaced by kandite-group clays with subordinate quartz. In some units feldspar destruction during diagenesis accounts for an apparent chemical maturity of the sediment. The variety and timing of diagenetic cements and replacement of framework components are strikingly similar to post-depositional alteration documented in the Athabasca Group (Ramaekers, 1981; oral communication, 1981).

In contrast, phosphate-bearing strata display distinctive morphological modifications to framework grains along with variations in the types and proportions of cements. The most characteristic feature unifying phosphate-cemented lithologies is the lack of silica cements so common throughout the Thelon Formation. Framework clasts in phosphate-bearing units may display traces of quartz overgrowths at pressure solution contact points but overall authigenic quartz overgrowths are absent (Fig. 62.4a, b). Also framework quartz clasts exhibit finely scalloped surfaces that indicate quartz was unstable during phosphate precipitation (Figure 62.5).

Fluorapatite, the most common phosphate cement, occurs as an unoriented mosaic of fine acicular crystallites (up to 0.15 mm in length) or as euhedral to subhedral hexagonal crystals. Goyazite, when present with or without fluorapatite in lithologies highly altered to clay occurs as blocky euhedra having an average grain size of 0.01 mm.

Textural variations in phosphate cements, along with those of the accompanying clay, hematite and minor quartz suggest multiple generations of these cements. Fluorapatite can occur as delicately zoned crystals with hematite-rich and hematite-poor growth bands commonly terminated by clear colourless rims (Figure 62.6). Veinlets of colourless fluorapatite crosscutting hematite-rich fluorapatite cements and geoid-like cavities infilled by fluorapatite crystals indicate remobilization and/or multiple generations of phosphate crystallization. Hematite, present as ultra fine disseminations in and cementing phosphate crystals, commonly occurs as bladed specularite or fine grained aggregates in later generations of fluorapatite crystals. Similarly illite and traces of a celadonite-like phyllosilicate, present as ultra fine platelets distributed throughout hematite-rich phosphate crystals, occur in later generations as very fine grained clay mats occupying intercrystal volumes and filling the central portions of geoid-like cavities.

Structurally controlled phosphate zones in the saprolitic basement complex range from irregular, finely branching, microveinlet networks to fracture-breccia zones tens of metres in width. Fracture zones adjacent to the basal Thelon Formation may contain angular, altered fragments of the adjacent country rock or polylithic, angular to rounded fragments of the basement lithologies and Thelon sediments. Oolitic to pisolitic and banded textures, consisting of radiating crystallites of hematitic fluorapatite, are recognized in some fracture zones. Some fracture zones filled by massive aggregates of specularite-clay-phosphate display spectacular rosettes of hematitic fluorapatite, fluorapatite rosettes attaining dimensions that can be measured in centimetres (Figure 62.7). No oolitic to pisolitic textures have been recognized within Thelon sediments.

Originally feldspar, a major component of basal Thelon sediments, is diagenetically replaced by a kandite group clay + quartz ± muscovite assemblage in non-phosphatic lithologies. However in phosphatic units, feldspar pseudomorphs are replaced by an euhedral fluorapatite + illite assemblage (Figure 62.8). These replacement assemblages suggest a post-diagenetic timing for the phosphorization.

Geochemistry

Table 62.1 lists whole rock chemical analyses of samples from a variety of radioactive phosphate-bearing lithologies in the Thelon Basin and sub-Thelon saprolite. Analyses were made by various methods at the Geological Survey of Canada Analytical Chemistry Section unless otherwise stated.

Highly variable quantities of phosphate cements are present within Thelon sediments as indicated by P_2O_5 contents ranging from 4.76 to 34.1 wt per cent. Accordingly, the abundances of Al_2O_3 and K_2O reflect variable illite group clay contents associated with the phosphates. Iron

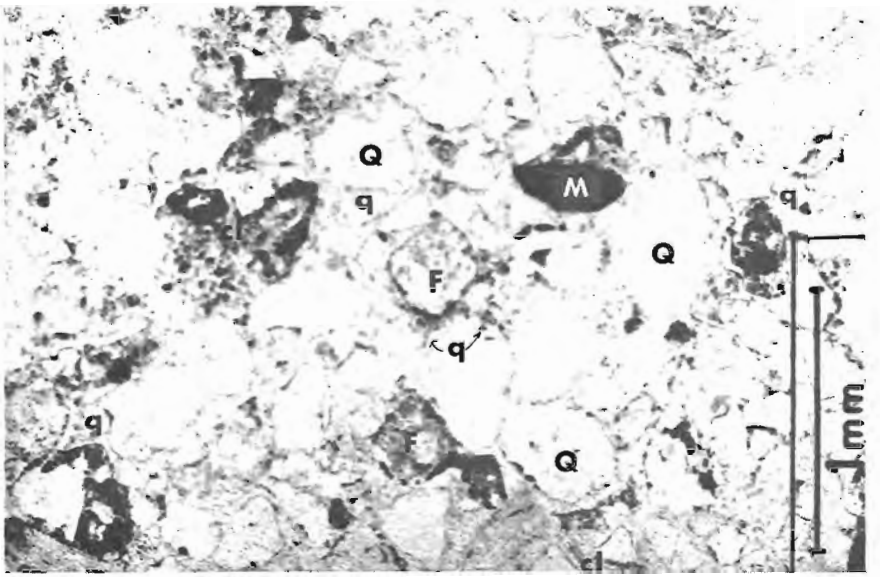

a. *lithic subarkose with framework quartz grains (Q), altered feldspar grains (F), and altered magnetite (M) cemented by authigenic quartz (q), clay (cl), and hematite (h)*

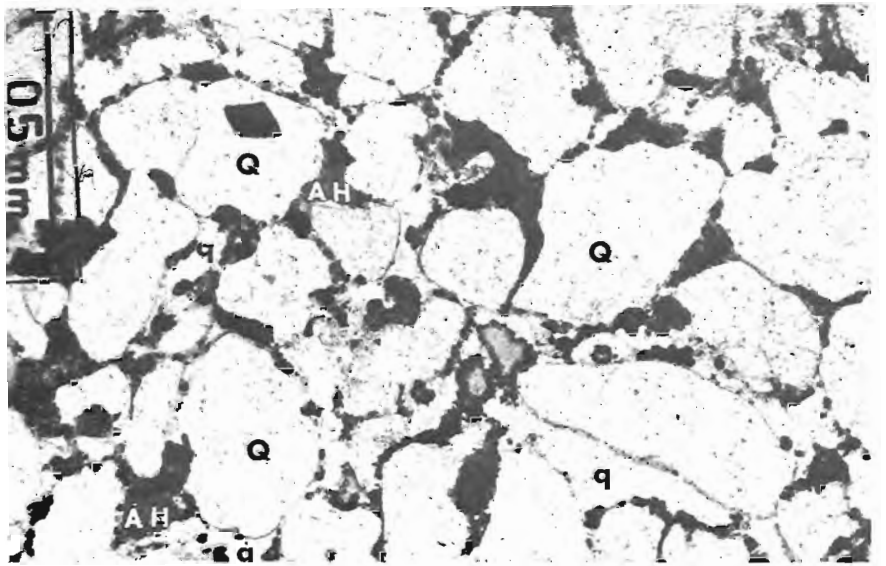

b. *lithic quartz arenite with framework quartz grains and lithic clasts (Q) cemented by fluorapatite-hematite (A-H) intergrowths occupying interstitial volumes remaining after authigenic quartz (q) cementation.*

Figure 62.4. *Photomicrographs of Thelon sediments displaying different cements.*

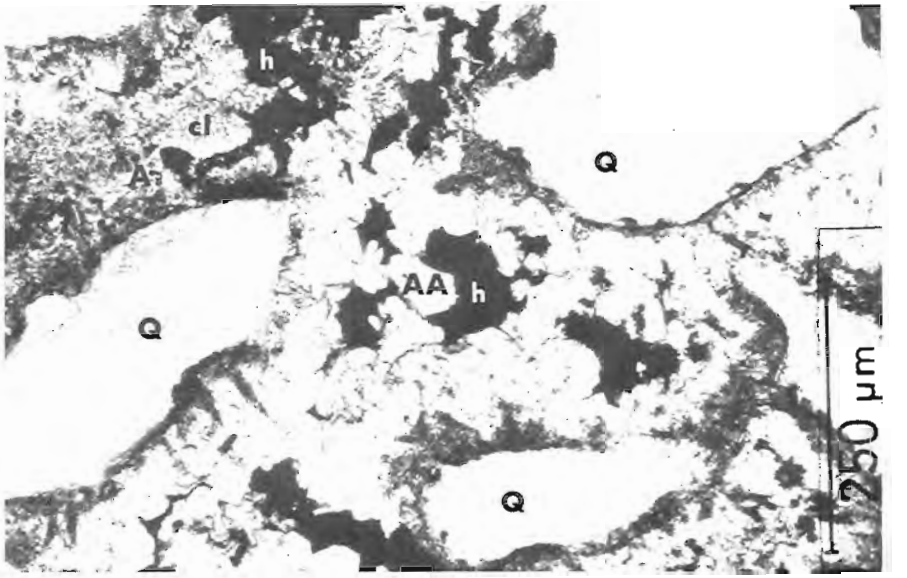

Figure 62.5. *Photomicrograph of lithic arkose with quartz (Q) grains cemented by fluorapatite crystals (A and AA) + illite (cl) + hematite (h). The scalloped margins of the quartz grains indicate the instability of quartz during phosphate deposition. Note the two generations of phosphate cement: ultra fine grained crystals rich in hematite (A) and later clear colourless crystals (AA).*

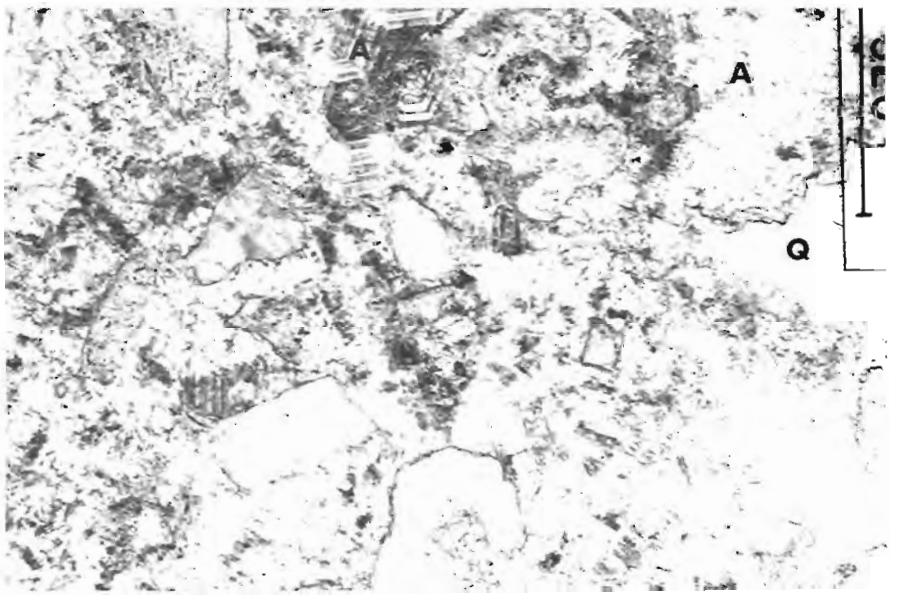

Figure 62.6. *Photomicrograph of zoned fluorapatite crystals (A) cementing corroded quartz grains (Q). Alternating dark and light bands in fluorapatite is due to hematite.*

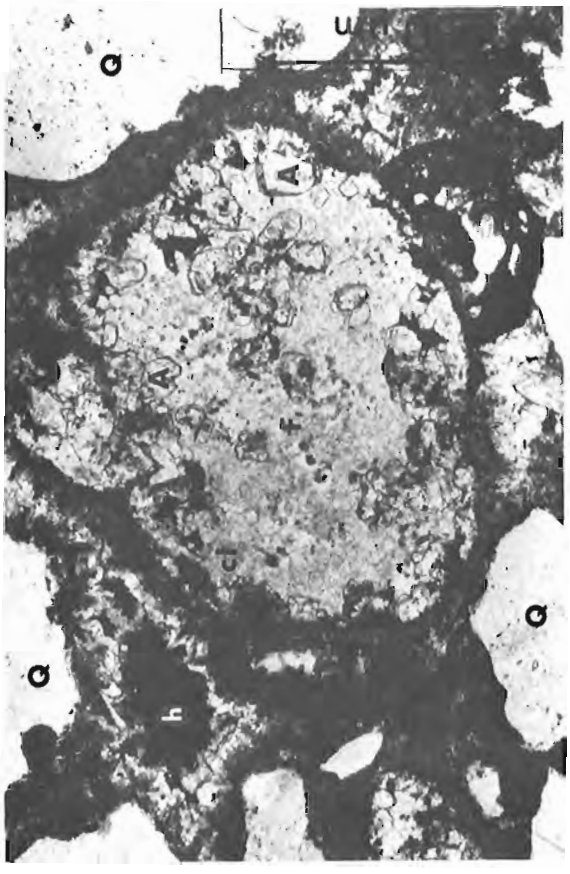

Figure 62.8. Photomicrograph of altered feldspar grain replaced by assemblage of euhedral fluorapatite (A) + illite (cl) + quartz (q) and cemented by fluorapatite (A) + illite (cl) + hematite (h).

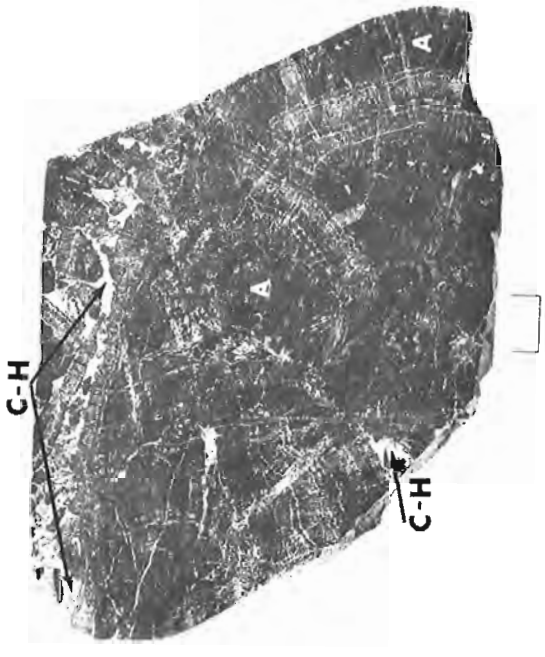

Figure 62.7. Polished slab of massive, banded radiating hematitic fluorapatite (A) with aggregates of clay-specularite (C-H). Sample from a fracture zone in the Thelon basement. GSC 203345-V

abundances are enhanced in most phosphate-bearing units except specimen 6 and the oxidized character of most strata is expressed by very high Fe^{+3}/Fe^{+2} ratios. Very low Na_2O contents in Thelon sediments reflect diagenetic feldspar destruction and the absence of smectite-type clay minerals.

The absence of authigenic carbonate cements in Thelon sediments and the negligible CO_2 contents of phosphate-bearing strata indicate little if any $CO_3^=$ substitution into the fluorapatite structure. X-ray identification of fluorapatite and low whole rock CO_2 contents indicate the absence of francolite, a carbonate-fluorapatite, common in marine phosphorites.

With respect to trace elements of Ag, Cu, Zn, Co, Ni, Cr, V and Mo the phosphate-bearing Thelon sediments show no anomalous concentrations relative to average abundances in marine phosphorites (Altschuler, 1980) or to non-phosphate bearing Thelon arenite. However, phosphatic Thelon sediments contain variable but anomalous abundances of B, Ba, Li, Rb and Sr compared to average marine phosphorite and non-phosphate bearing Thelon sediments. Very low chlorine contents, 100-300 ppm, are associated with phosphatic units. Qualitative electron microprobe energy dispersive investigations have shown trace chlorine in the spectra of illite and fluorapatite.

Uranium concentrations in 80 samples of non-phosphatic range from 0.2 to 3.5 ppm. However uranium content increases directly with P_2O_5, to a maximum value of 639 ppm U (Table 62.1). This relationship is shown in Figure 62.9 a plot of U vs P_2O_5 for phosphatic and non-phosphatic Thelon sediments. Autoradiographs of phosphate-bearing strata do not show discrete uranium phases but indistinct images in areas of phosphate cements. Spectra collected from fluorapatite grains using electron microprobe energy dispersive systems did not detect uranium. The positioning of uranium in the phosphatic phases has not been determined at this stage of study. However possible modes of occurrence may be: i) submicron sized grains of discrete uranium minerals situated along fluorapatite grain boundaries, ii) uranium absorbed onto fluorapatite grains, or iii) substituting for calcium within the fluorapatite lattice. Phosphatic units can be hematite-rich or hematite-poor with no significant difference in uranium content, suggesting that uranium is not absorbed onto fine grained iron oxide cements.

The common association of illite, hematite and quartz occurring with phosphate cements permits an interpretation of the chemical environment for phosphate formation. Nriagu (1976) and Nriagu and Dell (1974) outlined the geochemical conditions for phosphate-clay crystallization based on thermodynamic data. The illite-fluorapatite assemblage common throughout most Thelon sediments indicates a pH of 6.8-7.5. This neutral to slightly alkaline pH for phosphate crystallization explains the corroded texture margins of framework quartz clasts.

Diagenetically altered clay-rich units such as basal arkose, conglomerate or saprolite can contain fluorapatite and/or goyazite. Diagenetic formation of apatite by clay mineral phosphatolysis has been documented by Altschuler (1973) and Russell and Trueman (1971). Clay mineral alteration results in the formation of chert/quartz and Al-phosphate. The assemblage quartz + illite + phosphate and the total absence of diagenetic kandite group clays suggests that phosphatolysis of kandite group clay may explain the above mentioned mineral assemblages. Limiting conditions for the conversion of clay minerals to apatite in the presence of amorphous silica, ie. the assemblage quartz + illite + phosphate, indicates a pH of about ~8.5 Nriagu (1976). Hematite the principal iron cementing component in phosphatic rocks is not involved in direct reactions that precipitate Ca- or Al-phosphate and therefore phosphate crystallization is independent of Eh (Nriagu, 1976).

Age Dating

Because of these correlations a fluorapatite concentrate was obtained for isotopic analysis from sample 5 (Table 62.1), a lithic arkose at the base of the Thelon Formation. U-Pb isotopic analysis was attempted on fluorapatite because of the direct association of uranium with fluorapatite and because of the possibility that the phosphate system may have remained relatively closed.

The fluorapatite concentrate was obtained by crushing the pebbly arkose then washing the powder in methylene iodide. The isotopic analysis was conducted by Geospec Consultants Ltd., Edmonton Alberta and the data are listed in Table 62.2.

The concordia intercept of this single data point is ~1667 Ma whereas the $^{207}Pb/^{206}Pb$ model age is 1660 Ma. Because of the concordancy of the U/Pb and Pb/Pb ages, an age of ~1660 Ma is interpreted as a minimum age for cementation of the basal Thelon sediments.

Table 62.1

Geochemical expression of selected phosphate-bearing lithologies, Thelon Basin District of Keewatin

	Phosphate bearing Thelon sediments								
Rock type:	Lithic subarkose	Feldspathic lithic arenite	Lithic quartz arenite	Lithic arkose	Lithic arkose	Lithic quartz arenite	Lithic quartz arenite	Non-phosphatic lithic quartz arenite	Saprolitic granodiorite gneiss
Analysis	1	2	3	4	5	6	7	8	9
SiO_2	41.1	61.5	57.8	62.1	64.1	85.5	10.1	96.3	77.3
TiO_2	.40	.04	.11	.05	.32	.05	.20	.07	.25
Al_2O_3	11.2	5.3	1.8	2.2	4.3	1.1	4.7	1.3	14.6
Fe_2O_3	5.7	5.7	3.1	2.6	5.0	.8	6.2	1.7	1.3
FeO	.1	.1	.1	.4	1.1	.5	.6	.1	.1
MnO	.00	.01	.00	.01	.01	.01	.01	.00	.01
MgO	.21	.23	.20	.03	.13	.15	.28	.14	.13
CaO	20.9	13.9	20.2	17.5	12.8	6.59	40.0	.04	.12
Na_2O	0.0	0.0	0.0	0.0	0.0	.2	0.0	0.0	.4
K_2O	1.25	2.71	.64	.66	.27	.16	.74	.33	.92
H_2O Total	3.4	.8	.3	.4	1.4	.1	1.9	.2	4.8
CO_2	.2	.1	0.0	0.0	0.0	0.0	.3	0.0	.1
P_2O_5	15.0	9.90	14.6	12.6	9.17	4.76	34.1	.07	.12
S	.02	.16	.02	.02	.02	.02	.26	.02	.04
Total†	99.48	100.45	98.87	98.57	98.62	99.94	99.39	100.27	100.19
† by X-ray fluorescence									
Trace elements in ppm (method: emission spectroscopy unless as indicated)									
Ag	<5	<5	<5	<5	<5	<5	<5	<5	<5
B	120	170	120	150	<50	<50	67	80	77
Ba	880	200	50	96	130	37	210	37	100
Co*	NF	NF	NF	NF	NF	NF	NF	NF	NF
Cr	9	<5	<5	<5	21	16	30	8	<5
Cu*	8	8	5	6	8	6	8	6	NF
Li*	140	3	3	11	55	6	107	2	NA
Mo	<50	<50	<50	<50	<50	<50	<50	<50	<50
Ni*	5	2	0	1	3	4	9	2	NF
Pb*	124	149	111	19	145	38	71	10	30
Rb*	29	32	12	11	6	2	49	5	NA
Sr	1500	230	200	140	310	98	470	150	280
V	69	<20	<20	<20	<20	<20	47	<20	29
Zn*	15	16	17	9	19	9	33	7	10
U**	247	209	278	110	639	57.8	184	1.4	3.0
F*** (wt%)	1.85	1.25	1.90	1.63	1.13	0.43	3.50	0.02	NA
Cl†† (wt%)	0.02	0.02	0.02	0.01	0.03	0.01	.01	0.02	NA

NF = Not Found NA = Not Analyzed

* by atomic absorption
** by delayed neutron counting Atomic Energy of Canada Ltd. Ottawa
*** specific ion electrode
†† colorimetry

Table 62.2

Isotopic ratios from a fluorapatite concentrate, phosphate cemented Thelon lithic arkose

Sample ID	Wt. (mgm)	207/206	208/206	204/206	208/204	U(%)	Pb(%)	Common Pb(%)	$\frac{207Pb}{235U}$	$\frac{206Pb}{238U}$
Sample 5 Table 1	161.5	0.17586	0.20397	0.00537	38.0	0.13	0.03	26.26	2.3551	0.1676

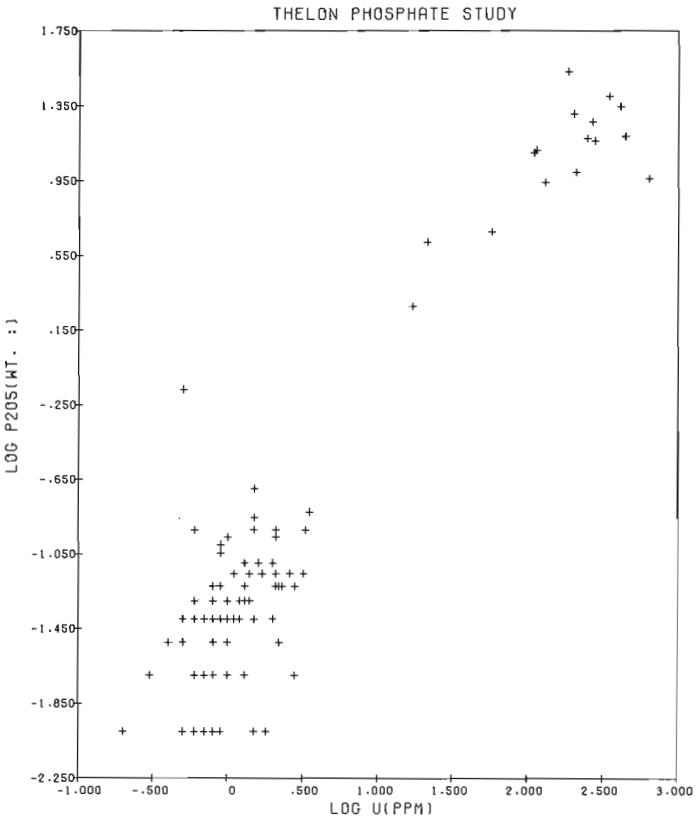

Figure 62.9. *Scattergrams of U vs P_2O_5.*

Possible Depositional Environment

Marine strata of different depositional regimes and facies associations are the most common hosts for phosphate deposition. Phosphorites deposited in water at least several hundred metres deep occur in black shales, chert and dolostone whereas shallow water phosphorites are recognized in siltstones, mudstones or limestones. Current ideas on the origin of phosphorites involve the upwelling of phosphorous-enriched deep ocean water along the continental shelf at low to equatorial latitudes and the diagenetic phosphorization of sediments occurring below the sediment-water interface (Birch, 1980).

However phosphate-bearing strata are not restricted to marine environments as evidenced by the Eocene uraniferous phosphatic lacustrine deposits of Wyoming and Utah (Love, 1964) and Pliocene lacustrine, phosphatic horizons of the Glenns Ferry Formation, southwestern Idaho (Swirydczuk et al., 1981). Both are interpreted to be part of a continental sequence of sediments deposited within intermontane basins. Phosphorization of coarse to fine clastic sediment is interpreted as diagenetic and commonly associated with organic-rich horizons.

Basal Thelon sediments were deposited in a continental, alluvial fan – braided river environment. The presence of major cataclastic zones transecting and bounding the Thelon Basin together with the distribution of coarse sediments suggests synchronous faulting and sedimentation (LeCheminant et al., 1983). This style of tectonism-sedimentation may have lead to the formation of closed subbasins somewhat similar to the multiple subbasins proposed in the Athabasca Basin (Raemakers, 1981; Tella et al., 1983; LeCheminant et al., 1983; Geological Survey of Canada Maps 1566A, 1567A). Fine grained red clastics present along the base of the Thelon Formation in the Aberdeen Lake map area (LeCheminant et al., 1983) and clasts of red siltstone-mudstone in coarse fluvial clastics indicate quiet water sedimentation. No evidence of organic-rich strata have been recognized associated with phosphatic zones of the Thelon Basin.

In the southwestern United States saline lakes of Tertiary to Recent age have been recognized (Bradley and Eugster, 1969; Love, 1964; Swirydczuk et al., 1981). Saline lakes can develop in closed basins in response to extensive block faulting with contemporaneous fluvial sedimentations as Deep Spring Lake, California (Jones, 1965) or in isolated depressions in desert plains as the Ubari Sand Sea, Libyan desert (Glennie, 1970). The paleolatitude of the Thelon Basin at ~1660 Ma would be subequatorial (Irving, 1979, p. 682, 688). The tectonic setting, sedimentology and latitude of modern saline lake environment is comparable to these features in the Thelon Basin.

Friedman et al. (1976) documented the compositional changes during dessication of the brines in Owens Lake, California. Progressive evaporation of the lake would lead to the precipitation of a variety of salts containing Ca, Na, HCO_3, SO_4 and Cl. However the resultant brine was highly concentrated in Li, F, PO_4 and B; increases in PO_4 were attributed to abundant organic activity in the lake. Thus the constituents concentrated in the Owens Lake brine are similar to variable but generally anomalous elements found in the phosphate-bearing Thelon sediments (Table 62.1) suggesting that the Thelon phosphate mineralization may have been related to a saline lake environment.

Due to the dynamic nature of sedimentation in an intermontane basin, various short lived sedimentary facies may not be preserved. Brines developed in alkaline lakes might be expected to undergo migration laterally or vertically in an environment of recurring faulting and fluctuating groundwater tables. Thus phosphatic brines could pervade strata that are facies equivalents to those at the site of generation. These brines could be channelled through Thelon strata which had an increased permeability due to feldspar diagenesis or which had escaped extensive early silicification. Alternatively the dense brines could migrate downward into structures beneath the Thelon Basin.

Summary

The available evidence suggests that phosphate mineralization in the Thelon Formation may have been related to ephemeral saline lakes. This evidence includes the following features: 1) the absence of marine rocks associated with phosphatic units in the Thelon Basin; 2) the variable but anomalous concentration of specific evaporite-related elements and 3) the analogous tectonic-sedimentological setting of the Thelon Basin to modern saline lakes. Phosphate-bearing strata examined in this report do not appear to contain any elements that may be diagnostic pathfinders for unconformity-type mineralization. However research is continuing on the geochemistry of remobilized phosphates to see if pathfinder elements can be recognized.

References

Altschuler, Z.S.

1973: Weathering of phosphate deposits – geochemical and environmental aspects; in Environmental phosphorus handbook, Wiley, p. 33-96.

1980: The geochemistry of trace elements in marine phosphorites, Part I. Characteristic abundances and enrichment; Society of Economic Paleontologists and Mineralogists, Special Publication No. 29, p. 19-30.

Birch, G.F.
1980: A model of penecontemporaneous phosphatization by diagenetic and authigenic mechanisms from the Western Margin of Southern Africa; Society of Economic Paleontologists and Mineralogists, Special Publication No. 29, p. 79-100.

Bradley, W.H. and Eugster, H.P.
1969: Geochemistry and paleoclimnology of the trona deposits and associated authigenic minerals of the Green River Formation of Wyoming; U.S. Geological Survey Professional Paper 496-B.

Christie, R.L.
1979: Phosphorite in sedimentary basins of Western Canada; in Current Research, Part B, Geological Survey of Canada, Paper 79-1B, p. 253-258.

1980: Paleolatitudes and potential for phosphorite deposition in Canada; in Current Research, Part B, Geological Survey of Canada, Paper 80-1B, p. 241-248.

Cecile, M.P.
1973: Lithofacies analysis of the Proterozoic Thelon Formation, Northwest Territories (including computer analysis of field data); unpublished M.Sc. thesis, Carleton University, 119 p.

Donaldson, J.A.
1965: The Dubawnt Group, Districts of Keewatin and Mackenzie; Geological Survey of Canada, Paper 64-20.

1966: Geology, Schultz Lake, District of Keewatin; Geological Survey of Canada, Map 7-1966.

1969: Descriptive notes (with particular reference to the late Proterozoic Dubawnt Group) to accompany a geological map of central Thelon Plain, District of Keewatin and Mackenzie (65M NW½, 66B,C,D, 75P E½); Geological Survey of Canada, Paper 68-49.

Douglas, R.J.W.
1973: Geological Provinces (sheet 28), in The National Atlas of Canada, Canada, Department of Energy, Mines and Resources.

Friedman, I., Smith, G.I., and Hardcastle, K.G.
1976: Studies of Quaternary saline lakes – II. Isotopic and compositional changes during description of the brines in Owens Lake, California, 1969-1971. Geochimica et Cosmochimica Acta, v. 40, p. 501-511.

Glennie, K.W.
1970: Desert sedimentary environments; Elsevier, New York, N.Y., 222 p.

Irving, E.
1979: Paleopoles and paleolatitudes of North America and speculations about displaced terrains; Canadian Journal of Earth Sciences, v. 16, no. 3 (Part 2), p. 669-694.

Jones, B.F.
1965: The hydrology and mineralogy of Deep Springs Lake, Inyo County, California; U.S. Geological Survey Professional Paper 502-A.

LeCheminant, A.N. and Ashton, K.E. with contributions by Chiarenzelli, J., Donaldson, J.A., and Best, M.; Tella, S. and Thompson, D.L.
– Geology of Aberdeen Lake map area, District of Keewatin, preliminary reports; in Current Research, Part A, Geological Survey of Canada, Paper 83-1A, report 16.

Love, J.D.
1964: Uraniferous phosphatic lake beds of Eocene age in intermontane basins of Wyoming and Utah; U.S. Geological Survey Professional Paper 474-E.

Nriagu, J.O.
1976: Phosphate-clay mineral relations in soils and sediments; Canadian Journal of Earth Sciences, v. 13, no. 6, p. 717-736.

Nriagu, J.O. and Dell, C.I.
1974: Diagenetic formation of iron phosphates in recent lake sediments; American Mineralogist, v. 59, p. 934-946.

Ramaekers, P.
1980: Sedimentary and tectonic history of the Athabasca Group (Helikian) of Northern Saskatchewan; in Summary of Investigations 1980, Saskatchewan Geological Survey, Miscellaneous Report 80-4, p. 99-106.

1981: Geochemistry of the Athabasca sandstones; implications for uranium genesis. (Abstract in CIM Geology Division Uranium Symposium and Field Tours, Saskatoon, Saskatchewan, Sept. 8-13, 1981, p. 18).

Russell, R.T. and Trueman, N.A.
1971: The geology of the Duchess phosphate deposits, Northwestern Queensland, Australia; Economic Geology, v. 66, p. 1186-1214.

Swirydczuk, K., Wilkinson, B.H., and Smith, G.R.
1981: Synsedimentary lacustrine phosphorites from the Pliocene Glenns Ferry Formation of Southwestern Idaho; Journal of Sedimentary Petrology, v. 51, no. 4, p. 1205-1214.

Tella, S., Ashton, K.E., and Thompson, D.L.
1983: Geology of the Deep Rose Lake map area, District of Keewatin, N.W.T.; in Current Research, Part A, Geological Survey of Canada, Paper 83-1A, report 56.

Wright, G.M.
1955: Geological notes on central District of Keewatin, Northwest Territories; Geological Survey of Canada, Paper 55-17.

1957: Geological notes on eastern District of Mackenzie, Northwest Territories; Geological Survey of Canada, Paper 56-10.

1967: Geology of the Southeastern Barren Grounds, Parts of the Districts of Mackenzie and Keewatin (Operations Keewatin, Baker, Thelon); Geological Survey of Canada, Memoir 350.

63. REGIONAL GEOLOGY OF THE EAST BULL LAKE AREA, ONTARIO

G.F.D. McCrank, Denver Stone, D.C. Kamineni, B. Zayachkivsky [1], and G. Vincent [2]
Atomic Energy of Canada Limited, Ottawa

McCrank, G.F.D., Stone, D., Kamineni, D.C., Zayachkivsky, B., and Vincent, G., Regional geology of the East Bull Lake area, Ontario; in Current Research, Part A, Geological Survey of Canada, Paper 83-1A, p. 457-464, 1983.

Abstract

The East Bull Lake map area is located within the Superior Structural Province but in proximity to the Southern Structural Province. It is underlain by Archean metavolcanic metasedimentary and granitic rocks which were deformed during the late Archean. These rocks were intruded, possibly during the early Proterozoic, by the East Bull Lake pluton, the Parisien Lake Syenite and an unnamed porphyritic granite.

The East Bull Lake pluton has been divided into seven textural and compositional units ranging from anorthosite to metagabbro. Anorthosite forms the outer margin on the north and northeast side of the pluton. The pluton becomes more mafic and more altered from north to south. Layering in the pluton, best developed in the anorthositic gabbro unit, is shallow to moderately dipping, generally to the southwest. The main units may also define major layers in the pluton.

Flat-lying Proterozoic sediments include quartzite and argillite, locally with basal conglomerate. This succession lies unconformably on Archean rocks and possibly on the East Bull Lake pluton. The maximum thickness is 80 m.

Numerous diabase dykes of gabbroic composition intrude all rocks in the map area. The most common orientation is from 300° to 320° and steeply dipping (70°-90°) though some have moderate dips. Dyke width is highly variable, ranging from 5 to 20 m. Sills of diabase intrusive into the volcanics may be 300 m wide.

Nipissing diabase forms large cliff bounded plateaus in the northeastern map area.

Faults are present in several parts of the map area. The Folson Lake Fault zone is the largest, and transects the map area. The fault is vertical with a large component of oblique-slip movement. It is characterized by tectonic breccia, quartz-filled fractures and red colouration of granitic rocks.

Linear features, visible on aerial photographs, are present throughout the map area. The most common orientation of these linears, dykes and faults is northwest.

Introduction

Regional mapping of the East Bull Lake area was performed during the summer of 1982 as part of the geological research for Atomic Energy of Canada Limited's Nuclear Fuel Waste Management Program. Mapping was carried out at 1:8000 scale based on aerial photography flown for the project and plotted on a base map derived from 1:10 000 and 1:20 000 scale base maps from the Ontario Ministry of Natural Resources.

Previous work in the area includes mapping around Whiskey Lake (Douglas, 1926), mapping of townships 123, 124, 130, and 131 (Moore and Armstrong, 1945), and mapping of the East Bull Lake pluton (Born, 1978). Remapping provided detailed information on structures, geochemistry and petrology of the area and in particular the East Bull Lake pluton. This report is concerned with the regional distribution of rock units and structures of the map area rather than detailed analysis of the East Bull Lake pluton.

The East Bull Lake map area is located about 35 km east-northeast of Elliot Lake, Ontario and about 26 km north-northwest of Massey, Ontario. Good access to the area is provided via Highway 553 north from the Trans-Canada Highway.

General Geology

The 198 km^2 map area is located entirely within the Superior Structural Province (Fig. 63.1). Supracrustal rocks of the Southern Structural Province occur south and immediately west of the map area. The Grenville Structural Province is 80 km to the southeast.

The area is underlain by Archean metavolcanic and metasedimentary sequences and Archean granitic rocks. These granites form the southern margin of the Superior Province and were emplaced at least 2500 Ma ago (Van Schmus, 1965; Card, 1978). Huronian sediments, members of the Quirke Lake Group, unconformably overlie the Archean rocks. Plutonic rocks of probable Proterozoic age intrude the Archean rocks. These include the East Bull Lake pluton, the Parisien Lake Syenite and an unnamed porphyritic granite. Numerous diabasic dykes of various ages intrude all rocks in the map area.

Geology

Whiskey Lake Greenstone Belt

Steeply dipping metavolcanic and metasedimentary rocks occur in the southwestern part of the map area. Mafic metavolcanics generally exhibit pillow or flow breccia textures. Intermediate metavolcanic rocks contain lapilli and bomb fragments and occur as narrow belt like domains within mafic metavolcanics. Several small enclaves of wacke and conglomerate, containing both metavolcanic and granitoid clasts, are present but in general metasediments are rare within the map area. Metavolcanic rocks were apparently intruded by medium- to coarse-grained gabbro prior to folding and metamorphism and subsequently intruded by diabase dykes and sills.

Archean Granitic Rocks

Granodiorite underlies large parts of the map area especially in the northwest and southeast. The granodiorite is generally medium grained, leucocratic with less than

[1] University of Toronto, Toronto, Ontario
[2] Laval University, Québec

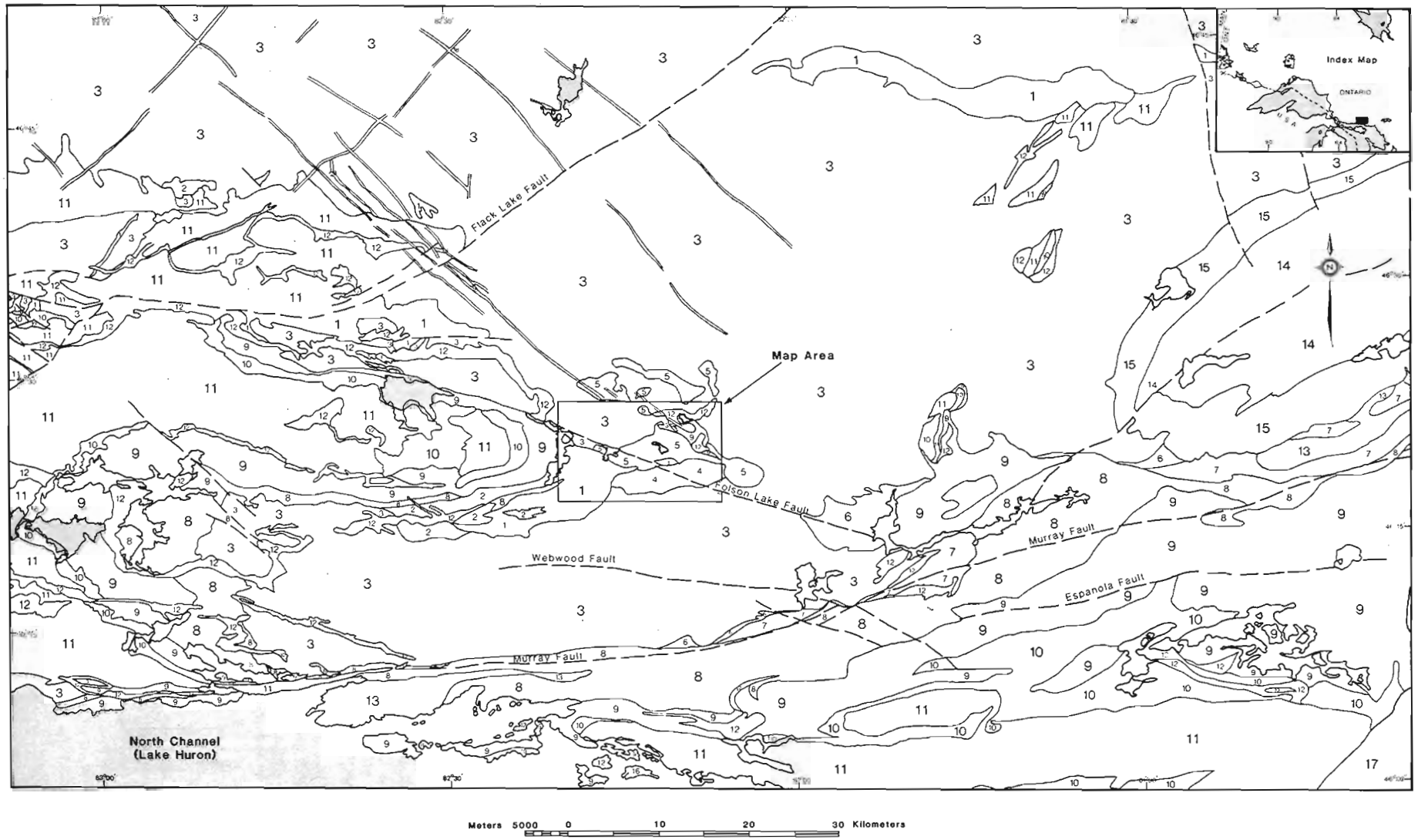
Index Map
ONTARIO
Flack Lake Fault
Map Area
Folson Lake Fault
Webwood Fault
Murray Fault
Espanola Fault
Murray Fault
North Channel
(Lake Huron)
Meters 5000 0 10 20 30 Kilometers

LEGEND FOR FIGURE 63.1

Figure 63.1. *Geological setting of the East Bull Lake map area. (after Card and Lumbers, 1977 and Giblin et al., 1979).*

10% biotite. It exhibits a weak to moderate metamorphic foliation defined by the long axes of quartz grains and aligned biotite. Xenoliths of amphibolite occur throughout the granodiorite although in the southeastern area they are particularly large and abundant. These may be scattered roof pendants of remnant volcanic flows into which the granodiorite intruded.

Porphyroblastic granite occurs in the northeast. It is beige to salmon pink, slightly foliated and contains undeformed porphyroblasts of subhedral to euhedral microcline, 1 to 10 cm long developed parallel to the foliation. The matrix is composed of quartz, plagioclase, microcline, biotite and subordinate hornblende. Porphyroblast content varies from about 10 to 20 per cent with local concentrations of 50 to 60 per cent. The foliation is defined by alignment of mafic minerals, porphyroblasts and occasionally by the long axis of elongate quartz grains. Xenoliths of amphibolite are present; some contain microcline porphyroblasts.

Archean gabbro occurs only in the western part of the map area and intrudes the granodiorite and supracrustals. The rock is a medium- to coarse-grained gabbro with original clinopyroxene altered to amphibole.

Intermediate intrusive rocks occur in the northwestern part of the map area. They are black weathering, medium grained dioritic rocks composed of plagioclase, hornblende and variable amounts of quartz.

Parisien Lake Syenite

The Parisien Lake Syenite outcrops directly south of the main gabbro intrusion. It is elongate, extending approximately 13.5 km in an east-west direction and 3.25 km wide. The syenite is compositionally homogeneous consisting of well twinned potassium feldspar phenocrysts and interstitial amphibole and biotite. The mafic mineral content is highly variable; it is generally less than 20 per cent although this percentage is exceeded in some outcrops. The syenite has been separated into 3 units based on the grain size of microcline feldspar. Coarse grained syenite is porphyritic with phenocrysts ranging from 5 mm to 4 cm. Medium grained syenite is less porphyritic with grains from 1.0 to 5.0 mm. A mixed unit consists of outcrops containing coarse- and medium-grained varieties. Primary alignment of potassium feldspar occurs locally and varies considerably over short distances.

Three small, isolated bodies of medium grained syenite occur along the north boundary of the map area immediately west of the Sauble River. These resemble the hornblende-rich phase of medium grained syenite which occurs north of Renault Lake.

East Bull Lake Pluton

The East Bull Lake pluton occupies the central part of the map area. It is elongate in an east-west direction, slightly more than 3 km wide with a minimum length of 13.5 km. The intrusion comprises various gabbroic rock units and two gabbro dykes which occur northwest and southeast of the main unit. Intrusive relationships with the surrounding rocks are rarely observed although the gabbro appears to intrude the volcanic rocks to the south.

Gabbro dykes strike 270° to 290°, apparently with steep dips, and vary from about 30 to 100 m wide. These dykes have an aphanitic chill margin and a gabbro core. They are essentially plagioclase and pyroxene rocks in which pyroxene is partly altered to amphibole. Crosscutting relations between these dykes and others in the area are rare, however some relationships suggest that the gabbro dykes are older.

The outer margin on the eastern side of the intrusion is composed mainly of anorthosite. Minor amounts of gabbroic anorthosite or gabbro occur in some outcrops where the increase in pyroxene content results in segregated, poorly defined layers within the anorthosite. The unit is generally medium- to coarse-grained although pyroxene-rich layers are finer grained.

Nodular anorthositic gabbro occurs only near the eastern map boundary. This unit is characterized by round- to oval-shaped, 3 cm to 10 cm nodules of anorthosite in a medium grained matrix of pyroxene gabbro.

A plagioclase-rich gabbro unit, gabbroic anorthosite, occurs within the outer margin of anorthosite. Plagioclase content ranges from 60 to 85 per cent with subophitic textures developed.

Anorthositic gabbro is concentrated around East Bull Lake and is characterized by metre-scale layers composed of thick gabbro layers and thinner anorthosite layers; both units


46° 25'
82° 15'
2000
1000
0
1000
Metres

are medium grained. The layers exhibit variable strike and dip though horizontal and subhorizintal dips are common. Fractures within the gabbro layers are generally filled while fractures within the anorthosite layers are normally short (20 cm), perpendicular to layering and not filled.

A relatively fresh gabbro occurs immediately west of Moon Lake. Ophitic and subophitic textures are commonly displayed and layering due to concentrations of medium- and fine-grained gabbro may be present.

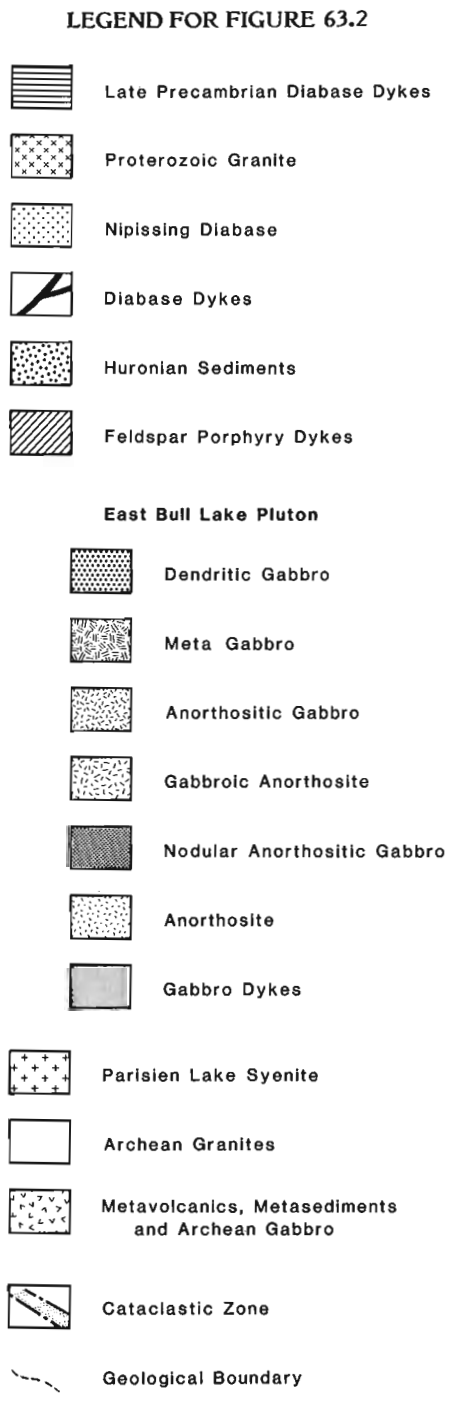

Figure 63.2. *Geology of the East Bull Lake map area.*

Most of the western part of the intrusion is a medium grained metagabbro. Primary pyroxene crystals are partly to completely converted to actinolitic amphibole and cummingtonite. These mafics commonly define a strong fabric with variable dips from subhorizontal to subvertical. The isolated gabbro lenses occurring in the northern part of the map area also belong to this unit.

Dendritic gabbro is located in the central region of the intrusion. It occurs as patchy areas in the central plateau west of Moon Lake and as an east-west linear band to the south. Amphibole dendrites of various sizes, although always coarse grained (greater than 1 cm), occur in a matrix of plagioclase. They are characteristically associated with potash feldspar which comprises 5 to 10 per cent of this rock unit. In some locales the dendrites and associated minerals are pegmatitic. Graphic intergrowths of quartz (granophyric) and feldspars are present.

Proterozoic Sedimentary Rocks

Huronian sediments occur extensively in the northeastern map area and sporadically in the southwest. In the northeast they form a sequence with a maximum thickness of 80 m that grades upwards from a basal conglomerate to argillite and quartzite. The sequence unconformably overlies the metavolcanics in the southwest, the Archean porphyroblastic granite and possibly the East Bull Lake pluton. Outliers of quartzite and argillite occur in the volcanics and the porphyroblastic granite. Contacts with the Nipissing diabase are sharp and vertical with diabase intruding the sediments.

The basal conglomerate consists of well rounded pebbles and boulders (1 cm to 1 m), of granite, with mafic volcanics, and amphibolite supported in a black, mudstone matrix. The conglomerate grades into a grey, flat lying massive argillite which in turn grades into a buff-white to green, massive to well-bedded quartzite. The quartzite exhibits primary structures such as graded beds, high-angle crossbeds, and ripple marks, all of which indicate that the unit has not been overturned.

Dykes

Two large feldspar porphyry dykes of gabbroic composition intrude the Parisien Lake syenite. The dykes appear to contain unaltered pyroxene and crystal aggregates of saussuritized plagioclase up to 3 cm in diameter.

Diabase dykes cut most rock units but occur most abundantly in granodiorite, granite, syenite and in the main body of the East Bull Lake pluton. Compositions range from 50 to 60 per cent plagioclase and 40 to 50 per cent pyroxene altered to amphibole. The dykes are often characterized by the presence of minor disseminated sulphides, mainly pyrite. Some dykes contain olivine.

The strike of these dykes varies from 270° to 360°, although by far the most common orientation is 300° to 320°. The dip of dykes can be measured only rarely but most seem to be steep (70° to 90°). Some have moderate dips and this is indicated by curvature in the trace of dykes where these are exposed in terrane of variable relief. Diabase dykes in the volcanic rocks (Fig. 63.1) are shallow dipping and some form subhorizontal sheets. Dyke width is highly variable from less than a metre to 300 m though most range from 5 to 20 m. True dyke width is rarely seen since dykes are generally incompletely exposed along the edges of outcrops. Dykes may attain lengths of 8 km. It is likely that dykes of several ages are present.

Nipissing diabase occurs in the northeastern part of the map area as high-cliff-bounded plateaus. The rock is mottled black and white, fine- to medium-grained with

diabase texture. The basal parts of several large cliffs are gabbro that contain occasional anorthosite lamallae. It is composed of plagioclase, pyroxene variably altered to amphibole, and variable amounts of quartz.

Late diabase dykes occur in the northeast. In one locale this type of dyke is a topographic high visible on aerial photographs. In other locales it is a topographic low occurring along valley bottoms or in swamps. The dykes strike northwest with steep to vertical dips and they postdate all rocks in the map area. The dykes have a minimum width of 20 m. The rock is rusty brown, highly weathered and porphyritic with laths of plagioclase in a diabase matrix of medium grained plagioclase, hornblende and pyroxene.

Late aplite dykes, too small to be indicated on the map, intrude the Parisien Lake syenite, porphyroblastic granite, and granodiorite. Felsic dykes, though present, are rare in the East Bull Lake pluton.

Proterozoic Granite

Proterozoic granite occurs southwest of Millen Lake and immediately west of the Sauble River in the northern part of the map area. It is porphyritic with red laths of poikilitic microcline and plagioclase phenocrysts (0.5 to 5 cm long) in a medium grained, generally massive matrix of plagioclase, potassium feldspar, quartz, and less than 5% biotite and/or hornblende.

Layering in the East Bull Lake Pluton

Layering (Fig. 63.3) is best developed in the anorthositic gabbro unit where it occurs as metre scale gabbro and thinner anorthosite layers. Individual layers are planar and continuous across outcrop, with uniform composition and texture. Contacts between layers are sharp and planar. The layering is rhythmic with several repetitions of the gabbro-anorthosite sequence.

The attitude of layering ranges from shallow to steeply dipping though most layers dip moderately to the southwest. In the vicinity of Moon Lake the layering is shallow to nearly horizontal. Layering in other units is indistinct and where present is discontinuous.

Layering has been used by several authors to estimate the thickness of the pluton. Born (1978) estimated a maximum thickness of 1060 m and a depth of 850 m. A. Brown (personal communication, 1981) estimated a maximum depth of about 1 km based on 20° dip of layering. Layering measured in this study ranges from horizontal to moderate, with an average of 35° which could indicate a depth of approximately 2.5 km. However, the high variability noted in the attitude of layers indicates that caution must be exercised in estimating thickness by this method.

Faulting

The map area is transected by several fault zones, the most notable of which trends 115° across the map area through Folson Lake (Fig. 63.1-63.3). A smaller fault zone splays southeast from it at Whiskey Lake and trends about 130° to terminate south of Folson Lake. Other fault zones occur in southeastern and northeastern parts of the map area. The faults in the northeast occur in the porphyritic granite and the Proterozoic granite. They are shorter than the Folson Lake Fault, and exhibit evidence of ductile deformation, with mylonite or ultramylonite.

Crystalline rocks affected by the Folson Lake fault such as the granodiorite and East Bull Lake pluton exhibit cataclastic textures including randomly oriented fractures, angular breccia fragments and numerous microfaults. Quartz veining in all faulted rocks and red colouration of granodiorite are common features. Amphibolite commonly develops a schistose texture. Slickensides and mineral lineations are common within the fault zones though orientations vary greatly.

The Folson Lake Fault zone exhibits an apparent dextral strike separation of about 3.2 km offsetting the western contact of the gabbro body from Shaule Lake on the north side of the fault to the western tip of Folson Lake on the south side. However the fault zone exhibits an apparent sinistral strike separation of about 1 km where it offsets the eastern contact of the gabbro body near Parisien Lake. Mineral lineations and slickensides in the Folson Lake fault zone have a NW-SE trend and variable plunge from 0° to 60° (Fig. 63.3).

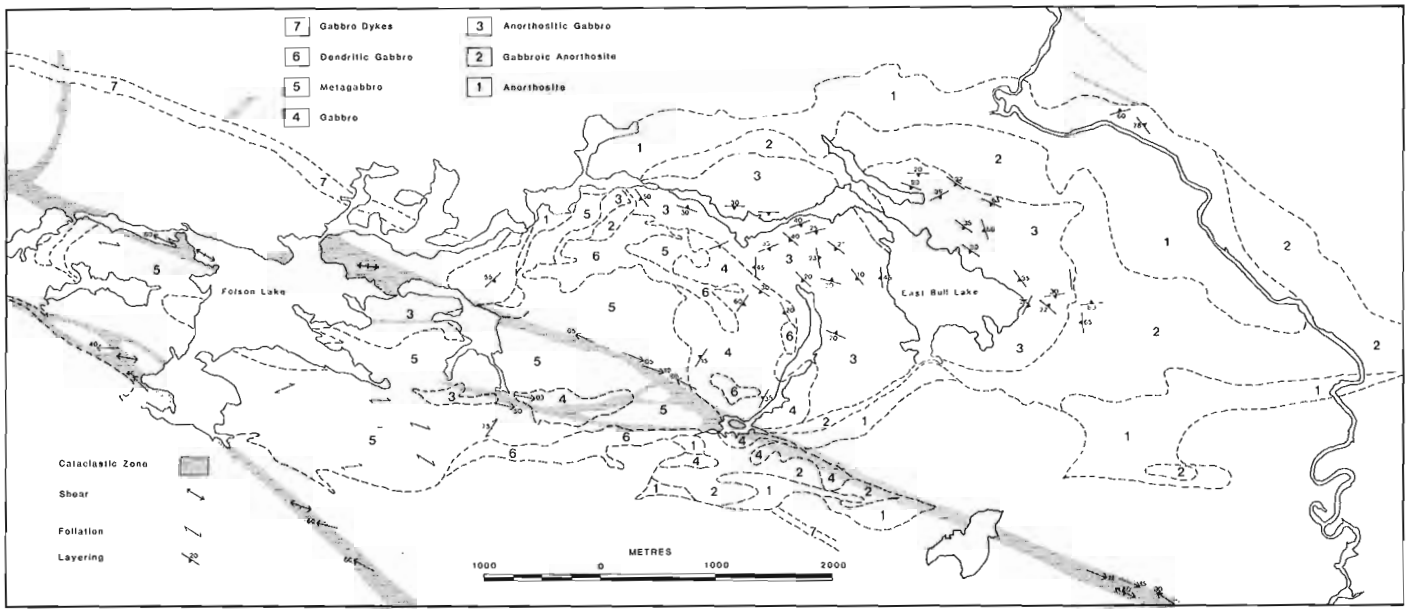

Figure 63.3. *Distribution of layering in the East Bull Lake pluton and mineral lineations and slickensides in the Folson Lake fault zone.*

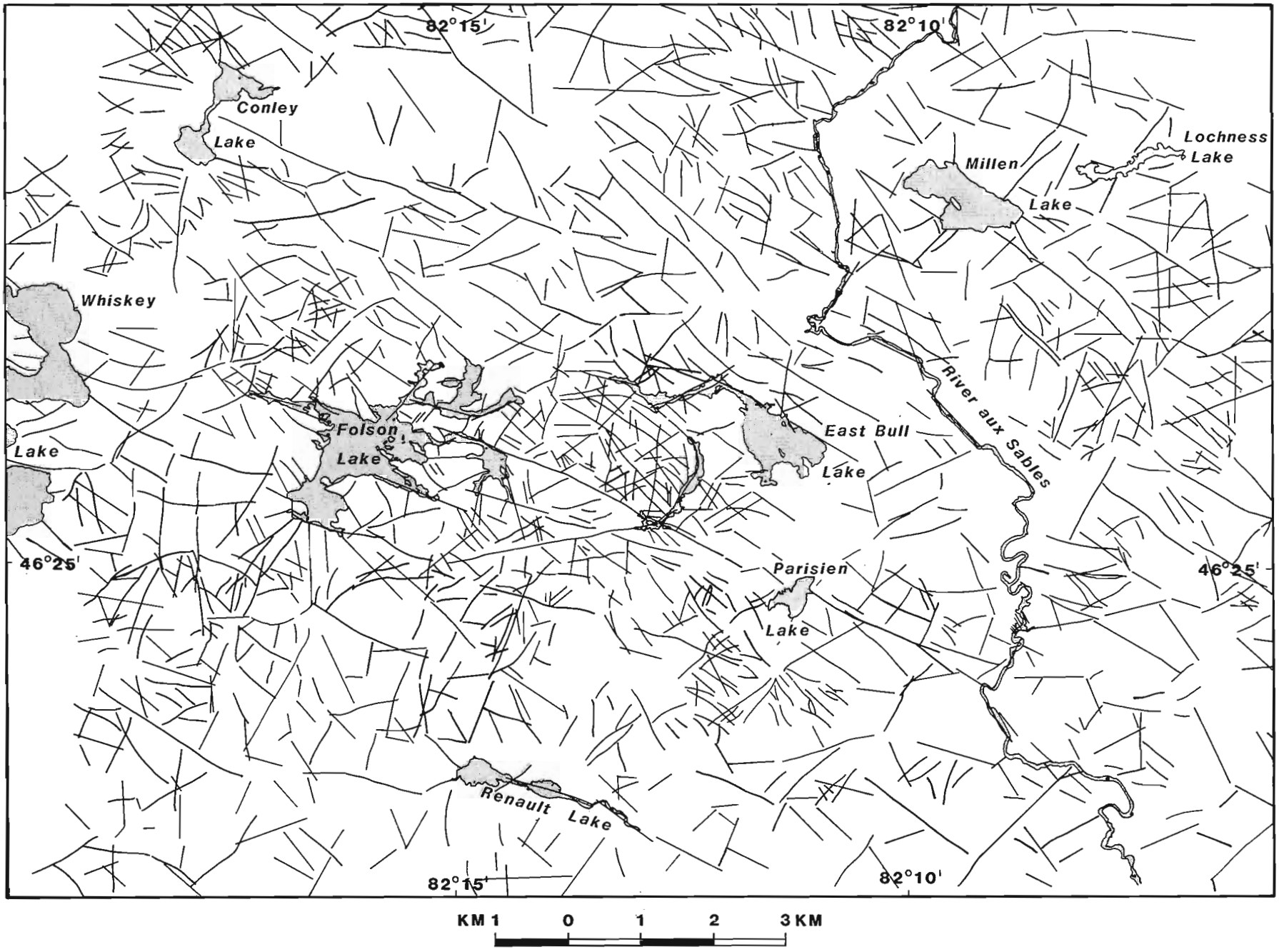

Figure 63.4. *Lineaments defined from 1:15 840 scale aerial photographs of the East Bull Lake map area.*

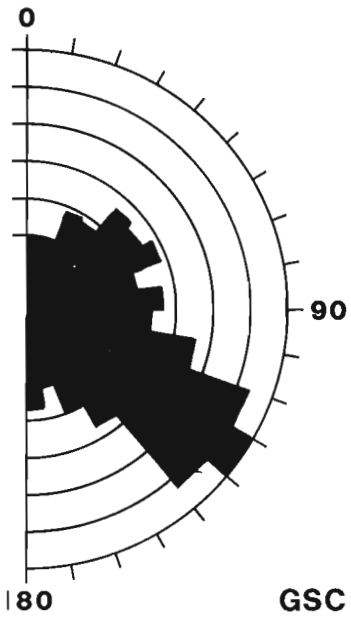

Figure 63.5. *Lineament orientations in the East Bull Lake map area.*

The present interpretation of movement on the fault zone is oblique-slip displacement, southside down, based primarily on apparent displacements of the pluton. Faults within southeastern parts of the map area exhibit vertical mineral lineations which may indicate primarily dip-slip displacement.

East Bull Lake Lineament Analysis

Lineaments were recorded from 1:15 840 scale aerial photographs (Ontario Ministry of Natural Resources), throughout the map area (Fig. 63.4). Lineament lengths have a log normal probability distribution. Ninety percent of the lineaments defined are less than 1 km long. Lineaments are oriented in all directions but a peak which ranges from 110° to 140° accounts for 36 per cent of the total lineament lengths (Fig. 63.5). Dykes and the Folson Lake fault zone tend to have similar orientations (120° to 140° and 115° respectively).

Acknowledgments

The authors thank R. Buchanan, M. Carter, J. Codere and R. Kat for assistance during the mapping program, C. Hamlin for assistance in drafting the figures, and I. Ermanovics for critical review of the manuscript.

References

Born, P.
1978: Geology of the East Bull Lake mafic intrusion, District of Algoma, Ontario; Unpublished M.Sc. Thesis, Laurentian University, Sudbury, Ontario.

Born, P. and James, R.S.
1978: Geology of the East Bull Lake layered anorthosite intrusion, District of Algoma, Ontario; in Current Research, Part A, Geological Survey of Canada, Paper 78-1A, p. 91-95.

Card, K.
1978: Geology of the Sudbury-Manitoulin area, Districts of Sudbury and Manitoulin; Ontario Geological Survey Report 166, 238 p.

Card, K.D. and Lumbers, S.B.
1977: Sudbury-Cobalt, Geological Compilation Series, Algoma Manitoulin, Nipissing, Parry Sound, Sudbury and Timiskaming Districts; Ontario Geological Survey, Map 2361, scale 1 inch to 4 miles.

Douglas, G.V.
1926: The Whisky Lake area, Algoma District, Ontario; Ontario Department of Mines, Annual Report, 1925, v. 35, pt. 4, p. 34-49, with colour map 34C.

Giblin, P.E., Leahy, E.J., and Robertson, J.A.
1979: Saulte Ste. Marie-Elliot Lake, Geological Compilation Series, Algoma, Manitoulin and Sudbury Districts; Ontario Geological Survey, Map 2419, scale 1 inch to 4 miles.

Moore, E.S. and Armstrong, W.S.
1945: Geology of the East Bull Lake area, Algoma District, Ontario; Ontario Department of Mines, Annual Report, 1943, v. 52, pt. 6.

Van Schmus, W.R.
1965: The geochronology of the Blind River-Bruce Mines area, Ontario; Canada Journal of Geology, volume 73, p. 775-780.

SCIENTIFIC AND TECHNICAL NOTES
NOTES SCIENTIFIQUES ET TECHNIQUES

SURFICIAL GEOLOGY MAPPING USING REMOTE SENSING

Project 780035

J.R. Bélanger
Terrain Sciences Division

Introduction

One of the objectives of this project is to look into the possibilities of using remote sensing in the mapping of surficial geology. In order to get a proper assessment of remote sensing in terrain mapping, several areas located throughout Canada are being considered. Although most of the studies are still in progress, it is possible to define a number of general principles concerning the approach to be used and the type of information that can be obtained from different geographical contexts.

Methodology

The mapping of surficial geology using remote sensing is done in the following way: an unsupervised map is produced which resembles a conventional false colour air photograph; the map is then interpreted by a geologist using ground information; and finally a new map (supervised) is generated by grouping spectral classes having similar geological meaning.

Unsupervised maps consist of an analog reproduction of MSS bands four (blue), five (red), and seven (infrared) for which the primary colours cyan, yellow, and magenta are assigned, respectively; the maps are produced on a Raster Scan Colour Plotter[1]. The reason for starting with an analog reproduction of the MSS Landsat scene is to get an image as close as possible to standard false colour photography, which permits the geologist to identify the various features appearing on the image. Unfortunately, even by using enhancement techniques, the analog reproduction of the MSS data commonly shows very little contrast between the various phenomena and requires some practice by the interpreter to separate the various geological units.

To overcome the lack of contrast in the unsupervised maps, a second map is produced on which similar spectral classes are grouped based on the judgment of the interpreter, and a new range of colours is assigned to these classes. This approach is preferred to methods based exclusively on cluster analyses (unsupervised classification) or ground information (supervised classification) because it gives the user better control over the formation and interpretation of the spectral classes and combines the advantages of spectral discrimination and of the geologist's experience.

Study Areas

Study areas have been chosen in various parts of the country in order to assess the potential of remote sensing in mapping surficial geology in different geographical contexts; an effort was made to distribute test sites over the Arctic Islands, the mainland of the Northwest Territories, and areas located south of the treeline. Except for a few images of areas in the south, most of the Landsat scenes were chosen of areas being presently mapped by the Terrain Sciences Division to permit an evaluation of remote sensing images at different stages of a mapping project. Figure 1 shows the locations of the study areas.

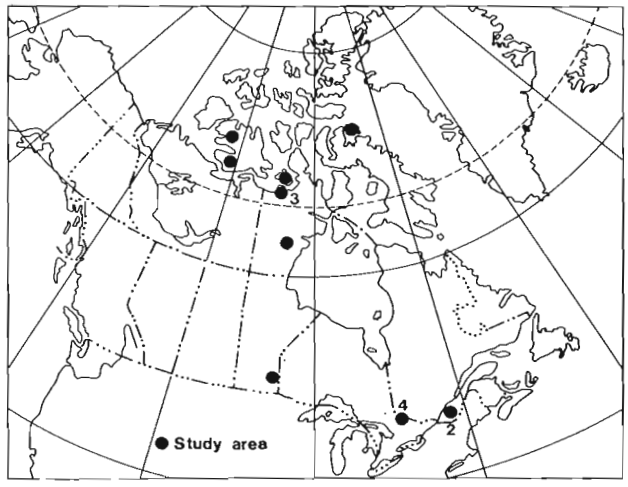

Figure 1. Location map showing study areas. Numbers refer to sites shown in Figures 2, 3, and 4.

Results

Although each area needs to be studied separately to assess properly remote sensing methodology in terrain mapping, it is possible to draw general conclusions which apply to all areas.

1. The country can be divided into two major regions with respect to the mapping using remote sensing imagery: one north and the other south of the treeline. The northern region is better suited to a direct interpretation of surficial geology since the vegetation is closely related to the underlying material because of climatic factors; the vegetation accentuates the contrasts between different types of surficial materials. In the southern region, the better formed soil profile and the well established vegetation, along with the disturbance by human activities, tend to mask the underlying geological materials (Fig. 2).

2. In the unsupervised classification, because the colour intensities are proportional to the reflectance values of the pixels and because the same primary colours are assigned to the same MSS bands, the resulting images will consistently represent similar features by similar colours regardless of the geographical context (for example, water in black, bedrock outcrops in red or white depending on the type of rock, vegetation in the various shades of green).

   On the unsupervised maps the various phenomena are presented in false colour because of the use of the invisible infrared, but once the user is accustomed to this new colour scheme, it becomes possible for him to distinguish new information provided by the infrared band which otherwise would be undetectable.

3. The analog reproduction of the MSS data on the unsupervised maps permits an analysis of the image at the pixel level, based on the individual spectral signature, as well as an interpretation at the regional level based on the structure of the phenomena. On the other hand, the digital registration of the signature permits the user to generate interpreted maps by grouping similar features and enhancing those that are of special interest, such as presented in Figure 3. The combination of the analog and digital processing of the MSS data permits a conventional interpretation of the image as well as the production of thematic maps (Bélanger, 1982).

[1] Figures 2, 3, and 4 were reproduced from colour maps, which explains the low contrast.

From: Scientific and Technical Notes in Current Research, Part A; Geol. Surv. Can., Paper 83-1A.

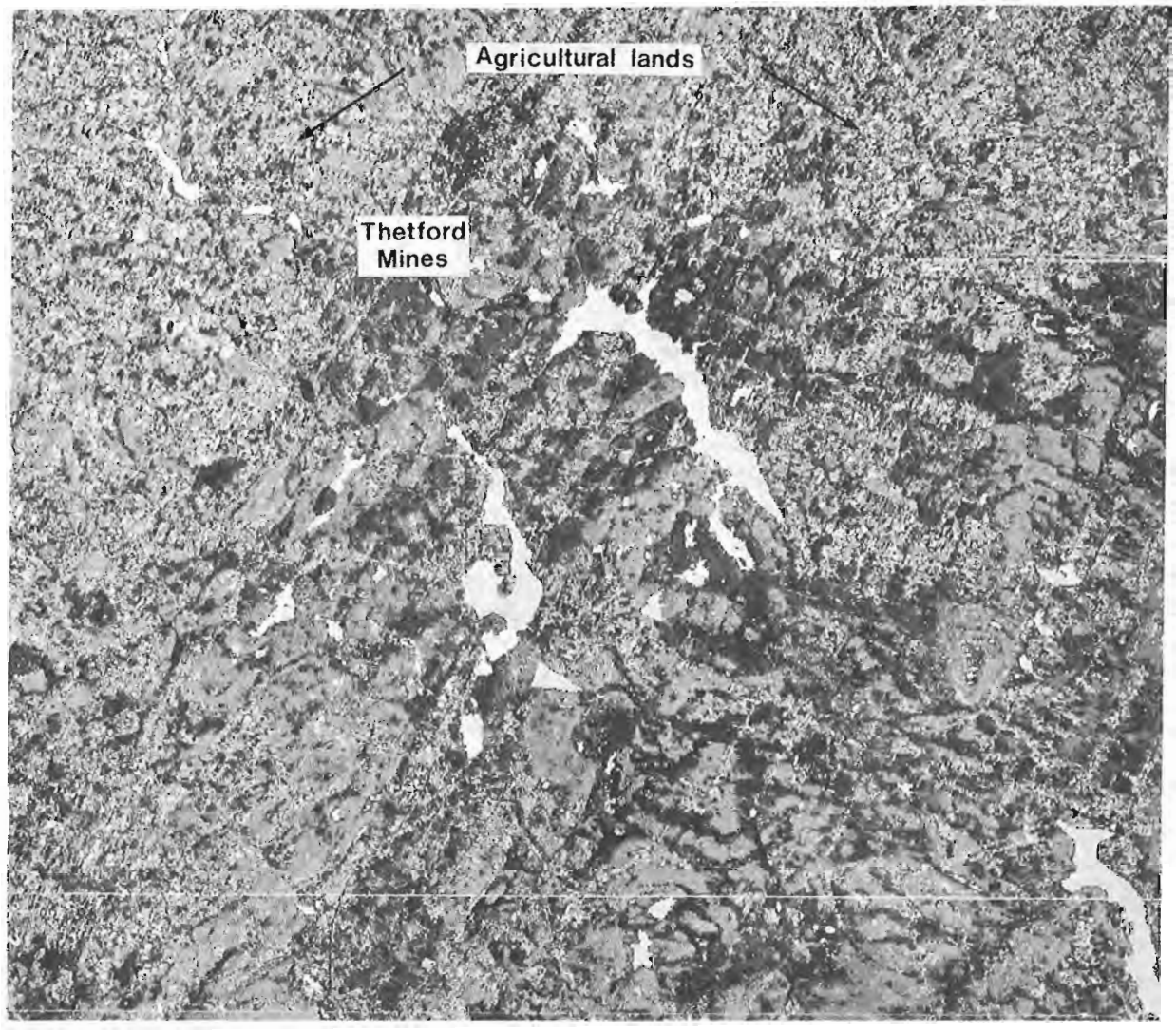

Figure 2. *Thetford Mines, Québec. Located in the Appalachian physiographic region, the area surrounding Thetford Mines is mostly covered by a sheet of till with numerous bedrock outcrops. Coniferous forests (dark tone) are commonly located in the lowlands where drainage is relatively poor and the till thickness exceeds 1.5 m. The deciduous hardwood species (medium tone) grow on hilly, till-veneered outcrops. Agricultural activities, mainly along river valleys, obscure the geology and make it impossible to use geobotanical indicators in these areas. A heavy metal dispersal train in the till immediately southeast of Thetford Mines makes the interpretation of the geology based on vegetation extremely difficult due to the toxic effect of heavy metals on vegetation (Bélanger et al., 1979). Landsat scene 14/28 taken on June 26, 1976.*

4. The rather coarse spatial resolution of the Landsat MSS pixel (57x79 m) makes the imagery unsuitable for detailed studies of local geological phenomena. On the other hand, the large area covered by each scene (186x186 km) and the little distortion of it makes the imagery an ideal replacement for an airphoto mosaic and permits regional studies of, for example, ice flow patterns (Fig. 3), till distribution, and morainic systems.

5. The date that a Landsat scene is taken plays a key role in the type of geological information that can be extracted. Other than during the winter, most of the ground surface, including the northern region, is covered by vegetation which is constantly changing. It is therefore important to select an image in which the vegetation can enhance the geology or interferes as little as possible.

Is has been noted, for example, that in areas of homogeneous forest cover on the Canadian Shield, bedrock lineaments can best be observed on images taken during the fall after defoliation (Fig. 4); in areas covered by discrete stands of deciduous trees and of coniferous trees, such as the Thetford Mines area (Fig. 2), surficial deposits can best be studied when vegetation is at its peak, enhancing natural segregation due to slope, drainage, soil type, etc. (Fig. 2).

Conclusion

The knowledge acquired to date shows that Landsat imagery can be useful in mapping surficial geology north of the treeline and, to a lesser degree, south of the treeline. The coarse resolution of the pixels and the impossibility of getting stereographic coverage makes Landsat data

Figure 3. *Adelaide Peninsula, District of Mackenzie. Ice flow direction has been enhanced on this image by assigning darker tones to the glacial fluting, which is covered by little vegetation, and lighter tones to the more densely vegetated surrounding land. Landsat scene 43/12 taken on July 7, 1976.*

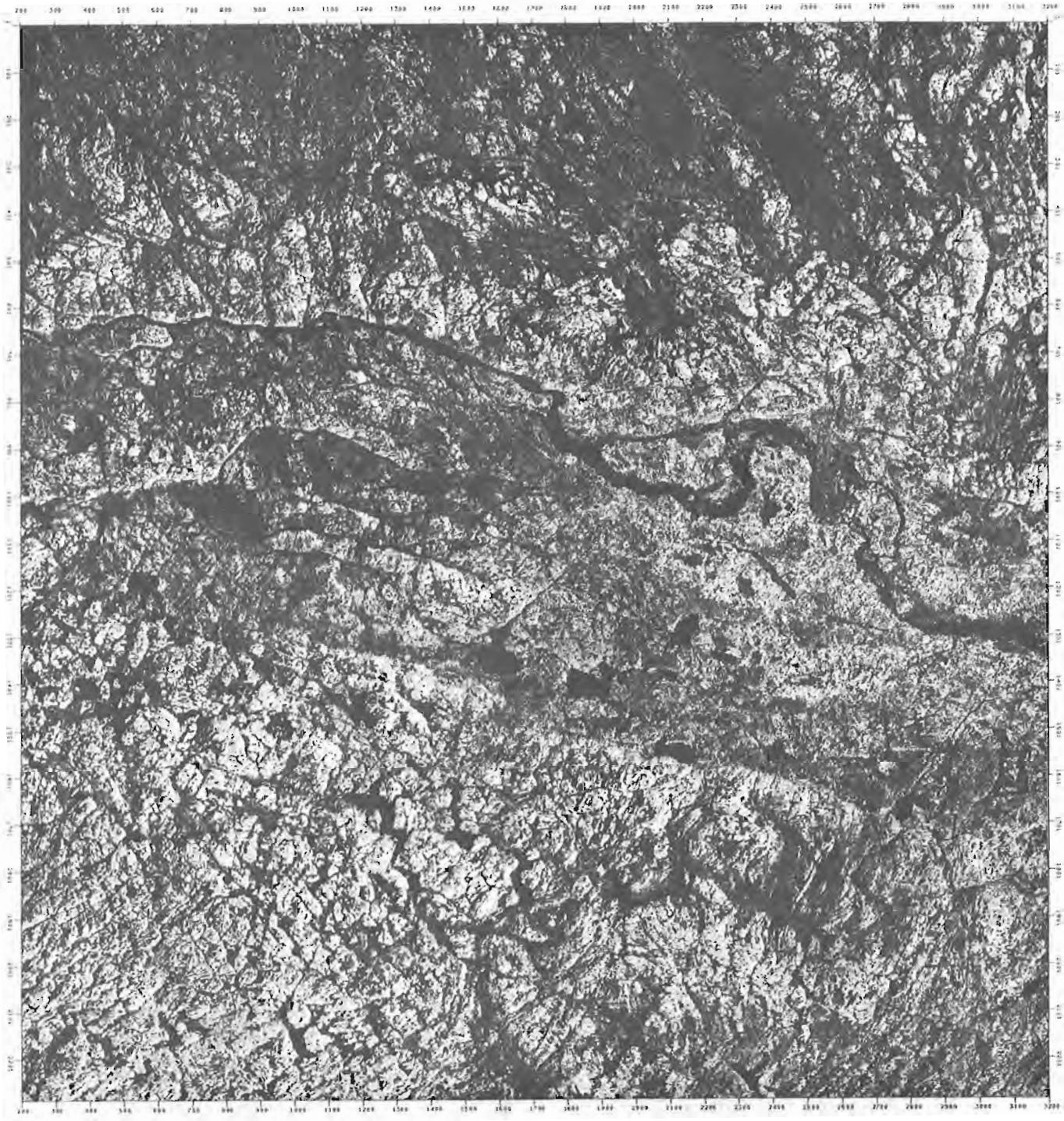

Figure 4. *Chalk River, Ontario-Quebec: Bedrock lineaments are evident after defoliation in an area of mixed deciduous-coniferous forests. Structure of Precambrian bedrock bordering Ottawa River valley is well exposed. Landsat scene 18/28 taken on October 8, 1973.*

unsuitable for detailed geological mapping; however Landsat imagery is well suited for small scale reconnaissance maps (i.e., scale 1:125 000 and smaller) covering large areas with little distortion. The availability of multiband data, mainly in the infrared portion of the spectrum, increases the potential of remote sensing for the mapping of surficial geology by revealing information that is absent on conventional black and white photography. The evaluation of remote sensing in Quaternary geology is still in progress and more detailed information on the various areas will be released as the studies are completed.

References

Bélanger, J.R.
1982: Les satellites à la rescousse de la cartographie; Geos. vol. 11, nº 1, p. 14-17.

Bélanger, J.R., Rencz, A.N., and Schilts, W.W.
1979: Patterns of glacial dispersal of heavy metals as reflected by satellite imagery; Télédétection et gestion des ressources, Association québécoise de télédétection, Ste-Foy, Québec.

RADIOCARBON DATING OF INTER-LABORATORY CHECK SAMPLES

Project 570148

W. Blake, Jr.
Terrain Sciences Division

Introduction

As part of the continuing program of the Geological Survey of Canada's Radiocarbon Dating Laboratory, an effort is made to determine the age of selected samples that have been dated already by other laboratories. Also, certain samples of which there is an abundance of material, usually a log, are supplied to other laboratories for cross-checking purposes. Previous cross-checks have been reported from time to time in our annual compilation of radiocarbon age determinations. Of particular interest in this regard is the series of dates on a 25 000 year-old log from British Columbia reported in list XIX by Lowdon and Blake (1979); five determinations by the GSC laboratory are included, the best one (because of the small error term) being a value of 25 200 ± 260 years (GSC-1802-2). In addition dates on this log from Brock University (BGS), Dalhousie University (DAL), Ministère des richesses naturelles, Québec (QU), and the University of Waterloo (WAT) are reported. Samples of the same log now have been sent to the other four laboratories in Canada: Simon Fraser University (SFU), the Alberta Environmental Centre (AEC), Saskatchewan Research Council (S), and Université du Québec à Montréal (UQ).

This note presents the results of a series of inter-laboratory age determinations (Table 1) in which the Geological Survey of Canada's Radiocarbon Dating Laboratory has been involved; all dates have been determined during the last three years. Another group of inter-laboratory checks on single pieces of driftwood were reported in Blake (1980), and they showed some serious discrepancies. In the new series of age determinations it is encouraging to find such good agreement between laboratories, although there may be other problems related to the interpretation of individual samples, as described in the following section.

Acknowledgments

The GSC age determinations reported here have been carried out under the direction of J.A. Lowdon (until October 1981) and R.N. McNeely. The careful work of laboratory staff members I.M. Robertson, A.M. Telka, and J. Tremblay is also acknowledged with thanks. Permission to use unpublished age determinations in this compilation has been granted by A.S. Dyke (GSC), H. Melville (Brock University, St. Catharines), and E. Nielsen (Manitoba Department of Energy and Mines, Winnipeg). Determination of the walrus species was done by C.R. Harington (National Museum of Natural Sciences, Ottawa), and of the wood samples by R.J. Mott (GSC). J.A. Lowdon and A. MacS. Stalker have provided helpful comments on the manuscript.

Results and Discussion

Walrus skull

The first comparative age determination listed in Table 1 was carried out because the young age (2420 ± 65 years; S-1392), obtained on the right tusk from a nearly complete walrus skeleton half imbedded in gravelly sand on a gentle slope, was far too young in relation to the elevation of 103 m at which the sample was collected (Dyke, 1979). On the basis of the ages of marine pelecypod shells collected at similar elevations near the northwest corner of Somerset Island, Northwest Territories, an age of the order of 9000 years could have been expected (Dyke, 1979; 1980). The check determination, made on part of the mandible (696.5 g) from the same skull, gave a nearly identical result of 2450 ± 180 years (GSC-3081).

As Dyke (1979) has indicated, some explanation must be sought for these anomalous dates, for not only do they agree, but other age determinations on walrus tusks in the Queen Elizabeth Islands show that no particular problem exists with dating the organic fraction derived from walrus bone or ivory. An age of 7320 ± 120 years (I-7796, Harington, 1975) was determined on bone from the maxillary region of a cranium found at an elevation of 53 m in Polar Bear Pass on Bathurst Island, and a date of 8690 ± 100 years (GSC-2899) was obtained on a tusk extracted by the author from marine sand at 5 m a.s.l. on Coburg Island (77°52.5'N, 79°02'W). Both dates were on the organic (collagen) fraction. On the other hand, the Somerset Island sample is not the only known example of 'young' walrus remains found at high elevations on raised beaches. A tusk from a nearly completely imbedded cranium (collected in 1976 by D.K. Elliott, M.R. Gibling, and G. Narbonne, then of the University of Ottawa) at approximately 170 m a.s.l. south of Read Bay, eastern Cornwallis Island (75°01.2'N, 93°34'W), gave an age of 3410 ± 50 years (GSC-2951; uncorrected). Also, Lauritzen et al. (1980) reported dates on vertebrae from two partly imbedded walrus skeletons in Svalbard; one at an elevation of 160 m and 7.5 km from the sea gave an age of 1330 ± 60 years (T-3452), and one at 200 m a.s.l. and 3.0 km from the sea gave an age of 540 ± 60 years (T-3453). In both areas age determinations on driftwood show that the beaches at those elevations are over 9500 years old (Salvigsen, 1978, 1981; cf. Table 1). Perhaps walrus do crawl far inland on occasion, as seals are known to do in Antarctica (Péwé et al., 1959). Otherwise it is necessary to attribute each of these finds to the activity of men or polar bears, which seems unlikely.

Larch driftwood

This driftwood sample (**Larix** sp.) was considered to be of particular importance as it was the highest single piece of Holocene driftwood collected in Svalbard (cf. Blake, 1961; Hoppe et al., 1969; Knape, 1971; Salvigsen, 1978; Häggblom, 1982a,b), an area where the oldest driftwood logs have proven to be approximately 1000 years older than any known logs from the raised beaches in the Canadian Arctic Archipelago (cf. Blake, 1972; Stewart and England, in press). The opportunity was taken to count the CO_2 derived from the sample in both of our counters as an internal cross-check, and the results agree closely (Table 1). The best determination, again because of the small error term, is that carried out in the 5L counter: 9850 ± 80 years (GSC-3039).

The age determinations show that the high-level beaches on Kongsøya, the island in the southeastern part of the Svalbard archipelago where the wood was found, are indeed Holocene in age. This fact is of interest since four pieces of driftwood from lower elevations, but still in the upper range (62 to 80 m a.s.l.) of the raised beaches on Kongsøya, are beyond the limit of the radiocarbon dating method (Salvigsen, 1981), and hence the upper beaches might have been considered as belonging to a separate, older generation (cf. Boulton, 1979; Salvigsen and Nydal, 1981; Schytt, 1981a, b).

Marine pelecypods

The next two examples listed in Table 1 are from sites close to Sundance Power Station on the Nelson River in Manitoba. The reason for the cross-checking in this case was

From: Scientific and Technical Notes in Current Research, Part A; Geol. Surv. Can., Paper 83-1A.

Table 1

Radiocarbon age determinations

Location	Approximate Co-ordinates	Collector	Material[1,2]	Field Sample No.	Laboratory designation[3]	Age (uncorrected)	$\delta^{13}C$ ‰	Age (corrected)[4,5]	Remarks
Near Cape Anne, Somerset Is., N.W.T.	74°02'N, 94°51'W elev. 103 m	A.S. Dyke, 1977	Walrus skull (**Odobenus rosmarus**)	DCA-77-B9 (NMC-34510-B)	S - 1392	2 420 ± 65			Determination on the organic fraction derived from the ivory of the right tusk (Dyke, 1979).
					GSC - 3081	2 440 ± 180	-24.7	2 450 ± 180	Determination on the organic fraction derived from 696.5 g of mandible from the the same skull. Sample mixed with dead gas for counting. One 3-day count in the 2 L counter.
Kongsøya, Svalbard	78°55'N, 29°04'E elev. 100 m	O. Salvigsen, 1979	Driftwood (**Larix** sp.)	-79,Sa. nr. 26	T - 3397		-26.1	9 790 ± 120	Salvigsen, 1981; Salvigsen and Nydal, 1981.
					GSC - 3039	9 840 ± 80	-24.4	9 850 ± 80	One 3-day count in the 5 L counter.
					GSC - 3039	9 900 ± 110	-24.4	9 910 ± 110	One 3-day count in the 2 L counter.
Nelson River (at Sundance Power Sta.), Manitoba	56°32'N, 94°01'W elev. 220 m	E. Nielsen, L.A. Dredge, 1981	Marine shells (**Hiatella arctica**)	EN 442	GSC - 3326	7 150 ± 70	+1.5	7 180 ± 70	Nielsen and Dredge, 1982. One 3-day count in the 5 L counter.
				EN442(c)	BGS - 714	6 900 ± 150			H. Melville, personal communication, 1982.
Nelson River (opposite Sundance Power Sta.), Manitoba	56°32'N, 94°00'W elev. 263 m	E. Nielsen, L.A. Dredge, 1981	Marine shells (**Hiatella arctica**)	EN 411(c)	GSC - 3367	6 750 ± 80	+0.3	6 760 ± 80	Nielsen and Dredge, 1982. Two 1-day counts in the 5 L counter.
				EN 411(c)	BGS - 791	6 760 ± 100			H. Melville, personal communication, 1982.
Webber Glacier Ellesmere Is., N.W.T.	80°53'N, 82°15'W elev. 175 m	R. Mäusbacher, D.Barsch, 1978	Wood (**Salix** sp.)		H 5607 - 5148	37 550 ± 1420			Völk, 1980; King, 1981; Barsch et al., 1981.
					GSC - 3427	38 200 ± 1240	-29.7	38 200 ± 1240	A portion of wood already pretreated at Heidelberg. GSC date based on one 7-day count in the 5 L counter.

[1] Determination of walrus species by C.R. Harington, National Museum of Natural Sciences, Ottawa; wood determinations by R.J. Mott, Quaternary Paleoecology Laboratory, GSC; marine pelecypods determined by W. Blake, Jr. The walrus is "almost certainly **Odobenus rosmarus rosmarus,** the Atlantic walrus" (C.R. Harington, personal communication, October 1982).

[2] The outermost 20% shell material in each sample was removed by HCl leach.

[3] Laboratory designations: S = Saskatchewan Research Council, Saskatoon, Sasktachewan; GSC = Geological Survey of Canada, Ottawa, Ontario; T = Laboratoriet for Radiologisk Datering, Trondheim – N.T.H., Norway; BGS = Brock Geological Sciences, Brock University, St. Catharines, Ontario; H = Institut für Umweltphysik der Universität Heidelberg, Heidelberg, Federal Republic of Germany.

[4] All age determinations from the Radiocarbon Dating Laboratory, Geological Survey of Canada, are based on a ^{14}C half-life of 5568 ± 30 years and 0.95 of the activity of the NBS oxalic acid standard. Ages are quoted in conventional radiocarbon years before present (BP), where "present" is taken to be 1950. All finite age determinations from this laboratory are based on the 2σ criteria, i.e., there is a 95% probability that the correct age in radiocarbon years lies within the stated limits of error. All $^{13}C/^{12}C$ ratios were determined under contract by R. Drimmie, Waterloo Isotope Analysts, Inc., using equipment at the Department of Earth Sciences, University of Waterloo. Relative to the PDB standard, it is GSC practice to normalize $\delta^{13}C$ values on terrestrial organic materials and bones of all types to -25.0 ‰, whereas marine shells are normalized to 0.0 ‰ (Lowdon and Blake, 1970).

[5] The $^{13}C/^{12}C$ value of -26.1 ‰ used by Trondheim is a mean value, based on results obtained beween 1975 and 1979 (Gulliksen, 1981).

that the first results, received by E. Nielsen (Manitoba Dept. of Energy and Mines) from Brock University indicated that both collections were in the 8000 to 9000 year range, i.e., at least 1000 years older than a number of previous age determinations on marine pelecypods along the southwest coast of Hudson Bay (cf. Craig, 1969; Lowdon and Blake, 1981, p. 7). Two previous determinations had also given results close to, or over 8000 years (Wagner, 1967; Lowdon and Blake, 1970, p. 64), and as the dates had major implications with regard to the timing of the Laurentide Ice Sheet's disintegration in the Hudson Bay region, a careful check was in order.

The first result, on shells of the common arctic pelecypod **Hiatella arctica** recollected in 1981 at the same site as the original collection, gave a date of 7180 ± 70 years (GSC-3326) – close to 2000 years younger than the original determination at Brock. For the second determination, also on a new collection of **Hiatella arctica** shells made in 1981, a different approach was tried, one that can only be done with a large collection: 533 individual valves, all measuring less than 2.5 cm in length, were broken in half, so that samples as nearly identical as possible could be dated in the two laboratories; 47.9 g was used by the GSC laboratory, 50.9 g was sent to Brock.

As it turned out, the source of the error was in the age calculation, specifically in applying a different factor for the activity of the new oxalic acid standard (cf. Stuiver, 1980). Once this correction was made, the recalculated value for BGS-714 (6900 ± 150 years) was reasonably close to the result on the recollected sample: GSC-3326 (7180 ± 70 years). In the case of the new collection that was split in half, the results were: BGS-791 (6760 ± 100 years) and GSC-3367 (6750 ± 80 years, uncorrected for isotopic fractionation; 6760 ± 80 years, corrected). Such close agreement is encouraging indeed! The new age determinations fit well into the regional pattern of marine incursions (Nielsen and Dredge, 1982).

Englacial arctic willow wood

The final cross-check reported here was carried out on a sample that was unusual both for the collection locale and the resultant age. During the course of the Heidelberg Ellesmere Island Expedition of 1978, a sample of wood – **Salix** sp., presumably of local origin – was collected from the lower, debris-laden zone of Webber Glacier in northern Ellesmere Island, Northwest Territories. This sample gave an age of 37 550 ± 1420 years (H 5607-5148; Völk, 1980; King, 1981; Barsch et al., 1981). A 9.3 g (dry weight) subsample, already pretreated with 0.3N HCl (boiling) and hot distilled water rinses at Heidelberg, was sent to the Geological Survey of Canada so that a separate age determination could be carried out. After our usual pretreatment, which includes both NaOH and HCl leaches, the sample was counted on two occasions, for a total of seven days. The result was 38 200 ± 1240 years (GSC-3427), a result that is well within the limits of error of the determination made in Heidelberg.

The implications of this sample are considerable. It is clear that part of the valley occupied by the snout of Webber Glacier was ice-free some 35 000 to 40 000 years ago, and this is the second such site discovered on Ellesmere Island (cf. Blake, 1982). Until the late 1970s no sites with terrestrial organic debris or buried tundra surfaces of finite mid-Wisconsin age has been found in the entire Canadian Arctic Archipelago (Blake, 1974; Blake and Matthews, 1979). Now, because of the relation of the dated organic materials to present-day outlet glaciers, it is clear that at these two sites, at least, there is more ice today than during the time interval corresponding to a period of ice withdrawal at many lower latitude northern hemisphere localities (cf. Dreimanis and Raukas, 1975).

References

Barsch, D., King, L., and Mäusbacher, R.
1981: Glaziologische Beobachtungen an der Stirn des Webber-Gletschers, Borup-Fjord-Gebiet, N-Ellesmere Island, N.W.T., Kanada; in Ergebnisse der Heidelberg-Ellesmere Island-Expedition, ed. D. Barsch and L. King; Heidelberger Geographische Arbeiten, Heft 69, p. 269-284.

Blake, W., Jr.
1961: Radiocarbon dating of raised beaches in Nordaustlandet, Spitsbergen, in Geology of the Arctic, ed. G.O. Raasch; Proceedings of the First International Symposium on Arctic Geology (Calgary, Alberta, 1960); University of Toronto Press, Toronto, p. 133-145.

1972: Climatic implications of radiocarbon-dated driftwood in the Queen Elizabeth Islands, Arctic Canada; in Climatic Changes in Arctic Areas During the Last Ten-Thousand Years, ed. Y. Vasari, H. Hyvärinen, and S. Hicks; Proceedings of a symposium held in Oulanka and Kevo, Finland, 1971; Acta Universitatis Ouluenis, Scientiae Rerum Naturalium No. 3, Geologica No. 1, p. 77-104.

1974: Studies of glacial history in Arctic Canada. II. Interglacial peat deposits on Bathurst Island; Canadian Journal of Earth Sciences, v. 11, p. 1025-1042.

1980: Radiocarbon dating of driftwood; inter-laboratory checks on samples from Nordaustlandet, Svalbard; in Current Research, Part C; Geological Survey of Canada, Paper 80-1C, p. 149-151.

1982: Terrestrial interstadial deposits, Ellesmere Island, N.W.T., Canada; American Quaternary Association, 7th Biennial meeting (Seattle, Washington, 1982), Abstracts, p. 73.

Blake, W., Jr. and Matthews, J.V., Jr.
1979: New data on an interglacial peat deposit near Makinson Inlet, Ellesmere Island, District of Franklin; in Current Research, Part A; Geological Survey of Canada, Paper 79-1A, p. 157-164.

Boulton, G.S.
1979: Glacial history of the Spitsbergen archipelago and the problem of a Barents Shelf ice sheet; Boreas, v. 8, p. 31-57.

Craig, B.G.
1969: Late-glacial and postglacial history of the Hudson Bay region; in Earth Science Symposium on Hudson Bay, ed. P.J. Hood; Geological Survey of Canada, Paper 68-53, p. 63-77.

Dreimanis, A. and Raukas, A.
1975: Did Middle Wisconsin, Middle Weichselian, and their equivalents represent an interglacial or an interstadial complex in the northern hemisphere?; in Quaternary Studies, ed. R.P. Suggate and M.M. Cresswell; The Royal Society of New Zealand, Wellington, p. 109-120.

Dyke, A.S.
1979: Radiocarbon-dated Holocene emergence of Somerset Island, central Canadian Arctic; in Current Research, Part B; Geological Survey of Canada, Paper 79-1B, p. 307-318.

Dyke, A.S. (cont.)
1980: Redated Holocene whale bones from Somerset Island, District of Franklin; in Current Research, Part B; Geological Survey of Canada, Paper 80-1B, p. 269-270.

Gulliksen, S.
1981: Korreksjon av dateringer for isotopisk fraksjonering; Daterings Nytt, Nr. 5, p. 7-10.

Häggblom, A.
1982a: Flytande ved och drivande is i Arktis; Fauna och flora, v. 77, p. 121-128.

1982b: Driftwood in Svalbard as an indicator of sea ice conditions; Geografiska Annaler, v. 64A, p. 81-94.

Harington, C.R.
1975: A postglacial walrus (**Odobenus rosmarus**) from Bathurst Island, Northwest Territories; Canadian Field-Naturalist, v. 89, p. 249-261.

Hoppe, G., Schytt, V., Häggblom, A., and Österholm, H.
1969: Studies of the glacial history of Hopen (Hopen Island), Svalbard; Geografiska Annaler, v. 51A, p. 185-192.

King, L.
1981: Gletschergeschichtliche Arbeiten im Gebiet zwischen Oobloyah Bay und Esayoo Bay, N-Ellesmere Island, N.W.T., Kanada; in Ergebnisse der Heidelberg Ellesmere Island Expedition, ed. D. Barsch and L. King; Heidelberger Geographische Arbeiten, Heft 69, p. 233-267.

Knape, P.
1971: C-14 dateringar av höjda strandlinjer, synkrona pimpstensnivåer och iakttagelser av högsta kustlinjen på Svalbard; öpublicerad Licentiatavhandling, Stockholms Universitet, Stockholm, 142 p.

Lauritzen, Ø., Salvigsen, O., and Winsnes, T.S.
1980: Two finds of walrus skeletons on high levels in Svalbard; Norsk Polarinstitutt Årbok 1979, p. 67-69.

Lowdon, J.A. and Blake, W., Jr.
1970: Geological Survey of Canada radiocarbon dates IX; Radiocarbon, v. 12, p. 46-86.

1979: Geological Survey of Canada radiocarbon dates XIX; Geological Survey of Canada, Paper 79-7, 58 p.

1981: Geological Survey of Canada radiocarbon dates XXI; Geological Survey of Canada, Paper 81-7, 22 p.

Nielsen, E. and Dredge, L.
1982: Quaternary stratigraphy and geomorphology of a part of the lower Nelson River; Geological Association of Canada Annual Meeting (Winnipeg, 1982); Guidebook, Trip 5, 56 p.

Péwé, T.L., Rivard, N.R., and Llano, G.A.
1959: Mummified seal carcasses in the McMurdo Sound region, Antarctica; Science, v. 130, p. 716.

Salvigsen, O.
1978: Holocene emergence and finds of pumice, whalebones, and driftwood at Svartknausflya, Nordaustlandet; Norsk Polarinstitutt Årbok 1977, p. 217-228.

1981: Radiocarbon dated raised beaches in Kong Karls Land, Svalbard, and their consequences for the glacial history of the Barents Sea area; Geografiska Annaler, v. 63A, p. 283-291.

Salvigsen, O. and Nydal, R.
1981: The Weichselian glaciation in Svalbard before 15,000 B.P.; Boreas, v. 10, p. 433-446.

Schytt, V.
1981a: Ymer-80's landbaserade naturgeografiska forskning; Ymer, Årsbok 1981, p. 51-66.

1981b: Studies of present and Pleistocene glaciation in Nordaustlandet and adjoining islands; in Geoscience during the Ymer-80 expedition to the Arctic, by V. Schytt, K. Boström, and C. Hjort; Geologiska Föreningens i Stockholm Förhandlingar, v. 103, Part 1, p. 109-119.

Stewart, T.G. and England, J.
– Holocene sea ice variations and paleo-environmental change,- northernmost Ellesmere Island, N.W.T., Canada; Arctic and Alpine Research, v. 15. (in press)

Stuiver, M.
1980: Workshop on ^{14}C reporting; Radiocarbon, v. 22, p. 964-966.

Völk, H.R.
1980: Records of emergence around Oobloyah Bay and Neil Peninsula in connection with the Wisconsin deglaciation pattern, Ellesmere Island, N.W.T., Canada: a preliminary report; Polarforschung, v. 50, p. 29-44.

Wagner, F.J.E.
1967: Additional radiocarbon dates, Tyrrell Sea area; Maritime Sediments, v. 3, p. 100-104.

INVESTIGATIONS IN THE VICINITY OF MOUNT SEDGWICK, YUKON TERRITORY

Projects 303121 and 750069

D.C. Findlay and R.T. Bell
Economic Geology Division

In an earlier assessment of the mineral and fuel resource potential of the proposed northern Yukon National Park, the Mount Sedgwick area was identified as having potential for tungsten, uranium, molybdenum and possibly placer gold mineralization (Geological Survey of Canada, 1980a). In July 1982, fieldwork was carried out in the vicinity of Mount Sedgwick in the area between Babbage and Crow (Tuluag) rivers (Fig. 1). The objective of the 1982 field work was to obtain geological and geochemical information for this area which lies within the eastern part of the proposed park.

The 1982 investigations comprised:

a. a study of local geological relationships and reported mineral occurrences;

b. the collection of stream sediments samples to increase the density of geochemical data over that which was obtained from a 1978 regional geochemical survey (Geological Survey of Canada, 1980a, b, 1981); and

c. the collection of heavy mineral samples (panned concentrates) from selected stream sites.

The stream silt and heavy mineral samples are currently being analyzed and results from this aspect of the 1982 work will be reported later. The following observations pertain mainly to (a) above:

1. fragments of a fine to coarse crystalline, biotite-feldspar-quartz gneiss (up to 40 cm diameter) were found on the northwest flank of Mount Sedgwick about 60 m below the summit area (Fig. 1, locality 1). They were initially detected by scintillometer as they display 3 to 5 times background (gamma) radioactivity. Preliminary mineral investigation has not identified any specific mineral that can account for the anomalous nature.

   These blocks are interpreted to come from xenoliths enclosed within the Sedgwick stock. The stock cuts only Precambrian rocks (Neruokpuk Formation) in this area.

2. Minor Cu-Mo-W-(U) mineralization was found at location 2 (Fig. 1) on Trail River on the south side of Sedgwick pluton. Previously Bell and Jones (1979) reported disseminated chalcopyrite and molybdenite in a sericitized zone at this location along with anomalous radiometric background (approximately 5 times background). During this 1982 investigation minor scheelite was also found at this location.

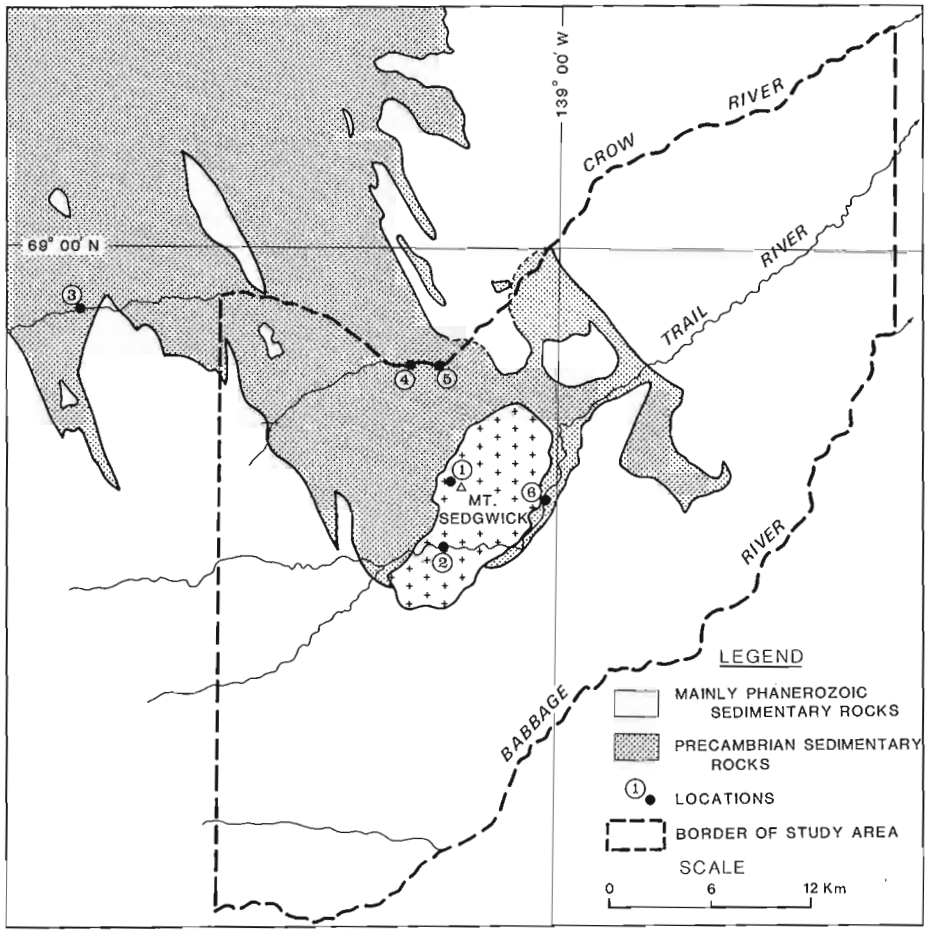

Figure 1. *General geology, of Mount Sedgwick area, Yukon. Crosses in centre of map area delineate Sedgwick stock. Numbered localities are described in text.*

From: Scientific and Technical Notes in Current Research, Part A; Geol. Surv. Can., Paper 83-1A.

3. Minor placer gold was found at four locations (locations 3, 4, 5, and 6, Fig. 1) during the routine sampling of heavy minerals by panning. At location 3, on Crow River) the visible gold comprised a single colour in samples from stream sediments in fractures in bedrock along the south riverbank upstream from the principal study area. At location 4 on Crow River, many colours and a few grains, one as large as 0.5 mm diameter, were obtained in panning sediments trapped in natural riffles formed by bedrock ledges. At location 5, a short distance farther downstream on Crow River, only a few colours were observed in samples from similar riffles. At location 6 on Trail River the visible gold comprised only 4 single colours in samples from stream sediments in fractures in bedrock along the south river bank. However, locations further downstream on Trail River failed to disclose any colours. These and other heavy mineral samples are currently being analyzed.

We express our thanks to A.T. Cross, field assistant and to J. Hodges, Okanagan Helicopter pilot, who aided in collecting heavy mineral samples.

References

Bell, R.T. and Jones, L.D.
1979: Geology of some uranium occurrences in western Canada; in Current Research, Part A, Geological Survey of Canada, Paper 79-1A, p. 397-399.

Geological Survey of Canada
1980a: Assessment of Mineral and Fuel Resource Potential of the Proposed Northern Yukon National Park and Adjacent Areas (Phase 1); Geological Survey of Canada, Open File 760, 35 p.

1980b: Regional stream sediment and water geochemical reconnaissance data, Yukon Territory – 117A and parts of 117B, C, and D; Geological Survey of Canada, Open File 565 (Rev. 1980), NGR45-1978, 89 p.

1981: National Geochemical reconnaissance, 1:2 000 000 coloured compilation map series, Northern Yukon and Northwest Territories – 117A and parts of 117B, C, and D; Geological Survey of Canada, Open File 730, 22 p.

Norris, D.K.
1981a: Geology, Blow River-Davidson Mountains, Yukon Territory and Northwest Territories; Geological Survey of Canada, Map 1516A, 1 250 000 scale.

1981b: Geology, Herschell Island-Demarcation Point, Yukon Territory; Geological Survey of Canada, Map 1514A, 1:250 000 scale.

NONCONFORMITY AT THE BASE OF UPPER PROTEROZOIC MISINCHINKA GROUP, DESERTERS RANGE, NORTHERN ROCKY MOUNTAINS

Project 700047

C.A. Evenchick[1]
Cordilleran Geology Division

Deserters Range

Mapping of the Deserters Range, which flanks the Northern Rocky Mountain Trench (NRMT) east of Williston Lake (Fig. 1), was started in the 1981 field season (Evenchick, 1982) and completed early in the 1982 season.

Detailed examination confirmed that quartzite (unit 2, Fig. 2, 3) which is the lowest stratigraphic unit of the upper Proterozoic Misinchinka Group overlies gneissic granite (unit 1) nonconformably. Quartz-feldspar pebble conglomerate about 15 cm thick overlies the granite and grades upward through gritty quartz-feldspar sandstone into relatively pure quartzite over a stratigraphic interval of several metres.

A U-Pb model age on zircons from the granite is 725 Ma (R. Parrish, personal communication, 1982). The gneissic granite appears to be exposed in the core of an anticline truncated by steep faults in the Northern Rocky Mountain Trench (Fig. 3, 4).

Summary

In the Deserters Range, basement gneiss, dated at 725 Ma, is overlain nonconformably by feldspathic quartzite and orthoquartzite. Orthoquartzite is the basal unit of a stratigraphic assemblage ranging from upper Proterozoic to Lower Cambrian.

Reference

Evenchick, C.A.
1982: Stratigraphy, structure and metamorphism in Deserters' Range, northern Rocky Mountains, British Columbia; in Current Research, Part A, Geological Survey of Canada, Paper 82-1A, p. 325-328.

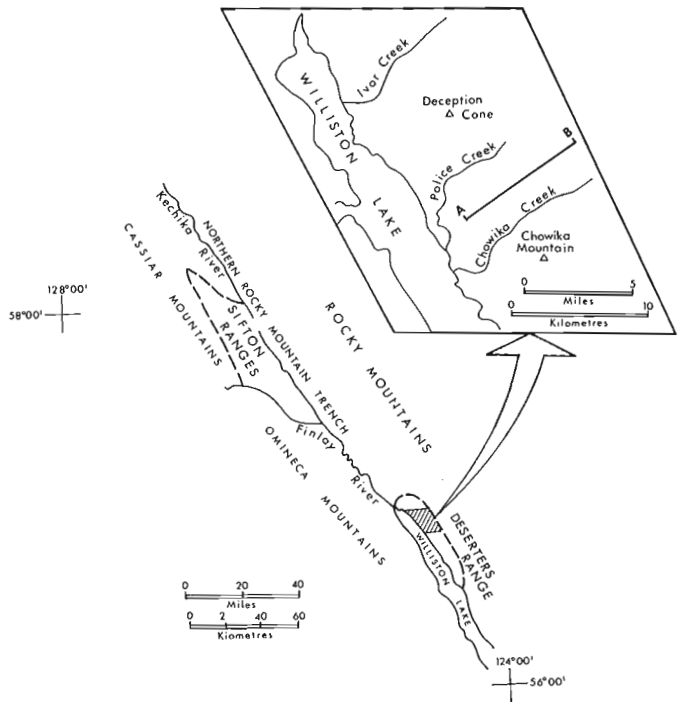

Figure 1. *Map of study area.*

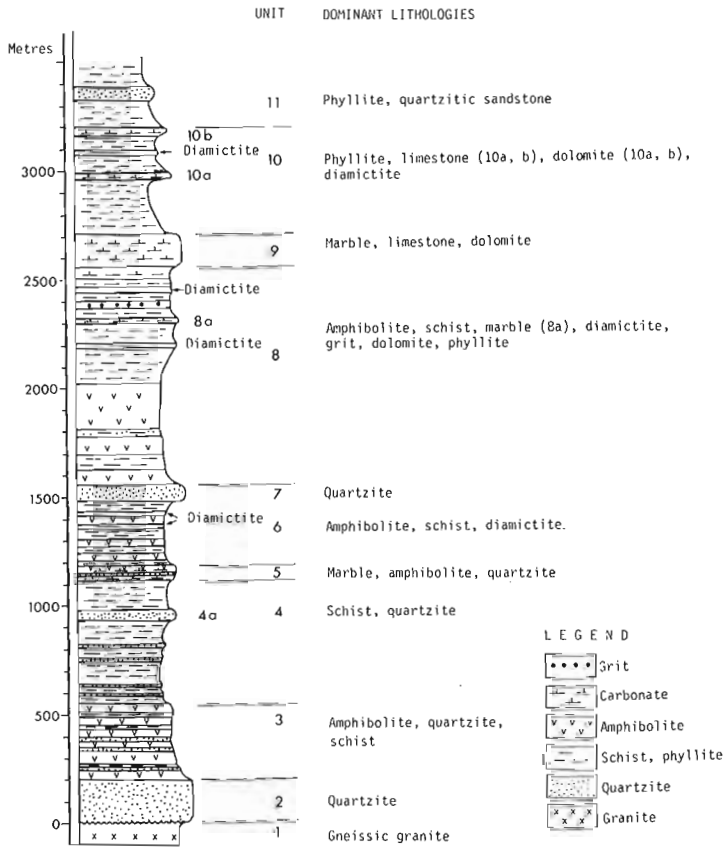

Figure 2. *Stratigraphic column, Deserters Range.*

[1] Department of Geological Sciences, Queen's University, Kingston, Ontario.

From: Scientific and Technical Notes in Current Research, Part A; Geol. Surv. Can., Paper 83-1A.

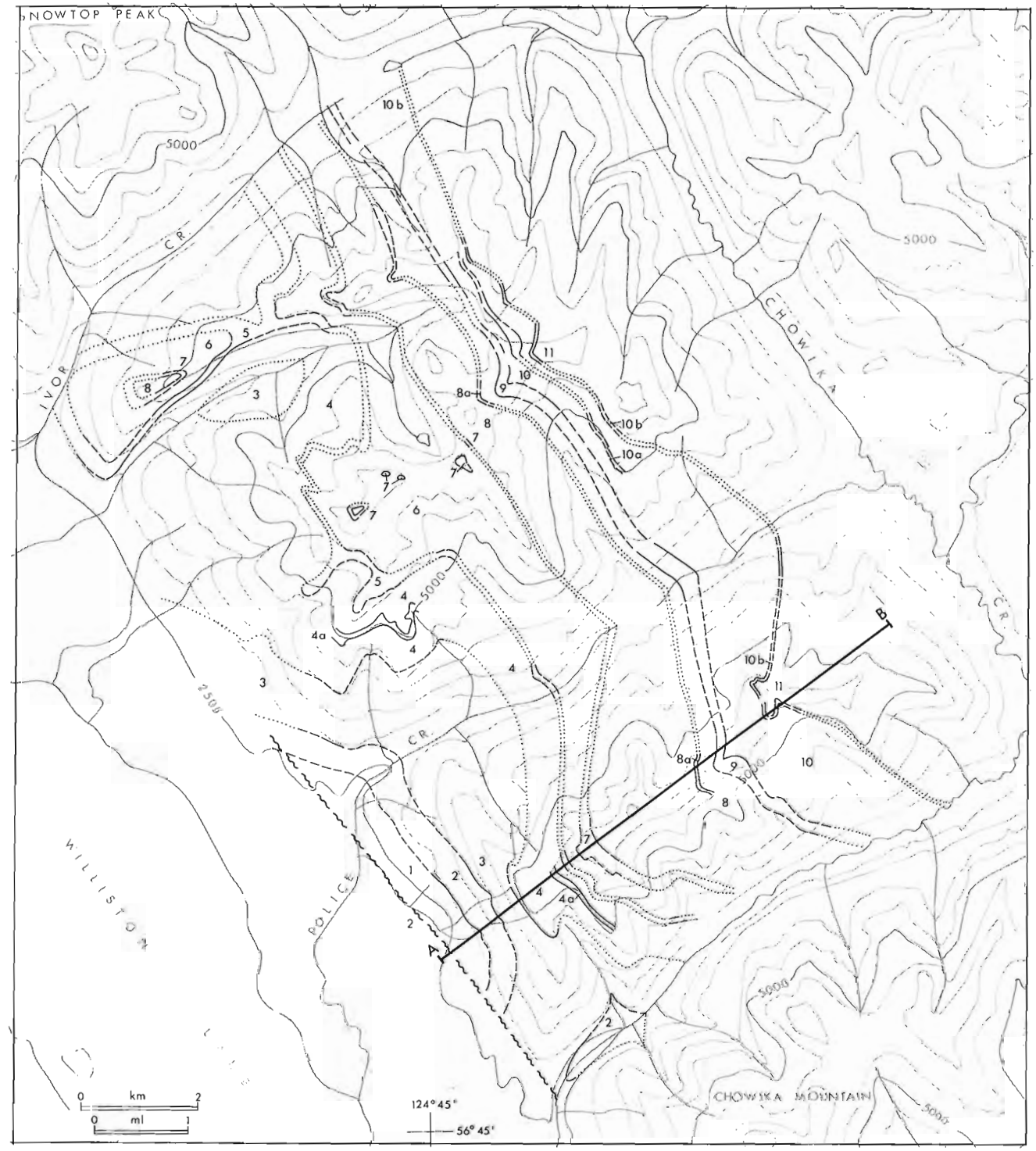

Figure 3. *Geology of study area and location of section AB.*

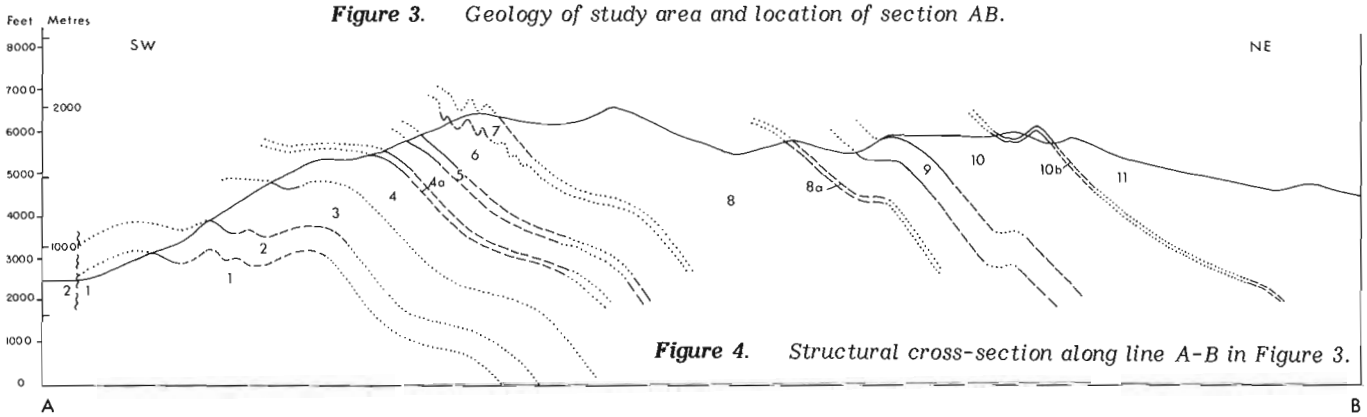

Figure 4. *Structural cross-section along line A-B in Figure 3.*

THE X-RAY CRYSTALLOGRAPHY OF A CHROMIAN ALUMOHYDROCALCITE FROM THE AKENOBE MINE, HYOGO PREFECTURE, JAPAN

Projects 680023 and 620308

A.C. Roberts and M. Bonardi
Central Laboratories and Technical Services Division

Introduction

Alumohydrocalcite, ideally $CaAl_2(CO_3)_2(OH)_4 \cdot 3H_2O$, has been systematically studied by numerous investigators since its original description by Bilibin (1926). It is known to occur at several localities within the U.S.S.R. (Bilibin, 1926; Lazarenko et al., 1963; Khomich and Cheglokov, 1969; Srebrodol'ski, 1971, 1976 and Popov, 1972), in Japan (Aikawa et al., 1972; Kato, 1973) and at single locations within Australia (Goldbery and Loughnan, 1977), Belgium (Fransolet and Melon, 1975), West Germany (Kautz, 1968, 1969), Italy (Vannucci et al., 1981), Pakistan (Paar, 1977), Poland (Hoehne, 1953; Morawiecki, 1962) and the United States (Dunning et al., 1975). General review articles of the known mineralogy, including comparative chemical analysis and X-ray powder diffraction data from various localities, are given by Srebrodol'ski (1976) and Vannucci et al. (1981). Nowhere, however, were crystals apparently coarse enough for X-ray crystallographic studies, hence the true symmetry and unit cell parameters are unknown.

The continuing study of the mineralogy of the silico-carbonatite sill exposed at the Francon quarry, Montreal has yielded yet another new species, APS #12, which appears at this time to be chemically and structurally the Sr-analogue of alumohydrocalcite. Because crystals of APS #12 are extremely fine grained, alumohydrocalcite specimens within the National Mineral Collection housed at the Geological Survey of Canada were examined in hopes that suitable material for single crystal studies would be available. Subsequently, the APS #12 powder pattern could then be indexed by reference to, and possible analogy with, the pattern of alumohydrocalcite. This search for suitable single crystals of alumohydrocalcite has proved successful and the X-ray results are reported herein.

The specimen used is from the Akenobe Mine, Hyogo Prefecture, Japan (Kato, 1973) and consists of four small pieces of tuffaceous rock with varying amounts of chromian alumohydrocalcite in each. It was received on exchange from A. Kato in 1968 and has been assigned National Mineral Collection catalogue #61906.

Acknowledgments

The senior author thanks J.L. Jambor, CANMET, for the specific gravity determination and A. Kato for the literature citation of alumohydrocalcite from the Akenobe Mine, Japan.

Physical Properties

Alumohydrocalcite occurs as pale to dark purplish red radiating crystal aggregates, anhedral crusts and rounded nodules on and in tuffaceous material. Within the tuff it is also found as thin monomineralic seams less than 1 mm in thickness. The total amount of sample available for study is less than 5 mg. Individual crystal fibres are very pale magenta, inclining to colourless; vitreous; transparent to translucent; and have a perfect cleavage parallel to the elongation (c). They rarely exceed 0.4 mm in length, with a length to width ratio approaching 100:1. The streak is pale purplish red, estimated hardness between 2 and 3, and the measured specific gravity determined by heavy liquids is 2.240 (4) g/cm^3.

Composition

A complete chemical analysis could not be obtained from the small amounts of alumohydrocalcite available. Cation percentages were determined by electron microprobe using the following procedure: several hand-picked crystal aggregates were mounted in cold-setting epoxy (Buehler Epo-kwick) and polished to yield a smooth surface. The carbon-coated samples were analyzed using a Material Analysis Company (MAC) electron microprobe equipped with a KEVEX energy dispersive spectrometer. Accelerating voltage was 20 KV with a specimen current of 10 nA (measured on a kaersutite standard) and a counting time of 100 seconds. A defocussed beam was utilized to minimize the effects of compositional changes and sample degradation due to electron bombardment.

Specimens were analyzed by EDA for the elements Al, Ca and Cr using the following standards: kaersutite (Al, Ca) and chromite (Cr). No other elements with atomic number greater than 11 were detected by energy dispersive analysis. The analytical raw data were processed using a modified version of the EMPADR computer program (Rucklidge and Gasparrini, 1969).

One of the crystal aggregates was X-rayed shortly after removal from the microprobe. The 57.3 mm Debye-Scherrer powder film confirmed the alumohydrocalcite structure thus indicating that any water loss due to vacuum or electron bombardment was minimal.

Two representative analyses gave CaO 14.8, 14.9; Al_2O_3 19.3, 19.0; Cr_2O_3 11.2, 11.0 wt %. The respective atomic ratios are Ca:(Al, Cr) = 1.00:1.99 and 1.00:1.94. The ratio of Al:Cr = 2.55:1 and 2.59:1, respectively.

The more recent chemical studies by Aikawa et al. (1972), Dunning et al. (1975), Kautz (1968), Srebrodol'ski (1974), and Vannucci et al. (1981) indicate that the ideal formula for alumohydrocalcite is $CaAl_2(CO_3)_2(OH)_4 \cdot 3H_2O$. Using this as a model, the analytical formula for Akenobe Mine material is then $Ca(Al_{1.44}Cr_{0.56})_{\Sigma 2}(CO_3)_2(OH)_4 \cdot 3H_2O$. This chromian-bearing alumohydrocalcite is similar in composition to the Californian material reported by Dunning et al. (1975).

It should be noted that complete confirmation of the ideal formula must await a detailed crystal structure analysis.

X-ray Studies

Numerous fibres were extracted from one of the coarser crystal aggregates and each checked for its degree of crystallinity and multiplicity by precession orientation methods. Only two elongate fibres, one mounted parallel to and the other normal to the glass spindle, gave satisfactory diffraction patterns and these were selected for detailed single crystal precession study. The levels photographed with unfiltered Cu radiation were 0kl, 1kl, h0l → h3l, hk0, hk1, $110^* \wedge c^*$ and $\bar{1}10^* \wedge c^*$.

Chromian alumohydrocalcite is triclinic, space group choices of P1(1) or $P\bar{1}(2)$ with the following reciprocal lattice cell parameters measured from precession single crystal films: $d_{(100)}$ = 6.45Å, $d_{(010)}$ = 14.31Å, $d_{(001)}$ = 5.66Å, α^* = 84°13', β^* = 87°35' and γ^* = 97°10'. The calculated direct cell parameters are: a = 6.50Å, b = 14.50Å, c = 5.68Å, α = 95.97°, β = 93.17° and γ = 82.59°.

From: Scientific and Technical Notes in Current Research, Part A; Geol. Surv. Can., Paper 83-1A.

Table 1

X-ray powder data for chromian alumohydrocalcite, Akenobe Mine, Hyogo Prefecture, Japan

Iest	dÅ meas.	dÅ calc.	hkl	Iest	dÅ meas.	dÅ calc.	hkl
80	7.15	7.13	020	5	2.642	2.640	$23\bar{1}$
80	6.44	6.43	100	3	2.618	2.618	221
100	6.18	6.17	$1\bar{1}0$	20	2.587	2.586	$12\bar{2}$
20	5.60	5.60	$\bar{1}10$	10	2.560	2.560	240
15	5.44	5.43	$01\bar{1}$			2.544	102
40	5.12	5.12	120	30	2.542	2.542	022
5	4.75	4.75	030			2.534	$03\bar{2}$
3	4.65	4.65	$02\bar{1}$	30	2.519	2.520	$\bar{1}12$
5	4.50	4.49	$\bar{1}20$			2.519	$\bar{1}1\bar{2}$
10	4.36	4.35	$11\bar{1}$	5	2.489	2.490	$\bar{1}50$
3	4.24	4.23	021			2.490	112
10	4.09	4.09	130	3	2.454	2.453	051
20	4.00	4.00	111			2.450	$13\bar{2}$
		4.00	$12\bar{1}$	15	2.422	2.422	$\bar{1}2\bar{2}$
3	3.82	3.82	$03\bar{1}$			2.377	060
15	3.61	3.61	$\bar{1}30$	3b	2.370	2.371	122
5	3.58	3.57	$\bar{1}21$			2.367	151
10	3.56	3.56	040			2.331	032
5	3.51	3.50	$13\bar{1}$	20	2.330	2.330	160
3	3.48	3.48	031			2.322	$04\bar{2}$
3	3.45	3.47	$\bar{1}21$	3	2.287	2.287	250
5	3.31	3.31	140	3b	2.271	2.269	$06\bar{1}$
30	3.225	3.229	210	3	2.247	2.242	$16\bar{1}$
50	3.216	3.216	200	10	2.195	2.197	$21\bar{2}$
10	2.999	3.000	$14\bar{1}$	3	2.169	2.172	$\bar{1}32$
10	2.958	2.959	$\bar{1}40$	3	2.158	2.162	310
3	2.885	2.885	$21\bar{1}$	3	2.143	2.144	300
40	2.851	2.852	050	3	2.128	2.131	320
10	2.819	2.822	002	10	2.104	2.104	$23\bar{2}$
		2.819	$01\bar{2}$	5	2.095	2.094	$\bar{2}12$
3	2.799	2.799	$\bar{2}20$	5	2.079	2.077	202
		2.724	141	3	2.057	2.058	330
5vb	2.711	2.719	012	70	2.037	2.037	070
		2.709	$\bar{2}11$	10	2.019	2.019	170
20	2.685	2.687	$14\bar{1}$	20	2.000	2.002	222

- Guinier camera, CoKα_1 radiation, Fe filter (λCoKα_1 = 1.78892Å)
- pattern run at CANMET by E.J. Murray
- b = broad line
- intensities estimated visually
- indexed on a = 6.499, b = 14.457, c = 5.678Å, α = 95.83°, β = 93.23°, α = 82.24°

These reciprocal cell parameters are completely unlike those reported by Kautz (1969) based on an electron diffraction study of alumohydrocalcite from Bergisch-Gladbach, Germany. He gave $d_{(100)}$ = 39.6Å, $d_{(010)}$ = 17.5Å, $d_{(001)}$ = 15.5Å, α^* = 93°, β^* = 96° and γ^* unknown. Because the powder patterns of the Japanese and German materials are very similar, especially for the stronger reflections, there appears to be little doubt that they represent only one mineral phase. Overexposed precession films of Japanese alumohydrocalcite failed to reveal additional weak diffraction nodes consistent with the electron diffraction results. The reciprocal lattice differences may then be attributed to multiple diffraction phenomena of the selected area electron diffraction patterns since the following general relationships appear to hold:

$d_{(100)}$	(this study)	$\approx \frac{1}{6} d_{(100)}$	(Kautz, 1969)
$d_{(010)}$	(this study)	$\approx d_{(001)}$	(Kautz, 1969)
$d_{(001)}$	(this study)	$\approx \frac{1}{3} d_{(010)}$	(Kautz, 1969)
reciprocal of β^*	(this study)	$\sim \alpha^*$	(Kautz, 1969)
reciprocal of α^*	(this study)	$\sim \beta^*$	(Kautz, 1969)

The Guinier diffraction pattern, presented in Table 1, was refined on 28 lines between 7.15Å and 2.000Å for which unambiguous indexing based on precession films was possible. The refined unit cell parameters are: a = 6.498(3)Å, b = 14.457(4)Å, c = 5.678(3)Å, α = 95.83(5)°, β = 93.23(3)°, γ = 82.24(3)°, V = 525.29Å^3 and a:b:c = 0.4495:1:0.3928. With Z = 2 and an Al:Cr ratio of 2.57:1, the calculated density is 2.213, in good aggreement with the measured result.

Debye-Scherrer powder patterns gave weak, somewhat diffuse arcs, except for the strongest reflections, and were considered unacceptable for film measurement and unit cell refinement.

References

Aikawa, N, Yoshida, M., and Ichikawa, K.
1972: Discovery of dawsonite and alumohydrocalcite from the Cretaceous Izumi Group in Osaka Prefecture, southwest Japan; The Journal of the Japanese Association of Mineralogists, Petrologists and Economic Geologists, v. 67, p. 370-385.

Bilibin, G.A.
1926: Alumohydrokalzit; Nowyi Miner. Sapiski Rossijkogo Mineralogitscheskogo Obschtschestwa, v. 4, p. 243-258.

Dunning, G.E., Cooper, J.F., and White, J.S.
1975: Chromian alumohydrocalcite from California, and knipovichite discredited; Mineralogical Record, v. 6, p. 180-183.

Fransolet, A.M. and Melon, J.
1975: Données nouvelles sur des minéraux de Belgique; Société Royale Sciences Liège, Bulletin, v. 44, p. 157-160.

Goldbery, R. and Loughnan, F.C.
1977: Dawsonite, alumohydrocalcite, nordstrandite and gorceixite in Permian marine strata of the Sydney Basin, Australia; Sedimentology, v. 24, p. 565-579.

Hoehne, K.
1953: Ein neues vorkommen von chromhaltigem alumohydrocalcit im Niederschlesischen Bergbau-Gebiet; Neus Jahrbuch für Mineralogie, Monatshefte, no. 1, p. 45-50.

Kato, A.
1973: Sakurai mineral collection; published by the Working Group for Commemoration of Dr. Sakurai's 60th Birthday; Tokyo, Japan, 173 p. (specifically p. 38).

Kautz, K.
1968: Ein vorkommen von alumohydrocalcit und allophan bei Bergisch-Gladbach; Neus Jahrbuch für Mineralogie, Monatshefte, no. 10, p. 350-358.

1969: Elektronenbeugung und infrarot-untersuchungen an alumohydrocalcit; Neus Jahrbuch für Mineralogie, Monatshefte, no. 3, p. 130-137.

Khomich, V.G. and Cheglokov, S.V.
1969: Formation of gypsum and alumohydrocalcite under supergene conditions in the Baley ore field; Izv. Zabayk. fil. Geograf. Obshch. SSSR, v. 5, no. 1.

Lazarenko, E.K., Lazarenko, E.A., Baryshnikov, E.K., and Malygina, O.A.
1963: Mineralogija Sakarpatija; Isd. Lwowskogo Universiteta.

Morawiecki, A.
1962: β-alumohydrocalcyt z Nowej Rudy; Kwartalnik geologiczny, Warszawa, v. 2, p. 539-570.

Paar, W.
1977: Ein vorkommen alumohydrocalcit von Chitral, Westpakistan, und neue beobachtungen an chromhaltigem alumohydrocalcit von Nowej Rudy, Polen (=Neurode, Schlesien); Aufschluss, v. 28, p. 269-272.

Popov, V.S.
1972: Alumohydrocalcite from the Gaurdak native sulfur deposit; Uzbek. Geol. Zh., no. 2, p. 65-69.

Rucklidge, J.C. and Gasparrini, E.L.
1969: Specifications of a computer program for processing electron probe analytical data: EMPADR VII; Department of Geology, University of Toronto.

Srebrodol'ski, B.I.
1971: The oxidized zone of sulfur ores of the Vodino deposit; Geol. Rudnykh Mestorozhd., no. 3.

1974: Alumohydrocalcites; Izvest. Akad. Nauk., SSSR, Ser. Geol., v. 10, p. 88-96. (English translation in International Geology Review, v. 18, p. 321-327 (1976))

Vannucci, S., Vannucci, R., and Franchi, R.
1981: L'alumohydrocalcite di Terlano (Bolzano); Rendiconti Società Italiana di Mineralogia e Petrologia, v. 37, p. 683-693.

POTASSIAN GAIDONNAYITE FROM THE KIPAWA AGPAITIC SYENITE COMPLEX, QUEBEC

Projects 680023 and 620308

A.C. Roberts and M. Bonardi
Central Laboratories and Technical Services Division

Introduction

During the latter stages of a comprehensive electron microprobe investigation of gittinsite from the Kipawa complex (Ansell et al., 1980), an unidentified Na-K-Zr silicate was encountered in polished thin section by energy dispersive analysis. X-ray powder diffraction dictated a gaidonnayite-like structure and, coupled with the qualitative chemical results, suggested that the silicate might be the potassium analogue of gaidonnayite ($Na_2ZrSi_3O_9 \cdot H_2O$). Subsequent quantitative electron microprobe analysis, however, indicated sodium greater than potassium; thus the Kipawa mineral is a potassian variety of gaidonnayite. This note details selected mineralogical properties as well as a paragenesis previously unrecognized for the mineral.

Gaidonnayite was originally described from Mont St. Hilaire, Quebec (Chao and Watkinson, 1974) and more recently has been found at Narsarsuk, Greenland (Mandarino and Sturman, 1978) and at several different localities in the U.S.S.R. (Khomyakov and Semenov, 1979).

Acknowledgments

The authors thank A.G. Plant for initial electron microprobe studies, J.D. Grice, National Museum of Canada, for the optical determinations, A.L. Littlejohn for discussion concerning paragenesis and G.Y. Chao, Carleton University, for the loan of Mont St. Hilaire gaidonnayite single crystal films.

Locality, Physical Description and Paragenesis

Potassian gaidonnayite occurs as an extremely rare constituent of eudialyte-rich pegmatitic lenses within a regionally metamorphosed agpaitic syenite complex at the Kipawa River, Villedieu Township, Témiscamingue County, Quebec, Canada. Associated minerals are vlasovite, gittinsite, apophyllite and traces of calcite and fluorite.

The mineral is found as 0.1 mm wide monomineralic rims separating massive vlasovite megacrysts from coexisting pods of gittinsite-apophyllite intergrowths. Individual randomly oriented crystal fibres average 40 μm long by 1 μm wide and show neither crystal faces nor prominent cleavage. Potassian gaidonnayite appears to be a late stage alteration-reaction product of the breakdown of vlasovite in the presence of gittinsite-apophyllite. Depletion of silica and the incorporation of potassium and water are essential to the mineral's formation but the exact nature of the chemical transformation is unclear at this time.

The optical refractive indices were determined with a spindle stage and Na light on a small fragment removed from a polished thin section. It is anisotropic with $\alpha = 1.574$ (1) and $\gamma = 1.580$ (1). The first order interference colours superficially resemble quartz; this is in marked contrast to the very dark vlasovite and the medium brown gittinsite-apophyllite mixtures.

Table 1

Chemical analysis of gaidonnayite

	Potassian Gaidonnayite (This study)	Gaidonnayite Mont St. Hilaire Chao & Watkinson (1974)	Gaidonnayite Narsarsuk, Greenland Mandarino & Sturman (1978)**
Na_2O	9.4	13.11	9.9
K_2O	6.1	2.20	6.1
CaO	2.1	–	0.4
SiO_2	42.6	42.51	43.1
ZrO_2	29.7	30.21	28.1
TiO_2	–	0.42	0.6
Nb_2O_5	–	3.00	0.9
H_2O	10.1*	9.25	n.d.
Total	100.0	100.70	89.1
	Cell content based on O = 9 in anhydrous part		
Na	1.27	1.72	1.33
K	0.54	0.19	0.54
Ca	0.15	–	0.03
Si	2.96	2.89	3.00
Zr	1.01	1.00	0.95
Ti	–	0.02	0.03
Nb	–	0.09	0.03
Σ	5.93	5.91	5.91

* H_2O calculated by difference.
** Analysis #13, page 197.

From: Scientific and Technical Notes in Current Research, Part A; Geol. Surv. Can., Paper 83-1A.

Table 2

X-ray powder data for potassian gaidonnayite

I obs.	dÅ meas.	dÅ calc.	hkl	I obs.	dÅ meas.	dÅ calc.	hkl
40	6.45	6.42	020	5	2.008	2.008	152
80	5.90	5.89	200	20	1.965	1.963	600
60	5.64	5.64	120	10	1.928	1.927	261
5	5.28	5.30	111			1.926	252
30	4.36	4.34	220	40	1.902	1.905	512
5	3.65	3.64	221			1.899	540
3	3.45	3.45	131	10	1.880	1.879	360
30	3.363	3.386	301			1.877	620
		3.350	320	5	1.857	1.857	323
10	3.238	3.238	012	5	1.807	several	
100	3.124	3.123	112	10	1.763	1.761	413
3	2.998	2.995	321	10	1.729	1.731	460
70	2.952	2.945	400	40	1.676	several	
3	2.889	2.895	041	3	1.627	several	
		2.878	122	5	1.608	several	
40	2.833	2.838	212	10	1.573	1.575	632
5	2.665	2.676	420			1.571	523
		2.656	331	3	1.551	several	
5	2.633	2.638	411	3	1.513	1.515	533
3	2.580	2.573	132	20	1.492	several	
40	2.496	2.498	312	20	1.472	1.472	800
20	2.408	2.406	232	20	1.452	several	
5	2.212	2.212	520	30	1.413	1.414	652
10	2.200	2.198	013				
3	2.168	2.170	440				
10	2.143	2.140	060				
20	2.105	2.106	160				
3	2.057	2.059	213				
10	2.039	2.039	061				
		2.038	052				

114.6 mm Debye-Scherrer camera, Cu radiation Ni filter
($\lambda CuK\alpha$ = 1.54178 Å)
intensities estimated visually
indexed on a = 11.778, b = 12.842, c = 6.693 Å

Chemical Composition

The cation weight percentages of potassian gaidonnayite were determined by energy dispersive analysis (EDA) using a Material Analysis Company (MAC) electron microprobe operated at 20 KV accelerating voltage and a counting time of 50 seconds. A defocussed beam was utilized to minimize the effects of compositional changes due to electron bombardment. The specimen current was 0.01 μA measured on a kaersutite standard. The following standards were used: biotite (K), kaersutite (Ca) and vlasovite (Na, Si and Zr). Vlasovite, which occurs in the same polished thin section as the potassian gaidonnayite, had previously been analyzed and the results compared to those reported by Gittins et al. (1973) from the same locality. Since the two analyses were virtually identical, the vlasovite adjacent to the potassian gaidonnayite was determined as a suitable standard. The raw data from the EDA were processed using a modified version of the EMPADR computer program of Rucklidge and Gasparrini (1969). The paucity of material dictated that water be determined by difference.

The average of 3 selected EDA analyses of potassian gaidonnayite is reported in column 1 of Table 1. The analytical formula derived from this analysis is $(Na_{1.23}K_{0.53}Ca_{0.15})\Sigma_{1.91}Zr_{0.98}Si_{2.87}O_{8.73}\cdot 2.26H_2O$. The general formula with O=9 in the anhydrous part is $(Na_{1.27}K_{0.54}Ca_{0.15})\Sigma_{1.96}Zr_{1.01}Si_{2.96}O_9\cdot 2H_2O$. Also reported in Table 1 for comparison purposes are the analyses of gaidonnayite from Mont St. Hilaire (Chao and Watkinson, 1974) and Narsarsuk, Greenland (Mandarino and Sturman, 1978). The latter was selected from numerous analyses as the closest to the Kipawa material.

X-ray Studies

The Kipawa material is too fine grained for X-ray single crystal study, but the X-ray powder diffraction pattern (Table 2) was successfully indexed by comparison with Mont St. Hilaire gaidonnayite (PDF 26-1387). Some inconsistencies exist between the two, most notably the absence on the Kipawa powder patterns of 5 weak to strong diffraction lines (5.84 (80), 4.64 (10), 4.17 (15), 3.094 (80) and 2.806 (30)) present on the Mont St. Hilaire powder pattern. These differences cannot be adequately explained at this time. The refined unit cell parameters, based on 16 lines between 3.238 and 1.413 Å for which unequivocal indexing was possible, are a = 11.778 (5), b = 12.842 (8) and c = 6.693 (4) Å. Single crystal precession and Weissenberg films of Mont St. Hilaire gaidonnayite were used to facilitate indexing of the powder pattern below 1.729 Å. With Z = 4, the calculated density, based on the analytical formula with Na : (K + Ca) = 1.84 : 1, is 2.701 g/cm^3. These cell parameters are slightly larger than those reported by Chao and Watkinson (1974) and obviously reflect the substitution of appreciable potassium for sodium within the crystal structure. This substitution may also account for the diffraction incongruities mentioned above.

References

Ansell, H.G., Roberts, A.C., Plant, A.G., and Sturman, B.D.
1980: Gittinsite, a new calcium zirconium silicate from the Kipawa agpaitic syenite complex, Quebec; Canadian Mineralogist, v. 18, p. 201-203.

Chao, G.Y. and Watkinson, D.H.
1974: Gaidonnayite, $Na_2ZrSi_3O_9 \cdot 2H_2O$, a new mineral from Mont St. Hilaire, Quebec; Canadian Mineralogist, v. 12, p. 316-319.

Gittins, J., Gasparrini, E.L., and Fleet, S.G.
1973: The occurrence of vlasovite in Canada; Canadian Mineralogist, v. 12, p. 211-214.

Khomyakov, A.P. and Semenov, E.I.
1979: First finds of gaidonnayite in the U.S.S.R.; Doklady Akademii Nauk SSSR, v. 248, p. 219-222.

Mandarino, J.A. and Sturman, B.D.
1978: The identity of α-catapleiite and gaidonnayite; Canadian Mineralogist, v. 16, p. 195-198.

Rucklidge, J.C. and Gasparrini, E.L.
1969: Specifications of a computer program for processing electron probe analytical data: EMPADR VII; Department of Geology, University of Toronto.

BOURGET AEROMAGNETIC CALIBRATION RANGE

Project 680081

Peter Hood and Peter Sawatzky
Resource Geophysics and Geochemistry Division

Introduction

The total field contours that appear on aeromagnetic maps are intended to accurately represent the configuration of the earth's magnetic field at a given level, usually 152 or 305 m (500 or 1000 feet) above the earth's surface. To an increasing extent regional magnetic anomaly maps are now being compiled in colour which utilize the results from adjoining surveys having a common boundary flown many years apart. It is important therefore in compiling such maps that there are not level shifts between the data in adjacent survey areas because these become immediately obvious in the final end product. Accordingly to ensure that aeromagnetic survey aircraft do in fact measure the total field values with an absolute accuracy of better than 10 gammas (N.B. accuracy as distinct from sensitivity), an aeromagnetic calibration range has been set up in a low gradient area near the village of Bourget about 45 km due east of Ottawa. A crossroads is used as a convenient reference point which is easily identified from the air and the values at 305 m and 152 m have been tied to the continously recording absolute magnetometers at the Ottawa Geomagnetic Observatory in Blackburn Hamlet operated by the EMR Earth Physics Branch. In order to obtain the actual total field values at a point 305 m above the crossroads at the instant the aeromagnetic survey aircraft passed over the crossroads, it is necessary to obtain the printout of the magnetic field values at Blackburn and this is done by pre-arrangement. It is now mandatory procedure prior to proceeding to the field that the Bourget Aeromagnetic Calibration Range be flown by contractors' survey aircraft on government aeromagnetic surveys. The Bourget Aeromagnetic Calibration Range appears to be the first such aeromagnetic calibration range set up for this purpose in the world and has seen continuous use during the past 4 years.

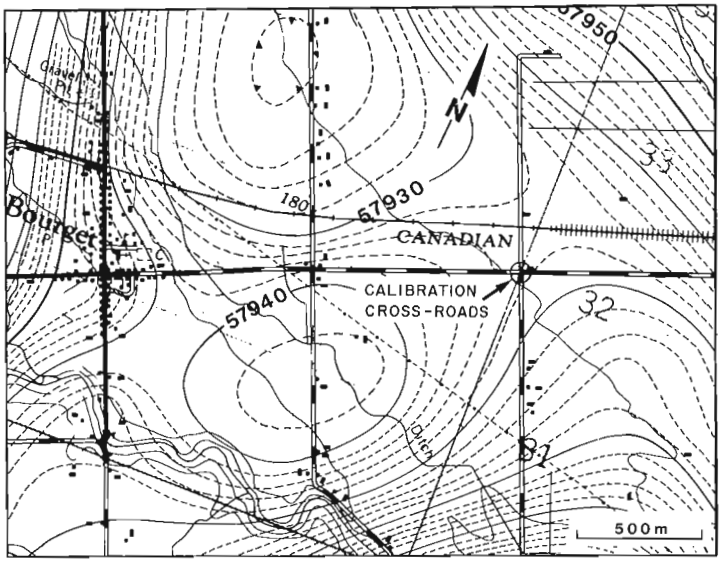

Figure 1. *High resolution total field aeromagnetic map of the Bourget area, about 45 km due east of Ottawa. The survey was flown at a height of 305 m with a 305 m flight line spacing, the contour interval for the map is 2 gammas.*

From: Scientific and Technical Notes in Current Research, Part A; Geol. Surv. Can., Paper 83-1A.

Aeromagnetic Surveying

Aeromagnetic surveys are carried out to map the small variations of the earth's magnetic field which are produced by the magnetic effects of the rocks close to the earth's surface. Presently the magnetometer most commonly utilized for airborne (and indeed for ground surveys) is the proton free-precession type whose output is a frequency (f) which is directly proportional to the ambient magnetic field (T). The constant of proportionality is the gyromagnetic ratio of the proton ($Y\rho P$) so that

$$T = \frac{2\pi}{Y_\rho} f = Kf$$

and the constant K = 23.4874. Thus the proton precession instrument is an absolute instrument and since frequency can be measured to a high degree of accuracy, its use permits magnetic fields to be accurately measured.

Magnetic Compensation of Aeromagnetic Survey Aircraft

In considering the influence of the survey aircraft itself on the magnetic field recorded by an inboard magnetometer, the interference can be divided into static and dynamic effects as follows:

1. the static effect is due to the permanent and induced magnetic fields produced by the ferrous components of the aircraft (and also by D.C. current loops) which slightly change the base level of the magnetic readings. The amplitude of the static effect will also depend on the heading of the aircraft with respect to magnetic north because the induced magnetization direction of the various ferrous components will change as the earth's magnetic field vector changes with respect to the aircraft flight direction.
2. the dynamic effect is produced by the unavoidable oscillatory manoeuvres of the aircraft as it flies. In order to estimate the magnitude of this effect, ±10° rolls, ±5° pitches and ±5° yaws are deliberately made in the four cardinal headings in a low magnetic gradient area and the sum without regard to sign of the (12) resultant magnetic excursions is called the figure of merit (FOM) of the aircraft. It is the dynamic effect which produces most of the noise swath which may be observed on the resultant analog profiles of the data. Thus a low FOM is required for the survey magnetometer to have a low noise swath. The remaining contributing cause of the noise swath is that produced by electrical interference from within the aircraft.

Thus the total field value recorded at any instant by an inboard magnetometer will differ somewhat from the true value due to the magnetic properties of the aeromagnetic survey aircraft itself. In any discussion of whether the measured total field values correspond to the actual total field values, there is also the question of the accuracy of the basic magnetometer circuitry utilized in measuring the frequency. Frequency measuring devices invariably require an accurate internal clock whatever the actual technique that is utilized. Consequently it follows that some form of calibration is required for an airborne magnetometer system. Helmholtz coils can and have been utilized for calibration purposes but they require that the aircraft be on the ground where the field is often disturbed and are really only suitable for the calibration of fluxgate magnetometers. Moreover although the Helmholtz coil calibration technique can ascertain that a change of one gamma (or one nanotesla in SI units) at the sensor will result in a one gamma change being recorded, it is rather difficult to ascertain that there is not an offset between the actual and measured total field value.

In the early days of aeromagnetic surveying following World War II, magnetometers were towed by a cable in a bomb-like housing known as a bird in order that the magnetic readings would be unaffected by the magnetic effects of the aircraft itself. However towing such devices behind aircraft proved troublesome, and required a motorized cable winch and a cradle for the bird mounted on the aircraft. When the techniques for nullifying or compensating the magnetic effects of the aircraft had been devised, the magnetometer was brought inboard to a position where the magnetic effect of the engines and other ferrous components was minimal. For most aircraft the aft end is the best place to locate a magnetometer and to maximize the separation from the magnetic components of the aircraft, it is usually placed in a cylindrical boom which protrudes from the tail section of the aircraft along its longitudinal axis; this is usually called a stinger by analogy with the anatomy of a bee.

To ensure that the reader is clear as to what we mean by accuracy as distinct from sensitivity, we define the terms as follows:

Accuracy. The total error of the recorded value from the true value of the quantity measured. This is normally expressed either as a ± quantity or as a percentage of the recorded value.

Sensitivity. The least change in the measured parameter occurring at the detector which the geophysical instrument is capable of accurately measuring in a repeatable fashion.

Thus a magnetometer may be capable of measuring the field strength change between two points with a sensitivity of one gamma or less although the accuracy of the individual measurements may only be 50 gammas. It follows that the accuracy of aeromagnetic survey measurements is mainly affected by the previously discussed static interference effect whereas the dynamic interference effect sets a limit on the effective sensitivity.

Calibration Range

It is clear that a good check on the accuracy of an aeromagnetic survey system may be obtained by flying the survey aircraft across an easily identifiable geographical location where the field is known at a given height. Due to diurnal variation effects however the reference value at the calibration point in question will change with the diurnal variation and also as years go by with the secular magnetic variation. The average total field value for the Ottawa Magnetic Observatory has decreased by approximately 96 gammas per year for the past three years. Thus it is necessary to tie the value at the calibration point to a permanent ground magnetic station. For best accuracy since an aeromagnetic survey aircraft travels about 75 m a second and in many airborne magnetometer systems the proton frequency is determined over a time period of about one second, it is necessary to choose a reference point in a low gradient area. With these requirements in mind, an aeromagnetic calibration range was set up at a crossroads near Bourget, Ontario which is about 45 km east of Ottawa and as the magnetic base station, the Ottawa Magnetic Observatory in Blackburn Hamlet is utilized. The procedure used in setting up the Bourget aeromagnetic calibration range was as follows.

The existing aeromagnetic contour map of the Ottawa area was first inspected and an area east of Ottawa in which the horizontal magnetic gradients were low was chosen for a high resolution aeromagnetic survey. The survey area was flown at a height of 300 m using the Queenair B80 aircraft of the Geological Survey of Canada and the lowest gradient area in which the horizontal gradient is about 1 gamma in 100 m was chosen as the location of the calibration point (see Fig. 1). A crossroads 2.6 km east of Bourget is conveniently located closeby although not exactly in the centre of the low gradient area. The geographic co-ordinates of the crossroads is 45°26'35"N, 75°07'40"W, in NTS sheet 31G/6e.

To tie the calibration point above the crossroads to the Ottawa Magnetic Observatory, a ground proton precession magnetometer was first taken to the observatory facility. Actually two vertically-separated calibration points were chosen, one at 150 m and one at 300 m above the crossroads. The sensor of the proton precession magnetometer, a Scintrex MP-2 (Serial No. 410119), was placed near the sensor for Magnetometer 1 in Building 5 and a number of readings and the time were recorded. This exercise established that the Scintrex MP-2 read 15γ too low. The Scintrex MP-2 magnetometer was then taken to the Bourget crossroads. During the complete duration of the exercise on July 17, 1979, the magnetometers in both Building 2 (AMOS or Magnetometer 2) and Magnetometer 1 in Building 5 were recording so that the readings obtained by the Scintrex MP-2 magnetometer could be corrected for diurnal variation changes. Magnetometer 2 in Building 2 produces a value every minute on a strip tape and Magnetometer 1 in Building 5 can be set to give an analog record at a speed of 12 inches per hour with 100γ across the chart.

It has been established that the total field value on the ground at Bourget crossroads is disturbed because of the presence of guard rails on the road to the south, steel culverts in the ditch to the north, and possibly due to the road material itself. However the aeromagnetic survey results show that these artifacts do not disturb the total field readings at the calibration points above the crossroads. In the past the value that it would be at the crossroads if those artifacts were not present was ascertained by carrying out road traverses in the two directions using the Scintrex MP-2 magnetometer and interpolating the value at the crossroads. However it is clear that more representative undisturbed values for the crossroads can be obtained by taking a series of measurements 75 m or so away from the roads in the four fields which bound the crossroads and so this was done. The repeated values obtained over a wide area in each of the fields corrected for the diurnal variation measured at the Ottawa Magnetic Observatory are shown in Figure 2.

It was found that the values in the SE field were disturbed by a few gammas possibly due to an old house site near the tree on the south road, so values obtained there have been ignored in obtaining the average for the crossroads. It is clear however that the horizontal gradients at Bourget are

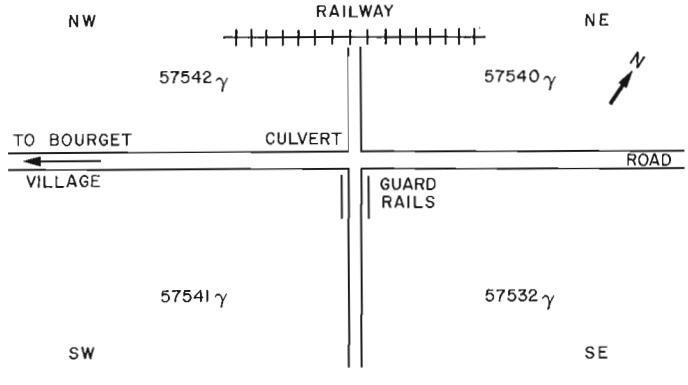

Figure 2. Sketch map showing the crossroads 2.7 km east-northeast of the village of Bourget, Ontario. The topographic map sheet is Russell, Ontario (NTS 31G/6e).

very low as the aeromagnetic map (Fig. 1) itself indicates and even at ground level vary by only one or two gammas in 200 m.

The results of the exercise established that the ground zero value at the Bourget crossroads at 1200 h EDT on July 17, 1979 approximated to 57 541γ when the Building 5 observatory value was 58 130γ. However, since the Scintrex MP-2 magnetometer read 15γ too low as ascertained by a comparison of the instrument values with the Building 5 observatory magnetometer values the actual values at Bourget ground zero was 57 556γ.

Having established the difference between the Ottawa Magnetic Observatory and crossroads values it was then necessary to measure the vertical gradient of the total field upwards to the calibration points at 150 and 300 m. This exercise was actually carried out on May 27, 1976 using the GSC Queenair aircraft which was flown along the four cardinal headings at heights of 152 m (500 ft), 228 m (750 ft), 305 m (1000 ft), 381 m (1250 ft), 457 m (1500 ft), 610 m (2000 ft) and 762 m (2500 ft). The results established that the gradient above the crossroads is linear being approximately 14 gammas positively upwards over the 305 m distance. Thus the difference between Building 5 observatory magnetometer value and Bourget 305 m value at 1200 h EDT on July 17, 1979 was therefore:

58130
57570
560γ

Similarly the difference at the 152 m calibration point is 553γ. Thus for an organization using the Bourget calibration range, the total field value from the Ottawa Magnetic Observatory must be obtained and the appropriate difference added to get the Bourget calibration value at the time the survey aircraft flew over the crossroads. Since this exercise was carried out, Magnetometer 1 has been moved from Building 5 to Building 4 where the magnetic field is 5γ lower. The respective difference values at the 305 m and 152 m levels are therefore respectively 555γ and 548γ. It is clear that the analog chart produced by Magnetometer 1 in Building 4 at the Ottawa Magnetic Observatory is the preferred reference magnetometer to obtain the Observatory value since the diurnal activity can also readily be viewed. This can be obtained by prior arrangement with Observatory staff at 613-824-2031 who will arrange for the analog chart to be run at 12 inches per hour instead of the normal 3 inches per hour. A 24 hour notice should be given.

In utilizing the Bourget aeromagnetic calibration range, survey aircraft are normally flown along the four magnetic cardinal headings across the crossroads with their flight path cameras operating and the field values for each cardinal heading is ascertained at the crossroads. The appropriate difference value (e.g. 555γ at 305 m) is subtracted from the Ottawa Magnetic Observatory reading at the exact time that the survey aircraft crossed the Bourget crossroads to get the true reading. The calibration errors for the airborne magnetometer when flown at the 305 m flight level may be ascertained from the following table when Magnetometer 1 in Building 4 is utilized:

Errors	Time over Bourget	A= T at Bourget in gammas	B= T at Blackburn in gammas	B+ 555γ	Errors in gammas = B+ 555γ -A	Errors in gammas
Magnetic						
N						$=N_E$
S						$=S_E$
E						$=E_E$
W						$=W_E$
					Average Error = _____	gammas

The crossroads are not oriented perfectly along the magnetic cardinal headings but are approximately 8°W of magnetic north. The aircraft heading errors are calculated from the following formulae:

$$\text{North/South Heading Error} = \frac{N_E - S_E}{2} \text{ gammas}$$

$$\text{East/West Heading Error} = \frac{E_E - W_E}{2} \text{ gammas}$$

In general the calibration errors should not exceed 10γ and the heading errors should be within 5γ in an acceptable aeromagnetic survey system.

A FAST POLYNOMIAL APPROXIMATION OF THE INTERNATIONAL GEOMAGNETIC REFERENCE FIELDS

Project 730081

K.G. Shih, Ford Doherty, and Ron Macnab
Atlantic Geoscience Centre, Dartmouth

Why Long Execution Times are Undesirable

In a recent investigation (Shih and Macnab, 1982) it was noted that the expressions which formulate the new International Geomagnetic Reference Field (IGRF) are mathematically more complex than the older models, and that their evaluation by computer can involve longer execution times.

These longer execution times have a non-trivial effect on the economics and scheduling of computer jobs that involve the manipulation of large data sets. For instance, the data set from just one of our major cruises (**Hudson** 75-009) contains in excess of 130 000 values of the total magnetic field. Deriving the magnetic anomaly from these readings using the older IGRF models took an estimated 500-600 CPU seconds on a Control Data Corporation Cyber 171 mainframe. The same process using the new reference field expressions took nearly 1200 CPU seconds.

Obviously, increased processing times can have a severe impact when operating on a limited computing budget. They can also affect turnaround times significantly, because the scheduling protocol employed by many computing centres defers longer jobs to the back of the input queue, at times into the overnight batch stream. Such delayed processing is often unacceptable.

Longer execution times also affect the processing of magnetic data on shipboard minicomputers, although in a different fashion. At sea, we tend to handle magnetic data in smaller blocks, typically the 1440 one-minute total field values collected during one day. Evaluating the new IGRF expression for this many data points consumes several minutes of CPU time on a slower minicomputer. With the machines and processing techniques in use aboard our ships, these extended execution times do not create problems in the scheduling or the availability of computer resources; however, they do manifest themselves as interruptions in an otherwise smooth sequence of interactive procedures, where an operator must sit and wait for this compute-intensive activity to run its course.

A Fast Approximation Technique

To circumvent the problems described above, we have implemented a fast approximation technique for calculating point values of the total geomagnetic reference field.

The technique involves the creation of a third-degree polynomial expression approximating the IGRF at any time with latitude and longitude as variables. The polynomial is derived by a least squares fit to the full IGRF expression over a limited region (typically ten degrees of latitude by ten degrees of longitude). Two such approximations are made, one year apart: the first polynomial approximates the IGRF at the beginning of a given year, the second at the end. Calculating an IGRF value for a specific location and date is thus reduced to evaluating the two polynomials according to position at the beginning and end of the appropriate year, and then performing a linear interpolation between the two results according to time.

For the 1980.0 – 1985.0 interval, this approximation yields total fields that are within 1 nanotesla of the full IGRF expression anywhere in the ten-degree by ten-degree area. Agreement can be improved to better than 0.25 nanotesla by incorporating correction factors that have been derived from the residuals of the least squares fits described above.

In our case, use of the approximation technique increases computer execution speeds by a factor of 40 to 45. For mainframe users, this translates into cheaper processing and faster turnaround for jobs involving large data sets. For example, the elapsed CPU time for the job described at the beginning of this note (i.e. the processing of 130 000 data points) is only 45 seconds using the approximation technique rather than 1200 seconds using the full IGRF expression. (Both times include fixed amounts for I/O and system overhead.) For minicomputer operators on our ships, the approximation method permits greater continuity in the flow if interactive data processing, because lengthy periods of 'dead' time are eliminated.

Software for Fast Approximation

The procedures for deriving the coefficients of the approximation polynomials and for the subsequent evaluation of these polynomials have been implemented in two sets of software: one for a Cyber 171 mainframe, the other for shipboard HP1000 minicomputers. The implementation and operating philosophies are not the same for these two classes of machine, because of the different kinds of data sets that each is called upon to handle.

Shipboard minicomputers are usually involved in the processing of data from one cruise in one area for one time period only. This can often be handled within the confines of a single ten-degree by ten-degree approximation area, valid for one year. (If necessary, a series of overlapping areas can be defined to cover the operating range of a given cruise.) At the beginning of a cruise, coefficients for the approximation polynomials are calculated and stored on disc. Then as each day's magnetic data are processed, the operator enters the name of the disc file containing the appropriate coefficients.

The shore-based mainframe, on the other hand, often handles multi-year data sets that may cover a region larger than the ten-degree by ten-degree approximation area. The approach here has been to create a library of subroutines that can approximate the IGRF over wide regions and over time intervals greater than one year. Each subroutine contains all the coefficients needed to create a range of ten-degree by ten-degree approximation polynomials; the appropriate coefficients are selected automatically according to the times and positions of the data points fed to the subroutine. We currently have three subroutines in use, applying to the following regions and time intervals:

i) northwest Atlantic (30-80°N, 40-80°W), 1980 – 1985
ii) Labrador Sea (45-65°N, 40-70°W), 1965 – 1985
iii) continental U.S.A. (25-55°N, 70-130°W), 1975 – 1980

Copies of the software related to this approximation method are available from the authors on request.

Summary

The longer execution times of computer programs that calculate the more complex formulae for the new International Geomagnetic Reference Fields cause increased processing costs as well as longer job turnaround times. They also cause prolonged intervals of 'dead' time while being executed on interactive processing systems. A simple polynomial technique has been devised that reduces execution times by a factor of 40 to 45 while approximating the full IGRF expressions to within 0.25 nanotesla. The technique has been implemented on a shore-based mainframe and on shipboard minicomputers.

Reference

Shih, K.G. and Macnab, R.
1982: The new International Geomagnetic Reference Fields: how good are they?; in Current Research, Part B, Geological Survey of Canada, Paper 82-1B, p. 167-168.

From: Scientific and Technical Notes in Current Research, Part A; Geol. Surv. Can., Paper 83-1A.

WEATHERING PIT FORMATION IN BEDROCK NEAR CORY GLACIER, SOUTHEASTERN ELLESMERE ISLAND, NORTHWEST TERRITORIES

EMR Research Agreement 52-4-81

Stephen H. Watts[1]
Terrain Sciences Division

Examples of intensely weathered terrain have been studied at widely scattered locations in east-central and southeastern Ellesmere Island during the past three field seasons (Watts, 1981a, b, in press). One such locality is a porphyritic granite ridge at 500 m a.s.l. immediately west of Cory Glacier (76°16'N, 80°8'W) on the southeast coast, some 75 km east-southeast of the settlement of Grise Fiord (Fig. 1). Preliminary bedrock mapping of this region has been done by Christie (1962, 1969) with more recent reconnaissance in progress (cf. Frisch et al., 1978). The most interesting, highly weathered nature of this site has been reported and illustrated by Blake (1978). This locality was examined briefly in July 1980 and was revisited in July 1981 to set up ongoing experiments for monitoring current rates of subaerial bedrock disintegration. In 1981 and 1982 data were also collected on the nature and distribution of pit features encountered.

Weathering pits have been found in most major rock types in virtually all climatic regions of the world, and their nature and occurrence have been reviewed by Hedges (1969). Such forms have been described from Arctic regions of Scandinavia and North America (e.g., Dahl, 1966; Watts, 1979) and in the latter region have been attributed to long continued subaerial weathering (Boyer and Pheasant, 1974; Sugden and Watts, 1977) in the presence of water ponded on upper outcrop surfaces.

One hundred and seven weathering pits developed in porphyritic granite were counted at the Cory Glacier site. The features range in size from a few centimetres to more than 160 cm across by up to 80 cm deep; average dimensions are 20 cm wide by 8 cm deep. The majority are circular to elliptical in outline and may be free of grus accumulations. The influence of wind deflation on grus removal was confirmed. Where grus was encountered in the pits, their floors were commonly sheltered by vertical to overhanging lips or by higher adjacent joint blocks (Fig. 2). Abundant grus was also noted in one pit containing a glacial erratic (Fig. 3).

Three distinct pit forms were observed. The smallest examples, measuring only a few centimetres in diameter by a few centimetres deep, are typically circular in outline with sharp rims and vertical walls. If it is assumed that the pits enlarge with time, it follows that these are incipient forms

Figure 1. Location map showing field study area.

[1] Geology Department, Sir Sandford Fleming College, P.O. Box 8000, Lindsay, Ontario K9V 5E6

From: Scientific and Technical Notes in Current Research, Part A; Geol. Surv. Can., Paper 83-1A.

Figure 2. Weathering pit measuring 50 cm across by 30 cm deep. Note the pronounced undercutting and grus accumulation. July 11, 1982.

Figure 3. Weathering pits developed in exposed, horizontal upper surface of a tor block in granite. A glacial erratic occupies one pit. Note the steep-sided and undercut walls of the pits which suggest that these pits are actively forming. Duplicate water samples obtained from the pit on the left were analyzed and revealed total dissolved salt concentrations of 215 ppm (cf. Table 1, Weathering Pit No. 3). Note also the grus present on the pit floor.

Figure 4. Four weathering pits occurring together and exhibiting similar dimensions. Here, pit walls are rounded indicative of a late destructive phase in pit development.

Figure 5. Large weathering pit, measuring 1.3 m across by 65 cm deep, with breached wall. July 15, 1981.

Figure 7. Weathering pits that have coalesced through breaching of walls into an elongated, trench-like form.

Figure 6. Same pit as illustrated in Figure 5 but containing rainwater to the level of the breached wall. July 10, 1982.

representing an early phase of weathering pit formation. It may be noteworthy that only eight such small features were recognized, suggesting that the majority of pits were initiated under earlier favourable conditions and have had sufficient time to grow beyond this initial form. Two large forms predominate. Some weathering pits have well defined lips with pronounced overhanging walls indicative of continued enlargement through lateral bedrock disintegration and undercutting (Fig. 2). This undercutting can be readily explained by the preservation of slightly indurated outcrop surfaces beneath which disintegration has proceeded. The largest examples of undercut pits are less than 35 cm in diameter, indicating that eventually undercut lips collapse, leaving a more typical third form. The majority of weathering pits reveal rounded rims suggestive of a later destructive phase during which deflation dominates (Fig. 4). The largest and deepest examples found are also of this type, implying that continued ponding of precipitation within the pits favours slow growth (Fig. 5, 6). Ultimate destruction of these forms can occur, as noted in 10 examples, through breaching of walls; moreover, these trench-like forms may channel water, resulting in further erosion (Fig. 7).

Ponding of precipitation would occur in small natural depressions in exposed horizontal joint block surfaces in the porphyritic granite typifying this ridge. Under arid to semi-arid high arctic conditions, slow evaporation would ensue with salts being concentrated about depression peripheries. Salt hydration and crystallization could in turn favour microfracturing, particularly in this coarsely textured rock type, leading to pit enlargement.

To begin to test this hypothesis, water samples were collected from rainfall, snowbanks, glacial meltwaters, and from a number of weathering pits at the Cory Glacier site for chemical analyses, the results of which are shown in Table 1.

Rainwater collected at the eastern base of the ridge is extremely soft, both in its cation concentration and in conductivity measurements completed in the field and in the laboratory. Similarly, snow obtained about both eastern and western flanks of the outcrop ridge and surface meltwaters, also originating from precipitation onto Cory Glacier, as taken in both 1980 and 1981, consists of nearly pure water. Over the short term, precipitation apparently does not contribute large amounts of salts to the exposures.

Indeed, water extracted from the weathering pits during rainfall was also nearly pure. In contrast, water from the same pit taken several hours after the storm showed a marked increase in total dissolved solids (cf. conductance values). Moreover, the salt concentrations of water samples from 9 weathering pits range from 80 to 335 ppm (125-500 - μmhos/cm) indicating that salts, particularly Na^+, $SO_4^=$ and Cl^- are concentrated in the pit waters. This can be explained by the evaporation of even nearly pure rainwater in the pit. Evaporation would, in turn, result in salt hydration and crystallization on pit walls, and from time to time on the pit bottoms, given total evaporation of pit waters. Subsequent precipitation would dissolve the salts and initiate the process over again. This might explain also why waters from larger pits were seen to have higher salt concentrations than waters from smaller ones. Moreover, eventual breaching of pit walls could result in greater flushing of salts out of these features during heavier rainfalls hindering further pit enlargement. The role of salt crystallization in bedrock disintegration under arid conditions is gaining recognition (e.g., Goudie, 1974, 1977; Sperling and Cooke, 1981a, b) and is currently under investigation by this author under controlled laboratory conditions of temperatures and humidities approaching those of the Cory Glacier site.

Table 1

Chemistry data based on 16 major ion analyses of water from weathering pits and other available sources at the Cory Glacier site

	Na^+	K^+	Ca^{++}	Mg^{++}	Total Fe	$SO_4^=$	NO_3^-	Alk.	Bicarb. Alk.	Cl^-		Conductivity - μmho/cm	TDS ppm	Remarks
Rainfall	< 0.5	0.1	< 1	< 1	0.08	< 1	< 0.1	2	2	< 1	<0.05	4	< 5	
Snowmelt, west side ridge	< 0.1	0.05	< 0.2	0.10	0.231	< 0.5	0.004	4	4	0.05	0.00	3.1	< 5	
Snowmelt, east side ridge	< 0.1	0.15	< 0.2	< 0.05	0.24	< 0.5	< 0.005	3	3	0.05	0.00	2.4	< 5	
Weathering Pit 1	1	0.1	< 1	< 1	0.04	< 1	< 0.1	1	1	2	0.70	8	< 5	Obtained during rainfall
Weathering Pit 1	42.5	1.9	12	7	0.05	24	0.5	5	5	83	1.50	335	225	Resampled 5 h after storm
Weathering Pit 2	16.5	1.5	10	2	5.40	14	< 0.1	7	7	34	1.70	170	110	
Weathering Pit 3	30	3.4	18	6	3.55	22	0.1	5	5	68	1.75	320	215	Fig. 3
Weathering Pit 4	60	2.7	18	9	0.07	35	0.8	4	4	111	2.35	500	335	Uppermost ridge location (Fig. 5, 6)
Weathering Pit 5	60	2.70	7.2	7.0	E	E	0.011	9	9	80.0	1.25	435	295	
Weathering Pit 6	14	0.70	2.6	2.1	1.0	E	0.004	4	4	25.0	0.60	125	80	
Weathering Pit 7	21	1.10	6.4	4.0	0.11	14.0	0.122	5	5	43.0	0.45	200	130	
Weathering Pit 8	28	1.40	7.0	4.25	0.07	18.0	0.065	4	4	53.5	0.50	245	162	
Weathering Pit 9	5.0	0.30	1.2	0.65	0.02	3.5	0.004	4	4	8.75	0.5	49	26	Small
Glacial meltwater, 1980	0.4	0.05	< 0.2	0.05	0.27	1.5	0.015	3	3	0.80	0.05	6	< 5	
Glacial meltwater, 1981	0.5	< 0.1	1	< 1	0.07	< 1	< 0.1	4	4	0.6	0.02	8.4	< 5	Same locality
Meltwater on Side Valley Glacier	0.5	< 0.1	< 1	< 1	0.02	< 1	< 0.1	3	3	1	<0.05	3.5	< 5	

E – insufficient sample to determine accurately

I wish to acknowledge the logistical air support provided by Polar Continental Shelf Project and the co-operation of the Ontario Ministry of the Environment in providing the water chemistry analyses presented.

References

Blake, W., Jr.
1978: Rock weathering forms above Cory Glacier, Ellesmere Island, District of Franklin; in Current Research, Part B, Geological Survey of Canada, Paper 78-1B, p. 207-211.

Boyer, S. and Pheasant, D.
1974: Delimitation of weathering zones in the fiord area of eastern Baffin Island, Canada; Geological Society of America, Bulletin, v. 85, p. 805-810.

Christie, R.L.
1962: Geology, southeast Ellesmere Island, District of Franklin; Geological Survey of Canada, Map 12-1962.

1969: Eastern Devon Island and southeastern Ellesmere Island, District of Franklin; in Report of Activities, Geological Survey of Canada, Paper 69-1, Part A, p. 231-4.

Cooke, R.U.
1979: Laboratory simulation of salt weathering processes in arid environments; Earth Surface Processes, v. 4, p. 347-359.

Dahl, R.
1966: Block fields, weathering pits and tor-like forms in the Narvik Mountains, Nordland, Norway; Geografiska Annaler, v. 48A, p. 55-85.

Frisch, T., Morgan, W.C., and Dunning, G.R.
1978: Reconnaissance geology of the Precambrian Shield on Ellesmere and Coburg Islands, Canadian Arctic Archipelago; in Current Research, Part A, Geological Survey of Canada, Paper 78-1A, p. 135-138.

Goudie, A.S.
1974: Further experimental investigation of rock weathering by salt and other mechanical processes; Zeitschrift fur Geomorphologie, Supplementband 21, p. 1-12.

1977: Sodium sulphate weathering and the disintegration of Mohenjo-daro, Pakistan; Earth Surface Processes, v. 2, p. 75-86.

Hedges, J.
1969: Opferkessel; Zeitschrift fur Geomorphologie, v. 13, p. 22-55.

Sperling, C.H.B. and Cooke, R.U.
1981a: Salt weathering in arid environments. I. Theoretical considerations; Bedford College Papers in Geography, no. 8, London, 60 p.

1981b: Salt weathering in arid environments. II. Laboratory studies; Bedford College Papers in Geography, no. 9, London, 60 p.

Sugden, D.E. and Watts, S.H.
1977: Tors, felsenmeer and glaciation in northern Cumberland Peninsula, Baffin Island; Canadian Journal of Earth Sciences, v. 14, p. 2817-2823.

Watts, S.H.
1979: Some observations on rock weathering, Cumberland Peninsula, Baffin Island; Canadian Journal of Earth Sciences, v. 16, p. 977-983.

1981a: Bedrock weathering features in a part of eastern High Arctic Canada: their nature and significance; Annals of Glaciology (Symposium on Glacial Erosion and Sedimentation, Geilo, Norway, 1980), v. 2, p. 170-175.

1981b: Near-coastal and incipient weathering features in the Cape Herschel-Alexandra Fiord area, Ellesmere Island, District of Franklin; in Current Research, Part A, Geological Survey of Canada, Paper 81-1A, p. 389-394.

– Weathering processes and products under arid Arctic conditions: A case from Ellesmere Island, Canada; Geografiska Annaler. (in press)

DISCUSSIONS AND COMMUNICATIONS
DISCUSSIONS ET COMMUNICATIONS

STRATIGRAPHY AND TECTONICS OF THE PEEL SOUND FORMATION, SOMERSET AND PRINCE OF WALES ISLANDS: DISCUSSION

Andrew D. Miall
Geology Department,
University of Toronto,
Toronto M5S 1A1

Manuscript received September 1, 1982

Introduction

A comprehensive re-evaluation of the Late Silurian and Early Devonian stratigraphy of the Boothia Uplift region was recently published by Thorsteinsson (1980). This is an important work as it incorporates, for the first time, biostratigraphic information derived from extensive conodont and vertebrate collections. Detailed correlations reported in this work led Thorsteinsson to make several suggestions regarding the timing and extent of diastrophic episodes of Boothia Uplift. The structural style of Boothia Uplift, and the origins of this tectonic element, were discussed by Kerr (1977). The writer has one area of disagreement with the conclusions presented in Thorsteinsson's (op. cit.) report, and suggests an origin for Boothia Uplift that differs from Kerr's (op. cit.) interpretations.

Using rather indirect evidence, Thorsteinsson interpreted the upper member of the Peel Sound Formation as late Lochkovian in age. The lower member of the formation on Prince of Wales Island is dated as no younger than early Pridolian, on the basis of conodonts and the trilobite **Hemiarges bigener** Bolton. Thorsteinsson (op. cit.) concluded that the time period corresponding to the late Pridolian and early Lochkovian is not represented by Peel Sound strata on either Somerset or Prince of Wales islands. Thorsteinsson (op. cit.) re-evaluated two localities where an angular unconformity had earlier been recorded involving the Peel Sound Formation, and stated that this was, in fact, a major regional unconformity between the two members.

Based on an evaluation of Thorsteinsson's data and field work carried out by the writer on both islands (Miall, 1969, 1970a,b; Miall and Gibling, 1978) the following points should be made:

1. The biostratigraphic correlation of the Upper Peel Sound Formation is inconclusive, and evidence presently available does not favour any time period between the early Pridolian and late Pragian.
2. The contact between the lower and upper members of the Peel Sound Formation can be demonstrated to be conformable at several localities close to Boothia Uplift.
3. The contact between the upper and lower members is defined on the basis of changes in conglomerate composition and grain size, but these may be markedly diachronous along strike.
4. Angular unconformities recorded at two localities are probably local structures and may have no regional significance.

Correlation of Upper Peel Sound Formation

Thorsteinsson (1980, p. 27) stated that, "the only evidence as to the age of the upper member of the Peel Sound Formation comes from one general fossil locality in Miall's (1970a) 'Sandstone-carbonate facies' near the north coast of Prince of Wales Island". A conodont identified from this locality is an indication of a late Lochkovian age. Thorsteinsson accepted the interpretation first proposed by Blackadar and Christie (1963), and adopted by Miall (1969, 1970a), that the nearly flat-lying strata exposed throughout most of northern Prince of Wales Island are all broadly comparable in age. Miall (1969, 1970a) subdivided these rocks into various facies belts and interpreted them in terms of a broad depositional systems tract, ranging from alluvial fans in the east to deltas and a carbonate platform in the west. Based on this interpretation, Thorsteinsson equated the conglomerates of the eastern outcrops with the conodont-bearing strata in the northern part of the island, and concluded that they were all late Lochkovian.

However, the Drake Bay Formation in the northwestern part of the island ranges up to late Pragian (Mayr, 1978) in age, implying a gentle westward regional dip, and Thorsteinsson (1980, Fig. 6) showed this dip as extending throughout northern Prince of Wales Island. There is, therefore, no reason why the conglomerates in the eastern part of the island could not include considerably older strata. A regional westward dip of only 2° would be adequate to accommodate a difference between a late Lochkovian age for the sandstone-carbonate facies and an early to middle Pridolian age for the upper Peel Sound conglomerate facies, 40 km to the east. This can be shown by the following simple estimate. Over a 40 km distance, a 2° dip results in a change in stratigraphic elevation of 1.4 km, meaning that the late Lochkovian horizon in the Sandstone-carbonate facies, exposed near sea level in western Prince of Wales Island, would be at an altitude of 1.4 km within the conglomerate facies. The base of the conglomerate facies is exposed near sea level, and so there would be 1.4 km of section representing the early Pridolian to late Lochkovian. This is equivalent to a sedimentation rate of about 0.7m/1000a, which is within the range of typical sedimentation rates for molasse basins (Schwab, 1976).

The nature of the regional dip is of crucial importance to the question of stratigraphic correlation, in the absence of fossils from the conglomerates of the upper Peel Sound, but it is of less importance to the paleogeographic reconstruction proposed by Miall (1969, 1970a), the essence of which would remain valid even if it could be shown that the upper Peel Sound Formation varied in age across Prince of Wales Island.

Conformable Contact Between Lower and Upper Members of the Peel Sound Formation

Thorsteinsson (1980) stated that a major unconformity exists between the two members of the Peel Sound Formation, and that it probably dies out to the west in Prince of Wales Island, because there is no evidence for it in the correlative Drake Bay Formation. However, the writer has documented several outcrops in eastern Prince of Wales Island where the contact is conformable and gradational over several tens of metres.

The upper and lower members are distinguished mainly on the basis of conglomerate character. Those of the lower members are pebble and cobble conglomerates consisting mainly of limestone and dolomite clasts, with up to 5 per cent of other clast types, including chert, Precambrian sandstones, and metamorphic rocks. The conglomerate units are interbedded with varying thicknesses of sandstone, limestone and dolomite. The upper member on Prince of Wales Island consists almost entirely of polymict cobble and boulder conglomerate, in which Precambrian clast types predominate.

From: Discussions and Communications in Current Research, Part A; Geol. Surv. Can., Paper 83-1A.

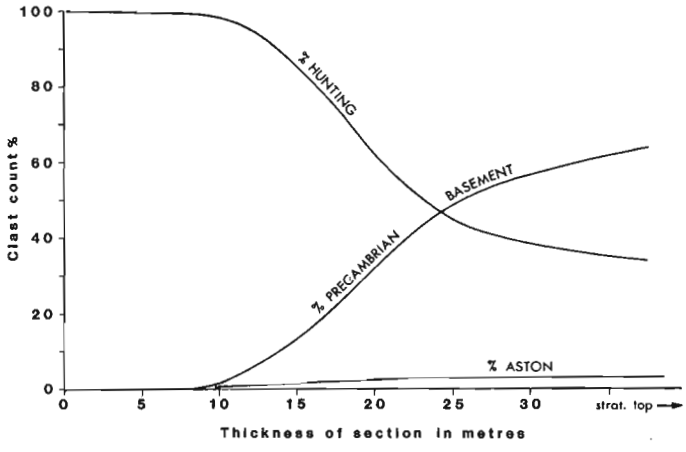

Figure 1. *Vertical clast changes between the upper and lower members of the Peel Sound Formation in a stratigraphic section at Cape Brodie.*

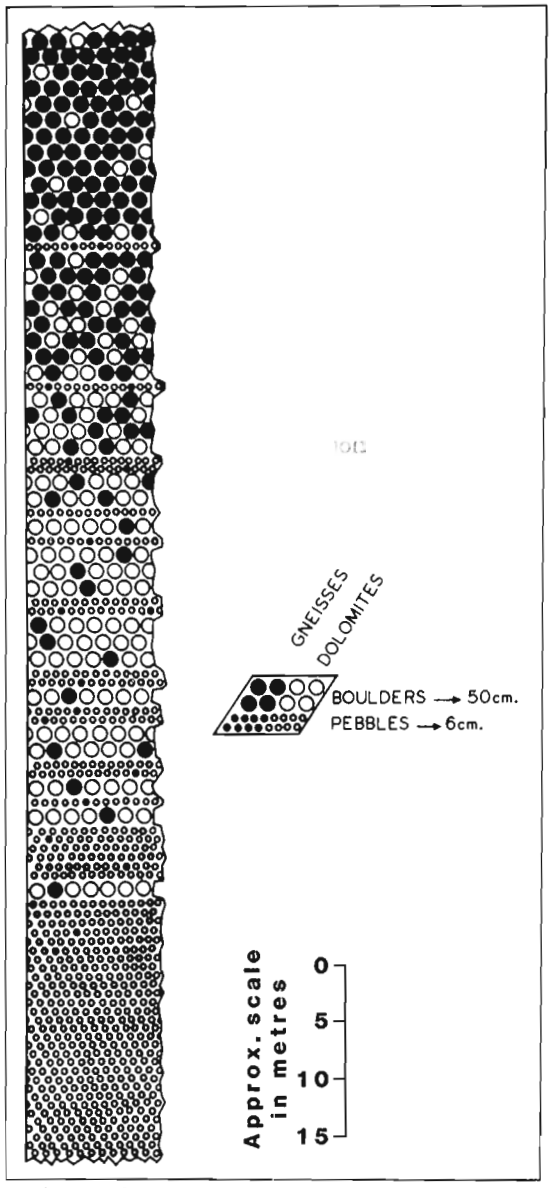

Figure 2. *Vertical clast changes at Transition Bay.*

Thorsteinsson (1980) implied that the contact between these different conglomerate types is abrupt, but this conflicts with a detailed documentation carried out at several localities by the writer (Miall, 1969). Sections measured across the contact at Mount Mathias, Cape Brodie, and Transition Bay, reveal gradational changes in clast composition and no angular discordance between the upper and lower members. Figure 1 illustrates clast changes recorded across the contact 16 km north of Cape Brodie, and Figure 2 summarizes data collected at several localities north of Transition Bay. Note that, in Figure 2, discrete beds of pebbly, dolomitic conglomerate are shown as interbedded with polymict boulder conglomerate over a vertical interval of more than 30 m. This has also been observed on southern Pandora Island. These vertical changes record the stripping away of the sediment cover from the Precambrian basement, resulting in a flood of basement detritus entering the Peel Sound drainage system. There is no reason why this event should have occurred everywhere at the same time. In fact, Miall (1969, 1979b) documented major lateral (north-south) changes in clast composition along the west flank of Boothia Uplift, reflecting variations in local source area geology. The contact between the lower and upper members of the Peel Sound Formation may therefore vary in age along strike. Similar vertical changes in clast composition occur east of the uplift in Somerset Island and their correlation is similarly uncertain.

Unconformities Within the Peel Sound Formation

Unconformities have been mapped at one locality in Prince of Wales Island, 11 km south of Bellot Cliff (Kerr and Christie, 1965; Miall, 1969), and in the Cape Anne syncline of northern Somerset Island (Miall and Gibling, 1978). At the Prince of Wales Island locality, the Peel Sound Formation rests on the Read Bay Formation (re-assigned to the Douro Formation by Thorsteinsson, 1980) with an angular discordance of over 20°. Miall (1969a) assigned the conglomerate above the unconformity to the lower Peel Sound, but Thorsteinsson (1980) interpreted it as part of the upper Peel Sound. In view of the unreliability of stratigraphic correlation based on conglomerate lithology, and the absence of any fossils, the precise age of this unconformity must remain uncertain.

In the Cape Anne syncline, mapping suggested that the polymict conglomerate in the uppermost part of the Peel Sound Formation (local member 4) rests conformably on older beds near the axis of the syncline, but cuts down unconformably into the oligomict conglomerate of member 2 toward Boothia Uplift, on the west flank of the syncline (Miall and Gibling, 1978).

Thorsteinsson (1980) suggested that both the Prince of Wales Island and Cape Anne observations represent exposures of a major regional unconformity of late Pridolian to early Lochkovian age. However, no biostratigraphic evidence is available to date the rocks above or below the unconformity at either location, so that we cannot be sure that the unconformities at the two locations are even of the same age.

To generalize about a regional unconformity from limited evidence such as this is a risky procedure. Many authors have commented on the difficulty of interpreting basin-wide events from the rocks exposed along basin margins. As Sloss (1963) noted, "the sedimentary records of basin margins and of the flanks of positive elements are punctuated by many unconformities," and "there is no apparent relationship between the prominence of the local evidences and the geographic scope of a given unconformity". These points were amply demonstrated by Riba (1976) who studied a well exposed succession of Tertiary alluvial fan conglomerates in the southern Spanish Pyrenees. There, syndepositional tectonism was very active, and several angular unconformities were mapped, none of which persisted down dip or along strike for more than a few kilometres. Riba showed angular discordances of 30° disappearing completely into a conformable contact 200 m down dip. Thus, although each unconformity represented a significant diastrophic episode, the extent of the tectonism may have been very limited. Uplift would have depended on the movement of particular fault blocks, and an unconformity would only have developed if the edge of the basin itself, on the downdip side of the fault, was partially

coupled to the fault and also underwent tilting. Accordingly, the writer's preferred interpretation of the Peel Sound unconformities is that they are local structures. This would seem to be confirmed by the conformable nature of the contact between the upper and lower members that has been recorded elsewhere, as noted above.

Implications for Boothia Uplift Tectonism

Thorsteinsson (1980) suggested that there were two episodes of diastrophism that affected Boothia Uplift, in the Late Silurian and Early Devonian. The first (late Ludlovian-early Pridolian) was restricted to the area south of Barrow Strait and formed the land area from which the lower Peel Sound Formation was derived. The second (late Lochkovian) is best dated in Cornwallis Island, where similar coarse clastics of the Snowblind Bay Formation occur. Thorsteinsson's correlations place the upper Peel Sound Formation in the same age bracket as the Snowblind Bay Formation, indicating that the second diastrophic episode was more widespread, affecting the whole of Boothia Uplift. The interpretation followed by the writer (following Miall and Gibling, 1978) is that the upper Peel Sound Formation is considerably older than the Snowblind Bay Formation, and that the evidence of the conglomeratic detritus suggests a single, extended period of diastrophism, that gradually extended northward along the uplift to Cornwallis Island.

The cause of this diastrophism remains a mystery. Plate tectonics theory cannot yet readily explain cratonic basement uplifts far from an active orogen. The structural and stratigraphic asymmetry of Boothia Uplift and its flanking clastic wedge south of Barrow Strait (Miall and Gibling, 1978), suggest that this was not a simple basement uplift as proposed by Kerr (1977). The writer would like to suggest, as an alternative model, to be explored by geophysical techniques, that Boothia Uplift may represent a deep-seated, east-dipping thrust block. Kerr (1977) compared the uplift to basement structures in Wyoming, but there the structural style has recently been shown by deep seismic reflection studies to be dominated by thrust faults extending to the base of the crust (Brewer et al., 1980; Smithson et al., 1978, 1979). Such a fault might have developed as an intraplate adjustment (along Precambrian lines of weakness) to the continental collisions that generated the Acadian Orogeny in Maritime Canada. Transmission of collisional stresses across the interior of a major continental plate has been well documented in Asia, where the docking of India with Tibet generated fault movements at least 3000 km north of the Indus Suture (Molnar and Tapponnier, 1975). Bache Peninsula Arch moved slightly later than Boothia Uplift (Trettin, 1978) and might have had a similar origin.

References

Blackadar, R.G. and Christie, R.L.
1963: Geological Reconnaissance, Boothia Peninsula, and Somerset, King William and Prince of Wales Islands, District of Franklin; Geological Survey of Canada, Paper 63-19, Report and maps 36-1963, 37-1963.

Brewer, J., Smithson, S.B., Oliver, J., Kaufman, S., and Brown, L.D.
1980: The Laramide orogeny: evidence from COCORP deep crustal seismic profiles in the Wind River Mountains, Wyoming; Tectonophysics, v. 62, p. 165-187.

Kerr, J. Wm.
1977: Cornwallis Fold Belt and the mechanism of basement uplift; Canadian Journal of Earth Sciences, v. 14, p. 1374-1401.

Kerr, J.W. and Christie, R.L.
1965: Tectonic history of Boothia Uplift and Cornwallis Fold Belt, Arctic Canada; American Association of Petroleum Geology, Bulletin, v. 49, p. 905-926.

Mayr, U.
1978: Stratigraphy of Lower Paleozoic formations, subsurface of Cornwallis, Devon, Somerset, and Russell Islands, Canadian Arctic Archipelago; Geological Survey of Canada, Bulletin 276.

Miall, A.D.
1969: The sedimentary history of the Peel Sound Formation, Prince of Wales Island, N.W.T.; unpublished Ph.D. thesis, University of Ottawa.

1970a: Continental marine transition in the Devonian of Prince of Wales Island, N.W.T.; Canadian Journal of Earth Sciences, v. 7, p. 125-144.

1970b: Devonian Alluvial Fans, Prince of Wales Island, Arctic Canada; Journal of Sedimentary Petroleum Geology, v. 40, p. 556-571.

Miall, A.D. and Gibling, M.R.
1978: The Siluro-Devonian clastic wedge of Somerset Island, Arctic Canada, and some regional paleogeographic implications; Sedimentary Geology, v. 21, p. 85-127.

Molnar, P. and Tapponnier, P.
1975: Cenozoic tectonics of Asia: effects of a continental collision; Science, v. 189, p. 419-426.

Riba, O.
1976: Syntectonic unconformities of the Alto Cardener, Spanish Pyrenees: a genetic interpretation; Sedimentary Geology, v. 15, p. 213-233.

Schwab, F.L.
1976: Modern and ancient sedimentary basins: comparative accumulation rates; Geology, v. 4, p. 723-727.

Sloss, L.L.
1963: Sequences in the Cratonic Interior of North America; Geological Society of America, Bulletin, v. 74, p. 93-113.

Smithson, S.B., Brewer, J.A., Kaufman, S., and Oliver, J.
1979: Structure of the Laramide Wind River Uplift, Wyoming, from COCORP deep reflection data and from gravity data; Journal of Geophysical Research, v. 84, p. 5955-5972.

Smithson, S.B., Brewer, J.A., Kaufman, S., Oliver, J., and Hurich, C.
1978: Nature of the Wind River thrust, Wyoming, from COCORP deep reflection and gravity data; Geology, v. 6, p. 648-652.

Thorsteinsson, R.
1980: Stratigraphy and conodonts of Upper Silurian and Lower Devonian rocks in the environs of the Boothia Uplift, Canadian Arctic Archipelago, Part I: contributions to stratigraphy; Geological Survey of Canada, Bulletin 292.

Trettin, H.P.
1978: Devonian stratigraphy, west-central Ellesmere Island, Arctic Archipelago; Geological Survey of Canada, Bulletin 302.

STRATIGRAPHY AND TECTONICS OF THE PEEL SOUND FORMATION, SOMERSET AND PRINCE OF WALES ISLANDS: EDITOR'S NOTE

R. Thorsteinsson has read A.D. Miall's Discussion and welcomes the additional information it contains and the suggested reinterpretation of the nature and timing of the episodes of diastrophism that affected the Boothia Peninsula.

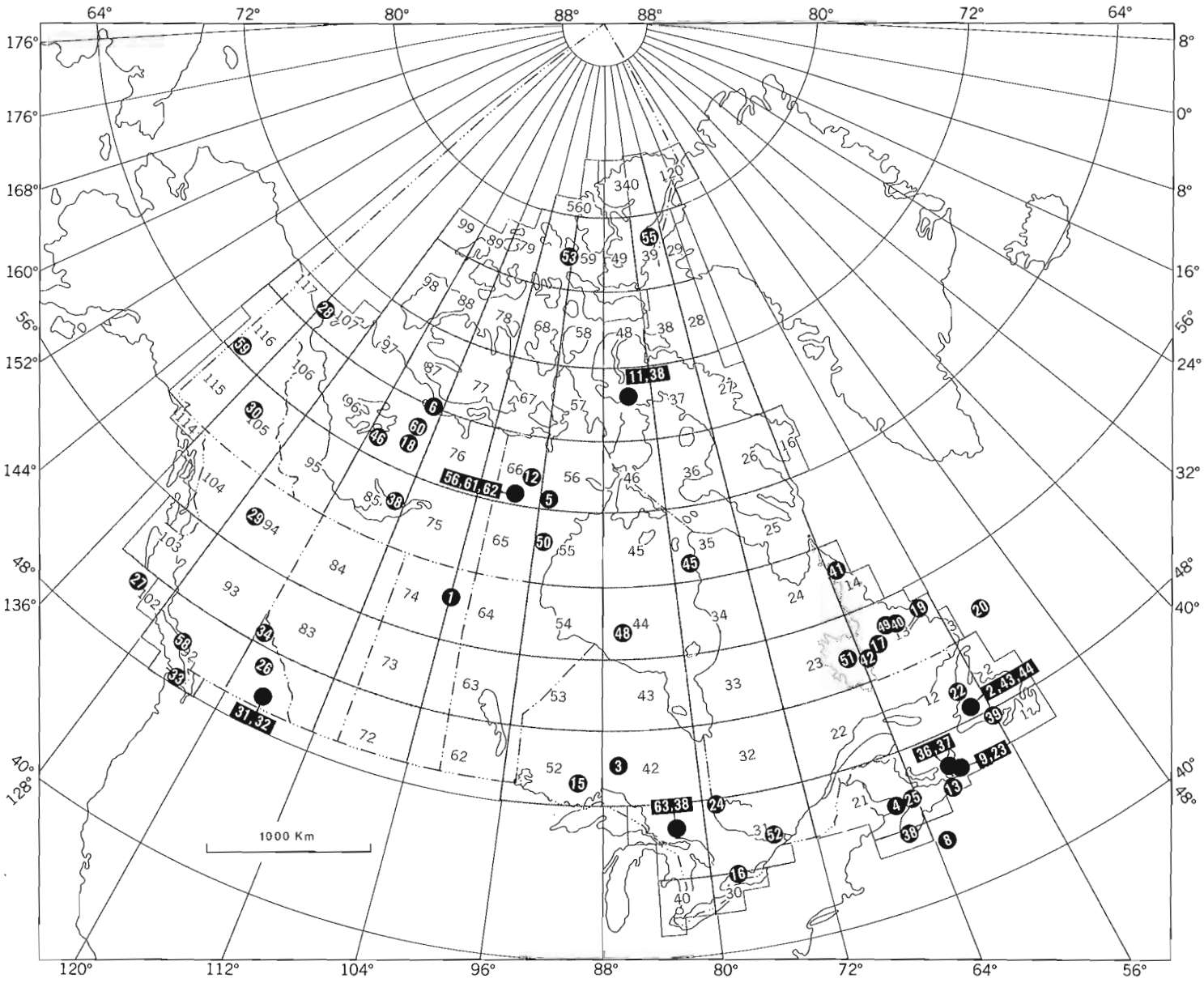
64°
72°
80°
88°
88°
80°
72°
64°
176°
176°
168°
160°
56°
152°
144°
48°
136°
40°
128°
8°
0°
8°
16°
56°
24°
32°
48°
40°
48°
120°
112°
104°
96°
88°
80°
72°
64°
56°
1000 Km

AUTHOR INDEX/INDEX DES AUTEURS

NOTE TO CONTRIBUTORS

Submissions to the *Discussion* section of *Current Research* are welcome from both the staff of the Geological Survey and from the public. Discussions are limited to 6 double-spaced typewritten pages (about 1500 words) and are subject to review by the Chief Scientific Editor. Discussions are restricted to the scientific content of Geological Survey reports. General discussions concerning branch or government policy will not be accepted. Illustrations will be accepted only if, in the opinion of the editor, they are considered essential. In any case no redrafting will be undertaken and reproducible copy must accompany the original submissions. Discussion is limited to recent reports (not more than 2 years old) and may be in either English or French. Every effort is made to include both *Discussion* and *Reply* in the same issue. *Current Research* is published in January, June and November. Submissions for these issues should be received not later than November 1, April 1, and September 1 respectively. Submissions should be sent to the Chief Scientific Editor, Geological Survey of Canada, 601 Booth Street, Ottawa, Canada, K1A 0E8.

AVIS AUX AUTEURS D'ARTICLES

Nous encourageons tant le personnel de la Commission géologique que le grand public à nous faire parvenir des articles destinés à la section discussion *de la publication* Recherches en cours. *Le texte doit comprendre au plus six pages dactylographiées à double interligne (environ 1500 mots), texte qui peut faire l'objet d'un réexamen par le rédacteur en chef scientifique. Les discussions doivent se limiter au contenu scientifique des rapports de la Commission géologique. Les discussions générales sur la Direction ou les politiques gouvernementales ne seront pas acceptées. Les illustrations ne seront acceptées que dans la mesure où, selon l'opinion du rédacteur, elles seront considérées comme essentielles. Aucune retouche ne sera faite aux textes et dans tous les cas, une copie qui puisse être reproduite doit accompagner les textes originaux. Les discussions en français ou en anglais doivent se limiter aux rapports récents (au plus de 2 ans). On s'efforcera de faire coincider les articles destinés aux rubriques* discussions *et* réponses *dans le même numéro. La publication* Recherches en cours *paraît en janvier, en juin et en novembre. Les articles pour ces numéros doivent être reçus au plus tard le 1er novembre, le 1er avril et le 1er septembre respectivement. Les articles doivent être renvoyés au rédacteur en chef scientifique: Commission géologique du Canada, 601, rue Booth, Ottawa, Canada, K1A 0E8.*

Energy, Mines and Resources Canada

Énergie, Mines et Ressources Canada